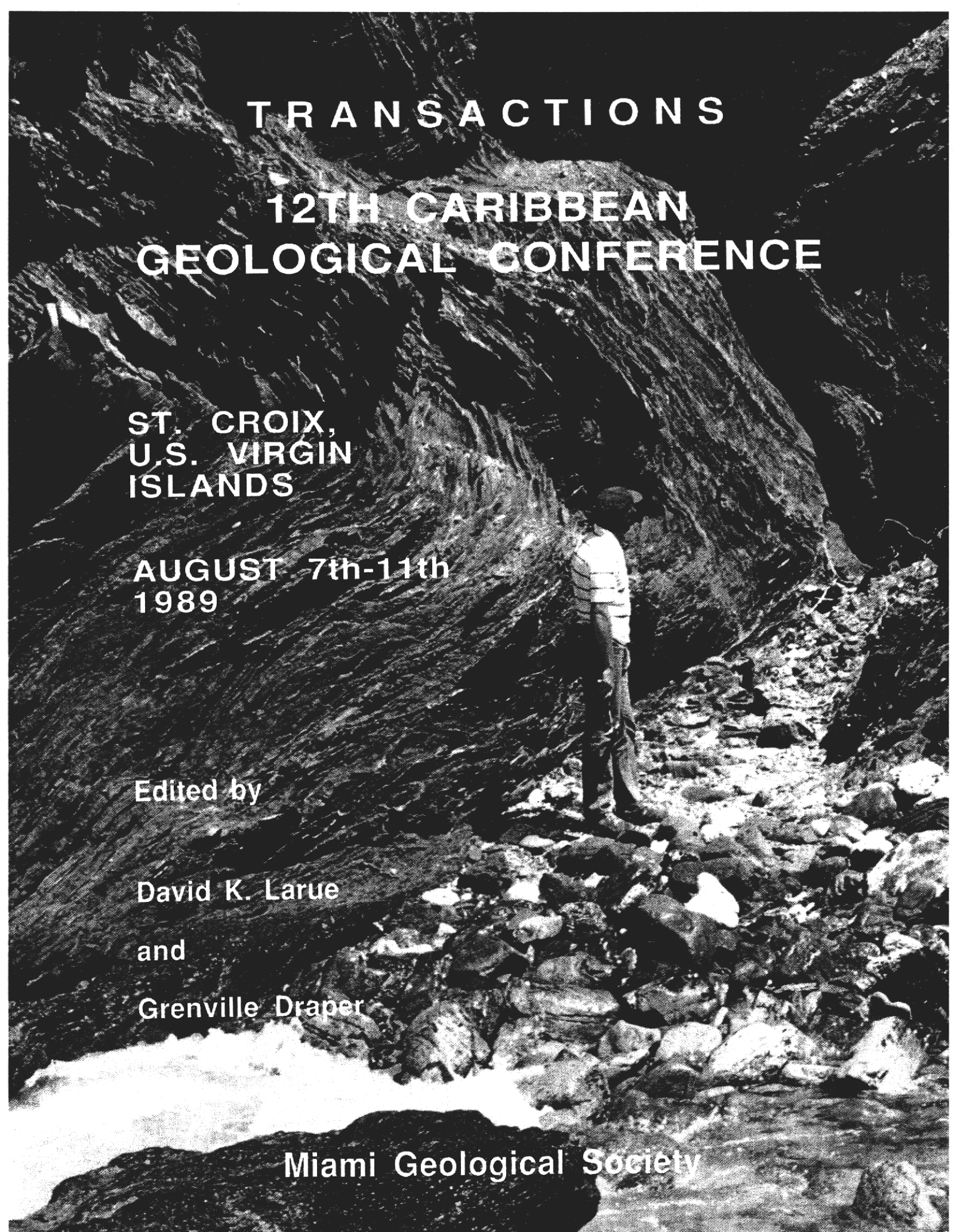

TRANSACTIONS

12TH CARIBBEAN GEOLOGICAL CONFERENCE

ST. CROIX,
U.S. VIRGIN
ISLANDS

AUGUST 7th-11th
1989

Edited by

David K. Larue

and

Grenville Draper

Miami Geological Society

12a Conferencia Geologica del Caribe

12th Caribbean Geological Conference

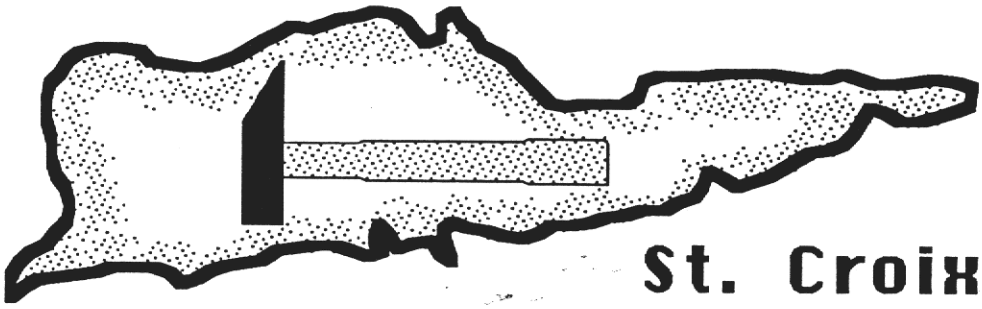

St. Croix

7th - 11th August, 1989

U.S. Virgin Islands

12me Conference Geologique de Caraibes

TRANSACTIONS OF THE 12TH CARIBBEAN GEOLOGICAL CONFERENCE

ST. CROIX, U.S. VIRGIN ISLANDS

August 7th - 11th, 1989

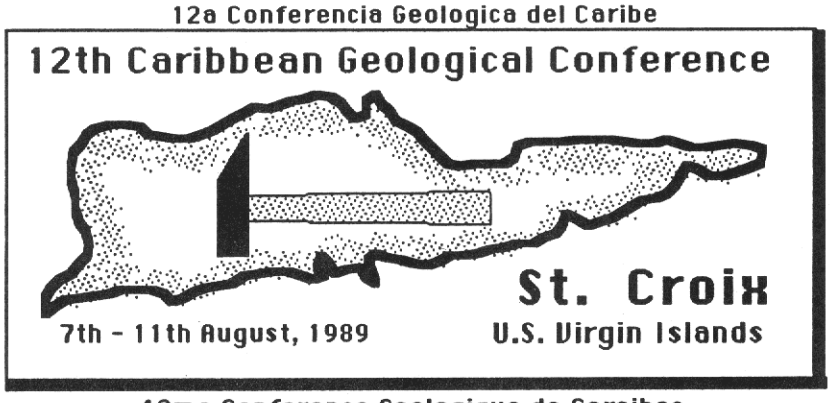

Edited by

David K. Larue
Department of Geology, University of Puerto Rico
Mayagüez, PR 00708, Puerto Rico

and

Grenville Draper
Department of Geology, Florida International University
Miami, FL 33199
U.S.A.

Additional copies of this book may be purchased from

Miami Geological Society
P.O. Box 431552
South Miami, FL 33243, U.S.A.

December 1990

COPYRIGHT © 1991 by the Miami Geological Society
All rights reserved

All materials subject to this copyright and included in this volume may be photocopied for the noncommercial purpose of scientific or educational advancement.

COVER

Looking East at deformed beds Cretaceous turbidites (Caledonia Formation) at Hams Bluff, West End St. Croix. Photo by Fred Nagle 1987; Gren Draper is scale.

Conference logo by Gren Draper created on a Apple Macintosh® computer with Superpaint®

12TH CARIBBEAN GEOLOGICAL CONFERENCE
August 7th - 11th, 1989
Christiansted, St. Croix, U.S. Virgin Islands

SPONSORS

Mobil Exploration and Producing Services, Inc.
United States Geological Survey
University of Miami
West Indies Laboratory, Fairleigh Dickinson University
Florida International University
University of Puerto Rico, Mayaguez

ORGANIZING COMMITTEE

Frederick Nagle, *General Chairman*
Dennis Hubbard, *Co-Chairman*
Grenville Draper, *Technical Program Chairman*
James Joyce, *Field Trip Chairman*
Claudia Johnson, *Technical Sessions*
Alan Smith, *Technical Sessions*

FIELD TRIPS

Ivan Gil
Dennis Hubbard
James Joyce
Alain Mascle
Gray Multer
Robert Speed
Malcom Weiss

TRANSACTIONS EDITORS

David Larue
Grenville Draper

CARIBBEAN GEOLOGICAL CONFERENCES PERMANENT STANDING COMMITTEE

John Saunders, *Chairman*

Leslie Barker • Alirio Belizzia. •. Jacques Butterlin • Salvador Brouwer •Thomas Donnelly •Grenville Draper •Hermann Duque-Caro • TrevorJackson • JamesJoyce • John Lewis • Henry MacvGillavry • Frederick Nagle • Edward Robinson • Kirton Rodriques • Carlos Schubert • Alan Smith • William Snow

Published by the Miami Geological Society, P.O. Box 431552, South Miami, FL 33243, U.S.A

Field guide:

Terrestrial and Marine Geology of St. Croix, U.S. Virgin Islands.
Dennis K. Hubbard (ed.) 213pp.

is available from:

Dr. D.K. Hubbard
5056 Cotton Valley 66
St. Croix, U.S. Virgin Islands
00820-4519

U.S. orders $25 Overseas orders $30
(shipping included)

Miami Geological Society

P.O. Box 431552, South Miami, FL 33243, U.S.A.

PUBLICATION LIST

JUNE 1988

DONATION
($US Drawn on US Banks Only)

1964 Field Guide to Geology and Geochemistry of the Bone Valley Formation and its Phosphate Deposits, West Central Florida: by S. Altschuler, J.B. Cathcart and E.J. Young, 68 pp..... $ 5.00

1964 Field Guidebook to Living and Fossil Reef Types of South Florida: by J.E. Hoffmeister, J.I. Jones, J.D. Milliman, D.R. Moore, and H.G. Multer, 28 pp..... $ 4.00

1964 Field Guidebook to Environments of Coal Formation in Southern Florida: by William Spackman, David W. Scholl, and William H. Taft, 67 pp..... $ 6.00

1971 Miami Geological Society Memoir 1, A Symposium of Recent South Floirda Foraminifera: by W.D. Bock, G.W. Lynts, S.L. Smith, R.C. Wright, W.W. Hay, and J.I. Jones, 245 pp..... $ 4.00

1977 Guatemala, Where Plates Collide: A Reconnaissance guide to Guatemalan Geology: by Frederick Nagle, Joshua Rosenfeld, and Jerry J. Stipp, 72 pp.
(without geologic map)..... $11.00
(with geologic map)..... $15.00

1979 A Field Guide with Road Log to the Pliocene Fossil Reef of Southwest Florida: by John F. Meeder (Barbara Lidz, ed.), 19 pp..... $ 6.00

1979 Hispaniola: Tectonic Focal Point of the Northern Caribbean - Three Geologic Studies in the Dominican Republic: by Frederick Nagle, H. Currie Palmer, and Gustavo A. Antonini (Barbara Lidz and Frederick Nagle, eds.) 96 pp., 3 maps..... $15.00

1980 The 1980 Field Trip Experience of the Miami Geological Society, "Water, Oil, and the Geology of Collier, Lee, and Hendry Counties:" edited and compiled by Patrick J. Gleason, 73 pp (out of print)..... $ 8.00

1981 Survey of Central Florida Geology - Miami Geological Society 1981 Field Trip: (with road log) 44 pp (out of print)..... $ 6.00

1982 Survey of the Geology of Haiti - Miami Geological Society 1982 Field Trip: by Florentin Maurrassee, 80 pp..... $10.00

1983 Miami Limestone: A guide to Selected Outcrops and Their Interpretations (with a discussion of diagenesis in the Formation): by Robert B. Halley and Charles C. Evans, 67 pp..... $10.00

1983 Miami Geological Society Memoir 2, Environments of South Florida: Present and Past: edited and compiled by Patrick J. Gleason, (revision of 1974 edition), about 500 pp..... $35.00

1988 Miami Geological Society Memoir 3, Symposium on South Florida Geology (ed: by F.J. Maurrasse) 233 pp..... $18.00

Overseas request: Please add $6.00 (U.S.) for shipping
U.S. orders: Please add 10% of purchase price for shipping

ACKNOWLEDGEMENTS

Late in July 1986, Nick Donnelly and I were on a flight together heading toward Bridgetown, Barbados for the 11th Caribbean Geological Conference. We were both concerned that all the pre-conference efforts of the Standing Committee to determine where the 12th Conference was to be held, a matter which was the major business item to be settled at the 11th Conference, had not resulted in a clear cut, single, choice. As I recall, he waited until we were on final approach (knowing full well of my general panic on all take-offs and landings) to ask me whether I thought it possible to have the next conference on St. Croix and whether I would volunteer to try to put it together. Now, I would never say "no" to anything during a landing or a takeoff, but I did manage to ask for two days to think about it. It is not bending the truth very much to say that I have thought about the 12th Conference every day since, in one way or another.

Although I felt honored to be asked to try to organize the Conference, it seemed to me an almost impossible situation, since there was no money in the bank, and I lived 1500 miles from the conference site. I took some hope from the knowledge that Donnelly had started from a similar position for the conference on St. Thomas some 20 years earlier. Frequent contact with and encouragement from members of the Standing Committee, especially Nick Donnelly and John Saunders, carried me through both some early and late moments of doubt. Bill Snow, Leslie Barker, and Hermann Duque-Caro were very generous in sharing budget information, mailing lists and hints gained from the experience of their earlier conferences.

I didn't realize it until much later, but my decision, made even before leaving the Barbados Conference, to dragoon Gren Draper and Dennis Hubbard into sharing the day to day organizational burden was the best and most important decision I was to make for the next three years. During that same time I extracted a promise of "support-in-kind" from the then Director of the West Indies Laboratory, John Ogden, which was later honored and delivered in a way that exceeded all my highest expectations by his successor Betsy Gladfelter, her colleagues, and her staff.

The day the check arrived from Mobil Exploration and Producing Services Inc., (MEPSI) was a high moment for us and when this check was followed by a generous contribution from the United States Geological Survey (U.S.G.S.), we knew we had a Conference and that it would be in St. Croix. I want to again thank Richard Kirk and C. P. Menard of MEPSI and Dallas Peck, Ben Morgan and Bob Halley from the U.S.G.S. for their help in obtaining these critical funds. We also received support from the West Indies Lab, the University of Miami, Florida International University and the University of Puerto Rico. We could not have gone forward with the conference without these funds.

My second best decision, closely rivaling the first best, was to ask my wife Rhoda and Dorothy Rowe from the West Indies Laboratory to handle all the day to day administration of the Conference during the two weeks of the actual conference. Those who were there know I did the right thing. In support of their effort and in order to make use of the computer talents of Rhoda and Gren Draper for last minute notices, program changes etc., we had a rental Mac SE flown in by seaplane from St. Thomas. That maneuver has to be a Conference first! Meanwhile, Hubbard and a team of helpers including Karla Parsons, Laura Venger and others were struggling night and day to put together the

Terrestrial and Marine Geology of St. Croix on a Mac II at the West Indies Laboratory. The conference owes a big collective thank you to Apple Computer Inc.

Another Conference "first" was the poster session arranged by Draper and Hubbard at The West Indies Laboratory. Although the whole conference had to be moved 8 miles for that afternoon, the effort was well worth it as that session added a new dimension to Caribbean Geological Conferences.

Randy Wheelis (Manager), Jim Schuck (Restaurant Manager) and Ada Ramos (Reservations) at our headquarters hotel went far beyond normal duties for our Conference and I want to thank them and their staff at Hotel-on-the-Cay for their help.

Field trips should be a heart of any conference and I think those of the 12th Conference were certainly that. My personal thanks to Dennis Hubbard, Bob Speed, Jim Joyce, and Ivan Gil, amongst others, for making the trips superior. And thanks also to Gray Multer, Malcolm Weiss and Alain Mascle who spent considerable effort planning trips to Antigua.

For the past year and one half, Dave Larue and Gren Draper, have been badgering the contributors to this volume, and each other, to get it together, and the fact that we have done so is due in no small way to their labors.

Art Snoke and Earl Kauffman have done us all a good service by writing Conference summaries which have appeared in the October 1990 issue of Geotimes, and the Journal of South American Earth Sciences, v. 3, no. 2/3, 1990. I am especially grateful to them for doing this since it would have been impossible for me to do. Conference chairpersons are too busy to attend many of the actual conference sessions, and therefore, I read their summaries with more than usual interest, simply to find out what had happened!.

Hurricane Hugo hit the island of St. Croix about a month after our Conference, severely damaging the West Indies Laboratory, flattening the rooms at Hotel on the Cay where we held our sessions, and destroying the Divi Hotel and the sea planes who brought us our computer. Although Hotel-on-the-Cay is back in business, and the Divi Hotel plans to rebuild, there is considerable doubt as to whether the West Indies Laboratory will ever function again as a research laboratory. Our best wishes go out to all our friends at these institutions and other businesses who helped the 12th Conference to be the success it was.

Finally, my heartfelt thanks to all of our delegates who came from 19 countries to participate in this Conference and in so doing made it for me something I now look back on as a highlight of 30 years of geologic work in the Caribbean.

Frederick Nagle
General Chairman

EDITORS' FOREWORD

Editing a volume such as this is a distinct pleasure. It is a chance to share ideas and discover the current thinking about the geology of the Caribbean developed by its multinational constituency. It allows one to correct the syntax of your English-speaking colleagues (and to admire the same of you Spanish- and French- speaking friends). Waiting for late manuscripts gives lessons in the art of patience and the science of pleading. Furthermore, it gives opportunities to puzzle through exciting, though thoroughly confusing concepts of Caribbean tectonic evolution, only to find that you are editing your own paper, at the same time waiting seemingly interminably for Art Snoke's paper and listening to Fred Nagle recite baseball statistics. And lastly, there is the experience of accepting papers with unsolicited modifications, no reference to your trials in the acknowledgements and having all your editing ignored in the final version anyway. Editing has indeed been a sincere pleasure. The result of over a year of work, this volume represents a kind of "Dorian Gray" literature in which the editors have aged and the volume remains timeless.

Despite our tribulations, we are happy to say that the experiment of assembling the volume from author prepared "camera-ready" copy has been a success and this owes much to the perseverance and cooperation of the authors. This is a "first" for the Caribbean conference transactions and it has enabled us to produce the volume much more rapidly and much more cheaply than would otherwise have been possible (and also with much less work on the part of the editors).

Another distinguishing feature of the transactions is the inclusion of several works by some of our Cuban colleagues. Despite the fact that they were unable to attend the meeting, we felt it important that we try to disseminate their findings, as information on Cuba is difficult to find outside the island. Unfortunately we were unable to publish all of the manuscripts that were given Gren Draper as we did not have the time or resources to prepare the camera-ready copy for the second batch.

Many people helped us in our labors. Fred Nagle provided a constant source of information, anecdotes and encouragement (even though he was late with his Acknowledgements foreword). We are especially indebted to those of our colleagues who we coerced into reviewing papers. These were Hans Schellekens, Alan Smith, Homer Montgomery and Jim Joyce of the University of Puerto Rico, Gautam Sen of Florida International University, and Claudia Johnson of the University of Colorado - Boulder. We are grateful to Ana Cortada and Leticia Flores who helped prepare several of the Spanish manuscripts. The assistance of Iris Diaz, Nydia Torres and especially Dimas Camacho was essential in preparing the final camera-ready state of the volume.

Lastly, we thank the Miami Geological Society for agreeing to be the publisher of the transactions and for providing that necessary additional finance to make publication possible

Dave Larue
Gren Draper

LIST OF ATTENDEES

Asencio, Eugenio, Law Environmental, 54-56 Bolivia St, Hato Rey, PR 00919; 809/758-2909

AveLallemant, Hans, Dept of Geol & Geophys, Rice Univ, PO Bx 1892, Houston, TX 77251; 713/527-4889

Barker, Leslie H., #35 Fairview Hgts., St.George, Barbados; 809/42-95254

Barreto Orta, Maritza, Marine Sci Dept, CAAM, Mayaguez, PR 00708; 809/729-6935

Baumgartner, Claudia Mora, Inst de Geol, Univ of Lausanne BFSH 2, CH-1015 Lausanne, Switzerland; 04121 692 4851

Baumgartner, Peter O., Inst de Geol, Univ of Lausanne BFSH 2, CH-1015 Lausanne, Switzerland; Phone: 04121 692 4852

Baxter, Carlton, Geol Survey Div, Hope Gardens, PO Box 181, Kingston 6, Jamaica; 92-71065

Bjorklund, Tom, Exptrte-Amoco Trinidad, PO Box 4381, Houston,TX 77210; 809/622-7331 FX908/628-5058

Black, John A., Suffolk College, Selden, NY 11784; 516/451-4120

Bloise, Giovanni E., PO Box 1343, Santo Domingo, DR; 809/682-6041 FAX 809/567-6905

Bonini, William E., Dept Geol., Princeton Univ., Princeton, NJ 08544; 609/452-3598

Brouwer, Salvador, PO Box 1343, Santo Domingo, DR; 809/525-4161 FAX 908/567-6905

Brueckmann, Warner, Geomar-Ctr for Marine Geosci Res, Wischhofsh 1-3, Bldg 9, D-2300 Kiel, FRG; 049/431-7202148 FAX 049/72025650

Burke, Kevin, NAS/NRC, 2101 Constitution Ave, NW, Washington, DC 20148; 202/334-3065

Burke, Randy, N.D. Geological Survey, PO Box 8156, Grand Fork, ND 58202-8156; 701/777-2231

Carr-Brown, Barry, c/o Trinidad & Tobago Oil Co., Pointe-A-Pierre, Trinidad and Tobago; 809/658-5241; FAX 809/658-1315

Cepeda, Rosa, Av. Central #39, Bo 30 de Mayo, Santo Domingo, DR; 809/685-8191

Chavez Castro, Cevero, PO Box 1343, Santo Domingo, DR; 809/525-4161 FAX 908/567-6905

Connor, Charles, Dept of Geol, Florida International Univ, Miami, FL 33199; 305/348-3089; FAX 305/348-3877

De la Bastide, Alan, c/o Trintopec, Santa Flora, PR; Phone 809/649-5500, FAX 809/649-5810

De Leon, Rafael Osiris, CORDE, Av Jiminez Moya esq Jose Contreras. Santo Domingo, DR; 809/535-9026; FAX 809/535-1656

DeZoeten, Ruurdjam(Rudi),Unocal Corp Int Oil&Gas Div,1201 W. 5 St., PO Bx 7600, Los Angeles, CA 90051; 231/977-5938

Dillon, William P., U.S. Geol.Survey, Woods Hole, MA 02543; 508/548-8700

Dingwall, Bruce, c/o Lasmo, 140 London Wall, London, England; Phone: 01-600-8021

Dolan, James F., US Geol Survey, MSGGG, 345 Middlefield Rd, Menlo Park, CA 94025; 415/354-3064

Dominguez, Hugo, PO Box 58, Santiage, Dominican Republic; 809/541-0403

Draper, Grenville, Dept of Geol, Florida International University, Miami, FL 33199; 305/348-3087; FAX 305/348-3877

Drobnyk, John, 140 Tuttles Pt. Rd., Guilford, CT; 203/397-4341

Droxler, Andre W., Dept of Geol & Geophys, Rice Univ, PO Bx 1892, Houston, TX 77251; 713/527-4885

Edgar, Terry, U. S. Geological Survey, Nat'l Center MS 914, Reston, VA 22092; 703/648-6508

Faugeres, Jean Claude, Dept de Geol, Univ de Bordeaux I, Ave des Facultes, 33405, Talence, France 56 806800

Frampton, John, Trinmar Ltd, Point Fortin, Trinidad, WI; Phone 648-2475

Franceschi, Guy, c/o Bugeco, Av Tervueren 206, Brussels Belgium; 02/707 5401, Fax 32 2 7123897

Geier, Lois J., 18911 NW 43 Avenue, Carol City, FL 33055; 305/554-2876

George, E. P., T. M. Brouwmeeslerlaan 26, 2597 G2, Den Haag, Nederland, 070/776033 FAX 070/774848

Gill, Ivan, Dept. of Geology, Tulane Univ., New Orleans, LA 70118; 504/865-5198

Gilzean, Mary, 5847 San Felipe, Suite 3820, Houston, TX77057; 713/268-5825

Glaser, Karen S., 2615 Heathergold, Houston, TX 77084; 713/527-4880

Gobel, Volker, Box 13011 SFA, Nacadoches, TX 75962; 409/568-3701

Gordon, Carla, 18 Richings Ave, Kingston 6, Jamaica, WI

Gordon, Mark, Dept Geol Sci, The Univ of Texas, Austin, TX 78713-7909; 512/471-0438

Grammer, Michael, Univ of Miami, Fisher Island Station, Miami Beach, FL 33139; 305/672-1840

Greenstein, Ben, Dept. of Geology, University of Cincinnati, OH 45221-0013; 513/556-3732

Greeson, Phillip E., U. S. Geological Survey, 75 Spring St, Suite 772, Atlanta, GA 30303; 404/331-3389

Guth, Lawrence R., Geol & Geophysics, Rice Univ PO Box 1892, Houston, TX 77251; 713/527-4880

Hall, Stuart A., Dept of Geosciences, Univ of Houston, Houston, TX 77204-5503; 713/749-4523

Harris, Norman, c/o Geol Survey Div, Hope Gardens, Kingston 6, Jamaica; 92-71936-9

Hayden, Joseph, 214/951-2814

Hendrickson, G., 642 English Bluff Rd., Delta, BC Canada V4M 2N4; /943-0983

Hendry, Malcolm, Cermes, Univ of West Indies, PO Box 65, Bridgetown, Barbados; Phone: 425-1310

Hodeson, C. Jay, Dept of Geol Sci, Queen's Univ, Kingston, Ontario, Canada K7L 3N6; 613/545-2601 FAX 613/545-6592

Hosein, Fazal, 9 Tamarind Ave., Pointe-A-Pierre, Trinidad W.I.; 658-5343

Hubbard, Dennis, West Indies Lab, Teague Bay, Christiansted, St. Croix USVI 00820; 809/773-9339

Hunter, Garry, Hunter & Assoc, 2695 North Sheridan Way, Mississnaga, Ontario, Canada; 416/855-2323; FAX 416/855-2411

Hupp, Cliff, R., US Geological Survey, 432 National Center, Reston, VA 22092; 703/648-5833

Jeremie, Jean-Jacques, Univ des Antilles Guyane, BP 592, 97167, Pointe a Pitie CEDEX FWI; 915696

Jimenez, Jorge, Dept de Expl Falconbridge Dom, Apto 1343, Santo Domingo, DR; 809/525-4161

John, Howard, c/o Ministry of Energy, Riverside Plaza, Port-of-Spain, Trinidad, WI 809/623-2727

Johnson, Claudia C., Dept Geol Sci, CB 250, Univ of Colorado, Boulder, CO 80309; 303/492-8141; FAX 303/492-2606

Jones, Brian, Dept of Geol, Univ of Alberta, Edmonton, Alberta, CN T6G 2E3; 403/492-7036

Jove', Carlos F., SC Bustamante #463, Hato Rey, PR 00918; 809/754-6299

Joyce, James, Dept of Geol, Univ of Puerto Rico, Mayaguez, PR 00709; 809/264-3845

Katz, Miriam, Lamont-Doherty Geol Obs., Palisades, NY 10964; 914/359-2900 x625

Kauffman, Erle G., Dept Geol Sci, CB 250, Univ of Colorado, Boulder, CO 80309; 303/492-6629; FAX 303/492-2606

Kellogg, James, Dept Geol Sci, Univ of S. Carolina, Columbia SC 29208; 803/777-4501 FAX 803/777-3065

Larson, Matt, USGS, PO Box 4424, San Juan, PR 00936; 809/749-4341

Larue, David K., Dept. of Geol, Univ of Puerto Rico, Mayaguez, PR 00709; 809/265-3845

Lawson, David, Dept Earth Sciences, Univ of Waterloo, Waterloo, Ont, Canada N2L 3G1; 519/885-1211 x3235

Lewis, John, Geol Dept, Geo Washington Univ, Washington DC 20052; 202/994-6987

Lidiak, Edward, Dept. of Geol. & Planetary Sci., Univ of Pittsburgh, Pittsburgh, PA 15260; 412/624-8871

Louca, Kyriacos, 45th Str 304E Rm FF1174, New York, NY 10017; 212/906-6390

Love, Karen, Dept Geosci, Univ of Houston, Houston,TX 77004; 713/749-4325

Lynch, Willy, 1636 Glen Ayr Dr, lakewood, CO 80215; 303/238-9419

Massa, Audrey A., Carleton College, Northfield, MN 55057; 507/663-4404, 5407

Maurrasse, Florentin, Dept of Geol, Florida International Univ, Miami, Fl 33199; 305/554-2365; FAX 305/348-3877

McLaughlin, Peter, Exxon Prod. Research Co., PO Bx 2189 (ST-4183A), Houston,TX 77252;713/966-6073

McNeill, Don, 4600 Rickenbacker Cswy, RSMAS/MGG, Miami, FL 33149; 305/672-1840

McVeigh, J. Garfield, (Falconbridge Dominicana) 1013 Club Crescent, New Minas, Nova Scotia Canada

Medina-Tyson, Dawn, #77 Fairview Park, Freeport, Trinidad, W.I.

Mercado, Reinaldo, Geol Dept., Michigan Tech Univ., Houghton, MI 49931, 906/487-2714

Merz, Martina, Fisher Island Station, Miami Beach, FL 33139; 305/672-1840

Meyers, Jayson B., 4600 Rickenbacker Cswy, RSMAS/MGG, Miami, FL 33149; 305/361-4683

Millman, Dean B., 18219 Wilstone Dr., Houston, TX 77084; 713/629-6600

Moore, Richard L., Jose Marti #9, Santo Domingo, Dominican Republic

Multer, Gray, 9855 Canaseraga Rd., Arkport, NY 14807; 607/295-7677

Munoz, Ivette, C 535 QM 16 Country Club, Rio Piedras, PR 00924; 768-9431, 265-2262

Nadai, Agi, 69 Greendale Rd., Scarsdale, NY 10583; 212/264-6730 Home phone 914/723-2477

Nadeau, Joseph, Dept. Geol & Marine Sci., Rider Coll, Lawrenceville, NJ 08648; 609/596-5314

Nagle, Frederick, Dept Geol Sci, Univ of Miami, Coral Gables, FL 33124; 305/284-4253

Ng, Samuel, Dept of Geol, Univ of Alberta, Edmonton, Alberta, Canada T6G 2E3; 403/492-7377

Nollsch, David, Pecten International, PO Box 205, Houston, TX 77001; 713/556-4742

Oostdam, B. L., Millersville Univ, Millersville, PA 17551; 717/989-6012 FAX 717/872-3985

Pascaline, Helene, Univ des Antilles-Guyane, B.P. 592, 97167, Pointe-A-Pitie, CEDEX FWI; 91 56 96

Persad, Krishna, 690 Ailgen Ave, Plimiste, Trinidad, WI; 809/657-4897 FAX 809/562-5613

Pindell, Jim, Earth Sciences, Dartmouth College, Hanover, NH 03755; 603/643-8514

Pittelli, Rosina, Maraven,SA, Filial de Petroleos de Venezuela, Dpto de Exploracion, Piso 9, Apartado 829, Caracas 1010A, Venezuela; Phone (58) (2) 9083223, FAX (58) (2) 9083150

Pizano, Orlando, PO Box 1343, Santo Domingo, DR; 809/682-6042 FAX 908/567-6905

Prieto, Rodulfo, Apdo 889, Lagoven S.A., Caracas, Venezuela; 582/606-4309

Puleo, Peggy, 5341 Gibson Hill, Edinboro, PA 16412; 814/732-2453

Renken, Robert A., 6481B Peachtree Indust Blvd., Doraville, GA 30360; 404/986-6860

Reyes, Elias, 809/682-6041 FAX 809/567-6905

Rhoades, Susan M., PO Box 757, Frederiksted, St. Croix USVI 00841; 809/778-1608

Robbins, Lisa L., Dept of Geol, Univ of South Florida, Tampa, FL 33620; 813/974-2238

Robertson, Richard, Ministry of Agric Ind & Labor, Richmond Hill, St. Vincent; Phone: 61410

Robinson, Edward, Dept of Geol, Florida International University, Miami, FL 33199; 305/271-0721

Rodrigues, Kirton, Gel Serv Lab TRINTOC, Pointe-A-Pierre, Trinidad; 803/6584230 x2367

Rodriguez Martinez, Jesus, GPO Box 4424 (USGS) San Juan, PR 00936; 749-4341

Rogers, James P., 810 Lincoln Tower Bldg, 1860 Lincoln St., Denver, CO 80295; 303/832-2328

Rohr, Gene M., 1105 Adams St, Denver, CO 80206; 303/377-2554

Rosenfeld, Joshua, 12419 Carriage Hill Dr, Houston, TX 77077; 713/556-2857

Roughgarden, Jonathan, Dept of Biol Sciences, Stanford Univ, Stanford, CA 94305; 415/723-3648

Santana, Jose Arismendy, Calle Caracas #122, San Carlos, Santo Domingo, DR; 809/685-8191

Saunders, John B., c/o Natural History Museum, Postfach 4001 Basel, Switzerland; 061 29-55-64; (Home) 061-22-58-86

Schellekens, Hans, Dept. of Geol, Univ of Puerto Rico, Mayaguez, PR 00709; 809/265-3845

Schubert, Carlos, Ecologia, IVIC, Apartado 21827, Caracas, 1020A, Venezuela

Sen, Gautam, Dept of Geol, Florida International University, Miami, FL 33199; 305/348-2299; FAX 305/348-3877

Shore, Patrick, Dept of Geol, Stephen F. Austin State Univ, Box 13011 SFA Station, Nacogdoches, TX 75961; 409/568-3701

Simon, Andrew, U.S. Geol Survey, WRD, A-413 Federal Bldg., Nashville, TN 37203; 615/736-5424

Smith, Alan L., Dept. of Geol, Univ of Puerto Rico, Mayaguez, PR 00709; 809/265-3845

Snoke, Arthur W., Dept of Geol & Geophysics, Univ of Wyoming, Laramie, WY 82071-3006; 307/766-5457

Soper, Elmer, Umpqua Comm College, PO Box 967, Roseburg, OR 97470; 503/440-4600

Speed, Bob, 1738 Chicago, Evanston, IL 60201; 312/491-5392

Taggart, Bruce, Dept of Marine Sci, Univ of Puerto Rico, Mayaguez, PR 5000-00709; 809/832-4040

Telemaque, Carol, c/o Geol. Dept., Trintopec, Santa Flora, Trinidad, WI 809/649-5500.FAX 809/649-5810

Thomas, Stefan, Zulpicherstrasse 46, Geol Institut, D-5000 Koln-1 West Germany

Tokarsky, Tim, 642 English Bluff Rd., Delta, BC, Canada V4M 2N4; 943-0983

Torres, Nalini, Calle Disneyland, N-20, Park Gardens, Rio Piedras, PR 00926

Tvrdik, Tim, 536 Oakcrest, Coppell, TX 75019; 214/951-2812

Tyson, Llewellyn, Geol Dept., Trintoc Adm. Bldg., Pointe A Pierre, Trinidad W.I.; 658-4220, x2253, 2217

van den Bold, W. A., 4646 Bennett Drive, Baton Rouge, LA 70808; 504/388-3417

Verdenius, Jacob, G., Continental Shelf Inst. Hakon Magnussons Gt 1B, 7000 Trondheim, Norway

Venger, Laura L., West Indies Lab, Teague Bay, Christiansted, St. Croix 00820; 809/773-9339

Vernette, Departement de Geologie et Oceanographie, Avenue des Facultes, 33405 Talence, France; 56806800

Ward, William C. , Dept of Geol & Geophysics, Univ of New Orleans, New Orleans, LA 70148; 504/286-6792

Warner, A. J., 809 Petroleum Bldg, Wichita, KS 67211; 316/265-9602 FAX 316/265-7014

Watlington, Roy A., Div of Sci & Math, U.V.I. Box 2321, St. Thomas, WI 00803; 776-9200

Webb, Richard, Calle Marina Oeste C-12, Levittown, PR 00949; 809/729-6935

Wegweiser, Art, 5341 Gibson Hill, Edinboro, PA 16412; 814/732-2453

Weiland, Thomas J., Dept of Geol, Georgia Southwestern College, Americus, GA 31709; 912/928-1613

Weiss, Malcolm P., Dept. of Geol., Northern Illinois Univ., DeKalb, IL 60115; 815/753-7937

Williams, Richard, 1201 West 5th St, Los Angeles, CA 90017; 213/977-5253

Whetten, John T., Mail stop A107, Los Alamos Natl. Laboratory, PO Box1663, Los Alamos, NM 87545; 505/667-3880

Woronow, Alex, Dept. Geosciences, Univ of Houston, Houston, TX 77004; 713/749-4325

Wright, Raymond, Petro Corp of Jamaica, 36 Trafalgar Rd, PO Bx 579, Kingston 10, Jamaica; 809/92-92411, FAX 9292409

TABLE OF CONTENTS
General Papers

Page

Geological Arguments Suggesting a Pacific Origin for the Caribbean Plate.....*James L. Pindell* 1

Hurricane Impacts on Caribbean Beaches: The Development of a Data Base and Guidelines for Coastal Area Planning and Management.....*Malcolm Hendry and Peter Bacon* 5

Origin of the Eastern Caribbean: Data from Reptiles and Amphibians.....*Jonathan Roughgarden* 10

Morphology and Development of Modern Carbonate Foreslopes, Tongue of the Ocean, Bahamas .....*G.M. Grammer, R.N. Ginsburg and D.F. McNeill* 27

Topical Papers
(approximately clockwise from Cayman Trough)

Cayman

Structure and Spreading History of the Central Cayman Trough.....*N. Terence Edgar, William P. Dillon, Colin Jacobs, Lindsay M. Parsons, Kathryn M. Scanlon and Troy L. Holcombe* 33

Cuba

Interpretación de los Datos Geofisicos con Fines de la Cartografia Geológo-Estructural de la Republica de Cuba .....*Manuel Pardo, Verania Bello, Hilda Amador, Sandor Taba, Oleg Sousin, Ileana Matamoros y Irio de Moya* 43

Geoquimica de la Asociación Ofiolitica de Cuba .....*E. Fonseca, F. Castillo, A. Uhanov, M. Navarrete and G. Correa* 51

Posición Estratigráfica de los Rudistas de Camaguey, Cuba.....*M.A. Iturralde Vinent y A. de la Torre y Callejas* 59

La Constitución Geologica del Macizo Isla de la Juventud y su Metalogenica Endogenia Vinculada al Magmatismo Acido .....*Manuel E. Pardo-Echarte* 68

Evolución de la Estructura del Macizo de Escambray Sur de Cuba Central.....*Guillermo Millán-Trujillo* 82

Correlación de las Metavulcanitas de la Sierra del Purial (Cuba Oriental) con las Rocas de la Asociación Ofiolitica .....*Mario Campos y Margarita Hernández* 95

Jamaica

Short Review of the Ostracoda of the Montpelier and Coastal Groups of Jamaica.....*W.A. van den Bold* 99

Grand Cayman

Sedimentology of the Late Pleistocene Ironshore Formation on Grand Cayman.....*Ian G. Hunter and Brian Jones* 104

Porosity and Permeability Development in the Oligocene-Miocene Bluff Formation, Grand Cayman .....*Kwok-Choi Ng and Brian Jones* 115

Geological Evolution of the Oligocene-Miocene Bluff Formation, Grand Cayman.....*Brian Jones, Ian G. Hunter and Kwok-Choi Ng* 125

Hispaniola

Morphology, structure and Active Tectonism of the Insular Margin Off Northwestern Hispaniola.....*William P. Dillon, Kathryn M. Scanlon, James A. Austin Jr., N. Terence Edgar, Lindsay M. Parson and Gordon E. Ness* 133

Tectonostratigraphy of the San Francisco Ridge Area in the Northeastern Cibao Valley, Dominican Republic .....*Agathe C. Nadai* 143

Preliminary Report on a Late Tertiary Plant Microfossil Assemblage from Haiti.....*Alan Graham* 156

Late Holocene Ostracoda In and Around Lake Enriquillo, Dominican Republic.....*W.A. van den Bold* 163

Petrography and Geochemistry of Mafic Rocks of the Peralvillo Formation in the Sabana Potrero Area, Central Dominican Republic.....*J, Espaillat, G. Bloise, and J.G. Macveigh and J.F. Lewis* 190

Geological Setting and Base and Precious Metal Deposits of Northern Haiti.....*Kyriacos Louca* 200

Puerto Rico

Landslide Processes in Saprolitic Soils of a Tropical Rain Forest, Puerto Rico.....*Matthew C. Larsen and Andrew Simon* 217

Extensional Tectonism in the Mona Passage, Puerto Rico and Hispaniola: A Preliminary Study.....*D.K. Larue and H. F. Ryan* 223

Neotectonics of the Puerto Rico Trench: Extensional Tectonism and Forearc Subsidence.....*D.K. Larue , J. Joyce and H.F. Ryan* 231

Radiometrically Dated Marine Terraces on Northwestern Puerto Rico.....*Bruce E. Taggart and James Joyce* 248

Depth of Emplacement of Granitoid Plutonic Rocks in the Eastern Greater Antilles Island Arc.....*Edward G. Lidiak* 259

Late Jurassic to Late Cretaceous Development of Island Arc Crust in Southwestern Puerto Rico.....*Johannes H. Schellekens, Homer Montgomery, James Joyce and Alan L. Smith* 268

Virgin Islands

Toxic Substances in the Coastal Environment of the US Virgin Islands, 1986.....*B. L. Oostdam* 282

Taphonomic Biasing of Subfossil Echinoid Populations Adjacent to St. Croix, U.S.V.I.....*Benjamin J. Greenstein* 290

Cretaceous Tectonic Complex, St. Croix.....*Robert Speed and James Joyce* 301

A Note of the Relative Timing of Cleavage Formation and Magmatism in the Cretaceous Rocks of St. Croix, U.S. Virgin Islands.....*Grenville Draper and Jamie M. Bartel* 314

Lesser Antilles

Characteristics of Volcanic Centers from the Lesser Antilles .....*A.L. Smith and M.J. Roobol* 319

Reefs of Antigua, West Indies: Changes over 40 years .....*Malcolm P. Weiss* 329

Map of Modern Reefs and Sediments of Antigua, West Indies .....*M. P. Weiss and H. Grey Multer* 340

The Cretaceous Age Sediments of the Saba Bank and Their Petroleum Potential.....*Ariel J. Warner Jr.* 341

Barbados

Stress Induced Modification of Sediment Mass Physical Properties During Accretion: A Reconstructional Approach.....*Warner Bruckmann* 355

Origin and Geologic Implications of Diagenetic Limestone in Fault Zones of Barbados.....*Rudolph Torrini, Jr, Robert C. Speed and George E. Claypool* 366

Staple Isotopic Compositions of Diagenetic Carbonate in Hemipelagic and Terrigenous submarine Fan Strata, Barbados, West Indies.....*Rudolph Torrini, Jr., Robert C. Speed and George E. Claypool* 371

Trinidad and Tobago

Patch Reef Ecology, Sedimentology and Distribution Buccoo Reef Complex, Tobago.....*D. Hudson and E.W. Mountjoy* 376

Stratigraphic and Structural Relationships on Tobago, West Indies, and Some Tectonic Implications .....*A.W. Snoke, J.D. Yule, D.W. Rowe G. Wadge and W.D. Sharp* 389

Structural Features Associated with the Los Bajos Fault and Their Interpretation in the Light of Current Theories of Strike-Slip Tectonics.....*Llewellyn Tyson* 403

An Evaluation of the Geological History and Hydrocarbon Potential of the Late Miocene - ? Plio/Pleistocene Sediments of the Goudron Field - Trinidad .....*Carol P. Telemaque* 415

Exploitation of the Middle Miocene Oil Bearing Intermediate Herrera Sandstone Reservoirs in Trinidad, West Indies .....*Fazal Hosein* 430

Significance of Geothermal Gradients in Petroleum Exploration in Trinidad.....*Kirton Rodrigues* 444

Southern Caribbean and Venezuela

Contribution of Paleomagnetism in the Relations Between the Piemontin and Internal Nappes of the Venezuelan Caribbean Chain: Synthesis and New Data .....*B.Blin, B. Sichler and J.F. Stéphan* 453

The Caribbean-South American Plate Boundary, Araya Peninsula, Eastern Venezuela.....*Hans G. Avé Lallemant* 461

A Kinematic History for Eastern Margarita Island, Venezuela .....*L.R. Guth and H.G. Avé Lallemant* 472

History of GoldMining on the Island of Aruba Dutch West Indies.....*Robert Salna* 481

Eocene Stratigraphical Studies, Maracaibo Basin, Northwestern Venezuela.....*Rosina Pittelli Viapiana* 485

Central America

Interpretation of Gravity Anomalies, Masaya Caldera Complex, Nicaragua.....*Charles B. Connor and Stanley N. Williams* 495

Active Tectonics of the Chortis Block.....*Mark B. Gordon, Michael J. Kozuch and William R. Muehlberger* 503

The Chortis Block is a Continental, Pre-Mesozoic Terrane .....*Mark B. Gordon* 505

Sedimentary Rocks of the Santa Cruz Ophiolite, Guatemala - A Proto-Caribbean History.....*Joshua H. Rosenfeld* 513

Tectonics and Petroleum Potential of Belize.....*R. Prasada Rao and R. Ramanathan* 520

Abstracts of the 12th Caribbean conference 528

GEOLOGICAL ARGUMENTS SUGGESTING A PACIFIC ORIGIN FOR THE CARIBBEAN PLATE

James L. Pindell
Department of Earth Sciences
Dartmouth College
Hanover, NH 03755 USA

ABSTRACT

In conjunction with an accurate assessment of relative motions between North and South America, seven arguments are presented that individually suggest that the Caribbean Plate has come from the Pacific realm to arrive at its present location after a long, relative eastward journey between the Americas. In a mantle reference frame, most of the relative motion has been due to westward translation of the Americas. While none of the seven arguments definitively proves Pacific provenance, none of the individual arguments can be explained adequately by more fixist, local (in situ) models for the origin of the Caribbean Plate. Therefore, the evidence is overwhelmingly in favor of a Pacific provenance, such that relative eastward migration of the Caribbean Plate to its present position occurred from Late Cretaceous to Recent times. Accordingly, field/marine studies and tectonic interpretations of local areas around the Caribbean must continue to test this hypothesis and attempt to reconcile what effects or implications a Pacific origin and relative eastward migration history may have had on the geological development of such areas.

INTRODUCTION

Pindell et al. (1988) defined the relative motion history between continental areas of the North and South American plates bordering the Caribbean. Their findings showed that relative plate divergence between North and South America occurred from Late Triassic to Late Cretaceous time (Early Campanian or just prior to Campanian), in a southeastward (present coordinates) direction. Since anomaly 34 time, or Early Campanian, relative motion has been either absent or minor. Motions between anomaly M-25 (Late Jurassic) and M-0 (Aptian) are well defined, but some uncertainty exists during the Cretaceous Quiet Period (Aptian to Santonian time). From the Early Campanian (anomaly 34) to the Eocene, relative motion is well constrained and was nearly absent. Since the Eocene, extremely slow north-south convergence has occurred, with the magnitude of motion increasing westwards away from a pole of rotation east of the Lesser Antilles. In the absence of significant magnitudes and rates of relative plate motion between adjacent parts of the North and South American Plates since the Campanian (Pindell et al., 1988), a distinct plate boundary probably has not existed between the two, and intense deformations within the Caribbean region since that time are likely due to tectonic interactions between the continental portions of the Americas with the Caribbean Plate, and not to motions between North and South America.

Caribbean plate evolution, having occurred within mainly oceanic terrains with all its arc magmatism, structural shortening at thrust belts, and evidence of strike-slip deformations, must have occurred within the above kinematic framework of the American plates. Two groups of tectonic models have evolved over the last two decades, one that views the Caribbean plate as having mainly developed between the Americas with only minor Cenozoic motion relative to the Americas (Klitgord and Schouten, 1987; Donnelly, 1989), and another that calls for a Pacific provenance for the Caribbean and subsequent long-distance migration into an oceanic gap (Proto-Caribbean seaway) between the Americas during Late Cretaceous and Cenozoic time (Wilson, 1966; Malfait and Dinkleman, 1972; Dickinson and Coney, 1980; Pindell and Dewey, 1982; Burke et al., 1984; Pindell and Barrett, 1990). In this paper, arguments are presented which support the latter group of models, and which suggest that a Pacific origin is necessary to understand the region's structural and stratigraphic evolution. Emphasis is placed upon possible plate boundary geometries and the existence of two unrelated suites of rock in the Caribbean, an autochthonous assemblage of passive margin sediments pertaining to the Proto-Caribbean seaway (Yucatan, northern South America, and the Florida/Bahamas Embankment), and an allochthonous collage of diverse rocks pertaining to the arcs and oceanic basement of the Caribbean plate itself. In onshore areas, a rough line can be drawn between these two suites, although sediments of the autochthon and syn-orogenic sediments are often incorporated in the thrusts that developed between the two suites during juxtaposition. Such rocks could be considered para-autochthonous.

ARGUMENTS FOR A PACIFIC ORIGIN FOR THE CARIBBEAN PLATE

1. Eastern Caribbean Volcanism

The Aves Ridge and Lesser Antilles volcanic arc complexes, although separated by the Grenada (intra-arc) Basin, collectively form the eastern portion of the Caribbean Plate. Intermediate magmatism and presumed subduction beneath these arcs (Figure 1) occurred in Upper Cretaceous-Paleogene and Eocene-Recent time, respectively (see data compilation, Figure 6, Pindell and Barrett, 1990). Polarity of subduction is clear for the Lesser Antilles arc (eastward facing arc, westward dipping subduction) based on seismicity, trench/Benioff zone morphology, accretionary prism, etc., but less clear for the Aves Ridge arc. Despite Donnelly's (1989) suggestion that the Aves Ridge was a west-facing arc based on a down to the east deepening of the eastern Venezuelan Basin's basement (possible former trench in his interpretation), such an eastward deepening of this basement is to be expected simply due to the load imparted on the eastern Venezuelan Basin from the magmatic/volcanic development of the arc. In favor of continuous westward dipping subduction, the Aves Ridge is located directly behind the Lesser Antilles arc, the latter of which began to develop immediately after volcanism had ceased in the Aves Ridge; a period of intra-arc spreading in the Grenada Basin during the Paleogene is the likely explanation for the shift in the active volcanic axis (Tomblin 1975; Speed and Westbrook, 1984). Furthermore, the Aves Ridge is slightly convex eastward, and there is no evidence for an accretionary prism along its west flank, as would be expected had subduction ever been from the west. Thus, most evidence indicates that a long, continuous history of westward dipping subduction of Atlantic crust has occurred beneath both the Aves Ridge and Lesser Antilles arcs since the early Late Cretaceous. In the framework of North and South American relative plate motions, this would require

Larue, D.K., and Draper, G. (eds.),
Transactions of the 12th Caribbean Geological Conference, St. Croix, U.S.V.I., Miami Geological Society, P.O. Box 431552, South Miami, FL 33243, U.S.A

eastward migration of the Caribbean Plate between the Americas from somewhere to the west. Assuming (1) an 80 million year period of subduction, as suggested by the isotopic and stratigraphic ages of arc magmatism, and (2) that a convergence rate of at least 10 mm/yr is required to produce arc magmas, a 800 km convergence is suggested for this arc system as an absolute minimum.

2. Cayman Trough and Strike-Slip Basins of the Northern Caribbean

Assessments of the history of the Cayman Trough (Rosencrantz et al., 1988; Wadge and Burke, 1983) and of the Tabera and northern San Juan Basins onshore Hispaniola (Mann et al., 1984; Dolan et al., 1990) and the "Eocene Belt" of Puerto Rico (Erikson, 1988; Erikson et al., 1990) suggest Late Eocene and Oligocene east-west, sinistral strike-slip motion in the northern Caribbean (Figure 1), in addition to similar Neogene motions which are more readily accepted (Speed, 1985; Donnelly, 1989). Offset on the order of 1000 km since Late Eocene is indicated from the length of the deeper, probably oceanic portion of the Cayman Trough, and from reconstructions of Cuba, Hispaniola, Puerto Rico and the Aves Ridge arc fragments into a single Greater Antillean arc (Pindell and Barrett, 1990; Draper and Barros, 1988). Such a relative motion history is expected judging from the Eocene to Recent volcanic activity of the Lesser Antilles arc.

3. Caribbean vs. Proto-Caribbean Stratigraphic Suites

Medial Cretaceous (Albian-Santonian) portions of the stratigraphies of two suites of rock in the Caribbean are genetically incompatible as presently juxtaposed (Figure 1). One suite, here called the Caribbean suite, occurs in most of the Caribbean islands/Central America, allochthonous thrusts in northern Colombia and Venezuela (such as Villa de Cura Complex), and the internal Caribbean Plate. The second suite, here called the Proto-Caribbean suite, occurs in the autochthonous sequences (overthrust by the Caribbean suite) of Yucatan (Maya Block), Florida/Bahamas, and the northern South American margin (passive margins of the original Proto-Caribbean Sea between the Americas; Pindell, 1985). The Caribbean suite, particularly the magmatic arc portions, is dominated by intrusive and volcanic rocks, volcanogenic sandstones, tuffs and minor limes often above Albian? and older metamorphic basement. In contrast, the Proto-Caribbean suite consists of Pre-Mesozoic basement, mainly Jurassic rift-related deposits, and Cretaceous non-volcanogenic shelf sediments, all overlain by clastics of various foredeep basins of Upper Cretaceous and Cenozoic age along the suture or boundary with the Caribbean Plate (Pindell, 1990). Of primary interest here is that evidence for volcanism (flows and more importantly tuffs) is predominant in the Caribbean suite, whereas evidence for volcanism is nearly absent in the Proto-Caribbean suite of rock. Thus, spatial separation during medial Cretaceous time (prior to Campanian) seems necessary to account for this primary difference. As this difference extends from around the Caribbean sea westward to at least the Guajira Peninsula of Colombia and to Chiapas, Mexico, it is probable that the Caribbean Plate was situated farther to the west, i.e. the Pacific, during medial Cretaceous time.

4. Geometrical Incompatibility Between a Pre-Aptian? Caribbean Plate and the Aptian Proto-Caribbean Seaway

Numerous faunal and isotopic dates have been obtained from rocks in areas presently encircling or formerly part of the Caribbean Plate (e.g., rocks from Costa Rica, Panama, Siquisique Complex, Venezuela, Curacao, Bonaire, La Blanquilla, Tobago, La Desirade, Bermeja Complex, Puerto Rico, Duarte Complex, Hispaniola, arc-related basement complexes, Cuba; see Donnelly, 1989 and references cited therein for review). A pre-Aptian age is not yet proved for the central portion of the plate (Colombian and Venezuelan Basins), as DSDP drilling has reached only Coniacian sediments and volcanics (seismic horizon B") that overlie a thick sequence of layered strata with intermediate velocities (Stoffa et al., 1981). Because of the pre-Coniacian (pre-layer B") layering and intermediate seismic velocities, it is not likely that horizon B" represents oceanic crust. Rather, the Caribbean crust is probably similar to western Pacific examples of areas of anomalously shallow oceanic plateaux where medial Cretaceous, off-spreading axis basalts and sediments overlie an older oceanic basement. If so, like the areas mentioned above, the entire Caribbean Plate may be pre-Aptian in age. However, plate separation between North and South America by Aptian time (marine magnetic anomaly M-0) and the production of the Proto-Caribbean Seaway was far insufficient (Figure 1) to have accommodated a Caribbean Plate approaching its present size (Pindell et al., 1988). In the absence of very large areas in the Caribbean having been produced by seafloor spreading, or by stretching of existing crust, after the Aptian, the Caribbean Plate must have been positioned (and presumably was formed) outside the present Caribbean area (i.e., Pacific) during Aptian time and older.

5. Truncation and Uplift of the Southwestern Margin of Mexico

Structural trends of the southwest margin of Mexico have been truncated either by subduction erosion (subduction of former forearc areas) or by strike-slip removal of forearc areas to the northwest or to the southeast (King, 1969; Anderson and Schmidt, 1983). In addition, the Trans-Mexican Volcanic Belt arc (King, 1969) is mainly Neogene in age, with volcanism commencing earlier in the west than in the east, implying an eastward migration of arc inception. Paleogene arc rocks in Mexico are largely restricted to the west, in the Sierra Madre Occidental. In the Chortis Block of Central America Paleogene arc activity is abundant, with volcanism extending back into the Cretaceous (see compilation in Pindell and Barrett, 1990). As pointed out by Wadge and Burke (1983), the Paleogene arc sequences likely were continuous from western Mexico into Chortis, prior to eastward strike-slip offset of Chortis to its present position (Figure 1) and progressive development of volcanism in the Trans-Mexican Volcanic Belt. In addition to the offset of the Paleogene arc, the Precambrian basement of the southwestern margin of Mexico (King, 1969) has yielded cooling ages that indicate uplift and erosion since Oligocene time (Damon and Coney, 1983). All of these observations are best explained by a model of continuous eastward migration of the Caribbean Plate, including the Chortis Block, relative to North America (Figure 1) during latter Cenozoic time (e.g., Wadge and Burke, 1983; Pindell and Dewey, 1982). Specifically, the eastward migration of the trench-trench-transform triple junction (Mexican Trench, Middle America Trench, Motagua/Polochic transform zone) since the Oligocene or Eocene would (1) truncate the basement of southwest Mexico, (2) provide a mechanism for the progressively eastward inception of arc magmatism in the Trans-Mexican Belt coeval with continued magmatism in the Chortis Block, and (3) cause uplift of the former northern wall of the transform margin during the onset of subduction behind the migrating triple junction.

6. Faunal provinciality: Pacific vs. Proto-Caribbean Realm

According to Johnson and Kauffman (1989; this volume; pers. comm., 1990), two differing faunal realms exist across the Mexican-Caribbean region that remained distinct until beginning to merge in Campanian time, indicating spatial separation of shallow water organisms prior to that time. The areas of occurrence for the two realms nearly exactly match the areas defined above for the two differing stratigraphic suites (Figure 1) of the Caribbean Plate and Proto-Caribbean Seaway (argument 3). Mexico, Chortis, and the Cretaceous Antilles define a more "Pacific" realm (see also Montgomery, this vol., for a discussion of Puerto Rican (Greater Antillean) cherts), whereas the carbonate or terrigenous passive margins of the Bahamas, eastern Yucatan, and northern South America define a Proto-Caribbean (Atlantic) faunal realm. The Campanian initiation of faunal merging of the two realms presumably is at least partially due to tectonic juxtaposition of the shelfal (and adjoining land) areas they occupied, during the relative eastward migration of the Caribbean Plate between the Americas.

7. Initiation of Foredeep Basins Around the Proto-Caribbean Seaway

Seafloor spreading and plate separation ceased between North and South America at about Campanian time. After this, the oceanic area and the margins of the Proto-Caribbean Seaway continued to subside thermally, probably without a central spreading

center (Pindell et al., 1988). North and South America essentially were part of a greater American Plate, with no significant plate boundary between them. As such, this oceanic basin would be expected to undergo a rapid load subsidence just ahead of the Caribbean Plate as it migrated progressively relatively eastwards across the Proto-Caribbean crust. In addition to the oceanic areas, adjoining shelf margins would undergo this load subsidence as well, for a distance of about 400 km "into" the passive margins (Yucatan, Bahamas, northern South America). As outlined in Pindell et al. (1988), foredeep basins with clastic flysch deposits developed at the onset of such subsidence around the Proto-Caribbean, as a direct consequence of the arrival of Caribbean crust at various portions of the Proto-Caribbean passive margins during this eastward migration. Specifically, the onset of rapid subsidence of previously shallow water areas and clastic flysch deposition occurred in northern Guatemala during the Campanian, in northern Cuba during the latest Cretaceous-Middle Eocene, in the Maracaibo area of Venezuela/Colombia in the Eocene, and in the Eastern Venezuela Basin during the Miocene (Pindell, 1990). The progressive eastward development of these basins (Figure 1) records the eastward migration of the Caribbean Plate across the Proto-Caribbean (Atlantic) Seaway, presumably from an origin within the Pacific realm. A total migration of about 1500 km since the Campanian, at rates of about 20 mm/yr average, is indicated from the development of these basins. Such a rate is in agreement with predictions of migration rate back into the Eocene from direct assessments of the Cayman Trough (Rosencrantz et al., 1988).

CONCLUSIONS

Although none of the above seven arguments for a Pacific origin of the Caribbean Plate is definitive proof for such an origin, none of the individual arguments can be adequately explained by more fixist models of plate boundary evolution within the Caribbean area (in situ origin). Therefore, the evidence is overwhelmingly in favor of a Pacific provenance. In the kinematic framework of Pindell et al., (1988), the first-order development of the Caribbean region is explained by using a perfectly rigid and non-deforming Caribbean plate during its eastward relative advance between the Americas since the Late Cretaceous. I see no need to impose ad hoc models for Caribbean evolution that do not adhere to the tenets of plate tectonics, i.e., ones that require internal deformations of oceanic crust on the order of hundreds of kilometers with little or no bathymetric expression of deformed zones, to explain the strong evidence of eastward translation that is clearly observable in some areas but less so in others. In light of a highly probable Pacific origin for the crust of the Caribbean Plate (except the oceanic floors of the Yucatan, Cayman and Grenada Basins which formed within the Caribbean Plate itself during migration), field/marine studies and tectonic interpretations of local areas around the Caribbean must continue to test the Pacific-origin hypothesis and attempt to reconcile what effects or implications, if any, a Pacific provenance may have had on the geological development of such areas.

Acknowledgements: The above arguments have developed over many years of interaction and geological synthesis among dozens of Caribbean workers, and it would be difficult to acknowledge everyone who has provided input. Particularly critical steps forward in the understanding of Caribbean evolution, however, have come from progressive refinement of the definition of relative motions between Africa and North and South America, and from studies indicating strike-slip motions in the Caribbean plate boundary zones, which have provided an increasingly accurate plate-kinematic framework for the Caribbean region in which a variety of other types of work can be set. Such studies now indicate that the primary, post-Campanian deformations of the Caribbean plate and its American continental borders pertain to interactions of the Caribbean Plate with the margins of North and South America, and not to motions between the two American plates themselves, as was once thought. Those who have helped in this refinement include John Ladd, Kim Klitgord, Steve Cande, Kevin Burke, Walter Pitman, John LaBrecque, Bill Haxby, John Dewey, Dave Rowley, Hans Schouten, Eric Rosencrantz, Paul Mann, Johan Erikson, Jim Dolan, Carlos Schubert, others. In addition, this refinement is largely responsible for the realization of the magnitude of the allochthoneity of rocks of the Caribbean Plate relative to the American margins, and for the recognition of the potential complexities of plate boundary developments in the northern and southern Caribbean. Like the Mediterranean and Asian regions, the Caribbean is an example where the geology is sufficiently complex to demand the deductive use of marine plate-kinematic assessments to provide first-order constraints on local development, upon which more local data sets and studies may be iteratively integrated.

REFERENCES CITED

Anderson, T. H., and Schmidt, V. A., 1983, The evolution of Middle America and the Gulf of Mexico-Caribbean Sea region during Mesozoic time: Geological Society of America Bulletin, v. 94, p. 941-966.

Burke, K., Cooper, C., Dewey, J. F., Mann, J. P., and Pindell, J., 1984, Caribbean tectonics and relative plate motions: in Bonini, W. E., Hargraves, R. B., and Shagam, R., eds., The Caribbean-South American Plate Boundary and Regional Tectonics: Geological Society of America Memoir 162, p. 31-64.

Damon, P., and Coney, P., 1983, Rate of movement of Nuclear Central America along the coast of Mexico during the last 90 Ma: Geol. Soc. America, Abstracts with Programs, v. 15, p. 553.

Dickinson, W. R., and Coney, P. J., 1980, Plate-tectonic constraints on the origin of the Gulf of Mexico: in Pilger, R. H., ed., The Origin of the Gulf of Mexico and the Early Opening of the Central North Atlantic: Louisiana State University, Baton Rouge, La., p. 27-36.

Dolan, J. F., Mann, P., Monechi, S., de Zoeten, R., Heubeck, C., and Shiroma, J., 1990, Sedimentologic, stratigraphic, and tectonic synthesis of Eocene-Miocene sedimentary basins, Hispaniola and Puerto Rico: in Mann, P., Draper, G., and Lewis, J., eds., Geology of Hispaniola: Geol. Soc. America Special Paper, (in press).

Donnelly, T. W., 1989, Geologic history of the Caribbean and Central America: in Bally, A. W., and Palmer, A. R., eds., The Geology of North America-An overview: Boulder, Colorado, Geological Society of America, Geology of North America, v. A., p. 299-321.

Draper, G., and Barros, J. T., 1988, Tectonic reconstruction of N. Hispaniola and S. E. Cuba: dissection of a Cretaceous island arc: Geol Society America, Abstracts with Programs, v. 20, no. 7, p. A60.

Erikson, J. P., 1988, Structural study of the Paleogene deformation in and around the Southern Puerto Rico Fault Zone: [M.S. Thesis], Stanford University, Stanford, California, 74 pp.

Erikson, J. P., Pindell, J. L., and Larue, D. K., 1990, Mid-Eocene-Early Oligocene Sinistral Transcurrent Faulting in Puerto Rico Associated with Formation of the Northern Caribbean Plate Boundary Zone: Journal of Geology, (in press).

Johnson, C., and Kauffman, E., 1989, Cretaceous Rudistid paleobiogeography of the Caribbean Province: Caribbean Geological Conference, 12th, Abstracts, St. Croix, p. 85.

Johnson, C., and Kauffman, E., 1990, this volume.

King, P. B., 1969, Tectonic Map of North America: United States Geological Survey, scale 1:5,000,000, Reston, Va.

Klitgord, K., and H. Schouten, 1987, Plate kinematics of the Central Atlantic: in Tucholke, B. E., and Vogt, P. R., eds., The Geology of North America: the Western Atlantic Region: Geol. Soc. America, Decade of North American Geology, v.

M, p. 351-378.

Malfait, B. T., and Dinkelman, M. G., 1972, Circum-Caribbean tectonic and igneous activity and the evolution of the Caribbean plate: Geological Society of America Bulletin, v. 83, p. 251-272.

Mann, P., Burke, K., and Matumoto, T., 1984, Neotectonics of Hispaniola: plate motion, sedimentation, and seismicity at a restraining bend: Earth and Planetary Science Letters, v. 70, p. 311-324.

Montgomery, H., 1990, (this volume).

Pindell, J. L., 1990, Circum-Caribbean sedimentary basin development and timing of hydrocarbon maturation as a function of the plate tectonic evolution of the Caribbean region: in Halbouty, M. T., ed., Geological resources of the Central American and Caribbean Region: Circum-Pacific Energy Council, American Association Petroleum Geologists, (in press).

_____ 1985, Alleghenian reconstruction and the subsequent evolution of the Gulf of Mexico, Bahamas and Proto-Caribbean Sea: Tectonics, v. 4, p. 1-39.

Pindell, J. L., and Barrett. S. F., 1990, Geologic evolution of the Caribbean Region: a plate-tectonic perspective: in Case, J. E., and Dengo, G., eds., Decade of North American Geology, volume H,Geological Society of America, Boulder, Co., (in press).

Pindell, J. L., Cande, S. C., Pitman III, W. C., Rowley, D. B., Dewey, J. F., LaBrecque, J., and Haxby, W., 1988, A plate-kinematic framework for models of Caribbean evolution: Tectonophysics, v. 155, p. 121-138.

Pindell, J. L., and Dewey, J. F., 1982, Permo-Triassic reconstruction of western Pangea and the evolution of the Gulf of Mexico/Caribbean region: Tectonics, v. 1, p. 179-212.

Rosencrantz, E., Ross, M., and Sclater, J. G., 1988, Age and spreading history of the Cayman Trough as determined from depth, heat flow, and magnetic anomalies: Journal of Geophysical Research, v. 93, p. 2141-2157.

Speed, R. C., 1985, Cenozoic collision of the Lesser Antilles Arc and continental South America and origin of the El Pilar Fault: Tectonics, v. 4, p. 40-70.

Speed, R. C., and Westbrook, G. K., et al., 1984, Lesser Antilles Arc and adjacent terranes, Ocean Margin Drilling Program, Regional Atlas Series, Atlas 10: Marine Science International, Woods Hole, Mass., 27 plates.

Stoffa, P. L., Mauffret, A., Truchan, M., and Buhl, P., 1981, "Sub-B" layering in the southern Caribbean: the Aruba gap and Venezuela Basin: Earth and Planetary Science Letters, v. 53, p. 131-146.

Tomblin, J. F., 1975, The Lesser Antilles and Aves Ridge: in: Nairn, A. E. M., and Stehli, F. G., eds., The Ocean Basins and Margins, vol. 3, Plenum, New York, p. 467-500.

Wadge, G., and Burke, K., 1983, Neogene Caribbean plate rotation and associated Central American tectonic evolution: Tectonics, v. 2, p. 633-643.

Wilson, J. T., 1966, Did the Atlantic close and then reopen?: Nature, v. 211, p. 676-680.

_____ 1990. Caribbean Geological Conference, 12th, Transactions, D. K. Larue, ed., St. Croix.

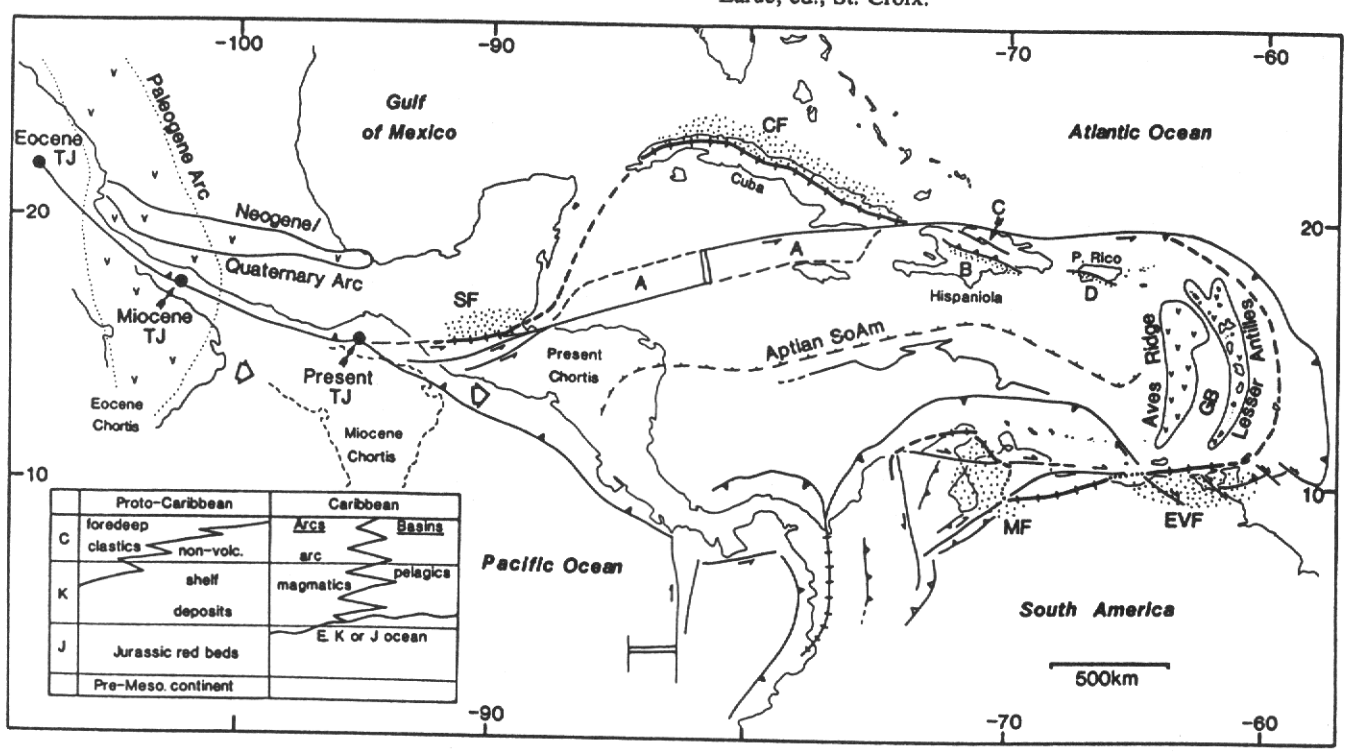

Fig. 1. Map with arguments/features discussed in text. Light lines = Present plate boundaries. Heavy lines = sutures between Caribbean arc/oceanic rocks and Proto-Caribbean shelf/foredeep rocks. Eastern Caribbean volcanism (argument 1) shown at Aves Ridge and L. Antilles. GB = Grenada Basin. Tertiary strike-slip basins (argument 2) = A, Cayman; B, San Juan; C, Tabera; D, Eocene Belt. Differences in Caribbean/Proto-Caribbean sections (argument 3), inset. Aptian S. American relative position (argument 4) = "Aptian SoAm". Migration of Chortis and TTF triple junction (TJ) (argument 5) shown SW of Mexico. Pre-Campanian Pacific/Proto-Caribbean faunal boundary (argument 6) matches suture zones. Foredeeps (argument 7) = dotted areas: SF = Sepur; CF = Cuban; MF = Maracaibo; EVF = Eastern Venezuelan.

HURRICANE IMPACTS ON CARIBBEAN BEACHES: THE DEVELOPMENT OF A DATA BASE AND GUIDELINES FOR COASTAL AREA PLANNING AND MANAGEMENT

Malcolm Hendry,
Center for Resource Management
and Environmental Studies,
University of the West Indies,
P.O. Box 64, Bridgetown, Barbados

Peter Bacon,
Zoology Department,
University of the West Indies,
Mona, Kingston 7, Jamaica

ABSTRACT

The incidence of severe Hurricanes in the Caribbean in recent years brings in to focus the need for informed decision making on pre-storm beach protection, coastal planning for beach development sites and post-storm renourishment and rehabilitation measures. This requirement is emphasized by the importance of beaches and the coastal zone in general in economies throughout the region, where tourism and residential development, particularly in the islands, depend heavily on coastal and in particular on beach resources as a focus for activity.

Our preliminary recommendations for data collection and interpretation include observations of the potential or observed tendency for sand bar formation and subsequent onshore migration as a result of storm events, and the time-frame in which this occurs. In addition, the potential for artificial and cost-effective beach renourishment measures at a site needs to be demonstrated particularly for new developments where post-storm sand bar migration may not occur. The development of a vulnerability index for possible hurricane impacts on beaches will be a useful addition to the tool kit of coastal managers and planners.

While recognising the usual constraints of trained manpower, institutional structures and financial resources needed to advance data collection in this area, we suggest that development of a data base and guidelines for management of hurricane affected beaches can be conducted within the framework of existing coastal monitoring projects within individual territories; as part of ongoing regional programs such as the UNEP climate change and IOCARIBE coastal geomorphology projects and that consideration of these problems should be built in to all environmental impact assessment's dealing with coastal area development.

INTRODUCTION

The economic importance of tourism in Caribbean islands is significant in terms of GNP (McElroy and de Albuquerque, 1989), and much of the focus is in coastal areas, where beaches are a, if not the, major tourist resource. In addition, due to physical (topographic) restrictions, major communication routes, residential districts and utility distribution networks are located in low lying coastal areas often adjacent to beaches. Recent record breaking hurricane events such as Gilbert in 1988 (Eyre, 1989) and Hugo in 1989 have highlighted the susceptibility of soft coastal substrates and their adjacent infrastructure to damage from storm surge and storm waves (Bacon, 1989; Hendry, 1989a). With the possibility of more frequent higher intensity storms due to climatic change (Shapiro, in press) the protection and rehabilitation of beaches susceptible to storm damage will be increasingly necessary.

The problems of inappropriate coastal planning for soft substrates have already manifested themselves in several islands, where inadequate set-back limits have placed coastal structures at direct risk from shoreline erosion. The most alarming example of this is in Barbados, which is currently implementing a US$7 million engineering feasibility study to advise on remedial measures for coasts of the island. Our observations and research following Hurricane Gilbert suggest that some emphasis also needs to be placed on understanding beach responses to storm events in the region. This need is further manifested by:

1. The importance of advising coastal landowner's, particularly those with property, of the likely risks of beach damage associated with hurricane events and whether short-term remedial measures are necessary after storm damage to restore degraded beach profiles. Such information will be increasingly valuable as the traditional winter tourist season is expanded into those months of the year during which hurricane activity normally occurs. It will be necessary to differentiate those beaches that are likely to display a naturally rapid post-storm recovery rate from those that recover slowly or not at all, as a basis for decision-making on whether short-term, expensive sand renourishment is required.

2. Future coastal planning that features beaches as a key resource, such as in a

Larue, D.K., and Draper, G., eds.,
Transactions of the 12th Caribbean Conference,
St.Croix U.S.V.I., Miami Geological Society,
P.O. Box 14433, Coral Gables, FL 33114

residential or hotel development should take potential hurricane-related beach damage into account. Far more guidance than presently provided is required, particularly when it is recognised that storm activity is an important mechanism for shoreline retreat under the rising sea-level scenario (Leatherman, 1981; Pilkey *et al.*, 1989; Hendry, in press). This is in addition to other storm-related problems such as flooding and damage to infrastructure from surge and storm waves.

DEVELOPMENT OF THE DATA BASE

While suggesting the need for information on hurricane-related beach changes for applied purposes in the region we are mindful of several major constraints on collection, interpretation and dissemination of data. One is the absence of baseline data on an historical time scale (eg. Hendry, 1979) on beach changes over large areas of the Caribbean. Larger scale pictures of shoreline behaviour over time scales of several thousand years (eg. Hendry and Digerfeldt, 1989) provide useful indicators for long-term shore management, but the site-specific surveyed or photographic data required for detailed local understanding and predictions are generally missing, especially in the context of high-magnitude, low-frequency events such as storms.

Equally important is the availability of personnel within regional Governments trained in observation of beach changes who regularly monitor them and take note of hurricane impacts. In addition, variability in application of descriptive and reporting techniques may reduce the value of observations made following storm events (Hendry, 1989a). This problem cannot be easily solved, except by improved training and the recognition by regional governments of beach management problems to the extent of providing full-time monitoring capability, such as with the Coastal Conservation Unit in Barbados. It is illuminating that the recently conducted Country Environment Profile in Jamaica (I.I.E.D., 1987) only mentioned hurricanes in the context of coastal stability in reference to one location in the north-west of the island. While there are many factors that may influence beach stability at any location, there is clearly a requirement for greater recognition of possible storm impact's at the Government level.

INFORMATION REQUIREMENTS

In order to answer questions as to vulnerability and relative effects on beaches of hurricane attack, we suggest the following lines of inquiry. This set of criteria will undoubtedly need refining, but it is a starting point. In several instances, the type of data needed may be readily accessed from, for example, existing bathymetric charts or aerial photographs or literature and records of coastal processes and resources. In some cases, fieldwork will be required and it is highly desirable that wherever possible some sites are established at which observations of pre- and post-storm beach behaviour are monitored, if only by photographic techniques (Hendry, 1989b). An initial approach should perhaps consider only those beaches which are presently of economic importance or for which some form of development is planned.

Potential for Sand Bar Migration

It is well known that some beaches respond to storm events by formation of shore-parallel bars that migrate onshore after the storm, partially or wholly replacing the pre-storm beach profile. This type of response has been observed in Jamaica for both west and east coast beaches (Hendry, 1982; Hendry, 1989a), where, in the west, recovery may be as rapid as 1-2 weeks. The timing of migration is crucial, especially where property owners fear loss of revenue from damaged beaches and are considering artificial nourishment. The following indicators are important in defining beaches that may respond in this way.

Gradient and Depth of Shelf

Basic bathymetric information is the pre-requisite for several of the investigations that follow. Generally speaking, detailed bathymetric information (say on scale of 1:12,500 or larger) is only available in the Caribbean for areas of interest to marine navigators such as at entries to ports and harbours, though coarser scale surveys are available for most of the region's shelves.

Normal Effective Wave Base

Onshore bar migration will not occur below the level of normal inter-storm effective wave base (depth at which onshore sediment movement can occur), which is dependant on the relationship between shelf bathymetry and characteristics (primarily wavelength) of approaching waves. Sediment deposited during a storm at a depth below this level will not return to the beach. Detailed, local wave climate data are infrequent for the region, but an approximation of approaching deep water waves can be had from the shipboard synoptic oceanographic data collected in the National Oceanographic Data Center in the U.S.A. Where fringing, barrier, bank barrier reefs or extensive patch reefs are found on the shelves, allowance must be made in the assessment for wave shoaling and breaking prior to interaction with the soft-sediment substrate inshore of the reefs that may be the site of sand deposition during a storm.

Sedimentary Sinks

There are many drowned rivers and gulleys on the shelves of Caribbean islands and continental margins that trace the course of former terrestrial run-off during times of lowered sea level. These features may be observable from bathymetric charts, but if the charts are not available, a look at coastal topographic maps will identify the landward continuation of such features and will indicate the need for further investigation offshore. Sediment finding it's way into these

features during storms will almost certainly be lost to the nearshore system by downslope processes and will therefore not be available for natural beach restoration. Beaches close to these natural sinks are potential high-risk areas for long-term damage.

Beach Sediment Storage

Successful formation of a longshore bar during a storm is partially a function of the volume of sediment available on the beach, particularly the subaerial portion. There are many examples where narrow stretches of sand back directly onto upland, for example old clifflines: if the sand is removed during a storm it may not readily be replaced due to increase in wave energy from wave reflection on the exposed surface. This stage may not be reached if approaching storm waves are sufficiently dampened by effective build up of the offshore bar prior to complete removal of sediments stored in the beach. If the back-beach scarp is exposed, recovery may be slower, if at all. Sand management, discussed below, is important in this context.

Direct Observations

While some good indications of potential beach response may be obtained from the approaches outlined above, wherever possible it is of course best to supplement the data with actual observations of beach behaviour due to storms. Trained beach geomorphologists can often identify features associated with previous storm action on a beach, though it is difficult to place a time scale on the rate of recovery (assuming this has occurred) if the observations do not follow soon after the incidence of damage. A useful additional source of data are local's, who qualitatively often provide very helpful observations on natural processes, even if the reason and manner of their observation does not follow solid scientific principles. As we recommend elsewhere in this paper, an attempt to incorporate at least some critical sites in future or ongoing beach monitoring programs should also be made by responsible agencies.

Potential for Artificial Renourishment

Where it is established that natural restoration of the beach profile does not occur (or appears unlikely to occur) after a storm, the possibility of artificial renourishment must be considered, though strong words of caution are clearly necessary based on the experience of expensive and not always successful renourishment programs in the U.S.A. (Pilkey, 1989). In the latter cases (Pilkey, 1989), the major problem appears to be that engineers have not always taken the incidence of storm activity into account in the design life of artificial shorelines. In our discussion, we are contemplating this as an option for beaches that we recognise as having potential to suffer long-term storm damage. In these cases, economic forecasting for cost of the renourished beach must take into account a realistic recurrence interval for potentially damaging storms. In the case of beach loss in front of existing property, the landowner, particularly a hotelier, may opt for soft engineering renourishment options even if only to satisfy short-term occupancy and to avoid possible law suits from visitors who have been attracted by brochures that display sandy beaches. It is in any case incumbent on the coastal scientist and engineer to advise appropriately on the potential long-term viability of the post-storm renourishment option.

Offshore Availability of 'Lost' Sand

Although sediment may be lost from the beach to sub-wave base shelf locations during a storm, it may still be close enough and shallow enough to consider dredging or pumping the sediment back to the beach (versus other sources). Clearly cost/benefits must be evaluated, as well as environmental consequences of such operations, though the latter *prima facie* may be hard to argue following a major perturbation such as a storm which moved sediment to that location in the first place. It will be interesting to see the discussions that might be generated on the relative impacts of the event that caused the beach loss versus the engineering process recommended for restoration. It may well be that these locations are also sites for storage of sediments that are lost by incremental processes from retreating shorelines, and again in this context their merit as borrow for renourishment needs to be evaluated against hard engineering options or alternative borrow sites.

Onshore Availability of Storm-Deposited Sand

Where berm overwash takes place during a storm sediment may be moved from the shoreface to the back beach area. It will thus be lost to the active shoreline, a process which may assist in overall retreat of the water line and beach face. This is clearly the most readily available and cheapest source of sand for immediate replenishment of the degraded beach profile. Sadly, poor sand management practices frequently result in the permanent loss of even this sediment to the beach system: following hurricane Gilbert in Jamaica, for example, the authors observed two sites where this occurred. The first was a north coast development project, where sediment transported by storm waves from the shoreface onto an access road behind the beach was spotted by others and illegally removed to other locations by truck. The other was on the east coast, where beach sand blocking the main coastal road was trucked away from the site to restore access to the area.

Other Sediment Sources

Few Government's in the region have adequately addressed the problem of demand for sand in the aggregate and construction industry, or in beach management and maintenance. Sand stealing is still a major problem, in rivers as well as from beaches or adjacent dune areas. Deane (1987) points out that successful implementation of beach

protection ordinances in the Lesser Antilles has only taken place in Barbados and Antigua where alternative sources of sediment have been delineated. Against this background, Governments must urgently seek, identify and legalize sand sources that may be used not just for post-storm beach rehabilitation, but for other beach management projects. Regardless of legislation and enforcement, coastal landowner's will find an alternative source to re-build their beach if the need is great enough, and illegal practices will continue until these needs are met. In the context of this paper, coastal researchers and agencies responsible for beach management in the Caribbean must continue to apply pressure for improvement of this contentious problem.

Long-Term Observations of Beach Behaviour

We have already recognised the limited resources available in the region for beach monitoring, but where such projects are in progress, and also at specific development sites where EIA data is required, ongoing observations of beach behaviour can provide valuable input to the coastal scientist's understanding of shoreline response to potential storm events, and on ways in which pre- and post-storm planning can take account of them. The mechanisms responsible for, and the rates of longshore and onshore-offshore sediment transport associated with inter-storm processes, combined with an understanding of sediment sources for the coastal area under consideration give useful clues to storm response and recovery.

VULNERABILITY INDEX AND PROJECT IMPLEMENTATION

In assembling data on storm effects on beaches that can assist coastal planners, managers, developers and landowners some expedient form of technical communication such as a 'vulnerability index' could be developed. Such indices are already well advanced for other purposes in coastal protection, including one for global coastal hazards associated with sea-level rise (Gornitz and Kanciruk, 1989). In the latter case, the data base requirements include information on 1) coastal relief (elevation), 2) rock type, 3) coastal landforms, 4) relative sea-level changes, 5) shoreline erosion or accretion, 6) tidal ranges, 7) wave heights and 8) storm frequencies and intensities. While the actual purpose of this particular data base is different, there is great similarity in the types of observations required, and there is much to be gained for an attempt to incorporate the needs of both in the same exercise, thus providing potential answer's to two separate problems at the same time. We do not recommend that the type of index under development by Gornitz and Kanciruk (1989) be used as a substitute for the one we are proposing here which addresses the very specific problem of Caribbean beach management in response to storms effects, but there is clearly complimentarity in the two approaches.

There is also much to be said for any effort to incorporate development of a hurricane vulnerability index into ongoing local and regional coastal research programs in the Caribbean, where assimilation of the data base requirements in routine information gathering will not require too much additional expenditure of effort. Regional programs at the present time include UNEP's Task Team on Implications of Climatic Changes in the Wider Caribbean (Maul, in press) and the Caribbean Secretariat of the IOC (IOCARIBE) programs on Climate and Physical Oceanography (I.O.C., 1987) and a newly developing one on Coastal Geomorphology. Opportunity also exists for research within International Geological Correlation Project #274 on Coastal Evolution in the Quaternary.

With the clear trend towards acceptable environmental standards in regional planning and development projects, spelled out in policy statements by such institutions as the World Bank (Warford, 1989) and Inter-American Development Bank (I.A.D.B., 1987), there is also a need for incorporation of data on hurricane vulnerability in environmental impact assessment (EIA) for coastal zones in the region and we hope that the approaches given an initial airing in this paper will assist towards that end.

REFERENCES

Bacon, P.R., 1989. Assessment of the economic impacts of Hurricane Gilbert on coastal and marine resources of Jamaica: UNEP Regional Seas Reports and Studies, No. 110, 78 p.

Deane, C., 1987. Coastal erosion and accretion in the Lesser Antilles: p. 138-147 in Coastal zone management of the Caribbean region: A status report: Commonwealth Science Council, Technical Publctns. Series No. 227, Commonwealth Science Council, London, 188 p.

Eyre, L.A., 1989. Hurricane Gilbert: Caribbean record-breaker: Weather, v. 44, p. 160-164.

Gornitz, V., and Kanciruk, P., 1989. Assessment of global hazards from sea-level rise: Proceedings, 6th Symposium Coastal and Ocean Management, American Society of Civil Engineers, p. 1345-1359.

Hendry, M.D., 1979. A study of coastline evolution and sedimentology: the Palisadoes, Jamaica: Ph.D. dissertation, University of the West Indies, Jamaica, 225 p.

Hendry, M.D., 1982. The structure, evolution and sedimentology of the reef, beach and morass complex at Negril, western Jamaica: Petroleum Corporation of Jamaica, Kingston, Jamaica, 185 p.

Hendry, M.D., 1989a. Coastal response to storm events: observations, planning and shore management procedures: Proceedings,

Seminar on Effects of Hurricane Gilbert on Buildings and Engineering Facilities in Jamaica, Jamaica Instituteof Engineers, Kingston, Jamaica, 14 p.

Hendry, M.D., 1989b. Beach resources management for tropical islands: Commonwealth Science Council, Training Course on Methodologies for Coastal Resources Management, Bellairs Research Institute, Barbados, 30 p.

Hendry, M.D., Geology: physical processes, coastal impacts, in Maul, G.A., editor, Implications of Climatic Changes in the Wider Caribbean, Regional Coordinating Unit, Caribbean Environment Program, UNEP, Kingston, Jamaica, inpress.

Hendry, M.D., and Digerfeldt, G., 1989. Palaeogeography and palaeoenvironments of a tropical coastal wetland and offshore shelf during Holocene submergence, Jamaica: Palaeogeography, Palaeoclimatology, Palaeoecology, v. 73, p. 1-10.

I.A.D.B., 1987. Conference on the environment, Proceedings of the Consultative Meeting with Public Agencies Responsible for Environmental Protection and Natural Resource Conservation in Latin America and the Caribbean: Inter-American Development Bank, Washington, D.C.,161 p.

I.I.E.D., 1987. Jamaica: country environment profile: Natural Resources Conservation Division, Jamaica and Ralph M. Field Associates, Inc., for International Institute for Environment and Development, London, 362 p.

I.O.C., 1987. Physical oceanography and climate: I.O.C. Workshop Report No. 45, Intergovernmental Oceanographic Institution, Paris, 1987.

Leatherman, S.P., 1981, editor. Overwash processes: Benchmark Papers in Geology, Hutchinson and Ross, Stroudsberg, Pa., 376 p.

Maul, G.A., Implications of climatic changes in the wider Caribbean: Report of the Task Team on Climatic Change, Regional Coordinating Unit, Caribbean Environment Program, UNEP, Kingston, Jamaica, in press.

McElroy, J., and de Albuquerque, K., 1989. Tourism styles and policy responses in the open economy-closed environment context: Conference on Economics and the Environment, Caribbean Conservation Association, Barbados, 18 p.

Pilkey, O.H., 1989. The engineering of sand: Journal of Geological Education, v. 37, p. 308-311.

Pilkey, O.H., Morton, R.A., Kelley, J.T., and Penland, S., 1989. Coastal land loss: American Geophysical Union, Short Course in Geology, Volume 2, American Geophysical Union, Washington D.C., 73 p.

Shapiro, L.J., Impact of climatic change on hurricanes, in Maul, G.A., editor, Implications of Climatic Changes in the Wider Caribbean: Regional Coordinating Unit, Caribbean Environment Program, UNEP, Kingston, Jamaica, in press.

Warford, J.J., 1989. Evolution of the World Bank's Environmental Policy: Conference on Economics and the Environment, Caribbean Conservation Association, Barbados, 11 p.

Origin of the Eastern Caribbean: Data from Reptiles and Amphibians

Jonathan Roughgarden

Departments of Biological Sciences and Geophysics
Stanford University

Abstract

Data on the ecology, systematics, and biogeography of *Anolis* lizards, combined with that on other reptiles and amphibians in the eastern Caribbean, suggest that:

1. The northeastern and southeastern Caribbean have had distinct geologic histories. The line separating these provinces starts between Dominica and Martinique and extends southwest to between Curacao and Bonaire.
2. Within the northeastern province, material in the Guadeloupe-Dominica region has split off from Puerto Rico. The fauna of Guadeloupe and Dominica has had a primarily vicariant origin (i.e., consists of the descendents of populations that were on Proto-Guadeloupe at the time of its original fragmentation from Puerto Rico). This region has then served as a biological source for the younger islands north of Guadeloupe up to the Anegada Passage. Propagules have come north from Guadeloupe by over-water dispersal, in accordance with the prevailing currents.
3. Within the southeastern province, St. Lucia, La Blanquilla and Bonaire seem to be members of a former island arc that was "upstream" of the eastward-moving Caribbean plate. Collision with this island arc resulted in the insertion of St. Lucia between Martinique and St. Vincent, while La Blanquilla and Bonaire were pushed down onto the Venezuelan shelf. The oceanic islands of the southeastern province thus consist of at least four classes of terrains: Curacao—related perhaps to Grand Cayman; Bonaire and La Blanquilla—related to St. Lucia; the triplet consisting of Martinique, St. Vincent, and Grenada; and Barbados—exposed accretionary prism that has formed *in situ* and been colonized recently through local over-water dispersal.

The colorful and small arboreal lizards of the genus *Anolis* found on all the islands of the Caribbean and in Central America may serve as "living strata." Here, information about eastern Caribbean anoles is offered to help in reconstructing the origin of the Lesser Antillean Island Arc in relation to Puerto Rico and the Netherlands-Venezuelan Antilles. A preliminary account has appeared in Roughgarden et. al. (1987).

For a biological population to mark a geologic entity, such as an island or island bank, it must be a ready colonist; it must rebuff subsequent colonizations from adjacent geological entities, for otherwise the labels would mix; and it must not be prone to extinction. Anoles are hardy survivors on tropical cays; ecological competition between anoles for limiting resources retards cross invasion between adjacent islands, and prevents cross invasion altogether between species of the same body size; and the huge population size on a Lesser Antillean island (estimated at 10^8 for a 400 km^2 island assuming 0.25 lizards per m^2) precludes chance extinction and increases the likelihood of contributing a propagule to newly opened habitat. Also, anoles are diverse, and thereby provide many labels. There are over 300 species of *Anolis*, about half of which are in the West Indies, and half in Central and northern South America. The genus is one of the largest of all vertebrate genera, and comprises about 5–10% of all lizard species in the world today.

Moreover, anoles have been in the Caribbean theater for a long time. A complete fossil *Anolis* encased in early Miocene amber (ca. 20–23 my BP) has been found in the Cordillera Septentrional of the Dominican Republic (Rieppel 1980). It may be even older than originally reported, lower Oligocene or upper Eocene (35–40 my BP), according to Poiner and Cannatella (1987). The specimen is a juvenile lizard indistinguishable from the green anoles now living in Hispaniola, *A. chlorocyanus* and *A. aliniger*. Skin fragments from another fossil anole have been described from Chiapas, Mexico; its amber has been dated as late Oligocene to early Miocene (Lazell 1965). Finally, the lineage (clade) consisting of the Iguanidae (including *Anolis*) is old, splitting from a sister lineage consisting of the Agamidae and Chamaeleonidae in the middle Jurassic (175 Ma) (Estes 1983). In contrast, old rock strata in the Caribbean are scarce, as Jurassic and Cretaceous materials have been lost to subduction or covered by more recent magmatic activity. Thus, anoles have been in place as the Caribbean itself has formed, and the systematics, ecology, and biogeography of these lizards may therefore provide sorely needed clues about the origin of the Caribbean to supplement geologic data.

The key conclusions offered here are:

- The northeastern and southeastern Caribbean have had separate geologic histories. The line separating these provinces starts between Dominica and Martinique and extends southwest to between Curacao and Bonaire, demarking a triangle at the southeastern corner of the Caribbean Plate.

Larue, D.K., and Draper, G. (eds.),
Transactions of the 12th Caribbean Geological Conference, St. Croix, U.S.V.I., Miami Geological Society, P.O. Box 431552, South Miami, FL 33243, U.S.A

- Within the northeastern Caribbean, material in the Guadeloupe-Dominica region split off from Puerto Rico. The fauna of this region has had a primarily vicariant origin (i.e., it consists of the descendents of populations that were on Proto-Guadeloupe at the time of its original fragmentation from Puerto Rico). The Guadeloupe region has itself served as the source for the biota on the younger islands north of Guadeloupe up to the Anegada Passage, and the propagules have come north from Guadeloupe by over-water dispersal, in accordance with the prevailing currents.

- Within the southeastern triangle of the Caribbean, St. Lucia, La Blanquilla and Bonaire are members of a former island arc that was upstream of the eastward-moving Caribbean plate. Collision with this island arc resulted in the addition of St. Lucia between Martinique and St. Vincent, and pushed La Blanquilla and Bonaire down onto the Venezuelan shelf.

The oceanic islands of the southeastern Caribbean thus consist of at least four classes of terranes: (1) Curacao—perhaps related to Grand Cayman; (2) Bonaire and La Blanquilla—related to St. Lucia; (3) the triplet consisting of Martinique, St. Vincent, and Grenada; and (4) Barbados—an exposed piece of accretionary prism that has formed in situ and has been colonized solely through over-water dispersal.

Also, biological data are consistent with speculation that some geologic material presently in the West Indies was in the neighborhood of nuclear Central America and northern South America during the Cretaceous, all of which comprised an archipelago in the Pacific. The southeastern triangle may have been sutured to the Caribbean plate.

1 Biological Data

We now review the main facts about the systematics, ecology, and biogeography of *Anolis* lizards, and of reptiles and amphibians in general, for the eastern Caribbean.

1.1 Systematics

1.1.1 Early Research on *Anolis*

Using squamation characters (number, size, shape, texture and arrangement of scales), Underwood (1959) proposed that the anoles of the eastern Caribbean comprise three sets having the relationship diagrammed in Figure 1.

The northern Lesser Antilles (Figure 2), from the Anguilla Bank through Dominica, are populated by the "bimaculatus group," which itself contains two series, the "wattsi series" and the "bimaculatus series."

The wattsi series are small brown lizards that typically perch near the ground and on the leaf litter. Each population from this series co-occurs with a population from the bimaculatus series; no population of the wattsi series occurs alone on an island.

The bimaculatus series consists of colorful large- and medium-sized lizards that are relatively arboreal. Some bimaculatus populations are alone on an island and others co-occur with a member of the wattsi series. Underwood (1959) envisaged that each of these series represented a separate invasion from Puerto Rico, and that the wattsi series was the more recent invasion.

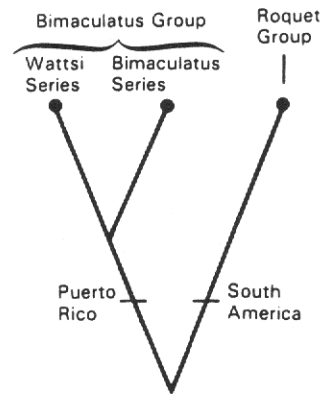

Figure 1. Relationship among eastern Caribbean *Anolis* from early systematic research. The wattsi and bimaculatus series of the northern Lesser Antilles were presumed to represent separate waves of invasion from Puerto Rico, with the wattsi series being the more recent invasion. The roquet series of the southern Lesser Antilles was presumed to be derived from South America.

The southern Lesser Antilles (Figure 2), from Martinique through Grenada, are populated by the "roquet group;" today it is also known that the anoles on Bonaire in the Netherlands Antilles and La Blanquilla in the Venezuelan Antilles are also members of this group. The roquet group was presumed to have colonized from South America.

1.1.2 Contemporary Studies of *Anolis*

Systematic research since the species were originally described has clarified the phylogenetic relationships of the species, and corroborates the early definitions of species groups based on squamation. The new data consist of karyotypes (descriptions of chromosomes), the immunological analysis of blood albumins, and the electrophoresis of proteins from over 20 loci (Gorman and Atkins 1969, Gorman 1973, Paull et al. 1976, Yang et al. 1974, Gorman and Kim 1976, Gorman et al. 1980, 1983, Shochat and Dessauer 1981).

Figure 3 offers my synthesis of the phylogenetic relationships entailed by this recent work (see also the extensive notes accompanying the figure). The taxa being classified are the populations on each of the island banks in the Lesser Antilles, together with all the Puerto Rican anoles. Geographically differentiated varieties (subspecies) are diagrammed as horizontal lines with vertical tick marks to indicate each named variety. Notice that the islands in the center of the arc, Guadeloupe, Dominica, and Martinique have species with geographical variation (i.e., multiple subspecies); the species on the other islands show little internal differentiation. The major branches express a strict consensus among the morphological, karyotypic, and biochemical data.

The most important new findings are: (1) the distinction between the bimaculatus and roquet groups reflects a deeply different chromosomal makeup, and great biochemical dissimilarity in blood albumins; (2) the bimaculatus group is sister to the cristatellus group of Puerto Rico, and both belong to a lineage termed the Central Caribbean Complex by Shochat and Dessauer (1981); (3) the genetic distances among the populations in the wattsi series are as great or greater than those

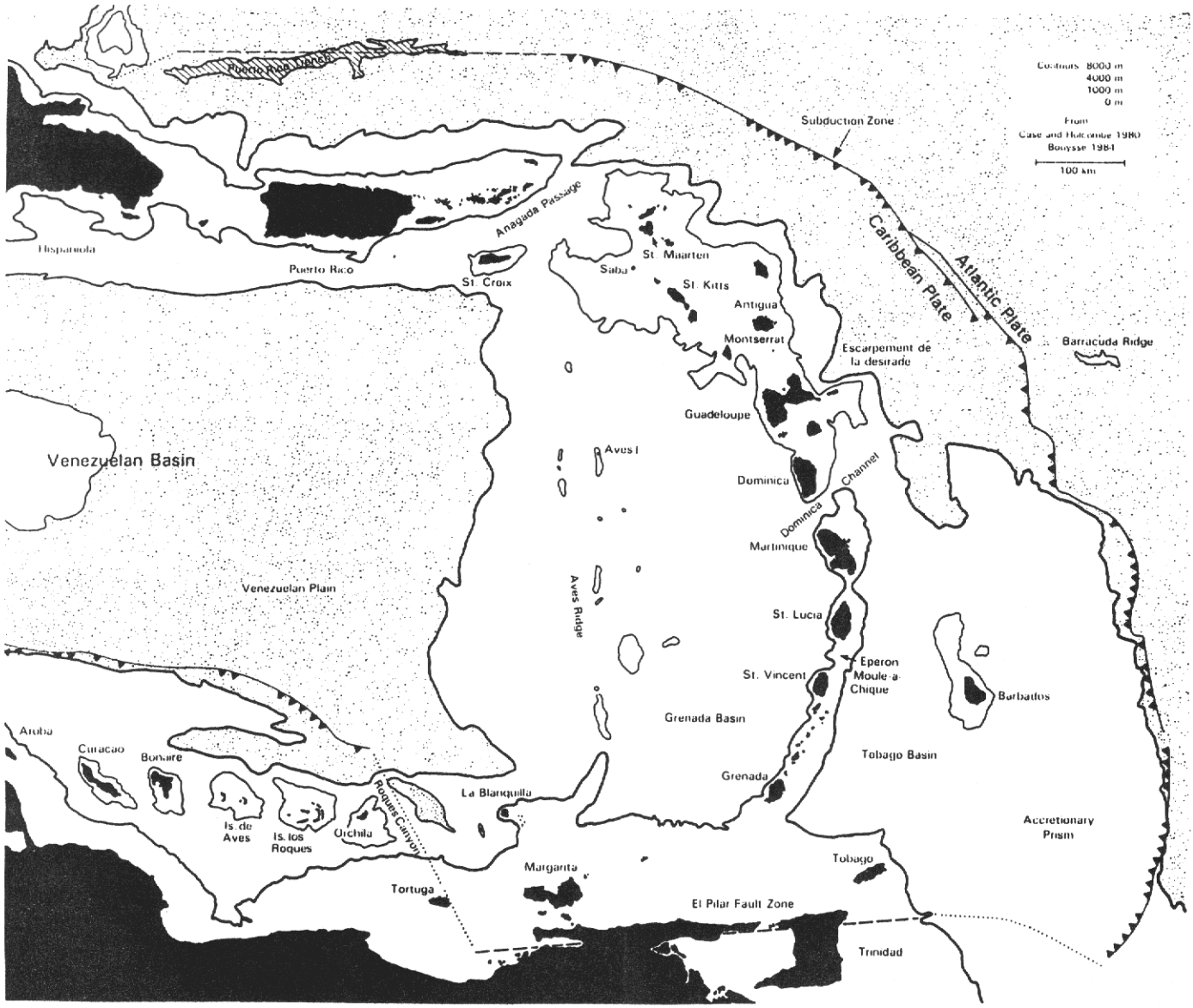

Figure 2. Tectonic map of Lesser Antilles. In the North, the Guadeloupe area has deposits as old as the oldest in the Greater Antilles. It is also a center of endemism for the bimaculatus group of *Anolis* lizards, a sister lineage of the cristatellus group of the Puerto Rico bank. In the South, the anoles come from the roquet group, and are not closely related to those in the North.

in the bimaculatus series; and (4) the roquet group subdivides into a "roquet" series and a "luciae" series, with the luciae series comprising the populations on St. Lucia, La Blanquilla, and Bonaire.

The distinction between the roquet and bimaculatus groups has proved so significant that Guyer and Savage (1986) recently suggested elevating the roquet group to generic status, and suggested the generic name, *Dactyloa* for the roquet group anoles.

Locating continental relatives of Caribbean anoles is difficult, even though over 150 species occur in Central and South America. The continental anoles are only distantly related to Caribbean anoles.

The closest known relative of an anole from the northeastern Caribbean, *A. evermanni* from Puerto Rico, is *A. gadovi*, from the Pacific versant [sic] of tropical Mexico. *A. gadovi* is itself a member of a cluster of rather closely related species in western Mexico, called the gadovi group. The albumin distance of the Puerto Rican anole to this Mexican anole is 29 units, a value far less than, for example, the typical albumin distance of about 55–60 units between a bimaculatus and roquet anole (Gorman 1984). (See notes to Figure 3 for other known albumin distances.) The karyotype of *A. gadovi* also includes sex chromosomes, which may be considered a derived characteristic shared with the eastern Caribbean anoles, all of which also have sex chromosomes (Lieb 1981).

Perhaps even more surprising, the closest known non-West Indian relative of an anole from the southeastern Caribbean is *A. agassizi* on the isolated island of Malpelo in the Pacific south of Panama and west of Columbia (Graham 1975). Shochat and Dessauer (1981) report an albumin distance of 40 units between *A. extremus* of Barbados (itself nearly identical to *A. roquet* of Martinique) and *A. agassizi* of Malpelo, and unpublished data of Gorman (personal communication) show an even closer relationship. The distance of *A. extremus* to a typical anole of

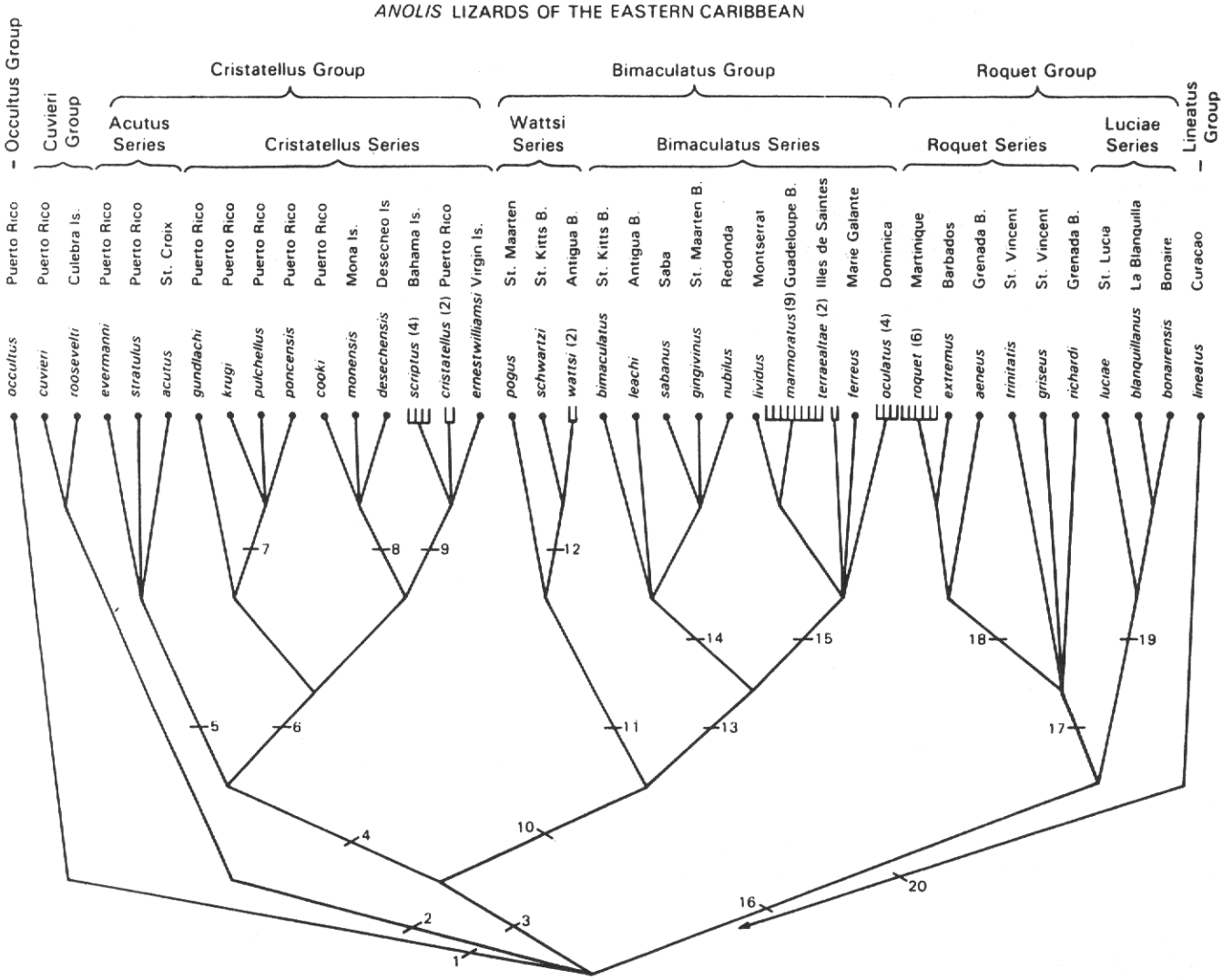

Figure 3. Phylogenetic Tree for *Anolis* in the Eastern Caribbean. The tree is derived from data on squamation, karyotypes, the electrophoresis of proteins, and the immunogenetic assay of albumins. The taxa being classified are the populations on present-day island banks, irrespective of their current nomenclatural status as "species" or "subspecies." Taxa having geographical variation within an island bank that resulted in the naming of subspecies (geographical races) are indicated as horizontal lines with vertical tick marks to denote each subspecific name that has been defined. The tree corroborates the early work depicted in Figure 1. Furthermore, the bimaculatus group is sister to the cristatellus group of Puerto Rico, and the roquet group is divided into the roquet series and the luciae series.

Venezuela, *A. chrysolepis*, is about 60 indicating a large distance. Thus, the preliminary indications are that the continental relatives of Caribbean anoles are on the Pacific coast of Central and northern South America.

The phylogenetic tree contributes to refuting the hypothesis that anoles colonize the Lesser Antilles by successive over-water dispersal from Puerto Rico in the north, and from Venezuela in the south. By this hypothesis, islands close to a source region should have more anole species than those far from a source (the classic distance effect of island biogeography) *and* the more recent invasions from a source region should still retain a close relationship to the taxa in the source region from which they were derived.

Instead, in both the north and south, islands with one anole species lie between the putative source areas and the islands with two species, indicating an absence of the classic distance effect in island biogeography. Moreover, in the north the anoles are more closely related to the species on Guadeloupe at the center of the arc than to anything in Puerto Rico, and in the south anoles are more closely related to the species on Martinique in the center of the arc than to anything in Venezuela. Thus, the sources for the Lesser Antillean anoles would appear to come from the center of the arc rather than from above or below, as traditionally thought.

Indeed, among the nine named varieties of *A. marmoratus* on Guadeloupe one can find every distinguishing trait possessed by its relatives to the north, suggesting that some of the northern members of the bimaculatus series have been derived from Guadeloupe. Dispersal from the Guadeloupe region north is also consistent with the prevailing currents (Richardson and Walsh

1986), whereas dispersal from Puerto Rico down into the Lesser Antilles is contrary to those currents.

Finally, the biochemical differentiation among the bimaculatus populations is appreciably less than that among the cristatellus populations or among the roquet populations, suggesting that the bimaculatus series is younger than the cristatellus or roquet series.

1.2 Ecology

1.2.1 Population Dynamics

Long-term monitoring of *Anolis* populations on St. Maarten has revealed a remarkable stability in the population dynamics of *Anolis* on a tropical island. Roughgarden and coworkers have censused two sites on St. Maarten once or twice a year from 1977–1987. Year after year the same cyclic pattern recurs even though two hurricanes passed the sites and the annual rainfall may vary by a factor of up to 2 in consecutive years. The abundance is lowest during the summer when the abundance is typically 0.5 lizards per m^2 and more than doubles during the winter with the production of juveniles. The between-year variation in abundance compared at the same point in the seasonal cycle is less than the within-year variation, and the summer abundance has been essentially constant (within 10%) at the two sites during 11 years. This abundance is what makes anoles likely colonists of new habitat as it forms, and makes chance population extinction unlikely.

1.2.2 Resource Limitation

Experimental studies point to food, and not space, as the principal limiting resource. Removal of lizards from experimental enclosures leads to a doubling of insect abundance on the forest floor and to a 10- to 30-fold increase in the quantity of spiders in the vegetation (Pacala and Roughgarden 1984, Schoener and Spiller 1987). Also, food augmentation increases lizard growth rates in nature (Licht 1974, Stamps 1977). In contrast, experimentally increasing the spatial overlap in perch positions of the two species on St. Eustatius produces little effect (Rummel and Roughgarden 1985) and interspecific territoriality cannot be detected except between animals of nearly identical body sizes (Bohlen 1983). The existence of food as a limiting resource is what underlies the existence of competition between lizard species.

1.2.3 Competition between Species

Experiments in which anoles were introduced to an offshore cay and to 12m × 12m enclosures experiments proved the existence of strong present-day competition between the two species on St. Maarten (where the body sizes of the two species are nearly the same) and also that competition between the two species on St. Eustatius (where the lizard species differ in size by a factor of nearly two) is weak and barely detectable (Roughgarden et al. 1984, Pacala and Roughgarden 1985, Rummel and Roughgarden 1985). This competition is what prevents islands from simply accumulating species without limit; it ensures that a species on an island becomes, in time, a unique label for that island.

1.2.4 Invasion

The record of recently introduced anoles supplies more evidence of interspecific competition. To aid the biological control of the fruit fly, *Ceratitis capitata*, in 1905 the Director of Agriculture of Bermuda liberated 71 individuals of *A. grahami* in public gardens (Wingate 1965). *A. grahami* is a medium sized lizard; it was collected from the Kingston area of Jamaica. By 1940 *A. grahami* was abundantly distributed throughout Bermuda. About 1940 the large anole from Antigua, *A. bimaculatus leachi*, first appeared. The species is now established in the center of Bermuda (Warwick area), primarily in woods. The spread of this large anole has taken place on territory already occupied by the medium sized anole. Finally, the solitary-sized anole, *A. extremus* from Barbados was noted in 1953 at the western end of Bermuda (Somerset and Ireland areas) where it still has a patchy distribution.

Hispaniola provides two well-documented instances of "enclaves" of introduced anoles; these typically form when natural habitat is cleared and replaced with plantings (Williams 1977). The Cuban green anole, *A. porcatus*, has been known since 1970 from a few city blocks in Santo Domingo at the site of former trade fairs. Its range has remained static through 1977 and is surrounded by the native green anole, *A. chlorocyanus*. The Puerto Rican trunk-ground anole, *A. cristatellus*, has been known since 1956 to be abundant in gardens in the port city of La Romana in the Dominican Republic. The town is the site of a sugar mill constructed by a Puerto Rican based company. The range of the anole has been static for over 20 years and is surrounded by the native trunk-ground anole, *A. cybotes*. Schoener and Schoener (1983a) also produced enclaves in the Bahamas with experimental introductions to tiny cays that were already inhabited by an anole. In contrast, introductions to empty cays large enough to support anoles invariably produced a population explosion of the introduced species.

Introduced small anoles evidently do not form enclaves when surrounded by larger anoles. A population of *A. wattsi* known from the botanical garden in St. Lucia has become extinct (Underwood 1959, Williams 1977). *Anolis wattsi* was introduced four times to a cay near Anguilla where *A. gingivinus* was already living and *A. wattsi* eventually became extinct each time. The waiting time to extinction could be doubled simply by removing half of the *A. gingivinus* at the site prior to the introduction (Roughgarden et al. 1984).

Thus, a large anole can become established in the presence of a smaller anole, an anole introduced to newly opened habitat can form a virtually static enclave in the range of another anole with similar size and habits, and a small anole evidently cannot be introduced successfully in the presence of a larger anole. Thus, competition between species ensures that the species, considered as labels for islands, remain as faithful markers of geologic structures.

1.2.5 Extinction

The tiny cays on the Puerto Rico Bank (British Virgin Islands) demonstrate how a complex herpetofauna responds to habitat fragmentation. These keys reveal that the species lists for a sequence of islands of decreasing area comprise, approximately, a sequence of nested subsets. The cays are not random subsets of some larger fauna. Specifically, all the cays with only one species of amphibian or reptile have precisely *A. cristatellus*, those with two species have both *A. cristatellus* and a gecko

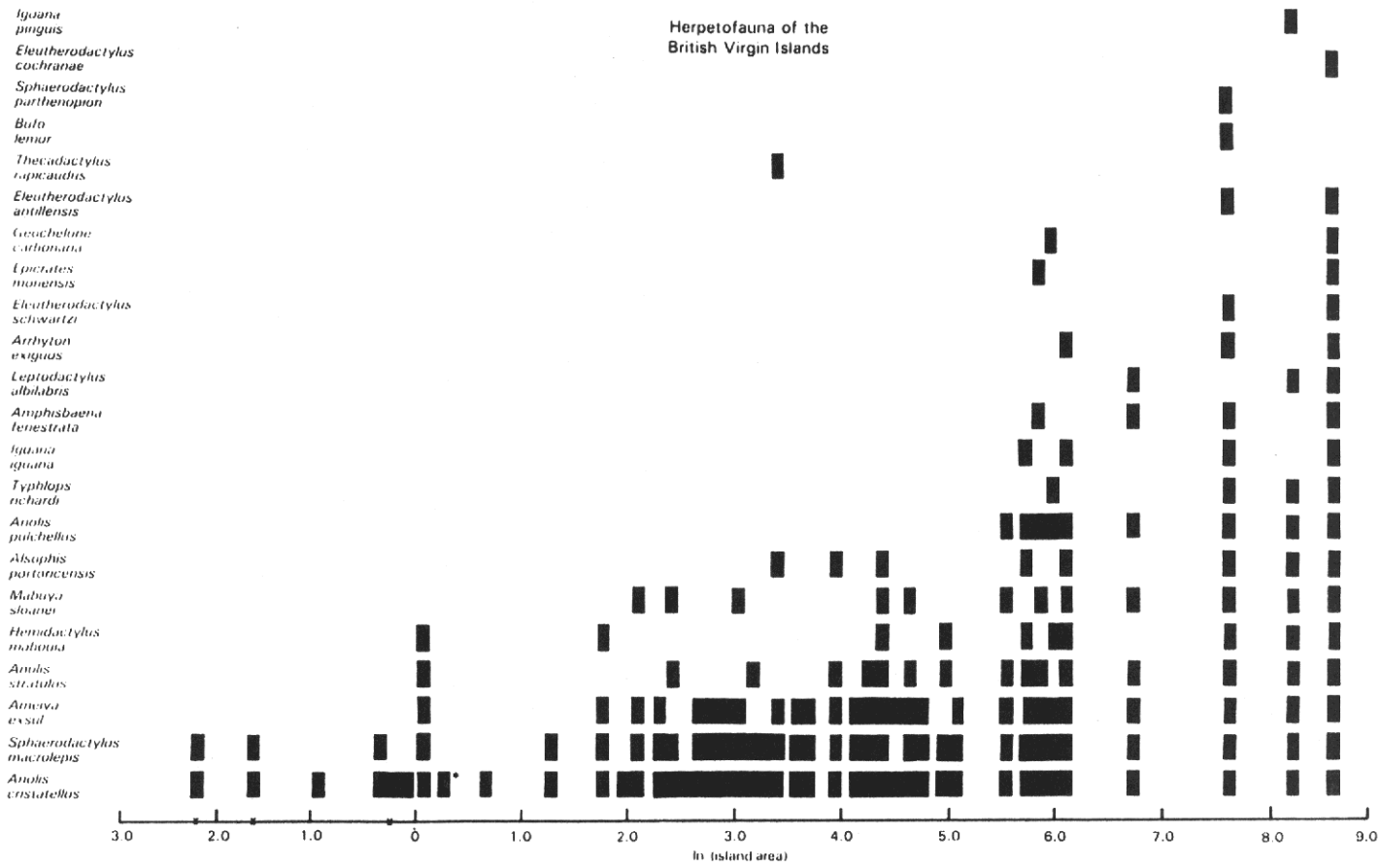

Figure 4. Nested subset pattern for the relation between island area and species occurrence for amphibians and reptiles in the British Virgin Islands. Notice that *Anolis cristatellus* is the species that can survive on the smallest cay; it has the best "bottle-necking" ability, and presumably for this reason is the parental lineage to the bimaculatus group centered in the Northern Lesser Antilles, as noted in Figure 2.

Sphaerodactylus macrolepis, those with three or more species have these plus certain others—each species seems to have a minimum island area at which is is first found, and is present on all islands larger than its minimum area. Thus, the islands with only one species do not possess random species, nor do islands with only two species possess random pairs, drawn, as it were, from some urn of all species in the region. Figure 4 presents the data from Lazell (1983) for the British Virgin Islands. Schoener and Schoener (1983b) discovered that the lizards on cays of the Bahama Bank also form nested subsets.

During the Pleistocene 15000 years ago, the Puerto Rico Bank extending to Anegada was above water (Heatwole and MacKenzie 1967). As the glaciers melted slight hilltops became the tiny cays of the British Virgin Islands today. The lizards on these cays presumably did not have to disperse there, they were there to begin with. The fauna on the cays consists of special species that have the property of not becoming extinct when the size of their habitat shrinks. They have, so to speak, a good "bottle-necking" ability—colonizing ability is probably irrelevant to their presence on the cays of the Puerto Rico Bank.

It is important to observe that *A. cristatellus*, the particular lizard that is retained on even the smallest of the Virgin Island cays, is the sister taxon to the bimaculatus group of the northern Lesser Antilles. This fact supports an hypothesis that the fauna in the northern Lesser Antilles is a differentiated fragment extracted from the Puerto Rican fauna.

1.3 Biogeography

1.3.1 Distribution of Amphibians and Reptiles

Table I presents all the amphibians and reptiles of the Lesser Antilles today compiled from the checklist of Schwartz and Thomas (1975) and the magnificent field guide of Schwartz and Henderson (1985).

The faunal break at Dominica marking the end of the bimaculatus group of anoles in the Lesser Antilles is observed by *Ameiva* ground lizards, *Typhlops* blind snakes, and *Alsophis* snakes. The *Ameiva* in St. Vincent and Grenada is South American, and the *Liophus* snakes of the southern islands are a South American genus.

Also, Dominica is the southern end of the *Sphaerodactylus fantasticus* complex, and the *S. vincenti* complex begins in the adjacent Martinique where seven subspecies are found. It would be useful to know if the *S. vincenti* complex is very distantly related to the *S. fantasticus* complex as are the anoles on these adjacent islands. Perhaps a difference between the *S. fantasticus* and *S. vincenti* complex is as great as that between the bimaculatus and roquet groups, and a test of this proposition would be very significant.

The Guadeloupe archipelago is unique among the northern islands in having a great endemic differentiation of anoles, *Sphaerodactylus* geckoes, *Alsophis* snakes and *Eleutherodactylus* frogs. *A. mormoratus* is recognized as one species having 12

Table Ia. Herpetofauna of Northern Lesser Antilles

	ANGUILLA	SABA	ST. KITTS	ANTIGUA	MONTSERRAT	GUADELOUPE	DOMINICA
Bufo			*marinus*[A]	*marinus*	*marinus*	*marinus*	
Hyla							
Leptodactylus			*fallax*[C]		*fallax*	*fallax*	*fallax*
Eleutherodactylus	*johnstoni*[E]	*johnstoni*	*johnstoni*	*johnstoni*	*johnstoni*	*johnstoni*	
				martinicensis[F]		*martinicensis*	*martinicensis*
Mabuya	*mabouya*[K]					*barlagnei*[G]	
Diploglossus						*pinchoni*[H]	
Ameiva	*corvina*[M]		*erythrocephala*[O]	*griswoldi*[P]	*mabouya*	*mabouya*	*mabouya*
	pleei[N]				*montisserrati*[L]		
Cnemidophorus					*pluvianotata*[Q]	*cineracea*[R]	*fuscata*[S]
Bachia							
Kentropyx							
Gymnophthalmus							
Thecadactylus	*rapicauda*[1]	*rapicauda*	*rapicauda*	*rapicauda*		*underwoodi*[X]	
Hemidactylus	*mabouia*[2]	*mabouia*	*mabouia*	*mabouia*	*rapicauda*	*rapicauda*	*rapicauda*
Phyllodactylus					*mabouia*	*mabouia*	*mabouia*
Sphaerodactylus	*sputator*[5]		*sputator*	*elegantulus*[8]			
	macrolepis[6]	*sabanus*[7]	*sabanus*		*fantasticus*	*fantasticus* spp.[9]	*fantasticus*
Iguana	*delicatissima*[c]		*delicatissima*	*delicatissima*			
		iguana[d]				*delicatissima*	*delicatissima*
Anolis	*gingivinus*[e]	*sabanus*[g]	*bimaculatus*[h]	*bimaculatus*[j]	*iguana*	*iguana*	
	wattsi[f]		*wattsi*[i]	*wattsi* spp.[k]	*lividus*[l]	*marmoratus* spp.[m]	*oculatus* spp.[n]
Typhlops			*monastus*[v]	*monastus*	*monastus*[w]	*dominicana*[x]	*dominicana*[y]
Leptotyphlops							
Bothrops							
Boa							*constrictor*[dd]
Corallus							
Alsophis	*rijersmai*[gg]	*rufiventris*[hh]	*rufiventris*	*antillensis*	*antillensis*	*antillensis* spp.[ii]	*antillensis*
Liophus						*juliae* spp.[jj]	*juliae*
Chironius							
Clelia							*clelia*[pp]
Mastigodryas							
Pseudoboa							

Table Ib. Herpetofauna of Southern Lesser Antilles

	MARTINIQUE	ST. LUCIA	ST. VINCENT	GRENADA	BARBADOS
Bufo	*marinus*	*marinus*	*marinus*	*marinus*	*marinus*
Hyla		*rubra*[B]			
Leptodactylus		*fallax*	*wagneri*[D]	*wagneri*	
Eleutherodactylus	*johnstoni*	*johnstoni*	*johnstoni*	*johnstoni*	*johnstoni*
	martinicensis		*urichi*[I]	*urichi*[J]	
		mabouya	*mabouya*	*mabouya*	*mabouya*
Mabuya			*ameiva*[T]	*ameiva*	
Diploglossus		*vanzoi*[U]			
Ameiva				*heteropus*[V]	
Cnemidophorus					*copei*[W]
Bachia		*pleei* spp.[Z]	*underwoodi*		*underwoodi*
Kentropyx		*rapicauda*	*rapicauda*	*rapicauda*	
Gymnophthalmus	*pleei*[Y]	*mabouia*	*mabouia*	*mabouia*	
Thecadactylus	*rapicauda*	*palaichthus*[3]			
Hemidactylus	*mabouia*				*pulcher*[4]
Phyllodactylus		*microlepis* spp.[b]			
Sphaerodactylus		*vincenti*	*vincenti*		
	vincenti spp.[a]				
Iguana	*delicatissima*	*iguana*	*iguana*	*iguana*	
		luciae[p]	*griseus*[q]	*richardi*[s]	*extremus*[u]
Anolis	*roquet* spp.[o]		*trinatatis*[r]	*aeneus*[t]	
Typhlops				*tasymicris*[z]	
Leptotyphlops	*bilineata*[aa]	*bilineata*			*bilineata*
Bothrops	*lanceolata*[bb]	*caribbaea*[cc]			
Boa		*constrictor*[ee]			
Corallus			*enydris*[ff]	*enydris*	
Alsophis					
Liophus	*cursor*[kk]	*ornatus*[ll]		*melanotus*[mm]	*perfuscus*[nn]
Chironius			*vincenti*[oo]		
Clelia		*clelia*		*clelia*	
Mastigodryas			*bruesi*[qq]	*bruesi*	
Pseudoboa				*neuwiedi*[rr]	

subspecies on Guadeloupe and the nearby islands, including the Ille de Saintes and Marie Galante. The species on Montserrat and Dominica are very close to *A. mormoratus*. Similarly, the *Sphaerodactylus* is recognized as one species having seven subspecies on Guadeloupe and nearby islands, together with subspecies on Montserrat and Dominica. The *Alsophis* is recognized as one species having two subspecies on Guadeloupe and nearby islands, together with subspecies on the Antigua bank, Montserrat, and Dominica. The *Eleutherodactylus* is recognized as four species including two species that occur only in middle elevation forest on Basse-Terre in Guadeloupe.

St. Lucia is as anomalous for other components of the herpetofauna as it is for *Anolis*. The closest relatives of *A. luciae* are the anoles of Bonaire and La Blanquilla near the coast of Venezuela, not the anoles from adjacent islands. St. Lucia is also anomalous in having the only hylid frog of the Lesser Antilles, *Hyla rubra* from South America; the only *Cnemidophorus* lizard of the Lesser Antilles, *C. vanzoi* similar to the widespread *C. lemniscatus* of South America; a South American gecko, *Hemidactylus palaichthus*; and a fere-de-lance, *Bothrops caribbaea*, nearly identical to the widespread South American *Bothrops atrox*.

Competition appears related to body size in some other lizards as it is in *Anolis*. The two species of *Iguana* having the same body size show a perfect checkerboard distribution. Every island has an iguana, but the two species do not co-occur anywhere. Even on Guadeloupe *I. delicatissima* occurs on Grand Terre while *I. iguana* is on Basse Terre. Similarly, no habitat has two species of *Ameiva* all of which have about the same body size in the Lesser Antilles. *Ameiva polops* is endemic to Sombrero and *A. corvina* occurs throughout the rest of the Anguilla bank. Yet on Hispaniola, where there are four species, the two extremes in body size coexist in the same habitat.

The Puerto Rico bank has five species of *Amphisbaena* burrowing lizards. One species is found today in the British Virgin Islands on cays larger than 300 ha. None, however, is found in the Lesser Antilles. The Puerto Rico bank also has four species of *Typhlops* blind snakes, and one occurs in the British Virgin islands on cays larger than 350 ha. The Lesser Antilles do have a *Typhlops* on the St. Kitts and Antigua banks through to Dominica.

1.3.2 Distribution of Other Groups

While it is beyond the scope of this article to review all known distributions of plants and animals in the Caribbean, the following paragraphs should help to place the data on amphibians and reptiles in perspective.

Perhaps the most intriguing biogeographic reference relative to today's tectonic setting is Alexander Agassiz's (1835–1910) "demonstration that the deep-water animals of the Caribbean Sea are more nearly related to those of the Pacific depths than they are to those of the Atlantic."—quoted from Singer (1931, p.255). Agassiz concluded that the Caribbean was once a bay of the Pacific that since the Cretaceous has been cut off from the Pacific by the uplift of the Isthmus of Panama. Today, of course, this observation would be taken as consistent with the hypothesis that much of the Caribbean sea floor was in the Pacific during the Cretaceous. The most recent analysis of tectonic implications for marine biogeography is offered by Durham (1985).

Howard (1973) noted 10 genera of plants from the Greater Antilles that reach the northern Lesser Antilles (Table VI, p. 23). Of these, five terminate at Guadeloupe and the rest north of Guadeloupe; that is, Guadeloupe is as far south as these genera reach.

Schwartz (1978) reviewed the distribution of amphibians and reptiles throughout the Greater and Lesser Antilles. Table I for the Lesser Antilles is drawn from this and his later work. For the Greater Antilles, highlights include the existence of endemic satellite genera to the anoles: *Chamaeleolis* with three species on Cuba, and *Chamaelinorops* from the south island of Hispaniola. Cuba also has an endemic genus of burrowing lizard, *Cadea*, with two species. And of special interest, Cuba has an endemic genus *Cricosaura* of the family Xantusiidae, the night lizards. The other three genera of this family occur in the southwestern United States, on the Channel Islands off southern California, and in central Mexico and Central America.

West Indian mammal and bird fossils come primarily from the Pleistocene and Holocene (Olson 1978). Extinct faunas in the Greater Antilles are generally rodents, insectivores, and edentates, together with raptorial birds, often of great size that presumably evolved in response to the lack of mammalian predators. Moreover, a dramatic bear sized-rodent *Anblyrhiza inundata* in an endemic Antillean family, Heptaxodontidae, was excavated from mines on Anguilla (Cope 1883). Still, Olson concludes that this fauna is the result of multiple overwater colonizations in the Oligocene and later, with the mammals having stronger affinities with South America and the birds with North America. These data indicate the limited value of mammals for tectonic reconstruction of the Caribbean. Mammals have only been available as colonists since the mid Tertiary after much of the tectonic events that created the Caribbean had already occured.

For bats, as with reptiles and amphibians, Guadeloupe is a center of endemism—six of 10 bat species are endemic to the Antilles (Baker and Genoways 1978) a significance to over water dispersal seems obvious. In contrast with anoles, 11 species in the southern Lesser Antilles show a classic distance effect with respect to South America, as illustrated in Baker and Genoways' Figure 2 (p. 77).

The freshwater fish of the Greater Antilles are "secondary" meaning that they are derived from salt water ancestors (Briggs 1984). Also, the diversity of endemic genera and species of fresh water fishes is highest in Cuba and declines progressively eastward. No endemic freshwater fish occur in the Lesser Antilles, and therefore can contribute limited information about the origin of the eastern Caribbean.

A suborder (Auchenorrhyncha) of the Homoptera that includes cicadas, treehoppers, spittlebugs, planthoppers, and leafhoppers for the Greater Antilles. is derived primarily from Central America and Mexico, with little or no affinity to North or South America (Ramos 1988). Ramos emphasized agreement with Metcalf (1947) who proposed defining a zoogeographic region, "the Caribbean", to include the West Indies, Mexico and Central America, and distinguished from the Neotropical region.

The Scaritinae, an old and cosmopolitan group of Carabid burrowing ground beetles that consists of over 1500 species through out the world has single island endemics in the Greater Antilles, Guadeloupe and Martinique (Nichols 1988). There is also an endemic genus, *Antilliscaris*, found on Puerto Rico and Hispaniola. The presence of three species in this genus on Puerto Rico, together with a 38% endemism in the fauna on Puerto Rico, led Nichols to suggest that Puerto Rico is the oldest emergent land mass in the West Indies.

Another large group of Carabid beetles, the genus *Platynus*, has over 300 species in Mexico and Central America and 1000

or more worldwide. Most are found at elevations >300m. Many endemic species are found in the Greater Antilles although, curiously, none occur in Puerto Rico (Liebherr 1988). Five endemic species occur on Guadeloupe, four on Dominica, and one each on Martinique, St. Lucia, and St. Vincent.

Fifty eight species of drosophilid flies are endemic to the Antilles (Grimaldi 1988). Also, an endemic genus of drosophilid in the Caribbean is *Mayagueza*—it has only one species and is endemic to Puerto Rico. Moreover, the *Drosophila repleta* group that feeds primarily on decaying cactus has *D. peninsularis* endemic in the Greater Antilles; it is related to Central American stocks.

The classic power law of island biogeography relating number of species to island area is valid in the West Indies for ant species (Wilson 1988). Curiously, no endemics are reported for the northern Lesser Antilles including Guadeloupe and Martinique, but endemic species are reported from St. Lucia, St. Vincent, Grenada, and Barbados—this suggests the need for further collection and analysis in the Lesser Antilles. On the Greater Antilles a wealth of fossil ants are preserved in Tertiary amber from the Dominican Republic. The late Tertiary fauna of the Greater Antilles is more characteristic of a continental fauna. Several genera were present on Hispaniola, including army ants, that are now absent from the West Indies but that remain abundant on the continent.

Other insect groups recently reviewed include the Lygaeidae where overwater dispersal is of primary importance (Slater 1988). There is limited endemism in the Lesser Antilles (only one in about 40 species on each of St. Kitts, Dominica, St. Vincent and Grenada) and a distance effect with respect to South America. Although the Lygaeids are a Lower Cretaceous group, their biogeography in the Lesser Antilles seems rather recent. In the Greater Antilles, however, 119 species are endemic to the islands, including four endemic genera two of which are in Cuba, one in Hispaniola, and the other more widely distributed in the West Indies. Similarly, the sweat bees (Halictidae) have also been interpreted primarily in terms of overwater dispersal in the Lesser Antilles (Eickwort 1988). Both these groups seem to accord with the butterflys, which have long been interpreted in terms of overwater dispersal (Brown 1978).

As a generalization then, Cuba and perhaps to a lesser extent, Puerto Rico, are old biologically as evidenced by the endemic genera on these islands. Also, the central islands of the Lesser Antilles are places of endemism at the specific and subspecific level in many groups.

Finally, the Antilles have long been conjectured as possibly providing land bridges between North and South America while they were west of their present positions closer to the continents. This issue is explored in detail in a marvelous volume edited by Stehli and Webb (1985a). Recently, Perfit and Williams (1989) have concluded that an isthmus of continuous dry land did not exist between North and South America during the latest Cretaceous and earliest Tertiary (Paleocene) based on mammalian data. Stehli and Webb (1985b), however, document substantial evidence from mammals, reptiles, nonmarine mollusks, and angiosperm plants that filtered in both directions between North and South America at this time. They envision island-arc stepping stones as the route of dispersal. Yet Perfit and Williams note the absence of mammalian evidence in the Antilles themselves for this dispersal. Again, the suitability of mammals for the reconstruction of late Cretaceous events is called into question.

Thus, this paper differs from previous biogeographic studies in focussing on a specific group, the anoles, that have enough antiquity to be relevant to Cretaceous as well as later events, that have desirable ecological characteristics to support their use as labels for tectonic units, and whose species relationships are nearly fully worked out for the eastern Caribbean. Also, this paper is as much concerned with the geologic origin of the Caribbean itself as it is with the origin of the Caribbean's biota.

2 Synthesis with Geologic Data

The phylogenetic tree of *Anolis* shows a major dichotomy between the cristatellus-bimaculatus lineage of the northeastern Caribbean from Puerto Rico through Dominica *versus* the roquet group of the southeastern triangle of the Caribbean from Martinique through Bonaire.

At the top of the southeastern triangle, between Dominica and Martinique, Tomblin (1975), Vierbuchen (1979), and Dorel (1981) have noted the deepest seismicity of the Lesser Antilles; the seismicity occurs there with an East-West trend and Stein et al. (1982) show that strike slip faulting occurs there at depth. This fault is labeled as the "Dominica Fault" in Figure 2.

A line extending southwest from the fault between Dominica and Martinique to some point between Bonaire and Curacao appears to coincide with a major difference in the crustal structure of the ocean floor in the Venezuelan Basin. Biju-Duval et al. (1978) discovered three parallel faults trending east northeast that they termed the "central Venezuelan Basin fault zone." Diebold et al. (1981) confirmed this discovery and characterized the very different crustal structure on opposite sides of this fault zone. West of the central Venezuelan Basin fault the so-called B" reflecting layer is smooth, as characteristic of most of the Caribbean, whereas it is described as rough east of this fault in the southeastern corner of the Caribbean. Moreover, this southeastern corner is a magnetically quiet zone, in contrast to the rest of the Venezuelan Basin where northeast-southwest trending magnetic anomalies parallel the central Venezuelan Basin Fault (Ghosh et al. 1984).

Although differing somewhat from the hypothesis offered here, Bouysse (1984) has suggested that the northern Lesser Antilles has developed separately from the southern Lesser Antilles, and Speed (1985) has alluded to a similar possibility. The data on *Anolis* strongly support this kind of hypothesis. Presumably, this southeastern triangle, that harbors the roquet group of *Anolis*, is a small separate plate or a piece of the South American plate that has become sutured to the present-day eastward-moving Caribbean plate.

Now focus on the northeastern part of Lesser Antilles. La Desirade, on the Guadeloupe archipelago, has Jurassic rock (Fink 1972). After repeated study, no doubt remains as to its magmatic origin, similar in appearance, chemical composition, and mineralogy to the basal units of the Greater Antilles, and especially Puerto Rico. (Bouysse et al. 1983). Although a tiny sliver of land on an aerial map (ca 30 km^2), La Desirade is the tip of an "iceberg" marking the edge of a cliff that drops 5000m to the ocean floor in less than 10 km horizontal distance, and is the site of a distinct local positive gravity anomaly (Bourguer anomaly). Tomblin (1975, p. 471) wrote "... in view of the long time interval between these and the next oldest rocks in the Lesser Antilles and the large horizontal movements which undoubtedly took place in the region during this interval ... it

is possible that the crust now exposed in Desirade represents a small block which was much closer to the Virgin Islands in Late Jurassic time and which subsequently separated from this area and moved relatively eastward." Alternatively, basement as old as that exposed on La Desirade may underly all the northern Lesser Antilles, but simply not be exposed between the Guadeloupe region and Puerto Rico. Many authors, including Bouysse (1979, 1984), Speed (1985), and Donnelly (1985), have referred to the origin of the northern Lesser Antilles as occurring together, in some way, with Puerto Rico.

The phylogenetic tree of *Anolis* supports an hypothesis that the Guadeloupe region has moved apart from the Puerto Rico bank because the bimaculatus group of the northern Lesser Antilles is sister to the cristatellus group of Puerto Rico. The bifurcation in the phylogenetic tree where these lineages split would seem to coincide with the movement of a small block representing proto-Guadeloupe away from the Puerto Rican area. This block would carry on it the ancestor of *A. cristatellus*, just as the small cays of the Puerto Rico bank today retain *A. cristatellus* itself. This ancestor of Puerto Rico's *A. cristatellus* developed in isolation on proto-Guadeloupe to become the present-day *A. mormoratus*. And this *A. marmoratus*, in turn, spawned propagules that dispersed north, with the prevailing currents, to islands younger than Guadeloupe as they surfaced. In fact, the entire range of the bimaculatus group coincides exactly with the geologic entity bounded by the 1000m depth contour encompassing the area from the Anegada passage to the passage between Dominica and Martinique.

The Anagada passage between the Virgin Islands and the northern Lesser Antilles is an extentional basin today (cf. Speed, this conference) and perhaps this type of expansion has occurred before. Alternatively, the Aves Ridge, when more exposed than at present, may have provided a stepping stone path for dispersal from Puerto Rico to Guadeloupe, assuming Guadeloupe was emergent before the islands north of it. This alternative would not require an expansion of the arc between Guadeloupe and Puerto Rico and would be consistent with common Jurassic basement to all the northern Lesser Antilles. Still, there is no evidence of a Jurassic basement common to the northern Lesser Antilles and the Puerto Rico bank; migration down an exposed Aves Ridge to Guadeloupe would run counter to the ocean currents; and such migration would have had to involve many species to account for the large fauna on Guadeloupe today. Thus, I feel the weight of the data favors an expansion of the arc between Guadeloupe and Puerto Rico.

I term the structure that contains the present-day islands of the Anguilla Bank down through Dominica as the "NLA platform." A "taxon cycle" involving an invasion, coevolution, and extinction of *Anolis* species seems to be occurring on the Anguilla, Antigua, and St. Kitts banks toward the northern part of this platform as a result of dispersal from the Guadeloupe Archipelago (Roughgarden and Pacala 1989). The dispersal of the bimaculatus series followed that of the wattsi series. The interval between these distinct waves of invasion from Guadeloupe north might represent the time needed for Guadeloupe to grow large enough in area and elevation for a subspecies of the anole there to evolve in montane habitat—such an anole is sufficiently different from a wattsi-series anole to invade successfully.

Turning now to the southeastern triangle of the Caribbean there is further heterogeneity. The coast of Venezuela, including the Netherlands-Venezuelan Antilles, appears to be the remnant of an island arc that collided with the coast of South America in the late Cretaceous (Maresch 1974). Curacao and Bonaire have different basements, formed at a mid-ocean spreading ridge and at a subduction zone respectively (Beets and MacGillavry 1977, Beets et al. 1984), and the anoles on these adjacent islands are not at all closely related. Also, in the Lesser Antilles, the chemical composition of the rocks on St. Lucia differ markedly from those of its neighbors (Figure 2 in Tomblin 1975) just as St. Lucia's anole is not closely related to those of its neighbors.

Bucher (1952) suggested that the motion of the Caribbean plate between the North and South American plates is analogous to the motion of a glacier in a valley. The analogy explains the opposite asymmetry of pull-apart basins with the strike-slip motion at faults in the north and south boundary zones of the Caribbean plate (Mann and Burke 1984). Perhaps the analogy can be extended by viewing the southern Lesser Antilles as the "terminal moraine" at the southern half of the leading edge of the Caribbean Plate. As this part of the Caribbean plate has moved eastward, it may have accumulated some islands in its path. The magmatic activity at the subduction zone adds an enormous amount of material tending to mask nuclei that may have both heterogeneous origins and times of entry into the island arc moraine. Specifically, St. Lucia (perhaps near Eperon Moule-a-Chique) may have a different geologic origin from its present-day neighbors of Martinique and St. Vincent, and instead, may have originated with Bonaire and La Blanquilla both of which are now lodged on the Venezuelan coast.

Figure 5 presents a reconstruction of the geologic origin of the eastern Caribbean that takes into account the points raised above. The two halves of the Lesser Antilles are hypothesized to develop separately. In the north, Puerto Rico and Desirade split. As they move apart, the NLA platform, containing the present-day Anguilla, Antigua, and St. Kitts banks, grows in area. Thereafter the *A. wattsi* lineage, and then the *A. bimaculatus* lineage colonize the exposed areas on the platform by overwater dispersal. In the south matters are more complex. An island arc consisting of basal elements of Bonaire, La Blanquilla, and St. Lucia is hypothesized to lie in the path of the material that contributes to Martinique and St. Vincent-Grenada. As the Caribbean plates moves east, it pushes the islands presently between Bonaire and La Blanquilla onto the Venezuelan shelf, and picks up St. Lucia.

3 Discussion

3.1 The Lesser Antilles—Not Homogeneous and Not Tertiary

Panoramic plate-tectonic reconstructions of the origin of the Caribbean generally view the Lesser Antillean island arc as a homogeneous grouping of islands that formed during the Tertiary (e.g. Pindell and Dewey 1982). Yet new discoveries point to an older age for the basement of the Lesser Antilles than previously believed. In 1975, the oldest material known in the Lesser Antilles, apart from the Aves Ridge and the then-controversial La Desirade find, was Eocene (ca 50 my BP), with large deposits on the NLA platform, and on the Grenada Bank. These facts contributed to the acceptance of a Tertiary origin for the Lesser Antilles. Now, Upper Cretaceous (ca 70 my BP) basement material has been obtained from both slopes of the Anegada Passage (Speed et al. 1979, Bouysse et al. 1980, 1985), and on Union Island in the Grenadines (Westercamp et al. 1985). Similarly,

the endemic vertebrate fauna of the Lesser Antilles primarily involves amphibians and reptiles, forms that were abundant and successful during the Cretaceous. These data are all consistent with the hypothesis that the Lesser Antillean island arc is Cretaceous, not Tertiary, and has been available as a terrestrial habitat since that time.

Furthermore, the geologic data reviewed above are not consistent with the view that the Lesser Antillean island arc is a homogeneous grouping of islands. The isolated occurrence of Jurassic material in La Desirade is one example of heterogeneity. The difference in earthquake frequencies between the northern and southern halves of the arc, the occurrence of distinctive ocean floor in the southeast corner of the Caribbean, the difference between the basements of Curacao and Bonaire, together with suggestions of a different lithic chemistry on St. Lucia, offer other examples. Biologically, the contrast between the bimaculatus anoles of the northern Lesser Antilles and the roquet anoles of the southern Lesser Antilles is stark, and the difference between the lineages of the anole on Curacao and that on the adjacent island of Bonaire is almost as dramatic. Thus, many data point to a heterogeneous history for the structures that are now aligned at the edge of the Caribbean plate.

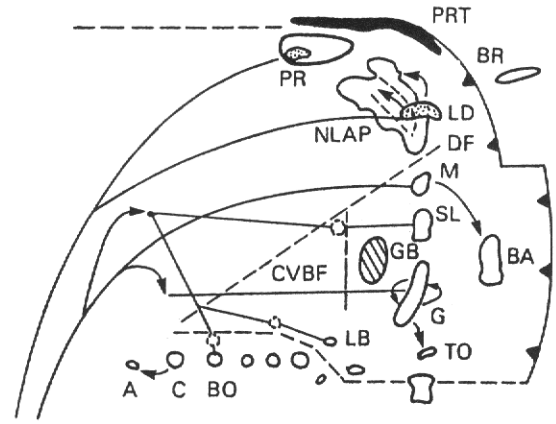

Figure 5. Schematic for proposed geologic origin of the eastern Caribbean. Abbreviations are: PR, Puerto Rico; PRT, Puerto Rico Trench; BR, Barracuda Ridge; LD, La Desirade; NLAP, Northern Lesser Antilles Platform; DF, Dominica Fault; M, Martinique; SL, St. Lucia; BA, Barbados; GB, Grenada Basin; G, Grenada-ST. Vincent; TO, Tobago; CVBF, Central Venezuelan Basin Fault; LB, La Blanquilla; BO, Bonaire; C, Curacao; A, Aruba. Lines ending in an arrow indicate overwater dispersal by anoles. Lines without arrows indicate the path traced by *Anolis* populations as they occupied basal elements of geologic structures that today are in the eastern Caribbean.

3.2 A Pacific Archipelago

Vertebrate paleontology and biogeography in Central America have focussed on the study of mammals as indicators of when the isthmus of Panama closed. This application of biogeography relies on the fact that mammal faunas of North and South America are distinctive, while Central American mammals are essentially a North American fauna. The closure of the isthmus is then indicated by dispersal of South American forms northward into Central and then North America, and North American forms into South America. This entire investigation has, however, diverted attention away a fundamental clue offered by the biogeography of other vertebrate groups. For amphibians, reptiles, and fresh water fish, Central America is a faunal province of its own, with many endemic genera, that have southern, not northern, affinity (Bussing 1976; Duellman 1966, 1979; Miller 1966; Savage 1966). To quote from Savage (1982),

> "The distributions of recent and fossil mammals for the region have been extensively reviewed by several workers, most recently by Savage (1974), Ferrusquia-Villafranca (1978), and Marshall et al. (1979). These studies all confirm that the South American mammal fauna was isolated from that of Central America until Pliocene; that no distinctive Middle American mammal fauna can be recognized; that no cluster of taxa of southern relationships, equivalent to the Middle American unit seen in the freshwater fishes and herpetofauna, can be distinguished; and that the region was dominated by groups of northern affinity until the interchange with South America."

Similarly, the Antillean herpetofauna is generally allied with Central America, and to some extent South America; for example, it does not contain the North American forms readily observed in the southwestern U. S.

These considerations led Savage (1982) to propose that

> "There was a continuous land connection or series of proximate islands extending from northern South America to the area of Nicaragua in late Mesozoic and/or early Tertiary. This land connection or island archipelago seems to have included the future Greater Antilles that were closely associated with the Nicaraguan region."

While this proposal may, of course, not be correct in detail, it is important to appreciate the point it is intended to convey—there has been a lot of evolutionary action in Central America by the very vertebrate groups that were abundant and successful during the Cretaceous (the so-called Age of Reptiles). In contrast, mammals are primarily creatures of the Tertiary (the so-called Age of Mammals) and they have not figured prominently in Central America. So, mammals apparently arrived in Central America with too little time for much evolution to occur. Hence, some material now in Central America and the Antilles appears to have been available to amphibians and reptiles during the Cretaceous before mammals became successful.

The evidence of interchange between North and South America at approximately the upper Cretaceous-Paleocene boundary argues that islands were present in the gap between North and South America at that time. Before that time this material had to be further west out in the Pacific. But was it exposed and available as habitat earlier in the Cretaceous? Quite possibly, in view of the relatives of cristatellus-bimaculatus anoles in western Mexico and roquet anoles on Malpalo off Columbia, the Pacific distribution of the relatives of the xantusid lizard of Cuba, and the extensive development of endemism in the Central American/Antillean province that Savage has emphasized in the quotations above. The suture of the southeastern corner of

the Caribbean plate also seems to have taken place in the Pacific because the Central Venezuelan Basin Fault separates smooth from rough B" material. This material that characterizes the Caribbean sea floor (Burke et al. 1978) was produced by an off-ridge episode of volcanism, called the B" event by Burke (1988), and the flood basalt event by Donnelly (1985), about 80 Ma. It appears to mark the initiation of the Galapagos hot spot (Duncan and Hargraves 1984) when the Caribbean ocean floor was in the Pacific. Given that both sides of the CVBF have B" material, both must have originated in the Pacific, even though they are not identical. The smooth B" sea floor may have been more northern, closer to the Nicaraguan block. The rough B" floor, with islands containing the roquet group of anoles, may have come more from the south, perhaps with affinity to the Cretaceous island arc now part of the Western Cordillera of Columbia and Ecuador (Bourgois et al. 1987, Lebras et al. 1987.)

The existence of a Cretaceous archipelago in the Pacific near South America as a theatre where small reptiles evolved and diversified might also be relevant to two of the classic mysteries of herpetology: the occurence of *Tropidurus* and iguanine lizards on the Galapagos (Wright 1984) and the iguanine *Brachylophus* of Fiji (Gibbons 1985). Such an archipelago would be well positioned to contribute fauna to both the Galapagos and the Fiji's.

3.3 A Grand Scenario

The preceding facts invite a conjecture—a grand scenario for how the origin of the eastern Caribbean might be spliced into the context of the origin of Central America. During the Cretaceous an archipelago formed west of the Americas, closer to South America than to North America. As North and South America moved westward, and while this archipelago was still in the Pacific, a piece of ocean floor containing the basement of the southern Lesser Antilles becomes sutured to the southeastern margin of the Caribbean plate. As the Caribbean plate moved between the Americas, some of the material remained at the gap between the Americas, to be incorporated into Central America, while other material continued through the gap to become the Antilles. As the Antillean material moved eastward relative to the Americas, it sent propagules to become the Jamaican radiation of anoles. Thereafter, the eastern margin of the Caribbean plate developed whereby the Guadeloupe region moved apart from Puerto Rico in the north, and in the south the Netherlands-Venezuelan Antilles are pushed onto the Venezuelan shelf while St. Lucia became lodged between Martinique and St. Vincent, as previously discussed.

3.4 Further Exploration and Dating

On a more empirical note, the reptile and amphibian faunas of Central and northern South America, and of Cuba and Hispaniola, need much more exploration. What is especially needed is collection and systematic study using modern molecular biology techniques. While conventional morphological analysis sufficies for naming and identifying species, determining lineage relationships requires molecular information. The molecular data for anoles is based solely on blood albumins. DNA hybridization studies would be even better. It cannot be over-emphasized that the lineage relationships combined with species range maps are what is needed to address geological processes using biological data. While most species of Caribbean, Central, and South American amphibians and reptiles have been collected and described, their lineage relationships have not been worked out. The data presented here for the eastern Caribbean is most of what is presently known about the lineage relationships of anoles. I believe that a large effort devoted to determining the species relationships of Caribbean, Central and South American anoles using molecular biology methods could quickly provide data of great relevance to reconstructing their plate tectonic origin.

Another potential value of lineage relationships based on molecular data is in providing dates for geologic events. The issues are whether the biochemical distance between two population on separate islands increases as a linear function of time since separation, and if so, what the speed of differentiation is. The mathematical formula for the "albumin immunogenetic distance" has been devised according to population-genetic theory in hopes that this distance does increase linearly with time (Wilson and Sarich 1969, Maxson and Wilson 1974, Wilson et al. 1977). Moreover, Shochat and Dessauer (1981) have even suggested that 1.7 units of distance accumulate per 1 million years. This speed is about twice the rate that seems appropriate for the reconstructions that are proposed in this paper. Clearly, more research here would valuable.

3.5 Historical Ecology of *Anolis*

We return now to the ecology of *Anolis* lizards, the subject that motivated this paper to begin with. Our findings suggest that the composition of *Anolis* communities in the Eastern Caribbean results from the combination of competition, habitat bottlenecking, and plate tectonics. Ecological competition prevents cross colonization by species of the same or very similar body size, but otherwise the strength of competition between anoles is slight. When a geologic fragment splits from a larger unit a very particular set of species is retained on the fragment, those with good "bottle-necking" ability. This special extraction then develops in isolation and need never represent an early stage in the buildup of a complex fauna. Thus, relatively fast-acting ecological interactions such as competition and predation are not sufficient to explain the composition and structure of ecological communities. Instead, ecological communities are fashioned as much by relatively slow geologic processes as by fast species interactions. We have thus come full circle. During the last two decades instances of fast evolution, on an ecological time scale, have been discovered. Now it is also clear that ecological change can itself be very slow, on an evolutionary time scale.

Finally, the explanation for why the eastern Caribbean has been a theater for the evolution of *Anolis* seems to involve a two-part relationship between anoles and birds. I hypothesize that the present-day dominance of anoles as the ground-feeding insectivorous vertebrates in Caribbean communities reflects a competitive superiority of arboreal lizards over birds in the ground-feeding insectivorous niche, provided the temperatures are mild and there is a relative absence of predation. North American birds are continually migrating through the Lesser Antilles, and do not establish there, supporting the idea that the lizards have pre-empted the ground-feeding insectivorous niche in the Lesser Antilles. But larger islands and continental regions support both a higher diversity and a higher abundance of birds of prey. These birds of prey can reduce anole abundance and thereby allow the competitively inferior insectivorous birds to occupy the ground-feeding insectivorous niche. The explanation for the reptile-dominated faunas of the Caribbean, that contrasts markedly

with the avian dominated faunas of the Pacific islands, is that the Caribbean islands are old enough to have accumulated a reptile fauna before birds and mammals diversified. Because the Caribbean islands remained at warm latitudes, and because the islands are small enough to lead to relatively little predation pressure on lizards, the islands today show communities that may resemble ecological communities of the Cretaceous.

4 Acknowledgments

I thank Dave Larue for helpful discussions on this work over a period of several years, and also Fred Nagle for the invitation to attend this wonderful conference. I gratefully acknowledge Joel Cracraft for stimulating this line of research, and for presenting it in my absence at a conference in New Orleans. Finally, I thank my students and colleagues for enjoyable companionship over the years the ecological work reported here has been carried out, and the National Science Foundation (General Ecology Program) for the continued financial support that has made these efforts possible.

5 References

Baker, R. and H. Genoways. 1978. Zoogeography of Antillean Bats. Pp. 53–97 in: F. B. Gill, ed., *Zoogeography in the Caribbean*, Spec. Pub. No. 13, Academy of Natural Sciences, Philadelphia.

Beets, D. J. and Mac Gillavry, H. J. 1977. Outline of the Cretaceous and Early Tertiary history of Curacao, Bonaire, and Aruba. Pp. 1-6 in *Guide to Geological Excursions on Curacao, Bonaire, and Aruba*, STINAPA Documentation Series No. 2, Caribbean Marine Biological Institute, Curacao (Also published as GUA Papers of Geology, Ser. 1, No. 10; Stichting GUA, Geologisch Institut, Amsterdam).

Beets, D. J., Maresch, W. V., Klaver, G. T., Mottana, A., Bocchio, R., Beunk, F. F. and Monen, H. P. 1984. Magmatic rock series and high-pressure metamorphism as constraints on the tectonic history of the southern Caribbean. *Geological Society of America Memoir*. 162:95-130.

Biju-Duval, B., Mascle, A., Montadert, L. and Wanneson, J., 1978. Seismic investigations in the Columbia, Venezuela and Grenada basins, and on the Barbados Ridge for future IPOD drilling. *Geologie en Mijnbouw* 57:105-116.

Bohlen, C. 1983. Competition for space in the anoles of the island of St. Maarten (Neth. Antilles). Unpublished Master's thesis, Stanford University, Stanford, California.

Bourgois, J., J Toussaint, H. Gonzalez, J. Azema, B. Calle, A. Desmet, L. Murcia, A. Acevedo, E. Parra, and J. Tournon. 1987. Geological history of the Cretaceous ophiolitic complexes of Northwestern South America (Columbian Andes). Tectonophysics 143:307–327.

Bouysse, P. 1979. Caracteres morphostructuraux et evolution geodynamique de l'arc insulaire des Petites Antilles. *Bureau de Recherches Géologiques et Miniéres Bulletin* Section IV, 3/4:185-210.

Bouysse, P. 1984. The Lesser Antilles island arc: Structure and geodynamic evolution. *Initial Reports, Deep Sea Drilling Project* (United States Government Printing Office) 78A:83-103.

Bouysse, P., Andreieff, P. and Westercamp, D. 1980. Evolution of the Lesser Antilles island arc, new data from the submarine geology. *Transactions of the 9th. Caribbean Geological Conference* (Santo Domingo, August 1980) pp.75-88.

Bouysse, P., Andreieff, P., Richard, M., Baubron, J., Mascle, A., Maury, R. and Westercamp, D. 1985. Geologie de la Ride d'Aves et des pentes sous-marines du nort des Petites Antilles et esquisse bathymetrique a 1/1.000.000 de l'Est-Caraibe. *Documents du Bureau de Recherches Géologiques et Miniéres*93.

Bouysse, P., Schmidt-Effing, R. and Westercamp, D. 1983. La Desirade island (Lesser Antilles) revisited: Lower Cretaceous radiolarian cherts and arguments against an ophiolitic origin for the basal complex. *Geology* 11:244-247.

Briggs, J. C. 1984. Freshwater fishes and biogeography of Central America and the Antilles. *Syst. Zool.* 33:428–435.

Brown, F. M. 1978. The origins of the West Indian butterfly fauna. Pp. 5–30 in: F. B. Gill, ed., *Zoogeography in the Caribbean*, Spec. Pub. No. 13, Academy of Natural Sciences, Philadelphia.

Bucher, W. H. 1952. Geological structure and orogenic history of Venezuela. *Geological Society of America Memoir* 49.

Burke, K. 1988. Tectonic evolution of the Caribbean. Ann. Rev. Earth Planet. Sci. 16:201–230.

Burke, K., P. J. Fox, A. Şengör, 1978. Buoyant ocean floor and the evolution of the Caribbean. J. Geophys. Res. 83:3949–3954.

Bussing, W. A. 1976. Geographic distribution of the San Juan ichthyofauna of Central America with remarks on its origin and ecology. In: E. B. Thorson (ed.) Investigations of the Ichthyofauna of Nicaraguan Lakes. Univ. Nebraska (10): 157.

Cope, E. D. 1883. On the contents of a bone cave in the island of Anguilla (West Indies). Smithson. Cont. Knowl. 489:1–30.

Diebold, J. B., Stoffa, P. L., Buhl, P. and Truchan, M. 1981. Venezuela Basin Crustal Structure. *Journal of Geophysical Research* 86:7901-7923.

Donnelly, T. W. 1985. Mesozoic and Cenozoic plate evolution of the Caribbean region. Pp. 89-121 in: F. G. Stehli and S. D. Webb (eds.) *The Great American Biotic Interchange*, Plenum Press, New York.

Dorel, J. 1981. Seismicity and seismic gaps in the Lesser Antilles arc and earthquake hazards in Guadeloupe. *Geophysical Journal of the Royal Astronomical Society* 67:679-696.

Duellman, W. E. 1966. The Central American herpetofauna: an ecology perspective. Copeia 1966:700-719.

Duellman, W. E. 1979. The South American herpetofauna: a panoramic view. Mus. Nat. Hist. Univ. Kansas. Monogr. 7:1-28.

Duncan, R. and R. Hargraves. 1984. Plate tectonic evolution of the Caribbean region in the mantle reference frame. Geol. Soc. of America, Memoir 162:81–93.

Durham, J. W. 1985. Movement of the Caribbean plate and its importance for biogeography in the Caribbean. *Geology* 13:123–125.

Eickwort, G. C 1988. Distribution patterns and biology of West Indian sweat bees. Pp. 231–253 in: J. K. Liebherr, ed., *Zoogeography of Caribbean Insects*, Comstock Publishing Associates, Cornell University Press, Ithaca, New York.

Estes, R. 1983. The fossil record and early distribution of lizards. Pp. 365-398 in: A. G. J. Rhodin and K. Miyata (eds.) *Advances in Herpetology and Evolutionary Biology*, Museum of Comparative Zoology, Harvard University, Cambridge, Mass.

Ferrusquia-Villafranca, I. 1978. Distribution of Cenozoic vertebrate faunas in Middle and North America and problems of migration between North and South America. Inst. Geol. Univ. Auto. Mexico. Biol. 101:193-321.

Fink, L. K. Jr. 1972. Bathymetric and geologic studies of the Guadeloupe region, Lesser Antilles island arc. *Marine Geology* 12:267-288.

Ghosh, N., Hall, S. A., and Casey, J. F. 1984. Seafloor spreading magnetic anomalies in the Venezuelan Basin. *Geological Society of America Memoir* 162:65-80.

Gibbons, J. R. H. 1985. The biogeography and evolution of Pacific island reptiles and amphibians. Pp. 125–142 in: G. Grigg, R. Shine, and H. Ehmann, eds., *Biology of Australasian Frogs and Reptiles*. Royal Zoological Society of New South Wales.

Gorman, G. C. 1973. The chromosomes of the Reptilia, a cytotaxonomic interpretation. Pp. 349-421 in A. Chiarelli and E. Capanna (eds.) Cytotaxonomy and Vertebrate Evolution. Academic Press, London.

Gorman, G. C. and L. Atkins. 1969. The zoogeography of Lesser Antillean *Anolis* lizards – an analysis based upon chromosomes and lactic dehydrogenases. Bull. Mus. Comp. Zool. 138:53-80.

Gorman, G. C., D. G. Buth, M. Soule, and S. Y. Yang. 1983. The relationships of the Puerto Rican *Anolis*: electrophoretic and karyotypic studies. Pp. 626- 642 in: A. G. J. Rhodin and K. Miyata (eds.) Advances in Herpetology and Evolutionary Biology, Museum of Comparative Zoology, Cambridge, Mass.

Gorman, G. C., D. G. Buth, and J. S. Wyles, 1980. *Anolis* lizards of the eastern Caribbean: a case study in evolution. III. A cladistic analysis of albumin immunological data, and the definition of species groups. Syst. Zool. 29:143-158.

Gorman, G. C., and Y. J. Kim. 1976. *Anolis* lizards of the eastern Caribbean: a case study in evolution. II. Genetic relationships and genetic variation of the *bimaculatus* group. Syst. Zool. 25:62-77.

Gorman, G. C., C. S. Lieb. and R. H. Harwood. 1984. The relationships of *Anolis gadovi*: albumin immunological evidence. Carib. J. Sci. 20:145-152.

Graham, J. B. 1975. The biological investigations of Malpelo Island, Columbia. Smithsonian Contributions to Zoology 176:1–98.

Guyer, C. and J. Savage. 1986. Cladistic relationships among anoles (Sauria: Iguanidae). Systematic Zoology 35:509-531.

Heatwole, H. and F. MacKenzie. 1967. Herpetogeography of Puerto Rico. IV. Paleogeography, faunal similarity, and endimism. Evolution 21:429–438.

Howard, R. A. 1973. The vegetation of the Antilles. Pp. 1–38 in: A. Graham, ed., *Vegetation and Vegetational History of Northern Latin America*. Elsevier Scientific Publishing Co., Amsterdam.

Lazell, J. D. Jr. 1965. An *Anolis* (Sauria, Iguanidae) in amber. J. Paleontology 39:379-382

Lazell, J. D. Jr. 1972. The Anoles (Sauria, Iguanidae) of the Lesser Antilles. Bull. Mus. Comp. Zool. 143:1-115.

Lazell, J. D. Jr. 1983. Biogeography of the herpetofauna of the British Virgin Islands, with description of a new anole (Sauria: Iguanidae). Pp. 99-117 in: A. G. J. Rhodin and K. Miyata (eds.) Advances in Herpetology and Evolutionary Biology, Museum of Comparative Zoology, Cambridge, Mass.

Lebras, M., F. Mégard, C. Dupuy, and J. Dostal. 1987. Geochemistry and tectonic setting of pre-collision Cretaceous and Paleogene volcanic rocks of Ecuador. Geol. Soc. of Amer. Bull 99:569–578.

Licht, P. 1974. Response of *Anolis* lizards to food supplementation in nature. Copeia 1974:215-221.

Lieb, C. S. 1981. Biochemical and karyological systematics of the Mexican lizards of the *Anolis gadovi* and *A. nebulosus* species groups. Ph. D. Thesis, Department of Biology, University of California–Los Angeles, (University Microfilms, Ann Arbor, Michigan. No. 8113869).

Liebherr, J. K. 1988. Biogeographic patterns of West Indian *Platynus* Carabid beetles (Coleoptera). Pp. 121–152 in: J. K. Liebherr, ed., *Zoogeography of Caribbean Insects*, Comstock Publishing Associates, Cornell University Press, Ithaca, New York.

Lister, B. 1976. The nature of niche expansion in West Indian *Anolis* lizards. II. Evolutionary components. Evolution 30:677-692.

MacArthur, R. H. and R. Levins. 1967. The limiting similarity, convergence and divergence of coexisting species. Amer. Natur. 101:377-385.

Mann, P. and Burke, K. 1984. Neotectonics of the Caribbean. *Reviews of Geophysics and Space Physics* 22:309-362.

Mann, P. and K. Burke. 1984. Neotectonics of the Caribbean. Rev. Geophys. Space Phys. 22:309-362.

Maresch, W. V. 1974. Plate tectonics origin of the Caribbean mountain system of Northern South America: Discussion and proposal. *Geological Society of America Bulletin* 85:669-682.

Marshall, L. G., R. f. Butler, R. E. Drake, G. H. Curtis, and R. H. Tedford. 1979. Calibration of the Great American Interchange. Science 204:272-279.

Maxson, L. R. and A. C. Wilson. 1975. Albumin evolution and organismal evolution in tree frogs (Hylidae). Syst. Zool. 24:1-15.

Metcalf, Z. P. 1947. The center of origin theory. Elisha Micthel Sci. Soc. J. 62:149–175.

Nichols, S. W. 1988. Kaleidoscopic biogeography of West Indian Scaritinae (Coleoptera: Carabidae). Pp. 71–120 in: J. K. Liebherr, ed., *Zoogeography of Caribbean Insects*, Comstock Publishing Associates, Cornell University Press, Ithaca, New York.

Olson, S. L. 1978. A paleontological perspective of West Indian birds and mammals. Pp. 99–117 in: F. B. Gill, ed., *Zoogeography in the Caribbean*, Spec. Pub. No. 13, Academy of Natural Sciences, Philadelphia.

Pacala, S. W. and J. D. Roughgarden. 1984. Control of arthropod abundance by *Anolis* lizards on St. Eustatius (Neth. Antilles). Oecologia 64:160-162.

Pacala, S. W. and J. D. Roughgarden. 1985. Population experiments with the *Anolis* lizards of St. Maarten and St. Eustatius. Ecology 66:129-141.

Paull, D., E. E. Williams, and W. P. Hall. 1976. Lizard karyotypes from the Galapagos islands: chromosomes in phylogeny and evolution. Breviora 441:1-31.

Perfit, M. R. and E. E. Williams. 1989. Geological constraints and biological retrodictions in the evolution of the Caribbean sea and its islands. Pp. 47–102 in: C. A. Woods, ed., *Biogeography of the West Indies*. Sandhill Crane Press.

Pindell, J. and Dewey, J. F. 1982. Permo-Triassic reconstruction of western Pangea and the evolution of the Gulf of Mexico/Caribbean region. *Tectonics* 1:179-211.

Poinar, G. O. Jr. and D. C. Cannatella. 1987. An upper Eocene frog from the Dominican Republic and its implications for Caribbean Biogeography. Science 237:1215-1216.

Ramos, J. A. 1988. Zoogeography of the Auchenorrhynchous Homoptera of the Greater Antilles (Hemiptera). Pp 61–70 in: J. K. Liebherr, ed., *Zoogeography of Caribbean Insects*, Comstock Publishing Associates, Cornell University Press, Ithaca, New York.

Richardson, P. L., and D. Walsh. 1986. Mapping climatological seasonal variations of surface currents in the tropical Atlantic using ship drifts. J. Geophys. Res. 91:10537-10550.

Rieppel, O. 1980. Green anole in Dominican amber. *Nature* 286:486-487.

Roughgarden J. and S. W. Pacala. 1989. Taxon cycle among *Anolis* lizard populations: Review of evidence. Pp. 403–432 in: D. Otte and J. Endler, eds., *Speciation and its Consequences*, Sinauer Associates, Sunderland Mass.

Roughgarden, J. D., S. W. Pacala, and J. D. Rummel. 1984. Strong present-day competition between the *Anolis* lizard populations of St. Maarten (Neth. Antilles). Pp. 203-220 in: B. Shorrocks (ed.) Evolutionary Ecology. Blackwell Scientific Publications, London

Roughgarden, J., S. Gaines, and S. Pacala. 1987. Supply-side ecology: the role of physical transport processes. In: P. Giller and J. Gee (eds.), Organization of Communities: Past and Present. Blackwell Scientific Publications. Pp. 459-486.

Rummel, J. D. and J. D. Roughgarden. 1985. Effects of reduced perch-height separation on competition between two *Anolis* lizards. Ecology 66:430-444.

Savage, J. M. 1966. The origins and history of the Central American herpetofauna. Copeia 1966:719-766.

Savage, J. M. 1974. The Isthmian Link and the evolution of neotropical mammals. Los Angeles County Mus. Contr. Sci. 160:1-51.

Savage, J. M. 1982. The enigma of the Central American herpetofauna: dispersals or vicariance? Ann. Missouri Bot. Gard. 69:464-547.

Schoener, T. W. and A. Schoener. 1983a. The time to extinction of a colonizing propagule of lizards increases with island area. Nature 302:332-334.

Schoener, T. W. and A. Schoener. 1983b. Distribution of vertebrates on some very small islands. II. Patterns in species counts. J. Anim. Ecol. 52:237-262.

Schoener, T. and D. Spiller. 1987. Effect of lizards on spider populations: manipulative reconstruction of a natural experiment. Science 236:949-952.

Schwartz, A. 1978. Some aspects of the herpetogeography of the West Indies. Pp. 31–51 in: F. B. Gill, ed., *Zoogeography in the Caribbean*, Spec. Pub. No. 13, Academy of Natural Sciences, Philadelphia.

Schwartz, A. and R. Thomas. 1975. A check-list of West Indian amphibians and reptiles. Carnegie Mus. Nat. Hist. Spec. Publ. 1:1-216.

Schwartz, A. and R. W. Henderson. 1985. A Guide to the Identification of the Amphibians and Reptiles of the West Indies exclusive of Hispaniola. Milwaukee Public Museum.

Shochat, D. and H. C. Dessauer. 1981. Comparative immunological study of albumins of *Anolis* lizards of the Caribbean islands. Comp. Biochem. Physiol. 68A:67-73.

Singer, C. 1931. *A Short History of Biology.* Oxford Clarendon Press.

Slater, J. A. 1988. Zoogeography of West Indian Lygaeidae (Hemiptera) Pp. 38–60 in: J. K. Liebherr, ed., *Zoogeography of Caribbean Insects*, Comstock Publishing Associates, Cornell University Press, Ithaca, New York.

Speed, R. C. 1985. Cenozoic collision of the Lesser Antilles arc and continental South America and the origin of the El Pilar Fault. *Tectonics* 4:41-69.

Speed, R. C., Gerhard, L. C. and McKee, E. H. 1979. Ages of deposition, deformation, and intrusion of Cretaceous rocks, eastern St. Croix, Virgin Islands. *Geological Society of America Bulletin* I, 90:629-632.

Stamps, J. A. 1977. Rainfall, moisture, and dry season growth rates in *Anolis aeneus*. Copeia 1977:415-419.

Stehli, F. G. and S. D. Webb. 1985a. eds., *The Great American Biotic Interchange.* Plenum Press, New York.

Stehli, F. G. and S. D. Webb. 1985b. A kaleidoscipe of plates, faunal and floral dispersals, and sea level changes. Pp. 3–16 in: Stehli, F. G. and S. D. Webb. 1985a. eds., *The Great American Biotic Interchange.* Plenum Press, New York.

Stein, S., Engeln, J., Wiens, D., Fujita, K. and Speed, R. 1982. Subduction seismicity and tectonics in the Lesser Antilles arc. *Journal of Geophysical Research* 87(B10):8642-8664.

Tomblin, J. F. 1975. The Lesser Antilles and the Aves Ridge. Pp. 467-500 in: Nairn, A. E. M. and Stehli, F. G. (eds.) *The Ocean Basins and Margins.* Vol. 3. The Gulf of Mexico and the Caribbean, Plenum Press, New York.

Underwood, G. 1959. Revisionary Notes. The anoles of the Eastern Caribbean (Sauria, Iguanidae). Part III. Bull. Mus. Comp. Zool. 121:191-226.

Vierbuchen, R. C. Jr. 1979. *The tectonics of north-eastern Venezuela and the southeastern Caribbean Sea.* Ph. D. thesis. 193 pp. Princeton University. Princeton N. J.

Westercamp, D., Andreieff, P., Bouysse, P., Mascle, A. and Baubron, J. 1985. Geologie de l'archipel des Grenadines (Petites Antilles meridionales). *Documents du Bureau de Recherches Géologiques et Miniéres* 92.

Williams, E. E. 1977. Anoles out of place: introduced anoles. Pp 110-118 in E. E. Williams (ed.) The Third *Anolis* Newsletter. Harvard University.

Wilson, A. C., S. S. Carlson, and T. J. White, 1977. Biochemical evolution. Ann. Rev. Biochem. 46:573-639.

Wilson, A. C., and V. M. Sarich. 1969. A molecular time scale for human evolution. Proc. Nat. Acad. Sci. (USA) 63:1088-1093.

Wingate, D. 1965. Terrestrial herpetofauna of Bermuda. Herpetologica 21:202- 218.

Wright, J. W. 1984. The origin and evolution of the lizards of the Galapagos Islands. TERRA March/April 1984:21–27.

Yang, S. Y., M. Soule, and G. C. Gorman. 1974. *Anolis* lizards of the eastern Caribbean: a case study in evolution. I. Genetic relationships, phylogeny, and colonization sequence of the *roquet* group. Syst. Zool. 23:387-399.

6 Notes on Phylogeny

0. Primitive anole karyotype = 12:24:0 (12 macrochromosomes, 24 microchromosomes, 0 sex chromosomes).

1. Twig Anoles. Primitive karyotype, short prehensile tail, reduced lateral exposure of coronoid bone, AID(*evermanni* → *occultus*) = 49, AID(*extremus* → *occultus*) = 51.

2. Giant Anoles. Primitive karyotype, AID(*evermanni* → *cuvieri*) = 45, AID(*extremus* → *cuvieri*) = 53, *A. rooseveltii* is recently extincto n Culebra.

3. Central Caribbean Complex. Derived karyotype: 14 or more macrochromosomes and sex chromosomes, AID(*evermanni* → *extremus*) = 59, AID (*cristatellus* → *extremus*) = 54, AID(*bimaculatus* → *extremus*) = 59, AID (*wattsi* → *extremus*) = 54.

4. Cristatellus Group. AID(*evermanni* → *cristatellus*) = 16, AID (*evermanni* → *bimaculatus*) = 33, AID(*cristatellus* → *bimaculatus*) = 41.

5. Acutus Series. Karyotype is 14 macrochromosomes but other aspects of the karyotype differ among members of this series: *evermanni* = 14:10:2, *acutus* = 14:10:3, *stratulus* 14:12:3, AID's within the group to *evermanni* = 13-14. The Jamaican anoles also have 14 macrochromosomes; their AID's to *evermanni* = 27- 30, to *cristatellus* = 34-41, and to *bimaculatus* = 42-44. Thus the Jamaican anoles appear to be a clade of the Acutus Series. *A. acutus* is on St. Croix.

6. Cristatellus Series. Each has 16 macrochromosomes, 8 to 10 microchromosomes, and 3 sex chromosomes. AID's within group to *cristatellus* = 11-13, Karyotypic, albumin and electrophoretic data corroborate a division into a gundlachi line and a cristatellus line.

7. Grass Anoles.

8. Trunk-ground Anoles. Karyotype = 16:10:3, Western Puerto Rico.

9. Trunk-ground Anoles. Karyotype = 16:8:3, Eastern Puerto Rico.

10. Bimaculatus Group. Karyotype = 18:8:3, except *oculatus* of Dominica = 20:8:3. AID's within group to *bimaculatus* = 10-12.

11. Wattsi Series. Small and brown with ventral scales strongly keeled. Division into wattsi series and bimaculatus series corroborated by electrophoretic data.

12. Genetic distance between *wattsi pogus* and other *wattsi* populations is greater than the distance between *w. schwartzi* and *w. wattsi*.

13. Bimaculatus Series. Large or solitary sized, often colorful, usually with green or grey-green tones. Division into northern and southern lines according to squamation and electrophoretic data.

14. Northern Bimaculatus Line. Ventral scales smooth. Two sublines: the large anoles – *A. bimaculatus bimaculatus* and *A. b. leachi*, frequently in upper canopy, and have large nuchal crests; medium-sized anoles *A. sabanus*, *A. gingivinus*, and *A. nubilus*, females with white lateral flank stripes, all three are electrophoretically closer to each other than are the two large anoles to each other.

15. Southern Bimaculatus Line. Ventral scales faintly keeled in at least some individuals. In spite of extensive differentiation in appearance as recognized by the subspecific nomenclature, electrophoretic distances among these taxa are slight. *A. lividus* from Montserrat and *A. marmoratus* of Guadeloupe are closest electrophoretically, *A. oculatus* of Dominica has karyotype = 20:8:3, and faintly keeled scales. *A. lividus* has the strongest keeling in the line, approaching, in some individuals, that of the wattsi series. The individuals from eastern half of Guadeloupe (Grande Terre) have smooth ventrals, and those from the western half (Basse Terre) are faintly keeled. *A. m. terraealtae* of the Ille des Saintes has smooth scales and some females have white lateral flank stripes. *A. m. alliaceus* from forests on Basse Terre in Guadeloupe is similar in appearance to *A. bimaculatus* and was considered a subspecies of *A. bimaculatus* by Underwood (1959) until

more extensive collections showed it to be conspecific with all the other anoles on Guadeloupe.

16. Roquet Group. Primitive karyotype, AID's to other lineages > 50, derived squamation on snout. Electrophoretic and albumin distances corroborate division into luciae and roquet series. AID's within roquet series to *extremus* = 0-14, and within luciae series to *extremus* = 26-35.

17. Roquet Series. Four unresolved lines according to electrophoretic and albumin distance data. *A. griseus* and *A. richardi* are large while *A. trinatatis* and the roquet line are medium-sized.

18. Roquet Line. Derived karyotype = 12:22:0. Electrophoretic and albumin data corroborate that *extremus* is nearly identical to *roquet*. *A. aeneus* shows extensive clinal variation in appearance but subspecies were not named.

19. Luciae Series. Electrophoretic and albumin data corroborate the relative closeness of *blanquillanus* to *bonairensis*.

20. Lineatus Series. *A. lineatus* has derived transverse processes on autotomic caudal vertebrae as do the anoles of Jamaica. AID(*lineatus* → *evermanni*) = 33, AID(*lineatus* → *cristatellus*) = 34, AID(*lineatus* → *valencienni* of Jamaica) = 22.

7 Notes on Biogeography

A. *Bufo marinus*. Large toad tolerant of brackish conditions; also in Greater Antilles except Cuba (where two large species of *Bufo* are endemic) and Central and South America.

B. *Hyla rubra*. Also Central and South America.

C. *Leptodactylus fallax*. Endemic in Lesser Antilles, recently extinct on St. Kitts, Guadeloupe, and St. Lucia.

D. *Leptodactylus wagneri*. Also South America.

E. *Eleutherodactylus johnstoni*. Endemic in Lesser Antilles.

F. *Eleutherodactylus martinicensis*. Endemic in Lesser Antilles, also on La Desirade, and Ille des Saintes.

G. *Eleutherodactylus barlagnei*. Endemic to Guadeloupe, 600-2100 ft. elevation on Basse Terre.

H. *Eleutherodactylus pinchoni*. Endemic to Guadeloupe, 600-2200 ft. elevation on Basse-Terre.

I. *Eleutherodactylus urichi schrevei*. Subspecies endemic to St. Vincent, *E. u. urichi* in Trinidad and Venezuela.

J. *Eleutherodactylus urichi euphronides*. Subspecies endemic to Grenada.

K. *Mabuya mabouya mabouya*. Also in Trinidad, Tobago, and South America.

L. *Diploglossus montisserrati*. Endemic to Montserrat. Genus occurs on Greater Antilles except Jamaica.

M. *Ameiva corvina*. Endemic to Sombrero.

N. *Ameiva pleei*. Endemic to Anguilla Bank.

O. *Ameiva erythrocephala*. Endemic to St. Kitts Bank.

P. *Ameiva griswoldi*. Endemic to Antigua Bank.

Q. *Ameiva pluvianotata*. Endemic to Lesser Antilles with distinct subspecies on Montserrat and Redonda.

R. *Ameiva cineracea*. Endemic to Guadeloupe, known only from Grand Ilet, off east coast of Basse-Terre, now extinct.

S. *Ameiva fuscata*. Endemic to Dominica. A specimen named "*A. major*" collected in 1839 may represent an extinct population from Martinique.

T. *Ameiva ameiva tobagana*. Subspecies endemic to St. Vincent and Grenada Bank, nominate subspecies occurs in Surinam.

U. *Cnemidophorus vanzoi*. Endemic to Maria Islands off St. Lucia.

V. *Bachia heteropus alleni*. Endemic subspecies to Grenada Bank, other subspecies on Trinidad and Venezuela.

W. *Kentropyx copei*. Endemic to Barbados, only Antillean representative of a genus widespread in South America.

X. *Gymnophthalmus underwoodi*. Also found in Surinam.

Y. *Gymnophthalmus pleei pleei*. Endemic subspecies to Martinique.

Z. *Gymnophthalmus pleei*. Distinct subspecies endemic to St. Lucia and to the Maria Islands off St. Lucia, species endemic to Martinique and St. Lucia.

1. *Thecadactylus rapicauda*. Also in Trinidad, Tobago, South and Central America, not in Greater Antilles, monotypic genus.

2. *Hemidactylus mabouia*. Also in Africa, Madagascar, Eastern South America, Trinidad and Tobago, Greater Antilles and Virgin Islands except Jamaica.

3. *Hemidactylus palaichthus*. On Maria Islands off St. Lucia, also in South and Central America, and Trinidad and Tobago.

4. *Phyllodactylus pulcher*. Endemic to Barbados.

5. *Sphaerodactylus sputator*. Endemic to Anguilla Bank and St. Kitts Bank.

6. *Sphaerodactylus macrolepis parvus*. Subspecies endemic to Anguilla Bank, other subspecies on Puerto Rico Bank.

7. *Sphaerodactylus sabanus*. Endemic to Saba and St. Kitts Bank.

8. *Sphaerodactylus elegantulus*. Endemic to Antigua Bank.

9. *Sphaerodactylus fantasticus*. Nine subspecies in total, two on Basse-Terre and two on Grand Terre in Guadeloupe, and one apiece on Ille des Saintes, Marie Galante, La Desirade, Montserrat, and Dominica.

a. *Sphaerodactylus vincenti*. Nine subspecies in total, seven on Martinique, and one apiece on St. Vincent and St. Lucia.

b. *Sphaerodactylus microlepis*. Endemic to St. Lucia, with distinct subspecies on St. Lucia and the Maria Islands off St. Lucia.

c. *Iguana delicatissima*. Endemic to Lesser Antilles, including Grande Terre in Guadeloupe, La Desirade, and Terre-de-Bas and Terre-de-Haute in the Illes des Saintes.

d. *Iguana iguana*. Also South America, also Lesser Antilles and Virgin Islands including Basse-Terre in Guadeloupe; La Coche, Grand Ilet, Terre-de-Haute, and Ilet a Cabrit in the Illes des Saintes; and the Maria Islands off St. Lucia.

e. *Anolis gingivinus*. Endemic to Anguilla Bank.

f. *Anolis wattsi pogus*. Subspecies endemic to Anguilla Bank.

g. *Anolis sabanus*. Endemic to Saba.

h. *Anolis bimaculatus bimaculatus*. Subspecies endemic to St. Kitts Bank, species endemic to Lesser Antilles.

i. *Anolis wattsi schwartzi*. Subspecies endemic to St. Kitts Bank.

j. *Anolis bimaculatus leachi*. Subspecies endemic to Antigua Bank.

k. *Anolis wattsi*. Species endemic to Lesser Antilles, distinct subspecies on Barbuda and Antigua.

l. *Anolis lividus*. Endemic to Montserrat.

m. *Anolis marmoratus*. Twelve subspecies total, two on Grand Terre and four on Basse-Terre in Guadeloupe, two in the Illes des Saintes, and one apiece on Ilet-a-Kohouanne, La Desirade, Les Iles de la Petite Terre, and Marie Galante.

n. *Anolis oculatus*. Endemic to Dominica with four subspecies.

o. *Anolis roquet*. Endemic to Martinique with six subspecies.

p. *Anolis luciae*. Endemic to St. Lucia.

q. *Anolis griseus*. Endemic to St. Vincent.

r. *Anolis trinatatis.* Endemic to St. Vincent.

s. *Anolis richardi.* Endemic to Grenada Bank.

t. *Anolis aeneus.* Endemic to Grenada Bank.

u. *Anolis extremus.* Endemic to Barbados.

v. *Typhlops monastus geotomus.* Subspecies endemic to Antigua and St. Kitts Banks.

w. *Typhlops monastus monastus.* Species endemic to Lesser Antilles, subspecies endemic to Montserrat.

x. *Typhlops dominicana guadeloupensis.* Subspecies endemic to Guadeloupe, known only from Grande-Terre.

y. *Typhlops dominicana dominicana.* Species endemic to Lesser Antilles, subspecies endemic to Dominica.

z. *Typhlops tasymicris.* Endemic to Grenada Bank, presumed close to South American forms.

aa. *Leptotyphlops bilineata.* Endemic to Lesser Antilles.

bb. *Bothrops lanceolata.* Endemic to Martinique, genus widespread in South America.

cc. *Bothrops caribbaea.* Endemic to St. Lucia, presumed close to *B. atrox* of South America.

dd. *Boa constrictor nebulosa.* Subspecies endemic to Dominica.

ee. *Boa constrictor crophias.* Subspecies endemic to St. Lucia.

ff. *Corallus enydris cooki.* Also South America, nominate subspecies in Amazonian region.

gg. *Alsophis rijersmai.* Endemic to Anguilla Bank.

hh. *Alsophis rufiventris.* Endemic to Saba and St. Kitts Bank.

ii. *Alsophis antillensis.* Five subspecies total, one apiece on the Antigua Bank, Montserrat, Guadeloupe & Marie Galante, Ille des Saintes, and Dominica.

jj. *Liophus juliae.* Three subspecies total, one apiece on Guadeloupe, Marie Galante, and Dominica.

kk. *Liophus cursor.* Endemic to Martinique.

ll. *Liophus ornatus.* Endemic to St. Lucia, collected on Maria Islands off St. Lucia.

mm. *Liophus melanotus.* Also Trinidad, Tobago, and South America.

nn. *Liophus perfuscus.* Endemic to Barbados.

oo. *Chironius vincenti.* Endemic to St. Vincent, a similar form, *C. carinatus* occurs in South and Central America, and Trinidad.

pp. *Clelia clelia.* Also South and Central America.

qq. *Mastigodryas bruesi.* Endemic to St. Vincent and Grenada Bank, genus in South America.

rr. *Pseudoboa neuwiedi.* Also in South and Central America.

MORPHOLOGY AND DEVELOPMENT OF MODERN CARBONATE FORESLOPES, TONGUE OF THE OCEAN, BAHAMAS

G. M. Grammer, R. N. Ginsburg, and D. F. McNeill
Comparative Sedimentology Laboratory
University of Miami/RSMAS
Fisher Island Station
Miami Beach, Florida

ABSTRACT

Using a small research submersible, we have found that the upper slopes surrounding the southern portion of the Tongue of the Ocean exhibit a distinctive morphology characterized by a near-vertical escarpment followed by steeply dipping hard rock slopes with declivities of 35-45^{0}. These slopes are believed to be modern counterparts to the clinoforms often observed in outcrop and seismic sections of fossil carbonate platforms.

Our observations indicate that the slopes formed by the synsedimentary amalgamation of localized, linear trains of sediment and talus derived from the marginal escarpment and not through the emplacement of large-scale mass flow deposits. Pervasive submarine cementation subsequently lithified the slope deposits resulting in the preservation of the steep slope angles. Distinct variations in the patterns of sediment accumulation along the foreslopes depending upon the windward or leeward orientation of the margin were also observed. These variations result from the increased sedimentation rates associated with open leeward margins.

INTRODUCTION

Carbonate foreslopes define an important transitional zone between shallow-water platform carbonates and deeper-water basinal and distal slope deposits. Because of its position adjacent to the margin, knowledge of the depositional and early diagenetic processes acting on the foreslope and how they influence overall slope morphology may provide valuable insight into the mechanisms by which carbonate platforms evolve. A review of the more recent literature on modern platform to basin transitions, however, indicates that with the exception of a very few studies utilizing research submersibles (e.g. Moore et al., 1976; James and Ginsburg, 1979), this part of the slope has been mostly overlooked.

Recent work in the southern portion (or cul-de-sac) of the Tongue of the Ocean has shown that the foreslopes on both windward and leeward margins are characterized by a consistent overall morphology. The profile is dominated by a near-vertical escarpment extending down from approximately 50 to 140 meters, followed by steeply dipping (35-45^{0}) hard-rock surfaces that may extend down to depths greater than 300 meters. These steeply dipping slopes are notable because of their similarity to the inclined beds or clinoforms (Rich, 1951) often observed in outcrop or seismic profiles of fossil platform margins (e.g. Sarg, 1988). The major emphasis of this study is to document the morphologic features characteristic of the foreslope and to discuss the mechanisms responsible for the development of the slope.

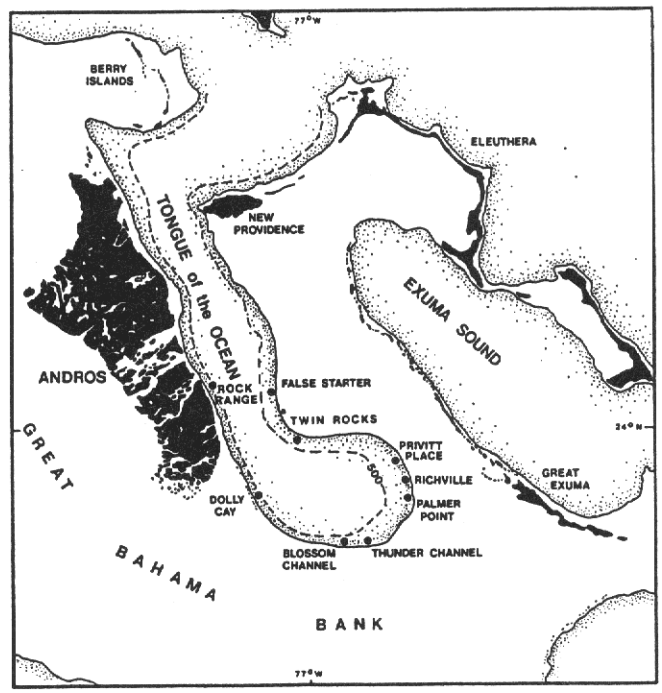

Figure 1. Map showing location of submersible dive sites in the Tongue of the Ocean, Bahamas. Depth in fathoms.

METHODS

A total of 94 dives with the research submersible DELTA were made at nine locations around the southern portion of the Tongue of the Ocean (Figure 1). Utilization of the DELTA enabled us to observe first hand the morphological features of the slopes, to document our observations via videotape and still photography, and to collect both sediment and rock samples from known locations along the slope. Slope profiles were constructed from a synthesis of initial dive observations combined with the evaluation of videotape documentation from all dives. Slope angles were measured using an inclinometer from inside the submersible.

Larue, D.K., and Draper, G. (eds.),
Transactions of the 12th Caribbean Geological Conference, St. Croix, U.S.V.I., Miami Geological Society, P.O. Box 431552, South Miami, FL 33243, U.S.A

Figure 2a-g. Profiles of upper slope from representative dive sites. Profiles were constructed from a synthesis of data accumulated during a total of 94 dives in the Tongue of the Ocean during 1987 and 1988. No vertical exaggeration.

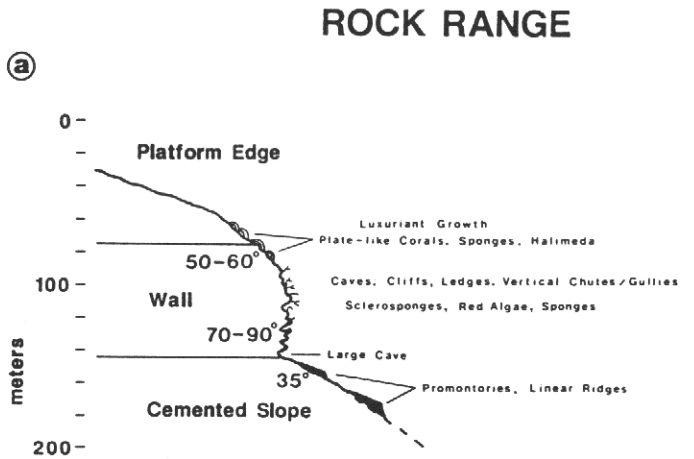

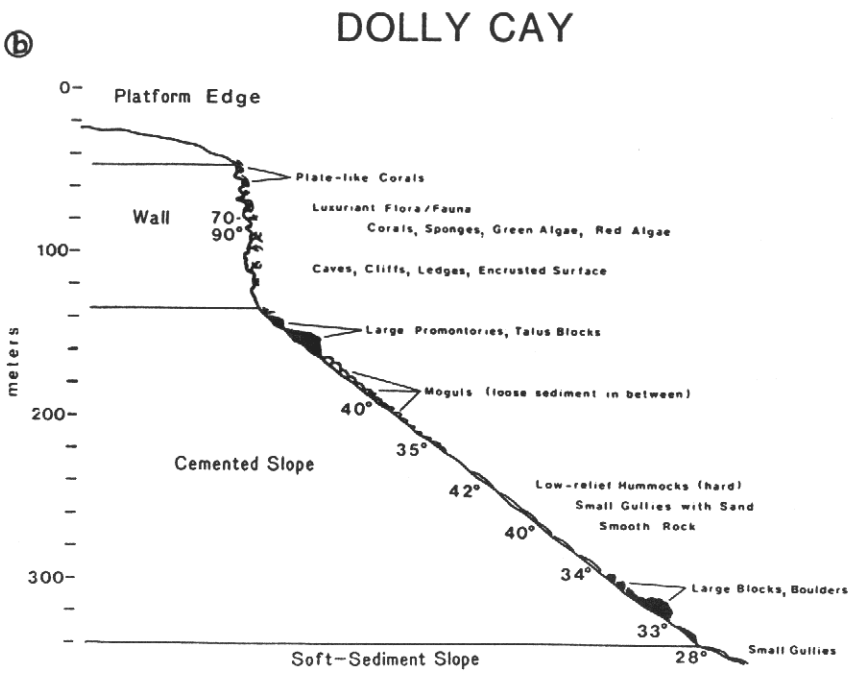

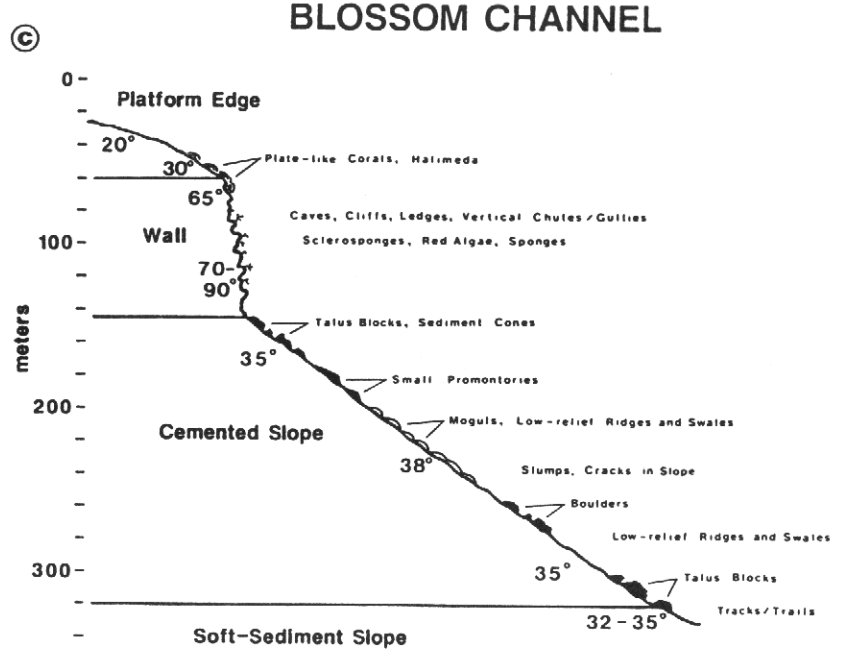

THUNDER CHANNEL

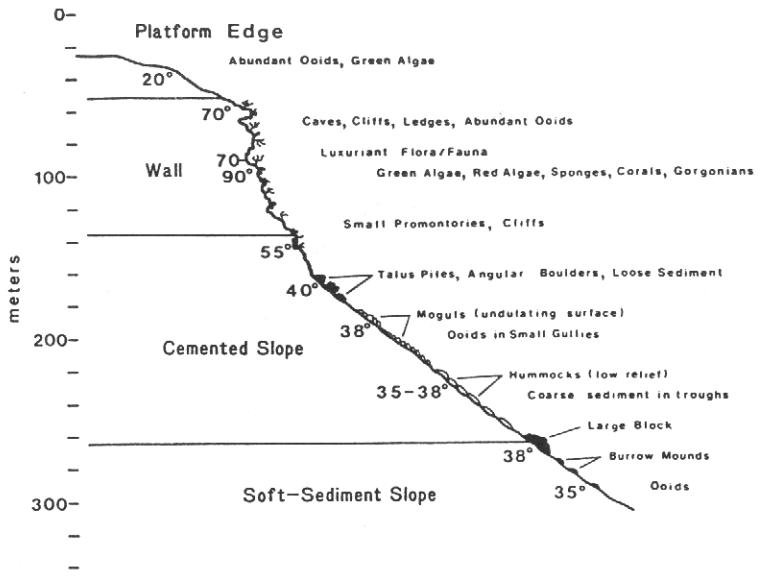

PALMER POINT

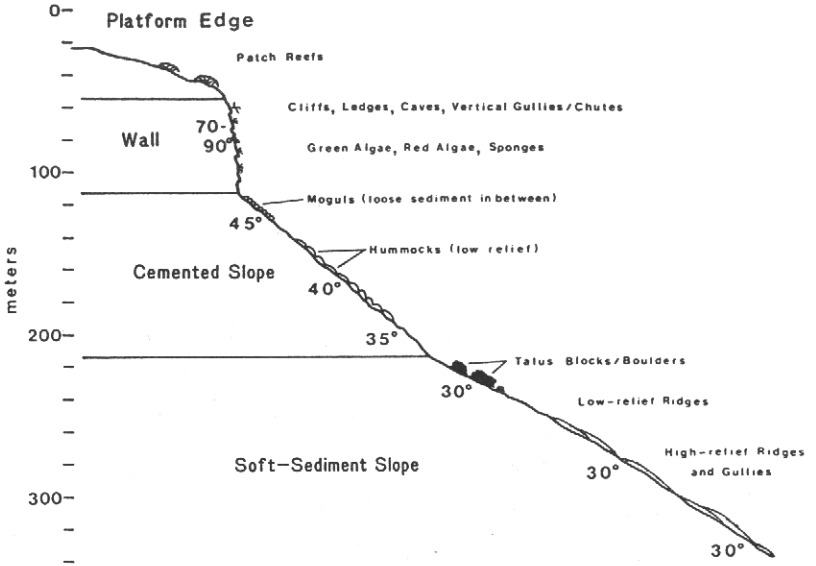

FALSE STARTER

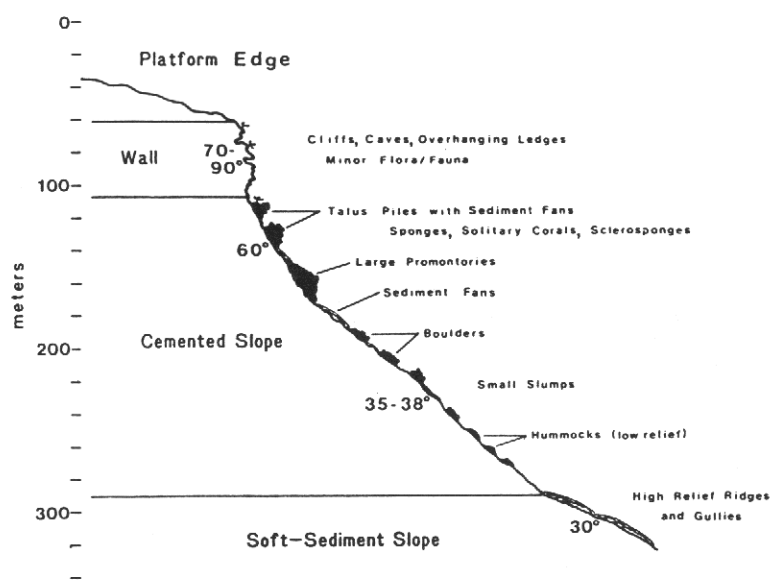

TWIN ROCKS

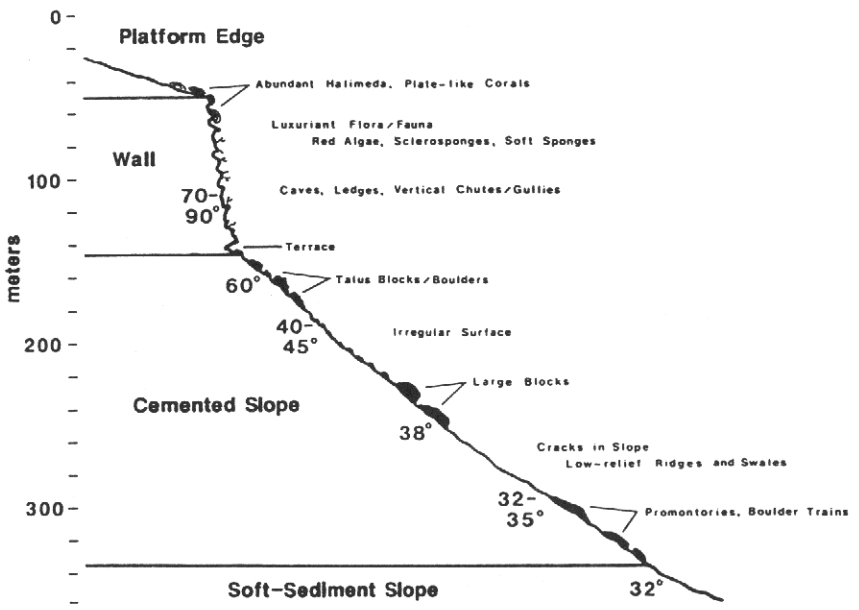

RESULTS AND INTERPRETATION

Morphology

Observations of the slopes around the Tongue of the Ocean indicate that the upper slope, or foreslope, is characterized by a distinctive morphology that may be subdivided into four zones (Figures 2a-g):

1. The platform edge, which consists of a Holocene sediment wedge, is situated in shallower water behind one or more areas of deep (40-60m) reef growth. These reefs, where present, are dissected by a series of sediment chutes that may extend to the edge of the platform. The sediment composition of the platform margin varies depending upon its windward or leeward positioning (see Figure 3).

2. The near-vertical wall, with slopes ranging from 70^{o} to 90^{o}, begins at water depths of 40-60 meters. This zone consists of variable types of deep-water corals, encrusting coralline algae, soft sponges, sclerosponges, and green algae. The surface of the wall is characterized by numerous small pits, caves, ledges, and vertical overhangs. Unconsolidated sediment derived both from the edge of the platform and the wall rests on all horizontal and sub-horizontal surfaces. Our observations suggest that the wall is capable of producing copious amounts of sediment, through both biological production (primarily Halimeda sp.) and bioerosion, which is subsequently transported further downslope.

The wall extends down to a depth of 135 to 145 meters except along the leeward margins where higher rates of sedimentation have effectively buried the lowermost portions. The base of the wall is commonly marked by near-horizontal ledges extending for tens of meters and flat-floored caves, suggesting that this may mark a previous lowstand of sea-level. The transition from the wall to the underlying cemented slope is often characterized by the presence of large talus blocks, some up to 30m high, that have apparently been derived through mass-wasting of the wall above.

3. The cemented slope is found at the base of the wall and is characterized by relatively consistent slope angles between 35^{o} and 45^{o}. The surface of the cemented slope often exhibits an irregular morphology of rounded to elliptical topographic highs (moguls) separated by trains of unconsolidated sediment in the adjacent troughs. Near the base of the wall, the moguls are mostly rounded and range in height from a few decimeters to over a meter. Downslope, the moguls are progressively more elongate.

In some areas, large promontories that are a few meters in height and up to several meters or tens of meters long project outward from the slope. These promontories may have been formed by the repeated deposition and subsequent cementation of numerous generations of sediment piled-up behind talus blocks.

The cemented slope is notable for its well-lithified surface, internal bedding, and steep slope angles. Only a thin veneer of unconsolidated sediment is present, primarily in localized topographic lows. Petrographic analysis of rock samples from this zone indicates pervasive submarine cementation dominated by micritic Mg-calcite cements. Lesser amounts of isopachous bladed Mg-calcite along with pore-filling fibrous and botryoidal aragonite cements are also present.

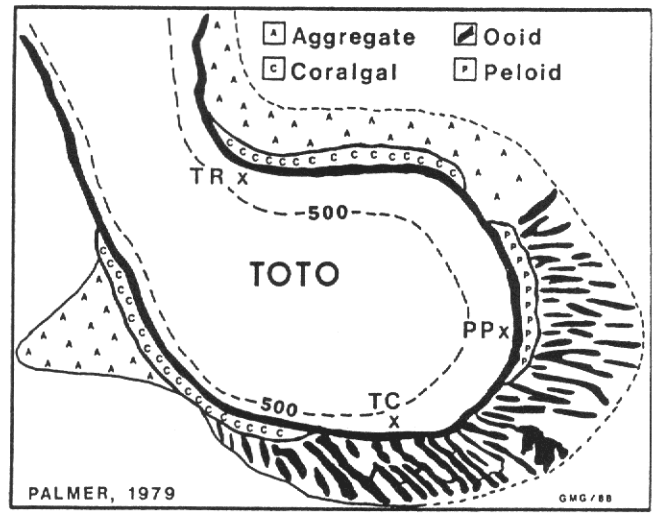

Figure 3. Map showing distribution of surface sediments in the southern portion of the Tongue of the Ocean. Thick dark line indicates slope break at top of wall. Depth in fathoms. TR - Twin Rocks; PP - Palmer Point; TC - Thunder Channel. Modified from Palmer (1979).

4. The soft-sediment slope is a wedge of unconsolidated sediment with slope angles of 25^{o} to 30^{o} that onlaps the overlying cemented slope. This sediment wedge exhibits varying surface morphologies ranging from a smooth sediment blanket to a series of large sediment ridges and erosional troughs that may be several meters high and extend downslope for many tens of meters. Active bioturbation in this zone is suggested by the presence of numerous tracks, trails and apparent burrows on the surface of the unconsolidated sediment. The transition between the cemented slope and the soft-sediment slope is often marked by an accumulation of talus blocks and reefal material derived from above. The soft-sediment slope consists of a mixture of platform-derived sands and muds, and deep water planktic material and defines the uppermost portion of the present-day, active depositional slope.

Development

The questions of how and when the cemented slope formed are of primary interest because of the similarity to steeply dipping slope deposits seen in the fossil record. Carbonate slopes from the Permian of West Texas/New Mexico (Yurewicz, 1977; Ward et al., 1986), the Devonian of Western Australia (Playford, 1980, 1989), and the Triassic Dolomites of northern Italy (Bosellini, 1984; Harris, 1988) all exhibit primary depositional slopes of $35\text{-}40^{o}$. This type of slope profile is also frequently observed in seismic profiles from ancient carbonate platforms in the subsurface (e.g. Sarg, 1988). Researchers working on both modern and ancient carbonate slopes have suggested a myriad of downslope, gravity-induced mechanisms for the deposition of sand-size and coarser sediments. On modern carbonate slopes, Cook and Mullins (1983) and Enos and Moore (1983) indicate that relatively large-scale turbidity currents and debris flows appear to be the dominant mechanisms for the downslope transport of coarse detritus.

Observations from the Tongue of the Ocean, however, suggest that the foreslopes formed by an alternative mechanism. In particular, the cemented slope appears to have formed in large part by the progressive amalgamation

of localized, linear trains or lobes of coarse sands and gravels rather than by emplacement of large-scale mass flow deposits. These sediment lenses are decimeters thick and average a few meters wide by a few tens of meters long and are oriented with their long axes parallel to the slope. They appear to form by the damming of sand and gravels behind large talus blocks or piles of rubble forming a framework that is subsequently "filled-in" by deposition of finer sands and muds. The sand-size and coarser material are derived from the wall and the margin of the platform and are dominated by Halimeda sands and coral rubble. The lobes of sediment are then rapidly lithified by pervasive submarine cementation. Repeated episodes of deposition and cementation result in the amalgamation of individual sediment packages that are linear in shape and discontinuous in both lateral and vertical dimensions along the slope. Because of the progressive infilling of the sieve-like internal structure of the lobes by fine sand and mud, the slope deposits are expected to have a considerably different internal fabric than those deposited by large-scale debris flows or turbidity currents.

Radiocarbon dating of skeletal components, utilizing accelerator mass spectrometer techniques to minimize the analytical error (Linick, et al., 1986), indicate that the cemented slope was an active depositional slope until approximately 10-11 ka. This suggests that the steep cemented slopes were actively forming while sea level was rising from the last lowstand of sea level (15-18 ka) and before the platform itself was flooded (6-8 ka). During this time, coarse sands and gravels derived from the wall were deposited primarily by grain flow and rock fall mechanisms on the steeply inclined slopes.

Another interesting and potentially significant feature observed along the Tongue of the Ocean slopes is the presence of rounded mounds that give the slope the appearance of a mogul field on an alpine ski slope. These moguls are found along the upper portions of the cemented foreslope (see slope profiles). They are nearly spherical at the top of the slope and gradually become more elliptical or elongate downslope with the long dimension oriented parallel to the slope. They are generally a meter or less in height and may be up to a few meters in diameter. Both dimensions decrease downslope. The surface of the moguls are typically covered by various encrusting and binding organisms.

Preliminary evaluation of these moguls suggests that they may have at least two possible origins. The first is that they may simply represent a "boulder field" of talus derived from above. Angular blocks derived from the wall could have been partially covered by prodigious amounts of sediment deposited on the slope. Progressive burial combined with surface colonization by encrusting organisms would have resulted in the rounded outline observed today.

Another possibility is that the moguls represent accretional features that formed by the sediment-trapping and binding of a community of turf-like organisms present on the surface of the slope. Subsequent cementation might lead to progressive formation of a hard, rounded, dome-like deposit similar to the observed moguls. Features similar to these have been described by Haddad et al. (1984) and James et al. (1988) from the Miocene in the Gulf of Suez, and from the Devonian of the Canning Basin, Australia (Playford et al., 1976). These features were interpreted by James (1988) and Playford (1976) to be deepwater "stromatolites" that formed along the foreslopes at depths approximately 50-100 meters below the level of the reef-crest. Continuing work on the moguls found in the Tongue of the Ocean should provide further insight into the evolution of these features.

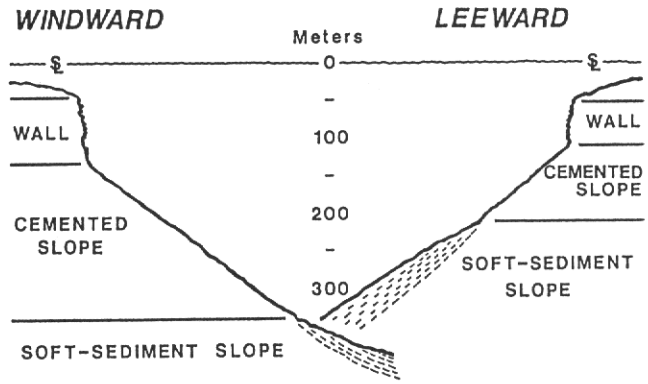

Figure 4. Schematic diagram showing variations in the slope profile related to windward or leeward positioning. Note that on leeward margins, the depth at which the soft-sediment onlaps the cemented slope is over 100m shallower than on windward margins and that the base of the wall appears to have been buried. Both results are presumably due to higher sedimentation rates along leeward margins.

WINDWARD VS. LEEWARD MARGINS

Our observations in the Tongue of the Ocean indicate that there are distinctive patterns of sediment accumulation related to the windward and leeward positioning of the margins (Figure 4). The most striking feature is the variable thickness in the wedge of unconsolidated, fine-grained sediment onlapping the cemented slope (see Figure 5). Leeward transects show a significantly higher upper limit of soft sediment onlap (about -215m) than the windward margin (about -320m), presumably as a result of greater amounts of fine-grained sediment being carried off the open leeward platform. Further north, where the leeward margin is partially sheltered by the Exuma chain, less fine-grained sediment accumulates (top at -275m). The depth to the base of the near-vertical wall also reflects variations due to windward versus leeward orientation. Figure 6 illustrates how the base of the wall is at a depth of 135-145m along the windward margins while it is considerably shallower on the leeward side. We believe that higher sedimentation rates along the leeward margins have resulted in the burial of the base of the wall along that side. This hypothesis is supported by the fact that in localized areas along the leeward margin, where there has apparently been some sheltering from sedimentation, the near-vertical wall extends down to depths equivalent to those found along the windward margin. These observations support the concept of rapid lateral growth on leeward margins and suggest that variations in sheltering effects may strongly influence carbonate platform growth.

ACKNOWLEDGEMENTS

This project has been funded as part of NOAA's National Undersea Research Program (SU-2-0887 and SU-2-0888 to RNG). Radiocarbon dating was performed by Tim Jull at the University of Arizona. We would like to acknowledge the valuable assistance provided by the captain and crew of the R/V Powell, and by the DELTA's support team, especially pilots Rich Slater and Doug Privitt. We are also indebted to our ship-board colleagues (Alton Brown, Paul Crevello, John Dunham, Gregor Eberli, Steve Murray, Harry Roberts, Art Saller, Stan Schumm, Peter Swart, and

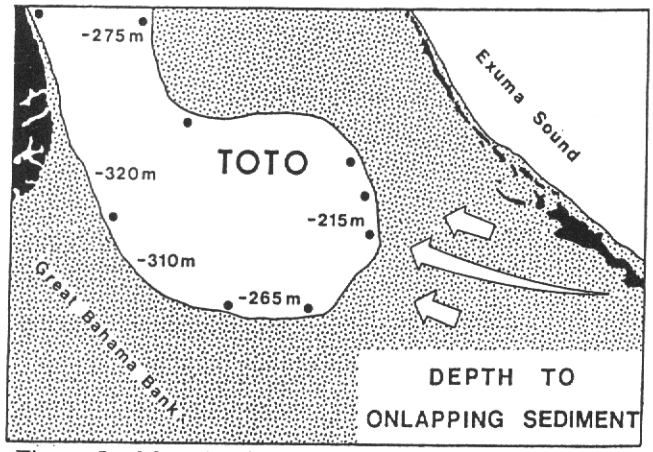

Figure 5. Map showing average depth to onlapping soft-sediment slope around TOTO. Depths determined from an analysis of all dives. Arrows indicate predominant winds (ESE). Note that on open leeward margins the soft-sediment has onlapped over 100m higher than on windward margins.

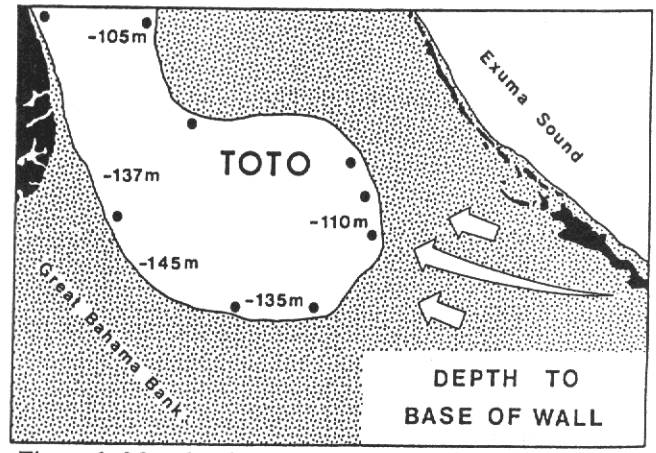

Figure 6. Map showing average depth to base of wall around the TOTO. Depths determined from an analysis of all dives. Arrows indicate the predominant winds (ESE). Note that the base of the wall has apparently been covered by greater amounts of sedimentation along the leeward margin.

Stuart Williams). Comments and suggestions by D. K. Larue improved the manuscript. A contribution from the Comparative Sedimentology Laboratory, Rosenstiel School of Marine and Atmospheric Science, University of Miami.

REFERENCES CITED

Bosellini, A., 1984, Progradation geometries of carbonate platforms: examples from the Triassic of the Dolomites, northern Italy: Sedimentology, vol. 31, p.1-24.

Cook, H. E., and H. T. Mullins, 1983, Basin Margin, in Scholle, P. A., Bebout, D. G., and C. H. Moore (eds.), Carbonate Depositional Environments: AAPG Memoir 33, p. 539-619.

Enos, P.. and C. H. Moore, 1983, Fore-reef Slope, in Scholle, P. A., Bebout, D. G., and C. H. Moore (eds.), Carbonate Depositional Environments: AAPG Memoir 33, p. 507-539.

Haddad, A., Aissaoui, M. D., and M. A. Soliman, 1984, Mixed carbonate-siliciclastic sedimentation on a Miocene fault-block, Gulf of Suez: Sedimentary Geology, vol. 37, p. 182-202.

Harris, M. T., 1988, Margin and foreslope deposits of the Latemar Carbonate Buildup (Middle Triassic), The Dolomites, Northern Italy: Ph.D. dissertation, Johns Hopkins University, 473 p.

James, N. P., and R. N. Ginsburg, 1979, The seaward margin of Belize barrier and atoll reefs: Int'l. Assoc. Sed., Special Publication no. 3, 191 p.

James, N. P., Coniglio, M., Aissaoui, D. M., and B. H. Purser, 1988, Facies and geologic history of an exposed Miocene rift-margin carbonate platform: Gulf of Suez, Egypt: AAPG Bulletin, vol. 72, p. 555-572.

Linick, T. W., Jull, A. J. T., Toolin, L. J., and D. J. Donahue, 1986, Operation of the NSF-Arizona Accelerator Facility for Radioisotope Analysis and results from selected collaborative research projects: Radiocarbon, vol. 28, p. 522-533.

Moore, C. H., Graham, E. A., and L. S. Land, 1976, Sediment transport and dispersal across the deep fore-reef and island slope (-55m to -305m), Discovery Bay, Jamaica: Journal Sed. Pet., vol. 46, p. 174-187.

Palmer, M., 1979, Holocene facies geometry of the leeward bank margin of Tongue of the Ocean: unpubl. M. S. Thesis, Univ. Miami, FL, 199 p.

Playford, P. E., Cockbain, A. E., Druce, E. C., and J. L. Wray, 1976, Devonian stromatolites from the Canning Basin, Western Australia, in M. R. Walter (ed.), Stromatolites: Elsevier, Amsterdam, p. 543-564.

Playford, P. E., 1980, Devonian "Great Barrier Reef" of Canning Basin, Western Australia: AAPG Bulletin, vol. 64, p. 814-840.

Playford, P. E., Hurley, N. F., Kerans, C., and M. F. Middleton, 1989, Reefal platform development, Devonian of the Canning Basin, Western Australia: SEPM Spec. Publ., no. 44, p. 187-202.

Rich, J. L., 1951, Three critical environments of deposition, and criteria for recognition of rocks deposited in each of them: GSA Bulletin, vol. 62, p. 1-20.

Sarg, J. F., 1988, Carbonate sequence stratigraphy, in Sea-Level Changes - An Integrated Approach: SEPM Spec. Publ., no. 42, p. 155-181.

Ward, R. F., Kendall, C. G. St. C., and P. M. Harris, 1986, Upper Permian (Guadalupian) facies and their association with hydrocarbons - Permian Basin, West Texas and New Mexico: AAPG Bulletin, vol. 70, p. 239-262.

Yurewicz, D. A., 1977, Origin of the massive facies of the Lower and Middle Capitan Limestone (Permian), Guadalupe Mountains, New Mexico and West Texas: SEPM (Permian Basin Section) Guidebook, no. 77-16, p. 45-92.

STRUCTURE AND SPREADING HISTORY OF THE CENTRAL CAYMAN TROUGH

N. Terence Edgar
U.. S. Geological Survey
Reston, Virginia 22092 USA

William P. Dillon
U.S. Geological Survey
Woods Hole, MA 02543 USA

Colin Jacobs
Institute of Oceanographic Sciences
Wormley, Surrey GU8 5UB, U.K.

Lindsay M. Parsons
Institute of Oceanographic Sciences
Wormley, Surrey GU8 5UB , U.K.

Kathryn M. Scanlon
U.S. Geological Survey
Woods Hole, MA 02543 USA

Troy L. Holcombe
National Geophysical Data Center
Boulder, Colorado 80303, USA

ABSTRACT

Based on newly acquired seismic, magnetic, and sidescan data in the central Cayman Trough, we are able to identify new relationships that bear on the recent development of the region. The presence of a crustal block within the rift valley, the absence of basalt on the top of faulted blocks on the inward-facing rift valley walls, and an offset of the south wall of the trough east of the rift-transform intersection may be explained by a ridge jump and subsequent oblique opening of the rift valley at about one million years ago. The oblique opening results from a right-lateral component of movement between the two walls of the valley.

Orientation of a nodal basin at the southern rift-transform intersection and depth relations west and east of the intersection support the argument in favor of principal transform motion being restricted to the northeast and southwest margins of the trough, as proposed by Holcombe and others (1973). Although there is sidescan-sonar evidence of structural activity along the south margin of the trough east of the rift-transform intersection, it is unlikely that there is any significant transform motion along this segment of the margin.

INTRODUCTION

The Cayman Trough is an easterly oriented strike-slip transform-spreading system (Holcombe and others, 1973) that has formed the northwestern Caribbean plate boundary (Fig. 1) since Eocene time (Molnar and Sykes, 1969; Malfait and Dinkelman, 1972). Almost centered along the trough at about 81°41'W is a north-trending rift valley (Fig. 2A). East of the rift valley, the Oriente Transform Fault extends along the northern wall of the trough where it forms the plate boundary and the boundary between the continental rocks of the Cayman Ridge and the oceanic rocks of the trough (Fig. 2) (Ewing and others, 1960; Eggler and others, 1973; Perfit, 1977). West of the rift valley, the Swan Islands Transform Fault forms the plate boundary located along the south wall of the trough, and, like the Oriente Transform Fault, it generally follows the boundary between oceanic crust of the Cayman Trough and continental rocks, in this case rocks of the Nicaraguan Rise (Fig. 2). An exception is noted where the fault appears to lie south of the Swan Islands microblock (Rosencrantz and Sclater, 1986), which is underlain by continental rocks.

The eastward motion of the Caribbean plate relative to the North American plate has formed a sea-floor spreading system at a jog on the plate boundary that has created new ocean crust that floors the entire trough. The rate at which sea-floor spreading has been taking place is equivalent to the rate at which the two plates are moving past each other. The spreading rate in the Cayman Trough has not been determined unequivocally because of the difficulty in identifying and correlating magnetic anomalies. However, Rosencrantz and others (1988) concluded that the spreading rate in the Cayman Trough has been 1.5 cm/yr for the past 26 Ma based on magnetic lineations, crustal subsidence, and bathymetry and by invoking several ridge jumps. Numerous estimates have also been made based on other lines of evidence such as geologic and geographic relations that give a range of 0.4- to 4.0 cm/yr. The object of this study is to examine the detailed structure of the central Cayman Trough in the light of new simultaneously gathered single-channel seismic, magnetic, and GLORIA (Geologic LOng-Range Inclined Asdic) sidescan-sonar data (Fig. 3). Based on already published data and these new data, we identified relationships that bear on the recent development of the Cayman Trough.

The GLORIA sidescan sonar system (Somers and others, 1978) is a broad-coverage (swath width of about 40 km in water depths greater than 3000 m), low-resolution system (pixel size is about 50- by 150 m in the field data) capable of rapidly surveying very large areas. Processing techniques to correct for geometric and radiometric distortions and to enhance the images were applied to the data followed by digital compilation into a map-coordinated system to create a sidescan-sonar mosaic.

Larue, D.K., and Draper, G. (eds.),
Transactions of the 12th Caribbean Geological Conference, St. Croix, U.S.V.I., Miami Geological Society, P.O. Box 431552, South Miami, FL 33243, U.S.A.

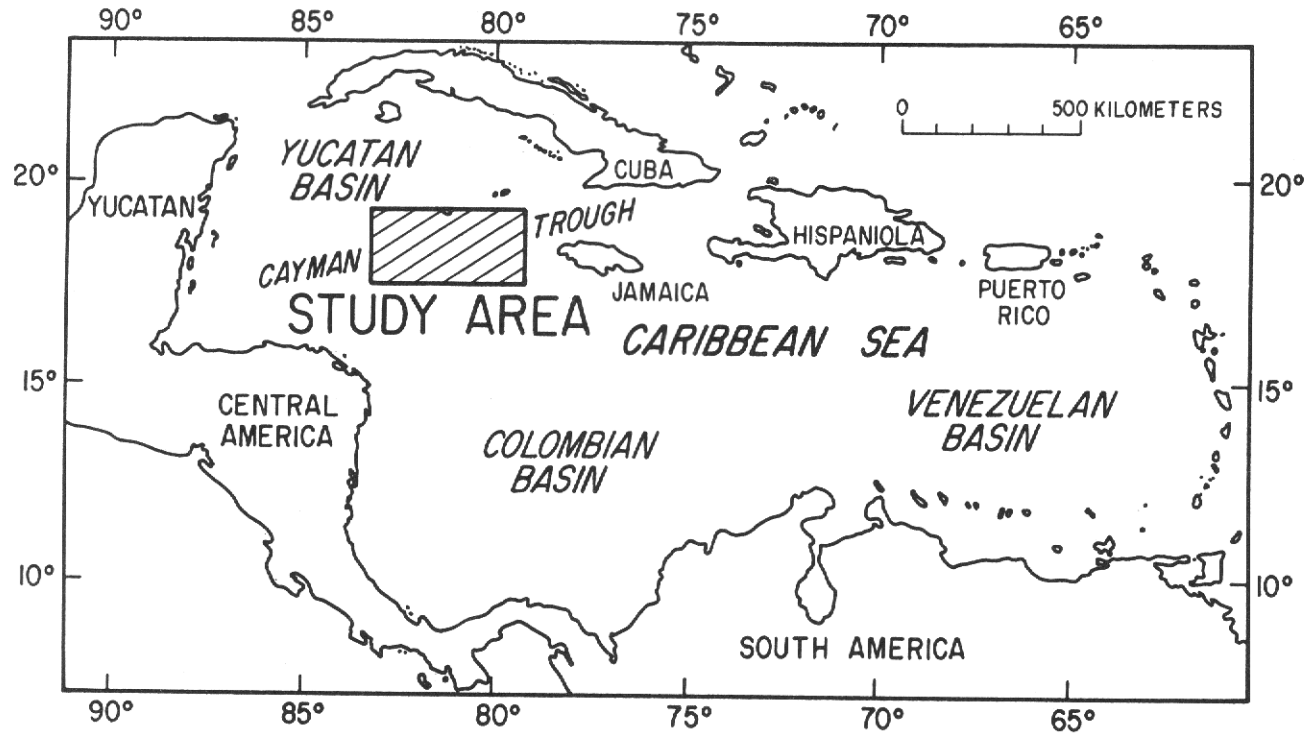

Figure 1. Map of the Caribbean region showing the area of study in the Cayman Trough

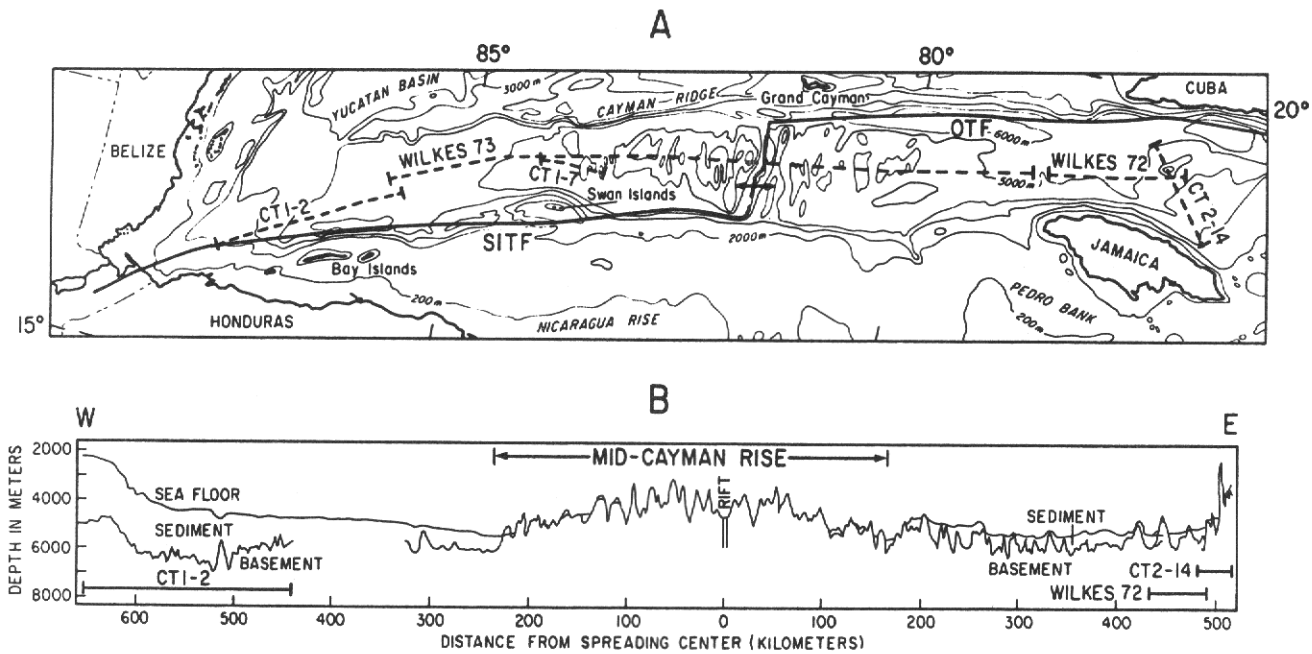

Figure 2. (A) Bathymetric map of the Cayman Trough showing the locations of U.S. Navy Wilkes single channel seismic line and two University of Texas multichannel seismic lines that are combined in part B of this figure. OTF= Oriente Transform Fault; SITF= Swan Islands Transform Fault. (Rosencrantz and Sclater, 1986). — (B) Line drawing of the U.S. Navy Wilkes single-channel seismic profile and the University of Texas multichannel seismic data showing the Mid-Cayman Rise and the more subdued, sediment-covered seafloor on each side of the rise. (Rosencrantz and Sclater, 1986).

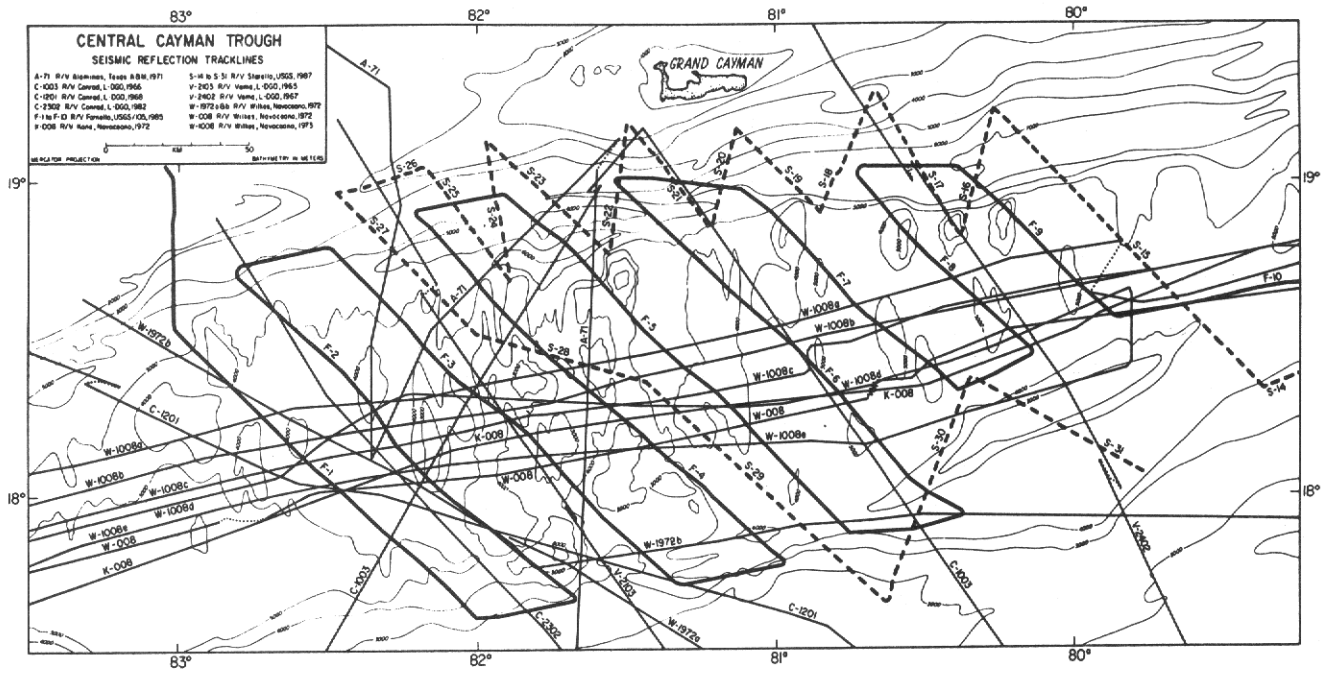

Figure 3. Seismic reflection track lines over the Central Cayman Trough. The Gloria sidescan tracks (R/V Farnella) are the heavy southeast oriented lines. The dashed lines are the R/V Starella lines. Bathymetry is after Jacobs and others (1989).

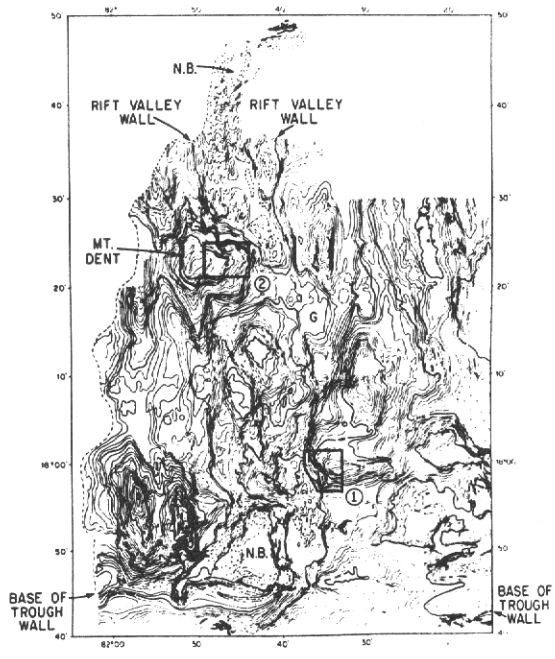

Figure 4. U.S. Navy multibeam bathymetry of the central region of the Mid-Cayman Rise, showing locations of the two ALVIN and one TRIESTE dive areas (CAYTROUGH, 1978). The walls of the rift valley have been stippled for clarification. Contour interval is 50 fm (uncorrected). N.B. = nodal basin; G = gap; W = base of the wall; boxes labelled 1 and 2 are ALVIN dive sites; dashed line is the track of TRIESTE II.

PREVIOUS STUDIES

The central Cayman Trough has been the subject of two important prior studies; the CAYTROUGH (1979) experiment, which utilized the deep-submersible ALVIN, dredging, and multibeam bathymetry in the rift valley area, and a geophysical study on the entire Cayman Trough conducted by Rosencrantz and Sclater (1986) and Rosencrantz and others (1988).

The multibeam bathymetric survey (Fig. 4) (CAYTROUGH, 1979) reveals bathymetric details within the valley that, combined with sampling and photography of the sea floor, delineate areas of very recent volcanic activity, which probably represent the location of the spreading axis. The survey also delineated a nodal basin (Fox and Gallo, 1986) at each of the two rift-transform intersections and revealed that the water depth east of the southern nodal basin is about 2000 m shallower than the depth west of the basin. The walls of the rift valley are also clearly identifiable, their continuity being interrupted only by a mountain, referred to here as Mt. Dent, at about the midpoint along the west wall and a gap on the east wall opposite Mt. Dent (Fig. 4).

Several observation, photographic, and sampling traverses (Fig. 4) were conducted from ALVIN over the western wall of the rift valley (east slope of Mt. Dent) and across the eastern rift valley wall in the southern part of the valley (CAYTROUGH, 1979). These traverses demonstrated that the walls are composed of gabbroic rocks capped by less than 200 m of basalt. Gabbroic oceanic crust is typically capped by about 500 m of basalt (Ballard and Van Andel, 1977). Fault blocks on the rift valley walls are also composed of gabbro, but they are not capped with basalt. The absence of basalt is unusual because fault blocks described on the walls of rift valleys at other locations are capped with about a half a kilometer of basalt, a

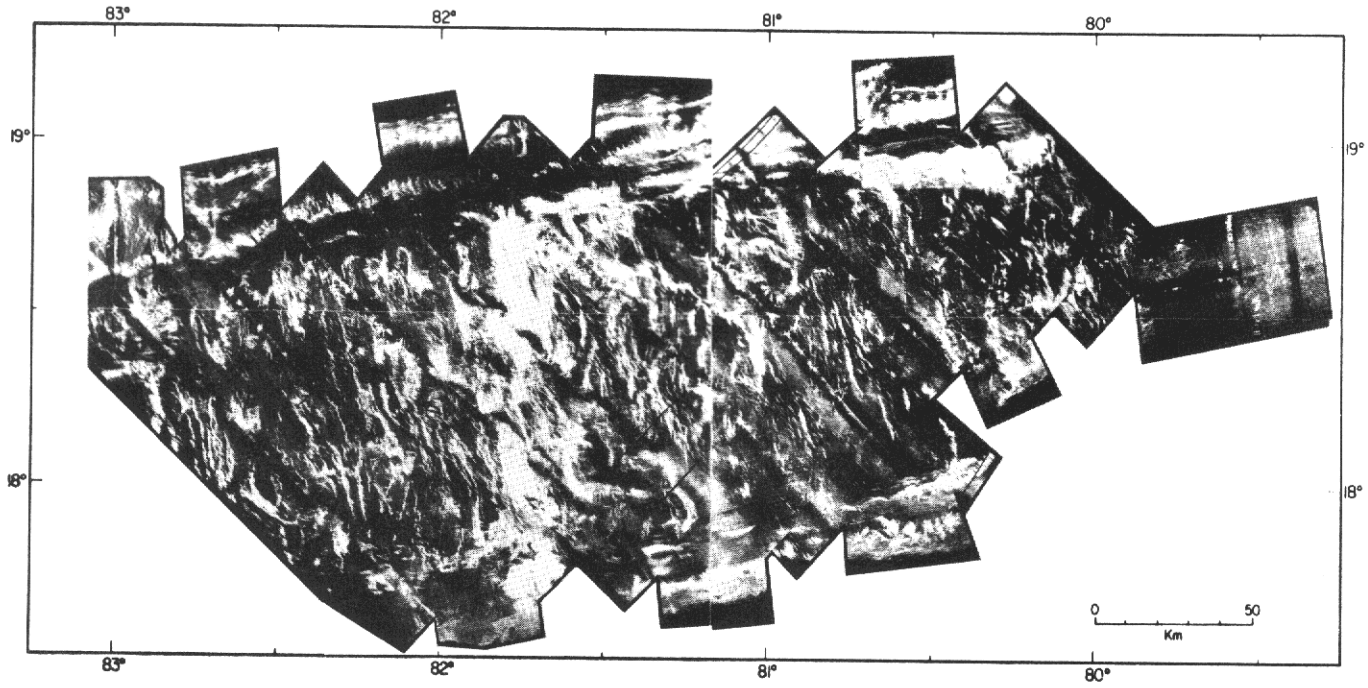

Figure 5(A) Processed GLORIA sidescan mosaic of the central Cayman Trough. White areas are caused by strong-returning acoustic signal, dark areas by weak returns. The north-trending bright zone in the central part of the mosaic is the sediment-free rift valley from which a strong reflection was recorded to the extent that most of the detail is masked. The dark areas are largely covered with sediment. It is virtually impossible to distinguish between pelagic and detrital sediments based solely on these images. Mercator projection.

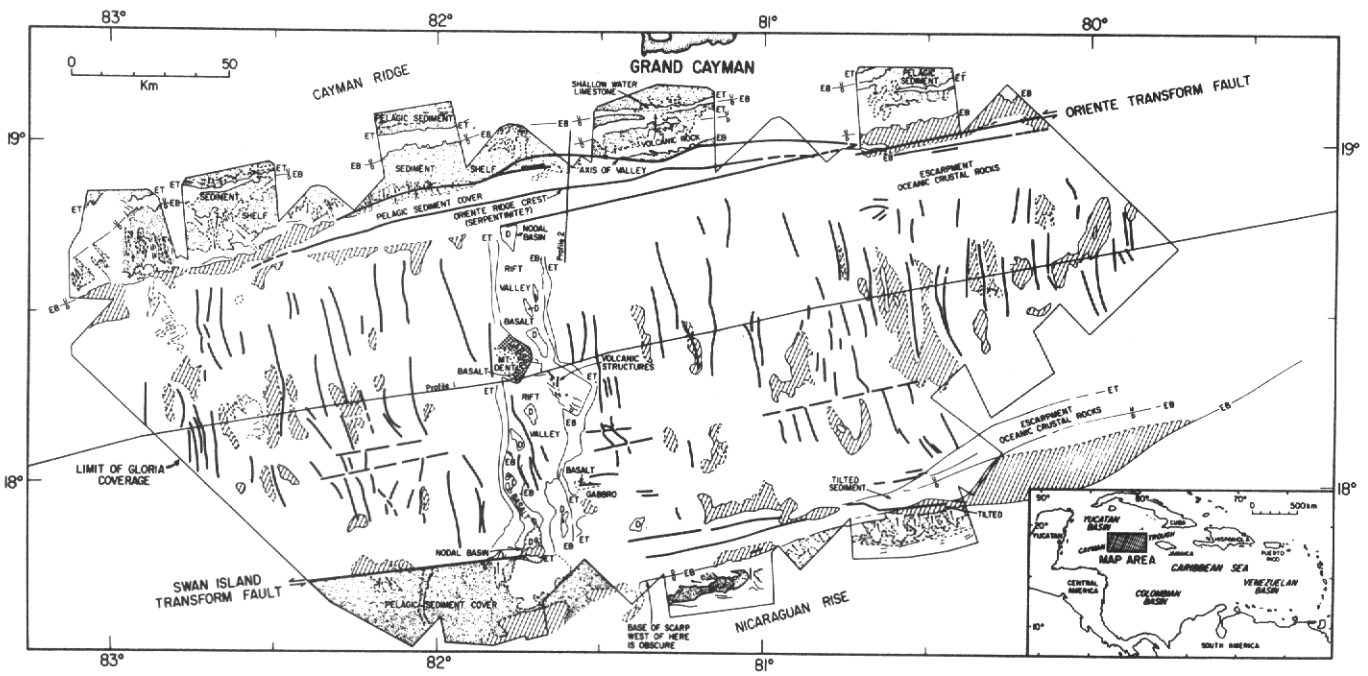

Figure 5(B). Interpretation of the sidescan mosaic. using seismic and bathymetric data. ET = top of escarpment; EB = bottom of escarpment; U = upthrown wall of fault; D = Downthrown wall of fault; stippled areas are sediment covered; areas covered with diagonal lines represent sediment ponds and abyssal plains; heavy lines are lineaments, including faults. Mercator projection.

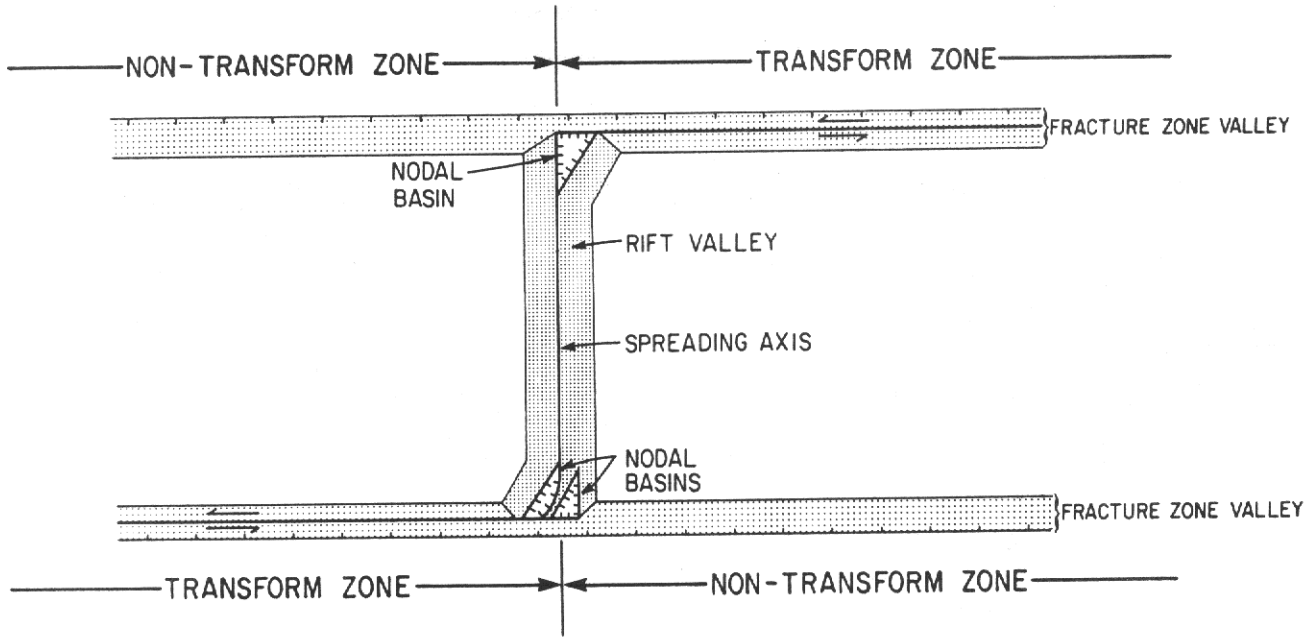

Figure 6. Diagram showing relationship of nodal basins to active transform faults in typical fracture zones. The hypotenuse of the triangular shaped nodal basin faces the active transform limb of the fracture zone valley. Widely spaced hatchures indicate a depression. In some cases, the spreading axis may pass through the nodal basin, splitting the basin as shown on this diagram (after Fox and Gallo, 1986).

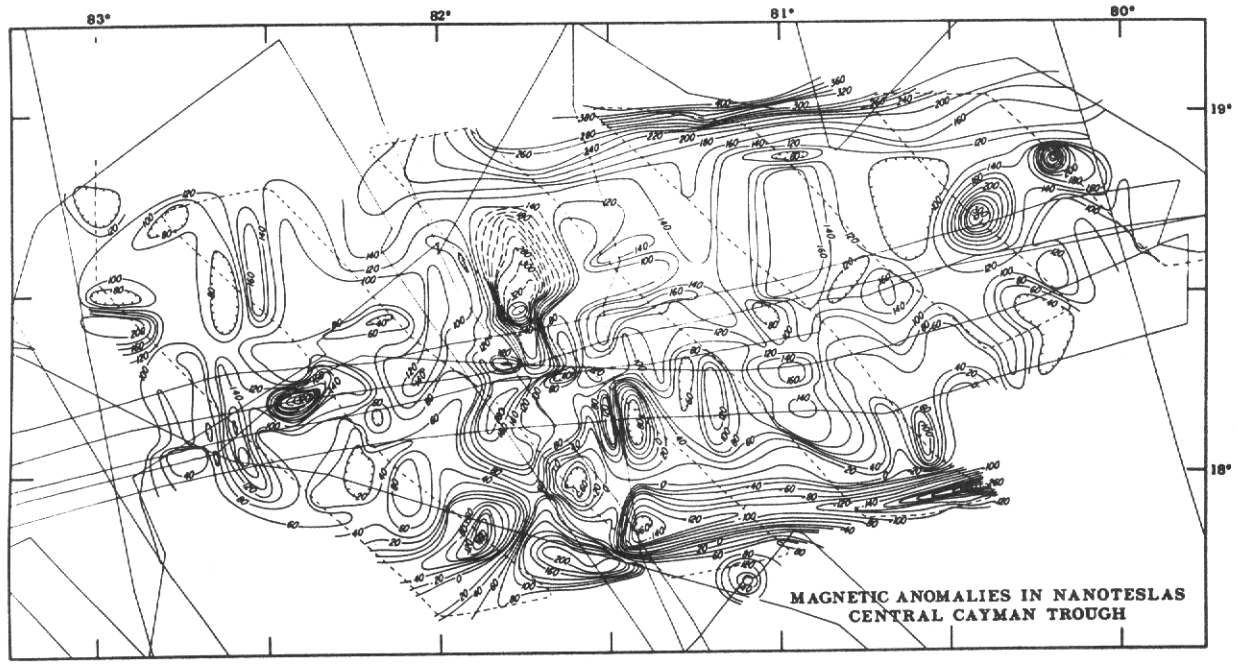

Figure 7. Magnetic anomaly contour map of the survey area in the central Cayman Trough. The area of simple magnetic anomaly pattern in the northern half of the trough is probably an artifact caused by insufficient data. Contour interval is 20 nanoteslas. Mercator projection.

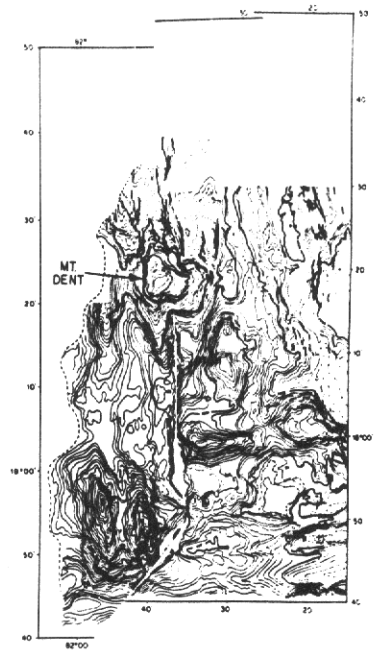

Figure 8. Multibeam bathymetric reconstruction of pre-rift jump (rift valley removed). Contour interval is 50 fm (uncorrected).

result that would be anticipated from the uplift of blocks from a basalt-covered rift valley floor.

NEW DATA AND OBSERVATIONS

GLORIA mosaic

The dominant lineament evident in the GLORIA mosaic (Fig. 5A) is a northerly trend that represents morphology resulting from the sea-floor spreading process between the east-northeast-trending walls of the Cayman Trough. The bright, northerly oriented band at 81°41'W is caused by strong reflections from the bare-rock surface of the rift valley. The trend of the lineaments east and west of the rift valley are parallel or subparallel to the rift valley, suggesting that there has been little change in the orientation of the spreading system within the survey area (20-26 Ma, Rosencrantz and others, 1988). The number and size of the sediment ponds trapped in valleys between ridges increases with increasing distance (increasing age) from the rift valley. Excluding the Oriente and Swan Islands Transform Faults, indications of strike-slip faulting in the Cayman Trough are few, and where evident, displacement does not appear to exceed 10 km (Fig. 5A and 5B).

The outline of the rift valley is well displayed, but details are obscured by the strength of the reflections from the young, bare-rock surface. A northerly trending line of volcanic structures, which probably formed along the spreading axis, is evident in the rift valley east of Mt. Dent. It is not known whether they are active. Lineaments of some of the larger features show a north-northwest trend in the rift valley south of Mt. Dent (Fig. 5A and 5b) that is consistent with the trend indicated by the multibeam bathymetry (Fig. 4). A crossing of one of these lineaments, a ridge south of Mt. Dent (Fig. 4), by the deep submersible TRIESTE II (CAYTROUGH, 1979) indicates that this volcanic ridge is no longer active, based on the evidence of a thin cover of pelagic sediment. Volcanically active or most-recently active, areas south of Mt. Dent lie in the western part of the rift valley at the base of the west rift valley wall and probably represent the active spreading axis in the rift valley (Stroup, 1981).

Particularly bright patches at the north and south ends of the rift valley (Fig. 5A) are strong reflections from depressions in the sea floor, or nodal basins. The existence of these basins is confirmed by the multibeam bathymetry (Fig. 4). Nodal basins are characteristic of rift-transform intersections (for a summary see Fox and Gallo, 1986) and their typical shape emulates a right triangle (Fig. 6).

Easterly trending ridges composed of oceanic rocks have been mapped and dredged (Perfit, 1977) along the north and south margins of the trough at about 80°25'W. The northern ridge is capped by north-elongated pinnacles, whereas the southern ridge does not appear to be capped with pinnacles (Fig. 3 and 5B). The southern ridge was referred to as the "east microblock" by Rosencrantz (1986). Although a direct correlation cannot be made, it is possible that the southern ridge is an extension of easterly oriented structures that parallel the southern margin at about 81°W (Figs. 4, 5A, and 5B), but there is no apparent topographic connection.

Topographic and structural features east and west of the southern nodal basin are quite different. The sidescan-sonar and multibeam data show a band of easterly trending ridges and valleys that parallel the southern margin of the Cayman Trough east of the southern nodal basin (Figs. 4 and 5a). These contrast with the northerly oriented features adjacent to the southern margin of the Cayman Trough west of the southern nodal basin. The south wall of the Cayman Trough appears to be offset to the south by about 5 km on the east side of the rift-transform intersection (Figs. 4, 5A, and 5B).

Magnetic anomaly map

The magnetic anomaly map (Dillon and others, 19xx) shows a strong positive anomaly of 320 nanoteslas located on the west side of the rift valley at the intersection with the northern slope of Mt. Dent and extending southward across the peak (Fig. 7). Mt Dent was demonstrated to be a gabbroic crustal block by ALVIN sampling (CAYTROUGH, 1979). There are no magnetic data across the rift valley north of Mt. Dent, and those tracks that cross the rift valley south of Mt. Dent show virtually no significant anomaly with a magnitude typical of a central anomaly in an active ocean-opening rift valley.

CONCLUSIONS

Ridge jump and oblique openingThree anomalous features of the rift valley, the presence of a crustal block within the valley (Mt. Dent), the absence of basalt on the top surface of the step-faulted gabbroic blocks on the inward wall of the valley, and the offset of the south wall of the Cayman Trough across the southern rift-transform intersection may be explained by a ridge jump and subsequent oblique opening. The displacement of the spreading center from its prejump position is probably relatively small, based on the gross bathymetric

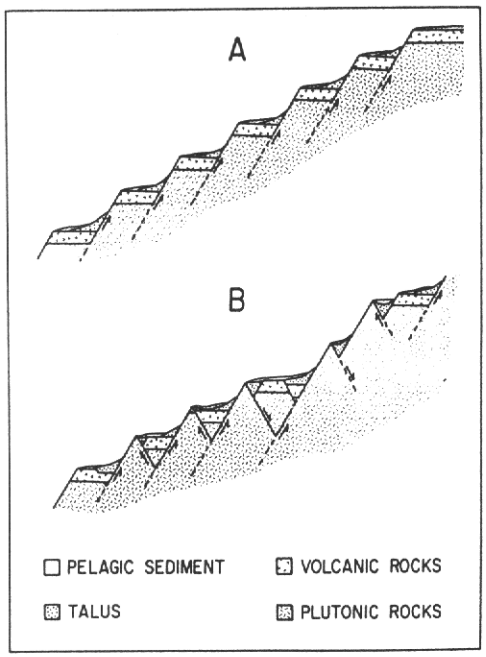

Figure 9. Diagram showing the White and Stroup (1979) model for explaining the absence of basalt on the crests of step-faulted blocks of gabbro on the walls of the rift valley. Blocks of gabbroic, basalt-capped crust are initially uplifted from the rift valley floor (A) according to the model of the mid-oceanic ridge system. Basalt on the crest of each of the fault blocks is downfaulted into grabens, then covered by talus (B). The result is the apparent absence of of basalt from the crest of the fault blocks.

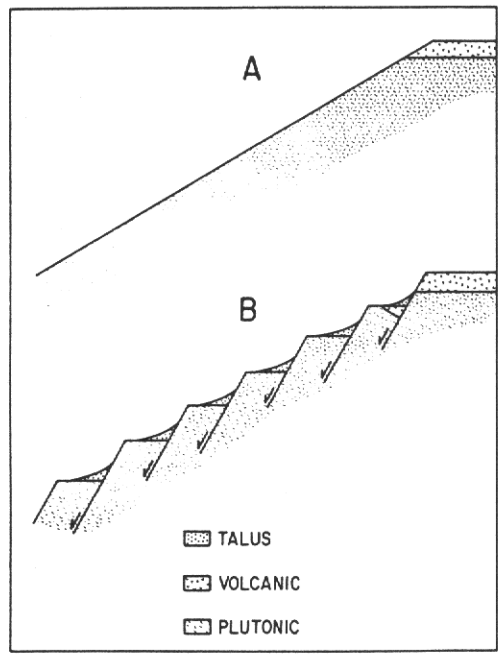

Figure 10. Diagram showing the model presented in this paper for the absence of basalt on the crests of step-faulted blocks of gabbro on the walls of the rift valley. Following the ridge jump (A), a tensional regime resulted in the downfaulting of gabbroic blocks from the escarpment of the rift valley wall (B). The result is a series of fault blocks composed of gabbroic rock.

symmetry of the Mid-Cayman Rise (Fig. 2), so the difference in age between the rocks of the walls and those of the rift valley floor should not be great.

On the assumption that the rift valley is the site of all of the most recently generated crust, the area can be restored to its prejump configuration (Fig. 8) by removing the rift valley area from the bathymetric map (Fig. 4). In so doing, it is apparent that, if the direction of closing is orthogonal to the valley walls, the closure cannot be completed because of the presence of Mt. Dent, assuming that Mt. Dent is older than the rift valley crust. However, if the direction of closure is about 117°, Mt. Dent fits snugly into the gap in the east wall of the valley and the closure can be completed as shown in Figure 8. It could be argued that Mt. Dent was uplifted after the initial formation of the rift valley, but if this were the case, then the gap in the east wall of the rift valley would remain unexplained. We also note that the distance between the east slope of Mt. Dent and the eastern end of the gap is the average width of the rift valley.

White and Stroup (1979) offered a rather contrived explanation for the absence of basalt on the top of the step-faulted gabbroic blocks on the inward-facing walls of the rift valley in which they called upon grabens at the crest of each gabbroic block into which the basalt was dropped and then covered with talus (Fig. 9). These authors assumed that the blocks were uplifted from the basalt-covered valley floor. However, the absence of basalt on the top of the blocks may also be explained by assuming that the blocks of gabbro dropped down from the face of the rifted escarpment (Fig. 10). Down-dropped blocks would result from the rifting apart (tension) of existing crust following the relocation of the spreading center.

By closing the rift valley obliquely so that Mt. Dent fits into the gap in the east wall, the south wall of the Cayman Trough east of the rift-transform intersection aligns with the wall west of the intersection (Fig. 11).

The combined evidence from these three observations strongly support the concept of a ridge jump into older crust and a subsequent oblique opening. Accepting Rosencrantz's spreading rate of 1.5 cm/y for the past 26 My and 15 km as an average width of the rift valley, the jump occurred about one million years ago. It is not clear from where the spreading center jumped, but the bathymetric symmetry about the rift valley (Fig. 2) would suggest that the previous location of the rift valley is not far from its present location.

Plate boundary

Burke and others (1980) proposed that the boundary between the North American and Caribbean plates is a zone about 200 km wide and that, in addition to the principal transform motion along the north wall of the trough, about 40

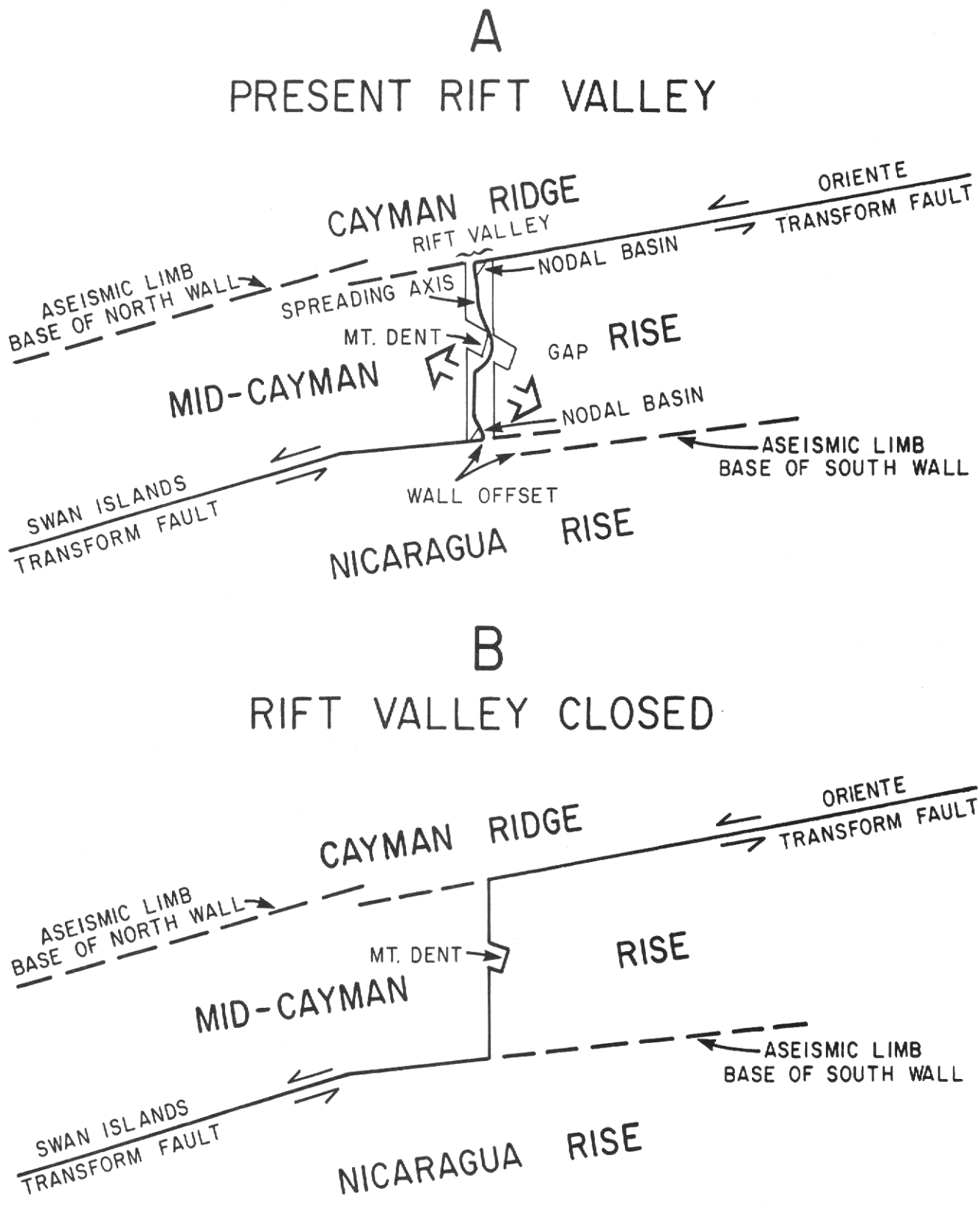

Figure 11. Diagram showing the present structural relationships in the rift valley (A) and when it was closed, at about 1 Ma (B).

km of transform motion has occurred in the Cayman Trough along the south margin east of the rift valley. This view was supported by Sykes and others (1982) who proposed that there is a significant component of left-lateral motion along the southeastern margin of the trough. However, two lines of evidence from bathymetric and sidescan data suggest that no significant component of motion occurs along the southeastern margin.

The orientation of nodal basins provides the first line of evidence. Nodal basins, discussed earlier, form at the intersection of spreading axes and transform faults, are shaped like right triangles with the hypotenuse of these triangular shaped basins facing toward the limb of the fracture zone valley on which there is active transform motion (Fig. 6). In the Cayman Trough (Fig. 4, 5A, and 5B), the hypotenuse of the nodal basin at the north end of the rift valley faces northeast towards the Oriente Transform Fault; at the southern terminus the hypotenuse faces southwest toward the Swan Islands Transform Fault. Hence, the orientation of the nodal basins indicates that the principal transform displacement zones are the Oriente Transform Fault and the Swan Islands Transform Fault and that there is no, or no significant, transform motion along the southern margin of the trough east of the rift valley as suggested by Burke and others (1980) and Sykes and others (1982).

The second line of evidence comes from the water depth associated with principal transform displacement zones. Transform fault zones are generally associated with greater water depths than adjacent areas (for summary see Fox and Gallo, 1986), probably because active fracture zones are underlain by shallow dense mantle rocks (Cochran, 1973; Robb and Kane, 1975). Meyerhoff (1966), Bowen (1966), Erickson (1972), and Holcombe and others (1973) noted that the deepest part of the Cayman Trough lies along the two bounding transform faults mentioned above and that the floor of the trough east of the rift valley slopes northward and west of the rift valley it slopes southward. The water depth along the southern margin east of the rift-transform intersection is about 1000 m shallower than that west of it and over 2000 m shallower than the northern boundary occupied by the Oriente Transform Fault, further supporting the statement that there is, or has been, little or no movement along the southeastern margin.

In the typical mid-oceanic ridge situation, ridge axis-parallel topographic features terminate at right angles against the aseismic limb of a transform fault (for summary see Fox and Gallo, 1986). This is not the case in the southern Cayman Trough where structures east of the rift valley are oriented orthogonal to the rift valley and extend eastward from the rift valley for tens of kilometers. Consequently, the structure of the rift-transform intersection along the southern margin of the Cayman Trough is different from that reported on the mid-oceanic ridge and may have resulted from some minor transcurrent movement along the southern aseismic limb of the fracture zone. In addition, there is evidence of topographic lineament in the abyssal plain along this aseismic limb that could be interpreted as resulting from transform motion. However, in view of the geometry of the nodal basin and water depth evidence cited above, it is unlikely that transform motion (displacement) has been, or is, significant.

SUMMARY

Evidence from sidescan sonar, seismic profiles, and bathymetry suggest that the present rift valley was created as a result of a ridge-axis jump about one million years ago. By fitting morphological features across the rift valley, we conclude that spreading has been oblique to the northerly trend of the valley. The depth pattern of symmetry of the Mid-Cayman Rise suggests that the spreading axis did not jump far from its previous position.

The primary motion along this segment of the northern Caribbean plate boundary is confined to the Oriente Transform Fault and the Swan Islands Transform Fault. Although the sidescan images show evidence of strike-slip movement along the southern aseismic limb east of the rift valley, the motion is probably not significant.

ACKNOWLEDGEMENTS

We wish to thank the captains and crews of the R/V FARNELLA and the R/V STARELLA and the USGS and IOS shipboard scientific staff. J. Zwinakis and D. Blackwood are credited with the excellent drafting and photography respectively. Reviews by R. Mattick and J. Robb are greatly appreciated.

References

Ballard, R.D. and Van Andel, T.H., 1977, Morphology and tectonics of the inner rift valley at latitude 36o 50'N on the Mid-Atlantic Ridge: Geological Society of America Bulletin, v. 88, p.507-530.

Bowin, C.O., 1968, Geophysical study of the Cayman Trough: Journal of Geophysical Research, v. 73, p. 5159-5173.

Burke, K., Grippi, J., and Sengor, A.M.C., 1980, Neogene structures in Jamaica and the tectonic style of the northern caribbean plate boundary zone: Journal of Geophysical Research, v. 88, p. 375-386.

CAYTROUGH, 1979, Geological and geophysical investigation of the Mid-Cayman Rise spreading center: initial results and observations: *in* Talwani, M. Harrison, C.G., and Hayes, D.E., eds., Deep Drilling Results in the Atlantic Ocean: Ocean Crust: American Geophysical Union Maurice Ewing Series 2, p. 66-93.

Cochran, J.R., 1973, Gravity and magnetic investigations of the Guiana Basin, western equatorial Atlantic: Geological Society of America Bulletin, v. 84, p. 3249-3268.

Dillon, W.P., Edgar, N.T., Parson, L.M., Scanlon, K.M., Driscoll, G.R., and Jacobs, Colin, 1990, Magnetic anomaly map of the central Cayman Trough, northwestern Caribbean Sea: U.S. Geological Survey, Miscellaneous Field Investigations Map, MF 2083-B.

Eggler, D.H., Falquist, D.A., Pequegnat, W.E., and Herdon, J.M, 1972, Ultrabasic rocks from the Cayman Trough, Caribbean Sea: Geological Society of America Bulletin, v. 84, p. 2133-2138.

Erickson, A.J., Helsley, C.E., and Simmons, G., 1972, Heat flow and continuous seismic profiles in the Cayman Trough and the Yucatan Basin: Geological Society of America Bulletin, v. 83, p.1241-1260.

Ewing, J.I., Antoine, J., and Ewing, M., 1960, Geophysical measurements in the western Caribbean Sea and in the Gulf of Mexico: Journal of Geophysical Research, v. 65, p. 4087-4126.

Fox, P.J. and Gallo, D.G., 1986, The geology of North Atlantic transform plate boundaries and their aseismic extensions: *in* Vogt, P.R. and Tucholke, B.E., eds., The Geology of North America, Volume M, The Western North Atlantic Region: Geological Society of America, p. 157-172.

Holcombe, T.L., Vogt, P.R., Mathews, J.E., and Murchison, R.R., 1973, Evidence for sea-floor spreading in the Cayman Trough: Earth and Planetary Science Letters, v. 20, p. 357-371.

Jacobs, C.L., Edgar, N.T., Parson, L.M., Dillon, W.P., Scanlon, K.M., and Holcombe, T.L., 1989, A revised bathymetry of the Mid-Cayman Rise and central Cayman Trough using long rang side-scan sonar: Institue of Oceanographic sciences, Deacon Laboratory, Report no. 272.

Meyerhoff, A.A., 1966, Bartlett fault system - age and offset: Transactions of the Third Caribbean Geological Conference, Jamaica Geological Survey Publication No. 95, p. 1-7.

Molnar, P. and Sykes, L.R., 1969, Tectonics of the Caribbean and Middle America regions from focal mechanisms and seismicity: Geological Society of America Bulletin, v. 80, p. 1639-1684.

Perfit, M.R., 1977, Petrology and geochemistry of mafic rocks from the Cayman Trench: evidence for spreading: Geology, v. 5, p. 105-110.

Robb, J.M. and Kane, M.F., 1975, Structure of the VEMA Fracture Zone from gravity and magnetic intensity profiles: Journal of Geophysical Research, v. 80, p. 4441-4445.

Rosencrantz, E., Ross, M.I., and Sclater, J.G., 1988, Age and spreading history of the Cayman Trough as determined from depth, heat flow, and magnetic anomalies: Journal of Geophysical Research, v. 93, p. 2141-2157.

Rosencrantz, E., and Sclater, J.G., 1986, Depth and age in the Cayman Trough: Earth and Planetary Science Letters, v. 79, p. 133-144.

Somers, M.L., Carson, R.M., Revie, J.A., Edge, R.H., Barrow, B.J., and Andrews, A.G., 1978, GLORIA II - an improved long-range sidescan-sonar: Proceedings of the Institute of Electrical Engineering on Offshore Instrumentation and Communications, Oceanology International Technical Session J: London, BPS Publications Ltd., p. 16-24.

Sykes, L.R., McCann,W.R., and Kafka, A.L., 1982, Motion of Caribbean plate during last 7 million years and implications for earlier Cenozoic movements: Journal of Geophysical Research, v. 87, p. 10,656-10,676.

Stroup, J.B. 1981, Geologic investigation of the Mid-Cayman Rise spreading center, Caribbean: Unpublished M.S. thesis, State University of New York, Albany, 173 pp.

White, G. W. and Stroup, J. B., 1979, Distribution of rock types in the Mid-Cayman Rise, Caribbean Sea, as evidence for conjugate normal faulting in slowly spreading ridges: Geology, v. 7, p. 32-36.

INTERPRETACION DE LOS DATOS GEOFISICOS CON FINES DE LA CARTOGRAFIA GEOLOGO-ESTRUCTURAL DE LA REPUBLICA DE CUBA

Manuel Pardo, Verania Bello, Hilda Amador, Sandor Taba, Oleg Sousin, Ileana Matamoros y Irio de Moya

Instituto de Geología y Paleontología, Ministerio de Industrias Básicas, La Habana, CUBA

RESUMEN

Se exponen los principales resultados en a interpretación geológica de los datos gravimétricos, aeromagnéticos y aerogamma-espectrométricos, con fines de la cartografía geólogo-estructural de la República de Cuba. Se incursiona en el problema de la naturaleza geológica de las principales fuentes de anomalías gravimagnetométricas residuales y, aero-espectrométricas. Como resultado, se establece el carácter, fundamentalmente, rocoso de las primeras y, la probable vinculación de las últimas con la concentración de distintos óxidos en la parte superior de la corteza de intemperismo (suelos), a consecuencia de su evolución en las condiciones de clima tropical. En base a la regionalización conjunta (visual) de los campos gravitatorio y aeromagnético se confecciona un esquema interpretativo geólogo-estructural de Cuba; se delimitan las principales unidades o bloques geólogo-geofísicos y, se comenta, especulativa-mente, sobre su posile naturaleza y relación. Finalmente, se aborda la idenficación de los complejos estructuro-rocosos reconocidos en el esquema anterior, con su homologos estructuro-metalogénicos.

ABSTRACT

Gravimetric, aeromagnetic and airborne gamma-spectrometry data, collected during structural-geological mapping of the Cuba, are interpreted. Gravimetric and magnetic amomalies are related to the character of the bedrock, and airborne gamma spectrometry anomalies are probably reflect concentrations of oxides developed in the overlying tropical soils. On the basis of a visual analysis of gravity and aeromagnetic fields, a scheme of geological-geophysical provinces is defined and their character discussed. This scheme correlates well with known metallogenic provinces.

INTRODUCCION

Durante los años 1986-1987, el Grupo de Geofísica de IGP realizó un trabajo dirigido al completamiento de la abase geofísico-cartográfica para el Mapa Metalogénico de la República de Cuba en escala 1:500 000. La confección de los materiales geofísicos y esquemas interpretativos geólogo-geofísicos) preveía la utilización de la información más actual del modo más integral posible con le fin de resolver las tareas planteadas en la etapa de confección de la maqueta de autor. Entre estas tareas se encontraba el apoyo de la cartografía de distintos complejos rocosos (ultramáfitico-mafítico, de granitoides, vulcanógeno-sedimentario, metamórfico, y sedimentario); contribuir al esclarecimiento de la estrucutura de los cinturones ultramáfitico-máfitico y de granitoides, así como al desciframiento de la tectónica y a la cartografía de otras estructuras geológicas (cuencas, domos, estructuras vulcano-tectónicas (plutónicas y otras). A tales propósitos se elaboraron los siguientes materiales:

-mapa esquemático de anomalías gravimétricas residuales (R = 2,5 km) de la Repblica de Cuba, en escala 1:250 000.

-Mapa esquemático (no unificado) de anomalías aeromagnéticas residuales (R = 3 y 5 km) de la República de Cuba, en escala 1:250 000 (polígonos aerogeofísicos).

-Mapa esquemático (no unificado) de anomalías aeroestrométricas (U (Ra), Th, y K) de la República de Cuba, en escala 1:250 000 (polignos aerogeofísicos).

Larue, D.K., and Draper, G. (eds.), *Transactions of the 12th Caribbean Geological Conference, St. Croix*, U.S.V.I., Miami Geological Society, P.O. Box 431552, South Miami, FL 33243, U.S.A

-esquemas interpretativos gelogo-geofísicos en escala 1:250 000.

El presente trabajo resume los principales resultados de la interpretación geológica de los datos geofísicos con fines de la cartografía geológo-estructural de la República de Cuba. Como quiera que el completamiente de la base geofísica resulta aún insuficiente para el cumplimiento de los objetivos propuestos, sumado a otros factores como son: su carácter esquemático, la no utilización de métodos numéricos para el análisis multivariado de la información; y dado el insuficiente nivel de generalización sobre el conocimiento de las propiedades físicas de las rocas, los resultados aquí presentados tienen un carácter preliminar, y deben verse sólo como una alternativa de contribución al conocimiento de las regularidades geológo-geofísicas en el territorio de la República de Cuba.

SOBRE LA INTERPRETACION GEOLOGICA DE LAS ANOMALIAS GRAVIMETRICAS Y AEROMAGNETICAS RESIDUALES

La distribución de las anomalías gravimétricas y aermagnéticas residuales refleja, en general, la regularidad espacial en la distribución de las heterogeneidades más superficiales del corte (0-2 km aproximadamente).

Las anomalías gravimétricas positivas responden, fundamentalmente, a la presencia de depresiones rellenas con rocas vulcanógeno-sedimentarias, y a la presencia o proximidad de ultramafitas poco serpentinizadas, mafitas, granitcides, y evaporitas. Las anomalías negativas responden, fundamentalmente, a la presencia de depresiones rellenas con rocas sedimentarias, y a la presencia o proximidad de granitoides y/o serpentinitas. En el campo gravimétrico residual, análisis, se reconocen sistemas anulares (semianulares) de anomalías (positivas y/o negativas) que se relacionan, al parecer, con estructuras morfotectónicas de distintos tipos.

Las anomalías aeromagnéticas positivas de mayor intensidad y extensión, frecuentemente dispuestas en forma de cadenas, responden a la presencia o proximidad de ultramafitas poco serpentinizadas, mafitas, granitoides, o rocas scarnizadas. Las anomalías negativas con iguales características responden, fundamentalmente, a la presencia de serpentinitas, o depresiones lineales con potentes espesores de rocas sedimentarias. El carácter de mosaico del campo aeromagnético residual resulta característico para las zonas de ultramafitas y mafitas afloradas, o muy proximas a a superficie. Del mismo modo, el carácter moteado, regularmente, es indicativo de la presencia o proximidad de vucanitas (fundamentalmente, de composición medio-básica). Dentro de las zonas de desarrollo de estas rocas, se reconocen sistemas anulares (semianulares) de anomalías, como regla, con un centro de anomalías negativas, y una zona exterior de anomalías positivas, los cuales se relacionan, probablemente, con estructuras morfotectónicas de carácter magmatógeno.

A modo de resumen, en la Tabla 1, se presenta la caracterización gravimétrica y aeromagnética (campo residual) - de algunos complejos recosos y estructuras morfotectónicas.

SOBRE LA INTERPRETACION GEOLOGICA DE LAS ANOMALIAS AEROGAMMA-ESPECTROMETRICAS

Debido a las condiciones climáticas de Cuba, la contribución fundamental al campo aerogammaespectrométrico está dada por la cortezas de intemperismo y los suelos, desarrollados, en mayor o menor grado (generalmente en condiciones autóctonas) sobre los distintos complejos rocosos. El estudio de la relación espacial de las anomalías aeroespectrométricas (U, Ra, Th y K) con la cortezas de intemperismo (y suelos correspondientes), permition establecer, al menos, en un nivel empírico, la probable vinculación las anomalías con la concentración de distintos óxides en los primeros horizontes del perfil de la corteza (suelo). De acuerdo con este resultado se plantea que:

-en general, una evolución prolongada de las cortezas (y suelos correspondientes) condiciona el enriquecimiento de Fe_2O_3 y Al_2O_3 en los primeros horizontes, favoreciendo así su capacidad para la retención del (Ra) y el Th en migración. En dependencia del predominio de uno de estos óxodos, la naturaleza de la anomalía tendra un carácter thoric-uranífero (Fe_2O_3) o urano-thorífero (Al_2O_3).

-la cortezas (y suelos correspondientes) desarrolladas sobre rocas calcáreas fosfatadas, tienen, como regla, una naturaleza uranífera, la cual puede tener su causa en la concentración superficial de P_2O_5). Igual naturaleza presentan los suelos Calizos Rojos y Latosólicos Típicos, desarrollados sobre calizas duras, pero aquí la causa se atribuye, probablemente, a la fertilización (aplicación de superfosfatos). En estos suelos (históricamente cultivados con cana de azúcar) los contenidos de Fe_2O_3 y Al_2O_3 son altos. Ambos

Tabla I. Caracterización gravimétrica y aeromagnética de los principales complejos rocosos y estructuras morfotectónicas.

DESCRIPCION GEOLOGICA.	CARACTERIZACION	
	GRAVIMETRICA	AEROMAGNETICA
Complejos ultramáfico-máfico y máfico.	Cadenas de anomalías residuales positivas (0-6 mgal)	Cadenas de anomalías residuales, fundamentalmente, positivas (50-500 nT). Campo residual tipo "mosaico" para las zonas afloradas o muy próximas a la superficie.
Complejo de granitoides.	Cadenas de anomalías residuales negativas (0-2 mgal). Cadenas de anomalías residuales positivas (0-4 mgal). Campo residual indiferenciado	Zona de mínimos del campo total anómalo. (+50-200nT). Cadenas de anomalías residuales positivas (50-300nT). Campo total anómalo de valores positivos bajos (0-100 nT) con un carácter moteado.
Complejo vulcanógeno-sedimentario (fundamentalmente, de composición medio-básico.)	Dentro de máximos regionales.	Campo residual moteado para las zonas afloradas o muy próximas a la superficie. Campo total anómalo > 100nT.
Complejo metamórfico meridional	Faja de mínimos gravimétricos regionales.	Campo total anómalo poco diferenciado de valores negativos bajos (0-100 nT).
Complejos sedimentarios.	Campo residual indiferenciado	Ausencia de anomalías residuales (> 50 nT).
Estructuras anulares de caracter magmatógeno.	Dentro de máximos regionales.	Sistemas anulares (semianulares) de anomalías positivas con un centro de anomalías negativas.
Estructuras anulares de caracter tectónico y no establecido.	Sistemas, anulares (semianulares) de anomalías residuales, positivas y/o negativas.	Campo indiferenciado.
Depresiones superpuestas.	Cadenas de anomalías residuales negativas (0-2 mgal).	Cadenas de anomalías residuales negativas (0-200 nT). Campo total anómalo <- 100 nT.

óxidos son grandes fijadores del fosfato, lo que dificulta su asimilación por las plantas. Se requiere entonces de una frecuente fertilización, la cual conlleva a una sobresaturación de P_2O_5 artificial en los primeros horizontes del perfil.

- las cortezas (y suelos correspondientes) desarrolladas sobre rocas predominantemente terrígenas, con abundancia de areniscas arcosicas, polimicticas, cuarzo-feldespáticas, aleurolitas carbonosas, y otras, tienen, como regla, una naturaleza potásica, la cual se explica por la acumulación de K_2O en los primeros horizontes del perfil. Lo mismo ocurre para las cortezas (y suelos correpondientes) poco evolucionadas, desarrolladas sobre rocas igneas intrusivas de composición ácido-media-alcalina (litomarge), así como sobre rocas máfico-alcalinas y vulcanogenas ácido-acalinas. Se conoce también que algunos suelos calizos pardos desarrollados sobre rocas calcáreas pobres en K_2O artificial, pudiera explicar entonces la contribución aumentada en este elemento para algunas localidades. Debe señalarse, además, que el fácil lavado y transporte del K_2O condiciona, en ocasiones, su concentración a lo largo de corrientes de agua depresines lineales del terreno que le sirven como cursos intermitentes.

- la cortezas (y suelos correspondientes) poco evolucionadas, desarrolladas sobre rocas con distintos tipos de alteraciones secundarias se reconocen, en ocasiones, por una contribución anomala (diagnostica) en algunos de los canales espectrométricos. Como ejempos, podemos citar: la naturaleza predominantemente uranífera de los sombreros de hierro; a naturaleza predominantemente potásica de muchas metasomatitas; y la naturaleza predominantemente thorifera de los sombreros de pirolusita.

- se reconocen por una contribución notablemente disminuida en todos los canales espectrométricos, las cortezas (y suelos correspondientes) poco evolucionadas, desarrolladas sobre rocas ultramáficas (y máficas) y sobre vulcanitas de composición medio-básica, así como las desarrolladas en sectores con conetraciones locales de SiO_2 y/o CO_3Ca.

En lo que respecta al canal total, su intrínseca naturaleza holística (integradora) favorece su utilización para la cartografía general del terreno, incluyendo a la cartografía geológica.

SOBRE LA REGIONALIZACION DE LOS CAMPOS GRAVIMETRICO Y AEROMAGNETICO Y SU INTERPRETACION GEOLOGICA

Algunos do los resultados de la interpretación geológica en base a la regionalización conjunta (visual) de los campos gravimétrico y aeromagnético, son presentados de forma simplificada en el esquema de la Fig. 1. En el mismo se ha minimizado, con toda intención, la carga tectónica, con el propósito de resaltar las regularidades en la distibución de distintos complejos rocosos, así como algunas estructurals morfotectónicas bien manifestadas en los campos físicos. Para la delimitacíon de los distintos complejos y estructuras se consideraron los criterios geofísicos resumidos en la Tabla 1. En lo relativo desciframiento de la tectónica disyuntiva, realizado, fundamentalmente, en base a los datos aeromagnéticos se revela un cuadro general de intenso desmembramiento, típico para una compleja geología alpina.

Partiendo de la generalización del esquema cartográfico referido (Fig. 1), se delimitan las principales unidades o bloques geólogo-geofísico (Fig. 2) y se establece su posible relación con la interpretación del cuadro geólogo-estructural de Cuba.

Unidad Pinar del Río

Esta compuesta por un complej carbonatado-terrígeno mesocenozoico con apariencia de cuña tectónica. A juzgar por el patrón de distrubución semianular de las anomalías gravimétricas residuales, parece constituir un domo regional elíptico deformado. La constitución paticular y la posición de esta unidad (formando un ángulo aproximado de 120^o con respecto a la dirección principal cubana), hace pensar en un brazo o rift abortado (aulacogeno) de una antigua unión triple. El límite meridional de esta unidad lo constituye la falla Pinar, interpretada como una falla transcurrente siniestra. Las rocas ultramáficas y máficas con que contacta este complejo, al norte, y supuestamente al sur, tienen una distribución lineal alargada, lo que hace suponer que puedan estar suturada. Analizando la correspondencia existente entre el cambio de la dirección del cordon ultramafítico-mafítico norte, con la distorsión en la configuración elíptica de la supuesta estructura dómica, (en la porción oriental donde ambos complejs rocosos contactan entre sí) surge la idea, de que la unidad Pinar del Río se comprimió cntra el borde de la plataforma de Bahamas producto de la colisión (desde el sur) de otro bloque continental.

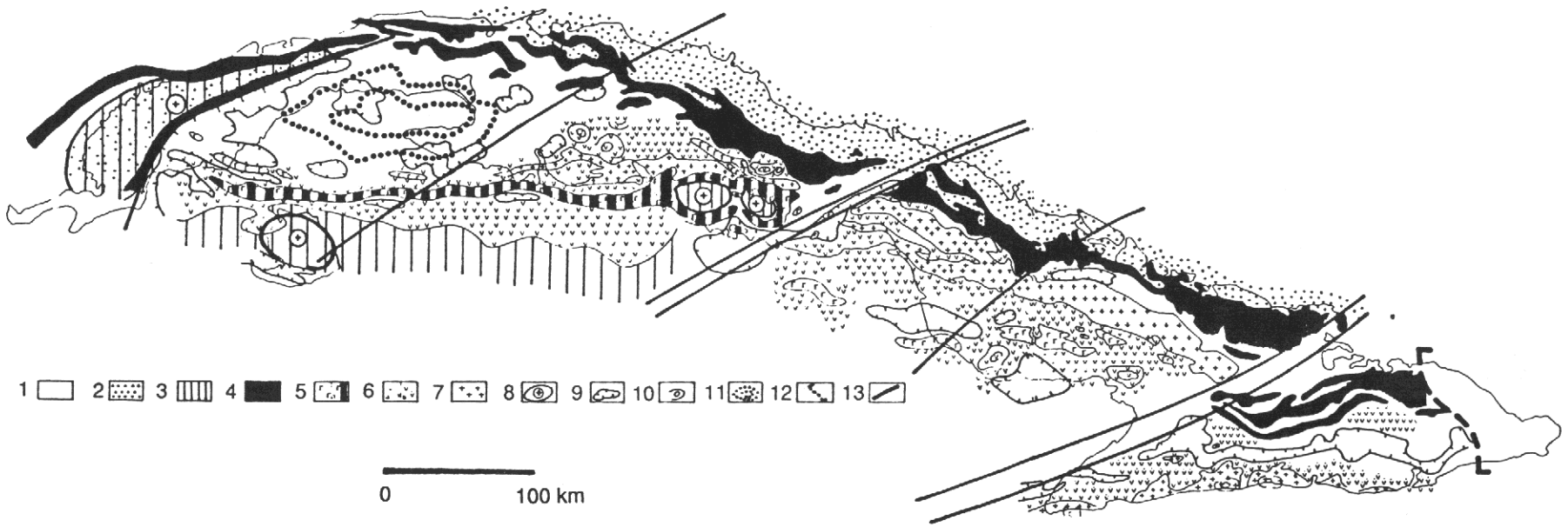

Fig. 1 Esquema interpretativo geólogo-geofísico (simplificado) en base a la regionalización conjunta (visual) de los campos gravimétrico y aeromagnético. (1) Rocas sedimentarias de la cobertura N-Q; (2) Rocas sedimentarias del margen continental de la Plataforma de Bahamas; (3) Rocas metamórficas; (4) Rocas ultramáficas-mafíticas; (5) Rocas mafíticas; a) supuestamente de la base del arco volcanico cretácico; (6) Rocas vulcanógeno-sedimentarias: a) del complejo de Arco Insular Paleógeno; (7) Granitoides; (8-11). Estructuras morfotectónicas: (8) Domos regionales; (9) Depresiones superpuestas; (10) Estructuras vulcano-tectónicas (plutónicas); (11) Configuración aproximada de la región central (núcleo) del "Macizo de Batabanó"; (12) Límite del territorio noestudiado; (13) Fallas transcurrentes.

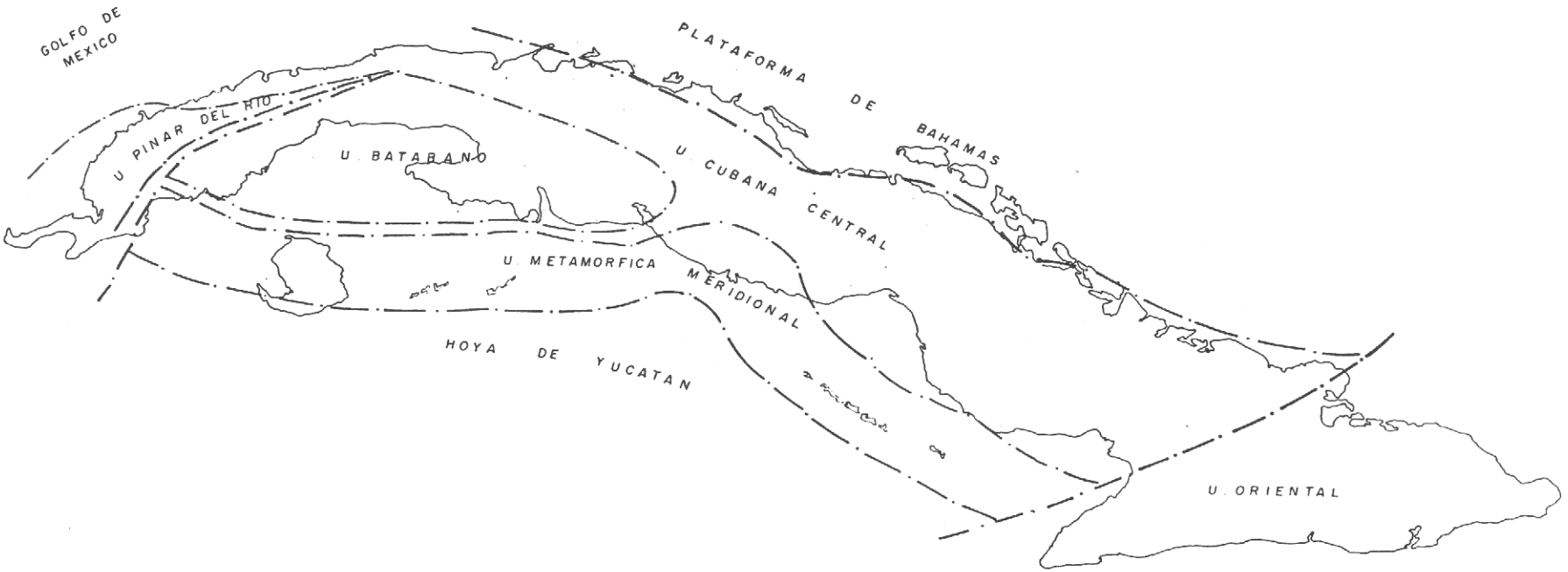

Fig. 2. Esquema de localización de las unidades geólogo-geofísicas propuestas.

Unidad Batabanó

Constituye un bloque con la forma aproximada de un gran triángulo isósceles, el cual controla gran parte del cuador geólogo-geofísico de las provincias occidentales. Desde el punto de vista geológico, se interpreta como un antiguo macizo, presumiblemente continental, enterrado ("Macizo de Batabanó"). La actual coincidencia espacial de un mínimo local del espesor de la corteza terrestre (por datos sismológicos y gravimétricos; Sousin y Sousina, 1988) con una nomalia local del geoide (por datos altimétricos de radar; Bowin, 1980), otorgan un carácter singular (único) a este bloque, y permiten suponer la ocurrencia de un proceso de basificación relacionado con un posible acercamiento local del manto. La aparente configuración triángular de esta unidad pudiera relacionarse con la supuesta unión triple antes referida. Su flanco meridional contacta, al parecer tectónicamente, con la Unidad Metamórfica Meridional. La presencia de un cinturón lineal y estrecho de rocas supuestamente mafíticas, (2 ultramafíticas?), que se extienden con rumbo sublatitudinal desde las immediaciones al sur de la ciudad de Pinar del Río hasta la provincia de Sancti Spíritus, se interpreta coo la sutura resultado de la colisión de dos bloque continentales: el "Macizo de Batabanó" y el Bloque Metamórfico Meridional. Con este cinturón mafítico (ultramafítico?) deben también relacionarse las rocas que presumiblemente corresponden a la base del arco volcánico cretácico, las cuales afloran en el extremo oriental del referico cinturón representadas por el complejo anfibolítico Mabujina. Como resultado de la mencionada colisión, debió ocurrir, posiblemente, la compresión y volcamiento de las secuencias del complejo de Arco Insular Cretácico en ambos sentidos, hacia el norte y hacia el sur, respectivamente, sobre el "Macizo de Batabanó" y sobre el Bloque Metamórfico Meridional. Con posterioridad, estas secuencias fueron recubiertas por depósitos neogénicos. Por la inerpretación de los datos gravimétricos, el bloque de Batabanó se concibe estructuralmente hundido (y adelgasado) en su parte central (núcleo), la cual presenta una configuración elíptica de grandes proporciones. Hacias los flancos, el macezo de Batabanó, presumiblemente, se extiende mucho más allá de los límites de la estructura elíptica mencionada. Cabria suponer entonces, que el cambio notorio de dirección del cinturón de granitoides con respecto a la dirección del cinturón ultramafítico-mafítico en los límites de las provincias Villa Clara y Cienfuegos (en toda la porción centro-oriental ambos con subparalelos) pudiera estar determinada por la terminación oriental, en forma de cuña, de este bloque. Analogamente, el aumento del espesor de la corteza terrestre (por datos sismológicos y gravimétricos; Sousin y Sousina, 1988) en las regiones de la Ciénaga de Zapata y de la Unidad Pinar del Río pudiera explicarse considerando que el basamento de las secuencias afloradas en estas dos regiones corresponde, al menos parcialmente, a este bloque.

Unidad Metamórfica Meridional

Por la interpretación de los datos gravimétricos y aeromagnéticos, este bloque de características continentales, se extiende con rumbo sublatitudinal, al menos entre los macizos metamórficos de la Isla de la Juventud y del Escambray, enlazando ambos macizos. Al norte contacta, presumiblemente de forma tectónica, en su extremo occidental, con la Unidad Cubana Central. Recubren parcialmente este bloque, supuestamente de forma tectónica (producto de la colisión), rocas vulcanógeno-sedimentarias del complejo de Arco Insular Cretácico en la Isla de la Juventud (Sabana Grande), y rocas del mismo complejo y el complejo anfibolítico en el Escambray. Los afloramientos del compejo metamórfico, al menos en los macizos de la Isla de la Juventud y el Escambray, se interpretan como ventanas tectónicas con apariencia cupular, desarrolladas, presumiblemente, como domos diapíricos regionales. Al sur esta unidad limita con la Hoya de Yucatan. Por el oeste contacta, presumiblemente de forma tectónica, con la Unidad Pinar del Río, y por el este, se extiende, al parecer cubierto por rocas vulcanógeno-sedimentarias del complejo de Arco Insular Cretácico y otros complejos más jóvenes, hasta la región oriental, pudiendo estar allí representada por las metamorfitas carbonato-terrígenas del extremo oriental del macizo del Purial.

Unidad Cubana Central

Se extiende desde la provincia de Pinar del Río hasta la provincia de Holguín, limitando: por el este, con la Unidad Oriental; por el norte, fundamentalmente, con la Plataforma de Bahamas; y por el sur, en su parte occidental, con las unidades Pinar del Río y Batabanó, y en su parte centro-oriental, con el Bloque Metamórfico Meridional. Esta unidad está constituida, básicamente, por el apilamiento tectónico de tres complejos estructuro-formacionales; de norte a sur: el complejo sedimentario del margen continental de la Plataforma de Bahamas, el complejo ultramafítico-mafítico, y el complejo de Arco Insular Cretácico. La manifestación en los campos geofísicos de sobre corrimientos respectivos de estos tres complejos de sur a norte, así como de los desplazamientos del bloque (en

igual dirección) en forma escalonada a lo largo de fallas transcurrentes siniestras (Isla de la Juventud-Rancho Veloz, L Troch, Camagüey, y Oriente), atestiguan sobre la colisión (desde el sur) del Bloque Metamórfico Meridional con el complejo de Arco Insular Cretácico, contra el margen continental de la Plataforma de Bahamas. El referido escalonamiento paece estar condicionado por las proprias irregularidades del frente de choque.

Unidad Oriental

La presencia de una brusca disminución del espesor de la corteza terrestre (por datas gravimétricos y sismológicos; Sousin y Sousina, 1988) a la cual se asocia una intensa anomalía local del geoide (por datos altimétricos de radar; Bowin, 1980), determinan la separación de esta unidad como un bloque independiente. Sus límites: al norte y al este con el Océano Atlántico; al sur con la Fosa de Bartlet, y al oeste con la Unidad Cubana Central, a través de un sistema de fallas transcurrentes, al parecer, siniestro. En lase de la interpretación de los datos gravimétricos y aeromagnéticos, la parte centro-septentrional de esta unidad, se compara, desde el punto de vista composicional, con el bloque anterior. En la parte meridional, estan presentes las rocas de complejo de Arco Insular Cretácico y ultramafítico-mafítico. A juzgar por los datos geofísicos, la estructuras asociadas al arco paleógeno pudieran estar presentes también al sur de la costa meridional de la provincia de Camagüey.

SOBRE LA INTERPRETACION METALOGENICA

El esquema geólogo-estructural confeccionado en base de la interpretación de los datos geofísicos (Fig. 1), toda vez que refleja la distribución y desarrollo de los principales complejos estructuro-rocosos, puede ser utilizado para la regionalización estructuro-metalogénica de Cuba. Con tal propósito se realizó la identificación de dichos complejos con los correspondientes estructuro-metalogénicos, reconocidos en el Esquema de Regionalizacion Metalogénica de Cuba en escala 1:2 500 000 (Cabrera, y otros, 1988):

Complejos Continentales (Pb, Zn, Cu, Au, W, Al)

-Complejo de rocas sedimentarias del margen continental de la Plataforma de Bahamas.

-Complejo de rocas metamórficas que componen el Bloque Metamórfico Meridional.

Complejos Oceánicos (Cr, Cu)

-Complejo de rocas ultrabásicas y básicas que componen el (¿s?) cinturón ultramafítico-mafítico cubano.

-Complejos de Arco Insulares (Cu, Fe, Mn, Pb, Zn, Au, Ag)

-Complejo de rocas vulcanógeno-sedimentarias y granitoides del Arco Insular Cretácico.

-Complejos de rocas vulcanógeno-sedimentarias y granitoides del Arco Insular Paleógeno.

Complejos de cobertura (Ni, Fe, Co, Au, Cr, Al, Mn)

-Complejo de rocas sedimentarias de la cobertura neogenocuaternaria.

REFERENCIAS

Bowin, C.,1982, Gravity and geoid anomalies of the Caribbean: Transactions, 9th Caribbean Geological Conf. , Santo Domingo, 1980.

Cabrera R., R. Lavandero, J.L. Kramer, y otros, 1988, Esquema de regionalización metalogénica de Cuba en escala 1:2 500 000; recuadro del Mapa Metalogénico de Cuba en escala 1:500 000: (original de autor - inédito), Instituto de Geología y Paleontología, La Habana, 1988.

Pardo, M., 1982, Investigaciones geofísicas regionales para minerales sólidos en la República de Cuba: (inédito), Instituto de Geología y Paleontlogia, La Habana.

Pardo, M., V. Bello, H. Amador, y otros, 1987, Nota explicativa de la base geofísica del Mapa metalogénico de Cuba en escala 1;500 000: (inédito), Instituto de Geología y Paleontología, La Habana, 33 p.

Susin, O.A. y E.A. Susina, 1988, Breve resumen y análisis del esquema de relieve de la superficie de Mohorovicic de la región Caribe-Mexicana y de Cuba, y la evaluación de su influencia gravitacional: (inédito), Instituto de Geología y Paleontología, La Habana 19 p., 1988.

GEOQUIMICA DE LA ASOCIACION OFIOLITICA DE CUBA

E. Fonseca[1], F. Castillo[1], A. Uhanov[2], M. Navarrete[3] and G. Correa[1]

[1]Instituto Geología y Paleontología, Ministerio de Industrias Basicas, La Habana, Cuba
[2]Instituto de Geoquímica y Química, Academia. de Ciencias, Moscú, URSS,
[3]Empresa de Geología. Ministerio de Industrias Basicas, Santiago de Cuba, Cuba

ABSTRACT

The ophiolites Cuba have two distinct modes of occurrence: 1) a discontinuous belt of ophiolite suites in northern Cuba, 2) isolated lenses or blocks within the metamorphic massifs in southern. Each of these occurrences have their own geochemical characteristics. Although the differences in the ultramafic components of the ophiolites are not significant, differences are apparent in the gabbroic rocks which suggests that they formed in different magma chambers. The basaltic rocks of the ophiolites exhibit a clear tholeiitic affinity.

(English abstract by Gren Draper)

INTRODUCCION

Las ofiolitas cubanas afloran en dos regiones principales; la primera y de major desarrollo corresponde al cinturón septentrional entre el margen continental y el arco volcánico cretacico (Fig. 1), y la segunda en fragmentos aislados asociados a los bloques metamórficos de la regíon meridional de Cuba - Guaniguanico, Isla de la Joventud, Escambray y Sierra del Convento (Fig. 1). En general ellas se caracterizan por la presencia de cuatro y a veces cinco complejos bien definidos, con una distrbución irregular, la que no está en dependencia de su grado de erosión, tectonismo o de su posición al norte o al sur del territorio nacional. Estos complejos son tectonitas, cúmulos ultramaficos y cúmulos maficos, gabros isotrópicos, diabasas y basaltos con sedimentos asociados.

CARACTERISTICAS GEOLOGICAS

Tectonitas Ultramáficas

Las tectonitas (complejos inferior de las ofiolitas) se distribuyen principalmente desde la región occidental hasta la región central del país. Por el Norte afloran en la Sierra de Cajalbana y sus alrededores, en las provincias de La Habana como aislados bloques mezclados con las secuencias del arco volcánico, en Villa Clara el complejo aflora como un melange unto conotros complejos de las ofiolitas.

En la parte septentrional de la región occidental de Cuba (Guaniguanico), las tectonitas afloran como bloques en harzburgitas intensamente tectonizadas en el contacto de la falla Pinar y en aislados bloques en la Sierra del Rosario.

En el Escambray ellas aparecen de igual forma, pero con alto grado de antigoritización (Somin y Millán, 1981). Hacia la región de Camaguey el dominio de este complejo va disminuyendo y empieza el predominio del complejo cumulativo. En Holguín, las tectonitas y los cumulos aparecen muy mezclados tectonicamente, pero con una marcada supremacía del complejo inferior (Andó y otros, 1988). En la región de la Sierra Nipe-Cristal, en el denominado macizo Mayarí coexisten espacialmente distribuídos los dos complejos en áreas independientes, en la parte occidental afloran las tectionitas u limitados por una falla diagonal de dirección SW-NE aparecen los cúmulos en la parte oriental (Sagua de Tánamo).

Larue, D.K., and Draper, G. (eds.),
Transactions of the 12th Caribbean Geological Conference, St. Croix, U.S.V.I., Miami Geological Society, P.O. Box 431552, South Miami, FL 33243, U.S.A

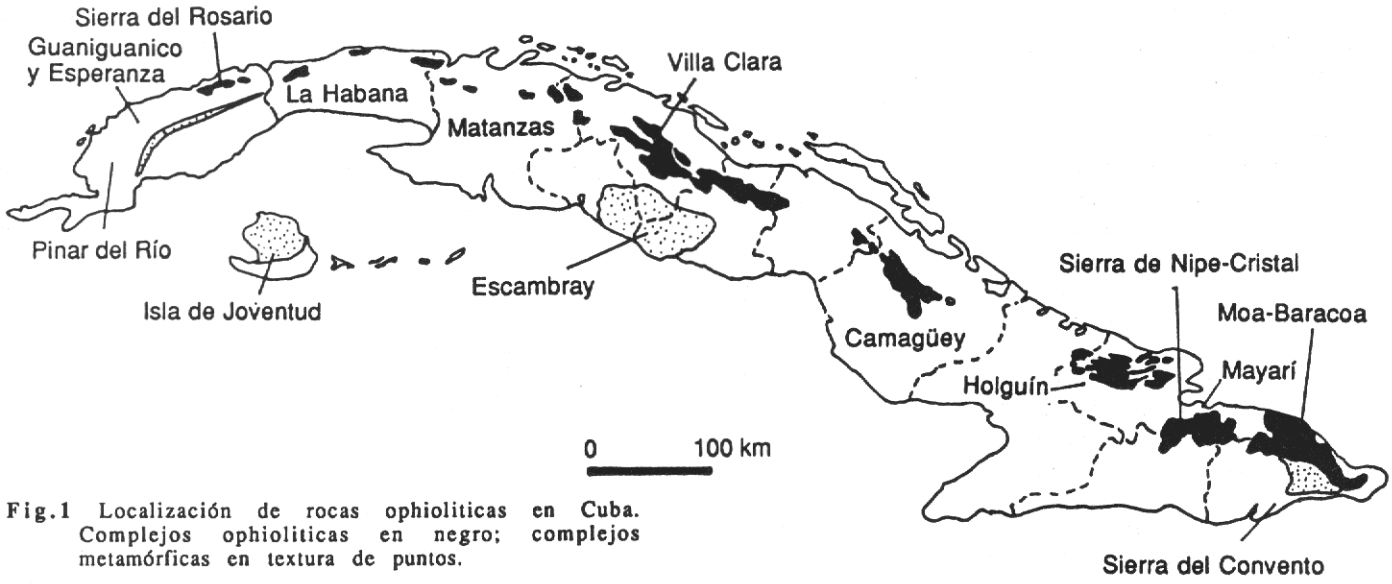

Fig.1 Localización de rocas ophioliticas en Cuba. Complejos ophioliticas en negro; complejos metamórficas en textura de puntos.

En Moa-Baracoa solo se han encontrado escasos afloramientos, que por las características estructurales se puede suponer su pertencia al complejo inferior.

En la Sierra del Convento afloran bloques de ultramafitas y gabros con alto grado de metamorfismo, lo que no ha permitido, hasta el momento establecer la pertenencia a las tectonitas o cúmulos (Teperin y Heredia, 1980).

Complejos cumulativos

El complejo cumulativo según lo expresado anterormente se distribye principalmente desde la región de Camaguey hasta Baracoa. Este complejo presenta particularidades estructurales, petrológicas y mineralógicas diferentes entre el cinturón septentrional y el meridional.

En la región de Pinar del Río en el contacto entre las zonas estructurales Guaniguanico y la Esperanza se observan escasos bloques de este complejo con mayor aflorabilidad de su parte superior (gabros, gabross olivínicos y troctolitas).

En la región de Villa Clara los cúmulos afloran como bloques al No de la región de Mabujina, con burna ritmicidad representada por troctolitas, pironxenitas, gabroides. Las piroxenitas aparecen como diques y como capas en este complejo (Millán comunicaión personal). El desarrollo y la ritmicidad de los cúmulos es diferente en Camaguey, Holguín y Moa-Baracoa. En la primera es notable la amplia distribución del complejo cumulativo ultrámafico (harzburgitas, dunitas, dunitas enstatícas) en menor grado el máfico (anortositas, gabros olivínicos, gabros). Las troctolitas aquí forman diques disordantes a los cúmulos (Haydutov y otros, 1981).

En Holguín los cúmulos ultramáficos están representados pro lherzolitas, dunitas, harzburgitas y el máfico se inicia con la transición de peridotitas plagioclásicas, troctolitas, gabros olivínicos y gabros hornbléndicos, concapitas de hornblenditas, estas últimas dan al corte características petrográficas diferentes al resto de los complejos cumulativos del país.

En Moa-Baracoa los cúmulos ultramáficos y maficos están bien desarrollados. En la parte inferior, se alternan las harzburgitas, ortopiroxenitas, dunitas, dunitas enstatíticas, pasando gradualmente a peridotitas plagioclásicas, troctolitas y gabros olivínicos.

Complejos Gábricos

El complejo gábrico propiamente dicho representado por gabros masivos isotrópicos con un tipo de piroxeno (clinopiroxeno)- aparece en Cuba independientemente de la presencia o no de los cúmulos máficos, en algunas oportunidades su presencia va acompañada por numerosos diques concordantes o discordantes a la pseudo-estratificación cumulativa.

En la región donde el desarrollo de los cúmulos es escaso, afloran abundantes cuerpos de gabroides (P. del Río, La Habana, Villa Clara, parte occidental del macizo Mayarí en Oriente. Es interesante notar que generalmente en estas mismas regiones, estos gabros están cortados por

diques de diabasas de dos sistemas, el primario: pseudoparalelo y el secundario discordante al anterior. Este sistema de diques ha sido descrito por muchos autores (Fonseca et al, 1985: Iturralde-Vinent, 1986; Andó y otros, 1988) como el llamado complejo de diques paralelos de diabasas, pero es claro que este no representa un complejo clásico segun la literatura.

Diabasas y basaltos

Las diabasas están presentes en todo el cinturón ofiolítico tanto al norte como al sur, pero exceptuando a los diques descritos anteriormente, estas rocas aparecen en general como bloques masivos, con contactos tectónicos entre los diferentes complejos ofiolíticos. El complejo superior de las ofiolitas, está representado por basaltos y sedimentos pelágicos asociados, estas rocas afloran en todo el cinturó ofiolítico septentrional, con diferentes espesores. En los bloques meridionales estas rocas están metamorfizadas hasta anfibolitas, su origen oceánico o de arco insular es discutido por algunos autores Millán y Haydutov, comunicación personal).

Los basaltos y sedimentos asociados espacialmente a las ultramafitas y relacionados por algunos autores (Fonseca y Zelepuguin, 1981: Iturralde-lVinent y otros, 1986; Andó y Navarrete, 1988) como el cuarto complejo de dicha asociación, están caracterizados como unidades litoestratigráficas en los diferentes bloques ofiolíticos del cinturón septentrional. En Pinar del Río, al norte de la Sierra del Rosario, la Formación Encrucijada aparece como una franja alargada muy tectonizada y representada por basaltos en almohadillas con hialoclastitas, silicitas y sedimentos pelágicos, de edad Ap-T.

Esta unidad aún debe ser subdividida ya que por sus características geoquímicas algunos niveles de lavas se acercan más a los basaltos del arco volcánico y otros son correlacionables con los de tipo ofiolítico (Fonseca, 1988).

En las formaciones de La Habana, los efusivos ofiolíticos aún no están cartografiados, pero se han encontrado basaltos oceánicos en los bloques alóctonos de la Formación Chirino (Arco volcánico cretácico, además es importante señalar que conjuntamente con basaltos y diabasas en contacto tectónico afloran boninitas, que supustamente representan la base del arco volcánico en esta región.

En Matanzas los basaltos corresponden a la Formación Margot, con características muy similares a Encrucijada, incluso en edad. En Villa Clara aparece la Formación Zurrapandilla, la que en proporción contiene más diabasas que basaltos Hatten, 1958; Zelepugin y otros, 1985). En Camaguey estos basaltos no afloran y han y han sido descritos por datos de pozos (Iturralde-Vinent y otros, 1986) como "Basitas Albaiza". En Holguín la nueva Formación Bariay representa a estos basaltos (Andó y Naverrete, 1988).

En la región oriental, aunque estos no están cartografiados afloran basaltos ofiolíticos en la parte norte del bloque Moa Biracoa (Torres y Fonseca, 1988).

GEOQUIMICA

Para realizar este estudio fueron recopiladas las mustras de los diferentes complejos en las regiones septentrional y meridional del país.

Las muestras de ultramafitas fueron analizadas por diferentes métodos en el Instituto de Geoguímica de la Academia de Ciencias de la URSS, y las de los complejos superiores fueron analizadas en los laboratorios del área geológica de Cuba.

Lo más complejo de este trabajo ha sido tratar de demostrar la pertenencia de las rocas ultramáficas, especialmente las dunitas y las harzburguitas a las tectonitas o a los cúmulos, debido a la complejidad tectónica con que ellas afloran.

De los complejos inferiores se utilizaron dunitas, harzburgitas, lherzolitas, dunitas-enstatíticas y sus serpentinitas, así como serpentinitas antigoríticas y crisotílicas.

En el gráfico de Skinner y otros (1978) se puede observar el carácter ofiolítico de todas las rocas ultramáficas de Cuba (Fig. 2). Las más empobrecidas en Ni, son las del Escambray, el resto presenta un comportamiento regular.

Para las rocas ultramáficas los elementos más discriminantes son el Cr, Ni, Co por una parte y por otral el Mg y Fe. También pueden servie para esta caracterización la suma de Al + Ti, (Fig. 3). Según este diagrama constuído con los valores en ppm, se puede observar que en línea decreciente por la relación Cr + Ni + Co las rocas transicionan en general desde dunitas, harzburgitas, lherzolitas y wherlitas y por último en el extremo opuesto aparecen los gabros.

En la linea Mg + Fe y Al + Ti las dunitas son igualmente las rocas con mayores contenidos de

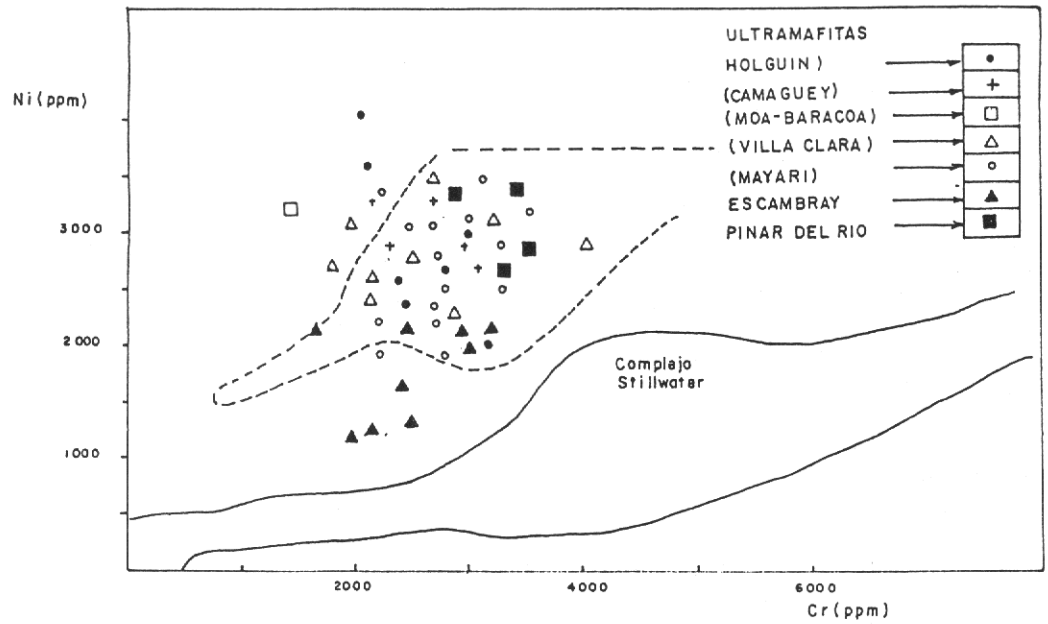

Fig. 2 Diagrama comparativo según Skinner e al. (1976), donde se incluyen las rocas ultramáficas de las tectonitas y los cúmulos.

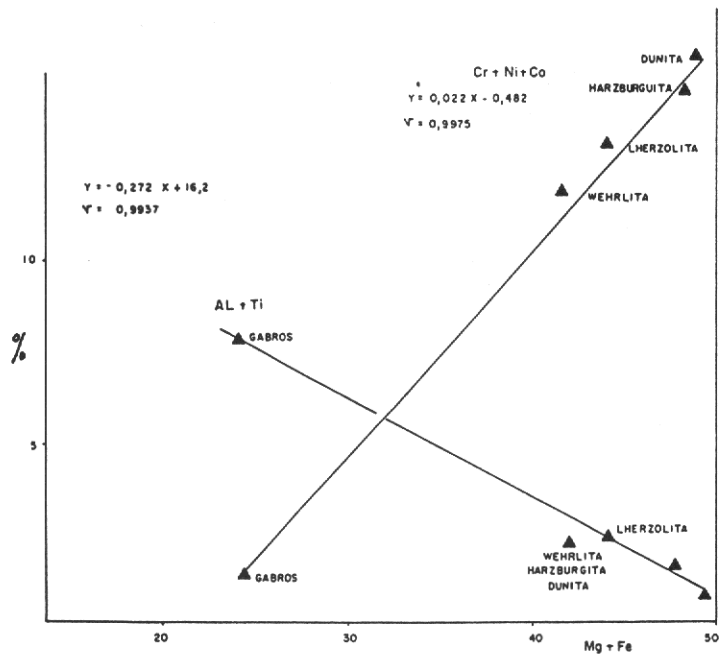

Fig. 3 Gráfico de compartamiento promedio para los principales elementos de las ultramafitas y los gabroides de Cuba.

estos elementos siguéndolas las harzburgitas, lherzolitas y por último las werhlitas que se separan un tanto de esta línea por sus contendidos promedio. Al igual que en el caso anterior los gabros ocupan el extremo de la línea.

Al estudiar el comportamiento de las serpentinitas duníticas según las diferentes regiones podemos observar como ellas (Fig. 4) en Mayarí y Holguín tienen un comportamiento similar y a la vez algo diferente con las de Camaguey. Los elementos que se diferencian son Ti, V, Cr, Cu y Nb. Las rocas de las dos primeras regiones pertenecen principalmente al complejo ultramáfico metamórfico y las de Camaguey son cumulativas. El comportamiento del V y el Ti, el similar, ya qye ellos se enriquecen progresivamente hacia los complejos superiores de las ofiolitas. Los contenidos promedio para otras regiones del mundo en estos elementos van desde 48 ppm en las tectonitas has 300 en los cúmulos; para el Ti y el V las varaiaciones son de 25 a 40 (Coleman, 1977). Las rocas cubanas presentan contenidos promedio de Ti de 45 ppm en las tectonitas hasta 700 ppm para los cúmulos y excepcionalmente suben los valores sobre 1000 ppm.

El vanadio por otra parte varía desde 40 hasta 130 aproximadamente. Este último elemento muestra un comportamiento interesante, no solo vertical en el corte ofiolítico, sino también lateral en el sentido geográfico, desde Occidente

hacia la parte Oriental de Cuba (Fig. 5). En este diagrama donde se unieron todas las ultramafitas, se observa un aumento de los contenidos de este elemento desde Villa Clara hacia Moa-Baracoa, especialmente en las lherzolitas, pero es interesante ver en las harzburgitas y en el promedio de todas ellas, el empobrecimento del elemento en Mayarí y el aumento brusco hacia Moa-Baracoa. Esto corrobora lo planteado por Fonseca y otros (1989), donde se expresa que en Mayari existe un prodominio del complejo inferior de las ofiolitas y también la cercanía de este bloque a su punto de origen en la zona del rift, caractrerizada por el quimismo de sus rocas y la posición de la mineralización cromitica. For otra parte las serpentinitas harzbugíticas desde Villa Clara hasta Moa-Baracoa, tienen un comportamiento muy similar (Fig. 6), solamente es interesante notar el mayor contenido de vanadio en estas últimas. En la regió de Moa-Baracoa se ha observado algún contendido de coulsonita (magnetita vanádica) entrecrecida con las menas cromíticas (Santa Cruz y otros, 1988), lo que pudiera influenciar tambíen en el contenido de este elemento en las rocas ultramáficas de la región.

Los valores de niobio en las harzburgitas y en las dunitas están dados por el mayor o menor grado de serpentinización, ya que en estas rocas la hidratación origina unenriquecimiento del elemento.

En el gráfico de la Fig. 7 se representan las variacines de los elementos para la región de Villa Clara, lugar en que se obtuvo una mayor

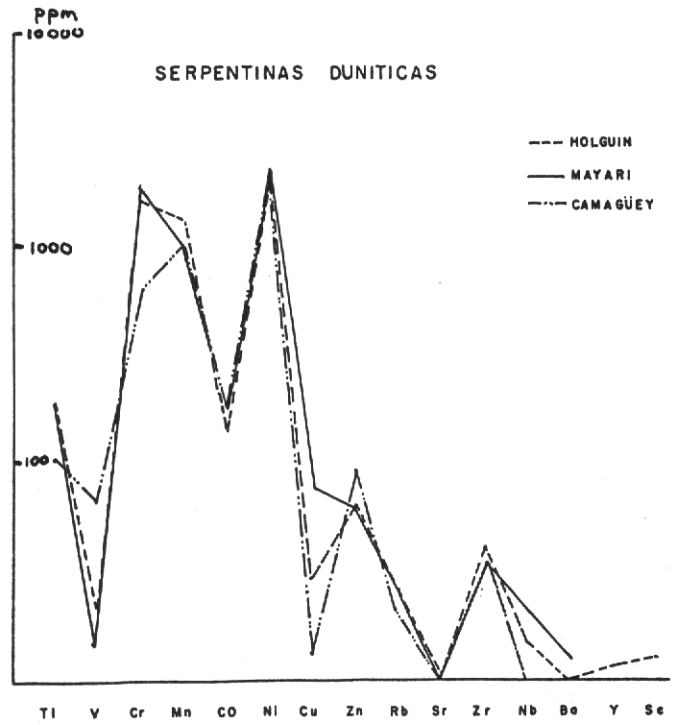

Fig. 4 Gráfico de variación de las serpentinitas dunítcas de tres regiones: Holguín y Mayarí (tectonitas), Camagüey (cumulativas).

variablilidad litológica. En general todas las rocas responden a un mismo patrón incluyendo las harzburgitas, las wehrlitas y las serpentinitas antigoríticas-crisotílicas del Escambray. Los gabros se utilizaron a modo de comparación, y es notable en ellos, el enriquecimiento en Ti, V, y Sr, así como el empobrecimiento en Cr, Ni, Co, Cu y anormalmente en Rb.

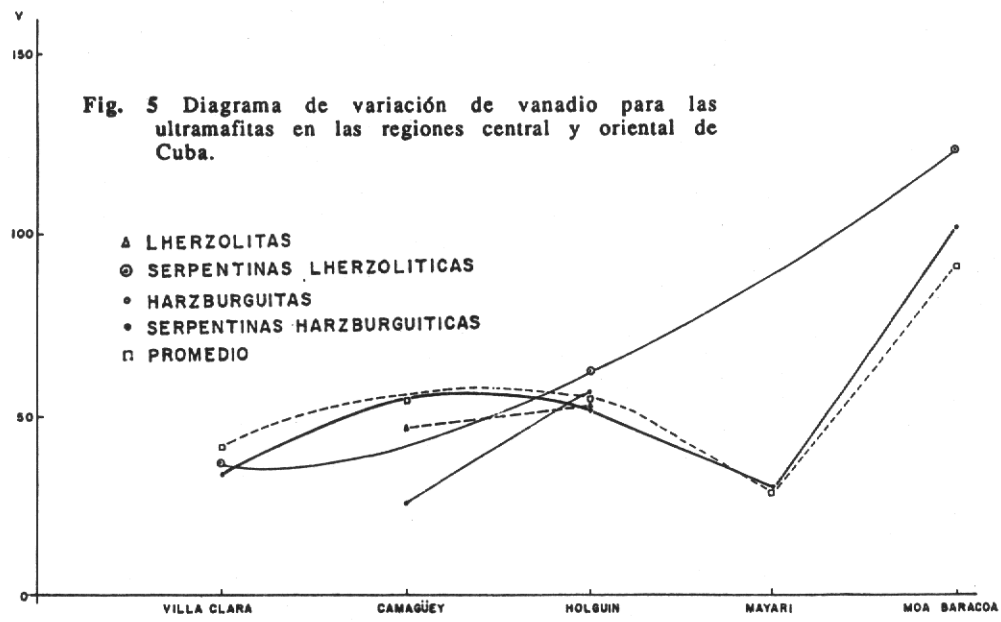

Fig. 5 Diagrama de variación de vanadio para las ultramafitas en las regiones central y oriental de Cuba.

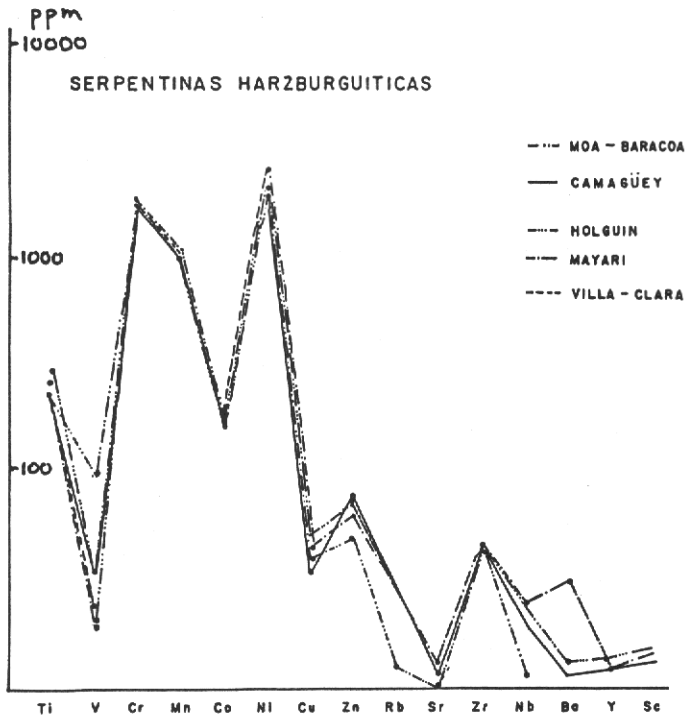

Fig. 6 Gráfico del contenido promedio de los principales elementos en las serpentinitas harzburgíticas de las regiones central y oriental de Cuba.

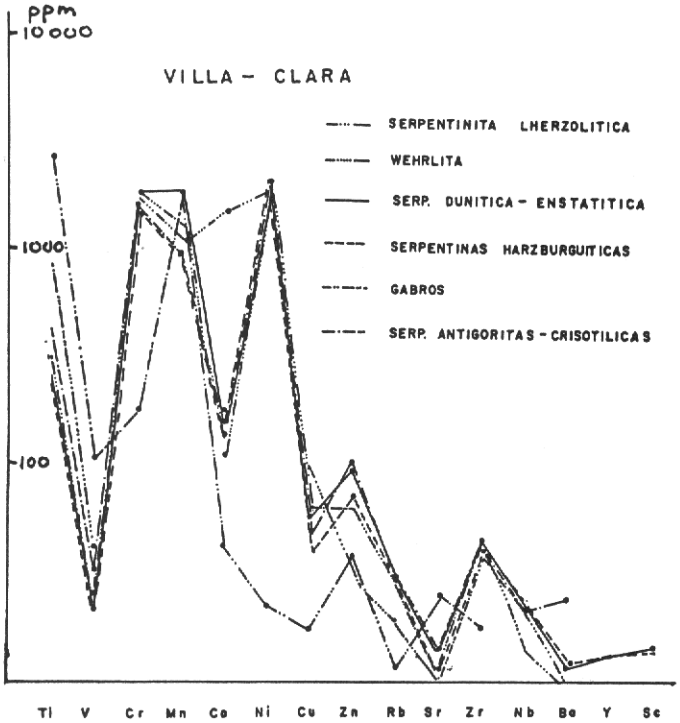

Fig. 7 Gráfico del compartamiento de las ultramafitas, de las tectonitas y los cúmulos en Villa Clara. Las serpentinitas antigoríticas-crisotílicas sn del Escambray.

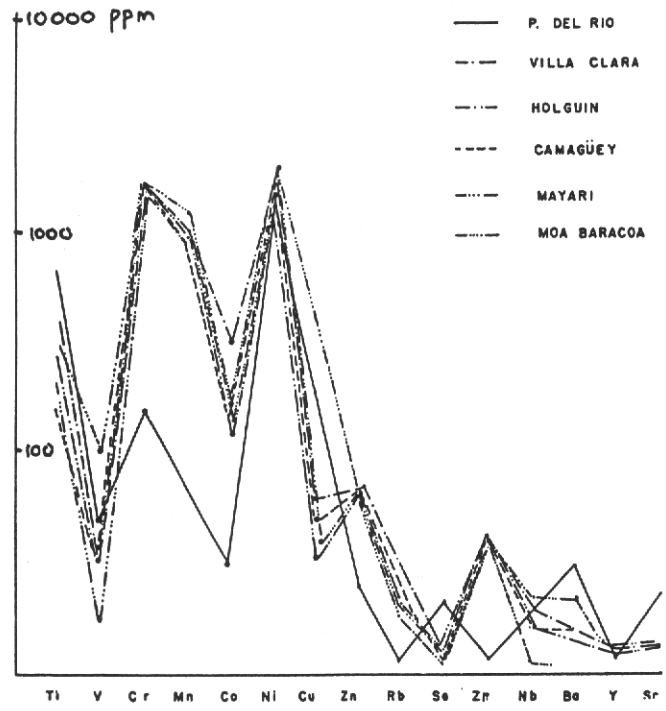

Fig. 8 Gráfico del contenido promedio de los elementos en las ultramafitas desde la región occidental hasta la oriental. Se observa la marcada diferencia en Pinar del Río.

La disminución de los elementos ferromagnesianos, como es conocido está dado por la cristalización fraccionada del olivino y de las familias de la enstatita y del diópsido tan abundantes en estas rocas. La enstatita e s junto con el olivino el mineral fundamental de estas rocas ultramáficas, pero debido a los intensos procesos tectónicos que ellas han sufrido en gernaral, se origina la deshidratación y por eso las rocas del Escambray (Mabujina) contienen major cantidad de talco, antigorita, tremolita-actinolita, observándose en ellas un empobrecimiento marcado del Ni, en comparación con rocas similares.

En el diagrama de la Fig. 8 se observa el comportamiento generalizado de todas las ultramafitas desde Pinar del Río hasta Moa-Baracoa notándose solo una diferencia en las rocas de Pinar, especialmente en los bajos contenidos de Cr, Co y Zn, así como los valores inversamente altos de Sc, Ba y Sr. Esto puede obedecer en el caso de los primeros elementos a que la composición del manto en esta región era algo diferente a la del resto de Cuba, posiblemente más cercana a las lherzolitas.

En el gráfico expuesto a continuación (Fig. 9) según Serri, 1982, el TiO_2 y la relación $FeO^{tot}/(FeO^{tot} + MgO)$ nos permite discriminar los

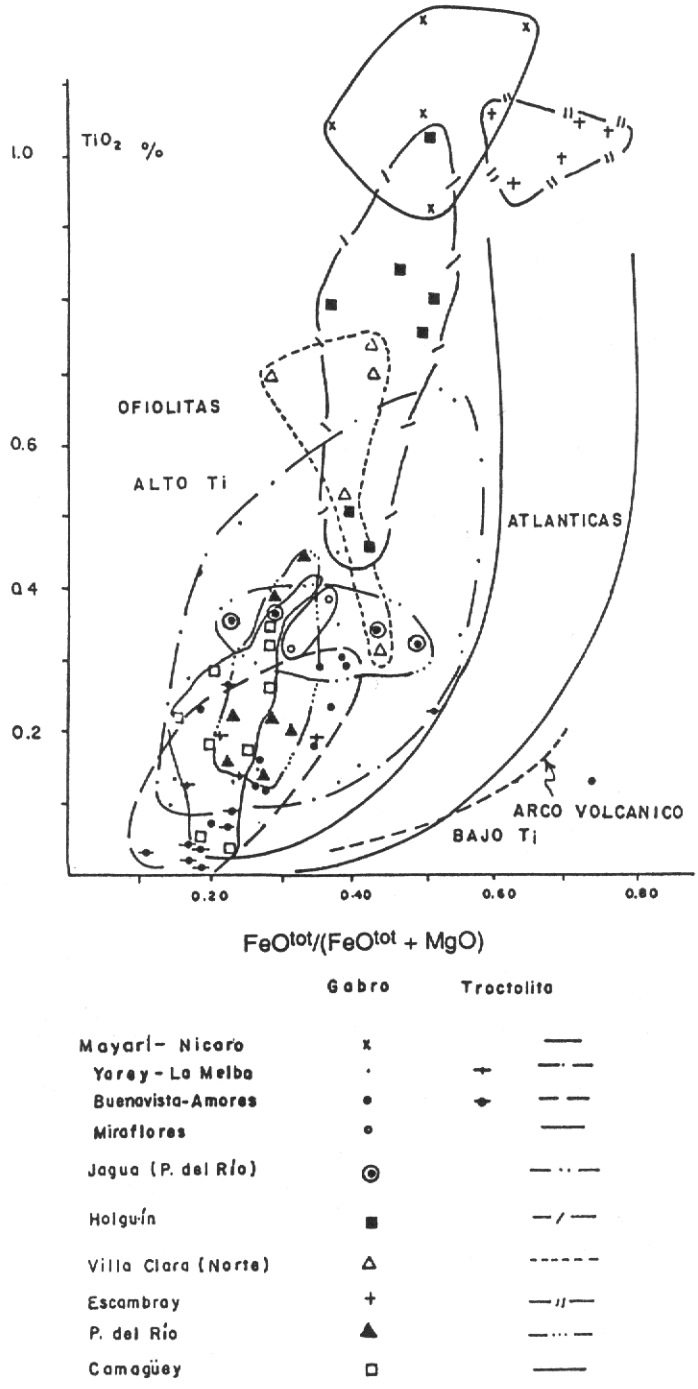

Fig. 9 Diagrama de Serri (1981) con las áreas de los cúmulos máficos y gabros isotrópicos para diferentes regiones de Cuba.

gabros ofiolíticos de los gabros de los arcos volcánicos. Aquí se tomaron todos los gabroides desde los que forman parte de los niveles superiores de los cúmulos hasta los gabros isotró que afloran en casi todo el cinturón sseptentrional y cuya presencia como se aclaró puede estar o no asociada con la aparación de los cúmulos. En general el desarrollo cumulativo en el territorio de Cuba, presenta interesantes variaciones geológicas desde Pinar del Río hasta Baracoa, como se ecplicó anteriormente.

Analizando el diagrama mencionado podemos ovservar un enriquecimiento progresivo de los contendidos de titanio desde Pinar del Río, Villa Clara, Holguín hasta Mayarí. En estas regiones excepto Holguín predominan los garos masivos.

En las áreas correspondientes a Camagüey y las diferentes zonas de Moa-Baracoa, donde los cúmulos afloran ampliamente, existe un solapamiento en la parte inferior del diagrama, donde los contenidos de Ti son menores. Los cúmulos de Mabujina (Escambray) ferromagnesianos, sin tomar en consideración las alteraciones que pueden originar este desplazamiento se puede suponer que los gabros de Mayarí y el Escambray son los más primitivos de todos ellos.

Del comportamiento de los gabroides se pudede concluir que ellos se han originado a partir de diferentes cámaras ígneas (criterio expuesto por Haydoutov para Camaguey) y que el magma

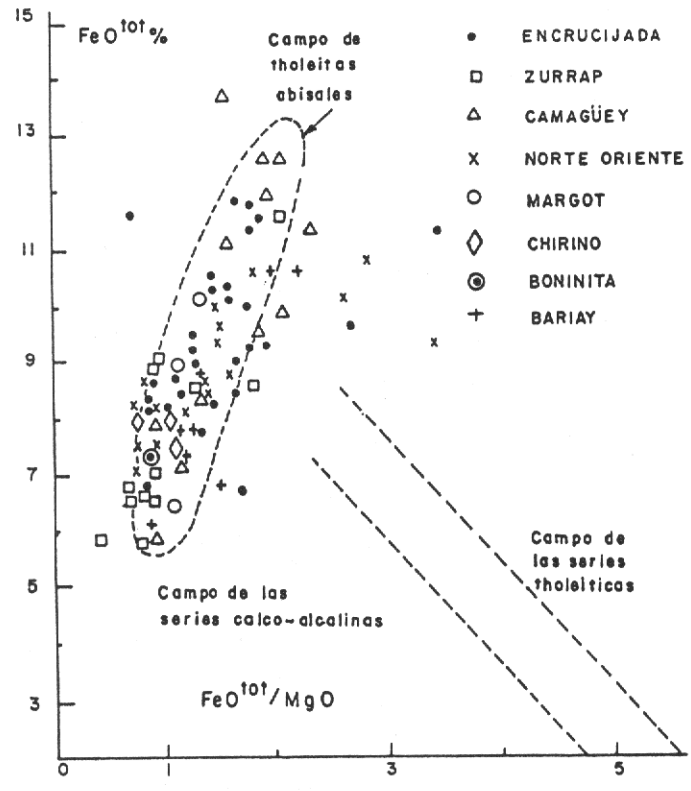

Fig. 10 Diagrama de Miyashiro y Shido (1975), se observa el comportamiento de los basaltos oceánicos en el cinturón ofiolítico septentrional.

de cada una de ellas erea empobrecido o enriquecido en algunos elementos, lo que permitió ihncluso en algunas regiones una amplia diferenciación de los cúmulos hasta rocas ácidas como en Holguín (Andó y Navarrete, 1988).

Los complejos efusivos están representados en la Fig. 10. En el estudio realizado se tomaron todas las formaciones estratigráficas, que por sus características geológicas y su comportamiento geoquímico pertenecen a la asociación ofiolítica. La Fm. Encrucijada de Pinar del Río, parte baja de Chirino de La Habana, Margot de Matanzas, Zurrapandilla de Villa Clara, las de Camaguey descritas en pozos, Bariay en Holguín, y por últimos las que aparecen en diferentes regiones de Moa-Baracoa asociadas a las ultramafitas y que aún no se ha concluído su cartografía.

Se incluyeron en estos diagramas las muestras de boninitas que se encontraron en la región de La Habana asociadas a los basaltos y diabasas ofiolíticas, cuya posición fue mencionada anteriormente. Para todas ellas es clara la marcada tendincia tholeítica.

REFERENCIAS

Andó J., y Navarrete, M., 1988,. Texto explicativo al levantamiento 1:50 000, región Holguín. Capítulo Asociación Ofiolítica (Informe inédito).

Coleman, R.,1977,. Ophiolites. Springer-Verlag, Berlín, Heidelberg, New York.

Fonseca, E., y Zelepugin, V., 1981,. Asociación de basaltos sódicos en la provincia de Pinar del Río. Resumen 1er Simposio Sociedad Cubana de Geología.

Fonseca, E, Zelepuguin, V. y Herdia, M., 1985,. Particularidades de la asociación ofiolítica de Cuba. Rev. Ciencia de la Tierra y el Espacio, no. 9,. La Habana.

Fonseca, E., y otros, 1988,. Geoquímica de la asociación ofilítica y la parte inferior del arco volcánico en Cuba centr-oriental,. Serie Geológica, No. 2. GIDP. La Habana.

Fonseca, E., 1988,. Geoquíimica de la asociación ofiolítica de Pinar del Río,. Revista Tecnológica, v.15, no. 4.

Fonseca, E, y otros, *en prensa*, Presencia de efusivos ofiolíticos en las provincias de La Habana y Matanzas, Boletín Geológico, MINBAS

Fonseca, E, y otros, 1989,. Geología y distribución de las cromitas de los macizos ofiolíticos de Mayarí y Moa-Baracoa, (resumen), Primer Congreso Cubano de Geología, La Habana

Hatten, C., Schooler, O. y otros, 1958, Geology of central Cuba: eastern Las Villas and western Camagüey provinces (informe inédito) C.F.N.G.

Haydoutov, Y., Kojujarova, E, y Cabrera, R., 1981, Capítulo corteza oceánica, Memoria explicativa al mapa geolólico 1:250,000 del territorio Ciego-Camagüey-Las Tunas, C.N.F.G.

Itturalde-Vinent, M., Hartwich, M. y otros, 1986, Ofiolitas de Camagüey: naturaleza, posición tectónica y sedimentos derivados, Rev. Tecnológica, v. 16, no. 2.

Santa Cruz-Pacheco, M., Fonseca, E., y Vega, N., 1988, Nuevos datos sobre la mineralización cromítitica del yacimiento Amores. (resumen) Primer Jornada Científica, Filial Habana, Soc. Cub. Geol.

Somin, M., y Millán, G., 1981, Geología de los complejos metamórficos de Cuba. (en ruso) Nauka, Moscú.

Teperin, A. y Heredia, M., 1980, Petrología de los complejos maficos de la provincia de Pinar del Río, los macizos Mayarí y Moa-Baracoa de Cuba Oriental (informe inédito) C.N.F.G., La Habana.

Torres, M., y Fonseca, E., *en prensa*, Caracteristicas de la asociacíon ofiolítica en la región norte de Moa-Baracoa y su relación con el arco volcánico.

Zelepuguin, V. y otros, 1985, Petrología de las rocas vulcanógenas y vulcanógeno-sedimentarias de Cuba (informe inédito), C.N.F.G., La Habana

POSICION ESTRATIGRAFICA DE LOS RUDISTAS DE CAMAGUEY, CUBA

M.A. Iturralde Vinent y A. de la Torre y Callejas
Museo Nacional de Historia Natural, La Habana, CUBA

RESUME

Los yacimientos de rudistas del territorio camagueyano se encuentran en dos paleoambientes distintos: como parte de un banco carbonatado perteneciente a la margen mesozoica de la plataforma de las Bahamas, y como intercalaciones de calizas entre y sobre una secuencia de rocas vulcanógeno-sedimentarias, propias de un antigua archipiélago volcánico. En el banco carbonatado hay un biostroma con *Biradiolites mooretownensis* de edad Campaniano a Maastrichtiano, asi como varios horizontes de calciruditas con fragmentos de radiolitidos demayor antigüedad. La secuencia vulcanógeno-sedimentaria incluye tobas, tufitas y lavas con tres horizontes intercalados de calizas biogénas, incluye *Sabinia* sp., *Tepeyacia corrugata* o *Ichthyosarcolites* sp. El otro nivel contiene *Durania curasavida, D. lopeztrigo, Vaccinites macgillavryi, Torreites tschoppi* y *Praebarrettia coralli*. La ausencia de foraminíferos orbitoidales hace suponer que su edad sea Coniaciano a Santoniano. Un horizonte Más joven incluye *Barrettia molilifera, Parastroma sanchezi, Antillocarpina acutodentata, Biradiolites acuticostatus, Lapeirousia nicholasi* y los foraminíferos orbitoidales *Pseudorbitoides* sp., *Sulcoperculina* sp. Es usual indentificar esta asociación como del Campaniano. Discordante sobre la secuencia anterior se encuentra un banco de calizas biostrómicas muy potente, que contiene *Biradiolites moretownensis, Titanosarcolites giganteus, Mitrocaprina tschoppi, Antillocaprina anulata, Bournonia thiadensis, Praebarrettia sparcilirata, Bournonia cancellata, Parastroma guitarti* y foraminíferos del Maastrichtiano.

ABSTRACT.

Rudist assemblages in the Camagüey region, central Cuba, are found in two different paleoenvironments: 1) a carbonate bank that belongs to the Bahamian mesozoic continental margin, and 2) as carbonate layer related to an island arc type volcano-sedimentary sequence. In the carbonate bank sequence there are biostromes of Campanian to Maastrichtien age with *Biradiolites mooretownensis*, and older layers of bioclastic rocks with radiolitids. The island arc vulcano-Sedimentary sequence contains three rudist limestones layers within tuffs, tuffites and flows. The older albian layer yield *Sabinia* sp., *Ichthyosarcolites* sp. and *Tepeyacia corrugata*. The second layer of probably Santonian age is characterized by *Durania curasavica, D. lopeztrigoi, Vaccinites macgillavryi, Torreites tschoppi and Praebarrettia coralli*. The third Campanian level yields *Barretia monilifera*, Parastroma *sanchezi, Antillocaprina acutodentata, Biradiolites acuticostatus, Lapeidrousia nicholasi* and foraminifers *Pseudorbitoides* sp. and *Sulcoperculina* sp. Unconformably over the volcano-sedimentary rocks a huge carbonate bank is developed with *Biradiolites mooretownensis, Titanosarcolites giganteus, Mitrocaprina tschopi, Antillocaprina anulata, Bournonia Thiadensis, Praebarrettia sparcilirata, Bournonia cancellata, Parastroma guitarti* and Maestrichtian foraminifera.

INTRODUCCION

Desde principios de siglo son bien conocidos los yacimientos de rudistas del territorio camagüeyano, que fueron estudiados por Sánchez Roig (1926), Palmer (1932), Chubb (1956), Torre (1960) y Chubb (1961), entre otros. Sin embargo, un problema surge de estos trabajos y es la falta de una buena base estratigráfica, de lo cual resulto alguna confusión en cuanto a la correlación de los horizontes con rudistas.

En los últimos años se han realizado levantamientos geológicos a distintas escalas (Iturralde-Vinent, Tchounev, Cabrera y otros, 1981; Iturralde-Vinent, Thieke y otros, 1987) que han permitido perfeccionar los conocimeintos sobre la estratigrafia y, de este modo, sentaron las bases para la mejor comprensión de la posición relativa de los yacimientos de rudistas.

Durante estas últimas investigaciones se colectaron nuevos ejemplares de rudistas que

Larue, D.K., and Draper, G. (eds.),
Transactions of the 12th Caribbean Geological Conference, St. Croix, U.S.V.I., Miami Geological Society, P.O. Box 431552, South Miami, FL 33243, U.S.A

fueron identificados hasta el nivel de genero por A. dela Torre, pero todo este material esta pendiente de un estudio adecuado. Los microfósiles bentónicos acompañates en las calizas fueron estudiados pro Consuelo Díaz (IGP, Cuba) en secciones delgadas, pero la conservación de los mismos en muchos casos no permitió definir las esepecies. Sin embargo, en las rocas deleznables asociadas a los bancos calcáreos fue posible encontrar microfósiles plantónicos que identifico Janka Vaptzarova (A.C., Bulgaria).

En este trabajo se presentan los resultados de estas investigaciones, que han permitido etablecer las posición estratigráfica y edad de los principales yacimientos de rudistas en el territorio camagüeyano. De ello se deriva la determinación de la edad de extinción del magmatismo del arco vulcano-plutónico del Cretacico. Asimismo, se adjunta un listado de localidades relevantes con rudistas, que prodrán simplificar la coleccta de nuuevos ejemplares en el futuro.

GENERALIDADES

En el territorio bajo consideración (Fig. 1), se encuentran elementos do dos terrenos y varias secuencias tectonoestratigráficas (Iturralde-Vinent, en prensa), que tienen sus propias asociaciones de rudistas. La porción septentrional está ocupada por el terreno "Estrecho de la Florida" donde las secuencias del Cretácico estan representadas por los ambientes propios de un margen continental pasivo, cuyo talud estaba inclindado hacia el sur. La configuración del relieve submarino durante el Cretácico superior se muestra en la Fig. 2. Observe la existencia de un promontorio o rampa marginal (secuencia de remedios) donde se desarollaron los rudistas. Los sedimentos propios de aquella rampa marginal son calizas (a veces dolomitizadas) que afloran en la Sierra de Cubitas y contienen rudistas del Maastrichtiano.

El resto del territorio camagüeyano está

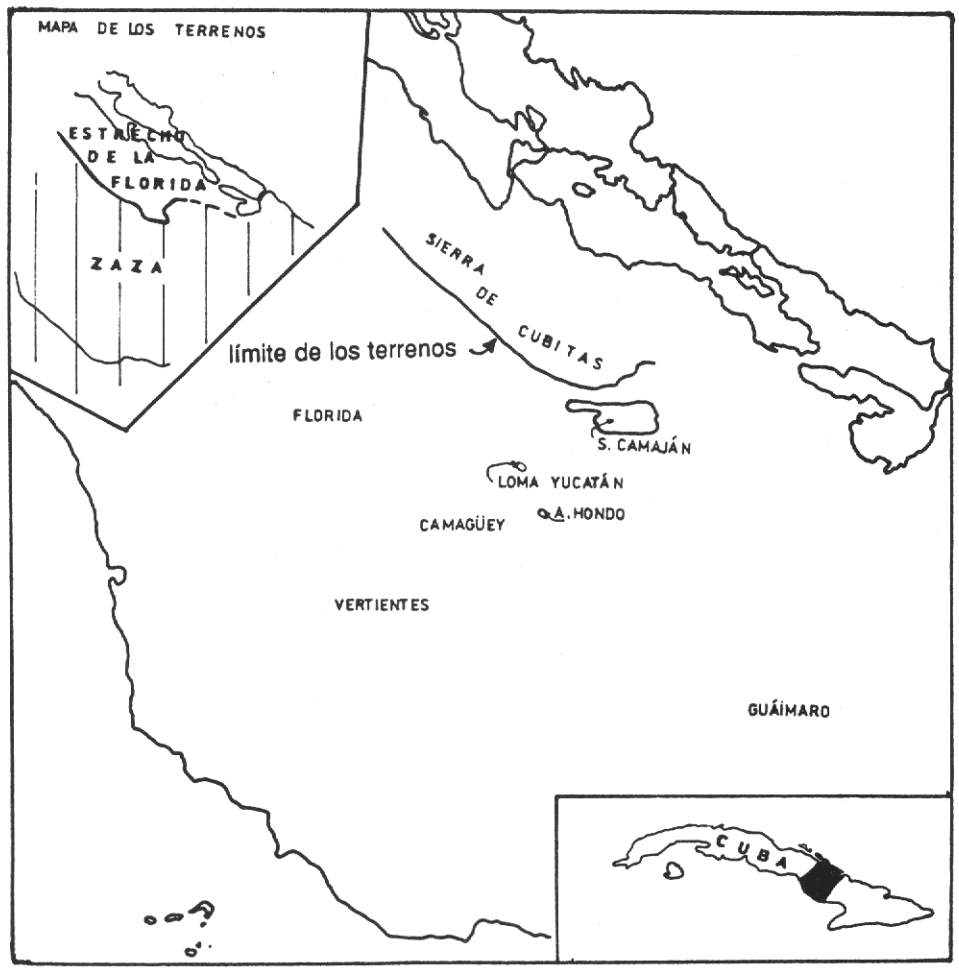

Fig.1 Mapa de las localidades mencionadas en el texto y los terrenos a que porresponden (A)

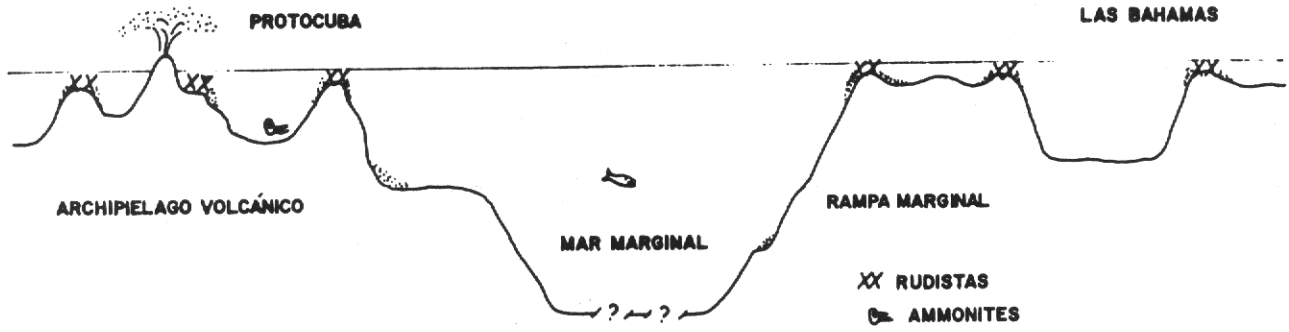

Fig. 2. Modelo de los ambientes de formación de los dépositos de rudistas camagüeyanos

ocupado por el terreno "Zaza", que yace parcialmente alóctono sobre el anterior (Fig. 1). Durante el Cretácico (Albiano-Campaniano) este constituyo un fondo oceanico y archipiélago de islas volcánicas, donde se recononocen tres niveles de callizas con rudistas intercalados entre las rocas efusivas y vulcanógeno-sedimentarias. Cuando el archipiélago volcánico se desactivó, sobre sus restos se desarrollo una plataforma de aguas poco profundas, donde progresó un nuevo nivel de rudistas en el Maastrichtiano. En la Fig. 2 se muestra una reconstrucción general de los ambientes del archipiélago volcánico.

Además de los lechos conrudistas mencionados, hay muchas secuencias del Maastrichtiano al Eoceno Medio yue contienen fragmentos de estos moluscos, los cuales no se han estudiado.

RUDISTAS DE LA SIERRA DE CUBITAS.

En estas elevaciones (Fig.1) aflora una potente secuencia de carbonatos de aguas poco profundas, que abarcan del Albiano al Maastrichtiano (secuencia de Remedios). Entre estas rocas se encuentran los ambientes de talud, laguna retroarrecifal y de bancos biostrómicos (Díaz Otero e Iturralde-Vinent, 1981). A pesar de que se han realizado trabajos detallados en la región, no se encontraron verdaderos arrecifes, lo que permite afirmar que durante el Cretácico representaba una rampa marginal con desarroloo de bancos biostromicos en su periferia. Un depósito de barrera con rudista debió existir durante el Cenomaniano, ya que en las rocas de dicha edad aparecen detritos de rudistas en facies de talud, en la Formación Vilató. Sin embargo, sólo se han podido edentificar come radiolitidos. Más arriba en el corte, en su sección superior, son calizas biogénas con *Biradiolites mooretownesis* (=? *B. lumbricoides*), masivas, que alcanzan 140 m de espesor. Junto con este rudista, muy abundante, se encuentran foraminíferos tipicos del Maastrichtiano al Campaniano tardió (Tablas 1 y 2). En la literatura geologica estas calizas con *Biradiolites* se han relaciónado a la Formación Remedios (Bermúdez, 1950; Meyerhoff y Hatten, 1974) o al Grupo Remedios, unidad "A" (Díaz Otero e Iturralde-Vinent, 1981). Según Furrazola-Bermúdez y Díaz Otero (1984) las calizas del Coniaciano al Maastrichtiano se deben denominar Formación Purio. No obstante, el autor consideral que al menos en Sierra de Cubitas la sección del Maastrichtiano es litológica y faunalmente muy característica y debe darsele el rango de formación. En la Tabla 3 se relacionan las localidades donde afloran las calizas con *Biradiolites*.

RUDISTAS DE LA SIERRA DE CAMAJAN

En estas alturas (Fig. 1) se desarrolla una secuencia de rocas de aguas profundas del Tithoniano al Turoniano, y sobre ellas, discordantes, calciruditas y calcarenitas del Maastrichtiano. Esta es la Formación Camaján (MacGillavry, 1937; Iturralde-Vinent, Tchounev, Cabrera y otros, 1981) que contiene fragmentos de radiolitidos y foraminíferos (Tablas 1 y 2). Parece corresponder a un ambiente de "brecha de talud". Hasta el presente no se han encontrado los lechos con rudistas in situ, ne en Camagüey, ne en las destintas localidades donde aflora esta secuencia en Cuba.

OTRAS LOCALIDADES CON RUDISTAS

El el resto del territorio camagüeyano, esencialmente al sur de las localidades descritas, se encuentran numerosos yacimientos de rudistas,

Tabla 1

Rudistas de Camagüey. Los rudistas de la formación Piragua señalados con el signo "0" pertenecen a la localidad Loma Yucatan. 1) Remedios; 2)Jimaguayú; 3) Durán; 4) Piragua 5) Guaimaro.

	Formaciones 1	2	3	4	5
Biradiolites mooretownesis	+	+			
Titanosarcolites giganteus		+	+		
Mitrocaprina tschoppi		+	+		
Antillocaprina anulata		+			
Bournonia thiadensis		+			
Bournonia cancellata		+			
Parastroma guitarti		+			
Praebarrettia sparcilirata		+			
Barrettia monilifera				+	
Biradiiolites acusticostatus				+	
Antillocaprina acusticostatus				+	
Lapeirousia nicholasi				+	
Parastroma sanchezi				+	
Durania curasavica				0	
Durania lopeztrigoi				0	
Vaccinites macgillavryi				0	
Praebarrettia coralli				0	
Torreites teschoppi				0	
Tepeyacia corrugata					+
Sabinia sp.					+
Ichthyosarcolites sp.					+

entre los límites del terreno Zaza (Fig. 1). Las investigaciones estratigráficas efectuadas durante los últimos años permiten establecer con bastante exactitud la posición relativa de las calizas con rudistas, que en el pasado se habian hecho corresponder con diversas unidades litoestratigráficas aparentemente inconexas.

La columna estratigráfica generalizada del Cretácico del área en cuestión se mustra en la Fig. 3, donde se reconocen tres secciones separadas por discordancias y conglomerados basales. La **sección inferior** (Formaciones Guaímaro y Camufiro), propia del arco volcánico, está incompleta, pues no aflora su base. Contiene un horizonte de calizas con rudistas que incluye *Tepeyacia corrugata, Ichthyosarcolites* sp. y *Sabinia* sp.del Albiano. Son calizas grises, recristalizadas, en forma de lentes, con espesor de una decena de metros que, enumero de dos o tres, se intercalan con tobas,, y todo el conjunto yace entre lavas, xenolavas y xenotobas andesitobásliticas y basálticas. A las calizas con *Tepeyacia* se asocian tobas con *Ticinella* sp., *Hedbergella*, sp. y otros microfósiles propios del Albiano al Cenomaniano.

La **sección media** (Formación Piragua) propia del arco volcánico maduro, contiene dos niveles con rudistas, así como un horizonte con ammonites. Las calizas conrudistas forman lentes de espesor variable entre unos metros y 20 a 50 m, de color gris oscuro, masivas o con capas medias a gruesas, pero pueden estar ausentes. El nivel más común se caracteriza por lla presencia muy estable de *Barrettia monilifera* junto a los foraminíferos *Pseudorbitoides* sp. indtm. y *Sulcoperculina* sp. indtm., entre otros. Según los criterios más modernos, esta asociacin es del Campaniano (Tabla 1). Sus localidades se relacionan en la Tabla 3.

Otro nivel de calizas con rudistas apareció en Loma Yucatán, donde se encuentra un potente espesor de calizas gris oscuro, que se intercalan con tufitas y tobas,, pero que afloran como un *klippen* alóctono, sobre las ofiolítas. Contienen *Durania curasavica* y otros rudistas (Tabla 1), pero carecen de foraminíferos orbitoidales. Chubb (1961) las data del Coniaciano o Santoniano. La litología de la secuencia presente en Loma Yucatan es commparable con la de la Formación Piragua.

En general, la Formación Piragua, que contine las calizas conrudistas, está constituida pro una secuencia de tobas y tufitas con sills, lavas y otros cuerpos de andesitas, basaltos y riolitas. Cuando faltan las calizas con rudistas, la secuencia tobacea puede sustituirse lateralmente por tufitas de color crema y carmelita claro, calcáreas, bien

Tabla 2.

Foraminíferos asociados a los rudistas en Camagüey. 1)Remedios, 2)Jimaguayú, 3)Durán, 4)Piragua, 5)Guaimaro, 6)Camajan.

	Formaciones					
	1	2	3	4	5	6
Vaughanina sp.						+
Vaughanina cubensis	+	+	+			
Vaughanina guatemalensis	+	+				
Orbitoides apicullata		+	+			
Orbitoides browni						+
Orbitoides media		+				
Orbitocyclina sp.						+
Pseudorbitoides spp.	+	+	+	+		+
Pseudorbitoides of P. Barkeri		+				
Orbitolina sp.				+		
Torreina torrei						+
Sulcoperculina sp.				+		
Sulcoperculina diazi		+				
Sulcoperculina dickersoni				+		
Sulcoperculina globosa	+	+	+			+
Chubbina cardenasensis	+					
Siderolites skoirensis	+					
Siderolites vanbelleni	+					
Raphydionina sp.	+					
Stomatorbina binkhorsti	+					
Rosita contusa			+			
Rosita fornicata		?	?			?
Globotruncanita conica		+				
Globotruncanita stuarti		+				
Globotruncanella petaloidea		+	+			
Globotruncana sp.				+		
Globotruncana arca			+			
Globotruncana gagnebini			+			
Globotruncana intermedia			+			
Globotruncana rossetta			+			
Globotruncana striata		+	+			
Globotruncana subcircumnodifer			+			
Globotruncana tricarinata			+			
Globotruncana ventricosa		+				
Rugoglobigerina macrocephala		+	+			
Rugoglobigerina penyi			+			
Rugoglobigerina pustulosa			+			
Rugoglobigerina scotti		+				
Psuedoguembelina costulata			+			
Heterohelix pulchra			+			
Heterohelix globulosa			+			
Heterohelix punctulata			+			
Globigerinelloides sp.					+	+
Globigerinelloides escheri			+			
Pseudotextularia elegans			+			
Hedbergella sp.						+
Ticinetta sp.						+

estratificadas, que contienen ammonites del Santoniano (*¿Paratexanites* sp. indet. y *¿Texasia dentatocarinata*, según A. C. Ricardi, de La plata, Argentina). En estos casos falta el conglomerado basal y parece que la sedimentación ocurrió enaguas profundas, pues los ammnonites están acoompanados pro radiolarios (vea las Figs. 2 y 3).

De aquí se deduce que las base de la Formación Piragua, y de sa sección media, corresponde con una transgresión que tuvo lugar sobre un relieve ondulado. En algunas localidades hay rocas del Santoniano de ambientes de aguas someras (con rudistas) y de aguas profundas (con radiolarios y ammonites); en tanto que en otras localidades aparece un conglomerado basal y directamente sobre él, las casizas con *Barrettia monilifera* de aguas poco profundas, del Campaniano.

Tabla 3. Localidades de rudistas de Camagüey.

Localidad	Hoja	Coordenadas X-Y	Fuente bibliográfica	Formación
F235a	4779-III	436,0-262,0	Hermes, J. (1945)	Guáimaro
F235c	4779-III	436,5-261,9	Hermes, J. (1945)	Guáimaro
H222	4778-IV	433,7-259,9	Hermes, J. (1945)	Guáimaro
C10-409	4779-III	435,2-263,1	Iturralde-Vinent, M. y otros (1981)	Guáimaro
V228	4779-IV	433,70-289,50	Vermunt (1937)	Piragua
H670	4679-I	420,7-285,2	MacGillavry (1947)	Piragua
H716b, c	4679-IV	393,35-294,3	MacGillavry (1937)	Piragua
L262	4680-III	399,0-299,0	MacGillavry (1937)	Piragua
L697	4680-III	395,7-314,6	MacGillavry (1937)	Piragua
L634	4680-III	395,7-314,6	MacGillavry (1937)	Piragua
L702	4580-III	369,8-305,5	MacGillavry (1937)	Piragua
L735	4580-II	362,36-310,31	MacGillavry (1937)	Piragua
M826	4679-IV	388,35-286,80	MacGillavry (1937)	Piragua
V461	4680-III	381,3-298,8	MacGillavry (1937)	Piragua
V499	4779-III	436,5-276,5	MacGillavry (1937)	Piragua
V523	4679-I	413,1-287,6	MacGillavry (1937)	Piragua
S/N	4679-I	419,7-286,5	Chubb (1961)	Piragua
S/N	4779-IV	422,5-286,5	Chubb (1961)	Piragua
S/N	4580-III	371,5-305,5	Chubb (1961)	Piragua
S/N	4580-II	363,5-310,5	Chubb (1961)	Piragua
S/N	4679-II	405,5-262,0	Chubb (1961)	Piragua
C8-1323	4678-I	424,2-254,50	Iturralde-Vinent, M. y otros (1981)	Piragua
T1425	4481-I	733,8-225,56	Van Wessen (1943)	Durán
V69	4481-I	732,82-226,14	Van Wessen (1943)	Durán
C3-967	4481-II	734,20-224,75	Iturralde-Vinent, M. y otros (1981)	Durán
C3-960	4481-II	737,30-216,30	Iturralde-Vinent, M. y otros (1981)	Durán
C3-1216F	4680-IV	827,300-206,300	Iturralde-Vinent, M. y otros (1981)	Remedios
C3-1220G	4681-II	836,50-213,50	Iturralde-Vinent, M. y otros (1981)	Remedios
L684	4679-III	403,15-266,45	MacGillavry (1937)	Jimaguayú
M873	4579-I	378,2-289,8	MacGillavry (1937)	Jimaguayú
M874	4579-I	377,4-289,5	MacGillavry (1937)	Jimaguayú
V469	4579-I	373,3-292,8	MacGillavry (1937)	Jimaguayú
H95	4580-IV	776,5-201,5	Van Wessen (1943)	Jimaguayú
H230, H689	4678-I	426,5-256,5	Hermes (1945)	Jimaguayú
H694	4678-I	424,85-256,10	MacGillavry (1937)	Jimaguayú
H697	4579-I	374,9-292,9	MacGillavry (1937)	Jimaguayú
H699	4579-I	375,5-293,75	MacGillavry (1937)	Jimaguayú
H421	4678-I	424,8-246,15	Hermes (1945)	Jimaguayú
H283	4778-IV	444,3-250,15	Hermes (1945)	Jimaguayú
H285	4778-IV	443,5-246,5	Hermes (1945)	Jimaguayú
S/N	4579-I	367,0-286,0	Chubb (1961)	Jimaguayú
C3-693A	4580-I	198,1-790,7	Iturralde-Vinent, M. y otros (1981)	Jimaguayú
C3-1303	4579-I	359,1-294,75	Iturralde-Vinent, M. y otros (1981)	Jimaguayú
C1-937	4579-I	375,90-292,30	Iturralde-Vinent, M. y otros (1981)	Jimaguayú
C3-734	4580-I	788,40-189,25	Iturralde-Vinent, M. y otros (1981)	Jimaguayú
C1-877	4579-I	292,5-373,5	Iturralde-Vinent, M. y otros (1981)	Jimaguayú
C8-1389	4678-I	427,0-246,4	Iturralde-Vinent, M. y otros (1981)	Jimaguayú
C3-1512	4679-II	377,15-263,30	Iturralde-Vinent, M. y otros (1981)	Jimaguayú
C10-620	4778-IV	439,15-247,15	Iturralde-Vinent, M. y otros (1981)	Jimaguayú
C7-661	4778-IV	447,0-246,10	Iturralde-Vinent, M. y otros (1981)	Jimaguayú
C8-1609	4678-I	409,85-257,95	Iturralde-Vinent, M. y otros (1981)	Jimaguayú
C1-966B	4579-I	375,0-292,95	Iturralde-Vinent, M. y otros (1981)	Jimaguayú
C3-1376	4579-II	378,0-267,26	Iturralde-Vinent, M. y otros (1981)	Jimaguayú

En los trabajos de los holandeses (MacGillavray, 1937;Wessen, 1943;Hermes, 1945) y demás estudiosos de los rudistas de Camagüey, las calizas mencionadas se incluyeron indistintamente en la formación Tobas, o en la formación Habana.

Despues se caracterizaron como lentes calcareos en las formaciones Guáimaro y Vidot principalmente (Iturralde-Vinent, Tchounov, Cabrera y otros, 1981). Sin embargo, las investigaciones detalladas realizadas posteriormente (Iturralde-Vinent, Thieke y otros, 1987), permitieron precisar la estratigrafía de las rocas vulcanógeno-sedimentarias. De esto resultó que: 1) se elevó al rango de Formación a los miembros Piragua y Camuujiro de la formación Vidot; 2) se estableció que el miembro Majasa de la Formación Guáimaro es sinónimo de la Formación Camujiro; y 3) que las formaciones Camujiro y Guáimaro tienen relaciones laterales muy estrechas.

La **sección superior** (Formaciones Jimaguayú y Durán)(Fig. 3) carece de rocas efusivas o piroclástias, y se originó después de cesada la actividad magmática, sobre la superficie erosionada del arco vulcano-plutónico extinto. Corresponde con una transgressión relativamente rápida que se estabilizó como una plataforma carbonatada en el Maastrichtiano tardió. En el potente banco de calizas se desarrollaron ambientes de barreras con abundantes rudistas, bajos de calizas bioclásticas y calcarenitas ricas en foraminíferos orbitoidales, ambientes de brecha de talud con fragmentos de rudistas, y paquetes de margas con abundantes microfósiles y rudistas, de ambiente lagunar. Este nivel corresponde a las calizas con *Titanosarcolites giganteus* (Tablas 1, 2 y 3).

Dentro de las sección superior, los conglomerados, areniscas y margas arenosas corresponden a la Formación Durán del Campaniano Más tardió (?) al Maastrichtiano; en tanto que las calizas, carciduritas y margas pertencecen a la Formación Jimaguayú del Maastrichtiano (Iturralde-Vinent, Tchonov, Cabrera y otros, 1981). En la literatura previa estas rocas se denominaron Formación Habana, o "upper Habana".

EL PROBLEMA DE LAS FAUNAS MEZCLADAS

En la localidad de Arroyo Hondo, al este de ciudad Camagüey, Sánchez Roig (1926) reporta *Barrettia monilifera, Titanosaricolites giganteus, Praebarrettia sparcilirata, Antillocaprina aff. occidentalis, Lapeirousia nichilasi, Biradiolites aff. cancellatus y Bouronia* sp. Esta es una de las pocas localidades conocidas donde se encuentran juntos representatantes de dos niveles estratigráficos, pero al inspeccionarla, se comprobó que allí yacen las calizas blancas y margas de la Formación Jimaguayú (con *Titanosarcolites*) discordantes sobre las tobas y calizas grises de la Formmación Peragua (con *Barrettia*). Es evidente que se trata de una mezcla de ejemplares durante la colecta.

El mismo problema lo presenta la localidad Ingenio Grande, de Sánchez Roig (1926), donde se mencionan *Biradiolites mooretownensis, Titanosarcolites giganteus* e *Ichthyosarcolites* sp., evidentemente mezclados durante la colecta.

En la región que colinda al este con el territorio estudiado, De la Torre y otros (1978) describen el "membro Cayojo" donde coexisten *Praebarrettia sparcilirata, Plagioptychus tschoppi, Titanosarcolites* sp. y *Barrettia multilirata*. Este afloramiento fue visitado y se comprobó que coincide con la Formación Jimaguayú, del Maastrichtiano. Dicho sea de paso, la otra loocalidad descrita por De la Torre y otros (1978), en la cantera Las Parras, con *Barrettia* monilifera, es un excelente representante de la Formación iragua, del Campaniano. Si *Barrettia multilirata* no está redepositada en el "miembro Cayojo", ello demuestra que se extiende al Maastrichtiano, lo cual no se aviene al caso de *B. monilifera*, al menos en Camagüey.

LA BIOESTRATIGRAFIA DE LOS RUDISTAS

Las investigaciones realizadas condirman las opiniones de Chubb (1961) sobre la existencia de cuatro niveles superpuestos de rudistas en Cuba, que en Camagüey son:

1 - fauna con *Titanosarcolites giganteus;*.
2 - fauna con *Barrettia monilifera;*
3 - fauna con *Durania curasavica;*
4 - fauna con *Tepeyacia corrugata;*

Al definir las faunas"según las especies, se elimina el rango de ambigüedad delas denominaciones propurstas pro (Chubb 1956), 1961) y De la Torre (1960), y se refleja el caso real en el territorio estudiado.

En las localidades camagüayanas estas "faunas" son relativemente fáciles de caracterizar y son excelente auxiliar durante los trabajos de campo. Sin embargo, es necesario referirse al problema de su datación.

La fauna con *Tepeyacia corrugata* se asignaba al Cenomaniano- Turoniano en trabajos

anteriores (Chubb, 1956; 1961), De la Torre (1960). Ahora bien, E. Kauffman, C. Johnson y N. Sohl (1989, comunicación personal) la datan dell Albiano Mediano. Los datos compilados en Camagüey no permiten tomar partido al respecto.

La fauna con *Durania curasavica* se reporta del Campaniano (MacGillavry, 1937; De la Torre, 1960) y del Santoniano o Coniaciano (Chubb, 1961; De la Torre y otros, 1978). Los datos existentes no permiten aportar nada nuevo al repecto, ya que estas ccalizas afloran desvinculadas de las restantes.

La fauna con *Barrettia monilifera* es del Maastrichtiano según De la Torre (1960) y De la Torre y otros (1978), probablemente coeval con la de *T. giganteus*. Según la opinión de Chubb (1961) su edad es Campaniano, pero E. Kauffman, C. Johnson y N. Sohl (1989, comunicación personal) extienden el rango de *B. monilifera* del Campaniano superior al Maastrichtiano inferior. El hallasgo en Camagüey de *Pseudorbitoides* sp. indtm., *Sulcoperculina* sp. indtm. en estas calizas, apunta más al Campaniano. Además, en la Formación piragua, que contiene a estas calizas, se han encontrado fósiles del Coniaciano o Santoniano (*D. curasavica*) y del Santoniano (ammonites), a un nivel estratigráfico ligeramente por debajo de las calizas con *B.monilifera*. Sobre estas últimas calizas hay unos 1000 m de espesor de tobas, tufitas y rocas sedimentarias, las que han sufrido los siguientes eventos posteriores: 1) intrusión del plutón granitoide; 2) dislocación y erosión hasta el nivel del Pluton; 3) sobre la superficie discordante así generada se depositaron las formaciones Durán y Jimaguayú, del Campaniano Tardió (?) al Maastrichtiano. En cosequencia, es muy poco proobable que las caizas con Barrettia monilifera de la Formación Piragua puedan extenderse al

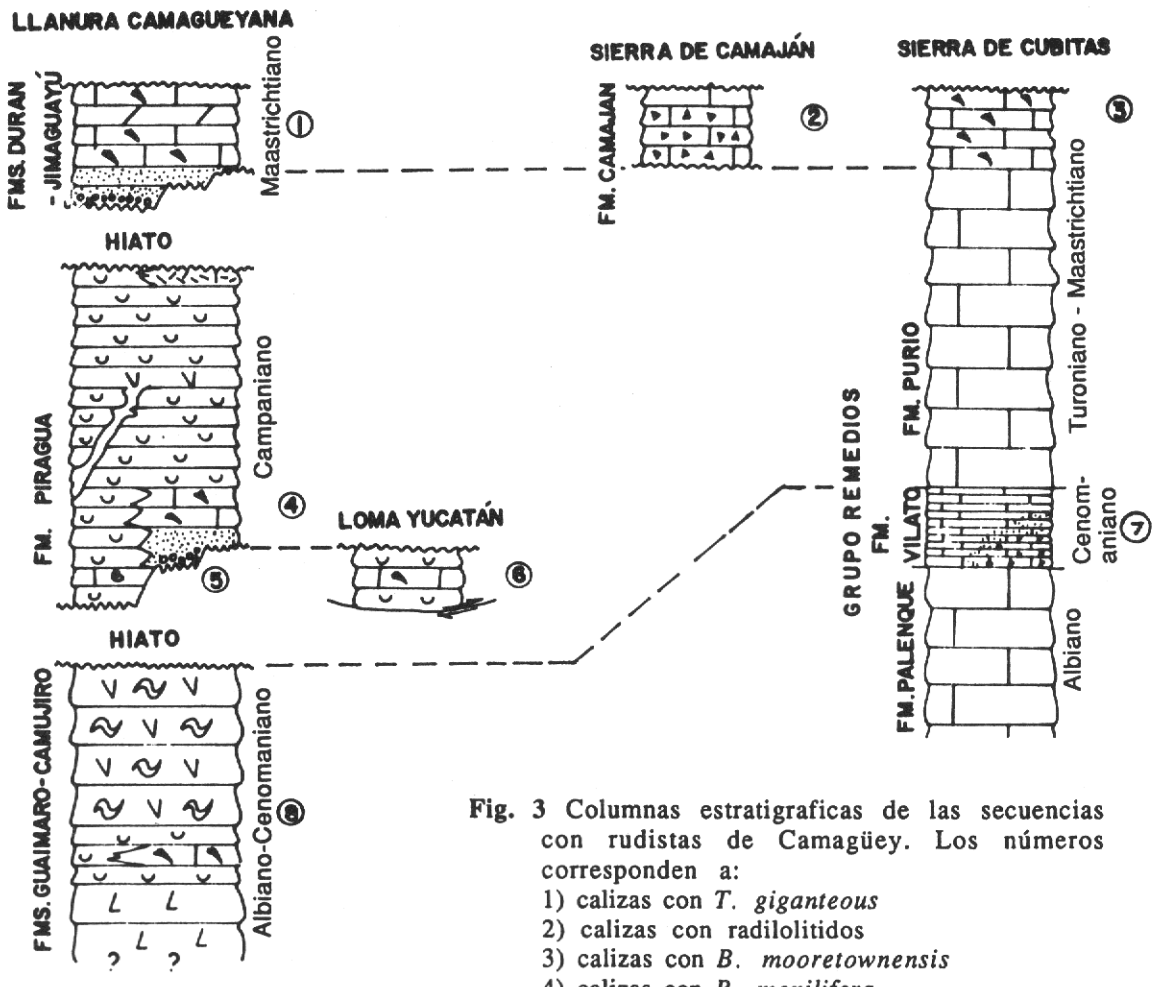

Fig. 3 Columnas estratigraficas de las secuencias con rudistas de Camagüey. Los números corresponden a:
1) calizas con *T. giganteous*
2) calizas con radilolitidos
3) calizas con *B. mooretownensis*
4) calizas con *B. monilifera*
5) tufitas con ammonites santonianos
6) calizas con *D. curasavica*
7) calciruditas con radiolitidos
8) calizas con *T. corrugata*

Maastrichtiano, y es razonable adoptar una edad Campaniano, al menos para el territorio bajo consideración.

La fauna con *Titanosarcolites* no es objeto de discusión en cuanto a su edad maestrichtiana (MacGillavry, 1937; Chubb, 1956, 1961; De la Torre, 1960 y otros). Lo mmismo se puede afirmar de las calizas con *Biradiolites mooretownesis* de la Sierra de Cubitas, que a lo sumo se pudieran extender al Campaniano tardió - Maastrichtiano.

Es importante notar que la edad de la discordancia entre las formacioanes Piragua, Durán y Jimaguayú marca la extinción del mmagmatismo del arco volcánico y de los movimientos tectónicos que lo dislocaron. Si el hiato está situado dentro del Campaniano, a dicha epoca corresponden esos eventos geológicos (Iturralde-Vinent, Tchounev, Cabrera y otros, 1981).

AGRADECIMIENTO

Los autores desean reconocer las valiosas sugerencias de C. Johnson (U.S.A.), S. Blanco y G. Fernandez (CIDP, Cuba) y G. Furrazola (I.G.P., Cuba) que permitieron mejorar el manuscrito original, asi como a C. Díaz (Cuba), Y. Voptzarova (Bulgaria) y A. Ricardi (Argentian) por sus determinaciones faunales.

REFERENCIAS

Albear, J.F. de, ,1947, Stratigraphic paleontology of Camagüey district, Cuba. AAPG Bull., v.31, no. 1, pp. 71-91

Bermúdez, P.J. ,1950, Contribución al estudio del Cenozoico cubano. Mem. Soc. Cubana Hist. Nat. "Felipe Poey", vol. 19, no. 3, pp. 205-375.

Chubb, L. J. ,1956,: Rudiest assemblages of the Antillean Upper Cretaceous. Bull. Amer. Pal.,v. 37, no. 161, pp. 1-23.

Chubb, L. J.,1961,: Rudist assemblages in Cuba. Bull. Amer. Pal., vol.43, no. 198, pp. 412-422.

Díaz, C. y m. Iturralde-Vinent, 1981, Estratigrafia, paleontología y paleogeografía del banco carbonatado Cretácico de Sierra de Cubitas. Resumenes Primer Simposio Soc. Cubana de Geología, p. 51.

Furrazola Bermúdez, G., C.Díaz Otero ,1984, Estudio bioestratigráfico y litofacial de la secuencia Cretácica de la zona Remedios. Inst. Geol. Paleont.,A.C.C., 68 pp.

Hermes, J. J. ,1945, Geology and paleontology of east Camagüey and West Oriente, Cuba. Geog. . Geol. Mededeel (Utrecht), Phys. Geol. Reeks, v. 2, no. 7 pp.1-45.

Iturralde-Vinent, M. (en prensa) Terrenos tectono-estratigráficos de Cuba.

Iturralde-Vinent, M. y otros ,1981, Resultados de las investigaciones y del levantamiento geológico a escala 1250 000 del territorio Ciego-Camagüey-Las Tunas. A.C.C., A.C.B., Centro Nacional del Fondo Geológico (en prensa). Boletin de la Academia de Ciencias de Bulgaria

Iturralde-Vinent, M., H. U. Thieke y otros ,1987, Informe sobre los resultados del levantamiento geológico complejo 1:50 000 sus busquedas acompanantes en el poligono Camagüey,Cuba-RDA. Centro Nacional del Fondo Geológico (inédito).

MacGillavry, H.J. ,1937, Geology of the province of Camagüey, Cuba, with revisional studies in rudist paleontology. Geogr. Geol. Mededeel (Utrecht), Phys. Reeks, no. 14, 169 pp.

Palmer, R. G. ,1932, Nuevos rudistas de Cuba. Rev. Agricultura, vol. 14, pp. 95-125.

Sánchez Roig, M. ,1926, La fauna Cretácica de la región central de Cuba. Mem. Soc. Cub. Hist. Nat.,v. 7, pp. 83-102.

De la Torre, A., 1960, Notas sobre rudistas. Mem. Soc. Cub. Hist. Nat., v. 25, no.1, pp.51-64

De La Torre, A. P. Jakus y J. F. de Albear, 1978, Nuevos datos sobre las asociaciones de rudistas en Cuba. Geol. en Mijnouw, v.57, no. 2, pp. 143-150.

Wessen, A. van ,1943, Geology and paleontology of Central Camagüey, Cuba. Geogr. Mededeel (Utrecht), Phys. Geol, Reeks 2, no. 5, pp. 1-91.

LA CONSTITUCION GEOLOGICA DEL MACIZO ISLA DE LA JUVENTUD Y SU METALOGENIA ENDOGENA VINCULADA AL MAGMATISMO ACIDO.

Manuel E. Pardo-Echarte
Instituto de Geologica y Paleontologia,
Ministerio de Industrias Basicas,
La Habana, CUBA

RESUMEN

Se argumenta la solución teórica del problema acerca del vínculo entre a estructura dómica regional más joven, superpuesta al cuadro de multiplegamiento y metamorfismo de la secuencias del macizo, y el desarrollo del magmatismo ácido y su metalogenia asociado en la región. Com resultado, se establece que, probablemente, a consecuencia del proceso de formación y evolución estructural del domo, tuvo lugar el emplazamiento de pequeños plutones graniticos (50-100 km^2), localizados en la intersección del sitema radial de grietas del domo con el sistema anular de fracturas profundas que lo delimita, a través del cual, presumiblemente, penetraron los fundidos anatécticos. A partir de sus apófisis subvolcánicos diferenciados. tuvo lugar, al parecer, la telescopisación de las intrusiones fisurales y de la mineralización, fundamentalmente, dentro del sistma radial de grietas. Basado en un mecanismo de herencia metalogénica, se supone que los plutones graniticos formados condujeron a concentraciones minerales, sólo donde éstos sobreyacían a zonas mineralisadas preexistentes y; que la regionalización geoquímica del territorio reproduce la zonalidad geoquimíca (y metalogénica) del basamento reelaborado.

ABSTRACT

A solution of the problem of the relation between of younger regional doming with regional granitic magmatism and associated metallogeny of the older polydeformed and metamorphosed rocks of the Isle of Youth (previously Isle of Pines) is presented. Intrusion of small small (50-100 km^2) granite plutons took place where radial fractures associated with the dome intersect an annular system which borders the dome. Differentiated apophyses and mineralized veins from the main intrusions were emplaced into the radial fracture system. It seems that granite plutons are associated with ore concentrations only only where they intrude previous ore zones. Moreover, the the geochemical zoning reflects the geochemical (and metallogenic) zonation in the reworked basement.

(English abstract by Gren Draper)

INTRODUCCION

El estudio de la constitución geológica del macizo Isla de la Juventud y su metalogenia endógena vinculade al magmatismo ácido, se aborda extensamente en un primer trabajo (Pardo, 1986) donde se formula, por primera vez, la hipotesis sobre el vínculo de la mineralización de metales raros y preciosos con el desarrolo de una estructura dómica regional más joven, superpuesta al cuadro de mutiplegamiento y metamorfismo de las secuencias del macizo. A juzgar por la regularidad regional de carácter radial en la distribución de las anomalías complejas geoquímico-geofísico-geomorfológicas (Fig. 1) establicida en este trabajo, la mineralización se localiza dentro del sistema de fracturas desarrollado, presumiblemente, durante la evolución del referido domo. El origen de éste, a su vez, se supone relacionado con un proceso profunde de distención localizada, con el cual podo tener lugar una desdensificación estructural-material local en la base de la coeteza, presumiblemente, como resultado del reajuste isostático de la misma al término de un estado compresivo. En el desarrollo del referido trabajo se argumenta la validez de la hipótesis planteada y, sobre su bse, se propone un modelo menífero-estructuro-metalogénico para la región. Por su parte, éste conduce al planteamiento de nuevas interrogantes; entre las que se encuentran:

-el posible patron de fracturas de la estrucutra cupular en el cual se vincula la mineralización;
-el posible desarrollo del magmatismo ácido en la región y su relación con a estructura dómica;
-el origen de los metales y la regionalización geoquímica del territorio, y;
-la determinación de la favorabiidad geológica para la ocurrejcia de la mineralización en le

Larue, D.K., and Draper, G. (eds.),
Transactions of the 12th Caribbean Geological Conference, St. Croix, U.S.V.I., Miami Geological Society, P.O. Box 431552, South Miami, FL 33243, U.S.A

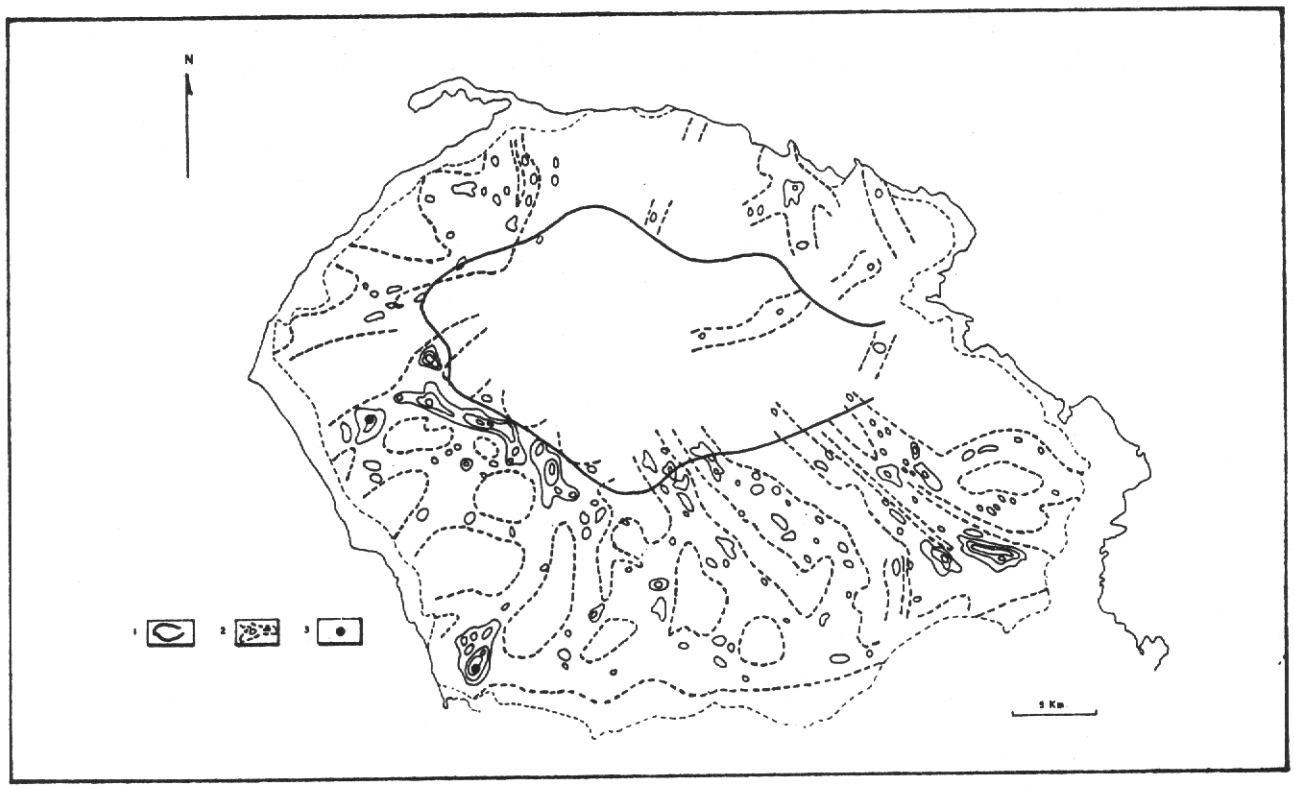

Fig. 1. Distribución de las anomalías complejas geoquímico-geofísico-geomorfológicas y su regularidad en el macizo Isla de la Juventud. **1.** Contorno del mínimo gravimétrico regional (isolínea de 16 mgal); **2.** Regularida en la distribución de las anomalías complejas; **3.** Depósito conocido.

macizo, en base al modelo ménifero-estruoturo-metalogénico propuesto.

El presente trabajo se propone, como objetivos principales, incursionar en la solución de los problemas planteados como vía para completar la argumentación de la hipótesis general de trabajo, y valorar preliminarmente la capacidad predictiva del modelo propuesto, con vistas a la ulterior evaluación de los recursos pronósticos en esta región. Comoquiera que en el trabajo se abordan una serie de aspectos teóricos (especulativos), de los cuales, en base al nivel de información disponible, no se tiene confirmación práctica, es también propósito del mismo, estimular la futura investigación y discusión en torno a estos aspectos.

MATERIALES Y METODOS

En la confección del travajo se utilizaron los materiales siguientes:

-mapa geológico de la Isla de la Juventud, en escala 1:100 000 (Garapko y otros, 1974).

-esquema geológico del macizo Isla de la Juventud, en escala 1:100 000 (Millán, 1979).

-mapa de yacimientos, manifestaciones y puntos de mineralización de la Isla de la Juventud, en escala 1:100 000 (Garapko y otros, 1974)/

-mapa gravimétrico de la Isla de la Juventud, en escala (no condicional) 1:100 000 (Garapko y otros, 1974).

-mapa de relieve residual del macizo Isla de la Juventud, en escala 1:50 000 (Pardo, 1986).

-mapa de anomalías gravimetricas residuales (R = 3 km) del macizo Isla de la Juventud, es escala 1:50 000 (variante autor, poligono - Cuba-URSS Pinar III, 1987).

-mapa de anomalías aero-gamma-espectrométricas de la Isla de la Juventud (canal total y de potasio), en escala 1:50 000 (Liubi y otros, - 1984),

-cartas topográficas de la Isla de la Juventud, en escala 1:100 000 (hojas 3581, 3680, 3681, Serie

ICGC E 621, 1968).

-mapa de anomalías geoquímicas complejas exógenas del macizo Isla de la Juventud, en escala 1:250 000 (Riftin y otros, 1988).

El proceso de trabajo consideró las etapas de elaboración, análisis e interpretación siguientes:

-generalización del mapa geológico con el apoyo de los datos aero-gamma-espectrométricos (cana total) para precisar el esquema geologo-estructural de la región.

-levantamiento de la red de drenaje del territorio, determinación del campo de divisorias de aguas y, establecimiento del posbile patrón de fracturas del domo con el cual se vincula la mineralizaqción. Análisis de la correspondencia espacial del campo de divisorias de aguas con las ocurrencias minerales y las anomalías del canal de potasio (>1%)

-discriminación de anomalías gravimetricas residuales negativas relacionadas con el relieve de la roca fresca. Análisis de la regularidad en la distribución de las anomalías geoquímicas complejas exógenas y gravimétricas residuales negativas (corregidas) con el propósito de evaluar el posible desarrollo del magmatismo ácido en la región y su tendencia. Análisis de la relación entre el posible desarrollo del magmatismo ácido y la probable evolución estrucutral del domo.

-Precisión del modelo menífero-estructuro-metalogénico propuesto y, determinación de la favorabilidad geológica para la ocurrencia de la mineralización en el macizo.

PRECISION DEL ESQUEMA GEOLOGO-ESTRUCTURAL DEL MACIZO

Aprovechando las posibilidades que ofrece para la cartografía general del terreno la intensidad de radiación gamma total, particularmente, en condiciones de desarrollo autóctono de las cortezas (y suelos), se realizó, previa generalización espacial del mapa de isoradas, su regionalización en base al nivel del cmapo. La comparación del esquema resultante con los datos geológicos anteriores (Garapko y otros, 1974 y; Millán, 1979) permitió, mediante una operación de generalización tipológica, su transformación en un esquema interpretativo geólogo-estructural (Fig. 2). En este se reconocen los principales bloques tectónicos, así como las distintas antiformas y sinformas establecidas en los trabajos anteriores de Millán (1981) y Pardo (1986). La falta de una información geológica más detallada impidió el desmembramiento de las partes media y superior de la Fm. Agua Santa. - Con fines comparativos se señalan en este equema, además, el contorno del minímo gravimétrco regional (con el perfil de estudio que atraviesa su región central) y la ubicación de los yacimientos conocido. Relativo a estos aspectos, resulta notorio la coincidencia espacial del mínim gravimétrico con un importante nudo tectónico en el centro del macizo, y la posición de los yacimientos, próxima al límite entre las capas Victoria y Loma (Fm. Canada) en los flancos de la Antiforma Río Los Indios.

EL POSIBLE PATRON DE FRACTURAS DEL DOMO CON EL CUAL SE VINCULA LA MINERALIZACION

Al enfocar este problema se parte de tres consideraciones básicas: (1) el intenso y prolongado proceso de erosión a que ha estado sometido el macizo, ha determinado el caracter escultural-estructural del relieve actual; (2) la ocurrencia del proceso de mineralización, poteríor, al metamorfismo regional (a lo cual acreditan los datos geológicos y radiométricos de Garapko y otros, 1974; Millán, 1975; Ananin y otros, 1976; Buguelsky y otros, 1985) ha favorecido el reconocimiento de los sectores metasomatizados, por formas positivas residuales del relieve actual, localizadas dentro del campo de divisorias de aguas. De ésto se infiere, que las zonas de agrietamiento tectónico desarrolladas con la estructura cupular tardía, las cuales, presumiblemente, sirvieron de canales principales para la circulación de las hidrotermas, deban tener, por consiguient, un claro reflejo en el sistema principal de divisorias de aguas, y; (3) la regularidad regional en la distribución de las anomalías aero-espectrométricas de potasio más intesa (> 1%), refleja, en gran medida, el desarrollo del proceso de metasomatismo en la región. De las consideraciones anteríores se infiere que deba existir una aceptable correlación espacial de las ocurrencias minerales y las anomalías de potasio (> 1%), con el campo de divisorias de aguas.

A partir de la red de drenaje del macizo se obtuvo, por transformación, el campo de divisorias de aguas, reprentado en la Fig. 3. La operación de transformación consistió en le trazado de los polígonos de influencia para los puntos de la red localizados en la desembocadura de los cursos de aguas. Con fines comparativos se ha senalado en esta figura, además, las ocurrencias minerales y en contorno del mínimo gravimétrico regiónal. en la misma se destaca la aparente correspondencia espacial de las ocurrencias minerales con el campo de divisorias de aguas, así como la convergencia

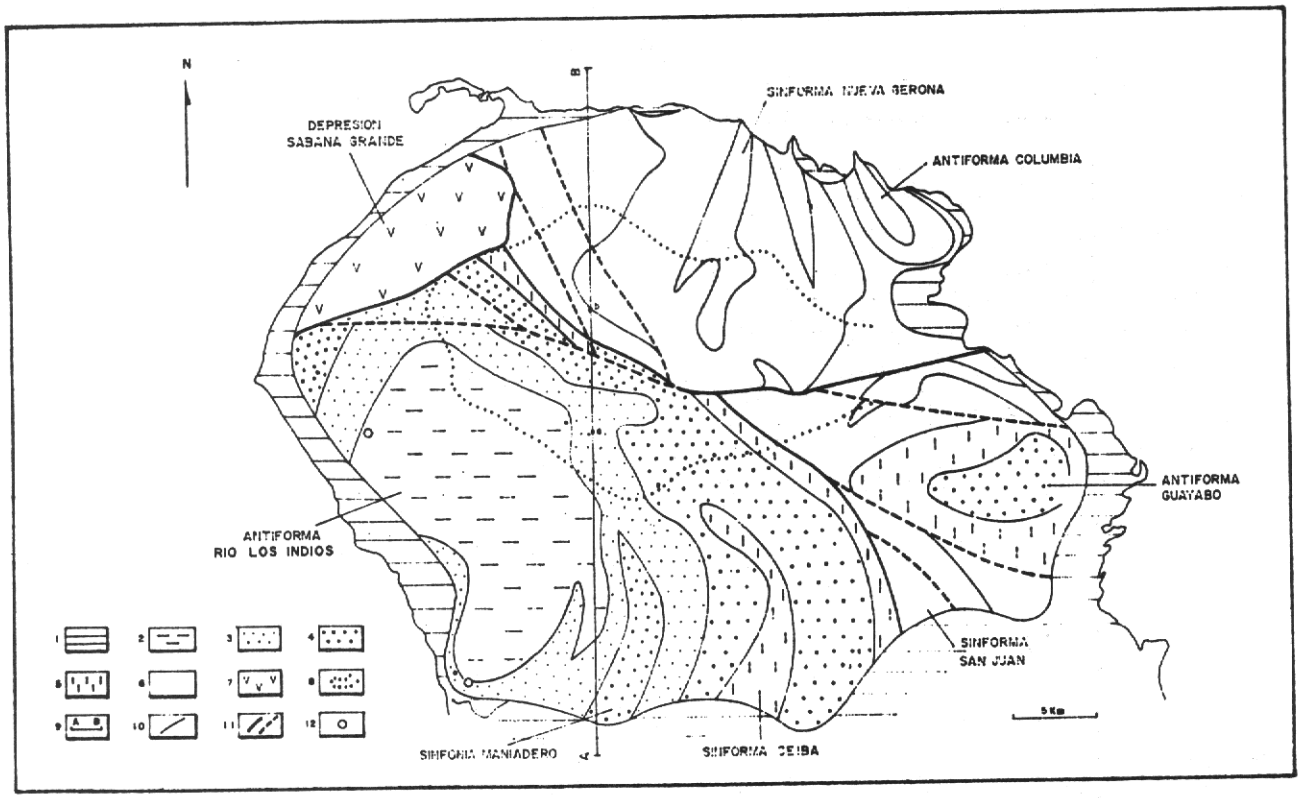

Fig. 2 Esquema geólogo-estructural (interpretativo) del macizo Isla de la Juventud. 1. Depósitos recientes; 2-4. Fm. Cañada: 2) parte inferíor, 3) parte media, 4) parte superíor; 5-6. Fm. Agua Santa: - 5) parte inferíor, 6) parte media y superíor; 7. Rocas volcanógen-sedimentarias; 8. Contorno del mínimo gravimétrico regional (isolínea de 16 mgal); 9. Perfil de estudio; 10. Límites litologo-estructurales; 11. Dislocaciones tectónicas; 12. Depositos conocidos.

de su distribución radial en torno a los límites del minimo gravimétrico regional.

El sistema axial principal de divisorias de aguas, representado en la Fig. 4, se trazó directamente a partir de las cartas topográficas. Tambien, con fines comparativos, se muestra en esta figura, el mínimo gravimétrico, las principales dislocaciones tectonicas que convergen en su región central y, los yacimientos conocidos. Del análisis de la mismas se destaca la semejanza con el cuadro de la regularidad regional en la distribución de las anomalías complejas geoquímico-geofísico-gemorfológicas (Fig. 1).

La regularidad regional en la distribución de las anomalías de potasio (≥1%) (pobtenida a partir de la correlación e las anomalías ≥0.5 %) se presenta en la Fig. 5. Como en las figuras anteríores, se han señalado, con fines compratívos, el mínimo gravimétrico y los yacimientos conocidos. Aquí se observa tambíen un cuadro muy parecido al de la Fig. 1., aunque, la convergencia de la regularidad radial se establece en torno a un núcleo anómalo que coincide especialmente con el mudo tectónico del centrl del macizo.

Con el propósito de argumentar el razonamiento expuesto al inicio de este epígrafe, se realizó el análisis de la correspondencia espacial del campo de divisorias de aguas con las ocurrencias minerales y las anomalías del canal de potasio (≥1%). A tal fin, se elaboraron las tablas de contingencia (Tablas 1 y 2) que sirven de base para el cálculo del coeficiente de correlación (r)

La expresión del coeficiente de correlación (r), segun Bondarenko y otros (1985), tiene la forma siguiente:

$$r = (AC \cdot BD \cdot AD)/(S1 \cdot S3 \cdot S2 \cdot S4)^{1/2} \qquad (1)$$

Evaluando la expresión (1) para los datos de las Tablas 1. y 2., se obtiene que:

$$r_1 = 0{,}22, \text{ y } r_2 = 0{,}17$$

Para el establecimiento de la dependencia significativa entre los atributos, se comparó el coeficiente de correlación estimado con el valor permisible para un nivel de significación del 95%.

Según Bondarenko y otros (1985), el valor permisible se determina en base a la expresión:

$$r_p = 3 (1 - r^2) / N^{1/2} \quad (2)$$

donde N es el total de celdas elementales en que ha sido subdividida el area de estudio.

Evaluando la expresión (2) para los datos anteríores, se obtiene que:

$$r_{p1} = 0{,}10 \text{ y } r_{p2} = 0,\ 11,$$

por consiguiente, dado que $r_1 > r_{p1}$ y $r_2 > r_{p2}$, se puede plantear que la correspondencia de la mineralización y de las anomalías de potasio (≥1%), con el campo de divisorias de aguas, al parecer, no es casual, sino que está condiciónada por causas geológicas.

Como resultad de todo el análisis anteríor (Figs. 3, 4 y 5) se puede concluir, a mode de síntesis, que:

- el sistema axial principal de divisorias de aguas (Fig. 4) refleja un cuadro, sino coincidente, muy parecido al posible patrón de fracturas del domo con el cual puede estar vinculada la mineralización;

- el mínimo gravimétrico regional parece estar provocado por una heterogeneidad local de la densidad, de grandes proporciones, localizada en la región núclear del domo, y;

- esta última, a juzgar por su posición, desplazada algo al sur, con respecto al nudo tectónico del centro del macizo, refleja, al parecer, la asimetría del domo, el cual se supone tenga un buzamiento más abrupto en su flanco septentríonal.

EL POSIBLE DESARROLLO DEL MAGMATISMO ACIDO EN LA REGION Y SU RELACION CON LA ESTRUCTURA DOMICA

La hipótesis general del trabajo planteada en la investigación precedente (Pardo, 1986), proponía, para expliar el desarrollo del magmatismo ácido en la region y la mineralización metálica vinculada al mismo, al siguiente modelo: la ocurrencia de la granitización metamorfogénica

Fig. 3. Campo de divisorias de aguas del macizo Isla de la Juventud. 1. Zona divisoria de aguas; 2. Contorno del mínimo gravimétrico regional (isolínea de 16 mgal); 3. Manifestaciones minerals: a) Sn, W, As, Au, Ag, Sb, b) Ni, Cu, Pb, Zn.

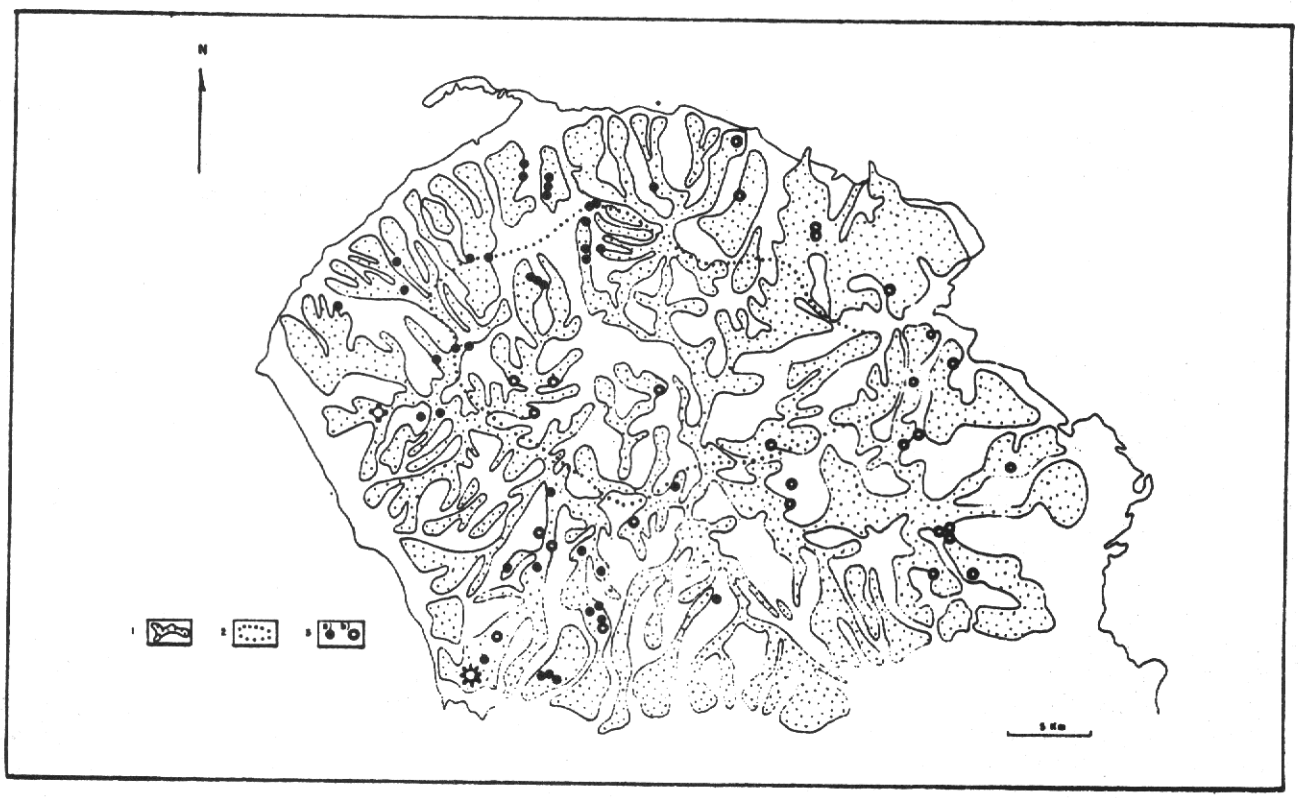

Tabla 1

Atributos	Presencia de divisorias de agua (C)	Ausencia de divisorias de aguas (D)	Total
Presencia de mineralización (A)	48	8	56 (S3)
Ausencia de mineralización (B)	300	396	696 (S4)
Total	348 (S1)	404 (2)	752 (N)

Tabla 2

Atributos	Presencia de dovisorias de aguas (C)	Ausencia de dovisoriasas de aguas (D)	Total
Presencia de anomalías (A)	64	30	94 (S3)
Ausencia de anomalías (B)	284	374	658 (S4)
Total	348 (S1)	404 (S2)	752 (N)

del basamento cristalino (como expresión de la densificación material local en la base de la corteza), la formación de fundidos anatécticos, su acumulación en cámaras, hibridismo, diferenciación, y posterior penetración el las grietas y fallas, a lo cual se superpuso, finalmente, la inyección de volátiles y soluciones hidrotermales metalíferas. El inicio de este proceso, a juzgar por los datos radiométricos y geológicos (Garapko y otros, 1974; Millán, 1975; Ananin y otros, 1976; Buguelsky y otros, 1985) se proponía, a fines del cretácico, y su desarrollo se extendía, hasta el paleógeno. Por su parte, el modelo menífero propuesto por Pardo (1986) suponía la presencia de rocas subvolcánicas ácidas cercanas a la superficie (<2 km), como representates de los apófisis diferenciados de pequenas intrusiónes hipoabisales, localizadas en la intersección de grietas y fallas profundas, formadas, presumiblemente, durante el desarrollo de la estructura dómica. Con estos subvolcánicos se relaciona la mineralización hidrotermal zonada de distintos tipos concebida como variedades faciales en función de la profundidad de formación. Aunque en el referido trabajo no se aborda el problema relativo a la fuente de los metales, se puede suponer implícito al modelo anterior, el mecanismo de herencia metalogénica concebido en la forma de su planteamiento original (Routhier, 1973). Este aspecto sera tratado más ampliamente en el siguiente epigrafe.

El modelo descrito trataba de explicar un conjunto de importantes - rasgos, característicos para esta región, como son - la asociación de los depósitos minerales con cuerpos subvolcánicos de granito-pórfiro (y no con granitos en sí); - la escala de la mineralización, significantemente pequeña en comparación con otras regiones granito metalíferas productivas, y su carácter disperso; la ausencia de una correspondencia espacial entre la mineralización y el mínimo gravimétrico regional, y la zonalidad vertical escalonada de los distintos tipos de mineralización observada en los depositos conocidos. El análisis de la regularidad regional en la distribución de las anomalías geoquímicas complejas (exógenas) y gravimétricas residuales negativas, aporta una mayor argumentación al

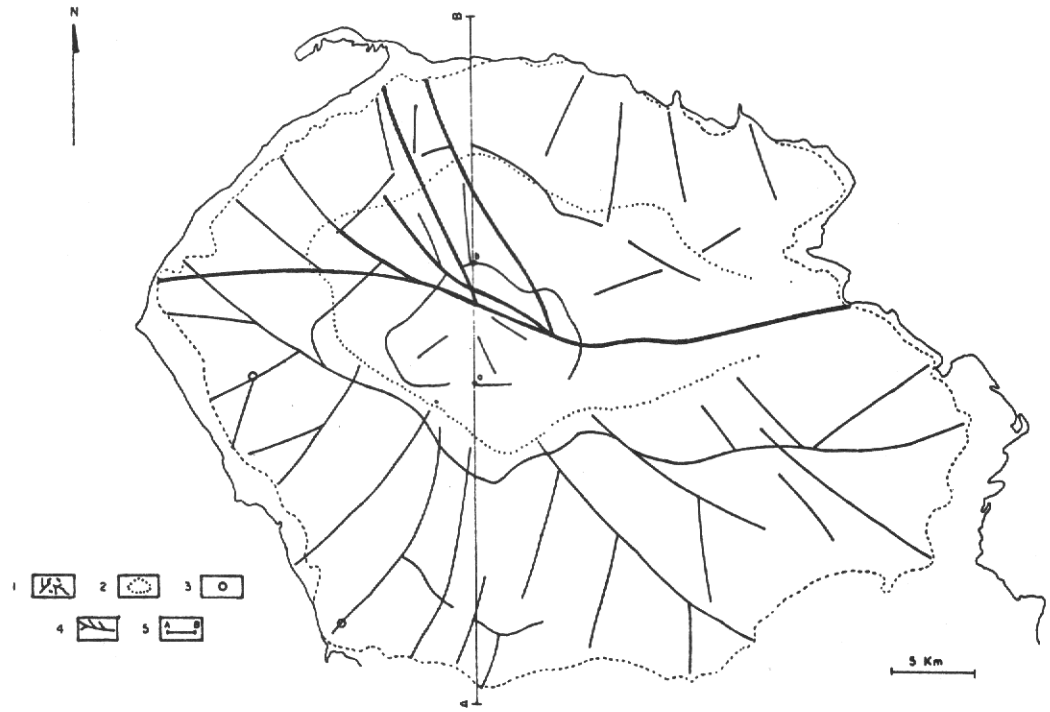

Fig. 4. Sistema axial principal de divisorias de aguas del macizo - Isla de la Juventud. 1. Ejes de las zonas divisorias de aguas; 2. Contorno del mínimo gravimétrico regional (isolínea de 16 mgal); 3. Depósito conocido; 4. Dislocaciones tectónicas; 5. Perfil de estudio.

Fig. 5. Distribución de las anomalías aeroespectrométricas de potasión (>1%) y su regularidad en el macizo Isla de la Juventud. 1. Regularidad en la distribución de las anomalías de potasio (>0, 5%); 2. Contorno del mínimo gravimétrico regional (isolínea de 16 mgal); 3. Depósito conocido.

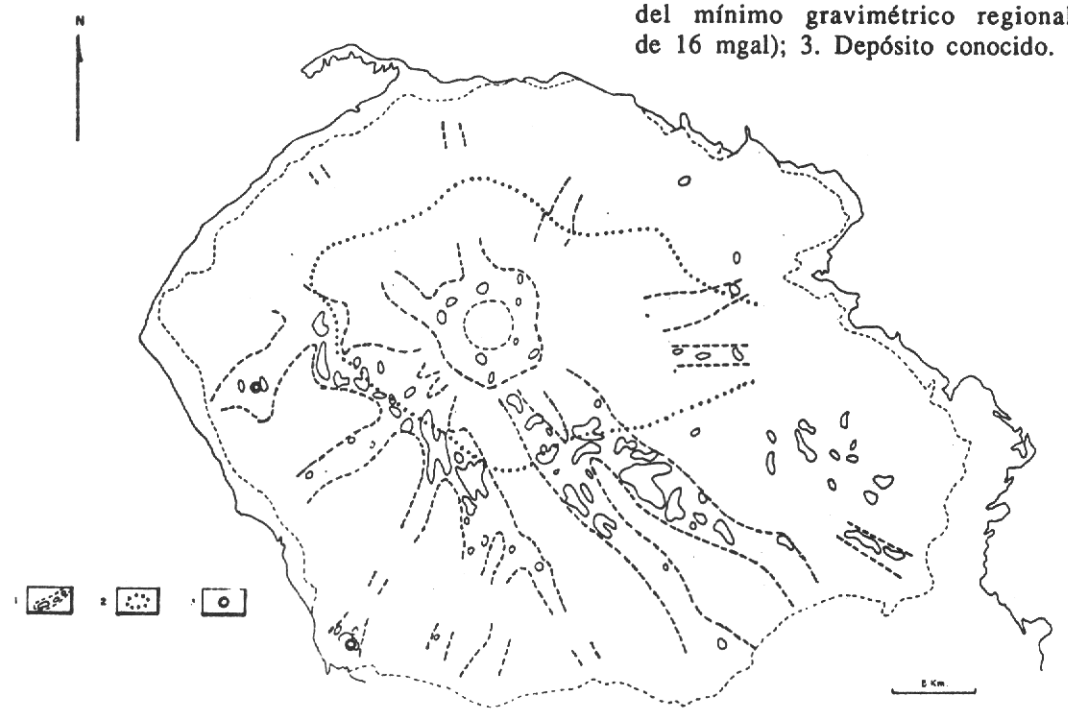

modelo planteado. Para ésto hagamos referencia a las correspondientes distribuciones de estas anomalías.

El mapa de anomalías geoquímicas compoehjas oxógenas (Fig. 6), confeccionado por Riftin y otros (1988) en base a la generalización de los levantamientos metalométricos realizados en el territorío, destaca una regularidad regional radial que converge en el nudo tectónico del centro del macizo, y una regionalización en la especialización geoquímica por la que se separan dos bloques, uno occidental (Mo, Sn, W, As, Au, Ag, Sb, Co, Ni Cu, Pb, Zn), y otro oriental (Mo, Sn, Co, Ni, Cu, Pb, Zn). Otro aspecto importante a considerar es la forma de las anomalías, las cuales se ensanchan y/o quedan abiertas próximo a su límite con la costa o con la Cienaga de Lanier, indicando la posible localización de las respectivas fuentes.

El esquema de anomalías gravimétricas residuales negativas presentado (Fig. 7), se obtuvo po modificación del original de autor (poligono Cuba-URSS Pinar III, 1987) basado en: el contorneo de las anomalías < -0,5 mgal; la incorporación de las anomalías en la zona costera marina (obtenidas por suavización manual del mapa gravimétrico del territorío de Garapko y otros, 1974) y; la discriminación de las anomalías vinculadas a depresiónes de la superficie de la roca fresca. Esta última operación se realizó mediante la comparación con el mapa del relieve residual de la región. elaborado en el trabajo precedente (Pardo, 1986). Al considerar las posibles fuentes de las anomalías grivimétricas residuales negativas y su naturaleza (una vez excluida la invluencia del factor anteríor), se establece, en base al conocimiento de las propiedades físicas de las rocas en la región (Pardo, 1986) y de la experiencia personal de trabajo en le territorío del investigador S. Akilbekov (comun. pers., 1987), el vínculo de las anomalías con heterogeneidades superficiales (0-2km) de naturaleza grafítica, granítica (subvolcánica), y/o metasomática, todas ellas con una desidad efectiva de -0,10 a -0,15 g/cm^3. La naturaleza grafítica, a juzgar por su amplio desarrollo en los sectores mineralizados conocidos, puede tener tambíen una contribución metasomática. Tambíen del análisis de esta figura se evidencia la regularidad radial en la distribución de las anomalías en torno al límite del mínimo gravimétrico regional donde éstas convergen. El aspecto más importante de la regularidad observada radica, como en el caso de la figura anteríor, en la continuidad de las zona anómalas hacia el mar y la Cienaga de Lanier, donde estas se ensanchan y/o se presentan como anomalías isométricas de mayores proporciones (10-20 km^2). En esta figura se trazó, además, la línea que une los epicentros de estas anomalías, la cual pudiera coincidir con un sistema anular de

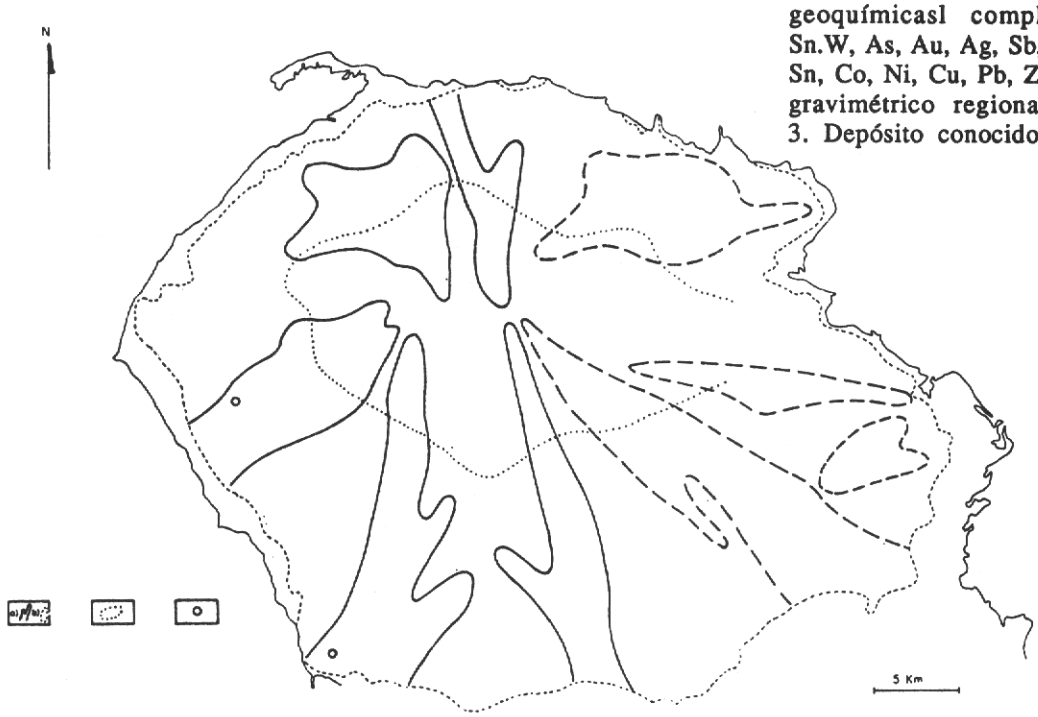

Fig. 6. Mapa de anomalías geoquímicas complejas exognas del macizo Isla de la Juventud (Riftin y otros, 1988). i. Anomalías geoquímicasl complejas exogenas: a) Mo, Sn.W, As, Au, Ag, Sb, Co, Ni, Cu, Pb, Zn, b) No, Sn, Co, Ni, Cu, Pb, Zn; 2. Contorno del minomo gravimétrico regional (isolínea de 16 mgal); 3. Depósito conocidos

fracturas profundas, originado, presumiblemente, durante el desarrollo del domo. Quizás no sea casual la virtual coincidencia de este límite con el actual contorno (fracturado) del macizo, establecido por los trabajos de levantamiento geológico de la plataforma marina de este territorío, en escala 1:100 000 (Hernandez y otros, 1988). A modo de síntesis de los resultados anterfores (Fig. 6 y 7) se puede inferir que:

- los focos principlaes del magmatismo ácido con los que, presumiblemente, se vincula la mineralización metálica endógena en el macizo, constituye, al parecer, pequeños plutones (50-100 km2) emplazados en la intersección del sistema radial de grietas del domo con el sistema anular de fracturas profundas que lo delimita, y;

- la naturaleza de la heterogeneidad local de la densidad, de grandes proporciones, localizada en la región nuclear del domo, al parecer, es granítica pero esteril, a juzgar por la ausencia de ocurrencias - minerales y de anomalías geoquímicas en esta area. La carácteristica morfológica del mínimo gravimétrico regional y su posición con respecto a la estructura geológica del macizo (Fig. 2), sugieren el posible emplazamiento del referico cuerpo granítico, a través de la falla profunda que separa los dos principales megabloques plegados en la parte central del macizo. Su forma, a juzgar por los resultados del modelaje volumétrico en el perfil de estudio (Fig. 8), simular la de una intrusión de tipo facolítico.

Para la solución de la tarea inversa de la gravimetría se utilizó el algoritmo de Sousin y Gross (1985). Dado el propósito orientativo de esta interpretación, no se intentó mejorar el ajuste de la curva calculada con la observada. Tambíen en esta figura se observan, próximo a los extremos del perfil, dos pequeños cuerpos cercanos a la superficie, interpretados como posibles apófisis subvolcánicos.

Intentemos, finalmente, explicar el proceso de evolución estructural del domo, con el cual, presumiblemente, se vínculó el desarrollo del magmatismo ácido en la región. Para ésto refiramonos a los resultados del trabajo de Hafner (1951) sobre el modelaje matemático de las deformaciones tectónicas, representados parcialmente en la Fig. 9. (modificada del original). En esta se presenta, en el caso I, el posible evento inicial de la formación del domo. Este considera la presencia de un campo de esfuerzos tangenciales, de carácter sinusoidal, con longitud de onda L_1, aplicado en la base de un bloque que representa, aproximadamente, las condiciones de espesor de la corteza y extensión de la región afectada al inicio del proceso de distensión localizada. En esta etapa no existen aún fuerzas verticales (A = 0), y la

Fig. 7. Distribución de las anomalías gravimétricas residuales negativas en el macizo Isla de la Juventud. 1. Línea que une los epicentros de la anomalías perifericas; 2. Anomalías residuales negativas; 3. Contorno del mínimo gravimétrico regional (isolínea de 16 mgal); 4. Depósitos conocidos.

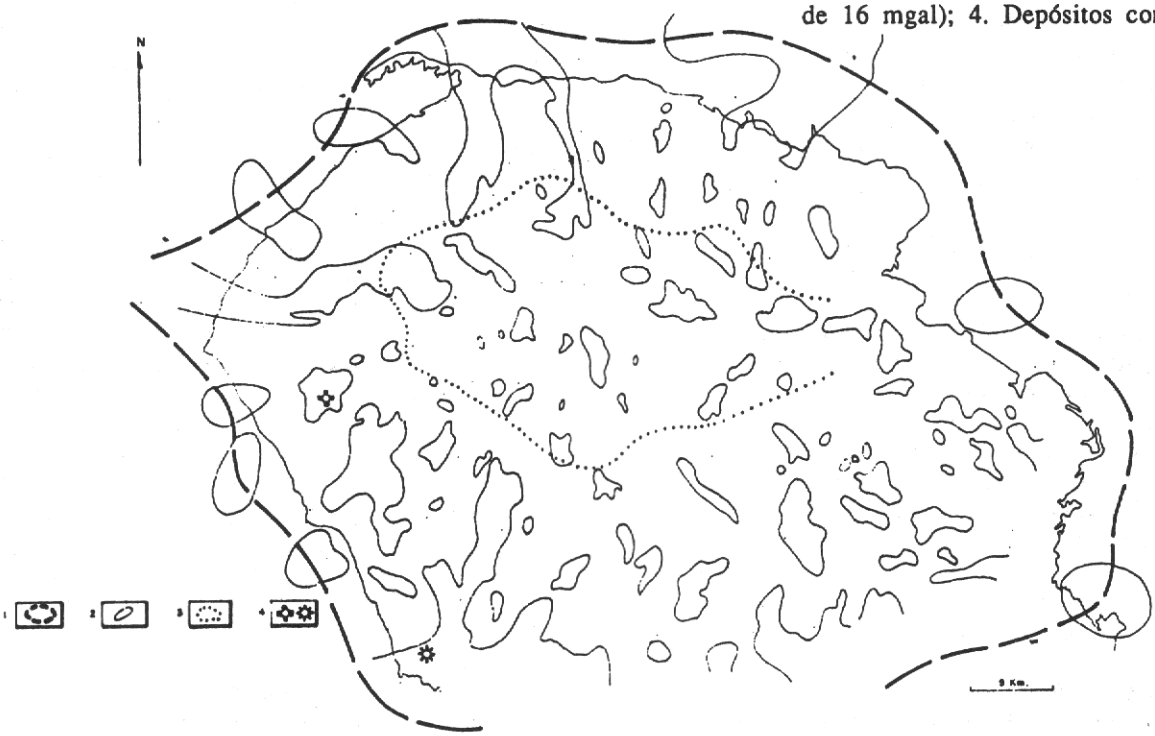

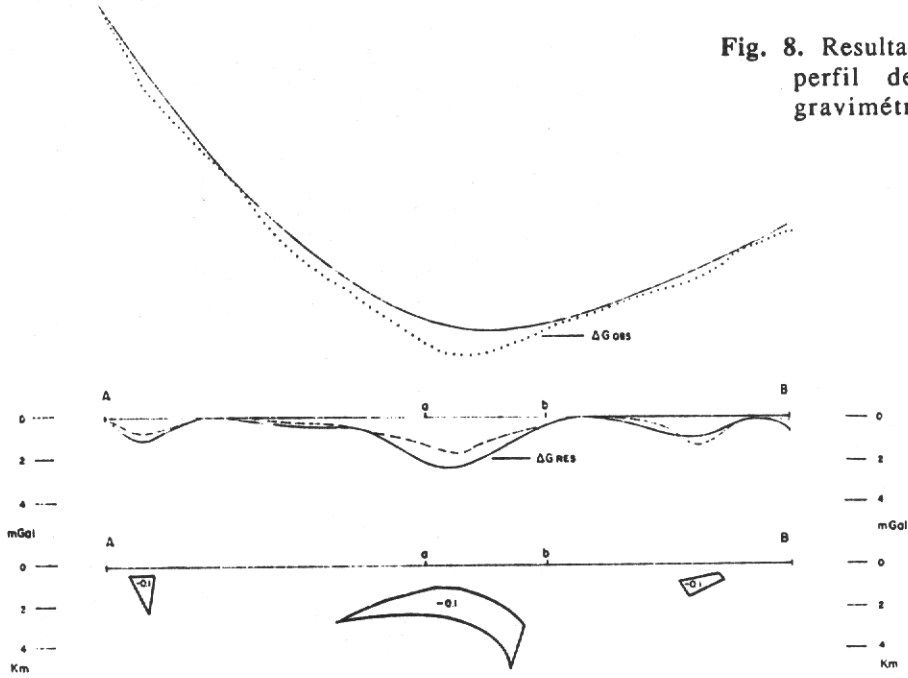

Fig. 8. Resultados del modelaje volumétrico en el perfil de estudio en base a los datos gravimétricos.

magnitud del esfuerzo tangencial (σ_{xy}) aumenta desde el centro hacia ambos extremos del bloque. La componente horizontal del edsfuerzo (σ_x) resultante de tal sistema según Hafner (1951), varia con la profundidad, tanto en signo como en magnitud, desde valores maximos de esfuerzos compresivos en la superficie, hasta valores máximos de esfuezos distensivos en la base. Un rasgo peculiar e importante de un sistema de esfuerzos de este tipo, de acuerdo con el referico autor, es que el mismo produce los niveles de fallamiento separados por una zona de estabilidad intermedia. Correspondientemente a las variaciones de σ_x señaladas, ocurre un nivel de fallamiento normal en la base del bloque (que se interpreta como causa de la desdensificación estructural), y una delgada zona de sobrecorrimientos en su parte superíor. Se presume, que conjuntamente cn la desdensificación estructural de la base del bloque, haya tenido lugar su desdensificación material (granitización metamorfogénica) en condiciones de un alto gradiente de temperatura. Esto coincidiría con el supuesto emplazamiento del focolito granítico en la región nuclear del domo, el cual requiere de condiciones muy parecidas a las desoritas para esta etapa.

El subsiguiente evento, representado en la Fig. 9 por el Caso II, considera el inicio de la acción de fuerzas verticales. En esta etapa el proceso de distensión se hace más local y el sistema de esfuerzos se transforma. Este se compone ahora por una presión vertical de carácter sinuscidal con longitud de onda L2 = $L_1/2$ y una presión tangencial de iguales características; ambas aplicadas en la base del bloque. La componente vertical del esfuerzo (σ_y) decrece gradualmente desde un valor máximo en el centro, has ca cero en ambos extremos del bloque. La componente tangencial (σ_{xy}) tiene igual comportamiento que en el caso anteríor. Estos dos esfuerzos primaríos, según Hafner (1951), dan lugar a una componente horizontal (σ_x) distensiva, aproximadamente constante con la profundidad. En opinión de este autor, durante el desarrollo gradual de un sistema de esfuerzos de este tipo se estable un régimen de inestabilidad con un fallamiento resultante, que se incia en un nivel superficial extenso, pero relativamente delgado. Con la continua intensificación de los esfuerzos primaríos, esta zona se expande con la profundidad y, en unmenor grado, lateralmente. Al alcanzar su valor máximo (3000 kg/cm3 en este ejemplo) esta zona se extiende hasta abarca completamente la base del bloque en sus partes extremas, pero sin cubrir la región central profunda la cual se mantiene estable. En la parte central y superíor del bloque ocurren fallas normales de dos conjuntos con buzamientos característicos. Alejado del centro, el buzamiento de las fallas de uno de estos conjuntos aumenta gradualmente hasta vertical, e incluso, se invierte ligeramente próximo al extremo del bloque, lo que da lugar, en regiones erodadas, a que sean interpretadas como fallas inversas. Es preciso destacar que solamente estas fallas cercanas a los límites del bloque logran alcanzar su base, por lo que se supone, constituyeron los

únicos posibles canales de ascenso a la superficie de los fundidos anatécticos, formados, presumiblemente, durante el evento anterior. Estas fallas con buzamiento abrupto, vertical e, incluso, ligeramente invertico, se observan frecuentemente, ségun Hafner (1951), en regiones con tectónica diapírica o sujetas a un levantamiento vertica diferencial. El conjunto complementarío de fallas normales, de acuerdo con este autor, disminuye progresivamente su buzamiento desde valores de 60^0 en el centro del bloque, hasta valores de 15^0 en sus partes profundas más alejadas; este conjunto tiene una rara ocurrencia.

CAPACIDAD PREDICTIVA DEL MODELO MENIFER-ESTRUCTURO-METALOGENICO

Al abordar este problema, el cual se vincula estrachamente con la de la región, espreciso considerar los siguentes aspectos basicos:
- rasgos particulares del desarrollo de la tectónica diapirica en la región,
- herencia metalogénica,
- estructuras plegadas preexistentes,
- propiedades físico-químicas del medio encajante,
- profundidad y amplitud vertical de la deposición menifera.

El desarrollo de la tectónica diapírica en la región condicionó, al parecer, la formación de un domo con elipticidad poco pronunciada, ligeramente asimétrico (buzamiento suave al sur), con una amplia región nuclear (bien definida por el contorno del mínimo gravimétrico regional fijado por la isolínea de 16 mgal) en cuyos límites converge un sistema radial de zonas de agrietamiento, con un mayor desarrollo en su flanco meridional. En la intersección de este sistema radial de grietas con la zona periférica anular de fracturas profundas, la cual sirvió, presumiblemente, de canal para el ascenso de los fundidos magmáticos, se crearon, al parecer, las condiciones favorables para el emplazamiento de

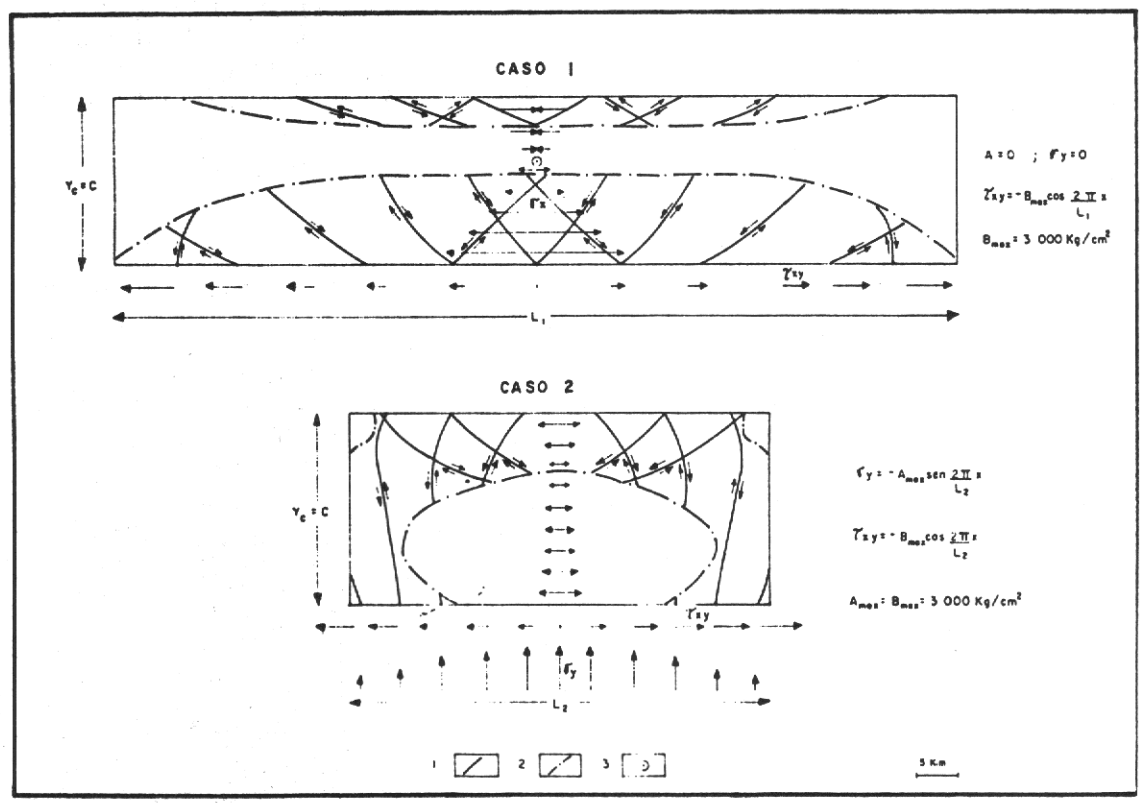

Fig. 9. Ejemplos de los resultados del modelaje matematico de las deformaciones tectónicas para los casos de un sistema de esfuerzos tangenciales y verticales variables actuando en la base de un bloque (Hafner, 1951; laminas 1Ab y 1Bb). 1. Posición de las superficies de fracturas potenciales, 0 = 30o; 2. Límite de las areas de estabilidad para valores de B max 3000 kg/cm^2 ; 3. Punto singular de cero esfuerzo cizallante.

pequeños plutones hipoabisales, cuyos apófisis subvolcánicos constituyeron los principales focos de la mineralización. Dentro del sistema radial de grietas tuvo lugar, al parecer, la telescopización de las intrusiones fisurales y de la mineralización, cuya magnitud, a juzgar por los datos geológo-geoquímico-geofísicos (Pardo, 1986), alcanza como promedio, una distancia de 15 km por la horizontal a partir de los supuestos focos subvolcánicos. La mayor favorabilidad para la ocurrencia de la mineralizacion debió tener lugar, por consiguiente, en el flanco meridional de la estructural dómica (donde están más desarrolladas estas zonas de agrietamiento) dentro de una "franja crítica" de aproximadamente 15km a partir de la línea que define la posición de la supuesta zona periférica anular de fracturas profundas. Resultan particularmente favorables aquellas zonas de agrietamiento reveladas por el complejo de datos geológo-geoquímico-geofísico-geomorfológicos.

Al considerar el proceso de transporte y deposición de los minerales metálicos desde su fuente granítica, se asume un modelo de diferenciación por cristalización fraccionada (Stemprok, 1982). Este supone la diferenciación del fundido magmático mediante la eliminación de cristales del sistema. La mezcla residual, como regla, rica en silicatos alcalinos (especialmente potasio) se concentra junto con grandes cantidades de metales (Mo, Sn, W, Au y otros) en el centro del granito solidificante y es expulsada hacia el techo de la masa rocosa. Junto con los metales se concentran, en esas mezclas residuales, el uranio y el thorío. De ahí que el enriquecimiento de la roca huesped en estos elementos, y en particular en uranio, sirva de índice, junto con el potasio, para el reconocimiento de las fuentes mencionadas. Este enriquecimiento en uranio tiene lugar, con preferencia (Yeates y otros, 1982) para los depósitos de F, Mo, Sn, W. y otros metales raros.

Para explicar el origen de los metales, se acepta el mecanismo de herencia propuesto por Routhier (1973), el cual considera que el basamente reelaborado durante el proceso de granitización contiene depositos de los mismos metales. Así, los plutones graníticos formados condujeron a concentraciones minerales, al parecer, solo donde éstos sobreyacían a las zonas mineralizadas preexistentes; fuera de estos lugares son, presumiblemente, estériles. De este mode se explican las diferencias en las escala de la mineralización de distintos sectores (incluyendo la región nuclear del domo), y la regionalización geoquímica del territorío, la cual, presumiblemente, reproduce la zonalidad geoquímica (y metalogénica) del basamento.

Los estructuras plegadas preexistentes (de diferente órdenes) sirvieron, presumiblemente, de trampas estructurales para la deposición menífera. En correspondencia con una regularidad mundial (Rundkvist, 1971; Groves et al., 1987), la mayor favorabilidad debió correponder a los bloques hórsticos, en particular, po su amplitude, a la Antiforma Río Los Indios (Millán, 1981); y dentro de éstos a los cierres, flancos, y/o flexiones bruscas de las capas en las antiformas y, en menor grado, sinformas, de orden menor.

La deposición menífera, tambíen en corresondencia con una regularidad mundial (Runskvist, 1971; Volfson y Yakovlev, 1982; Groves et al., 1987) debio estar condicionada, presumiblemente, or los siguientes factores: un ambiente reductor dentro de rocas con un grado metamórfico nunco mayor que el límite entre las facies esquistos verdes y anfibolítica; una brusca variación en el pH de las soluciones metalíferas, y; la presencia de rocas impermeables que pudieran actuar como sello de las mismas. De acuerdo con ésto, y en ese mismo orden, la mayor favorabilidad debió tener lugar para: la potente secuencia carbonosa Victoria (Fm. Canada) con abundante contenido de pirita singenética, y la secuencia volcanógena andesito-basáltica (Fm. vulcanógena-sodimentaria Sabana Grande) dada la presencia de silicatos ferruginosos y pirita singenetica; el paso de las soluciones metalíferas de secuencias metaterrígenas a metacarbonáticas, o de alguna de éstas a secuencias volcanógenas y; la presencia, dentro de las secuencias anteríores, de paquetes de esquistos cuarcíferos metapsamíticos, de marmoles, y, de sedimentos tobáceos (dentro de la formación vulcanógena-sedimentaria) como posibles sellos. Al analizar de conjunto los aspectos antes señalados, se deriva que los límites litólogo-estratigráficos más favorables para deposición menífera fueron, probablemente, el contacto entre la parte inferíor de la Fm. Cañada y sus partes media y superíor; el contacto entre las formaciones Cañada y Agua Santa; el contacto vulcanitas-metamorfitas y, finalmente; el contacto entre paquetes andesito-basálticos y paquetes tobaceos dentro de la formación vulcanógena-sedimentaria.

En correspondencia con una regularidad mundial (Smirnov, 1980; Kitaev, 1982; Volfsen y Yakovlev, 1982) y en base al análisis de la reconocida zonalidad vertical del sistema de formacin menífera de metales preciosos y raros en esta región, se establecen, al menos dos zonas de deposición menifea (Pardo, 1986): una subvolcánica suprayacente (0,5 - 1,2 km) y otra subvolcánica infrayacente (1,0 - 2,0 km). Estas resumen las particularidades individuales morfoestructurales y mineralogo-geoquímicas de

la mineralización en los depósitos conocidos, Delita y Lola, respectivamente. Tal planteamiento se ve confirmado por los resultados de investigaciones recientes, sobre la composición sustencial de las monas, la isotopica de azufre y oxígeno, así como de las inclusiones gaseoso-líquidas, realizadas a las menas del yacimiento aurífero Delita (Kramer, 1988). De acuerdo con estas investigaciones, la deposición menífera tuvo lugar: a profundidades medias; bajo condiciones de presión y temperatura oscilando, respectivamente, entre 210 - 400 ^{0}C y, 0,9 - 1,5 kb; a partir de soluciones con gran cantidad de ácido carbónico y metano y, principalmente, como resultado de un mecanismo de efervecencia. De acuerdo con las dos zonas reconocidas, a amplitud vertical de la deposición menífera en la región se establece entre 0,7 y 1,5 km. El nivel del corte erosiónado, estimado para los depósitos de Delita y Lela (Pardo, 1986) oscila, respectivamente, entre 0,7 y 1,2 km, de lo que se infiere que el actual corte de erosión alcanza las anomalías geoquímicas y mineralógicas, haciendo detectable la mineralización oculta por los métodos de investigación de superficie, preferentemente, en zonas algo más alejadas de la costa y de la Ciénaga de Lanier. Finalmente, la profundidad de los focos magmáticos se estima (Pardo, 1986), para los apófisis subvolcánicos, entre 1,5, y 2,5 km, y para su fuente hipoabisal, entre 2,5 y 4,5 km; en ambos casos con respecto a la superficie original. Aunque no se ha podido establecer en base a los datos disponibles (Garapko y otros, 1974; Riftin y otros, 1988) la zonalidad geoquímica-mineralógica regional (en el plano local fue establecida por el autor en el trabajo procedente) que delimita las zonas críticas para a ocurrencia de la mineralización metálica de distintos tipos, por ejemplo, de Mo-W y Au-Ag-Sb; éstas pueden determinarse, orientativamente, en base al modelo propuesto, tomando en consideración los estimados anteríores.

CONCLUSIONES

El modelo menífero-estructuro-metalogénico propuesto para el macizo Isla de la Juventud, ofrece una alternativa teórica a la explicación de los rasgos principales del desarrollo tectóno-magmático tardío de esta región y su metalogenia asociada. Su capacidad predictiva no se restringe a la delimitación de los sectores más favorable para la ocurrencia de la mineralización, sino que tambíen proporciona un metodo para el reconocimiento y estudio de otras regiones con una evolución geológica tardia semejante. No obstante, su definitivo valor se establecerá a partir de una confrontación más precisa con la realidad geológica de este territorío.

REFERENCIAS

Ananin, V., 1976, M. Gajardo, M. Pardo, y otros, Informe sobre los trabajos de busqueda-exploración en escala 1:10000-1:2000 en el yacimiento aurífero Delita, Isla de Pinos (inedito). Centro Nacional del Fondo Geológico, La Habana.

Bondarenko, V.N., R.I. Kogan, y otros, 1985, Métodos estadísticos durante las búsquedas geoquímicas de los yacimientos minerales, Oriente, Santiago de Cuba, 183 p.

Buguelsky, Y., O. Vazquez, y otros, 1985, Yacimientos minerales metálicos de Cuba (en ruso), Nauka, Moscú, 246 p.

Expedición Cuba-URSS Pinar III, 1987, Mapa (preliminar) de anomalías gravimétricas residuales (R=3Km) del macizo Isla de la Juventud en escala 1:50 000 (inédito), Establecimiento de Geología Isa de la Juventud, La Demajagua.

Garapko, I., O. Buliga, y otros, 1974, La composición geológica y los minerales útiles de Isla de Pinos; informe del levantamiento en escala 1:100 000 (inédito), Centro Nacional del Fondo Geológico, La Habana.

Groves, D.I., N. Phillips, et al., 1987, Graton scale distributión of Archean greenstone gold deposits; predictive capacity of the metamorphic model, Econ. Geol., v.82, 2045-2058.

Hafner, W., 1951, Stress distributions and faulting, Bull. of the Geol. Soc. of America, v.62, 373-398.

Hernandez, C., M. Cabrera, y otros, 1988, Informe sobre los trabajos geológicos regionales para minerales sólidos en la plataforma marina suroccidental de la República de Cuba, GEOMAR IV (inédito), Centro Nacional del Fondo Geológico, La Habana.

Kitaev, N.A., 1982, Sobre las zonas de mineralización aurífera en Transbaikalia Oriental (en ruso), Geología y Geofisica, v.2, 53-60.

Kramer, J.L., 1988, Composición sustancial y asociaciones minerales de los yacimientos auriferos cubanos (en ruso), tesis presentada en opción al grado de CSc (inédito), Instituto de Geología y Paleontología, La Habana.

Liubi, L.I., T.V. Martinova, y otros, 1984,

Resultados del levantamiento aerogeofísico complejo en escala 1:25 000 en la Isla de la Juventud (en ruso) (inédito), Centro Nacional del Fondo Geológico, La Habana.

Millán, G., 1975, El complejo cristalino mesozoico de Isla de Pinos; su metamorfismo, Serie Geológica ACC, no.23, 16p.

Millán, G., 1981, Geología del macizo metamorfico Isla de la Juventud, Ciencias de la Tierra y el Espacio. v.3, 3-22.

Pardo, M., 1986, La constitución geológica y la metalogenia endogena del macizo Isla de la Juventud, tesis presentada en opción al grado de CSc (inédito), Instituto de Geología y Paleontología, La Habana.

Riftin, V., G. Correa, y otros, 1988, Mapa de anomalías geoquímicas de la Republica de Cuba en escala 1:500 000 (inédito), Instituto de Geología y Paleontología, La Habana.

Routhier, P., 1973, Some major concepts of metallogeny, Miner. Deposita, v.8, 237-258.

Rundkvist, D.V., et al., 1971, Depositos de greisen; ontologia y filogenia (en ruso), Nedra, Moscú, 349 p.

Smirnov, V.I., 1980, Geología de los yacimientos minerales, MIR, Moscú, 654 p..

Stemprok, M., 1982, Yacimientos minerales asociados a los granitos, Boletin del PICG: La naturaleza y sus recursos, v.18 (3), 29-34.

Susin, O.A., y S.S. Gross, 1985, Algoritmo y programa para la solución de la tarea inversa (tridimensional) de la gravimetria (en ruso) (inédito), VINITI, Tadzhiquistan.

Volfson, F.I., y P.D. Yakovlev, 1982, Estructuras de los campos y yacimientos metaliferos, MIR, Moscú, 332 p.

Yeates, A.N., et al., 1982, Applicatión of gamma-ray spectrometry to prospecting for tin and tungsten granites, particulary within the Lachlan fold belt, New South Wales, Econ. Geol., v.77, p. 1725-1738.

EVOLUCION DE LA ESTRUCTURA DEL MACIZO DE ESCAMBRAY, SUR DE CUBA CENTRAL.

Guillermo Millán-Trujillo
Instituto de Geología y Paleontología,
Ministerio de Industrias Basicas, La Habana, CUBA

RESUMEN

Las secuencias jurásico-cretácicas del macizo del Escambray conformaron primeramente una sucesión de nappes y escamas apilados uno sobre el otro, destacándose 6 nappes principales (el más superior se emplazó posteriormente) y diferentes tipos de secuencias. Luego se sometieron a un proceso metamórifico con la ocurrencia de 5 fases (6 etapas) de plegamiento, cada una de las cuales se asocia con un sistema de esquistosidad o clivaje con sus tendencias definidas. El estilo de los pliegues varia en dependencia de la fase y del área; sus órdenes alcanzan hasta muchos centenares de metros. La fase 1 dió lugar a una esquistocidad con una tendencia NE a N-NE y pliegues isoclinales. La fase 2 conformó 2 grandes antiformas con una estrecha sin forma intermedia que se acuna hacia el Norte. La occidental es cupular elongada hacia el NO; mientras que la oriental está elongada más hacia el N-NO, desapareciendo al norte para formar parte del plan estructural de la primera. El sistema de esquistosidad relacional contornea a las antiformas y se asocia con pliegues isoclinales. En ambas antiformas se destaca otra esquistosidad más tardía en su parte axial, dispuesta concordantemente con sus ejes de elongación. La fase 3 se dispone siguiendo una tendencia arqueada independiente en cada mega-estructura. Esta fue intensa en la antiforma occidental y su efecto incrementó el desarrollo de la sinforma hacia el Norte. Las fases 4 y 5 imprimieron la elongación final hacia el O-NO de las antiformas. Finalmente las rocas fueron intensamente fracturadas.

Las secuencias primarias del macizo se depositaron en un margen continental. Su apilamiento en nappes, metamorfismo y plegamientos asociados, son consecuencia de una colisión ocurrida en el Cretácico Superior entre este margen y el arco volcánico cretácico; en la parte basal de este último ya se disponía el complejo anfibolítico Mabujina (CM). Debido a ello estas secuencias infracorrieron debajo del CM, metamorfizándose y multiplegandose en condiciones de un bajo gradiente temperatura/presión. El CM fue deformado conjuntamente con las mismas y su parte basal parcialmente reelaborada por el metamorfismo. Al desaparecer el estado compresivo vinculado con la colisión, las 2 megaestructuras positivas emergieron en forma diapirica, atravesando las rocas más densas del CM durante la busqueda del equilibrio gravitacional.

ABSTRACT

The Jurassic-Cretaceous rocks of the Escambray massif were first imbricated into a series of 6 thrust sheets (nappes), the highest of which was emplaced last; later, they experienced metamorphism and 5 phases (6 stages) of folding, each one associated with a set of schistosities or cleavages with characteristic orientations. The style of the folds varies, depending.on thier phase and location. The scale of the folding may be up to several hundreds of meters. Phase 1 formed NE to NNE trending schistosity and isoclinal folds. Phase 2 formed two megastructural, antiformal domes with an intervening synformal structure. The western dome is elongate NW, while the eastern dome is elongate in a NNW direction. The related set of schistosities wrap around the antiforms and is associated with isoclinal folds. In the center of both antiforms, a later cleavage is developed which is parallel to the elongation. Phase 3 structures follow an independent arcuate trend in each megastructure.This deformation was intense in the western antiform and enhanced the development of the synform to the north. Phases 4 and 5 produced the present ENE elongation of the antiforms. Finally, the rocks were intensely fractured.

The primary sequences of the were deposited on a continental margin. Thrusting, metamorphism and associated folding were the result of collision between this margin and a south facing (north dipping) island arc.whose basal part of the latter is represented by the amphibolitic Mabujina Complex (MC).The Escambray sequences were underthrust beneath the MC, metamorphosing and folding the rocks under high P/T conditions. The MC was thrust together with the Escambray nappes and its basal part partially deformed during the later metamorphism.After the compression resulting from the collision the two megastructural domes developed from the diapiric rise of the less dense Escambray sequences through the the denser rocks of the MC.

(English abstract by Gren Draper)

INTRODUCCION

El macizo de Escambray (Fig.1) está constituido por secuencias jurásico-cretácicas, metamor-fizadas en condiciones de baja relación Temperatura/Presión durante el Cretácico Superior. Su estructura interna es de tipo nappe-excamada, destacándose además diferentes fases superpuestas de

Larue, D.K., and Draper, G. (eds.),
Transactions of the 12th Caribbean Geological Conference, St. Croix, U.S.V.I., Miami Geological Society, P.O. Box 431552, South Miami, FL 33243, U.S.A

deformaciones relacionadas con el propio proceso metamórfico. Sin lugar a dudas, ésta es mucho mas complicada que la de cualquier otra región de Cuba, resultado estremadamente difícil realizar una cartografía del mismo que refleje de forma adecuada la realidad de su constitución geológico-estructural, hecho que se acentúa por la escasez de restos fósiles que permitan resolver adecuadamente la sucesión estratigráfica de sus secuencias. De aquí tambien la especulación que tradicionalmente ha existido, y que aún persiste, en cuanto a la edad de su protolitos. A pesar de que en la actualidad existen suficientes argumentos que confirman la tesis de que dentro de este maciso no afloran representates de su fundamento cristalino (ver Millán y Somin, 1985 a,b), hay algunos autores que, de una forma poco argumentada, recientemente consideraron que dentro del mismo afloran ampliamente metamorfitas que corresponden con us basamento prejurásico o premesozoico (Linares et al., 1985; Mossakovskii et al., 1986)

En cuanto a la estructura interna del macizo, Hill (1959 fue el primer geólogo que reportó la existencia de pliegues isoclinales dentro del mismo, así como de sobrecorrimientos tardíos, en su trabajo realizado en el extremo noroccidental de la magnestructura de Trinidad. Anteriormente se consideraba la misma de una manera muy simple (Thiadens, 1937), tendencia que se manifestó incluso con posterioridad (Maximov et al., 1968; Bolotin et al., 1970). Somin y Millán (1974) destacaron la existencia de plegamientos superpuestos de varias etapas de una zonación metamórfica invertida que disminuye hacia las partes internas de ambas magnestructuras. En Millán (1978) y Millán y Somin (1981) se destacaron algunas regularidades superpuestas, señalandose la existencia de grandes pliegues isoclinales y apretados de 2 fases diferentes, cuya superposición originó complicadas figuras cartográficas de interferencea. En esos mismo trabajos se consideró, equivocadamente, que las do megaestructuras que constituyen al macizo tuvieron un origen tardío, posterior al proceso metamórfico con sus plegamientos superpuestos asociados. Por otra parte, Suchanek (1980) en su trabajo estructural realizado en la megaestructura occidental, señaló también la presencia de varias fases de plegamiento superpuestas, destacando regularidades que muchas veces no coincidían con las establicidas en los trabajos señalados más arriba, ni tampoco en el presente trabajo. Este autor fue el primero en demostrar que la megaestructura cupular de Trinidad tuvo su génesis durante el propio proceso metamórfico. De acuerdo con el mismo, esta cupula se originó a partir de final de la primera fase de plegamiento (F_1), considerando además que ella tuvo su desarrollo más intenso durante las etapas más tardías de plegamientos sinmetamórficos, lo cual no concuerda con los materiales expuestos en el presente texto, Según Suchanek, la primera etapa de plegamiento (que según este trabajo corresponde realmente con la segunda fase F_2) está relacionada con la generación de grandes pliegues isoclinales, recumbentes, cuyos planos axiales tienen una vergencia dirigida hacia el centro de la cúpula debido a que se formaron durante el comienzo de la gestación de la misma.

En cuanto a la estructura nappe-escamada interna, en Millán y Somin (1981) se señaló la necesaria existencia de escamas y nappes de diferentes órdenes, los cuales se consideraron, en gran parte, premetamórficos, sobre la base de oriterio litológicos y estructurales. Estos autores consideraron que la zonación metamórfica invertida que caracteriza al macizo, como regla, es de tipo transicional, o sea, sin saltos abruptos en el grado metamórfico. Por otra parte, Stanik et al. (1981) sostuvo la idea acerca de la existencia de diferentes nappes-postmetamórficos de orden principal, con diferentes grados de metamorfismo, los cuales rigieron el carácter de la zonación metamórfica invertida. Más recientemente, nosostros hemos sostenido el punto de vista, que en este trabajo apoyames en principio, de que las secuencias del Escambray fueron despegadas de su basamento y escamadas antes

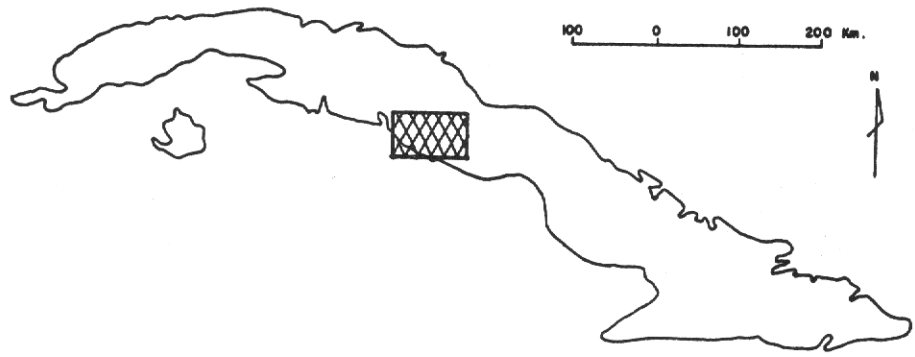

Fig. 1. Ubicación de area abarcada en el esquema geológico.

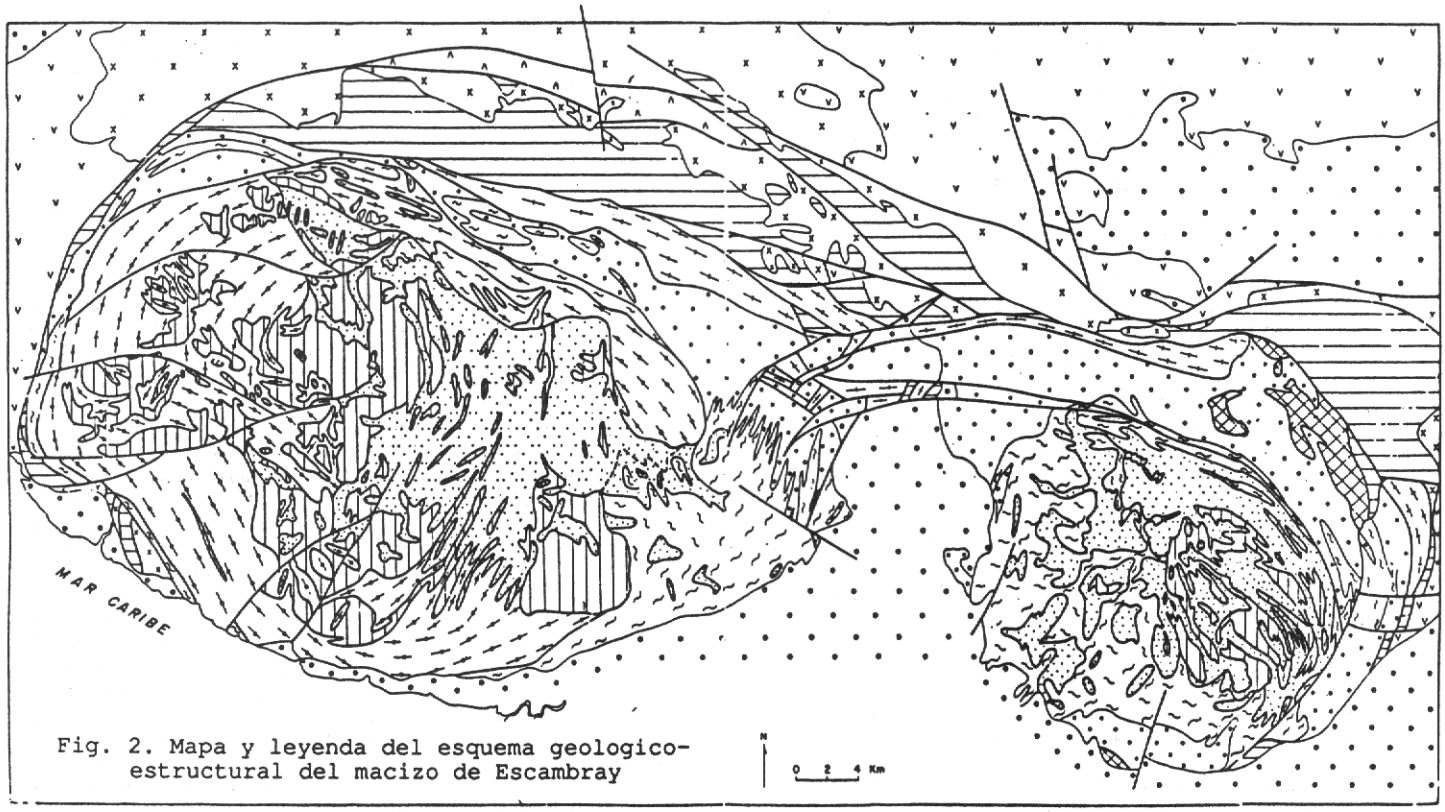

Fig. 2. Mapa y leyenda del esquema geologico-estructural del macizo de Escambray

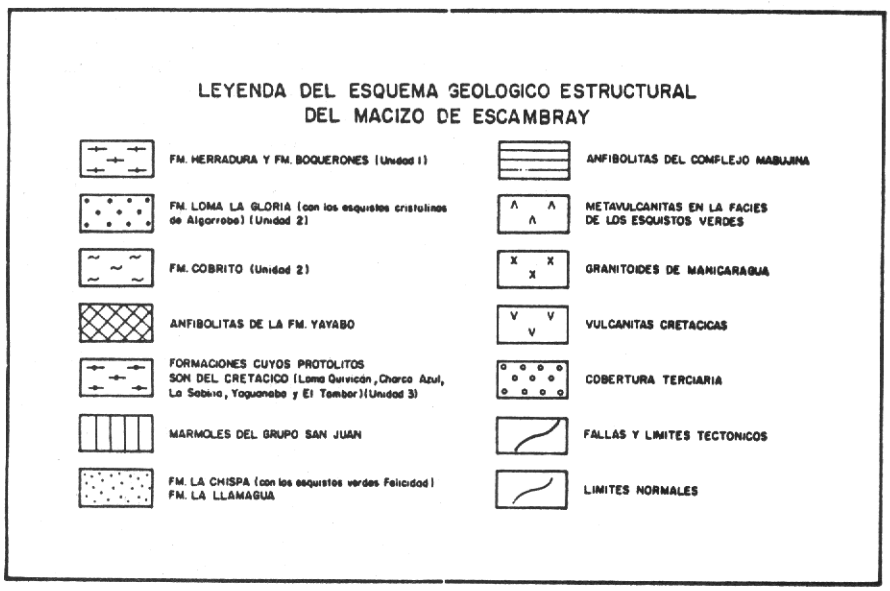

de metamorfismo, formando así una sucesión de nappes y escamas premetamórficas apilados uno sobre el otro, aunque consideramos también la existencia de mantos y escamas más tardías (Millán y Somin, 1985 a y b). En Millán y Somin (1985 b) se intentó, por primera vez, separar los mantos tectónicos principales del macizo, los cuales en gran parte coinciden con los destacados en este trabajo.

En el presente texto, se precisa más la caracterización de los principales mantos tectónicos o nappes, así como su orden y posición estructural. Se definen y caracterizan para todo el macizo la existencia de 6 diferentes tendencias estructurales que corresponden a distintas fases o etapas de plegamientos superpuestos (con esquistosidad o clivage asociados) relacionadas con el propio proceso de metamorfismo regional, estableciéndose sus regularidades y su superposición en el tiempo. Se demuestra que la fase más importante fue la segunda (F_2), toda vez que con ella está relacionada la propia generación de las 2 antiformas que caracterizan al macizo, así como de la depresión sinfórmica intermedia; además de ser la que desempeñó el rol principal en la cartografía geologica (Fig.1).

Para la preparación del presente texto realizamos un análisis y sistematización de los datos geológicos y estructurales de nuestras observaciones y trabajos realizados anteriormente (tanto de forma independiente, así como conjuntamente con M.L. Somin). Además tomamos en cuenta el mapa geológico de Stanik et al.(1981), así como el de Dublan et al.(1986), principalmente en cuanto a los elementos yaciencia de las esquistosidades medidos en el terreno. De gran ayuda y utilidad nos sirvió el estudio minucioso de las fotos aéreas en las escalas 1:26 000 y 1:37 000 para la definición de las diferentes tendencias estructurales y sus regularidades, así como las mediciones de diferentes elementos estructurales en afloramientos donde se destaca su orden de superposición.

Finalmente, debemos subrayar, que el esquema litoestratigráfico seguido en este texto corresponde con el establecido por Millán y Somin (1985a,b), ya que no disponemos de datos más recientes que permitan enriquecerlo o modificarlo.

PRINCIPALES UNIDADES ESTRUCTURALES Y CARACTERIZACION DE LAS MISMAS.

Las secuencias que actualmente constituyen al macizo metamórfico Escambray, fueron, inicialmente, escamadas y despegadas de su basamento cristalino premesozoico por cizallamiento, apilándose en una sucesión de nappes y escamas tectónicas uno sobre el otro. Esto ocurrió, en gran medida, precediendo justo al proceso metamórfico (o durante la etapa más inicial deel mismo), aunque en etapas más tardías también ocurrieron escamas y mantos tectónicos cuyos órdenes pudieron llegar a ser considerables. De esta forma se gestó una típica estructura de tipo nappe-escamada, con diferentes tipos de secuencias representadas, la cual se podría considerar similar, en principio, a la que caracteriza la Zona de Guaniguanico en Cuba Occidental (Hatten, 1957; Rigassi-Studer, 1963; Piotrowska, 1957, 1978; Pszczolkowski, 1976, 1978). La ocurrencia de este tipo de estructura explica por que dentro del macizo no afloran fragmentos de su fundamento premesozoico, lo cual también sucede en la Zona de Guaniguanico cuya superficie es mucho mayor que la de este ultimo (ver Millán y Somin, 1985 a).

Las particularidades de la estratigrafía del macizo de Escambray y la propia distribución de sus diferentes unidades litoestratigráficas y distintos tipos de secuencias, guardan una relación directa con su estructura interna nappe-escamada. Cada uno de los mantos tectónicos de orden principal presenta sus particularidades, ya sea por contener una parte definida de la sucesión estratigráfica, o por las características de su secuencia primaria y sus especifidades faciales (Fig.4).

A continuación pasaremos a la caracterización de las principales unidades estructurales (mantos tectónicos) por su orden de sucesión en la estructura interna del macizo (Figs. 3 y 4).

Unidad 1

La unidad estructural más superior (unidad 1) se trata de un nappe integrado por las formaciones Herradura y Boquerones, bien caracterizado por Millán y Somin (1985 b). La primera es una sucesión de esquistos cuarcíferos y cuarzo moscovíticos, cuyo proltolito es similar a la Formación San Cayetano del J_1-J_3 ox. La segunda se trata de una sucesión de esquistos calcáreo grafíticos, cuyo protolito es una facies carbonatada flyschoídica en estatos muy finos a laminares, con restos de radiolarios, entre ellos, muy probables Nassellaria sp. de edad mesozoica (Millán y Somin, 1985 b), y restos de palinomorfos de edad jurásico-cretácica (Dublan et al., 1986). Esta formación pudiera tratarse de un equivalente por su edad a los mármoles del Grupo San Juan del Jurásico Superior, aunque se trata de facies carbonatadas diferentes. La parte posiblemente más alta de la columna estratigráfica expuesta en la unidad 1, parece ser una sucesión de esquistos metasilicíticos que afloran en diferentes sectores, aunque muy subordinadamente a las dos formaciones señaladas.

Esta unidad, en su área de desarollo, es la que contacta directamente con el complejo anfibolitico Mabujina. La misma se expone en forma de una estrecha faja en el borde septentrional de ambas megaestructuras y, presumiblemente, también, en el borde oriental de la Sancti Spíritus, constituyendo la unidad más externa del macizo. Por el otro lado, ella contacta siempre con la unidad estructural 2 del macizo, la cual constituye el nappe que le infrayace en la sucesión de mantos tectónicos. En el mismo limite entre ambos nappes, con frecuencia aparecen afloramientos de un melange serpentinítico que contiene bloques de rocas eclogíticas (Millán y Somin, 1985 b). Un fragmento de uno de esos bloques arrojó una edad de 255±7 millones de años, utilizando el método K-Ar en un concentrado de hornblenda (Hatten et al., en prensa). De acuerdo con nuestras observaciones, la hornblenda constituye aquí unos cristales gigantes relícticos ((de hasta 3 cm de diámetro). los cuales son más antiguos que la propia asociación eclogítica, alterandose parcialmente por la misma. Esto podría indicar una edad Paleozoico Superior para su protolito, el cual pudiera tratarse de una roca gabroídica. Estos bloques deben tener una procedecis similar a otros semejantes encontrados enn diferentes regiones cubanas donde afloran melange serpentinniticos con inclusiones de metamorfitas de alta presión (incluyendo rocas eclogíticas) con un grado metamórfico variable, pero no tienen por que tratarse se representantes del basamento premesozoico de lad secuencias del Escambray.

Se destaca claramente un salto en el grado de metamorfismo en el límite entre las unidades estructurales 1 y 2, toda vez que la

parte superior y externa de la unidad 2 (que contacta directamente con la unidad 1) está carácterizada por el más alto grado metamórfico de alta presion de todo el macizo de Escambray, indudablemente major que el de la unidad 1. Esto rompe con el carácter de la zonación metamórfica (invertida y gradual) característico para el resto de esta región. Además, entre las unidades 1 y 2 se destaca también una discordancia estructural, principalmente manifiesta en la parte septentrional de la megaestructura de Sancti Spírutus. Todo ésto poermite considerar, que el manto tectónico más superior fue emplazado más tardíamente con respecto a los restantes nappes y escamas principales expuestos en el macizo. Su emplazamiento probablemente tuvo lugar en la época correspondiente al empolazamiento definitivo de las anfibolitas del complejo Mabujina sobre las secuencias del Escambray, después de la ocurrencia de la primmera fase de plegamientos (F_1).

Unidad 2

El nappe que constutye a la unidad 2 (infrayacente a la unidad 1) está integrado por las formaciones Loma La Gloria y Cobrito, destacandose además dentro de su área de distribución los cuerpos de los esquistos cristalinos de Algarrobo y de las anfibolitas de la Formación Yayabo. El mismo constitye una faja bien expuesta en las partes periféricas de ambas megaestructuras; en la occidental su distribución concuerda aproximadamente con la configuración de la antiforma generada durante de la fase de plegamiento y esquistosidad F_2. La parte externa de la faja (parte superior del nappe) está carácterizada por el mayor grado metamórfico del macizao, el cual disminuye hacia las prociones interiores de la misma. Este cambio gradual en el grado de metamorfismo se aprecia muy bien dentro de los cortes de la Formación Cobrito (formación más interna e inferior estructuralmente), con excepción de la parte norte de la megaestructura de Sancti Spiritus donde se destaca un salto en este ultimo debido a una importante falla. Inculso dentro de los cortes de la Formación Loma la Gloria a veces se caraprecia una disminución en el grado metamórfico en sus porciones mad internas e inferiores estructuralmente. Una carácteristica general de este nappe es que la secuencia estratigráfica primaria parece encontrarse invertida.

El protolito de la Formación Loma La Gloria es muy similar a la Formación San Cayetano, por ello se considera también del J_1-J_3ox, aunque contiene intercalaciones basálticas (transformadas en qran parte en rocas eclogíticas), carbonáticas y pedernálicas. La Formación Cobirito es muy similar a la Formación Boquerones por su constitución. La misma también con tiene con frecuencia restos de radiolarios, entre ellos, muy probables Nassellaria sp. (destaccados recientemente por N. Braguin en una muestra que tomamos en las cercanías de su contacto con la Formación Loma La Gloria en la parte norte de la megaestructura de Trinidad), Este hecho debe confirmar, con un alto grade de probabilidad, la edad mesozoica del protolito de la Formación Corbrito, así como del resto de la secuencia carácterizada en este nappe. Los esquistos crista linos de Algarrobo se tratan de intercalaciones estratigráficas dentro de la Formación Loma La Gloria. En cuanto a la Formación Yayabo, aunque sus cuerpos también aparecen destacados dentro de los cortes de la citada formación, consideramos que la misma formaba parte de otra secuencia diferente, emplazada como una escama tectónica independiente antes del metamorfismo (Millán y Somin, 1985 a y b). Los cuerpos de esta última algunas veces son considerables y de gran potencia, mientras que su protolito consiste de una secuencia basáltica con capas subordinadas de silicitas, sin intercalaciones carbonaticas niterrrigenas.

Unidad 3

Debajo estructuralmente de la unidad estructural 2 se destaca la unidad estructural 3, la cual constituye otro manto tectónico independiente de orden principal,, cuyos cortes solamente afloran en la megaestructura occidental, no así en la oriental (Millán y Somin, 1985 b). El mismo está integrado por las formaciones cuyos protolitos osn de edad probablemente cretácica. También se destaca en su secuencia la parte estratigráfica mas superior de los mármoles del Grupo San Juan, aunque solo aflora ocasionalmente. Este nappe se carácteriza por una faja de ancho variable, dispuesta siempre más internamente que la unidad estructural 2 y en contacto directo con esta última. La misma se ensancha considerablemente en la porción occidental de la megaestructura y se acuna hasta desaparecer completamente en su parte oriental. Esto explica por que su área de distribución no se extendio hacia la región de la megaestructura de Sancti Spíritus, donde nunca afloran las formaciones que intergran este nappe.

La parte más baja estratigráficamente del corte de las secuencias presumiblemente cretácicas está dada por las formaciones Charco Azul (intercalaciones de mármoles achocolatado oscuros hasta grises, esquistos metasilicíticos, metapelíticos y raras capas metavulanógenas) y Loma Quivicán (mármoles de tonos claros variados a veces con capillas de de metapedernal, e esquistos metapsamiticos y bancos ocasionales de metabrechas intraformacionales). Ambas formaciones sobreyacen estratigráficamente, en la secuencia del propio nappe, a los mármoles negros de la Formación Collantes (tope estratigráfico del Grupo San Juan). Más arriba el corte consiste en una sucesión donde predominan los esquistos cuarcíticos metasilicíticos bandeados, algunas veces ricos en manganeso (Formación La Sabina y parte alta de la Formación Charco Azul). Este último transisiona lateral y verticalmente hacia una sucesión de esquistos verdes derivados de metavulcanitas básicas (Formación Yaguanabo). El tope de esta secuencia estratigráfica está dada por una

sucesión cuto protolito es un flysch terrígeno convertido en esquistos verdes (Formación El Tambor), cuyas facies más distales (estratos muy finos a laminares de metapsamitas finas, metapelitas y veces metasílicitas) las reportamos recientemente con el apelativo informal de Formación San Blas, en los alrededores de la localidad homónima (Millán y Díaz Machín, 1988). La sucesión de metaflysch sobreyace estratigráficamente tanto a la Formación Yaguanabo, así como a la Formación La Sabina, en dependencia del área.

Cabe señalar, que en el área de distribucción de la propia unidad estructural 3 se destaca una clara disminución en el grado metamórfico de las rocas hacia sus porciones más internas e inferiores estructuralmente. Es interseante el hecho de que con mucha frecuencia no se destacan asociaciónes con minerales metamerficos tipomorfos de alta presión en las rocas de esta unidad. Como ejemplo de ello tenemos a las áreas de San Blas y Yaguanabo, en las cuales hemos descrito decenas de secciones delgadas de metavulcanitas básicas y de metaflysch, en contando siempre asociaciones típicas para la facies de los esquistos verdes con clinozoisita y actinolita, pero sin lawsonita ni glaucofana.. Estos dos ultimos minerales, como regla, sólo aparecen raramente en otras localidades. En las áreas más esternas y con mayor grado metamórfico puede puede destacarse granate en las asociaciones metabasíticas, e incluso un anfibol más parecido a la hornblenda que a la actinolita típica.

Unidades 4 a 6

Las unidades estructurales más inferiores se carácterizan por la distribución de los cuerpos de mármoles del Grupo San Juan y de los esquistos metaterrígenos de las formaciones La Chispa (con los esquistos verdes lawsoníticos Felicidad) y La Llamagua. Los mármoles del Grupo San Juan tienen una edad Jurásico Superior, bien determinada en 2 localidades diferentes de la megaestructura de Trinidad en las cuales se destacaron restos de amonites del Oxfodianoi y del Tithoniano, respectivamente (Millán y Myczynski, 1978): la edad tithoniana corresponde con la Formación Mayarí, la más ampliamente distribuida del grupo. Recientemente, en una trcera localidad de la propia megaestructura occidental, en las cercanías del caserío de San Blas , encontramos restos de microfauna dentro de una muestra tomada en la propia Formación Mayarí. La misma fue estudiada por G. Furrazola-Bermúdez, quien señaló que se trata de moldes de radiolarios y de Cadosina sp.; los últimos se asemejan a las especies C. nagyi Borza (J_3-K_1), C. heliosphaera Vogler (K_1v-h) o C. carpathica (Borza) (J_3k-t). Con major probabilidad parecen tratarse de la última especie referida, lo que indicaría una edad Kimerigdiano-tithoniano para la Formación Mayarí en el área de San Blas.

Los mármoles del Grupo San Jua siempre aparecen en una posición estructural más interna e inferior que los esquistos calcáreos de las formaciones Cobrito y Boquerones en ambas megaestructuras. Su grado metamórfico, en sentido general, también es menor que en las últimas. Es probable que sus protolitos sean equivalentes pro su edad, tratándose de distintas facies carbonátadas depositadas en ambientes diferentes. Cada una de estas unidades litoestratigráficas carbonáticas sobreyacen estratigráficamente en el corte, en distintas unidades estructurales, a diferentes formaciones cuyos protolitos consideramos equivalents a la Formación San Cayetano. Las formaciones Cobrito y Boquerones

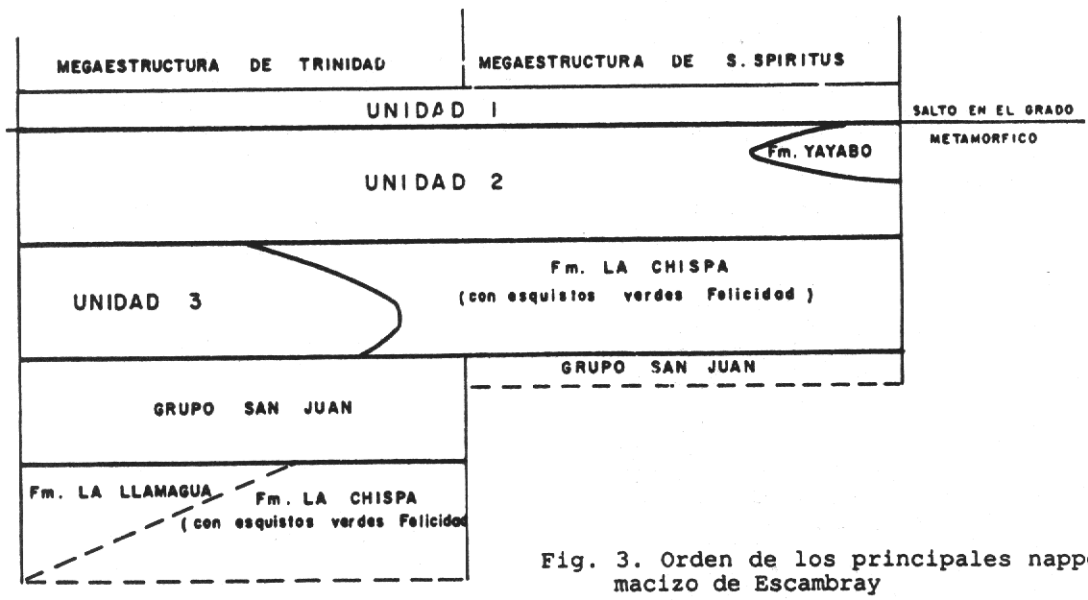

Fig. 3. Orden de los principales nappes del macizo de Escambray

carácterrizan el corte carbonático en los dos mantos tectónicos principales superiores de la sucesio de nappes superpuestos del macizo; mientras que los mármoles del Grupos San Juan forman parte de la secuencia de los mantos tectónicos inferiores (a partir de la propia unidad tectónica 3), aflorando siempre en posiciones estructurales más internas en ambas megaestructuras. Esto pudiera tratarse de una verdadera zonación estructuro-formacional dentro de los cortes primarios que carácterizan al macizo. Esta zonación también se manifiesta en los propios cortes de esquistos metaterrígenos equivalentes a la Formación San Cayetano, los cuales tienen sus propias especificidades en diferentes nappes.

En la magaestructura de Trinidad, los cuerpos de mármoles del Grupo San Juan Se distribuyen ampliamente en todo el interior de la misma, y, en sentido general, deben formar parte de mismo nappe de orden principal. Sin embargo, es necesario señalar, que en la porción nororiental sus cuerpos son relativamente pequeños y bastante escasos, lo cual contrasta marcadamente con el resto. No se descarta que ello sea una consecuencia de la propia estructura nappe-escamada del macizo y que esta área nororiental este representada principalmente por los cortes de un nappe o escama compuesto por la Formación La Chispa (junto con los esquistos verdes Felicidad) que sobreyace estructuralmente al nappe del Grupo San Juan (tal como veremos más adelante esto último es carácteristico para el extremo oriental de la propia megaestructura y para toda la megaestructura de Sancti Spíritus). Los cuerpos de estos mármoles se distribuyen conjuntamente con afloramientos de las formaciones metaterrígenas del J_1-J_3ox (La Chispa y la Lamagua) y una p0arte de los cortes de la faja de las formaciones cretácicas que constituyen a la unidad estructural 3 (principalmente en porciones internas de las misma), ya que se multiplegaron con comp[etencia conotras litologías, los mármoles de este grupo con frecuencia fueron escamados durante las deformaciones, formando sobrecorrimientos más tardíos.

En la propia megaestructura occidental, la unidad estructural más inferior pareece estar constituida por cortes de la Formación La Chispa (con cuerpos intercalados de los esquistos verdes lawsoníticos Felicidad) y por la denominada Formación La Llamagua. La premera es una sucesión de esquistos metaterrígenos que contiene intercalaciones de esquistos verdes metavulcanógenos, de metasílicitas (a veces muy abundantes y también de mármoles gris oscuros; mientras que la segunda se trata de unos esquistos metaterrígenos de muy bajo grado de metamorfismo, casi identicos a la Formación San Cayetano, que a diferencia de la anterior no contiene intercalaciones de otros tipos de roca. La transición entre ambas formaciones no está clara, considerándose que podrían correspondera diferentes secuencias y distintas unidades estructurales, o a una misma secuencia con variaciones laterales o verticales (Millán y Somin, 1985). Por o disponer de elementos concretos a favor de

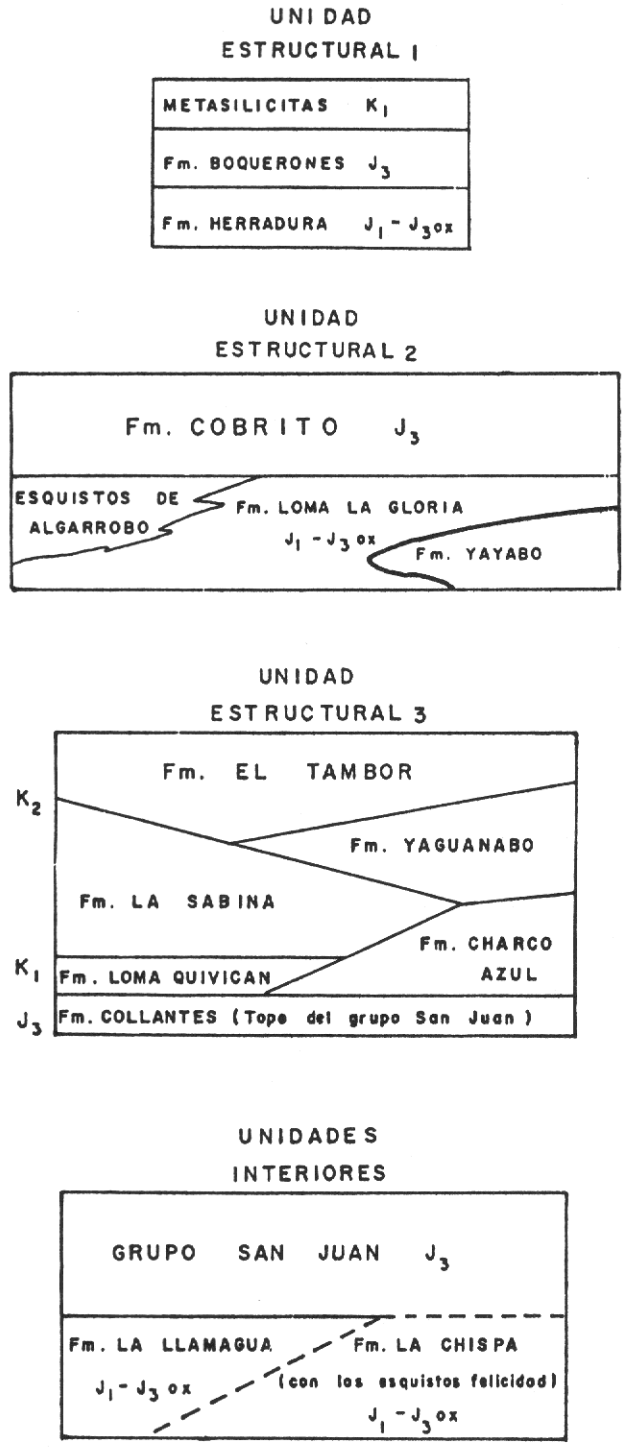

Fig. 4.Diferentes secuencias estratigráficas destacadas en el macizo Escambray.

una u otra alternativa, las consideramos aquí, de forma convencional, formando parte de una supuesta secuencia única corresondiente a misma unidad estructural de orden principal. Sin embargo, debemos señalar que los cortes referidos a la Formación La Llamagua aparecen restringidos a la porción suroccidental del área de distribución de esta última y siempre aparecen afactados por el menor drado de metamorfismo carácterizaddo dentro del macizo. En localidades aislada parecen destacarse los contactos estratigráficos normales entre la base del Grupo San Juan y la citada formación.

Cabe destacar, que en la porción oriental de la megaestructura occidental, precisamente, donde ocurre el acuñamiento y desaparición de la faja del nappe de las secuencies cretácicas (unidad 3), la formación La Chispa contacta directamente con las porciones más interiores de la Formación Cobrito (correspondienntes a la parte más inferior del nappe de la unidad 2); disposición similar a la que ocurre en toda la megaestructura de Sancti. Spíritus. De aquí que, por lo menos, en esta área, la primera formación deba constituir otro manto tectónico diferente, dispuesto estructuralmente por encima de los mármoles del Grupo San Juan y por debajo de la Formación Cobrito, tal como ocurre en la megaestructura oriental. Aunque el área de este nappe la restringimos, convencionalmente, a la porción más oriental de los cortes de La Chispa, cabe la posibilidad, de acuerdo con lo que señalamos anteriormente, que esta incluya una gran parte de los cortes de la citada formación que afloran en su porción septentrional, donde apenas se exponen los cuerpos de mármoles del Grupo San Juan.

La megaestructura de Sancti Spíritus se comporta, por su constitución nappe-escamada, como una prolongación de la porción más oriental de la megaestructura de Trinidad. La Formación La Chispa (con los esquistos verdes lawsoníticos Felicidad) contacta también directamente con la parte interior de la Formación Cobrito, distribuyéndose en una posición estructural más interna. Está claro que la primera infrayace aqui tectónicamente a la segunda y que ambas aparecen metamorfizadas y multiplegadas conjuntamente. Por otra parte, los mármoles del Grupo San Juan constituyen la unidad más inferior expuesta en la megaestructura, subyaciendo estructuralmente a la Formación La Chispa (y los esquistos verdes Felicidad). Estos mármoles sólo afloran en el área nuclear de la antiforma generada en la fase F_2, sin sobrepasar los límites de la misma. La geología de este sector se caracteriza pro grandes plieges isoclinales o apretados de varies etapas, bien definidos en la figura cartográfica de ambas formaciones, Entre esas dos unidades litoestratigráficas, en el propio núcleo de la antiforma, a veces afloran los restos de una escama tectónica constituida por una serpentinita antigorítica (a veces muy esquistosa) y por una metabasita enriquecida en un agregado jadeítico fino, con abundantes restos de clinopiroxenio y plagioclasa magmáticos y de una eestructura brechosa magmática relíctica. Cabe señalar, que la sucesión de nappes premetamórficos establecida en el presente trabajo para el enterior de esta megaestructura, difiere de la propuesta anteriormente en Millán y Somin (1985 b), la cual había sido fundamentada por observacioones geológicas locales.

El grado más bajo de metamorfismo regional encontrado en las rocas del macizo, sólo tuvo lugar en las áreas donde afloran los cortes estructuralemente más inferiores, expuestos en el interior de la megaestructuras de Trinidad, pero no en la de Sancti Spíritus. El menor grado metamórfico ocurre en una parte de los cuerpos de mármoles del Grupo San Juan, parte de los cortes de la Formación La Chispa y, principalmente, en los cortes de la Formación La Llamagua, ocupando concretamente un área en la porción centro-meridional de la megaestructura occidental. En cuanto al carácter gradual e invertido de la zonación metamórfica, se puede apreciar come el grado de metamorfismo aumenta paulatinamente desde los mantos o escamas más inferiores hasta el nappe que constituye la unidad estructural 2 en su porción externa y superior. Como ejemplo de ello se podría trazar un perfil hipotético con rumbo Noreste franco, a partir de unos 3 Km al Suroeste de Topes de Collantes (donde el metamorfismo alcanzó su menor grado), atravesando diferentes nappes y escamas premetamórficos hacia niveles estructurales cada vez más superiores (exceptuando al nappe más superior que constitue la unidad 1). Este hecho está avalado por observaciones en el terreno, así como por el estudio de numerosas secciones delgadas al microscopio.

DEFORMACIONES RELACIONADAS CON EL PROPIO PROCESO METAMORFICO

Las secuencias nappe escamadas del Escambray fueron sometidas a un proceso de metamorfismo al ser enterradas a gran profundidad, en el transcurso del cual ocurrieron 5 fases (6 etapas) de plegamientos superpuestas una sobre la otra. Cada una de ellas se carácteriza por su propio sistem de esquistosidad metamórfica o por un clivaje de intensidad variable, con una tendencia bien definida en todo el macizo (Fig. 5). El estilo de los pliegues, así como su intensidad y magnitud, son variables, dependiendo ello de la fase que se trate y del sector del macizo propiamente. En el caso de las fases más antiguas, éstos son, come regla, isolinales o similares apretados, con una verdadera esquistosdidad metamórfica asociada dispuesta paralelamente a sus planos axiales. En las fases más jóvenes, los pliegues son más variables por su intensidad en dependencia del sector del macizo, aunque generalmente son más abiertos y, a menudo, consisten en verdaderos pliegues concéntricos; la esquistosidad relacionada se trata principalmente de un clivaje de plano exial con diferente grado desarrollo. La magnitud de los pliegues es variable, pudiendo variar desde milímetros hasta centenares de metros. En diferentes porciones del macizo puede predominar en los

cortes rocoso la tendencia correspondiente a una u otra fase, existiendo un grado variable de transposición estructural de los elementos estructurales de las etapas más antiguas por las más jóvenes. Este cuadro estructural tan complicado se refleja muy bien en la propia cartografia geológica de las diferentes unidades litoestratigráficas y cuerpos rocosos, la cual está carácterizada por figuras de interferencia muy complicadas y de forma a veces muy caprichosas.

A continuación pasaremos a la carácterización de las diferentes fases:

Primera fase (F_1).

La primera fase tiene un carácter precupular o preantifórmico. La misma está dada pro una verdadera esquistosidad metamórfica (S_1), cuya tendencia primaria es de N-NE NE en la megaestructura de Trinidad y de NE a E-NE en la megaestructura de Sancti Spíritus. a mejor expresión de S_1 y de la fase F_1 con su tendencia primaria la tenemos en el extremo oriental de la primera y en el extremo occidental de la segunda, donde incluso F_1 controla y domina las principales representaciones cartográficas. En esa parte de la cupula de Trinidad los buzamientos locales de S_1, como regla, son hacia el SE, mientras que en la de Sancti Spíritus, al parecer, S_1 buza suavemente hacia el NW en un sentido regional. En el resto del macizo, S_1 tiene un carácter principalmente relíctico y como regla aparece transpuesta o desaparece, aunque la existencia de la fase F_1 se refleja en la cartografía geológica.

Los pliegues de esta fase son siempre isoclinales y sus demensiones varían desde pocos milímetros hasta centenares de metros. En el borde oriental de la megaestructura de Trinidad, el límite entre las Formaciones Loma La Gloria y Cobrito está dado por una serie de pliegues isoclinales F_1, cuyos órdenes son de decenas y centenas de metros, expresándose muy bien en la cartografía geológica. Muchas veces se preserva la lineación L_1, originada por la intersección de S_1 con la estratificación primaria; cuando no aparece transpuesta se orienta según un azimut NE a N-NE dispuesta subhorizontalmente.

Segunda fase (F_2).

La fase F_2 es la de mayor importancia en el macizo, tratándose de la fase antifórmica propiamente. El sistem a de esquistosidad S_2 relacionado con ella está vinculado con la génesis de la antiforma cupular de Trinidad (occidental) y de la antilforma cupular incompleta de Sancti Spíritus (oriental). La tendencia de esta esquistosidad metamórfica, la cual es perfectamente concordante con la configuración de las antiformas, se expresa muy bien in ambas megaestructuras, desempeñando un rol principal, tanto en las mediciones realizadas en el terreno, la cartografia-geológica, así como en las fotos aéreas.

El núcleo de la antiforma cupular F_2 de Trinidad está ubicado practicamente en su mismo centro, purs parece ser bastante concentrica. Su eje de elongación está orientado hacia el NW ($N50^0W$ aproximadamente). El sistema de esquistosidad S_2 sigue el conterno de la antiforma en toda su extensión, con sus buzamientos dispuestos de forma periclinal con respecto a su núcleo.

La antiforma cupular (F_2) de Sancti Spíritus se desarrolló sólo en su parte sur, ya que en la parte norte desaparece como tal la estructura y la tendencia de S_2 pasa a formar parte del proppio plan estructural de la antiforma occidental. Su porción meridional tiene un carácter similar a la anterior por su configuración, con una disposición periclinal de la esquistosidad S_2 conterneando a la estructura. Sin embargo, a diferencia de ella, su eje de elongación está dispuesto más hacia el N-NW (aproximadamente $N30^0W$). De aquí que los ejes de ambas tengan una diferencia de unos 20^0 en su orientación. La tendencia correspondiente a S_1 se manifiesta pobremente en la porción más noroccidental de la megaestructura.

El núcleo de la antiforma incompleta F_2 de Sancti Spíritus coincide perfectamente con la distribución de los afloramientos de los mármoles del Grupo San Juan, los cuales nunca afloran más alla de los limites del mismo. Cabe señelar, que en esta área nuclear las tendencias de F_1 y F_2 se cortan bajo angulos cercanos a los 90^0. Este último, unido a la magnituud que alcanzaron los pliegues de ambas fases en este sector (del orden de los centenares de metros y quizas hhasta más de un kilómetro), condicionó que el horizonte de mármoles del Grupo San Juan tenga una figura cartográfica muy complicada (en la cual influencio también la fase F_4) que coincide con uno de los patrones típicos de interferencia de Ramsay (1967).

Cabe destacar el desarrollo de un clivaje o esquistosidad axial en ambas antiformas F_2, dispuesto concordantemente con respecto a su eje de elongación respectivo, el cual se manifiesta intensamente en las porciones cercanas al propio eje. En las dos megaestructura el buzamiento de esta esquistosidad es, como regla, hacia el NE con ángulos medios. Al parecer, la misma se asocia con mesopliegues apretados. Este sistema axial se desarrolló tardíamente con respecto a la generación de las antiformas F_2 y con posterioridad al sistema de esquistosidad S_2 concordante con la configuración de las últimas. Sin embargo, auque se trata realmente de una esquistosidad S_3, el mismo corresponde también con la propia fase F_2 y no con la fase F_3 más joven. De aquí podemos decir que la fase F_2 comprende dos diferentes sistemas o tendencias de esquistosidad generados en distintas etapas: uno prinicipal y más antiguo, que es el propiamente S_2, vinculado directamente con la propia generación de las antiformas; otro, más tardío, desarrollado como una esquistosidad o clivaje exial con repecto a las últimas.

La fase F_2 dió lugar a la formación de pliegues isoclinales a similares apretados, cuyo orden alcanza las centenas de metros, al igual que en la fase F_1. Una intensa lineación tectónica L_2 aparece relacionada don esta fase, muy prominente en ambas megaestructuras en sus diferentes sectores, la cula tiene una tendencia general hacia el NW.

Las dos antiformas aparecen separadas pro una estrecha de presión estructural entermedia, la cual se generó conjuntamente con las premeras durante la fase F_2. Esta depresión sinfórmica se extiende hacia el sur y se acuñó estructuralmente hacia el norte. En la misma afloran actualmente depositos de rocas terciarias conjuntamente con rocas vulcanógenas cretácicias y del complejo anfibolítico Mabujina. El acuñamiento de la sinforma F_2 hacia el norte está relaciónado con la propia configuración de la antiforma F_2 de Sancti Spíritus, la cual deja de existir como tal en la parte norte de la megaestructura, pasando así a formar parte del propio plan estructural de la antiforma F_2 de Trinidad que es de major tamaño y más acabada. Este condicionó finalmente que la actual megaestructura de Trinidad tenga el doble del área que la de Sancti Spíritus y que en la primera alforen niveles estructurales más inferiores que no se exponen en la segunda.

Tercera fase (F_3)

La fase F_3 está mucho mejor desarrollada en la megaestructura de Trinidad que en la de Sancti Spíritus. En la primera su tendencia se dispone, en toda su extensión, formando una disposición arqueada que sugiere una porción limitada de una gigantesca antiforma cupular que se extiende mucho más allá de los límites de la megaestructura actual, cuyo núcleo estaría ubcado en el extemo occidental de esta última. La tendencia de la esquistosidad o clivaje relacionado, así como de las esquistosdiades más antiguas transpuestas, se dispone en forma de arco con los buzamientos inclinados, como regla, hacia el este. Su expresión es acentuada en la cartografía geológica y en las fotos aéreas, con excepción de su área nuclear en el extremo occidental de la cúpula. El arqueamiento de su tendencia se incrementa gradualmente hacia el oeste, a medida que nos acercamos hacia el supuesto núcleo. Con esta fase se vinculan pliegues apretados de estilo similar ocn una esquistosidad o clivaje axial asociado, destacándose como regla una transposición variable, en ocasiones intensa, de las fases más antiguas. El mismo extremo oriental de la megaestructura de Trinidad parece coincidir con el propio límite oriental de la supuesta estructura cupular gigantesca F_3.

En la megaestructura de Sancti Spíritus, la fase F_3 está pobremente desarrollada, reflejándose solamente en su porción occidental con una tendencia alrededor del N-S, la cual manifiesta un ligero arqueamiento de carácter invertido con respecto al de la megaestructura anterior y cuyos buzamientos son hacia el Oeste. Esta fase podira representar aquí, en sentido regional, una porción limitada del extremo occidental de otra gigantesca antiforma cupular, la cual se extendería mucho más alla de los límites de la megaestructura actual y cuyo mucleo estaria muy alejado al este de la última.

El carácter e individualidad de esta fase en cada una dde las dos megaestructuras del macilzo, parece haber conducido a una intensificación del desarrollo de la depresión sinfónica intermedia (generada durante la fase F_2) hacia el Norte. Según parece, durante la fase F_3 esta depresio adquirió una dirección N-S.

Fases cuarta y quinta (F_4 y F_5).

Las fases F_4 y F_5 que afectaron al macizo condicionaron, en gran medida, la configuración final del mismo y de sus dos megaestructuras.

En la megaestructura de Trinidad, ambas fases no pudieron ser separadas, al parecer, debido a que sus tendencias se intersectaron bajo ángulos muy bajos. De aquí que en la leyenda se considerasen conjuntamente. Su rol fue aquí considerable, toda vez que la configuración actual de esta megaestructura tiene su eje de elongación orientado según un azimut W-NW, concordante con esta tendencia. La misma puede variar a lo largo de la cúpula en un orden cercano a los 20^0 , desde una dirección W-NW, hasta bien definida hacia el NW, destacándose claramente en toda su extensión en las fotos aéreas. Su reflejo es variable en la cartografía y en las esquistosidades medidas en el terreno; aunque como regla tiene una menor expresión que las fases F_2 y F_3, en ocasíones puede ser intenso. Con frecuencia se destacan pliegues apretados asociados con un clivaje intenso paralelo a sus planos axiales. La transposición de las tendencia más antiguas a veces pude ser considerable, al menos a escala de los afloramientos. El clivaje (o esquistosidad más antigua-transpuesta) relacionado con esta fase, generalmente buza hacia el Sur bajo ángulos medios.

En la megaestructura de Sancti Spíritus las fases F_4 y F_5 se separan claramente a lo largo de toda su extensión. El ángulo de intersección de sus tendencias es de un orden de los 20^0.

La fase cuarta presenta una tendencia muy regular con un azimut NW ($N50-60^0W$) bien definido en las fotos aéreas en toda la megaestructura, aunque con una expresión mucho mayor en su porción norte-central, donde se destaca una transposición intensa de las esquistosidades más antiguas S_1 y S_2. En otros sectores su wxpresión en los afloramientos puede ser bastante pobre. El buzamiento del sistema S_4 (clivaje relacionado y esquistosidad más antigua transpuesta) es regularmente hacia el SW bajo angulos medios a abruptos. La fase F_4 generó

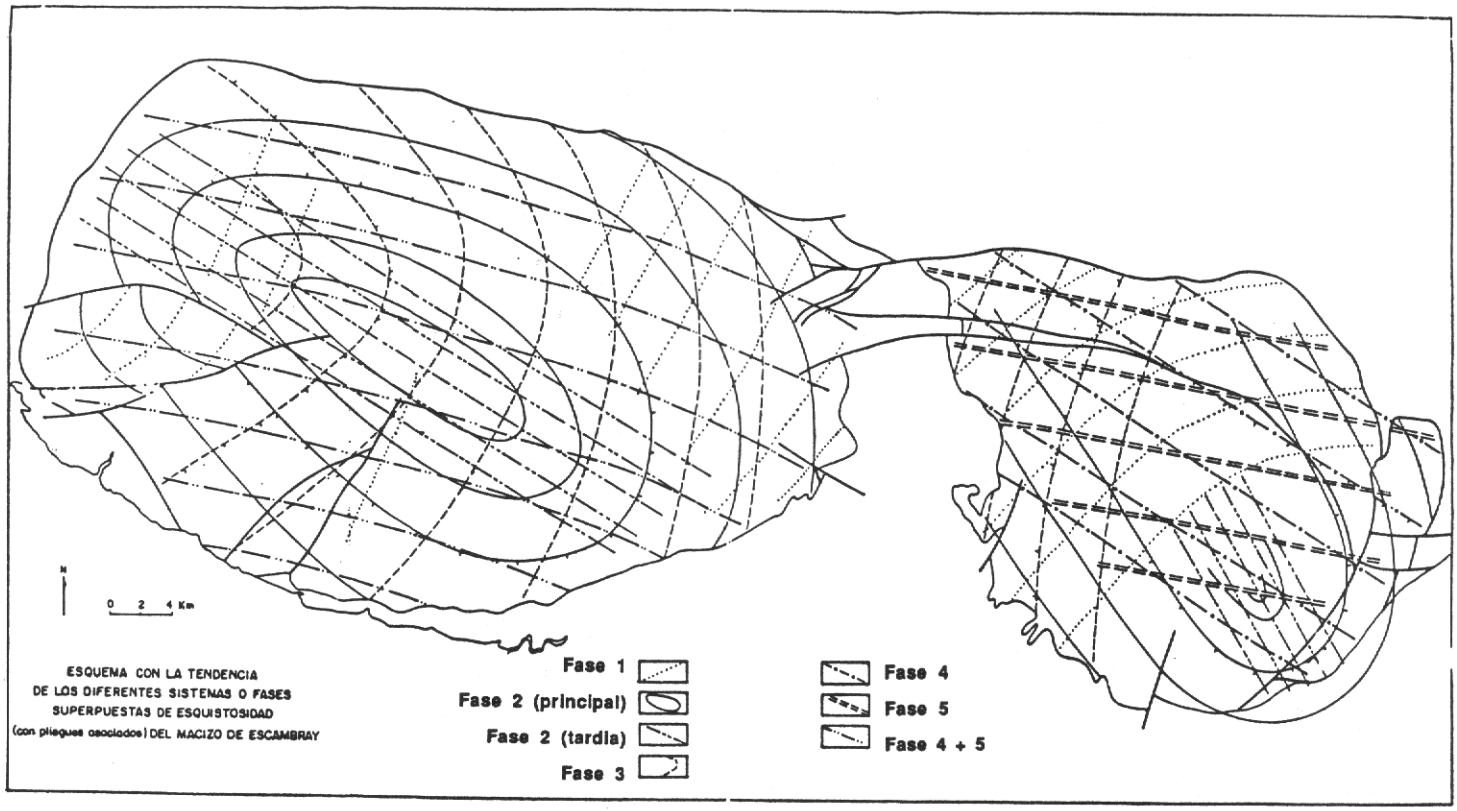

Fig. 5. Esquema con la tendencia de los diferentes sistemas o fases superpuestas de esquistosidad (con plegues asociadas) del macizo de Escambray.

pliegues apretados con un clivaje axial intenso en las áreas de mayor expresión. La magnitud máxima de los mismos no está definida, sin embargo, esta claro que F_4 jugó también su papel en la figura cartográfica de interferencia dada por los mármoles del Grupo San Juan el el área nuclear de la antiforma incompleta F_2 de Sancti Spíritus. Cabe señelar, que el eje de elongación de la actual megaestructura coincide, en sentido general, con la tendencia F_4.

La fase F_5 en la magaestructura de Sancti Spíritus corresponde con la tendencia W-NW. La misma se refleja bien en las fotos aéreas en gran parte de la cúpula, principalmente en sus porciones norte-central. Se relaciona con un clivaje S_5, a veces intenso, y pequeños plieguecillos cuyas dimensiones maximas no estan definidas. La expresión cartográfica de la fase F_5 sólo se destaca en algunos sectores de la parte más septentrional de la megaestructura. El buzamiento de la tendencia S_5 pride ser tanto al norte como al sur, con ángulos medios a abruptos.

Relaciones con el Complejo Mabujina

Los hechos permiten confirmar que el complejo anfibolitico Mabujina (de alta relación Temperatura/Presión) fue deformado conjuntamente con las secuencias del Escambray durante el metamorfismo, al menos a partir de la F_2, lo cual está avalado por los datos estructurales, así como por los estudios de las fotos aéreas. Este concuerda con la reelaboración metamórfica parcial, en condiciones de baja relación Temperatura/Presión, de las anfibolitas en la parte más baja del citado complejo, encontrada en diferentes localidades contiguas al límite con el macizo de Escambray, Aquí tales rocas preden contener abundante mica blanca, y en ocasiones también granate, clinozoisita, rutilo e incluso plagioclasa ácida; minerales atípicos para el complejo Mabujina, pero característicos para el macizo de Escambray.

Agrietamientos

Con posterioridad a las fases de plegamientos con sus tendencias definidas y esquistosidad o clivaje relacionados, ocurrio un agrietamiento intenso de las rocas del macizo, tratandose en ocasiones de grietas selladas por venillas. En total se destacan entre 10 y 12 sistemas diferentes de agrietamiento, con diferente grado de desarrollo y expresión geomorfologica en distintos sectores.

En la megaestructura de Sancti Spíritus son particularmente prominentes dos sistemas: uno con grietas orientadas hhacia el NE (N 30-40 grados E), el cual es muy acentuado en su extremo oriental; el otro, con las grietas oreintadas alrededor del azimut N-S franco,

muy acentuado en toda a parte central y oriental y que muchas veces parece relacionarse con desplazamientos rocosos de cierta consideración. En ambos casos, a veces parecen haverse originado unos plieguecillos pequenos de tipo concentrico, crenulaciones o chevron, con clivaje de r=fractura asociado dispuesto de forma abrupta.

CONCLUSIONES.

La evolución geológico-estructural del actual macizo metamórfico de Escambray se pude resumir de la forma siguiente:

Las secuencias primarias que hoy dia forman parte del actual macizo son jurásico-cretácicas y fueron depositadas en un ambiente geotectónico de tipo margen continental, donde tuvo lugar una zonacio estructuro-formacional con la ocurrencia de diferentes secuencias isocronas con variaciones faciales. El despegue de tales secuencias de su basamento premesozoico por cizallamiento, su apilamiento en nappes, así como su metamorfismo y deformaciones multiples asociadas, ocurrileron como consecuencia de una colisión que tovo lugar durante el Cretácici Superior entre dicho margen y el arcovolcanico cretácico; en la parte basal de este ultimo ya se disponia el complejo anfibolitico Mabujina. En virtud de esta colisión, las secuencias del Escambray infracorrieron debajo la forma de diferentes mantos tectónicos y escamas, metamorfizándose y multiplegándose a gran profundidad en condiciones de una baja relación Temperatura/Presión. Esta situación propieio que las anfibolitas del complejo Mabujina fuesen deformadas conjuntamente con las secuencias del macizo melanocratico fuese parcialmente reelaborada durante el metamorfismo de las última. El emplazamiento definitivo de tales anfibolitas sobre las secuencias nappe-escamadas del Escambray, según parece, ocurrió, de hecho,, simultaneamente con el del nappe que consituye la unidad estructural más superior del actual macizo (unidad 1), con posterioridad a los restantes mantos tectónicos principales carácterizados en este último e incluso después de la fase de plegamiento F_1.En la etapa final de la compresión vinculada con la co lisión, las dos megaestructuras del macizo comenzaron a fracturarse intensamente. Luego, al desaparecer totalmente el estado compresivo, las dos prominentes elevaciones estructurales de metamorfitas siálicas, conformadas en la profundidad desde la fase F_2 de plegamiento sinmetamórfico, se hicieron especialmente inestables al infayacer a las anfibolitas del complejo Mabujina mucho más densas. Debido a ello ambas megaestructuras antifórmicas se despegaron del medio como un conjunto uniltario y emergieron en forma diapirica, atravesando un potente espesor de anfibolitas densas del complejo Mabujina e incluso de las secuencias suprayacentes del arco volcanico cretácico. De esta manera el macizo de Escambray aflora, en su disposición actual, bajo la forma de una ventana tectónica en medio del complejo Mabujina y de las secuencias del arco volcánico. Los datos geológicos (área de distribución del nappe más superior y más tardío del macizo de Escambray, así como su emplazamiento directo debajo del Complejo Mabujina; el ancho y la potencia de las anfibolitas del complejo Mabujina al norte del macizo de Escambray y su reducción estema en otros sectores, así como su probable distribución y prolongación el la profundidad hacia el Oeste de acuerdo con los datos geofísicos; la distribución y sentido de la polarización al norte del macizo, de las secuencias del arco volcánico cretácico y de los granitoides relacionados) favorecen la idea de que el Complejo Mabujina y las secuencias suprayacentes del arco volcánico se desarrollaron al Norte del margen continental donde se depositaron las secuencias del actual macizo de Escambray, y que, además, previamente a la colisión, existio una zona de subducción buziado hacia el Norte.

REFERENCIAS

BOLOTIN, Y.A.; YIDKOV, A.Y.; MAXIMOV, A.A.; SOSA, R. ,1970, Yacimientos de minerales sulfurosos de la serie metamórfica Escambray, en la parte noroeste del macizo montanoso del mismo nombre: Rev. Tecnologica, v. 8, N.2, p.35-48.

DUBLAN, L.; et al.,1986, Informe final del levantamiento geológico y evaluación de los minerales utiles en escala 1: 50,000 del Poligono CAME + I, Zona Centro. Archivo Instituto de Geología y Paleontologia y Fondo Geológico Nacional (inedito).

HATTEN, C.W.,1957, Geology of the Central Siera de los Organos. Fondo Geológico Nacional (inedito).

HATTEN, C.W.; et al. (en presa) Tectonostratigraphic units of Central Cuba.

HILL, P.A.,1959, Geology and structure of the northwest-Trinidad Mountains, Las Villas Province, Cuba. Geol. Soc. Amer. Bull., v. 70, p. 1459-1478.

LINARES, E.; et al.,1985, Mapa geológico de la Republica de Cuba a escala 1:500 000.

MAXIMOV, A.; CRACHEV, G.; SOSA, R.,1968, Geología y minerales utiles de las pendientes noroccidentales del sistema montanoso Escambray. Informe sobre los trabajos de busqueda-levantamiento a escala 1:50 000 realizados en la parte sur de la provincia de Las Villas en 1966-67. Fondo Geológico Nacional (inedito).

MILLAN, G.,1978, Tectónica y metamorfismo de las secuencias mesczoicas de las montanas del Escambray, Cuba:. (en ruso) C. Sc. Tesis, Instituto Fisica de la Tierra, AN. SSSR, Moscu, 134 pp. (resumen en ruso 23 pp.).

MILLAN, G.; MYCZYNSKI, R.,1978, Fauna jurasica y cosideraciones sobre la edad de las secuencias metamórficas del Escambray:. Acad. Ciencias Cuba, Inf. Cient. Tecn. 80, 14 pp.

MILLAN, G.; SOMIN, M.L.,1985 a, Nuevos aspectos sobre la estratigrafia del macizo metamórfico de Escambray. En: Contribución al conociiento geológico e las metamorfitas del Escambray y del Purial:. Instituto de Geología y Paleontologia, Reporte de Investigación No. 2, p. 1-42.

MILLAN, G.; SOMIN, M.L.,1985 b, Condiciones geológicas de la constitución de la capa granite-metamórfica de la corteza terrestre de Cuba. Instituto de Geología y Paleontología, 83 pp.

MILLAN, G.; DIAZ-MACHIN, J.,1988, Estudio de factibilidad de la C.H.A. Centro. Variante San Blas (capitulo sobre las carácteristicas geológicas de la región): Instituto de Hidroeconomía (inedito).

MOSSAKOVSKII, A.A.; NEKRASOV, G.E.; SOKILOV, S.D.,1986, Los complejos metamórficos y el problema del fundamente de las estructuras alpinas del sector central de Cuba (en ruso): Geotektonika, No. 3, p. 5-24.

PIOTROWSKA, K.,1978,, Nappe Structures in the Sierra de los Organos, Western Cuba:. Acta Geol. Polon., v. 28, No. 1, p. 97-170.

PSZCZOLKOWSKI, A.,1976, Nappe structure of Sierra del Rosario (Cuba):. Bull. Acad. Polon. Sci., ser. Sci. Terre, v. 24, No. 3-4, p 205-215.

PSZCZOLKOWSKI, A.,1978, Geosynclinal sequences of the Cordillera de Guaniguanico in Western Cuba; their lithostratigraphy, facies development, and paleogeography: Acta Geol. Polon., v. 28, No. 1, p. 1-96.

RAMSAY, J.G.,1967, Folding and fracturing of rocks. Mc Graw-Hill, 568 pp.

RIGASSI-STUDER, D.,1963, Sur la geológic de la Sierra de los Organos, Cuba: Arch. Sci. Geneve, vol. 16, fasc. 2, p. 339-350.

SOMIN, M.L.; MILLAN, G.,1974, Algunos rasgos estructurales de los complejos metamórficos mesozoicos de Cuba-(en ruso):. Geotektonika, No. 5, p. 19-30.

STANIK, E., et al.,1981, Informe del lavantamiento geológico, geoquimico y trabajos geofisicos realizados en la parte sur de Cuba Cental, en las provincias Cienfuegos, Sancti Spíritus y Villa Clara: Fondo Geológico Nacional,inedito).

SUCHANEK, Z.,1980, Semistatistical method of the processing of small-tectonic data:. Cas. pro mineralogii a geologii, roc. 25, c. 3, p. 253-262.

THIADENS, A.A.,1937, Geology of the southern part of the province of Santa Clara (Las Villas): Geogr. Geol.- Meded., Phys. Geol. Reeks, ser 2, No. 12, 69 pp.

CORRELACION DE LAS METAVULCANITAS DE LA SIERRA DEL PURIAL (CUBA ORIENTAL) CON LAS ROCAS DE LA ASOCIACION OFIOLITICA.

Mario Campos y Margarita Hernández
Instituto Superior Minero Metalurgico,
Moa, CUBA

RESUMEN

Ideas preliminares acerca de la posible correlación de las metavulcanitas de la Sierra del Purial con las rocas de la asociación ofiolítica se exponen, a partir de las comparación de las peculiaridades petroquímicas de las mismas; en los diagramas AFM y SiO_2-K_2O. En dichos graficos fueron ploteados muestras de anfibolitas, esquistos metavulcanógenos y vulcanitas de la Fm. Quibiján, comparándose en los diagramas AFM, con los campos en que se distribuyen los diferentes complejos de la asociación ofiolítica, en regiones tipicas de desarrollo de las ofiolitas en el mundo.

Se concluye que existe una buena correlación entre las anfibolitas y los complejos basáltico, diabásico y de graboides de las ofiolitas, en tanto que los esquistos metavulcanógenos y las rocas de la Fm. Quibiján no tienen una tendencia definida, esistiendo mezcla de rocas ofiolíticas y de aquellas que son típicas de los arcos insulares.

ABSTRACT

A preliminary comparison is made of the meta-igneous rocks of the Sierra Purial (eastern Cuba) using AFM and SiO_2-K_2O diagrams. Compositions of the metavolcanic rocks of the Quibiján Formation and the Mocambo and Güira de Jauco Amphibolites are compared with the compositional fields of ocean floor rocks and classic ophiolite regions of the world. The amphibolites compare well with the basalts, diabases and gabbros of ophiolites while the rocks of the Quibiján Formation show no definite affinities and are composionally a mix of ophiolitic rocks and those typical of island arcs

(English abstract by Gren Draper)

La Sierra del Purial ubicada en la porción central y suroriental de la provincia de Guantánamo constutuye, después del Escambray, una de las regiones de Cuba conextensos afloramientos de metamorifitas regionales (figura 1), en la misma están representados los complejos metavulcanógeno,, metaterrígeno y metacarbonatado propuestos por Somin y Millán (1981).

Las rocas del complejo metavulcanógeno están representadas por anfibolitas, y una potente secuencia de esquistos verdes los cuales proceden del metamorfismo de rocas volcanicas y vulcanógeno-sedimentarias.

Localmente y asociado a zonas de contacto tectónico dentro de los esquistos verdes, las anfibolitas y serpentinitas han sido reportados esquistos glaucofanicos y bloques de rocas eclogíticas (Cobiella et al., 1984).

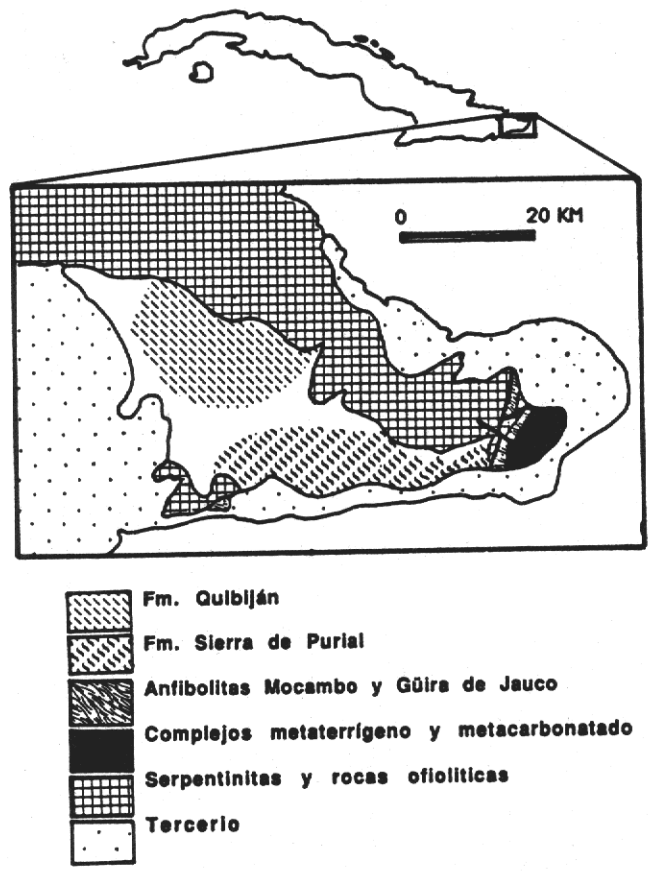

Fig. 1 Esquematico del mapa geologico de la región de Cuba Oriental

Larue, D.K., and Draper, G. (eds.),
Transactions of the 12th Caribbean Geological Conference, St. Croix, U.S.V.I., Miami Geological Society, P.O. Box 431552, South Miami, FL 33243, U.S.A

Las rocas de los complejos metaterrígeno y metacarbonatado, que no analizaremos en este trabajo, afloran en el borde oriental de la Sierra del Purial estando representados por filitas, pizarras mármoles pertenecientes a la facies esquistos verdes. Estas secuencies yacen tectónicamente sobre las metavulcanitas.

Investigaciones petrográficas y petroquímicas detalladas realizadas por M. Hernández (Hernandez, 1987) han demostrado, que parte de las metavulcanitas del complejo metavulcanógeno se derivan de vulcanitas básicas de composición toleítica y parcialmente de la serie calco-alcalina. En relación con esto, una buena correlación ha sido obtenida al comparar el quimismo de las anfibolitas del Purial con el quimismo de las toleitas abisales propuesto por otros autores.

Una correlación similar se ha obtenido para las metavulcanitas que sufrieron el metamorfismo el la facies esquistos verdes, y localmente en la facies esquistos glaucofánicos, los cuales proceden del metamorfismo de basaltos toleíticos.

Los datos de campo han revelado, además, la presencia en las anfibolitas y esquistos verdes de algunas texturas relícticas tales como el bandeamiento que exhiben las primeras y la textura almohadiforme de los segundos, las cuales recuerdan a aquellas que son características para el complejo de gabroides y de basaltos de las ofiolitas. Es muy probable que los esquistos recubran a las anfibolitas.

Las partes restantes del corte metavulcanógeno, no poseen estas características y desde el punto de vista petrográfico y petroquímico son muy variadas, con predominio de las metavulcanitas y metapiroclasititas de composición andesítica. En estas rocas tambien se pueden apreciar texturas relícticas, tales como aglomeratica, brechosa, diaclasamiento columnar e incluso estratiforme.

No obstante las diferencias señaladas, dada la extremada complejidad tectónica del Purial, hasta el presente la cartografia geológica efectuada a escales pequeñas, no ha logrado la separación de las diferentes secuencias adecuadamente, aunque se han dado pasos en este sentido.

Teniendo en cuenta lo anterior en el presente trabajo se analiza la probable existencia de rocas metamórficas en el Purial que puedan correlacionarse con las rocas de la asociación ofiolítica, lo cual ya desde hace algunos años, a partir de algunas observaciones preliminares fue señalado por especialistas franceses (Boiteau et al., 1972), los cuales interpretaron las anfibolitas y las ultramafitas relacionadas y otras metabasitas como bloques de la corteza oceánica.

A continuación pasaremos a analizar el comportamiento petroquímico de las metavulcanitas del Purial, sobre la base de los diagramas AFM.

En la figura 2 han sido ploteadas en el diagrama AFM, 25 muestras de anfibolitas correspondientes a las Formaciones Anfibolitas Macambo y Güira de Jauco, pertencientes al complejo metamórfico de la Sierra del Purial. En el diagrama a manera de comparación han sido trazados los compos de localización de los diferentes miembros de la asociación ofiolítica correspondientes a los complejos de Papua y Omán, observándo se como la mayoría de las muestras caen dentro de los campos definidos en el diagrama para las ofiolitas de los complejos citados anteriormente.

Este hecho unido a la composición petrográfica, quimismo y posición estructural de las anfibolitas de la Sierra del Puria 1, indica con toda probabilidad que dichas rocas son equivalentes metamorifizados de parte del corte tipico de las rocas de la asociación ofiolítica.

En el caso de las rocas de la Formación. Anfibolitas Macambo se puede

Tabla 1 Composión química promedio de las anfibolitas del complejo Sierra del Purial y su comaración con las toleítas abisales. **1**: Anfibolitas Mocambo, **2**: Anfibolitas Güira de Jauco, **3**: Toleitas abisales de crestas medias oceánicas (segun Miyashiro, 1975), **4**: Toleitas abisales (Engel et al, 1965)

	1	2	3	4
SiO_2	41.8	50.21	47-51	49.34
TiO_2	1.72	0.21	0.7-2.3	1.49
Al_2O_3	13.66	16.00	-	17.04
Fe_2O_3	3,47	2.05	-	1.99
FeO	9.70	5.74	-	6.22
MnO	0.14	0.05	-	0.17
MgO	8.13	8.14	-	7.17
CaO	9.80	10.60	-	11.72
Na_2O	2.56	2.89	1.7-3.3	2.75
K_2O	0.32	0.35	0.07-0.4	0.16
FeO*/MgO	1.57	1.05	0.8-2.1	-
FeO*	13.20	7.76	6.0-14.0	-

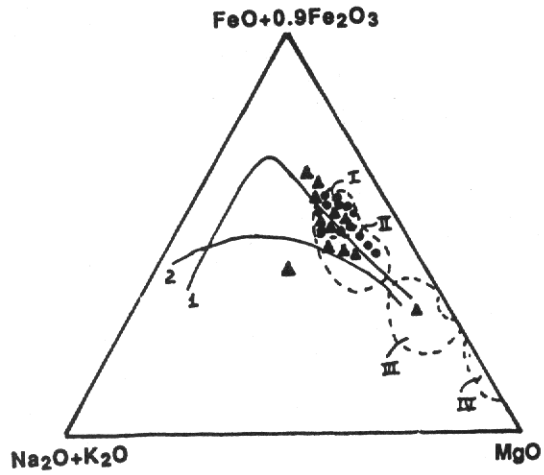

Fig. 2 Diagrama AFM para las anfibolitas del, Purial y su comaparación con otros complejos ofiolitícios conocidos (Coleman, 1977). ▲ = Anfibolitas Mocambo, ● = Anfibolitas Güira de Jauco, 1 = Toleitas Hawaianas, 2.= Rocas alcalinas Hawaianas, I = Basaltos de Papua,II. Diabasas de Omán, III = Gabroides de Papúa y Omán, IV = Ultrabasitas de Papúa y Omán

apreciar que la totalidad de las muestras analizadas se ubican en el campo de las vulcanitas básicas relacionadas con las ofiolitas, manifestándose su tendencia toleítica.

Para las rocas de la Fm. Güira de Jauco es caracteristica una mayor dispersión, abarcando los campos de los complejos basáltico, diabasico y gabroides de la asociación ofiolítica, manifestandose su tendencia toleítica.

En el diagrama AFM de la figura 3 se comparan las metavulcanitas de la Fm. Sierra del Purial, y las vulcanitas de la Fm. Quibiján con las rocas pertenecientes a la asociación ofiolítica.

Como se puede apreciar en el diagrama AFM las rocas de la Fm..Sierra del Purial muestran una gran dispersión, manifestandose tanto la tendencia toleiticia como calco-alcalina de su composición. Una parte de las muestras analizadas manifies tan asociación con los complejos basáltico y diabásico de las ofiolitas, no sucede así con el resto. En nuestra opinión esto refleja lo expresado anteriormente en relación con que en la Fm. Sierra del Púrial están mezcaldas tectónicamennte rocas de diversos origenes, que incluyen parte de rocas de la corteza oceánica, del arco insular y de sedimentos derivados de lla erosión del mismo qe sufrieron los procesos del metamorfismo regional.

En el diagrama además aparecen las rocas volcánicas básicas no metamorfizadas de la llamada Fm. Quibiján, las cuales incluyen rocas de la serie toleítica y calco-alcalina existiendo una situación similar a la que presentan las rocas de la Fm. Sierra del Purial, puesto que en el área de afloramiento de la Fm. Quibiján aparecen mezcladas tectónicamente vulcanitas ofiolíticas y del arco insular volcánico cretácico.

En la figura 4 se muestra el diagrama SiO_2 - K_2O (Engel et al., 1965) utilizado con el objetivo de caracterizar las metabasitas de Cuba Oriente (en especial las de la región de la Sierra del Purial).

En este diagrama se representan las anfibolitas de las Formaciones Güira de Jauco y Macambo, las vulcanitas de la Fm. Quibiján, y las metavulcanitas de la Fm. Sierra del Purial.

Se puede observar que las rocas metavolcánicas del macizo Sierra del Purial tienen una tendencia toleítica, de naturaleza preferentemente basaltica y en manos proporción andesítica.

Las anfibolitas y las roas volcánicas de la Fm. Quibiján caen en el campo de los basaltos toleiticos, que son caracteristicas de las asociaciones ofiolíticas.

Las metavulcanitas de la Fm. Sierra del Purial tienen una amplia dispersión en el diagrama SiO_2 - K_20, estando representadas estas rocas tanto en el campo de la serie toleítica, como en el campo de la serie calcoalcalina.

Las metavulcanitas de esta formación que se corresponden con una naturaleza basaltica toleítica son esquitos de la

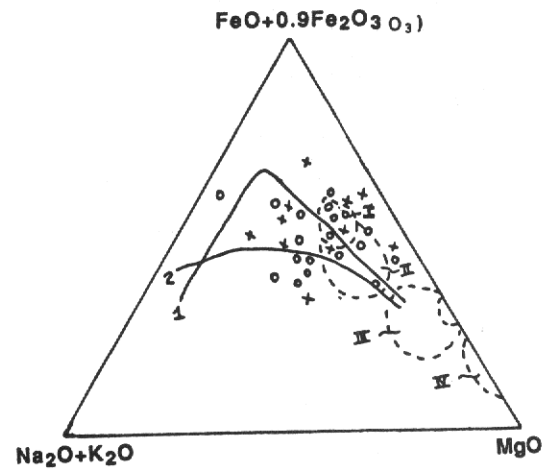

Fig. 3 Diagrama AFM para las rocas volcanicas de la Fm. Quibiján y las metavulcanitas de la Fm. Sierra del Purial y su comparación con otros complejos ofioliticos conocidos (Coleman, 1977). x = Fm. Quibiján, o = Fm. Sierra del Purial, 1 = Toleitas Hawaianas, 2.= Rocas alcalinas Hawaianas, I = Basaltos de Papua,II. Diabasas de Omán, III = Gabroides de Papúa y Omán, IV = Ultrabasitas de Papúa y Omán

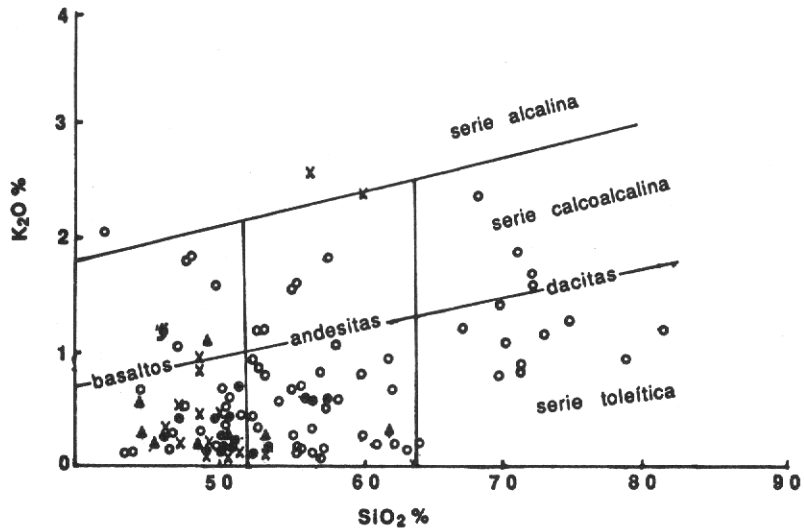

Fig 4 Diagrama SiO2-K2O. con campos de composiciones según Engel et al (1965). o = Fm. Sierra del Purial, x = Fm. Quibiján, ▲ = Anfibolitas Mocambo. ● = Anfibolitas Güira de Jauco.

localidad de La Tinta y la parte más baja de la vía La Farola (esquistos de Cajobabo, Veguita del Sur, entre otros). En un trabajo anterior M. Hernández (Coleman, 1977) plantea un caracter oceánico para las anfibolitas y para algunas secuencias de la Fm. Sierra del Purial aspecto este en el cual actualmente se sigue trabajando.

REFERENCIAS

Boiteau, A., Michard, A. and Saliot, P., 1972b, Metamorphisme de haute presion dans le complexe ophiolitique du Purial (Oriente, Cuba): Comptes Rendus de l'Academie de Science de Paris, v. 274, series D, p. 2137-2140.

Coleman, R.G.,1977, Ophiolites; Springer - Verlag, Berlin - New-York, 229pp.

Cobiella, J.L.; Hernández, M. M., Campos, M., Quintas, F,1984, Geología de la porción sur-central de la provincia de Guantanamo: Ed. Oriente, 125pp. .

Engel, A.E.J., Engel, C.G. y Havens, R.G.,1965, Chemical characteristic of oceanic basalts and the upper mantle Bull. Geol. Soc. America, v.76, p.719-734.

Hernández, M.,1987, Algunas particularidades petroquímicas de las metavul canitas de la Sierra del Purial: Revista Minería y Geología, v.5, no. 1, p.3,

Miyashiro, A., 1975, Classification, characteristics and origin of ophiolites: Journal. of Geology, v.83, 249-281.

Somin, M. y G. Millán, 1981, Geología de los complejos metamórficos de Cuba. Editorial Nauka, Moscú, 219pp. (en ruso)

SHORT REVIEW OF THE OSTRACODA OF THE MONTPELIER AND COASTAL GROUPS OF JAMAICA

W. A. van den Bold

The Montpelier Group (see Steineck, 1981) contains a mixture of dominant bathyal taxa (large Krithe, Abyssocypris, Argilloecia, Agrenocythere, Bradleya, Bythocypris, Cardobairdia etc., Table 1), minor outer neritic taxa (Costa, Cytheropteron, Loxoconcha (Palmoconcha), Trachyleberidea, etc.) and a sprinkling of inner neritic taxa (Aurila, Caudites, Hemicytherura, Loxoconcha (Loxocorniculum), Jugosocythereis, Orionina, Pokornyella, Procythereis?, Triebelina (Table 2). The neritic forms are probably derived from contemporaneous deposits on the shelf. However, in the Basal Spring Garden Formation (N8) some of them are clearly reworked from older deposits (indicated with X in Table 2 - note that these are all shallow water species). The increase of neritic species in N1-2 (Fig. 1) is probably due to uplift in the shelf area whereas the presence of deep water taxa such as Krithe reversa and K. trinidadensis indicates that no shallowing took place in the area of deposition and that it remained at bathyal depths. Also the redeposited species in the basal Spring Garden are apparently derived from N1-2 zone sediments.

In the Buff Bay Formation, after an increase of neritic forms in the Upper Spring Garden Formation and lower Buff Bay (N14), the number of neritic forms drops in the middle part (N15) and then increases again in the upper part, which increase continues in the San San clay and Bowden Formation, where it is probably related to an increase of land derived sediment (Fig. 1). Reduction of the larger Krithe species and the presence of small Krithe (K. dolichodeira) suggests upper bathyal deposition. Bathyal species continue to be present, but most of them disappear in the San San Clay (N18, 19). Radimella appears in the upper Buff Bay (N 17) in its normal position of appearance in the Caribbean.

No deeper water taxa are present in the Bowden shell bed (Bold, 1971) and the fauna here is typically inner neritic. However, above the shell bed in the Bowden Formation deeper water taxa (Cardobairdia, Messinella, Trachyleberidea, Ambocythere) return in a fauna that appears outer neritic. The same type of fauna persists in the Manchioneal Formation, but with an increased influx of inner neritic forms (Glyptobairdia, Triebelina, Uroleberis, Propontocypris) which suggests the vicinity of reefs.
Based on the distribution of ostracodes the Bonny Gate and Lower Sign Formations of the Montpelier group appear upper bathyal, upper Sign and lower and middle Spring Garden middle bathyal, Upper Spring Garden and lower and Middle Buff Bay upper bathyal, San San clay upper bathyal, upper San San, Bowden and Manchioneal outer neritic. In these deeper water deposits the biostratigraphy based on shallow marine ostracodes is rather unsatisfactory (see Table 2). In the Montpelier group the Bonny Gate and lower Sign formations belong to the Pokornyella poagi zone (P 19/18 -N5, Bold, 1983), with the Bonny Gate in the Loxoconcha (Loxocorniculum) lienenklausi-Triebelina howei zones. Note that Triebelina howei occurs here earlier than indicated by the boundaries of the zone (Bold, 1983, N3-4). The Spring Garden belongs to the Procythereis? deformis zone (N6-16). In the lower Coastal group more neritic forms occur and the zonation is more reliable. The upper Buff Bay and lower San San belong to the Radimella ovata subzone (N17-18) of the Radimella confragosa zone, and correlate with the Uppermost Cercado in the Dominican Republic and the Springvale of Trinidad. The Manchioneal belongs to the Radimella wantlandi zone (N22 - Recent).

Note on Nomenclature:

Pokornyella poagi Bold, new name
Aurila saginata (Stephenson), Butler, 1963, p. 74, pl. 2. fig. 19-21
Procythereis saginata (Stephenson), Bold, 1965, p. 396; 1975, table 4.
Trachylebereis saginata (Stephenson, Lubimova and Sánchez. 1974, pl. 14, fig. 6, 6a.
Pokornyella "saginata" (Butler, not Stephenson), Bold, 1983, p. 400, 401, 407, 409.
Not Hemicythere saginata Stephenson, 1944, p. 158, pl. 28, fig. 16, 17.

REFERENCES

Bold, W. A. van den, 1965. Middle Tertiary Ostracoda from northwestern Puerto Rico. Micropaleontology, vol. 11, no. 4, p. 381-414, pls. 1-7, 1 text fig.., 5 tables

Bold, W. A. van den, 1971. Ostracoda of the Coastal Group of Formations of Jamaica. Transaction Gulf Coast Association of Geological Societies, vol. 21, p. 3250348, pls. 1-3, 8 text-figs. 6 tables.

-----, Shallow marine biostratigraphic zonation in the Caribbean Post Eocene. Proceedings Eighth International Symposium on Stracoda, p. 400-416, 9 text-figs.

Larue, D.K., and Draper, G. (eds.), *Transactions of the 12th Caribbean Geological Conference, St. Croix, U.S.V.I.*, Miami Geological Society, P.O. Box 431552 South Miami, FL 33243 U.S.A.

-----, 1975. Remarks on the ostracode-biostratigraphy of the late and middle Tertiary of Southwest Puerto Rico. Caribbean Journal of Science, Vol. 15, no. 1-2, p. 31-36, 2 text-figs. 1 table.

-----, 1983. Shallow-marine biostratigraphic zonation in the Caribbean Post-Eocene. Proceedings 8th International Symposium on Ostracoda, p. 400-416, 9 text-figs.

Butler, E. Ann, 1963. Ostracoda and correlation of the Upper and Middle Frio from Louisiana to Florida. Louisiana State Geological Survey, Geological Bulletin, no. 39, p. 1-100, pls. 1-6, 9 text-figs., 1 map.

Poag, C. W., 1974. Late Oligocene Ostracoda from the United States Gulf Coastal Plain. Revista Española Micropaleontologîa, vol.6, no. 1, p. 39-74, pls. 1-10, 2 text-figs.,, 1 map.

Steineck, P. L., 1981. Upper Eocene to middle Miocene ostracode faunas and paleoceanography of the north coastal belt, Jamaica, West Indies. Marine micropaleontology, vol. 6, p. 339-366, pls. 1, 2, 10 text-figs.

Stephenson, M. B., 1944. New Ostracoda from subsurface middle Tertiary strata of Texas. Journal of Paleontology, vol. 18, no. 2, p. 156-161, pl. 28.

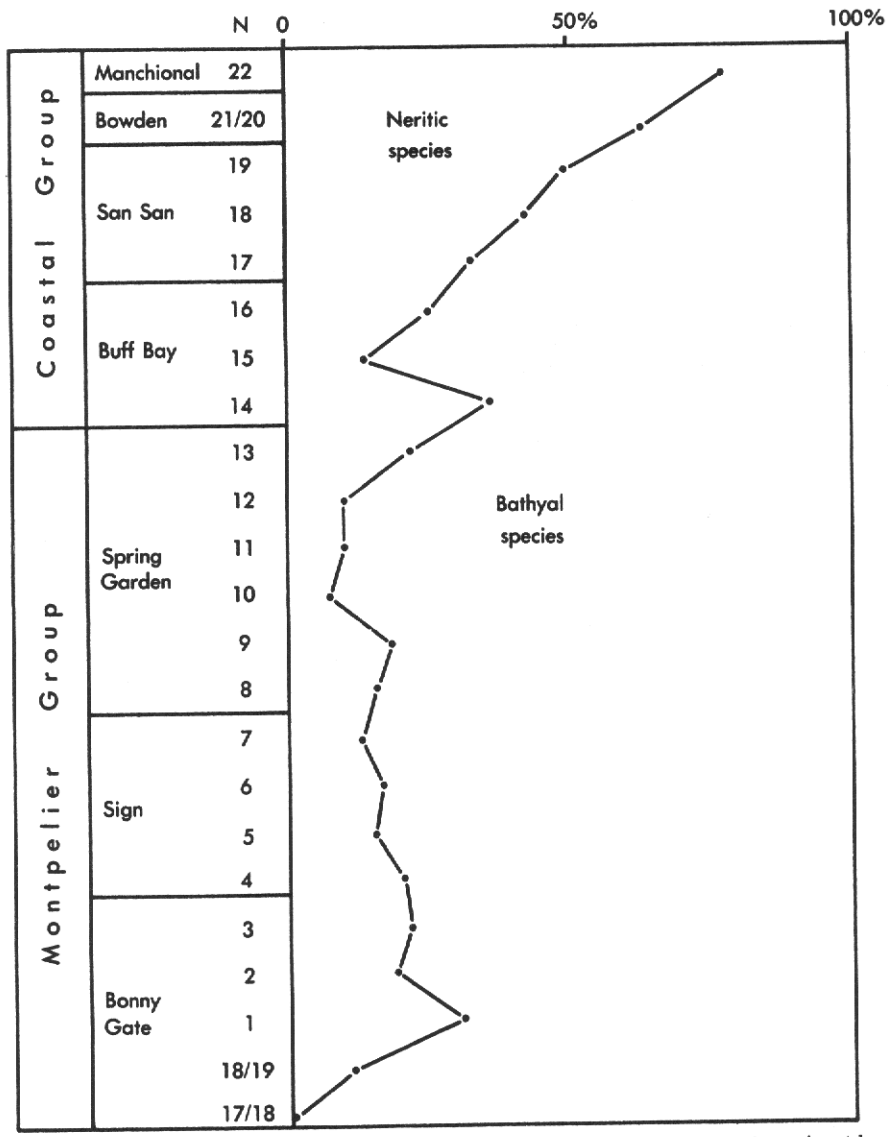

Fig. 1: Percentage of neritic vs. bathyal ostracodes in the Montpelier and Coastal Groups of Jamaica.

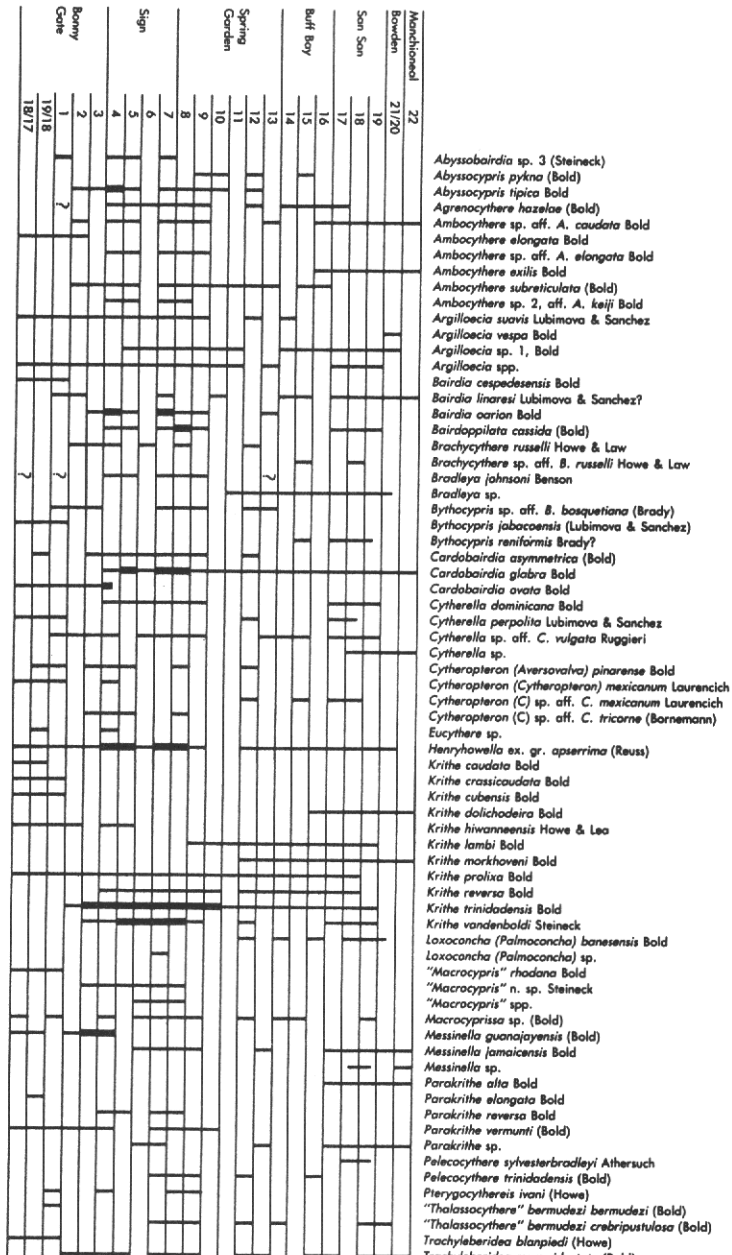

Table 1: Distribution of bathyal to outer neritic species of ostracodes in the Montpelier and Coastal Groups of Jamaica.

Table 2: Distribution of neritic species of ostracodes in the Montpelier and Coastal Groups of Jamaica.

SEDIMENTOLOGY OF THE LATE PLEISTOCENE IRONSHORE FORMATION ON GRAND CAYMAN

Ian G. Hunter and Brian Jones
Department of Geology, University of Alberta,
Edmonton, Alberta, T6G 2E3, Canada

ABSTRACT

The Ironshore Formation on Grand Cayman comprises 13 facies which were deposited in the Ironshore Lagoon. Bivalve Facies A and B, in the interior of the lagoon, consist of abundant bivalves in a matrix of poorly to moderately sorted carbonate silt to fine-grained sand. These allochems are predominantly micritized skeletal grains, Halimeda, and benthic foraminifera. Bivalve Facies A is located in the extreme interior of the lagoon and is finer grained and contains more foraminifera and fewer corals than Bivalve Facies B.

Coral Facies A includes a series of patch reefs, which formed near the westward opening of the lagoon. These patch reefs, from 2-3 m to over 300 m in diameter, are dominated by Montastrea, Diploria, Porites, Siderastrea, and Agaricia. The larger patch reefs, which show a distinct zonation, have a higher diversity than the smaller patch reefs, which are commonly monospecific. The Skeletal Grainstone, Moderately Burrowed Grainstone, or Highly Burrowed Grainstone facies were deposited between the patch reefs.

Coral Facies B comprises a diverse assemblage of corals, similar to those in the patch reefs, but also containing Meandrina, Acropora, Pocillopora, and Dendrogyra. These corals grew in a reef tract across the western edge of the lagoon, in a back reef environment. The Well Sorted Skeletal Grainstone Facies crosses Coral Facies B and was deposited in a series of channels through the reef tract.

The Multidirectional Cross-bedded Grainstone Facies consists of ooid grainstones that probably formed in an upper shoreface environment. This facies, which overlies Coral Facies A and B and associated facies, contains abundant marine trace fossils, which are found up to 4 m above present-day sea level. Erosional channels into this facies contain the Unidirectional Cross-bedded Grainstone, Lithoclast Rudstone, and Bioclast Floatstone facies.

The Multidirectional Cross-bedded Grainstone Facies is overlain by the Laminated Grainstone Facies, also consisting of ooid grainstones. This facies, which occurs up to 6.5 m above present-day sea level, is interpreted to be a foreshore (beach) deposit.

INTRODUCTION

Matley (1926) named the Ironshore Formation for the Pleistocene limestones that overlie the Oligocene-Miocene Bluff Formation on the Cayman Islands. The formation, which is up to 30 m thick (Brunt et al., 1973), is best exposed on the western part of Grand Cayman where the bedding is horizontal. The formation, 125,000 years old according to U-Th dating (Woodroffe et al., 1983), correlates with many other late Pleistocene sequences in the Caribbean (e.g. Broecker et al., 1968; Neumann and Moore, 1975; Harmon et al., 1981). Although Brunt et al. (1973), Rigby and Roberts (1976), Woodroffe et al. (1980), Jones and Goodbody (1984), Jones and Pemberton (1988a, 1988b, 1989), Hunter and Jones (1988, 1989), and Jones and Hunter (in press) discussed various aspects of the sedimentology of the Ironshore Formation, there has been no attempt to produce an overall synthesis.

The height of sea level in the Caribbean, 125,000 years ago, was approximately 5-6 m above current sea level (e.g. Neumann and Moore, 1975; Harmon et al., 1981; Carew et al., 1984; Brasier and Donahue, 1985). On Grand Cayman, however, Woodroffe et al. (1983) and Woodroffe (1988) placed the last interglacial sea level at 2-3 m above present day sea level. This was based on an erosional terrace at about 2 m (Emery, 1981) and a wave cut notch at 2.3-2.5 m on the southwest coast (Woodroffe et al., 1983, p. 71). There is, however, a 6 m terrace (Emery, 1981) and a wave cut notch at about 6 m on the northwest coast of Grand Cayman (Jones and Hunter, in press) which corresponds to a wave cut notch at 5.5-7 m on Cayman Brac (Woodroffe et al., 1983). These data supplemented with sedimentological data, suggest that the sea level during the deposition of the Ironshore Formation was at about +6 m on Grand Cayman (Jones and Hunter, in press).

Following a preliminary study of the Pleistocene geology of Grand Cayman, Hunter and Jones (1988) suggested that most of the Ironshore Formation was deposited in a lagoon, which they termed the Ironshore Lagoon. With respect to the Ironshore Formation, this paper (1) compares the facies as described by different authors, (2) describes the sedimentology of these facies, and (3) comments on the paleogeography at the time of deposition.

METHODS

The western part of Grand Cayman is low lying (most < 2 m above sea level) and usually covered with mangrove swamps. Thus, apart from coastal exposures on the southwest and northwest coasts and two quarries, good exposures of the Ironshore Formation are rare. Data for this study were obtained from (1) transects of 3 km along the southwest coast and 4 km along the northwest coast, (2) excavations associated with the construction of canals in the interior of the island, (3) exposures along the west coast of North Sound, and (4) exposures in Paul Bodden Quarry (PBQ, PBA) and Botabano Quarry (BQ). One hundred thirty eight localities were examined in the Ironshore Formation (Fig. 1B).

Grain size and sorting was determined qualitatively from thin sections using a microscope with a micrometer eyepiece. Skeletal types were determined from thin section microscopy by comparing them to thin sections of known skeletal material and published descriptions (Bathurst, 1975; Scholle, 1978). Two hundred thirty three thin sections were used in these analyses.

FACIES OF THE IRONSHORE FORMATION

Introduction

Thirteen facies are present in the Ironshore Formation on Grand Cayman (Table 1, 2). Although some facies have been described before, they were used for different purposes and thus simplified and generalized (Table 1). A detailed geology map of the island has been drawn based on extensive field work completed on the island (Fig. 2, 3).

Bivalve Facies A

This limestone, which is only found in the extreme interior of the Ironshore Lagoon, is characterized by abundant bivalves in a skeletal wackestone to packstone matrix (Table 2). This facies occurs at Midland Acres (MA) and Tarpon Springs Estates (TSE - Fig. 1B).

Bivalve Facies A contains a diverse assemblage of molluscs (70 species), that is dominated by Linga pensylvanica, Anodontia alba, Bulla striata, Cerithium spp., and Tellina candeana (Rehder,

Larue, D.K., and Draper, G. (eds.),
Transactions of the 12th Caribbean Geological Conference, St. Croix, U.S.V.I., Miami Geological Society, P.O. Box 431552, South Miami, FL 33243, U.S.A

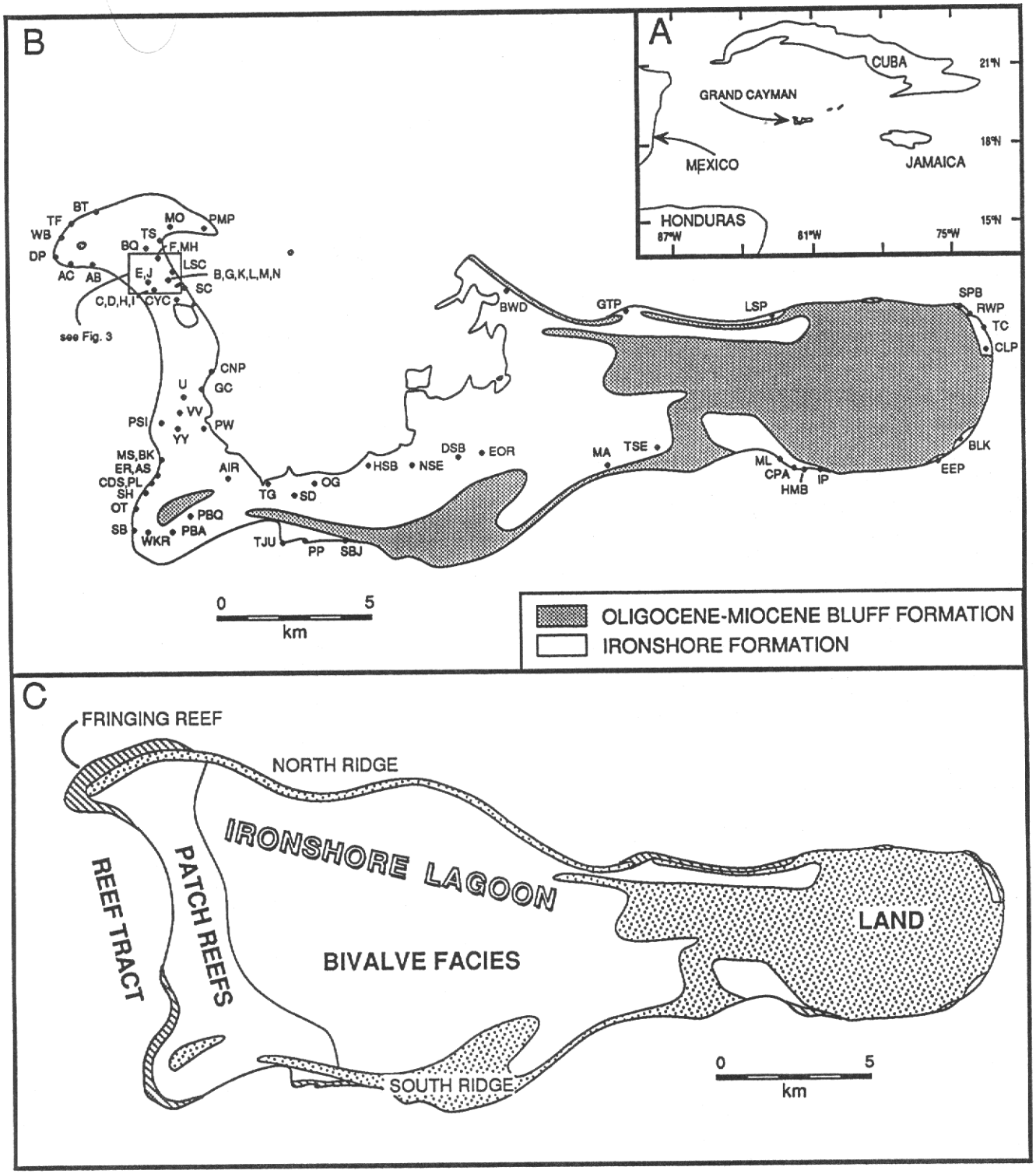

Figure 1. A) General location of the Cayman Islands in the Caribbean. B) Geological map of Grand Cayman with locations mentioned in the text. C) Paleogeographic map of Grand Cayman 125,000 years ago (modified after Hunter and Jones, 1988).

1962; Brunt et al., 1973; Cerridwen, 1989). The bivalves, commonly articulated, show no evidence of abrasion. Although molluscs generally lose their colour quickly (Parsons, 1989), some bivalves, such as Argopecten nucleus and Chione paphia (Cerridwen, 1989), retained their original colour. This may reflect rapid burial and little mechanical movement. This bivalve assemblage, dominated by burrowing bivalves, is indicative of a lagoonal environment, either in grass meadows or on a sandy bottom (Hunter and Jones, 1988; Cerridwen, 1989). Corals are very rare in this facies.

The dominant allochems in the matrix of this limestone are micritized skeletal grains, foraminifera, and Halimeda fragments,

<table>
<tr><th>Brunt et al. 1973</th><th>Woodroffe et al. 1980</th><th>Jones and Goodbody 1984</th><th>Hunter and Jones 1988</th><th>Hunter and Jones 1989</th><th>Jones and Hunter in press</th><th>Jones and Pemberton 1989</th><th>This paper</th></tr>
<tr><td rowspan="4">Lagoonal Facies</td><td rowspan="2">N/A</td><td rowspan="2">N/A</td><td rowspan="2">Bivalve Facies</td><td>Facies A</td><td rowspan="2">Bivalve Facies</td><td>N/A</td><td>Bivalve A</td></tr>
<tr><td>Facies B</td><td>N/A</td><td>Bivalve B</td></tr>
<tr><td>Coral bearing facies</td><td rowspan="2">N/A</td><td rowspan="2">Lagoonal environment Patch reefs</td><td>Facies C</td><td>Coral Facies A</td><td>N/A</td><td>Coral A</td></tr>
<tr><td>Lagoonal facies</td><td>Facies D</td><td>Laminated to highly burrowed grainstone</td><td>N/A</td><td>Skeletal Grainstone</td></tr>
<tr><td>Reef Facies</td><td rowspan="2">N/A</td><td rowspan="2">N/A</td><td rowspan="3">Reef Tract</td><td>Facies E</td><td rowspan="3">Coral Facies B</td><td>N/A</td><td>Coral B</td></tr>
<tr><td>Back-reef Facies</td><td rowspan="2">N/A</td><td rowspan="2">N/A</td><td rowspan="2">Facies F</td><td rowspan="2">N/A</td><td rowspan="2">Well Sorted Skeletal Grainstone</td></tr>
<tr><td>N/A</td><td>N/A</td></tr>
<tr><td rowspan="6">Shoal Facies</td><td rowspan="6">Oolitic Facies</td><td>Facies B</td><td rowspan="6">Ooid Facies</td><td rowspan="6">Facies G</td><td rowspan="2">Laminated to highly burrowed grainstone</td><td>Facies A</td><td rowspan="2">Moderately Burrowed Grainstone</td></tr>
<tr><td>Facies A</td><td>Facies B</td></tr>
<tr><td>Facies C</td><td>Facies C</td><td>Highly Burrowed Grainstone</td></tr>
<tr><td>N/A</td><td>Unidirectional high-angle cross-bedded grainstone</td><td>Facies D</td><td>Unidirectional Cross-bedded Grainstone</td></tr>
<tr><td rowspan="2">Multidirectional high-angle cross-bedded grainstone</td><td>Facies E</td><td rowspan="2">Multidirectional Cross-bedded Grainstone</td></tr>
<tr><td rowspan="3">Rudstone</td><td>Facies F</td><td>Lithoclast Rudstone</td></tr>
<tr><td>Facies G</td><td>Bioclast Floatstone</td></tr>
<tr><td>Laminated to low-angle cross-bedded grainstone</td><td>N/A</td><td>Laminated Grainstone</td></tr>
</table>

Table 1. Correlation of facies names of the Ironshore Formation as used by different authors on Grand Cayman. N/A = not applicable.

along with lesser amounts of red algae, mollusc, coral, and echinoid fragments (Fig. 4A). The rock contains up to 20% benthic foraminifera, mainly peneroplids (Fig. 4B). The micritized skeletal grains (1) are 30-125 μm in diameter, (2) contain no skeletal fragments, (3) are angular in shape, and (4) do not contain canal systems. Collectively, this suggests that they are micritized skeletal grains rather than pellets.

Bivalve Facies B

Between the extreme interior of the Ironshore Lagoon (Bivalve Facies A) and the area of patch reefs (Coral Facies A) is a facies characterized by bivalves in a skeletal packstone to grainstone matrix (Table 2). This facies occurs at the End of the Road (EOR), Duck Pond Bight (DSB), North Sound Estates (NSE), Head Sound Barcadere (HSB), Omega Gardens (OG, OGA), Tropical Gardens (TG), and Bowseland (BWD - Fig. 1B).

The main difference between the Bivalve Facies A and Bivalve Facies B is that the former is finer grained, contains more foraminifera (up to 20% of the rock), and has fewer corals.

Bivalve Facies B contains a diverse assemblage of molluscs (Rehder, 1962; Brunt et al., 1973; Cerridwen, 1989), with 79 species of molluscs recorded by Cerridwen (1989). The preservation of the molluscs is similar to that in Bivalve Facies A (Hunter and Jones, 1988). Although this facies and Bivalve Facies A were grouped together by Cerridwen (1989), the mollusc assemblage is slightly different, being dominated by Chione spp., Codakia spp., Anodontia alba, Crassinella martinicensis, and Cerithium spp.

FACIES	LOCALITIES	LITHOTYPE	SORTING	GRAIN SIZE	SEDIMENTARY STRUCTURES	FOSSILS		TRACE FOSSILS*	ENVIRONMENT
						DOMINANT	MINOR		
Bivalve A	MA, TSE	skeletal wackestone to packstone	poor	silt to very fine	N/O	bivalves	gastropods, foraminifera	N/O	Lagoon
Bivalve B	EOR, DSB, NSE, OG, OGA, HSB, BWD, TG	skeletal packstone to grainstone	moderate to poor	very fine to fine	N/O	bivalves	corals, Halimeda, gastropods	N/O	Lagoon
Coral A	MOS, MH, A, B, C, D, E, F, G, I, J, K, CYA, CYB, CYC, PSI, VV, YY, PBA, PBQ, WKR, SDA, SDB	coral floatstone	poor	fine to coarse	N/O	corals	bivalves, gastropods	Gastrochaenolites Entobia Trypanites	Patch reefs
Skeletal Grainstone	H, MOA, MOC, MON, TS, CYC, U, CNP, GC, PWA,PWD, SD, SDC	skeletal grainstone	moderate	fine to coarse	moderate burrowing	none	corals, bivalves	Polykladichnus Skolithos	Inter-reef
Coral B	GTP, LSP, SPB, RWP, CPA, HMB, TC, SBJ, IP, ML, PP, TJU, SB, SH, EOT, TOT, CDS, PL, ER, AS, MS, AB, AC, DP, WB, TF, BT	coral boundstone	poor	fine to coarse	N/O	corals	gastropods, red algae	N/O	Reef tract
Well sorted Skeletal Grainstone	SBB, SBD, ACB, ACF, ABB, ABC, TFB, MS	skeletal grainstone	well	fine to medium	N/O	none	corals	N/O	Reef channel
Moderately Burrowed Grainstone	SC, L, M, N, PBQ, BQ	ooid grainstone	well	fine to medium	laminated moderate burrowing	none	none	Ophiomorpha Polykladichnus Skolithos Conichnus	Subtidal
Highly Burrowed Grainstone	SC, LSC, BQ, PBA, PBQ	ooid grainstone	well	fine to medium	high burrowing	none	none	Ophiomorpha Polykladichnus Skolithos Planolites	Subtidal
Unidirectional Cross-bedded Grainstone	SC	ooid grainstone	well	fine to medium	unidirectional high-angle cross-bedding low burrowing	none	none	Polykladichnus Skolithos Conichnus Bergaueria Psilonichnus	Subtidal
Multidirectional Cross-bedded Grainstone	SC, LSC, PBQ, PBA, PMP, SB, SBA, SBF, ACA, ACH, WRS, BQ	ooid grainstone	well	fine to medium	multidirectional high-angle cross-bedding moderate burrowing	none	none	Ophiomorpha Skolithos	Upper shoreface
Lithoclast Rudstone	SC	lithoclast rudstone	moderate	fine to medium	high burrowing	none	none	Ophiomorpha Polykladichnus Conichnus	High energy subtidal
Bioclast Floatstone	SC	bioclast floatstone	moderate	fine to medium	high-angle cross-bedding moderate burrowing	none	corals, bivalves	Ophiomorpha Polykladichnus Skolithos	High energy subtidal
Laminated Grainstone	LSC, PBQ, PBA, BQ, SBA	ooid grainstone	well	fine to medium	laminated to low-angle cross-bedding	none	none	none	Foreshore-backshore

Table 2. Summary of lithology, fossils, and trace fossils of the facies in the Ironshore Formation on Grand Cayman. N/O = not observed due to poor exposure. * Trace fossils in Coral A Facies from Jones and Pemberton (1988a, 1988b); all other trace fossils from Pemberton and Jones (1988) and Jones and Pemberton (1989).

This mollusc assemblage, however, is also indicative of a lagoonal environment. Corals are slightly more abundant in this facies than in Bivalve Facies A (Hunter and Jones, 1988).

The dominant allochems in the matrix between the bivalves are micritized skeletal grains and Halimeda fragments, with lesser amounts of foraminifera, red algae, mollusc, and coral fragments (Fig. 4C).

Coral Facies A

This facies, dominated by a diverse assemblage of corals (Hunter and Jones, 1988), occurs in patches up to 300 m in diameter on the western part of Grand Cayman. This facies, which also contains a diverse assemblage of molluscs, occurs at Barker's (MOS), Morgan's Harbour (MH), localities B, C, D, E, F, G, I, J, and K near Salt Creek (Fig. 3), the Cayman Yacht Club (CYA, CYB, CYC), the Pump Station (PSI) along West Bay Road, localities A, VV, and YY near the cinemas, Walker's Road (WKR), Paul Bodden Quarry (PBA, PBQ), and Selkirk Drive (SDA, SDB - Fig. 1B). These patches of coral, considered to be patch reefs, were briefly mentioned by Brunt et al. (1973) and described by Woodroffe et al. (1980).

Coral Facies A is a coral floatstone with a grainstone matrix (Table 2). The abundant, diverse coral fauna of the patch reefs is

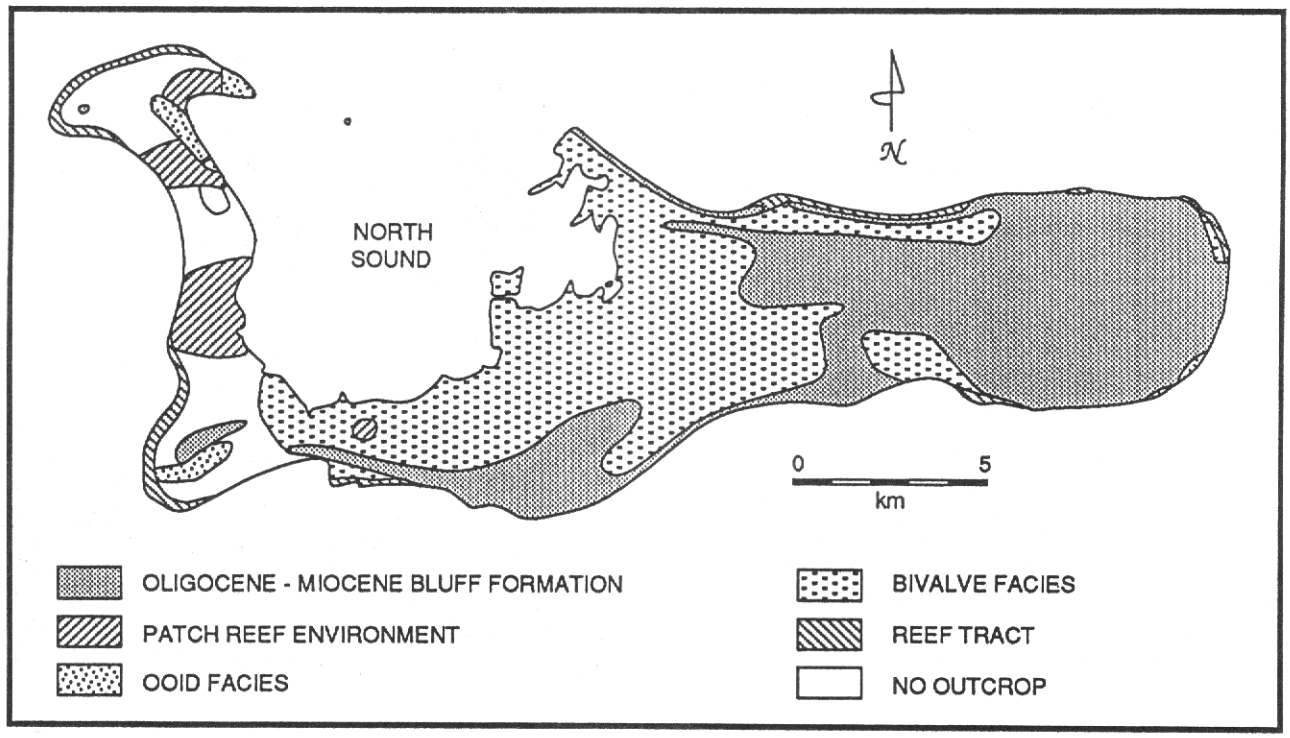

Figure 2. Facies map of the Ironshore Formation.

dominated by Montastrea, Diploria, Porites, Siderastrea, and Agaricia (Fig. 5 - Hunter and Jones, 1988). The patch reefs vary from 2-3 m in diameter at Walker's Road (WKR) and Paul Bodden Quarry (PBA, PBQ) to over 300 m in diameter near Salt Creek (Fig. 3). The amount of coral varies from 20-30% in the reefs at localities MOS, VV, and YY to 50-60% in the reef at localities C and D. Coral diversity in the patch reefs varies from nearly monospecific (e.g. Walker's Road - WKR, Paul Bodden Quarry - PBQ, or locality I), to high diversity (e.g. 21 species at Cayman Yacht Club - CYC). Many of the larger patch reefs have a distinct zonation, being dominated by massive and hemispherical corals (Montastrea, Diploria, and Siderastrea) in the center of the reefs and branching corals (Porites) and cementing bivalves (Chama and Pseudochama) on the outer parts of the reef. All the corals found in the patch reefs are capable of significant sediment rejection (Hubbard and Pocock, 1972; Hunter and Jones, 1988).

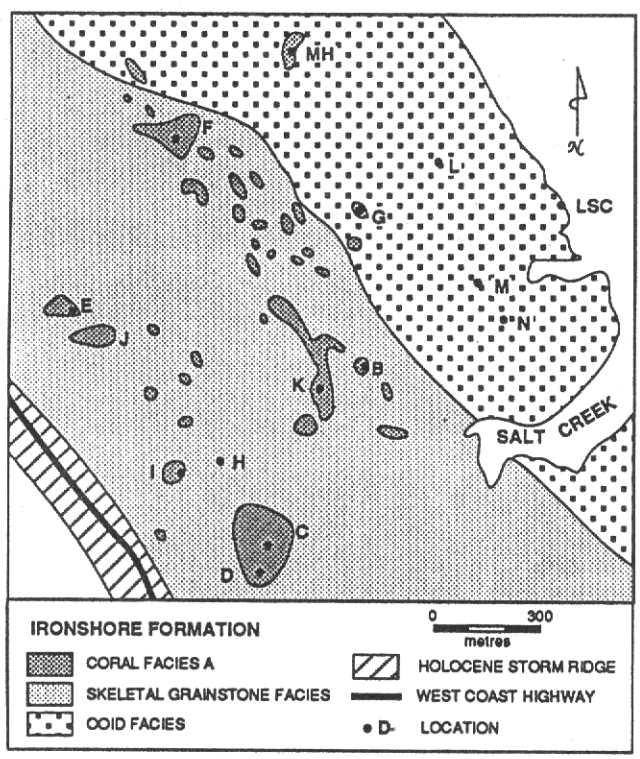

Figure 3. Paleogeographic map of a portion of the western peninsula of Grand Cayman (modified after Woodroffe et al., 1980).

Coral Facies A contains a diverse assemblage of molluscs (Woodroffe et al., 1980; Cerridwen, 1989), with 148 species of molluscs recorded by Cerridwen (1989). The mollusc fauna of the patch reefs is dominated by forms which cemented themselves to hard substrates (e.g. Chama spp. and Pseudochama radians) or lived in crevices between the corals (e.g. Arca spp. and Barbatia spp. - Cerridwen, 1989). Many reef localities include molluscs which are found in the associated sediments just off the patch reef, including Americardia guppyi, Chione spp., Codakia spp., Ervilia concentrica, Crassinella martinicensis, Linga pensylvanica, Pitar fulminatus, and Cerithium spp.

The skeletal sand between the corals is usually poorly sorted (Fig. 4D), but locally well sorted. The dominant allochems are micritized skeletal grains. The remainder of the allochems are Halimeda, mollusc, red algae, and coral fragments along with lesser amounts of echinoid fragments, worm tube fragments, and foraminifera. Comparison of well preserved fecal pellets (Fig. 6A), with modern thalassinid anomuran crustacean fecal pellets (Moore, 1932, 1939; Shinn, 1968), suggests that they are crustacean pellets. These pellets indicate the importance of burrowing crustaceans around the patch reefs.

Many large hemispherical corals, such as Montastrea annularis, M. cavernosa, Diploria strigosa, D. labyrinthiformis, and

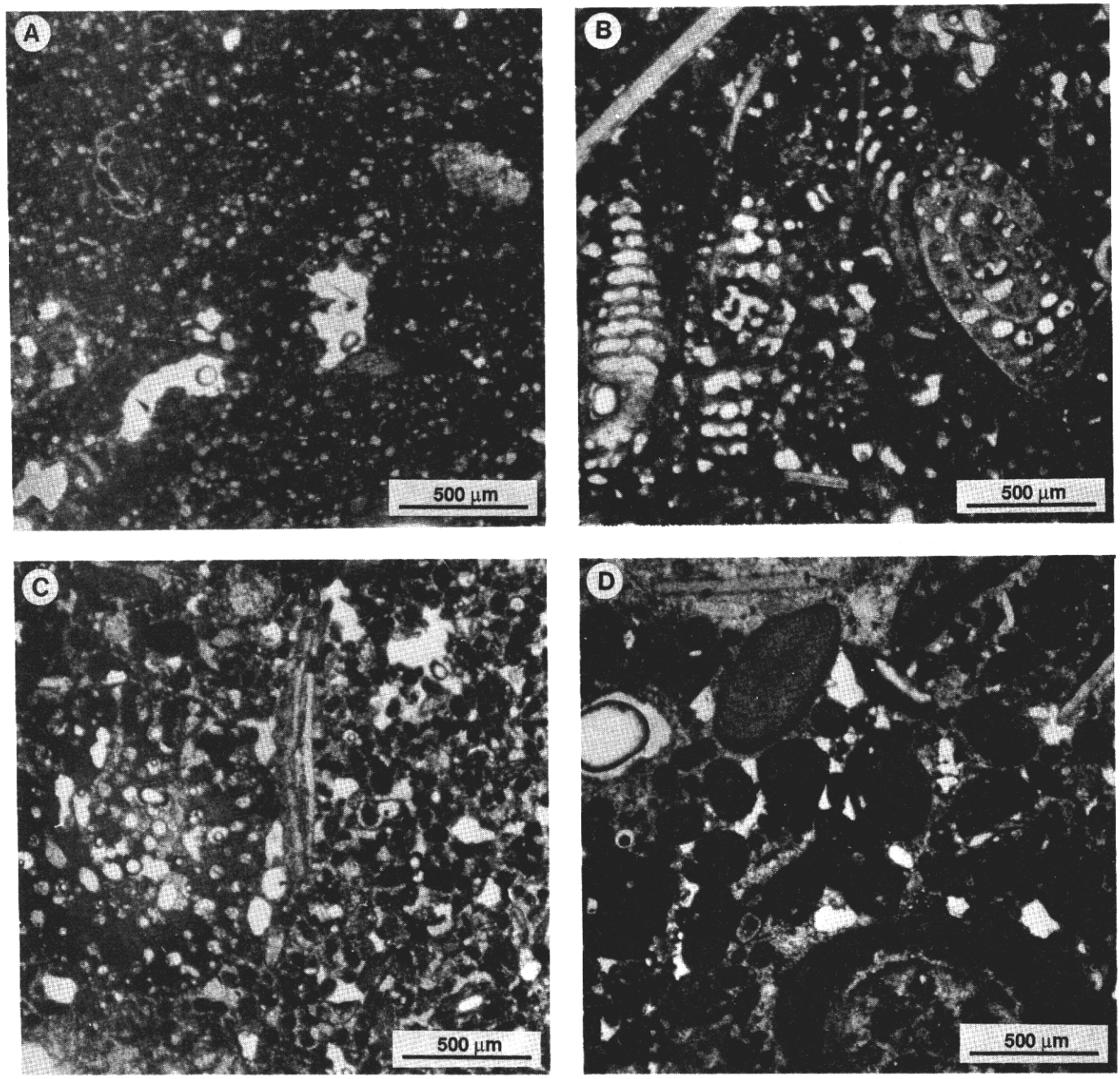

Figure 4. A) Skeletal wackestone in Bivalve Facies A. Sample CI 2236, locality TSE. B) Abundant Peneroplid foraminifera in Bivalve Facies A. Sample CI 2208, locality TSE. C) Skeletal packstone in Bivalve Facies B. Sample CI 2198, locality OGA. D) Poorly sorted skeletal grainstone in Coral Facies A. Sample CI 1976, locality B.

Siderastrea siderea, were extensively bored by Lithophaga (Jones and Pemberton, 1988a, 1988b), sponges, and worms. The Lithophaga (1) bored into dead colonies, because the borings are found around the entire colonies, (2) substantially weakened the coral heads thereby making them more susceptible to erosion, (3) bound the substrate by virtue of the dense calcareous linings in the borings, (4) liberated substantial amounts of calcium carbonate from the coral heads, (5) increased the rock-area available for further bioerosion by sponges, algae, and fungi, and (6) by virtue of the empty borings provided protected sites for sediment accumulation (Jones and Pemberton, 1988a, 1988b).

Skeletal Grainstone Facies

Between the patch reefs on the west side of Grand Cayman, is the Skeletal Grainstone Facies (Table 2). This facies is present at Barker's (MOA, MON, MOC) near the patch reef at MOS, The Shores (TS), locality H near the patch reefs at B, C, D, E, F, G, I, J, and K near Salt Creek (Fig. 3), Canal Point (CNP), Golf Course (GC), locality U near the patch reefs at A, VV, and YY near the cinemas, localities PWA and PWD near the Public Works Department, and Selkirk Drive (SD, SDC, SDD) near the patch reefs (SDA, SDB - Fig. 1B).

FACIES	CORAL A					CORAL B						
LOCATION	SB	SH	DP	TF	BT	C,D	F	MH	B	K	SD	I
Stephanocoenia michelini					R							
Acropora palmata	S	A	A	S								
Acropora cervicornis	S	A	A	C	C							
Pocillopora sp.	C		R									
Agaricia agaricites		S	S	S	S	C	S	R		S	S	R
Agaricia fragilis				R		S	R					R
Leptoseris cucullata											R	
Siderastrea siderea		S	C		S	C	C	C		S	C	
Siderastrea radians				S							S	
Porites astreoides		S	S	S	S	S	S	C	S	S	S	
Porites porites	A	C	C	A	C	A	C	S	C	A	S	A
Favia fragum	S	S	S	S	S	S	S	S	S		S	
Diploria clivosa	C		C				S	S				
Diploria strigosa	C	C	C	C	C	C	C	A	C	C		
Diploria labyrinthiformis	S	S	S	C	S	S	C	C	C	S		
Manicina areolata	S	S	R	R	S	S	S	R	S	S	S	S
Colpophyllia natans	S	S	S		S	S	C					
Montastrea annularis	A	A	A	A	A	A	C	A	A	A	A	C
Montastrea cavernosa	S	C	C	S	C		R	C				
Oculina diffusa	R										R	
Meandrina meandrites			R	R	R							
Dichocoenia stokesi			R	R	R						R	
Dendrogyra cylindrus	C	C	R		S							
Mussa angulosa					R							
Scolymia cubensis						R	R				R	
Isophyllastrea rigida	R	R	R	R				R				
Isophyllia sinuosa	R		R	R	R						R	
Mycetophyllia spp.	R	S	S			C	S	R			S	
Eusmilia fastigiata				R	R	R		R		R	R	

Figure 5. Distribution of corals at selected localities as Coral Facies A and B on the western part of Grand Cayman. A = abundant; C = common; S = Scarce; R = Rare. (Modified after Hunter and Jones, 1988).

The Skeletal Grainstone Facies contains a diverse assemblage of molluscs (Woodroffe et al., 1980; Cerridwen, 1989), with 118 species of molluscs recorded by Cerridwen (1989). These molluscs are usually articulated and well preserved, although some of the thin shelled molluscs have been broken (Cerridwen, 1989). This mollusc assemblage is dominated by Chione spp., Codakia spp., Crassinella martinicensis, Linga pensylvanica, and Cerithium spp. Locally, these limestones are highly bioturbated, with Skolithos and Polykladichnus being abundant.

The limestone between the patch reefs is usually a grainstone, but is locally a packstone. The allochems, dominated by micritized skeletal grains, are usually poorly to very poorly sorted, but in some areas are moderately to moderately well sorted. Other allochems include mollusc, coral, red algae, and Halimeda fragments, and rare foraminifera, echinoid and worm tube fragments, and pellets. Less Halimeda fragments are present in this facies than in Bivalve Facies A or B. In some areas (e.g. Canal Point, CNP) ooids with thin oolitic coatings are present. In fact, there is probably a transition between the Skeletal Grainstone Facies and the Highly Burrowed Grainstone Facies. The sediment surrounding the reefs at Selkirk Drive (SD, SDC, SDD) is finer, consisting of sediment very fine to medium grained in size.

Corals are rare in this facies. The corals were deposited as rubble from the patch reefs or isolated growth on the sea floor.

Coral Facies B

This facies, which contains a diverse coral fauna (Fig. 5; Hunter and Jones, 1988), occurs in a linear outcrop belt along the west, northwest, and southwest coasts of Grand Cayman. This facies is present at West Bay (ABA, ABB, ABC, ABD, ACA, ACB, ACC, ACD, ACE, ACF, ACG, ACI), Dolphin Point (DP, DPQ, DPA, DPB, DPC, DPD, DPE, DPF), West Bay (WBA, WBB), Turtle Farm (TF, TFN, TFA, TFB), Birch Tree Hill (BTH, BTA, BTB, BTC, BTD, BTE, BTF), Georgetown (BK, MS, AS), Eden Rock (ERN, ERS), Cayman Diving School (CDS), Parrot's Landing (PL), Sunset House (SH, SHA, SHB), Esso Oil Tanks (EOT), Texaco Oil Tanks (TOT), Smith's Barcadere (SB, SBA, SBB, SBC, SBD, SBE, SBF, SBG), Prospect Point (PP, TJU), Spotts Bay Jetty (SBJ, SBK), Frank Sound (ML), Cottage Point (CPA), Half Moon Bay (HMA, HMB), Ironshore Point (IP), Tortuga Club (TC), Rodger's Wreck Point (RWP), Spotter Bay (SPB), Little Spot Point (LSP), and Grape Tree Point (GTP) (Fig. 1B). This linear outcrop of corals is considered to be a reef tract. Channels which are filled with the Well Sorted Skeletal Grainstone Facies transect the reef tract.

Facies of the reef crest have been eroded through much of the reef tract. The preserved portion of the reef tract is probably back-reef in origin, because of substantial erosion of the Ironshore Formation since the Pleistocene (Hunter and Jones, 1988).

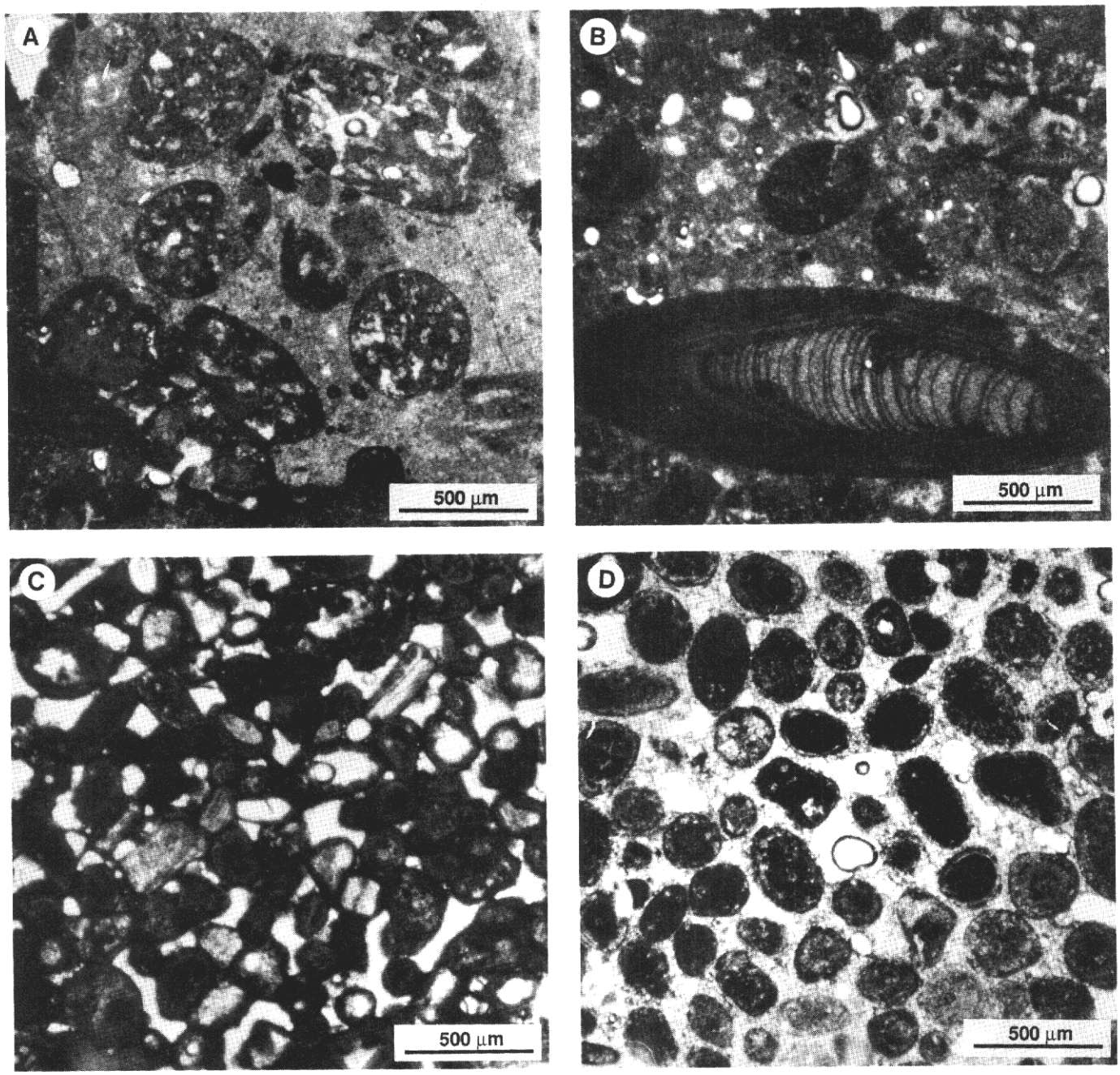

Figure 6. A) Shrimp pellets in Coral Facies A. Sample 2085, locality G. B) Poorly sorted skeletal grainstone in Coral B Facies. Sample CI 2673, locality WBB. C) Well sorted ooid and skeletal grainstone in Well Sorted Skeletal Sand Facies. Sample CI 1753, locality ABB. D) Ooids with a thin oolitic coating in the Moderately Burrowed Grainstone Facies. Sample CI 1324, locality SC.

This facies is a coral framestone to rudstone with a grainstone matrix (Table 2). The sediment surrounding the corals is usually a poorly sorted carbonate sand (Fig. 6B), but is locally well sorted. The dominant allochems are micritized skeletal grains, coral and red algae fragments, with lesser numbers of foraminifera, Halimeda, and mollusc fragments. Between the abundant coral skeletons is a diverse mollusc fauna, dominated by gastropods and lesser numbers of bivalves (77 species - Cerridwen, 1989).

Coral diversity in the reef tract varies from nearly monospecific patches of Porites porites, Pocillopora sp., or Dendrogyra cylindrus (e.g. Smith's Barcadere SBB, SBD, SBE, SBF) to areas of high diversity (e.g. 21 species at Dolphin Point DP - Fig. 5). The corals, which occur in the reef tract but not in the patch reefs, are Meandrina meandrites, Dendrogyra cylindrus, Pocillopora sp., Acropora cervicornis, and A. palmata. The Acropora spp. and M. meandrites are incapable of sediment rejection (Hubbard and Pocock, 1972).

Different coral communities (Fig. 5), occur in different areas of Coral Facies B. These communities are:

(1) Acropora community, dominated by A. cervicornis and A. palmata;

(2) Porites community, dominated by P. porites;

(3) Dendrogyra community, dominated by D. cylindrus and Pocillopora sp.;
(4) Montastrea community, dominated by hemispherical corals of M. annularis, M. cavernosa, Diploria spp., and Siderastrea siderea; and
(5) Diploria community, dominated by D. clivosa and D. strigosa.

Stromatolites formed around many coral fragments (Pocillopora sp. and Acropora cervicornis) in this facies. These stromatolites, up to 3 cm thick and 10 cm long, are composed of alternating layers of carbonate silt and micrite, and darker algal-rich layers. Some layers within the stromatolites are encrusted by foraminifera (Homotrema and Carpentaria) or red algae. The structure of these stromatolites suggest that they were formed in a low energy environment.

Well Sorted Skeletal Grainstone Facies

This facies, located along the reef tract, consists of well sorted ooid and skeletal grainstones, with few corals. This facies is present at Smith's Barcadere (SBB, SBD), West Bay (ABB, ABC, ACB, ACF), and the Turtle Farm (TFB - Fig. 1B). This facies, restricted to areas 10-25 m wide, is interpreted to have been deposited in reef channels. Corals are rare, being mostly debris from the nearby reef.

This facies consists of well sorted ooid or skeletal grainstones (Table 2). The ooids have thick cortical layers making up approximately 50% of the ooid (Fig. 6C). The nuclei of the ooids are coral and mollusc fragments and micritized skeletal grains. Other allochems include coral, red algae, and mollusc fragments.

Moderately Burrowed Grainstone Facies

This facies, which consists of moderately burrowed ooid grainstones (Table 2), is present at Salt Creek (SC). Jones and Pemberton (1989 - Table 1) divided this facies based on the thickness of the laminations.

The dominant allochems in this facies are ooids. They average 125-250 µm in diameter (Fig. 6D), although they are up to 550 µm in diameter (Jones and Goodbody, 1984). The ooids typically have a (1) slightly irregular ovoid outline, (2) matt surface, (3) large nucleus, and (4) thin cortex of only a few cortical layers (Jones and Goodbody, 1984; Jones and Pemberton, 1989). Small skeletal fragments of mollusc shells, corals, and Halimeda form less than 5% of this facies. Jones and Goodbody (1984) suggested that the thin oolitic coatings on the ooids may have been developed because of bacterially induced calcite precipitation intimately associated with pellets produced by Callianassa.

The nuclei of the ooids are masses of dense, dark-coloured cryptocrystalline calcite or aragonite. These were considered to be fecal pellets (Jones and Goodbody, 1984), because the nuclei of the ooids (1) have an ovoid shape comparable to that associated with pellets, (2) have a high organic content, (3) are well sorted, (4) contain detrital fragments of skeletal material that are randomly scattered throughout the nuclei, and (5) many contain small (30-50 µm) circular to ovate openings that are comparable to canal systems found in pellets produced by Callianassa (Shinn, 1968).

These ooids are different from the ooids in the Well Sorted Skeletal Grainstone Facies. The ooids from the Moderately Burrowed Grainstone Facies have thin cortical layers (as opposed to thick cortical layers) and have pellets as nuclei (as opposed to skeletal fragments as nuclei).

This facies, which is moderately burrowed (5 on the scale of Frey and Pemberton, 1985 - Table 2), has low angle to parallel laminations (Jones and Pemberton, 1989). The Ophiomorpha are dominantly vertical in the upper part of this facies and usually extend down to the lower section of the outcrop where they become horizontal. This facies probably originated in a quiet-water lagoon (Jones and Goodbody, 1984; Jones and Pemberton, 1989).

Highly Burrowed Grainstone Facies

This facies, characterized by a sequence of highly burrowed ooid grainstones, is present at Botabano Quarry (BQ), Paul Bodden Quarry (PBQ, PBA), Salt Creek (SC), and Little Salt Creek (LSC).

The dominant allochems are ooids (Table 2), similar to those in the Moderately Burrowed Grainstone Facies. These oolitic limestones have been moderately to highly burrowed (7-9 on the scale of Frey and Pemberton, 1985), with vague laminations remaining. This facies is interpreted to be deposited in a quiet-water lagoon (Jones and Pemberton, 1989).

Unidirectional Cross-bedded Grainstone Facies

This facies, characterized by a sequence of unidirectional cross-bedded ooid grainstones, is restricted to Salt Creek (SC). Woodroffe (1988) attributed a subaerial origin to this facies by incorrectly citing and interpreting information from Jones and Goodbody (1984).

The ooids (Table 2) in this facies are similar to those in the Moderately Burrowed Grainstone Facies. At the base of this facies, there are scattered tabular lithoclasts, up to 30 cm x 30 cm x 10 cm. They are composed of well sorted cemented ooids similar to those in the matrix. Although their appearance suggests derivation from beachrock, they contain no features that would support this suggestion (Jones and Pemberton, 1989).

The ooid grainstones are characterized by high-angle cross-bedding, locally with back-flow ripples (Jones and Pemberton, 1989). This facies has low burrowing (1-2 on the scale of Frey and Pemberton, 1985), but the trace fossil assemblage is unequivocally marine in origin (Pemberton and Jones, 1988; Jones and Pemberton, 1989). This facies is interpreted to be deposited in a (tidal?) channel (Jones and Pemberton, 1989).

Multidirectional Cross-bedded Grainstone Facies

The Multidirectional Cross-bedded Grainstone Facies, occurs at Salt Creek (SC), Little Salt Creek (LSC), Botabano Quarry (BQ), West Bay (ACA, ACH), Palmetto Point (PMP), Smith's Barcadere (SBA, SB, SBF), Paul Bodden Quarry (PBQ, PBA), and Walker's Road School (WRS - Fig. 1B). It overlies the lagoonal deposits of the Skeletal Grainstone, Moderately Burrowed Grainstone, and Highly Burrowed Grainstone facies and the reefal deposits of the Coral A and B facies.

This facies, containing well sorted ooids, similar to those in the Moderately Burrowed Grainstone Facies, is characterized by trough cross-bedding, planar cross-bedding, and parallel laminations (Jones and Pemberton, 1989). These oolitic limestones, with low burrowing (3 on the scale of Frey and Pemberton, 1985 - Table 2), are interpreted to be upper shoreface (Jones and Hunter, in press).

Lithoclast Rudstone Facies

This facies, characterized by irregular-shaped lithoclasts with a well sorted ooid grainstone matrix, is only present at Salt Creek (SC). These lithoclasts, up to 10 cm x 10 cm x 10 cm, consist of well sorted cemented ooids similar to those in the matrix. These lithoclasts extend though the entire thickness of the facies. There are no sedimentary structures (Jones and Pemberton, 1989), because it is highly burrowed (8 on the scale of Frey and Pemberton, 1985). These rudstones were deposited at the base of a high-energy channel (Jones and Pemberton, 1989).

Bioclast Floatstone Facies

These bioclast floatstones occur only at Salt Creek (SC) as a channel fill. The bioclasts of molluscs and corals are in a matrix of well sorted ooids, similar to those in the Moderately Burrowed Grainstone Facies. At the base of this facies there are scattered tabular lithoclasts, similar to those in the Unidirectional Cross-

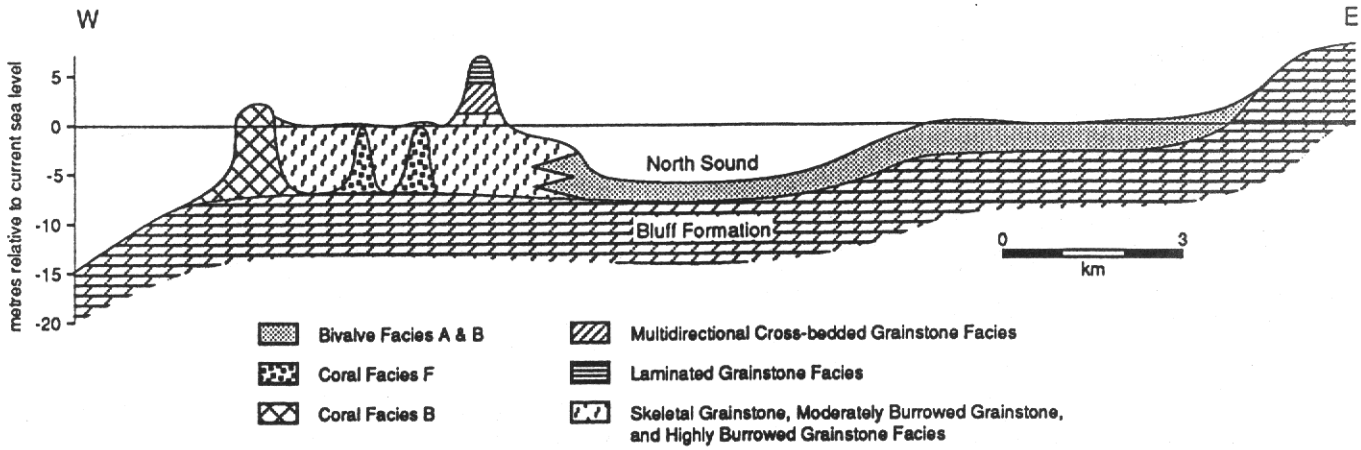

Figure 7. Schematic east-west cross-section across the western half of Grand Cayman showing the lateral and vertical relationships of the main facies in the Ironshore Formation (modified after Jones and Hunter, in press).

bedded Grainstone Facies. These limestones contain large scale cross-bedding, locally with planar laminations (Jones and Pemberton, 1989), and are interpreted to have been deposited in a channel (Jones and Pemberton, 1989).

Laminated Grainstone Facies

These laminated ooid grainstones are present at Little Salt Creek (LSC), Paul Bodden Quarry (PBA, PBQ), Botabano Quarry (BQ), and Smith's Barcadere (SBA - Fig. 1B) overlying the Multidirectional Cross-bedded Grainstone Facies. At Paul Bodden Quarry (PBA) they attain a maximum elevation of 6.5 m above present-day sea level.

These grainstones, dominated by well sorted ooids similar to those in the Moderately Burrowed Grainstone Facies, are characterized by horizontal to low-angle laminations. No burrows have been observed, even though all outcrops were examined in great detail. This facies of subparallel to low-angle cross-bedded laminated grainstones is interpreted to be a foreshore (beach) deposit and indicative of sea level (Jones and Hunter, in press).

DISCUSSION

Erosion of the Bluff Formation between middle Miocene and late Pleistocene times produced a highly irregular topography, upon which the limestones of the Ironshore Formation were deposited (Jones and Smith, 1988). Although the Ironshore Formation occurs in small embayments on the east, south, and north coasts of Grand Cayman, the main area of deposition was in a large lagoon that covered the western half of Grand Cayman. This lagoon was named the Ironshore Lagoon (Fig. 1C, 7 - Hunter and Jones, 1988).

In the interior of the lagoon, Bivalve Facies A and B were deposited in quiet shallow water conditions. These sediments were deposited in either grass meadows or sediment banks, similar to those in North Sound. The western portion of the Ironshore Lagoon was characterized by patch reefs (Coral Facies A) and inter-reef sediments (Skeletal Grainstone, Moderately Burrowed Grainstone, and Highly Burrowed Grainstone). These patch reefs are similar to patch reefs found in many lagoons around Grand Cayman today. At the margin of the Ironshore Lagoon was an extensive barrier reef with a series of tidal channels (Well Sorted Skeletal Grainstone) through the reef. Little of the reef crest and shallow fore-reef sediments are now preserved, but an extensive reef tract (dominantly shallow back-reef) with a diverse assemblage of corals (Coral Facies B) is still preserved.

Subsequent to the deposition of the temporal equivalent facies described above, the lagoon was filled by ooid grainstones to a maximum elevation of 6.5 m above present day sea level. This shallowing upward sequence comprises (1) lagoonal deposits described above, (2) an upper shoreface facies (Multidirectional Cross-bedded Grainstone Facies), and (3) a foreshore-backshore deposit (Laminated Grainstone Facies). The Laminated Grainstone Facies occurs 4-6.5 m above sea level and puts constraints on the height of sea level during the Sangamon.

The outcrop of the Ironshore Formation at Salt Creek contains a good exposure of a series of channels, probably formed by storm activity (Jones and Pemberton, 1989). In these channels the Unidirectional Cross-bedded Grainstone Facies, Lithoclast Rudstone, and Bioclast Floatstone were deposited.

CONCLUSIONS

Detailed study of the Ironshore Formation on Grand Cayman has shown that:

(1) it can be divided into thirteen distinct facies, representing environments from a lagoon to a reef tract,
(2) the coral communities in the patch reefs and the reef tract can be differentiated by the presence or absence of corals incapable of sediment rejection, and
(3) sea level, 125,000 years ago, can be estimated at about 6 m above present day sea level.

ACKNOWLEDGEMENTS

We are indebted to the Natural Sciences and Research Council of Canada who financially supported the fieldwork and preparation work needed for this study (grant A6090 to Jones), the Mosquito Research Control Unit of the Cayman Islands which provided accommodation during the course of the fieldwork, Mr. Richard Beswick, Director of the Water Authority of the Cayman Islands for logistical support, and Sam Ng, Jill Rehman, and Sarah Cerridwen who provided assistance in the field.

REFERENCES CITED

Bathurst, R.G.C., 1975, Carbonate Sediments and their Diagenesis, Second Edition: Elsevier, N.Y., 658 p.

Brasier, M. and Donahue, J., 1985, Barbuda - an emerging reef and lagoon complex on the edge of the Lesser Antilles island arc: Jour. Geol. Soc. London, v. 142, p. 1101-1117.

Broecker, W.S., Thurber, D.L., Goddard, J., Ku, T.-L., Matthews, R.K., and Mesolella, K.J., 1968, Milankovitch hypothesis supported by precise dating of coral reefs and deep-sea sediments: Science, v. 159, p. 297-300.

Brunt, M.A., Giglioli, M.E., Mather, J.D., Piper, D.J., and Richards, H.G., 1973, The Pleistocene rocks of the Cayman Islands: Geol. Mag., v. 110, p. 209-221.

Carew, J.L., Mylroie, J., Wehmiller, J.F., and Lively, R.S., 1984, Estimate of Late Pleistocene sea level high stands from San Salvador, Bahamas, in Teeter, J.W., ed., Proc. 2nd Symp. Geol. Bahamas: CCFL, Bahamian Field Station, San Salvador, Bahamas, p. 153-175.

Cerridwen, S.A., 1989, Paleoecology of Pleistocene Mollusca from the Ironshore Formation, Grand Cayman, B.W.I.: Unpubl. M.Sc. Thesis, Univ. Alberta, Edmonton, 271 p.

Emery, K.O., 1981, Low marine terraces on Grand Cayman Island: Estuarine Coast. Shelf Sci., v. 12, p. 569-578.

Frey, R.W. and Pemberton, S.G., 1985, Biogenic structures in outcrops and core. I. Approaches to ichnology: Bull. Can. Petrol. Geol., v. 33, p. 72-115.

Harmon, R.S., Land, L.S., Mitterer, R.M., Garrett, P., Schwarz, H.P., and Larson, G.J., 1981, Bermuda sea level during the last interglacial: Nature, v. 209, p. 481-483.

Hubbard, J.A.E.B. and Pocock, Y.P., 1972, Sediment rejection by recent scleractinian corals: a key to paleo-environmental reconstruction: Geol. Rund., v. 61, p. 598-626.

Hunter, I.G. and Jones, B., 1988, The corals and paleogeography of the Ironshore Formation on Grand Cayman, B.W.I.: Proc. 6th Inter. Coral Reef Symp., Townsville, Australia, v. 3, p. 431-435.

_____ 1989, Sedimentology of the late Pleistocene Ironshore Formation on Grand Cayman: 12th Carib. Geol. Cong., St. Croix, Abstracts, p. 78.

Jones, B. and Goodbody, Q.H., 1984, Biological factors in the formation of quiet-water ooids: Bull. Can. Petrol. Geol., v. 32, p. 190-200.

Jones, B. and Hunter, I.G., in press, Pleistocene paleogeography and sea level on the Cayman Islands, British West Indies: Coral Reefs.

Jones, B. and Pemberton, S.G., 1988a, Lithophaga borings and their influence on the diagenesis of corals in the Pleistocene Ironshore Formation of Grand Cayman: Palaios, v. 3, p. 1-19.

_____ 1988b, Bioerosion of corals by Lithophaga: example from the Pleistocene Ironshore Formation of Grand Cayman, B.W.I.: Proc. 6th Inter. Coral Reef Symp., Townsville, Australia, v. 3, p. 437-440.

_____ 1989, Sedimentology and ichnology of a Pleistocene unconformity bounded shallowing upward carbonate sequence: the Ironshore Formation, Salt Creek, Grand Cayman: Palaios, v. 4, p. 343-355.

Jones, B., and Smith, D.S., 1988, Open and filled karst features on the Cayman Islands: implications for the recognition of paleokarst: Can. Jour. Earth Sci., v. 25, p. 1277-1291.

Matley, C.A., 1926, The geology of the Cayman Islands (British West Indies) and their relation to the Bartlett Trough: Quart. Jour. Geol. Soc. London, v. 82, p. 352-386.

Moore, H.B., 1932, The faecal pellets of the Anomura: Proc. Royal Soc. Edinburgh, v. 52, p. 296-308.

_____ 1939, Faecal pellets in relation to marine deposits, in Trask, P.D., ed., Recent Marine Sediments: Amer. Assoc. Petrol. Geol., p. 516-524.

Neumann, A.C., and Moore, W.S., 1975, Sea level events and Pleistocene coral ages in the Northern Bahamas. Quat. Res., v. 5, p. 215-224.

Parsons, K.M., 1989, Taphonomy as an indicator of environment: Smuggler's Cove, St. Croix, U.S.V.I. in Hubbard, D.K., ed., Terrestrial and Marine Geology of St. Croix, U.S. Virgin Islands: West Indies Laboratory, Spec. Publ. 8, 12th Carib. Geol. Conf., Teague Bay, St. Croix, U.S.V.I., p. 135-143.

Pemberton, S.G. and Jones, B., 1988, Ichnology of the Pleistocene Ironshore Formation, Grand Cayman Island, British West Indies: Jour. Paleont., v. 62, p. 495-505.

Rehder, H.A., 1962, The Pleistocene mollusks of Grand Cayman Island, with notes on the geology of the island: Jour. Paleont., v. 36, p. 583-585.

Rigby, J.K., and Roberts, H.H., 1976, Geology, Reefs, and Marine Communities of Grand Cayman Island, British West Indies: Brigham Young Univ., Geol. Stud., Spec. Publ. 4, p. 1-95.

Scholle, P.A., 1978, A Color Illustrated Guide to Carbonate Rock Constituents, Textures, Cements, and Porosities: Amer. Assoc. Petrol. Geol., Mem. 27, 241 p.

Shinn, E.A., 1968, Burrowing in recent lime sediments of Florida and the Bahamas: Jour. Paleont., v. 42, p. 879-894.

Woodroffe, C.D., 1988, Vertical movements of isolated oceanic islands at plate margins: evidence from emergent reefs in Tonga (Pacific Ocean), Cayman Islands (Caribbean Sea) and Christmas Island (Indian Ocean): Z. Geomorph. N. F., v. 69, p. 17-37.

Woodroffe, C.D., Stoddart, D.R., and Giglioli, M.E.C., 1980, Pleistocene patch reefs and Holocene swamp morphology, Grand Cayman Island, West Indies: Jour. Biogeogr., v. 7, p. 103-113.

Woodroffe, C.D., Stoddart, D.R., Harmon, R.S., and Spencer, T., 1983, Coastal morphology and late Quaternary history, Cayman Islands, West Indies: Quat. Res., v. 19, p. 64-84.

POROSITY AND PERMEABILITY DEVELOPMENT IN THE OLIGOCENE-MIOCENE BLUFF FORMATION, GRAND CAYMAN

Kwok-Choi Ng and Brian Jones
Department of Geology, University of Alberta,
Edmonton, Alberta, T6G 2E3, Canada

ABSTRACT

Present day porosity and permeability in the Bluff Formation of Grand Cayman is a result of numerous constructive and destructive processes. Porosity was created by (1) preferential dissolution of aragonite fossils, (2) solution widening of joints and fissures, (3) development of solution caverns and passages, (4) tree root borings, (5) microborings, and (6) selective dissolution of the cores of dolomite rhombs. The high permeability is related to extensive network of joints which transect the island and the well developed karst system. Porosity and permeability destruction occurred through the (1) deposition of caymanite, grainstones and terra rossa, and (2) precipitation of speleothemic calcite and carbonate cements.

The creation and destruction of the porosity in the Bluff Formation was controlled by the interplay of climatic conditions and the successive cycles of regressions and transgressions that have affected Grand Cayman over the last 30 million years. During some regressions porosity was created because the carbonates were dissolved during influx of fresh water. At other times, however, conditions were suitable for the formation of speleothemic calcite, calcite and dolomite cements and/or terra rossa and this led to porosity reduction. The onset of transgressive conditions led to porosity destruction because marine sediments were commonly brought onshore and flushed into the cavities via the well developed joint and cave systems.

The combination of constructive and destructive processes has produced a heterogeneous aquifer of which the hydraulic information is difficult to interpret. The integration of hydrogeological data, hydrochemical information and the geological evolution of the island has led to an improved understanding of the manner in which the ground water behaves because water-rock interactions affects the hydrogeological properties of the aquifer and hence, the ground water flow. Such information is invaluable in the development and management of this valuable resource.

INTRODUCTION

An effective prediction of porosity and permeability distribution in the Oligocene-Miocene Bluff Formation (Fig. 1) is essential to the management of ground water resources on Grand Cayman. Conversely, chemical characteristics of the present-day ground water can be used to examine the conditions for the formation of diagenetic fabrics present in the rocks. The present day porosity and permeability distribution in the Bluff Formation is a result of the numerous constructive and destructive processes which produced heterogeneous aquifers. Interpretation of the porosity and permeability distribution in the dolostones of the Bluff Formation, therefore, requires a detailed study of the mechanisms involved in porosity creation and destruction. These mechanisms are controlled by extrinsic (climate, vegetation, and time) and intrinsic (lithology, structure, and stratigraphy) factors.

This study (1) identifies the porosity styles and evaluates their conditions of development, (2) identifies the cavity fills and evaluate the conditions for their formation, (3) highlights the relationship between porosity distribution and ground water flow regime, and (4) emphasizes the effect of sea level fluctuations on diagenetic modification of the Bluff Formation. This study is based on hydrological and hydrogeological data collected over a three year period from 1985 to 1988. The petrographic signatures of the rocks were determined from some 160 thin sections.

GEOLOGICAL FRAMEWORK

Grand Cayman (Fig. 1A) is formed of the Oligocene-Miocene Bluff Formation and Pleistocene Ironshore Formation (Fig. 1B; Matley, 1926; Vaughan, 1926; Brunt et al., 1973; Rigby and Roberts, 1976; Jones et al., 1984; Jones and Hunter, 1989). A disconformity divides the Bluff Formation into the early late Oligocene Cayman Member and the middle Miocene Pedro Castle Member (Jones and Hunter, 1989). The lithology of the Bluff Formation is typically a dense, white to light tan, finely crystalline dolostone. The Pleistocene Ironshore Formation, which unconformably overlies the Bluff Formation, is formed of limestone (Brunt et al., 1973; Jones et al., 1984).

HYDROLOGICAL REGIME

The fresh ground waters are recharged by infiltration of precipitation not lost to evapotranspiration or surface runoff. The patchy soil cover together with the intense jointing and karsting (Folk et al., 1973; Rigby and Roberts, 1976; Jones and Smith, 1988) suggest that the Bluff Formation should have a high infiltration capacity. Rapid recharge, recorded by water table hydrograph of well 7-84EE following each rainfall (Figs. 1B, 2), probably occurs when rain water infiltrates through the fissures or caverns. The rapid decline of the water table demonstrates the efficient transmission of the ground water in the aquifer (Fig. 2).

Recharge is also indicated by the improvement of water quality recorded by piezometer 4-84LV (Figs. 1B, 3). The rain water probably causes dilution of water salinity in the shallow aquifer during rapid recharge. The sharp decrease in salinity at the end of May, 1986 (Fig. 3) was in response to a storm that lasted for 12 days with a total rainfall of 246 mm.

A significant part of the precipitation generally is lost through evapotranspiration. On Grand Cayman, where the temperature averages about 28°C, evapotranspiration is an active process. Evapotranspiration also has a significant impact on the chemical quality of the ground water. The fluctuation of water salinity with time recorded by piezometer 4-84LV (Fig. 3) is caused by the interplay between the rain water recharge and evapotranspiration.

HYDROGEOLOGICAL REGIME

Fresh water accumulations on Grand Cayman (Mather, 1972) are typically lens shaped and entirely land locked (Fig. 1B); features that are common on small limestone oceanic islands (Mather and Buckley, 1973; Vacher, 1978; Lloyd, 1980; Ayers and Vacher, 1986). The major fresh water lenses on Grand Cayman are developed in an unconfined condition in the Bluff Formation (Fig. 4A), where the land surface elevations are highest.

Fresh water lenses developed on Grand Cayman typically have an irregular configuration (Fig. 4A) that is controlled by the attitude and orientation of the joints and fissures. Commonly, the lens thickness is not in agreement with the general theories of the Ghyben-Herzberg principle (Fig. 4B) as developed by Herzberg (1901). This is probably because of the continual changes in the ground water compositions, the mixing effect of the fresh and underlying saline water, and the heterogeneity and anisotropy of the aquifers.

The highly permeable nature of the karstic bedrocks prevents the development of surface streams. Thick soil cover is also

Larue, D.K., and Draper, G. (eds.),
Transactions of the 12th Caribbean Geological Conference, St. Croix, U.S.V.I., Miami Geological Society, P.O. Box 431552, South Miami, FL 33243, U.S.A

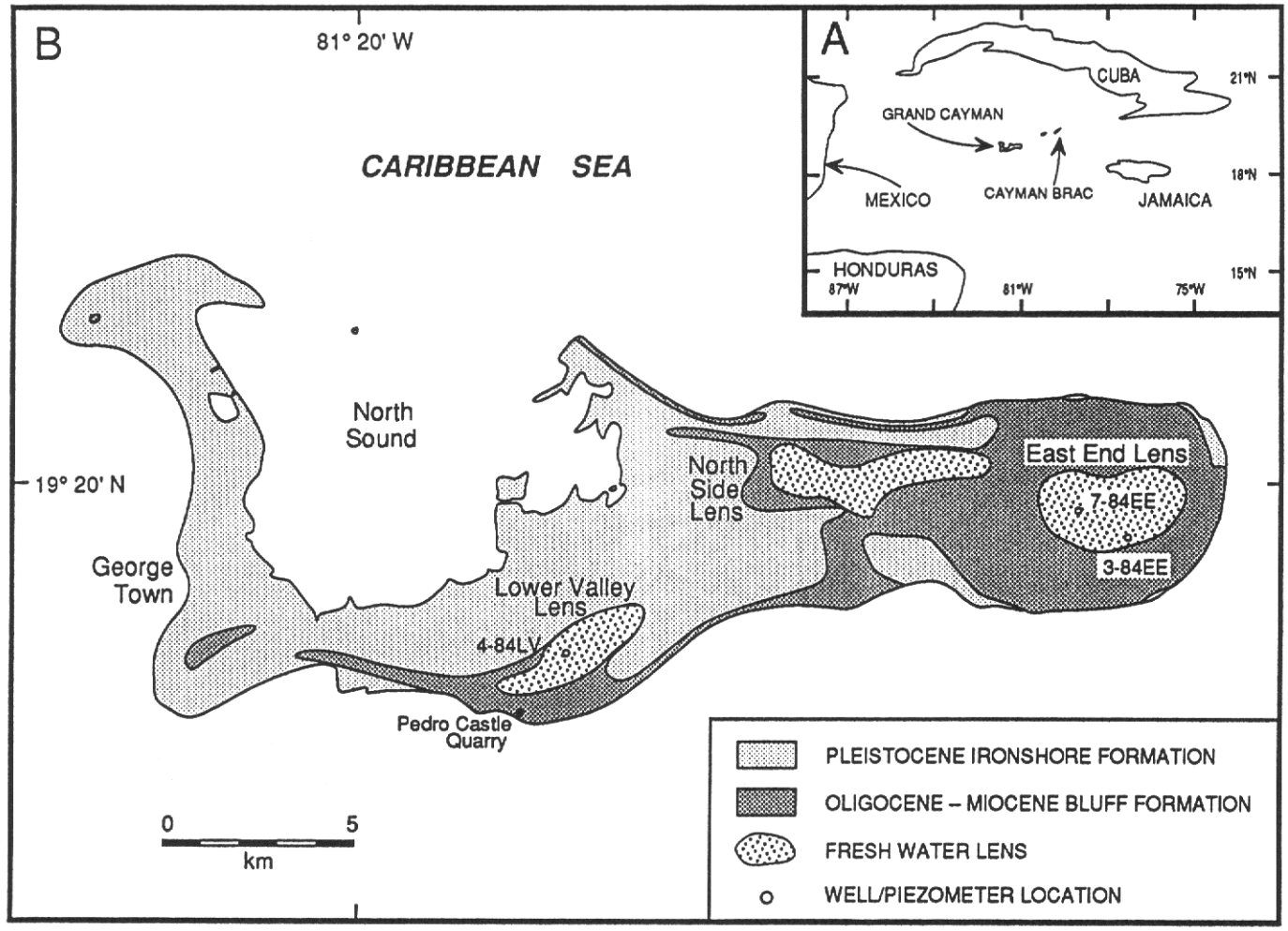

Fig. 1. (A) Geographic location of the Cayman Islands. (B) Hydrogeological setting of the fresh ground water occurrences on Grand Cayman and location of wells and piezometers cited in text.

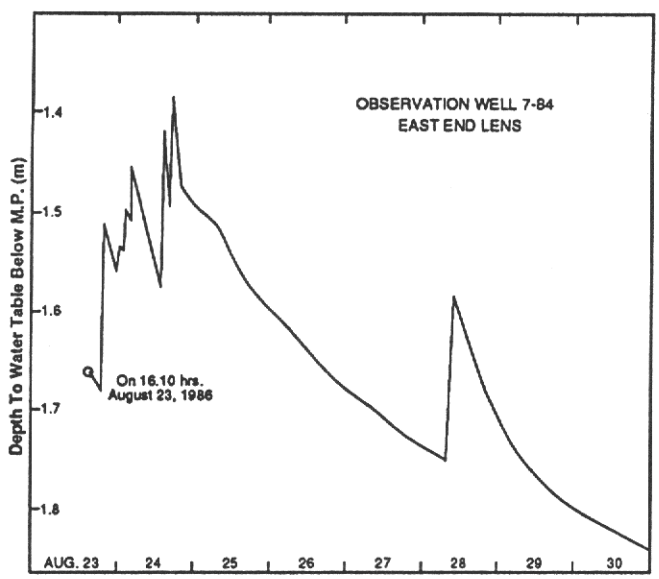

Fig. 2. Water table hydrograph of well 7-84EE showing rapid infiltration and discharge of rain water in response to rainfall events. M.P. is measuring point at top of the well casing.

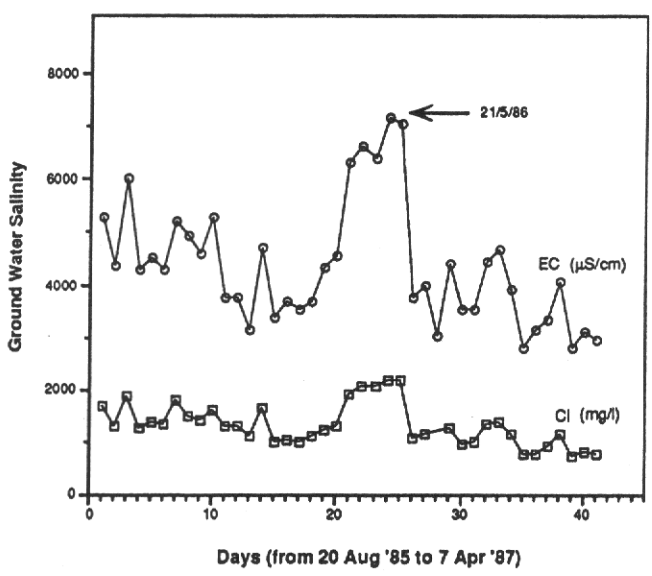

Fig. 3. Temporal variation of ground water salinity in the Lower Valley lens recorded by piezometer 4-84LV in stalled in the lightly brackish water zone.

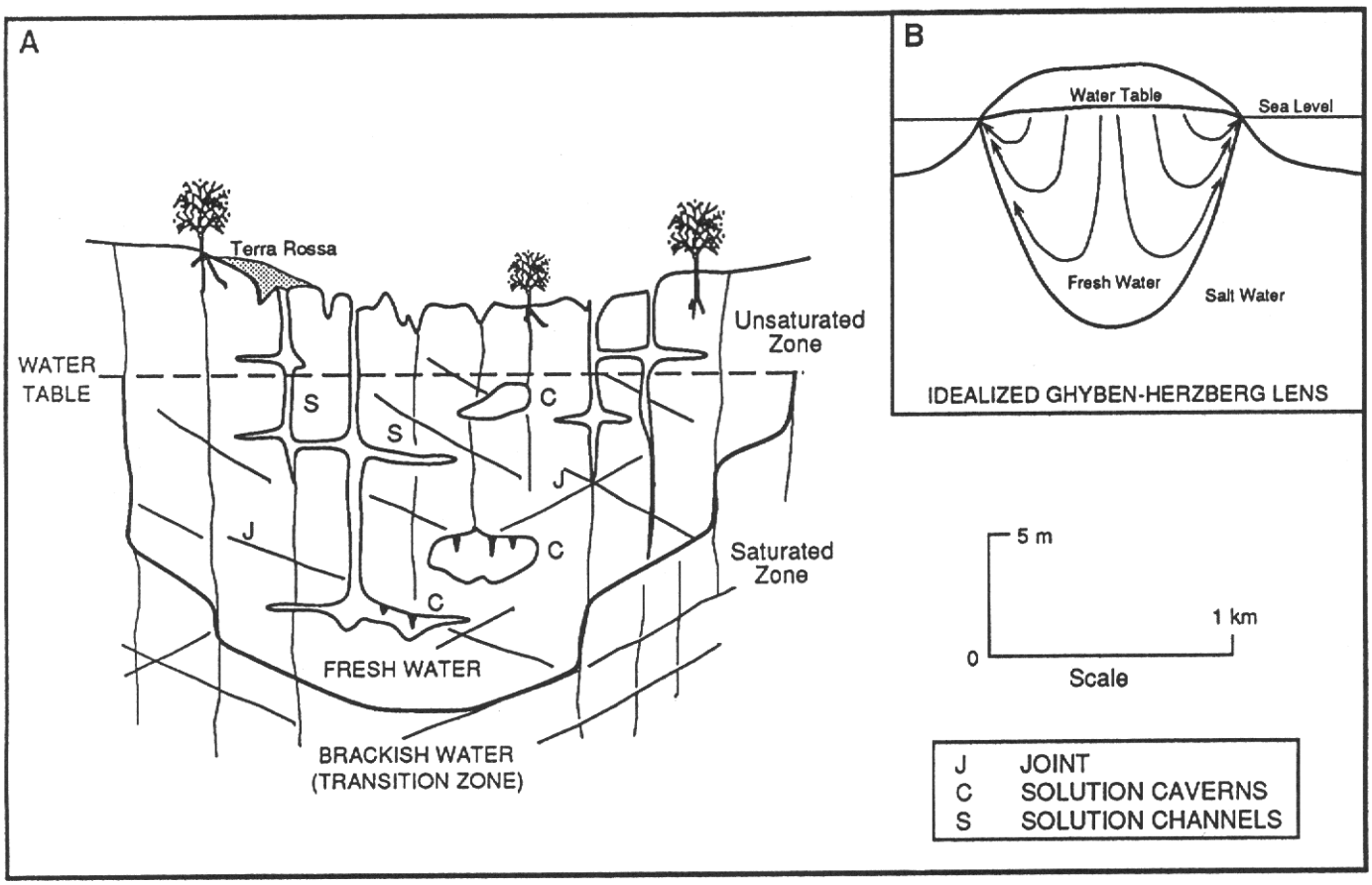

Fig. 4. (A) Schematic representation of joint and karst controlled lens configuration on Grand Cayman. (B) Idealized Ghyben-Herzberg lens.

absent because of the high infiltration rate of rain water. The high transmissivity of the aquifer, which results in limited storage of fresh water in the aquifer, is well exemplified by the low ground water table elevations (Fig. 5).

The sea around Grand Cayman generally experiences an average semi-diurnal tide range of 0.2 m and a seasonal fluctuation of about 0.4 m (Fig. 5). The ground water table fluctuates in response to the sea tides (Fig. 5) because the aquifers are hydraulically linked to the surrounding ocean. As a result, a thick transition zone of brackish water develops between the fresh and sea water (Fig. 4A) in response to tide generated hydrodynamic dispersion. A similar phenomenon occurs in the Bahamas (Mather and Buckley, 1973), Bermuda (Vacher, 1978), Enewetak (Wheatcraft and Buddemeier, 1981), and Majuro Atoll (Anthony et al., 1989).

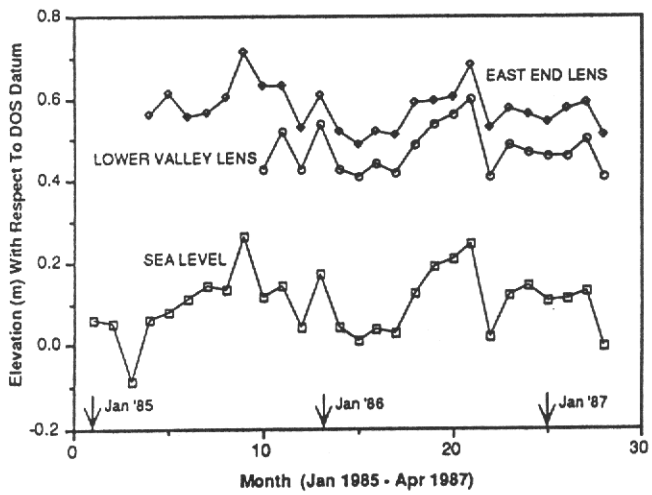

Fig. 5. Average monthly sea level around Grand Cayman and water table elevation of Lower Valley and East End Lens. DOS refers to Directorate Overseas Survey datum.

POROSITY STYLE

Dolostones of the Bluff Formation have variable porosity owing to the diversity of pore types. Most primary intergranular porosity was obliterated through pervasive dolomitization (Jones et al., 1984; Pleydell, 1987). Primary intergranular porosity does, however, occur in a rubble facies (rhodolite rudstone) on Cayman Brac and, locally, in skeletal grainstone which is composed of fragments of red algae and foraminifera. Most porosity was created by (1) preferential leaching of metastable carbonates prior to dolomitization, (2) jointing and fracturing, and (3) karsting. Tree root borings and microborings can be important in creating porosity in the surface and near-surface zones. Locally, secondary intracrystalline porosity formed by selective dissolution of the unstable zones of dolomite are common.

Skeletal Moldic Porosity

Preferential dissolution of original skeletal aragonite in the molluscs, gastropods, and corals was common in the Bluff Formation (Folk et al., 1973; Jones et al., 1984; Jones and Hunter, 1989). Conversely, skeletal components formed of high-magnesian calcite, such as red algae and most foraminifera, have been dolomitized and their textures preserved. Locally, up to 25% moldic porosity occurs in the dolostones.

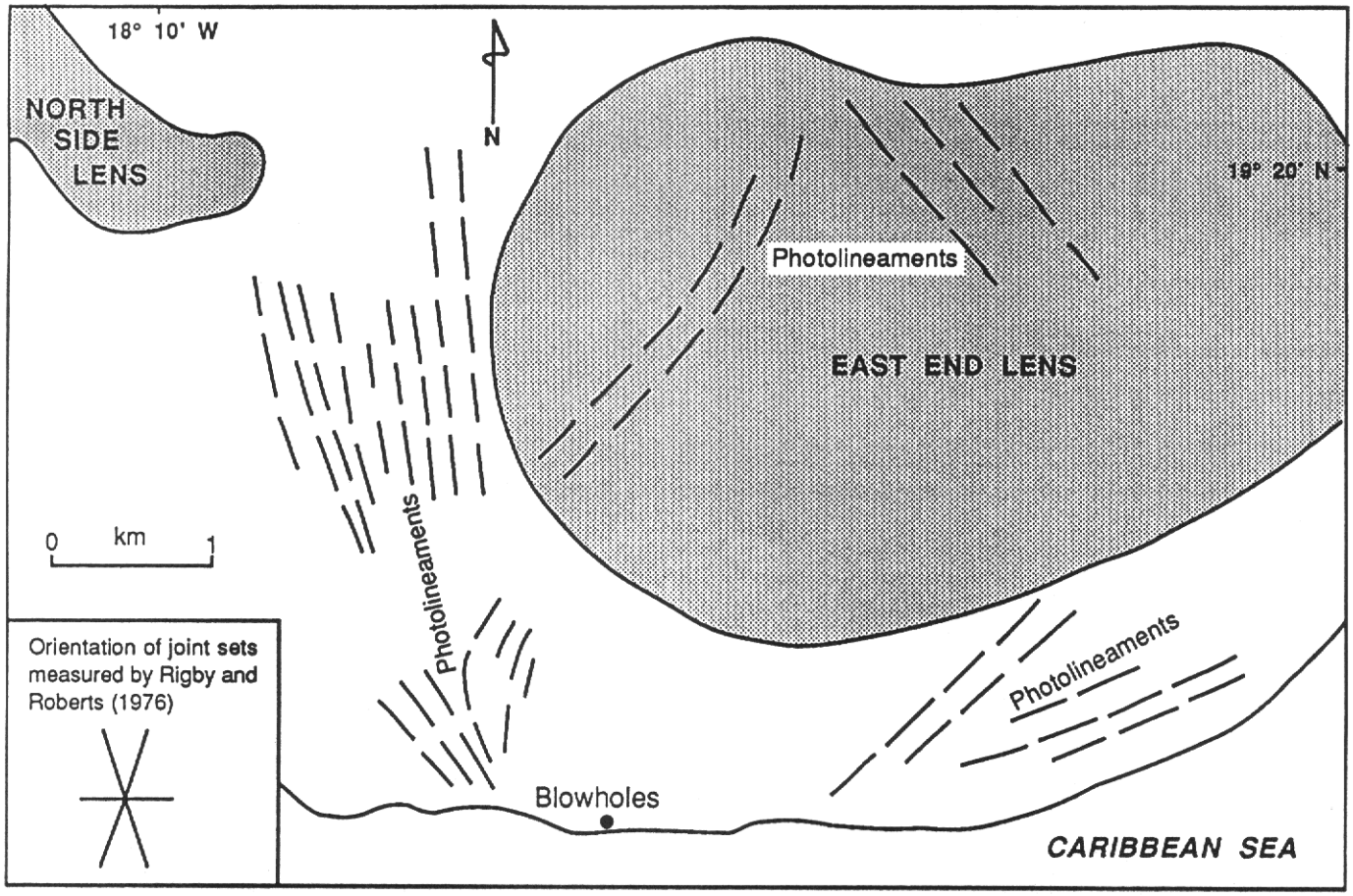

Fig. 6. Structural photolineaments near the East End lens on Grand Cayman. Inset shows joint directions determined by Rigby and Roberts (1976).

Fissures and Joints

Detailed joint measurement on the coastal exposures of the Bluff Formation on Grand Cayman showed three major joint sets trending at about 20°, 90° and 160° (Rigby and Roberts, 1976). Structural photolineaments, which are surface expressions of subsurface joints and fissures, are particularly pronounced on the eastern half of Grand Cayman where the Bluff Formation is exposed. Near the East End lens (Fig. 1B), two vertical conjugate photolineaments striking 030-040° and 175° (Fig. 6) are particularly well developed. Southward to the coast, besides the east-west trending joint set, two joint groups trending 050° and 160° are present (Fig. 6). Around the Lower Valley lens (Fig. 1B), dominant photolineaments, commonly indicated by the alignment of small ponds, trend at 020° and 150°.

Karst Porosity

Cave systems, preferentially developed along joints and at water table zones, are common in the dolostone of the Bluff Formation. At depth, extensive networks of solution passages and chambers (Fig. 4A) are commonly indicated by the sudden drop of drilling tools and the lack of cutting returns.

Root Moldic Porosity

Plant (trees, bushes and grasses) commonly root directly into the dolostones of the Bluff Formation and penetrate the rocks either through existing joints or by chemically excavating the substrate as they grow. Porosity in the upper 3 m can be as high as 50% due to the actions of plant roots.

Microborings

Microborings (generally <10 μm diameter), formed by the action of algae, fungi and bacteria are common in the surface zones of the Bluff Formation (Folk et al., 1973; Viles and Spencer, 1983; Jones, 1989). The density of microborings tends to be high around the tree roots because many of the micro-organisms are symbiotically associated with the plant root systems.

Hollow Dolomite Rhombs

Locally, the dolomite rhombs in the Bluff Formation have had their cores removed by selective dissolution (Jones et al., 1989). Such dissolution typically occurs in dolostones on weathered surfaces or joint surfaces.

CONDITIONS FOR POROSITY CREATION

Selective dissolution of the aragonitic skeletal materials reflects the thermodynamical instability of aragonite under earth surface conditions (Bathurst, 1975; Berner, 1981). Subaerial exposure of metastable carbonate sediments of the Bluff Formation undoubtedly occurred during the relative sea level drops in late Oligocene and late Miocene times.

Studies of Pleistocene limestones led Land (1970), Steinen and Matthews (1973), and Pingitore (1976) to conclude that dissolution of biogenic aragonite is more effective in the fresh water phreatic environment than in the vadose setting. It is possible, therefore, that dissolution of aragonitic skeletal components in the Bluff Formation may have occurred in a similar setting.

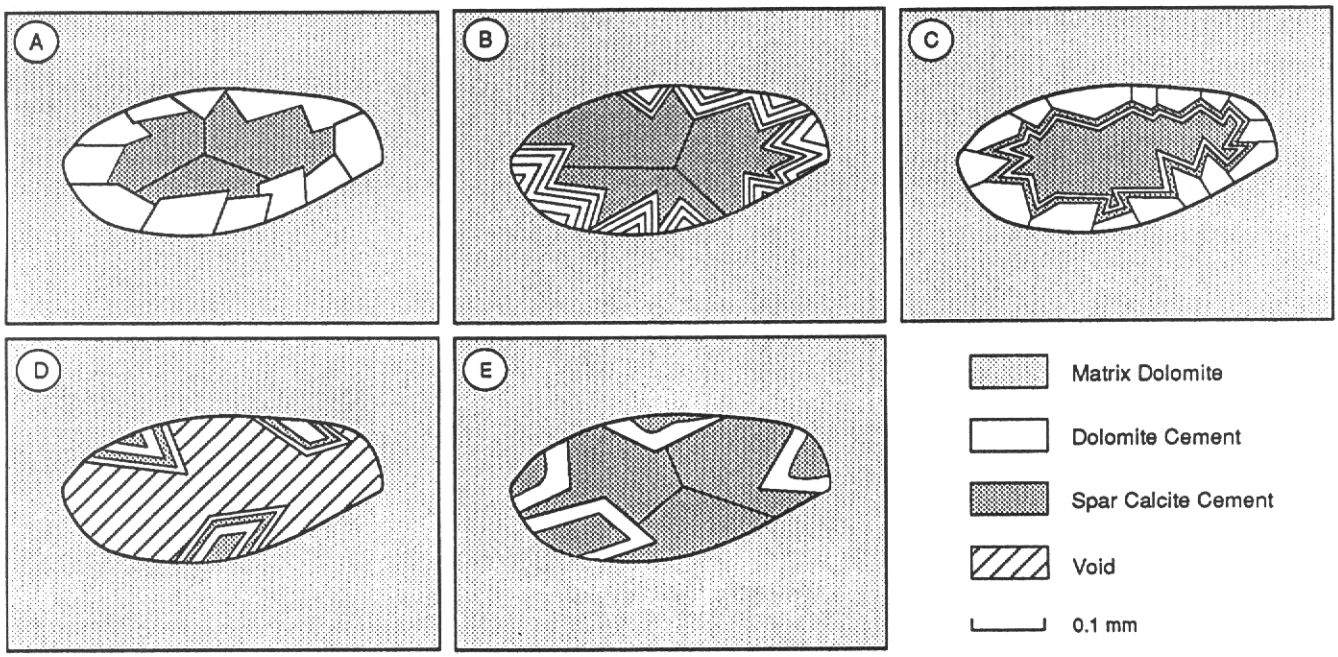

Fig. 7. Schematic diagram showing cement types in the Bluff Formation. (A) Clear euhedral dolomite and sparry calcite. (B) Zoned euhedral dolomite and sparry calcite. (C) Alternating bands of dolomite and calcite. (D) Intracrystalline zoning of dolomite and calcite. (E) Poikilotopic calcite-dolomite.

Joints and fissures are important in porosity creation because they provide avenues for fluid movement. Uniformity and intensity of the joint sets present in the Bluff Formation (Fig. 6) and the fact that the Cayman Islands are sited on the Cayman Ridge (Uchupi, 1975; MacDonald and Holcombe, 1978) suggest that the joints are probably related to past tectonism of the Cayman Trench. Differential enlargement of fissures by solution resulted in concentrated flow, which increased dissolution rates and further enlarged the incipient caverns and channels. This dissolution phenomenon leads to the development of permeable zones in the aquifer system.

On the Cayman Islands, there is clear evidence that caves were developed both pre- and post-dolomitization of the host rocks (Jones and Smith, 1988). Therefore, karsting in the Bluff Formation is a multiple phase phenomenon. The fact that the largest caves on Grand Cayman and Cayman Brac formed after dolomitization of the Bluff Formation suggests that climatic conditions, and density and openness of joints probably were more dominant in controlling the extent of karsting than lithology.

Biological control has been largely ignored by many workers in evaluating porosity distribution in carbonates. Extensive dissolution of spar calcite mediated by fungi was experimentally demonstrated by Jones and Pemberton (1987a, 1987b). More importantly, Jones and Pemberton (1987a) suggested that under the mediation of fungi, dissolution of calcite occurs via surface reaction controlled kinetic processes without the intervention of vast quantities of fluid. Besides being a source of CO_2 through root respiration, root borings also provide avenues for water flow.

Where ground water is in continual motion through pores, it dissolves and carries away soluble material, which in turn increases ground water circulation and the permeability in the rock. The zone of greatest permeability tends to develop in the zone of greatest circulation, which is commonly just below the water table (Thrailkill, 1968; Stringfield and Rapp, 1977; Esteban and Klappa, 1983; LeGrand, 1983). Rapid rain water recharge through open fractures can also cause significant undersaturation at the water table zone by introducing water of low salinity. Furthermore, the shallow water zone is most likely to receive CO_2 from the respiration of plant roots and organic decay.

In the brackish water transition zone which develops between fresh and sea water, Runnells (1969), Hanshaw et al. (1971), Badiozamani (1973), and Plummer (1975) suggested that undersaturation with respect to calcite occurs as a result of mixing. Stoessell et al. (1989) showed that aragonite is preferentially dissolving throughout the modern mixing zone along the Caribbean coast of the Yucatan Peninsula. Furthermore, Sanford and Konikow (1989) suggested that significant porosity development occurs when a large influx of fresh water occurs in the aquifers.

Jones and Smith (1988) suggested that mixing corrosion, which occurs in the mixing zone, was probably responsible for the development of most caves on Grand Cayman. A similar mechanism was proposed for the karst features formed on the Bahamas (Palmer, 1984; Mylroie, 1984) and the Yucatan Peninsula (Hanshaw and Back, 1980; Back et al., 1986). Ford (1988), however, argued that such mixing is physically infeasible unless the rock mass has very high effective porosity. Furthermore, on small islands like Grand Cayman, mixing corrosion is less effective because of the absence of large hinterland for fresh water recharge.

At the ground water discharge zone, permeability increases as a result of concentrated flow (Chidley and Lloyd, 1977; Lloyd, 1980). On Grand Cayman, there is no geological boundary in defining the base of the mixing zone; therefore, porosity enhancement is probably most favourable near the coast at the discharge zone where flow rate is high. Indeed, cave development on Grand Cayman tends to be locally extensive along the coast. Paleoclimatic conditions are equally important. The karsting and speleothemic deposits on Grand Cayman suggest that they did not develop under present day climatic regime, but probably developed in the past when the rainfall was much higher. Therefore, karstification on the Bluff Formation is predominantly controlled by sea level elevation and climatic conditions. Cave geometry is controlled by jointing and ground water flow regime.

CAVITY FILLS

Secondary pores, irrespective of their origin, were commonly filled or partly filled by multi-phase carbonate cements, flowstone, and internal sediments (Fig. 7; Jones et al., 1984; Jones and Smith, 1988).

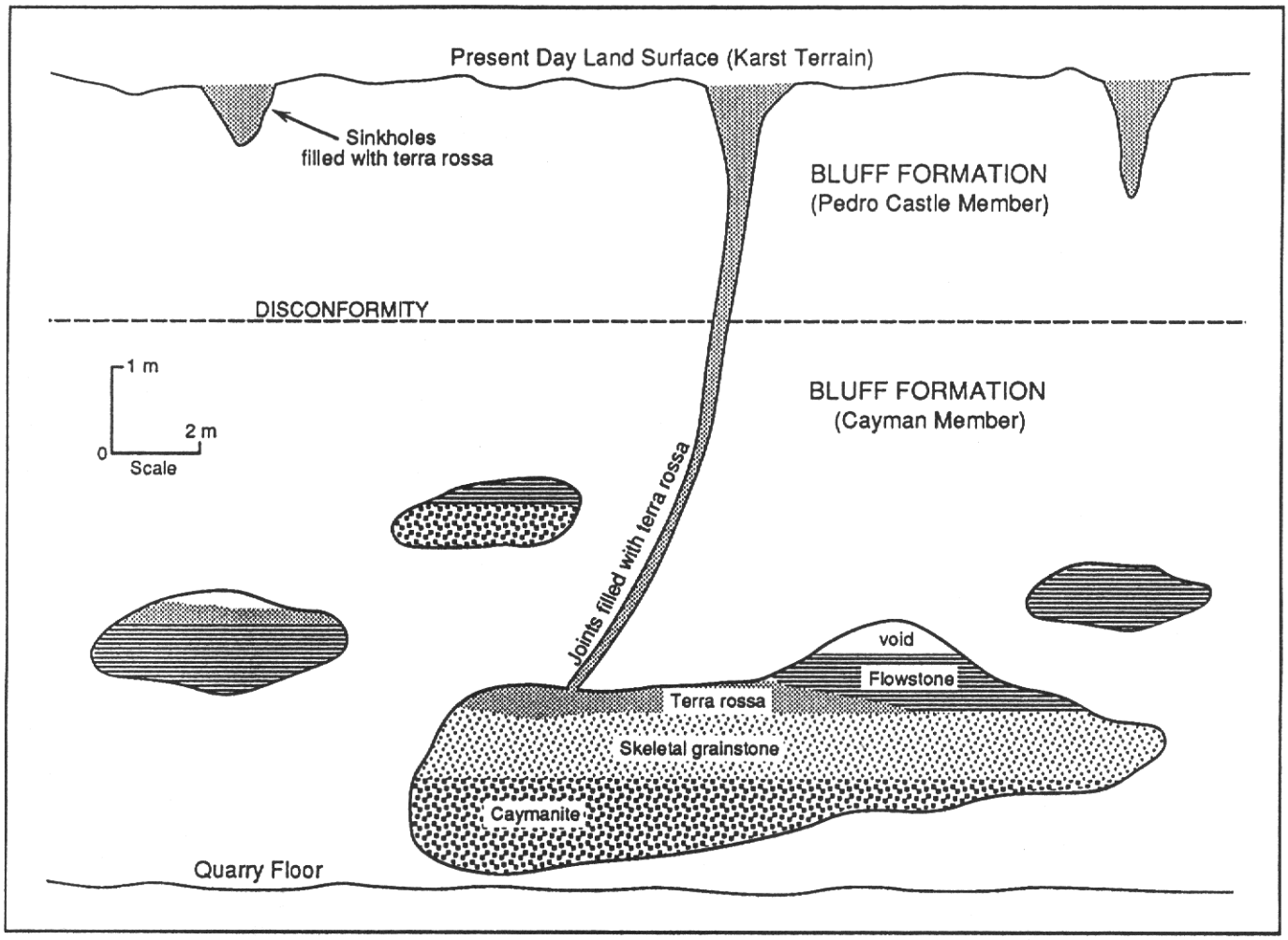

Fig. 8. Schematic diagram of quarry wall exposure at Pedro Castle Quarry (Fig. 1B) showing cave fills in the Cayman Member of the Bluff Formation.

Carbonate Precipitates

Euhedral, clear or zoned dolomite typically developed as the first phase of cement lining cavities (Figs. 7A, 7B). At least two generations of dolomite cement occur in some cavities. The first generation of dolomite cement precipitated prior to internal sedimentation whereas the second generation of dolomite cement formed on top of the internal sediments.

Precipitation of sparry calcite cements, which followed the dolomite cements, commonly occluded the cavities (Figs. 7A, 7B). This dolomite-calcite couplet, previously documented by Jones et al. (1984) in the Bluff Formation, also occurs in other dolomitic limestone sequences (e.g. Land, 1973; Kaldi and Gilman).

Alternating zones of dolomite and calcite occur in two forms. The first type of alternating zones (10 μm thick) that are laterally continuous from crystal to crystal (Fig. 7C). The second type of alternating zones occurs in a single crystal (Fig. 7D).

Poikilotopic calcite that encases dolomite cement and matrix dolomite produced fabrics (Jones et al., 1989) comparable to those considered indicative of dedolomite (e.g. Shearman et al., 1961; Evamy, 1967). The poikilotopic calcite-dolomite commonly associated with the zoned dolomite-calcite cements (Fig. 7E).

Flowstone commonly filled cavities, joints and caverns in the Bluff Formation (Fig. 8; Lockhart, 1986; Jones and Smith, 1988). Some caves are decorated with various forms of speleothems (Jones and Motyka, 1987; Jones and Smith, 1988; Jones and MacDonald, 1989).

Internal Sediments

Caymanite, formed of tightly interlocking anhedral microcrystalline dolomite, is a common cavity and cave fill in the Bluff Formation (Fig. 8). It is characterized by (1) white, orange/red and black colour bands, (2) geopetal texture, (3) cross bedding, and (4) cut and fill channels. Rare examples also contain foraminifera and gastropods. Dolomitized skeletal grainstone is commonly associated with caymanite (Fig. 8). The skeletal components are predominantly red algae and foraminifera.

Terra rossa in the Bluff Formation is formed of organic rich glaebules embedded in microcrystalline carbonate and clay matrix. However, it is not clear if the terra rossa is of residual or foreign origin. Terra rossa breccia, which has dolostone fragments embedded in the soil, is common in some cavities and open joints.

CONDITIONS FOR POROSITY DESTRUCTION

Carbonate Precipitation

Speciation calculations for ground waters from Grand Cayman indicate that almost all the fresh to saline waters are supersaturated with respect to calcite. Thus, according to thermodynamic

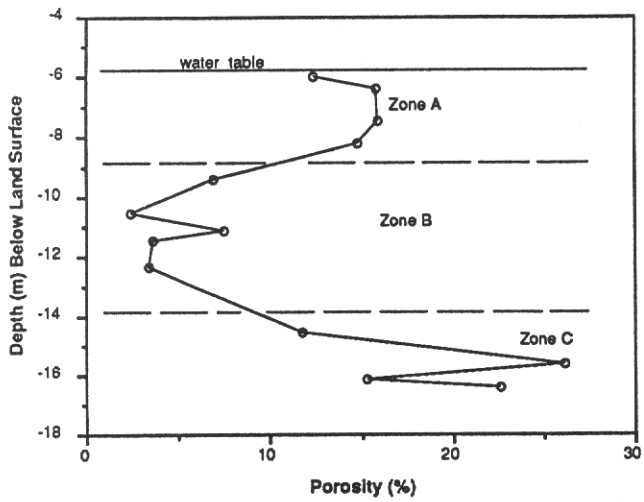

Fig. 9. Porosity distribution with depth shown by analysis of rock cores from well 3-84EE.

considerations, calcite precipitation should be common throughout all hydrochemical zones. Folk and Land (1975) suggested that sparry calcite precipitation occurs in meteoric waters or dilute subsurface waters with Mg/Ca ratios from 1:1 to 1:10. The common occurrence of calcite cement in present day fresh water zone also suggests that precipitation of sparry calcite probably occurs in water of low salinity.

Most waters from the dolostone aquifer of the Bluff Formation are supersaturated with respect to dolomite. Therefore, theoretically, the ground waters are also capable of precipitating dolomite. Dolomite cements may form in mixing zones (Folk and Land, 1975; Land 1985; Machel and Mountjoy, 1986; Hardie, 1987). The decrease in the content of dolomite cement as the last cement phase from the slightly brackish to saline water zones in the Bluff Formation also suggests that dolomite cement in the Bluff Formation probably formed in the brackish water zone.

The alternating growth of dolomite and calcite cement probably represents periods of ionic depletion followed by subsequent ionic replenishment of the pore solutions. During cement growth in the cavities, the degree of supersaturation of the pore solutions with respect to the precipitating mineral decreases. This decrease in ionic concentration may lead to the formation of another mineral variety or complete cessation of cement growth.

Dissolution of unstable dolomite zones in zoned dolomite crystals probably occurred during periodic influxes of CO_2-charged rain water, which is most effective at the water table zone or along joints. Furthermore, rain water recharge would have caused undersaturation of the ground water with respect to dolomite at the water table zone. Shallow ground waters on Grand Cayman are commonly supersaturated with respect to calcite and have a relatively low Mg/Ca ratio, which are most favourable for precipitating calcite that filled the leached zones and remaining cavity.

The precipitation of speleothemic calcite is typically regarded as an abiogenic process (e.g. White, 1976; Kendall and Broughton, 1978). Studies on Cayman speleothems by Jones and Motyka (1987) and Jones and MacDonald (1989), however, demonstrated that formation of speleothems may, to some extent, be biogenically controlled.

Internal Sedimentation

The presence of normal marine skeletal components (foraminifera and red algae) in the grainstone led Jones and Hunter (1989) to suggest that the skeletal sands were deposited during the early part of a marine transgression. The origin of caymanite, however, is less certain. Folk and McBride (1976) and Lockhart (1986) suggested that caymanite was formed from materials washed from swamps into the cavities and caverns via the well-developed joint system during seasonal storms. The presence of terra rossa at various stratigraphic levels suggests that the soils probably entered the cavities and caverns via the well developed joint and karst systems in a manner similar to the transport of caymanite (Fig. 8).

The multiple cycles of caymanite formation is best illustrated by the distinct laminations and cut and filled channels. The presence of (1) erosional features and cross-bedding, (2) large angular fragments, and (3) fragments probably removed from irregular projections on cavity walls suggests that sedimentation occurred under high-stage flow conditions.

The variation in grain size of sediments in the same layer indicates that the sediments were transported in steady turbulent flow in a manner suggested by Bridge (1981). Gales (1984) also suggested that finer sediment can be deposited simultaneously with the coarser sediment where flow expansion resulted in a sudden reduction in flow competence, such as at the exit to the phreatic zone. A similar mode of flow and transport was probably responsible for the caymanite sedimentation in the Bluff Formation. Cross-bedding in the caymanite further indicates high fluid flow regime during its deposition.

POROSITY DISTRIBUTION AND FLOW REGIME

Porosity distribution in cores from well 3-84EE (Fig. 1B) indicates three distinct porosity zones, herein termed A, B and C (Fig. 9). An examination of the rock cores shows that the porosity in zone A developed near the water table zone probably resulted from active ground water circulation at the water table. Active dissolution due to mixing corrosion and high hydraulic erosion is a characteristic of the shallow phreatic zone (Thrailkill,1968; Stringfield and Rapp, 1977; Esteban and Klappa,1983). The differences in porosity between zones B and C (Fig. 9) appears to be facies control. Zone C has a high content of leached corals whereas zone B has only scattered, leached mollusc fragments. This vertical variability of porosity in the Bluff Formation shows that ground water flow in the aquifer system is heterogeneous even over a short distance.

Parizek (1976), LaRiccia and Rauch (1977) and LeGrand (1979) demonstrated that wells penetrating fractures generally have high flow rates. On Grand Cayman, the joints, fissures, caverns and solution channels probably affected the ground water flow regime by: (i) providing a direct hydraulic connection between the aquifer and the surrounding ocean (Fig. 5), (ii) creating semi-confined conditions in an unconfined aquifer (Fig. 4A), (iii) providing avenues for mixing of water from different hydrochemical zones, (iv) allowing rapid recharge of rain water into the aquifer (Fig. 2), (v) defining the lens geometry as shown by the irregular lens geometry and sharp lens boundary (Figs. 1B, 4A), (vi) being responsible for the intrusion of the saline water which divides and prevents linkage of the North Side and East End lenses (Fig. 6), and (vii) facilitating leaching process by providing pathways for fluid flow.

RECORDS OF SEA LEVEL FLUCTUATIONS

In order to unravel the diagenetic history of the Bluff Formation, it is imperative to reconstruct the paleohydrogeology which controlled the diagenetic regime. Past tectonic activity caused differential uplift or down faulting of the Cayman Islands prior to the late Pleistocene (Stoddart, 1980; Woodroffe, 1988), and resulted in the development of joints and fissures (Rigby and Roberts, 1976).

For the Tertiary period, the most significant sea level fall of nearly 400 m took place in the late Oligocene (Vail et al., 1977). Olsson et al. (1980), however, argued that a rapid sea level drop of up to 150 m occurred in the early Oligocene. The major regression

near the end of the Miocene is well documented (Adams et al., 1977; Vail et al., 1977; Loutit and Keigwin, 1982; Haq et al., 1987). Jones and Hunter (1989) suggested that the stratigraphic record in the Bluff Formation is in agreement with the global pattern of sea level changes as postulated by Vail et al. (1977) and Haq et al. (1987). Thus, according to Jones and Hunter (1989), the Cayman Member of the Bluff Formation was subaerially exposed in late Oligocene and early Miocene times. Subsequent to transgression in Miocene times led to the deposition of the Pedro Castle Member. The entire sequence was exposed in late Miocene as a result of the late Miocene regression (Jones and Hunter, 1989).

Although the records of Pleistocene sea level fluctuation on the Cayman Islands are less complete than those on Barbados (e.g. Mesolella et al., 1969; Bender et al., 1973), there are several lines of evidence to suggest that the islands were subjected to fluctuating sea levels during the Quaternary. They include: (i) well defined wave cut notches on the north coast of Grand Cayman and around Cayman Bac (Fig. 1A) at about 6 m above present sea level (Woodroffe et al., 1983), which probably developed at the time when the Ironshore Formation (125,000 years old) was being deposited (Jones and Smith, 1988); (ii) wave-cut notch at about 2.5 m above present sea level on the southeastern coast of Grand Cayman (Woodroffe et al., 1983); (iii) two levels of caves along the cliff face on Cayman Brac (Fig. 1A) at about 18 m and 30 m above present sea level, probably related to past sea levels as suggested by their horizontal orientation; (iv) submerged wave cut notches around Grand Cayman at about 19 m below present sea level and possibly at about 150 m below present sea level (reported by pilots of the research submersible submarine); and (v) low marine terraces (six levels at 2 m, 4 m, 6 m, 8 m, 11 m and 15 m) above present sea level (Emery, 1981) and submerged terraces around Grand Cayman (Rigby and Roberts, 1976).

DISCUSSION

Available evidence suggests that the Bluff Formation has been subjected to more than one cycle of subaerial exposure since late Oligocene times because of sea level fluctuations. Precise dating of the different stages of karstification is difficult, because each stage of karst development further modified the inherited karst features. Stringfield et al. (1979) noted that in areas where paleokarst is not too deeply buried, it may be incorporated into the present circulation system such as the artesian aquifer of Tertiary age in southeastern Georgia and Florida. Thus, the present day hydrogeological regime on Grand Cayman is the end product of numerous past and present processes. It is also difficult to assess the depth of karstification in response to each sea level change because of the overlapping karst effect. Furthermore, changes in the surface and ground water drainage began as soon as the carbonate rocks were elevated above sea level and circulation was established.

In addition to the effect of past sea level high stands, the extensive networks of cave systems are probably related to solution features preferentially developed along joints and fractures in a manner suggested by Ford and Ewers (1978) and Ford (1988). Jointing on Grand Cayman is a multi-phase phenomenon and is one of the pre-requisite parameters for cave formation by providing avenues for fluid flow, and hence, carbonate dissolution. Joints of different attitudes near Blowholes (Fig. 6) contain diverse fills which are similar to those filling caves in the Cayman Member of the Bluff Formation (Fig. 8). This relationship suggests that jointing and karsting are closely related to one another. The karsting and speleothemic deposits on Grand Cayman also suggest that they did not develop under present day climatic regime, but were probably developed in the past when the rainfall was much higher.

The various high stands of sea level in the past suggest that there were different established ground water circulation systems. As a result, the rocks were subjected to various diagenetic regimes and fluids in response to emergence and/or submergence. The complex distribution of the diagenetic fabrics in individual cavities is an excellent indication of the heterogeneity of the Bluff Formation which results in variations of ground water chemistry in close proximity.

CONCLUSIONS

Integration of hydrogeological data, hydrochemical information and the geological evolution of Grand Cayman allows the following conclusions:

(1) ground water lens development is controlled by porosity and permeability distribution in the Bluff Formation,
(2) ground water chemistry is influenced by rain water recharge, evapotranspiration, and mixing effect.
(3) porosity creation processes include (i) leaching of aragonitic skeletal components, (ii) jointing, (iii) karsting, (iv) root boring, (v) microboring, and (vi) leaching of unstable zones in dolomite crystals,
(4) porosity destruction processes include (i) precipitation of carbonate cements and speleothemic calcite and (ii) deposition of internal sediments,
(5) the Bluff Formation has been subjected to numerous cycles of sea level changes since the deposition of the Cayman Member in Oligocene times,
(6) the rocks have been subjected to various diagenetic regimes in response to successive cycles of emergence and submergence, and
(7) the complex distribution of the diagenetic fabrics in the rocks is due to the variability of fluid chemistry in the joint and karst controlled aquifer.

ACKNOWLEDGEMENTS

We are indebted to the Water Authority of the Cayman Islands and the Natural Science and Engineering Research Council of Canada (grant A6090 to Jones) for the support of this study. Part of the expense for participating at the conference was provided by the Unversity of Alberta Alma Mater Fund and the Faculty of Graduate Studies and Research (to Ng).

REFERENCES

Adams, C.G., Benson, R.H., Kidd, R.B., Ryan, W.B.F. and Wright R.C., 1977, The Messinian salinity crisis and evidence of late Miocene eustatic changes in the world ocean: Nature, v. 269, p. 383-386.

Anthony, S.S., Peterson, F.L., MacKenzie, F.T. and Hamlin, S.N., 1989, Geohydrology of the Laura fresh water lens, Majuro atoll: A hydrogeochemical approach: Geol. Soc. Am. Bull. v. 101, p. 1066-1075.

Ayers, J.F. and Vacher, H.L., 1986, Hydrogeology of an atoll island: a conceptual model for detailed study of a Micronesian example: Ground Water, v. 24, p. 185-198.

Back, W., Hanshaw, B.B., Herman, J.S. and van Driel, J.N., 1986, Differential dissolution of a Pleistocene reef in the ground water mixing zone of central Yucatan, Mexico: Geol., v. 14, p. 137-140.

Badiozamani, K., 1973, The Dorag dolomitization model application to the Middle Ordovician of Wisconsin: J. Sed. Petrol. v. 43, p. 965-984.

Bathurst, R.G.C., 1975, Carbonate Sediments and Their Diagenes: (2nd ed.): Elsevier, N.Y., 658 p.

Bender, M.L., Taylor, F.T. and Matthews, R.K., 1973, Helium-Uranium dating of corals from Middle-Pleistocene Barbados reef tracts: Quat. Res., v. 3, p. 142-146.

Berner, R.A., 1981, Kinetics of weathering and diagenesis, in Lasaga, A.C. and Kirkpatrick, R.J. eds., Kinetics of Geochemical Processes: Mineral. Soc. Am., Rev. Mineral., v. 8, p. 111-134.

Bridge, J.S., 1981, Hydraulic interpretation of grain-size distribution using a physical model for bedload transport: J. Sed. Petrol., v. 51, 1109-1124.

Brunt, M.A., Giglioli, M.E.C., Mather, J.D., Piper, D.J.W. and Richards, H.G., 1973, The Pleistocene rocks of the Cayman Islands: Geol. Mag., v. 110, p. 209-221.

Chidley, T.R.E. and Lloyd, J.W., 1977, A mathematical model study of fresh-water lenses: Ground Water, v. 15, p. 215-222.

Emery, K.O., 1981, Low marine terraces of Grand Cayman Island: Estuar. Coast. Shelf Sci., v. 12, p. 569-578.

Esteban, M. and Klappa, C.F., 1983, Subaerial exposure, in Scholle, P.A., Bebout, D.G. and Moore, C.H. eds., Carbonate Depositional Environments: Am. Assoc. Petrol. Geol., Mem. 33, p. 1-54.

Evamy, B.D., 1967, Dedolomitization and the development of rhombohedral pores in limestones: J. Sed. Petrol., v. 37, p. 1204-1215.

Folk, R.L. and Land, L.S., 1975, Mg/Ca ratio and salinity: two controls over crystallization of dolomite: Bull. Am. Assoc. Petrol. Geol., v. 59, p. 60-68.

Folk, R.L. and McBride, E.F., 1976, The Caballos Novaculite revisited. Part. 1: Origin of Novaculite Members: J. Sed. Petrol., v. 46, p. 659-669.

Folk, R.L., Roberts, H.H. and Moore, C.H., 1973, Black phytokarst from Hell, Cayman Islands, British West Indies: Geol. Soc. Am. Bull., v. 84, p. 2351-2360.

Ford, D.C., 1988, Characteristics of dissolutional cave systems in carbonate rocks, in James, N.P. and Choquette, P.W. eds., Paleokarst: Springer-Verlag, N.Y., p. 25-57.

Ford, D.C. and Ewers, R.O., 1978, The development of limestone cave system in the dimensions of length and depth: Can. J. Earth Sci., v. 15, p. 1783-1798.

Gale, S.J., 1984, The hydraulics of conduit flow in carbonate aquifers: J. Hydrol., v. 70, p. 309-327.

Hanshaw, B.B. and Back, W., 1980, Chemical mass-wasting of the northern Yucatan Peninsula by groundwater dissolution: Geol., v. 8, p. 222-224.

Hanshaw, B.B., Back, W. and Deike, R.G., 1971, A geochemical hypothesis for dolomitization by groundwater: Econ. Geol., v. 66, p. 710-724.

Haq, B.U., Hardenbol, J. and Vail, P.R., 1987, Chronology of fluctuating sea level since the Triassic: Sci, v. 235, p. 1156-1167.

Hardie, L.A., 1987, Dolomitization: a critical view of some current views: J. Sed. Petrol., v. 57, p. 166-183.

Jones, B., 1989, The role of micro-organisms in phytokarst development on dolostones and limestones, Grand Cayman, British West Indies: Can. J. Earth Sci., v. 26, p. 2204-2213.

Herzberg, A., 1901, Die Wasserversorgung einiger Nordseebader: J. Gasbeleucht. Wasserversorg., v. 41, p. 815-819.

Jones, B. and Hunter, I.G., 1989, Oligocene-Miocene Bluff Formation on Grand Cayman: Carib. J. Sci., v. 25, p. 71-85.

Jones, B., Lockhart, E.B. and Squair, C., 1984, Phreatic and vadose cements in the Tertiary Bluff Formation of Grand Cayman Island, British West Indies. Bull. Can. Petrol. Geol., v. 32, p. 382-397.

Jones, B. and MacDonald, R.W., 1989, Micro-organisms and crystal fabrics in cave pisoliths from Grand Cayman, British West Indies: J. Sed. Petrol., v. 59, p. 387-396.

Jones, B. and Motyka, A., 1987, Biogenic structures and micrite in stalactites from Grand Cayman Island, British West Indies: Can. J. Earth Sci., v. 24, p. 1402-1411.

Jones, B. and Pemberton, S.G., 1987a, Experimental formation of spiky calcite through organically mediated dissolution: J. Sed. Petrol., v. 57, p. 687-694.

Jones, B. and Pemberton, S.G., 1987b, The role of fungi in the diagenetic alteration of spar calcite: Can. J. Earth Sci., v. 24, p. 903-914.

Jones, B., Pleydell, S.M., Ng, K.-C. and Longstaffe, F.J., 1989, Formation of poikilotopic calcite-dolomite fabrics in the Oligocene-Miocene Bluff Formation of Grand Cayman, British West Indies: Bull. Can. Petrol. Geol., v. 37, p. 255-265.

Jones, B. and Smith, D.S., 1988, Open and filled karst features on the Cayman Islands: implication for the recognition of paleokarst: Can. J. Earth Sci., v. 25, p. 1277-1291.

Kaldi, J. and Gidman, J. 1982. Early diagenetic dolomite cements: examples from the Permian Lower Magnesian Limestone of England and the Pleistocene carbonates of Bahamas: J. Sed. Petrol., v. 52, p. 1073-1085.

Kendall, A.C. and Broughton, P.L., 1978, Origin of fabrics in speleothems composed of columnar calcite crystals: J. Sed. Petrol., v. 48, p. 519-538.

Land, L.S., 1970, Phreatic versus vadose meteoric diagenesis of limestones: evidence from a fossil water table: Sedimentology, v. 14, p. 175-185.

Land, L.S., 1973, Contemporaneous dolomitization of Middle Pleistocene reefs by meteoric water, North Jamaica: Bull. Mar. Sci., v. 23, p. 64-92.

Land, L.S., 1985, The origin of massive dolomite: J. Geol. Educ., v. 33, p. 112-125.

LaRiccia, M.P. and Rauch, H.W., 1977, Water well productivity related to photolineaments in carbonates of Frederick Valley, Maryland, in Dilamarter, R.R. and Csallany, S.C. eds., Hydrologic Problems in Karst Regions: p. 228-234.

LeGrand, H.E., 1979, Evaluation techniques of fractured-rock hydrology: J. Hydrol., v. 43, p. 333-346.

LeGrand, H.E., 1983, Perspective on karst hydrology: J. Hydrol., v. 61, p. 343-355.

Lloyd, J.W., 1980, Problems of the quantitative assessment of fresh groundwater resources on small limestone islands, Proceedings of the Seminar on Small Islands Water Problems: Bridgetown, Barbados. U.N. and Commonwealth Sci Council, p. 337-351.

Lockhart, E.B., 1986, Nature and genesis of caymanite in the Oligocene-Miocene Bluff Formation of Grand Cayman Island, British West Indies: Unpublished M.Sc. thesis, University of Alberta, Edmonton, Alberta, 111 p.

Loutit, T.S. and Keigwin, L.D., 1982, Stable isotope evidence for late Miocene sea level fall in the Mediterranean region: Nature, v. 300, p. 163-166.

MacDonald, K.C. and Holcombe, T.L., 1978, Inversion of magnetic anomalies and sea-floor spreading in the Cayman Trough: Earth Planet. Sci. Lett., v. 40, p. 407-414.

Machel, H.-G. and Mountjoy, E.W., 1986, Chemistry and environ-

ments of dolomitization - a reappraisal: Earth Sci. Rev., v. 23, p. 175-222.

Mather, J.D., 1972, The geology of Grand Cayman and its control over the development of lenses of potable groundwater: Mem. VI Conf. Geol. Del Caribe - Margarita, Venezuela, p. 154-157.

Mather, J.D. and Buckley, D.K., 1973, Tidal fluctuations and groundwater conditions in the Bahamian archipelago: Trans. 2nd Inter. Conf. Groundwater, Palermo, Sicily, 7 p.

Matley, C.A., 1926, The geology of Cayman Islands (British West Indies) and their relation to the Bartlett Trough: J. Geol. Soc. London, v. 82, p. 352-387.

Mesolella, K.J., Matthews, R.K., Broecker, W.S. and Thurber, D.L., 1969, The astronomical theory of climatic change: Barbados data: J. Geol., v. 77, p. 250-274.

Mylroie, J.E., 1984, Hydrologic classification of caves and karst, in Lafleur, R.G. ed., Groundwater as a Geomorphic Agent: Binghampton Symp. in Geomorph., Inter. Ser., v. 13, p. 157-172.

Olsson, R.K., Miller, K.G. and Ungrady, R.E., 1980, Late Oligocene transgression of middle Atlantic coastal plain: Geol., v. 18, p. 549-554.

Palmer, J. 1984. Geomorphic interpretation of karst features, in Lafleur, R.G. ed., Groundwater as a Geomorphic Agent: Binghampton Symp. in Geomorph., Inter. Ser., v. 13, p. 173-209.

Parizek, R.R., 1976, On the nature and significance of fracture traces and lineaments in carbonate and other terranes, in Yevjevich, V. ed., Proceedings of the U.S.-Yugoslavian Symposium, Dubrovnik, June 1975, Karst Hydrology and Water Resources: Water Resources Publications, Fort Collins, Colorado, p. 3.1-3.62.

Pingitore, N.E., Jr., 1976, Vadose and phreatic diagenesis: Processes, products and their recognition in corals: J. Sed. Petrol., v. 46, p. 985-1006.

Pleydell, S.M., 1987, Aspects of diagenesis and ichnology in the Oligocene-Miocene Bluff Formation of Grand Cayman Island, British West Indies: Unpublished M.Sc. thesis, University of Alberta, Edmonton, Alberta, 205 p.

Plummer, L.N., 1975, Mixing of sea water with calcium carbonate ground water: Geol. Soc. Am., Mem 142, p. 219-236.

Rigby, J.K. and Roberts, H.H., 1976, Geology, reefs and marine communities of Grand Cayman Island, British West Indies: Brigham Young University, Geol. Stud. Spec. Publ. 4, 95 p.

Runnells, D.D., 1969, Diagenesis, chemical sediments, and the mixing of natural waters: J. Sed. Petrol., v. 39, p. 1188-1201.

Sanford, W.E. and Konikow, L.F., 1989, Porosity development in coastal carbonate aquifers: Geol., v. 17, p. 249-252.

Shearman, D.J., Khouri, J. and Tahas, S., 1961, On the replacement of dolomite by calcite in some Mesozoic limestones from the French Jura: Proc. Geol. Assoc. London, v. 12, p. 1-12.

Steinen, R.P. and Matthews, R.K., 1973, Phreatic vs. vadose diagenesis: stratigraphy and mineralogy of a cored bore hole on Barbados, West Indies: J. Sed. Petrol., v. 43, p. 1012-1020.

Stoddart, D.R., 1980, Geology and geomorphology of Little Cayman, Atoll Res. Bull., v. 241, p. 11-16.

Stoessell, R.K., Ward, W.C., Ford, B.H. and Schuffert, J.D., 1989, Water chemistry and $CaCO_3$ dissolution in the saline part of an open-flow mixing zone, coastal Yucatan Peninsula, Mexico: Geol. Soc. Am. Bull., v. 101, p. 159-169.

Stringfield, V.T. and Rapp, J.R., 1977, Progress of knowledge of hydrology of carbonate rock terranes - a review, in Dilamarter, R.R. and Csallany, S.C. eds., Hydrologic Problems in Karst Regions: p. 1-9.

Stringfield, V.T., Rapp, J.R. and Anders, R.B., 1979, Effects of karst and geologic structure on the circulation of water and permeability in carbonate aquifers, J. Hydrol., v. 43, p. 313-332.

Thrailkill, J., 1968, Chemical and hydrologic factors in the excavation of limestone caves, Geol. Soc. Am. Bull., v. 79, p. 19-46.

Uchupi, E., 1975, Physiography of the Gulf of Mexico and Caribbean Sea, in Naim, A.E.M. and Stehli, F.G. eds., The Ocean Basins and Margins, 3, The Gulf of Mexico and the Caribbean: Plenum Publications, N.Y., p. 1-64.

Vacher, H.L., 1978, Hydrogeology of Bermuda - significance of an across-the-island variation in permeability, J. Hydrol., v. 39, p. 207-226.

Vail, P.R., Mitchum, R.M., Jr. and Thompson, S. III., 1977, Relative changes of sea level from coastal onlap, in Payton, C.E., ed., Seismic Stratigraphy - Application to Hydrocarbon Exploration: Am. Assoc. Petrol. Geol., Mem. 26, p. 83-98.

Vaughan, T.W., 1926, Species of Lepidocyclina and Carpentaria from the Cayman Islands and their significance: Geol. Mag., v. 82, p. 388-400.

Viles, H.A. and Spencer, T., 1986, 'Phytokarst', blue green algae and limestone weathering, in Paterson, K. and Sweeting, M.M., eds., New Direction in Karst: Proceedings of the Anglo-French Karst Symp., p. 115-140.

Ward, W.C. and Halley, R.B., 1985, Dolomitization in a mixing zone of near seawater composition, Late Pleistocene, northeastern Yucatan Peninsula: J. Sed. Petrol., v. 55, p. 407-420.

Wheatcraft, S.W. and Buddemeier, R.W., 1981, Atoll island hydrology: Ground Water, v. 19, p. 311-320.

White, W.B., 1976, Cave minerals and speleothems, in Ford, T.D. and Cullingford, C.M.D., eds., The Science of Speleology: Acad. Press, N.Y., p. 267-327.

Woodroffe, C.D., 1988, Vertical movement of isolated oceanic islands at plate margin: evidence from emergent reefs in Tonga (Pacific Ocean), Cayman Islands (Caribbean Sea) and Christmas Islands (Indian Ocean): Z. Geomorph. N.F., v. 69, p. 17-37.

Woodroffe, C.D., Stoddart, D.R., Harmon, R.S. and Spencer, T., 1983, Coastal morphology and late Quaternary History, Cayman Islands, West Indies: Quat. Res., v. 19, p. 64-84.

GEOLOGICAL EVOLUTION OF THE OLIGOCENE-MIOCENE BLUFF FORMATION, GRAND CAYMAN

Brian Jones, Ian G. Hunter, and Kwok-Choi Ng
Department of Geology, University of Alberta,
Edmonton, Alberta, T6G 2E3, Canada

ABSTRACT

The core of Grand Cayman, like the other Cayman Islands, is formed of dolostones which belong to the Bluff Formation. On Grand Cayman a major disconformity divides it into the lower Cayman Member and the upper Pedro Castle Member.

The Cayman Member is formed of hard, massive, white, microcrystalline dolostone that contains abundant massive and branching corals, bivalves, gastropods, foraminifera, and red algae. This member has high porosity because of (1) leaching of fossils that originally had aragonitic skeletons and (2) dissolution of bedrock associated with karst development. Many of the fossil molds and caves have been partly or totally filled with caymanite (red, white, and black laminated dolostone), fossiliferous grainstone, terra rossa, and/or flowstone.

The disconformity separating the Cayman and Pedro Castle members is a distinct planar surface that was bored by sponges, worms, and bivalves and locally encrusted by red algae. Sedimentological and diagenetic evidence suggest that the Cayman Member was subaerially exposed and subjected to karst development prior to deposition of the Pedro Castle Member. Corals in the upper part of the Cayman Member suggest that it is of early late Oligocene age whereas those in the Pedro Castle Member suggest a middle Miocene age.

The Pedro Castle Member is formed of relatively soft cream to white coloured dolostones that are characterized by abundant foraminifera, rhodolites, and free-living corals. Although porosity is high because of leaching of the corals, there is no evidence of dissolution associated with karst development. Only small amounts of white caymanite are present in a few of the coral molds. Multicolored caymanite fills some of the westward dipping joints that occur on the south coast between Pedro Castle and Spotts Bay. Although terra rossa occurs in some cavities, no fossiliferous grainstone or flowstone has been found.

Petrographic and geochemical evidence suggest that the original limestones of the Bluff Formation underwent only one phase of pervasive dolomitization. $^{87}Sr/^{86}Sr$ isotope ratios suggest that the dolomitization occurred 2 to 5 million years ago.

INTRODUCTION

Matley (1926) originally named the Bluff Limestone for poorly bedded, white to cream coloured, hard, microcrystalline, porous carbonates that formed the core of each of the Cayman Islands (Fig. 1). Although these carbonates have been called limestones (e.g. Mather, 1972; Brunt et al., 1973; Bugg and Lloyd, 1976; Rigby and Roberts, 1976; Stoddart, 1980; Woodroffe et al., 1980; Emery, 1981; Woodroffe, 1981; Woodroffe et al., 1983; Spencer, 1985) recent studies have shown that they are largely dolostone (e.g. Jones et al., 1984; Pleydell, 1987; Pleydell and Jones, 1988; Pleydell et al., in press). Areas of calcareous dolostone or dolomitic limestone are the product of dedolomitization (Jones et al., 1989). Following Jones and Hunter (1989) these strata are referred to as the Bluff Formation because this removes the lithologic connotation associated with the use of the term Bluff Limestone.

The Bluff Formation crops out on the eastern part of Grand Cayman, along a ridge on the southwest coast, and in small outliers at Hell and south of George Town (Fig. 1B). Information on the stratigraphy and sedimentology of the Bluff Formation comes from scattered coastal outcrops and quarries. A quarry near Pedro Castle (Figs. 1B, 2) contains the type section of the Cayman and Pedro Castle members as designated by Jones and Hunter (1989). There, the members are well exposed along with the disconformity which separates them (Fig. 2).

THE CAYMAN MEMBER

Distribution

The Cayman Member forms most of the Bluff Formation which crops out on Grand Cayman (Fig. 1B) and all of the Bluff Formation on Cayman Brac (Fig. 1C). Preliminary field studies on Little Cayman suggest that it forms all of the Bluff Formation on that island.

Lithology

At its type section in Pedro Castle Quarry, the Cayman Member is formed of two units which Jones and Hunter (1989) designated I and II (Fig. 2A). Unit I, 3 m thick, is a microcrystalline, hard, white dolostone that was originally a packstone to grainstone. Colonial corals (e.g. Montastrea, Leptoceris, Agathiphyllia, Favia, Diploastrea crassolamellata (Duncan, 1863), Diploria), branching corals (e.g. Stylophora and Porites), gastropods, and rare bivalves occur throughout unit I (Fig. 2A). Many corals were encrusted by red algae. Molds of corals, gastropods, and bivalves contain casts of borings (e.g. Entobia, Trypanites and Uniglobites) such as those described by Pleydell (1987) and Pleydell and Jones (1988). The dolomitized allochems include foraminifera (primarily miliolids), fragments of red algae, Halimeda, and echinoid plates and spines. Many echinoid fragments were enlarged by syntaxial overgrowths.

Porosity (up to 25%) and permeability are high in unit I because of leaching of the corals, gastropods, and bivalves. Most pores and cavities in unit I are lined with two types of euhedral dolomite cements (Fig. 2B); type 1 being an inclusion-free, limpid dolomite whereas type 2 is a zoned dolomite (cf. Jones et al., 1984). Many cavities are filled or partly filled with laminated, white caymanite and more rarely red and black caymanite (Fig. 2B).

Filled cavities and caves occur in unit I (Figs. 2A, 2B). Prior to blasting in late 1984 or early 1985, the southwest wall of Pedro Castle Quarry, provided a section through a cave that was 22 m long and 4.5 m high (Jones and Smith, 1988). That cave was filled with caymanite and dolomitized skeletal sands (predominantly foraminifera) overlain by undolomitized flowstone and terra rossa (Lockhart, 1986; Jones and Smith, 1988). This was probably part of a larger cave system.

Unit II (1.75 m thick), formed of white microcrystalline dolostone, contains abundant branching corals (Stylophora and Porites), rare colonial corals, bivalves, gastropods, rare complete echinoids, and poorly preserved foraminifera (Fig. 2A). The associated sediment was originally a mudstone to wackestone. This unit probably represent thickets of Stylophora and Porites that promoted deposition of fine grained sediment by baffling currents.

Unit II, like unit I, has high porosity because the corals, gastropods, and bivalves were leached. Casts of borings occur in most corals. Pores and cavities are lined with dolomite cements that are similar to those in unit 1. Many cavities are filled or partly

Larue, D.K., and Draper, G. (eds.),
Transactions of the 12th Caribbean Geological Conference, St. Croix, U.S.V.I., Miami Geological Society, P.O. Box 431552, South Miami, FL 33243, U.S.A

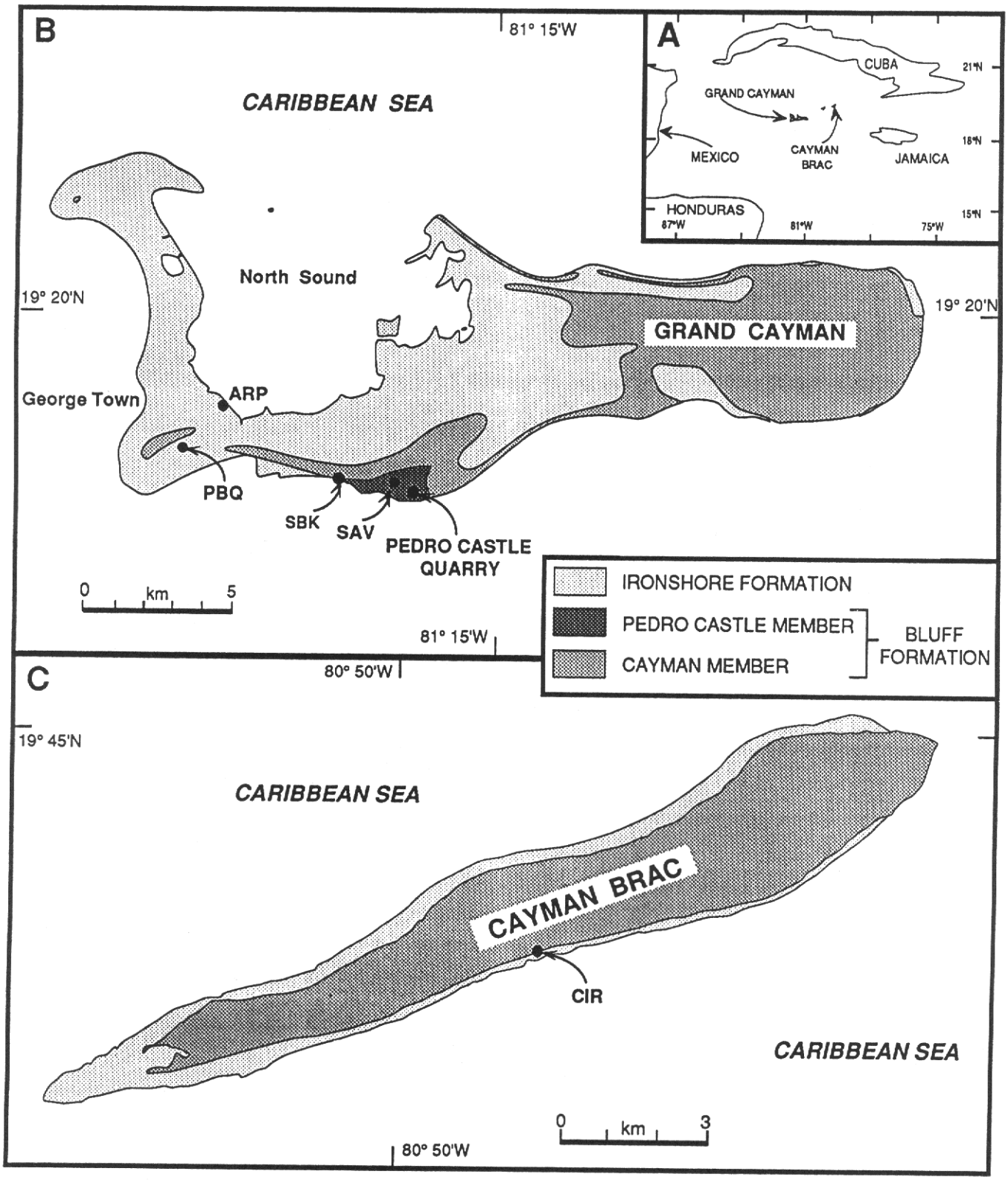

Figure 1. (A) Map of central Caribbean showing positions of Grand Cayman and Cayman Brac. Sketch maps of (B) Grand Cayman and (C) Cayman Brac showing the distribution of the Cayman and Pedro Castle members of the Bluff Formation and Ironshore Formation. ARP = Airport locality; PBQ = Paul Bodden's Quarry; SAV= Savannah; SBK = Spotts Bay; CIR = Cross-island Road

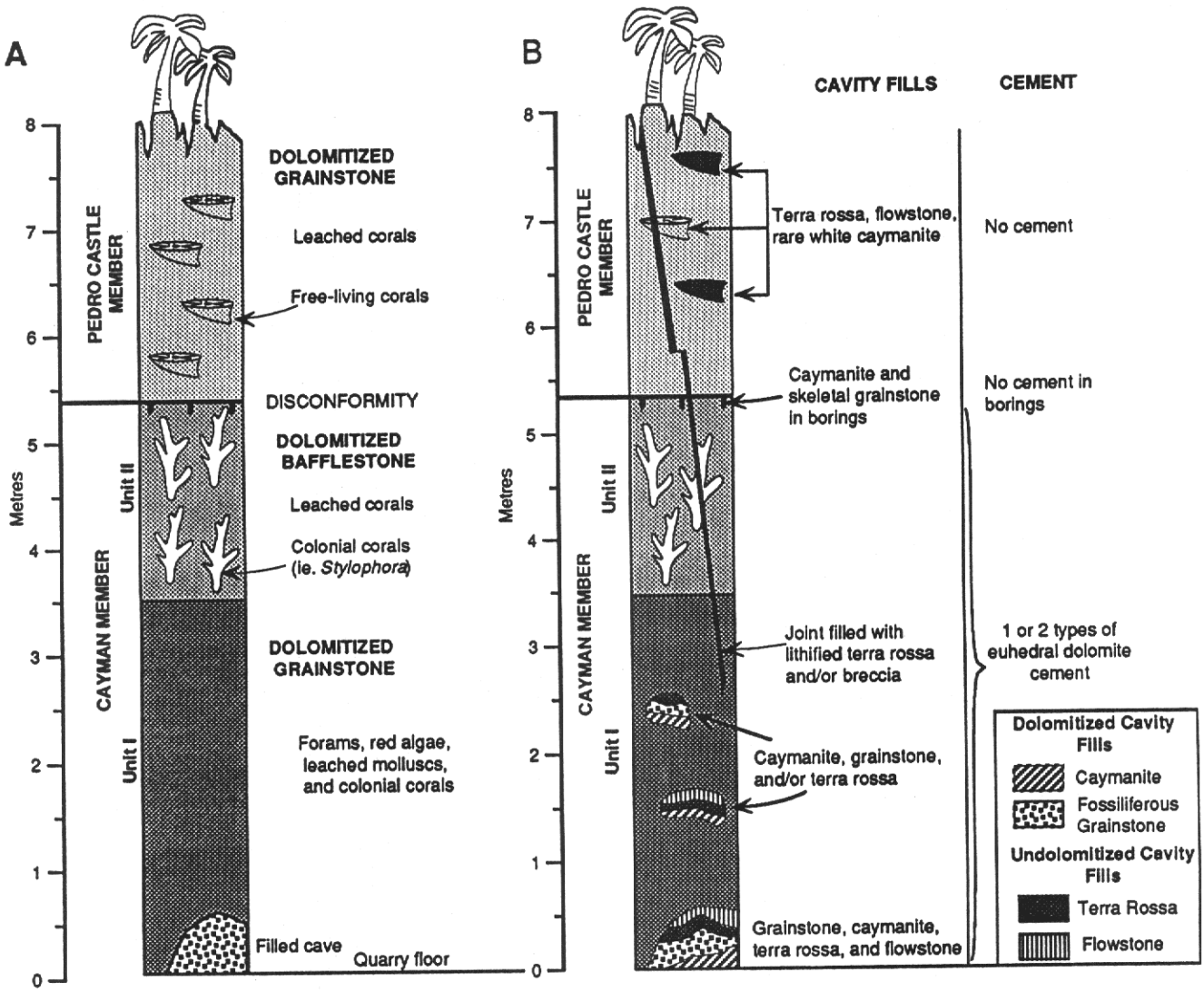

Figure 2. (A) Lithologies and faunal elements, and (B) diagenetic features in the type section of the Bluff Formation in the Pedro Castle Quarry as designated by Jones and Hunter (1989).

filled with laminated, white caymanite, and more rarely red and black caymanite.

Age

Dolostones of the Cayman Member on Cayman Brac contain benthic foraminifera which Vaughan (1926) considered to be of late Oligocene age and correlative with the Antigua Formation on Antigua (Fig. 3). Jones and Hunter (1989), based in part on the coral fauna in the Cayman Member, concluded that it was probably of early late Oligocene age.

THE PEDRO CASTLE MEMBER

Distribution

Besides the type section in Pedro Castle Quarry, the Pedro Castle Member crops out along the south coast between Pedro Castle and Spotts Bay (SBK on Fig. 1). It has also been found in house excavations around Savannah (SAV on Fig. 1) and in the southeast corner of the airport at George Town (ARP on Fig. 1). The former now has houses built on them, whereas the latter was excavated and material removed during drainage work on the airport.

Lithology

The Pedro Castle Member (Fig. 2A), 2.5 m thick in Pedro Castle Quarry, is formed of off-white to cream coloured, relatively soft (compared to dolostones in the Cayman Member), rubbly weathering dolostone that contains numerous large free-living corals such as Trachyphyllia, Thysanus, Teliophyllia, and Antillocyathus. Foraminifera (mostly miliolids), rare fragments of red algae, rare colonial corals, echinoid fragments that lack syntaxial overgrowths, and bivalves also occur. Rhodolites, up to 5 cm in diameter, are common in the basal part of the member. Allochem preservation is poorer than in the Cayman Member. Entobia and Trypanites casts occur in some corals molds.

Porosity is high in the Pedro Castle Member because the corals, gastropods, and bivalves have been leached. Some fossil molds are lined, partly filled or completely filled with unconsolidated terra rossa (Fig. 2B). The pores or cavities in this member are not lined with dolomite cements. White caymanite and/or

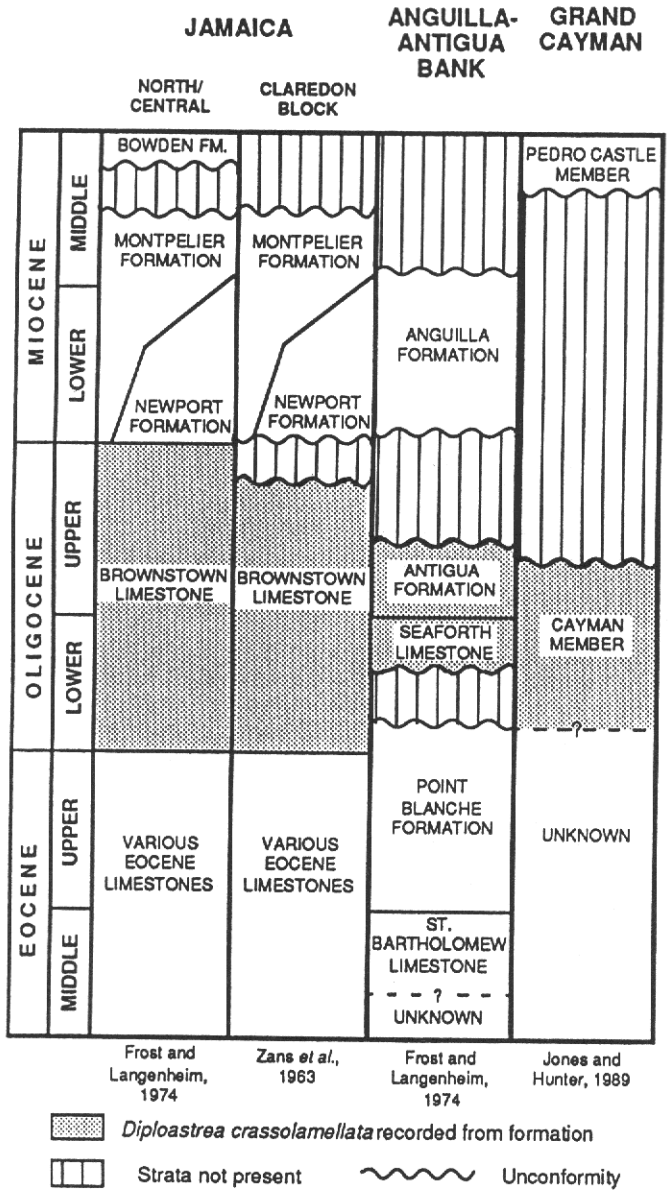

Figure 3. Suggested correlation of the Bluff Formation of Grand Cayman with other Oligocene-Miocene successions on Jamaica and theAnguilla-Antigua Bank.

grainstone are rare, being found in only a few of the hundreds of cavities examined. No red or black caymanite has been found in cavities in this member. On the south coast between Pedro Castle Quarry and Spotts Bay, however, some of the westward dipping joints are filled with white, red, and black caymanite.

Age

Jones and Hunter (1989) suggested that the Pedro Castle Member was of middle Miocene age (Fig. 3) because it contains a coral fauna that (1) is significantly different from that in the underlying Cayman Member, (2) includes the same corals as those from the Bluff Formation around Bodden Town which Matley (1926) considered to be of Miocene age, and (3) is dominated by large free-living corals which are typical of the Miocene in the West Indies (e.g. Frost and Langenheim, 1974; Frost, 1977, p. 96; Vaughan and Hoffmeister, 1926; Vaughan, 1919, p. 212-213).

COMPARISON OF THE CAYMAN AND PEDRO CASTLE MEMBERS

The Cayman Member is distinguished from the Pedro Castle Member because (1) it is massive and hard rather than rubbly and relatively soft (Fig. 4), (2) it is off-white to light grey in colour rather than white to cream in colour (Fig. 4), (3) it contains branching and massive corals rather than large free-living corals (Figs. 2A, 2B, 4), and (4) its cavities contain a wide variety of cements (Fig. 5). In addition, multicoloured caymanite and coarse, dolomitized skeletal grainstone, common in cavities in the Cayman Member are rare in cavities in the Pedro Castle Member (Fig. 2B). Multicolored caymanite does, however, occur in the westward dipping joints that locally cut the Pedro Castle Member.

DISCONFORMITY BETWEEN THE CAYMAN AND PEDRO CASTLE MEMBERS

In the Pedro Castle Quarry, the contact between the Cayman Member and Pedro Castle Member is a sharply defined disconformity (Figs. 2A, 2B) that contrasts with the vaguely defined bedding that is the norm in the Bluff Formation. The disconformity dips 2° to the northwest in the Pedro Castle Quarry (Jones and Hunter, 1989). Entobia, Uniglobites, Trypanites and Gastrochaenolites with their apertures at the disconformity, penetrate into the Cayman Member. These borings, which were probably produced by sponges, worms, and bivalves, are like those which occur in many of the corals in the Bluff Formation (e.g. Pleydell, 1987; Pleydell and Jones, 1988). Such borings could only exist if the upper surface of the Cayman Member was lithified prior to deposition of the overlying Pedro Castle Member.

All borings are filled or partly filled with white, laminated caymanite that is identical to that in cavities in the Cayman Member (Fig. 2B). Partly filled borings display a geopetal fabric with the upper surface parallel to the disconformity. Skeletal sands in the borings contain well preserved foraminifera (miliolids and rare Lepidocyclina) and fragments of red algae. Locally, the disconformity surface is encrusted by red algae.

Determining the time period represented by the disconformity between the Cayman and Pedro Castle members is difficult because of the uncertainty regarding the age of the Pedro Castle Member (Jones and Hunter, 1989). Nevertheless, consideration of available evidence suggests that it records a time span of 13 to 14 million years (Jones and Hunter, 1989). A time gap of this magnitude is consistent with the suggestion that the rocks of the Cayman Member underwent considerable diagenetic modification prior to deposition of the Pedro Castle Member.

DIAGENETIC FABRICS IN THE CAYMAN AND PEDRO CASTLE MEMBERS

The Cayman and Pedro Castle members both exhibit a complex array of diagenetic fabrics, including those caused by pervasive dolomitization. Petrographic and geochemical (C, O, and Sr isotopes - Pleydell et al., in press) analyses did not reveal any significant differences between the dolostone of the two members. These data may indicate that the rocks of the Cayman and Pedro Castle members underwent only one phase of dolomitization (Jones et al., 1984; Pleydell, 1987; Jones and Hunter, 1989). Alternatively, the rocks may have been subjected to more than one phase of dolomitization but retained petrographic and geochemical signatures of only the last phase. The lack of dolomite in the overlying Ironshore Formation means that dolomitization of the Bluff Formation must have been completed prior to deposition of that formation approximately 125,000 years ago (Jones et al., 1984; Pleydell, 1987; Jones and Hunter, 1989).

The Bluff Formation on Grand Cayman has undergone a complex paragenetic sequence (Fig. 6) which reflects successive transgressive - regressive cycles and ever changing climatic conditions (Jones and Hunter, 1989). The contrast in the diagenetic fabric of the Cayman Member and the Pedro Castle Member adds further credence to the suggestion that the disconformity between the

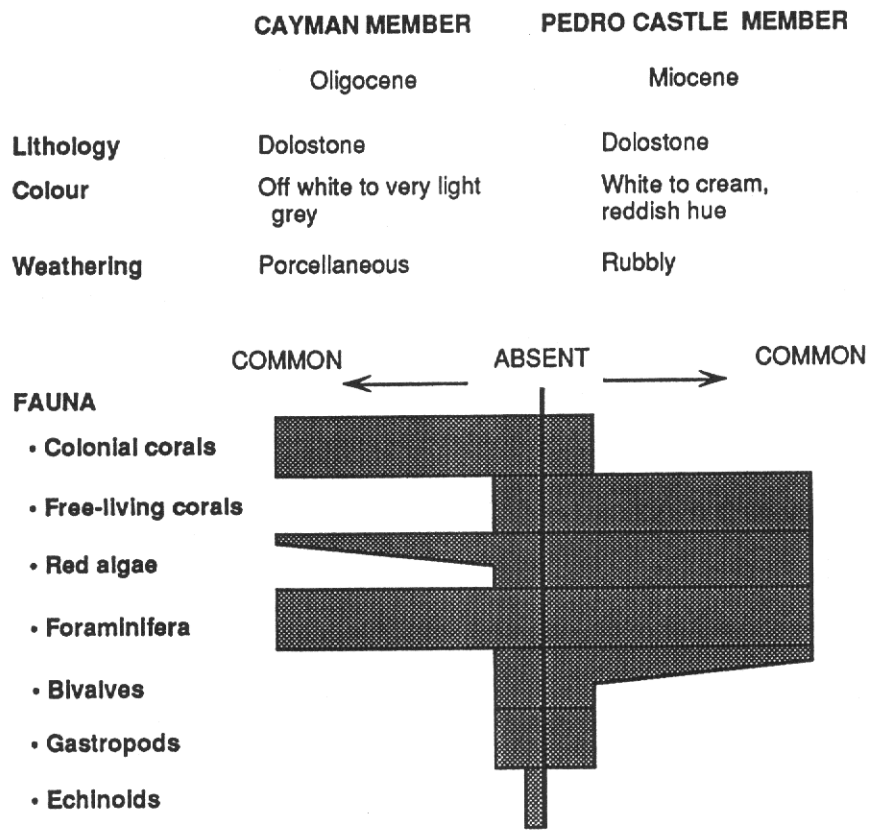

Figure 4. Comparison of depositional features in the Cayman and Pedro Castle members.

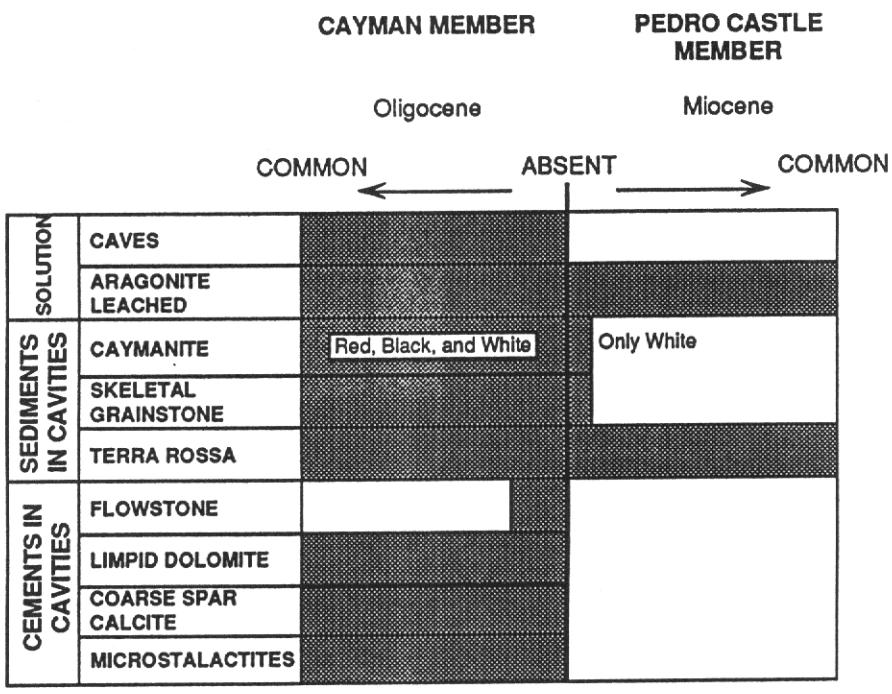

Figure 5. Comparison of diagenetic features in the Cayman and Pedro Castle members.

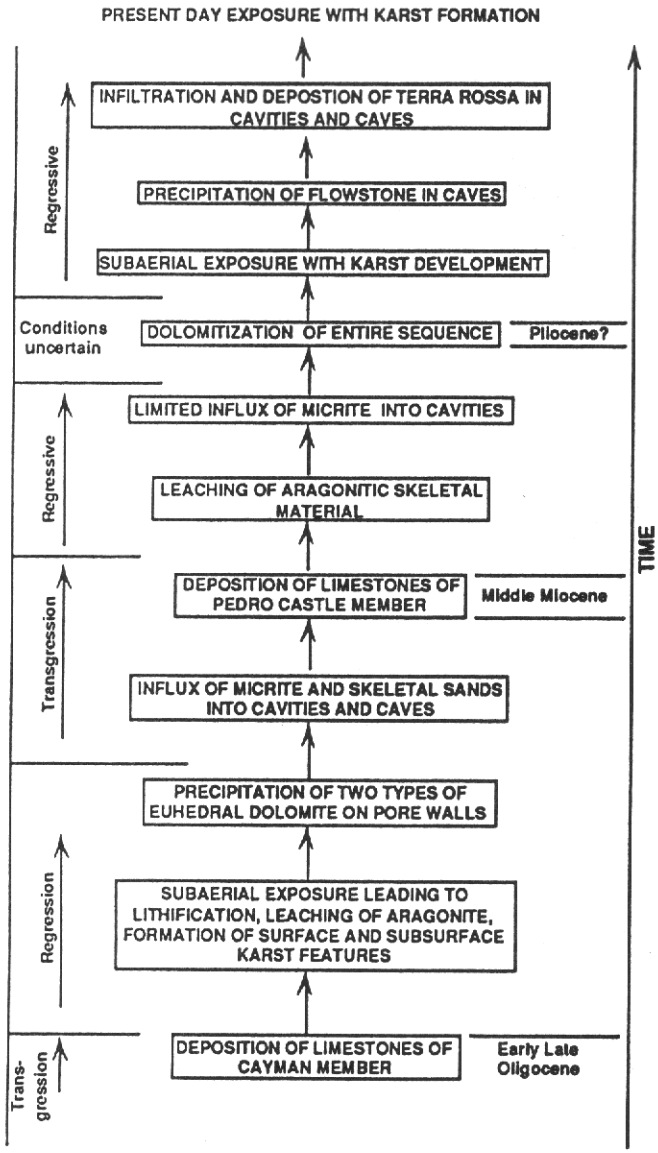

Figure 6. Suggested paragenetic sequence for the Bluff Formation of Grand Cayman.

two members represents a substantial period of time. In this respect, the following comparisons are important:

1. pores and cavities in the Cayman Member are lined with one or two generations of euhedral dolomite cement (cf. Jones et al., 1984) whereas the borings at the disconformity and cavities in the Pedro Castle Member lack these cements (Fig. 2B),

2. multicoloured caymanite is common in cavities throughout the Cayman Member but absent from the Pedro Castle Member apart from rare cavities which contain small amounts of white caymanite (Fig. 3) and westward dipping joints that contain red, white, and black caymanite,

3. caves, cavities, and fossil molds in the Cayman Member are filled or partly filled with multicoloured caymanite, dolomitized skeletal grainstone, flowstone, and terra rossa whereas those in the Pedro Castle Member are either open or contain only minor amounts of white caymanite, flowstone, or terra rossa (Fig. 6).

The contrast in diagenetic styles of the Cayman and Pedro Castle members suggests that the Cayman Member was lithified prior to deposition of the Pedro Castle Member because (1) the caves, cavities, and moldic porosity could only have maintained their form if the rocks were lithified, (2) the dolomite cements lining the caves, cavities, and fossil molds indicate that the surrounding sediments must have been lithified; if not, the sediment would have collapsed and the cavities destroyed, and (3) the borings at the disconformity could only have been made into lithified sediment.

As in most examples of dolomitization it is difficult to determine the time period during which the original limestones were converted to dolostone. Analysis of 16 samples of dolostone from the Cayman and Pedro Castle members yielded an average $^{87}Sr/^{86}Sr$ value of 0.70905. If it is assumed that (1) dolomitization was mediated by seawater, and (2) the $^{87}Sr/^{86}Sr$ represents the time of dolomitization (cf. Saller, 1984), the comparison with the $^{87}Sr/^{86}Sr$ curve of Koepnick et al. (1985) suggests that dolomitization occurred 2 to 5 million years ago.

CORRELATION OF BLUFF FORMATION BETWEEN GRAND CAYMAN AND CAYMAN BRAC

The Bluff Formation is well exposed on Cayman Brac in steep cliffs that rise to about 50 m above sea level. There is no evi-

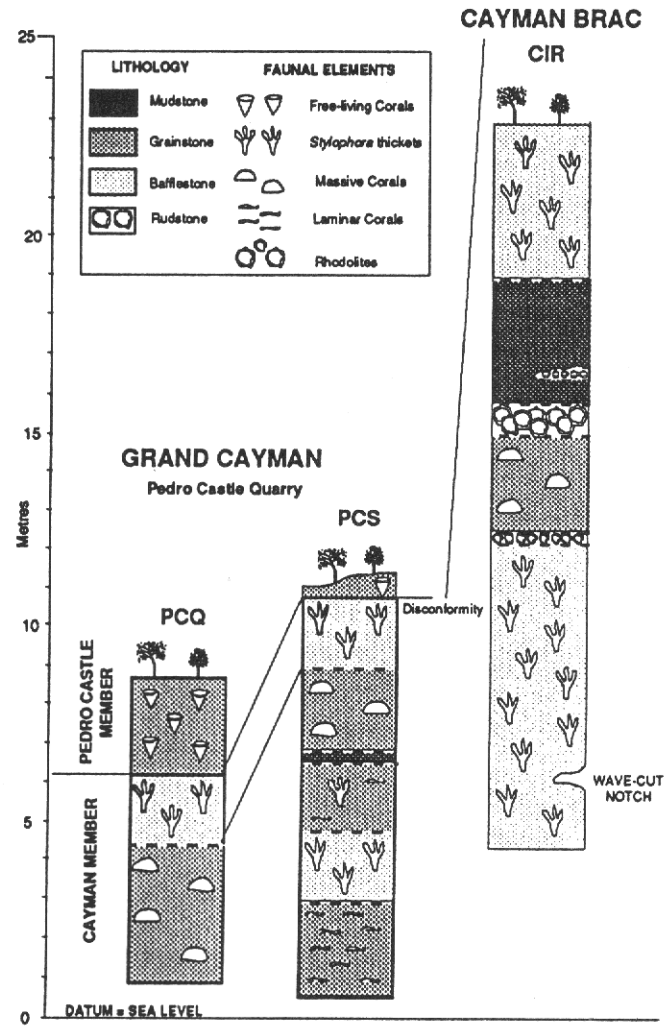

Figure 7. Comparison of the Bluff Formation in Pedro Castle Quarry, Grand Cayman and the south shore of Cayman Brac (locality CIR on Figure 1C).

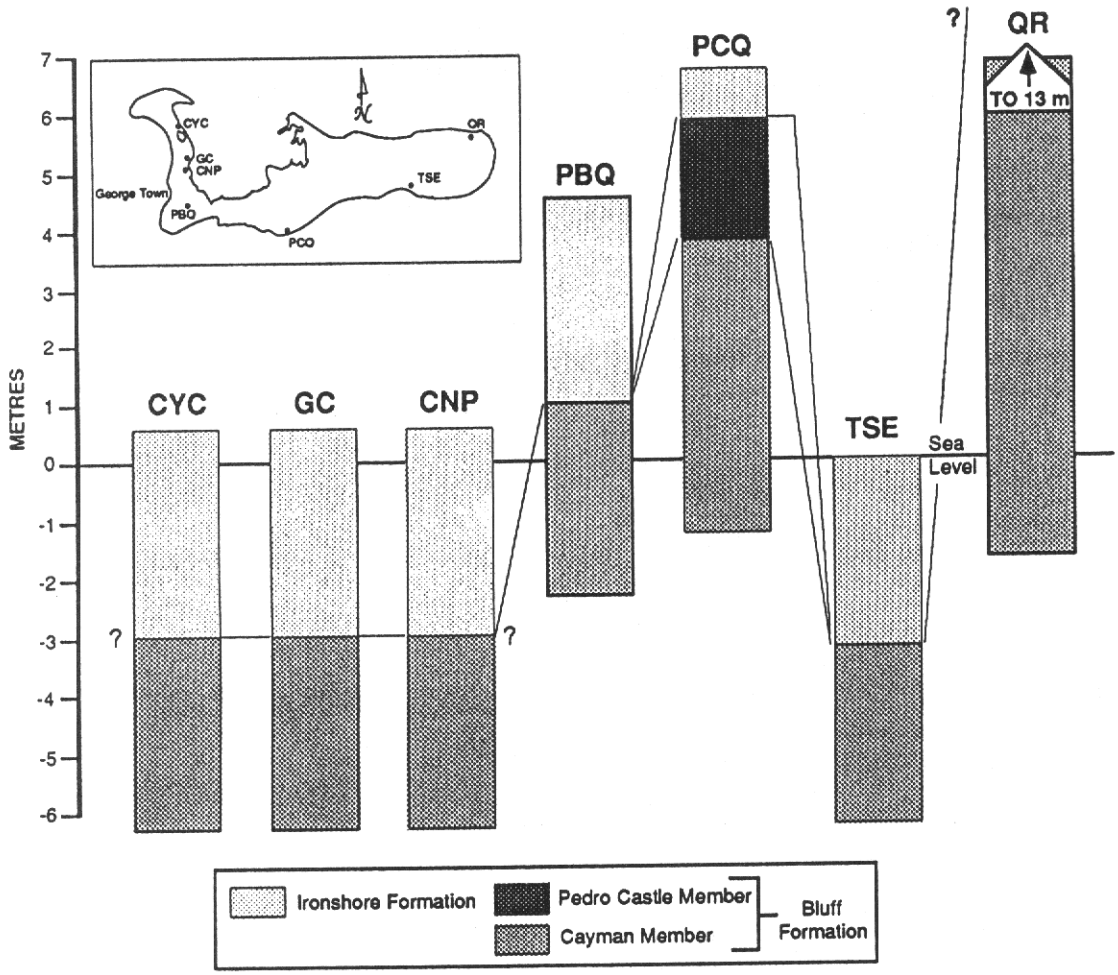

Figure 8. Distribution of the Cayman Member and Pedro Castle Member (Bluff Formation) and the Ironshore Formation relative to present day sea level at selected localities (see inset) on Grand Cayman. CYC = Cayman Yacht Club; GC = Golf Course; CNP = Canal Point; PBQ = Paul Bodden's Quarry; PCQ = Pedro Castle Quarry; TSE = Tarpon Spring Estate; and QR = Queen's Road.

dence of any break in the succession and examination of the dolostones suggest that they all belong to the Cayman Member. In general, the Cayman Member on Cayman Brac appears to encompass a wider range of facies than on Grand Cayman (Fig. 7). With our present state of knowledge it is impossible to accurately correlate the succession on Cayman Brac with the type section on Grand Cayman (Fig. 7) because there are no distinctive units or markers.

DISCUSSION

On Grand Cayman there is considerable evidence that the Bluff Formation has, during the various periods of exposure, been eroded down to different levels (Fig. 8). In the area around Pedro Castle both the Cayman and Pedro Castle members occur. Elsewhere, however, this is not the case. For example, in excavations at Tarpon Springs Estate (TSE - Fig. 8) limestones of the Pleistocene Ironshore Formation rest on dolostones of the Cayman Member. It would appear that the Pedro Castle Member was either never deposited or was removed by erosion prior to deposition of the Ironshore Formation because there is no evidence of the disconformity or the Pedro Castle Member. In a quarry south of George Town (PBQ - Fig. 8) dolostones of the Cayman Member are unconformably overlain by limestones of the Pleistocene Ironshore Formation. The unconformity surface, which has a local relief of up to 1 m, is highlighted by a thin layer of white caymanite and numerous borings (primarily Entobia) filled with white caymanite. These features are akin to those which characterize the disconformity that forms the contact between the Cayman and Pedro Castle members in the quarry near Pedro Castle. Thus, in the quarry near George Town, it is evident that the Pedro Castle Member was completely removed prior to deposition of the Pleistocene Ironshore Formation.

Along Queen's Road (QR - Fig. 8), the Cayman Member is exposed in road cuts that are up to 13 m above sea level. At Canal Point (CNP - Fig. 8), Golf Course (GC - Fig. 8), and the Cayman Yacht Club (CYC - Fig. 8) the contact between the Ironshore Formation and the Bluff Formation is 2 to 4 m below sea level. Dolostones from the upper part of the Bluff Formation are lithologically similar to those from the Cayman Member at its type section.

CONCLUSIONS

Detailed study of the Bluff Formation on Grand Cayman has shown that:

1. it can be divided into the Cayman and Pedro Castle members,
2. the Cayman Member is probably of early late Oligocene age,
3. the Pedro Castle Member is probably of middle Miocene age,
4. the disconformity between the Cayman and Pedro Castle members represents a hiatus of 13 to 14 million years,
5. the diagenetic history of the Cayman Member is different from

that of the Pedro Castle Member,

6. the Cayman Member crops out over most of Grand Cayman whereas the Pedro Castle Member is restricted to scattered remnants that survived post-Miocene erosion,

7. all of the Bluff Formation on Cayman Brac belongs to the Cayman Member.

ACKNOWLEDGEMENTS

We are indebted to the Natural Sciences and Engineering Research Council of Canada for the financial support of the field-work and preparation work needed for this study (grant A6090 to Jones), the Mosquito Research Control Unit of the Cayman Islands which provided accommodation during the course of the field-work.

REFERENCES CITED

Brunt, M. A., Giglioli, M. E. C., Mather, J. D., Piper, D. J. W., and Richards, H. G., 1973, The Pleistocene rocks of the Cayman Islands: Geol. Mag., v. 110, p. 209-221.

Bugg, S. F., and Lloyd, J. W., 1976, A study of freshwater lens configuration in the Cayman Islands using resistivity methods: Quart. J. Eng. Geol., v. 9, p. 291-302.

Emery, K. O., 1981, Low marine terraces of Grand Cayman Island: Estuar. Coast. Shelf Sci., v. 12, p. 569-578.

Frost, S. H., 1977, Cenozoic reef systems of the Caribbean - Prospects for Paleoecologic Synthesis, in Frost, S. H., Weiss, M. P., and Saunders, J. B., eds., Reefs and Related Carbonates - Ecology and Sedimentology: Amer. Assoc. Petrol. Geol., Stud. Geol. No. 4, p. 93-110.

Frost, S. H., and Langenheim, R. L., 1974, Cenozoic Reef Biofacies. Tertiary Larger Foraminifera and Scleractinian Corals from Chiapas, Mexico: Northern Illinois Univ. Press, 388 p.

Jones, B., and Hunter, I. G., 1989, The Oligocene-Miocene Bluff Formation on Grand Cayman: Carib. J. Sci., v. 25, p. 71-85.

Jones, B., Lockhart, E. B., and Squair, C., 1984, Phreatic and vadose cements in the Tertiary Bluff Formation of Grand Cayman Island, British West Indies: Bull. Can. Petrol. Geol., v. 32, p. 382-397.

Jones, B., Pleydell, S. A., Ng, K. C., and Longstaffe, F. J., 1989, Formation of poikilotopic calcite-dolomite fabrics in the Oligocene-Miocene Bluff Formation of Grand Cayman, British West Indies: Bull. Can. Petrol. Geol., v. 37, p. 255-265.

Jones, B., and Smith, D. S., 1988, Open and filled karst features on the Cayman Islands: implications for the recognition of paleokarst: Can. J. Earth Sci., v. 25, p. 1277-1291.

Lockhart, E. B., 1986, Nature and genesis of caymanite in the Oligocene-Miocene Bluff Formation of Grand Cayman Island, British West Indies: Unpublish. M. Sc. Thesis, Univ. Alberta, Edmonton, 111 p.

Koepnick, R. B., Burke, W. H., Denison, R. E., Hetherington, E. A., Nelson, H. F., Otto, J. B., and Waite, L. E., 1985, Construction of the seawater $^{87}Sr/^{86}Sr$ curve for the Cenozoic and Cretaceous: supporting data: Chemical Geol. (Isotope Geoscience section), v. 58, p. 55-81.

Mather, J. D., 1972, The geology of Grand Cayman and its control over the development of lenses of potable groundwater: Trans. VI Carib. Geol. Conf., Isla de Margarita, Venezuela, p. 154-157.

Matley, C. A., 1926, The Geology of the Cayman Islands (British West Indies) and their relation to the Bartlett Trough: Quart. J. Geol. Soc. London, v. 82, p. 352-386.

Pleydell, S. M., 1987, Aspects of diagenesis and ichnology in the Oligocene-Miocene Bluff Formation of Grand Cayman Island, British West Indies: Unpublish. M. Sc. Thesis, Univ. Alberta, Edmonton, 209 p.

Pleydell, S. M., and Jones, B., 1988, Boring of various faunal elements in the Oligocene-Miocene Bluff Formation of Grand Cayman, British West Indies: J. Paleont., v. 62, p. 348-367.

Pleydell, S. M., Jones, B., Longstaffe, F. J., and Baadsgaard, H., in press, Dolomitization of the Oligocene-Miocene Bluff Formation on Grand Cayman, British West Indies: Can. J. Earth Sci.

Rigby, J. K., and Roberts, H. H., 1976, Geology, reefs and marine communities of Grand Cayman Island, British West Indies: Brigham Young Univ., Geol. Stud., Spec. Publ. 4, 95 p.

Saller, A. H., 1984, Petrologic and geochemical constraints on the origin of subsurface dolomite, Enewetok Atoll: An example of dolomitization by normal seawater: Geology, v. 12, p. 221-225.

Spencer, T., 1985, Marine erosion rates and coastal morphology of reef limestones on Grand Cayman Island, West Indies: Coral Reefs, v. 4, p. 59-70.

Stoddart, D. R., 1980, Geology and geomorphology of Little Cayman: Atoll Res. Bull. No. 241, p. 11-16.

Vaughan, T. W., 1919, Fossil corals from Central America, Cuba and Puerto Rico with an account of the American Tertiary, Pleistocene and recent coral reefs: U. S. Nat. Mus. Bull. 103, p. 189-524.

Vaughan, T. W., 1926, Species of Lepidocyclina and Carpenterea from the Cayman Islands, and their geological significance: Quart. J. Geol. Soc. London, v. 82, p. 388-400.

Vaughan, T. W., and Hoffmeister, J. E., 1926, Miocene corals from Trinidad: Papers from the Depart. Mar. Biol. Carnegie Inst. Washington, v. 23, p. 107-134.

Woodroffe, C. D., 1981, Mangrove swamp stratigraphy and Holocene transgression, Grand Cayman Island, West Indies: Mar. Geol., v. 41, p. 271-294.

Woodroffe, C. D., Stoddart, D. R., and Giglioli, M. E. C., 1980, Pleistocene patch reefs and Holocene swamp morphology, Grand Cayman Island, West Indies: J. Biogeogr., v. 7, p. 103-113.

Woodroffe, C. D., Stoddart, D. R., Harmon, R. S., and Spencer, T., 1983. Coastal morphology and Late Quaternary history, Cayman Islands, West Indies: Quat. Res., v. 19, p. 64-84.

Zans, V. A., Chubb, L. J., Versey, H. R., Williams, J. B., Robinson, E., and Cooke, D. L. 1963, Synopsis of the geology of Jamaica: Geol. Surv. Dept. Jamaica Bull. No. 4, 72 p.

MORPHOLOGY, STRUCTURE AND ACTIVE TECTONISM OF THE INSULAR MARGIN OFF NORTHWESTERN HISPANIOLA

William P. Dillon
U.S. Geological Survey
Woods Hole, MA 02543

Kathryn M. Scanlon
U.S. Geological Survey
Woods Hole, MA 02543

James A. Austin Jr.
Institute for Geophysics
University of Texas
Austin TX 78759

N. Terence Edgar
U.S. Geological Survey
Reston, VA 22092

Lindsay M. Parson
Institute of Oceanographic Sciences,
Wormley, Surrey, GU8 5UB, U.K.

Gordon E. Ness
Oregon State University,
Corvallis OR 97333

ABSTRACT

Long-range sidescan sonar, multichannel and single channel seismic reflection profiles and bathymetric surveys were carried out off northwestern Hispaniola (north of Haiti and the westernmost Dominican Republic. The morphology and structure of the insular slope define three distinct and abruptly bounded compartments. In the central compartment (Type I), the insular slope surface (the sea floor) is approximately planar, dipping about 4°, and internal structure consists of broad anticlines between thrust faults, with a gradational structural contact to undisturbed basin strata to the north. In the eastern and western compartments (Type II), the insular slope is convex and much steeper (9° to 16° for the lower slope) internal structure appears chaotic (presumably complexly folded and faulted), and the foot of the slope marks an abrupt structural front against undisturbed basin strata. The insular slope has formed as a tectonic accretionary wedge resulting from motion between the North American and Caribbean plates which has caused continuing crumpling of Hispaniola Basin sediments (dominantly turbidites) against the backstop formed by the island of Hispaniola. Although overall motion at the plate boundary is primarily transcurrent, the study region is a zone of transpression, and the structure of the insular slope has been dominated by compressional effects. We speculate that the difference in dip of the sea floor between compartments may result from variations in dip of the main decollement at the base of the tectonic accretionary wedge, and that the differences in internal structure may, in turn, result from the differences in sea-floor dip.

INTRODUCTION

The insular margin north of western Hispaniola (off Haiti and the western Dominican Republic) lies in the plate-boundary region between the North American and Caribbean plates. The dominant motion between these plates along the northern boundary of the Caribbean region is left-lateral transcurrent. However, apparently due to a slight convergence of plate trajectories and the presence of a restraining bend, the insular slope north of western Hispaniola is affected by compression, although probably not by subduction (Bracey and Vogt, 1970; Mann et al. 1984; Pindell and Barrett, 1988), and its structure is that of a tectonic accretionary wedge (Austin, 1983). This paper examines the morphological and structural variation in this region using sidescan-sonar imagery, seismic profiles, and echo-sounder bathymetry.

DATA

Long-range sidescan-sonar data were obtained during a U.S. Geological Survey cruise using the GLORIA system (Somers and others, 1978), which provided sea-floor images having a swath width of 40 km in the deep-water part of the Hispaniola Basin. Initial picture-element (pixel) size is about 50 m across-track by 150 m along-track; this is the effective resolution. The digital data were processed to present a 50- by 50-m pixel size (Chavez, 1986). Four multichannel seismic-reflection profiles were obtained by the University of Texas using a seismic source consisting of four 1500-in^3 airguns and a 48-trace streamer having 70-m group intervals. Data were

Larue, D.K., and Draper, G. (eds.),
Transactions of the 12th Caribbean Geological Conference, St. Croix, U.S.V.I., Miami Geological Society, P.O. Box 431552, South Miami, FL 33243, U.S.A

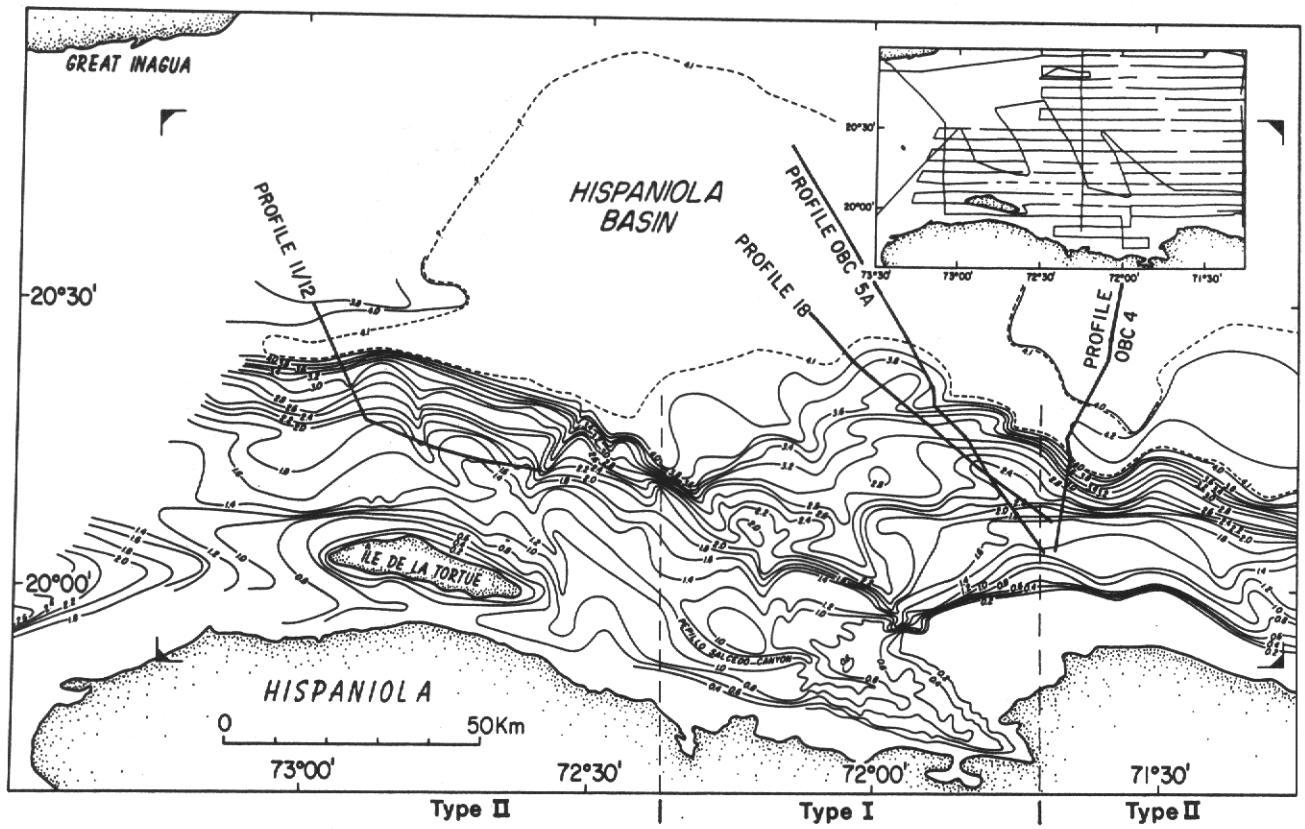

Figure 1. Contours of depth in kilometers of the continental margin off northwestern Hispaniola. Inset map shows data tracks. These were supplemented by a survey and contouring by N.T. Edgar in the Pepillo Salcedo Canyon area. The supplementary 4.1 km contour (dashed) indicates the approximate boundary of the flat-floored part of the Hispaniola Basin.

stacked 24-fold. Single-channel seismic profiles were collected along all GLORIA tracks using a 180-in^3 airgun. For purposes of structure mapping and creation of bathymetric sections across the margin, seismic profiles previously collected by Woods Hole Oceanographic Institution also were consulted (Uchupi, et al., 1971; Goreau, 1981). Digital bathymetric data were collected during Oregon State University and U.S. Geological Survey cruises (bathymetry coverage is shown in the inset map of Figure 1).

MORPHOLOGY OF THE INSULAR MARGIN

A bathymetric map of the study area (Fig. 1) discloses that the morphology of the insular slope comprises two distinctly different styles that occupy abruptly bounded compartments of the slope. A central compartment from about 71°42'W to 72°22'W (marked Type I in Fig. 1) extends farther north than the Type II areas to either side. Contours are more broadly spaced on the lower slope and generally are more random, defining irregular ridges. In the Type II areas to the east and west, lower-slope contours are more even and closely packed than in Type I, indicating a steepening of the slope toward the base. The differences between types are displayed in Figure 2 in a series of profiles plotted on north-south lines of projection from west (line A) to east (line I). Profiles in the Type I area (starred profiles E, F and G) show that the insular slope is planar or slightly concave, and has a dip angle of about 4°, whereas in the Type II area, (profiles A,B,C,D, H, and I) the slope is convex and has an angle near its base of 9° to 16°. The contact of the base of the slope and the Hispaniola Basin floor is gradational in Type I, but forms a very abrupt angle in Type II.

GLORIA sidescan-sonar imagery has been used to guide the contouring of Figure 1 and a portion of the GLORIA data is shown in Figure 3 to demonstrate the contrast between Type I and II areas at a boundary between compartments. The broad ridges and valleys of Type I contrast with the smaller scale roughness of Type II, and the generally greater breadth of the slope in Type I is apparent. The ridges in Type I are roughly parallel to the insular margin, but a break through them has created a submarine canyon that

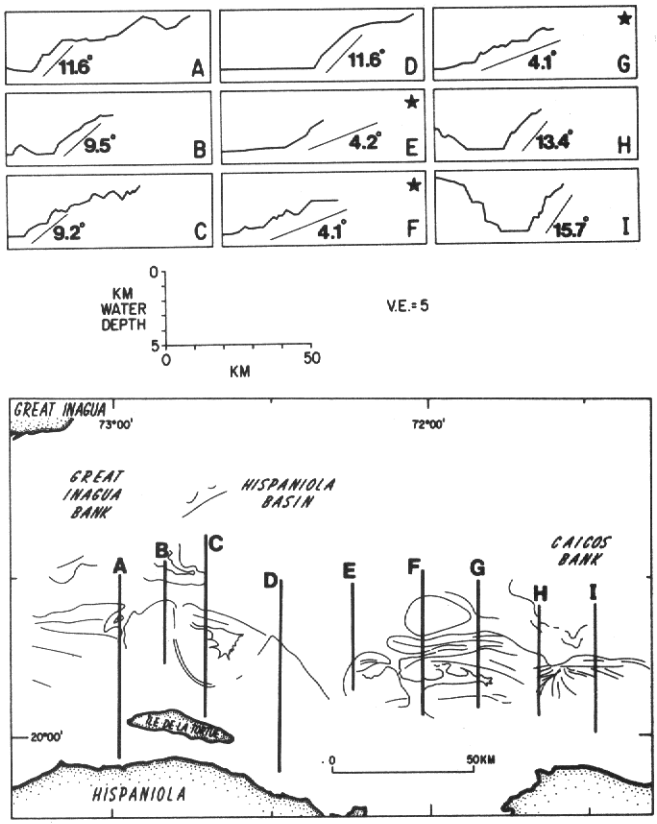

Figure 2 Bathymetric profiles of the insular margin off northwestern Hispaniola in the study area. The profiles are along north-south lines of projection from west (line A) to east (line I). Estimated average dip of the lower slope is indicated by a fine line and indication of angle in degrees in each profile. Starred profiles are in the Type I area; other profiles are in the western Type II area (profiles A-D), and eastern Type II area (H and I). Locations of lines of projection are shown in the map below the profiles. This map also indicates as light lines the principal sea-floor reflections observed in our GLORIA sidescan-sonar survey.

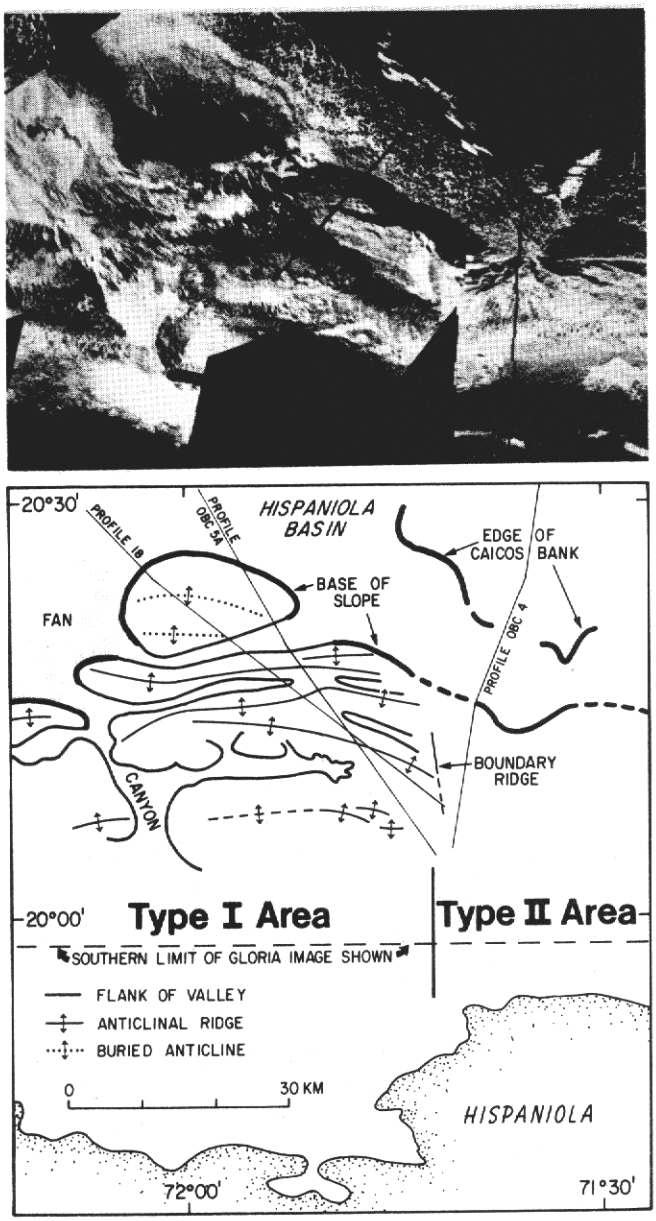

Figure 3. A portion of the GLORIA sidescan sonar mosaic and interpretation covering part of the central (Type I) area and eastern (Type II) area. The GLORIA image (top) covers the area above the dashed line in the interpretation (bottom). The limit of the deep (approximately 4100m), flat-floored, part of the Hispaniola Basin is indicated by a heavy line at the base of the Hispaniola insular slope or edge of Caicos Bank.

feeds turbidity flows to a fan at its mouth and to the floor of the Hispaniola Basin (see "canyon" and "fan" in Figure 3) (Bennetts and Pilkey, 1976; Ditty et al., 1977). The floor of the canyon and the fan are strongly reflective, probably because they are covered by a coarse lag deposit resulting from turbidity current flow.

STRUCTURE OF THE INSULAR MARGIN

Seismic-reflection profiles across the Type I area show that the broad ridges that are characteristic of this area are formed by anticlines (Figs. 4 and 5; locations of profiles shown in Figs. 1 and 3). Some buried anticlines that presumably have not yet grown upward enough to form ridges also were identified (note mapped anticlines shown in Figure 3). The amplitudes of the folds increase continuously toward the south from the flat, undisturbed strata of the

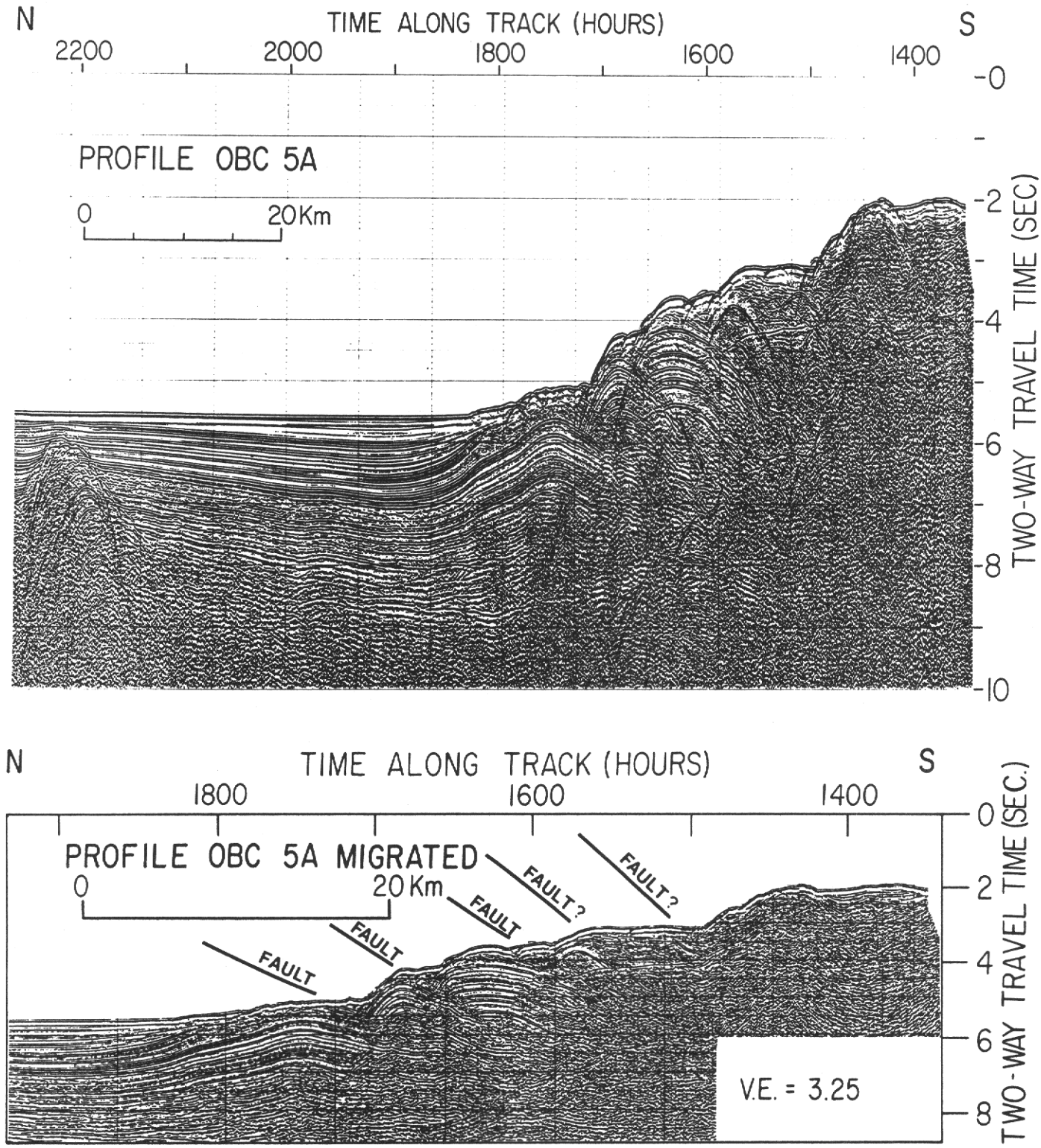

Figure 4. Multichannel seismic-reflection profile OBC 5A showing folds and thrust faults of the Type I area. Upper section received standard processing (Austin, 1983); vertical exaggeration is 8.4:1. Lower section is a migrated version of the central and southern part of the upper profile at lower vertical exaggeration; vertical exaggeration is 3.25:1. See Figures 1 and 3 for location.

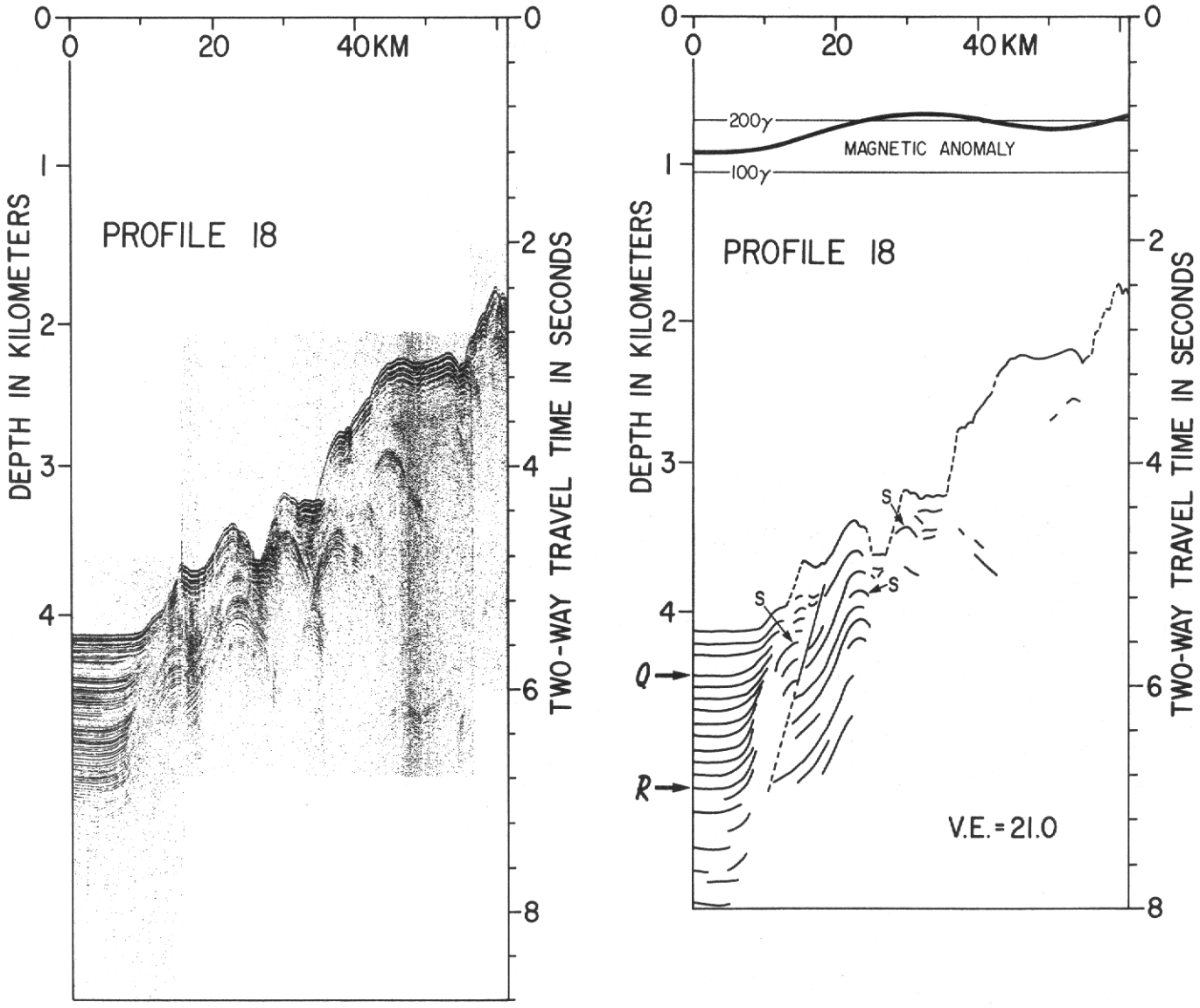

Figure 5. Single-channel seismic-reflection profile 18 and interpretation in Type I area. Vertical exaggeration is 21:1. See Figures 1 and 3 for location. A distinctive reflecting horizon (labeled S) appears to be recognizable at several locations. Its distribution suggests that it has been thrust up by the folding and faulting.

Hispaniola Basin, suggesting that folding has been progressive, occurring earliest at the south. Fold amplitudes also increase downward (Figs. 4 and 5), further indicating that folding has been continuous for some time and that the folds are syndepositional. The deeper-penetrating, multichannel profile shown in Figure 4, is interpreted to indicate that the anticlines are separated by thrust faults. The lack of correspondence of magnetic anomaly pattern to structure and the small amplitudes of the anomalies suggest that the basement beneath the insular slope is not involved in the folding (Fig. 5).

Seismic-reflection profiles in the Type II areas also show the smaller scale roughness of these insular slopes that was noted in GLORIA images, and the profiles display the greater steepness and convexity of this type in cross-section (Figs. 6 and 7). The abrupt angular contact of the slope to the basin floor is interpreted to be a structural front. Neither the large-source multichannel profiles nor the smaller-airgun, higher-resolution, single-channel profiles show significant subbottom structure in the Type II areas. Most subbottom reflections in the multichannel profile (Fig. 6) represent diffractions.

The boundaries between compartments are extremely abrupt and probably require structural

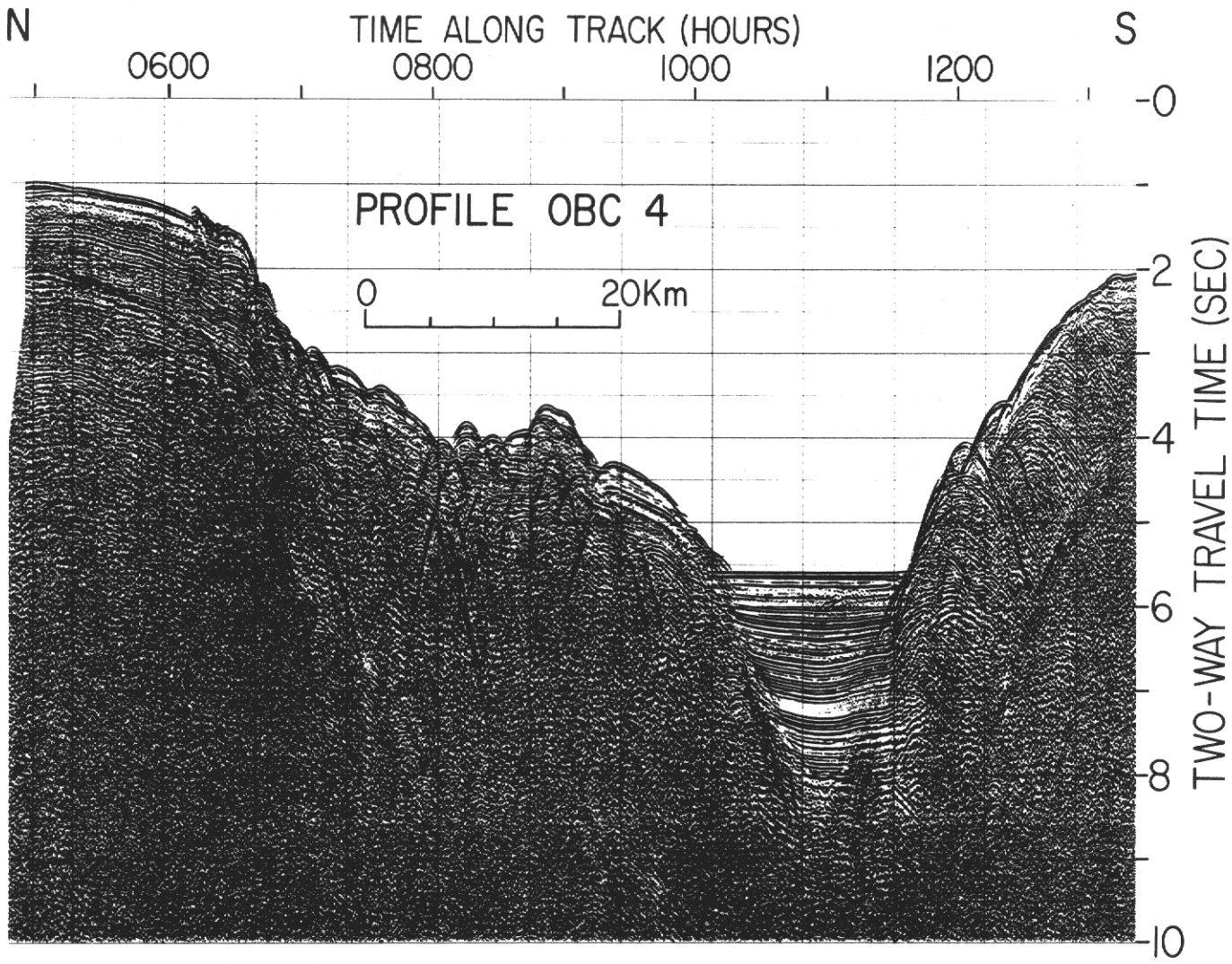

Figure 6. Multichannel seismic-reflection profile OBC 4 in eastern Type II area. Processing and vertical exaggeration are comparable to those of the upper profile of figure 4; vertical exaggeration is 8.9:1. The Hispaniola insular margin is on the right, showing a convex form and general lack of coherent internal structure. Caicos Bank is on the left, showing the typical collapse features of carbonate bank margins. See Figures 1 and 3 for location.

breaks that cross the insular margin. Evidence for such a break is present at least at the east side of the Type I area, where a north-trending ridge probably marks the structural feature that bounds the compartments. This ridge is apparent in the GLORIA image ("boundary ridge" in Figure 3) and is crossed by profile 18 at its southern end (Fig. 5).

MORPHOLOGY AND STRUCTURE OF THE INSULAR MARGIN: REVIEW AND IMPLICATIONS

We have observed very distinct differences in morphology and structure in well-defined compartments of the northwestern Hispaniola insular margin. These are summarized in Table 1 and sketched in the conceptual block diagram (Fig. 8).

The insular margin off northwestern Hispaniola clearly is a tectonic accretionary wedge. The sediments of the Hispaniola Basin are being compressed against the backstop of Hispaniola by motions of the North American and Caribbean plates. In the Type I area, the basin strata are being folded into broad anticlines, then the folds are truncated by thrust faults and shoved beneath a pile of earlier-formed folds that previously had been sliced off in their turn as the plates moved toward each other. The resulting Type I structure is well displayed in Figure 4. The anticlinal ridges that dominate Type

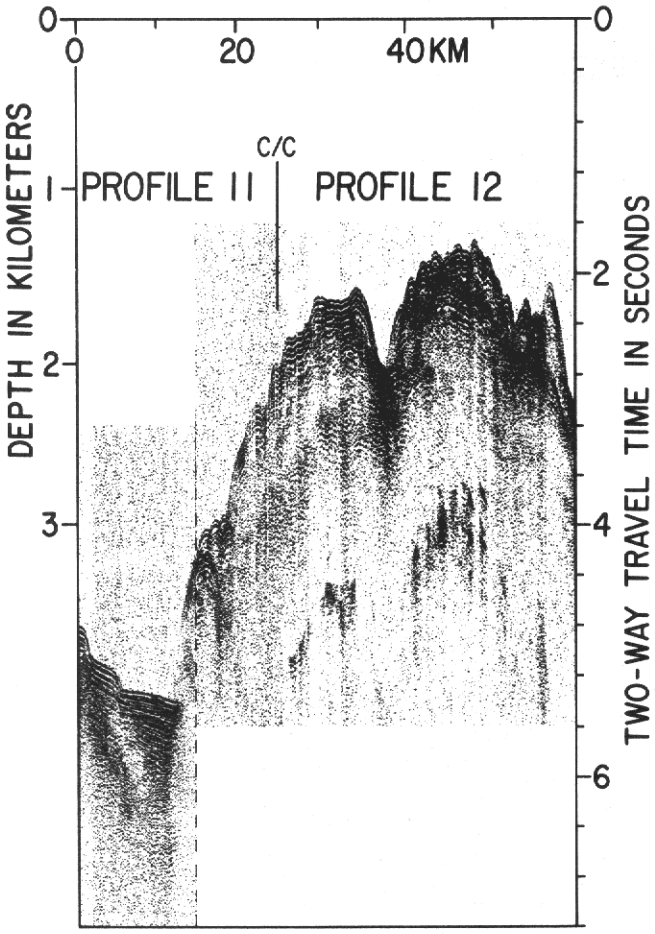

Figure 7. Single-channel seismic-reflection profiles 11/12 in western Type II area. C/C indicates course change. Vertical exaggeration is 20:1. See Figure 1 for location.

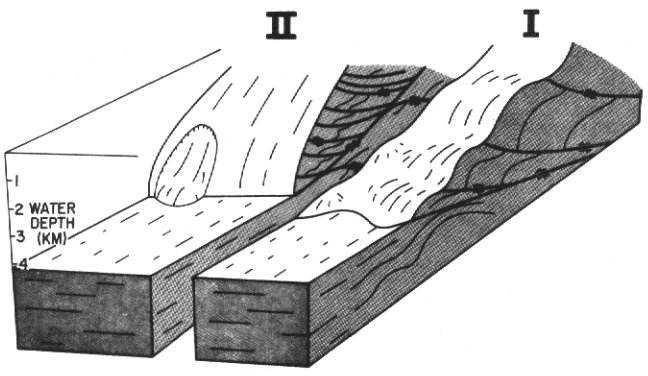

Figure 8. Conceptual block diagrams showing interpreted structure of the two morphological/structural types of the insular margin off northwestern Hispaniola.

COMPARISON OF INSULAR SLOPE TYPES, NORTHWESTERN HISPANIOLA

TYPE I	TYPE II
GENTLE SLOPE, ABOUT 4°	STEEP SLOPE, 9°-16°
INTERNAL STRUCTURE: THRUST FAULTS BETWEEN BROAD ANTICLINES	INTERNAL STRUCTURE: APPEARS CHAOTIC IN SEISMIC PROFILES
GRADATIONAL STRUCTURAL CONTACT TO BASIN STRATA	ABRUPT STRUCTURAL FRONT AGAINST BASIN
PLANAR TO CONCAVE	CONVEX

Table 1.

I morphology result in the formation of a structurally-controlled submarine canyon system. The internal structure of Type II insular slopes is not displayed by either of the seismic-reflection systems that we used. Thus we refer to this structure as chaotic; it consists, perhaps, of tight folds and complex faults. However, in such a small area, both Types I and II insular slopes and their internal structures must have been formed by the same plate interactions.

Although this insular margin is located near a plate boundary that is dominantly transcurrent, no structural features typical of strike-slip faulting, such as evidence of linear, vertical faults, or flower structures, have been observed in seismic profiles. Rather all structure in the insular slope seems to be related to compression. The actual strike-slip motion at the plate boundary may be marked by the trend of seismicity along the coastline; very few earthquakes occur on the insular slope (Sykes et al., 1982; National Geophysical Data Center, Boulder, CO, Earthquake Data Base). In a region of transpression, broad zones of pure compression flanking a narrow zone of pure transcurrent motion may be the common situation, in any case (Mount and Suppe, 1987).

SPECULATION ON CAUSES OF STRUCTURAL AND MORPHOLOGICAL VARIATION

Two principal questions arise: (1.) Why are the slope angles so different between types? (2.) Why are the internal structures apparently so different?

Differences in slope angle

Tectonic accretionary wedges are common features of collisional plate interactions. As noted above, even in oblique collision, strains tend to be organized into a narrow zone of pure transcurrent

motion at the plate boundary, with broader, flanking zones where shortening is normal to the plate boundary, and accretionary wedges can form. Such a wedge is comparable to the pile of snow in front of a constantly moving snowplow, in which the pile will maintain its shape in front of the moving blade in a dynamic way, as long as all factors remain the same. At the front of a tectonic accretionary wedge, the angle between the sediment surface and the decollement is referred to as the taper. The critical taper is the constant angle that will be maintained at steady state when the basal decollement and the sediments of the wedge are everywhere at the point of failure (Davis et al., 1983; Dahlen et al., 1984). Critical taper depends on the internal strength of the wedge balanced against four forces, the compressive push of a backstop (of Hispaniola in this case), the basal frictional resistance (at the decollement), the gravitational body force (the tendency for any slope to spread out flat under the influence of gravity), and the pressure of overlying water. Hence, at the front of a tectonic accretionary wedge such as that north of Hispaniola, abrupt changes in sea-floor dip could result from abrupt changes in any of the four forces or in the internal strength of the wedge, any of which would cause changes in the critical taper. Alternatively, such a change in sea-floor dip could result from a change in the dip of the decollement while critical taper remained constant.

Which of these factors seems likely to be responsible for the major variations along the northwestern Hispaniola insular slope? Water depth at the top and bottom of the wedge does not change along the margin, so pressure does not vary, and it is difficult to visualize how the gravitational body force could change abruptly . The Hispaniola backstop apparently is rigid and continuous along this segment of the plate boundary, as structures, including faults, trend parallel to the insular margin within the island, affording no opportunity for the segmentation of the backstop (e.g. Bowin, 1975). Therefore, distinct variations in compressive push seem unlikely. Basal frictional resistance can be affected by fluid on the decollement, but it is not clear how this would be compartmentalized. Therefore, the four forces do not seem to be good candidates for abrupt change, and we are left with a need to vary the internal strength of the wedge or the dip of the decollement. Internal strength might change if material entering the accretionary wedge at two points were radically different. If, for example, a component of the carbonate Bahama Banks had been dragged into the wedge, such a block would be stronger than the Hispaniola Basin turbidite sediments and therefore would cause a large increase in critical taper and in the stable angle for the insular slope. Thus a Type II area might be formed. Although this could have happened, we have no evidence for it in the seismic profiles and, therefore, do not propose such a scenario.

Variations in any of the factors considered in the previous paragraph would have modified the dip of the slope by changing the angle of the critical taper, but a change by a very large value would be required to account for the observed insular slope morphology -- a change of more than 11° at some locations on the basis of the angles indicated in Figure 2. Such a large change seems unlikely, as most critical tapers reported are within a fairly small range (e.g., in 10 of 12 cases reported by Davis et al., 1983, critical tapers were in the range of 7° to 10° and none exceeded 10°). In this study area, north of Hispaniola, where apparently similar basin deposits are being crumpled into a small wedge, which has apparently similar conditions along it, we expect that the critical taper would not vary radically.

If the critical taper does not vary extremely, as seems likely, then the decollement must dip at varied angles so that the top of the tectonic accretionary wedge (the insular slope) can vary in dip as it does. The structure of the margin in the Type I area, with a 4° surface slope, is considered to be that sketched in the idealized block diagram (Fig. 8, right block), in which the decollement dips toward the south. However, Type II slopes range from 9° to 16° (Fig. 2). If the critical angles in both the Type I and Type II areas are similar to those indicated in the literature as noted above (less than 10°), this would require that, in many Type II cases, the decollement must rise toward the south (dip northward toward the toe of the wedge). The space beneath such a southward-rising decollement would have to be filled by some structure such as a duplex. The proposed situation is sketched in the left block of Figure 8. Although our seismic profiles do not display this duplex (and probably no profiles could, in an area with such a complex topography, structure, and velocity field), it seems to be the most logical solution to the structural problem. Presence of a similar duplex beneath the accretionary wedge northwest of the Nankai Trough off Japan has been interpreted by Leggett et al. (1985).

Differences in internal structures

Whereas the Type I internal structure is characterized by broad folds separated by major thrust faults, the Type II appears to be chaotic, presumably consisting of tight folds and intensive, complex faulting, as sketched in Figure 8. The difference in structure may result directly from the differences in slope angles because increase in strength in sediments is strongly affected by overburden loading. On moving landward across a steep Type II slope, overburden will thicken much faster above a horizontal plane than on crossing a flatter Type I. For a unit amount of thickening, one would have to move 3.6 times farther across a 4° Type I slope than across a 14° Type II. In a Type I slope, the broader zone of weaker sediments, which is perhaps more appropriate for folding, may account, in part, for the broader wavelength of folds. The cohesive strengthening of

sediments in the Type II situation is demonstrated by the convex curve of the slope profile, which actually results from a decrease in the critical taper resulting from the increase in strength on proceeding into the wedge, as demonstrated by Zhao et al. (1986).

SUMMARY

The insular slope north of western Hispaniola is a tectonic accretionary wedge, formed as a result of compressional components of transpression between the North American and Caribbean plates. Two very different morphological/structural types exist in distinct, adjacent compartments along the insular slope. In the central part of the study area, the Type I slope is planar, has a dip of about 4°, and its structure consists of broad anticlines separated by thrust faults. To the east and west of the central compartment, the Type II slope is convex (indicating a progressive landward increase in cohesive strength), has a dip of 9° to 16°, and has an internal structure that, in seismic profiles, appears chaotic (probably formed of short-wavelength folds and abundant, small faults). The compartment boundaries are abrupt, a condition that probably requires faults that cross the insular margin; evidence for one such structure is noted in sidescan sonar. We suggest that the difference in slope between the two types may result from differences in dip of the decollement beneath the tectonic accretionary wedge, because very large changes in the critical angle at the front of the wedge are unlikely. If this is correct and if the critical angle is comparable to others discussed in the literature (less than 10°), then the decollement would be expected to rise toward the south (dip toward the toe of the wedge) in some Type II areas. Such a structural model would require a complicating structure, such as a duplex, beneath the decollement in order to fill the space. We infer that the difference in structure within the wedge between Types I and II may depend on the variations in slope steepness, such that flatter slopes allow a broader zone in which sediments are weaker and therefore more easily folded.

ACKNOWLEDGEMENTS

We wish to thank William Schwab and Arthur Snoke for suggestions regarding geological interpretations. Excellent editorial, drafting, secretarial, and photographic assistance by Elizabeth Winget, Patricia Forrestel, Jeffrey Zwinakis, Margaret Wengler and Dann Blackwood is gratefully acknowledged. The paper was reviewed by Robert Oldale and John Schlee, and they are thanked for their comments.

REFERENCES CITED

Austin, J. A., Jr., Overthrusting in a deep-water carbonate terrane, in Bally, A.W., ed., Seismic expression of structural styles: American Association of Petroleum Geologists, Studies in Geology No.15, v.3, p. 3.4.2-167 - 3.4.2-172, 1983.

Bennetts, K.R. and Pilkey, O.H., Characteristics of three turbidites, Hispaniola-Caicos Basin: Geological Society of America Bulletin, v. 87, p. 1291-1300, 1976.

Bowin, C., The geology of Hispaniola, in Nairn, A.E.M.,and Stehli, F.G., eds., The Ocean Basins and Margins, v. 3, p. 501-552, Plenum Publishing Co., New York, 1975.

Bracey, D.R. and Vogt, P.R., Plate Tectonics in the Hispaniola area: Geological Society of America Bulletin, v. 81, p. 2855-2860, 1970.

Chavez, P.S., Jr., Processing techniques for digital sonar images from GLORIA: Photogrammetric Engineering and Remote Sensing, v. 52, p. 1133-1145, 1986.

Dahlen, F.A., Suppe, J., and Davis D., Mechanics of fold-and-thrust belts and accretionary wedges: Cohesive Coulomb theory: Journal of Geophysical Research, v. 89, p. 10,087-10,101, 1984.

Davis, D.M., Suppe, J. , and Dahlen, F.A., Mechanics of fold-and-thrust belts and accretionary wedges: Journal of Geophysical Research, v. 88, p. 1153-1172, 1983.

Ditty, P.S., Harmon, C.J., Pilkey, O.H., Ball, M.M. and Richardson, E.S., Mixed terrigenous-carbonate sedimentation in the Hispaniola-Caicos turbidite basin, Marine Geology, v. 24, p. 1-20, 1977.

Goreau, P.D.E., The tectonic evolution of the north central Caribbean plate margin [Sc. D. thesis], Massachusetts Institute of Technology and Woods Hole Oceanographic Institution, 244 p. 1981.

Leggett, J., Aoki, Y. and Toba, T., Transition from frontal accretion to underplating in a part of the Nankai Trough accretionary complex off Shikoku (SW Japan) and extensional features on the lower trough slope, Marine and Petroleum Geology, v. 2, p. 131-141, 1985.

Mann, P., Burke, K., and Matumoto, T., Neotectonics of Hispaniola: plate motion sedimentation and seismicity at a restraining bend, Earth and Planetary Science Letters, v. 70 p. 311-324, 1984.

Mount, V.S. and Suppe, J., State of stress near the San Andreas fault: implications for wrench tectonics, Geology, v. 15, p. 1143-1146, 1987.

Pindell, J.L. and Barrett, S.F., Geological evolution of the Caribbean region: A plate-tectonic perspective, in Dengo, G. and Case, J.E., eds. The Caribbean Region, Geological Society of America, The Geology of North America, v. H, 1988.

Somers, M.L., Carson, R.M., Revie, J.A., Edge, R.E., Barrow, B.J. and Andrews, A.G., GLORIA II - An improved long-range side-scan sonar, Proceedings of the IEEE/IERE sub-conference on offshore instrumentation and communications, Oceanology International, Technical Session J, p. 16-24, London, BPS Publications, 1978.

Sykes, L.R., McCann, W.R., and Kafka, A.L., Motion of the Caribbean plate during the last 7 million years, and implications for earlier Cenozoic movements, Journal of Geophysical Research, v. 87, p. 10,656-10676, 1982.

Uchupi, E., Milliman, J.D., Luyendyk, B.P., Bowin, C.O. and Emery, K.O., Structure and origin of southeastern Bahamas, American Association of Petroleum Geologists Bulletin, v. 55, p. 687-704, 1971.

Zhao, W.-L., Davis, D.M., Dahlin, F. A. and Suppe, J., Origin of convex accretionary wedges: Evidence from Barbados, Journal of Geophysical Research, v. 91, p. 10,246-10,258.

TECTONOSTRATIGRAPHY OF THE SAN FRANCISCO RIDGE AREA IN THE NORTHEASTERN CIBAO VALLEY, DOMINICAN REPUBLIC.

Agathe C. Nadai
Residence: 69 Greendale Rd.,
Scarsdale, New York 10583.

ABSTRACT

Neogene strata exposed along the San Francisco ridge (SFR) in northeastern Hispaniola record the tectonostratigraphic evolution of a former marine basin, the present day Cibao Valley, which is adjacent to a now uplifted subduction complex, the Cordillera Septentrional. Deep-water calciclastic strata of Miocene age are unconformably overlain by shallow-marine carbonate strata of early Pliocene age. These strata are in turn unconformably overlain by mainly fluvial channel deposits of later Pliocene age or younger.

In the SFR, Miocene strata are folded and faulted which indicates that uplift and deformation occurred since latest Miocene time. The intense deformational event ceased by early Pliocene time as indicated by the much less deformed Pliocene strata. A Pliocene or later deformational event resulted in the present relief of the SFR as evidenced by the broad warping of the Pliocene strata over the SFR.

The topographic expression of the SFR dies out west of Samana Bay, yet this structure, by correlation with seismic data, appears to continue to the east offshore beneath the bay.

INTRODUCTION

The area of study forms an irregular quadrangle of 300 km located in the eastern Cibao Valley of the northeastern Dominican Republic (Fig. 1). Much of the terrain lies along a topographic high up to 400 m in elevation that is dissected by deep river valleys which give rise to the hilly landscape and includes a narrow strip of the southern part of the Cordillera Septentrional. This ridge is part of the northern slope of the Cibao Valley which is bounded to the north by the Septentrional fault system. Because of its location near the city of San Francisco de Macoris this ridge was called the " San Francisco Ridge" (SFR) by Winslow and McCann 1985. This study covers the Western half of the SFR.

The purpose of this study is to provide brief descriptions of the formations informally defined by the author for 300-600 m of exposed Neogene strata. The stratigraphic and structural framework are presented on a 1:50,000 scale map and offer an interpretation of the tectonostratigraphic evolution of the area.

The field data of this study are correlated with the seismic profile SS' (Edgar and Rodriguez, 1990), through Samana Bay located 55 km east of study area (Fig. 1B).

TECTONIC SETTING

The SFR is part of the northern flank of an uplifted marine basin, the Cibao Valley, and is separated from the uplifted subduction complex of the Cordillera Septentrional by the Septentrional fault system (Bowin, 1966; Bowin and Nagle, 1980; Nagle, 1971, 1974; Nagle et al., 1979). This complex was formed by the southward subduction of the North American Plate beneath the Caribbean Plate during Cretaceous to about late Eocene time (Bowin, 1975; Draper and Lewis, 1982; Rosencrantz et al., 1988). By late Eocene time, plate motion changed so that the Caribbean Plate began to move eastward with respect to the North and South American Plates (Burke et al., 1984; Duncan and Hargraves, 1984; Joyce, 1990; Malfait and Dinkelman, 1972; Mattson, 1984; Ross et al., 1986; Sykes et al., 1983; see Fig. 1A). Many authors suggest that the collision of the Bahama Bank, a buoyant feature on the North American Plate, caused a slowing of lateral motion and contributed to the uplift of the subduction complex (Dolan et al., 1990; McCann and Sykes, 1984; Mann et al., 1984; Nagle, 1974). By Neogene time, the northern margin of the Caribbean Plate in northern Hispaniola became a tranpressional boundary caused by local convergence at a restraining bend along the east-west Septentrional strike-slip fault system (De Zoeten and Mann, 1990; Evans, 1990; Lewis, 1980; Mann, et al., 1984; Redmond, 1980).

LITHOSTRATIGRAPHY

Lithostratigraphic data were principally collected by traverses of rivers which parallel and cut across the strike of the rock units. These data were combined with aerial photo interpretations to construct the geologic map (Fig. 2) and the cross-sections (Fig. 3). Field descriptions, measured sections, petrographic and micropaleontological data (Fig. 4; Appendix A) were used to determine the stratigraphic framework of the SFR which is expressed in the composite columnar section shown on Fig. 5.

Within the area of study, seven informal formations have been defined (Figs. 2 and 5). Of these, the El Firme and Cinta Negra formations (both named and described by Guglielmo, 1988) are located to the east of the study area and in a structurally complex area northwest of the SFR. At this time their stratigraphic relationships are incompletely understood.

Of the remaining formations, the Arroyon, Los Cafes, and Castillo formations (named and described by Guglielmo, 1988 and Nadai 1987), consist of a conformable

Larue, D.K., and Draper, G. (eds.),
Transactions of the 12th Caribbean Geological Conference, St. Croix, U.S.V.I., Miami Geological Society, P.O. Box 431552, South Miami, FL 33243, U.S.A.

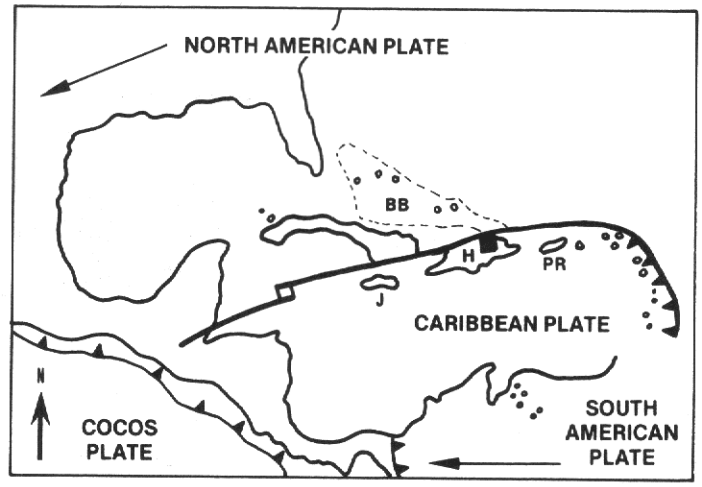

Figure 1A. Tectonic setting of study area. Area of Fig. 1B is represented by box; H=Hispaniola, BB=Bahama Bank, J=Jamaica, PR=Puerto Rico. Arrows indicate plate motions in reference to the Galapagos hot spot frame (Duncan and Hargraves, 1984).

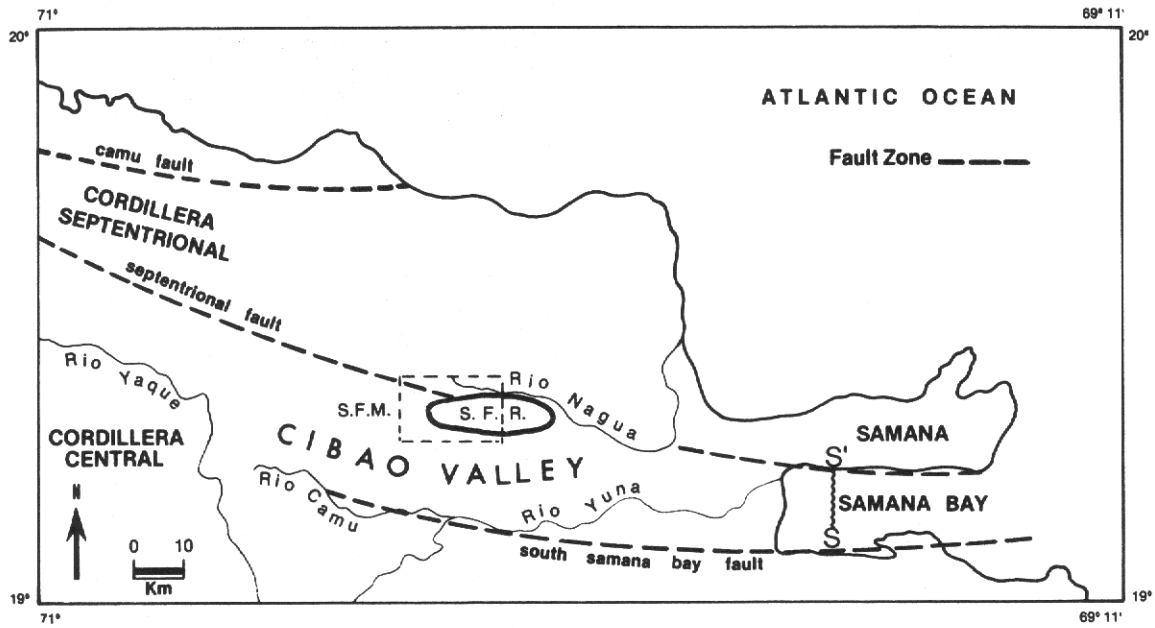

Figure 1B. Northeastern Dominican Republic. Dashed outline indicates study area SFM = San Francisco De Macoris; SFR=San Francisco Ridge.

Figure 1C. Photograph of the San Francisco Ridge. View is southward.

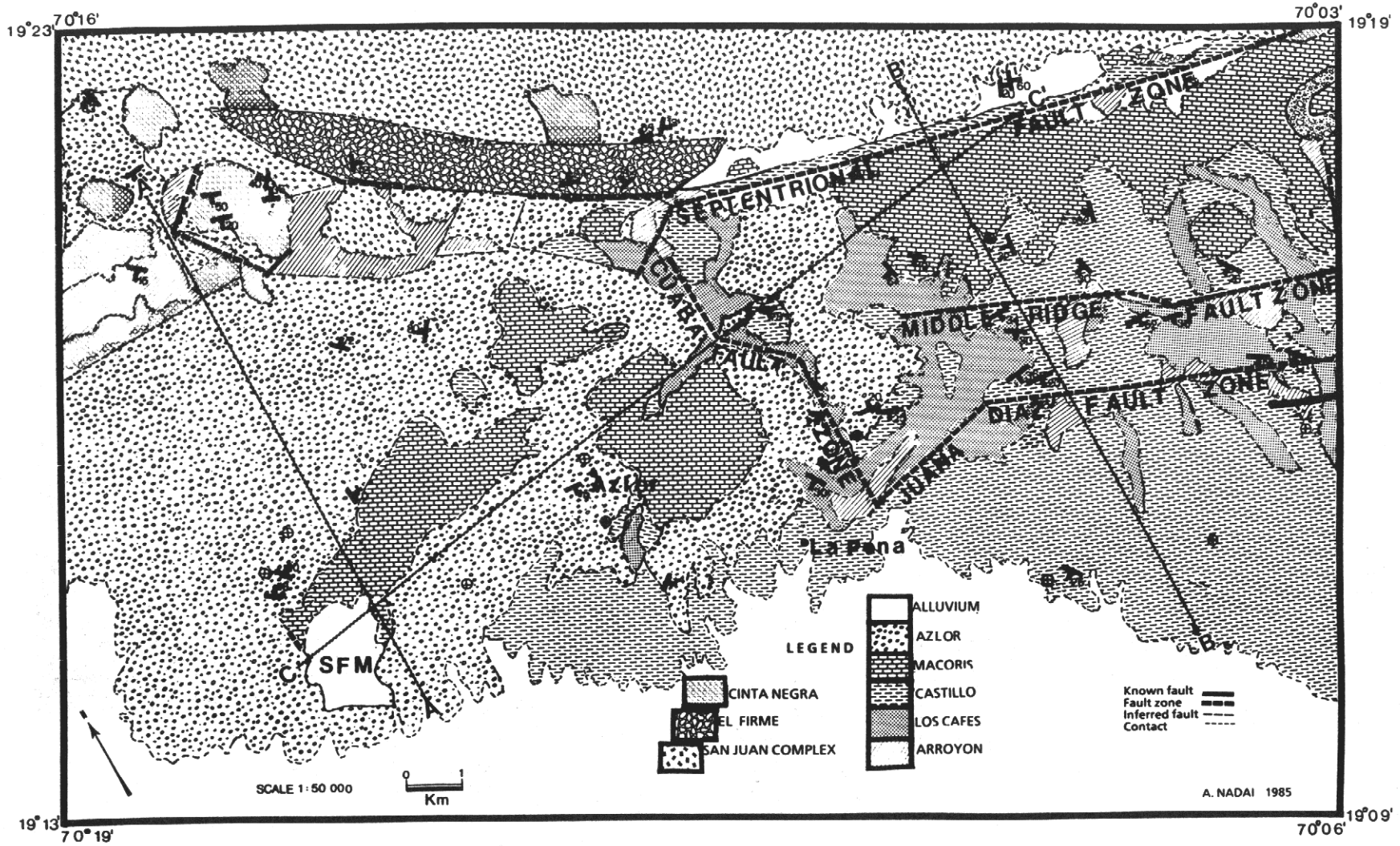

Figure 2. Interpretative geologic map of the western half of the SFR.

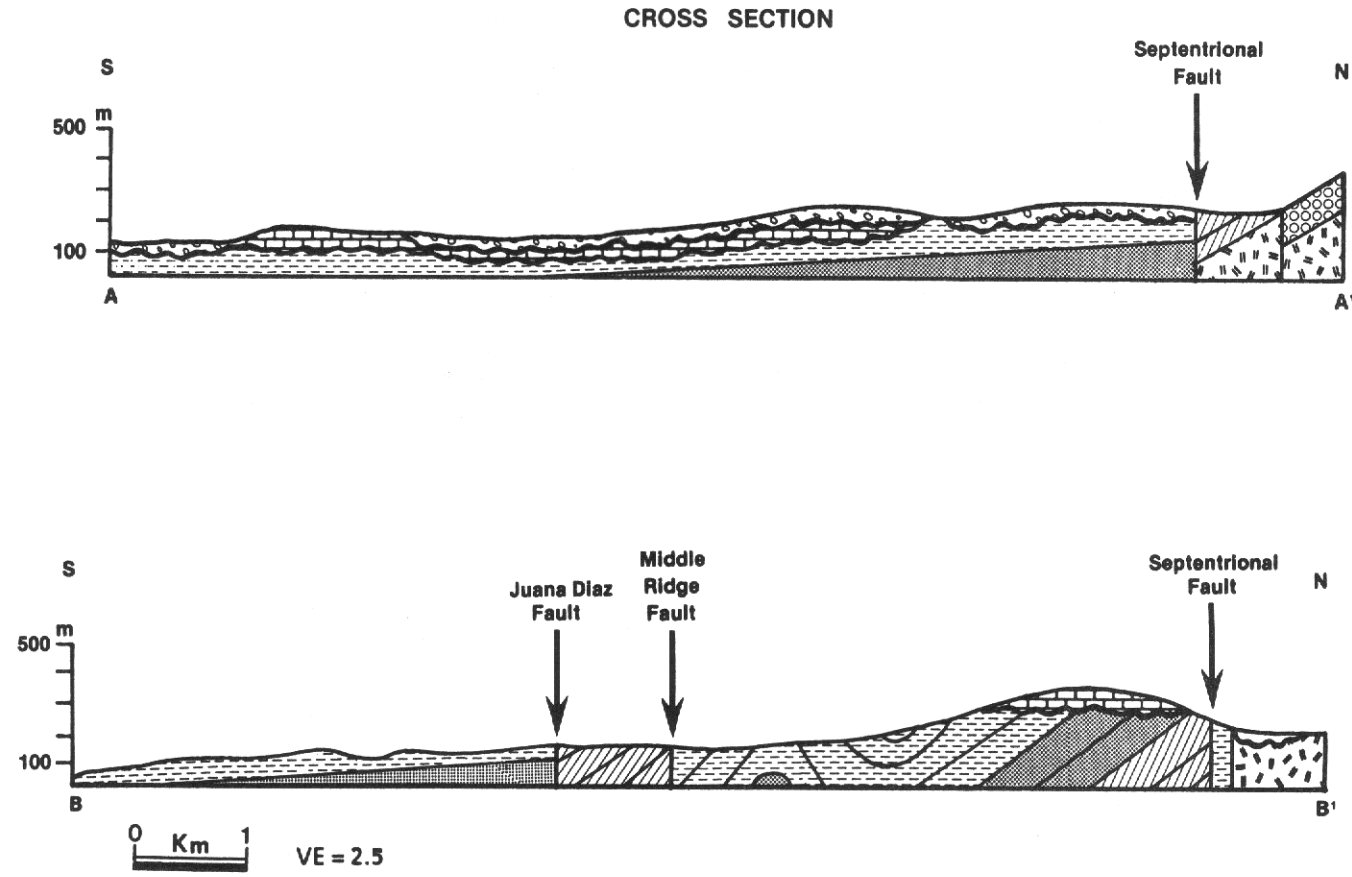

Figure 3. Cross-sections AA' and BB' cut through the entire width of the SFR. See Fig. 2 for line of section. Symbols same as in Figs. 2 and 5.

sequence of deep-water calciclastics. They are unconformably overlain by the Macoris formation (named and described by Nadai, 1987), which is a shallow-marine carbonate. The Macoris is in turn unconformably overlain by the Azlor formation (named and described by Nadai, 1987), which consists mainly of fluvial channel deposits (Fig. 5).

The oldest rocks exposed in the northern part of the study area occur in the Cordillera Septentrional and form the Rio San Juan Complex which was mapped and described by Bowin and Nagle (1982), Draper and Nagle (1985, 1988) and Draper and Lewis (1990). It consists of a gneissic unit, the Cuaba Amphibolite, and a series of banded gabbros, diorites, and ultramafic cumulites called the Rio Boba Intrusive Suite. These units range in age from middle-late Cretaceous to Paleocene (Fig. 2).

The El Firme formation, consists of more than several hundred meters of polylithic diamictite which contains a variety of volcanic, plutonic, metamorphic, and sedimentary rock clasts. All clast types are angular to subangular and range in size from 1 to 30 cm. The matrix consists of sand to silt-sized siliciclastics with minor amounts of carbonate and glauconite grains. The unit is massive with little evidence of stratification or grading. The El Firme formation is still being studied and at this time no firm conclusion can be reached as to the environment of deposition or precise age, although a post-Cretaceous to pre-Miocene age is most likely. This formation crops out along the Septentrional fault and in the Cordillera Septentrional (Fig. 2).

The Cinta Negra formation, is estimated to be more than 300 m thick. It is a massive reefal limestone that has been partially dolomitized and recrystallized. The presence of Montastraea annularis suggests an age of Miocene or younger and indicates that deposition occurred in a shallow-marine environment (J. Wells, pers. comm., 1986). The Cinta Negra formation crops out along the western section of the Nagua River in the Septentrdional fault zone and in the Cordillera Septentrional (Fig. 2).

The Arroyon formation, and is more than 100 m thick. It consists of interbedded calcarenites, calcisiltites, and calcilutites (Fig. 6). Beds range in thickness from 10 to 30 cm and consist of complete or incomplete Bouma sequences. The stratigraphic position as well as the presence of Globigerinoides of the trilobus group date these units as Miocene (R. Liska, pers. comm., 1986). This formation crops out in the SFR and along the Septentrional fault and is conformably

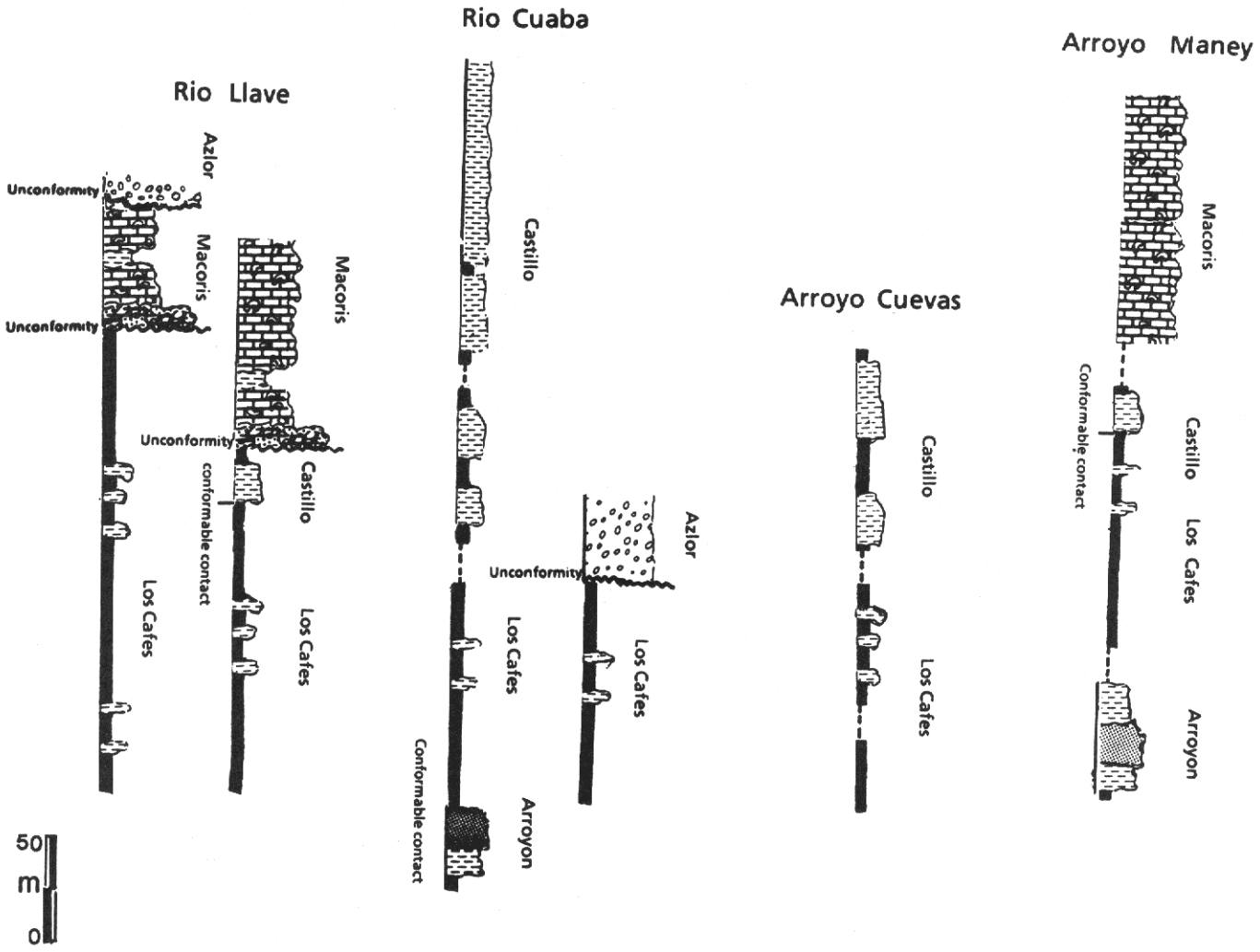

Figure 4. Columnar sections of four river traverses in the study area. a) Rio LLave, b) Rio Cuaba, c) Arroyo Cuevas, d) Arroyo Maney. See Fig. 10 for localities. See Figs. 2 and 5 for descriptions of lithologic symbols.

overlain by the Los Cafes formation (Figs. 2 and 5).

The Los Cafes formation, varies from 100 to 200 m in thickness. It consists of gray to green calcilutite. Conchoidal fracturing on weathered surfaces gives the characteristic texture of this formation. Locally, 2 to 3 cm thick beds of laterally continuous calcisiltite break the monotony of this unit's massive appearance. Based on its stratigraphic position, the Los Cafes formation is tentatively considered to be of Miocene age. This formation crops out along the axis of the SFR and is conformably overlain by the Castillo formation (Figs. 2 and 5).

The Castillo formation, ranges from 50 to 150 m in thickness. It consists primarily of interbedded, bioclastic calcisiltites and calcilutites. Beds vary in thickness from 20 to 40 cm for the calcisiltites and 15 to 30 cm for the calcilutites. In places, bedding is indiscernible and the formation appears massive. Based on the presence of a planktonic foraminiferal assemblage (Globigerinoides, Orbulina universa, Sphaeroidinellopsis penediscens, Globorotalia margaritae, Globigerina nepentes, Neogloquadrina humerosa) the Castillo formation is dated as late Miocene (Zone N-17 fide Blow: 7.1 to 5.4 Ma; R. Liska and E. Robinson, pers. comm., 1986; Saunders et al., 1986). The Castillo formation is unconformably overlain by either the Macoris formation or the Azlor formation (Fig. 7). In southernmost exposures, it is unconformably draped by alluvium. It crops out along the southern flank of the SFR and the Nagua River (Fig. 2).

The Macoris formation is named for exposures near the city of San Francisco de Macoris (Fig. 2) and ranges from 50 to 150 m in thickness. It is a rough-surfaced, grayish-yellow, vuggy, fossiliferous limestone that contains many calcarenite and calcisiltite layers. Its rough texture is due to the presence of the cigar-shaped fossil, Kuphus incrassatus (Vokes, 1972) which can be up to 20 cm long and have a diameter ranging from 1 to 4 cm (Fig. 8). These limestones are partially

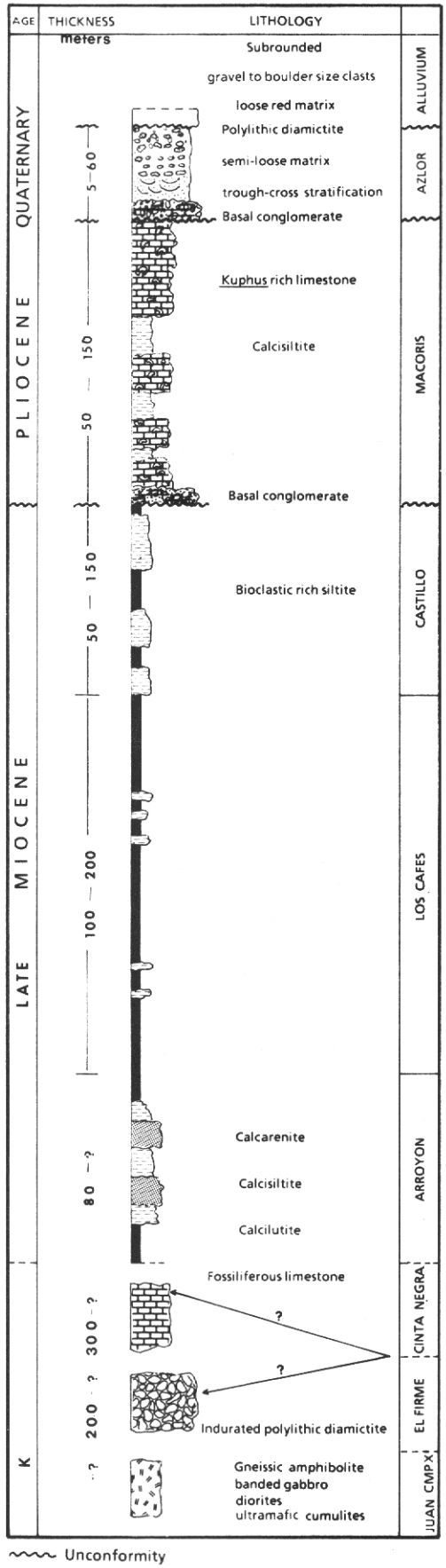

Figure 5. Composite columnar sections for the western SFR area, north slope of Cibao Valley, Dominican Republic.

Figure 6. Arroyon formation. Bedded calcarenite, calcisiltite and calcilutite; interpreted as a deposit of deep-water turbidity currents. This exposure was taken at the northwestern end of the SFR and the fault lies in the Septentrional Fault Zone area.

recrystallized and in places dolomitized and where weathered become loose and chalky. The Macoris formation can be bedded or massive. Where bedded, the layers rich with Kuphus are 30 to 40 cm thick and alternate with silty limestone layers that are 10 to 20 cm thick. The massive appearance of the Macoris formation occurs where Kuphus-rich beds thicken upward to form a massive Kuphus coquina that locally contains an oolitic facies.

The base of the Macoris formation is interpreted as an erosive unconformity (Fig. 7). This interpretation is based on the observations that: (1) The basal beds of the Macoris formation display erosive channeling and contain clasts of the Castillo and Los Cafes formations; (2) along the flanks and axis of the SFR, the flat to moderately tilted Macoris strata overlie more steeply dipping and faulted beds of the underlying formations (Fig. 3); and (3) the abrupt change to shallow-marine carbonates (Macoris formation) from deep-water calciclastics (Arroyon, Los Cafes, and Castillo formations) is incompatible. Because the Macoris formation unconformably overlies the late Miocene Castillo formation, it is most likely early (?) Pliocene in age. The Macoris formation is unconformably overlain by the Azlor formation (Fig. 5).

The Azlor formation is named for exposures near the village of Azlor (Fig. 2) and ranges in thickness from 5 to 60 m. It is a loose to semi-indurated, poorly-sorted polylithic diamictite composed of a variety of sedimentary, igneous, and metamorphic rock clasts. The matrix consists of red sand

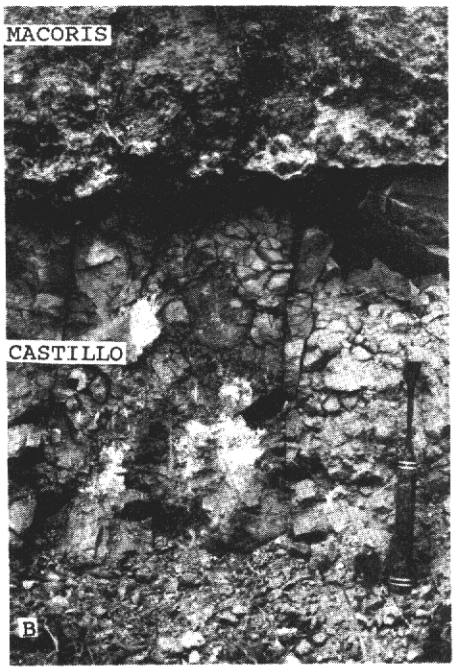

Figure 7. Unconformity between the Castillo and Macoris formations. The former is interpreted as a deep-water calciclastic deposit and the latter as a shallow-marine carbonate. A. View of the outcrop. B. Boxed area shown in A.

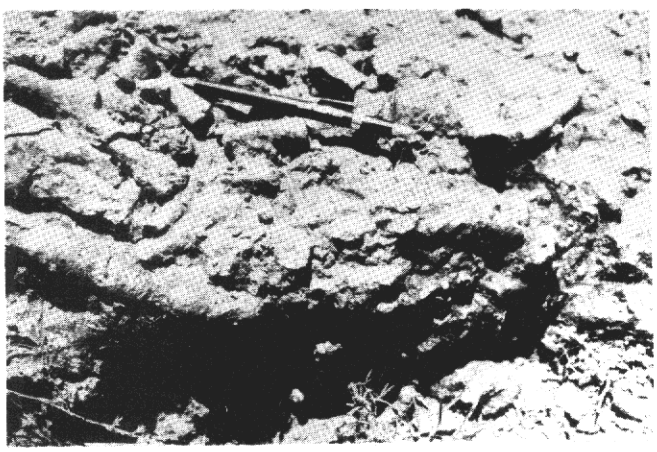

Figure 8. Macoris formation, a Kuphus-rich limestone.

Figure 9. Azlor formation, a semi-indurated, polylithic diamictate interpreted as a fluvial channel deposit.

and silt. The Azlor formation is poorly bedded to massive and displays a range of sedimentary structures from disorganized fabric to trough cross-bedding and clast imbrication (Fig. 9). Because of its stratigraphic position, the Azlor formation can be no older than early Pliocene. This formation is interpreted as a fluvial deposit. The basal erosive contact is in the form of channels that have carved into the older formations. The Azlor covers most of the western half of the study area.

STRUCTURES

The outstanding structural features which characterize the study area of the San Francisco Ridge are five faults (Fig. 2): the Septentrional and Juana Diaz faults that run along its entire length; the Cuaba fault which crosses the ridge to the east of San Francisco de Macoris; the Middle Ridge fault which cuts the ridge lengthwise in an E-W direction; and an unnamed fault which trends N-S through the middle of the ridge.

The Septentrional fault was described by Bowin in 1966 and mapped by Blesch in 1966; but it was recognized in unpublished reports since 1943 (De Zoeten and Mann, (1990). The Juana Diaz fault was identified in the field by Guglielmo et al., (1986), the Cuaba fault and the Middle Ridge fault were identified and mapped in this study and the unnamed fault was observed in the field by Winslow (pers. comm., 1987); the latter two faults need further investigations. The change in drainage patterns, field mapping of structurally deformed formations and tectonized zones, and lineaments observed on aerial photos on a scale of 1:40000 and on SEASAT-SAR images, are used collectively as evidence for the existence of these faults (Fig. 10). These faults cut across the topography at high angles, but their displacements were not established. The presence of triangular facets on the southern flanks of the Cordillera Septentrional with their bases parallel to the fault trace suggests a dip-slip component to the mainly left-lateral strike-slip displacement observed west of this study area (Eberle et al. 1980; Mann et al. 1984; Winslow and McCann, 1985; Fig. 11). The displacement of the Septentrional fault separates the Cordillera Septentrional from the Cibao Valley. The Juana Diaz and Cuaba faults separate the intensely deformed Miocene formations of the SFR (Arroyon, Los Cafes and Castillo) from the much less deformed Pliocene or younger formations of the Cibao Valley (Macoris and Azlor).

The trend of the three subparallel, E-W faults and the SFR structure ranges between N75W to N85W. In the study area, none of the five faults appear to cut across the Pliocene or younger formations (Macoris and Azlor; Fig. 3).

CORRELATIONS

Cross-section BB', across the SFR structure matches remarkably well with the N-S seismic profile SS'of the Samana Bay (Figs. 12 and 13). The Septentrional, Middle Ridge and Juana Diaz faults align with the three steep south-dipping faults offshore with a slight change in strike from WNW to approximatly E-W, a trend previously observed by Mann et al. (1984). The topographic high of the SFR aligns with the subsurface uplifted basement. Both profiles BB' and SS' show the deformed Miocene strata to be overlain by the relatively nondeformed Pliocene or younger strata and separated from it by an unconformity. The Juana Diaz and Middle Ridge faults and their inferred extensions along the seismic profile do not cut across Pliocene formations. However, in the seismic profile, the inferred extension of the Septentrional fault does cut across the Pliocene or younger formations. This agrees with the field observations west (Winslow and Mc Cann, 1985) and east (Guglielmo and Winslow, 1986) of this study area which also have shown that the Septentrional fault cuts the Pliocene or younger formations.

The proposed correlation of the field data in the west with seismic interpretations in the east suggests that the SFR, which is expressed topographically in the study area, continues eastward as a structure in the subsurface and offshore beneath Samana Bay (Fig. 13).

The Miocene-Pliocene carbonate strata identified in this study are coeval with the Villa Trina Formation located in the Cordillera Septentrional, which lies unconformably (Vaughan et al. 1921) and in places conformably (De Zoeten and Mann, in prep.) over the 4000 m thick deep-marine siliciclastics, the Altamira and La Toca Formation of upper Eocene to middle Miocene age.

TECTONOSTRATIGRAPHIC EVOLUTION

The lateral and vertical facies characteristics as well as the faunal assemblages indicate a relatively deep-water marine depositional environment for the Miocene strata (Arroyon, Los Cafes, and Castillo formations). During latest Miocene time, this deep marine basin was uplifted and deformed. The deformational event must have ceased or diminished by Pliocene time because the folded and highly faulted Miocene strata exposed along the SFR are erosionally truncated and unconformably overlain by the much less deformed Macoris formation (Fig. 3). The interpretation of the Macoris as a shallow-marine carbonate and the observation that it is relatively thin (<200 m) indicate that tectonism was minimal and that the basin maintained shallow-marine conditions. The area became subaerial during post-Macoris time (mid-late Pliocene ?) as evidenced by the unconformably overlying fluvial channel deposits of the Azlor formation.

Both unconformities (base of the Macoris formation and base of the Azlor formation) rise topographically along the SFR, which suggests a post-Azlor warping (Fig. 14). This event is responsible for the topographic expression of the SFR. The age and nature (block rotation, fault reactivation, compressional folding, etc.) of this latest deformation, however, remain to be determined.

It does appear though, that tectonism dramatically overprinted the relative global eustatic sea level changes proposed by Vail, Mitchum and Thompson (1977).

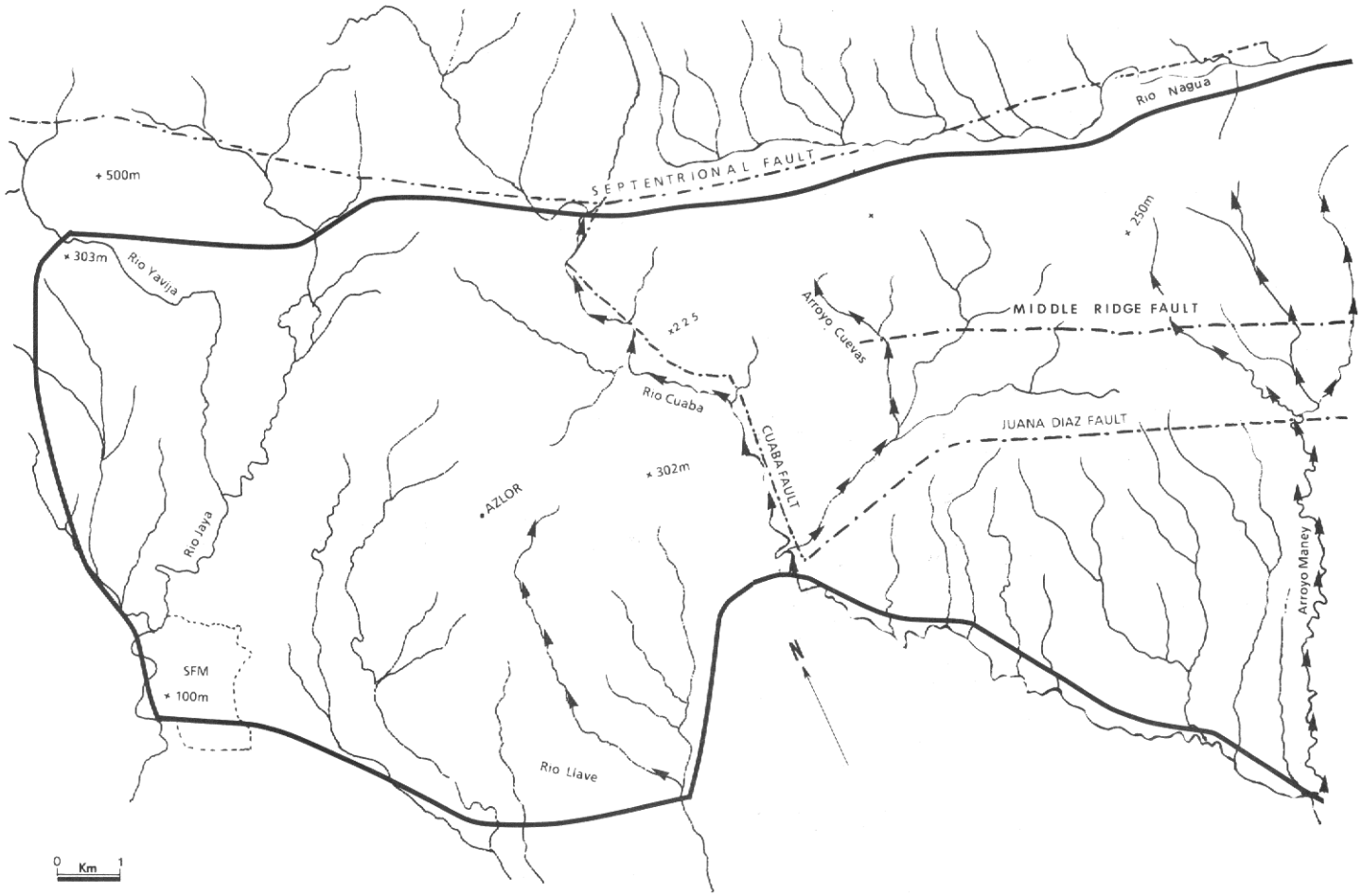

Figure 10. Drainage patterns and faults along the western SFR region. The solid line outlines the area of the western half of the SFR. The arrow points indicate the river traverses interpreted in Fig. 4.

Figure 11. Cordillera Septentrional with faceted spurs, view northward from the Cibao Valley.

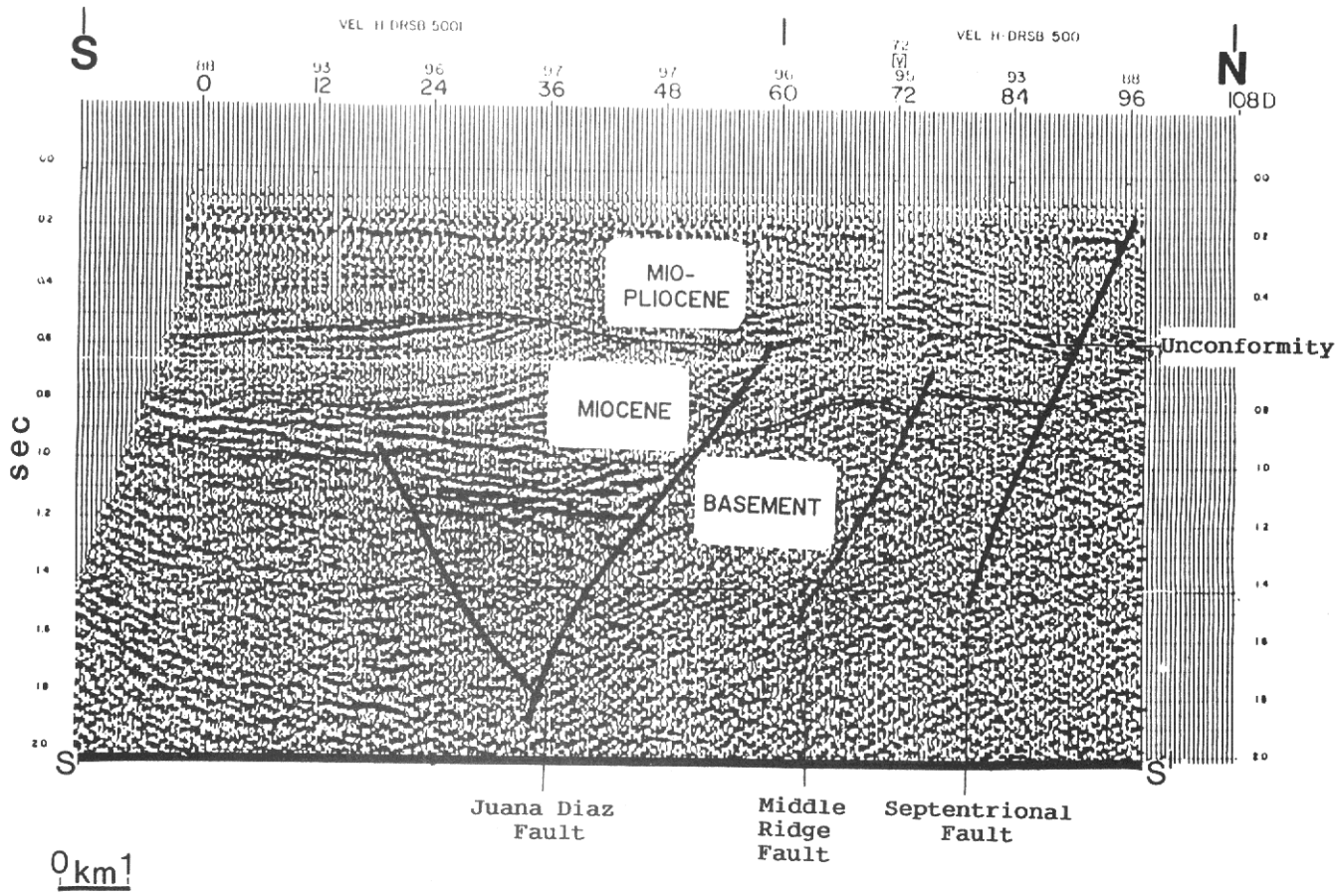

Figure 12. N-S seismic profile through Samana Bay with stratigraphic interpretation by Edgar and Rodriguez, (1990). Location of SS' profile shown in Fig. 1B.

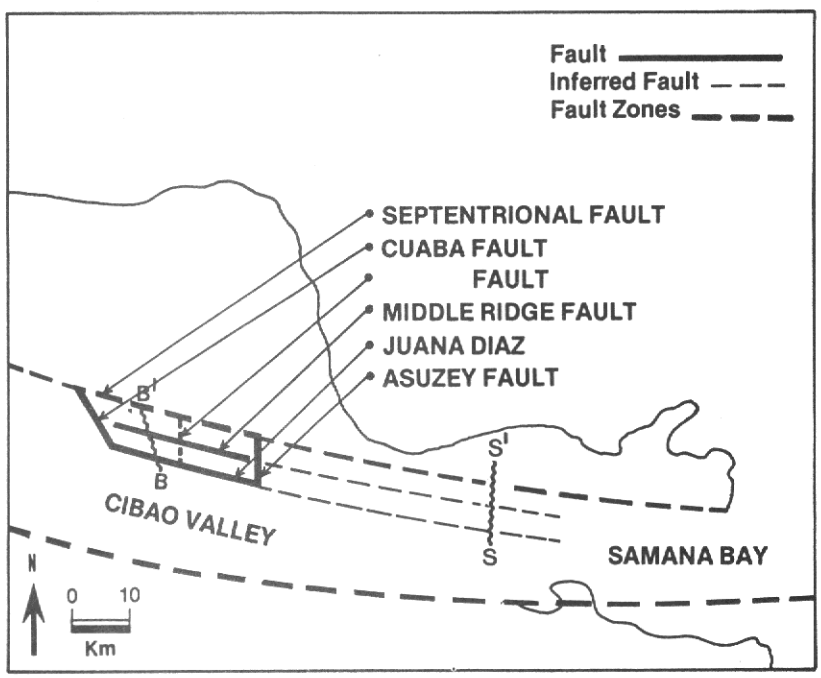

Figure 13. Suggested correlation of the faults of the SFR with the faults of the Samana Bay seismic profile. The Asuzey fault is east of the study area and is described by Guglielmo and Winslow (1988).

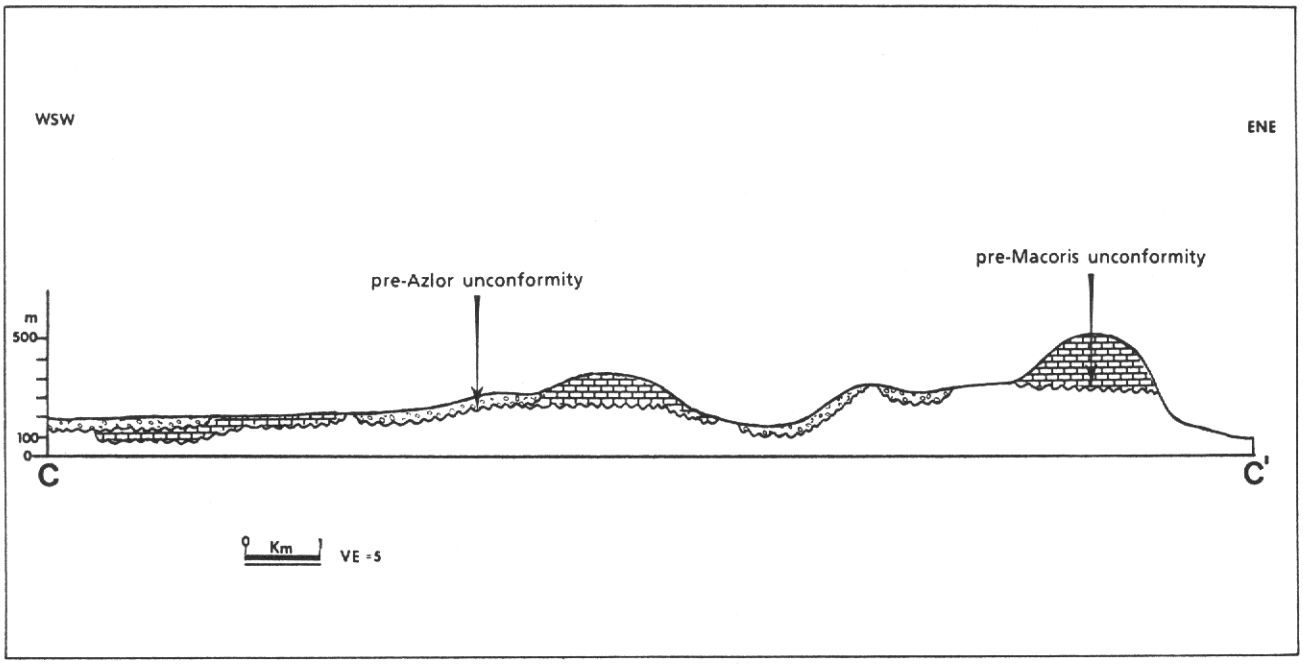

Figure 14. Cross-section showing the topographic variation of the Pliocene or younger unconformities. Lithologic symbols the same as in Figs. 2 and 5.

CONCLUSION

The Neogene strata exposed along the San Francisco Ridge on the northern slope of the Cibao Valley, which is part of the uplifted subduction complex of northeastern Hispaniola, have been divided into seven formations. These strata reveal the following tectonostratigraphic evolution:

1) During the Miocene, this area was a relatively deep-marine basin as evidenced by a conformable sequence of turbidite strata. 2) A late Miocene tectonic event deformed those strata in the SFR. 3) During the early Pliocene, the deformational event ended and shallow-marine carbonates were unconformably deposited on the deformed Miocene strata. 4) The basin subsequently became subaerial as indicated by a series of unconformably overlying fluvial channel deposits. 5) The Pliocene or later uplift is ultimately responsible for the SFR relief. This is revealed by the varying topographic location off and on the SFR of the two Pliocene or later unconformities. The mechanisms of the pre-Pliocene uplift of the deep-marine Cibao Basin and the later uplift of the SFR have not been identified. The topographic expression of the SFR dies out about 10 km west of Samana Bay yet this structure, by correlation with seismic data, appears to continue to the east offshore beneath the bay.

ACKNOWLEDGEMENTS

I acknowledge Prof. Margaret Winslow for giving me the opportunity to work on the San Francisco ridge. This project was funded by the City University of New York faculty research award # 665185 and Petroleum Research Fund grant # 775520. I thank Professor Anthony R. Prave who guided me into the stratigraphic interpretation or my study. I acknowledge my colleague Giovanni Guglielmo for his cooperation during our field work. Above all I would like to express my gratitude to Robert Liska and Dr. Edward Robinson who dated my samples and made my stratigraphic interpretation sound. I am thankful to Dr. Terence Edgar for allowing me to use his data and to Prof. Grenville Draper who supplied me with the most recent literature and constructively reviewed earlier versions of this work .

APPENDIX A

Age and paleobathymetry of the SFR formations:

El Firme formation (Guglielmo and Winslow 1986).
Bathymetry: shallow water benthic and planktic foraminifera and calcareous algae. (C.B. Schreiber, pers. comm., 1986).

Arroyon formation (poor preservation of fossils, reworked or diagenetically altered)
Age: based on one Globigerinoides of the trilobus group, dates the fauna as Miocene or younger (R. Liska, pers. comm., 1986).
Bathymetry: middle shelf environment of deposition (R. Liska, pers. comm., 1986).
Indeterminate benthic fauna: Uvigerinids, Cassidulinids, Buliminids, Miliolids and Anomalinids.

Los Cafes formation
(probably equivalent to the Castillo formation).

Castillo formation
Age: 7.1-5.4, my bp, late Miocene, (Zone N-17 fide Blow), suggested from planktic assemblage.
(R. Liska and E. Robinson pers. comm.,1986).

Bathymetry: open marine shelf environmnent 200 m depth or deeper, depends on location as suggested from benthic assemblage.
Planktic Foraminifera: Globigerinoides ? canimarensis, G. obliquus, G. quadrilobatus, G. trilobus, Orbulina universa, Sphaeroidinellopsis penedehiscens, Globorotalia cf margaritae, G.scitula, G. pseudomiocenica, Globigerina nepenthes, G. eamesi, Neogloboquadrina humerosa.
Benthic Foraminifera: Nodosaria spp, Siphonina pulchra Cibicidoides, Hoeglundina elegans, Planulina ariminensis, P. cf foveolata, Pullenia bulloides, Melonis barleeanus, Valvulineria sp., Sphaeroidina bulloides, Discorbis sp., Uvigerina peregrina, Globocassidulina subglobosa.

Macoris formation
Age: Middle Miocene or younger, suggested by the foraminifera assemblages (R. Liska and E. Robinson, pers. comm., 1986).
Bathymetry: shelfal environments, suggested by benthic foraminifera (R. Liska, pers. comm., 1986), intertidal suggested by various bioclasts analysed in thin sections coralline algae, Halimeda (0.5 to 10 m deep), Kuphus (intertidal), Miliolids (C.B. Schreiber, pers. comm., 1986).
Planktic Foraminifera: Orbulina spp., Globigerinoides trilobus trilobus, Globigerinoides trilobus immaturus, Hastigerina siphonifera.
Benthic Foraminifera: Heterostegina spp., Amphistegina spp.

REFERENCES

Blesch, R.R., 1966, Mapa geologico preliminar, Republica Dominicana, 1:250,000 in: Mapas, II, Reconocimiento y Evaluacion de los Recursos Naturales de la Republica Dominicana, Union Panamericana.

Bowin, C.O., 1966, Geology of the Central Dominican Republic, Geol. Soc. America, Memoir 98, p. 11-84.

Bowin, C.O., 1975, The Geology of Hispaniola, in, Naim, A.E.M. & Stehli, F.G., eds., The Ocean Basins and Margins, 3: Plenum Publishing Corp., New York, p. 501-552.

Bowin, C.O., and Nagle, F., 1982, Igneous and metamorphic rocks of northern Dominican Republic: an uplifted subduction complex, Transactions of the 9th Caribbean Conference 1980, Santo Domingo, Dominican Republic, v. 1, p. 39-50.

Burke, K., Cooper, C., Dewey, J. F., Mann, P., and Pindell, J.L., 1984, Caribbean tectonics and relative plate motions, Geol. Soc. America Memoir 162, p. 31-63.

De Zoeten, R., and Mann, P., 1990, Structural geology and Cenozoic tectonic history of the Central Cordillera Septentrional, Dominican Republic, in, Mann, P., Draper, G. and Lewis, J., eds., Geologic and Tectonic Studies in Hispaniola: Geol. Soc. America Special Paper, in press.

Dolan, J., Mann, P, Monech, S., Shiroma,J., and Keller, G., 1990, Paleogene sedimentary basin development in the Greater Antilles: record of a collisional to strike-slip transition, in, Mann, P., Draper, G. and Lewis, J., eds., Geologic and Tectonic Studies in Hispaniola: Geol. Soc. America Special Paper, in press.

Draper, G., and Lewis, J.F., 1982, Cenozoic tectonic evolution and sedimentation in Hispaniola, Transactions of the 9th Caribbean Geologic Conference 1980, Santo Domingo, Dominican Republic, v. 1, p. 53-65.

Draper, G., and Nagle, F., 1988, Blueschist and eclogite bearing melanges in northern Hispaniola, Transactions of the 11th Caribbean Geologic Conference 1986, Barbados, v. 33, p. 1-9.

Duncan, R.A., and Hargraves, R.B., 1984, Plate tectonic evolution of the Caribbean region in the mantle reference frame, in, Bonini, R., Hargraves, R.B., and Shagam, R., eds., Caribbean-South American Plate Boundary and Regional Tectonics: Geol. Soc. America Memoir 162, p. 1-93.

Eberle, W., Hirdes, W., Muff, R., and Pelaez, M., 1982, The geology of the Cordillera Septentrional (Dominican Republic), Transactions of the 9th Caribbean Geologic Conference 1980, Santo Domingo, Dominican Republic, v. 2, p. 619-632.

Edgar, T., and Rodriguez,R.W., 1990, Structure and Stratigraphy of the Cibao Basin, in, Mann, P., Draper, G., and Lewis, J., eds., Geologic and Tectonic Studies in Hispaniola: Geol. Soc. America Special Paper, in press.

Evans, C., 1990., Facies evolution in a Neogene transpressional Basin: Cibao Valley, Dominican Republic, in, Mann, P., Draper, G., and Lewis, J., eds., Geologic and Tectonic Studies in Hispaniola: Geol. Soc. America Special Paper, in press.

Guglielmo, G. Jr., and Winslow, M.A., 1988, Push-Up structure in a transpressional environment: Northeastern Hispaniola, Transactions of the 11th Caribbean Geologic Conference 1986, Barbados, v. 18, p. 1-21.

Guglielmo, G. Jr., Winslow, M.A., Castelli-Nadai, A., and McCann, W.R., 1986, Push-Up structure in a transpressional environment: Northeastern Hispaniola, Geol. Soc. America, Abstracts with Programs, 18, p. 622.

Joyce J., 1990, Blueshist metamorphism and deformation on the Samana Peninsula - A record of subduction and collision in the Greater Antilles, in, Mann, P., Draper, G., and Lewis, J., eds., Geologic and Tectonic Studies in Hispaniola: Geol. Soc. America Special Paper, in press.

Lewis, J.F., 1982, Cenozoic tectonic evolution and sedimentation in Hispaniola, Transactions of the 9th Caribbean Conference 1980, Santo Domingo, Dominican Republic, v. 1, p. 65-75.

Malfait, B.T., and Dinkelman, M.G., 1972, Circum-Caribbean tectonic and igneous activity and the evolution of the Caribbean plate, Geol. Soc. America Bull., v. 83, p. 251-272.

Mann, P., Burke, K., and Matsumoto, T., 1984, Neotectonics of Hispaniola: plate motion, sedimentation, and seismicity at a restraining bend, Earth and Planetary Sci. Letters, v. 70, p. 311-3244.

Mattson, P.H., 1984, Caribbean structural breaks and plate movements, in, Bonini, R., Hargraves, R.B., and Shagam, R., eds., Caribbean-South American Plate Boundary and Regional Tectonics: Geol. Soc. America Memoir

162, p. 131-152.
McCann, W.R., and Sykes, L.R., 1984, Subduction of aseismic ridges beneath the western Caribbean plate: Implications for the tectonics and seismic potential of the northeastern Caribbean, Jour. Geophys. Research, v. 89, p. 4493-4519.
Nagle, F., 1971, Geology of the Puerto Plata Area, Dominican Republic, relative to the Puerto Rico Trench, Transactions of the 5th Caribbean Geologic Conference, Geol. Bull. No. 5, Queens College Press, p. 79-84.
Nagle, F., 1974, Blueschist, eclogite, paired metamorphic belts and the early tectonics of Hispaniola, Geol. Soc. America Bull. v. 85, p. 1461-1466.
Nagle, F., Palmer, C.N., and Antonini, G.A., 1979, Hispaniola: Tectonic Focal Point of the Northern Caribbean, three geologic studies in the Dominican Republic, in, Lidz, B., and Nagle, F., eds., Miami Geol. Soc., 28 p.
Nadai, A.C., 1987, Tectonostratigraphy of the San Francisco ridge area in the northeastern Dominican Republic (M.A. Thesis): City College of the City University of New York, New York, 33 p.
Redmond, B., 1982, The Tertiary of the Central Cordillera Septentrional, in Transactions of the 9th Caribbean Conference 1980, Santo Domingo, Dominican Republic, v. 1, p. 199-210.
Rosencrantz, E., Ross, M.I., and Sclater, J.L., 1988, Age and spreading history of the Cayman Trough as determined from the depth, heat flow, magnetic anomalies, Jour. Geophys. Research, v. 93, p. 2141-2157.
Ross, M., Rosencrantz, E., Scotese, C.R., and Sclater, J., 1986, New interpretation of spreading rates in the Cayman Trough, Geol. Soc. America, Abstracts with Programs, v. 18, 733 p.
Saunders, J., Jung P., and Biju-Duval, B., 1986, Neogene paleontology in the northern Dominican Republic, Bull. American Paleont., v. 89, No.323, 78 p.
Sykes, L.R., McCann, W.R., and Kafke, A.L., 1892, Motion of Caribbean plate during the last 7 million years and implications for earlier Cenozoic movements, Jour. Geophys. Research, v. 70, p. 5065-5074.
Vail, P.R., Mitchum, R.M., Jr. and Thompson, III, S., 1977, Global cycles of relative changes of sea level, in. Payton C.E., ed., Seismic stratigraphy-applications to hydrocarbon exploration: American Assoc. Petrol. Geologists, Memoir 26, p. 399-444.
Vaughan, T.W., Cooke, W., Condit, D.D., Ross, C.P., Woodring, W.P., and Calkins, F.C., 1921, A geological reconnaissance of the Dominican Republic, Geological Survey of the Dominican Republic, Memoir 1, prepared by the U.S. Geologic Survey, Washington, D.C., 268 p.
Vokes, H.E., 1972, On the presence of Kuphus incrassatus gabb: Tulane Studies in Geol. and Paleont., v. 10., No. 1, p. 41-46.
Winslow, M.A., and Mc Cann, W.R., 1985, Neotectonics of a subduction/strike-slip transition zone: the northeastern Dominican Republic, Geol. Soc. America, Abstracts with Programs, v. 17, p. 753.

PRELIMINARY REPORT ON A LATE TERTIARY PLANT MICROFOSSIL ASSEMBLAGE FROM HAITI

Alan Graham
Department of Biological Sciences
Kent State University
Kent, Ohio 44242

ABSTRACT

Twenty-five fossil pollen and spore types have been recovered from the late Tertiary Artibonite flora of Haiti. These are monolete fern spore (36%), Alsophila (6%), Pteris types 1-3 (type 1= 11%), cf. Antrophyum, trilete fern spore (types 1, 2), Pinus (16%), Palmae (types 1, 2), Hygrophila, Chenopodiaceae/Amaranthaceae, Compositae (types 1-4; 9%), Alchornea, Alfaroa/Oreomunnea, Oryctanthus, Malpighiaceae, Allophylus, and unknown types 1-3. The principal vegetation types suggested by the fossil flora are pine forest and cloud forest, with a fern marsh bordering the depositional basin. Communities of drier to arid aspect, savannas, and high altitude vegetation are not represented. The age of the flora is estimated as late Miocene to possibly middle Pliocene. Annual temperatures ranged between about 23-26° C at 400 m elevation, and 17-19° C at elevations of about 1,400 m. Annual rainfall is estimated at about 1,300 ml and was seasonal. The affinity of the flora is distinctly North American, consistent with plate tectonic models showing the proto-Greater Antilles located off southwestern Mexico during the early Tertiary and moving eastward at an average rate of 2-3 cm/yr. The development of South American affinities, other than by long-distance dispersal throughout the Cenozoic, was facilitated in later Tertiary times by eastward movement away from Mexico/proto-Central America and emergence of the Lesser Antilles in the Eo-Oligocene.

INTRODUCTION

In the early 1900's the United States Geological Survey carried out field studies in Hispaniola under the direction of T. Wayland Vaughan. The Haitian phase of the project was supervised by W. P. Woodring, and in 1920 and 1921 he made collections of fossil plants from 13 localities which were sent to E. W. Berry for study. The specimens were few in number and generally fragmentary and poorly preserved, but from them Berry (1923) identified nine species (Table 1). Almost all of the better preserved specimens came from a locality designated W 185 F (station 7544). The location is given as "Department de l'Ouest, cut along road from Mirebalais to Las Cahobas, on north side of ravine at foot of mountain on north side of gap. W. P. Woodring, collector. January 8, 1921" (Berry, 1923, p. 2; Fig. 1). In 1981 permission was granted to remove small pieces from the outer matrix of the Haiti specimens, presently in the collections of the Smithsonian Institution, for pollen and spore analysis. A small assemblage of fair diversity and preservation was recovered. The flora is considered important, nonetheless, because it is the first paleopalynological study for Hispaniola, and provides the only paleobotanical information for the island since the publication of Berry (1923).

MATERIALS AND METHODS

Small pieces from the outer matrix were broken off and scraped clean to remove contaminants and oxidized plant microfossils. The material was then broken in a mortar and pestle, transfered to 400 ml Nalgene beakers, and placed in HCl for one hour for removal of carbonates, overnight in HF for removal of silicates, and for one hour in HNO_3 for oxidation of organic debris. The samples were centrifuged for 4 minutes at 1,400 rpm in 150 ml Nalgene centrifuge tubes and washed four times with distilled water between each acid treatment. The material was then acetolyzed (nine parts of acetic anhydride to one part concentrated H_2SO_4) for three minutes in a water bath at ca. 85° C, preceded and followed by rinses in glacial acetic acid, and treated with 10% KOH at ca. 85° C for three minutes for final breakdown of organic debris. After the final centrifuging, the tubes were inverted and allowed to drain for four hours. Warm (melted) glycerine jelly was then added (about twice the amount of jelly for the amount of material in the centrifuge tube), stirred, two drops placed on a slide on a warming table, a cover slip added, and the slides allowed to cool to solidify the jelly. The slides were labeled (Haiti, Miocene, Berry specimen, Smithsonian, USGS 7544-station 185, and slide number), and sealed with CoverBond. The specimens were photographed with a Leitz Orthoplan microscope with automatic camera using Panatomic X film. Location of the specimens on the slides is by England Slide Finder coordinates (e.g., N-25). All materials are deposited in the palynology collections at Kent State University.

RESULTS

The ferns are represented in the Artibonite microfossil flora by eight kinds of spores, including two unknowns (Table 1). Laevigatisporites (Fig. 2) is a smooth, reniform spore produced by many genera in at least three families- Blechnaceae, Polypodiaceae, and Pteridaceae. Laevigatisporites ranges from Paleozoic to Recent, and is of limited stratigraphic or paleoecologic value. Three kinds of Pteris spores are present, and the most common form is illustrated in Fig. 3. Pteris is a genus of ferns, with three species in Hispaniola having spores similar to the most abundant fossil specimens (Fig. 3), P. podophyla Sw., P. stridens J. G. Agardh, and P. tripartita Cav. (Mickel, pers. comm., 1989). Judd (1987) lists two additional species growing on Haiti, P. hispaniolica Maxon and P. longifolia L. Pteris stridens occurs at 1,400 to 2,300 m elevation in humid, broadleaf forests with Podocarpus, tree ferns, and Brunellia. Pteris podophyla grows at elevations of 500 to 1,500 m in very humid, broadleaf forests. Pteris tripartita occurs from sea level to about 800 m in humid, broadleaf forests with Prestoea (Palmae), but it is an Old World fern

Larue, D.K., and Draper, G., eds.,
Transactions of the 12th Caribbean Conference,
St.Croix U.S.V.I., Miami Geological Society,
P.O. Box 14433, Coral Gables, FL 33114

Table 1. Composition of the megafossil and microfossil Artibonite flora, Republic of Haiti. Spellings and family assignments for megafossils follow original assignments in Berry (1923)

Megafossils

Characeae
Chara woodringi Berry

Polypodiaceae
Gymnogramme woodringi Berry

Lauraceae
Mespilodaphne hispaniolana Berry

Nyctaginaceae
Pisonia conditi Berry

Rubiaceae
Guettarda cookei Berry

Simarubaceae
Simaruba haitensis Berry

Sapotaceae
Bumelia cuneatafolia Berry
Chrysophyllum cahobasensis Berry
Mimusops praeparvifolia Berry

Microfossils

Monolete fern spore

Cyatheaceae
Alsophila

Pteridaceae
Pteris (types 1-3)

Vittariaceae
Antrophyum

Trilete fern spore (types 1, 2)

Pinaceae
Pinus

Palmae (types 1, 2)

Acanthaceae
Hygrophila

Cheno/am

Compositae (types 1-4)

Euphorbiaceae
Alchornea

Juglandaceae
Alfaroa/Oreomunnea

Loranthaceae
Oryctanthus

Malpighiaceae

Sapindaceae
Allophylus

Unknowns (types 1-3)

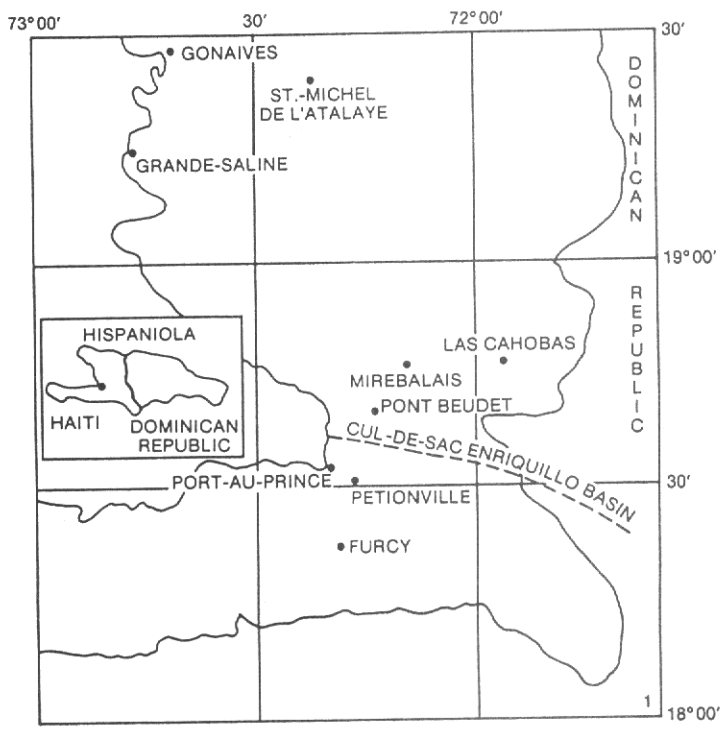

Figure 1. Index map of place names cited in text. The fossil locality is about mid-way on a road connecting Mirebalais and Las Cahobas. The dot on the inset map shows the location of Port-au-Prince.

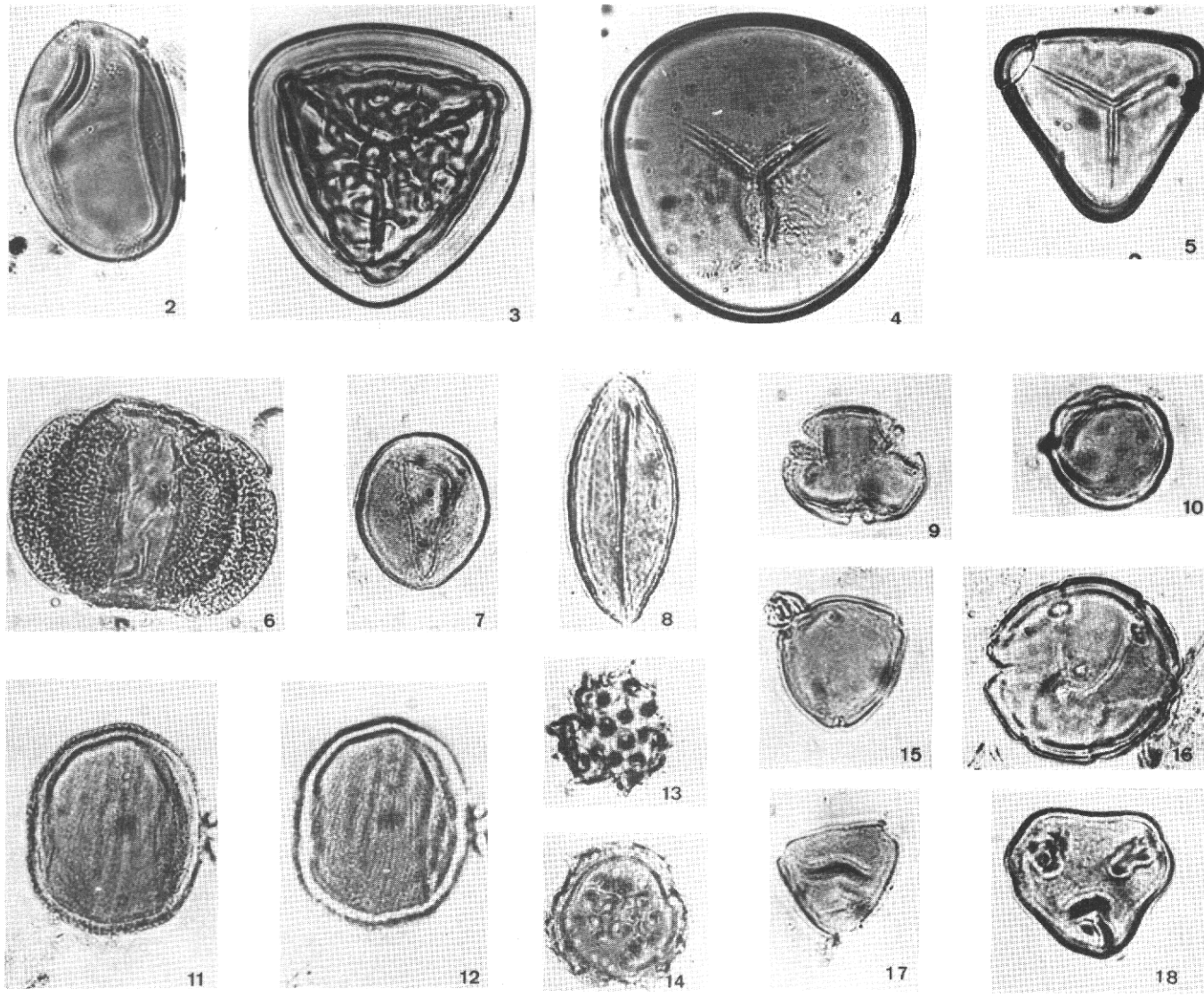

Figures 2-18. Fossil pollen and spores from the upper Tertiary (upper Miocene to middle Pliocene) Artibonite group, Republic of Haiti. (2). Monolete fern spore (Laevigatisporites), slide 1, England Slide Finder coordinates N-25, size: 60 x 38 um. (3). Pteris (Polypodiaceoisporites; Pteridaceae), slide 3, ESF M-26, size: 65 um. (4). cf. Antrophyum (Triletes; Vittariaceae), slide 8, ESF J-50, size: 81 um. (5). Alsophila (Cyatheaceae), slide 8, ESF N-35, size: 48 um. (6). Pinus (Pinaceae), slide 9, ESF V-45, size: 68 x 50 um. (7). Palmae, slide 8, ESF K-46, size: 38 x 32 um. (8). Palmae, slide 1, ESF G-47, size: 58 x 26 um. (9). Alchornea (Psilatricolporites operculatus; Euphorbiaceae), slide 10, ESF N-36, size: 32 um. (10). Chenopodiaceae/-Amaranthaceae (Psilaperiporites), slide 3, ESF G-52, size: 24 um. (11). Hygrophila (Acanthaceae; no previous reports in the Gulf/Caribbean microfossil record), slide 7, ESF F-52, size: 52 x 42 um, equatorial view. (12). Hygrophila, surface view showing numerous pseudocolpi giving striate appearance to exine sculpture. (13). Compositae (Echitricolporites), slide 5, ESF U-28, becoming common as a microfossil in the Gulf/Caribbean area only in the early Miocene, and in association with Cheno/ams (Psilaperiporites) more typically in the late Miocene, size: 30 um. (14). Compositae, slide 9, ESF U-47, size: 38 um. (15). Alfaroa/Oreomunnea (Momipites; Juglandaceae), slide 9, ESF P-38, size: 30 um; the only microfossil in the Artibonite flora whose modern analog does not occur in the modern vegetation of Haiti (present range: cloud forests of Mexico and Central America, northern Colombia). (16). Malpighiaceae, slide 8, ESF J-34, size: 50 um; note distinctive arcing colpi connecting pores. (17). Allophylus (Sapindaceae), slide 1, ESF G-24, size: 26 um. (18). Oryctanthus (Loranthaceae), slide 5, ESF R-48, size: 32 um; note distinct apertures set off the equatorial plane (heterocolpate).

naturalized in the American tropics. Pteris hispaniolica and P. longifolia are both found in moist habitats, typically associated with the pine forest at elevations between 1,000 to 2,150 m. Pteris is known in the stratigraphic literature as Polypodiaceoisporites (e.g., Lorente, 1986, p. 154), and in our other Caribbean studies it ranges from middle(?) to upper Eocene (Gatuncillo Formation, Panama; Graham, 1985) to Recent. Spores of cf. Antrophyum (Fig. 4) are large (ca. 80 um), smooth, and with a trilete mark that is small in relation to the size of the spore. About 10 species occur in the neotropics, usually in moist or wet forests, often in deep shade, in rain or cloud forests (Tryon & Tryon, 1982). Antrophyum feei Schaffner is listed for Haiti (Judd, 1987, p. 78) as occasional in the cloud forest at ca. 2,210 m elevation. In the stratigraphic literature Antrophyum would probably be classified as Triletes, and in our studies it ranges from middle(?) to upper Eocene to Recent. Spores similar to those of the tree fern Alsophila (Fig. 5) are common in the fossil flora. The spores are trilete, smooth, and frequently bear a row of minute pits bordering the triradiate scar. The genus is represented in the neotropics by about 13 species, typically growing in cloud forests, wet montane forests, or elfin forests, commonly as an understory plant (Tryon & Tryon, 1982, p. 184). Judd (1987) lists three species for the Morne La Visite and Pic Macaya National Parks in Haiti, growing in the moist pine and cloud forests at elevations between about 950 to 2,200 m.

The gymnosperms are represented in the fossil flora by abundant pollen of Pinus (Fig. 6). Pine forests are one of the principal communities in the modern vegetation of Haiti, consisting of the single species P. occidentalis Sw. It occurs either as a dominant, forming pine forests, or as an overstory tree in the cloud forest, typically at elevations between 1,000 to 2,340 m, although in the Cordillera Central of the Dominican Republic it occurs locally at elevations as low as 500 m (Judd, pers. comm., 1989). Another conifer with winged pollen, Podocarpus aristulatus Parl., grows on Haiti but was not present in the fossil flora.

Thirteen types of angiosperm pollen were recovered, including two kinds of palm (Figs. 7, 8), which cannot be identified to genus. Coccothrinax and Prestoea are among cloud forest palms presently growing on Haiti. The specimens are more similar to the scabrate pollen of Prestoea than to the finely reticulate pollen of Coccothrinax examined in our reference collection. The finely striate pollen of Hygrophila (Figs. 11, 12) is of interest because the genus has never been reported in the megafossil record, or as a microfossil from the New World. Hygrophila pollen is known from the Miocene of Senegal (Médus, 1975; see Muller, 1981, p. 97; 1984, p. 430). It grows in marshes, along the margins of ponds and lakes, and in waterways, often partly submerged and sometimes floating, from sea level to about 1,500 m (Durkee, 1978). The common Caribbean species is H. costata Nees (H. guianensis Nees). The spherical, periporate pollen of the families Chenopodiaceae and Amaranthaceae usually cannot be distinguished, and the microfossils are commonly designated as Cheno/am (Fig. 10; Psilaperiporites; upper Oligocene to Recent for northern Venezuela; Lorente, 1987, p. 179). In our studies from northern Latin America it ranges from lower Miocene (Culebra Formation, Panama, Graham, 1988) to Recent. Pollen of the various Compositae types (Figs. 13, 14) are referred to Echitricolporites, Fenestrites, and other genera in the stratigraphic literature. In the Caribbean region they first appear in the latest Oligocene, become more common and diverse in the early Miocene, and are best represented, along with the Cheno/ams, beginning in the middle to late Miocene. Pollen of Alchornea (Fig. 9) is distinguished by an operculum within the colpus, and is one of the most frequent, but not abundant, components of Gulf/Caribbean Tertiary deposits. Alchornea is known in the stratigraphic literature as Psilatricolporites operculatus and ranges from middle Eocene to Recent. Alchornea is a common tree in the Gulf/Caribbean region, growing in moist lowland and premontane forests. Alchornea is represented in Haiti by the widespread A. latifolia Sw. in moist forests on limestone at elevations between about 930 to 1,370 m (Judd, 1987, p. 52). The presence of Alfaroa/Oreomunnea (Fig. 15) pollen in the late Tertiary of Haiti is of interest because neither genus presently occurs on the island. Alfaroa is a genus of about 7 species in the highlands of Mexico, Central America, and northern Colombia. Oreomunnea comprises two species in cloud forests from southern Mexico to central Costa Rica. It is known in the stratigraphic literature as Momipites, and in our studies ranges from middle(?) to late Eocene to Recent. Oryctanthus (Fig. 18) is a parasitic shrub of moist to drier, premontane forests and is widespread throughout the Gulf/Caribbean area. The Malpighiaceae (Fig. 16) is represented by pollen that presently cannot be referred to any one modern genus. Allophylus (Sapindaceae, Fig. 17) is a common member of the modern pine and cloud forests of Haiti (A. rigidus Sw., 950 to 4,000 m; A. crassinervis Radlk., 1,660 to 1,740 m; Judd, 1987). Three unknowns are also present whose affinities even at the family level have not been established.

DISCUSSION

Age of the Flora

Strata at the fossil plant locality are part of the Artibonite group (Woodring et al., 1924), which was considered at that time to consist of three formations: Madame Joie (basal), Thomonde, and Las Cahobas. The relationship of the plant-bearing beds to these formations was uncertain: "On the east side of the road from Mirebalais to Las Cahobas and immediately north of the small stream at the foot of the mountains, on the north side of the gap, soft sandy and clayey beds in the Thomonde formation strike N. 30° W and dip 32° NE. At the same locality but on the west side of the road, there is finely laminated buff or yellowish clay from which the plants ... were collected. The clay can hardly belong to the Thomonde formation because of its stratigraphic relations and because the Thomonde formation not far distant along the strike carries a relatively deep-water fauna. It may represent some part of the Miocene series not known elsewhere in the Central Plain. Its stratigraphic relations led to the supposition in the field that it was of Pliocene age, but overwhelming evidence shows that the sea withdrew from the area now embraced by the Central Plain before Pliocene time. It is unfortunate that the age of these beds is not known, as they furnish the largest collection of fossil plants obtained in the Republic" (Woodring et al., 1924, p. 166). The stratigraphic charts prepared by Cooke et al. (1943) place the Madame Joie Formation in the lower part of the lower Miocene, the Thomonde Formation in the upper lower Miocene, and the Las Cahobas Formation in the lower middle Miocene. Bowin (1975)

recognizes four formations within the Artibonite group, elevating the Maissade tongue of the Thomonde of earlier authors to formation status. The Madame Joie is considered late late Oligocene to early early Miocene in age; the Thomonde as middle early Miocene to middle Miocene; the Maissade as middle Miocene; and the Las Cahobas as late Miocene (Fig. 19). The position of the plant-bearing beds is not mentioned in these later publications.

On the basis of the plant megafossil material, Berry considered the flora to be Miocene in age, and probably late Miocene, consistent with estimates by Woodring et al. (1924) based on field observations and other paleontological evidence. Efforts at age determination from the plant microfossil assemblage are equally equivocal. As noted earlier, the types of Compositae pollen recovered from the Artibonite strata first appear in the Gulf/Caribbean region in the uppermost Oligocene, but do not become abundant (as in the Artibonite assemblage) until the early Miocene. Compositae pollen in association with that of the Chenopodiaceae/Amaranthaceae is typical of even later floras. For this reason, the microfossil flora is regarded as probably late Miocene to possibly Pliocene in age, and the strata may represent a facies of the Las Cahobas Formation.

Paleocommunities and Paleoenvironments

The composition of the fossil flora suggests a mosaic of pine and cloud forests. All genera presently occur in that vegetation type, either in Haiti, or in the case of Alfaroa/Oreomunnea, in similar communities elsewhere in the Caribbean.

There were no representatives of the xerophytic vegetation that now characterizes many lowland areas to the lee of mountains (e.g., in the Artibonite Plain southeast of Grande-Saline, Woodring et al., 1924, pl. IV; Cul-de-Sac Plain near Pont Beudet, pl. V; northeast of Gonaines, pl. V). No pollen of the Gramineae was recovered, a family which is the principle component of savannas (e.g., southwest of St.-Michel de l'Atalaye; Woodring et al., 1924, pl. VI). Based on studies of other Gulf/Caribbean Tertiary microfossil floras (Figs. 20, 21), it is likely that savannas and dry to arid communities developed in the Pliocene and Quaternary, with maximum range expansion in very recent times as a result of anthropogenic factors.

Little is known of the lowland paleocommunities except for the nine genera of megafossils reported by Berry (1923; Table 1). In evaluating the megafossil record it must be noted that in the few instances where a re-study has been made of these older works, the percentage of misidentifications is high. In the Eocene Wilcox flora of the southeastern United States, Dilcher (1973) estimates that 60% of Berry's determinations may be incorrect, and the figure likely would not be any lower for the Haiti material. None of the genera identified by Berry were encountered as microfossils (Table 1). If the megafossil assemblage were larger and more diverse, it would be possible to suggest broad paleoclimatic conditions based on leaf physiognomy (Wolfe, 1971). For the few fragmentary specimens in Berry (1923), all are described as entire-margined and coriaceous to subcoriaceous in texture, two have prominent drip tips, and size ranges from 3.25 x 1.1 cm to 9 x 3 cm. These specimens are probably remnants of a lowland paleocommunity growing close to the margins of the depositional basin.

General parameters for the late Tertiary paleoclimate of Haiti can be established from modern temperature and rainfall records at sites bracketing the altitude ranges suggested by the fossil flora (to the extent these data are available for Haiti). Pétionville (18° 31' N, 72° 17' W; altitude 400 m) is located just to the southeast of Port-au-Prince. The average monthly temperature, based on an eight year record from 1909 to 1916 (Woodring et al., 1924, p. 39), ranges from a December/January minimum of 23.1° C to a July maximum of 26.5° C. At Furcy (18° 25' N, 72° 17' W; altitude 1,540 m) the values are a December/January minimum of 17.5° C and a summer maximum of 19.8° C. Records from Port-au-Prince (18° 32' N, 72° 26' W), Pétionville, and Furcy indicate an average lowering of the annual mean temperature of about 1° C for each 150 m increase in altitude (at its present latitude of ca. 18+° N). Annual rainfall at Pétionville (based on 20-21 year records) is 1,327.5 ml, with the driest months (December/January) receiving 26.1 and 28.9 ml, respectively, and the wettest months (April/May) receiving 183.2 and 220.6 ml. Comparable rainfall figures are not available for Furcy, but annual rainfall is about 2,100 ml, with December/January dry and April/May wet periods. Mirebalais (18° 55' N, 72° 36' W; 100 m elevation), closest to the fossil locality, is one of the wettest places in Haiti, receiving about 2,659 ml of annual rainfall, while the driest is at Gonaives (19° 27' N, 72° 41' W; 524 ml). None of these extremes support (or, rather, supported in the recent past) vegetation similar to the paleocommunities, especially the deserts near Gonaives.

The paleoaltitude for the Artibonite flora cannot be established from the limited information available. The modern analogs grow between sea level and 2,300 m, with an average lower elevation of 700 m and an average higher elevation of 1,900 m. A zone from about 1,200 to 1,300 m would accommodate all components of the flora. The present altitude at Mirebalais is only 100 m, so the palynoflora probably reflects an upland community growing on slopes adjacent to the depositional basin. No pollen of mangroves (Rhizophora, Avicennia, Conocarpus, Laguncularia), or plants with species associated with the mangroves (Hibiscus, Mimosa, Sapium, and others), which do occur in other Gulf/Caribbean Tertiary floras, were found in the Haiti material.

Paleoenvironmental reconstructions, and especially biogeographic models, for the Caribbean must take into account the former position and the submergent/-emergent history of the islands. In the case of Hispaniola, its northern and southern portions, divided at the Cul-de-Sac--Enriquillo Basin (Pindell & Dewey, 1982; Mann & Burke, 1984), have had similar but independent histories. Southern Hispaniola is constituted of uplifted ocean floor emergent only since the Pliocene. Several models show southern Hispaniola, and Jamaica, moving "several hundred kilometers eastward into their present positions during the last 30 million years", at an estimated rate of about 3 cm/year (Buskirk, 1985). Collision of southern Hispaniola with northern Hispaniola occurred in the late Miocene. It is not possible to reconstruct paleophysiographic detail to the degree of locating precisely the fossil site during this period. However, the reconstructions suggest the locality may have been on the southern shore of the northern fragment of proto-Hispaniola, with the fossil flora being deposited during or just prior to the accretion of southern Hispaniola. Most tectonic models for the early and middle Tertiary (see

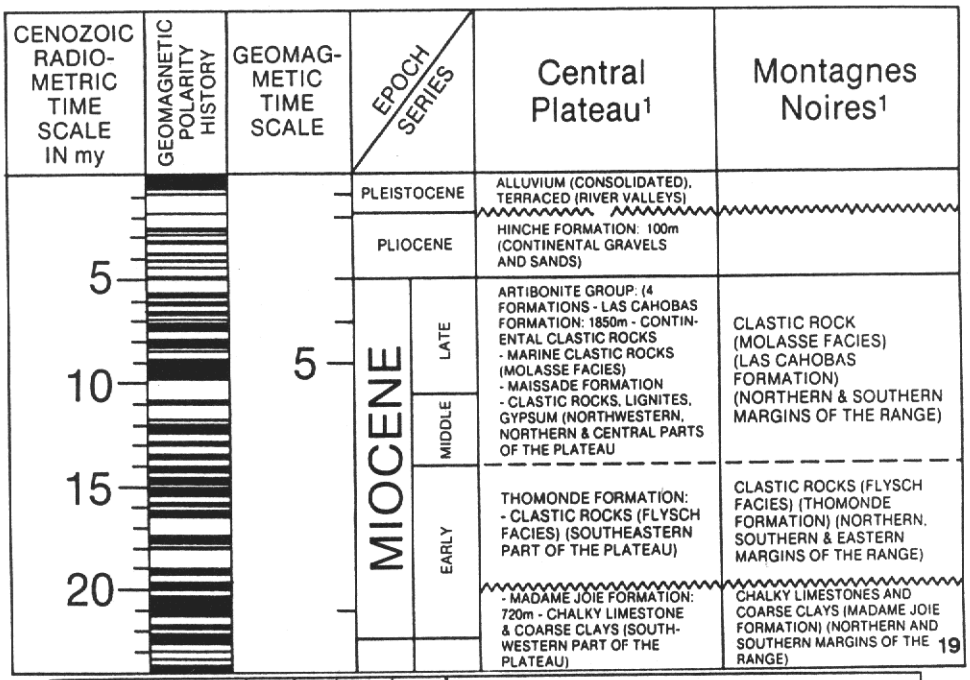

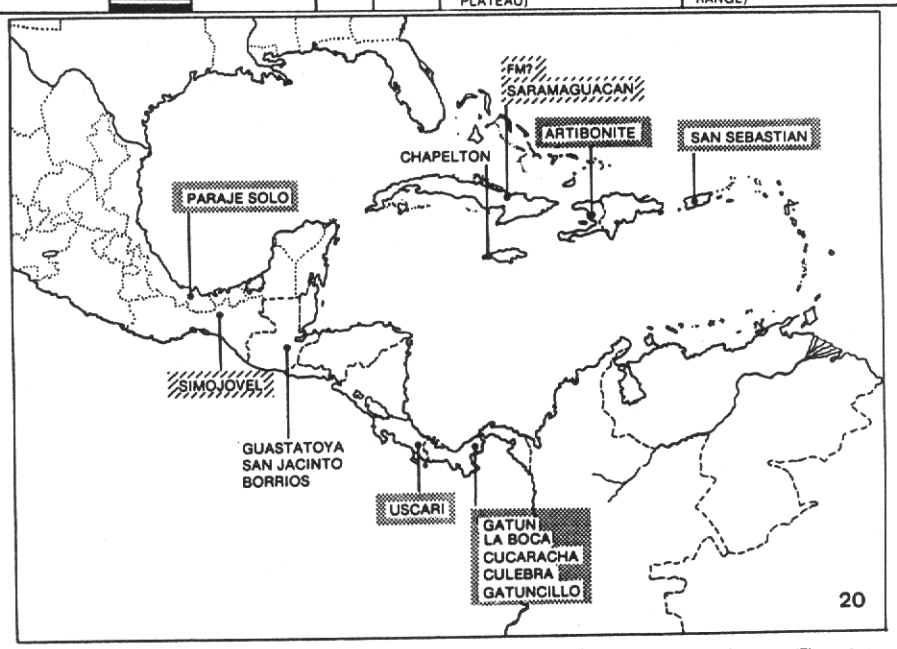

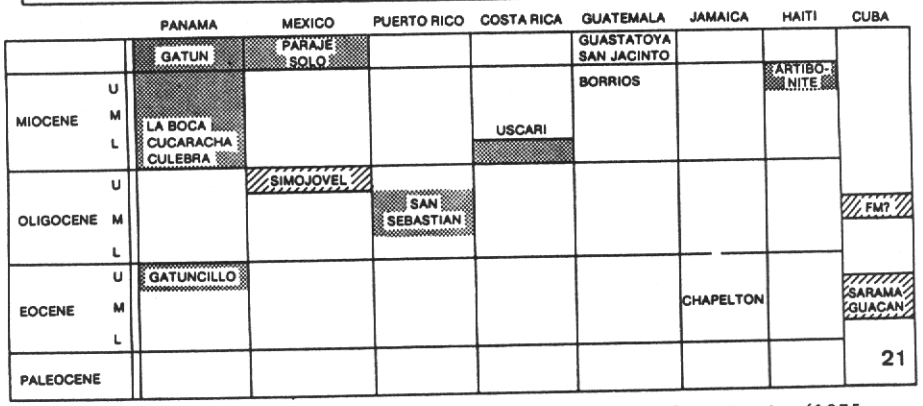

Figure 19. Stratigraphic relations of the Artibonite group formations. After Bowin (1975, used with permission).

Figure 20. Geographic distribution of Caribbean microfossil floras. Stippling indicates study complete.

Figure 21. Stratigraphic distribution of Caribbean microfossil floras; position does not imply formal correlation

summary in Buskirk, 1985; Rosen, 1985) show the Greater Antilles further to the west, off the southern coast of Mexico, and moving east along the Motagua-Polochic/Cayman fault zone. In this case the affinities of early and middle Tertiary fossil floras should be primarily with Mexico and northern Central America, with a South American component becoming progressively more prominent in latest Tertiary and Quaternary times. Although the data base is meager, the Antillean Tertiary floras studied to date (Figs. 20, 21) have almost exclusively northern Central American and Mexican affinities. This observation forms one component of a preliminary biogeographic model to be tested as future studies are completed.

In summary, the twenty-five fossil palynomorphs recovered from the Artibonite flora, in association with other limited paleontological and stratigraphic evidence, suggest an age of late Miocene to possibly middle Pliocene. The principal paleocommunities were pine and cloud forests, with a fringing fern marsh. Annual paleotemperatures are estimated from 23° C to 26° C at elevations of about 400 m, and from 17° C to 19° C at elevations of about 1,400 m. Rainfall is estimated at 1,300 ml and was seasonal. All modern analogs of the Artibonite flora grow between sea level and about 1,200 to 1,300 m, consistent with values based on Tertiary paleopalynological evidence from other Caribbean localities. The affinities of the Artibonite flora are with northern Central America and Mexico, as opposed to South America, supporting reconstructions that place the proto-Greater Antilles to the west along southern Mexico during the lower and middle Tertiary.

ACKNOWLEDGEMENTS

The author is grateful for comments on the manuscript and for information on the modern vegetation of Haiti provided by Walter S. Judd (University of Florida, Gainesville) and Dan Skean, Jr. (Albion College, Albion, Michigan), and for information on Pteris provided by John T. Mickel (N. Y. Botanical Garden). Research was supported by NSF grant BSR-8819771.

REFERENCES CITED

Berry, E. W., 1923, Tertiary fossil plants from the Republic of Haiti: Proc. U. S. Natl. Mus., v. 62, p. 1-10.

Bowin, C., 1975, The geology of Hispaniola, in Narin, A.E.M., and Stehli, F.G., eds., The Ocean Basins and Margins: Plenum Press, p. 501-552.

Buskirk, R. E., 1985, Zoogeographic patterns and teconic history of Jamaica and the northern Caribbean: Jour. Biogeography, v. 12, p. 445-461.

Cooke, C. W., Gardner, J., and Woodring, W. P., 1943, Correlation of the Cenozoic formations of the Atlantic and Gulf coastal plain and the Caribbean region: Geol. Soc. Amer. Bull., v. 54, p. 1713-1723.

Dilcher, D. L., 1973, A paleoclimatic interpretation of the Eocene floras of southeastern North America, in Graham, Alan (ed.), Vegetation and Vegetational History of Northern Latin America: Elsevier, p. 39-59.

Durkee, L. H., 1978, Acanthaceae, in Woodson, R. E. and Schery, R. W. (eds.), Flora of Panama: Ann. Missouri Bot. Gard., v. 65, p. 155-283.

Graham, A., 1985, Studies in neotropical paleobotany. IV. The Eocene communities of Panama: Ann. Missouri Bot. Gard., v. 72, p. 504-534.

Graham, A., 1988, Studies in neotropical paleobotany. V. The lower Miocene communities of Panama--the Culebra Formation: Ann. Missouri Bot. Gard., v. 75, p. 1440-1466.

Judd, W. S., 1987, Floristic study of Morne La Visite and Pic Macaya National Parks, Haiti: Bull. Florida State Mus. Biol. Sci., v. 32, p. 1-136.

Lorente, M. A., 1986, Palynology and palynofacies of the upper Tertiary in Venezuela: Dissertationes Botanicae (J. Cramer, Berlin), v. 99, p. 1-222.

Mann, P., and Burke, K., 1984, Neotectonics of the Caribbean: Rev. Geophys. Space Phys., v. 22, p. 309-362.

Médus, J., 1975, Palynologie de sédiments Tertiaires du Sénégal méridional: Pollen et Spores, v. 17, p. 545-608.

Muller, J., 1981, Fossil pollen records of extant angiosperms: Bot. Rev., v. 47, p. 1-142.

Muller, J., 1984, Significance of fossil pollen for angiosperm history: Ann. Missouri Bot. Gard., v. 71, p. 419-443.

Pindell, J., and Dewey, J. F., 1982, Permo-Triassic reconstruction of western Pangea and the evolution of the Gulf of Mexico/Caribbean region: Tectonics, v. 1, p. 179-211.

Rosen, D. E., 1985, Geological hierarchies and biogeographic congruence in the Caribbean: Ann. Missouri Bot. Gard., v. 72, p. 636-659.

Tryon, R. M., and Tryon, A. F., 1982, Ferns and Allied Plants, with special reference to tropical America: Springer-Verlag.

Wolfe, J. A., 1971, Tertiary climatic fluctuations and methods of analysis of Tertiary floras: Palaeogeogr., Palaeoclimatol., Palaeoecol., v. 9, p. 27-57.

Woodring, W. P., Brown, J. S., and Burbank, W. S., 1924, Geology of the Republic of Haiti: Port-au-Prince.

LATE HOLOCENE OSTRACODA IN AND AROUND LAKE ENRIQUILLO, DOMINICAN REPUBLIC

W. A. van den Bold

Louisiana State University, Baton Rouge

Abstract.

Fifteen short cores (-35 cm) and one longer one (-115 cm) in Lake Enriquillo show ostracode faunas of very low diversity. The top 10-15 cm of 5 cores exhibits dominant Cyprideis salebrosa, suggesting low salinities. Bottom parts show dominant Cyprideis edentata, indicative of hypersalinity; it occurs throughout some cores. The middle, and sometimes upper, parts exhibit a fauna of Dolerocypria inopinata and Perissocytheridea cribrosa probably indicative of intermediate salinities, usually with Cyprideis similis. The surface sections around the lake show a more diverse fauna, from almost totally marine (with some brackish water species, e.g. Perissocytheridea exilis n. sp.) in the Holocene coral reef, to lacustrine in the upper part of the overlying sediments with Cyprideis salebrosa, Limnocythere sp. aff. L. ceriotuberosa, Cytheridella boldi, Cyclocypris sp. 1, Cypridopsis vidua, Strandesia pistrix, Darwinula stevensoni etc. This fauna is similar, but much more diverse than that of the bottom part of the longer core in the lake, and identical to that of a sample from Isla Cabritos. There is a transition from marine to lacustrine fauna with Cyprideis similis, C. mexicana, C. salebrosa and Peratocytheridea setipunctata. An attempt is made to correlate the surface sections on the basis of faunal characteristics, and to correlate the short sections of lake mud on the basis of dominance of Cyprideis species. However, no direct correlation is possible between the surface sections and the lake section.

I. Geological setting.

The Enriquillo Basin is part of an elongate depression, which separates the Massif de la Selle of Haiti and the Sierre de Bahoruco of the Dominican Republic from the main body of the island of Hispaniola. The depression is bordered on the north by the Sierre de Neiba, the Montagnes du Trou d'Eau and the Chaîne des Mattheux. It is partially filled by two lakes, the Etang Saumâtre in Haiti and the Lago de Enriquillo in the Dominican Republic. The surface of the latter lies about 45 m below sea level and is dammed-off on its east side by deposits of the Rió Yaque del Sur and separated from the Etang Saumâtre on its west side by low hills in which the Jimaní Formation is exposed. South of the Lake are low mountains composed mainly of rocks of the Las Salinas and Jimaní Formations. To the north the foothills of the Sierre de Neiba are mainly formed by Paleogene and early Neogene limestones with some Plio-Pleistocene beds, tentatively correlated with the Arroyo Blanco Formation. The Enriquillo basin was flooded by the sea several times in the Miocene and Pliocene; afterward the deposited sediments were folded and faulted. The last invasion was accompanied by the growth of a fringing coral reef (text-fig. 1), the crest of which lies at about 5 m below present sea level (B.S.L.), which is believed to be the position of sea level about 5000 Y. B. P. After the separation from the sea by river deposits (mainly of the Rio Yaque del Sur), a decrease in salinity killed the reef, and lacustrine sediments were deposited on top of it. Later evaporation caused the lake level to drop to its present position and increase the salinity to about 49‰ (Condit & Ross, in Vaughan et al. 1921). The level of Lake Enriquillo was reported by Wells (1892) to be at sea level, Tippenhauer (1900) reported it at 34 m (B.S.L.) and Condit and Ross (1919) at 43 m (see Bold, 1975a, text-fig. 2). The level of the Etang Saumâtre over the same period was and is about 60 m higher.

II. Introduction to present studies.

In 1987 geologists of the University of Texas measured, described and sampled a number of sections of sediments overlying the subaerially exposed Holocene reef around Lake Enriquillo. These sections

Larue, D.K., and Draper, G. (eds.),
Transactions of the 12th Caribbean Geological Conference, St. Croix, U.S.V.I., Miami Geological Society, P.O. Box 431552, South Miami, FL 33243, U.S.A

were those of the Arroyo el Aculadero, "Big Bend", Cañada Honda, Cañada del Benito and part of a gully west of Villa Jaragua (Text-fig. 1: 2-7). At the same time they took fifteen short cores (25-35 cm) and one slightly longer one (115 cm) in the lake (Text-fig. 1). They also collected samples from sediment between coral heads within the reef itself in the Cañada Honda and Cañada del Benito sections, and in one case in the Cañada Honda from Quaternary sediments below the reef. Later, Barun Sen Gupta collected samples inside the reef in the Arroyo el Aculadero, and I added to the post-reef sections by completing the Villa Jaragua section and sampling the Canada de Charco Salido section on the south side of the lake, east of Arroyo el Aculadero. In the reef below the villa Jaragua section I found a large, silty-marly lens with a rich fauna of ostracodes. The age of the Holocene coral reef has been determined to lie roughly between 9000 and 4800 Y. B.P. (Mann et al, 1984, Taylor et al, 1985).

The lake cores were split lengthwise into 2 halves, one of which was stored for future reference. The other half was sampled at 5 cm intervals, washed and examined for microfauna. They contain a low diversity fauna of ostracodes and mostly very small, foraminifera: Ammonia, Bolivina and Miliolids. Ammonia is dominant in samples with Cyprideis salebrosa assemblage, Miliolids in the other assemblages. In one sample a few specimens of Globorotalia crassaformis and G. tumida were found. They represent late Pliocene or younger reworked material, which creates an additional problem as deep water deposits of this age are unknown in the vicinity of the lake. Of the 225 samples studied, 100 came from the lake cores, the rest from surface sections.

Types and figured specimens are deposited in the H.V. Howe collections, Museum of Geoscience, Louisiana State University, Baton Rouge, HVH nos. 10927-10957.

III. Ostracodes in Recent and Subrecent sediments of Lake Enriquillo (Table 1)

These include: Cyprideis edentata Klie, C. salebrosa Bold, C. similis (Brady) Dolerocypria inopinata Klie. Heterocypris? sp. = Ostracode sp. B, Bold, 1975a, p. 616, pl. 58, fig. 4. Limnocythere floridensis Keyser. Perissocytheridea cribrosa (Klie). Potamocypris sp., Bold, pl. 59, fig. 11. Cyprideis edentata and C. salebrosa are mutually exclusive, but both occur with Cyprideis similis, Dolerocypria inopinata and Perissocytheridea cribrosa. Heterocypris? sp. and Linmocythere floridensis are only associated with C. salebrosa. There is also some negative correlation between abundances of Dolerocypria inopinata and Cyprideis edenata; in fact, D. inopinata is more abundant in samples where Cyprideis similis is the dominant Cyprideis species and in some where only C. similis - Dolerocypria and Perissocytheridea are found. The Cyprideis edentata - C. similis - Dolerocypria inopinata- Perissocytheridea cribrosa assemblage is identical to that of the saline lagoons of Aruba, Bonaire and Curacao (Klie, 1939b) and indicative of hypersalinities of the order of 49% as reported by Condit and Ross from Lake Enriquillo (Vaughan et al., 1921, p. 191). Perissocytheridea cribrosa and Dolerocypria inopinata also occur in low salinity environment such as is found in the tops of cores 8, 9, 19 and 21, where they occur with Cyprideis salebrosa and Limnocythere floridensis or in the upper part of the sediment sections above the exposed reef, where they occur together with Cytheridella boldi Purper and several fresh water ostracodes in addition to the two species mentioned above. This assemblage may indicate oligohaline conditions. The hypersaline Cyprideis edentata assemblage is found in the bottom of most of the short cores, and sometimes also in the top part (See Table 2 and Text-fig. 2). the assemblage of dominant Cyprideis similis generally occurs in the middle part of the cores (and sometimes the upper part). In cores 8, 9, 19 and 21 it separates the Cyprideis salebrosa assemblage from the C. edentata assemblage, probably representing salinities intermediate between oligohaline and hypersaline. The low salinity environment of these 4 cores is attributed to upwelling fresh water in the deeper parts of the basin, possibly associated with the fault zone that crosses Lake Enriquillo from west to east just north of Isla Cabritos.

The fauna of the longer core is slightly anomalous in that Cyprideis salebrosa is dominant both in the top 10 cm and from 25 to 115 cm, separated by an interval in which Cyprideis similis is the dominant Cyprideis species. Therefore, the top 25 cm are similar to those in neighboring core 9. The possibility exists that the lower C. salebrosa assemblage could correlate with those at the tops of the subaerially exposed sections around the lake. However, given the total absence of the fresh water species that accompany this assemblage in those sections (especially Cypridopsis sp. 1) this appears not very likely.

Hydrobid gastropods and a species of bivalves are common in most cores. The gastropods are dominant in samples with Cyprideis salebrosa and in some with intermediate faunas, usually with Cyprideis similis. The bivalves are dominant in samples with Cyprideis edentata and in some of the intermediate faunas. In intermediate faunas they often occur together.

All samples have a very low diversity. The Cyprideis edentata assemblage never contains more than four species, the C. salebrosa assemblage not more than seven. The more common ostracodes are accompanied by complete or almost complete sets of molt stages; gastropods and bivalves include numerous young individuals of all sizes. Therefore post portem transport may be excluded. Bioturbation has disturbed some layers and individual samples may have a somewhat mixed fauna. Rare reworked ostracodes occur in several samples, all single valves with a more milky color, which are filled with slightly indurated sediment. Only in one case are they suspected to be derived from the exposed sections around the lake: interval 20-35 cm of the longer core with Limnocythere sp. aff. L. ceriotuberosa.

IV. Ostracodes in sediments overlying the Holocene reef around Lake Enriquillo (Tables 3-9).

They include:

Bairdia sp.
Bairdoppilata cushmani (Tressler)
Cryptocandona sp.
Cyclocypris sp. 1, Bold, 1975a, p. 605, pl. 58, fig. 2a-d; Cyclocypris sp. 2, Bold, 1975a, p. 606, pl. 58, fig. 5a, b. Cyclocypris occurs mostly in mesohaline waters of very low alkalinity (Carbonel et al, 1988).
Cyprideis mexicana Sandberg, C. salebrosa Bold, C. similis (Brady), See VII.
Cypridopsis vidua (Müller), Cypridopsis sp.
Cytherella sp.
Cytheridella boldi Purper (See VII).
Cytherura sp.
Darwinula stevensoni (Brady and Robertson) (See, Sohn, 1987). Darwinula seems to prefer oligohaline (Keyser, 1975), clear, calm waters (Carbonel et al, 1988). Pl. 1, fig. 6.
Dolerocypria inopinata Klie (See VII).
Hemicypris reticulata Klie (See VII).
Heterocypris? sp. = Ostracode sp. B, Bold, 1975a, p. 616, pl. 58, fig. 4)
Jugosocythereis pannosa (Brady)
Limnocythere floridensis Keyser, L. sp. aff. L. ceriotuberosa Delorme (Bold, 1975a, p. 613, pl. 59, fig. 9). See remarks to L. floridensis in section VII, Pl. 1, fig. 8.
Loxoconcha (Loxoconcha) levis Brady
Loxoconcha (Loxocorniculum) dorsotuberculata (Brady), L. (L.) fischeri (Brady), L. (L.) tricornuta (Krutak).
Orionina bradyi Bold, O. fragilis Bold, O. serrulata (Brady)
Paracytheridea tschoppi Bold, P. sp.
Paracytheroma sp.
Paranesidea bradyi (Bold), P. bensoni (Teeter).
Peratocytheridea setipuncata (Brady). Pl. 2, fig. 6-8.
Perissocytheridea cribrosa (Klie), P. rugata Swain (=P. sp., Bold, 1975a, p. 612, pl. 62,, fig. 4a, b), P. subrugosa (Brady), P. sp. A.
Propontocypris sp. (See VII).
Potamocypris sp. (Bold, 1975a, pl. 59, fig. 11).
Puriana minuta Bold.
Strandesia pistrix Broodbakker, S. venezolana Broodbakker?, Strandesia sp. (See VII).
Xestoleberis antillea Bold, X. punctata Tressler, X. sp.

The most common species Cyprideis salebrosa, Perissocytheridea cribrosa, P. subrugosa, Cyclocypris sp.) are always accompanied by numerous molds, and they probably were living near the place of their thanatocoenosis.

The important difference with the fauna of the bottom part of the longer core in Lake Enriquillo is the continuous presence in the upper part of the subaerially exposed sections of Cyclocypris sp. 1, Cytheridella boldi, and other freshwater species, such as Strandesia pistrix and Darwinula stevensoni. Instead of Limnocythere floridensis a more spinosa form occurs in the surface sections (L. sp. aff. L. ceriobuberosa Delorme). The marine taxa, such as Paranesidea, Propontocypris, Orionina, Jugosocythereis, and Loxoconcha (Loxocorniculum), are almost totally confined to the basal strata, immediately overlying the reef. Their higher occurrences probably represent reworked reefal material; there are also layers of reworked Acropora cervicornis.

Correlation among the seven sections of post-reef sediments is based on the occurrence of 1) horizons of razor clams (Tagelus plebius) in life position. 2) the presence of hydrobid gastropods, with Cyprideis salebrosa and with or without the presence of Cytheridella boldi; 3) the temporary disappearance of Cyprideis mexicana, C. similis and Peratocytheridea setipunctata.

This level of disappearance is found at a somewhat varying distance (40-150 cm) below the upper Tagelus horizon, but is not observed in the Villa Jaragua section (see below). An upper Cytheridella boldi horizon occurs some distance (25-100 cm) above the Tagelus horizon(Text-fig. 1, sections 1-3, Tables 3-5). In the "Big Bend" section a lower Tagelus horizon is found about 150 cm below the upper one. In the Cañada del Benito section (Table 8) two Cytheridella boldi horizons occur, the upper one about 70 cm above the Tagelus horizon, the lower one about the same distance below it. The two Cañada Honda sections show (Tables 6, 7,) show a single Cytheridella boldi horizon just above the single Tagelus horizon. Therefore it seems almost certain, that both these horizons represent the lower ones, and that the Tagelus horizon in the Cañada del Benito is

the upper one, which was not reached in the short Cañada Honda sections.

In the Villa Jaragua section (Table 8) two Tagelus horizons and two Cytheridella boldi horizons occur. Both are found just above layers of reworked A. cervicornis. It is not clear if the lower one represents the C. boldi horizon of the Cañada Honda and Cañada del Benito sections, and the upper one the apparently continuous horizon in the top of the more westerly sections, or if there may be three different occurrences of Cytheridella boldi. C. boldi horizons represent a drop in salinity and the Tagelus horizons a slight increase in salinity. As marine influences would come from the east the presence of two Tagelus horizons there instead of one as in the west, does not seem illogical.

The level of temporary disappearance of Cyprideis mexicana, C. similis and Peratocytheridea setipunctata occurs below the upper Tagelus horizon and just above the top of the lower one. This disappearance is probably related to a lowering of the salinity and a possible increase in salinity may be indicated by the re-appearance of (some of) these species near the top in the Arroyo Aculadero section and in the upper Tagelus horizon in other sections. The distribution of Perissocytheridea subrugosa and P. sp. A, is similar to that of the above named species, but in the Villa Jaragua section the level of temporary disappearance is not observed, and Perissocytheridea sp. A is confined to the upper part of the section and P. subrugosa to the lower part. It should be emphasized, that the Villa Jaragua section is a composite one. The lower part was surveyed by Glenn and Maddox, the upper part, at a slightly different location, by me. Therefore although Table 9 shows a logical succession, it should be treated with some caution.

A limestone on Isla Cabritos (Text-fig. 1) sampled by J. W. Hunter (Bold, 1975a, H 10287) contains Cyclocypris sp. 1, Cyprideis salebrosa, Limnocythere floridensis and Cytheridella boldi, and is almost identical in fauna to the upper Cytheridella boldi horizon in the post reef sections.

In all sections Cyprideis salebrosa is ubiquitous. The relative abundance of the smooth, punctate and nodose forms is recorded in the tables, and appear to indicate an increased salt concentration between the two Tagelus horizons, but no firm conclusions have been reached about the environmental significance. The faunas in the surface sections are more diverse than corresponding asesemblages in the cores (always more than 10 species in individual samples).

V. Ostracode fauna of Holocene reef sediments around Lake Enriquillo (Tables 10-12).

They include:Bairdia laevicula Edwards, B. sp.
Bairdoppilata cushmani (Tressler)
Basslerites minutus Bold
Campylocythere sp., Bold, 1975a, p. 615, pl. 59, fig. 5a, b
Candona sp.
Caribecandona sp.
Carilella yoni (Puri)
Cativella navis Coryell and Fields
Coquimba sp.
Cyprideis mexicana Sandberg, C. portusprospectuensis Bold, C. salebrosa Bold, C. similis (Brady)
Cytherella harpago Kornicker, C. pandora Kornicker, C. polita Brady, C. sp. aff. C. pulchra Brady
Cytherelloidea sp. aff. C. leonensis Howe
Cytheridella boldi Purper
Cytherura sp.
Heterocypris? sp.
Jugosocythereis pannosa (Brady)
Loxoconcha (Loxoconcha) levis Brady
Loxoconcha (Loxocorniculum) fischeri (Brady), L. (L.) tricornuta (Krutak)
Occultocythereis angusta Bold
Orionina bradyi Bold, O. serrulata (Brady)
Paracytheridea calcitrapa Bold, P. tschoppi Bold
Paradoxostoma sp.
Paranesidea bradyi (Bold)
Pellucistoma sp. aff. P. howei Coryell and Fields
Peratocytheridea setipunctata (Brady)
Perissocytheridea cribrosa (Klie), P. exilis n. sp., P. n. sp. (rew.), P. plauta Forester, P. subrugosa ((Brady), P. sp.
Propontocypris sp. (See VII)
Semicytherura sp.
Triangulocypris keiji (Bold)
Triebelina rugosa Allison and Holden
Xestoleberis antillea Bold, X. punctata Tressler, X. sp.

The fauna comes from marly and silty pockets within the reef and from a large marly-silty lens inside the reef in the Villa Jaragua section (species marked with an asterisk) This fauna is always nearly totally marine with a small admixture of brackish water species and a few occurrences of rare fresh water species, obviously washed into the reef. Jugosocythereis pannosa is the dominant species in nearly all samples. Typical Caribbean reef forms (e.g. Paranesidea, Propontocypris, Tribelina, etc.) are rare or absent (compare Bold, 1988b). However, some modern ubiquitous forms (e.g. Morkhovenia inconspicua, Neomonoceratina mediterranea) may have been introduced in the Caribbean after the closing of the Enriquillo Basin. The diversity of the faunas is less than what might be expected in modern Caribbean coral reefs; compare the Alacran (Bold, 1988b) or Belize reefs (Teeter, 1975).

This somewhat impoverished reef fauna may be the result of slow colonization of the Enriquillo Basin when the sea invaded it for the last time some 10,000 years ago. This could also be a possible explanation for the absence of typical Caribbean reef corals (Acropora palmata, Meandrina and Diploporal) as noted by Mann et al (1984).

The fauna of the sediments immediately underlying the reef in the Cañada Honda (Table 11) is similar to the reef fauna with Jugosocythereis pannosa dominant, but lacking typical reef forms. The age of these sediments was determined as 9760 ± 110 Y.B.P. (Taylor et al, 1985). In other instances the reef lies unconformably on older (Pliocene or Pleistocene) sediments.

VI. CONCLUSIONS.

The last invasion of the sea into the Enriquillo Basin took place about 10,000 years ago and reef growth around the rim of the depression continued for about 5000 years. About 5700 Y.B.P., alluvial deposits of the Rio Yaque del Sur cut-off the supply of marine water, lagoonal conditions began and brackish water environment gradually changed to lacustrine. There were at least two periods of temporarily increased salinity during which Tagelus plebius became prominent, the last one determined as taking place at 2820 + 40 Y.B.P. (Taylor et al, 1985). Lacustrine conditions continued for at least the time needed to deposit one more meter of sediment above this horizon. The hypersaline conditions in at least the upper 35 cm of the lake deposits are a very recent event. The distribution of ostracodes suggests that this late development followed the neutral saline path of the evaporation cycle (see Carbonel et al, 1988). Local lower salinity conditions may be caused by upwelling fresh water. More precise timing of the beginning of hypersaline conditions, and possible correlation of lake sediments with the subaerially exposed sections around the lake can only be accomplished by collecting some longer cores in the lake.

VII. Systematics.

Only some of the fresh- and brackish water species and one marine species are treated here. For some others references have been given in the lists of species of parts III-V. Very rare species are not considered here.

CYPRIDACEA BAIRD, 1859
CYPRIDIDAE Baird, 1850
CYPRIDINAE Baird, 1850
Genus DOLEROCYPRIA Kaufmann, 1900
Dolerocypria inopinata Klie
Pl.1, fig. 9, Pl. 2, fig. 9-10

Dolerocypria inopinata Klie, 1939b, p. 6, figs. 1-8; Teeter, 1975, p. 426, figs, 5c, 6g; Sanger and Teeter, 1982, figs. 2f-j.

Remarks: Teeter's identification suggests that this species can tolerate extreme differences in salinity. This is confirmed by its presence in the Enriquillo Lake with both Cyprideis edentata and Cyprideis salebrosa and with distinct fresh water species in the subaerially exposed sections above the reef. According to Keyser (1975) this species is systematically closer to Parapontoparta than to Dolerocypria.

Distribution: Recent of Aruba, Bonaire, Curacao, Belize, Bahamas and Hispaniola, subrecent Hispaniola.

Genus HEMICYPRIS Sars, 1903
Hemicypris reticulata (Klie)

Heterocypris reticulata Klie, 1930, p. 228, figs. 10-13.

Hemicypris reticulata (Klie), Bate, 1970, p. 292; Broodbakker, 1983a, p. 143, figs. 5A-F, 6A-H, 9C.

Remarks: H. reticulata has been reported from temporary and semipermanent small and large pools and basins, mostly without vegetation in muddy sediments of waterdepth 0.1-2 m, chlorinity 10-725 mg Cl/l.

Distribution: Paragray, Aruba, Bonaire, Curacao, St. Croix, Puerto Rico (Recent); Hispaniola (subrecent).

Genus STRANDESIA Stuhlman, 1888
Strandesia pistrix Broodbakker
Pl.1, fig. 7

Strandesia pistrix Broodbakker, 1983c, p. 438, figs. 10A-F, 11A-D.

Remarks: S. pistrix has only been reported from a large, open karst spring with low chlorinity and much vegetation. Although it is oculate, Broodbakker supposes it to be epigean. Its fossil occurrence in the Dominican Republic, however, suggests that it belongs to the lacustrian fauna (with Cytheridella and Limnocythere).

Distribution: Hispaniola (Recent and subrecent).

Strandesia venezolana Broodbakker?

Strandesia venezolana Broodbakker, 1983c, p. 351, figs. 12A-L.

Remarks: Only fragments of this large species have been found and determination therefore is questionable. It has been reported from a karst spring, a "limnocrene" well and river sediments of varying chlorinity.

Distribution: Venezuela (Recent),? Hispaniola (subrecent)

CANDONINAE Daday, 1900
Genus CARIBECANDONA Broodbakker

Caribecandona ansa Broodbakker, 1983b, p. 314, figs. 7E-F, 8H-M, 10H, 11A, C.

Remarks: C. ansa may be epigean and interstitial. It was reported from a water well with no other ostracodes present.

Distribution: Hispaniola (Recent and subrecent).

PONTOCYPRIDIDAE Müller, 1894
Genus PROPONTOCYPRIS Sylvester-Bradley, 1947
Propontocypris sp.
Pl.1, fig. 1-5

Diagnosis: Left valve elongate trapezoid in side view, right valve elongate subtriangular; greatest height at 3/8 of the length from the anterior, postdorsal angulation at 1/5 of the length from the posterior.
Dimensions: Left valve: L: 0.64; H: 0.33; Right valve: L: 0.63; H: 0.32.
Affinities: Similar to the P. dispar (Müller) complex (Maddocks, 1969, p. 15), but slenderer in side view and with a distinct, though weak, posterodorsal angulation.
Distribution: Interreef sediments and basal sediments overlying the reef in the "Big Bend" section.

CYTHERACEA Ulrich and Bassler, 1923
CYTHERIDEIDIDAE Sylvester-Bradley and Harding, 1953
Genus CYPRIDEIS Jones, 1857
Cyprideis edentata Klie
Pl. 2, fig. 3-5

Cyprideis edentata Klie, 1939b, p. 11-13, figs. 9-15; Sandberg, 1964, p. 113-115, pl. 6, fig. 1-8, pl. 16, fig. 8, pl. 21, fig. 6a-d, pl. 22, fig. 6; Bold, 1976, p. 23; Maddocks and Iliffe, 1986, p. 69.
Remarks: Klie (1939) reports it in chlorinities of 26-80 g/l.
Distribution: Salinas of Aruba, Bonaire and Curacao, Bermuda caves, Dominican Republic (Recent).

Cyprideis mexicana Sandberg
Pl. 1, Fig. 10-11

Cyprideis mexicana Sandberg, 1964, p. 125, pl. 11, fig. 11-14, pl. 12, fig. 1-5, pl. 17, fig. 1, pl. 20, fig. 1, 2, pl. 22, figs, 2, 4a, b.
Cyprideis bensoni Sandberg, King and Kornicker, 1970, pl. 12, figs. 7, 10
Cyprideis sp. King and Kornicker, 1970, pl. 13, figs. 7, 8.
Cyprideis sp. aff. C. mexicana Sandberg, Machain, 1986, p. 138; 1988, p. 102, pl. 1, fig. 9.
Distribution: Late Pliocene - Recent, Mexico; Upper Las Salinas and Jimani Formations and Subrecent deposits, Enriquillo Basin, Dominican Republic.

Cyprideis salebrosa Bold.
Pl. 2, fig. 1. 2

Cyprideis salebrosa Bold, 1963, p. 377, p. 7, fig. 9a-d, p. 11, fig. 1a-c; 1976, p. 22 (with synonymy); Kusnetsov et al, 1977, p. 55; Bold, 1981, p 60, p. 2, fig. 5a, b, table 10; Stout, 1981, p.898, text-fig. 1; Bold, 1983, p. 413, figs, 8, 9; Cronin, 1986, pl. 6, fig. 4, Machain, 1986, p. 101, pl. 1, fig. 8; Diaz-Brito, Maura and Würdig, 1988, pl. 1, fig. 14 (Not fig. 15); Bold, 1988, p. 58.
Distribution: Santiago Formation (Cuba), Upper Las Cahobas and Morne Delmas formations (Haita), Jimani, Upper Las Salinas and Arroyo Blanco formations, and recent and subrecent deposits (Dominican Republic), Lajas beds (Puerto Rico), Talparo Formation (Trinidad), Encanto, Concepción and Agueguexquite formations (Mexico). Late? Pliocene - Recent. Known in recent deposits from Kansas to Argentina.

Cyprideis similis (Brady)

Cytheridea similis Brady, 1869, p. 147, pl. 14, fig. 19, 20.
Cyprideis similis (Brady), Bold, 1976, p. 22 (with synonymy); Sánchez, 1977, table 2; Bold, 1988, p. 58.
Remarks: Klie (1939) reports Cyprideis inermis (= C. similis) in chlorinities of 20-44 g/l.
Distribution: Unnamed beds in Pozo Catalina no. 5 (6-160 m) (Cuba); Upper Morne Delmas and Las Cahobas formations (Haiti). Upper Las Salinas. Jimaní and Arroyo Blanco formations and recent and subrecent deposits (Dominican Republic); Talparo formation (Trinidad), Cumaná and Guiria formation (Venezuela). Late Pliocene to Recent. Known from recent deposits in the Gulf of Gascogne, Magellan Straits, Mauritius, Java, Brazil (Klie, 1939a), and throughout the Caribbean.

Genus LIMNOCYTHERIDAE Klie, 1938
Limnocythere floridensis Keyser

Limnocythere santipatricii Brady and Robertson, Swain, 1955, p. 613, pl. 60, figs. 1a-f, text-figs. 32a, 38.4; Swain, 1967, p. 90, figs. 47b, pl. 4, figs. 5a-c; Engel and Swain, 1967, p. 413, pl. 2, figs. 30a-c; King and Kornicker, 1970, p. 39, pl. 8, figs. 1a, b, pl. 18, figs. 9, 10, pl. 19, figs. 1, 2; Keyser, 1975, p. 490, text-fig. 3.
Limnocythere cf. santipatricii Brady and Robertson, McKenzie and Swain, 1967, p. 298, pl. 29, fig. 9.
Limnocythere sp., King and Kornicker, 1970, p. 40, pl. 8, figs. 2a, b, pl. 19, figs. 3-6.
Limnocythere cf. friabilis Benson and MacDonald, Bold, 1975a, p. 612, pl. 59, fig. 10.
Limnocythere floridensis Keyser, 1975, p. 259, pl. 20, figs, 5-11, test-fig. 3; 1976, p. 60, pl. 2, figs. 3-10, text-fig. 24; 1977, p. 208, text-figs. 1-5; Garbett and Maddocks, 1979, p. 863, pl. 1, figs. 5-8; Sanger and Teeter, 1982, figs. 1a, b; Cronin, 1986, pl. 1, figs. 5,6.
Limnocythere sp., Kontrovitz, 1978, p. 156, pl. 5, fig. 3.
Distribution: Quaternary (southern U.S., Cuba, Dominican Republic).
Remarks: Limnocythere floridensis has been reported to tolerate salinities up to 13‰.
Limnocythere sp. aff. L. ceriotuberosa Delorme (Bold, 1975, p. 613, pl. 59, fig. 9) is believed to be a variant of L. floridensis, differing in the development of two spines, one ventral and one dorsal, just behind the depressed muscle scar area (Pl. 1, fig. 8). The development of these spines is quite variable and in some specimens of L. floridensis a weak ventral spine is present. However, in the present study, the distribution of the two forms is quite different. Only a few specimens of real L. floridensis have been found in the sediments overlying the reef, whereas the spinose form is absent in the lake cores.

Therefore the two species have been kept separate until more is known about the influence of the environment on the development of the spines. One probably redeposited specimen of L. sp. aff. L. ceriotuberosa was found at 30-35 cm depth in the longer core. In the interval 20-35 cm many reworked specimens of Cyprideis salebrosa, Dolerocypria inopinata and Perissocytheridea cribrosa occur.

Genus CYTHERIDELLA Daday, 1905
Cytheridella boldi Purper

Metacypris? sp., Bold, 1958, p. 74, text-figs a-f.
Cytheridella sp., Pinto and Sanguinetti, 1962, p. 32.
Cytheridella boldi Purper, 1974, p. 654, pl. 10, figs, 1-4; Bold, 1986, p. 154, pl. 2, figs. 9, 10.
Cytheridella ilosvayi Daday?, Bold, 1975a, p. 613, pl. 58, figs. 1a-g, pl. 6, figs. 3a, b.
Distribution: Morne Delmas Formation (upper part) (Haiti), Las Salinas Formation?, Jimaní Formation (Dominican Republic), Talparo Formation (Trinidad), Siguire Formation (Venezuela) (Pliocene Pleistocene), Subrecent (Dominican Republic), Recent (Venezuela, Trinidad).

CYTHERIDAE Baird, 1850
PERISSOCYTHERIDEINAE Bold, 1963
Genus PERISSOCYTHERIDEA Stephenson,
Perissocytheridea cribrosa (Klie)
Pl. 3, fig 1-4

Leptocythere cribrosa Klie, 1933, p. 383, figs. 22-25 (Not Cythere cribrosa Brady, Grosskey and Robertson, 1874, place in Leptocythere by Herrig, 1977, p. 1256); Klie, 1939a, p. 16.
Ilyocythere cribrosa (Klie), Klie, 1939b, p. 370.
Perissocytheridea bicelliforma Swain, 1955, p. 621, pl. 61, figs. 3a, b, pl. 64, fig. 4; Bold, 1958a, table 1, 3; Morales, 1966, p. 36, pl. 3, figs. 1a-c; Swain and Gilby, 1967, p. 323, pl. 31, figs. 4a, b, text-fig. 11c; Krutak, 1971, p. 17, pl. 3, figs. 3a, b; Bold, 1972, table 2; Garbett and Maddocks, 1979, p. 893, pl. 8, figs. 7-10, text-fig. 41; Bold, 1981, p. 22, table 5; Sanger and Teeter, 1982, figs. 1 g, h; Crotty and Teeter, 1984, table 2; Teeter, 1987, p. 138; Teeter et al, 1987, table 1; Machain, 1986, p. 139; 1988, p. 108, pll. 2, fig. 5.
Perissocytheridea bicelliforma Swain?, Bold, 1963, p. 380, pl. 4, figs. 1a-d; pl. 12, fig. 11; 1964, table 2; 1966, table 1, 2; 1971, pl. 1, figs. 8a-d; 1975a, p. 609, table 2, 3, 5-8.
Perissocytheridea cf. bicelliforma Swain, Krutak, 1982, p. 270, pl. 6, figs. 4-9.
Perissocytheridea sp. aff. P. bicelliforma Swain, Bold, 1968, p. 29; Cronin, 1986, pl. 5, fig. 5.
Perissocytheridea sp. cf. P. matsoni (Stephenson), Bold, 1969, p. 121, pl. 1, figs. 10a-d.
Perissocytheridea matsoni (Stephenson), Bold, 1975a, table 1.
Perissocytheridea sp., Bold, 1971b, table 6.
Perissocytheridea cribrosa (Klie), Bold, 1972a, table 3; table 3; Keyser, 1976, p. 55, pl. 1, figs. 8-10; 1977, p. 52, pl. 1, figs. 8-12, text-fig. 4.
Not Perissocytheridea bicelliforma Swain?, Hulings and Puri, 1964, fig. 16; Keyser, 1975, p. 490, fig. 3.
Remarks: This species has been reported from very varying salinities: 1-20‰ (Swain, 1958), 5-48‰ (Keyser, 1975), 26-80‰ (Klie, 1939).
Distribution: Recent Trinidad, Venezuela, Aruba, Bonaire, Curacao, Costa Rica, Mexico, U.S. Gulf Coast, Florida, Cuba, Hispaniola, St. Croix, St. Martin; Upper Las Cahobas and Morne Delmas formations (Haiti), Angostura, Las Salinas and Jimaní Formations (Dominican Republic), Lajas beds (Puerto Rico), Springvale and Talparo formations (Trinidad), Cubagua and Cumaná formations (Venezuela), unnamed Pleistocene beds, Goajira (Colombia), Concepción and Agueguexquite formations (Mexico).
Pliocene - Recent.

Perissocytheridea exilis n. sp.
Pl. 4, fig. 1-10

Name: exilis (L) - slender, thin.
Holotype: HVH no. 10946, right valve female, pl. 4, fig. 1.
Paratypes: HVH nos. 10947 - 10953; pl. 4, figs. 2, 4-8, 10.
Type locality: BSG 88/66, Arroyo El Aculadero, Enriquillo Basin, Dominican Repubic.
Stratigraphic horizon: Holocene coral reef.
Diagnosis: A small, rather heavily reticulate species of Perissocytheridea.
Description: Female carapace small, elongate subovate, highest at 1/4 of the length from the anterior extremity, somewhat pointed subposteroventrally. Anterior end slightly obliquely rounded, dorsal margin straight, slightly obscured in posterior half by the swollen posterodorsal portion of the valve, ventral margin gently convex, curving upward to the subventral posterior angulation. Dorsal part of posterior margin short and straight. Surface regularly reticulate with mostly hexagonal fossae, which are about the same size throughout, and rather coarse for such a small species. There is a median sulcus into which bend the more or less longitudinal rows of fossae of the posterodorsal swelling. Greatest width subventrally at 7/20 of the length from the posterior 1/4 of the carapace. Male, very similar in shape to the female, but slightly slenderer; the anterior cardinal angle is slightly elevated and rounded, giving a weak sinuation to the anterior part of the dorsal margin; the median sulcus is more distinct than in the female and the greatest width is situated at medium height instead of subventrally.
Dimensions: Female, left valve: L: 0.47; H: 0.27; W: 0.15; right valve: L: 0.46; H: 0.26; W: 0.14.
Male: Left valve: L: 0.48; H: 0.25; W: 0.14; Right valve: L: 0.47; H: 0.24; W: 0.13.
Remarks: This species is very similar to

Perissocytheridea pumila Bold, but differs by the absence of a median ridge and a more pronounced median sulcus, especially in the male. It is also slightly larger. P. pumila has been encountered in the La Cruz and Santiago formations of eastern Cuba and in the Cibao basin of the Dominican Republic. (Upper Miocene and Pliocene).
Distribution: Holocene reef around Lake Enriquillo and pre-reef sediments in the Cavellina section (? Pleistocene).

Perissocytheridea sp. A.

Pl. 3, Fig. 5-9, Pl.4, fig. 11, 12.
Perissocytheridea sp. A, Bold, 1975a, p. 611, pl. 62, figs. 3a-d.
Remarks: This species consistently occurs with P. cribrosa and the development of its ventral node varies. It is believe to be a variant of P. cribrosa, with the ventral node developing under conditions of environmental stress. It appears that this form occurs in brackish water deposits of moderately high salinity, however, it is not found in the lake sediments.
Distribution: Lower part of post-reef sections. Generally occurring together with Cyprideis mexicana, C. similis and Peratocytheridea setipunctata, often common in the Tagelus horizons. Las Salinas and Jimaní formations (Enriquillo Basin, Dominican Republic).

VIII. ACKNOWLEDGEMENTS

Paul Mann, Charlotte Glenn and Ross Maddox (University of Texas, Austin) collected the greater part of the samples used in this report and I am very grateful for the meticulous description of the sections. F. W. Taylor gave information on the position of the longer lake core. The samples were eventually conveyed to Baton Rouge through the courtesy of Rosalie Maddocks (University of Houston, Texas). Ivan Tavares of the Dirección General de Minería (Santo Domingo) very generously provided part of the transportation in the Dominican Republic and assigned a driver (Aquiles Mejía Ogando) and an assistant (Frederico Echevaría), who were very helpful in carrying out the fieldwork. Barun Sen Gupta and Peter McLaughlin (Louisiana State University, Baton Rouge) assisted in part of the fieldwork and gave helpful suggestions during the study. Sen Gupta also reviewed an early draft of this paper. Preparation of the samples was done by student workers for the Department of Geology and Geophysics at LSU, Baton Rouge. This study was supported by NSF Grant AER-8720201.

REFERENCES

Baker, J. H. and Hulings, N. C., 1966. Recent Marine Ostracod Assemblages of Puerto Rico. Publication Institute Marine Science, Texas, vol. 11, p. 108-125, 6 text-figs.

Bate, R. H., 1970. A new species of Hemicypris (Ostracoda) from the ancient beach sediments of Lake Rudolf, Kenya. Palaeontology, vol. 13, no. 2, p. 289-296, 4 text-figs.

Bold, W. A. van den, 1957. Oligo-Miocene Ostracoda from southern Trinidad. Micropaleontology, vol. 3, no. 3, p. 231-254, pls. 1-4, 2 text-figs.

-----, 1958a. Distribution of freshwater ostracodes in Trinidad. Micropaleontology, vol. 4, no. 1, p. 71-74, 3 text-figs.

-----, 1958b. Ostracoda of the Brasso Formation of Trinidad. Micropaleontology, vol. 4, no. 4, p. 391-418, pls. 1-5.

-----,1963. Upper Miocene and Pliocene Ostracoda of Trinidad. Micropaleontology, vol. 9, no. 4, p. 361-424, pls. 1-12, 6 text-figs.

-----,1964. Nota preliminar sobre los ostrácodosdel Miocene-Reciente de Venezuela. Geos, no. 11, p. 7-13.

-----1966. Miocene and Pliocene Ostracoda from Northeastern Venezuela. Verhandelingen Koninklijke Nederlandse Akademie van Wetenschappen, ser. 1, vol. 23, no. 3, p. 1-43, pls. 1-5.

-----1968. Ostracoda of the Yaque Group (Neogene) of the northern Dominican Republic. Bulletins of American Paleontology, vol. 54, no. 239, p. 1-106, pls. 1-10, 18 text-figs.

-----, 1969. Neogene Ostracodes from Southern Puerto Rico. Caribbean Journal of Science, vol. 9, no. 3/4, p. 117-125, pls. 1, 2, 5 text-figs.

-----, 1972. Ostrácodos del Post-Eoceno de Venezuela y regiones vecinas. Congreso Geológico Venezolano, vol. 2, mem. 4, special publication no. 5, p. 999-1063, pls. 1-4, text-figs. 1-3.

-----, 1975a. Neogene biostratigraphy (Ostracoda) of southern Hispañola. Bulletins of American Paleontology, vol. 66, no. 286, p. 549-625, pls. 58-62, 19 text-figs.

-----, 1975b. Ostracoda from the late Neogene of Cuba. Bulletins of American Paleontology, vol. 68, no. 289, p. 121-167, pls. 14-19, 4 text-figs.

-----, 1975c. Remarks on ostracode-biostratigraphy of the late and middle Tertiary of Southwest Puerto Rico. Caribbean Journal of Science, vol. 15, no. 1/2, p. 31-36, 2 text-figs.

-----, 1976. Distribution of species of the tribe Cyprideidini (Ostracoda, Cytherideinae) in the Neogene of the Caribbean. Micropaleontology, vol. 22, no. 1, p. 1-43, pls. 1-5, 19 text-figs.

-----, 1977. Cenozoic marine Ostracoda of the South Atlantic. in: ; F. M. Swain (edit.) Stratigraphic

micropaleontology of Atlantic Basin and Borderlands. Developments in Paleontology and Stratigraphy, 6, Elsevier, p. 495-519, 6 text-figs.

-----, 1981. Distribution of Ostracoda in the Neogene of Central Haita. Bulletins of American Paleontology, vol. 79, no. 312, p. 1-136, pls. 1-6, 18 text-figs.

-----, 1983. Shallow marine biostratigraphic zonation in the Caribbean Post-Eocene. In: R. F. Maddocks (edit). Applications of Ostracoda. Proceedings Eighth International Symposium on Ostracoda, p. 400-416, 9 text-figs.

-----, 1986. Fresh and brackish water Ostracoda from the Neogene of northern Venezuela. Tulane Studies in Geology and Paleontology, vol. 19, no. 3, p. 141-157, pls. 1-3, 3 text-figs.

-----, 1988a. Neogene Paleontology in the northern Dominican Republic, 7. The subclass Ostracoda. Bulletins of American Paleontology, vol. 94, no. 329, p. 1-105, pls. 1-13, 15 text-figs.

-----, 1988b. Ostracoda of Alacran Reef, Campeche Shelf, Mexico. Tulane Studies in Geology and Paleontology, vol. 21, no. 4, p. 143-155, 2 text-figs.

Brady, G. S., 1868. Description of Ostracoda in: De Folin et Périer: Les Fonds de La Mer, vol. 1, p. 49-112.

-----, 1869. Description of Ostracoda, in: De Folin et Périer: Les Fonds de La Mer, vol. 1, p. 113-176.

Brady, G. S., Crosskey, H. W. and Robertson, D., 1874. A Monograph of the Post-Tertiary Entomostraca of Scotland, including species from England and Ireland. Palaeontographical Society, London, vol. 28, p. i-v, 1-2342, 16 pls.

Broodbakker, N., 1983a. The genus Hemicypris (Crustacea, Ostracoda) in the West Indies. Bijdragen tot de Dierkunde, vol. 53, no. 1, p. 135-157.

-----, 1983b. The subfamily Candoninae (Crustacea: Ostracoda) in the West Indies. Bijdragen tot de Dierkunde, vol. 53 (2), p. 287-326.

-----, 1983c. The genus Strandesia and other Cypricercini (Crustacea, Ostracoda) in the West Indies. Part I: Taxonomy Bijdragen tot de Dierkunde, vol. 53, no. 2, p. 327-368.

Carbonel, P., Colin, J. P., Danielopol, D. L., Löffler, H. and Neustrueva, I., 1988. Paleoecology of limnic ostracodes: A review of some major topics. Palaeogeography, Palaeoclimatology, Palaeoecology, vol. 62, p. 413-461, 26 text-figs.

Cronin, T. M., 1986. Ostracodes from Late Quaternary Deposits, South Texas Coastal Complex, Stratigraphic studies of a Late Quaternary barrier-type coastal complex, Mustang Island - Corpus Christi Bay area, South Texas, Gulf Coast. United States Geological Survey, Professional Paper 1328-C, p. 132-42, pls. 1-11, 1 text-fig.

Crotty, K. J. and Teeter, J. W., 1984. Post Pleistocene variations in a Blue Hole, San Salvador Island, Bahamas, as interpreted from the ostracode fauna. IN: Teeter, J. W. (edit): Proceedings of the second symposium on the Geology of the Bahamas. College Center of the Finger Lakes, Bahamian Field Station, San Salvador, Bahamas, p. 3-16.

Dias-Brito, D., Maoura, J. A. and Würdig, N., 1988. Relationships between ecological models based on ostracods and foraminifers from Sepetiba Bay (Rio de Janeiro-Brazil). Proceedings of the ninth International Symposium on Ostracoda, p. 467-484, pls. 1, 2, 14 text-figs.

Garbett, E. C. and Maddocks, R. F., 1979. Zoogeography of Holocene Ostracodes in the bays of Texas. Journal of Paleontology, vol. 53, no. 4, p. 841-919, pls. 1-15, text-figs. 1-49.

Hanai, T., Ikeya, N., and Yajima, M., 1980. Checklist of Ostracoda from Southeast Asia. Bulletin University Museum Tokyo, no. 17, 242 pp., 4 text-figs.

Hulings, N. C. and Puri, H. S., 1964. The ecology of shallow water ostracods of the West Coast of Florida. Pubblicazione Stazione zoologica di Napoli, 33 supplement, p. 308-344, 17 text-figs.

Keyser, D., 1975. Ostracoden aus den Mangrovegebieten von Südwest-Florida (Crustacea, Ostracoda, Podocopa). Abhandlungen Verh. naturwissenschaflischen Verein Hamburg (NF), 18/19, p. 255-290, pls. 20-22, 13 text-figs.

-----, 1976. Zur kenntnis der brackigen mangrovebewachsenen Weichböden Südwest-Floridas unter besonderer Berücksichtigung ihrer Ostracodenfauna. Disseration Universität Hamburg (Biologie), p. 1-142, pls. 1-9, 34 text-figs.

-----, 1977. Brackwasser-Cytheracea aus Süd-Florida (Crust.: Ostracoda: Podocopa). Abh,. Verh. naturwissenschaftlichen Verein Hamburg (NF), vol. 20, p. 43-85, pls. 1-3, 10 text-figs.

-----, 1978. Ecology and zoogeography of recent brackish-water Ostracods (Crustacea) from South-west Florida. Sixth International Symposium on Ostracoda, 1976, Junk, p. 207-222, 5 text-figs.

King, C. E. and Kornicker, L. S., 1970. Ostracoda in Texas Bays and Lagoons: An Ecological Study. Smithsonian Contributions to Zoology, no. 24, p. 1-92, pls. 1-21, 15 text-figs.

Klie, W., 1930. Ostracoden aus dem Paraguayischen Teile des Qran-Chaco. Archiv für Hydrobiologie, vol. 22, p. 221-258, 40 text-figs.

-----, 1933. Süss- und Brackwasserostracoden aus Bonaire Curaçao und Aruba. Zoologisches Jahrbuch, Systematik, vol. 64, p. 369-390, 25 text-figs.

-----, 1939a. Brackwasserostracoden von Nordostbrasilien. Zoologisches Jahrbuch, Systematik, vol. 72, p. 359-372, 10 text-figs.

-----, 1939b. Ostracoden aus den marinen Salinen von Bonaire, Aruba und Curaçao. Capita Zoologica, vol. 8, no. 4, p. 1-19, 28 text-figs.

Krutak, P. R., 1971. The Recent Ostracoda of Laguna Mandinga, Veracruz, Mexico. Micropaleontology, vol. 17, no. 1, p. 1-30, pls. 1-4.

-----, 1982. Modern ostracodes of the Veracruz-Anton Lizardo reefs, Mexico. Micropaleontology, vol. 28, no. 3, p. 258-266, pls. 1-7, 12 text-figs.

Kusnetzov, V. I., Bassov, V. A., Furrazola Bermúdez, G., García-Sanchez, R. and Sánchez Arango, J. R., 1977. Resumen estratigráfico de los sedimentos mesozóicos y cenozóicos de Cuba. La Minería en Cuba, vol. 3, no. 4, p. 44-61, 7 text-figs.

Machain-Castillo, M. L., 1986. Ostracode biofacies and paleoecology of the Pliocene of the Isthmian salt basin, Verazcruz, Mexico. Tulane Studies in Geology and Paleontology, vol. 19, no. 3, p. 123-139, 9 text-figs.

-----, 1988. Pliocene Ostracoda of southeastern Mexico. Part I. Encanto and Concepcion biofacies. Contribution 575 of the Instituto de Ciencias del Mar y Limnología, Universidad Nacional Autonoma de Mexico. Revista de la Sociedad mexicana de Historia Natural, vol. 38, p. 81-138, pls. 1-4.

Maddocks, R. F. and Iliffe, T. M., 1986. Podocopid Ostracoda of Bermudian caves. Stygologia, vol. 2, p. 26-76.

Mann, P., Taylor, P. W., Burke, K., Kulstad, R., 1984. Subaerially exposed Holocene coral reef, Enriquillo Valley, Dominican Republic. Geological Society of America, Bulletin, vol. 95, no. 9, p. 1084-1092, 9 text-figs.

Morales, G. A., 1966. Ecology, Distribution and Taxonomy of Recent Ostracoda of the Laguna de Terminos, Campeche, Mexico. Universidad Nacional Autonoma de Mexico, Instituto de Geología, Bol. 81, p. 1-103, pls. 1-8, text-figs. 1-46.

Morkhoven, F. P. C. M., van, 1963. Post-Palaeozoic Ostracoda, their morphology, taxonomy and economic use. Vol. 2: Generic descriptions. Elsevier, Amsterdam, p. 205-478, 684 text-figs.

Müller, G. W., 1912. Ostracoda, In: Schulze, F. E. (edit), Das Tierreich, eine Zusammenstellung und Kennzeichning der rezenten Tierformen, vol. 31, R. Friedlander u. Sohn, Berlin, p. i-xxxiii, 1-434.

Pinto, I. D. and Sanguinetti, Y. T., 1862. A complete revision of the genera Bisulcocypris and Theriosynoecum (Ostracoda) with the world geographical and stratigraphical distribution (including Metacypris, Elpidium, Gomphocythere and Cytheridella). Universidade do Rio Grande do Sul, Escola de Geologia, Publicada especial, no. 4, p. 1-97, pls. 1-3.

Purper, I., 1974. Cytheridella boldi Purper, sp. nov. (Ostracoda) from Venezuela and a Revision of the genus Cytheridella Daday, 1905. Anales Academa brasileno Ciencias, vol. 46, no. 3/4, p. 635-662, pls. 1-10.

Sánchez Arango, J. R., 1977. Estudio bioestratigráfico del Pozo Catalina No. 5 (Cuenca Central). La Minería en Cuba, vol. 3, no. 4, p. 15-24, 3 text-figs.

Sandberg, P. A., 1864. The Ostracod genus Cyprideis in the Americas. Acta Universitata Stockholmiensis, Stockholm Contributions in Geology, vol. 12, p. 1-178, pls. 1-23, 33 text-figs.

Sanger, D. B. and Teeter, J. W., 1983. The distribution of living and fossil Ostracoda and their use in the interpretation of the Post-Pleistocene of Little Lake, San Salvador, Bahamas. Proceedings First Symposium Geology of the Bahamas. College Center of Finger Lake, Bahamas, Field Station, San Salvador, Bahamas, p. 27-31.

Sohn, I. G., 1987. The ubiquitous ostracode Darwinula stevensoni (Brady and Robertson, 1870), redescription of the species and lectotype designation. Micropaleontology, vol. 33, no. 2, p. 150-163, pls. 1-3, 1 text-fig., 3 tables.

Swain, F. M., 1955. Ostracoda of San Antonio bay, Texas. Journal of Paleontology, vol. 29, no. 4, p. 561-646, pls. 59-64, 39 text-figs.

Swain, F. M. and Gilby, J. M., 1976. Recent Ostracoda from Corinto Bay, western Nicaragua, and their relationship to some other assemblages of the Pacific Coast. Journal of Paleontology, vol. 41, no. 2, p. 306-334, pls. 31-34, 266 text-figs.

Taylor, F. W., Mann, P., Valastro, S. and Burke, K., 1985. Stratigraphic and radiocarbon chronology of a subaerially exposed Holocene coral reef, Dominican Republic. Journal of Geology, vol. 93, p. 311-321.

Teeter,, J. W., 1975. Distribution of Holocene Marine Ostracoda from Belize. In: Wantland, K. F. and Pusey, W. C. Belize Shelf Carbonate sediments, clastic sediments and Ecology. American Association of Petroleum Geologists, Studies in Geology, no. 2, p. 400-499, 23 figs.

-----, 1981. Ostracoda of the Lake Flirt Formation (Pleistocene) of southern Florida. Micropaleontology, vol. 26, no 4, p. 337-355, pls. 1-6, 3 text-figs.

-----, 1987. Holocene lacustrine depositional history. In: Currant, H. A. (edit.) Pleistocene and Holocene carbonate environments on San Salvador Island, Bahamas. Geological Society of America, Guide book of field trip, Orlando Meeting. College Center of Finger Lake, Bahamas Field Station, p. 133-145.

Teeter, J. W., Beyke, R. J., Bray, T. F., Brocculeri, T. F., Bruno, P. W., Dremann, J., and Kendall, R. L., 1987. Holocene depositional history of salt pond, San Salvador, Bahamas. Proceedings Third Symposium on the Geology of the Bahamas. College Center of Finger Lake, Bahamian Field Station (H. A. Curran, edit.), p. 145-150, 4 text-figs.

Vaughan, T. W., Cooke, W., Condit, D. D., Ross, C. P., Woodring, W. P. and Calkin, F. C. 1921. A geological reconnaissance of the Dominican Republic. Geological Survey of the Dominican Republic, vol. 1, 168 pp.

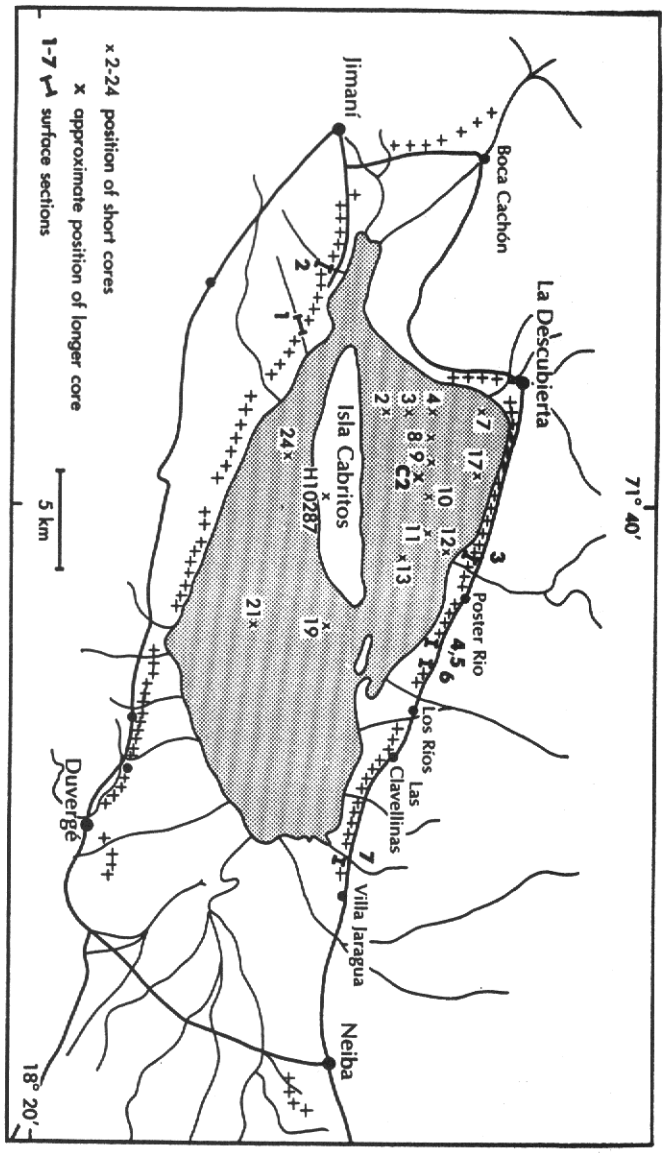

Text-fig. 1: Location of lake cores and surface section in and around Lake Enriquillo.
x 2-24 lake cores; C2: slightly longer core, I 1-7: surface sections: 1 Cañada de Charco Salido; 2 Arroyo el Aculadero (Table 4), 3 "Big Bend" (Table 5); 4 Cañada Honda (Table 6); 5 Cañada Honda (Table 7); 6 Cañada del Benito (Table 8); Villa Jaragua section (Table 9). xxx: position of Holocene reef.

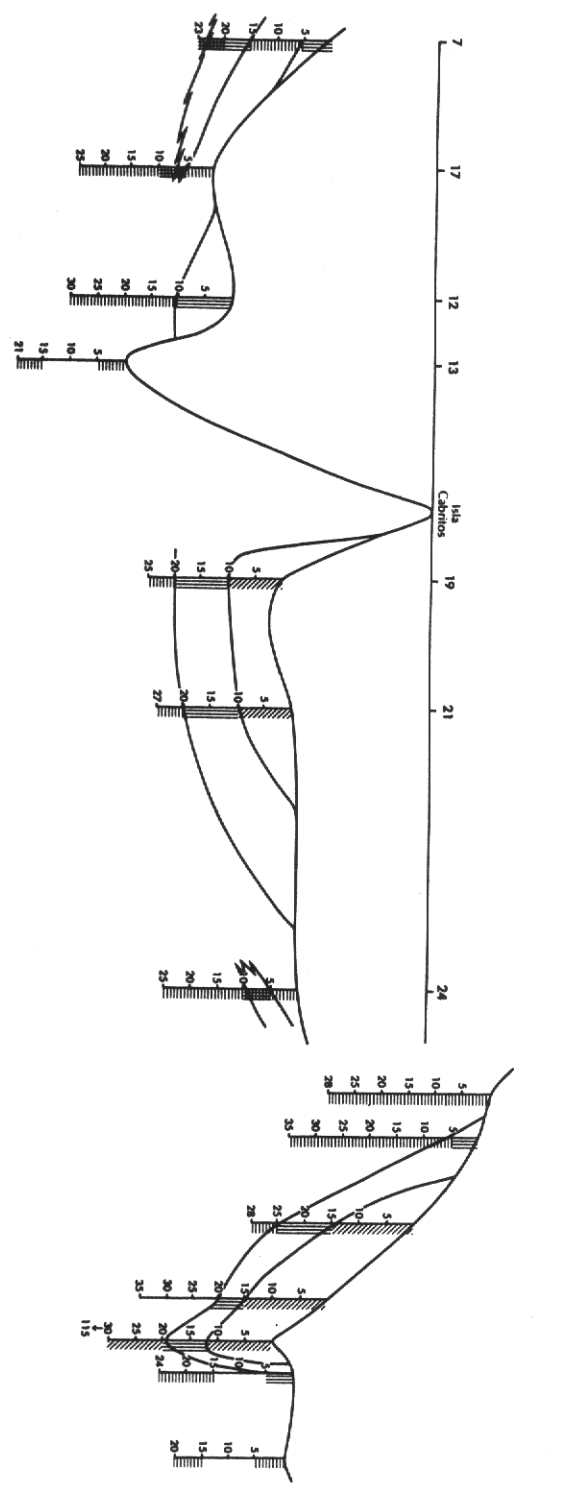

Text-fig. 2: Distribution of ostracode zones in Lake Enriquillo mud. Note the difference between the horizontal scale and two vertical scales (water depths and core lengths).

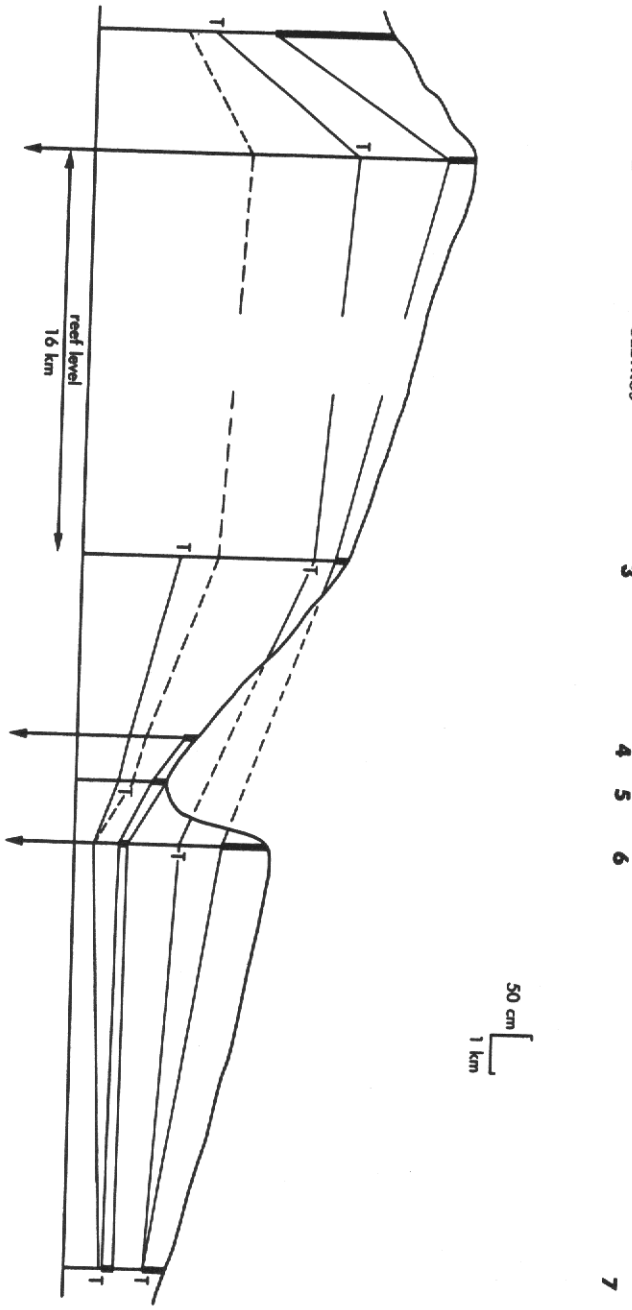

Text-fig. 3: Correlation of subaerially exposed sections above the Holocene reef.
I Cytheridella boldi horizons
T Tagelus plebius horizons
-----temporary disappearance of Cyprideis mexicana, C. similis and Peratocytheridea setipunctata.

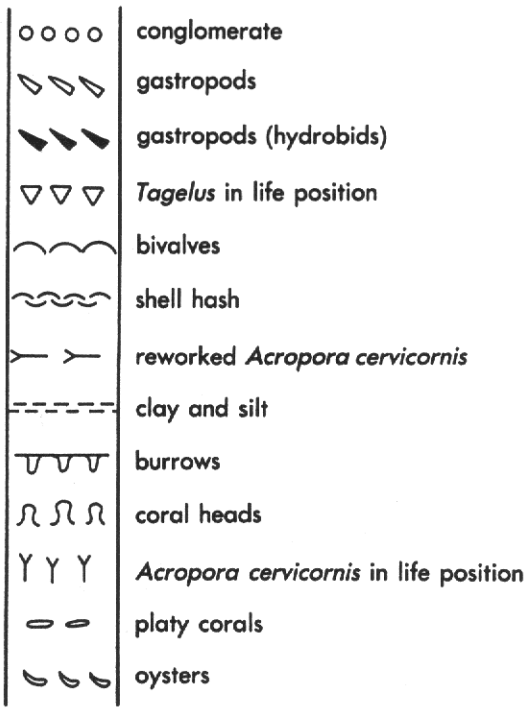

Text-fig. 4: Legend for the lithological columns of Tables 3-12.

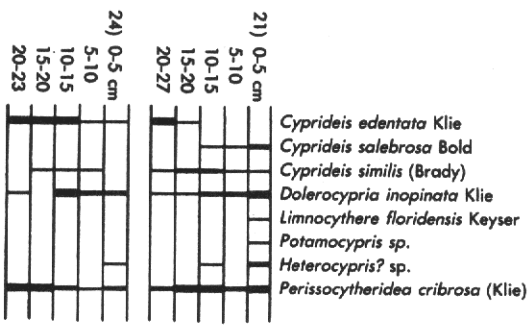

Table 1: Distribution of ostracodes in two short cores of Lake Enriquillo mud.

core no.	Depth in m.	0-5 cm	5-10 cm	10-15 cm	15-20 cm	20-25 cm	25-30 cm	30-35 cm
2	5	ED	ED>SM	ED	ED	ED	ED	ED
3	5	SM>ED	ED>SM	ED>SM	-	ED>SM	ED	ED
4	5.5	SM..ED						
7	5	SM>ED	ED>SM	ED>SM	SM>ED	SM=ED		
8	8.5	SA	SA	SA>SM	SM>ED	SM>ED	ED>SM	
9	12.5	SA	SM>SA	SM>SA	SM	-	-	-
10	14	SM	-		ED	ED	ED	
11	13	SM	SM	-	ED	-	-	
12	9	SM	SM	ED>SM	ED	ED		ED
13	14.5	ED	-	-	ED			
15	14.5	SM>ED	-	ED	ED	ED		
17	10.5	ED	SM=ED	ED	ED	ED		
19	7	SA	SA	SM	SM	ED>SM		
21	6.5	SA>SM	SA=SM	SM>ED	SM>ED		ED>SM	
24	6	ED>SM	SM=ED	ED>SM	ED	ED		
C2	15	SA>ED	SA	SA=SM	SM	SM	SA>SM	SA
		35-40	40-45	45-50	50-55	55-60	60-65	65-70
		SA	SA	SA	SA	SA	SA	SA
		70-75	75-80	80-85	85-90	90-95	95-100	10-105
		SA	SA	SA	SA	SA	SA	SA
		105-110	110-115					
		SA	SA					

Table 2: Dominant species of Cyprideis in cores of Lago de Enriquillo mud.

SA= C. salebrosa; SM= C. similis; ED= C. edentata; - no Cypridesi present.

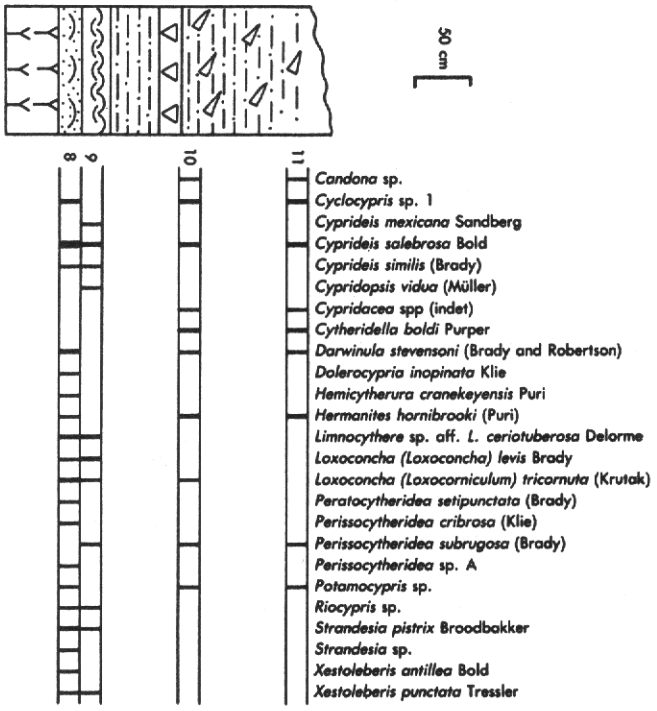

Table 3: Distribution of ostracoda in post reef sediments of the Cañada de Charco Salido section, and lithological column (Legend, see Text-fig. 4)

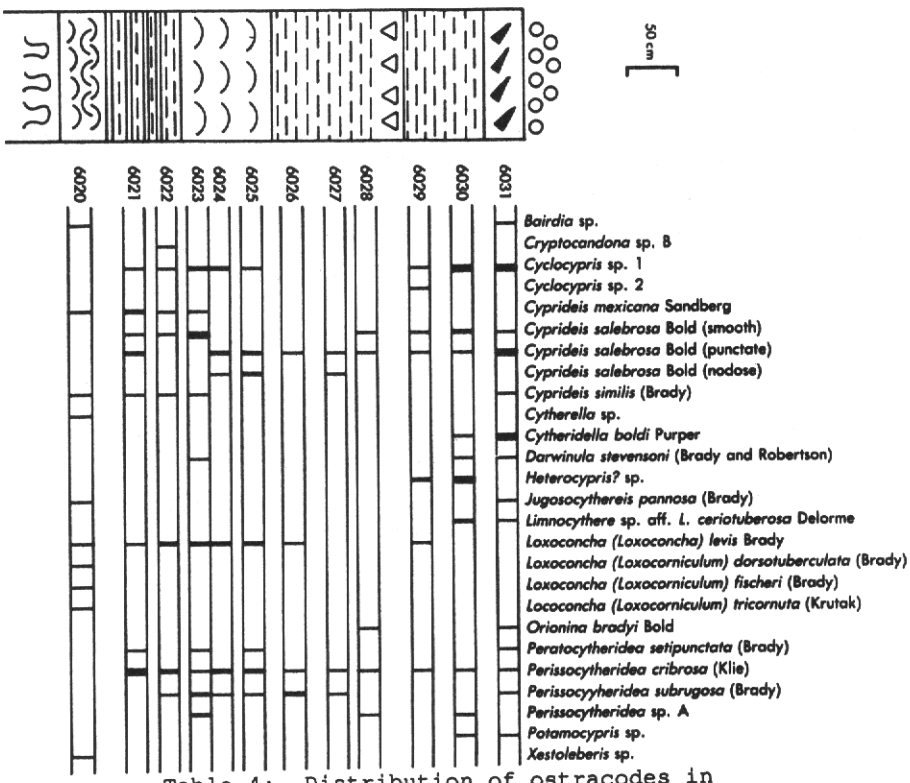

Table 4: Distribution of ostracodes in post reef sediments of the Arroyo el Aculadero section, and lithological column (Legend, see Text-fig. 4)

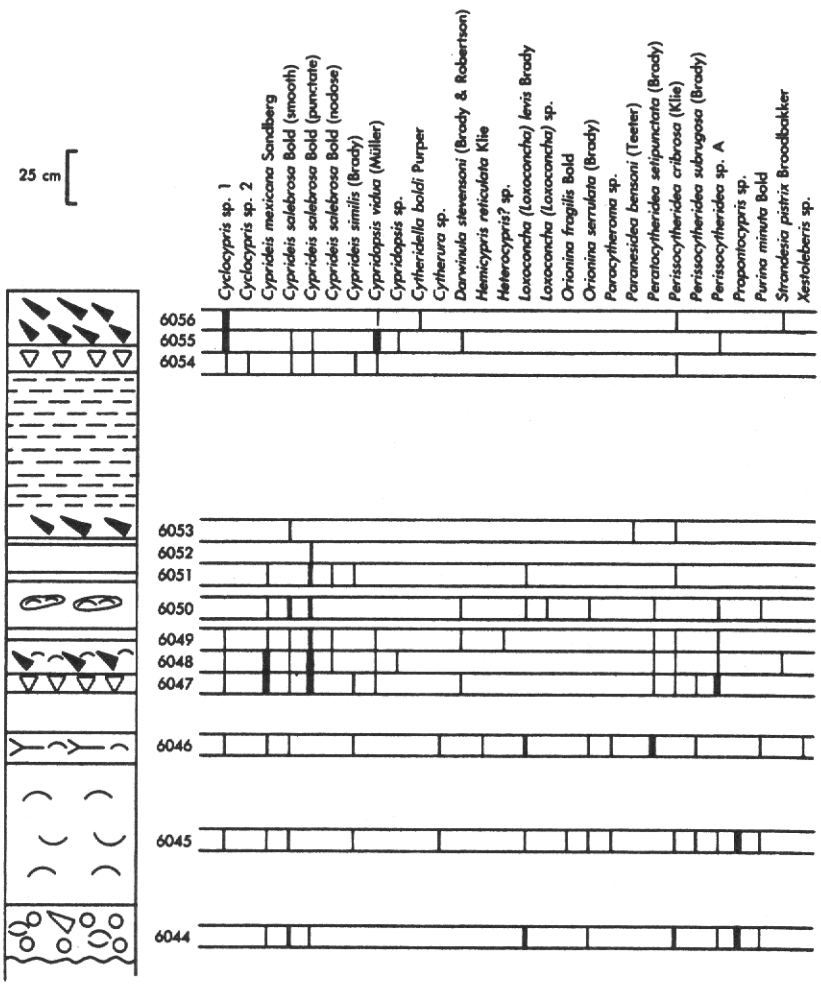

Table 5 Distribution of ostracodes in post reef sediments of "Big Bend" section with lithological column

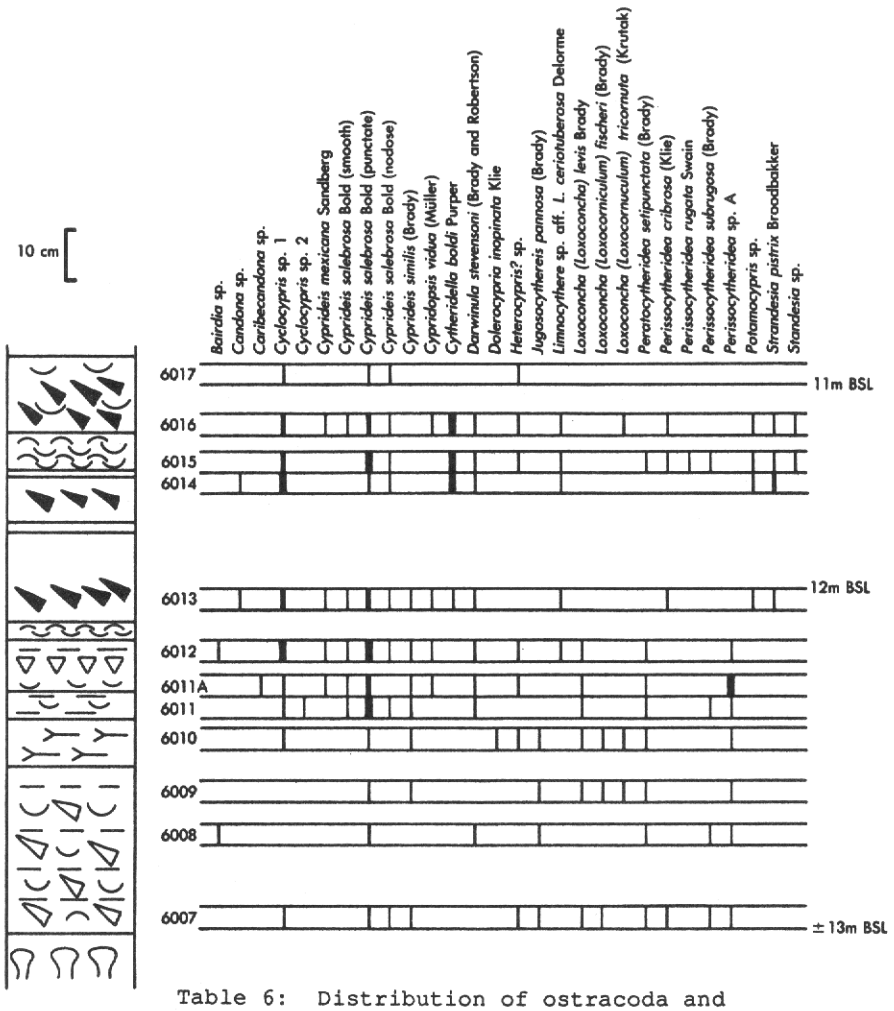

Table 6: Distribution of ostracoda and lithological column of post reef sediments in Cañada Honda, section I. (Legend, see Text-fig. 4)

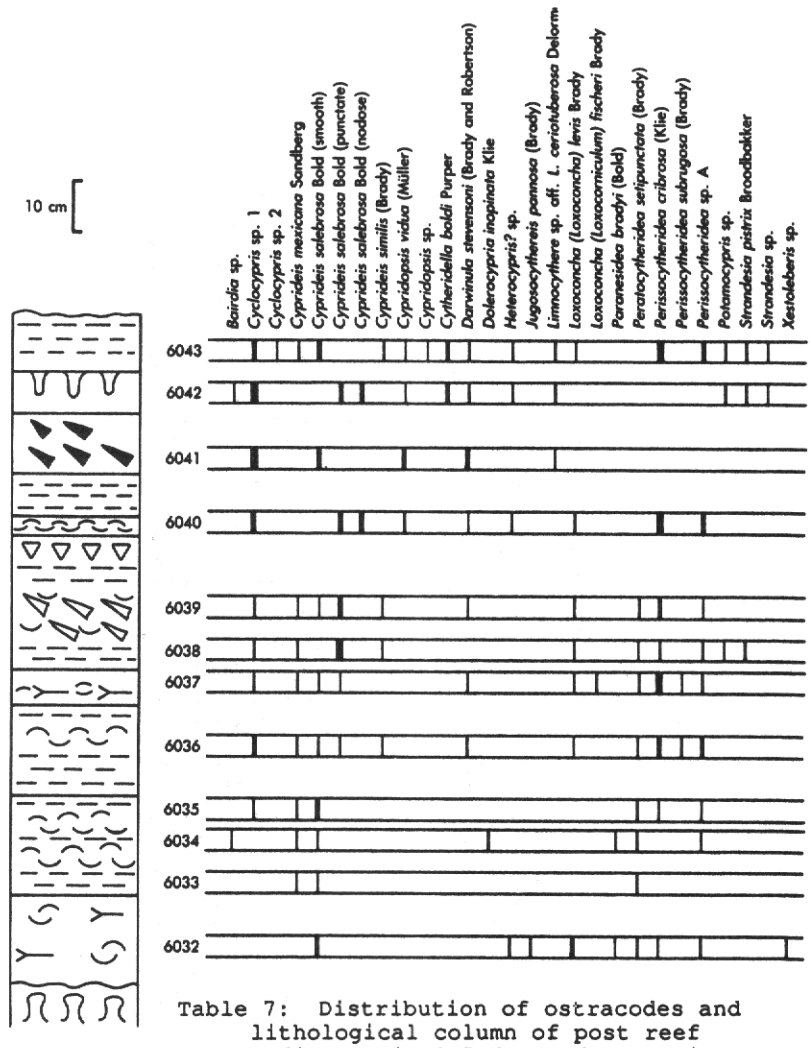

Table 7: Distribution of ostracodes and lithological column of post reef sediments in Cañada Honda, section II. (Legend, see Text-fig. 4)

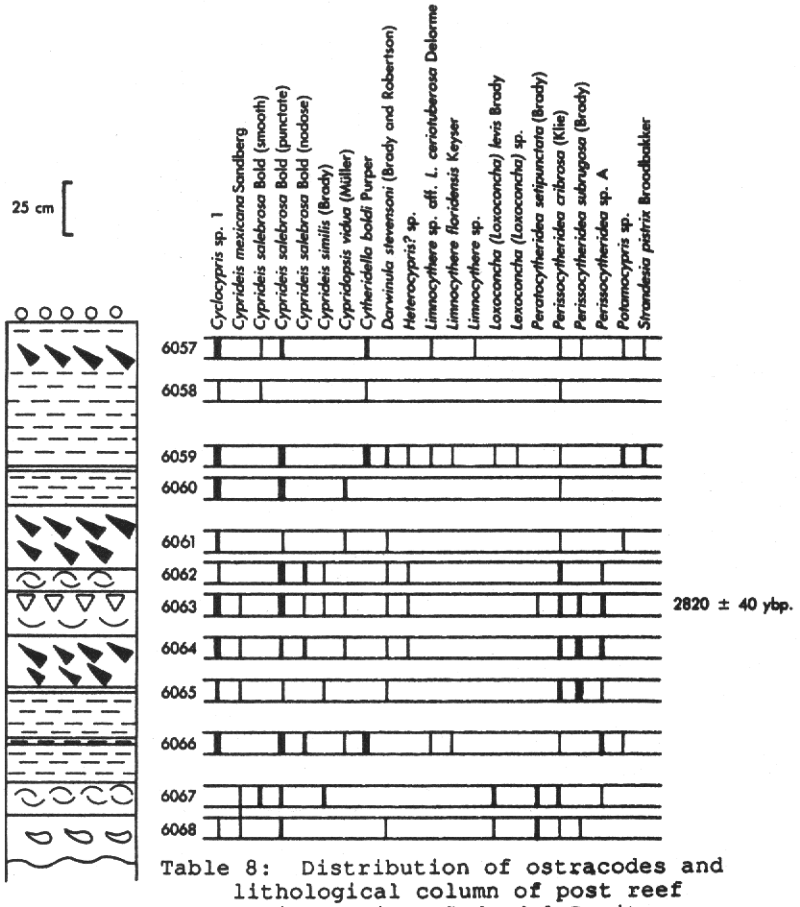

Table 8: Distribution of ostracodes and lithological column of post reef sediments in Cañada del Benito. (Legend, see Text-fig. 4)

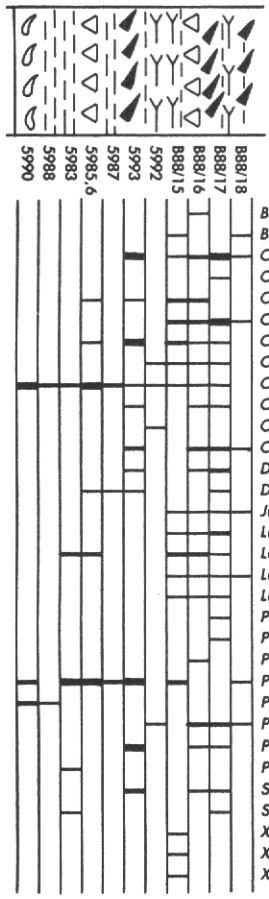

Table 9: Distribution of ostracodes and lithological column of post reef sediments in the Villa Jaragua section. (Legend, see Text-fig. 4)

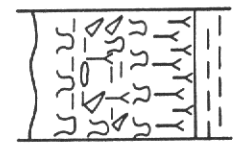

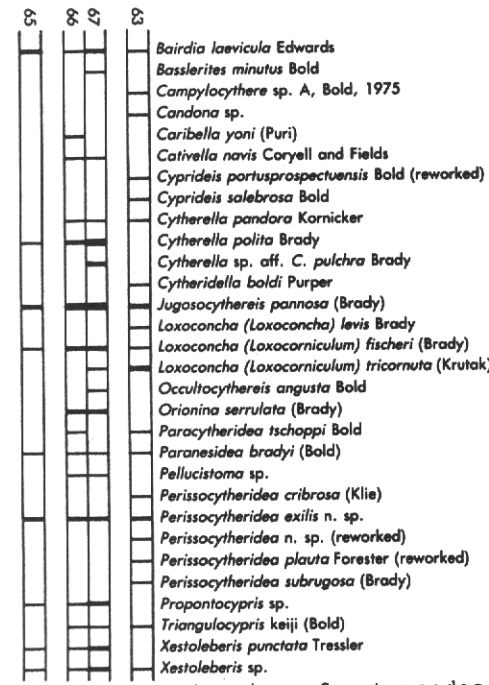

Table 10: Distribution of ostracodes and lithological column of reef sediments in the Arroyo el Aculadero section. (Legend, see Text-fig. 4)

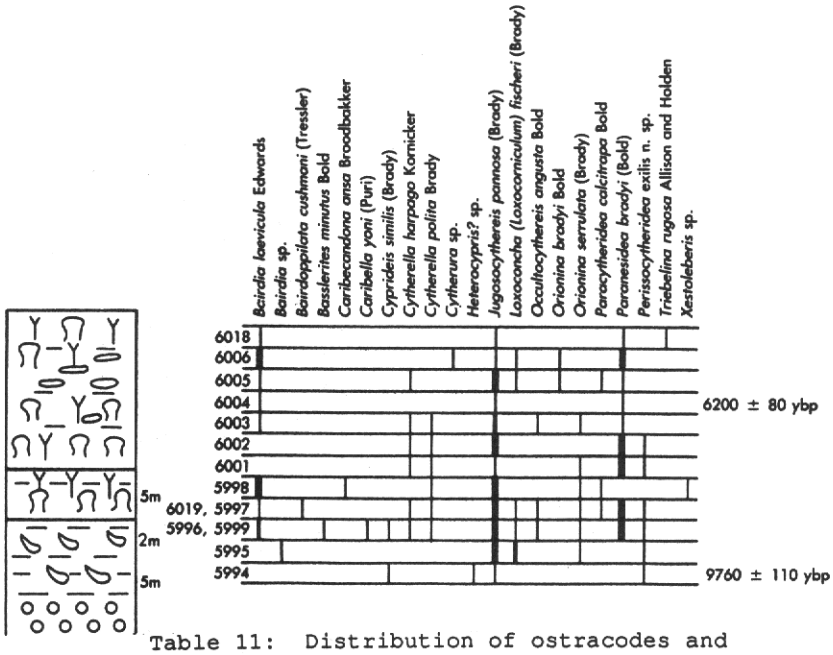

Table 11: Distribution of ostracodes and lithological column of reef and pre-reef sediments in the Cañada Honda section. (Legend, see Text-fig. 4)

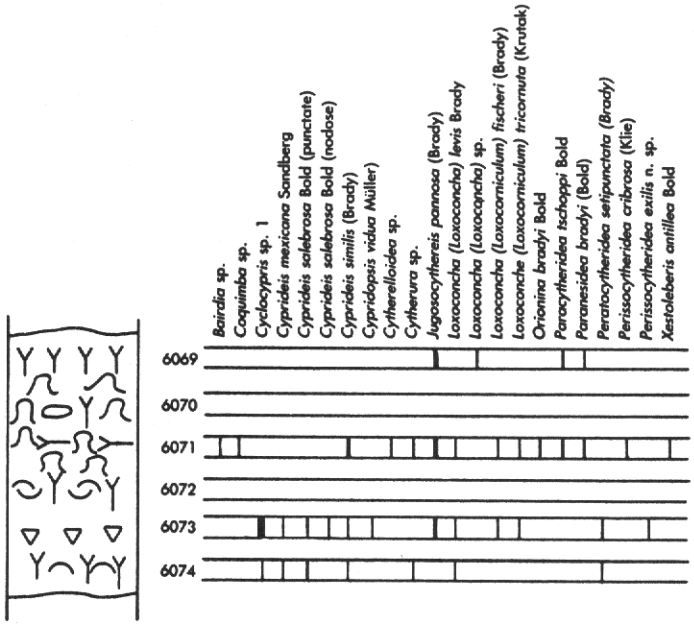

Table 12: Distribution of ostracodes and lithological column in reef sediments of the Cañada del Benito section (Legend, see Text-fig. 4)

Plate 1

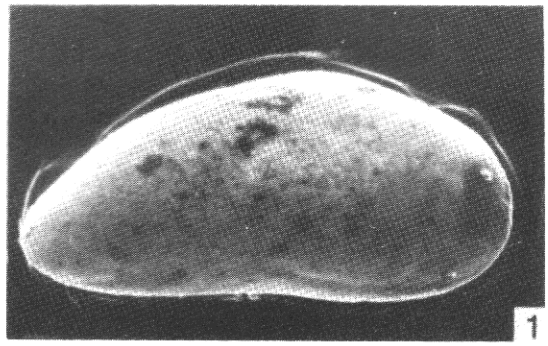
1

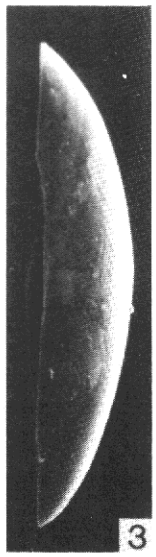
3

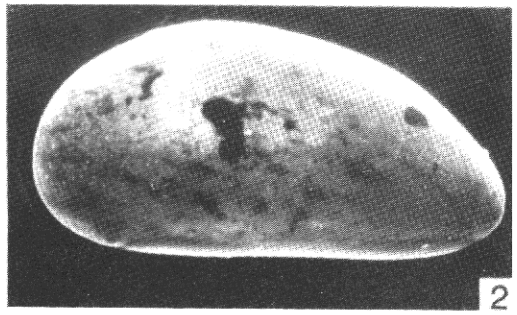
2

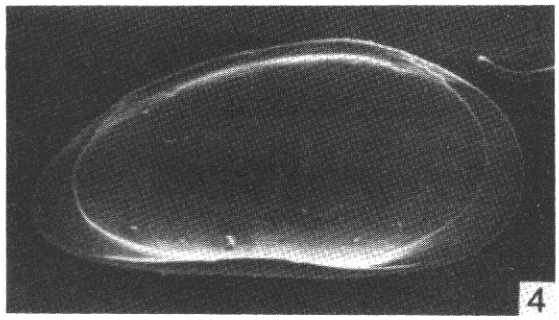
4

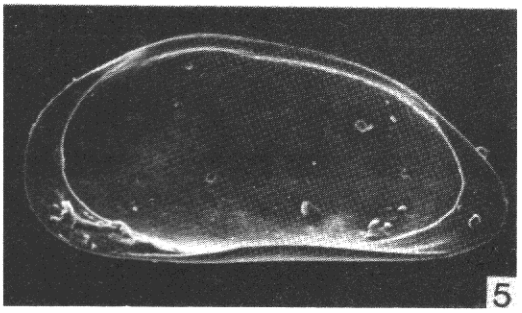
5

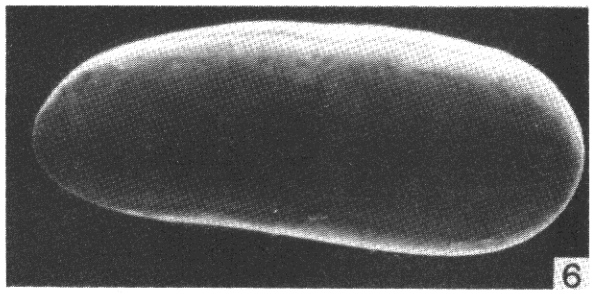
6

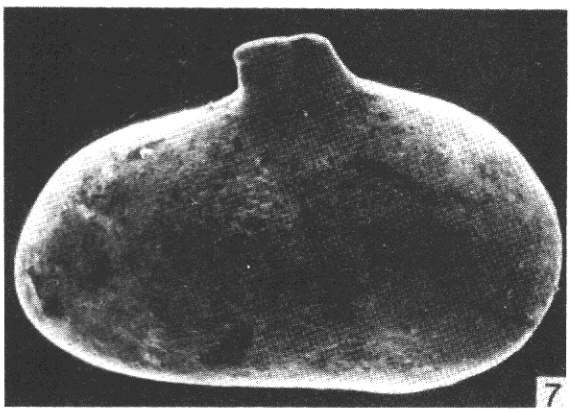
7

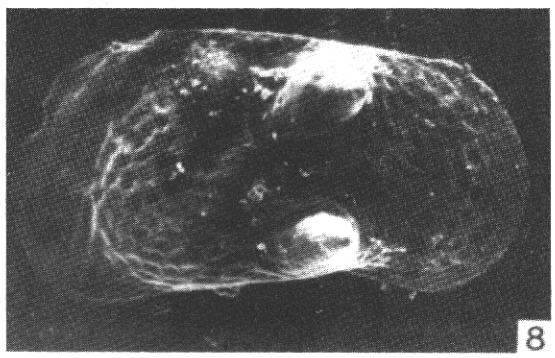
8

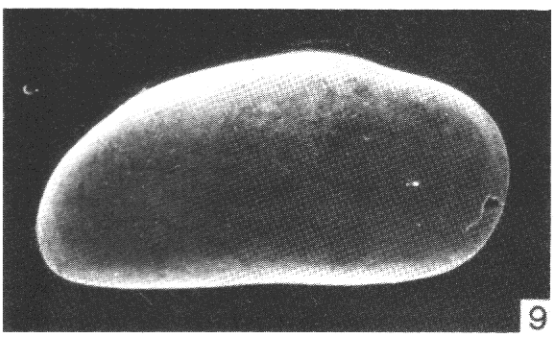
9

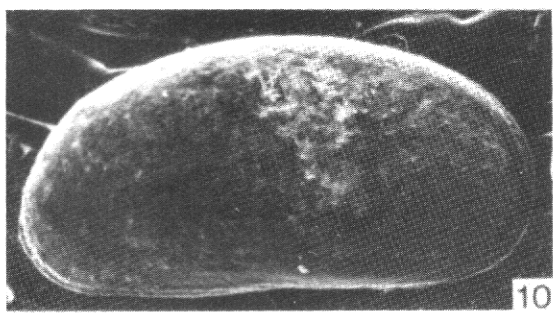
10

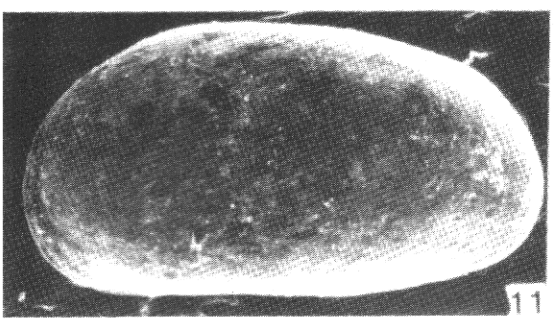
11

Plate 2

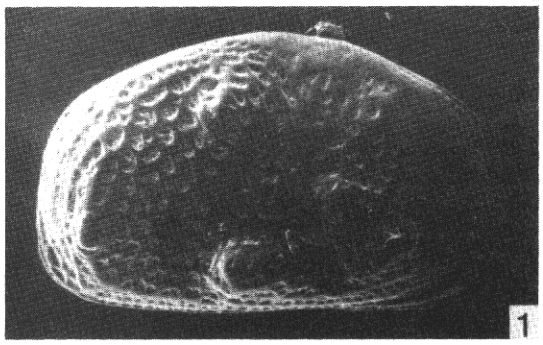
1

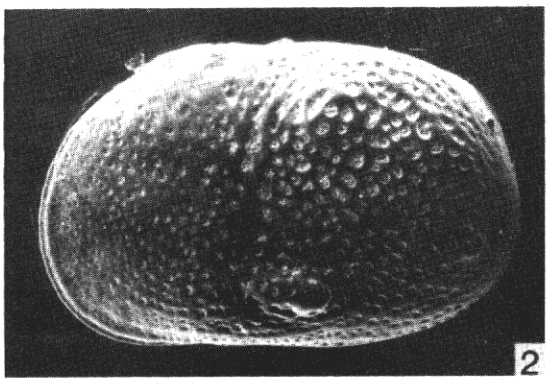
2

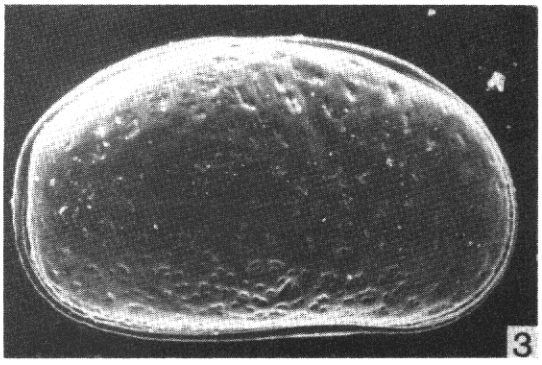
3

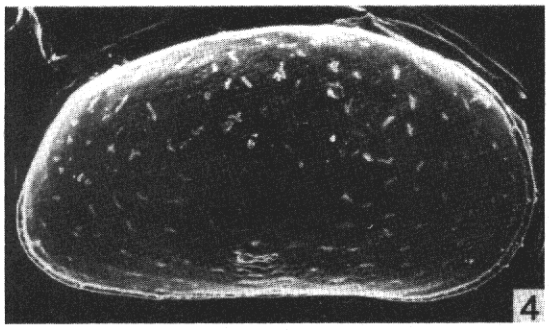
4

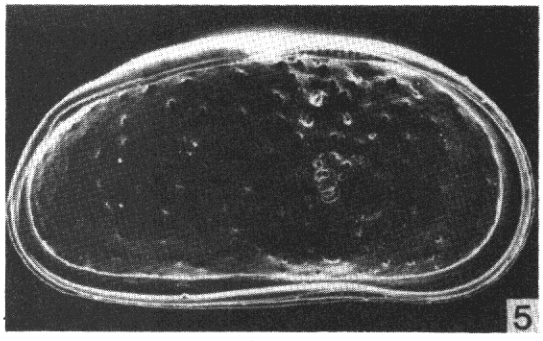
5

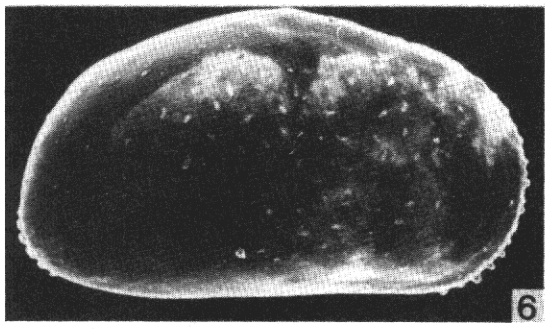
6

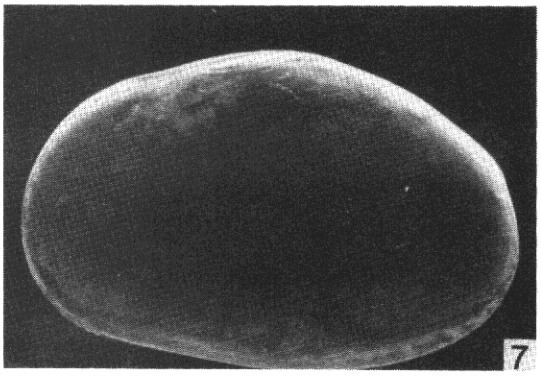
7

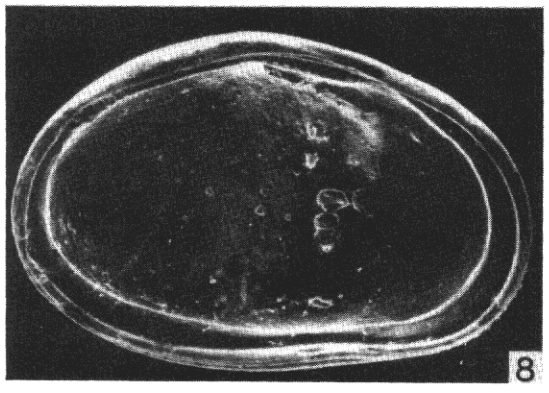
8

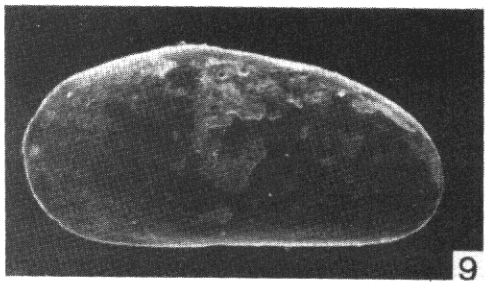
9

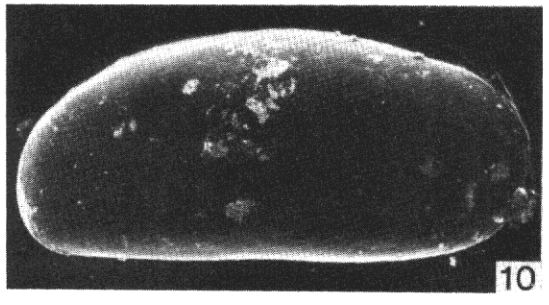
10

Plate 3

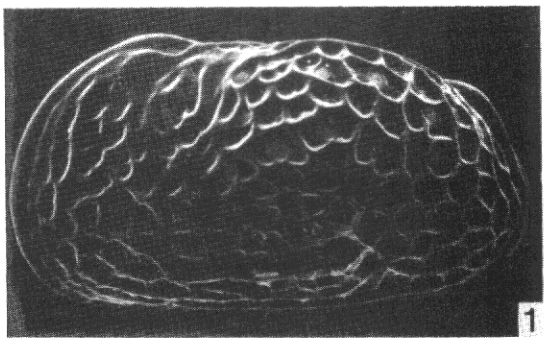
1

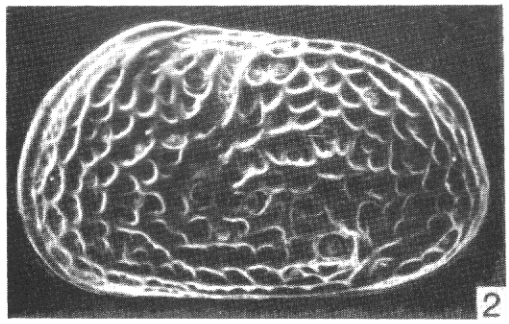
2

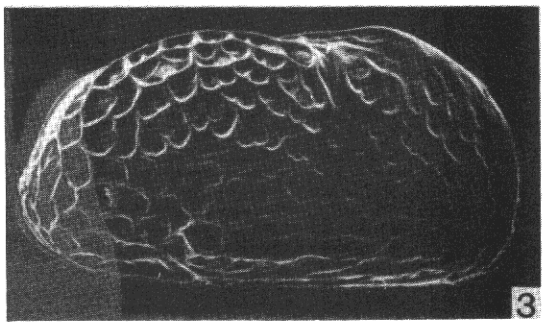
3

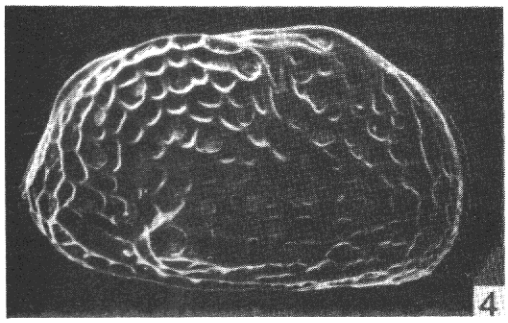
4

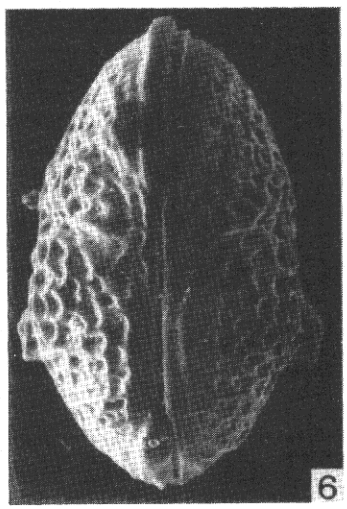
6

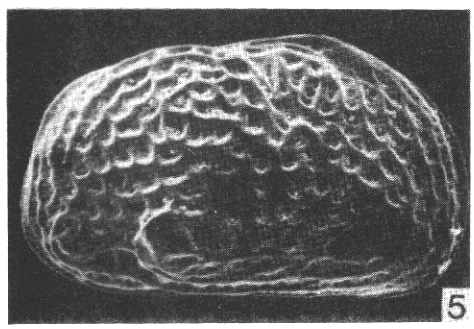
5

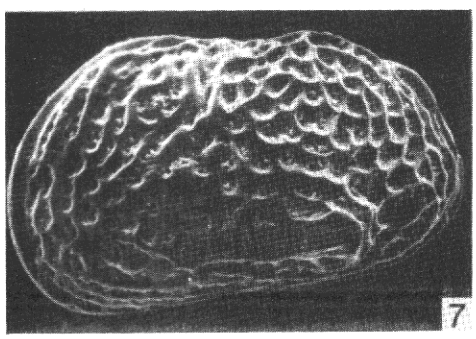
7

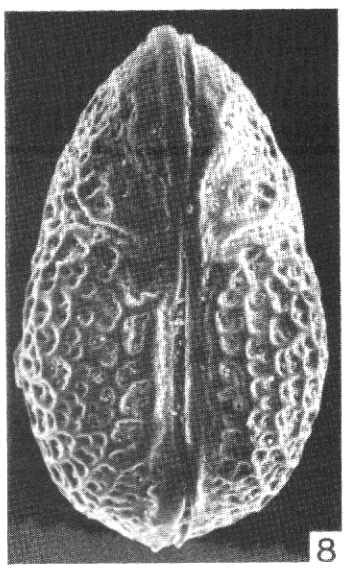
8

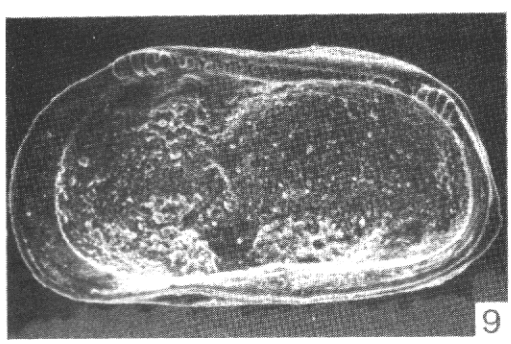
9

Plate 4

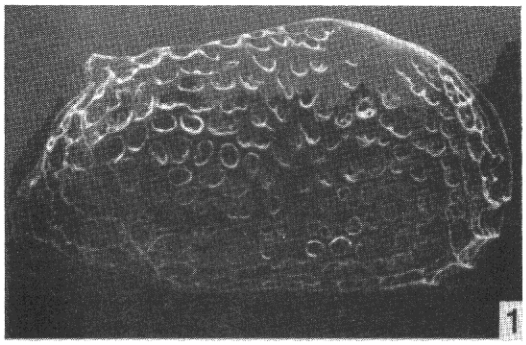
1

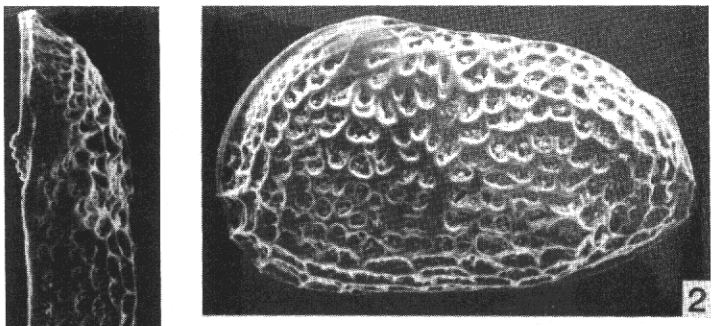
2

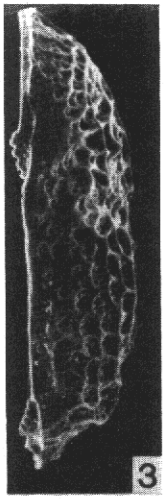
3

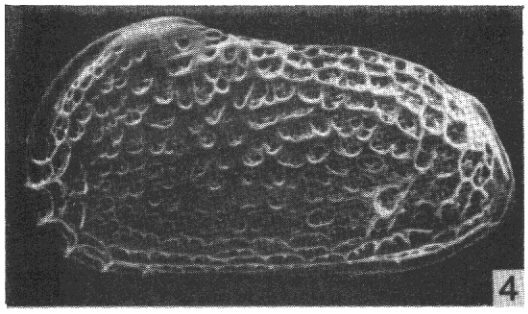
4

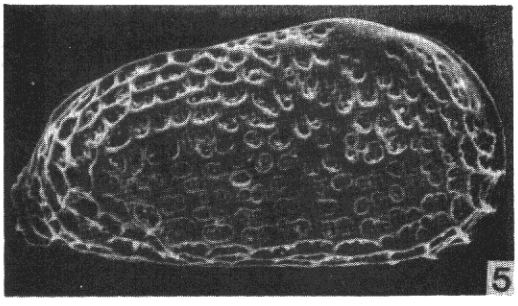
5

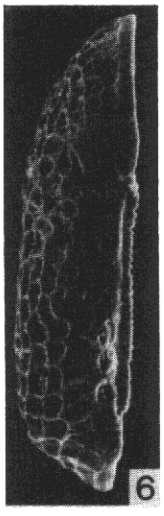
6

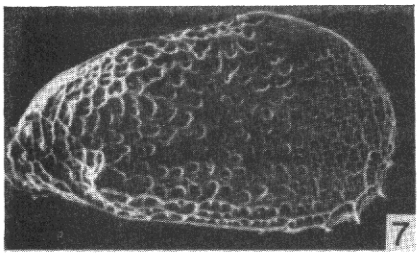
7

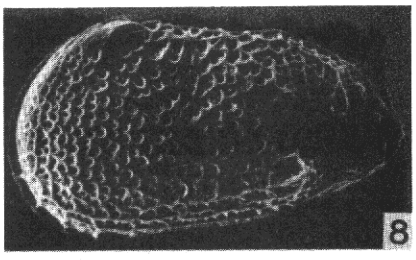
8

9

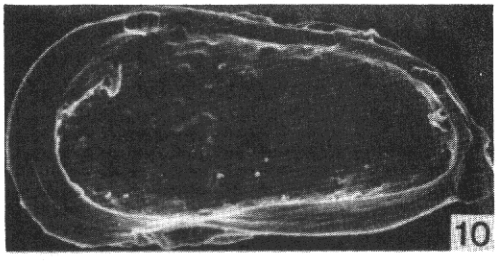
10

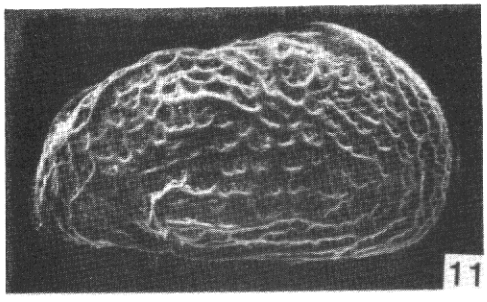
11

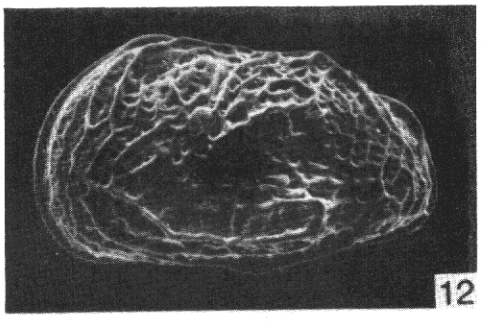
12

PLATE 1

Figs. 1-5: Propontocypris sp.; Bold, 88/7, marly lens in Holocene reef, illa Jaragua section; Magn. 150X. 1. outside of right valve, HVH no. 10927; 2. outside of left valve, HVH no. 10928; 3. dorsal view of right valve, HVH no. 10927; 4. inside of left valve, HVH no. 10928; 5. inside of right valve, HVH no. 10927.

Fig. 6: Darwinula stevensoni (Brady and Robertson); HVH no. 10930, Glenn 6030, Cañada del Benito. Outside of left valve; Magn. 150X.

Fig. 7: Strandesia pistrix Broodbakker; HVH no. 10931, Maddox 6014, Cañada Honda, upper hydrobid gastropod layer; outside of right valve; Magn. 150X.

Fig. 8: Limnocythere sp. aff. L. ceriotuberosa Delorme; HVH no. 10932, Glenn 6074, layer of mixed clams and A. cervicornis; outside of left valve; Magn. 200X.

Fig. 9: Dolerocypria inopinata Klie; HVH no. 10933, Core 2: 20-25 cm. Outside of left valve; Magn. 200X.

Fig. 10-11: Cyprideis mexicana Sandberg; HVH no. 10934, Glenn 6073, Cañada del Benito, Tagelus horizon. 10. outside of right valve; 11. outside of left valve; Magn. 100X.

PLATE 2

Figs. 1-2: Cyprideis salebrosa Bold; HVH no. 10935, Maddox 6025, Arroyo El Aculadero. Magn. 100X. 1. outside of female right valve; 2. outside of female left valve.

Figs. 3-5: Cyprideis edentata Klie; HVH no. 10936, Core 2: 20-25 cm; Magn. 100X. 3. right valve view of female carapace; 4. outside of male right valve; 5. inside of male right valve.

Figs. 6-8: Peratocytheridea setipunctata (Brady); HVH no. 10937, Maddox 6064, Cañada del Benito: Magn. 100X. 6. outside of female right valve; 7. outside of male left valve; 8. inside of female left valve.

Figs. 9-10: Dolerocypria inopinata Klie; HVH no. 10933, Core 2: 20-25 cm; Magn. 150X. 9. outside of juvenile left valve; 10. outside of male (?) right valve.

PLATE 3

Figs. 1-4: Perissocytheridea cribrosa (Klie); Core 2: 20-25 cm; Magn. 200 X. 1. outside of male left valve, HVH no. 10939; 2. outside of male right valve, HVH no. 10939; 3. outside of female left valve, HVH no. 10938; 4. outside of female right valve, HVH no. 10938.

Figs. 5-9: Periossocytheridea sp. A; Maddox 6023, Arroyo El Aculadero; Magn. 200X. 5. outside of female right valve, HVH no. 10940; 6. dorsal view of female carapace, HVH no. 10841; 7. outside of male left valve, HVH no. 10942; 8. dorsal view of male carapace, HVH no. 10943; 9. inside of male right valve, HVH no. 10944.

PLATE 4

FIGS. 1-10: Perissocytheridea exilis n. sp.; Magn. 200X.
1. outside of female right valve, holotype, HVH no. 10946, Sen Gupta 88/66, Arroyo El Aculadero, silty-marly pocket in Holocene reef; 2. outside of female left valve HVH no. 10947, same sample; 3. dorsal view of female right valve, HVH no. 10955, Glenn 5999, Cañada Honda, top of red oysterbed; 4. outside of male left valve, HVH no. 10948, Sen Gupta 88/66; 5. outside of male right valve, HVH no. 10949, same sample; 6. dorsal view of male left valve, HVH no. 10950, same sample; 7. outside of juvenile right valve, HVH no. 10951, same sample; 8. outside of juvenile left valve, HVH no. 10951; 9. inside of female right valve, HVH no. 10954, Glenn 5999; 10. inside of male right valve, HVH no. 10952, Sen Gupta 88/66.

Figs. 11-12: Perissocytheridea sp. A, HVH no. 10945, Glenn 6023, Arroyo El Aculadero. Magn. 200X. 11. outside of juvenile right valve; 12. outside of juvenile left valve.

PETROGRAPHY AND GEOCHEMISTRY OF MAFIC ROCKS OF THE PERALVILLO FORMATION IN THE SABANA POTRERO AREA, CENTRAL DOMINICAN REPUBLIC

J. Espaillat, G. Bloise, and J.G. Macveigh, Falconbridge Dominicana, C por A., Dominican Republic
Lewis, J.F., The George Washington University, Washington, D.C., U.S.A.

ABSTRACT

Mafic volcanic rocks composed of pillowed and massive units together with minor hyaloclastites, with a thickness of between about 1200-2300 m form a narrow belt immediately north of the Loma Caribe serpentinized peridotite within the Median Belt, in the central Dominican Republic. At Sabana Potrero a zone of altered rock with disseminated sulfide and stockwork, structurally overlies massive sulfide ore bodies within the mafic volcanic rocks. The structural and stratigraphic information indicates that these mafic and volcanic rocks form the base of the Peralvillo formation of apparent Late Cretaceous age and are probably equivalent to the vitric and crystalline basalts of the Siete Cabezas Formation to the south of the peridotite belt.

The texture of the volcanic rocks ranges from fine-grained microporphyritic to poorly-developed sub-ophitic to granular textures in the coarse-grained varieties. Clinopyroxene and plagioclase make up 90% of the rocks. The dominant alteration minerals are chlorite, prehnite, and epidote. Iron titanium oxide minerals are ubiquitously replaced by leucoxene. Mafic lavas and intrusives (diabases) have been analyzed for major and trace elements mainly from the drill cores of the Sabana Potrero area, but also from surface exposures. Most of the rocks are olivine-hypersthene normative and some contain normative quartz. TiO_2 ranges from 0.43 to 2.8% and varies with the Fe/Mg ratio allowing correlations of different flow units between drill holes. Variation diagrams show that both the lavas and intrusive phases belong to a comagmatic sequence.

Chondrite-normalized Rare Earth plots show enrichment in Ce over La, depletion in Nd and a positive Eu anomaly. Trace element spider diagrams, normalized to N Type MORB, show consistent patterns for all samples. Characteristic features are relative enrichment of Ce over La, 2 to 7 times enrichment in Nb and Ta, and slight depletion in Nd. Relative concentrations of Ti, Zr, Hf, Y are constant and similar to those of present-day ocean floor (MORB) basalts. Sabana Potrero basalts are chemically distinct from Duarte metabasalts.

INTRODUCTION

Peralvillo (mispelled as Peravillo) Formation was the name given by Bowin (1966) to a narrow belt of essentially unmetamorphosed rocks that lie between the Loma Caribe peridotite and the schistose rocks of the Maimon Formation within the Median Belt of the Cordillera Central (Fig. 1).

Bowin (1966) recognized three volcanic rocks types within the Peralvillo Formation, namely fine and course tuff, lapilli-tuff and microporphyritic aphanitic volcanic rocks. The most common volcanic flow rocks were described as pyroxene andesite with microphenocrysts of plagioclase and clinopyroxene. An outcrop of calcareous black pelite with abundant carbonaceous material from south of Yamasa was also described.

Boisseau (1987) reported on several measured sections in the Peralvillo Formation. He described the sequence exposed in the Arroyo Toro as consisting of layered gabbro at the base and overlain by basalts intruded by diabase. These basic rocks are in contact with the Loma Caribe peridotite to the south. This is similar to the section measured by Jimenez from the Arroyo Los Martinez (Jimenez and Lewis, 1989), except that Jimenez did not find gabbro at the base of the section in contact with peridotite. Even though the exact nature of the gabbroic rocks and the nature of the contact with the peridotite to the south is not clearly established the association of basic rocks with the peridotite is suggestive of an ophiolitic sequence as pointed out by Boisseau (1987). The upper part of the sequence above the basalts in the Arroyo Toro and Arroyo Los Martinez consists of volcaniclastic and epiclastic sedimentary rocks including varicoloured cherts. Unfortunately, radiolaria from these cherts did

Larue, D.K., and Draper, G. (eds.), ***Transactions of the 12th Caribbean Geological Conference, St. Croix, U.S.V.I.***, Miami Geological Society, P.O. Box 431552, South Miami, FL 33243, U.S.A

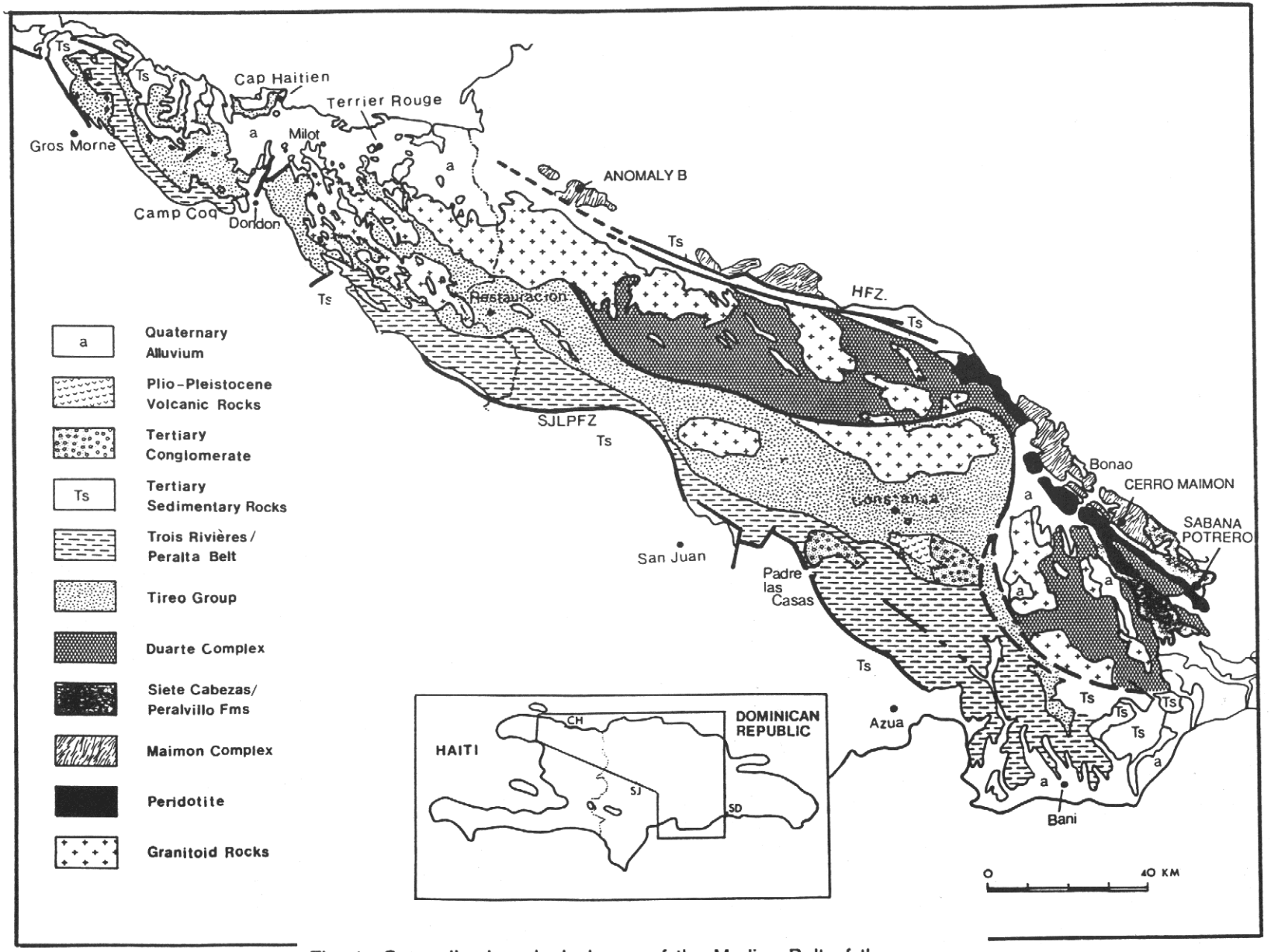

Fig. 1 Generalized geological map of the Median Belt of the Dominican Republic showing the Peralvillo Formation north of the peridotite belt and the location of the Sabana Potrero, Cerro Maimon and Anomaly B prospect areas (Brouwer and others, 1989).

not give an age more precise than Cretaceous (determinations by P. de Wever, in Boisseau, 1987). However, Boisseau (1987) tentatively correlated these cherty beds in the Peralvillo with similar sedimentary rocks in the upper part of the Siete Cabezas Formation which gave a Cenomanian-Turonian age (Boisseau, 1987).

In the quest for massive sulfide mineral deposits geologists from Falconbridge Dominicana have had the opportunity to examine the rock types within the Peralvillo belt in two areas, namely at Cerro Maimon, east of the town of Maimon, and at Sabana Potrero. A summary of the recent work on the geology at Cerro Maimon was presented at the 12th Caribbean conference by Jimenez and Lewis (1989). The work in both these areas has shown the geology is far more complicated than in the preliminary description given by Bowin (1966).

GEOLOGY

This is an initial report concerned within the small area under prospection by Falconbridge Dominicana at Sabana Potrero located 4.5 km southwest of the town of Yamasa (Fig. 1), and 25 km east of Cerro Maimon and the Arroyo Los Martinez. A preliminary map of the geology over an area of just less than one square kilometer at Sabana Potrero is given in Figure 2. The dominant rocks in the area are aphanatic pillow basalts intruded by diabase, but details of the alteration and contacts between pillows and intrusive phases are best studied in drill cores. The mafic rocks lie to the north of, and for the most part are in fault contact with an arm of the Loma Caribe serpentinized peridotite. Small bodies of metamorphosed diabase and gabbroic rock, some with banding, are included in the serpentinized peridotite.

A narrow east-west belt, about 100-150 meters wide at the surface, and more than 100 m thick, of altered (bleached) rock with disseminated sulfide and stockwork (quartz-sulfide veins), structurally overlies restricted massive sulfide ore bodies (Figs. 2 and 3). Boulders of highly oxidised mafic rocks (gossan) occur at the surface above the massive sulfide deposits. The mineralization in the stockwork is irregular and patchy and is mainly in the form of anastomizing veins and veinlets of silica (both quartz and jasper) and sulfide (mainly pyrite with minor chalcopyrite). Chlorite is pervasive through the stockwork zone and occurs within the veins, often as large clots. Epidote is rare in the stockwork zone. The massive sulfide is composed of mainly pyrite with chalcopyrite and minor sphalerite.

The massive sulfide ore bodies are distributed at depth along a north-west trend (parallel to the regional trend) and dip to the south. The trend and position of the massive sulfide deposits have been interrupted and restricted by the mafic intrusive bodies. The southerly dip and the form of the stockwork above the massive sulfide suggests the sequence is overturned.

The mafic volcanic rocks are composed of pillowed and massive flow units (eg drill hole SP-19). The pillowed units can be subdivided on the basis of their selvage characteristics into those consisting of thick well-developed selvages with massive epidote, jasper and chert and those containing irregular cavities with epidote-quartz-chlorite. Laminated cherts within the flow units in hole SP-17 indicate a sedimentary origin for at least some of the chert. In places the pillows are brecciated and in thin section appear granulated and sheared. Fracture fillings composed of quartz, epidote and carbonate are common.

The flow units are fine to medium-grained rocks . Chilled flow contacts can be observed within the flow units with epidote alteration prominent along contacts. Flow textures are most prominent in the fine-grained rocks beneath the massive sulfide, although textures in the mafic volcanic rocks above the massive sulfide have been obscured by the more extensive alteration in these rocks.

In the footwall to the massive sulfides the mafic volcanic rocks are cut by coarse-grained massive mafic rocks. The intrusive phases are recognised by their coarse grain size, relative freedom from alteration and mineralization, and cross-cutting contacts. These rocks show the same basic mineralogical features as the flow units. In the hanging wall, the alteration is similar in both fine and coarse-grained rocks so that it is difficult to distinguish the intrusive phases.

The medium- and course-grained rocks are composed of mainly clinopyroxene and plagioclase and show a sub-ophitic texture. Skeletal ilmenite/titanomagnetite, almost entirely altered to leucoxene is prominent in some rocks. Chlorite alteration is pervasive and chlorite makes up to 25 per cent of some rocks. Plagioclase is commonly albitised. Finer-grained rocks are microporphyritic with laths of plagioclase and pyroxene in a fine-grained

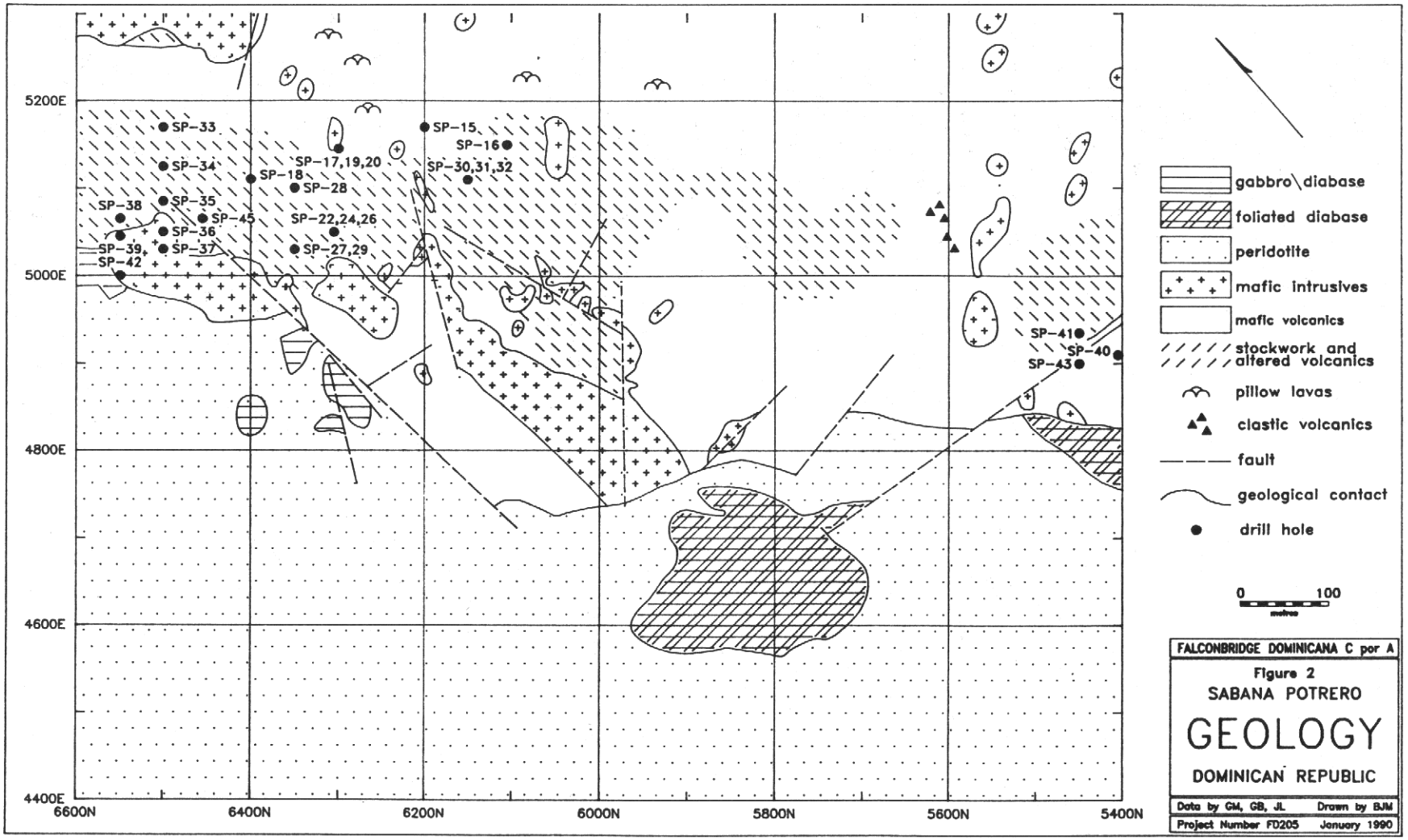

Fig. 2 Geological map of the Sabana Potrero area. Numbers (SP-15 etc.) give location of drill holes.

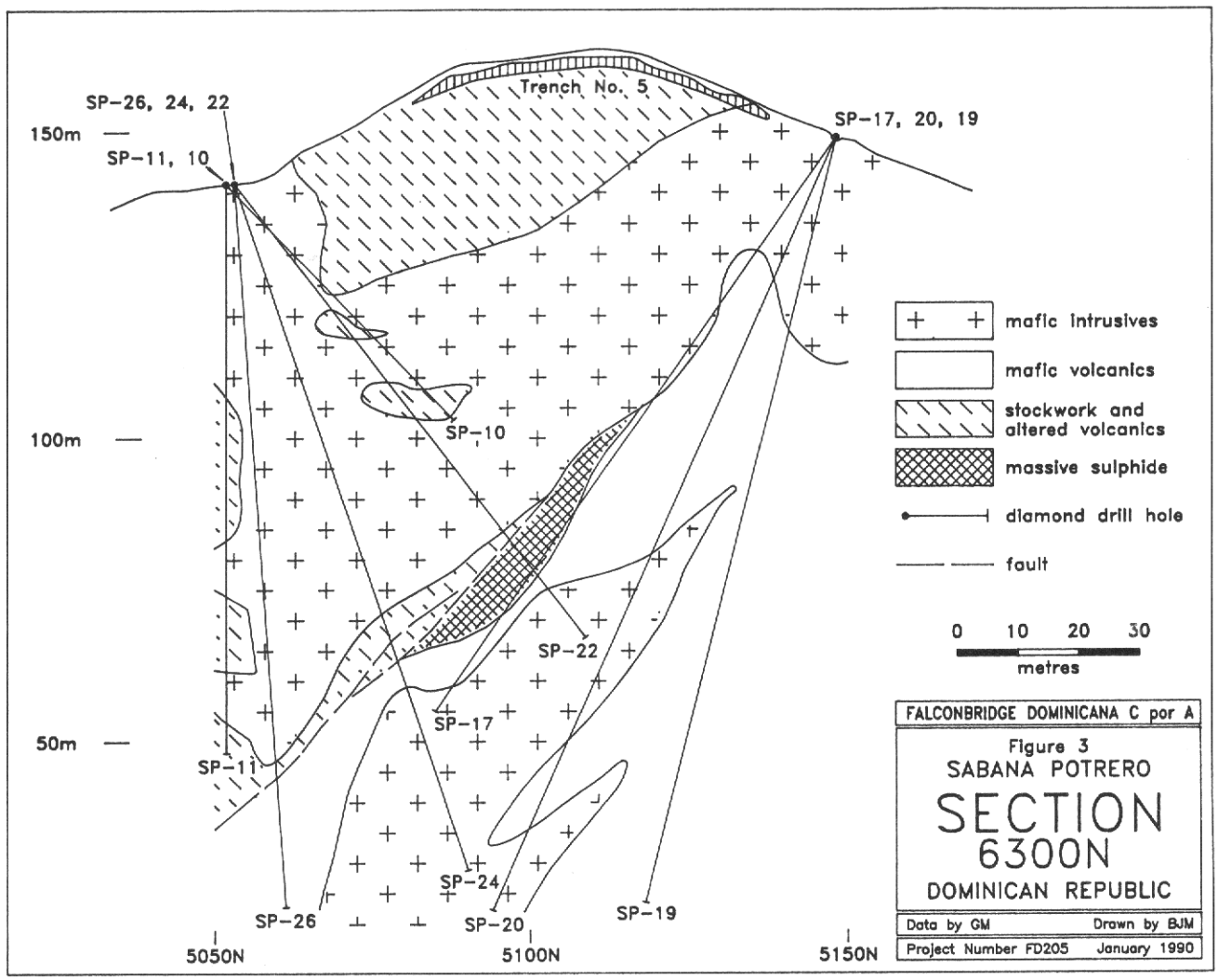

Fig. 3 North-south cross section through drill holes SP-17,19,20 and SP-22,24,26 showing relations between basalt flows, mafic intrusive phases, stockwork and massive sulfide ore.

matrix. Thus the rocks have a low grade greenschist assemblage and can be loosely referred to as spilites.

This pervasive alteration and the extensive veining in the Sabana Potrero basalts is common in mafic rocks erupted on the sea flow described from other areas. However, at this time the nature of the alteration at Sabana Potrero and degree of mobility of the elements has been examined in only a general way.

GEOCHEMISTRY

At the time of writing thirteen drill holes have been sampled for chemical analysis. Forty-two whole rock analyses of all textural types have been made for both major and trace elements. Of these, 30 samples have been analyzed for trace elements including Rare Earth elements (REE). Major elements were determined by X-ray Fluorescence on fused powders. Representative analyses are given in Table 1. The Loss on Ignition (LOI) value, which varies between 2 to 3 percent in most of the rocks is due to water present in alteration minerals, mainly chlorite. The overall similarity in the analyses is immediately apparent but there is some significant variation. The rocks are hypersthene-olivine normative tholeiites. Only two of the analyses (from core SP-36) are quartz normative, showing that the rocks are basalts even though some samples show up to 54% SiO_2 when calculated on a water-free basis.

TiO_2 varies from 0.43% to 2.31% and is highest in the main flow rocks analysed from cores SP-16, SP-17 and SP-22. The MgO content ranges from 4.63% to 9.31% and varies inversely with TiO_2. The highest MgO content is in sample SP-28/70.2 and this lava has the lowest TiO_2 content (Table 1). Na_2O is relatively high in comparison with most present day fresh young basalts suggesting that this element might have been concentrated by sea water alteration.

Variations in major element chemistry and the chemical relations between the flows and intrusive phases can be examined using a TiO_2:FeO/MgO diagram (Fig. 4). Samples showing the lowest TiO_2 and lowest FeO/MgO ratio are those from the middle flows from drill cores SP-27 and SP-28. Samples from flows lower down in these cores contain almost twice as much TiO_2 with only slightly higher FeO/MgO ratios and presumably represent a different magma batch.

In contrast, definite flow rocks from drill holes SP-17, 19 and 20 show the highest TiO_2 contents and highest FeO/MgO and must represent the most differentiated lavas. Unique parallel trends can be distinguished for the flow rocks from drill holes SP-17 and SP-19 (although some points lie off the trends). These linear trends are surprising since the rocks are altered to low grade greenschist assemblages which would suggest that Fe and Mg would probably have been mobilised. Samples SP-26/28.65 and SP-24/113.5 are gabbroic rocks and represent an intrusive phase into the lavas. These rocks have a lower TiO_2 content and lower FeO/MgO ratio than most of the lavas analyzed from SP-17, 19 and 20. On the other hand sample SP-26/105.6 (lower in the drill hole) is a definite volcanic rock and is assumed to lie below the sulfide zone (Fig. 3). The chemistry of this rock is very similar to the intrusive sample above and different from most of the more fractionated lavas from higher in drill holes SP-17 and 19 and discussed earlier. Sample SP-19/19.38 from the top of hole SP-19 is correlated with the intrusive rock in holes SP-24 and SP-26 (Fig. 3).

The three samples analysed from drill hole SP-30 are from both the volcanic and diabase facies of the drill core. All three analyses are similar in composition and plot in a field along with other analyses approximating 1.3 to 1.6% TiO_2 and an FeO/MgO ratio ranging from 1.6 to 1.9. In fact, one half of the Sabana Potrero samples so far analysed fall in this compositional range. This could therefore be the main parental magma composition from which the magmas such as represented in the cores from drill holes SP-17, 19 and 20 with higher FeO/MgO fractionated.

Analyses for 25 trace elements were made on 30 samples using multi-element techniques. Most trace elements, including the Rare Earth Elements (REE), were determined by Instrumental Neutron Activation Analysis at the McMaster University Reactor Facility by Neutron Activation Services (NAS). Rb, Sr, Ba, Cr, Zr, Nb and Y were determined by X-ray Fluorescence. In order to demonstrate the characteristic features and comparisons the trace element data of representative samples have been normalized to N-Type MORB and plotted in a multi-element (spider) diagram (Fig. 5). Because the rocks have undergone low grade metamorphism, which probably included sea water alteration, the least mobile elements such as Nb, Ta, Zr, Hf, Ti, Y, Th and the REE's should be used as discriminants.

Important features are:

1) Sabana Potrero basaltic rocks display relatively high Nb-Ta concentrations. Nb in all samples ranges from two times to almost seven times N-Type MORB.

2) La/Ce ratios (N-Type MORB normalized) are negative, in contrast to Duarte metabasalts, in which they are positive.

3) In a few samples HFS elements show concentrations slightly above those of N-Type MORB but in most samples the concentrations are almost equal to, or are lower, than N-Type MORB. Sample 28/70.2 is distinctly depleted in P, Ti, Y and Tb with respect to N-Type MORB.

4) On the Rare Earth Element (REE) plot, normalized to chondrite (Fig.6), the samples show flat to jagged (sea-saw) patterns and concentrations of between about five times and twenty-five times chondrite. Most samples show relatively high concentrations of Ce and Eu, and depletion in Nd. Three samples from drill holes SP-27 and SP-28 show depletion in the light REE.

5) The variation in REE's in the Sabana Potrero basalts differs from the typical patterns of metabasalts from the lower unit of the Duarte Complex which shows smooth rotated patterns with high concentrations of light REE's (Draper and Lewis, 1989; 1990 submitted).

6) In terms of their Ti-Y-Zr ratios (Fig. 7) (using the discriminant diagram of Pearce and Cann, 1973) most of the Sabana Potrero basalts fall in the Ocean Floor basalt field (OFB).

One chemical analysis is presented (Table 1) of an altered volcanic rock (SP-26/22.16) from the stockwork zone. In comparison with the analyses of the main zone of mafic volcanic rocks (Table 1) this rock has lost most of its Ca, Na, K, and some Al and Mn. The rock has gained some Si, Fe, possibly Mg and H_2O and other volatiles. Except for an apparent loss of some Ni the trace elements seem to be relatively immobile. Note the difference in the chemistry of this type of alteration associated with the stockwork as opposed to the alteration associated apparently with sea water, producing greenschist-type mineral assemblages through the major zone of mafic volcanic rocks.

SUMMARY AND CONCLUSIONS

The data presented here are the initial results of a detailed study over a limited area of a sequence of submarine tholeiitic basalts of apparent Late Cretaceous age within the Peralvillo Formation.

The basaltic pile at Sabana Potrero which approximates 1200-2300 m in thickness, consists of pillow basalts, fine-grained volcanic rocks without pillows, and coarser-grained rocks (diabases) which are intrusive into the volcanic pile. The chemical data show that the basaltic rocks are a consanguinous suite presumably erupted over a short time interval. Most of the rocks show a consistent composition but certain of the lavas from drill holes SP-15,16,17,19 and 20 represent more fractionated liquids. Certain rocks from cores SP-27 and 28 are distinctly depleted in Ti, P, Y, and Tb compared with the other Sabana Potrero basalts and probably represent a separate magma batch. In terms of their trace element chemistry the Sabana Potrero basaltic rocks show many of the features of MORB basalts but exhibit anomalously high Nb-Ta contents with respect to N-Type MORB.

The field association of massive sulfide ore bodies within pillowed and massive flows juxtaposed against serpentinized peridotite points toward a Cyprus type of ophiolitic association. The structure suggests the sequence is overturned. The structural,textural and compositional relations clearly indicate that the massive sulfide bodies are synvolcanic in origin. Although massive gabbro bodies are present in the association, layered gabbroic cumulates, sheeted dikes and more felsic differentiates which should be present in the ophiolitic sequence have not been located at Sabana Potrero. However, Boisseau (1987) has reported layered gabbros at the base of the basaltic rock sequence at Arroyo Toro, near Cerro Maimon, 25 kms to the north-west of Sabana Potrero.

ACKNOWLEDGEMENTS

This work was supported by Falconbridge Dominicana and Falconbridge Limited, Canada, and we wish to acknowledge the continued interest and support of J. McLelland and S.A. Brouwer of Falconbridge Dominicana. Travel and subsistence to Lewis was provided by the University Facilitating Fund of the Committee on Research of The George Washington University. The chemical analytical work was funded by Falconbridge Dominicana. Barbara Moore drafted the maps using the new computer equipment at Falconbridge Dominicana. The final typing and reduction for camera ready printing was done on the MacIntosh computer by Joanne Ristorcelli at The George Washington University. We thank S.A. Brouwer, H. Sehelekens and D. Larue for useful comments on the script.

REFERENCES

Boisseau, M., 1987, Le plane nord-est de la Cordillère Centrale dominicaine (Hispaniola, Grande Antilles): Un édifice de nappes Crétacé polyphase (Doctoral thesis): Paris, Université Pierre et Marie Curie, 200 p.

Bowin, C., 1966, Geology of the central Dominican Republic (A case history of part of an island arc), *in* Hess, H.H., ed., Caribbean Geological investigations: Geol. Soc. Amer. Mem. 98, p. 11-84.

Brouwer, S.B., MaCveigh, J.G., Espaillat, J., Jimenez, J., Pizano, O. 1989. Geological setting of some polymetallic massive sulfide occurrences in the Median Belt, central Dominican Republic12th Caribbean Geological Conference, Abstracts, St. Croix, V.I. August, 1989, p. 18.

Draper, G., and Lewis, J., 1989, Petrology and structural development of the Duarte Complex, central Dominican Republic: A preliminary account and some tectonic implications. Transactions 10th Caribbean Geological Conference Cartagena, Colombia 1983, p. 103-112.

_____, 1990, Metamorphic belts in central Hispaniola (paper submitted to Geol. Soc. Amer. Special Paper, Geologic and Tectonic Studies in Hispaniola).

Jimenez, J., and Lewis, J.F., 1989, Lithologies and stratigraphy of the Peralvillo Formation in the Cerro de Maimón area, central Dominican Republic. 12th Caribbean Geological Conference, Abstracts, St. Croix, V.I. August, 1989, p. 84.

Pearce, J.A. and Cann, J.R., 1973. Tectonic setting of basic volcanics determined using trace element analysis: Earth and Planetary Science Letters, v. 19, p. 290-300.

Table 1
Chemical analyses of basaltic rocks from Sabana Potrero.

Variation		SP-17/26.73m	SP-28/70.20m	SP26/28.65m	SP36/22.16m
SiO_2	47.6-53.9	49.4	51.5	51.3	55.88
TiO_2	0.43-2.31	2.31	0.43	1.49	0.93
Al_2O_3	12.6-15.5	12.8	13.9	14.7	11.8
FE_2O_3	7.8-14.6	14.6	7.8	11.4	15.3
MnO	0.16-0.24	0.24	0.16	0.21	0.11
MgO	4.63-9.31	5.93	9.31	5.96	9.02
CaO	5.9-11.5(16.2)	7.94	9.24	8.87	0.56
Na_2O	2.59-4.83	3.5	3.67	3.61	0.09
K_20	0.08-0.89	0.13	0.33	0.39	0.03
P_2O_5	0.04-0.39	0.2	0.04	0.15	0.08
L.O.I.	1.7-3.4	2.7	2.8	2.4	5.8
	Total	99.8	99.2	100.5	100
Cr	38-480	87	480	130	63
Ni	21-120	44	110	47	28
Y	12-40	36	12	35	16
Nb	5-18	7	13	7	6
Zr	18-143	143	18	73	75
La	0.6-4.6	4.5	0.9	2.8	0.6
Ce	4-22	20	4	15	5

Notes: SP-17/26.73 and SP-28/70.20 are basalt flows, Sabana Potrero
SP-26/28.65 is a coarse grained rock (diabase) apparently intrusive into the flow rocks, stockwork and massive sulfides.
SP-36/22.16 is a sample of altered basalt--part of the stockwork.

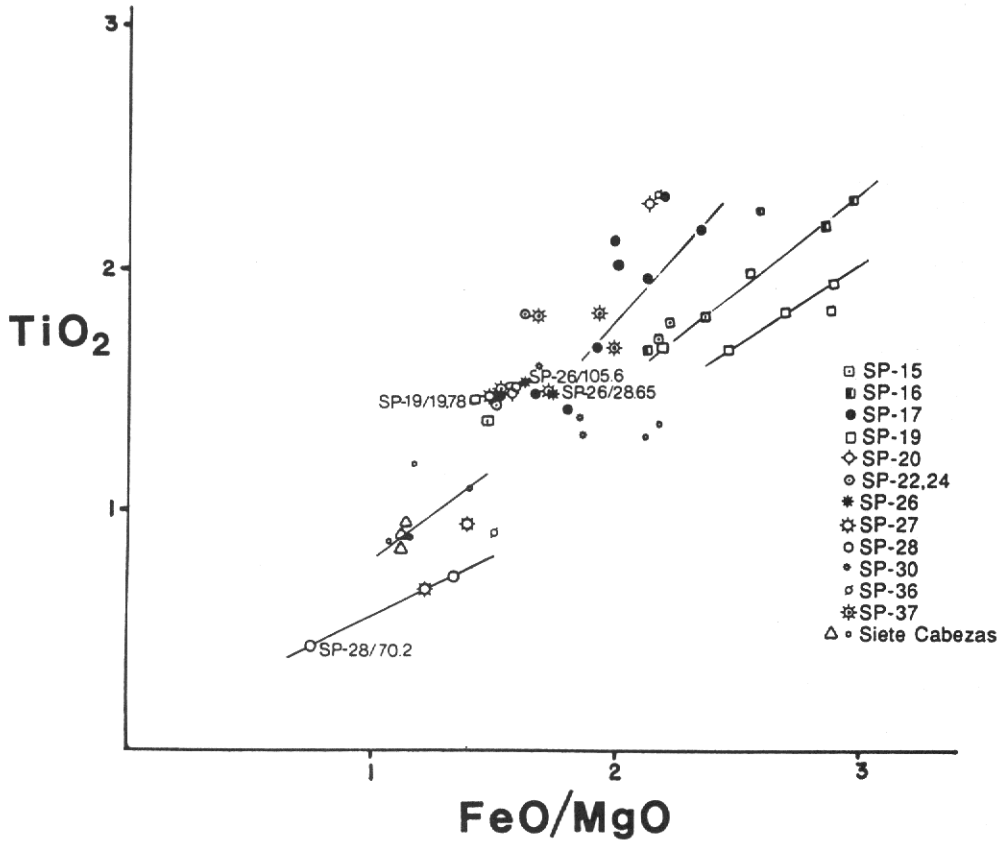

Fig. 4 Plot of TiO_2: FeO/MgO for the basaltic rocks from the Sabana Potrero area.

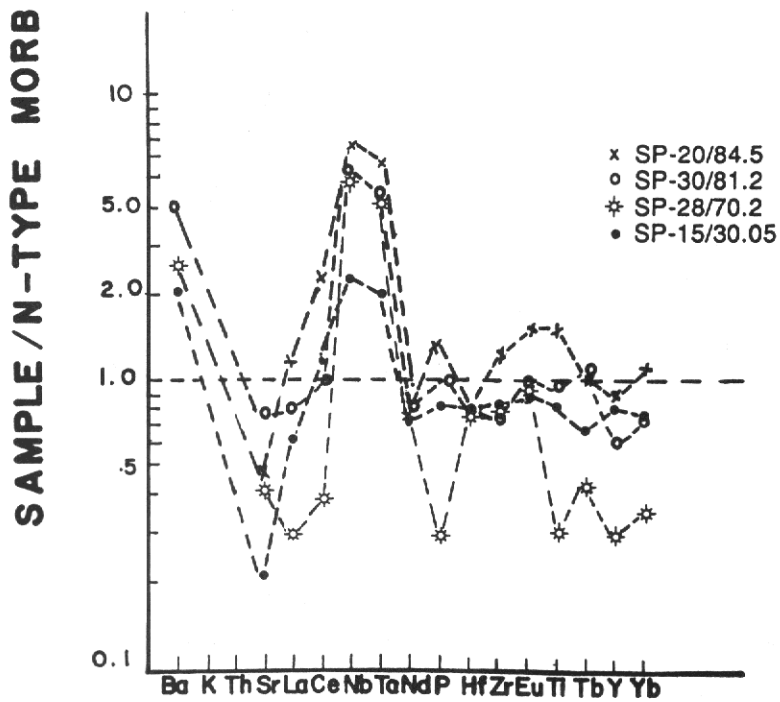

Fig. 5 Multi-element plot, normalised to N-Type MORB, showing element variation for representative basaltic rocks from the Sabana Potrero area.

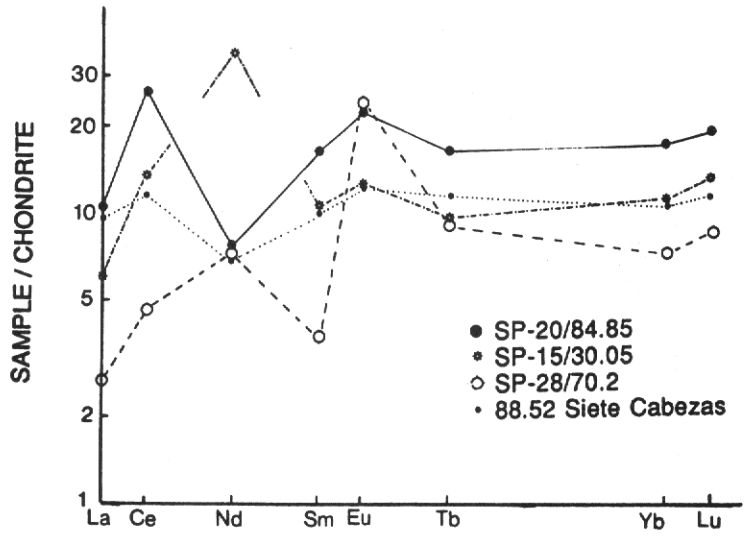

Fig.6 REE plot, normalised to chondrite, for representative basaltic rocks from the Sabana Potrero area.

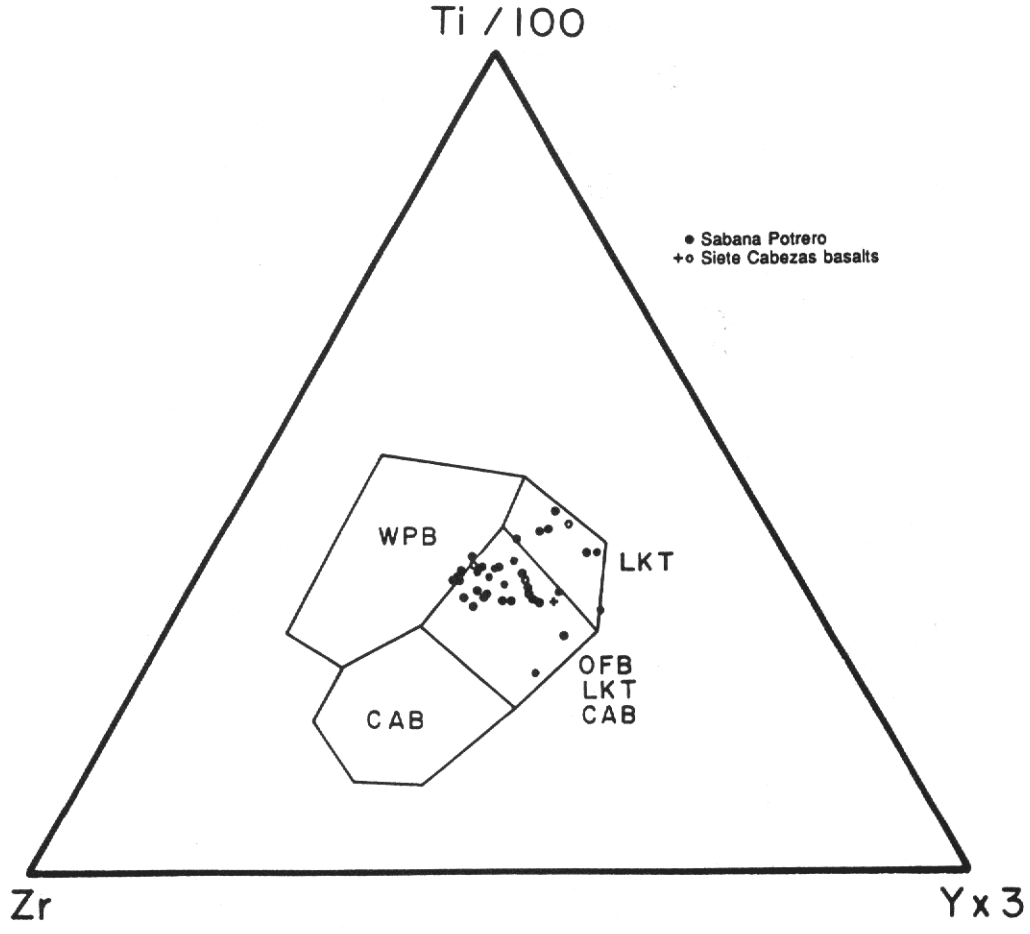

Fig. 7 Ti-Y-Zr plot (after Pearce and Cann, 1973) for the basaltic rocks from the Sabana Potrero area. OFB = ocean floor basalts; LKT = low potassium tholeiites; WPB = within plate basalts; CAB = calc-alkaline basalts.

GEOLOGICAL SETTING AND BASE AND PRECIOUS METAL DEPOSITS Of NORTHERN HAITI

Kyriacos Louca
United Nations Revolving Fund for Natural Resources Exploration
304 E 45th Street, New York, New York 10017, U.S.A.

ABSTRACT

Northern Haiti is dominated by the Massif du Nord, a major anticlinal structure which represents the northwestern extension of Cordillera Central, the "backbone" of the Hispaniola segment of the Greater Antilles Cretaceous-Early Tertiary calc-alkaline volcanic arc. The core of the Massif du Nord is made of the extensive Loma de Cabrera batholith, partly enveloped by Pre-Albian ophiolite suite rocks, black shale units and Upper Cretaceous andesitic volcano-sedimentary series rocks. Its periphery is marked by a more or less continuous belt of Upper Cretaceous, intermediate to felsic volcano-sedimentary series (La Mine Series) bordered by the overlying Late Cretaceous-Paleocene Trois Rivières flysch series and Tertiary limestones.

A spectrum of base and precious metal deposits in the Massif du Nord, is spatially and genetically related to two types of high-level magmatic systems, each characterized by distinct lithologies, alteration assemblages, mineral and geochemical associations. The first system is centered on quartz diorite porphyry stocks, high level periplutonic intrusions of the tonalite batholith, emplaced in Pre-Albian formations and in the deeper zones of the Upper Cretaceous andesitic volcanic pile. Mineral deposits related to this system comprise porphyry copper bearing stocks, limestone replacement deposits (Cu-Au-Ag skarns), copper-rich veins and auriferous quartz veins. Examples of these deposits are Douvray and Blondin with reserves of 200 million tonnes at 0.60% Cu and 50 million tonnes at 0.66% Cu respectively, Mémé former underground mine with potential resource of 3.5 million tonnes at 2% Cu, 2 g/t Au, 10 g/t Ag and Faille B gold deposit with drill indicated reserves of 520,000 tonnes grading 14.0 g/t Au.

The second major system sits higher in the stratigraphic sequence and represents epithermal polymetallic mineralization associated with stocks and domes of dacite hosted by the La Mine Upper Cretaceous volcano-sedimentary series. Mineralization exhibits volcano-tectonic fracture control and features strong Cu-Zn-Pb-Au-Ag barite associations and enrichment in Sb-Hg-As-Mo. The maximum gold and silver contents reported from this type of mineralization are 48.5 g/t Au and 640 g/t Ag. Mineralization is characterized by a large halo of advanced argillic alteration containing zones of chalcedony silica alteration, sulphide stockworks, massive powder-fine pyritization, barite veins, barite-sulphide lenses and stratabound replacements. Gold oxide deposits of this type of mineralization are Morne Bossa and Grand Bois with 2 million at 2.25 g/t Au and 4.5 million tonnes at 2.3 g/t Au respectively.

INTRODUCTION

Although Haiti has been celebrated since Columbus time for its historical workings of gold objects, it has had recorded only a few artisanal placer gold working in the Acul de Pins, Valliéres and Mont Organisé areas of northeast Haiti. Butterlin (1954) reported that approximately 2000 artisans were recovering 700-800 g of gold daily from Riviére de l'Acul de Pins. The only two significant metalliferous mines were the Reynolds bauxite mine in the Miragoane district of the Jacmel Peninsula in the south, and Sedren Mémé copper mine in the northewestern part of the country near Gonaives, which operated for a short time in the late 1960's. Increased interest in the mineral resource of Haiti started in 1975 and with various intensity has been continued through the present. With the discovery of important metallic mineral deposits made during the last ten years, northern Haiti is now recognized as a precious and base metal province, but until recently, its commercially extractable gold deposits have not gone into production.

The exploration models adopted and tested by the previous investigators in northern Haiti included among others Pueblo Viejo-type (Russel et al., 1976) and Kuroko-type (Ohashi, 1920) mineralization, but all efforts in locating economic deposits of this type of mineralization failed. Evidence obtained from studies performed by the United Nations-assisted projects throughout the Massif du Nord, as well as the discovery of the Faille B gold deposit by the United Nations Revolving Fund for Natural Resources Exploration (UNRFNRE) in the ultrabasic basement complex, necessitates the updating of previously reported information. Ideas on the Kuroko-type mineralization and the emphasized significance of the felsic volcano-sedimentary series in the localization of the most potential gold deposits in Haiti are subject to review. The importance of a genetic model for an effective and efficient exploration is well recognized by all exploration geologists. Exploration models are key to any exploration programme as they can help investigators focus

Larue, D.K., and Draper, G. (eds.),
Transactions of the 12th Caribbean Geological Conference, St. Croix, U.S.V.I., Miami Geological Society, P.O. Box 431552, South Miami, FL 33243, U.S.A

on critical geological attributes and conserve funds that might otherwise be spent collecting data not critical to discovering an economic ore body.

The purpose of this paper is to provide a comprehensive review of the principal characteristics of all important deposit types of northern Haiti and to present a unified deposit model concept which hopefully would increase the effectiveness of exploration efforts and enhance the understanding of the metallogenesis and geological setting of Hispaniola. In the present review attention is focused on the epithermal mineralization system, which for first time is announced through this study and on the Faille B auriferous quartz vein system. The paper is mainly based on a mass of data generated by integrated exploration programmes carried out by the United Nations Development Programme and the Revolving Fund for Natural Resources Exploration during the last ten years and on field work conducted by this author between 1983 and 1988 in northern Haiti.

REGIONAL GEOLOGICAL SETTING

Haiti, the western third of Hispaniola, represents a segment of the Greater Antilles Cretaceous-Tertiary calc-alkaline volcanic arc formed at the convergent plate margins of North America and the Caribbean (Bowin 1975; Kesler 1978). Northern Haiti is dominated by the Massif du Nord which represents the northwestern extension of the Cordillera Central, the "backbone" of Hispaniola (Fig. 1). Massif du Nord displays an anticlinal structure of folded Mesozoic and Tertiary volcano-sedimentary series, intruded by the Loma de Cabrera tonalite batholith. Its most prominent structural feature is the NW-SE trending pattern of synclines and anticlines and the alignment of major fault zones in this direction. The synclines are usually marked by well-preserved volcano-sedimentary rocks, whereas the anticlines are almost exclusively intruded by the batholith. The principal faults of the Massif du Nord are the major Hispaniola Fault, Faille Fault Zone and Cerca Caraval-Monpin Crochu Fault, all striking NW-SE. The Hispaniola Fault bounds the Massif du Nord on the north and is inferred to extend from the Dominican Republic through Ouanaminth to Fort Liberté. The Faille B Fault Zone, up to 1.2 km wide and 40 km long, occurs along the central axis of the Massif du Nord from Trou du Nord to Mont Organisé located close to the border of the Dominican Republic. The Cerca Caraval-Monpin Crochu Fault Zone borders the southeastern part of the Massif du Nord on the south and apparently extends to Padre las Casas in the Dominican Republic (Fig. 2).

The geological features and history of the Massif du Nord were comprehensively reviewed by Woodring et al. (1924) and Butterlin (1954). In broad terms the geological setting and base and precious metal potential of the Massif du Nord may be understood better in the context of a simplified division shown in Figures 3 and 4. The earliest known rocks in the Massif du Nord, apart from the schists of Ile de la Tortue (uncertain age) are represented by the Jurassic Morne Cabrit Series of ophiolites, inferred to correspond to the Duarte Formation in the Dominican Republic, where K-Ar age dating indicated metamorphism of 125 Ma. The Morne Cabrit ophiolitic suite consists of peridotites, serpentinites,

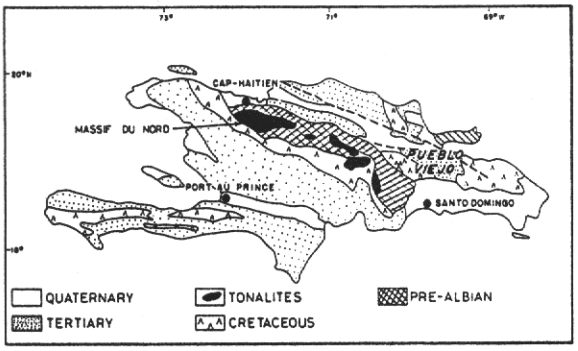

Figure 1. Simplified geological map showing major features of Hispaniola, from Donovan and Louca (1989).

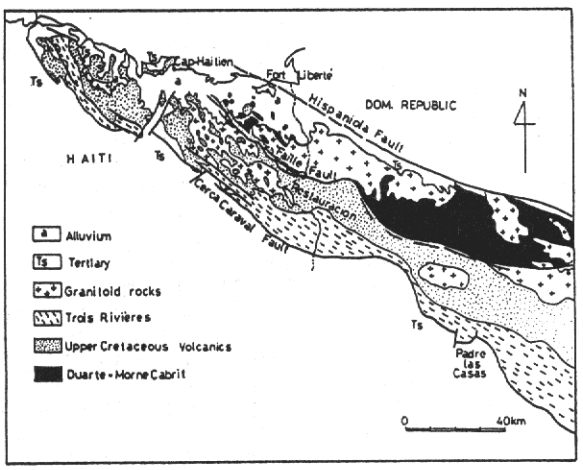

Figure 2. Generalized geological map of the Massif du Nord and Cordillera Central. Geology of the Cordillera modified after Lewis (1989).

harzburgites and dunite at its base, overlain by pyroxenites, hornblendites and gabbros. Dolerites, basalts and locally basic tuff and radiolarites form the uppermost part of the sequence. The rocks underwent metamorphism varying from greenschist to epidote-amphibolite facies and in hydrothermally altered zones are transformed to tremolite-chlorite schists, talc schist and sericite (fuchsite) schists. Contact metamorphism has been superimposed on the regional effects at the contacts with the tonalite intrusions, resulting into amphibolites. The most frequent occurrences of the Morne Cabrit ophiolites are confined to the eastern part of the Massif du Nord, and their present disposition is in the form of discrete roof pendants and linear septa of the batholith and tectonic slices associated with major fault zones.

The Morne Cabrit Series is overlain by the Lower Cretaceous Perches Series, consisting mainly of carbonaceous shales and felsic

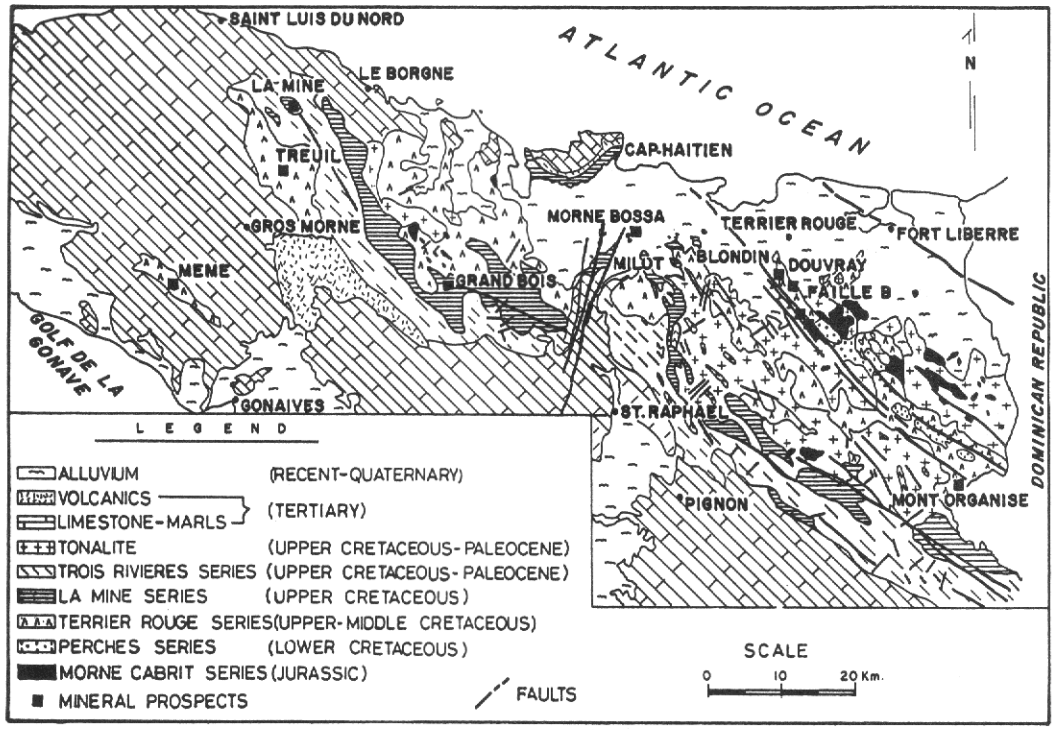

Figure 3. Geological map of the Massif du Nord. Modified after UNDP maps (1977).

SYSTEM/SERIES		STRATIGR. NAME	LITHOLOGY
QUATERNARY			Marine and continental alluvium
TERTIARY	PLIOCENE TO EOCENE		Undifferentiated reef limestones, sandstones, marl with minor basic volcanics
	PALEOCENE	Loma de Cabrera	Tonalite porphyry (c) Dacite (d)
			Tonalite granodiorite, quartz-diorite(e)
		Trois Rivieres	Marls, mudstone, siltstone, shales, marly limestones.
CRETACEOUS	UPPER	La Mine	Crystal-lithic tuff, breccias, unsorted pyroclastics dacite flows and subvolcanic stocks(b)
			Cherts and cherty tuffites.
		Terrier Rouge	Andesites, andesitic tuff, tuffite, agglomerates, mudstones, basalts intercalated limestone
	LOWER	Perches	Carbonaceous shale, acid tuff and alkaline igneous rocks.
JURASSIC		Morne Cabrit	Ophiolitic complex: serpentinites peridotites pyroxenite, gabbros, basalts, tuffs
PALEOZOIC		Ile de la Tortue	Calcareous schist, chlorite amphibolite schist

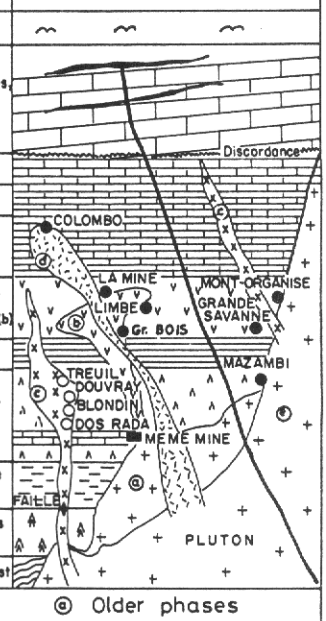

● Epithermal deposits ♦ Gold vein deposits ◎ Older phases of tonalite
○ Porphyry copper deposits ■ Skarn deposits

Figure 4. Generalized lithostratigraphic column and mineralization systems of the Massif du Nord (Louca 1988).

volcaniclastics. In the Faille B area (Grand Bassin) important lithologies include intercalated cherts and well laminated barite, ranging from few centimeters to two meters in thickness. Perches Series has limited distribution in the Massif du Nord and is preserved as thin patchy outliers over the ophiolite complex and as tectonic slices and microbreccias. The distribution of the individual lithostratigraphic members of this unit is very irregular and there is no evidence of a completely developed succession. Nicolini (1977) considered the Perches Series to be an equivalent of the Los Ranchos Formation, which is the host of the Pueblo Viejo gold deposit in the Dominican Republic.

Upper Cretaceous volcanism in the Massif du Nord, largely basaltic and andesitic at the beginning, was succeeded by dacites. The volcanic activity was interspersed with sedimentation and a thick volcano-sedimentary pile was constructed. The basalto-andesitic member of this volcano-sedimentary pile was named the Terrier Rouge Series by previous workers (Nicolini, 1977) and the upper felsic member was termed the La Mine Series by this author, who also considers it to be equivalent to the upper part of the Tireo Formation in the Dominican Republic (Louca, 1985 and 1987).

The Terrier Rouge Series with a total thickness near one kilometer, is very widespread in the Massif du Nord and in general forms huge septa and segments of synclines in the Loma Cabrera batholith. It consists of green and red vitric tuffs, tuffites, agglomerates, basalt and andesite flows, with interstratified mudstones, polymict conglomerates and limestones. The conglomerates represent both marine and subaerial facies and include hematitic and multicolored varieties consisting of andesitic and more basic material. The andesite flows vary in composition and texture between various outcrops. Fine-grained homogeneous andesite showing doleritic textures and amygdaloidal andesite and ophitic textures are the most frequent types. Mineralogically, the flows consist of andesine, augite, amphibole, orthorombic pyroxene and quartz. The Terrier Rouge rocks have undergone greenschist facies metamorphism characterized by the following mineral assemblage: albite-quartz-chlorite-epidote (actinolite)-calcite. In proximity to the batholith the rocks are traversed by a network of quartz-epidote veinlets and in direct contact with the batholith they have been transformed into hornfels. The Terrier Rouge Series correlates with the Lower Tireo Group rocks in the Dominican Republic, consisting of a sequence of red and green vitroclastic tuffs, andesite flows and agglomerates with intercalated mudstones, siltstones and limestones (Lewis et al., 1989). The paleontological determinations cited by Lewis et al. (1989) on the Lower Tireo Group rocks suggest a Turonian to early Senonian age for the main volcanism.

Upward passage from the Terrier Rouge Series to the La Mine Series varies from sharp to gradational and in a few areas is marked by a horizon of black cherts and cherty tuffites which vary from a few meters to 50 m in thickness. La Mine Series has a total estimated thickness of 500 meters and forms a more or less continuous belt confined to the outer periphery of the Massif du Nord. The belt consists of coalesced products of several discrete centers of Upper Cretaceous dacite volcanism and its principal components are tuff breccias, crystal-lithic tuffs, dacite flows and stocks, unsorted pyroclastics, laharic deposits and locally ignimbrites. In the La Mine area a porphyritic dacite (Morne Petriac) constitutes the base of the succession, overlain by a coarse monomict lahar breccia of this parent rock. The breccia is overlain by unsorted pyroclastics which are in turn overlain by crystal-vitric-lithic tuffs, grading upwards into the Trois Riviéres flysch series. Pyroxene dacite stocks with associated pyritization cut through this sequence. Variations displayed in the Camp Coq (Grand Bois) area include the presence of quartz-eye crystal tuff and ignimbrites. Tuffites and cherts are locally interbedded in the crystal tuffs. No useful fossil data are available to constrain the age of the La Mine Series, nor its equivalent Upper Tireo volcanism in the Dominican Republic. K/Ar age data from Camp Coq suggest that the main volcanism in the Massif du Nord did not begin before early Santonian. In the Restauracion area (Dominican Republic) the Upper Tireo volcanism is dated at 81.2 + 0.8 Ma by Ar^{40}/Ar^{39} on a hornblende separate (Jimenez and Lewis, in press).

The Trois Riviéres Series (Late Cretaceous-Paleocene) overlies conformably the La Mine Series and marks the beginning of prevailing marine conditions in the Tertiary. The series mainly represents turbiditic sediments consisting of mudstones, marls, limestones and locally greywackes. Thin-bedded ferruginous limestones and intercalated tuffites are confined to the base of this sequence. The maximum thickness of the Trois Riviéres Series exceeds 500 m.

The Upper Cretaceous-Paleocene period was marked by the most important geological event in the evolution of the Massif du Nord, the emplacement of the Loma de Cabrera batholith and the associated high-level periplutonic stocks. The batholith was emplaced not only into the Morne Cabrit Series but also into the Upper Cretaceous volcaniclastics and the lower members of the Trois Riviéres Series. A number of K-Ar age determinations have been made on the tonalites of Hispaniola (Bowin, 1966, Kesler and Sutter, 1977) and the age of the batholith has been examined using Rb/Sr isotope methods (Feigenson, 1978). The available data indicate that the tonalites were emplaced as magmas between 90 and 48 million years before present (Lewis, 1982). In the Massif du Nord, hornblende tonalite with small amounts of biotite is the dominant rock type and locally may grade to quartz diorite and quartz monzonite, in the Streickeisen (1974) classification. It varies texturally from medium to coarse grained and from equigranular to porphyritic types. In general it is quite inhomogeneous containing high amounts of quartz-epidote stringers and partially assimilated xenoliths of older rocks and resultant, hybrid products. As a result of the regional metamorphism the tonalite has undergone strong chloritization and epidotization. Clear intrusive deformation effects are seen in some

areas where the country rocks were raised to amphibolites whereas in others, passive emplacement of tonalite into host-rocks is apparent. Occurrences of small porphyry stocks of similar composition as the batholith but with associated copper and gold mineralization are abundant in the Massif du Nord and are described further in this study.

From the early Eocene onward calc-alkaline magmatism declined and was replaced by widespread limestone and marl sedimentation. Minor isolated acid and basaltic volcanism occurred in the Tertiary.

METALLOGENIC SETTING

Metallogenically, Massif du Nord exhibits many similarities to the Dominican Republic and to the other Caribbean volcanic arcs but it has also its own peculiarities in both style and time of deposition of mineralization. Temporal correspondence is seen with the Dominican Republic in the development of porphyry copper deposits and epithermal-polymetallic deposits, during the latest phases of the Upper Cretaceous magmatism and the occurrence of auriferous quartz veins in ultrabasic and basic rocks. Differences between the metallogenic evolution of these two parts of Hispaniola include the absence of volcanogenic massive sulphides and Pueblo Viejo-type mineralization in the Massif du Nord. These peculiarities of the Massif du Nord are related directly to its tectonic evolution which includes among others the absence of the Pre-Albian Maimon Formation, host of volcanogenic massive sulphides, and very limited occurrence of the Lower Cretaceous Los Ranchos Formation, host of Pueblo-type epithermal mineralization in the Dominican Republic. The absence or weak development of these formations was probably related to the lack of significant fragmentation of the Massif du Nord during the Lower Cretaceous subduction process.

A spectrum of base and precious metal deposits in the Massif du Nord is spatially and genetically related to two distinct types of high level Upper Cretaceous magmatic systems: the lower consists of quartz diorite and tonalite stocks with associated porphyry copper mineralization and the upper of dacitic stocks and domes with associated epithermal-polymetallic mineralization hosted in the La Mine Series (Fig. 4). The only authentic occurrences of syngenetic stratabound precious metal mineralization in the Massif du Nord are thinly laminated barite-chert seams which are found locally in the Lower Cretaceous Series. The polymetallic mineralization associated with the La Mine Series was regarded by previous exploration groups as submarine volcanogenic and was compared to a Kuroko-style mineralization (Société Minière d'Haiti, 1977 and Société Franco-Haitienne des Mines, 1980). Our recent work has shown no evidence supporting this genetic model.

DISTRIBUTION AND DESCRIPTION OF BASE-PRECIOUS METAL MINERALIZATION

This section of the study attempts to classify the various styles of primary base and precious metal mineralization and describes their principal characteristics and geological setting. In the following discussion, base and precious metal deposits and occurrences have been divided into the following major groups: syngenetic stratabound mineralization in the Lower Cretaceous Perches Series, deposits associated with Upper Cretaceous granitoid-porphyry stocks and polymetallic-epithermal mineralization associated with the Upper Cretaceous La Mine Series. It should be emphasized that all significant mineral deposits and occurrences in the Massif du Nord can be included within these categories. The classification scheme adopted in this study is based on both lithological and structural criteria, as well as on alteration types, geochemical and mineral associations.

Stratabound Base-Precious Metal Mineralization

This type of syngenetic mineralization has been recorded only in one locality in the Faille B area of the Grand Bassin mineral district. It is composed of thinly laminated barite seams, varying in thickness from a few centimeters to 2 m, which occur in the Perches Series covering an area of 150 x 100 m. The barite beds occur in metatuffs and metasediments of various stratigraphic horizons and grade laterally to recrystallized grey cherts which resemble jasperoids. Fine-grained pyrite with delicate layering occurs as thin interlayers up to 0.5 m thick, in metatuffs. The barite is variegated with alternating brown, tan, grey, light grey and dark grey aphanitic laminae. The laminations result from fine hematite, graphite and tiny interlayers of chert and carbonate. The barite contains up to 5 g/t Au, 40 g/t Ag, 0.28% Pb and 0.16% Zn.

Brecciation and recrystallization which occurred during folding, intense faulting and intrusion of tonalitic stocks modify and obscure the original character of this type of mineralization. The possibility of an affinity with the Carlin model was initially considered but later rejected on the basis of petrographic and mineragraphic work which indicated that the lamination of barite and sulphides is sedimentary. (Dressler, 1985 and Harris, 1986). The writer interprets the mineralization as having submarine hot spring origin.

Mineralization Associated with Granitoid-Porphyry Stocks

Copper mineralization with appreciable amounts of gold and silver in the Massif du Nord, is centered on small, shallow granitoid intrusives that range from hornblende microtonalites and quartz diorites to less common granodiorites and quartz monzonites. They are mainly fine-grained and porphyritic but locally are heterogeneous displaying variations in texture, grain size and modal composition. Leucocratic and mafic varieties and hybrid rocks occur locally. The intrusives vary in surface area from a few tenths of a square kilometer to 2 square kilometers and are often elongated in a northwest-southeast direction, representing forceful injections along pre-existing fault zones. Discontinuous sets of both elongated and oval-shaped stocks occur along well defined

northwest-southeast lineaments, particularly along the central axis of the Massif du Nord. According to the mode of mineral occurrence and composition, the deposits associated with these shallow-level stocks have been sub-divided into limestone replacements, porphyry copper, copper veins and auriferous quartz-sulphide veins.

Limestone Replacement Deposits

The limestone replacement deposits are found in the Terre Neuve Mountains, on the southwestern flanks of the Massif du Nord, where the Cretaceous volcanics are exposed in a narrow window through the Eocene limestones. The area exhibits a complex structural history characterized by northwest-southeast trending fold axes and fault traces. The volcanic rocks show an apparent compositional gradation from andesite to dacite, contain intercalations of siltstones and limestones and they are intruded by the Terre Neuve stock. The stock varies in composition from quartz monzonite to quartz diorite and forms three small elongate bodies along the axis of a broken anticline. Kesler (1968) cited an age of 66 Ma from this stock. Mineral deposits associated with the Terre Neuve stock include the dormant Mémé copper mine and three other prospects of which Causseus is the most developed (Fig. 5).

Base and precious metal mineralization has been emplaced in both stock and altered volcanics but mostly in skarns developed in blocks of recrystallized limestone and marble that were tapped into the stock during the intrusion. The skarn-intrusion contacts are sharp but show mineral zonations and two gradational types of skarns. The skarns contain garnet, epidote, chlorite diopside, wollastonite, tremolite, magnetite and hematite. Sulphides include pyrite, chalcopyrite, bornite, chalcocite, digenite and locally molybdenite. The sulphides occur as disseminations, irregular massive replacements, interstitials and veinlets in the skarn, and as disseminations and parallel veinlets banded with quartz, in the intrusive. The deposition of metallic minerals began during the waning stages of skarn formation and continued after the cessation of skarn mineral deposition (Kesler, 1968). The skarn-sulphide paragenesis, as well as other characteristics clearly point to the transitional nature of this mineralization and its intriguing link between contact - localized ore and porphyry copper ore.

Based on drilling and underground development work the original ore reserves at Mémé, are estimated to be 3.5 million tonnes grading 2% copper, 2 g/t gold and 15 g/t silver. Certain portions of the mineralized skarns contain up to 23 g/t gold. To date the indicated resources in the Terre Neuve mineral district, computed from data on Mémé Mine and the other prospects, are 6.0 million tonnes with ore grades similar to those of Mémé Mine. Mémé was brought into production by SEDREN S.A. in 1960 and operated until December 1971. Approximately 2 million tonnes of ore at 2% Cu was mined from underground workings. The mine appears to have closed in early 1972, when it failed to meet a concentrate shipment during a period of low copper prices and the Bank d'Haiti assumed all assets. The geology and mineralization at Mémé Mine have been described and illustrated in a number of publications including those by Kesler (1966, 1968).

Porphyry Copper Deposits

Porphyry copper deposits and occurrences are widespread in the Massif du Nord and they are related to small, irregular, porphyritic hornblende tonalite and quartz diorite stocks, that are emplaced in the Terrier Rouge or earlier metabasaltic rocks. In the western part of the Massif du Nord they occur as isolated stocks cutting volcanic terrain and in the east are clustered close to the border of the Loma de Cabrera batholith. The latter intrusive environment is presumably indicative of a deeper regional erosion level.

The northern Haitian deposits belong to a distinct porphyry copper deposit class, lacking the typical concentric alteration-mineralization zoning and extensive feldspar-destructive alteration. The deposits are typified by propylitic alteration characterized by epidote, chlorite, calcite, quartz and albite with an intimate association with sulphides. The stocks and their host rocks are both altered and mineralized in parts and it is difficult to formulate a general rule governing sulphide distribution. The dominant sulphides are chalcopyrite, pyrite and bornite occurring as fine disseminations, small blebs, patches, veinlets, either alone or with quartz and/or epidote and calcite. The amount of chalcopyrite and pyrite as well as their ratio vary considerably from deposit to deposit. Pyrite and chalcopyrite contents range from 0-10% and 1-5% respectively. Geochemical associations include Zn, Mo, Au and Ag.

Deposits of this sub-group, considered to possess the greatest potential, are Douvray and Blondin, located 40 km southeastward of Cap-Haitien (Fig. 6). At Douvray the potential exists for some 200 million tonnes of 0.6% copper ore and at Blondin the drill-indicated resource is on the order of 50 million tonnes averaging about 0.66% Cu. Systematic assaying for gold has not been done but to date the highest average grades of these deposits are about 0.30 g/t Au. Quartz veins carrying up to 9.0 g/t Au and 42 g/t Ag occur locally at Blondin. Oxidation is shallow, ranging from 5 to 20 m and supergene sulphide mineralization is limited.

Other occurrences of porhyry copper mineralization in the Grand Bassin area include Dos Rada (Louca, 1988), and Philippe (Fig. 6). Copper-bearing porphyritic tonalite and quartz diorite intrusives of much smaller dimensions such as dykes and elongated narrow bodies occur in several other locations in the Massif du Nord. Within one of these stocks is the Treuil prospect located due north of Gros Morne town (Fig. 3). Treuil prospect is found within a quartz diorite stock with associated rich supergene sulphides in irregular fracture fillings up to 2.0 m in width, carrying more than 10% Cu and several ounces per tonne silver. Host rock lithologies include andesitic and basaltic tuffs.

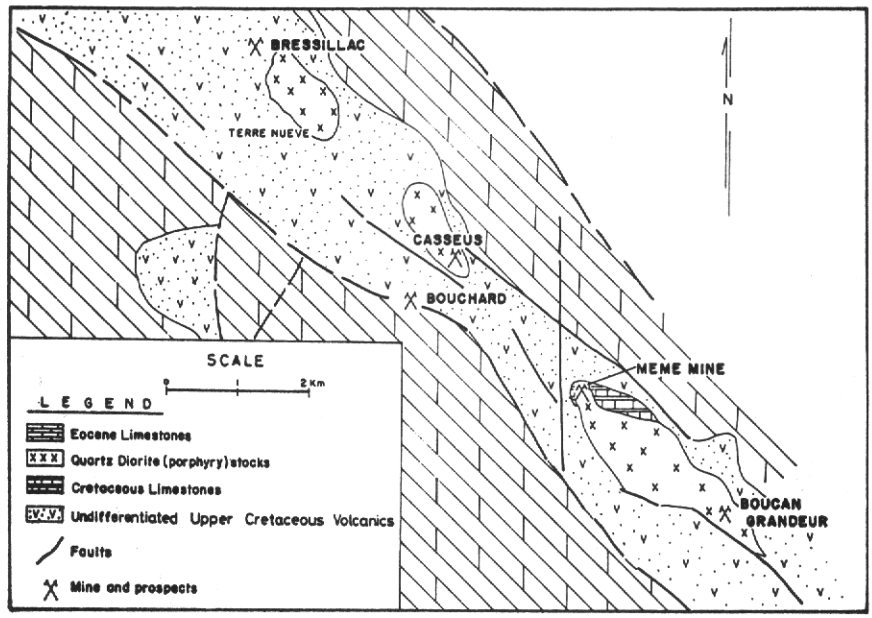

Figure 5. Simplified geological map of Terre Neuve Mountains. Modified after Kesler (1968).

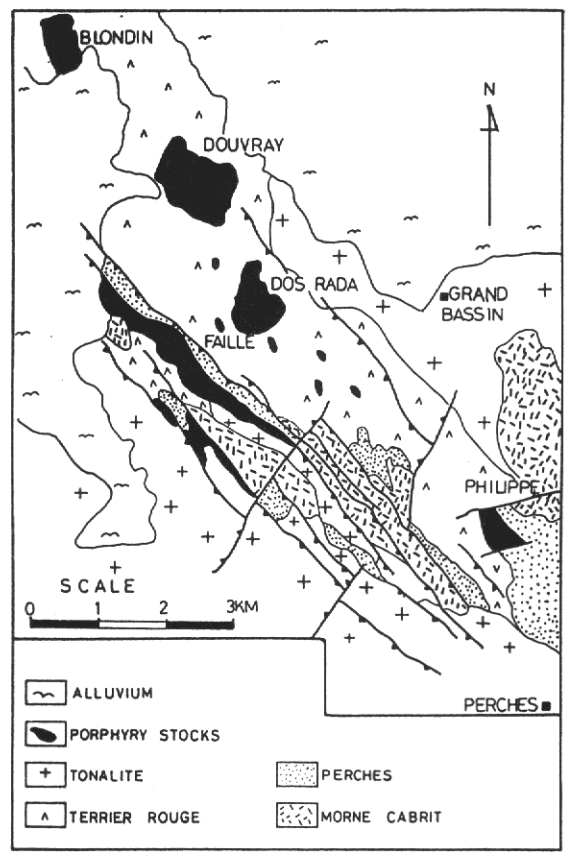

Figure 6. Geological map of the Grand Bassin area. Reduced from 1:50,000 map (Louca, 1988).

The Mont Organisé prospect located in northeastern Haiti, along the border with the Dominican Republic, although not yet thoroughly defined, can be provisionally classified as a porphyry type deposit (Fig. 3). Alteration and sulphide mineralization is apparently confined to the contact zone between the Upper Cretaceous volcano-sedimentary series and a porphyritic tonalite. Disseminated sulphides are mainly pyrite whereas copper and gold mineralization is more sporadic and follows the fracture systems.

Vein Copper Mineralization

Copper-bearing veins and shear zones represent the second main type of widespread copper mineralization in the Massif du Nord. They are found mainly in the lower stratigraphic units (Morne Cabrit and Terrier Rouge Series) and they occur within and are marginal to porphyry copper systems, as well as in fault zones without obvious relation to copper-bearing stocks.

The veins are represented by several varieties of fissure veins such as single fractures, sheeted zones of closely spaced joints and veinlets, varying in width from a few centimeters to a few meters. They range from a few tens of meters to a few hundreds of meters in length. The main copper mineral is chalcopyrite and it is locally accompanied by minor bornite and pyrite. Gangue minerals include quartz, chlorite and calcite occurring in various proportions with sulphides. The oxidized zone of the veins is characterized by copper carbonates, pitch limonite and goethite. This class of veins shows strong silver enrichment, up to 62 g/t but in most cases their gold content is less than 0.20 g/t. The deposits are generally small and vary from 15,000 tonnes to 50,000 tonnes at 2% Cu.

Auriferous Quartz-sulphide Veins

This type of gold mineralization is associated with a microtonalite stock hosted in the Morne Cabrit ophiolites and its major occurrence is Faille B gold deposit located in the Grand Bassin mineral district (Fig. 6). Douvray and Blondin porphyry copper deposits are located only 2 km north-northeast and 4 km north of Faille B. The deposit occupies the eastern part of the Faille Fault Zone, marked by a series of NW-SE faults which bring various lithostratigraphic units into juxtaposition as tectonic sheet-like bodies, aligned parallel to the regional trend (Fig. 7). The most characteristic geological feature of Faille B is the elongate and tabular wedge-like body of hornblende microtonalite, emplaced along a major shear zone in ophiolites and other Lower Cretaceous rocks. The microtonalite is more than 2 km long and varies in width from 250 m on the northwest and 25 m on the southeast. It has a relatively fine-grained porphyritic texture but is locally quite heterogeneous, with variations in texture and grain size. It is generally characterized by strong chloritization, moderate propylitization and zones of sericitic alteration and contains tiny stringers and impregnations of pyrite and chalcopyrite (Louca, 1988, Donovan and Louca, 1989).

The microtonalite and its wall rocks, particularly the Morne Cabrit ophiolites are the principal hosts of most of the auriferous quartz veins. The Morne Cabrit ophiolites consist mainly of sheared rocks mapped collectively as "metabasites". They include meta-peridotites, meta-gabbros, meta-basalts, actinolite-chlorite schists and tremolite-chlorite schists. Veins in "metabasites" at the surface have been found to cut the microtonalite at depth in some cases.

The veins range from simple to exceedingly complex systems, such as multiple lenticular veinlets, sheeted banded veins and systems of quartz veinlets. Most of the veins strike NW-SE, comformably with the structural grain of the area and have westerly dips ranging from 40 to 65 degrees. Steeper veins with opposite dips, however, also occur and in some cases vein material passes with many changes of dip and strike from one fracture to the other. The simple massive veins, or the veinlets which constitute the sheeted veins, vary in width from a few centimeters to one meter, while the vein systems reach up to 3 m in width. There are at least five principal quartz vein systems in the microtonalite. Although the quartz veins occur over a distance of more than 2 km, individual veins can usually be traced from trench to trench for only 50 to 70 m before pinching out (Fig. 8).

Quartz is the principal gangue mineral, occurring as several distinct textural types, of which a rather fine-grained variety predominates. It exhibits heterogeneous grain variations, fragmentation and incipient brecciation and ranges in colour from grey to light grey and glassy, with delicate chlorite and sulphide banding. Chlorite is an abundant gangue mineral and is widely distributed throughout the vein selveges and as a vein mineral replaced by quartz or vice versa. Barite and calcite occur locally in some of the quartz veins. Pyrite is the most abundant sulphide, generally comprising 3 to 15% of the vein. Chalcopyrite and sphalerite locally form concentrations up to 5% and 10% respectively.

Gold occurs as the native metal and exists in the primary mineralization mainly as grains from 2 to 50 microns in diameter. In the oxidized veins it is rarely visible to the naked eye. The distribution and size of gold grains determined from microphotographs suggests that the gold is less than minus 200-mesh in size and much would pass through minus 400-mesh screen. Gold shows diverse associations: specks within chlorite wisps and quartz, on contacts of sulphide grains, and less frequently as inclusions in microfractures in pyrite.

The distribution of gold in quartz veins along strike and dip is erratic, as demonstrated by both trenching and drilling (Fig. 9). The gold within a sheeted or multiple vein section tends to be confined to a single vein component and is often concentrated in the chloritic walls of the veins. The amount of chalcopyrite generally increases sympathetically with gold grades, but the reverse is not always true, at least according to the assays, although this

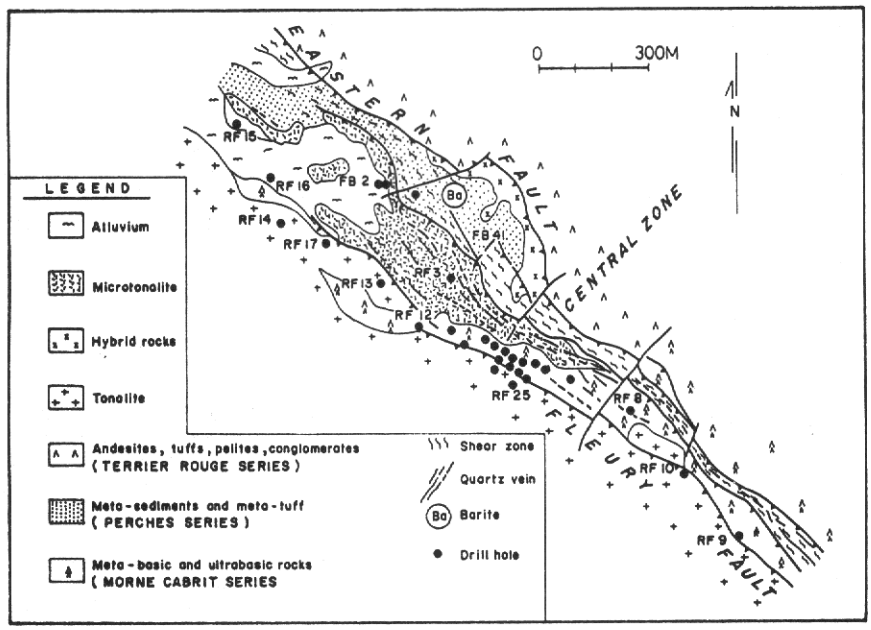

Figure 7. Geological map of Faille B area. Reduced from 1:2,000 maps (Louca 1985-1988).

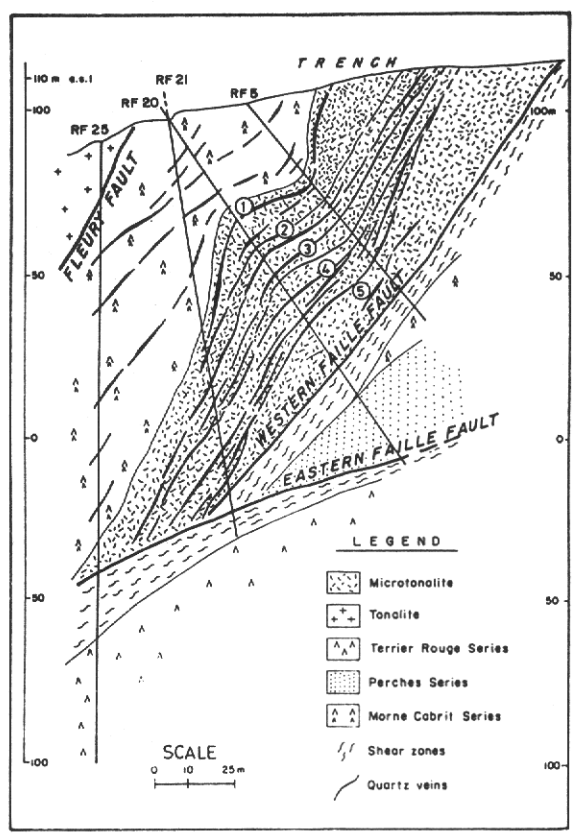

Figure 8. Cross-section of the Central Zone of Faille B gold deposit (Louca 1985-1988).

effect may be due to the spotty distribution of the gold particles. Gold contents in quartz veins from trenches range from traces to 230 g/t. Gold values persist with depth and only in a few cases was secondary enrichment of gold suggested in the oxidized zone, which varies from 15 to 25 m depth. Gold values up to 200 g/t were encountered at depths of 120 m in the primary zone. The auriferous quartz vein mineralization shows enrichment of Ag, Cu, and Te. The following elements appear to be somewhat enhanced: As, Sb, and F.

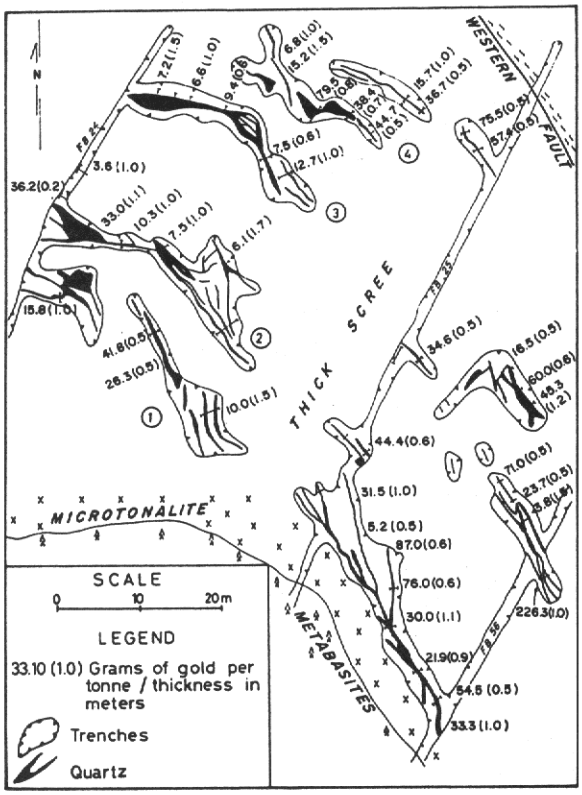

Figure 9. Distribution of gold and quartz veins in the Central Zone of Faille B (Louca 1985-1988).

Positive gold mineralization was encountered by drilling and trenching over a strike length of 1.8 km but the wide spaced drilling does not allow reliable calculation of grade and tonnage for the entire belt. Estimates of grade and tonnage were made in the Central Zone of Faille B (300 m strike length) where there is a higher concentration of gold and frequency of drillholes. Drill-indicated tonnages are 520,000 tonnes at 14.0 g/t Au.

The textural and geochemical characteristics of the Faille B auriferous quartz veins are similar to veins associated with dioritic intrusions in an active tectonic environment. The syntectonic emplacement of the quartz vein material is evidenced by textures indicative of plastic deformation, cataclastic textures and the development and closing of open spaces for vein formation by tectonic movement. Textural relationships of mineralized quartz veins suggest overlapping paragenesis of gold and vein constituents and two phases of gold deposition. The earlier phase of gold introduction is represented by the small inclusions of gold in pyrite and the later phase is associated with chalcopyrite and chlorite wisps and quartz. The stronger development of quartz veins within the stock is thought to be due to the relatively brittle character of this intrusive compared to the ductile nature of the sheared metabasites and metasediments.

Epithermal-Polymetallic Mineralization

General Statement

Oxidized ore of the epithermal-polymetallic mineralization is an important part of the mineral resource endowment of the country. So far, two such deposits have been discovered and thoroughly evaluated with respect to their tonnage, grades and gold leacheability characteristics. These are Grand Bois and Morne Bossa (Fig. 3), containing 4.5 million tonnes of extractable oxide ore with 2.3 g/t Au and 2.0 million tonnes with 2.25 g/t Au respectively.

Although the association of this type of mineralization with the Upper Cretaceous La Mine Series is well known in Haiti, its volcanogenic setting and characteristics are not available in the literature and its specific deposit type has not been classified until now. The superficial resemblance of local occurrences of black massive sphalerite with the black Kuroko-type ores, the presence of massive pyrite and barite, as well as the close association of the mineralization with the relatively felsic volcano-sedimentary series led previous investigators to relate this mineralization to a Kuroko model. Both Société Minière d'Haiti (S.M.H., 1977) and Société Franco-Haitienne des Mines (S.F.H.M., 1980) engaged in the exploration of massive sulphides in the Camp Coq-Limbe area, and mapped and interpreted all sulphide stockwork zones as exhalite horizons and divided the La Mine Series into pre- and post-mineralization units. All undeformed massive barite-sulphide mineralization was interpreted as being syngenetic ore and the fragmented and cataclased massive mineralization as distal "conglomeratic" Kuroko-type ore.

Our studies throughout the La Mine volcanic belt, from the Dominican border in the southeast, to the Colombo prospect 110 km to the northwest, have shown that the mineralization does not fit the definitions of Kuroko-type or any other sub-type of stratabound-syngenetic sulphide mineralization. Extensive detailed geological mapping supported by petrological and mineragraphic studies, and geochemical and geophysical data, support the interpretation that the north-Haitian mineralization belongs to a unique replacement-deposit type. The present study favours a shallow epithermal origin, which is based on diagnostic features in the nature of both host volcanics and sulphide-barite mineralization, as well as in the overall structural setting and geochemical and mineralogical association of the deposits. Epithermal mineralization of similar characteristics and age to the mineralization of

northern Haiti, has been described by Amarante et al. (1989), in the Upper Tireo Group rocks of the Restauracion area in the Dominican Republic. This section will briefly describe the geological, mineralogical and geochemical characteristics of this north-Haitian mineralization, so that it may be easily related to other epithermal, precious-metal deposit types.

Depositional Environment of Host Rocks

The mineralized portions of the La Mine Series consist of multicyclic volcanic accumulations, predominantly dacitic in composition, which grade laterally and vertically from subaerial tuffs and pyroclastics to submarine volcanic sediments. A subaerial depositional environment prevails at the base of the volcanic pile and in some areas also at the upper part of the sequence. Purely sedimentary components include interbeds of siltstones, greywackes and cherts varying in thickness from one meter to a few meters. The maximum thickness attained by the volcanic pile at La Mine and Grand Bois area is 500 m and 400 m respectively.

Typically, the first and lowermost portions of the sequence are tuff breccias, and heterolithologic lahars, followed upwards by flow breccias, unsorted fine pyroclastics and dacite flows. The uppermost portion of the pile contains abundant massive or bedded lithic-crystal tuffs and ignimbrites. A characteristic feature of the La Mine Series is that it is intruded by subvolcanic stocks and dome-like protrusions of quartz porphyry, rhyodacite and porphyritic quartz-hornblende dacite. In many areas these shallow intrusives form local extrusive accumulations and result in both intrusive and extrusive equivalents of the same lithology.

Distribution of Mineralization

This type of sulphide mineralization has the tendency to occur in swarms or clusters in structurally complex areas of which the best known are La Mine-Colombo area, Limbe-Camp Coq area, Milot-Grande Riviére area, and Bois Laurence-Grande Savane area. The two oxide gold deposits mentioned above, Grand Bois and Morne Bossa, occur in the Limbe-Camp Coq and Milot-Grande Riviére areas respectively.

Unlike the various forms of exhalite deposits, including stratiform massive sulphides which occur within a fairly narrow stratigraphic interval or even along a single horizon, the north-Haitian sulphide mineralization has a demonstrable structural control and cross-cuts all distinct lithostratigraphic members of the La Mine Series (Fig. 10). The structural control is seen as a concentration of high angle faults and fractures, fault intersections and intersections of faults with relatively permeable or reactive rocks. The general disposition of the mineralization is in the form of linear fault and fracture zones up to 3 km in length, whose orientation is partly oblique or is conformable with the regional structural grain. The mineralized zones are usually bound by faults and their overall position is discordant to the orientation of the volcaniclastic series rocks. Stratiform replacements are very restricted and present as thin discontinuous zones of jasperoids and small lenses of barite with sulphides. Also,

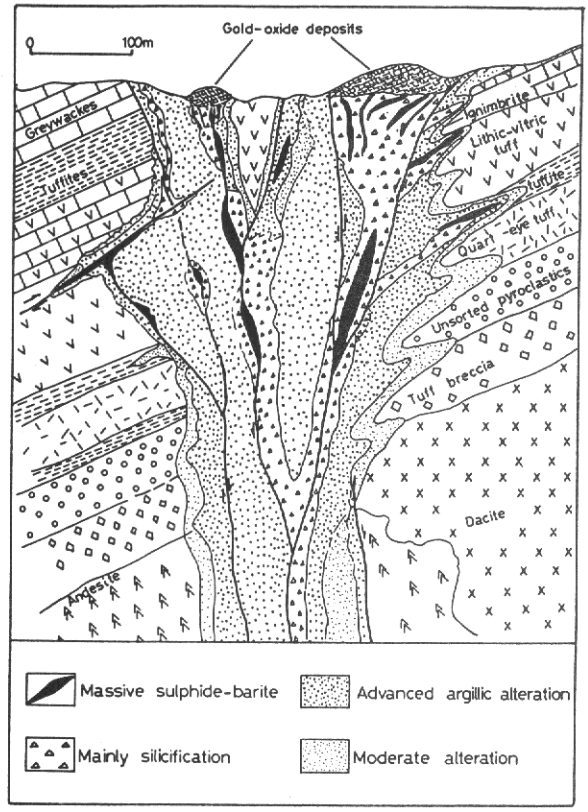

Figure 10. Schematic cross-section of the epithermal mineralization system in the La Mine Series (Louca 1987).

there is a striking spatial association between the mineralization and the dacite stocks and domes. At Morne Bossa the mineralization took place on the edge of a circular dacite porphyry dome, which constitutes the arcuate hills north and west of Morne Bossa. At La Mine the mineralization is closely associated with the Colombo stock of pyroxene dacite.

Hydrothermal Alteration

Mineralization is strongly characterized by a large halo of advanced argillic alteration, containing zones of massive chalcedonic silicification, stockworks, and open-growth barite along multi-generational breccias. The dominant clay mineral is illite with small amounts of alunite. Diaspore and sericite have been reported from the alteration zones of Camp Coq area by Société Minière d'Haiti (1977) and Société Franco-Haitienne des Mines (1980) respectively. All gradations exist between argillization and silicification along strike and dip of the hydrothermally altered zones, as well as from a fresh host rock through chloritized and partly altered rock to a rock completely replaced by silica and clay minerals. Chloritization is mainly confined to the immediate wall rocks but chlorite also mantles sulphide stringers and

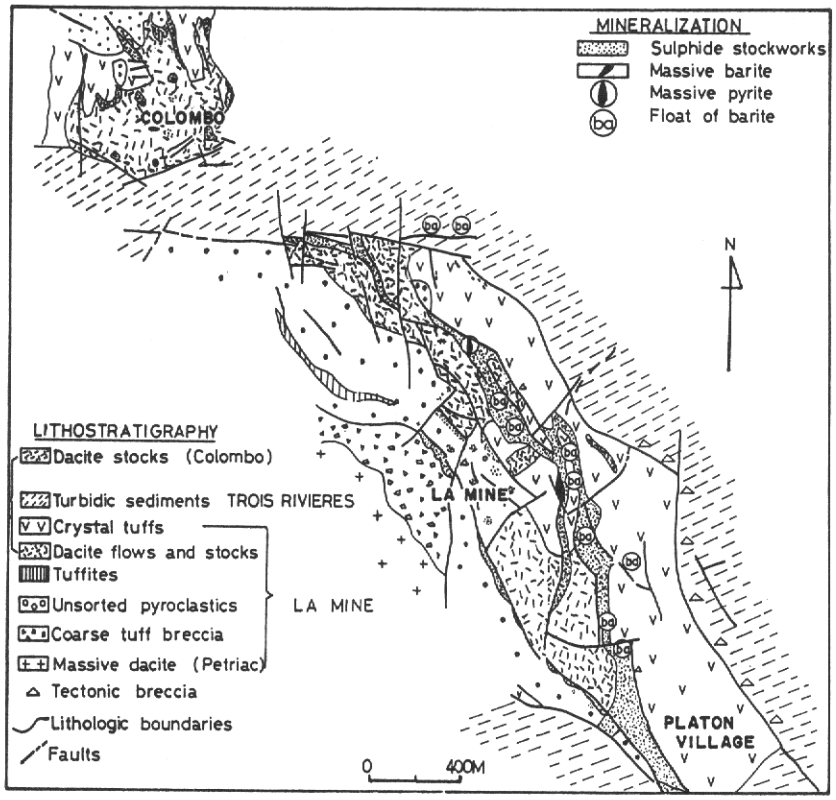

Figure 11. Geological map of La Mine-Colombo area. Reduced from 1:2,000 maps (Louca 1985).

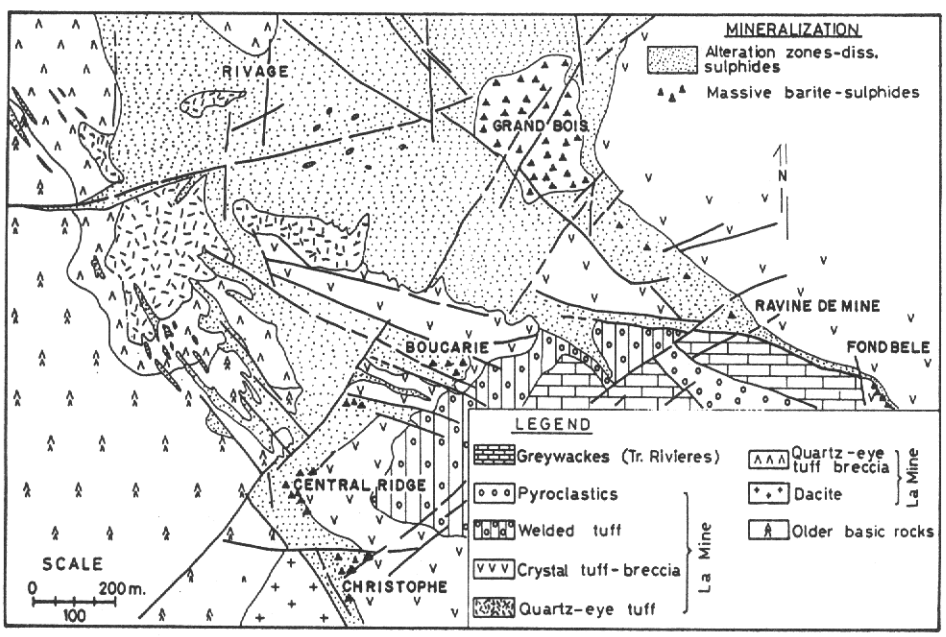

Figure 12. Geological map of Grand Bois-Camp Coq area. Reduced from 1:2,000 maps (Louca 1987).

occurs as filling fractures, and along slips and joint planes.

Sulphide Stockwork

Sulphide stockwork mineralization with variable amounts of barite, is the most widespread and characteristic type of north Haitian epithermal mineralization and is hosted in pervasively altered zones, fault zones, and tectonic and hydrothermal breccias. Mineralization varies from a few tens of meters to 200 meters in width and it may exceed 2 km and 200 meters in strike length and depth respectively. The stockwork zones of La Mine (Fig. 11) consist of a number of bifurcating, steeply dipping fault strands varying in width from a few meters to 100 meters. In the Camp Coq area the focus of the mineralization is centered over the Grand Bois gold deposit, where it extends southwestward and southeastward along fault zones up to 200 m in width (Fig. 12).

Sulphide mineralization consisting mainly of pyrite with small amounts of chalcopyrite, sphalerite and galena, takes the form of heavy disseminations, fracture and cavity infillings and a random network of stringers. The total sulphide content ranges from 3 to 50% and varies considerably along strike and depth, lacking any zonation. Pyrite content increases directly with the intensity of silicification and argillization. Chalcopyrite and sphalerite are more frequent in narrow veinlets and irregular fracture fillings than in disseminations and locally attain widths up to one meter. Although copper and zinc may attain grades of 10 to 25% in the individual fractures and veinlets, their average contents in the stockwork zones are less than 1%. The overall gold contents of the stockwork zones are generally less than 1 g/t. Higher gold values which range up to 9.0 g/t are always associated with the abundant barite.

Barite is widespread in the stockwork zones and in the immediately adjacent hydrothermally altered rocks and occurs in the following more frequent forms: interstitial material with sulphides, stringers, veinlets, veins and gangue in the sulphide stringers. The barite veins range up to three meters in width and are usually enveloped by zones of "mixed" silica and barite. Vein-type and cavity-filling barite is coarse-grained and varies in colour from grey to white according to its sulphide content.

Massive Sulphide-Barite Mineralization

The massive sulphide-barite occurrences have restricted and patchy distribution in the stockwork zones and take the form of irregular fracture-fillings and in-situ replacements and veins. In general, they show lensoid and tabular bodies which range in thickness from 0.6 m to 6.0 m and have strike lengths which vary from 10 m to 90 m. Their contacts with the stockwork zones or hydrothermally altered rock are usually sharp but in some cases gradational. At La Mine a massive powder-fine pyrite body (20 x 10 x 5 m) grades in all directions through semi-massive pyrite to silica with high amounts of pyrite and at Grand Bois (Camp Coq area) irregular bodies of massive barite grade laterally and vertically through semi-massive barite to baritized - silicified and pyritized tuff. The massive sulphide-barite mineralization occurs at various stratigraphic horizons even within the same locality. In the Camp Coq area, the massive sulphide-barite occurrences have a general tendency to concentrate at the outer margins of the stockwork zones but their hanging walls are always formed by pervasive argillic alteration and in most cases are marked by low-angle microshears or steep by dipping fault. In most cases the massive mineralization is oblique to the strike and often to the bedding of host rocks but in a few cases is conformable with the bedding, forming stratiform replacement bodies. Perhaps the best examples of stratiform replacement bodies are those of Christophe and Rosses in the Camp Coq area. An example of cross-cutting relationships between massive ore and host rock is La Cour in the La Mine area. Here a barite-sulphide lense 100 m long and 2 to 6 m wide enveloped by argillic alteration is dipping steeply to the southwest whereas the host volcaniclastics are dipping 50° to 60° to the northeast.

Barite and sulphides occur together in various mineral associations and proportions forming massive ore composed of up to 87% $BaSO_4$ and up to 70% sulphides by volume. In general the barite-sulphide ores are massive and compact but with the leaching of sulphides in the zones of intensive oxidation, the barite may be very porous and spongy. They vary in colour from grey to black dependent on the amount of sulphides, particularly of black sphalerite. The most common sulphides associated with the barite are: pyrite, chalcopyrite, sphalerite, and galena. Sulphosalts of the tennantite series that are present include tetrahedrite and enargite. Geochemical associations are Hg, Sb, As and Mo. Base and precious metal contents vary considerably on an outcrop and district-scale. Copper contents range up to 9%, zinc up to 22%, lead up to 2%, gold up to 12.0 g/t and silver up to 150 g/t. An intimate association of precious metals with barite is typical of all epithermal occurrences in northern Haiti, and in the zone of oxidation leached barite contains up to 48.5 g/t Au and 640 g/t Ag. High gold concentrations occur in locally developed silica boxworks in the oxidation zone of Morne Bossa. Gold in the hypogene zone is bound with sulfosalts and silver sulphides and in the oxidation zones occurs as native gold.

Textures and structures also vary considerably. In general, barite is holocrystalline, medium to coarse grained, and consists of euhedral to subhedral crystals intergrown with sulphides or replacing sulphides. Barite zonally replaces sphalerite and chalcopyrite. Colloform textures and banding of barite with sulphides occur locally in the finer varieties but cataclastic textures and multi-generational breccias occur frequently in all types of ores. Multi-generational breccias in the stockwork zones point to prolonged and episodic mineralization with emplacement of massive barite-sulphides following an initial brecciation and pyritization.

INTERPRETATION

The most important events in the geological and metallogenic evolution of the Massif du Nord of northern Haiti are the La Mine dacite volcanism (Upper Cretaceous) and the Loma de Cabrera tonalite magmatism (Upper Cretaceous - Paleocene). One of the most important contributions of our studies is the recognition and classification of the two principal mineralization systems - epithermal and porphyry copper - and the important role played by the above geological events in their formation in this region. However, the volcanological evolution of La Mine Series and its magmatic affinities are poorly understood and there is only limited information from which we can deduce the relationship of the two principal mineralization systems and constrain their ages. Detailed geological mapping and extensive radiometric dating will be necessary to supplement the available data before final conclusions can be made.

The epithermal mineralization cuts the entire Upper Cretaceous volcanic sequence and the base of the Trois Rivières Series, suggesting that hydrothermal activity occurred during the later stages of acid volcanism. Based on their studies in the Dominican Republic, Amarante et al. (1989) and Lewis et al. (1989), consider that the main fractures providing fluid conduits for hydrothermal activity in the Upper Tireo (La Mine Series) would have been developed in the Campanian at the latest. The available age dating on the epithermal-polymetallic mineralization in both Haiti and Dominican Republic show dates that extend from 85 to 59.4 Ma, spanning the entire Campanian - Lower Paleocene (Danian) period and indicating more than one episode of hydrothermal activity. Reported ages in Haiti include K/Ar dates of 84 Ma on sericite from the hydrothermal alteration at Camp Coq (Société Minière d'Haiti, 1977) and concordant Rb/Sr and K/Ar ages of 59.4 Ma on mineralized dacite stocks at Mazambi (Cheilletz et al., 1978). Whole rock K/Ar dates ranging from 71 to 85 Ma were reported on mineralized felsic intrusions of the Tireo Group in the Dominican Republic (Electroconsult, in Lewis et al., 1989).

Information on the epithermal mineralization suggests times of hydrothermal activity which coincide with the main phases of the Loma de Cabrera magmatism. In a subjective way the writer feels that some of the dacite stocks with associated mineralization, may represent a shallow level manifestation of the tonalite magmatism or subjacent porphyry copper stocks (Louca, 1985). Similar conclusions have been reached by Lewis et al., (1989), who also considers that it is likely that the dacite volcanism of the Upper Tireo unit (La Mine Series) is the volcanic equivalent of the tonalite plutonism. It would appear that the early phases of the Loma de Cabrera tonalite magmatism gave way to the La Mine volcanics which, at a much later stage, were intruded by their parent tonalite rocks (Fig. 13).

Although the relation between the tonalite batholith and the small shallow porphyry stocks of microtonalite and quartz diorite, as well as many aspects of the associated porphyry copper

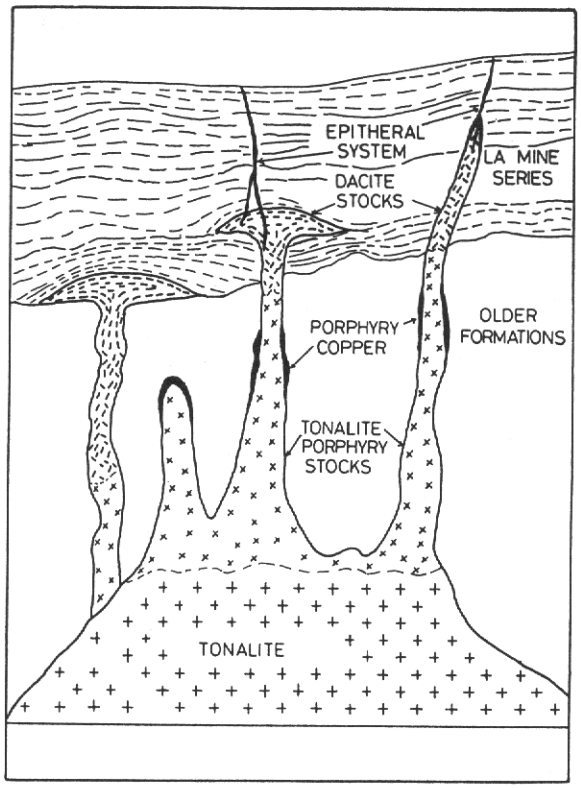

Figure 13. Idealized model of possible relationships between the epithermal and porphyry copper mineralization (Louca 1987).

mineralization have been a source of heated controversy, there seems little doubt that these stocks represent high level periplutonic intrusions of the tonalite magmatism. This relationship is not always obvious because the ages of both stocks and batholith are poorly constrained and the various generations of tonalites have not yet been differentiated in the Massif du Nord. Field evidence partly supported by radiometric age dating point to emplacement times of both the stocks and the batholith that range from Upper Cretaceous to Paleocene. Age dating of Rb/Sr and K/Ar on the Terre Neuve stocks (Kesler, 1968) and Jean Rabel stocks (Cheilletz et al., 1978) gave 66 Ma and 67 + 4 Ma respectively.

With regard to the origin of precious metals of the two principal mineralizations of northern Haiti, our studies allow interpretations only for the porphyry copper group deposits. Lithogeochemical work on rock samples from the Grand Bassin area shows that the ultrabasic and basic rocks, as well as the lower members of the Perches Series can be chemically distinguished from the other formations by their high Ni and Au contents which range up to 1600 ppm and 50 ppb respectively. In the Faille B area the hydrothermally unaltered Perches Series containing intercalated thin barite layers, is characterized by values up to 1700 ppm Pb, 1000 ppm Zn, 7 ppm Ag and 200 ppb Au. Within the hydrothermally or sheared Perches Series and ultrabasic rocks, Ni decreases to 360 ppm, Zn to 50 ppm, Pb to 26 ppm Au to 30 ppb respectively.

This phenomenon of depletion of base and precious metals from the hydrothermally altered rocks and their concentration in quartz veins, as well as the close spatial relationship of these gold-bearing veins with ultrabasic and basic rocks, suggest that at least part of the gold in quartz veins was generated from these rocks. This interpretation of metal source rocks applies equally well to both gold bearing stocks and silver-rich vein deposits hosted in metabasic and ultrabasic rocks elsewhere in the Massif du Nord.

Although our studies have demonstrated an intimate association between gold and barite in the epithermal mineralization system, additional information is needed in order to understand the factors affecting the mobilization and Olocalization of the gold during the various episodes of hydrothermal activity.

SUMMARY AND CONCLUSIONS

The present study has isolated two principal genetic types of economic sulphide and gold mineralization in northern Haiti: porphyry copper-bearing stocks and epithermal-polymetallic sulphide-barite mineralization. The first one is related to quartz diorite stocks and includes a continuum between porphyry copper deposits, limestone replacement (skarn) deposits and gold bearing quartz-sulphide veins. These deposits are known from the deeper and central parts of the Upper Cretaceous volcano-sedimentary pile (andesites and basalts) and from tectonic zones in older formations. Epithermal-polymetallic mineralization exhibits volcano-tectonic control and is characteristically associated with zones of silicification and advanced argillic alteration at the higher levels of the same volcanic pile (dacitic La Mine Series).

Although the author's studies on northern Haiti have given a better appreciation of the classification of the mineral deposit types and their association with certain lithologic units and rock types, considerably more work needs to be done on the individual mineralized systems to better understand their genesis and emplacement history in terms of time. The time of emplacement of the porphyry copper-bearing stocks and the dacite stocks with related epithermal mineralization falls within the Upper Cretaceous-Paleocene interval, coinciding with the tonalite plutonism. However, the genetic and temporal relationships between the two principal mineralized systems have not yet been defined. The epithermal system may be underlain at depth by porphyry copper stocks in a polygenetic volcanic setting such as a stratovolcano-flow dome complex similar to those described by Sillitoe and Bonham (1984) in the western Americas and the southwest Pacific.

Further exploration for base and precious metal mineralization in northern Haiti is considered to be a worthwhile undertaking. Despite the unanswered questions on the emplacement history and origin of the north-Haitian mineralization the present work has provided valuable information and features which have an important bearing on future exploration programmes. Utilizing this information the exploration strategy should be modified in accordance with the following:

a. Mémé skarn deposit reported in literature as a copper mine, contains appreciable amounts of gold and silver. Resampling of various parts of the deposit indicated gold contents up to 23 g/t and sizeable portions of the mine may average about 10 g/t Au. So far, exploration efforts have been focused only on skarn mineralization with surface expression and even in those cases, mineralization has not been fully delineated. The structural disposition of the quartz diorite stocks and related skarn deposits, suggest possible sub-surface extension of the mineralization between the individual stock outcrops and additional ore potential.

b. The evaluation of the two major porhyry copper deposits, Douvray and Blondin, carried out in the late 1970's aimed at their copper ore reserves and the information on their precious metal content is very sporadic. Selected drill holes from Blondin deposit analyzed for gold show intersections over one meter in width with 9.0 g/t Au. In view of the significant potential of mineralized ground (combined 250 million tonnes with 0.6% Cu) the assessment of these two deposits for their precious metal content is strongly warranted.

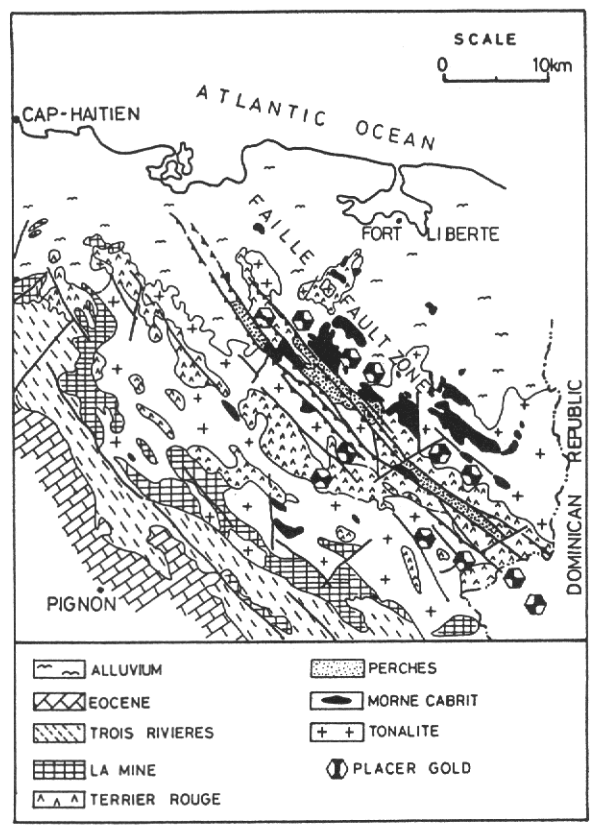

Figure 14. Geological map of Northeastern Haiti (Louca 1988).

c. Field evidence supported by regional air photo interpretation and geochemical data suggest that the Faille Fault Zone containing the Faille B gold deposit, extends northwest towards the Blondin porphyry copper deposit and to the southeast through Mont Organisé to the Dominican Republic (Fig. 14). The projection of a major fault zone is further supported by the distribution of the occurrences of alluvial gold at Acul de Pins, Vallières and Mont Organisé.

d. Although the targets sought in the primary zone of the epithermal mineralized system are small, their high gold contents make them deserving of further attention. The lack of exploration success in locating economic ore bodies may be attributed to the fact that exploration to date has been concentrated on the search for syngenetic and concordant bodies of massive mineralization instead of focusing on steep fault zones and planes of the mineralized structures within which the massive sulphides-barite replacements are likely to be elongated.

ACKNOWLEDGEMENTS

The author is greatly indebted to Mr. Briand Lafalaise, Director General of the Bureau des Mines et de l'Energie of Haiti and to Mr. Shigeaki Tomita, Director of the United Nations Revolving Fund for Natural Resources Exploration for permission to publish this work. Sincere thanks are due to Dr. John F. Lewis (Professor of Geology, George Washington University) and his co-workers from the Dominican Republic for discussion of the results of their work in the Restauracion area.

REFERENCES

Amarante, J.A., Jimenez, J. and Lewis, J.F., 1989. Geology, hydrothermal alteration and geochemistry of epithermal Au-Ag mineralization in the Restauracion area, Dominican Republic, Trans. 11 Carib. Geol. Conf.

Bowin, C.O., 1966. Geology of the Central Dominican Republic, Geol. Soc. Amer. Mem 98, p.11-84.

____ 1975. The geology of Hispaniola in, The Ocean Basins and Margins, Vol. 3, A.E. Nairn and F.G. Stehli, eds., Plenum Publishing Corp., N.Y.,p. 501-552.

Butterin, J., 1954. La géologie de la République d'Haiti, Mem. Inst. Franc. d'Haiti no. 1, 446p.

Cheilletz, A., Kachrillo, J.J., Sonet, J. and Zimmermann, J.L., 1978. Pétrographie et géochronologie de deux complèxes intrusifs à porphyres cuprifères d'Haiti. Contribution à la connaissance de la province cuprifére laramienne de l'arc insulaire des Grandes Antilles, Bull. Soc. géol. Fr., no. 6.

Donovan, P. R., and Louca, K., 1989. The Faille B Gold Deposit, Northern Haiti: An Exploration Case History; p. 898-911 in Proceedings of Exploration '87: Third Decennial International Conference on Geophysical and Geochemical Exploration for Minerals and Ground Water, edited by G.D. Garland, Ontario Geol. Surv. Special Vol. 3, 960p.

Dressler, B., 1986. Petrography of igneous rocks suites from the Faille B, La Mine, Plaisance and Grande Savane areas. UNRFNRE Tech. Rep. No. 11.

Feigenson, M., 1978. Petrology and strontium isotope geochemistry of the Loma de Cabrera batholith, Dominican Republic, M.S. thesis. G. Washington Univ.

Harris, J. F., 1986. Mineragraphy and petrography of drill core samples from the Faille B gold prospect, Zone A, Perches, UNRFNRE, Tech. Rep. No. 24.

Jimenez, G.J., and Lewis, J.F., Petrologia del area de Restauracion, Republica Dominicana, Trans. 10 Carib. Geol. Conf., in press.

Kesler, S.E., 1966. Geology and ore deposits of the Memé-Casseus district, Haiti: Ph.D. dissertation Stanford Univ. 156p.

____ 1968. Contact-localized ore formation at Mémé Mine, Haiti, Econ. Geol. 63, p. 541-552.

Kesler, S.E. and Sutter, J.F., 1977. Progress report on radiometric age determinations in the Caribbean region, (Abs) 8 Carib. Geol. Conf., pp. 85-86.

Lewis, J.F., 1982. Granitoid rocks in Hispaniola, Trans.9 Carib. Geol. Conf.Lewis, J.F., Amarante, A., Bloise, G., Jimenez, G.J. and Dominguez, H.D., 1989. Lithology and stratigraphy of Upper Cretaceous volcanic and volcaniclastic rocks of the Tireo Group, Dominican Republic and Haiti, unp. rep.

Louca, K., 1985. Geology, exploration and mineral resources of La Mine. UNRFNRE Tech. Rep. No. 15, 53p.

____ 1987. Geology and mineralization of Camp Coq Area, UNRFNRE Tech. Rep. No. 26, 31p.

____ 1988. Geology and mineralization of Faille B Gold Prospect, UNRFNRE Rep. No. 25, 112p.

Nicolini, Ph., 1977. Les porphyres cuprifères et les complexes ultrabasiques du Nord Est d'Haiti, Essai de Typologie Prévisionelle Thèse Doct. Univ. P. et M. Curie, Paris, V1, 203p.

Ohashi, R., 1920. On the origin of the Kuroko of the Kosaka copper mines, northern Japan. Akita Mining College Jour., v. 2, pp.11-18.

Russell, N., Seaward, M., Rivera, J.A., McCurdy, K., Kesler, S.E. and Cloke, P.L., 1981. Geology and geochemistry of the Pueblo Viejo gold-silver oxide deposit, Dominican Republic. Inst. Min. and Met. Trans., Section B, v 90, pp.B153-B162m.

Streckeisen, A.L., 1974. Classification and nomenclature of plutonic rocks. Recommendations of the IUGS Subcommission on the Systematics of igneous rocks. Geol. Rund., 63 pp773-786.

Sillitoe, R.H. and Bonham, H.F., 1984. Volcanic landforms and ore deposits, Econ. Geol., v. 79, p 1286-1298.

Société Minière d'Haiti (S.M.H.), 1977. Exploration Progress Report, November 1975 through December 1976, Limbe Project, Haiti, Unp. Rep., Company Report, Port-au-Prince, Haiti.

Société Franco-Haitienne des Mines (S.F.M.H.), 1980. Les minéralisations volcanosédimentaires sulfurées des permis de la Société Minière d'Haiti, Unp. Rep., Company Report, Port-au-Prince, Haiti.

Woodring, W.P.B. and Brown, J.S., and Burbank, W.S., 1924. Geology of the Republic of Haiti, Dept. Publ. Works, Geol. Haiti, Port-au-Prince.

LANDSLIDE PROCESSES IN SAPROLITIC SOILS OF A TROPICAL RAIN FOREST, PUERTO RICO

Matthew C. Larsen, USGS, San Juan, Puerto Rico and
Andrew Simon, USGS, Nashville, Tennessee

ABSTRACT

Shallow soil slips, earth and debris slides appear to be a primary mechanism of hillslope denudation in the rainforest of eastern Puerto Rico. Annual rainfall in excess of 4,000 mm, and thick sequences (up to 20 m) of residual soils (saprolite) combine to produce these landslides. Shear-strength testing and observations of tension cracks indicate that landslides may start as tensile failure of saprolite material. The tension cracks provide avenues for rapid infiltration of rainwater and saturation of the underlying soil. During or shortly after intense and prolonged precipitation, shear failure then occurs as a result of pore-pressure buildup along zones of low permeability within the saprolite.

Tensile stresses in the unsaturated, low-density, upper saprolite zone range from 3 to 10 kPa, and mean seismic-refraction velocities are 476 +/- 127 m/s. Denser, clay-rich, less permeable saprolitic zones having mean seismic velocities of 1420 +/- 157 m/s represent zones that are commonly associated with perched ground water and are zones where excess pore-water pressure is most likely to trigger movement. These zones of translocated clay show marked density increases.

Slickensides are present in the saprolite along relict fractures and joints derived from the parent rock; they are common in quartz-diorite bedrock, and less so in marine-deposited volcaniclastic bedrock. The failure planes of many landslides have exposed these relict fractures and joints as slickensides, and landslides appear to move on these pre-existing planes of weakness in the saprolite. The largest landslides (areas greater than 20,000 m^2), however, are those that fail along saprolite-bedrock boundaries, which are zones of contrasting density and permeability within or at the base of the weathered profile.

INTRODUCTION

Landslides are a common problem in the Caribbean National Forest (CNF), an 11,330-hectare tropical rain forest in northeastern Puerto Rico (fig.1). More than 170 landslides have been mapped in this area using aerial photography and field observation (Guariguata and Larsen, 1990)(fig.1). Numerous sections of roadway have been damaged or destroyed, and lives have been lost as a result of these landslides. Rainfall, relict structures in saprolite, bedrock and soil type, and road-construction practices appear to be important controlling factors for landslide occurrence and location. These factors have been examined, and are discussed below, as part of a regional study of landslide hazards conducted by the U. S. Geological Survey in cooperation with the Planning Board of Puerto Rico.

Several investigators have described CNF landslides. St. John and others (1969) discussed the role of relict structures in residual soil as a control in small-scale landslides. Deere and Patton (1971) related landslide processes to intense rainfall and certain characteristics of the weathering profile. Sowers (1971) described various types of small slumps and earth slides as well as rock falls that hampered construction of a CNF highway begun in 1960. Most recently, in an island-wide map showing landslide susceptibility, Monroe (1979), classified the CNF as having moderate overall susceptibility, with a few areas of high and highest susceptibility.

SETTING

The CNF ranges in elevation from 100 to 1,075 m (meters) above mean sea level. Mean annual temperature and rainfall range from 26.5°C and 2,500 mm (millimeters) respectively in the lower elevations to 17.5°C and 4,500 mm at higher elevations (Brown and others, 1983). Intense precipitation may occur throughout the year but generally is associated with tropical depressions, hurricanes, or less intense tropical waves (Miller, 1965). These types of storms are most common between June and November and can result in 24-hour rainfall totals of more than 300 mm (Calvesbert, 1970).

Bedrock in the study area consists of marine-deposited andesitic to basaltic volcaniclastics of Cretaceous age (Seiders, 1971). In the upper Rio Blanco basin, these rocks have been intruded by the Rio Blanco stock, a light-gray, medium- to coarse-grained quartz-diorite that covers about 20 km (square kilometers) and is bounded by a metamorphosed zone extending 0.5 to 3.5 km into the surrounding volcaniclastics. Slopes in the CNF are mantled with a shallow [40 cm (centimeters)] but dense root zone (Brown and others, 1983) within the A and B soil horizons in the upper meter. This soil is derived from the underlying colluvium and and silt-clay saprolite. This sequence of saprolitic material overlies weathered and unweathered bedrock and ranges in thickness from 1 to 24 m (fig.2)(Dames and Moore, 1980; Larsen, 1989a,1989b; U. S. Dept. of Transportation, written comm., 1988).

METHODOLOGY

Data used in this study were obtained from bore-hole shear tests (BST); analyses of soil samples for grain size, Atterberg limits, moisture content, and bulk density; seismic-refraction surveys; landslide field surveys; and aerial photography. Bore-hole shear tests were conducted at depths ranging from 0.5 to 3 m, at several locations along slope profiles to measure in-situ shear strength (friction angle and cohesion). Detailed discussions of the BST are in Lohnes and Handy (1968), Lutenegger and Hallberg (1981), and Lutenegger (1987). Soil samples collected from the same depths as those used in the BST were analyzed as described by Lambe (1951).

Seventeen seismic-refraction surveys were conducted, generally along lines of equal elevation, to determine (1) depth to bedrock or weathered bedrock; (2) depth to water table, if present; and (3) depth to intermediate weathering zones within the saprolite and/or weathered rock. A signal-enhancing 12-channel seismograph was used in conjunction with an array of 12 geophones. The energy sources used were blows from a 3.6 kg (kilogram) sledge hammer on a steel plate and a seismic shotgun using 8- and 12- gage shells. Seismic data were analyzed using the delay-time method and a ray-tracing procedure (Scott, 1977).

Aerial photographs for seven different years between 1936 and 1988 were examined for this study. More than 170 landslides identified on these photographs were mapped on topographic quadrangles and then field checked (fig. 1)(Guariguata and Larsen, 1990). After field work was completed for this article, Hurricane Hugo struck eastern Puerto Rico in September 1989, with maximum sustained winds of over 225 km per hour. The 3-day rainfall total associated with the hurricane ranged from 165 to 344 mm. More than 200 landslides occurred within and near the CNF during this storm; most of these were shallow soil slips, as well as shallow earth slides and

Larue, D.K., and Draper, G. (eds.),
Transactions of the 12th Caribbean Geological Conference, St. Croix, *U.S.V.I.*, Miami Geological Society, P.O. Box 431552, South Miami, FL 33243, U.S.A

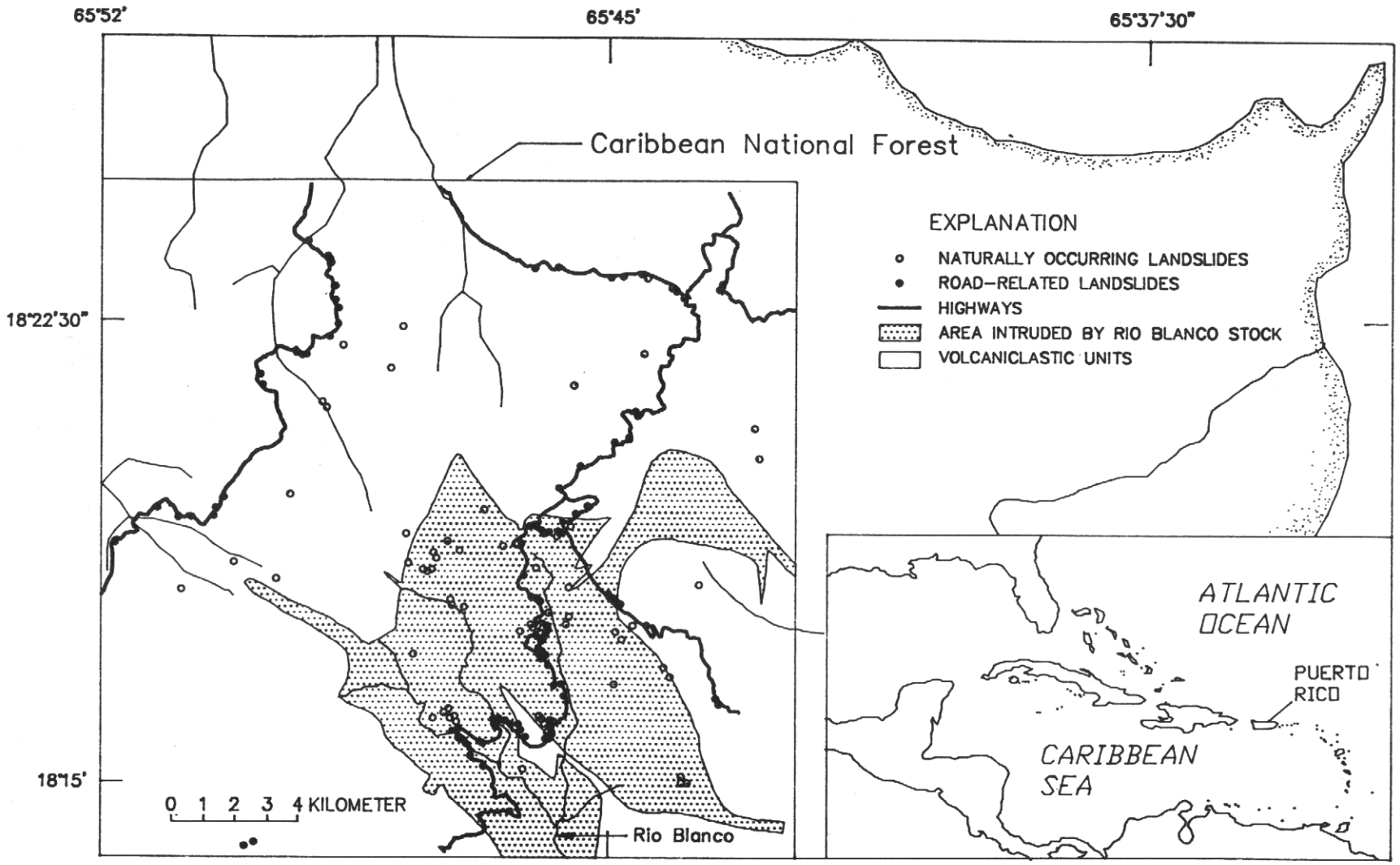

Figure 1. Map showing location of landslides in the Caribbean National Forest (from Guariguata and Larsen, 1990).

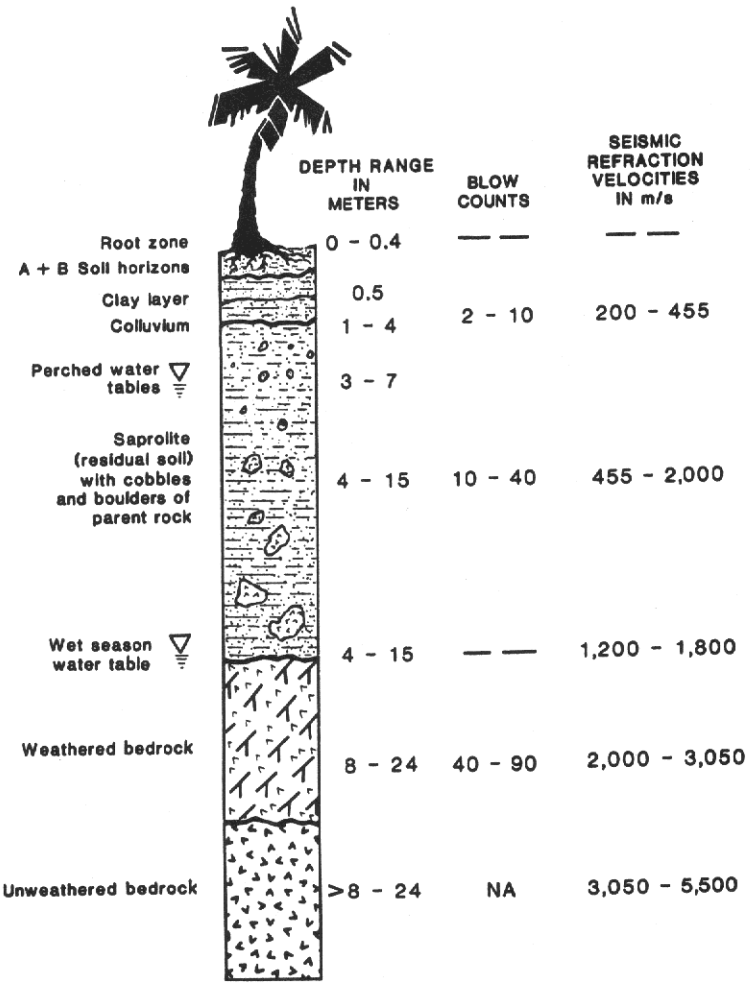

Figure 2. Generalized stratigraphic column for the Caribbean National Forest.

debris flows (Larsen, 1990). These recent landslides are not included in this study.

RESULTS

In the soils overlying quartz-diorite bedrock, friction angles obtained with the BST range from 5.3 to 39° and cohesion values range from near 0 to 21.4 kPa (kilopascals) (fig. 3a,b). The data are sharply skewed towards low strengths and generally indicate soils of low cohesion (mean cohesion was 6.29 +/- 1.59 kPa). Soils overlying volcaniclastic bedrock tend to have greater mean cohesive strengths (9.35 kPa) but a friction angle range (11° to 38°) similar to that of soils overlying the quartz-diorite bedrock. Although friction angles for both soil types do not differ significantly, the frequency distribution of friction angles for quartz-diorite soils shows a marked skewness for higher values (fig. 3a). Friction angle data for volcaniclastic soils are more equally distributed (fig. 3a). Cohesion values for the two soil types show higher values for those soils overlying volcanic bedrock (fig. 3b). Saprolite above and near headscarps is considerably drier and is subject to tensile stresses, (mean of -4.9 +/- 0.7 kPa) (Simon and Larsen, 1988). Tension cracks are visible at some sites, particularly those that have had recent landslides. These tension cracks provide avenues for rapid infiltration of rainwater into the subsurface, which thus increases the potential for more rapid saturation and the build up of pore-water pressure.

On the basis of field observations, lithologic data, and seismic velocities, substrate materials fall into three general categories, outlined in figure 3. Unsaturated soil, colluvium, and upper-saprolite materials have a mean seismic velocity of 476 +/- 127 m/s (meters per second). The lower saprolite, which includes denser, clay-rich, less-permeable zones, has mean seismic velocity of 1,420 +/- 157 m/s and ranges from 4 to 15 m below ground surface (Larsen, 1989a, 1989b). Where drilled, the clay-rich layers show a 2- to 3-fold increase in blow counts [Blow count is an engineering term which describes the number of blows required to drive a drill-rig sampling spoon a distance of 30 cm (centimeters) with a 64 kg hammer falling 76 cm]. At several sites, a perched water table was encountered at the top of these clay-rich horizons. Bedrock mean seismic velocity is 3,930 +/- 1625 m/s. Average depth to bedrock is 15 m, but this depth varies from 8 to 24 m because of undulating bedrock weathering-surfaces, formed by uneven weathering rates.

Field examination and testing of exposed relict structures in saprolite using a pocket penetrometer reveal black, clay-rich layers several centimeters thick having higher density and strength [average values for unconfined compressive strength of 3 kg/cm^2 (kilograms per square centimeter) as compared with 1 kg/cm^2] than the overlying saprolite. Chemical analyses of these black layers in saprolite from Georgia and Puerto Rico indicate that the dominant component is manganese oxide, with iron oxide and humic compounds also present (St.

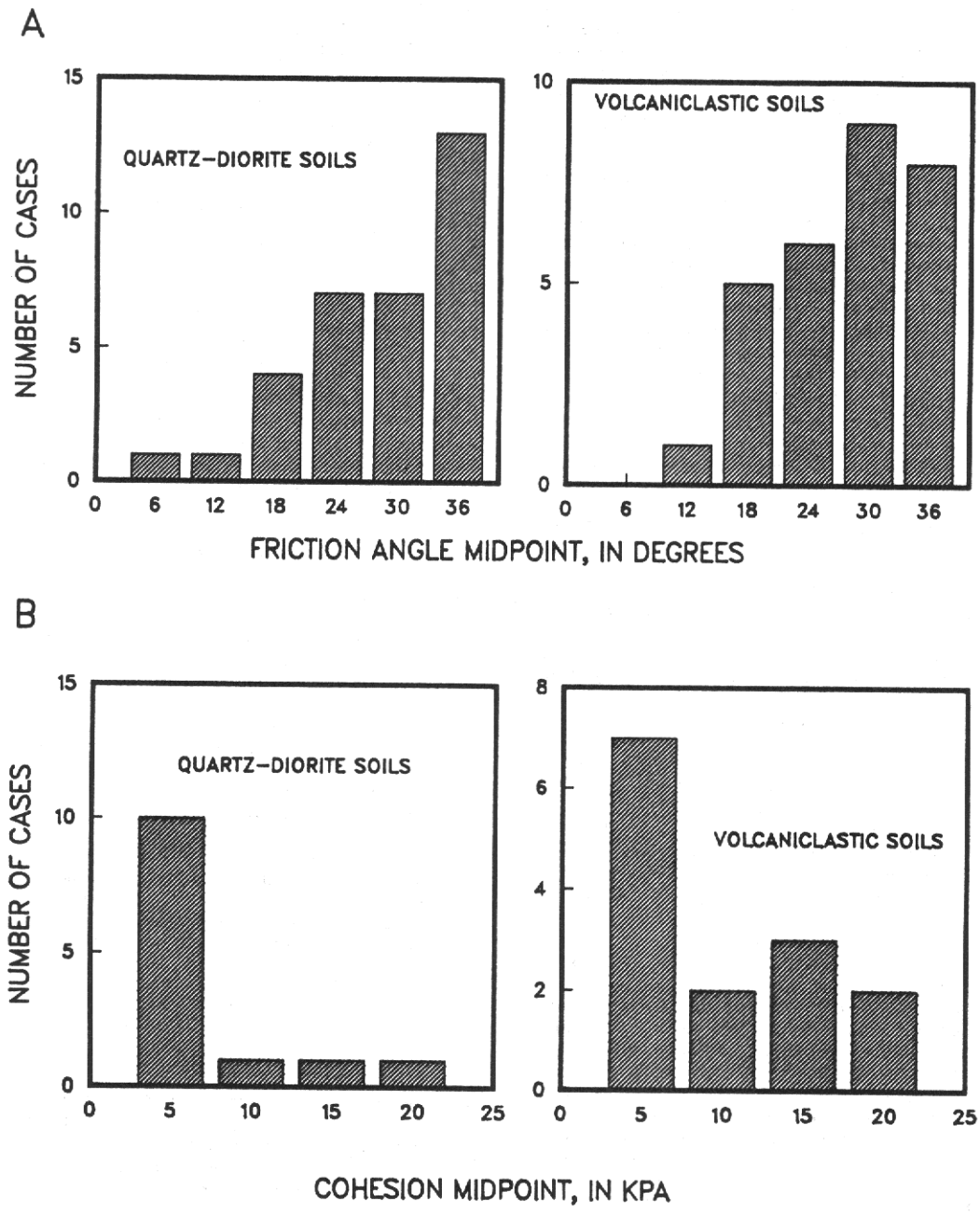

Figure 3. Frequency distribution for (a) friction angle and (b) cohesion in soils overlying quartz-diorite and volcaniclastic bedrock.

John and others, 1969). Discontinuous zones of this material generally are associated with perched water and increased pore-water pressure during and after intense and prolonged rainfall. This implies that smaller landlides within the saprolite probably occur along zones of increased pore pressure immediately overlying saprolite layers having decreased permeability and increased density.

Data from five drill-holes that encountered water show two perched water tables at depths of 9 and 12 m at the lower segments of slopes. These depths, noted during periods of wet-season (June to November) normal rainfall, are several meters deeper than most observed landslide failure planes. Preliminary piezometer data from recent storms of small to moderate rainfall accumulation and intensity indicate a significant water-table rise often occurs within 1 to 5 days after the storm. One such storm (Hurricane Hugo) triggered numerous landslides with failure planes that are 0.5 to 2 m deep, presumably the depth of a zone of increased pore pressure (Larsen, 1990). The largest landslide that resulted from Hurricane Hugo, a 23,000 m^3 debris avalanche, occurred three days after the passage of the storm.

Preliminary field and air photo surveys of recent landslides and adjacent areas reveal trends in landslide type, location, dimensions, relation to highway construction, timing in relation to intense rainfall, apparent failure mechanisms, and failure planes. The majority of landslides observed in the CNF are shallow soil slips, earth slides, debris slides, and earth slumps which occur mainly along planar or concave slopes

(classification after Varnes, 1978; Campbell, 1975). They commonly are from 0.5 to 7 m deep, are tens of meters long, and range from 5 to 25 m wide. Also present, but less common, are debris avalanches as well as rock falls and slow earth flows found mainly along roadcuts. More than 60 percent of the mapped landslides are associated with highway construction (fig. 1).

Once initiated by buildup of hydrostatic pressure within tension cracks, earth slides commonly fail along planes of weakness in the saprolite. These planes of weakness are former fracture or joint planes that remain evident in the saprolite after the rock has been weathered. Because stress-release fractures that form in parent rock as it weathers generally are parallel or subparallel to the slope surface, the fractures provide an optimal orientation for a sliding mass. Other evidence of earth slides are trees rafted downslope in upright position on intact blocks of soil. Since the majority of the forest root zone is less than 40 cm thick (Brown and others, 1983), these trees continue to grow at their new location, which contributes to the forest canopy recovery.

Evidence from headscarps and exposed unweathered, or slightly weathered, bedrock on failure planes indicates that the largest landslides (areas greater than 20,000 m^2) usually start as slumps and fail along the saprolite/bedrock boundary. Several such landslides, located along a CNF highway, are 300 to 600 m long and become debris avalanches downslope with long and narrow run-out zones. They are all located above roadway sections where slope toes were removed, and all occurred during or shortly after hurricane-related rainfall.

Most landslides (54 percent of road-related and 77 percent of naturally-occurring landslides) are within the area of the quartz-diorite intrusion which indicates a strong lithologic control (fig. 1)(Guariguata and Larsen, 1990). Landslides associated with road construction are almost exclusively on slopes subjected either to toe removal or to surcharge by fill material on their upper segments.

Most of the dated landslides can be associated with specific storm events in which one-to five-day total rainfall ranged from 100 to 1000 mm. Actual timing of the landslides cannot be determined in most cases due to their remote location. For most known cases, the failures occurred within several hours to 5 days after the rainfall. A notable exception is one of the largest landslides, a 300,000 m^3 debris avalanche which occurred five weeks after the passage hurricanes David and Frederick in 1979. These hurricanes struck the island within a period of five days and each produced more than 300 mm of rainfall. This indicates that slow infiltration of rainfall (over a period of five to six weeks) may have resulted in pore-pressure buildup along deep failure surfaces and the subsequent large landslide.

ACKNOWLEDGMENTS

The U.S. Geological Survey gratefully acknowledges the support and interest of Ariel Lugo and Frederick Scatena, of the U.S. Forest Service, Puerto Rico. Additionally, we thank Thomas Fennessey, U.S. Dept. of Transportation, for providing drill-hole data. The authors thank Randall Jibson and Allen Gellis for valuable review comments.

REFERENCES

Brown, Sandra, Lugo, A.E., Silander, Susan, and Liegel, Leon, 1983, Research history and opportunities in Luquillo Experimental Forest, U. S. Department of Agriculture, Forest Service, General Technical Rept. SO-44, 128 p.

Calvesbert, R. J., 1970, Climate of Puerto Rico and the U.S. Virgin Islands, U.S. Dept. of Commerce, Climatography of the U.S. no. 60-52.

Campbell, R. H., 1975, Soil slips, debris flows, and rainstorms in the Santa Monica Mountains and vicinity, southern California, U. S. Geological Survey Prof. Paper 851, 51 p.

Dames and Moore, 1980, Report on the rehabilitation of Rio Blanco hydroelectric project for Puerto Rico Electric Power Authority, Houston, Texas, Job No. 11905-002-14.

Deere, D.U. and Patton, F.D., 1971, Slope stability in residual soils, Proceedings of the 4th Panamerican Conference on Soil Mechanics and Foundation Engineering, vol. 1, p.87-170.

Guariguata, M.R, and Larsen, M.C., 1990, Preliminary map showing landslides in El Yunque quadrangle, Puerto Rico, U.S. Geological Survey Open-File Report, 89-257, scale 1:20,000.

Lambe, T.W., 1951, Soil testing for engineers, John Wiley and Sons, New York, 165 p.

Larsen, M.C., 1989a, Use of seismic refraction techniques for investigating the morphology of recent landslides in a tropical rain forest in Puerto Rico, Geological Society of America, Abstracts with Programs, v. 21, no. 3, p.46.

Larsen, M.C., 1989b, Use of seismic refraction techniques for investigating recent landslides in a tropical rain forest in Puerto Rico, Energy and Mineral Potential of the Central American-Caribbean Region, San Jose, Costa Rica, March 5-9, 1989, Proceedings volume.

Larsen, M.C., 1990, Landslides caused by the intense precipitation of Hurricane Hugo, September 1989, Eastern Puerto Rico, abstract, EOS, Transactions, American Geophysical Union, vol.71, no.7, p.256.

Lohnes, R.A., and Handy, R.L., 1968, Slope angles in friable loess, Journal of Geology, v. 76, no. 3, p.247-258.

Lutenegger, A.J., and Hallberg, G.R., 1981, Borehole shear test in geotechnical investigations, in Laboratory Shear Strength of Soil: ASTM STP 740, R.N. Yong and F.C. Townsend, Eds., American Society for Testing and Materials, 1981, p.566-578.

Lutenegger, A.J.,1987, Suggested method for performing the borehole shear test, Geotechnical Testing Journal, GTJODJ, vol.10, no.1, p.19-25.

Miller, J.F., 1965, Two- to ten-day rainfall for return periods of 2 to 100 years in Puerto Rico and Virgin Islands, Weather Bureau, U.S. Dept. of Commerce, Technical Paper 53, 35 p.

Monroe, W. H., 1979, Map showing landslides and areas of susceptibility to landsliding in Puerto Rico, U.S. Geological Survey Miscellaneous Investigations Map I-1148, scale 1:240,000.

Murphy, V.J., and Holt, R.J., 1960, Engineering seismology applications in deep weathered rock areas, First Panamerican Conference on Soil Mechanics and Foundation Engineering, Proceedings vol. 2, p.889-901.

St. John, B.J., Sowers, G.F., and Weaver, C.E., Slickensides in residual soils and their engineering significance, Seventh International Conf. Soil Mechanics and Foundation Engineering, Mexico, vol.2, p.591-597.

Scott, J.H., 1977, SIPB-- A seismic inverse modeling program for batch computer systems, U.S. Geological Survey Open-File Report 77-366,40p.

Seiders, V.M.,1971, Geologic map of the El Yunque quadrangle, Puerto Rico, U.S. Geological Survey Miscellaneous Geologic Investigations Map I-658, scale 1:20,000.

Simon, Andrew and Larsen, M.C., 1988, Shear strength and slope stability at sites in the Caribbean National Forest and Coamo area, Puerto Rico, Geological Society of America Abstracts with Programs, vol. 20, no. 7, p.A-144.

Sowers, G.F., 1971, Landslides in weathered volcanics in Puerto Rico, Proc. of 4th Panamerican Soil Mechanics and Foundation Engineering Conference, v. 2, p.105-115.

Varnes, D.J., 1978, Slope movement types and processes, in, Schuster, R.L., and Krizek, R.J., eds., Landslides, Analysis and Control Special Report 176, Transportation Research Board, National Academy of Sciences, Washington, D.C., p.12-33.

Extensional Tectonism in the Mona Passage, Puerto Rico and Hispaniola: A Preliminary Study

D.K. Larue
Geology Dept.
University of Puerto Rico
Mayaguez, PR 00708

H.F. Ryan
U.S.Geological Survey
345 Middlefield Rd
Menlo Park, CA 94025

ABSTRACT

The Mona Passage, separating the Puerto Rican block from Hispaniola, is dominated by three sets of active normal faults. The northernmost is the 19° lat (latitude) Fault, a south-dipping normal fault separating a metamorphic complex on the north from an arc complex on the south. The second is the Mona Canyon, a relatively straightforward north-south trending graben (Gardner and others, 1980) that cuts the 19° lat Fault, and has a throw of over 2 kms and cumulative heave on the order of 10 kms. South of the Mona Canyon is a complex of normal faults, some with throws up to more than 2 kms. This complex of normal faults reaches from the southern termination of the Mona Canyon south to the uppermost limit of Muertos Trough (trench) accretion, crosses southwest Puerto Rico and heads offshore in the southcentral Puerto Rico region, and has not been traced as of yet to the west. This extension complex, a myriad of normal faults probably connected by transfer zones, is here proposed to represent a large (over 100 km by 100 km) extensional allochthon, sliding into the Muertos Trough. The 19° lat Fault may indicate that a larger extensional allochthon underlies much of the Mona Passage. The relationship between the two extensional allochthons is not known with certainty.

INTRODUCTION

This is a preliminary description of the geology of the Mona Passage, which lies between the islands of Puerto Rico and Hispaniola (Fig. 1). The Mona Passage provides a continuous seaway from the Muertos Trough (Trench) to the south, across the non-volcanic arc massif of the eastern Greater Antilles, to the Puerto Rico Trench on the north. Most previous studies have emphasized the important of convergence in the trenches (Ladd and others, 1977; Ladd and Watkins, 1978; Ladd and others, 1981; McCann and Sykes, 1984) and strike-slip faulting (Mann and Burke, 1984; Mann and others, 1984). Herein, we present evidence for large magnitude normal faults in the Mona Passage. Much of our study is based on analysis of seismic reflection lines collected by Western Geophysical Inc. for the Puerto Rico Electric Power Authority in the 1970's, and two seismic lines presently owned by the Texas Institute for Geophysics.

SEISMIC STRATIGRAPHY OF THE MONA PASSAGE

Based on preliminary study of seismic lines in conjunction with information from dredge hauls, and submersible surveys (Fox and Heezen, 1975; Weaver and others, 1975; Perfit and others, 1980; Heezen and others, 1985), a two-part stratigraphic sequence is recognized in the Mona Passage. The lower part of the seismic stratigraphy is acoustic basement, which can be shown through correlating rock data from dredge hauls and seismic lines, to represent island arc basement, except in the far nothern part of the Mona Passage, where the acoustic basement is a metamorphic complex (Perfit and others, 1980). The acoustic basement is generally structureless, though in a few seismic lines reflectors are observed which may be faults. Lying above acoustic basement is layered, shallow-water-facies, middle Tertiary rocks (Oligocene, Miocene), again correlating dredge haul and seismic information. Because these rocks are found in scarps of normal faults, it is known that at least some of the normal faulting in the Mona Passage is Miocene or younger.

Larue, D.K., and Draper, G. (eds.),
Transactions of the 12th Caribbean Geological Conference, St. Croix, U.S.V.I., Miami Geological Society, P.O. Box 431552, South Miami, FL 33243, U.S.A

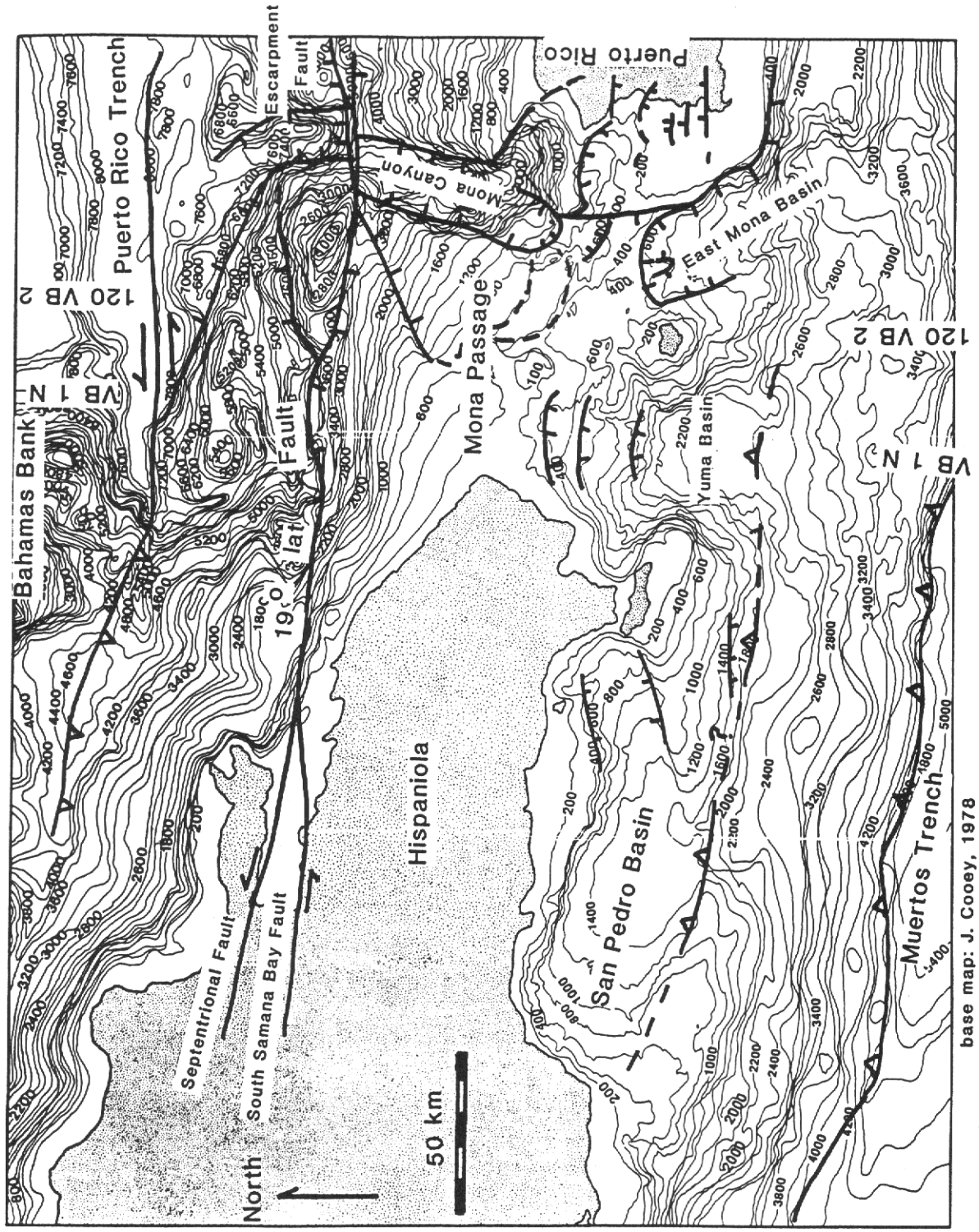

1. Location map of the Mona Passage between Hispaniola and Puerto Rico (bathymetry from Cooey, 1978, unpublished). Tectonics south of eastern Hispaniola are from Ladd and others (1981). VB 1 N and 120 VB 2 are two seismic lines owned by Texas Institute for Geophysics, and studied with their permission here. Positions of Septentrional and South Samana Bay Faults from Mann and others 1984. The Escaprment Fault is a north-dipping normal or oblique normal fault, responsible for the northward downward step in the Mona Canyon across the 19° lat Fault (Larue and others, 1990).

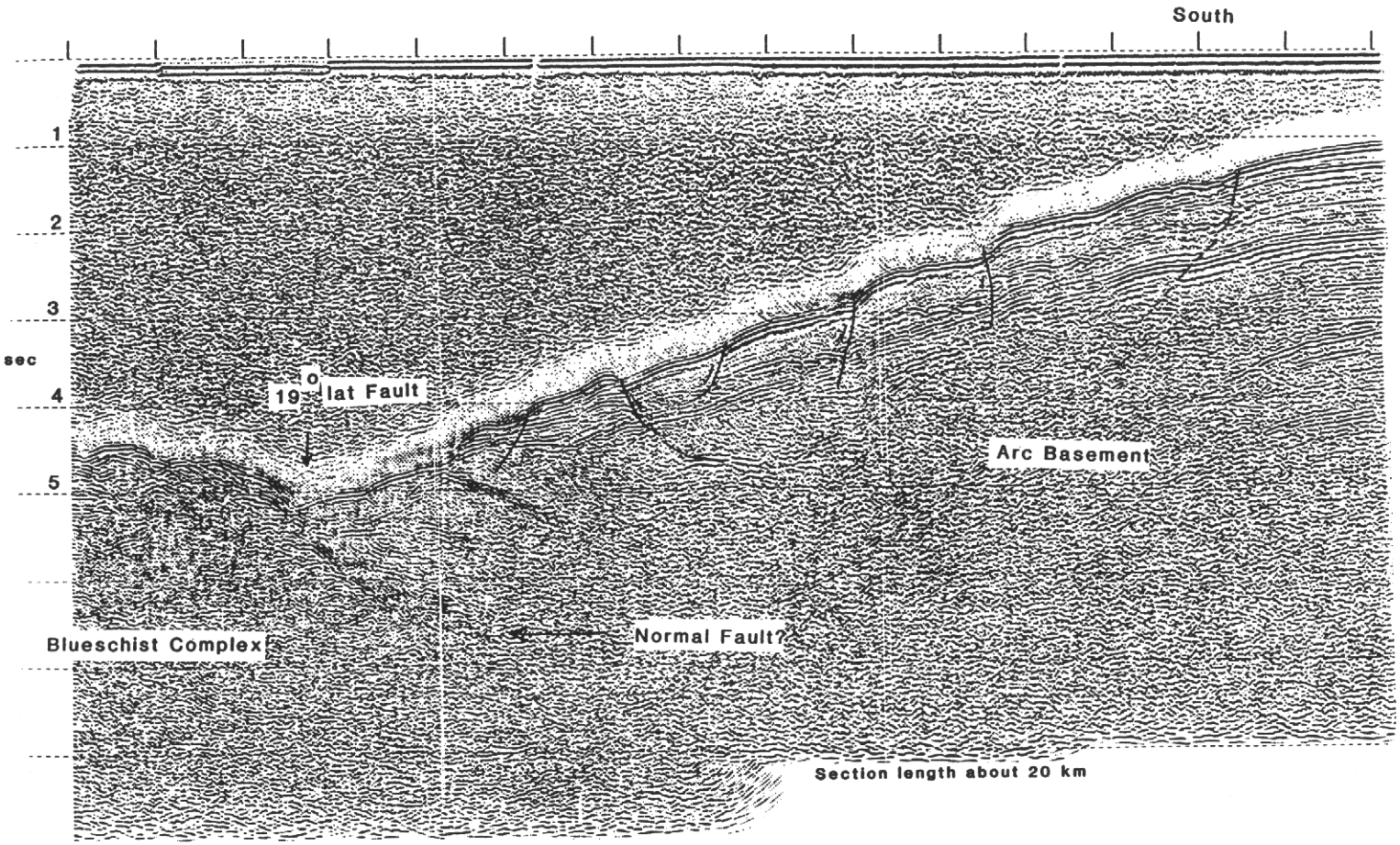

2. Line VB 1 N. Image of the 19° lat Fault, showing southward dip and rollover of Tertiary strata. Evidence for blueschist complex is from Perfit and others (1980) based on dredge hauls.

19° LATITUDE FAULT

The 19° lat (latitude) Fault is the offshore extension of the Septentrional and Samana Faults of Hispaniola (Fig. 1). Based on dredge haul information, the fault separates a metamorphic basement terrane to the north from an arc basement terrane on the south (Perfit and others, 1980). Migration of a seismic line crossing the fault indicates that it is probably a normal fault, dipping south (Fig. 2). Layered Oligo-Miocene strata define a rollover, indicating the 19° lat Fault is probably listric at depth. It is estimated that if the fault is indeed listric, the decollement could be as deep as the base of the arc crust near 30 km. This may indicate that in the Mona Passage, the arc massif is part of an extensional allochthon.

Normal faulting on the 19° lat Fault may be responsible for regional subsidence of Late Miocene age to the south of the 19° lat Fault originally described by Schneiderman and others (1972), Perfit and others (1980), Le Pichon and others (1985), Birch (1986), Moussa and others (1987).

MONA CANYON

The Mona Canyon can be divided into a northern and southern section, separated by the 19° lat Fault. The canyon trends NW, north of the 19° lat Fault, and N, south of the 19° lat Fault. Abundant multichannel seismic data are available for the southern part of the graben, and limited single-channel data are available for the northern part (Fig. 3,4). Wall rocks of the canyon have been dredged and described by Weaver and others (1975), Fox and Heezen (1975) and Perfit and others (1980). In addition, Heezen and others (1985) described observations from a submersible investigation. The structure of the canyon seems to be a simple graben (Figs. 3,4) indicating E-W extension. As indicated by a large earthquake in 1918 (magnitude 7.5; Gardner and others, 1980), and a moderate earthquake in 1987, the graben is seismically active.

The southern termination of the graben is peculiar. The graben faults fan to the east and west, and form a "Y" pattern. The origin of this fanning pattern is uncertain, and has not been addressed in previous work.

NORMAL FAULTS BETWEEN ISLA DESECHEO AND THE MUERTOS TROUGH: THE MONA ALLOCHTHON

South of the "Y" shaped termination of the Mona Canyon, there are an abundance of normal faults with arcuate bathymetric traces. These faults have maximum throws of greater than 2 kms, and clearly cut deeply into basement. These have been mapped by Western Geophysical Company and Fugro (1974), but not interpreted. Their work relied only on the seismic reflection data, and did not stress the correlation between bathymetry and active faulting. In a preliminary map, we restudied all the seismic lines, and have reinterpreted the map traces of the faults (Fig. 3). All seem to have normal displacements, and if the arcuate patterns are indeed correct, little strike-slip displacement is indicated.

Normal faults occur in southwest Puerto Rico, cut rocks as young as Miocene, and some are seismically active. Several onland lineaments can be traced offshore, and linked to faults seen in seismic records.

The depth to the base of the Mona allochthon decollement can be approximated by using balanced cross-sections (Fig. 4). Preliminary calculations indicates a decollement depth around 6 kms, which correpsonds to the depths of the Muertos Trough. It is thus possible that this purported large slide block is contributing to the deformation in the Muertos Trough (Fig. 5).

TENTATIVE EXPLANATIONS FOR NORMAL FAULTING IN THE STUDY AREA

We tentatively conclude that two directions of extension are indicated: E-W for the Mona Graben, and N-S for the region south of the Mona Canyon and the 19°lat Fault. A number of explanations can be proposed for these two extension directions. Faults south of the Mona Canyon may have formed by slope failure (mentioned briefly for smaller normal faults southeast of Hispaniola by Ladd and others, 1977). However, simple slope failure cannot explain the vertical throws of 2 kms on the Desecheo Ridge fault, and the southern "Y" part of the Mona Canyon fault, where it opens into an east-west orientation. Furthermore, simple slope failure does not explain why most of the normal faults cut arc basement rocks. Thus, we tentatively conclude that simple slope failure cannot explain the province of normal faults south of the Mona Canyon graben.

The two directions of extension may be related to a single NW-SE extension, where the sums of their extensions are additive. Rotation of the Puerto Rico block could also conceivably explain some of the normal faults. The solution we

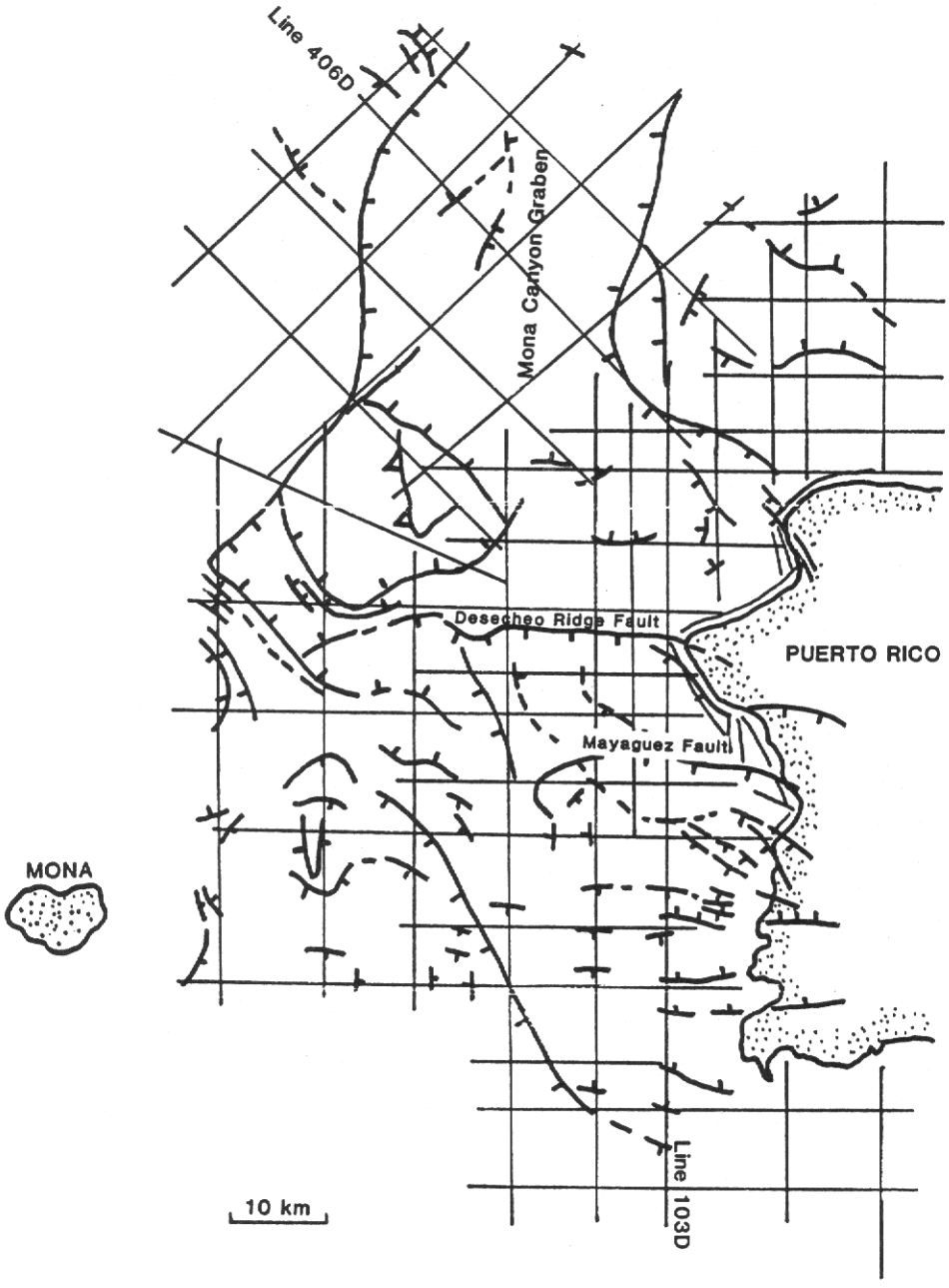

3. Interpretation of normal fault patterns in the Puerto Rican territorial waters of the Mona Passage. Note grid coverage. Data collected by Western Geophysical Inc., and owned by the Puerto Rico Electric Power Authority.

tentatively propose is that the faults south of the Mona Canyon represent an extensional allocthon (Fig. 5), slipping toward the Muertos Trough. This allochthon is structurally on top of an extensional boundary, represented by the Mona Canyon north of the allochthon, between Hispaniola and the Puerto Rican block.

The 19° lat Fault, which has an apparent extension direction parallel to that of the Mona allochthon (although motion probably is oblique left-lateral, based on plate motion studies), is thought to represent extensional tectonism in the Puerto Rico Trench, either associated with Caribbean plate motion or related to rotation of the Puerto Rico block (Larue and others, 1990).

SIMILAR STRUCTURES FOUND ELSEWHERE

Large extensional allochthons similar to the Mona allochthon have been observed in several other places in the world. First, and most obviously, there is soft-sediment deformation of significant scale associated with delta fronts such as the Gulf Coast and the Niger Delta. Deformation in these delta fronts is probably as deep as several kilometers, and thus similar to what is described herein. The Mexican Ridges (Buffler, 1979; Buffler, 1983) are especially interesting, because at the base of a large gravity slide, a thrust belt is developed. Also off southwest Africa, a large extensional allochthon with a fold and thrust belt at the toe is developed (Coffin and Rabinowitz, 1983), probably the largest submarine extensional allochthon recognized, according to the authors. However, these examples involve weakly lithified materials, in contract to the arc basement lithologies involved in the Mona allochthon.

Normal faults with large offset are found in arc platform settings. For example, the summit basins of the Aleutian arc, described by Geist and others (1988), are bound by oblique normal faults with large displacements.

We must also consider the possibility that the accretionary complex of the Muertos Trough is not a typical one formed by plate convergence, but instead, simply the toe of the extensional allochthon (the continuation of the accretionary complex to the east would be due to the coalition of various extensional allochthons). No Benioff zone has been recognized beneath the Muertos Trough, and few earthquakes have been associated with the subduction (Ascencio, 1980; Byrne and others, 1984). This interpretation is not favored at present, because the accretionary complex seems to be too large to be associated with the extension observed in the Mona Passage, even if extension from the 19°lat Fault is included. The upper limits of accretion extend some 40 kms inboard from the base of the accretionary complex, and it is unlikely that all accretion is related to the proposed extensional allochthon. Rather, we think it likely that the Muertos trough accretionary complex is accentuated by deformation at the toe of the proposed Mona allochthon.

REFERENCES

Ascencio, E., 1980, Seismicity of western Puerto Rico: U.S. Geological Survey Open File Report, 80-192, p. 1-135.

Birch, F.S., 1986, Isostatic, thermal and flexural models of the subsidence of the north coast of Puerto Rico: Geolog, v. 14, p. 427-429.

Byrne, D.B., Suarez, G., and McCann, W.R., 1985, Muertos Trough subduction-microplate tectonics in the northern Caribbean: Nature, v. 317, p. 420-421.

Fox, P.J., and Heezen, B.C., 1975, Geology of the Caribbean crust, *in* Nairn, A.E.M., and Stehli, F.G.., eds., The ocean basins and margins, v. 3. The Caribbean and the Gulf of Mexico: New York, Plenum Press, p. 421-466.

Gardner, W.O., Glover, L. K., and Hollister, C.D., 1980, Canyons off northwest Puerto Rico: studies of their orgin and maintenance with the nuclear research submarine NR-1. Marine Geology, v. 37, p. 41-70.

Geist, E. Childs, J., and Scholl, D., 1988, The origin of summit basins of the Aleutian Ridge: implications for block rotation of an arc massif: Tectonics, v. 7, p. 327-342.

Heezen, B.C., Nesteroff, W.D., Rawson, M., and Freeman-Lynde, R.P., 1985, Visual evidence for subduction in the western Puerto Rico trench, *in* Mascle, A., ed., Caribbean Geodynamics Symposium, Paris March 5-8, 1985: Paris, France, Editions, Technip, p. 287-304.

Ladd, J.W., Shih, T., and Tsai, C.J., 1981, Cenozoic tectonics of central Hispaniola and adjacent Caribbean Sea: American Association of Petroleum Geologists Bulletin, v. 65, p.466-489.

Ladd, J.W., Worzel, J.L., and Watkins, J.S., 1977, multifold seismic reflection records from the northern Venezuela basin and the north slope of Muertos Trench: *in* Island Arcs, Deep-Sea trenches and Back-arc basins (eds., M. Talwani and W.C. Pitman)., American Geophysical Union, Wasington, D.C., p. 41-56.

Ladd, J.W., and Watkins, J.S., 1978, Active margin structures within the north slope of the Muertos Trench: Geologie and Mijnbouw, v. 57, p.

Line ID 103D

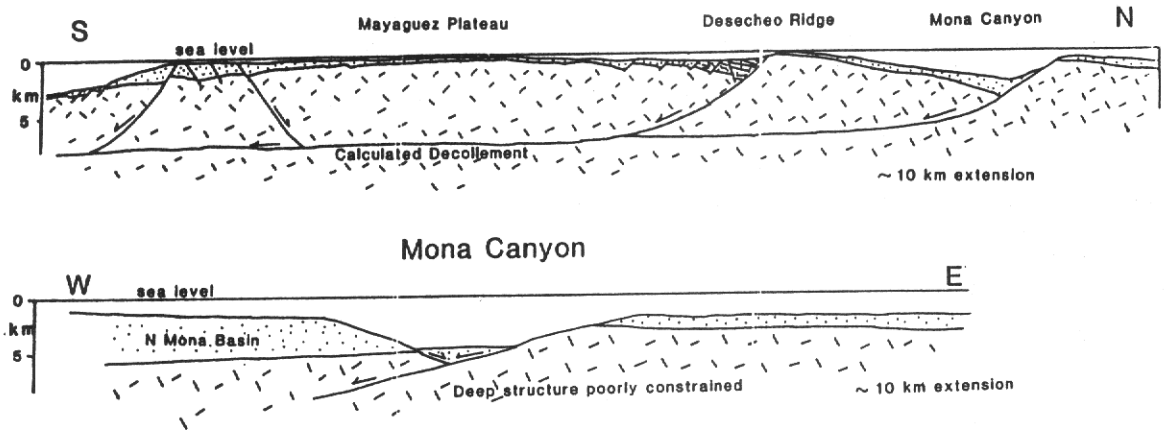

4A,B Interpreted line drawings for Line 406D and 103D of Figure 3.

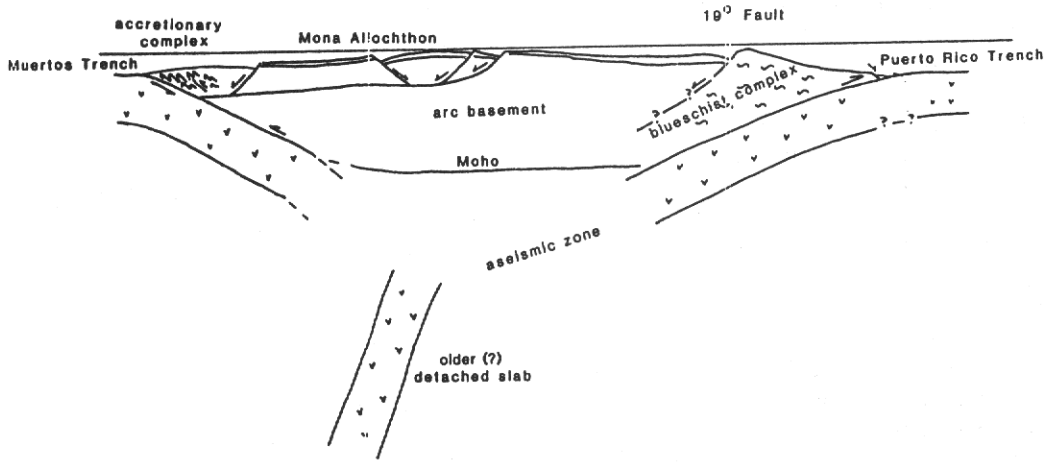

5. Cross-section through the Mona Passage. Positions of down-going slabs from seismic data (McCann and Sykes, 1984; Byrne and others, 1985). Base of Moho from gravity and refraction data (Talwani and others, 1959). Line of section is generalized to include several features.

255-260.
Larue, D.K., Joyce, J., and Ryan, H.F., 1990, Neotectonics of the Puerto Rico Trench: extensional tectonism and forearc subsidence: *in* Larue, D. K., and Draper, G., eds., 12th Transactions of the Caribbean Conference, in press.
Le Pichon, X., Iiyama, J., Bourgois, Mercier de Lepinay, B., Tournon, J., Muller, C., Butterlin, J., and Glacon, G., 1985, First results of the test dives of the French submersible Nautile in the Puerto Rico trench (Greater Antilles): Academie de Sciencees Paris transactions, 301, Serie II, number 10, p. 743-749.
Mann, P., and Burke, K., 1984, Neotectonics of the Caribbean, Reviews of Geophysics and Space physics, v. 22, p. 309-362.
Mann, P., Burke, K., and Matumoto, T., 1984, Neotectonics of Hispaniola: plate motion, sedimentation and seismicity at a restraining bend: Earth Planetary Science Letters, v. 70, p. 311- 324.
McCann, W. R., and Sykes, L. R., 1984, Subduction of aseismic ridges beneath the Caribbean plate: implications for the tecotnics and seismic potential of the norther eastern Caribbean: Journal of Geophysical Research, v. 89, p. 4493-4519.
Moussa, M.t., Seiglie, G.A., Meyerhoff, A.A., Taner, I., 1987, The Quebradillas Limestone (Miocene-Pliocene), northern Puerto Rico, and tectonics of the northeastern Caribbean margin: Geological Society of America Bulletin, v. 99, p. 427-439.
Perfit,, M.R., Heezen, B.C., Rawson, M., and Donnelly, T.W., 1980, Chemistry, origin, and tectonic significance of metamorphic rocks from the Puerto Rico Trench: Marine Geology, v. 34, p. 125- 156.
Schneidermann, N., Beckmann, J.C., and Heezen, B.C., 1972, Shallow water carbonates from the Puerto Rico Trench region, *in* Petzall, C., ed., Caribbean Geological Conference, 6th, Isla de Margarita, Venezuela, 1971, Transactions: Caracas, Venezuela, Chromotip, p. 423-425.
Talwani, M., Sutton, G.H., and Worzel, J.L., 1959, a crustal section across the Puerto Rico Trench: Journal of Geophsyical Research, v. 64, p. 1545-1555.
Weaver, J., Smith, A., and Seiglie, G., 1975, Geology and tectonics of the Mona Passage: Transactions of the American Geophysical Union, v. 56, p. 451.

NEOTECTONICS OF THE PUERTO RICO TRENCH: EXTENSIONAL TECTONISM AND FOREARC SUBSIDENCE

D. K. Larue
Geology Dept
University of Puerto Rico
Mayaguez, PR 00708

J. Joyce
Geology Dept
University of Puerto Rico
Mayaguez, PR 00708

H.F. Ryan
U.S.G.S.
Menlo Park, CA 94025

ABSTRACT

Study of multichannel seismic-reflection profiles indicate underthrusting in the Puerto Rico Trench diminishes from east to west. GLORIA sidescan studies suggest that strike-slip tectonism is more predominant toward the west. Faults present along the north and south walls of the trench slope are extensional. The south-dipping 19° latitude Fault on the trench slope break probably has a history of both normal and strike-slip motion. This fault juxtaposes a metamorphic terrane found beneath the lower trench slope and the arc massif complex. The arc massif near the 19° lat Fault has differentially subsided about 4 km since the Late Miocene, with the hinge line near the present shoreline of Puerto Rico. This subsidence may have occurred during: 1) a tectonic erosion event beneath the trench slope; 2) 'folding' accompanying compression of the arc massif platform; 3) rollover associated with normal movement on the 19° lat Fault.

Overall, the Puerto Rico Trench represents a transtensional environment. The history of the trench has been complicated by subduction of buoyant oceanic crust ca. 40 mybp, accompanied by plate margin truncation, and deformation, rotation and uplift of the arc massif on the order of 2-4 km. About 9 mybp, the arc massif of Puerto Rico rotated an addional 20° counterclockwise, such that many of the features observed today are relict from that event.

INTRODUCTION

The Puerto Rico Trench is located in a corner zone, where the orientation of the Caribbean-North America plate boundary abruptly changes from east-west to north south (Fig. 1). Study of multichannel seismic-reflection profiles of the Puerto Rico Trench and surrounding areas reveals an extremely complicated structural evolution since the Miocene. Three important features we recognize are 1) the lateral and temporal transition from underthrusting to strike-slip deformation; 2) 4 km of subsidence of the arc massif platform near the trench slope break since the Late Miocene; and 3) a plate margin erosion event in the trench, probably of Late Eocene age .

REGIONAL GEOLOGY

In this paper we will present information about the Puerto Rico Trench from the area north of the Virgin Islands, to the Mona Passage (Fig. 1). North of the Puerto Rico Trench is Atlantic oceanic crust, which passes laterally eastward to attentuated continental crust or thick oceanic crust of the Bahama bank (Uchupi and others, 1971; Freeman-Lynde and Ryan, 1988). The Puerto Rico Trench east of the northern Virgin Islands curves toward the south, as shown by both bathymetric and gravity data, into the north-south oriented Lesser Antilles subduction zone (Bowin, 1972). West of the Mona Passage, the Bahama bank is probably colliding with Hispaniola at the Puerto Rico Trench (Dolan and others, 1989). The exact nature of this collision zone, whether mostly thrust, strike-slip, or both, is uncertain. However, a steeply inclined seismic zone exists at least in eastern Hispaniola (Schell and Tarr, 1978; McCann and Sykes, 1984), indicating that subduction is occurring. The Hispaniola basin lies west of the collision zone and is being underthrust beneath Hispaniola (Austin, 1983; Dillon and others, this volume).

Hispaniola is cut by a number of strike-slip faults; two important ones, the Septentrional and South Samana Bay faults, are shown in Figure 1 (Mann and Burke, 1984). As shown in this study, these faults can be traced eastward using bathymetry, dredge sample compositions, and seismic reflection studies, into what is defined here as the 19° lat (latitude) Fault. The 19° lat Fault can be traced further east, where it nearly coincides with the Escarpment Fault. North of the 19° lat fault and east of the Mona Canyon are a series of basins and ridges on the southern wall of the Puerto Rico Trench. Unlike most ridges in subduction zone settings, these ridges and basins locally do not parallel the strike of the trench, and trend northeast (Anomalous Block) and northwest (Main Ridge).

Profound tectonic subsidence (approximately 4 km) occurred between the island of Puerto Rico and the 19° lat Fault in the Neogene. Evidence for this is discussed below, but consists of dredge hauls and submersible observations of in-place shallow-water carbonates of Miocene age along the 19° lat Fault and in the walls of the Mona Canyon. To the south of Puerto Rico, a second subduction zone is observed, the Muertos Trough or Trench (Ladd and Watkins, 1978; Ladd and others, 1977; Ladd and others, 1981; Biju-Duval and others, 1982). The Virgin Island basin, between Puerto Rico and St. Croix, probably formed as a pull-apart (Case, 1975; Jany and others, 1987), or as interpreted here, is mostly extensional.

Tectonic Evolution of the Eastern Greater Antilles

The eastern Greater Antilles consists largely of a suite of rock types thought to have formed in oceanic island arc and trench settings. Arc-related rocks of Cretaceous to Eocene age occur in central Hispaniola, Puerto Rico, and the Virgin Islands (Joyce, 1985). North of the Septentrional fault in Hispaniola (Fig. 1) is a complicated terrane containing both arc-related lithologies and high-pressure, low-temperature metamorphic rocks (Nagle, 1974; Eberle and others, 1980; Joyce, 1980). Such metamorphic rocks are thought to represent products of

Larue, D.K., and Draper, G. (eds.),
Transactions of the 12th Caribbean Geological Conference, St. Croix, U.S.V.I., Miami Geological Society, P.O. Box 431552, South Miami, FL 33243, U.S.A

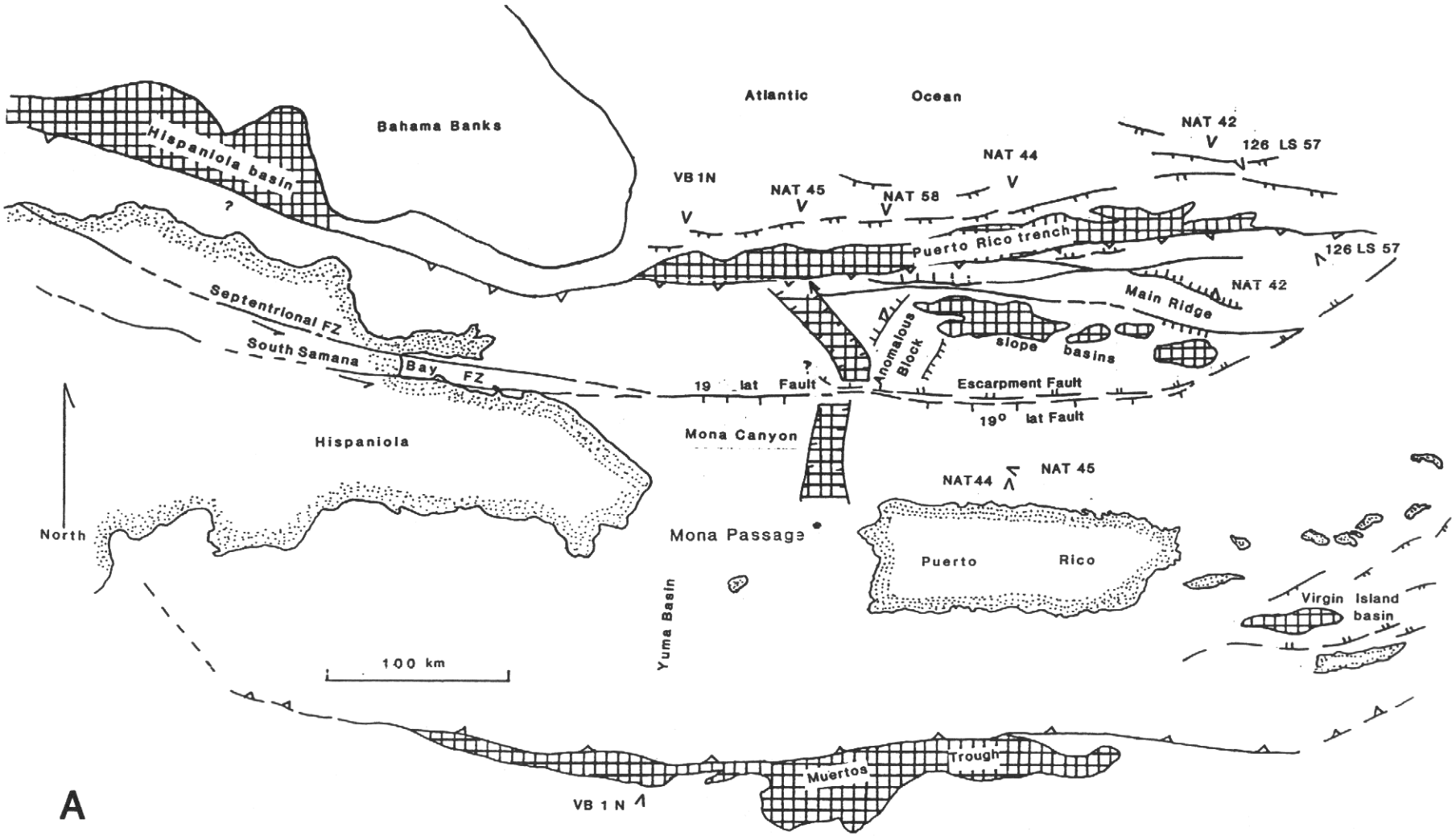

Figure 1. Location map of features of geologic interest in the area around Puerto Rico, with location of seismic lines of Figure 4.

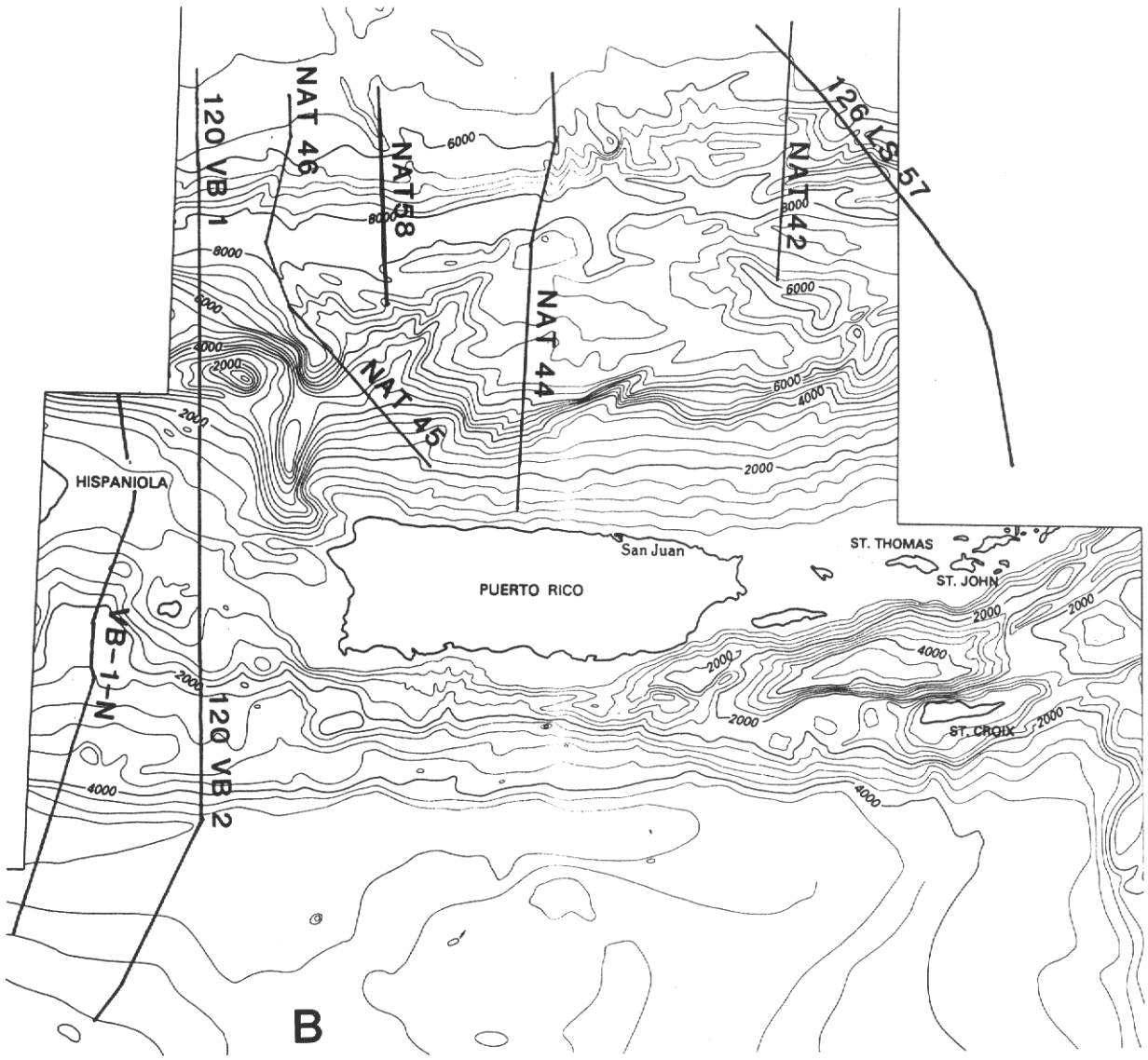

recrystallization in a subduction zone setting. South of the Septentrional fault in central Hispaniola is the Cordillera Central, where Cretaceous arc volcanism was pronounced (Lewis, 1980).

During the Late Eocene, a poorly understood event resulted in the end of arc magmatism and uplift of subduction-zone rocks. Earlier studies proposed that, like Cuba, the eastern Greater Antilles collided with the Bahama bank in the Early Tertiary (Pindell and Dewey, 1982). However, that does not explain the presence of over 250 km of slab subducted below eastern Hispaniola since the middle Tertiary (McCann and Sykes, 1984). That is, if true collision occurred with the Bahama bank, further subduction would be inhibited.

The Oligo-Miocene history of Hispaniola is characterized by subduction and accretion in southern Hispaniola (Biju-Duval and others, 1982) and the formation of carbonate banks and strike-slip basins toward the north (Lewis, 1980). On Puerto Rico, Oligo-Miocene basins were apparently formed through extensional processes (Birch, 1986; Moussa and others, 1987).

PUERTO RICO TRENCH

The Puerto Rico Trench is a flat-lying submarine valley, filled with turbidites (Connolly and Ewing, 1967) surrounded by great topographic relief (Figs. 1, 3). North of the trench, the Atlantic Ocean crust is broken into a number of blocks by normal faulting, as indicated by offsets in seismic stratigraphy (Fig. 4).

The south wall of the trench also exhibits extreme relief, the most profound associated with the Puerto Rico scarp (Ewing and Heezen, 1955; Ewing and others, 1965), which is shown here to be a fault scarp (that is, the 19° lat Fault and Escarpment Fault) associated with the continuation of the Septentrional and Samana Bay fault zones.

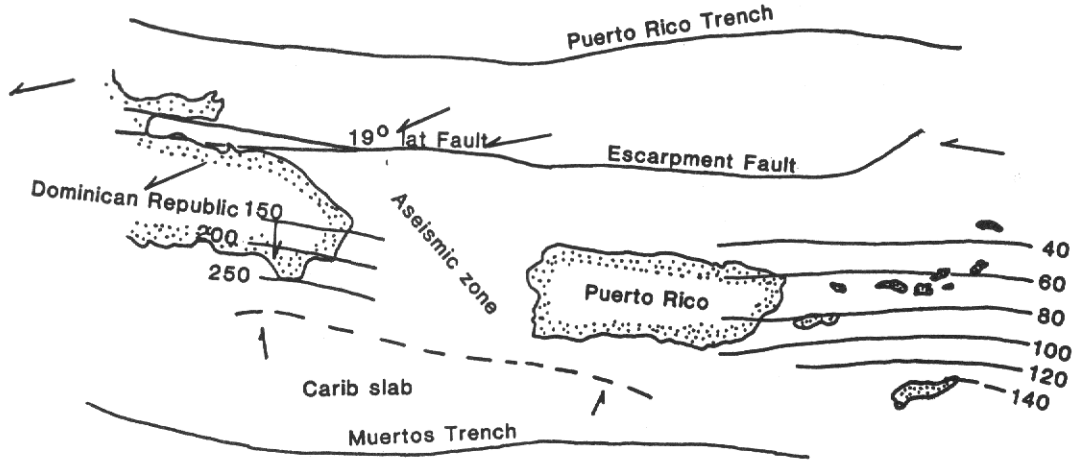

Figure 2. Summary of information concerning inclined seismic zones beneath Puerto Rico and the Virgin Islands. Focal mechanisms give motion of lower plate (arrows). From Molnar and Sykes (1969), Bracey and Vogt (1970), Schell and Tarr (1978), Sykes and others (1982), McCann and Sykes (1984), Byrne and others (1985) and Ascencio (1980). "Carib slab" in the Muertos trough is based on earthquakes located and focal mechanisms done by Ascencio (1980) and Byrne and others (1985) and based on seismic reflection studies by Ladd and Watkins (1978) who noted the presence of inclined reflectors below the Yuma basin (located in Figure 1).

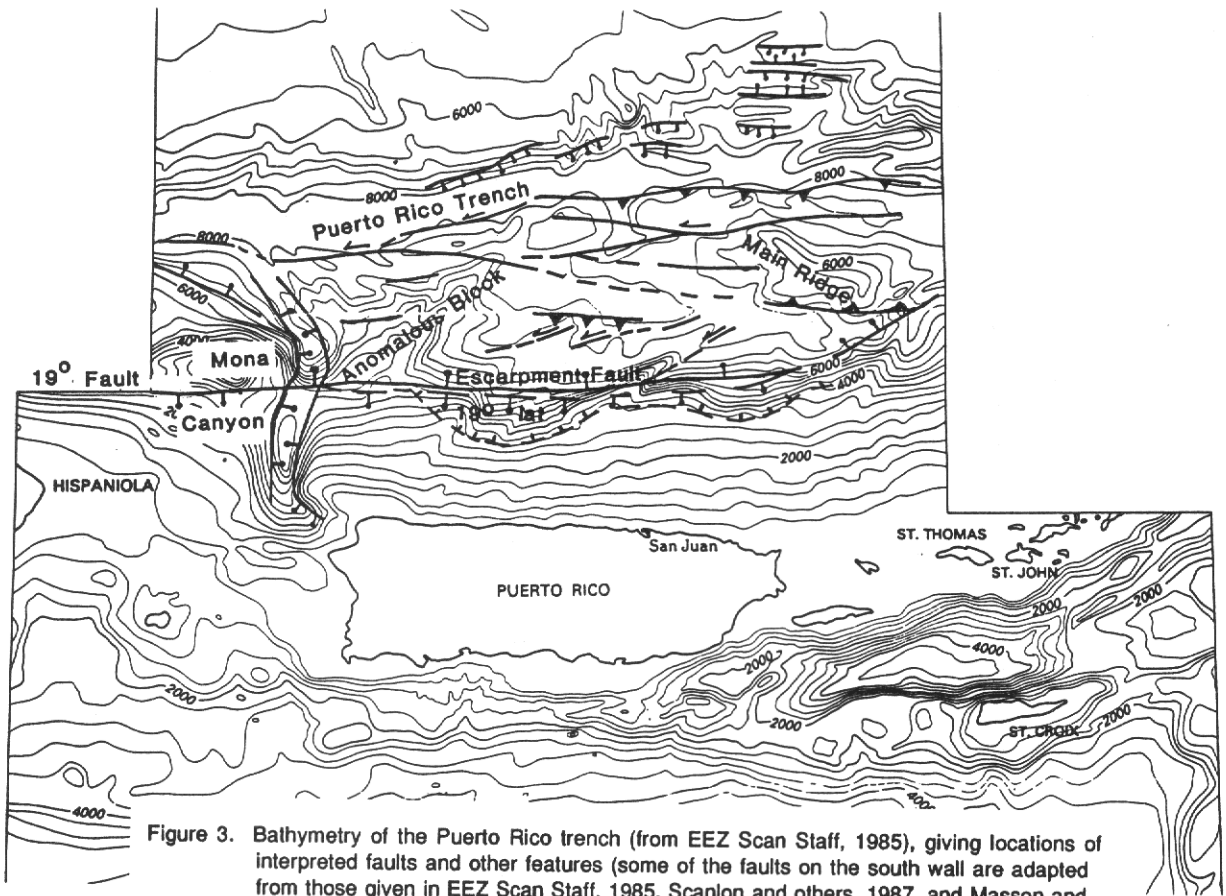

Figure 3. Bathymetry of the Puerto Rico trench (from EEZ Scan Staff, 1985), giving locations of interpreted faults and other features (some of the faults on the south wall are adapted from those given in EEZ Scan Staff, 1985, Scanlon and others, 1987, and Masson and Scanlon, in press; all faults on the north wall of the trench are from EEZ Scan Staff, 1985).

BENIOFF ZONE AND SUBDUCTION DIRECTION

An inclined seismic zone below Puerto Rico has been documented by Sykes and Ewing (1965), Schell and Tarr (1978), Ascencio (1980) and McCann and Sykes (1984). Fault plane solutions show mostly left-lateral strike-slip faulting parallel to the trench on inclined planes (Molnar and Sykes, 1969) (Fig. 2). From central Puerto Rico to eastern Hispaniola, the inclined seismic zone is discontinuous, which indicates that the steeply-dipping slab is detached at it's eastern end(McCann and Sykes, 1984)(Fig. 2). The origin of this slab is debatable: McCann and Sykes (1984) suggested that the detachment occurred during an earlier collision/accretion event with the Bahama banks. Bracey and Vogt (1970), suggested it was a small subduction zone, which Schell and Tarr (1978) and Mann and others (1984) related to a strike-slip restraining bend in Hispaniola.

The rate of underthrusting can be estimated from the direction and rate of relative plate motion, presuming that the motion is all taken up along the Puerto Rico Trench. Estimates of Caribbean plate motion relative to North American plate motion range from N 65° E (Sykes and others, 1982) to ESE (Jordan, 1975; Stein and others, 1988). To generalize these two different vectors, the plate motion is about east-west with an uncertainty of about 25°. Estimates of rates of relative plate motion range from approximately 1.5 to 4 cm/yr (McCann and Sykes, 1984; Jordan, 1975; Stein and others, 1988). From this, one can conclude that present day rates of underthrusting on the Puerto Rico Trench are well under 1 cm/yr.

DREDGE HAULS, SUBMERISBLE OBSERVATIONS AND PISTON CORING IN THE PUERTO RICO TRENCH AREA

On the north wall of the Puerto Rico Trench, Bowin and others (1966), Chase and Hersey (1968), Nalwalk (1969) and Perfit and others (1980) described dredged rocks attributed to an origin at a mid-ocean ridge spreading center, later covered by pelagic sediments. Dredge samples containing oceanic crustal rocks such as serpentinites and serpentinized peridotites support the presence of normal faults imaged seismically, that have up to several kilometers of throw.

Perfit and others (1980; see also Fox and Heezen, 1974; Weaver and others, 1975; Heezen and others, 1985; Le Pichon and others, 1985) noted two principal basement rock lithologies on the south wall of the trench: arc-related rocks and metamorphic rocks similar to blueschist grade metamorphic rocks identified on the north coast of Hispaniola (see Perfit and others, 1980; Joyce, 1985; Joyce and Aronson, 1987) . The boundary between these two basement rock lithotypes north of Puerto Rico is the 19° lat and Escarpment Faults (Fig. 1,2,3). On Hispaniola, the Septentrional and South Samana Bay Faults separate a dominately metamorphic complex to the north from an arc terrane to the south. Both basement rock types are overlain by Tertiary limestones.

Intact Miocene shallow-water limestone sequences at water depths of greater than 4 km, are present on the south wall of the Puerto Rico Trench (Moussa and others, 1987). The Puerto Rico slope extends from the island of Puerto Rico to the 19° lat and Escarpment Faults. Apparently, in the Miocene, the Puerto Rico shelf extended 50 km further to the north, and subsided since that time (Meyerhoff and others, 1983; Birch, 1986; Moussa and others, 1987). Birch (1986) and Moussa and others (1987) argued that the subsidence was Pliocene or younger. However, based on review of dredge haul and piston core data the conclusion is reached that subsidence probably began in the Late Miocene. For example, piston core number V3-2 is a foraminiferal lutite of Late Miocene age (Ewing and Heezen, 1955), and dredge samples 5, 11 and 23 (Perfit and others, 1980), both indicate open marine deposition in the Late Miocene. Interesting, at 9 ma, a change in North American plate motion occurred toward more southerly motion (Pollitz, 1988), which may have caused flexure in the Puerto Rico arc massif platform, with resulting subsidence.

Heezen and others (1985) described an intact coral reef in the Mona Passage near the 19° lat Fault at a depth of 3652 m of post-Pliocene age based on paleontologic data, and older than 700,000 yrs based on U/Th studies. The rapid subsidence indicated by this submerged reef is perhaps related to the 19° lat Fault or perhaps Mona Canyon subsidence, and not directly to the regional subsidence of the Puerto Rico slope.

GLORIA STUDIES

Studies of the Exclusive Economic Zones off Puerto Rico by the U.S. Geological Survey using GLORIA reveal pronounced continuous lineations in the Puerto Rico Trench, possibly related to strike-slip faulting (EEZ Scan Staff, 1985; Scanlon and others, 1987, Masson and Scanlon, in press). Unfortunately, the 19° lat and Escarpment Faults, were not observed by the GLORIA scans because the ship tracks converge and parallel 19° (thus 19° is a zone of no data collection). Given that the Puerto Rico Trench is undergoing left-lateral shearing accompanying E-W motion of the Caribbean plate relative to the North American plate, the lineations are presumed to be left-lateral shear zones (Fig. 3). The orientation of the Escarpment Fault near the Main Ridge indicates it may be a releasing bend along the primary strike-slip fault zone. The fault at the base of the Main Ridge is probably a reverse or thrust fault based on its orientation and on the pronounced topography on the south side of the lineation. Using the above assumptions, the slope basins (Figs. 1,3) to the west of the Main Ridge therefore represent pull-apart or fault-wedge basins, relative to the releasing bend and the complex system of faults on the landward wall of the trench (nomenclature after Mann and Burke, 1984).

Folding is not prevalent in the GLORIA data from the Puerto Rico Trench, although folds and a well-developed deformation front is observed in the Muertos Trough to the south on the same data set. The lack of folds in the Puerto Rico Trench is puzzling, but may reflect the occurrence of indurated rock in the trench slope, and absence of accreted sediment. One fold associated with a probable reverse fault (Fig. 4F) was imaged in multichannel seismic profile at the base of the Puerto Rico scarp, and that fault is shown in Figure 3.

SINGLE AND MULTICHANNEL SEISMIC LINES CROSSING THE TRENCH

A number of studies have used single channel data to study the Puerto Rico Trench (most recently, McCann and Sykes, 1984; and EEZ staff, 1987). The present study relies on multichannel data (see Fig. 1) owned by the Texas Institute of Geophysics, and reprinted with their permission here.

Figure 4A-J show unmigrated seismic lines and interpretations. The 19° lat and Escarpment Faults are imaged as transitions from parallel-layered reflectors over acoustic basement to acoustic basement exposed at the seafloor (Figs. 4 E,F,G,H,K,L). The south-dipping 19° lat Fault is separated from the north-dipping Escarpment Fault by an inferred horst block.

The Mona Canyon graben (Fig. 1) is over 100 km long, and several kilometers deep. The graben is segmented by the 19° lat fault, yet is not appreciably offset laterally, indicating no lateral movement on the fault since the graben formed.

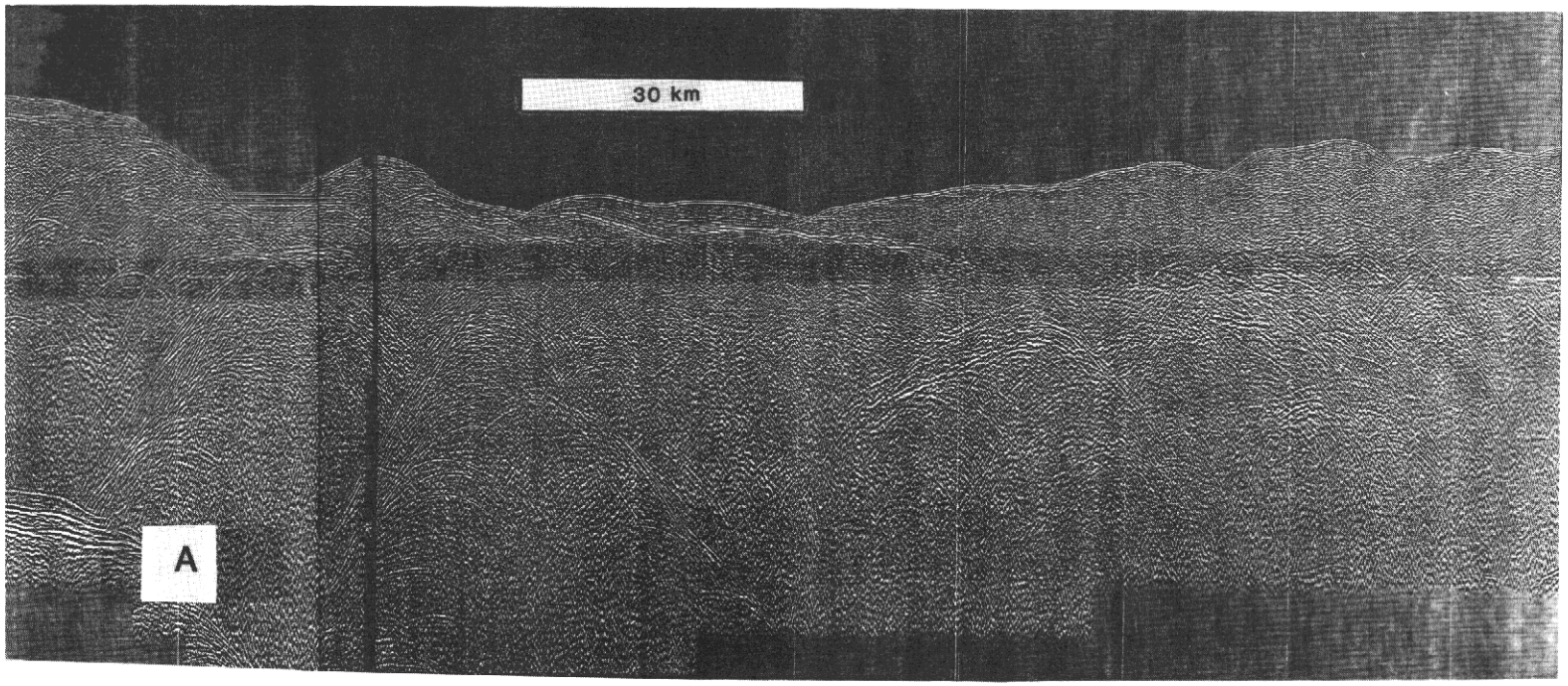
30 km
A

126 LS 57

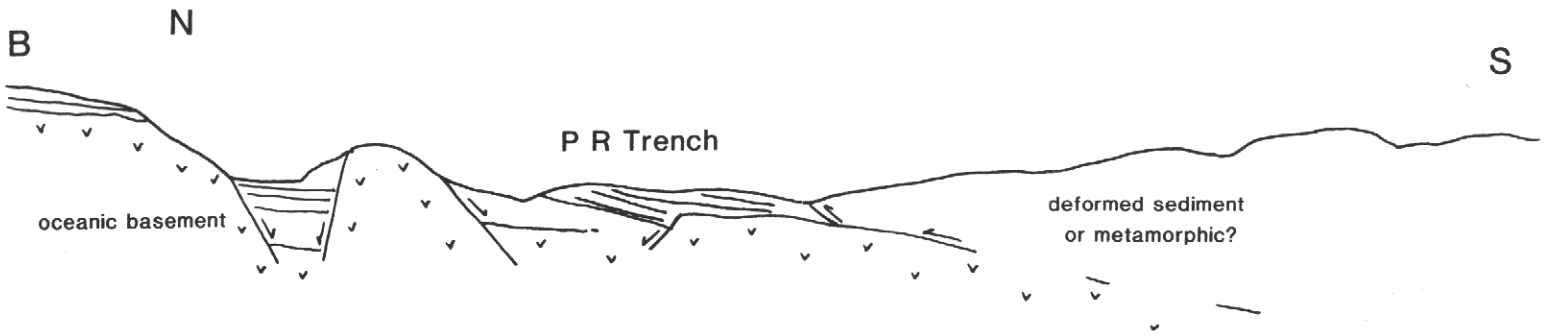
B
N
S
P R Trench
oceanic basement
deformed sediment
or metamorphic?

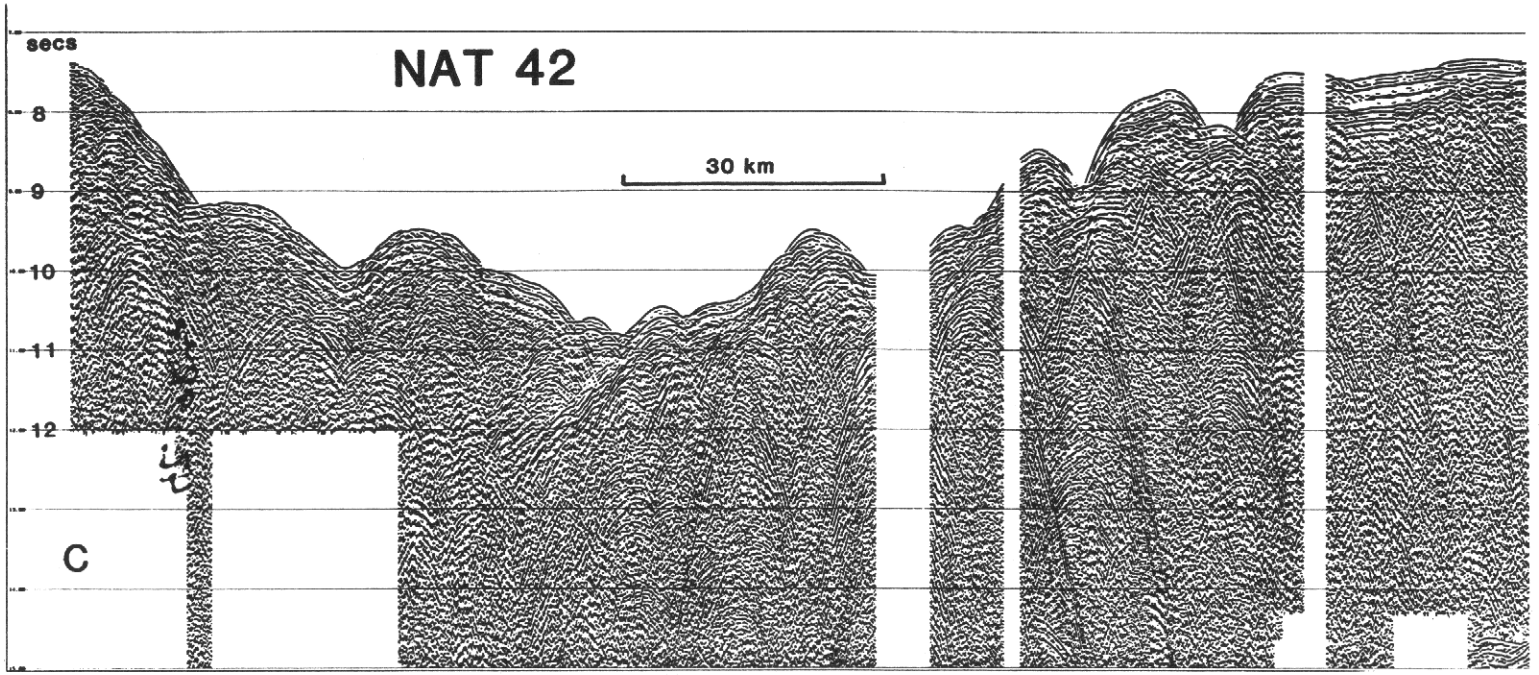
secs
NAT 42
8
9
10
11
12
30 km
C

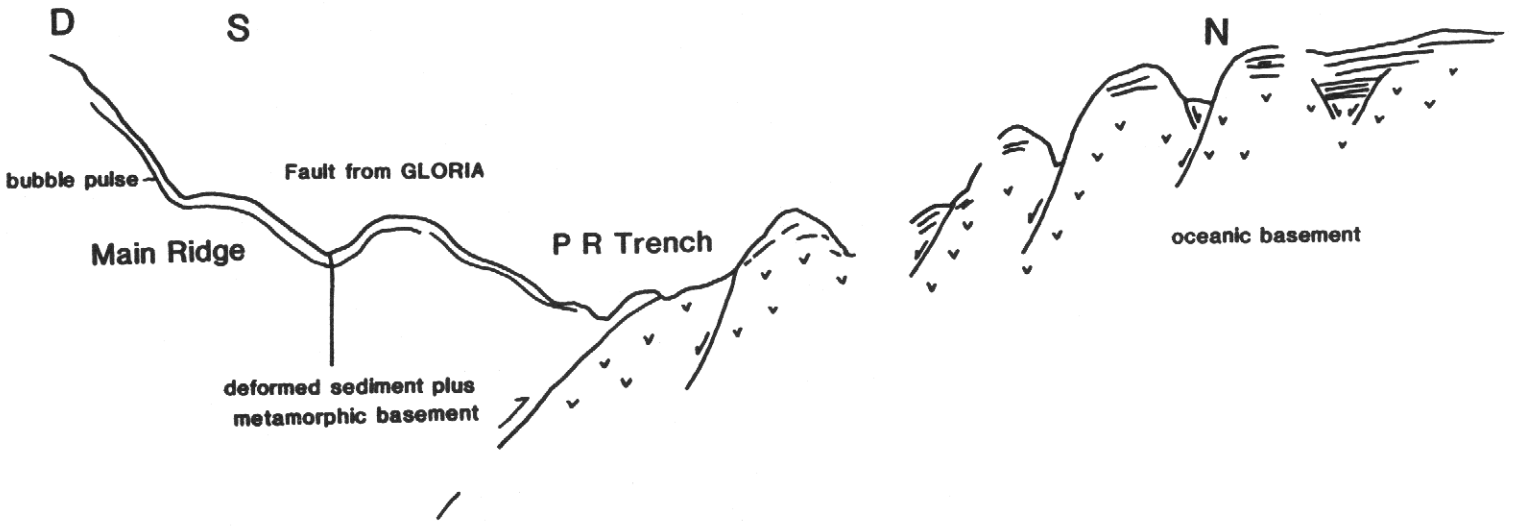
D
S
N
bubble pulse
Fault from GLORIA
Main Ridge
P R Trench
oceanic basement
deformed sediment plus
metamorphic basement

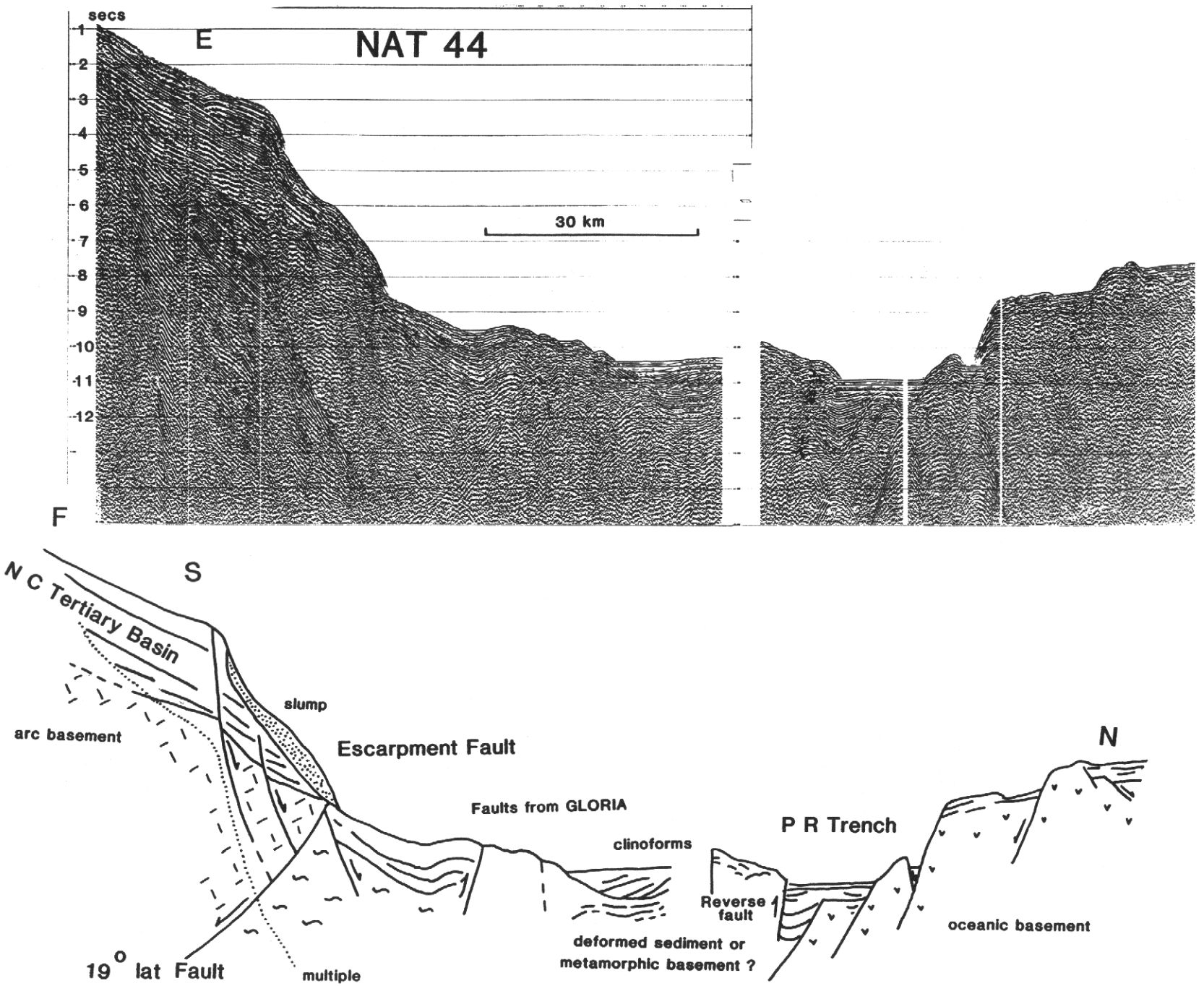
secs
1
2
3
4
5
6
7
8
9
10
11
12
E
NAT 44
30 km
F
S
N C Tertiary Basin
slump
arc basement
Escarpment Fault
Faults from GLORIA
clinoforms
P R Trench
N
Reverse fault
oceanic basement
deformed sediment or
metamorphic basement ?
19° lat Fault
multiple

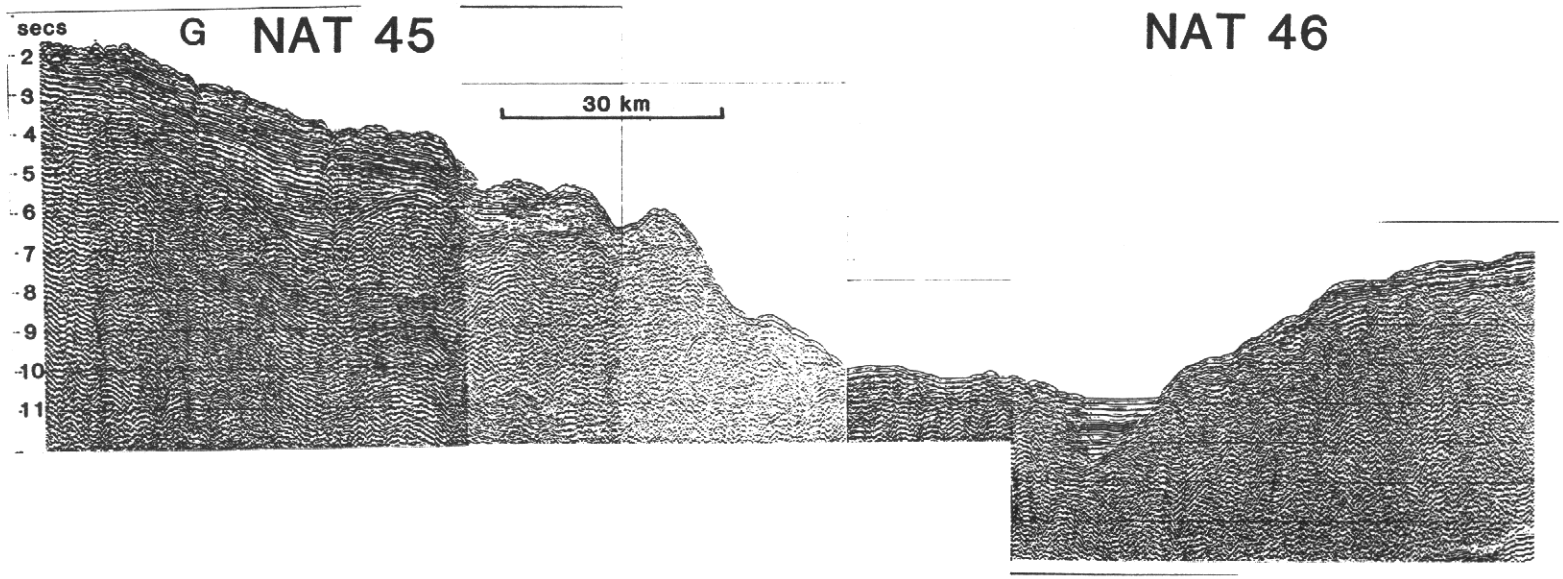
secs
2
3
4
5
6
7
8
9
10
11
G
NAT 45
NAT 46
30 km

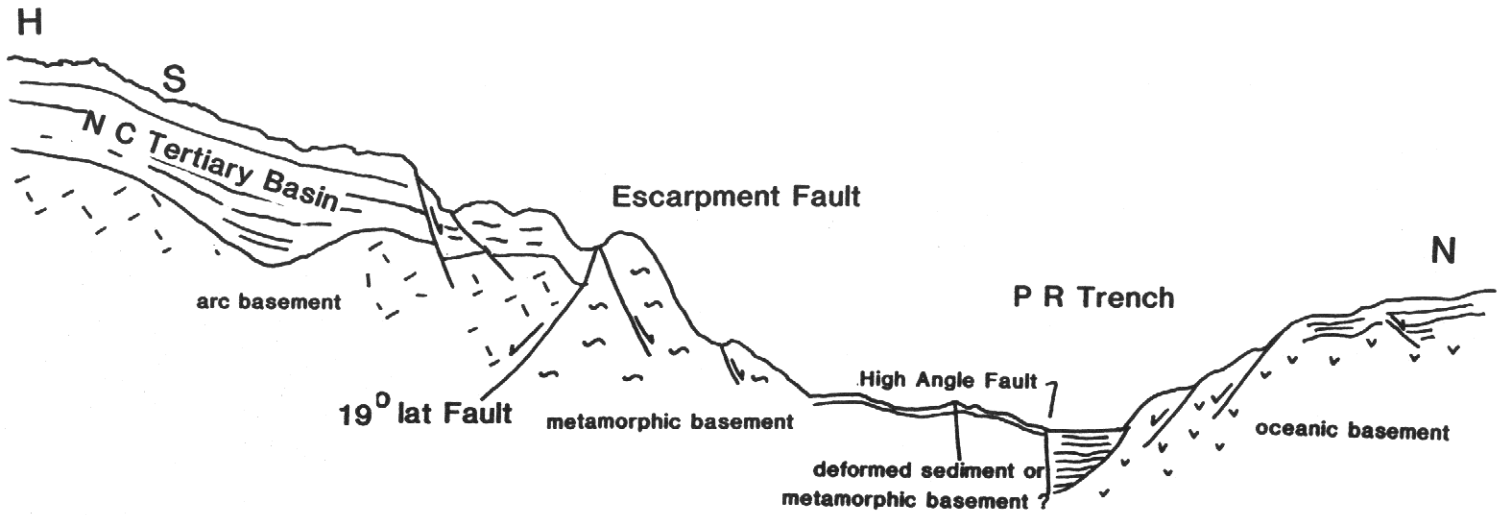
H
S
N C Tertiary Basin
Escarpment Fault
N
P R Trench
arc basement
High Angle Fault
19° lat Fault
metamorphic basement
oceanic basement
deformed sediment or
metamorphic basement ?

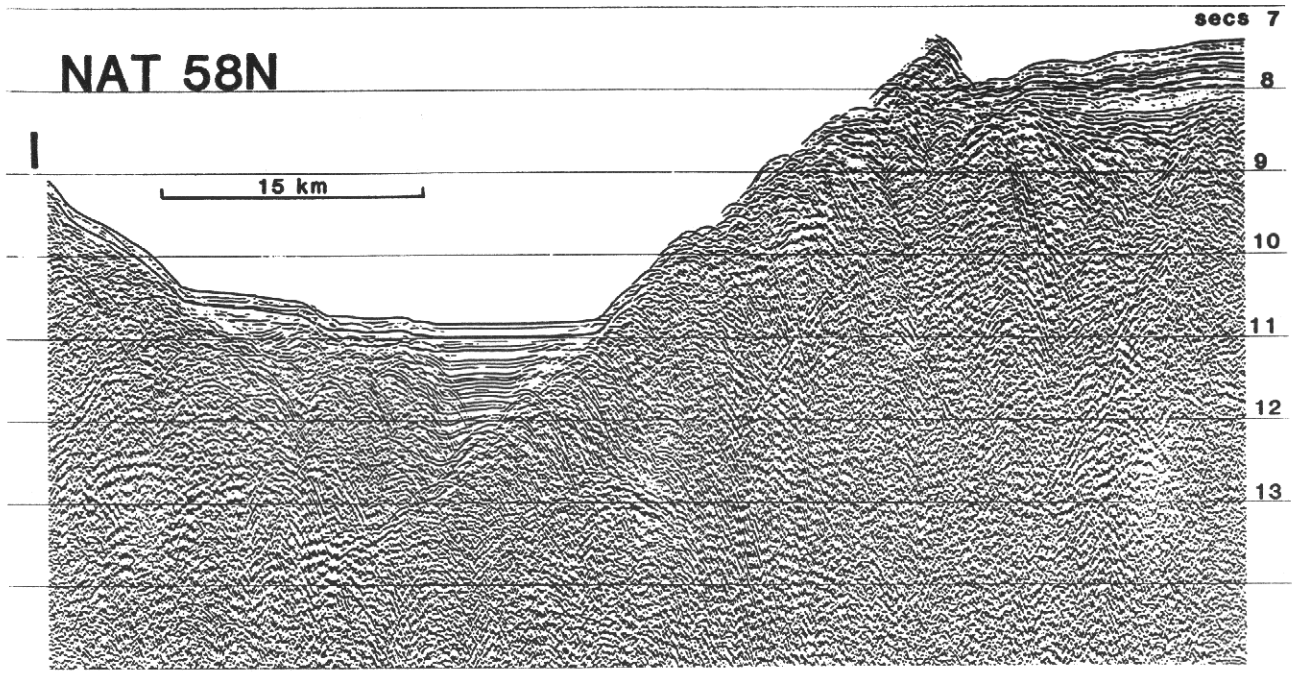
NAT 58N
I
15 km
secs 7
8
9
10
11
12
13

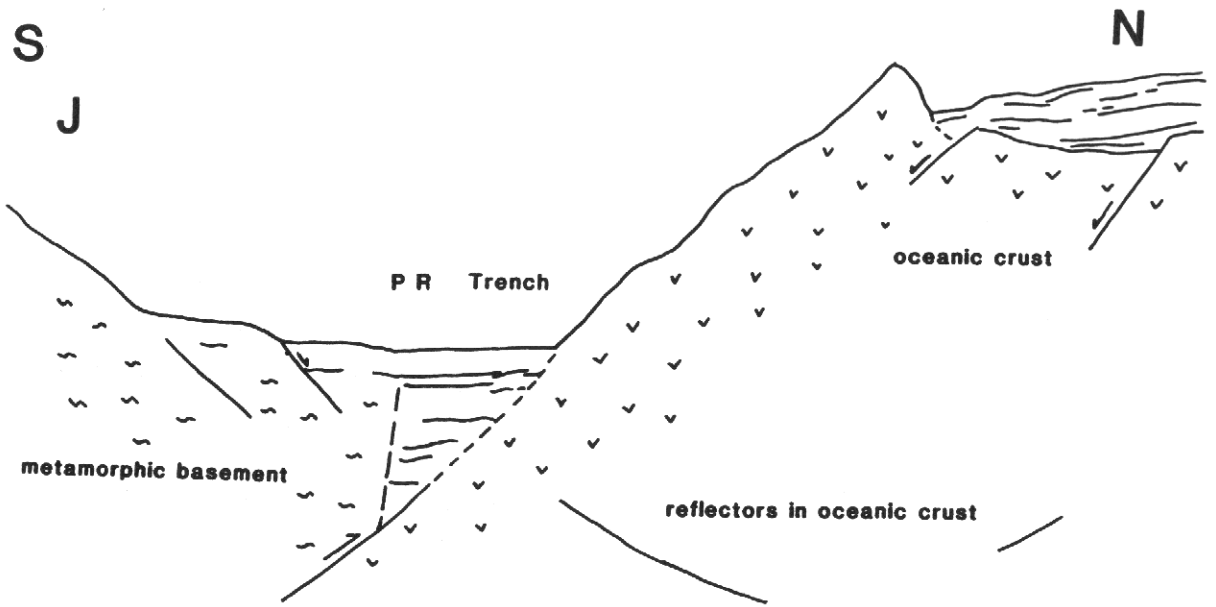
S
J
N
P R Trench
oceanic crust
metamorphic basement
reflectors in oceanic crust

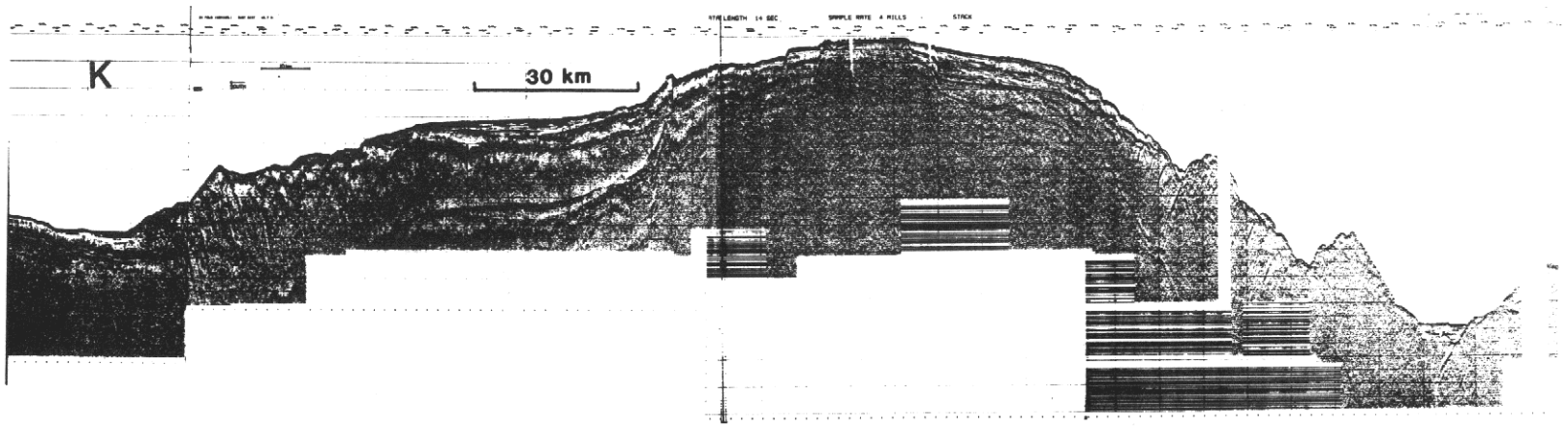

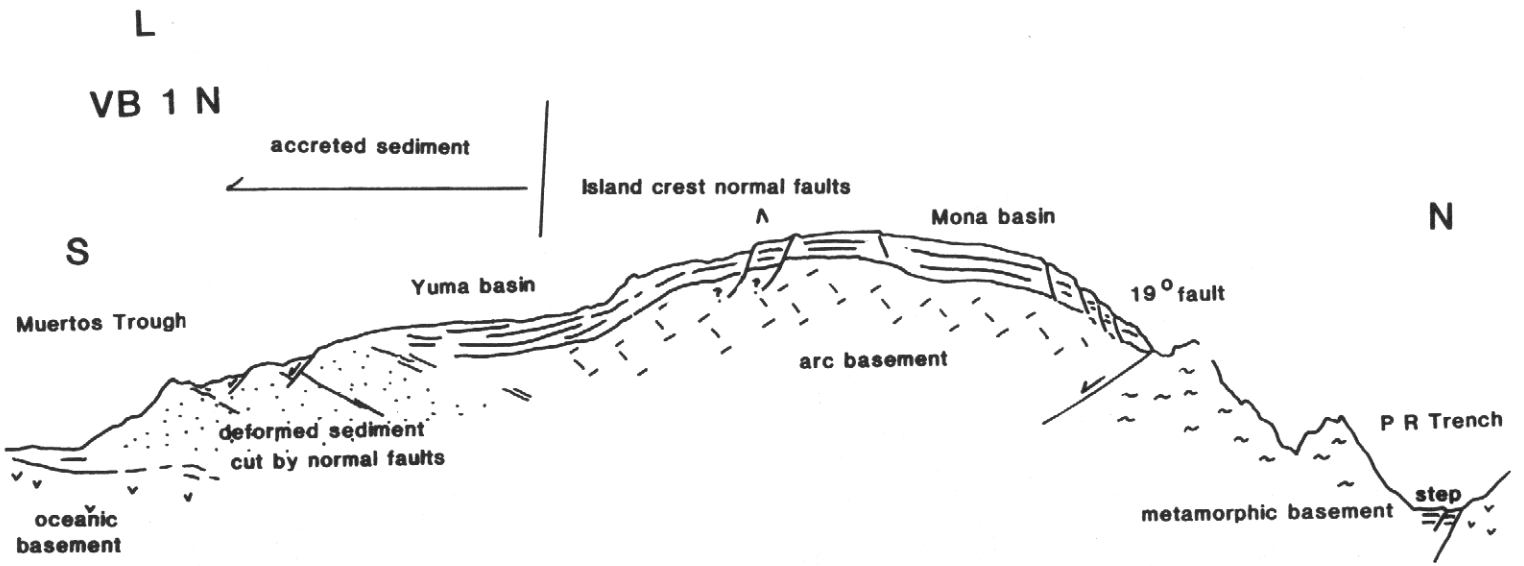

Figure 4. Seismic reflection profiles, located in Figure 1. Property of the Texas Institute of Geophysics and reprinted here with permission. See text for discussion. Figures A,C,E,G,I,K show data and B,D,F,H,J,L show interpretations. Important note: some of the interpreted faults are based on crossing of presumed faults shown in Figure 3, but can not be observed on the seismic lines. Dip of frontal fault in Puerto Rico Trench in F and H are from other lines (not shown here) with less vertical exaggeration. Dip of 19° Iat Fault is from migration of K (Larue and Ryan, work in progress).

Migration of seismic profile VB-1-N (line interpretation shown in Fig. 4 K,L) suggests that the 19° lat Fault is a south-dipping normal fault (Larue and Ryan, work in progress). The antiformal strata above this south-dipping fault (Fig. 4L) is proposed to result from rollover accompanying motion on a listric fault (see also, Speed, 1989). However, the floor of the Mona Canyon is characterized by a downward step to the north at 19° lat based on bathymetric data. Because the anticlinal rollover can be traced by bathymetry and seismic reflection profiles along 19° latitude to longitudes slightly east of Puerto Rico, it seems that the 19° lat Fault has to exist in this area as a south-dipping listric normal fault. The topographic steps toward the north (floor of Mona Canyon and steep south trench slope) are thus associated with the inferred Escarpment Fault, which is thought to be separated from the 19° lat Fault by a narrow horst block (Fig. 4 E,F,G,H). The western edge of the Escarpment Fault crosses the Mona Canyon (as shown by a downward step to the north down the axis of the canyon), and perhaps loses displacement further west, as it is not imaged well by bathymetry. The eastern part of the 19° lat Fault is defined by the disappearance of the rollover structure described herein. Possibly the rollover is progressively truncated by the Escarpment Fault, or the 19° lat Fault loses displacement toward the east.

The layered reflectors south of 19° (for example, Fig. 4 E,F,G,H) can be traced via other seismic lines (unpublished data, University of Puerto Rico in Mayaguez) to the island of Puerto Rico, and correlated with formations in outcrop and in borehole (for example, Moussa and others, 1987).

The multichannel lines show that the Puerto Rico Trench contains about 1 or 2 seconds of trench facies strata (Ewing and others, 1965). Well-developed thrust faults are only imaged on the easternmost lines (Fig. 4A,B,C,D,E,F), and length of the imaged thrust zone diminishes toward the west. West of Puerto Rico in the trench, there is little evidence for significant amounts of underthrusting (Fig. 4 G,H,I,J,K,L). Linear features interpreted as faults on the GLORIA scans are not obvious on most of the multichannel seismic lines; these faults are shown in the interpreted seismic profiles to document their relative positions. If the linear features from the GLORIA studies are indeed mostly strike-slip faults, it is well-known that strike-slip faults are not easily imaged using seismic reflection techniques (for example, Sylvester, 1988).

The slope basins of Figure 1 are not clearly imaged in Figure 4E,F,G,H (see also, Figure 4 of Murphy and McCann, 1979). Thus it cannot be proven based on seismic data that the slope basins are indeed strike-slip related, related to pull-aparts and fault divergence, and not solely related to accretion as was previously suggested (McCann and Sykes, 1984). A strike-slip origin to the slope basins is therefore based on bathymetric patterns, GLORIA scan studies, and inferences based on directions of plate motion.

Line 45 (Fig. 4C,D) shows the North Coast Tertiary basin, north of Puerto Rico. Birch (1986) argued that the basin contains two sequences: an older extension-related sequence (Late Eocene through Oligocene) followed by a sequence deposited during cooling of the magmatic arc (Oligocene-Miocene). Recently it has been shown through drilling on the north coast of Puerto Rico that lower series of reflectors in the basin is of Lower to Middle Eocene age (Larue, 1990). The north side of the basin is truncated by the 19° lat Fault, however, clear northward stratigraphic thinning and onlap onto basement south of the fault is indicated.

Line VB-1-N (Fig. 4K,L) shows a complete seismic reflection record from the Muertos Trough to the Puerto Rico Trench. The southern part of this line was described by Ladd and Watkins (1978) who noted the presence of inclined reflectors in sedimentary rock beneath the Yuma basin. Here, it is concluded that from these inclined reflectors beneath the Yuma basin to the Muertos Trough, all rocks are accreted (Fig. 2), and thus the northern limit of the subducting Caribbean plate is given. From the Yuma basin to the 19° lat Fault, the arc massif has a bowed appearance, with an anticlinal drape of sedimentary rocks over arc basement. Based on studies on land on Puerto Rico, on dredge hauls in the Mona Canyon and along the Puerto Rico scarp and limited information on the south slope of Puerto Rico, it is concluded that a platform of shallow water carbonates was flexed into this anticlinal orientation (that is, these are not depositional slopes). Age of this flexure, based on the above, is assumed to be approximately Late Miocene.

DISCUSSION

Evidence for Plate Margin Truncation

The Puerto Rico Trench underwent one or perhaps two plate margin truncation events. The metamorphic rocks exposed beneath the south trench wall formed at pressures of 3 to 7 kb (burial of 12-25 km) and temperatures of 400 to 550° C (Perfit and others, 1980). If such conditions apply to a subduction zone setting, as suggested by Perfit and others (1980), the original trench was probably located 50 to 100 km north of its position prior to uplift of the metamorphic rocks. That is, metamorphism occurred 50-100 km down slab, in the hanging wall of the original trench. Uplift probably occurred in the Early Tertiary, possibly the Eocene or Oligocene, as indicated by a few K-Ar dates, shut off of volcanism, and regional geologic relations (Joyce, 1985). Figure 5A shows one such means in which plate margin truncation can occur during and accompanying subduction of oceanic topography (von Huene, 1986; Lallemand and Le Pichon, 1987). According to these workers, margin truncation follows subduction of the tail of the the anomalous topography.

A second period of margin truncation may have occurred in the Miocene to Pliocene, and is indicated by shallow water facies strata deposited at least as far north as 19°, only 70 km from the present trench.

Faulting in the Puerto Rico Trench region

The north and south walls of the Puerto Rico Trench are characterized by normal faults with cumulative vertical diplacements of several kilometers. Relative plate motions indicate that left-lateral strike-slip faulting is important as well. Although dominantly normal faults bound the walls of the Puerto Rico Trench, the trench floor appears to be dominated by thrust-faults in the east that progressively change to strike-slip faults in the west. Although the Puerto Rico Trench is not characterized by active underthrusting (as revealed by seismic reflection profiles), an inclined seismic zone exists below Puerto Rico. In summary, the Puerto Rico Trench is essentially an inclined strike-slip fault in transtension (supporting the plate motion vectors of Jordan, 1975).

The Main Ridge is probably a fragment of the metamorphic complex that has been uplifted along a reverse or thrust fault. The slope basins to the south and west of the Main Ridge are probably related to the releasing bend of the 19° lat and Escarpment Faults, and thus are pull-apart (or fault wedge) basins (nomenclature of Mann and Burke, 1984).

The Mona Canyon is not visibly offset by the 19° lat Fault using bathymetric data (and if it is offset, it's offset is right-lateral). There is a topographic step of approximately 2 km in the Mona Canyon as it crosses the 19° lat fault, thus some

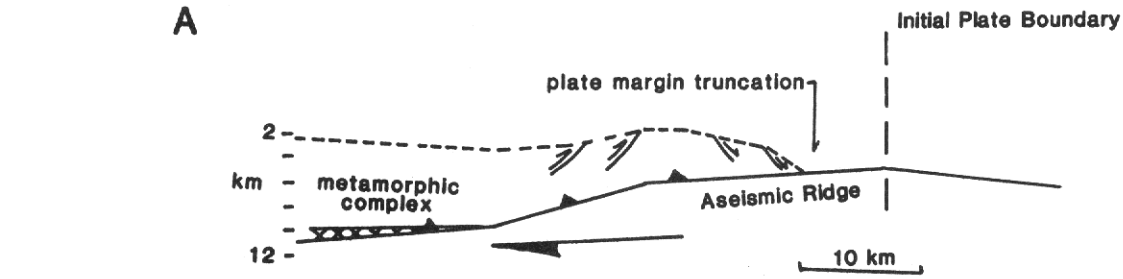

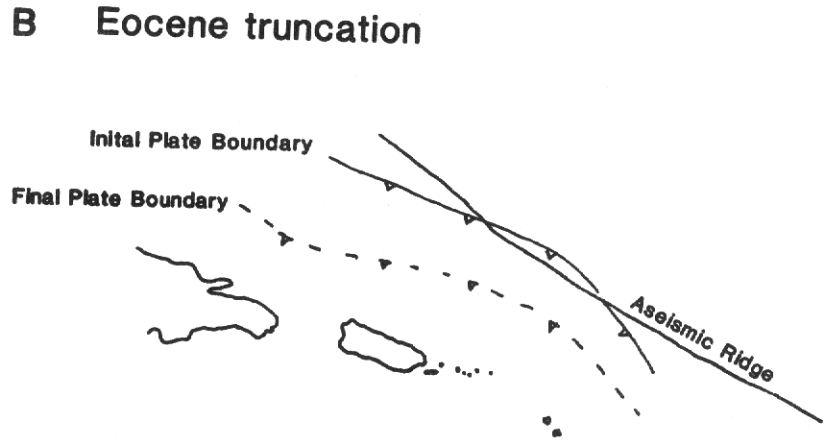

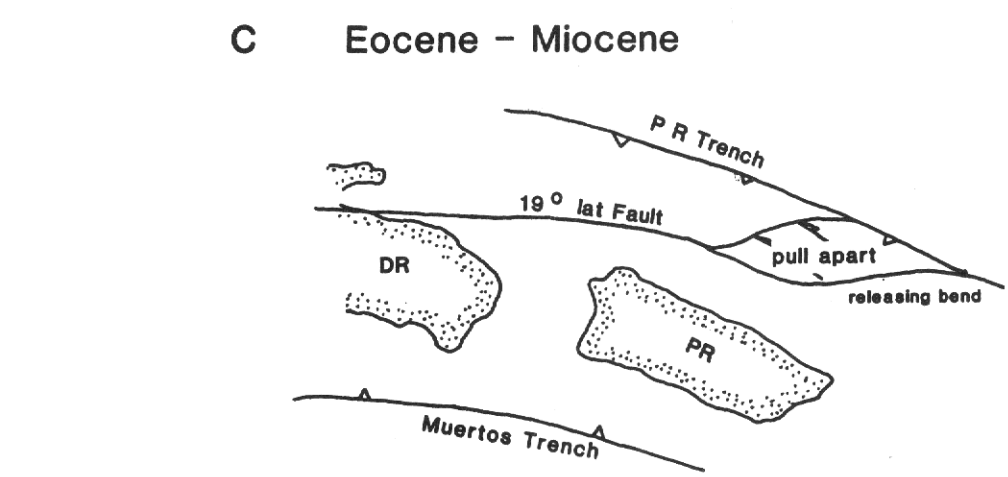

Figure 5. A. Model from Lallemand and Le Pichon (1987) for plate margin truncation associated with subduction of anomalous seafloor topography. Diagram has been modified, showing upper limit of metamorphic rocks now present in the Puerto Rico Trench wall. Subduction of the ridge is thought to have caused uplift and exposure, mostly through extensional processes, of the metamorphic complex in the present day trench wall. B. Subduction of an aseismic ridge in the Eocene (to perhaps Oligocene) results in a plate margin truncation event. C. Oblique subduction in the Eocene through Miocene results in formation of a pull-apart region on the 19° lat Fault, with attendant formation of slope basins (see Fig. 1). The Muertos Trench is located closer to Puerto Rico prior to formation of accretionary complex. D. Miocene through Pliocene events: 20° counter clockwise rotation of Puerto Rico (from Reid and others, 1988), opening of Virgin Island, Whiting, St. Croix, and other basins southeast of Puerto Rico. 19° lat Fault is hinged on the east and moves normally on the west (that is, displacement increases to west), probably also associated with rotation of Puerto Rico block. Mona Canyon graben opens because Hispaniola moves more slowly than Puerto Rico owing to underthrust Bahama Bank (a drag effect). Rotation of Puerto Rican block is taken up in Puerto Rico trench by overthrusting Atlantic crust, and overthrusting in Muertos

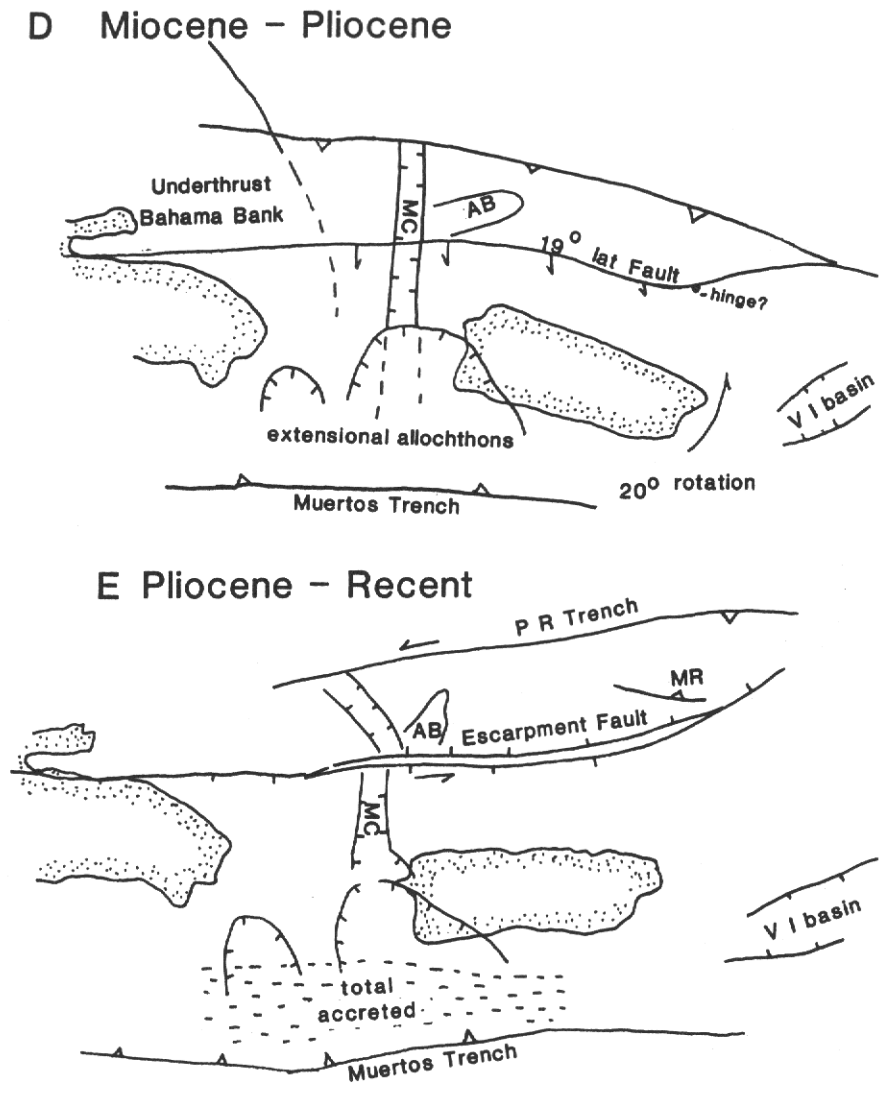

Trench, and rotation on the 19° lat Fault. Extensional allochthons form between Hispaniola and Puerto Rico (Larue, 1989), obscuring location of the Puerto Rico block boundary. E. Pliocene to Recent reconstruction. North America-Caribbean plate motion is nearly pure East-West, with overthrusting in Puerto Rico trench associated with rotation of the Puerto Rico block. Main Ridge (MR) is uplifted on a splay thrust. Mona Canyon (MC) north of 19° lat Fault and anomalous block (AB) rotate by simple shear into northwest-trending structure. Muertos Trough has developed significant accretionary complex. Extensional allocthons cut older accreted material (Larue, 1989).

vertical motion is indicated. It is concluded that strike-slip motion along the 19° lat Fault must have occurred prior to formation of the Mona Canyon, if the Mona Canyon formed as a continuous feature across the 19° lat Fault. The change in orientation of the Mona Canyon from N-S, south of the 19° lat Fault to NW-SE, north of the 19° lat Fault could conceivably be due to rotation of the Mona Canyon accompanying shear between the 19° lat Fault and the Puerto Rico Trench, or alternatively, the Canyon could have formed in this kinked position.

Forearc Subsidence

The shelf north of Puerto Rico once extended to the 19° lat fault, and this shelf subsided approximately 4 km in the Late Miocene to form a slope environment. Birch (1986) has shown that this forearc subsidence is best modelled using flexural isostasy of an elastic plate subject to a small upward load in the south and a large downward one in the north, and suggested several tectonic mechanisms to accomplish such flexure. One obvious means in which tectonic subsidence could occur is through tectonic erosion (for example, Scholl and others, 1980). Alonso and others (1987) suggested the interesting hypothesis that subduction may have been initiated in the trench at about the same time as subsidence, such that the downbowing of the Puerto Rico shelf was in response to the formation of the trench. Such an hypothesis is acceptable and could explain the detached slab of McCann and Sykes (1984); that is, a period of nonsubduction was followed by continued subduction and formation of the trench.

The hypothesis favored here for forearc subsidence is that subsidence occurred during extension on the 19° lat Fault, and the flexure is due to extensional rollover. This hypothesis indicates that the change in plate motion at 9 m.y.b.p. (Pollitz,1988) did not cause relative compression between North America and the Caribbean plate, but extension.

CONCLUSIONS

A summary of the neotectonic history of the Puerto Rico Trench area is as follows (Fig. 5B-F, 6). 1)The metamorphic complex was uplifted to its position on the south trench wall during extension associated with subduction of an aseismic ridge, probably in the Late Eocene (Fig. 5B). This aseismic ridge could have formed as a transform boundary separating older rocks to the southeast from younger more buoyant rocks to the northeast, during the opening of the Atlantic Ocean (Pindell and others, 1989). 2) Deposition of shallow water Oligocene through Middle Miocene carbonates as far north as 19° latitude, accompanied strike-slip motion on the 19° lat Fault including motion around a releasing bend (Fig. 5C). Oblique subduction occurred in the Puerto Rico Trench. 3) Motion on the 19° lat Fault in the Late Miocene (Fig. 5D) was normal oblique, with accompanying extensional rollover and subsidence of shallow-water Oligocene-Miocene strata south of the fault. Normal movement was hinged in the east, increasing toward the west, indicating counter-clockwise rotation. Paleomagnetic data onland Puerto Rico indicates nearly 20° of counter-clockwise rotation during this period (Reid and others, 1988). Also associated with the rotation of the Puerto Rico block was the opening of basins southeast of Puerto Rico (Whiting basin, Virgin Island basin, St. Croix basin) and overthrusting in the eastern Puerto Rico Trench. The Mona Canyon Graben formed as the Puerto Rico block rotated and moved away from Hispaniola. 4) In the Pliocene to Recent (Fig. 5F), as Puerto Rico rotated into its present position, faults north of Puerto Rico in the Puerto Rico Trench which previously showed a component of shortening became strike-slip faults. Distributed shear between the 19° lat Fault and the Puerto Rico trench, caused rotation accompanying shear of the Mona Canyon graben north of 19° latitude. Further down-dropping of the trench region occurred associated with normal motion on the trench slope walls (including Escarpment Fault), associated with transtensional tectonism in the Puerto Rico Trench.

ACKNOWLEDGEMENTS

We are indebted to Eric Rosencrantz for obtaining copies of the seismic reflection profiles reproduced herein, and the Texas Institute for Geophysics for allowing their publication. Discussions with colleagues at the University of Puerto Rico were helpful in the refinement of the interpretations presented herein. This study was supported by a National Science Foundation EPSCoR Grant to the Department of Geology at the University of Puerto Rico. D. K. Larue was strongly moved by a paper by R.C. Speed (1989), who inferred the Puerto Rico Trench was an extensional allochthon, and discussions with J. Oldow initiated the senior author to the concept of orogenic float and dipping strike-slip systems.

REFERENCES

Alonso, R.M., Krieg, E.A., and Meyerhoff, A.A., 1987, Post-early Pliocene age of the Puerto Rico Trench: 10th Carib. Geol. Conf., Cartagena, Colombia (in press).

Ascencio, E., 1980, Seismicity of western Puerto Rico: U.S. Geol. Survey Open File Report, 80-192, p. 1-135.

Austin, J.A., Jr., 1983, OBC-5A: Overthrusting in a deep-water carbonate terrane: *in* Bally, A.W., ed., A picture and work atlas of seismic expression of structural styles: American Assoc. Petroleum Geol. Studies in Geology Series #15, v. 3,3.4.2-163.

Biju-Duval, B., Bizon, G., Mascle, A., and Muller, C., 1982, Active margin processes: field observation in southern Hispaniola:*in* J.S. Watkins and C.L. Drake, eds., Studies in Continental Margin Geology, American Assoc. Petroleum Geol. Memoir 34, p. 325-344.

Birch, F.S., 1986, Isostatic, thermal and flexural models of the subsidence of the north coast of Puerto Rico: Geology, v. 14, p. 427-429.

Bowin, C., 1972, Puerto Rico Trench netative gravity anomaly belt: Geol. Soc. America Memoir 132, p. 339-350.

Bowin, C.O., Nalwalk, A.J., and Hersey, J.B., 1966, Sepentinized peridotite from the north wall of the Puerto Rico Trench: Geol. Soc. America Bull., v. 77, p. 257-270.

Bracey, D.R., and Vogt, P.R., 1970, Plate tectonics in the Hispaniola area: Geol. Soc. America Bulletin, v. 81, p. 2855-2860.

Byrne, D.B., Suarez, G., and McCann, W.R., 1985, Muertos Trough subduction-microplate tectonics in the northern Caribbean: Nature, v. 317, p. 420-421.

Case, J.E., 1975, Geophysical studies in the Caribbean Sea: *in* A.E.M. Nairn and F.G. Stehli, eds., The Ocean basins and margins, v. 3, The Gulf of Mexico and the Caribbean: Plenum Press, New York, p. 107-180.

Chase, R.L., and Hersey, J.B., 1968, Geology of the north slope of the Puerto Rico Trench: Deep-Sea Research, v. 15, p. 297-317.

Conolly, J.R., and Ewing, M., Sedimentation in the Puerto Rico Trench: Journal of Sed. Petrology, v. 37, p. 44-59.

Dolan, J.F., Breen, N.A., Mullins, H.T., 1989, Oblique collision between the southeastern Bahamas and Hispaniola: Preliminary SeaMARC II/single channel seismic-reflection results: EOS, v. 70, p. 1313.

Eberle, W., Hirdes, W., Muff, R., and Pelaez, M., 1980, The geology of the Cordillera Septentrional (Dominican Republic): *in* 9th Caribbean Geological Conference, Santo Domingo, Dominican Republic, Transactions, p. 619-632.

EEZ SCAN 85 Scientific Staff 1987, Atlas of the U.S. Exclusive Economic Zone, eastern Caribbean: U.S. Geol. Survey Miscellanceous Investigation Ser. I-1864B, 58 p.

Ewing, M., and Heezen, B.C., 1955, Puerto Rico Trench topograhic and geophysical data: Geol. Soc. America Spec. Paper 62, p. 255-268.

Ewing, W.M., Lonardi, A., and Ewing, J.I., 1966, The sediments and topography of the Puerto Rico Trench and Outer Ridge: Trans. Fourth Caribbean Geological Conference, Port-of-Spain, Trinidad, p. 325-334.

Fox, P.J., and Heezen, B.C., 1975, Geology of the Caribbean crust, *in* Nairn, A.E.M., and Stehli, F.G.., eds., The ocean basins and margins, v. 3. The Caribbean and the Gulf of Mexico: New York, Plenum Press, p. 421-466.

Heezen, B.C., Nesteroff, W.D., Rawson, M., and Freeman-Lynde, R.P., 1985, Visual evidence for subduction in the western Puerto Rico trench, *in* Mascle, A., ed., Caribbean Geodynamics Symposium, Paris, March 5-8, 1985: Paris, France, Editions, Technip, p. 287-304.

Jany, I., Mauffret, A., Bouysse, P., Mascle, A., Mercier de Lepinay, B., Renard, and Stephan, F., 1987, Seabeam survey and wrench tectonics south of the Virgin Islands (northeastern Caribbean): C.R. Acad. Sc. Paris, t. 304, Serie II, p. 527-532.

Jordan, T.H., 1975, The present day motions of the Caribbean plate: Journal of Geophysical Research, v. 80, p. 4433-4440.

Joyce, J., 1980, The lithology and structure of the eclogite and glaucophanite-bearing rocks on the Samana Peninsula, Dominican Republic: 9th Transactions of the Carib. Conf., Dominican Republic, p.417-422.

Joyce, J., 1985, High pressure-low temperature metamorphism and the tectonic evolution of the Samana Peninsula, Dominican Republic, Greater Antilles, University Microfilms, Ann Arbor, Michigan, 250p.

Joyce, J., and Aronson, J., 1987, K-Ar dates for blueschist metamorphism on the Samana Peninsula, Domincan Republic: 10th Carib. Geol. Conf., Cartagena, 1983, in press.

Ladd, J.W., Shih, T., and Tsai, C.J., 1981, Cenozoic tectonics of central Hispaniola and adjacent Caribbean Sea: American Assoc. Petrol. Geol. Bull., v. 65, p.466-489.

Ladd, J.W., Worzel, J.L., and Watkins, J.S., 1977, Multifold seismic reflection records from the northern Venezuela basin and the north slope of Muertos Trench: *in* M. Talwani and W.C. Pitman, eds., Island Arcs, Deep-Sea trenches and Back-arc basins: American Geophys. Union, Washington D.C., p. 41-56.

Ladd, J.W., and Watkins, J.S., 1978, Active margin structures within the north slope of the Muertos Trench: Geologie and Mijnbouw, v. 57, p. 255-260.

Lallemand, S. and Le Pichon, X., 1987, Colomb wedge model applied to the subduction of seamounts in the Japan Trench: Geology, v. 15, p. 1065-1069.

Larue, D.K., 1989, Extensional allochthon in the Mona Passage: 12th Carib. Geol. Conf. Abs., St. Croix, p. 99.

Larue, D. K., 1990, Toa Baja Drilling Project, Puerto Rico: EOS, v. 71, p. 233-234.

Le Pichon,, Iiyama, J., Bourgois, Mercier de Lepinay, B., Tournon, J., Muller, C., Butterlin, J., and Glacon, G., 1985, First results of the test dives of the French submersible Nautile in the Puerto Rico trench (Greater Antilles): Acad. de Sciencees Paris trans., 301, Serie II, number 10, p. 743-749.

Lewis, J.F., 1980, Cenozoic tectonic evolution and sedimentation in Hispaniola: 9th Trans. Carib. Conf., Santo Domingo, Dominican Republic, p. 65-74.

Mann, P., and Burke, K., 1984, Neotectonics of the Caribbean, Rev. Geophys. Space phys., v. 22, p. 309-362.

Mann, P., Burke, K., and Matumoto, T., 1984, Neotectonics of Hispaniola: plate motion, sedimentation and seismicity at a restraining bend: Earth Planet. Sci. Letters, v. 70, p. 311-324.

Masson, D.G., and K.M., Scanlon, in press, The regional tectonic setting of Puerto Rico: submitted to Geol. Soc. America Bull.

McCann, W. R., and Sykes, L. R., 1984, Subduction of aseismic ridges beneath the Caribbean plate: implications for the tecotnics and seismic potential of the north eastern Caribbean: J. Geophys. Res., v. 89, p. 4493-4519.

Meyerhoff, A.A., Krieg, E.W., Cloos, J.D., and Taner, I., 1983, Petroleum possibilites of Puerto Rico: Oil and Gas journal, v. 81, no. 51, p. 113-120.

Molnar, P., and Sykes, L.R., 1969, Tectonics of the Caribbean and Middle America regions from focal mechanisms and seismicity: Geol. Soc. America Bull., v. 59, p. 801-854.

Moussa, M.t., Seiglie, G.A., Meyerhoff, A.A., Taner, I., 1987, The Quebradillas Limestone (Miocene-Pliocene), northern Puerto Rico, and tectonics of the northeastern Caribbean margin: Geol. Soc. America Bull., v. 99, p. 427-439.

Murphy, A. J., and McCann, W.R., 1979, Preliminary results from a new seismic network in the northeastern Caribbean: Bull. Seismol. Soc. America, v. 69, p. 1497-1513.

Nagle, F., 1974, Blueschist, eclogite, paired metamorphic belts and the early tectonic history of Hispaniola, Geol. Soc. America Bull., v. 89, p. 1155-1174.

Perfit,, M.R., Heezen, B.C., Rawson, M., and Donnelly, T.W., 1980, Chemistry, origin, and tectonic significance of metamorphic rocks from the Puerto Rico Trench: Marine Geol., v. 34, p. 125-156.

Pollitz, F.F., 1988, Episodic North America and Pacific plate motions: Tectonics, v. 7, p. 711-726.

Scanlon, K.M., Masson, D.G., and Rodriguez, R.W., 1987, GLORIA sidescan-sonar survey of the EEZ of Puerto Rico and the U.S. Virgin Islands: Transactions of the 11th Carib. Geol. Conf., Barbados, p.321-329.

Schell, B.A., and Tarr, A.C., Plate tectonics of the northeastern Caribbean Sea region: Geologie en Mijnbouw, v. 57, p. 319-324.

Schneidermann, N., Beckmann, J.C., and Heezen, B.C., 1972, Shallow water carbonates from the Puerto Rico Trench region, *in* Petzall, C., ed., 6th Carib. Geol. Conf., Isla de Margarita, Venezuela, 1971, Trans: Caracas, Venezuela, Chromotip, p.423-425.

Scholl, D., Huene, R. von, Vallier, T.L., and Howell, D.G., 1980, Sedimentary masses and concepts about tectonic processes at under-thrust ocean margins: Geology, v. 8, 564-568.

Speed, R.C., 1989, Tectonic evolution of St. Croix: implications for tectonics of the northeastern Caribbean: *in* Hubbard, D.K., ed., Terrestrial and marine geology of St. Croix, U.S. Virgin Islands: Spec. Publication Number 8, West Indies Laboratory, Teague Bay, St. Croix, p. 9-22.

Sykes, L. R., and Ewing, M., 1965, The seismicity of the Caribbean region: Jour. Geophys. Res., v. 70, p. 5065-5074.

Sykes, L.R., McCann, W.R., and Kafka, A.L., 1982, Motion of the Caribbean plate during last 7 million years and implications for earlier Cenozoic movements: Jour. Geophys. Res., v. 87, p. 10656-10676.

Sylvester, A. G., 1988, Strike-slip faults: Geol. Soc. America Bull., v. 100, p. 1666-1703.

Uchupi, E., Milliman, J.D., Luyendyk, B.P., Bowin, C.O., and Emery, K.O., 1971, Structure and origin of southeastern Bahamas: American Assoc. Petrol. Geol. Bull., v. 55, p. 687-704.

Von Huene, R., 1986, To accrete or not accrete, this is the question: Geol, Rundschau, v. 75, p. 1-15.

Weaver, J., Smith, A., and Seiglie, G., 1975, Geology and tectonics of the Mona Passage: Trans. American Geophy. Union, v. 56, p. 451.

RADIOMETRICALLY DATED MARINE TERRACES ON NORTHWESTERN PUERTO RICO

Bruce E. Taggart
Department of Marine Sciences
University of Puerto Rico
Mayagüez, PR, 00709-5000

James Joyce
Department of Geology
University of Puerto Rico
Mayagüez, PR, 00709-5000

ABSTRACT

A detailed study of Pleistocene marine terraces on northwestern Puerto Rico is in progress focusing on the correlation of wave-cut geomorphic features and marine terrace deposit stratigraphy. Stratigraphic control is based on ^{14}C and $^{230}Th/^{234}U$ coral dates from four localities; Rincón, Punta Borinquen, Quebradillas and Palmas Alta.

Radiometric age ranges have been obtained for the 2-3 m and 10 m marine terrace levels. The 10 m marine terrace level has produced $^{230}Th/^{234}U$ ages ranging from 114,000 YBP (± 3,495) to 134,500 YBP (± 2,825). The 2-3 m marine terrace level has produced two groups of radiometric ages. A younger group of ^{14}C ages ranging from 1,460 YBP (± 80) to 2,050 YBP (± 80) and an older group of $^{230}Th/^{234}U$ ages of 115,000 YBP (± 2,955) to 123,000 YBP (± 4,514). The older group of corals were eroded from the 10 m level and subsequently incorporated into the younger 2-3 m level during its formation. Radiometric data and field observations from the Punta Gorda and Punta Borinquen localities, as well as previously published data from northern Puerto Rico and Isla Desecheo, suggest that sea level in northwestern Puerto Rico was 2-3 m higher than present between 1,460 and 3,300 YBP.

Using the data from these marine terrace deposits, a minimum rate of uplift of between 0.03 mm/yr and 0.05 mm/year has been determined for northwestern Puerto Rico during the late Pleistocene. The Pliocene Quebradillas Limestone occurs at elevations of up to 200 m in northwestern Puerto Rico and has marine terrace surfaces developed in it as high as 140 m. These elevations are in agreement with the computed average rate of uplift determined from late Pleistocene marine terrace deposits and suggest that the rate of uplift in northwestern Puerto Rico has been consistent since the mid-Pliocene.

INTRODUCTION

Numerous marine terrace levels and deposits have been observed along all coastal regions of Puerto Rico (Table 1). However, they are most extensively preserved on northwestern Puerto Rico, Isla Desecheo and Isla de Mona (Kaye, 1959a; Kaye, 1959b; Monroe, 1968; Seiders et al., 1972).

In northwestern Puerto Rico marine terrace deposits known to be of Holocene and late Pleistocene age occur at 2-3 m, 10 m, 25-30 m, 36.5 m and 45 m (Kaye, 1959a; Monroe, 1968; Weaver, 1970). The age of the other marine terrace levels shown in Table 1 are not known exactly, but are thought to range from Neogene to early Pleistocene in age. Pleistocene marine terrace deposits occur throughout the northeastern Caribbean Islands (Horsfield, 1975) and have been radiometrically dated on the Cayman Islands (Woodroffe et al., 1985), Jamaica (Cant, 1973), Haiti (Dodge et al., 1983), the Dominican Republic (Schubert and Cowart, 1980) and St. Croix (Hubbard et al., 1989).

We have undertaken a detailed study of marine terraces on northwestern Puerto Rico focusing on correlation of wave-cut geomorphic features and terrace stratigraphy. Stratigraphic control is based on ^{14}C and $^{230}Th/^{234}U$ coral dates. These coral dates indicate the time of deposition on marine terrace surfaces at four localities; Rincón, Borinquen, Quebradillas and Palmas Alta (Figure 1). Table 2 summarizes the radiometric age data determined from coral samples collected at each of the field sites. The elevations of the various deposits and marine terrace surfaces discussed herein were measured from mean sea level using a stadia rod, a tape measure and an inclinometer and are accurate to ± 0.05 m.

The deposits at Rincón, Borinquen and Quebradillas are dominantly calcareous siliciclastic sandstones and conglomerates derived from mixed marine and terrigenous sources. Coral rich layers occur in these deposits immediately above unconformities. Conglomeratic units, especially basal conglomerates, contain numerous corals. The Palmas Alta site consists of an elevated reef tract overlain by lithified beach and eolianite deposits. The Rincón Region contains the best exposures of terrace deposits and has yielded most of the radiometrically dated corals.

These data, along with geomorphic and stratigraphic observations, have been used to correlate deposits and wave-cut features from all other localities to the Rincón deposits. They have then been used to ascertain the amount, and nature, of vertical tectonic movement in northwestern Puerto Rico during the late Quaternary. These data are summarized and discussed for each field site in the following section.

Larue, D.K., and Draper, G., eds.,
Transactions of the 12th Caribbean Conference,
St.Croix, U.S.V.I., Miami Geological Society,
P.O. Box 14433, Coral Gables, FL 33114

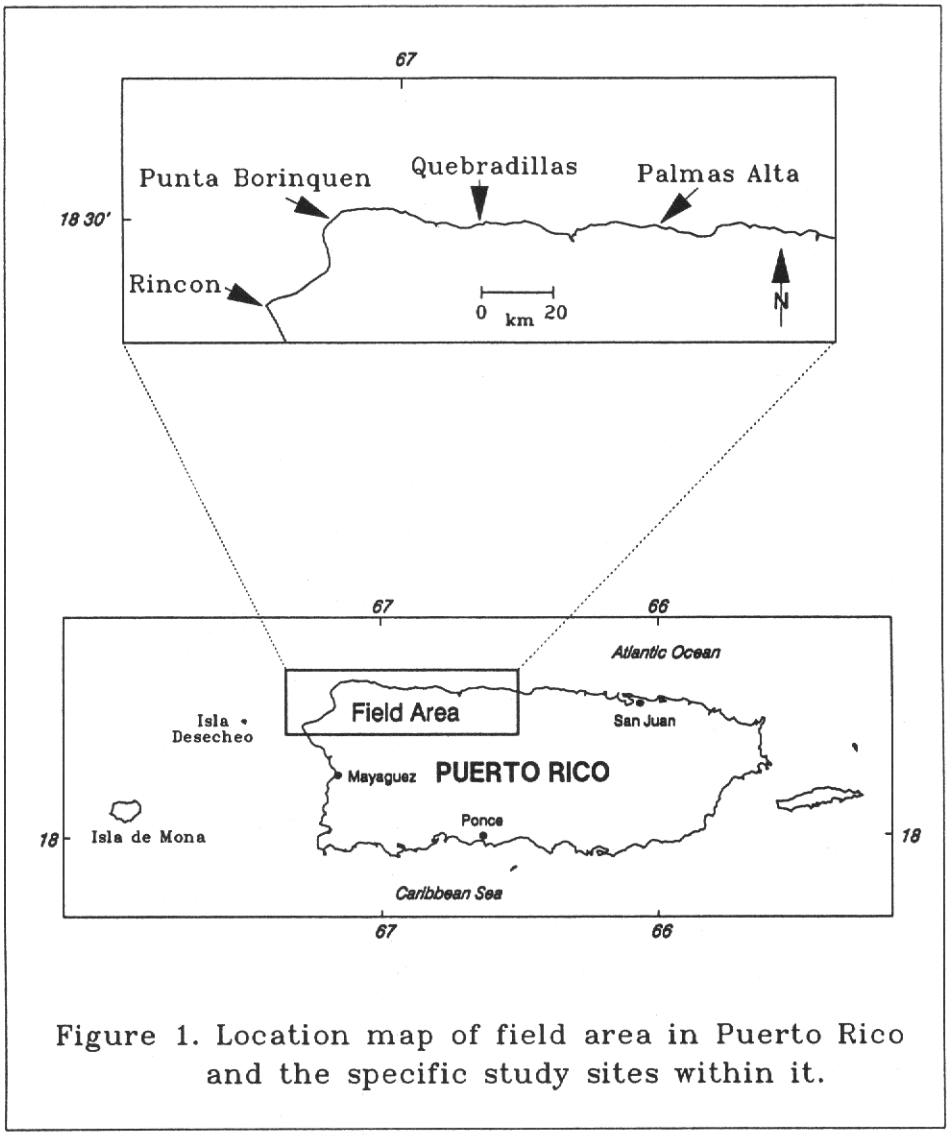

Figure 1. Location map of field area in Puerto Rico and the specific study sites within it.

RESULTS AND DISCUSSION

Rincón Region

The most extensive sequence of Quaternary marine terrace deposits identified are found in the Rincón region. These deposits are best exposed between Punta Ensenada and Punta Gorda (Figure 2). Four marine terrace depositional units are recognized at Rincón: Gorda (Qg), Higüero One (Qh_1), Higüero Two (Qh_2) and Martinica (Qm). Qg is an undifferentiated marine sand and reef rock deposit that is found at elevations ranging from 1 m to 2 m at Punta Gorda. The type section for Qh_1 and Qh_2 is found at Punta Higüero. Qh_1 extends from an elevation of 1 m to 8 m and is a calcareous sandstone containing abundant marine fossil fragments. The upper surface of this unit contains large vertical solution pits that mark the unconformable contact between Qh_1 and the overlying Qh_2 unit. The basal portion of Qh_2 fills the solution pits and grades upwards into a middle zone containing abundant Acropora palmata and other corals in a lithic calcarenite. Above this middle zone, Qh_2 grades into a cross-bedded medium-grained lithic carbonate sand containing granules, pebbles and marine fossil fragments. This unit extends from about 8 m to 10 m elevation. A composite stratigraphic cross-section of these units is presented in Figure 3. Qm consists of small scattered exposures of marine sands and coral fragments unconformably deposited on the Culebrinas Formation of Eocene age. It is found at elevations of up to 25 m along a distinctive slope break throughout the hinterland between Punta Higüero and Punta Ensenada (Figure 4). Weaver (1970) described this unit as a raised beach deposit of Pleistocene age. Based on its location at higher, and more landward, elevations relative to Qh deposits and its association with a distinct break in slope we conclude that Qm constitutes a Pleistocene marine terrace deposit that is older than the Qh deposits. Datable corals have not been recovered from Qm deposits so its exact age

Table 1. Elevated marine terrace (M) and accordant summit levels (A) reported for Puerto Rico. An accordant summit surface consists of summits of equal elevation in a region of high topographic relief that suggest they are remnants of an erosion plain formed in a previous erosion cycle. Kaye (1959a) not only cites his own observations of marine terrace levels but provides an excellent summary of previously reported ones and is cited in their stead for purposes of brevity where appropriate.

Elevation (m)	Surface Type	Reference
760	A	Weaver (1966)
620	A	Weaver (1966)
470	A	Weaver (1966)
330	M	Weaver (1966, 1970)
300	M	Weaver (1966, 1970)
280	M	Weaver (1970)
200	M	Weaver (1970)
190	M	Weaver (1970)
160	M	Weaver (1970)
140	M	Weaver (1970)
120	M	Weaver (1966)
100	M	Weaver (1971)
80	M	Weaver (1971)
50-60	M	Lobeck (1922), Hubbard (1923), Monroe (1968), Weaver (1970, 1971)
36.5	M	Kaye (1959a)
25	M	Weaver (1970)
20	M	Kaye (1959a), Williams (1968)
12	M	Seiders et al. (1972)
8-10	M	Kaye (1959a), Williams (1968)
4-5	M	Kaye (1959a)
2-3	M	Kaye (1959a), Williams (1968), Weaver, (1970), Seiders et al. (1972)

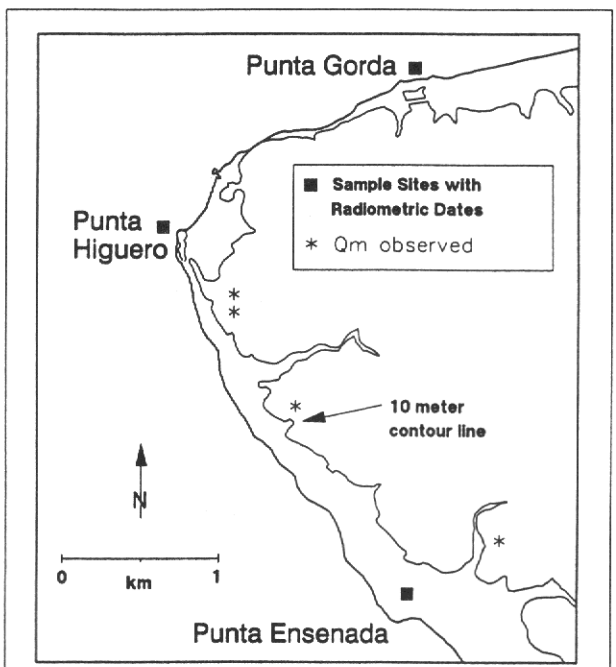

Figure 2. Generalized map of the Rincon Region showing sites of interest discussed in text.

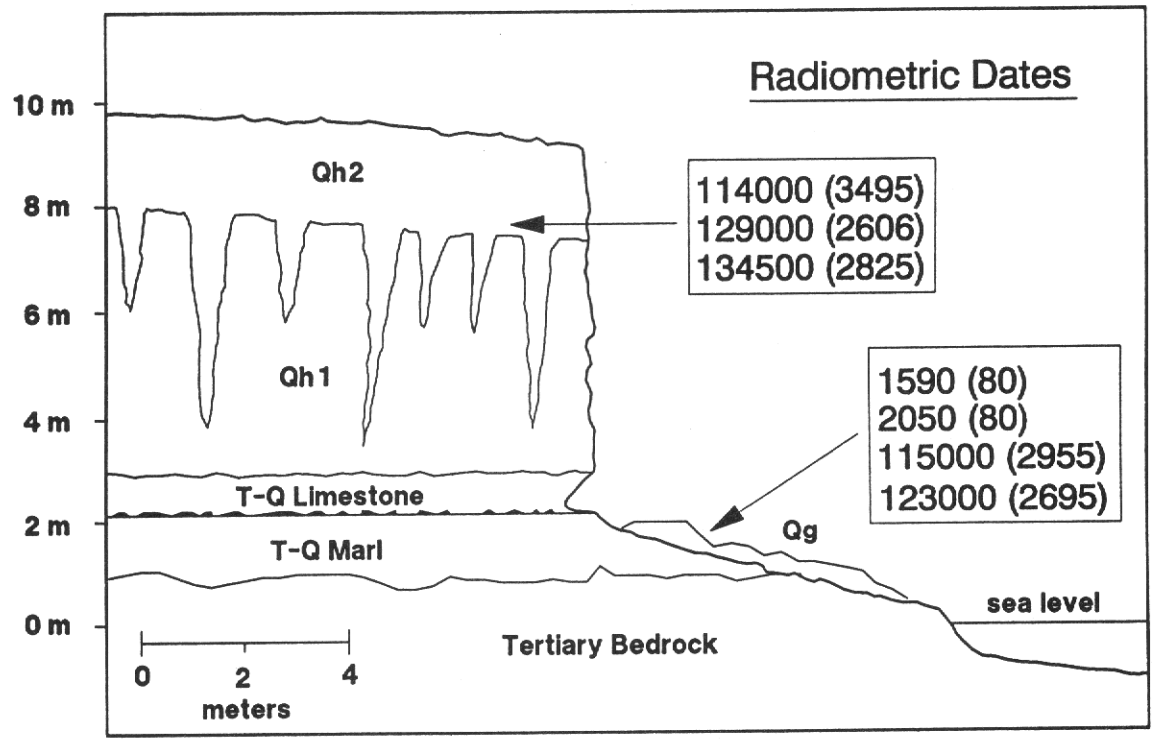

Figure 3. Composite cross-section of the Rincon Region Quaternary deposits on the west coast of Puerto Rico.

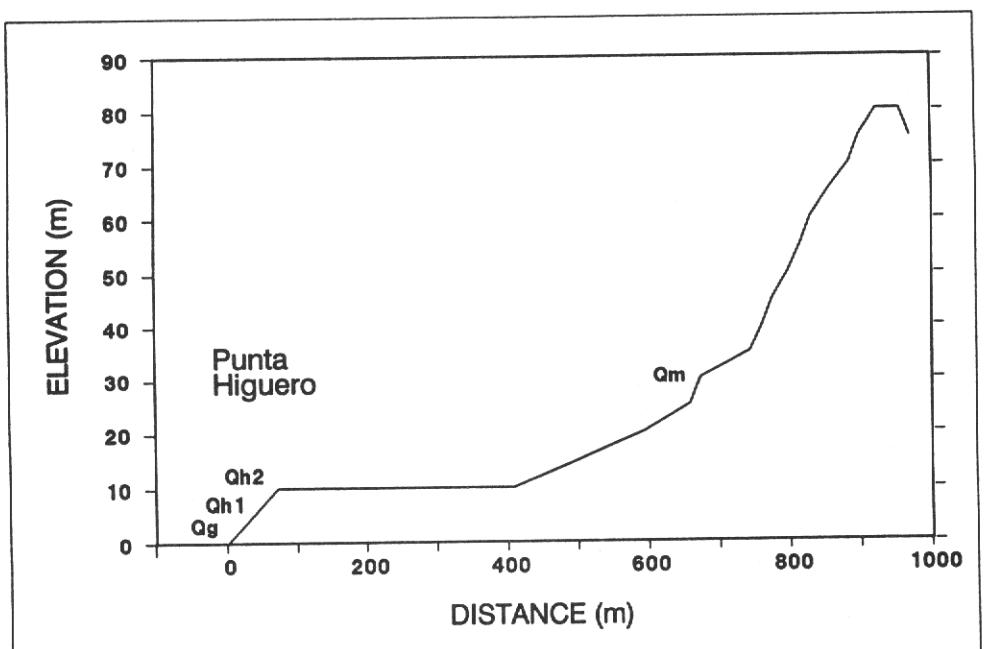

Figure 4. Topographic profile at Punta Higuero, Puerto Rico.

Table 2. Summary of data obtained from corals retrieved from various marine terrace deposits in northwestern Puerto Rico.

Sample Number	Sample Site	Coral Sp.	Sample Elevation (m)	Percent Aragonite	Th-230 (dpm/gm)	Std. Dev.	U-234 (dpm/gm)	Std. Dev.	U-234 / U-238	Std. Dev.	Th-232 / Th-230	Std. Dev.	Th-230 Age	Std. Dev.	C-14 Age	Std. Dev.
1	RH	S	8.8	96.9	1.909	2.53	2.883	1.72	1.13	*	0.662	3.07	114000	3495	33060	670
7	RG	D	1	99.9	0.061	4.90	2.384	1.10	1.15	*	0.026	5.02	3000	150	1590	80
8	RG	Mc	1	99.7	0.054	4.88	2.139	1.10	1.13	*	0.025	5.00	3000	150	2050	80
9	RG	Ap	1	100	1.684	1.73	2.439	1.79	1.12	*	0.690	2.19	123000	2695	35290	1150
10	RG	Ss	1	100	1.444	1.77	2.171	1.87	1.15	*	0.665	2.57	115000	2955	30360	1100
11	PB	Ma	1.4	100	0.146	5.56	2.045	1.93	1.10	*	0.071	5.88	8000	470	1460	80
12	PB	Ap	1.4	100	0.050	5.60	2.637	1.79	1.12	*	0.019	5.88	2000	118	1680	70
13	PH	D	2.7	99.6	1.163	1.80	2.381	1.87	1.09	*	0.677	2.46	120000	2950	33940	800
14	PH	D	2.7	100	1.525	1.77	2.224	1.87	1.09	*	0.680	2.57	120000	3064	39100	1340
25	PB	D	1.4	97.7	1.657	2.31	2.402	2.87	1.08	2.91	0.690	3.68	124000	4563	---	---
28	PA	D	1	100	1.584	2.41	2.215	2.34	1.09	2.53	0.715	3.36	133000	4469	---	---
29	PA	D	1	100	1.525	2.30	2.096	2.95	1.06	3.20	0.728	3.74	138000	5161	---	---
30	PH	D	3.0	100	1.639	1.89	2.291	2.32	1.08	2.50	0.716	2.99	133000	3977	---	---
31	PH	Ma	3.0	100	1.520	1.99	2.130	2.32	1.08	2.56	0.714	3.06	132500	4055	---	---
38	RE	Sr	5.0	98.8	1.896	1.83	2.399	1.42	1.10	1.49	0.790	2.32	162500	3770	---	---
39	RH	Ap	6.7	100	1.745	1.83	2.463	1.19	1.13	1.27	0.709	2.02	129000	2606	---	---
41	RH	Ap	6.7	100	1.744	1.82	2.425	1.34	1.09	1.43	0.719	2.10	134500	2825	---	---

(a) RE = Punta Ensenada RH = Punta Higuero RG = Punta Gorda
PB = Punta Borinquen PH = Puerto Hermina PA = Palmas Altas

* Value not provided with processed data

(b) S = Siderastrea sp. Mc = Montastrea cavernosa Ap = Acropora palmata
Ss = Siderastrea sideria Ma = Montastrea annularis D = Diploria sp.
Sr = Siderastrea radians

is not known.

Coral samples have been retrieved from Qg, Qh_2 and Qm deposits at Punta Higüero and Punta Gorda. However, only samples retrieved from Qg and Qh_2 exposures have proven to be radiometrically datable. At Punta Higüero three corals retrieved from basal Qh_2 deposits have produced $^{230}Th/^{234}U$ ages of 114,000 ± 3,495 YBP, 129,000 ± 2,606 YBP and 134,500 ± 2,825 YBP (Table 2). Sample #1 was also dated by the ^{14}C method and yielded an age of 33,060 ± 670 YBP (Table 2).

At Punta Gorda a wave-cut notch is preserved at an elevation of 1.5 to 2.0 m. The Qg (undifferentiated marine sand and reef rock) deposit lies seaward of, and abuts, this wave-cut notch. Two coral samples retrieved from Qg yielded ^{14}C ages of 1,590 ± 80 YBP and 2,050 ± 80 YBP and $^{230}Th/^{234}U$ ages of 3,000 ± 150 YBP and 3,000 ± 150 YBP. Two additional samples yielded $^{230}Th/^{234}U$ ages of 123,000 ± 2,695 YBP and 115,000 ± 2,955 YBP and ^{14}C ages of 35,290 ± 1,150 YBP and 30,360 ± 1,100 YBP respectively (Table 2). According to Pierce (1986) many ^{14}C dates that fall within the 25-40 YBP range may be the result of contamination of older coral samples (> 50 ka) with between 0.5-2.0 percent young carbon. Therefore, the ages of coral samples retrieved from Punta Gorda that were analysed by both radiometric dating methods appear to be in agreement inasmuch as the young ^{14}C ages are supported by young $^{230}Th/^{234}U$ ages and the older $^{230}Th/^{234}U$ ages are supported by ^{14}C ages in Pierce's (1986) questionable range of 25-40 YBP. These older $^{230}Th/^{234}U$ dates are identical with those determined for Qh deposits at Punta Higüero. The bimodal nature of the dates and the presence of a wave-cut notch at the base of Qh deposits at Punta Gorda suggest reworking of Qh deposits into Qg during the late Holocene.

One coral suitable for radiometric dating was recovered at Punta Ensenada. It was found in a small reef rock exposure located about 200 m inland of Punta Ensenada at an elevation of 5 m. It produced a $^{230}Th/^{234}U$ age of 162,500 ± 3,770 YBP (Table 2). This reef rock exposure contains A. palmata, M. annularis, S. radians and Diploria sp. corals. Based on the elevation of the exposure (lower than Qh_2) and its age (older than Qh_2) we suggest that it is either a Qh_1 deposit or that it represents a pre-Qh deposit. More dates are needed to verify which of these two hypotheses is correct.

Marine terrace deposits on Isla Desecheo, located 21 km west of Punta Higüero, occur at elevations of 2-3 m and 10-12 m (Seiders et al., 1972). These deposits were called the Lower Desecheo Stage (2-3 m)

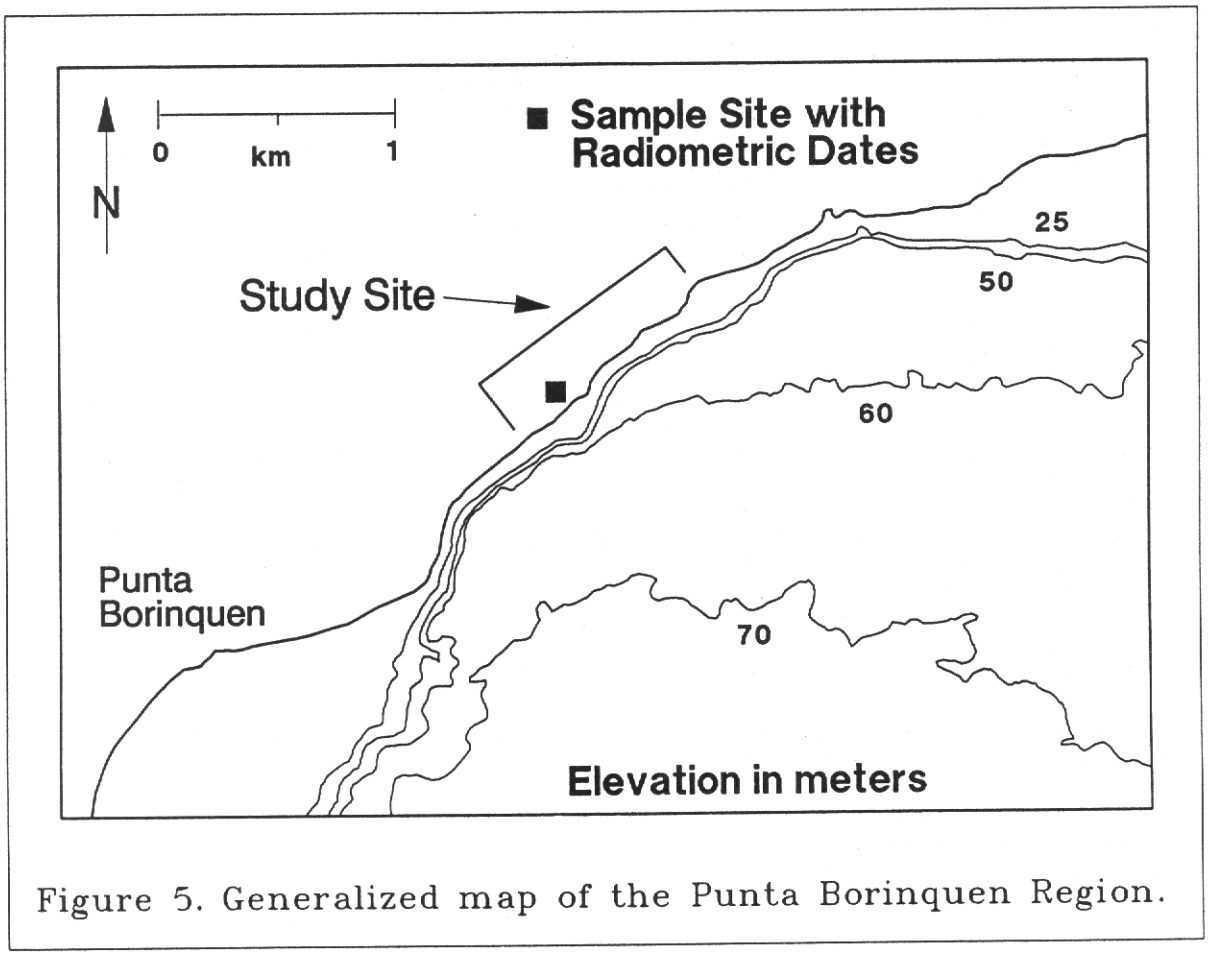

Figure 5. Generalized map of the Punta Borinquen Region.

and the Upper Desecheo Stage (10-12 m) by Hubbard (1923). Seiders et al. (1972) concluded that the Lower Desecheo Stage is Holocene in age and the Upper Desecheo Stage is late Pleistocene in age. They based their conclusion on geomorphic and stratigraphic observations of the deposits and one ^{14}C age of 3,300 ± 300 YBP from a 2 m coastal swamp deposit in north-central Puerto Rico (Seiders et al., 1972; p. 21). We conclude that the Lower Desecheo Stage and the Upper Desecheo Stage correlate with Qg and Qh deposits.

Punta Borinquen Region

Immediately north of Punta Borinquen deposits correlated to Qg are found at elevations of up to 2.7 m within a wave-cut notch that begins at 2.5 m (Figure 5). Marine debris deposits, often overlain by colluvium, are discontinuously exposed in the cliffs throughout this region at an average elevation of 5 m and are correlated to Qh. Two coral samples retrieved from the Qg deposit yielded ^{14}C ages of 1,460 ± 80 YBP and 1,680 ± 70 YBP and $^{230}Th/^{234}U$ ages of 8,000 ± 470 YBP and 2,000 ± 118 YBP. A third sample yielded a $^{230}Th/^{234}U$ age of 124,000 ± 4,563 YBP (Table 2). The distribution of ^{14}C ages here is similar to that found at Punta Gorda and supports correlation with Qg.

At the Punta Gorda and Punta Borinquen sites the radiometric ages fall into two distinct populations on the 2-3 m terrace level. They are late Holocene (1,500 to 2,000 YBP) and late Pleistocene (115,000 to 123,000 YBP) in age. We conclude that the older corals were eroded from the adjacent Pleistocene Qh deposits and subsequently incorporated into the younger surface as it formed during the late Holocene. The presence of a well-developed wave-cut notch at the landward edge of Qg at Punta Gorda and Punta Borinquen, the occurrence of Qh blocks in Qg at Punta Gorda, adjacent Qh deposits and the congruence of coral ages between the two sites support this conclusion. The low average rate of uplift established for northwestern Puerto Rico for the late Pleistocene suggests that this feature must have formed at a higher stand of sea level or been co-seismically uplifted. The lack of surficial features favoring the occurrence of co-seismic movement in this region during the Holocene does not support uplift of 2-3 m during the last 2,000 years. Also, there is no reason to suspect that the average rate of tectonic uplift should increase by two orders of magnitude during the late Holocene. This suggests that local sea-level was locally 2-3 m higher than present between 1,460 YBP and 3,300 YBP.

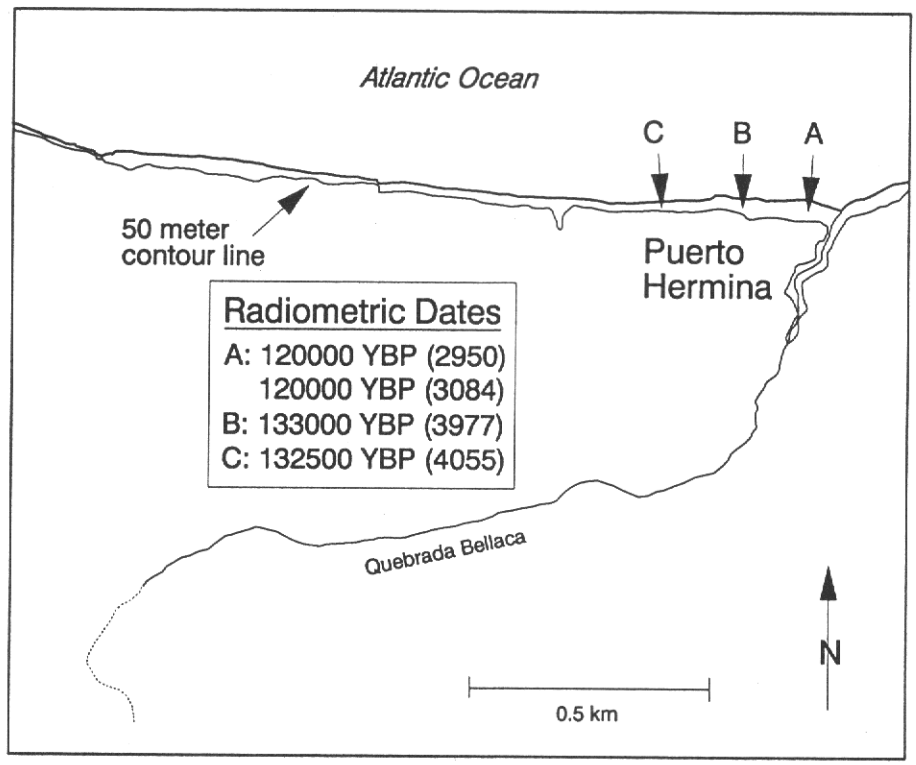

Figure 6. Generalized map of the Puerto Hermina study site in the Quebradillas Region.

Quebradillas Region

On the coast immediately northeast of the town of Quebradillas, at Puerto Hermina, four coral samples suitable for radiometric dating were retrieved from the base of the 10 m marine terrace deposit (Figure 6). $^{230}Th/^{234}U$ ages of 120,000 ± 2,950 YBP, 120,000 ± 3,084 YBP, 133,000 ± 3,977 YBP and 132,500 ± 4,055 YBP were determined for these samples (Table 2). The deposits at Puerto Hermina are correlated with the Qh deposits at Punta Higüero based on radiometric ages of dated corals, the presence of wave-cut notches at 8-10 m elevation and small exposures of marine sand deposits at up to 12 m.

Palmas Alta Region

Palmas Alta differs from the three preceding sites in that it is a reef-rock exposure consisting of large coral heads in a sand matrix rather than marine deposits veneering a wave-cut platform. Corals were collected from the reef tract at Palmas Alta at an elevation of one meter (Figure 7). These samples produced $^{230}Th/^{234}U$ ages of 133,000 ± 4,469 YBP and 138,000 ± 5,161 YBP (Table 2). This reef tract exposure is conformably overlain by lithified Pleistocene beach deposits. The beach deposits are unconformably overlain by late Pleistocene eolianite deposits described by Kaye (1959) that extend along much of the north coast. The radiometric ages effectively establish a maximum age of a late Pleistocene regression and the formation of the overlying eolianite ridge.

The ages available for this deposit indicate that it formed at the same time as Qh deposits at Punta Higüero and Puerto Hermina. The total absence of A. palmata from the deposit suggests that this reef exposure may have formed at depths greater than 5-10 m below the paleosea-level (Lighty et al., 1982). It is also possible that sediment stress and/or the wave-energy environment inhibited the development of A. palmata at this site.

CONCLUSIONS

Elevated marine terraces with deposits 125,000 ± 10,000 YBP occur in northwestern Puerto Rico and on Isla Desecheo at elevations of 10-12 m above present sea level (Seiders et al., 1972). These deposits establish a lower limit constraint on sea level around Puerto Rico 125,000 YBP. Sea level may have been even a few meters higher than the top of the deposits. The age and

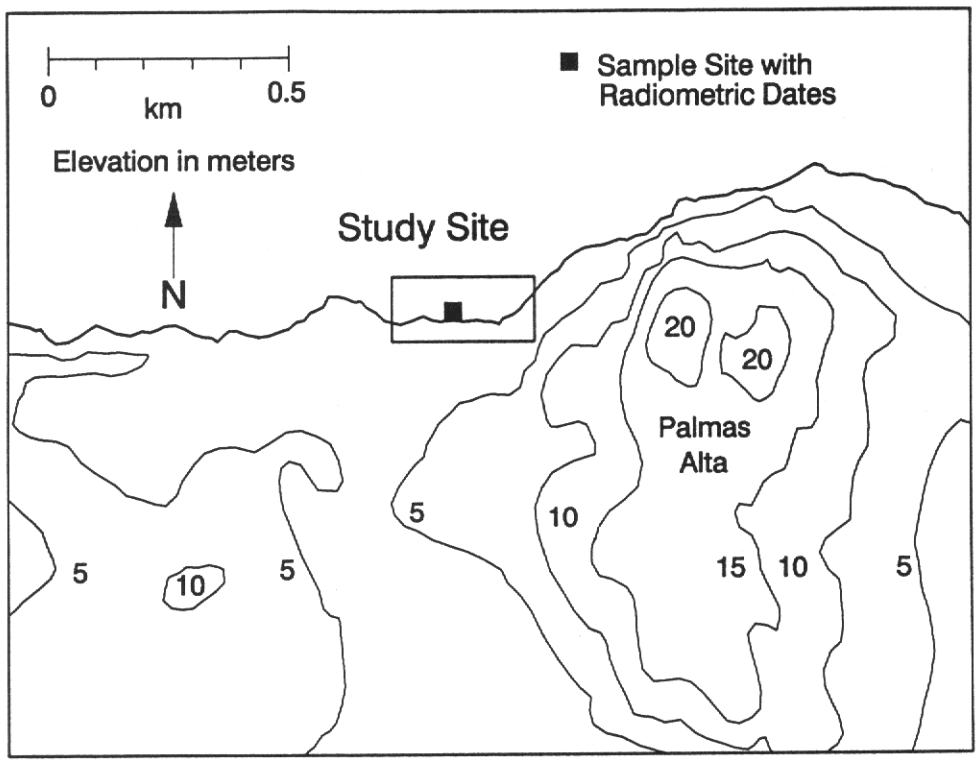

Figure 7. Study site location in the Palmas Alta Region. The hills are composed of Pleistocene eolianite.

elevation of the deposits are compared with the sea-level curve synthesized by Moore (1982) (Figure 8). We have chosen Moore's (1982) sea-level curve, rather than the more recent one published by Chappell and Shackleton (1986), because it incorporates data from both the Pacific and Atlantic Ocean basins and is probably more applicable to Puerto Rico. It is generally accepted that sea level was 6 ± 4 m higher than present approximately 125,000 ± 10,000 YBP (Bloom et al., 1974; Yonekura, 1983; Lajoie, 1986; Edwards et al., 1987) (Figure 8). These data indicate that northwestern Puerto Rico has been uplifted by at least 4 m to 6 m during the last 125,000 years. Performing the calculations on these data produces a minimum rate of uplift of between 0.03 mm/year and 0.05 mm/year during the late Pleistocene. This is a relatively low rate of tectonic uplift when compared to 0.14 mm/year for Jamaica (Cant, 1973) and 0.3 mm/year for Haiti (Dodge et al., 1983). However, it is on the same order of magnitude as the southeastern Dominican Republic (Schubert and Cowart, 1980; F.W. Taylor, personal comm., 1990) and St. Croix (Hubbard et al., 1989) which are in the immediate vicinity of Puerto Rico. This variability of tectonic uplift rates in the northeastern Caribbean is due to the complex tectonic structure of the Northern Caribbean Plate Boundary Zone (Mann et al., in press).

Neritic limestone deposited during the Pliocene (Quebradillas Limestone) is now found at elevations of up to 200 m in northwestern Puerto Rico (Monroe, 1969). The upper member of the Quebradillas Limestone was largely deposited in deep water about 4 million years ago (Moussa et al., 1987). The presence of cross-stratified beach calcarenites and calcareous sandstones and shallow water foramiferal assemblages (10 m to 35 m depths) at the top of the upper member of the Quebradillas Limestone (Seiglie and Moussa, 1984) suggests that it was deposited during a regression. According to Haq et al. (1987) sea level 4 million years ago was approximately 60 m higher than present. All of these data taken together indicate tectonic uplift of at least 130 m, and possibly as much as 200 m, of the Quebradillas Limestone following its deposition and provide a minimum uplift rate of between 0.03 mm/year and 0.05 mm/year. This is in virtual agreement with the minimum rate of uplift range determined for northwestern Puerto Rico during the late Pleistocene. Therefore, we suggest that the rate of tectonic uplift has been slow and consistent in northwestern Puerto Rico during

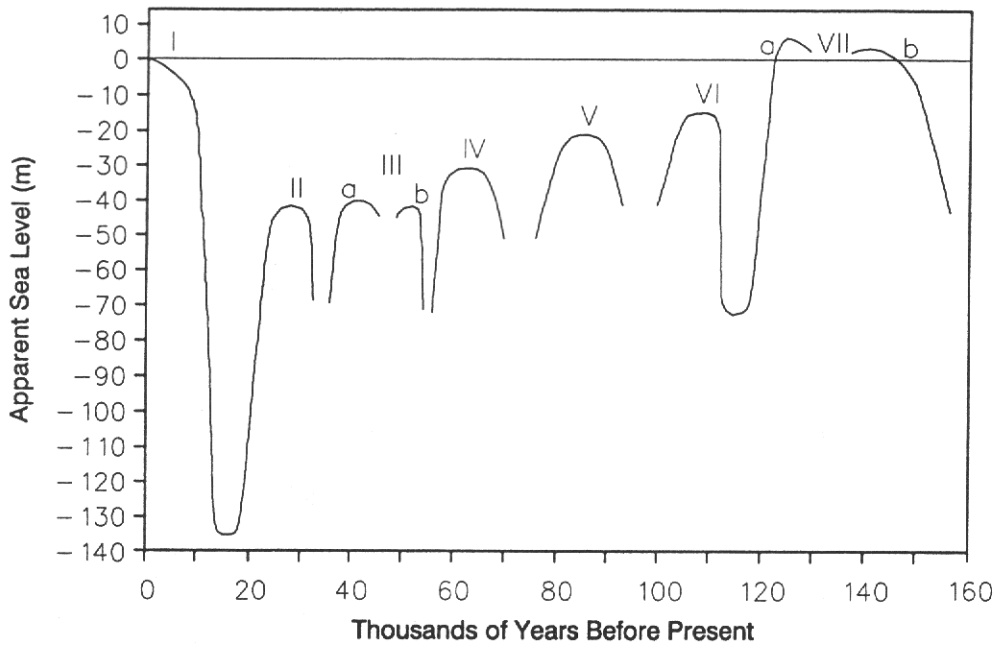

Figure 8. Late Pleistocene sea-level curve relative to present sea level (after Moore, 1982). Roman numerals follow the designations assigned by Chappell (1974) to the Huon, New Guinea terraces. This sea-level curve is used instead of the more recent sea-level curve of Chappell and Shackleton (1986) because it incorporates data from the west-central Atlantic Ocean and Caribbean Sea regions.

the last 4 million years.

Marine terrace deposits, elevated beach deposits and wave-cut notches are found at elevations of 2-3 m throughout the coast of Puerto Rico and on its associated islands (Kaye, 1959a; Williams, 1965; Seiders et al., 1972). As previously discussed, the 2-3 m marine terrace and coastal swamp deposits in northwestern and north-central Puerto Rico have been radiometrically dated and are late Holocene in age. Based on the pervasive presence of this coastal feature around Puerto Rico and the lack of any evidence supporting its co-seismic uplift we conclude that sea level was 2-3 m higher than present between 1,500 and 3,300 YBP.

ACKNOWLEDGEMENTS

Funding for the radiometric dating of coral samples was provided by a National Science Foundation EPSCoR Grant to the Department of Geology at the University of Puerto Rico. ^{14}C dates were determined by Beta Analytic Inc.. $^{230}Th/^{234}U$ dates were determined by Willard S. Moore of the Department of Geological Sciences at the University of South Carolina in Columbia.

REFERENCES

Birch, F.S., 1986, Isostatic, thermal, and flexural models of the subsidence of the north coast of Puerto Rico: Geology, v. 14, p. 427-429.

Bloom, A.L., Broecker, W.S., Chappell, J.M.A., Matthews, R.K. and Mesolella, K.J., 1974, Quaternary sea level fluctuations on a tectonic coast: New $^{230}Th/^{234}U$ dates from the Huon Peninsula, New Guinea: Quaternary Research, v. 4, p. 185-205.

Cant, R.V., 1973, Jamaica's Pleistocene reef terraces: Geologie en Mijnbouw, v. 52, p. 157-160.

Chappell, J.M.A., 1974, Geology of coral terraces, Huon Peninsula, New Guinea: A study of Quaternary tectonic movements and sea level changes: Geological Society of America Bulletin, v. 85, p. 553-570.

_____ and Shackleton, N.J., 1986, Oxygen isotopes and sea level: Nature, v. 324, p. 137-140.

Dodge, R.E., Fairbanks, R.G., Benninger, L.K. and Maurrasse, F., 1983, Pleistocene sea levels from raised coral reefs of Haiti: Science, v. 219, p. 1423-1225.

Edwards, R.L., Chen, J.H., Ku, T.-L. and Wasserburg, G.J., 1987, Precise timing of the last interglacial period from mass spectrometric determination of Thorium-230 in corals: Science, v. 236, p. 1547-1553.

Fox, P.J. and Heezen, B.C., 1975, Geology of the Caribbean crust in A.E.M. Nairn and F.G. Stehli (eds.), The ocean basins and margins, v. 3, New York, Plenum Press, 706 p.

Horsfield, W.T., 1975, Quaternary vertical movements in the Greater Antilles: Geological Society of America Bulletin, v. 86, p. 933-938.

Haq, B.U., Hardenbol, J. and Vail, P.R., 1987, Chronology of fluctuating sea levels since the Triassic: Science, v. 235, p. 1156-1167.

Hubbard, B., 1923, The geology of the Lares District: New York, New York Academy of Sciences, Scientific Survey of Porto Rico and the Virgin Islands, v. 2, part 1, 115 p.

Hubbard, D., Venger, L, Parsons, K. and Stanley, D., 1989, Geologic development of the West End Terrace System on St. Croix, U.S. Virgin islands, in D.K. Hubbard (ed.), Terrestrial and Marine Geology of St. Croix, U.S. Virgin Islands: Teague Bay, St. Croix, Special Pub. No. 8, West Indies Laboratory, p. 73-83.

Kaye, C.A., 1959a, Shoreline features and Quaternary shoreline changes, Puerto Rico: Washington D.C., U.S. Printing Office, U.S. Geological Survey Professional Paper 317-B, p. 49-140.

_____ 1959b, Geology of Isla Mona Puerto Rico, and notes on age of Mona Passage: Washington D.C., U.S. Printing Office, U.S. Geological Survey Professional Paper 317-C, p. 141-178.

Lajoie, K.R., 1986, Coastal tectonics, in R.E. Wallace (ed.), Active Tectonics: Washington D.C., National Academy Press, p. 95-124.

Lighty, R.G., Macintyre, I.G. and Stuckenrath, R., 1982, Acropora palmata reef framework: A reliable indicator of sea level in the Western Atlantic for the past 10,000 years: Coral Reefs, v. 1, p. 125-130.

Lobeck, A.K., 1922, The physiography of Porto Rico: New York, New York Academy of Sciences, Scientific Survey of Porto Rico and the Virgin Islands, v. 1, part 4, p. 301-384.

Mann, P., Schubert, C. and Burke, K., in press, Review of Caribbean neotectonics, in G. Dengo and J.E. Case (eds.), The Caribbean region: Boulder, Colorado, G.S.A., The Geology of North America, v. H.

McCann, W.R. and Sykes, L.R., 1984, Subduction of aseismic ridges beneath the Caribbean plate; Implications for the tectonics and seismic potential of the northeastern Caribbean: Journal of Geophysical Research, v. 89, p. 4493-4519.

Meyerhoff, A.A., Krieg, E.A., Cloos, J.D., and Taner, I., 1983, Petroleum potential of Puerto Rico: Oil and Gas Journal, p. 113-120.

Monroe, W.H., 1968, High level Quaternary beach deposits in northwestern Puerto Rico: Washington D.C., U.S. Govt Printing Office, U.S.G.S. Prof. Paper 600-C, p. C140-C143.

_____ 1969, Geologic map of the Moca and Isabela Quadrangles Puerto Rico: Washington D.C., U.S. Geological Survey, Miscellaneous Geologic Investigations Map I-565, 1 sheet.

Moore, W.S., 1982, Late Pleistocene sea-level history, in M. Ivanovich and R.S. Harmon (eds.), Uranium Series Disequilibrium: Applications to Environmental Problems: Oxford, Clarendon Press, p. 481-496.

Moussa, M., Seiglie, G.A., Meyerhoff, A.A., and Taner, I., 1987, The Quebradillas Limestone (Miocene-Pliocene), northern Puerto Rico, and tectonics of the northeastern Caribbean margin: GSA Bull., v. 99, p. 427-439.

Perfit, M.R., Heezen, B.C., Rawson, M., and Donnelly, T.W., 1980, Chemistry, origin and tectonic significance of metamorphic rocks from the Puerto Rico trench: Marine Geology, v. 34, p. 125-166.

Pierce, K.L., Dating methods, in R.E. Wallace (ed.), Active Tectonics: Washington D.C., National Academy Press, p. 195-214.

Schneidermann, N., Beckmann, J.P., and Heezen, B.,C., 1972, Shallow water carbonates from the Puerto Rico Trench region: Margarita, Venezuela, Sixth Caribbean Geology Conference, p. 423-425.

Schubert, C. and Cowart, J.B., 1980, Terrazas marinas del Pleistoceno a lo largo de la costa suroriental de la Republica Dominicana; Cronologia preliminar: Transactions of the 9th Caribbean Geological Conference, Santo Domingo, Dominican Republic, p. 681-688.

Seiders, V.M, Briggs, R.P., and Glover, L., III., 1972, Geology of Isla Desecheo, Puerto Rico, with notes on the Great Southern Puerto Rico Fault Zone and Quaternary Stillstands of the sea: Washington D.C., U.S. Printing Office, U.S. Geological Survey Professional Paper 739, 22 p.

Seiglie, G.A. and Moussa, M.T., 1984, Late Oligocene-Pliocene transgressive-regressive cycles of sedimentation in northwestern Puerto Rico, in J.S. Schlee (ed.), Interregional Unconformities and Hydrocarbon Accumulation: Tulsa, Oklahoma, The American Association of Petroleum Geologists, AAPG Memoir 36, p. 89-95.

Sykes, L.R., McCann, W.R., and Kafka, A.L., 1982, Motion of Caribbean plate during last 7 million years and implications for earlier Cenozoic movements: Journal of Geophysical Research, v. 87, p. 10,656-10,676.

Weaver, J.D., 1966, Higher level erosion surfaces in the Caribbean: Third Caribbean Geological Conference, Jamaica Geol. Survey Pub. 95, p. 10-12.

_____ 1970, Terraces in western Puerto Rico: Fourth Caribbean Geology Conference, Port of Spain, Trinidad, p. 243-245.

_____ 1971, Review of geomorphological and Pleistocene research in the Caribbean: Transactions of the Fifth Caribbean Geological Conference, Geol. Bull. No. 5, Queens College Press, p. 201-206.

Williams, R.S., Jr., 1965, Geomorphology of a portion of the northern coastal plain of Puerto Rico: Pennsylvania State University, unpub. Ph.D. dissertation, 191 p.

Woodroffe, C.D., Stoddart, D.R., Harmon, R.S. and Spencer, T., 1983, Coastal morphology and late Quaternary history, Cayman Islands, West Indies: Quaternary Research, v. 19, p. 64-84.

Yonekura, N., 1983, Late Quaternary vertical crustal movements in and around the Pacific as deduced from former shoreline data in Thomas W.C. Hilde and S. Uyeda, (eds.), Geodynamics of the Western Pacific-Indonesian Region: Washington D.C., American Geophysical Union, Geodynamics Series, Volume 11, p. 41-50.

DEPTH OF EMPLACEMENT OF GRANITOID PLUTONIC ROCKS IN THE EASTERN GREATER ANTILLES ISLAND ARC

Edward G. Lidiak
Department of Geology and Planetary Science
University of Pittsburgh
Pittsburgh, Pennsylvania 15260

ABSTRACT

Electron-microprobe analyses of magmatic hornblende from granitoid rocks of the Morovis stock, San Lorenzo batholith, Vieques pluton, Utuado pluton, Rio Blanco stock, and Virgin Islands batholith have been carried out for the purpose of estimating the pressure at which the intrusions were emplaced. The intrusions have calc-alkalic chemical affinities and consist mainly of granodiorite and quartz monzodiorite, with lesser amounts of quartz diorite, tonalite, and gabbro. Hornblende, with different Al content in the various plutons, typically occurs in association with quartz, plagioclase, K-feldspar, biotite, magnetite, and sphene.

Analyses of the total Al content of hornblende, which may be used as an empirical geobarometer, suggest that the intrusions were emplaced at low to medium pressures and show a progressive decrease in depth of emplacement from about 10 km for the oldest pluton to about 4 km for the youngest pluton. These geobarometric data help characterize the evolution of the crust in the eastern Greater Antilles island arc in late Cretaceous and early Tertiary time and indicate an average uplift rate of 0.01-0.02 cm/yr.

INTRODUCTION

The Caribbean region encompasses a complex of Cretaceous to Cenozoic island arc rocks which includes both active and inactive arc segments that developed by interaction of the Pacific, proto-Caribbean, and Atlantic oceanic plates, the Caribbean oceanic plateau, and the bounding continental plates (Burke, 1988; Donnelly, 1989). Each of the various arc segments or terranes that are presently preserved evolved in response to a related series of tectonic events but each has its own geological, geochemical, and geophysical characteristics. Considerable attention has justifiably been given to reconstruction of the Caribbean plate and its highly mobile history in which various geologic elements have been displaced by hundreds of kilometers.

Also of considerable interest is the origin and evolution of the Caribbean lithosphere and specifically its crust. Seismic refraction studies (Officer and others, 1959; Edgar and others, 1971; Boynton and others, 1979) have demonstrated that the Caribbean crust is thicker than typical oceanic crust and that beneath islands such as Puerto Rico crustal thickness approaches 30-35 km. It seems evident that if the Caribbean evolved as an ocean-ocean arc system as most researchers have proposed, then the thickened Caribbean crust owes its origin not only to tectonic processes but also to igneous and metamorphic processes that occurred during island arc formation. Knowledge of the composition as well as the intensive parameters of temperature and pressure are thus critical to understanding the origin of the crust in the Caribbean as these parameters can provide constraints on the evolution of the various rock systems.

The igneous geology of the Caribbean region has been summarized in a series of papers by Donnelly (Donnelly and Rogers, 1978; Donnelly and Rogers, 1980; Donnelly and others, 1990). Most of the research has been carried out on the volcanic rocks which include oceanic plateau basalts, primitive island arc suite, calc-alkaline suites, and rift-related suites. Comparatively little emphasis has been given to the intrusive rocks, and only limited data are available.

In this paper some preliminary results are presented on the chemical mineralogy of hornblende from a suite of granitoid plutons in Puerto Rico, including Vieques, and the nearby Virgin Islands with the purpose of presenting estimates on the pressures (and depths) at which the plutons were emplaced. The use of hornblende as a geobarometer is based on the correlation between the total Al (Al^T) content of hornblende and the estimated pressures of crystallization of calc-alkaline plutons (Hammarstrom and Zen, 1986; Hollister and others, 1987; Rutter and others, 1989). Data of this type which permit the estimation of depths of plutonic emplacement and the average rates of uplift since late Cretaceous time have not previously been published for any igneous rocks in the Caribbean region.

GEOLOGIC SETTING

Puerto Rico and the Virgin Islands form the eastern part of the inactive Greater Antilles island arc. The earliest arc deposits are the pre-Albian submarine keratophyres and spilites (Water Island Formation) of the Virgin Islands and their pre-Robles equivalents of Puerto Rico. These rocks comprise the primitive island arc suite of Donnelly and Rogers (1980). The primitive suite is overlain by Albian to Paleocene shallow-water submarine and terrestrial deposits with distinct calc-alkaline affinities and which reflect an emergent island arc. The main granitoid plutons, which are the topic of this report, were emplaced during this second main phase of arc evolution. The intrusive igneous activity in Puerto Rico occurred mainly during late Cretaceous time but continued on a lesser scale into the Eocene. Plutonism in the Virgin Islands continued into the Oligocene. Active vulcanism ceased by late Oligocene time and was succeeded by platform-type clastic and carbonate sedimentation.

The plutons discussed in this report are, from west to east, the Utuado pluton, Morovis stock, San Lorenzo batholith, Rio Blanco stock, Vieques pluton, and Virgin Islands batholith (Figure 1). They occupy the core of the eastern Greater Antilles island arc. The plutons vary in size and compositional complexity from the large San Lorenzo batholith having an outcrop area of 500 km^2 and composed of at least three distinct compositional units, through the medium-size Utuado pluton with an outcrop area of about 200 km^2 and containing two mappable units, to the smaller and essentially compositionally uniform Morovis and Rio Blanco stocks each having outcrop areas of about 20 km^2 (Cox and others, 1977; Kesler and Sutter, 1979). The Virgin Islands batholith occupies about 35 km^2 of land area, but large parts of the batholith may be submerged (Longshore, 1965). It is compositionally diverse.

The effects of contact metamorphism along the margins of the plutons are minor. Assemblages corresponding to the hornblende hornfels facies are present locally adjacent to the San Lorenzo batholith (Fettke, 1924), the Utuado pluton (Chen, 1969), and the Rio Blanco stock (Seiders, 1971). Both hornblende hornfels and pyroxene hornfels occur locally adjacent to the Virgin Islands batholith (Longshore, 1965). Pressure

Larue, D.K., and Draper, G. (eds.),
Transactions of the 12th Caribbean Geological Conference, St. Croix, U.S.V.I., Miami Geological Society, P.O. Box 431552, South Miami, FL 33243, U.S.A

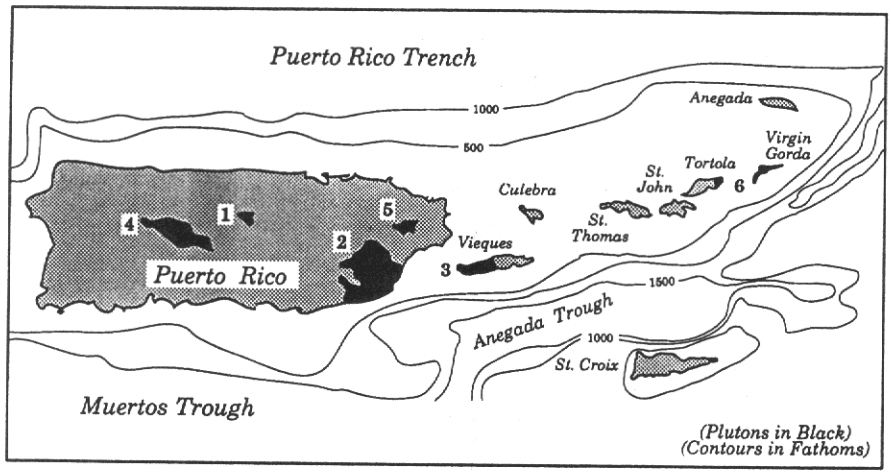

Figure 1. Location map of Puerto Rico and the Virgin Islands. Plutons discussed in text: 1, Morovis stock; 2, San Lorenzo batholith; 3, Vieques pluton; 4, Utuado pluton; 5, Rio Blanco stock; 6, Virgin Islands batholith.

estimates based on critical mineral assemblages from the contact aureoles are not presently available. Longshore (1965), however, on the basis of general facies associations, concluded that pressures were 1-3 kbar during contact metamorphism of the Virgin Islands batholith. Field relationships suggest that the other plutons were also emplaced at shallow levels.

Samples used in this study were selected in so far as possible on (1) the basis of location within the interior of each pluton and away from possible thermal effects of later igneous activity, (2) lack of alteration (both surficial and otherwise), and (3) their being compositionally representative of the main phase or phases of each pluton. The U. S. Geological Survey quadrangle maps were used where available for geologic control.

ANALYTICAL METHODS

Hornblende crystals were analyzed for Si, Al, Ti, Cr, Fe (total), Mn, Mg, Ca, Na, and K using an automated CAMECA SX-50 electron probe microanalyser fitted with four wavelength dispersive spectrometers and one energy dispersive spectrometer. Operating conditions were set at 15-kV accelerating voltage and 20 nannoamps beam current and with a spectrum accumulation time of 20 seconds.

Between three and six different thin sections (rock samples) from each pluton were analyzed. For samples used in the pressure determinations, at least two hornblende crystals were examined in each thin section and a minimum of eight separate spot analyses were made of each thin section. Results are summarized in Tables 1 and 2. Hornblende analyses reported here are from the rims of crystals, all analyses being from within 20 μm of a crystal edge. Systematic study of the interiors of hornblende crystals were not carried out as part of this study; however, it is apparent from random spot analyses that the hornblende is typically zoned with respect to Si, Al, Fe, and Mg.

APPLICABILITY OF THE GEOBAROMETER

The hornblende geobarometer proposed by Hammarstrom and Zen (1986) is based on the correlation between estimated pressures of crystallization of calc-alkalic granitoid rocks and the Al^T content of hornblende. For the geobarometer to be applicable to a suite of calc-alkalic plutons, the following conditions should be satisfied (Hammarstrom and Zen, 1986; Hollister and others, 1987): (1) bulk rocks must have calc-alkalic compositions; (2) hornblende must be magmatic and not modified by sub-solidus reaction; (3) the primary phases quartz, plagioclase, K-feldspar, hornblende, biotite, sphene, and magnetite must be co-magmatic; (4) hornblende rims only should be used in order to reflect more closely final crystallization conditions; (5) plagioclase compositions should be essentially constant; and (6) pressures of emplacement should be greater than ~2 kbars to reduce the effects of temperature variability. The hornblende studied by Hammarstrom and Zen (1986) show a strong linear correlation between Al^T and Al^{iv}, and they determined that the correlation between pressure and Al^T in hornblende can be described by the linear regression $P = -3.92 + 5.03Al^T$. This regression equation is used in the present paper to calculate pressures of emplacement.

HORNBLENDE COMPOSITIONS

Average hornblende analyses that were used in the pressure calculations are listed in Table 1. Cation proportions were calculated on a basis of 23 oxygens, with total Fe as FeO. Total Al in these hornblende crystals varies from a high of 1.36 cations in the Morovis stock to a low of 0.99 cations in the Virgin Islands

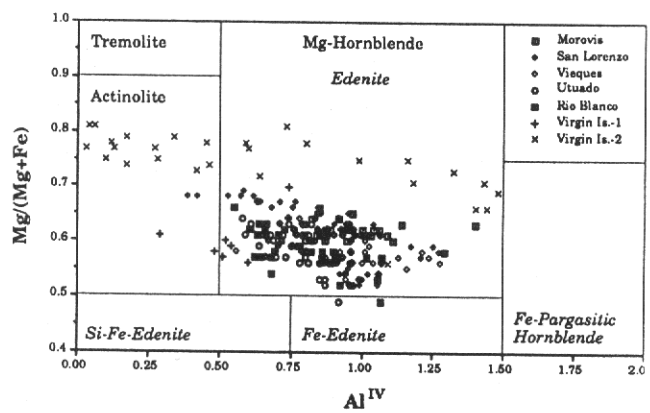

Figure 2. Compositions of hornblende from intrusive granitoids of the eastern Greater Antilles island arc. Modified IMA classification of calcic hornblendes (Leake, 1978; Hammarstrom and Zen, 1986). Italicized type is nomenclature for (Na + K) ≥ 0.50; plain type is for (Na + K) ≤ 0.50. Virgin Is.-1, analyses in Table 1; Virgin Is.-2, analyses in Table 2.

Table 1. Hornblende Analyses, Eastern Greater Antilles Granitoids

Pluton	Morovis	San Lorenzo	Vieques	Utuado	Rio Blanco	Virgin Is.
Samples (n)	3	4	4	5	3	3
Analyses (n)	25	49	43	42	33	12
SiO_2	46.35	47.23	46.69	47.87	48.24	50.78
TiO_2	1.27	1.23	1.21	1.23	1.04	0.55
Al_2O_3	7.64	7.35	7.35	7.18	6.81	5.69
Cr_2O_3	0.01	0.00	0.01	0.02	0.00	0.00
FeO_T	12.84	12.81	13.70	13.31	14.36	14.15
MnO	0.82	0.94	1.11	0.74	0.86	1.37
MgO	11.63	11.39	10.81	10.57	11.46	12.11
CaO	12.30	11.96	12.15	12.26	11.77	11.48
Na_2O	1.63	1.62	1.40	1.43	1.35	1.18
K_2O	0.85	0.68	0.63	0.73	0.33	0.39
F	0.34	0.14	0.12	0.23	0.07	0.06
Sum	95.69	95.36	95.20	95.57	96.31	97.43
Cations Based on 23 Oxygens:						
Si	7.00	7.12	7.09	7.20	7.20	7.45
Al^{iv}	1.00	0.88	0.91	0.80	0.80	0.55
Al^{vi}	0.36	0.43	0.41	0.48	0.40	0.44
Ti"	0.14	0.14	0.14	0.14	0.12	0.05
Cr	0.00	0.00	0.00	0.00	0.00	0.00
Fe	1.62	1.62	1.74	1.68	1.80	1.73
Mn	0.10	0.12	0.14	0.09	0.11	0.14
Mg	2.62	2.56	2.45	2.37	2.55	2.65
Ca	1.99	1.93	1.98	1.98	1.88	1.80
Na	0.48	0.47	0.41	0.42	0.39	0.34
K	0.16	0.13	0.12	0.14	0.06	0.07
Sum	15.48	15.40	15.39	15.30	15.31	15.22
Al^T	1.36	1.31	1.32	1.28	1.20	0.99
Sigma (Al^T)	0.08	0.19	0.11	0.14	0.15	0.12
Pressure (kbar)	2.92	2.67	2.72	2.52	2.12	1.06
Depth (km)	10.25	9.37	9.54	8.84	7.42	3.72

batholith. A plot of Al^T vs. Al^{iv} yields a least-square regression line for these analyses of $Al^{iv} = -0.54 + 1.09Al^T$, $r^2 = 0.94$. The slope of this equation is steeper than the one reported by Hammarstrom and Zen (1986), possibly because of generally lower Al^{vi} content and more restricted range of Al^T, however, its linearity and similarity to the Hammarstrom and Zen curve suggest that the barometer is also applicable to these Caribbean plutonic rocks.

The range of hornblende compositions in the six plutons is shown on Figure 2, a modified version of the IMA classification of calcic amphiboles (Leake, 1978; Hammarstrom and Zen, 1986). Each point represents an individual spot analysis. Essentially all of the analyses used in the pressure calculation are edenites. Samples from a gabbro, a diorite, and a tonalite from the Virgin Islands batholith are also plotted (Fig. 2; Table 2) but were excluded from the calculations because of the previously noted compositional and mineralogical constraints imposed by the geobarometer (see subsequent discussion of Virgin Islands batholith).

DESCRIPTION OF INDIVIDUAL PLUTONS

General

All of the intrusions discussed in this report, with the exception of the Vieques pluton, have been the subject of field mapping and at least reconnaissance major element and K-Ar geochronologic studies (references for each pluton is given below). Unfortunately, only a limited amount of published modal, mineralogical, or textural data are available on the plutons (Nelson, 1968; Chen, 1969). It is therefore difficult to evaluate the distribution, abundance, and mineral assemblages of the main rock types in each of the plutons. However, major element analyses and calculated CIPW norms provide an alternative basis for characterizing the plutons according to major rock types. Figure 3 is a plot of the normative proportions of quartz, plagioclase, and K-feldspar utilizing the IUGS classification scheme (Streckeisen, 1976). This normative plot approximates closely the standard modal plot because there are only minor differences in the specific gravity of the three end components and because the K-feldspars in the plutons is only sparsely perthitic.

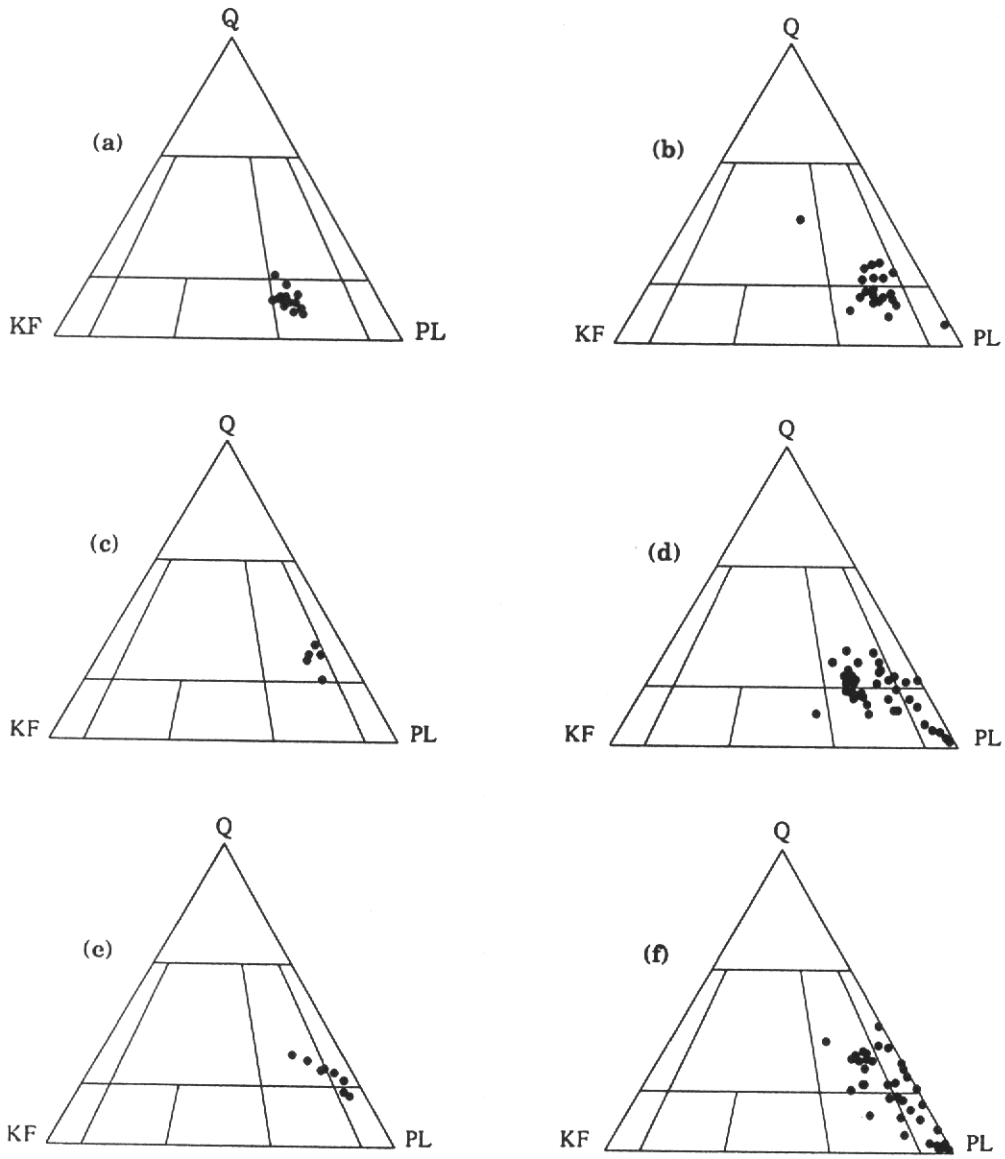

Figure 3. Quartz-K-Feldspar-Plagioclase compositions of eastern Greater Antilles granitoid rocks. All plotted data are CIPW norms except Fig. 3c which are modal compositions. (a), Morovis stock (Kesler and Sutter, 1979); (b), San Lorenzo batholith (Kesler and Sutter, 1979); (c), Vieques pluton (this report); (d), Utuado pluton (Chen, 1969); (e) Rio Blanco stock (Kesler and Sutter, 1979); (f), Virgin Islands batholith (Longshore, 1965). Classification field boundaries are from Streckeisen (1976).

Morovis Stock

The Morovis stock (Fig. 4) is a relatively small unit of about 20 km^2 that is intrusive into the potassic Rio Orocovis Formation (Berryhill, 1965; Lidiak, 1965). The stock is medium grained and texturally homogeneous and contains conspicuous laths of K-feldspar and subparallel crystals of hornblende throughout. Normative data (Fig. 3a) indicate that the stock consists primarily of quartz monzodiorite. The stock is the oldest of the intrusives considered in this report, having a K-Ar date on hornblende of 88 Ma (Cox and others, 1977), and is one of the most potassic intrusives in the eastern Greater Antilles. The average K_2O content is 3.9 percent (Kesler and Sutter, 1979).

The mineral assemblage is quartz, zoned plagioclase (An_{45}-An_{35}), K-feldspar, hornblende, chloritized biotite, sphene, magnetite, and zircon. Quartz is mainly intergranular and commonly adjacent to hornblende. Hornblende is greenish-brown and is mainly subhedral to euhedral, zoned, and less commonly poikilitic.

San Lorenzo Batholith

The San Lorenzo batholith (Fig. 5) is the largest pluton in the eastern Greater Antilles having an outcrop extent of about 500 km^2. It is a complex intrusion and has been divided into three mappable units: granodiorite-quartz diorite (comprising 75 percent of the batholith), a quartz monzonite-quartz diorite, and a small unit of diorite-gabbro (Cox and others, 1977). K-feldspar is a prominent mineral in most of the granitoid rocks. The available normative compositions (Fig. 3b) of samples from the two main granitoid units plot in the quartz monzodiorite and granodiorite fields. Some of the rocks are distinctly potassic and similar to rocks of the Morovis stock. An average K-Ar date on hornblende from the main granodiorite-quartz diorite unit is about 73 Ma (Cox and others, 1977). The batholith has had a more complex history;

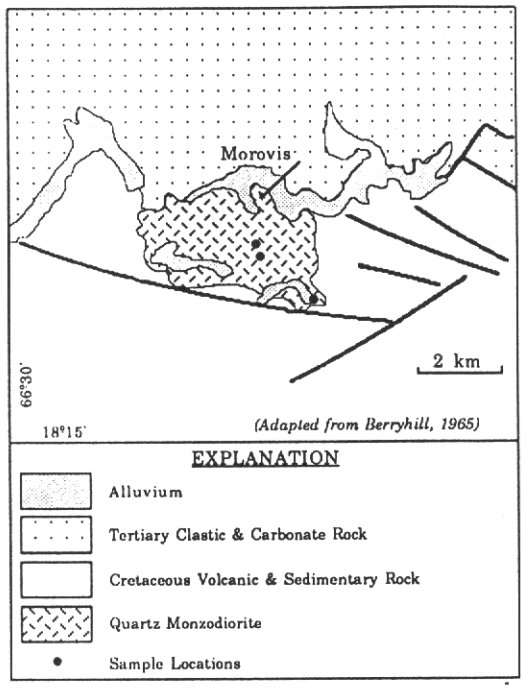

Figure 4. Generalized geologic map of Morovis stock.

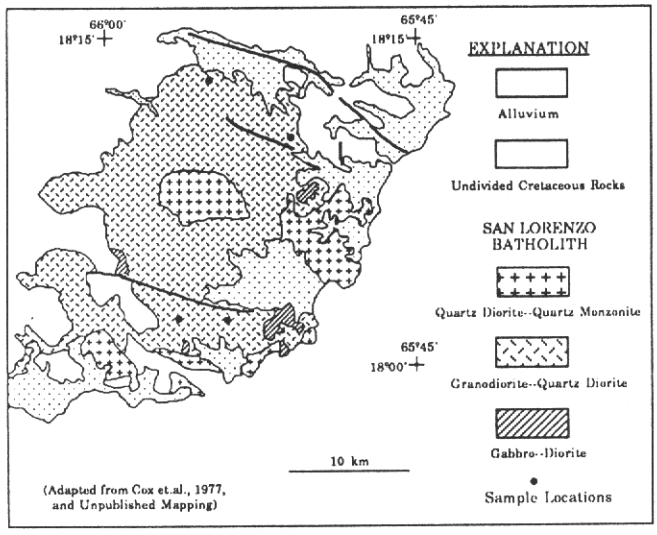

Figure 5. Generalized geologic map of San Lorenzo batholith.

for example, the diorite-gabbro unit yields K-Ar ratios older than 78 Ma and the quartz monzonite-quartz diorite unit has values as low as about 66 Ma (Cox and others, 1977). The average K_2O content of the main-phase granodiorite-quartz diorite is 2.5 percent (Kesler and Sutter, 1979).

Only samples from the main-phase granodiorite-quartz diorite unit were studied in this report. They are mainly medium to coarse grained and only moderately porphyritic. Samples from which hornblende was analyzed contain the assemblage quartz, zoned plagioclase (An_{40}-An_{50}), K-feldspar, hornblende, biotite, sphene, magnetite, apatite, and zircon.

The hornblende is mainly euhedral to subhedral, some with locally resorbed edges, and poikilitic. In one of the unanalyzed samples, the typical greenish-brown hornblende is partially replaced by a light green-blue amphibole having uneven extinction or by a complex intergrowth of actinolite, chlorite, epidote and an opaque mineral.

Vieques Pluton

The Vieques pluton (Fig. 6) crops out in an area of about 80 km^2 in the western part of Isla Vieques, but it probably underlies most of the island. The pluton has been mapped only in reconnaissance (Briggs and Akers, 1965) and chemical analyses are not yet available. The few modal analyses that are available (Fig. 3c) plot in the granodiorite field and these determinations are in agreement with observations by the author that granodiorite is the main phase of the pluton. However, portions of the pluton are not accessible because of military restrictions. K-feldspar is a subordinate phase in most of the rocks.

Rock samples are typically medium to coarse grained and moderately porphyritic with distinctly aligned hornblende crystals. In thin section, the primary mineral assemblage consists of quartz, zoned plagioclase (An_{40}-An_{50}), K-feldspar (subordinate), hornblende, biotite, magnetite, sphene (rare), and zircon. Hornblende is mainly poikilitic and moderately zoned. In some sections the primary greenish-brown hornblende is partly to completely replaced by light green amphibole, chlorite, epidote, and an opaque mineral.

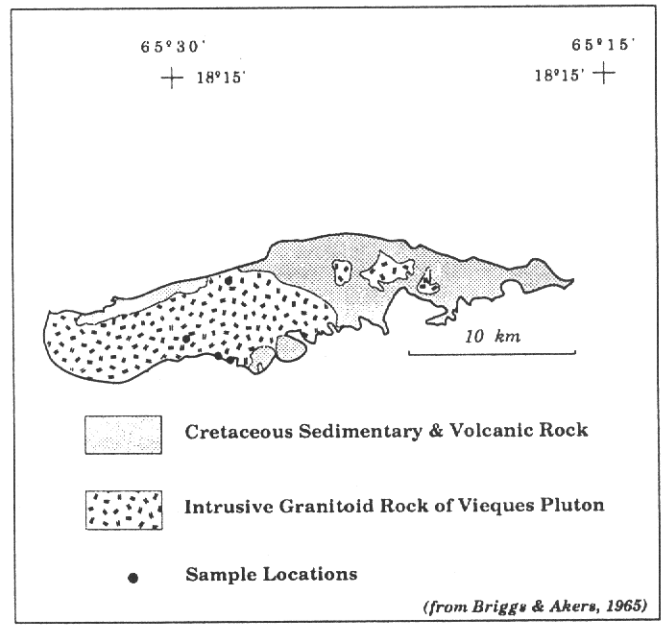

Figure 6. Generalized geologic map of Vieques pluton.

Utuado Pluton

The Utuado pluton (Fig. 7) occupies an area of about 200 km^2 and is a composite pluton that is elongate in the direction of the regional structure. The main phase of the pluton has been mapped as quartz diorite, granodiorite, and quartz monzonite (Weaver, 1958; Chen, 1969; Cox and others, 1977) which has an average K-Ar hornblende date of 67 Ma (Cox and others, 1977). The CIPW normative plot (Fig. 3d) indicates that the pluton is comprised of gabbro, diorite, tonalite, quartz monzodiorite, and granodiorite. Many of the rocks have a distinct potassic signature, and the average K_2O content of granitoid rocks from the main-phase pluton is 2.4 percent (Chen, 1969).

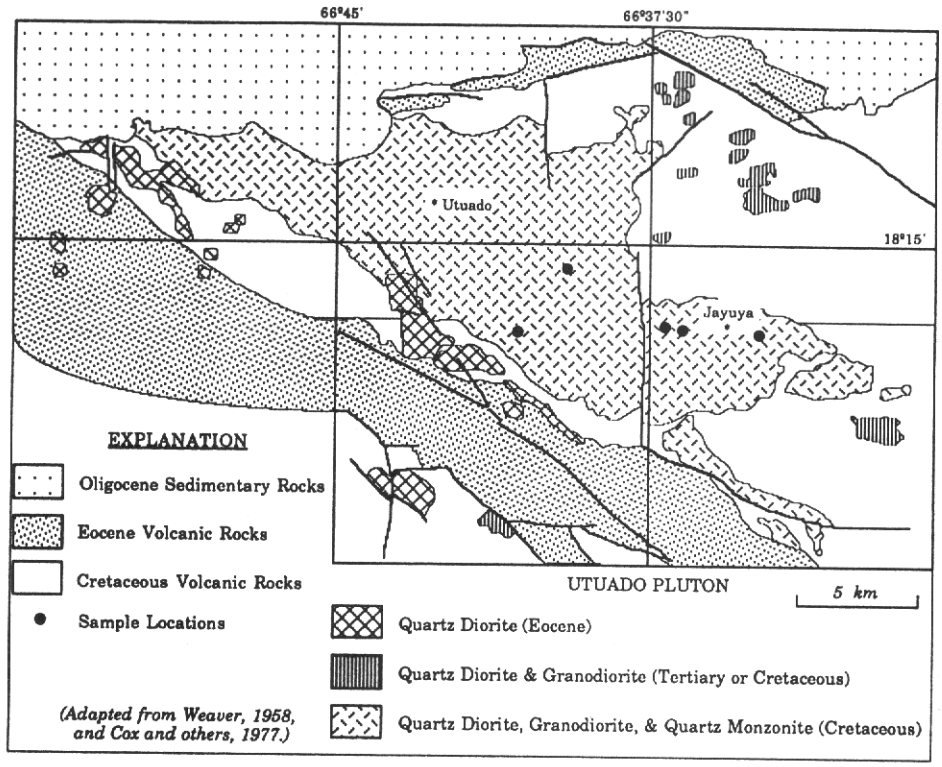

Figure 7. Generalized geologic map of Utuado pluton

The granitoid rocks are mainly medium to coarse grained and equigranular. Samples studied in this report have a generally consistent mineral assemblage of quartz, zoned plagioclase (An_{25}-An_{40}), K-feldspar, hornblende, biotite, sphene, and magnetite. The biotite is commonly chloritized and both biotite and hornblende are locally replaced by intergrown chlorite, epidote, and opaques. The analyzed hornblende is moderately zoned, euhedral to subhedral, poikilitic, and some crystals show resorption effects along rims.

Rio Blanco Stock

The Rio Blanco stock (Fig. 8) crops out north of the San Lorenzo batholith in an area of about 20 km^2. Seiders (1971) mapped the stock as a quartz diorite and diorite. CIPW norms (Fig. 3e) plot within the quartz diorite, tonalite, and granodiorite fields. These rocks contrast with the other Puerto Rican intrusives discussed here in containing less normative and modal K-feldspar. The average K_2O content is 1.2 percent (Kesler and Sutter, 1979). Co-existing hornblende and biotite yield concordant K-Ar dates of 46 Ma (Cox and others, 1977).

The rocks are medium to coarse grained and equigranular to porphyritic with phenocrysts of both plagioclase and hornblende. Aligned mafic inclusions and large hornblende megacrysts are abundant in some samples. The minerals present are quartz, complexly zoned plagioclase (An_{35}-An_{50}), K-feldspar, hornblende, biotite, magnetite, sphene (±), apatite, and zircon. Glomeroporphyritic aggregates consist of hornblende, plagioclase, biotite, and magnetite. Hornblende occurs both as large crystals with slightly poikilitic cores and thin exsolution lamellae, surrounded by complexly poikilitic zones, and clear, slightly zoned margins, and as small, slightly zoned, clear crystals. Only the latter were analyzed. Replacement patches of chlorite, epidote, and opaques (±) are minor.

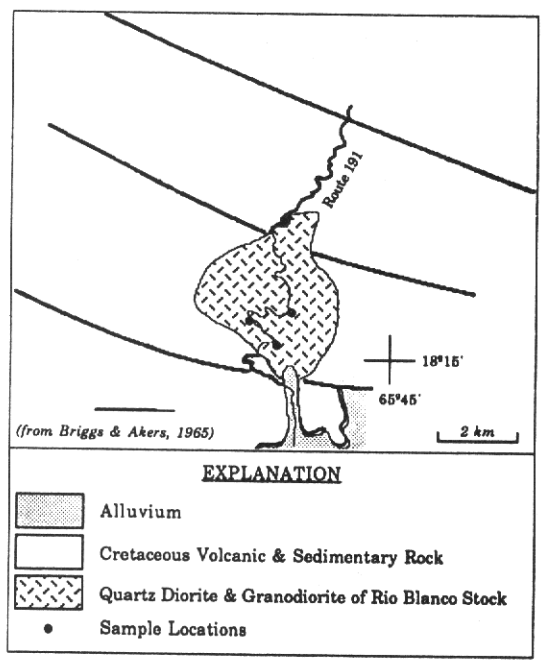

Figure 8. Generalized geologic map of Rio Blanco stock.

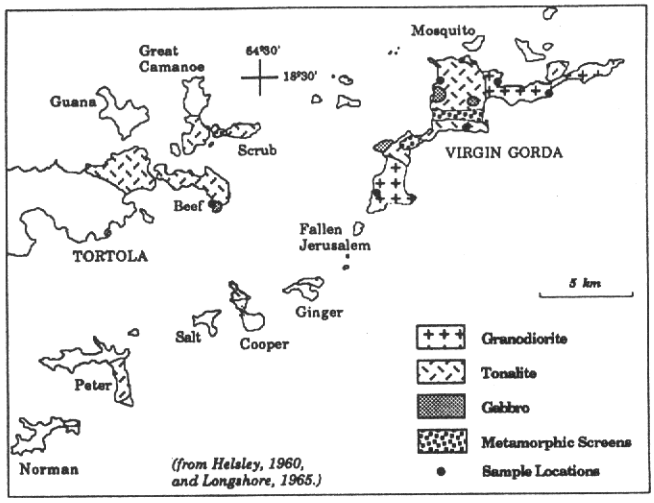

Figure 9. Generalized geologic map of Virgin Islands batholith.

Virgin Islands Batholith

The Virgin Islands Batholith (Fig. 9) is exposed mainly on the islands of Virgin Gorda, Tortola, Great Camanoe, Scrub , and Peter. The distribution of the contact aureole and magnetic anomaly patterns suggest that large portions of the batholith are submerged and that the intrusive rocks on each of the islands are interconnected and part of a composite batholith having an extent of about 160 km^2 (Helsley, 1960; Longshore, 1965). The batholith was emplaced as a discordant, flat-lying, sill-like body prior to regional tilting of about 90^0 about an axis approximately parallel to the strike of the enclosing sedimentary rocks (Helsley, 1960; Longshore, 1965). The western part of the batholith is intrusive mainly into the Cretaceous Tutu Formation; in the eastern portions it is progressively more discordant and intrusive into the 7,600-meter-thick Eocene Tortola Formation.

The main rock types of the batholith consist of gabbro (10%), diorite and tonalite (65%), and granodiorite (65%) with the main compositional and textural phases commonly being gradational (Helsley, 1960; Longshore, 1965). Figure 3f shows the normative compositions. The granitoid rocks form a generally low-potassic suite and have an average K_2O content of about 1.2 percent (Longshore, 1965). K-Ar dates from the eastern part of the batholith indicate emplacement at about 35 Ma (Cox and others, 1977; Kesler and Sutter, 1979).

The rocks are texturally diverse and vary from fine to coarse grained, equigranular to porphyritic, and massive to layered. Of the samples studied in this project, only three were included in the pressure calculations (Table 1). Their primary mineralogy consists of quartz, zoned plagioclase (An_{35}-An_{45}), K-feldspar, hornblende, chloritized biotite, magnetite, sphene, apatite, and zircon. The hornblende is unaltered, medium greenish-brown, slightly zoned, subhedral, and free of inclusions. The biotites are commonly chloritized and some are altered to chlorite + epidote.

Three other amphiboles (Table 2) were not included in the calculations. Samples BI-22 and VG-168 are hornblende from a quartz-free gabbro and a quartz-free diorite, respectively. The hornblende in thin section is colorless to light green brown and occurs as marginal to interstitial replacements of primary hypersthene and augite. The compositions indicate that the crystals are aluminous magnesio-hornblende. The third sample (VG-329), an amphibole from a tonalite having a largely recrystallized texture is compositionally an actinolite (Table 2, Fig. 2). The actinolite is colorless to light green, forms elongate crystals with acicular edges, and has uneven to patchy extinction.

Table 2.Magnesio-hornblende and actinolite analyses, Virgin Islands batholith

Sample	BI-22	VG-168	VG-329
Rock	Gabbro	Diorite	Tonalite
Mineral	Mg-Hornblende	Mg-Hornblende	Actinolite
Analyses (n)	6	4	18
SiO_2	46.35	47.23	46.69
TiO_2	1.16	1.51	0.68
Al_2O_3	10.68	10.76	2.82
Cr_2O_3	0.04	0.01	0.00
FeO	8.73	10.45	8.52
MnO	0.18	0.13	0.39
MgO	12.33	13.40	15.87
CaO	13.39	12.26	12.05
Na_2O	1.54	2.62	1.32
K_2O	0.19	0.28	0.23
F	0.06	0.07	0.31
Sum	92.82	98.32	94.14
Cations Based on 23 Oxygens:			
Si	6.76	6.75	7.69
Al^{iv}	1.24	1.25	0.31
Al^{vi}	0.68	0.58	0.18
Ti	0.13	0.16	0.08
Cr	0.00	0.00	0.00
Fe	1.11	1.26	1.06
Mn	0.02	0.02	0.05
Mg	2.77	2.88	3.50
Ca	2.18	1.89	1.91
Na	0.45	0.73	0.38
K	0.04	0.05	0.04
Sum	15.39	15.57	15.20
Al^T	1.92	1.83	0.49
Sigma (Al^T)	0.28	0.16	0.16

The presence of several augite relicts indicates that the amphibole is of replacement origin. It is clear that none of the amphiboles listed in Table 2 equilibrated with a quartzose calc-alkalic magma.

DISCUSSION

The total Al content of hornblende and the corresponding calculated pressures at which hornblende crystallized show a distinguishable trend of decreasing Al^T content and pressure with decreasing K-Ar date of the plutons (Tables 1 and 3). Although there is some overlap in the Al^T values at the one sigma level, particularly for the higher Al^T values, as well as uncertainty in the K-Ar ages at which the plutons were emplaced, the overall trend in the data seems clear.

Table 3 shows that there is a progressive decrease in both pressure and K-Ar date of plutons from the Morovis stock (oldest), through the San Lorenzo batholith, Utuado pluton, and Rio Blanco stock, to the Virgin Islands batholith (youngest). The pressures (and inferred depths of emplacement) are: Morovis, 2.9 kbars (10.3 km); San Lorenzo, 2.7 kbars (9.4 km); Utuado, 2.5 kbars (8.8 km); Rio Blanco, 2.1 kbars (7.4 km); and Virgin Islands, 1.1 kbars (3.7 km).

An independent check of the pressure data is Longshore's (1965) estimate of 1-3 kbars for the formation of the contact aureole associated with the Virgin Islands batholith. The maturation of organic material in Puerto Rican sedimentary rocks (Hayes and others, 1986) has also been used to infer a shallow

Table 3. Relation among pressure and depth of emplacement, K-Ar date, and average K_2O content of eastern Greater Antilles granitoid rocks and their estimated rate of uplift

Pluton	Pressure (kbars)	Depth* (km)	K-Ar Date (Ma)	K_2O (%)	Uplift Rate (cm/yr)
Morovis	2.92	10.3	88	3.9	0.012
San Lorenzo	2.67	9.4	73	2.5	0.013
Utuado	2.52	8.8	67	2.4	0.013
Rio Blanco	2.12	7.4	46	1.2	0.016
Virgin Is.	1.06	3.7	35	1.2	0.011

*Depth based on a density of 2.85 gm/cm^3.

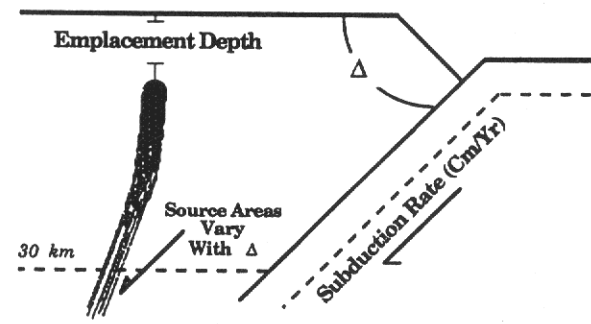

Figure 10. Schematic diagram showing proposed relation of depth of emplacement of plutons to angle and rate of subduction. An increase in rate of subduction causes a flattening of the angle of subduction (Δ) which results in a change in magma source areas, less interaction of the magma with the upper lithosphere, and a shallower depth of plutonic emplacement.

depth of burial of the sedimentary and volcanic sequence. There is, however, some uncertainty in such estimates as an appropriate geothermal gradient and an applicable temperature/reflectance curve must be assigned. Utilizing mean reflectance values of 1.5-2.5 (Hayes and others, 1986), the temperature/reflectance curves of Barker and Pawlewicz (1986), and a hypothetical geothermal gradient of 50^{0}C/km, yields a depth of burial of about 5-6 km for the Eocene-late Cretaceous and middle Cretaceous sequences. Lower geothermal gradients of 30-40^{0}C/km yield values more closely comparable to the Al^T data.

A second important correlation summarized in Table 3 is that there is also a relationship among the composition (as expressed in average K_2O content), depth of emplacement, and K-Ar date. The older Morovis, San Lorenzo, and Utuado intrusives are all more potassic than the less-potassic and younger Rio Blanco and Virgin Islands intrusives (Table 3). Of the former, the Morovis is the oldest and most potassic and was emplaced at the greatest depth. There is thus a pattern of evolutionary change in both composition and depth of emplacement during the main plutonic phases of eastern Greater Antilles island arc development.

TECTONIC IMPLICATIONS

The pressure data presented here indicate that about 10 km of unroofing occurred in portions of the eastern Greater Antilles since late Cretaceous time. Assuming a simple linear relationship between depth (pressure) and age, a surprisingly consistent rate of uplift of 0.01-0.02 cm/yr for all five plutons is obtained (Table 3). Although this rate is decidedly minor compared to estimated lateral plate movements in the Caribbean during the same time span (Burke, 1988; Donnelly, 1989) and to vertical movements in other tectonically active areas (Zen, 1985), it is nevertheless reflective of the tectonic history and perhaps characteristics of active oceanic orogenic areas.

A further consequence is the inter-relation among depth of plutonic emplacement, K-Ar date, and average K_2O content of the plutons. The reason for this relationship is not entirely straight forward and may be the result of a variety of factors. Previous work on both the volcanic (Lidiak, 1972) and the intrusive rocks (Kesler and Sutter, 1979) of Puerto Rico has shown that the K_2O content changes through time and may be related to changes in depth of magma generation. The new Al^T hornblende data is clear indication that pressure (depth) is an important factor in the equation.

My current interpretation is that the depth and composition parameters are related to magma generation associated with a change in the angle of the Benioff zone and a change in the rate of subduction. The earlier plutons are derived and emplaced by interaction of a steeply-dipping subduction zone. An increased rate of subduction results in flattening of the subduction angle, a changing source area of magma generation, shallower depths of pluton emplacement, and possibly less interaction of the upwelling magma with the enclosing upper lithosphere. These relations are shown schematically on Figure 10. The proposed decrease in subduction angle is, in general, consistent with changes in relative motions of the major plates (Pindell and others, 1988; Donnelly, 1989) during the interval 100 to 35 Ma. Accordingly to Donnelly (1989), the rate of convergence changed from about 6 cm/yr 102 to 72 Ma ago to 12-13 cm/yr between 72 and 35 Ma ago.

Other parameters such as age of the subducted lithosphere, thermal regimes, and magma viscosity also need to be evaluated to obtain a better understanding of evolution of the plutons in the eastern Greater Antilles island arc.

Acknowledgments. I thank John Longshore of Humboldt State University for providing some of the Virgin Islands samples. Dave Little of Ohio State University helped in the use of the electron probe microanalyser.

REFERENCES CITED

Barker, C. E., and Pawlewicz, M. J., 1986, The correlation of vitrinite reflectance with maximum temperature in humic organic matter, *in* Buntebarth, G., and Stegena, L., eds., Lecture notes in earth sciences: Berlin, Springer-Verlag, v. 5, paleogeothermics, p. 79-93.

Berryhill, H. L., Jr., 1965, Geology of the Ciales quadrangle, Puerto Rico: U. S. Geol. Survey Bull. 1184, 116 p.

Boynton, C. H., Westbrook, G. K., Bott, M. H. P., and Long, R. E., 1979, A seismic refraction investigation of crustal structure beneath the Lesser Antilles island arc: Geophys. Jour. Royal Astron. Soc., v. 58, p. 371-393.

Briggs, R. P., and Akers, J. P., 1965, Hydrologic map of Puerto Rico and adjacent islands: U. S. Geol. Surv. Hydrol. Inv. Atlas, Map HA-197, scale 1:240,000.

Burke, K., 1988, Tectonic evolution of the Caribbean: Ann. Rev. Earth Planet. Sci., v. 16, p. 201-230.

Chen, J.-C., 1969, Petrological and chemical studies of Utuado pluton, Puerto Rico: Acta Geol. Taiwanica, v. 13, p. 21-41.

Cox, D. P., Marvin, R. F., M'Gonigle, J. W., McIntyre, D. H., and Rogers, C. L., 1977, Potassium-argon geochronology of some metamorphic, igneous, and hydrothermal events in Puerto Rico and the Virgin Islands: Jour. Research U. S. Geol. Survey, v. 5, p. 689-703.

Donnelly, T. W., 1989, Geologic history of the Caribbean and Central America, *in* Bally, A. W., and Palmer, A. R., eds.,

The Geology of North America--An overview: Boulder, Colorado, Geol. Soc. America, v. A, p. 299-321.
Donnelly, T. W., and 10 others, 1990, History and tectonic setting of Caribbean magmatism, *in* Case, J. E., and Dengo, G., eds., The Caribbean Region: Boulder, Colorado, Geol. Soc. America, v. H, p. (in press).
Donnelly, T. W., and Rogers, J. J. W., 1978, The distribution of igneous rocks throughout the Caribbean: Geol. Mijnb., v. 57, p. 151-162.
Donnelly, T. W., and Rogers, J. J. W., 1980, Igneous series in island arcs: the northeastern Caribbean compared with worldwide island-arc assemblages: Bull. Volcanol., v. 43-2, p. 347-382.
Edgar, A. D., Ewing, J. I., and Hennion, J., 1971, Seismic refraction and reflection in Caribbean Sea: Am. Assoc. Petroleum Geologists Bull., v. 55, p. 833-870.
Fettke, C. R., 1924, The geology of the Humacao district, Porto Rico: New York Acad. Sci., Sci. Surv. Porto Rico and the Virgin Islands, v. II (2), p. 117-197.
Hammarstrom, J. M., and Zen, E., 1986, Aluminum in hornblende: an empirical igneous geobarometer: Am. Mineralogist, v. 71, p. 1297-1313.
Hayes, J. A., Larue, D. K., Joyce, J., and Schellekens, J. H., 1986, Puerto Rico: reconnaissance study of the maturation and source rock potential of an oceanic arc involved in a collision: Jour. Marine Pet. Geol., v. 3, p. 126-139.
Helsley, C. E., 1960, Geology of the British Virgin Islands [Ph. D. Dissertation]: Princeton, New Jersey, Princeton University, 219 p.
Hollister, L. S., Grissom, G. C., Peters, E. K., Stowell, H. H., and Sisson, V. B., 1987, Confirmation of the empirical correlation of Al in hornblende with pressure of solidification of calc-alkaline plutons: Am. Mineralogist, v. 72, p. 231-239.
Kesler, S. E., and Sutter, J. F., 1979, Compositional evolution of intrusive rocks in the eastern Greater Antilles island arc: Geology, v. 7, p. 197-200.
Leake, B. E., 1978, Nomenclature of amphiboles: Mineralog. Mag., v. 42, p. 533-563.
Lidiak, E. G., 1965, Petrology of andesitic, spilitic, and keratophyric flow rock, north-central Puerto Rico: Geol. Soc. America Bull., v. 76, p. 57-88.
Lidiak, E. G., 1972, Spatial and temporal variations of potassium in the volcanic rocks of Puerto Rico: Caribbean Geol. Conf. Trans., v. 6, p. 203-209.
Longshore, J. D., 1965, Chemical and mineralogical variations in the Virgin Islands batholith and its associated wall rocks [Ph. D. Dissertation]: Houston, Texas, Rice University, 94 p.
Nelson, A. E., 1968, Intrusive rocks of north-central Puerto Rico: U. S. Geol. Survey Prof. Paper 600-B, v. p. B16-B20.
Officer, C. B., Jr., Ewing, J. I., Hennion, J. L., Harkrider, D. G., and Miller, D. E., 1959, Geophysical investigations in the eastern Caribbean--summary of the 1955 and 1956 cruises, *in* Ahrens, L. H., Press, F., Rankama, K., and Runcorn, S. K., eds., Physics and Chemistry of the Earth: v. 3, p. 17-109.
Pindell, J. L., Cande, S. C., Pitman, W. C., III, Rowley, D. B., Dewey, J. F., La Brecque, J., and Haxby, W., 1988, A plate-kinematic framework for models of Caribbean evolution: Tectonophysics, v. 155, p. 121-138.
Rutter, M. J., Van der Laan, S. R., and Wyllie, P. J., 1989, Experimental data for a proposed empirical igneous geobarometer: aluminum in hornblende at 10 kbar pressure: Geology, v. 17, p. 897-900.
Seiders, V. M., 1971, Geologic map of the El Yunque quadrangle, Puerto Rico: U. S. Geol. Survey Misc. Geol. Inv., Map I-658, scale 1:20,000.
Streckeisen, A. L., 1976, To each plutonic rock its proper name: Earth Sci. Rev., v. 12, p. 1-34.
Weaver, J. D., 1958, Utuado pluton, Puerto Rico: Geol. Soc. America Bull., v. 69, p. 1125-1142.
Zen, E., 1985, Implications of magmatic epidote-bearing plutons on crustal evolution in the accreted terranes of northwestern North America: Geology, v. 13, p. 266-269.

LATE JURASSIC TO LATE CRETACEOUS DEVELOPMENT OF ISLAND ARC CRUST IN SOUTHWESTERN PUERTO RICO.

Johannes H. Schellekens, Homer Montgomery,
James Joyce, and Alan L. Smith
Department of Geology,
University of Puerto Rico,
P.O.Box 5000, Mayaguez,
Puerto Rico 00709-5000.

ABSTRACT

Based on fossil assemblages, radiometric ages, and rock and mineral chemistry, three stages can be distinguished in the development of the island arc crust in southwest Puerto Rico. Records of the first and second stage are preserved in the cherts and metamorphic rocks of the Bermeja Complex. The third stage is represented by the volcanic and sedimentary rocks, that unconformably overlie the Bermeja Complex, and by the intrusive rocks, associated with the volcanics. Radiolarian assemblages suggest three chert forming periods: 1) Kimmeridgian - Tithonian, with northern Tethyan to Boreal paleogeographic origin, deposited at abyssal depths; 2) Hauterivian - Aptian, deposited at bathyal depths; and 3) Cenomanian to Campanian in the Tethyan Realm. The basaltic rocks of the Bermeja Complex range in metamorphic grade from weakly metamorphosed prehnite - bearing rocks, through greenstones, to amphibolites. Although the whole rock geochemistry is not conclusive, the major, trace, and REE data for the higher grade metamorphic rocks suggest a possible ocean floor origin, whereas the lower grade grade metamorphics may have originated in an island arc setting. Clinopyroxene compositions for the low grade rocks (greenstones, dikes, and two pyroxene gabbro) confirm an island arc origin. Radiometric ages indicate a magmatic and metamorphic event in the Early Cretaceous corresponding to the second chert forming period, whereas the third chert forming period is coeval with the radiometric age for the intrusion of the Maguayo Porphyry diorite, and resetting of the metamorphic ages. Volcanics associated with the intrusions were probably subaerial and are partly covered by Santonian and Campanian reef and shelf limestones.

INTRODUCTION

Puerto Rico, the easternmost island of the Greater Antilles is located at the northern margin of the Caribbean Plate. The island consists of a deformed core of volcanic, volcaniclastic, and sedimentary rocks of Late Jurassic to Early Tertiary age, which was intruded in the Late Cretaceous and Early Tertiary by felsic plutons. This core, which extends in an east-west direction across the center of the island, is overlain on the north and south coasts by slightly tilted Oligocene and younger sedimentary rocks and sediments (Fig.1) (Briggs and Akers, 1965, Mattson, 1966). The southwestern part of the island consists of three linear belts of serpentinite separated by rocks of Late Cretaceous age, which are locally overlain by younger sedimentary rocks and sediments. The serpentinite, with rafts of amphibolites, greenstones, and cherts, belongs to the Bermeja Complex, which represents the oldest dated rocks on Puerto Rico. Previous workers (eg. Mattson, 1973, Mattson and Pessagno, 1974, 1979, Wadge and others, 1983) have regarded the Bermeja Complex as representing a dismembered ophiolite complex. However, the evidence is ambiguous and it could also represent island arc basement. Based on petrology, geochemistry, and fossil and radiometric ages this study attempts to compile the geologic history of southwestern Puerto Rico.

BERMEJA COMPLEX

The Bermeja Complex (Fig. 1a) was first described by Mattson (1960), who distinguished four rock types: serpentinized peridotite (Mattson,

Larue, D.K., and Draper, G. (eds.),
Transactions of the 12th Caribbean Geological Conference, St. Croix, U.S.V.I., Miami Geological Society, P.O. Box 431552, South Miami, FL 33243, U.S.A

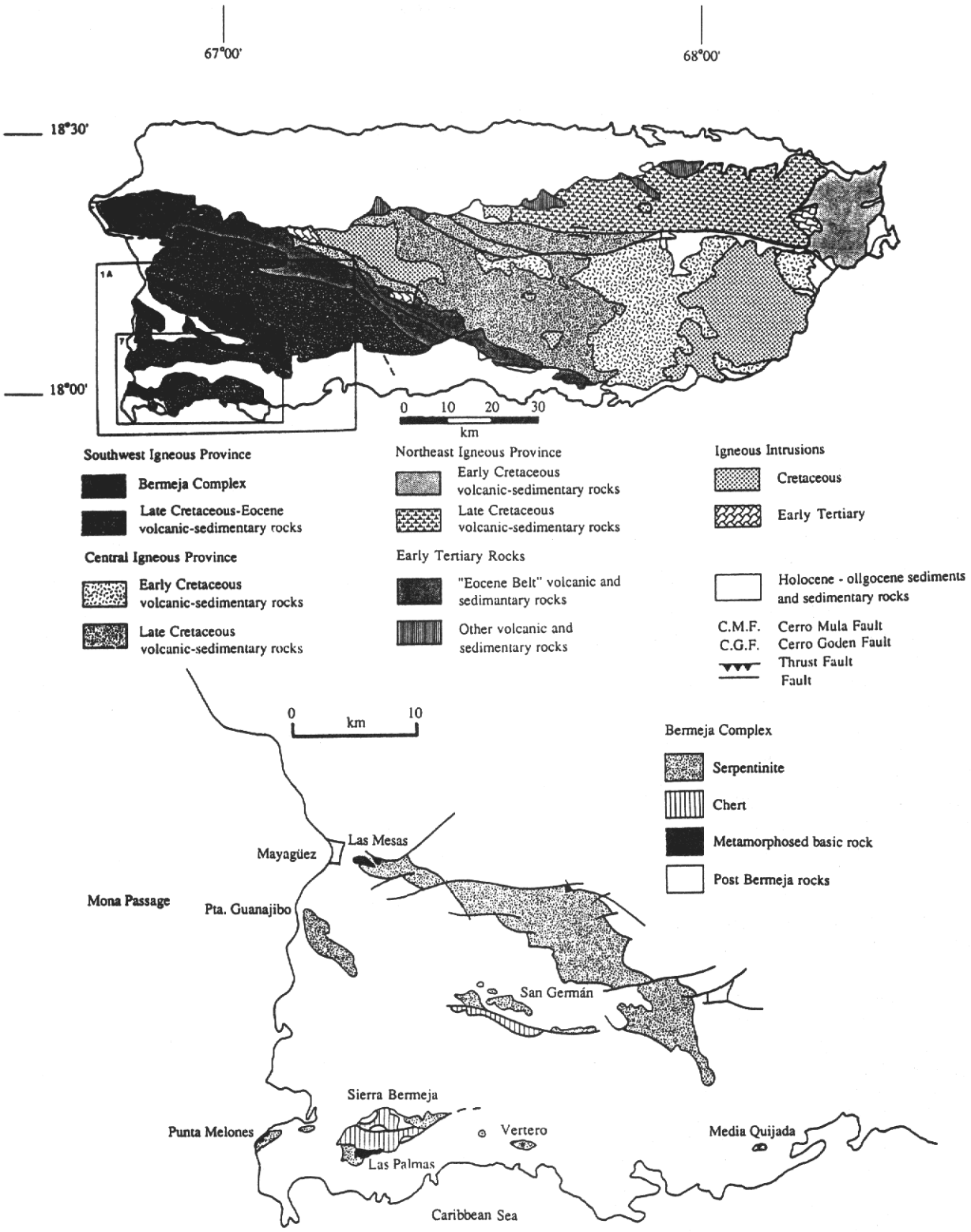

Fig.1: Geologic map of Puerto Rico. Insets: Figure 1A: Bermeja Complex, and figure 6: Maguayo Volcanic Center.

1960, 1964), spilite (here named the Las Mesas Greenstone), amphibolite (later named the Las Palmas Hornblende Schist and Amphibolite; Mattson, 1973), and silicified volcanic rock and/or chert (later named the Mariquita Chert by Mattson, 1973).

Of the three serpentinite belts, the northern one consists predominantly of serpentinite, and extends from the city of Mayaguez, ESE towards Sabana Grande (Mattson, 1960, McIntyre, 1975, Curet, 1986). Greenstone and amphibolite occurring within the serpentinite of this belt are exposed in two quarries just east of Mayaguez (Mattson, 1960, Curet, 1981, 1986). In the northern quarry, non-foliated greenstones comprise a bedded sequence, with beds from 20 cm to several meters in thickness, of basaltic flow rocks, volcaniclastic conglomerates and sandstones. In the southern quarry metamorphosed and veined volcaniclastic sandstones are associated with non-foliated amphibolite. About 3 Km. ESE of Maricao an outcrop of "amphibolite" -breccia in serpentinite was described by McIntyre (1975). A restudy of this outcrop has identified the "amphibolite" as a hornblende-two-pyroxene gabbro, with prehnite and hydrogrossular veining giving it a foliated impression.

The other two serpentinite belts are discontinuous. One runs from Punta Guanajibo, eastward through San German, where outcrops of Mariquita Chert occur (Volckmann, 1984c) to join the northern belt near Sabana Grande. (Mattson, 1960, Krushensky and Monroe, 1979, Volckmann, 1984c). Locally the serpentinite is cut by small basaltic and andesitic intrusions. The third, southernmost, belt extends from Punta Melones across the Sierra Bermeja (Fig. 1) (Mattson, 1960, 1973, Volckmann, 1984 b,d); east of the Sierra Bermeja, only a few patchy exposures of the Bermeja Complex are encountered at Cerro Vertero, (Volckmann, 1984b), and Media Quijada (Krushensky and Monroe, 1979). At both Punta Melones and Sierra Bermeja the serpentinite, which contains amphibolite blocks some of which are on the order of tens of meters in diameter (Mattson, 1960, Renz and Verspyck, 1962, Tobisch, 1968), is overlain by chert. In the largest amphibolite raft, near barrio Las Palmas, foliated amphibolites are cut by meta-basaltic dikes, which cross-cut the foliation, and they themselves may be off-set along small faults. The serpentinite of this southern belt is intruded by Late Cretaceous intrusions, the most prominent of which is the diorite stock of the Maguayo Porphyry.

Petrology of the metamorphosed rocks

The petrography of representative samples of the Bermeja Complex is summarized in Table 1. The amphibolites have a medium-grade metamorphic paragenesis of green hornblende and calcic plagioclase, sometimes with relics of clinopyroxene, brown hornblende, and plagioclase. Two varieties of amphibolite can be distinguished based on the texture: foliated and non-foliated, there is however no difference in mineralogy between the two varieties. Many of the amphibolites show evidence of retrograde metamorphism. In the southern serpentinite belt

Table 1: Petrography of representative samples of the Bermeja Complex.

No:	Location:	paragenesis + relics	retrograde minerals:
Foliated amphibolite			
VP1	Las Palmas	green hnbl.-plag.(labr.)-Qtz-sphene-magnetite	chlorite-calcite
VP3	Las Palmas	brown hnbl.cores-cpx.relics-green hnbl.-plag.-mgnt.	
VP4	Las Palmas	browngreen hnbl.-plag.-Qtz.-mgnt.	
VP85	Media Quijada	br.green hnbl.-plag.(labr.-bytw.)-cpx.relics	calcite
EC14	Punta Melones	green hnbl.-cpx.relics-sphene	prehnite
Non-foliated amphibolite			
VP66	vertedero Lajas	green hnbl.-plag.-sphene-cpx.relics	sericite
VP78	Punta Melones	green hnbl.-plag.-cpx.relics	serpentine?-sericite
VP80	Punta Melones	green hnbl.-plag.(olig.-and.)-sphene-cpx.relics	
VP180	Las Mesas	green hnbl.-plag.-cpx.relics	actinolite-chlorite-albite
Meta-basalt porphyry			
VP2	Las Palmas	actinolite-green hnbl.-plag.(alb.)	chlorite-Qtz.
VP117	Las Palmas	actinolite-green hnbl. plag.(alb.)-cpx.relics	
Greenstones			
EC13	Las Mesas	cpx-plag.(alb.)	calcite-chlorite-prehnite-epidote
Two pyroxene gabbro			
VP179	Maricao	brown hnbl.-cpx-opx-plag.(bytw.)	prehnite-chlorite-hydrogrossular

this is evidenced by the presence of chlorite. The amphibolites from the northern belt, associated with the greenstones (eg. VP180) contain actinolite, chlorite, and albite, indicating they were probably remetamorphosed during the greenschist metamorphism. The meta-basalt porphyry dikes in the Las Palmas area, are metamorphosed to a low grade metamorphic facies with a paragenesis of actinolite, green hornblende, and albite, sometimes with clinopyroxene relics preserved. The greenstones of the northern serpentinite belt are composed of clinopyroxene and plagioclase, the latter is often albitized, together with veins of epidote, chlorite, and prehnite. The gabbro near Maricao (VP179) consists of clinopyroxene, orthopyroxene, and calcic plagioclase. The pyroxenes are rimmed by brown hornblende, of a composition falling in the pyroxene miscibility gap, on the tie-line between the orthopyroxene and clinopyroxene, suggesting the amphibole to be of late magmatic origin. Secondary chlorite and prehnite, and thin, parallel prehnite and hydrogrossular veins indicate a very low-grade metamorphism.

Whole rock geochemistry

Fourteen new major and trace element analyses (obtained by X-ray fluorescence at Mich. Tech. Univ., Rose and others, 1986) for the basic rocks of the Bermeja Complex are presented in Table 2. In order to try and determine the tectonic environment of the rocks of the Bermeja Complex immobile trace elements were plotted on discriminant diagrams (Fig. 2). The Ti vs Zr, and the Cr vs Y (Pearce, 1982) , and the log (Zr/Y) vs log Zr diagrams (Pearce and Norry, 1979) show most analyses clustering in the Mid Ocean Ridge Basalt (MORB) field. The lower grade metamorphic basaltic rocks fall in the island arc-field, or where the island arc-field overlaps the MORB-field. When the composition of the amphibolites only, so without the greenstones, dikes, and two-pyroxene gabbro, are plotted on a TiO_2 vs Y diagram (Perfit, 1980) the analyses show a trend similar to that of E-type MORB.

Thirteen samples were analyzed by neutron activation for rare earth elements (M.I.T. laboratory, Ila and Frey, 1984). Overall the chondrite-normalized patterns for the various Bermeja rock types are similar (Fig.3). Enrichment above chondrite ranges from 6 to 20 times, with flat, slightly LREE depleted patterns. These patterns are compatible with both those of N-type MORB (Basaltic Volcanic Study Project, 1981), and island arc tholeiites (Jakes and Gill, 1970). However within this group the field of foliated amphibolites of the Las Palmas area are distinctly more enriched in REE than the other rocks (Fig.3). The gneissic texture and the higher REE content may suggest an origin near a transform fault (Langmuir and Bender, 1984), this is supported by the occurrence of gneissic amphibolites, dredged from the deepest part of the VEMA Fracture Zone (Honorez and others,1984).

Clinopyroxene discrimination

Leterrier and others (1982) have shown that calcic pyroxene compositions in rocks that have only undergone low-grade metamorphism can discriminate between various tectonic

Table 2: Anhydrous analyses Bermeja Complex

	VP1	VP-3	VP-4	VP-2	VP-66	VP-7E	EC-14	VP-79	VP-80	VP-85	EC-13	VP-17E	VP-180
SiO2	50.43	45.45	49.46	51.29	51.28	47.77	47.17	40.63	50.11	50.09	50.31	48.11	49.52
TiO2	1.96	2.19	2.37	1.42	1.86	1.43	1.25	1.3	1.45	1.75	1.23	1.45	1.03
Al2O3	12.90	11.89	12.37	14.35	14.18	12.92	10.57	11.82	14.18	13.76	12.80	16.02	14.72
FeO*	14.00	15.94	16.24	10.84	13.02	12.30	10.3	11.37	10.91	12.87	11.82	9.67	9.67
MnO	0.25	0.23	0.23	0.18	0.2	0.22	0.18	0.21	0.18	0.20	0.20	0.15	0.16
MgO	7.70	10.34	6.76	8.29	7.25	13.27	12.29	26.12	8.52	7.48	12.04	8.46	9.35
CaO	9.72	11.81	9.55	10.28	8.03	8.90	17.29	7.71	10.72	10.01	7.19	13.49	8.59
Na2O	2.63	1.59	2.53	3.05	3.47	2.76	0.6	0.63	3.57	3.47	4.02	2.47	5.74
K2O	0.15	0.32	0.10	0.33	0.49	0.24	0.08	0.08	0.19	0.18	0.23	0.23	0.22
P2O5	0.25	0.24	0.38	0.16	0.23	0.19	0.26	0.13	0.17	0.19	0.15	ND	ND
Total	99.99	100.00	99.99	99.99	100.01	100.00	99.99	100.00	100.00	100.00	99.99	100.05	100.00
Sc	45	57	47	39	ND	ND	41	ND	ND	ND	37	ND	ND
V	448	507	543	294	401	343	185	304	317	395	179	326	244
Cr	168	227	134	221	162	116	129	150	206	140	159	199	316
Ni	53	70	44	57	75	53	64	85	65	38	60	61	102
Cu	7	62	46	70	46	65	<11	58	62	48	29	78	89
Zn	123	102	94	89	83	76	59	67	72	62	84	61	65
Rb	<5	<5	<5	<5	<5	<5	<5	<5	<5	<5	<5	<3	<3
Sr	110	89	93	180	338	451	59	28	275	1016	89	364	779
Y	29	28	36	22	26	24	19	21	22	25	16	24	20
Zr	112	74	199	77	122	113	58	64	88	156	59	76	115
Nb	8	5	8	3	0	0	9	8	2	<	11	4	<2
Ba	150	153	167	783	368	132	289	235	985	650	179	179	179
La	4.97	3.08	7.75	2.77	3.38	2.83	<10	2.79	2.58	2.87	2.57	1.89	2.80
Ce	17.90	13.60	27.50	9.80	13.00	10.00	40.00	10.70	9.10	10.70	9.30	9.70	8.70
Nd	13.70	12.40	20.30	7.20	10.60	8.50	ND	8.30	7.50	8.90	7.90	7.20	7.20
Sm	5.02	4.83	6.59	2.91	3.76	3.08	ND	2.84	2.91	3.32	2.86	2.80	2.40
Eu	1.65	1.66	2.02	1.07	1.34	1.08	ND	1.08	1.06	1.19	0.98	1.05	0.91
Tb	1.06	1.10	1.65	0.85	0.88	0.79	ND	0.61	0.66	0.77	0.61	0.69	0.62
Yb	5.10	5.25	6.69	2.87	3.77	3.28	ND	2.89	3.10	3.58	2.94	2.75	2.35
Lu	0.73	0.76	0.98	0.41	0.55	0.47	ND	0.43	0.44	0.53	0.42	0.42	0.37
Hf	3.80	2.70	5.10	2.00	2.80	2.40	ND	2.00	2.10	2.40	1.90	1.37	1.65
Th	ND	ND	ND	0.20	ND	ND	ND	ND	ND	NC	0.10	ND	ND

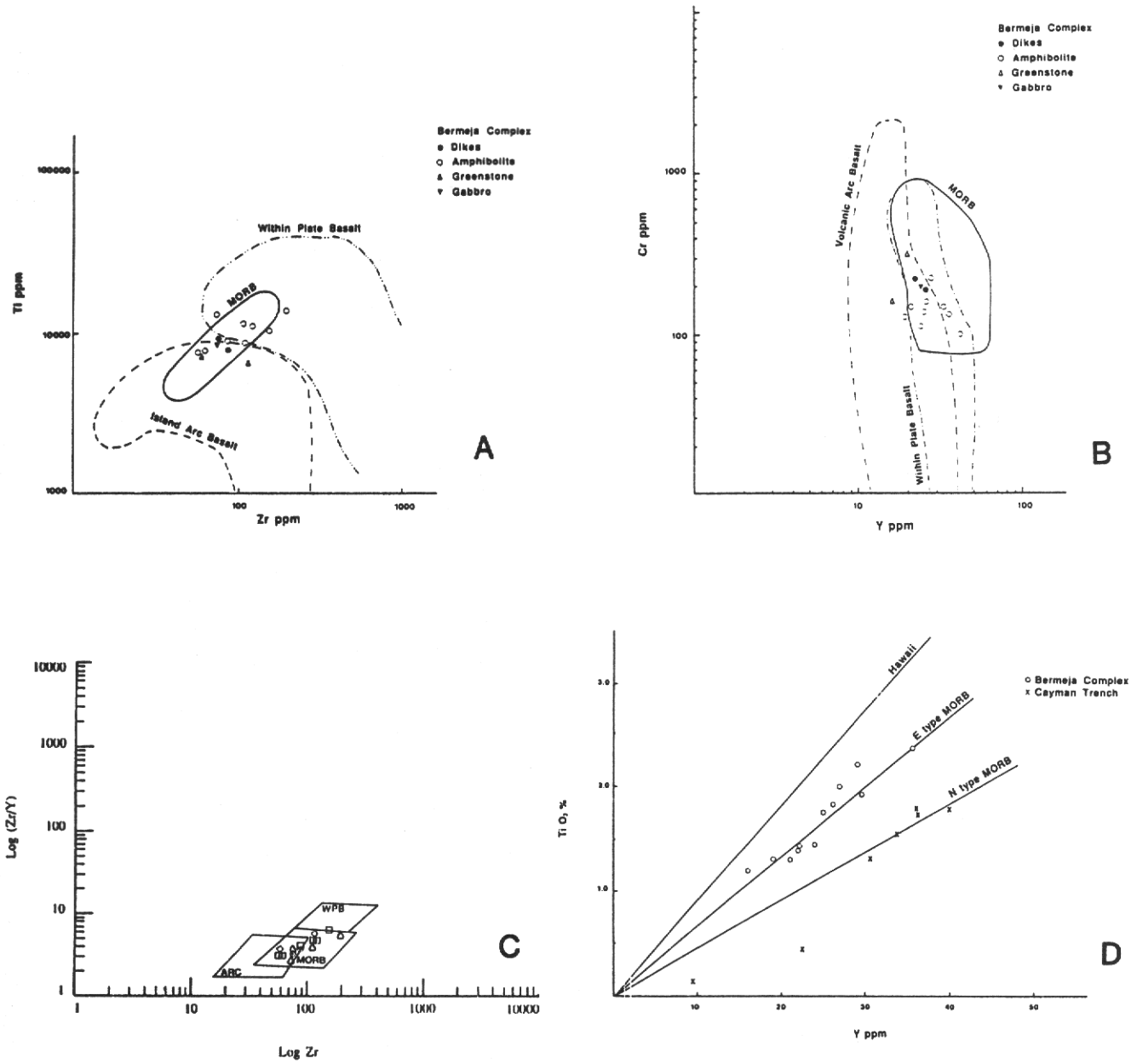

Fig.2: Chemical variation diagrams: 2A and B: Pearce (1982); 2C Pearce and Norry (1979); 2D: Perfit and others (1980).

environments. Calcic clinopyroxenes are preserved in a number of rock types in the Bermeja Complex. The metamorphic grade of these rocks ranges from very low (prehnite and chlorite), through low (chlorite, actinolite and albite), to medium (green hornblende and Ca- plagioclase). Clinopyroxene compositions were determined using a microprobe (Jeol Superprobe, Cornell University). The clinopyroxene relics from the amphibolites in Media Quijada, and Cerro Las Mesas do not give balanced analyses, indicating that the composition of the clinopyroxene has been affected by metamorphic processes. Analyses from pyroxenes of rocks with lower metamorphic grades (Table 4), the two pyroxene (VP179) gabbro breccia, the greenstones (VP259), and the meta-basaltic dikes (VP117), were plotted on the diagrams of Leterrier and others (1982). These plots suggest the host rocks were originally tholeiitic island arc basalts (Fig 4), a conclusion not contradicted by the whole rock chemistry.

MARIQUITA CHERT

The Mariquita Chert (Mattson, 1973) is a fine-grained greenish-gray or black radiolarian bearing rock, consisting of fine recrystallized quartz with minor iron oxides. It was named after Cerro Mariquita, the highest peak of the Sierra Bermeja, where it overlies the serpentinite. Other

Table 3: Anhydrous analyses Maguayo Volcanic Center

	VP114	VP-113	VP-112	VP-110	VP-120	VP-119	VP-105	VP-122	VP-124	EC-15	VP-118	EC-11	EC-12
SiO2	56.50	53.65	60.14	59.74	54.95	55.05	59.79	54.53	58.85	56.79	62.44	57.14	57.89
TiO2	0.98	0.88	0.96	1.16	1.34	1.17	0.82	1.39	0.90	0.70	0.69	0.76	0.77
Al2O3	17.85	16.87	18.14	16.93	17.24	17.59	16.12	16.75	16.57	16.72	17.16	16.99	16.58
FeO*	6.51	8.47	4.83	4.74	8.17	8.29	6.13	9.01	6.39	6.83	4.52	6.16	6.82
MnO	0.16	0.16	0.19	0.31	0.15	0.12	0.14	0.32	0.25	0.11	0.18	0.23	0.15
MgO	3.56	6.64	1.01	1.95	4.93	4.10	4.55	6.06	5.46	5.38	4.05	4.89	3.90
CaO	6.70	8.99	7.84	8.27	7.91	8.69	4.49	7.48	3.82	6.28	4.27	7.71	6.93
Na2O	4.79	2.62	4.78	5.81	2.85	3.00	5.29	3.63	4.21	4.31	3.87	3.37	3.35
K2O	2.59	1.38	1.64	0.61	2.05	1.56	2.40	0.54	3.33	2.62	2.54	2.45	3.30
P2O5	0.35	0.35	0.46	0.48	0.40	0.42	0.27	0.29	0.23	0.28	0.28	0.31	0.30
Total	99.99	100.01	99.99	100.00	99.99	99.99	100.00	100.00	100.01	100.02	100.00	100.01	99.99
V	189	174	175	207	253	226	142	268	157	114	117	107	110
Cr	236	232	21	0	23	51	55	18	20	170	35	91	105
Ni	57	92	3	8	13	14	29	13	23	59	13	24	20
Cu	57	55	38	177	50	8	21	77	26	0	28	0	0
Zn	86	60	80	72	81	78	68	74	73	69	116	77	58
Rb	33	17	27	1	24	1999	33	4	53	48	53	47	79
Sr	580	543	585	511	448	554	599	670	569	498	489	508	548
Y	18	17	17	18	19	18	16	16	18	16	17	15	23
Zr	162	171	176	246	185	166	161	168	149	140	153	143	159
Nb	12	0	10	30	19	15	13	1	11	14	24	17	16
Ba	1091	591	834	584	1155	883	976	1292	1579	1075	1410	717	806
La	14.00	19.90	30	37	24	19	27	21.50	23	25	13	28	19
Ce	88.00	43.10	68	70	93	68	78	45.00	110	93	91	75	91
Nd	ND	21.40	ND	ND	ND	ND	ND	21.60	ND	ND	ND	ND	ND
Sm	ND	4.13	ND	ND	ND	ND	ND	4.60	ND	ND	ND	ND	ND
Eu	ND	1.20	ND	ND	ND	ND	ND	1.38	ND	ND	ND	ND	ND
Tb	ND	0.46	ND	ND	ND	ND	ND	0.59	ND	ND	ND	ND	ND
Yb	ND	1.68	ND	ND	ND	ND	ND	1.68	ND	ND	ND	ND	ND
Lu	ND	0.26	ND	ND	ND	ND	ND	0.26	ND	ND	ND	ND	ND
Hf	ND	3.49	ND	ND	ND	ND	ND	3.18	ND	ND	ND	ND	ND
Th	ND	3.40	ND	ND	ND	ND	ND	3.40	ND	ND	ND	ND	ND

Table 4: Representative analyses clinopyroxenes, Bermeja Complex

	Hornblende -Two pyroxene Gabbro (VP179)			Dikes (VP117)				Greenstones (VP259)			
sample #	179-1	179-2	179-3	117-1 core	117-1 rim	117-2.3	117-7.2	259-1 core	259-1 rim	259-3 core	259-5 rim
mineral#											
SiO2	52.01	52.18	51.25	53.43	51.52	52.74	52.82	52.46	51.89	52.95	51.81
CaO	21.00	19.58	21.06	19.73	19.20	20.24	21.00	20.86	19.96	20.12	20.63
Al2O3	1.11	1.57	1.64	1.80	3.05	1.98	2.02	2.14	2.93	2.21	3.36
FeO	10.28	12.33	11.59	5.53	5.89	5.81	5.57	5.00	7.67	5.31	6.47
K2O	0.00	0.00	0.01	0.02	0.02	0.01	0.00	0.03	0.02	0.00	0.00
MgO	13.44	13.35	12.99	17.26	16.71	17.23	17.06	17.93	16.48	18.01	16.90
Cr2O5	0.08	0.00	0.01	0.19	0.27	0.17	0.16	0.27	0.03	0.21	0.02
Na2O	0.32	0.30	0.29	0.24	0.26	0.26	0.22	0.25	0.26	0.25	0.28
TiO2	0.16	0.25	0.34	0.19	0.28	0.19	0.24	0.28	0.56	0.28	0.55
MnO	0.34	0.33	0.29	0.09	0.09	0.11	0.12	0.14	0.22	0.15	0.14
Oxygen			0.00					0.00	0.00	0.00	0.00
TOTAL	98.74	99.89	99.47	98.48	97.29	98.74	99.21	99.36	100.02	99.49	100.16
cpx structure based on 6 O											
SI	1.9746	1.9656	1.9452	1.9743	1.9331	1.9515	1.9485	1.9299	1.9143	1.9410	1.9011
AIIv	0.0254	0.0344	0.0548	0.0258	0.0669	0.0485	0.0516	0.0701	0.0858	0.0591	0.0989
AIvI	0.0244	0.0354	0.0185	0.0528	0.0680	0.0377	0.0363	0.0229	0.0416	0.0363	0.0466
TI	0.0044	0.0072	0.0098	0.0053	0.0079	0.0053	0.0065	0.0077	0.0155	0.0077	0.0151
Fe	0.3263	0.3884	0.3678	0.1709	0.1849	0.1798	0.1717	0.1540	0.2367	0.1626	0.1986
Cr	0.0023	0.0000	0.0004	0.0055	0.0079	0.0051	0.0047	0.0078	0.0008	0.0060	0.0006
Mg	0.7605	0.7496	0.7352	0.9510	0.9346	0.9503	0.9380	0.9834	0.9062	0.9841	0.9247
Mn	0.0109	0.0106	0.0094	0.0028	0.0028	0.0034	0.0038	0.0045	0.0068	0.4700	0.0043
Ca	0.8541	0.7903	0.8563	0.7812	0.7717	0.8064	0.8298	0.8221	0.7891	0.7902	0.8108
Na	0.0240	0.0216	0.0211	0.0170	0.0187	0.0187	0.0160	0.0178	0.0183	0.0181	0.0199
K	0.0000	0.0000	0.0003	0.0010	0.0009	0.0003	0.0000	0.0013	0.0008	0.0001	0.0000
O	6.0000	6.0000	6.0000	6.0000	6.0000	6.0000	6.0000	6.0000	6.0000	6.0000	6.0000

chert occurrences mapped originally as Mariquita chert are at Punta Melones (El Combate), Media Quijada, and San German (Krushensky and Monroe, 1979, Volckmann, 1984a,b,c).

Based on radiolarian chronostratigraphy (Mattson and Pessagno, 1974, 1979, Pessagno written comm. in Volckmann, 1984c, Schellekens and others, 1989, Montgomery, this volume)

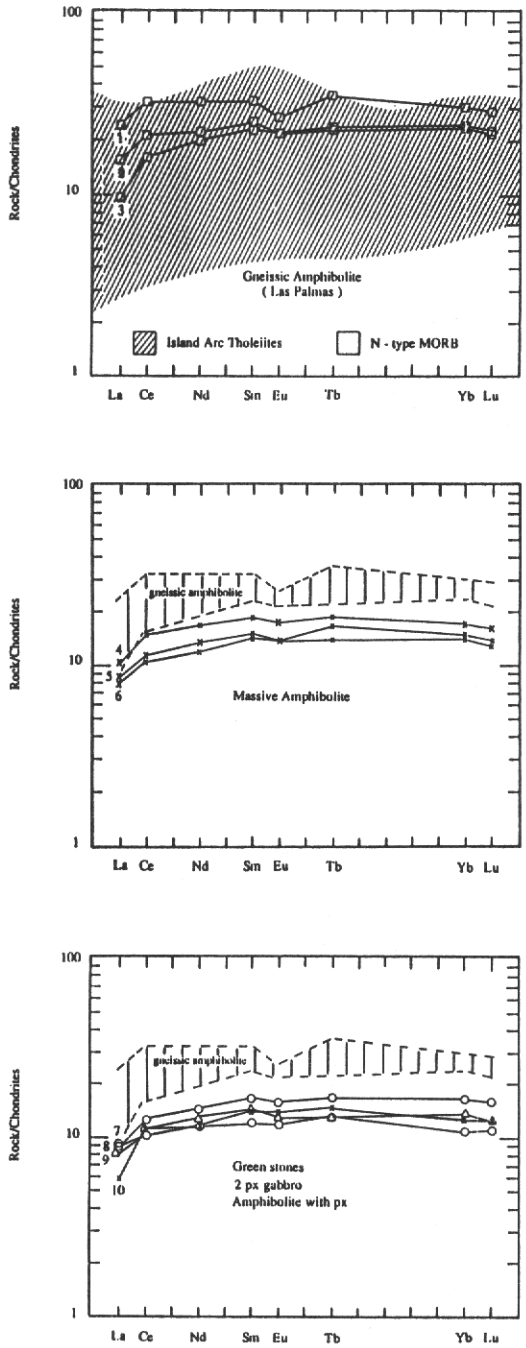

Fig.3: Chondrite normalized REE patterns for rocks of the Bermeja Complex. Normalization values from Nakamura (1974). 1:VP4; 2:VP1; 3:VP3; 4:VP66; 5:VP78; 6:VP80; 7:VP85; 8:EC13; 9:VP117; 10:VP179

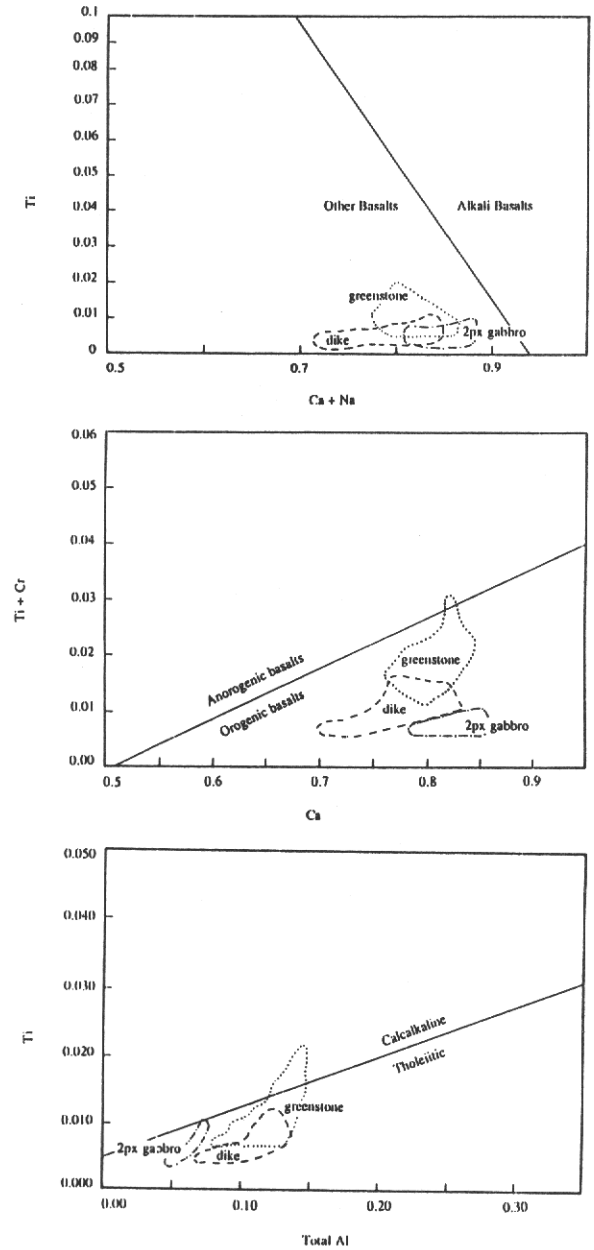

Fig.4: Clinopyroxene discrimination diagrams after Leterrier and others (1982). greenstones: Las Mesas Greenstone, (VP-259); dikes: metabasaltic dikes in amphibolite near Bo. Las Palmas (VP-2, VP-117); 2px gabbro: amphibole two pyroxene gabbro near Maricao (VP-179).

three chert forming episodes can be distinguished (Fig.5).

Kimmeridgian to Tithonian radiolarian chert in central northern Sierra Bermeja was interpreted as having been deposited in an abyssal depositional environment, at northern Tethyan paleolatitudes (approx. 22 - 30°N). A second sequence of chert from the southern Sierra Bermeja of Hauterivian to lower Albian age, suggests they were deposited in a bathyal environment. Mattson and Pessagno (1979) described radiolarians of this age from cherts that are intercalated with volcanic sandstones.

A third period of chert formation occurred in the Upper Cretaceous. Cenomanian radiolarian cherts overly a serpentinite conglomerate in Media Quijada; Campanian chert overlies the

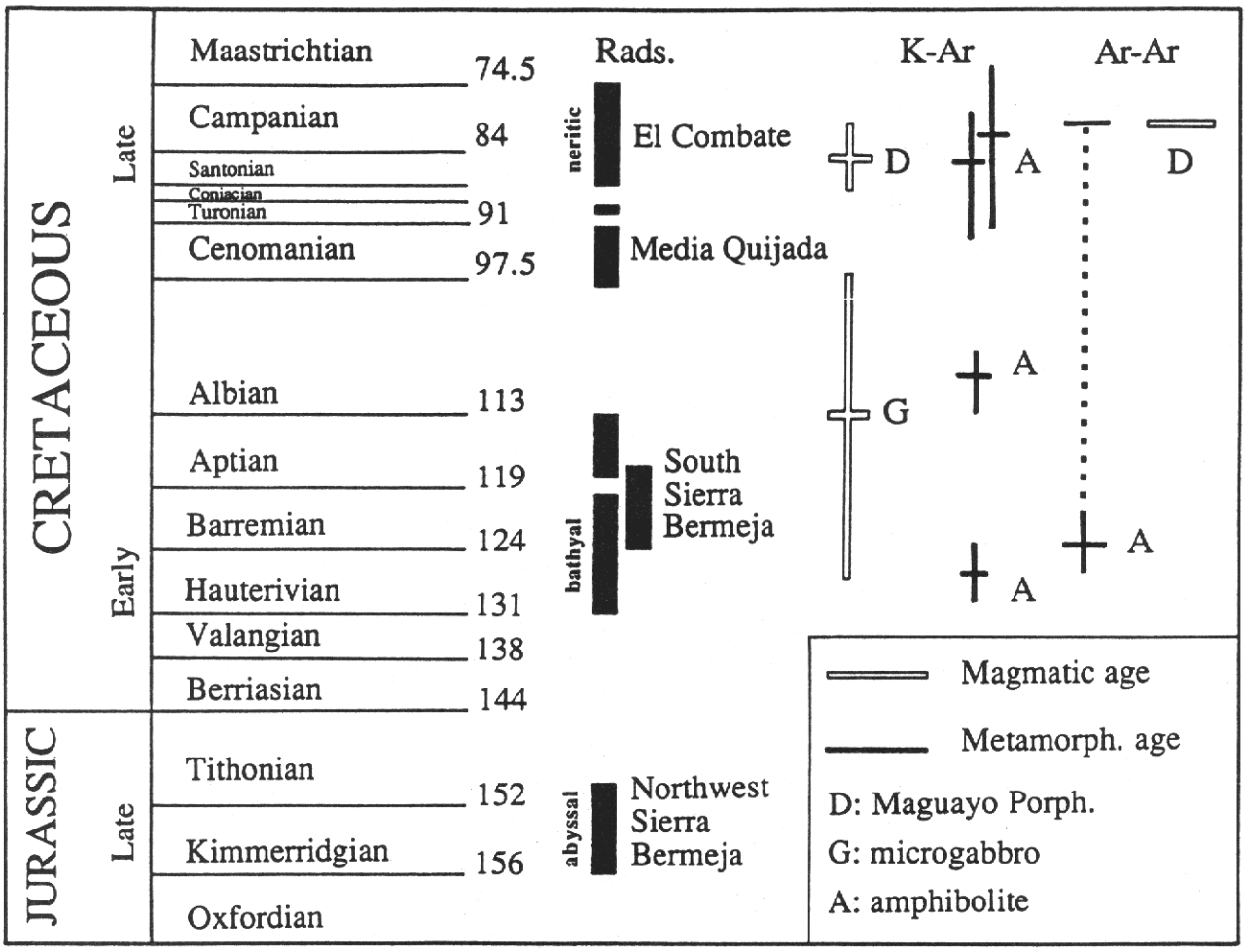

Fig.5: Radiolarian chronostratigraphy and radiometric age dates for SW Puerto Rico. Data from Mattson (1964), Tobisch (1968), Cox and others (1976), Mattson and Pessagno (1979), Schellekens and others (1989), Montgomery (this volume) and Schellekens (unpublished).

serpentinite near El Combate (Schellekens and others, 1989, Montgomery, this volume; Turonian chert is found near San German (Pessagno writ. comm.in Volckmann, 1984c).

MAGUAYO VOLCANIC CENTER

In southwest Puerto Rico, north and south of the Valle de Lajas, a sequence of volcanic rocks unconformably overlies the Bermeja Complex. North of the Valle de Lajas, the volcanic rocks are mapped as Boqueron Basalt and Lajas Formation, and are overlain disconformably and locally conformably by the Cotui Limestone (Volckmann, 1984 a,c,d). South of the valley the volcanic rocks are mapped as basaltic andesite (Kba) by Volckmann (1984b) and as augite-hypersthene andesite, augite andesite, and augite-hornblende andesite by Almy (1965). These are overlain by the Parguera Limestone (Almy, 1965, 1969, Volckmann, 1984b). The Cotui Limestone, the base of which is of Campanian age (Santos and Kauffman, 1989), transgressively overlies the northern volcanic sequence. The age of the Parguera Limestone is also reported as lower Campanian (Almy, 1965, 1969) suggesting that these two limestone formations are correlatable. As no radiometric ages for the volcanic rocks are available, their minimum age can only be assigned as at least lower Campanian. Based on the stratigraphic position of these volcanic rocks, and their similar petrographical, and geochemical characteristics, the northern and southern volcanic sequences are tentatively correlated.

The name Maguayo Volcanic Center was given for the Maguayo Porphyry stock. This stock, based on its geochemistry, its radiometric ages (K-Ar age of 86.1 $\pm$ 2.1 Ma, Cox and others, 1977, Ar-Ar age of 83 Ma, Schellekens, unpublished), and its central geographic position with respect to the volcanics, probably represents the volcanic

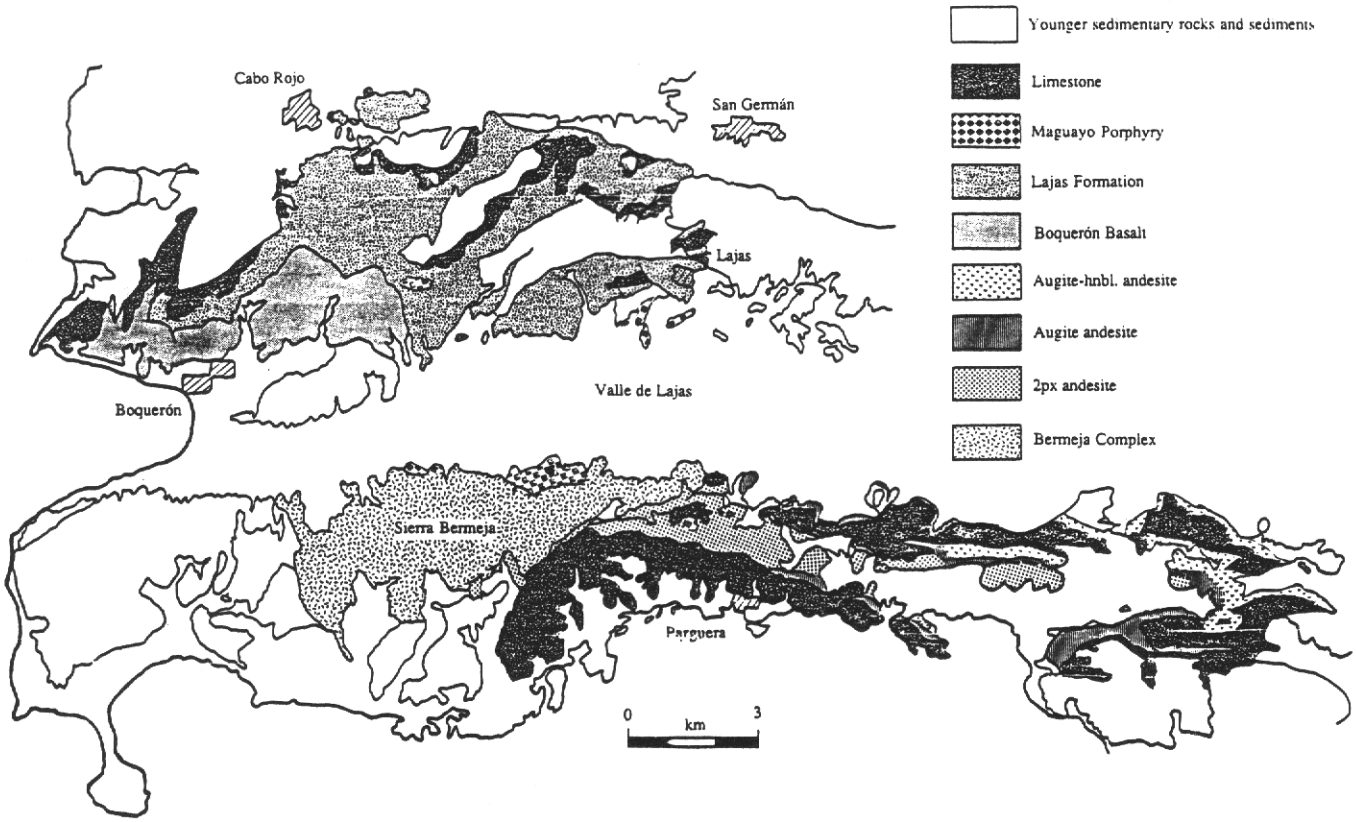

Fig.6: Geologic map of southwest Puerto Rico (see inset fig. 1 for location) showing outcrop areas of rocks assigned to Maguayo Volcanic Center (Redrawn after Almy, 1965, and Volckmann, 1984abc).

complex from which these volcanics were erupted. The Maguayo Porphyry of dacitic composition (Mattson, 1973, p.23), intrudes amphibolites and serpentinites of the northern end of the Sierra Bermeja. It consists of feldspar and hornblende, rare biotite, and quartz phenocrysts in a felsic groundmass. Rocks correlated with the Maguayo Porphyry also occur as dikes and sills cutting the Cajul Volcanics and the Mariquita Cherts. Dikes and small intrusions north of the Valle de Lajas have also been tentatively correlated with the Maguayo Porphyry. Volckmann (1984c) suggests that part of the Valle de Lajas may be underlain by this intrusion.

Geochemistry

Thirteen new whole rock analyses were obtained for rocks considered to belong to the Maguayo Volcanic Center (Table 3). Geochemically the rocks range in composition from basaltic andesite to dacite. All major elements and many trace elements show evidence, on geochemical diagrams, of element mobility (Wood and others, 1976). Those trace elements, that suggest that they behaved on a refractory manner include Sr, Y, and Zr. Spider plots of rocks, normalized to primordial mantle, for the Maguayo Porphyry and related volcanic rocks, all show a similar pattern. In order to facilitate comparison between the different units, the band of compositions for the entire Volcanic Center is drawn on the diagrams for the individual mapped formations (Fig. 7). REE patterns for the Boqueron Basalt and the rocks of the Lajas Formation, are almost identical, and show a LREE enriched pattern characteristic of calc-alkaline volcanics (Fig. 8).

AGES

Radiometric and fossil age determinations are summarized in figure 6. The oldest radiometric age of 126 $\pm$ 3 Ma (K-Ar date on hornblende in the amphibolites of the NE Sierra Bermeja, Cox and others, 1977) is interpreted as a metamorphic age. The other ages for the amphibolites, 110 $\pm$ 3.3 Ma (Mattson, 1964), and 86.3 $\pm$ 8.6, and 84.9 $\pm$ 8.5 Ma (Tobisch, 1968) are all considered to be reset, possibly by the intrusion of the Maguayo Porphyry dated at 86.1 $\pm$ 2.1 Ma (K-Ar: Cox and others, 1977), and 83 Ma (Ar-Ar: Schellekens, unpubl.). Based on the reinterpretation of the hornblende in the two-pyroxene gabbro near Maricao as a late-magmatic mineral, the 112 $\pm$ 15 Ma K-Ar (Cox and others,

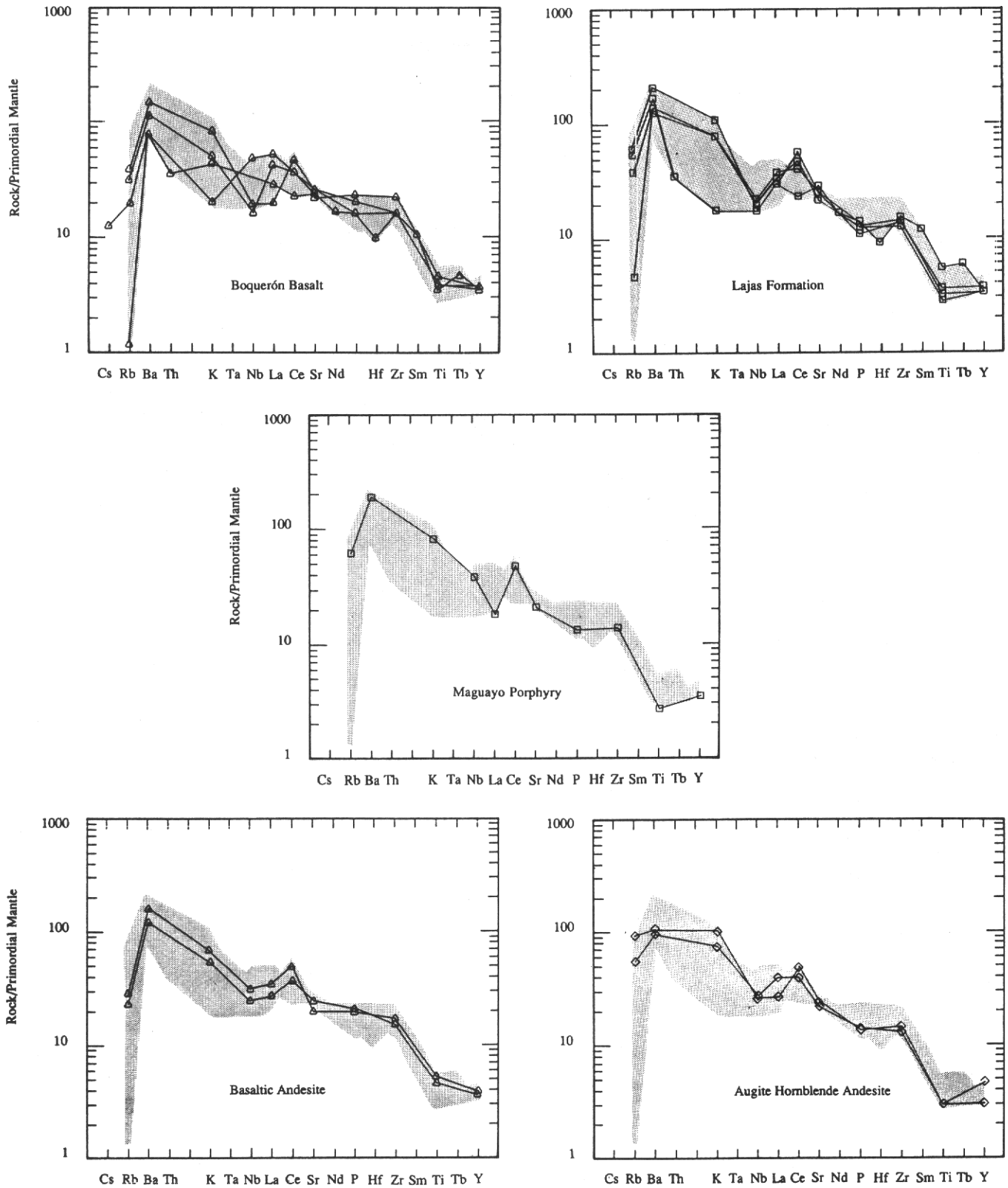

Fig.7: Primordial mantle normalized spider plots of Maguayo Volcanic Center rocks (after Wood and others, 1979). To facilitate comparison the boundaries of the entire field of Maguayo Volcanic Center rocks are drawn on each separate diagram. NB. Not all trace elements were analyzed for all samples.

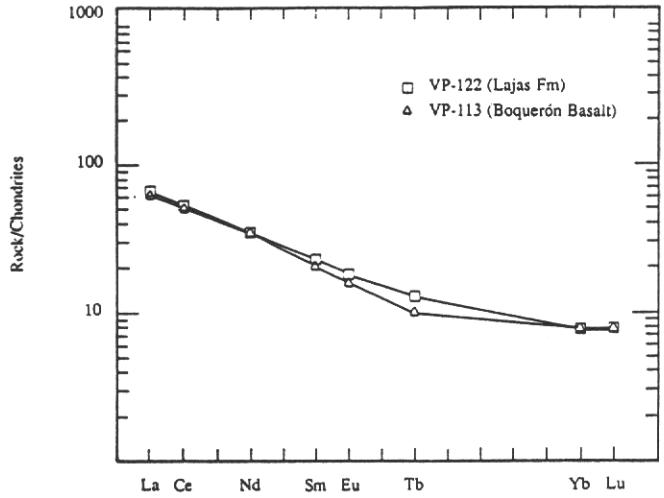

Fig.8: Chondrite normalized REE patterns for rocks of the Maguayo Volcanic Center. Normalization values from Nakamura (1974).

1977) is reinterpreted as a magmatic age. The massive amphibolite of Cerro Las Mesas was dated by Ar-Ar at 123.1 ± 2.6 Ma, with a second plateau age of 80 Ma (Schellekens, unpublished). This younger age presumably represents the age of the retrograde greenschist metamorphism of the amphibolites.

CONCLUSIONS

The formation of the rocks from southwest Puerto Rico can be divided into three stages (Fig. 9):

A first stage, characterized by Late Jurassic (156 - 146 Ma) abyssal chert deposition, is interpreted to have occurred at northern Tethyan latitudes. This conclusion is compatible with the paleomagnetic data for the Colombian Basin (Ghosh and Hall, 1989). The ocean floor on which these cherts were deposited may be present in the

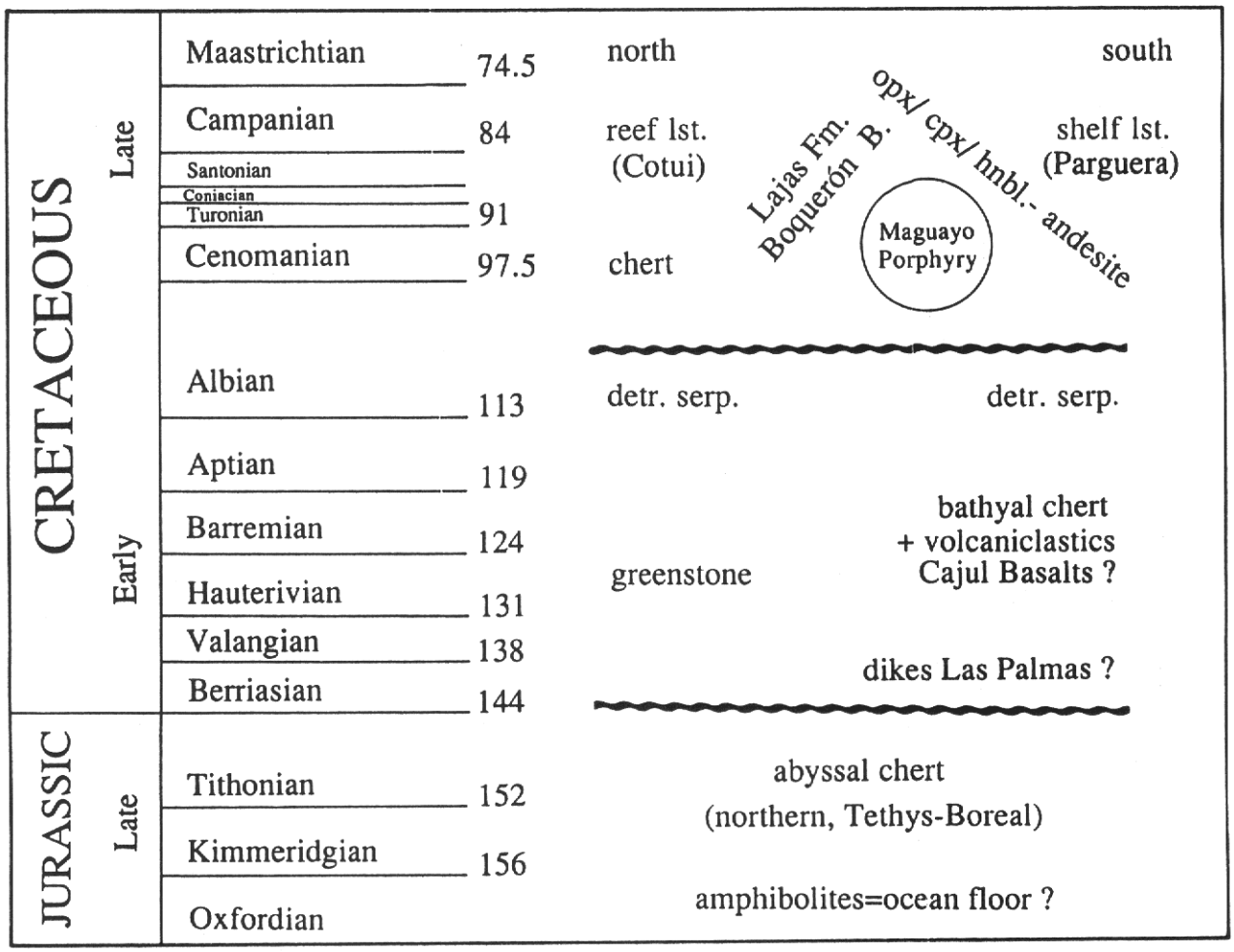

Fig.9: Summary of the stratigraphy of southwest Puerto Rico.

Bermeja Complex, as the amphibolites showing oceanic heritage.

The second stage is represented by cherts containing intercalated volcanic-derived material, that were deposited in a bathyal environment, during the Hauterivian to early Albian (131 - 113 Ma). Other rocks of this stage are amphibolites from both the northern and southern serpentinite belts, which give metamorphic radiometric ages of 123 and 126 Ma respectively, and the microgabbro from Maricao with an age of 112 Ma. The amphibolites of the northern belt are associated with the Las Mesas Greenstones, both have undergone greenschist metamorphism, presumably at around 80 Ma. Geochemical evidence indicates that the greenstones and the microgabbro represent island arc magmatic rocks. Other rocks with an island arc signature occur as low grade metamorphosed dikes, cutting the amphibolites of the southern belt.

The third stage is represented by the Maguayo Volcanic Center, an island arc volcanic complex of pre-Lower Campanian age, that intrudes and overlies the Bermeja Complex. This volcanic center was flanked by a carbonate platform to the (present day) north (Cotui Limestone), and a reef, carbonate shelf, slope to basinal environment to the (present day) south (Parguera Limestone).

Acknowledgement

This research was supported by grants from the University of Puerto Rico to J.H.S and A.L.S., Syracuse University to J.H.S., and EPSCoR grant (RII-85-13533) to all authors. J.H.S. would like to acknowledge discussions with John Dickey, and Fred Frey. H.M. would like to thank Emile Pessagno, and Donna Meyerhoff for helpful discussions. Gladys Otero, Edgar Carlo, and Enrique Collado skilfully drafted the figures.

REFERENCES

Almy, C.C., Jr, 1965, Parguera Limestone, Upper Cretaceous Mayaguez Group, Southwest Puerto Rico: Ph.D-thesis Rice University, Houston, Texas, 203 p.

Almy, C.C., Jr., 1969, Sedimentation, tectonism in the Upper Cretaceous Puerto Rican portion of the Caribbean island Arc: Transact. Gulf Assoc. Geol. Sci., v. XIX, p. 269-279.

Briggs, R.P., 1965, Geologic map of the Barceloneta quadrangle, Puerto Rico: U.S. Geol. Survey Misc. Geol. Inv. Map I-421.

Briggs, R.P. and Akers, J.P., 1965, Hydrogeologic map of Puerto Rico and adjacent islands: U.S. Geol . Survey Hydrologic Investigation Atlas HA-197.

Cox, D.P., Marvin, R.F., M'Gonigle, J.W., McIntyre, D.H., and Rogers, C.L., 1977, Potassium-argon geochronology of some metamorphic, igneous, and hydrothermal events in Puerto Rico and the Virgin Islands: U.S. Geol. Survey Journal Research, v. 5, p.689-703.

Curet, A.F., 1981, The geology of a Cretaceous-Tertiary volcano sedimentary sequence in the Mayaguez - Rosario quadrangles in west- central Puerto Rico: Unpubl. Ph.D.

_____ 1986, Geologic map of the Mayaguez and Rosario quadrangles, Puerto Rico: U.S. Geol. Survey Misc. Geol. Inv. Map I-421.

Ghosh, N. and Hall, S.A., 1989, Magnetic anomalies over the Colombian Basin, Western Caribbean Sea [Abstr.] : Abstracts 12th Caribbean Geological Conference, St. Croix, U.S. Virgin Islands, p. 55

Honorez, J., Mevel, C., and Montigny, R., 1984, Occurrence and significance of gneissic amphibolites in the VEMA fracture zone, equatorial Mid-Atlantic Ridge, in Gass,I.G., Lippard, S.J., and Shelton, J.W., eds. Ophiolite and oceanic lithosphere: Geol. Soc. London Special Publ., v. 13 , p. 121-130.

Ila, P. and Frey, F., 1984, Utilization of neutro activation analysis in the study of geologic material, in O. Harling and others, eds., Use in development of low and medium flux research reactors: Supplement to vol. 44, Atomkern Energie Kerntechnik, p.710-716.

Jakes, P. and Gill, J., 1970, Rare earth elements and the island arc tholeiitic series: Earth Planet. Sci. Letters, v. 9, p.17-22.

Krushensky, R.D., and Monroe, W.H., 1979, Geologic map of the Yauco and Punta Verraco quadrangles, Puerto Rico: U.S. Geol. Survey. Misc. Geol. Inv. Map I-1147.

Langmuir, C.H. and Bender, J.F., 1984, The geochemistry of oceanic basalts in the vicinity of transform faults, observations and implications: Earth Planet. Sci. Letters, v. 69, p. 107-127.

Leterrier, J., Maury, R.C., Thonon, P., Girard, D., and Marchal, M., Clinopyroxene composition as a method of identification of magmatic affinities of paleo-volcanic series: Earth Planet. Sci. Letters, v. 59, p. 139-154.

Lee, V.B.J. and Mattson, P.H., 1976, Metamorphosed oceanic crust or early volcanic products in Puerto Rican basement rock association: Transactions 7th Carib. Geol. Conference, Guadaloupe, 1974, p. 263-270.

Mattson, P.H., 1960, Geology of the Mayaguez area, Puerto Rico: Geol. Soc. America Bull., v. 71, p. 319-362.

Mattson, P.H., 1964, Petrography and structure of serpentinite from Mayaguez, Puerto Rico, in Burke, C.A. ed. , A study of serpentinite: NAS-NRC Publ. , v. 1188.

Mattson, P.H., 1966, Geological characteristics of Puerto Rico, in Poole, W.H. (ed.) Continental margins and island arcs: Canada Geol. Survey Paper, v. 66-15, p. 49-54.

Mattson, P.H., 1973, Middle Cretaceous nappe structures in Puerto Rican ophiolites and their relation to the tectonic history of the Greater Antilles: Geol. Soc. America Bull., v. 84, p. 21-38.

Mattson, P.H. and Pessagno, E.A. Jr., 1974, Tectonic significance of Late Jurassic - Early Cretaceous radiolarian chert from Puerto Rican ophiolite [Abstr.]: Geol. Soc. America Abstracts with programs, v. 6 (7), p. 859.

Mattson, P.H. and Pessagno, E.A. Jr., 1979, Jurassic and Early Cretaceous radiolarians in Puerto Rican ophiolite - Tectonic implications: Geology, v. 7, p. 440-444.

McIntyre, D.H., , 1975, Geologic map of the Maricao quadrangle Puerto Rico: U.S. Geol. Survey Misc. Geol. Inv. Map I-918.

Montgomery, H. , (this volume), Late Jurassic radiolarian-based paleogeography of the Sierra Bermeja, southwestern Puerto Rico: Transactions 12th Caribbean Geol. Conf. , St. Croix, 1989.

Nakamura, N., 1974, Determination of REE, Ba, Fe, Mg, Na, and K in carbonaceous and ordinary chondrites: Geochim. Cosmochim. Acta, v. 38, p.757-775.

Palmer, A.R., 1983, The decade of North American Geology 1983 geologic time scale: Geology, v. 11, p. 503-504.

Pearce, J.A. and Cann, J.R., 1973, Tectonic setting of basic volcanic rocks using trace element analyses: Earth Planet. Sci. Letters, v. 19, p. 290-300.

Pearce, J.A. and Norry, M.J., 1979, Petrogenetic implications of Ti, Zr, Y, and Nb variations in volcanic rocks: Contrib. Mineral. Petrol., v. 69, p. 33-47.

Perfit, M.R., Gust, D.A., Bence, A.E., Arculus, R.J., and Taylor, S.R., 1980, Chemical characteristics of island arc basalts, Implications for mantle source: Chem. Geol., v. 30, p. 227-256.

Renz, O. and Verspyck, G.W., 1962, The occurrence of gneissic amphibolites in southwest Puerto Rico: Geologie en Mijnbouw, v. 41, p. 315-320.

Rose, W.I.Jr., Bornhorst, T.J., and Sivonen, S.J., 1986, Rapid, High quality major and trace element analysis of powdered rock by X-ray Fluorescence Spectrometry: X-Ray Spectrometry, v. 15, p. 55 -60.

Santos, H. and Kauffman, E.G., 1989, Regional structural and volcanic events within the Cotui Limestone - Sabana Grande contact interval (Late Campanian), southwest Puerto Rico [Abstr.]: 12th Caribbean Geol. Conf. St.Croix, Abstracts, p. 149.

Schellekens, J.H., Montgomery, H., Joyce, J., and Smith, A.L., 1989, Petrology and paleontology of the Bermeja Complex, Puerto Rico, Questions about the origin of basal terranes of the northern Caribbean [Abstr.]: Abstracts with programs Geol. Soc. America, v. 21 (1) p. 40.

Tobisch, O.T., 1968, Gneissic amphibolite at Las Palmas, Puerto Rico, and its significance in the early history of the Greater Antilles island arc: Geol. Soc. America Bull., v. 79, p. 557- 574.

Volckmann, R.P., 1984a, Upper Cretaceous stratigraphy of southwest Puerto Rico, in Stratigraphic notes 1983: U.S. Geol. Survey Bull. , v. 1537A, p. A73-A83.

Volckmann, R.P., 1984b, Geologic map of the Cabo Rojo and Parguera quadrangles, southwest Puerto Rico: U.S. Geol. Survey Misc. Geol. Inv. Map I-1557.

_____ 1984c, Geologic map of the San German quadrangle, southwest Puerto Rico: U.S. Geol. Survey Misc. Geol. Inv. Map I-1558.

_____ 1984d, Geologic map of the Puerto Real quadrangle, southwest Puerto Rico: U.S. Geol. Survey Misc. Geol. Inv. Map I-1559.

Wadge, G., Draper, G., and Lewis, J.F., 1983, Ophiolites of the northern Caribbean, A reappraisal of their roles in the evolution of the Caribbean plate boundary, in Gass, I.G., Lippard, S.J., and Shelton, J.W. eds., Ophiolites and oceanic lithosphere: Geol. Soc. London Special Publication, v. 13, p.367-380.

Wood, D.A., Gibson, I.L., Thompson, R.N., 1976, Elemental mobility during zeolite facies metamorphism of the Tertiary basalts of eastern Iceland: Contrib. Mineral. Petrol., v. 55, p. 241-254.

Wood D.A., Joron, J.L., and Treuil, M., 1979, Reappraisal of the use of trace elements to classify and discriminate magmas erupted in different tectonic settings: Earth Planet. Sci. Letters, v. 45, p. 326-336.

TOXIC SUBSTANCES IN THE COASTAL ENVIRONMENT OF THE US VIRGIN ISLANDS, 1986

B.L. Oostdam
Millersville University
Millersville, Pennsylvania 17551

ABSTRACT

A two phase investigation was made of the concentration levels of toxic substances in the marine sediments and coastal waters around the U S Virgin Islands. The Pilot Phase, March 1986, served to screen six composites of three bottom samples each, representing the main pollution impact areas and a control, for all 129 EPA priority toxic substances. Based on the virtual absence of any toxic organics in any of these composites, the Main Phase, July/August 1986, concentrated on sampling and analyzing for the 13 priority toxic trace elements in pairs of samples of seawater and marine sediment at 24 locations around the three islands.

Locally elevated concentrations were found of several trace elements, especially Ni, Pb, Hg, Zn and Cu. Highest contamination occurred in the fine muds off HOVIC, St Croix and Mangrove Lagoon, St Thomas. By contrast, concentrations at the Sewage Treatment Plant (STP) outfall off St Croix were significantly below average. The order of degree of pollution by island was St Croix > St Thomas > St John.

Very low correlation was found for trace element levels in marine sediments and in adjacent terrestrial rocks and soil analyzed by USGS, suggesting that erosion contributes little to the trace element distribution pattern, with the possible exception of Ni. Distribution of Hg and Pb can be partly explained from transport by the predominant trade winds. Other 'hot spots', e.g. Cu and Zn in harbors, clearly result from point sources of anthropogenic inputs.

In conclusion, the USVI marine environment is relatively pure and impacts of inorganic trace elements are largely localized.

INTRODUCTION

An investigation was made of the toxic substances in the sediments, seawater and biota of the coastal environment of the US Virgin Islands (USVI). The project was carried out by a combined team from the College of the Virgin Islands (CVI)[1] and Millersville University (MU), under contract to the Department of Conservation and Cultural Affairs (DCCA)[2] of the USVI. It comprised sampling and chemical analysis, review of available relevant data, and recommendations on required legislation, monitoring and research.

The U S Virgin Islands are located in the Caribbean at a latitude of 18 to 19 degrees North about 70 km east of Puerto Rico (Fig. 1). The three main islands are St Thomas, with a population of 51,020 (1985) and area of 83 km^2, St Croix: 57,020 and 218 km^2 and St John: 2,760 and 52 km^2. Because of the tropical setting, clear waters, attractive beaches and protected bays, tourism is the main source of income, reflected in 1,220,586 visits during 1985. By contrast, industry and manufacturing have declined in the last decade - which witnessed the discontinuation of Martin Marietta's Aluminum smeltery as well as Hess Oil refineries-, while agriculture and fisheries are negligible.

[1] now University of the Virgin Islands
[2] now Department of Planning and Natural Resources

Two major sets of environmental problems associated with the increase in population and tourism are water supply and waste disposal. The principal **point sources** of pollution, requiring discharge permits from the DCCA under the NPDES (National Pollutant Discharge Elimination System) are WAPA (Water and Power Authority, desalination plants on St Croix and St Thomas), POTW's (Publicly Owned Treatment Works), sanitary landfills, and a few industries, chiefly HOVIC (Hess Oil of the Virgin Islands)(Fig. 1). **Non-point sources** include atmospheric input, natural drainage, urban runoff, vessel waste and floating oil and tar (USVI Department of Health, 1972; DCCA, 1979; Wernicke, 1986; Wernicke & Towle, 1983).

Previous investigations of toxic substances in USVI coastal waters are reported by USEPA (1973) and Alonso (1983), and compiled in EPA's STORET data bank. Site-specific studies which include some data on toxics were made by Nichols and Towle (1977) and USACE (1982) on Mangrove Lagoon/Benner Bay, St Thomas, Beck (1974) on WAPA, and USEPA (in STORET), chiefly on HOVIC Harbor. Soils, river sediments and rocks on St John and St Thomas were analyzed by the USGS (Hopkins et al., 1984)

Our results indicate that all USEPA defined priority organic toxic substances were below detection limits. As to inorganic toxics, however, local elevated concentrations were found of several trace elements, including Ni, Pb, Hg, Zn and Cu. The highest degree of contamination occurred in the fine muds off HOVIC, St Croix and Mangrove Lagoon, St Thomas. By contrast, concentrations were significantly below average at both POTW outfalls.

PROCEDURES

The study consisted of two parts: the Pilot Phase, conducted in March, 1986, and the Main Phase, July/August 1986. Because of the high cost of a complete analysis for all 129 EPA priority toxic substances - in excess of $1,000 for a single sample - only few samples could be completely analyzed. We, therefore, opted to combine sample sets into composites. In the first phase, five composites of three sediment samples each from four main impact areas and the St John control site were analyzed for all 129 EPA priority toxic substances. Based on the initial results, the second phase emphasized the 13 EPA priority toxic trace elements in both sediment and seawater at 24 sample sites (Fig. 1).

Sampling around St Thomas and St John was done from the CVI's R.V. 'Burkholder', while the DCCA's monitor vessel was used around St Croix. SCUBA divers wearing disposable plastic sterile gloves used appropriate pre-

Larue, D.K., and Draper, G., eds.,
Transactions of the 12th Caribbean Conference, St.Croix U.S.V.I., Miami Geological Society,
P.O. Box 14433, Coral Gables, FL 33114

cleaned containers to take water samples at mid-depth, as well as a teflon-coated scoop to collect a surface sediment layer of about 5-10 cm into a large plastic jar. Although occasionally biota were collected and analyzed, results are not reported here. All samples were kept refrigerated and hand-carried to the EPA - certified Radiation Management Corporation (RMC) Laboratory in Pottsville, PA for analysis in accordance with EPA's (1982) specified procedures for storage, holding time and method of analysis.

Associated field measurements included position by handbearing compass, depth by Lowrance CG 336-2003 portable fathometer, dissolved oxygen by YSI Model 54A oxygen analyzer, salinity and temperature by YSI Model 33 in situ conductivity-salinometer, and water transparency by standard Secchi disc. Grainsize analyses were performed at CVI and MU by sieving at 1/2 phi intervals or, in the case of muds, by pipette (Folk, 1952)

RESULTS

Station locations for the four composites collected in March and for all 24 stations sampled in July/August 1986 are plotted in Figure 1. Table 1 shows specific details of the 24 stations, including latitude and longitude, water depths and type of pollution activity.

The water column was characterized by temperatures ranging from 25.5 to 31.5^0 C, salinities from 31.8 to 37.9 %o, and generally excellent visibility. Most of the sediments consisted of medium - to fine-grained sands (Table 1), very poorly to moderately well-sorted, and principally biogenous in composition (fragmented shell, algae, foraminifera, corals, echinoids and sponge-spicules). Odiferous anaerobic muds were found in HOVIC Harbor, St Croix, and Mangrove Lagoon, St Thomas, and slightly smelly, greasy silts in Coral Harbor and Cruz Bay, St John.

Because of financial restrictions only the four composite bottom sample shown in the inset of Figure 1, as well as one water sample from HOVIC Harbor were tested completely for all 129 EPA priority toxic substances. All organic toxic substances occurred in concentrations below detection limits, but the 13 toxic inorganic trace elements did not and therefore required more detailed studies, which are summarized in Table 2. Based on replicate sampling and interlaboratory comparison (Oostdam, 1986), all elemental analyses except those for Antimony (Sb) were accepted as reliable. The latter are included, however, because of their internal consistency.

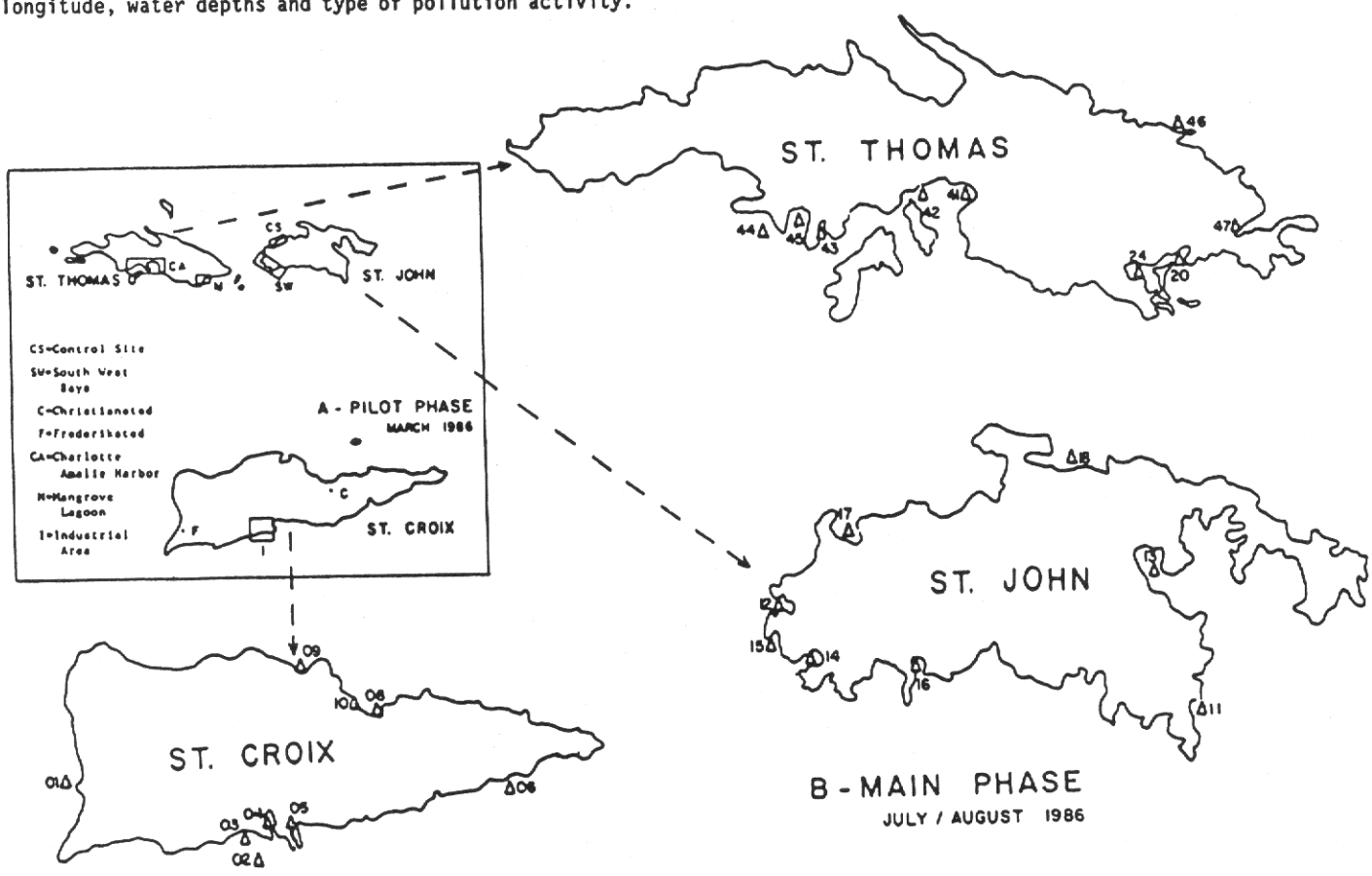

Figure 1. Station Locations, U.S.V.I. Toxic Substances Project,1986
Quadrangles of inset represent pollution impact areas and the overall control site of the Pilot Phase.
Triangles on main part of map are individual sampling sites of the Main Phase. Note: main map is not to scale.

DISCUSSION

Disregarding values below the lower detection limits, there is a considerable variation in the concentrations of several of the trace elements. Pb, Ni and Cu vary through three orders of magnitude, As, Cr and Hg through two; in fact, the ratio of the highest Pb measured to lowest amounts to 7,470, almost four orders. These high variabilities strongly suggest anthropogenic effects, even though natural variability of trace elements is also high.

Comparison with earlier data sets, e.g. EPA's 1972, 1979 and 1982 results, suffer from differences caused by improved analytical techniques (Amore, 1976) which render them inadequate for assessing temporal variations (Oostdam, 1986).

By contrast, areal variations can be more reliably evaluated. In general, trace element concentrations in sediments were highest in St Croix and lowest in St John, as expected on the basis of degree of pollution activity and impact. The worst polluted sites were the industrial complex off southern St Croix, specifically HOVIC Harbor and vicinity (Figure 2). On St Thomas, Benner Bay, Mangrove Lagoon and Careening Cove showed elevated concentrations. Each of these sites also displayed high percentages fines &/or low percentages solids (Tables 1 and 2), which contributes to the adsorption capacity of the sediments.

TABLE 1: STATION LOCATIONS AND RELATED DETAILS, US VIRGIN ISLANDS TOXIC SUBSTANCES PROJECT (July 15-August 7, 1986)

STA	LATITUDE (N)	LONGITUDE (W)	WATER DEPTH (M)	LOCATION	DATE	SEDIMENTS(1): % FINES	SEDIMENTS(1): MEAN PHI	REMARKS
				ST. CROIX:				
01	17 42.9	64 53.2	9.2	Frederiksted	July 15	0.40	1.65	harbor
02	17 40.8	64 47.0	7.9	STP Outfall	July 16	0.02	1.18	sewage
03	17 41.7	64 47.2	1.5	off Anguilla	July 16	0.16	1.96	dumpsite
04	17 42.0	64 46.0	0.9	Krause Lagoon	July 16	3.0	-0.35	former Al.Smeltery
05	17 42.1	64 45.1	7.6	HOVIC Harbor	July 16	49.0	3.49	oil refinery
06	17 43.7	64 37.6	2.4	Robin Bay	July 16	0.27	1.36	Control site
08	17 45.4	64 42.9	7.0	Gallows Bay	July 15	12.1	2.01	marina
09	17 46.5	64 45.4	2.7	Salt River	July 15	7.33	1.32	yacht basin
10	17 45.2	64 42.8	1.5	Christiansted	July 15	4.86	1.41	desal. plant
				ST. JOHN:				
12	18 19.4	64 47.4	5.8	Great Cruz Bay	August 6	12.8	2.25	harbor
13	18 20.7	64 42.7	4.9	Coral Harbor	August 5	31.5	3.45	harbor
14	18 20.1	64 47.8	4.6	Cruz Bay	August 5	16.5	3.32	harbor
15	18 19.7	64 47.9	4.9	Turner Bay	August 5	0.62	1.30	sewage discharge
16	18 19.3	64 45.8	1.5	Fish Bay	August 6	4.65	2.16	dumpsite
17	18 21.0	64 46.8	4.9	Hawksnest Bay	August 5	0.62	1.87	CONTROL SITE
				ST. THOMAS:				
20	18 19.2	64 52.1	1.5	Benner Bay	August 6	11.4	1.83	marina
24	18 19.1	64 52.9	1.2	Mangrove Lagoon	August 6	2.61	0.33	dumpsite
41	18 20.2	64 52.2	9.2	Long Bay	July 30	14.1	0.64	harbor, marina
42	18 20.3	64 56.4	6.1	Careening Cove	July 30	10.1	2.13	marina
43	18 20.0	64 57.7	5.5	Krum Bay	July 30	11.5	1.93	desal. plant
44	18 20.0	64 58.5	20.7	off Red Point	July 31	17.2	1.99	sewage outfall
45	18 20.0	64 57.9	4.3	Lindbergh Bay	July 31	1.29	1.38	WAPA discharge
46	18 21.1	64 52.0	5.5	Coki Bay	August 7	0.14	1.17	control site
47	18 19.5	64 51.2	1.2	Vessup Bay	August 7	1.27	0.85	marina

(1) % FINES = fraction finer than 4 phi (very fine sand):
PHI = $-\text{LOG}_2$ (diameter in mm): e.g. 4 phi = 0.125mm

TABLE 2: USEPA PRIORITY TOXIC TRACE ELEMENT CONCENTRATIONS IN USVI MARINE SEDIMENTS, July/August, 1986
(mg. kg^{-1}, or ppm, dry weight)

SAMPLE (NOTE 1)	% SOLIDS (NOTE 2)	SB (NOTE 3)	AS	BE	CD	CR	CU	PB	HG	NI	SE	AG	TL	ZN
01-30	80.9	148	0.37	0.04	<0.012	5.32	5.32	1.48	<0.025	0.74	0.74	<0.012	<0.062	4.25
02-26	84.6	160	0.07	<0.012	<0.012	0.59	0.17	0.01	<0.015	3.07	1.00	<0.012	<0.059	2.91
03-05A	67.5	76.1	8.9	0.089	0.415	14.8	24.4	17.0	0.015	5.19	2.15	0.030	<0.044	91.1
04-03	7.1	625	28.2	<0.141	<0.141	50.7	69.0	2.39	0.141	8.45	6.90	<0.141	<0.704	49.2
05-25	29.8	179	10.1	0.340	0.30	90.6	117	40.3	0.77	60.4	3.36	0.067	<0.168	386
06-08 cs	76.9	148	1.43	<0.013	<0.013	7.54	0.78	0.156	<0.143	0.78	2.08	<0.013	<0.065	3.95
08-23	73.6	123	5.43	0.14	0.04	14.9	312	40.8	0.48	5.71	2.58	0.08	<0.068	79.8
09-09	49.0	20.4	14.3	0.82	0.06	23.5	198	13.5	0.08	15.3	1.00	0.04	<0.102	10.6
10-05	78.9	44.0	6.34	0.51	0.03	35.5	45.6	10.1	<0.005	20.3	3.04	0.013	<0.063	47.4
12-19B	70.7	68.4	4.26	0.07	0.03	14.2	17.0	0.47	<0.006	2.70	2.98	<0.014	<0.071	32.3
13-16B	71.2	59.7	5.62	0.08	<0.013	7.02	14.0	0.58	0.125	84.3	4.78	<0.014	<0.070	21.2
14-15B	71.0	78.6	1.13	0.04	0.03	9.86	11.3	0.66	0.023	1.27	5.63	<0.014	<0.070	26.2
15-16B	75.1	87.6	5.33	0.03	<0.013	5.19	4.53	0.21	<0.005	21.3	4.93	<0.013	<0.067	6.13
16-05B	72.2	82.0	2.77	0.04	<0.013	9.70	11.1	0.15	<0.006	1.25	6.09	<0.014	<0.069	19.7
17-16B CS	76.9	103	1.30	0.01	<0.013	5.20	0.91	0.08	<0.005	0.39	5.85	<0.013	<0.065	3.51
20-05	49.8	51.0	9.04	0.42	0.08	14.1	98.4	26.1	0.18	8.03	4.82	0.100	<0.100	8.23
24-04	43.2	72.7	13.9	0.19	0.09	18.5	55.5	5.09	0.063	764	4.17	0.116	<0.116	81.0
41-30	79.6	43.6	7.54	0.10	0.05	12.6	151	50.3	0.33	6.03	1.88	0.163	<0.063	95.7
42-20B	50.9	48.5	13.8	0.20	0.18	31.4	157	74.7	0.59	15.7	2.36	0.33	<0.099	356
43-18B	57.6	60.2	8.51	0.10	0.07	19.1	71.2	26.0	0.28	13.9	3.65	0.07	<0.087	104
44-68B	73.4	76.0	3.00	0.04	0.03	8.2	6.8	5.4	0.03	1.36	5.86	0.14	<0.068	28.1
45-14B	72.5	78.5	0.69	0.03	<0.014	6.5	6.8	0.69	<0.005	1.38	6.34	<0.014	<0.069	14.8
46-18B cs	79.6	85.6	0.25	<0.013	<0.013	13.8	0.75	0.10	<0.005	0.25	6.16	<0.013	<0.063	3.6
47-04B	70.7	57.0	3.54	0.03	0.057	5.52	45.3	4.38	0.10	0.99	4.10	0.057	0.071	55.2

Note 1: 45-14B represents sample Number 45, waterdepth 14 feet, replicate B
cs = control station for island, CS = control station for three islands

Note 2: data are calculated on dry weight basis, accounting for water in muddy sediments
this column details the % solids of the entire sample - the rest is water

Note 3: based on replicate - and interlaboratory comparison, values for Sb are considered spuriously high, because they are internally consistent, however, they are included for the purpose of comparing areal variations.

Based on an intercomparison of concentrations of **sewage-related trace elements** in the STP outfalls off St Croix (Figure 2) and St Thomas with sewage disposal sites off the continental USA and in Solway Firth, U.K. (Table 3), the USVI sites, especially St Croix, showed surprisingly little impact from the marine discharge operations. This fact is attributed to the lower discharges and better dispersal, and is clearly relevant to future licensing and exemption considerations.

Comparing the **specific toxic trace elements** from USVI averages and control (sample 17-16B) with STORET means for ambient USA ocean sediments and with worldwide means (Table 4), USVI sediments appear enriched - though not dangerously so - in Se and Ni (and possibly Sb), but much below STORET values in the elements Be, Cd, Hg and Ag.

TABLE 3: COMPARISON OF SEWAGE - RELATED TRACE ELEMEMENTS IN SEDIMENTS NEAR USVI STP OUTFALLS WITH THOSE OF SIMILAR SITES WORLDWIDE

(mean concentrations, in mg. kg^{-1}, (ppm) dry weight)

Trace Element:	Cr	Cu	Ni	Pb	Zn	
Average Daily Ingestion: ($ug.d^{-1}$)	144	2,100	460	138	16,900	(1)
US VIRGIN ISLANDS:						
- Control, STA 17:	5.2	0.91	0.39	0.08	3.51	
- St. Croix STP, STA 02:	0.59	0.17	3.07	0.01	2.91	
- ST. Thomas STP, STA 44:	8.2	6.8	1.36	5.4	28.1	
FORMER PHILADELPHIA DUMPSITES:						(2)
- Off Delaware Bay (n=25):	1.11	-	1.56	2.84	4.02	
- Off Ocean City MD (n=6):	1.22	-	2.20	2.80	6.0	
NEW YORK BIGHT:						(3)
- Unaffected	6	3	3	12	18	
- Center of Former Dump: (n=21)	105	141	24	157	259	
S. CALIFORNIA BIGHT:						
- Los Angeles Harbor (n=5):	123	99	31	174	202	(4)
- Whites Point (1 km from Los Angeles City Outfall):						(5)
-Sediments	730	590	84	430	1,800	
-Wastewater Particulates	1,700	1,120	220	570	4,100	
SOLWAY FIRTH, UK: (n=53):	39	10	-	40	66	(6)

(1) Anon., 1974 (2) Oostdam et al., 1975 (3) Carmody et al., 1973

(4) Emerson et al ., 1976 (5) Bruland et al., 1974 (6) Halcrow et al., 1973

A search for possible sources indicated very low correlations between trace element concentrations in marine sediments and in adjacent terrestrial rocks and soil (Hopkins et al. 1984; also see Ramos-Perez and Gines-Sanchez, 1988), with the possible exception of high values for Ni on St John and St Thomas. The distribution pattern of Pb and Hg suggests the influence of transport by the prevailing trade winds. Other distribution patterns are best explained by local anthropogenic inputs, e.g. Cu and Zn in harbors and marinas.

CONCLUSION

The USVI marine environment in general is relatively pure, especially with respect to organic toxic substances. Impacts of inorganic toxic trace elements on bottom sediments is largely localized, e.g. HOVIC Harbor.

Anthropogenic inputs of some trace elements, e.g. Cu, Pb and Hg, exceed natural inputs from erosion and cause fluctuations in concentrations through three or more orders of magnitude. Although sediments with elevated toxic trace element concentrations need not be inherently dangerous to man, consumption of shellfish caught in such sediments should be avoided.

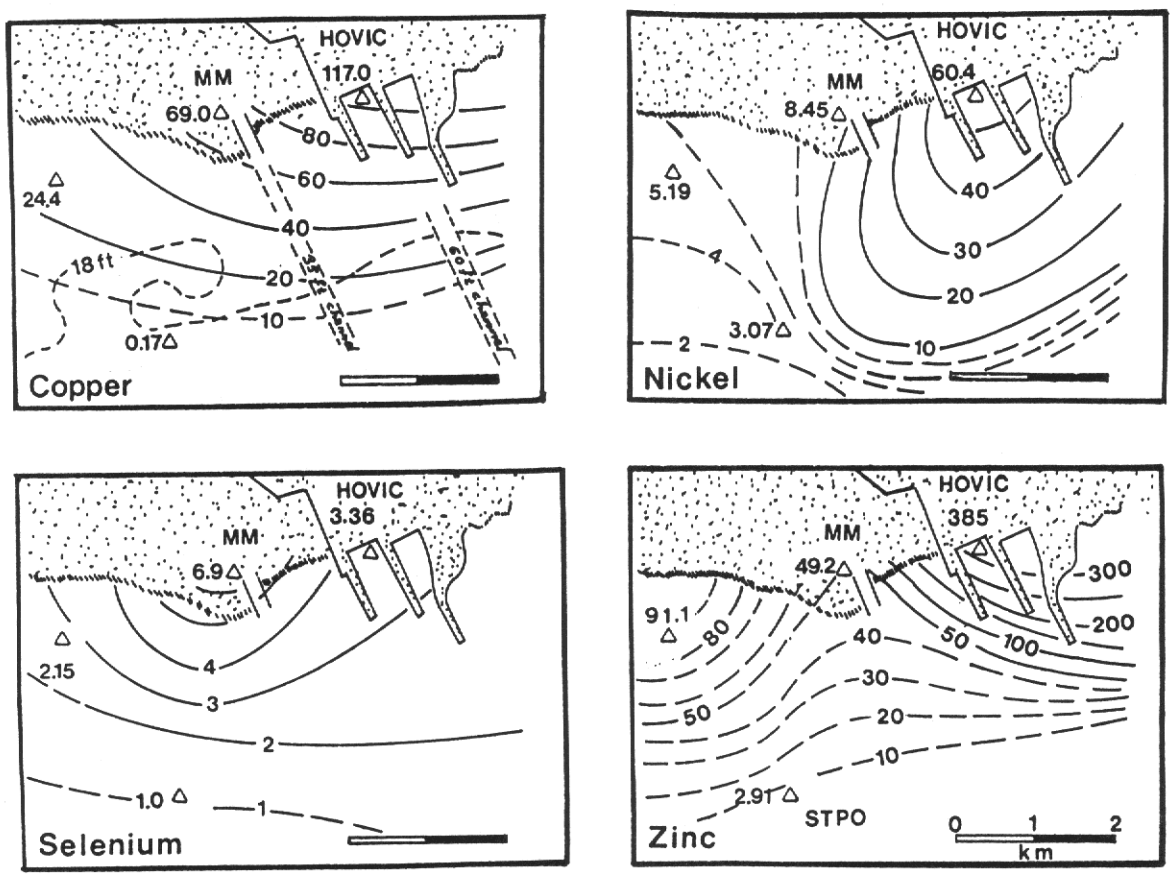

Figure 2. Concentration Contours for Selected Toxic Trace Elements in Nearshore Sediments off Southern St. Croix, U.S.V.I., 1986. Concentrations are in mg per kg dry weight (ppm). The area shown corresponds to rectangle 1 on inset of Figure 1. Triangles represent sampling sites.
MM = Martin Marietta Aluminum Smelter (now VIALCO)
HOVIC = Hess Oil of the Virgin Islands Corp., oil refinery
SL = site directly off Sanitary Landfill
STPO = Sewage Treatment Plant Outfall

TABLE 4: COMPARISON OF TOXIC CONCENTRATION MEANS OF USVI SEDIMENTS WITH STORET AND WORLDWIDE MEANS.

Toxic trace element or compound	C O N C E N T R A T I O N (milligram per kilogram (ppm) dry) USVI mean (n=24)	USVI control <STA 17> (n=1)	Storet ambient ocean seds 1)	W O R L D W I D E M E A N S continental rock 2)	continental soil 2)	rivers susp. sed. 2)	deep sea clay 2)
Sb*	<101.	103	4.66	0.90	1.00	2.50	0.80
As	6.49	1.30	8.22	7.90	6.00	5.00	13.0
Be	<0.146	0.01	1.57	-	-	-	-
Cd	<0.072	<0.013	6.37	0.20	0.35	1.00	0.23
Cr	17.7	5.20	489.2	71	70	100	100
Cu	59.2	0.91	12.1	32	30	100	200
Pb	13.4	0.08	13.9	16	35	100	200
Hg	<0.143	<0.005	1.44	-	-	-	-
Ni	43.4	0.39	18.2	49	50	90	200
Se	3.85	5.85	0.91	-	-	-	-
Ag	<0.062	<0.013	3.09	0.070	0.050	0.070	0.100
Tl	<0.103	<0.065	0.18	-	-	-	-
Zn	63.8	3.51	118	127	90	250	120

*USVI - values for Sb are considered spuriously high

1) From USEPA STORET sample data for ambient ocean samples collected between 1967 and 1986, using all values (including >, <, and est.). The number of samples ranges from minimum of 8 for Tl to a maximum of 3,984 for Zn, Courtesy Mr. John Higgins, USEPA, Edison, NJ..

2) After Martin and Whitfield, Tables 5 and 6, in Wong, C.S. et al., 1983.

Additional Studies should include investigation of:

(1) The interrelation between toxic substances in sediments and their superjacent waters.

(2) The causes of variation in concentrations of toxic trace elements in water, sediment and biota.

(3) The optimization of sampling and monitoring operations.

(4) Mechanisms of effective regulation and enforcement, including setting of realistic criteria, standards and guidelines.

(5) Improvements in emergency preparedness for spills of toxic substances, including oil and raw sewage, caused by such disasters as the recent Hurricane

ACKNOWLEDGEMENTS

The author thanks the University of the Virgin Islands, the Department of Planning and Natural Resources and Millersville University for financial support. Professor Helen Gjessing acted as project manager, Dinah Johnson as program supervisor. On and in the water, Dan O'Sullivan, Steve Mowry, Mark Sabino and Ellis Webster proved indispensable. At MU, Dr. Thomas Greco, Doug Brodhecker, Andy Driscoll, Wallace Koster and Linda Sheets provided useful consultation and assistance, at UVI Drs. Bill MacLean and LaVerne Ragster, and at DCCA Kurt van Gelder, Phyllis Hall-Brin and Marcia Gilnack. Data and information were generously made available by Aristotle Harris, John Higgins and Lloyd Kahn of EPA, Bob Neuman of the USACE, Jim Audet and Robert Kornspan of NOAA and various staff-members of the Caribbean Research Institute, the West Indies Laboratory, the Island Resources Foundation and the National Park Service.

REFERENCES

Alonso, John C., 1983, Toxic Pollutants in Sediment, St. Croix, USVI., Unpubl. Report, USEPA/DCCA, 8 pp.

Amore, F., 1976, Losses, Interferences and Contamination in Trace Analysis- Some Examples. Nat. Bur. of Standards Spec. Publ. 442: Accuracy in Trace Analysis: Sampling, Sample Handling and Analysis, Vol.1, p.661-669.

Anon., 1974, Chemistry, Vol.47, no.6, p.4-5.

Beck, R.W. and Associates, 1974, NPDES Environmental Analysis for the Virgin Islands Water & Power Authority.

____,1986, Review and Evaluation of the Wastewater Discharge Monitoring at the St. Thomas and St. Croix Power Plants, VI Water and Power Authority.

Bruland, Kenneth W., 1983, Trace Elements in Sea-Water, in Chemical Oceanography, Vol.8, p.157-220, Academic Press, London.

Carmody, D.J., Pearce, J.B. and Yasso, W.E., 1973, Trace Metals in Sediments of the New York Bight. Mar. Pollut. Bull., Vol.4, no.9, p.132-135.

Department of Conservation and Cultural Affairs, USVI, 1979, Virgin Islands' Lead Implementation Plan.

____, 1984, Handbook for Homebuilders and Developers. VI Coastal Zone Management Program, 153 pp.

Department of Health, USVI, 1972, Contingency Plan for the Control of Oil and Other Hazardous Materials in the US Virgin Islands, 20 pp.

Federal Register, Nov. 28, 1980, Guidelines for Deriving Numerical National Water Quality Criteria for the Protection of Aquatic Life and Its Uses. Vol.45, p.79341 (revised in 50 FR 308784, July 29, 1985).

Folk, Robert L., 1974. Petrology of Sedimentary Rocks. Hemphill Publ. Co., Austin, Texas, 182 pp.

GESAMP (IMCO/FAO/UNESCO/WMO/WHO/IAEA/UN) Joint Group of Experts on the Scientific Aspects of Marine Pollution, 1976, Review of Harmful Substances. Reports and Studies no. 2, 80 pp.

Halcrow, W., MacKay, D.W., and Thornton, I., 1973, The Distribution of Trace Metals and Fauna in the Firth of Clyde in Relation to the Disposal of Sewage Sludge. Jour. Mar. Biol. Assoc. U.K., Vol.53, p.721-739.

Hopkins, R.T., Tucker, R.E., Roemer, T.A., Sharkay, J.D., and Aubin, L.L., 1984, Analytical Results from a Geochemical Survey of St. Thomas and St. John, USVI, Using Soil, Rock and Panned Concentrate Samples. Open File Report 84-784, US Dept. Interior, Geol. Survey, 64 pp.

Ketchum, Bostwick H., 1977, The Water Environment, in The Integrity of Water, USEPA Symp., p.25-32.

Martin, J.M., and Whitfield, M., 1983, The Significance of the River Input of Chemical Elements to the Ocean, in Trace Metals in Sea Water (Wong et al., editors), Plenum Press, New York, p.265-296.

Nichols, Maynard and Towle, Edward, 1977, Water, Sediments and Ecology of the Mangrove Lagoon and Benner Bay, St. Thomas, Rept. By Island Resources Foundation to Dept. of Conservation and Cultural Affairs, USVI, 159 pp.

Oostdam, B.L., 1983, Sewage Sludge Dumping in the Mid-Atlantic Bight in the 1970's: Short-, Intermediate- and Long-term Effects, in Wastes in the Ocean, vol. 1, (Duedall, I, editor) Proc. Second Internat. Symp. on Ocean Dumping, Woods Hole, Mass, 1980, p.196-209.

Ramos-Perez, Carlos and Cindy Gines-Sanchez, 1988, Geochemistry of St. John and Influence on Marine Systems, Virgin Islands Resource Management Cooperative, Biosphere Reserve Research Rept. no. 28, 34 pp.

US Army Corps of Engineers, 1982, Section 107, Reconnaissance Report, Benner Bay, St. Thomas, USVI., U.S. Engnrs. District, Jacksonville, FL.

US Environmental Protection Agency, 1980, Ambient Water Quality Criteria For....[individual publications for each of the thirteen toxic trace elements].

____, 1982, Water Quality Standards Handbook. Off. of Water Regulations and Standards, Washington, DC.

Wernicke, W., 1986, Urban Pollution Survey, Christiansted and Charlotte Amalie, USVI. Rept. by Donald L. Hamlin Consulting Engnrs. for Dept. of Conservation and Cultural Affairs, USVI.

Wernicke, W. and Towle, E.L., 1983, Vessel Waste Control Plan for the USVI. Rept. by Island Resources Foundation for Dept. of Conservation and Cultural Affairs, USVI.

Wong, C.S., Boyle, Edward, Bruland, Kenneth W., Burton, J.D. and Goldberg, Edward D. (editors), 1982, Trace Metals in Sea Water. NATO Confer. Series, no. 12, Elsevier Scient. Publ. Co., New York.

==========

TAPHONOMIC BIASING OF SUBFOSSIL ECHINOID POPULATIONS ADJACENT TO ST. CROIX, U.S.V.I.

Benjamin J. Greenstein
Department of Geology
University of Cincinnati
Cincinnati, Ohio 45221-0013

ABSTRACT

The distribution of live- and dead-echinoid populations occurring in forereef, reef and shallow subtidal environments in Smuggler's Cove and Rod Bay, St. Croix, was determined along 720 m and 50 m transects, respectively. Although echinoids are generally regarded as ubiquitous in shallow reef and adjacent environments, their distributions in Smuggler's Cove and Rod Bay are patchy. No intact tests of dead individuals were found associated with living populations and constituent particle analysis reveals a lack of correspondence between live echinoid distribution and sediment composition. Additional experiments conducted in the laboratory indicate that taxonomically-controlled differences in the size distribution of echinoid skeletal elements could play a role in determining their style of preservation. The lack of association of live and dead faunas as well as the results of field and laboratory experiments suggest that echinoids are quickly acted on by biostratinomic processes; their preservation, therefore, may require extraordinary circumstances. One such circumstance possibly occurred during 1983-84, when mass mortality decimated populations of *Diadema antillarum* adjacent to St. Croix. Tests and spines of *D. antillarum* were observed accumulating in seagrass beds immediately leeward of the reef tract in Smuggler's Cove in 1984. A piston core taken in 1988 from a seagrass bed leeward of the reef tract was analyzed centimeter by centimeter to determine if a horizon unusually rich in *Diadema* skeletal elements has been preserved as a result of the baffling and binding properties of the bed. No horizon is evident in the macro- or microscopic components of the core. The lack of a "*Diadema* spike" in an environment of net sediment accumulation suggests that individual tests of *Diadema* degrade so rapidly that increasing the amount of subfossil material as a consequence of the mass mortality alone was insufficient to preserve the event. Results of field and laboratory work are currently being synthesized into a predictive model for taphonomic overprint affecting fossil echinoids. A test of the model using literature-derived data of echinoid fossil occurrences is ongoing.

INTRODUCTION

The Class Echinoidea originated in the Ordovician and has a long and abundant fossil record. Their evolutionary history as interpreted through the fossil record is necessarily influenced by taphonomic bias. Kier (1977) demonstrated that, although both regular (generally epifaunal, radially symetrical) and irregular (generally infaunal, bilaterally symetrical) echinoids have rich fossil records, fossil regular echinoids are less abundant than their irregular counterparts. Kier also suggested that life habit and test construction of regular echinoids are, in part, responsible for their lower preservation potential. Thus, biostratinomic processes would be expected to particularly affect regular echinoids, rapidly obscuring any recognizable remains.

Schäfer (1972) described that, in the absence of rapid burial, echinoids disarticulate readily once decay sets in. Work by Greenstein and Meyer (1985a, b) extended this conclusion by demonstrating that scavengers greatly accelerate the disarticulation of the echinoid skeleton. Greenstein (1989) concluded that no recognizable signature of the mass mortality of *Diadema antillarum* remained in sediments surrounding a fringing reef in Bonaire, suggesting that increasing the amount of subfossil material alone was insufficient to overcome the taphonomic processes at work biasing the sedimentary record of the event. These studies intimate that each occurrence of a fossil regular echinoid is also a record of extraordinary taphonomic circumstances, a presumption contradicted by their abundance as fossils throughout most of the post-Paleozoic. Further study of taphonomic processes affecting populations of echinoids occurring in various reef subenvironments is clearly needed.

The reef and near-reef environments adjacent to St. Croix, U.S.V.I. are ideal areas in which to study echinoid taphonomy because of their abundant and

Larue, D.K., and Draper, G. (eds.),
Transactions of the 12th Caribbean Geological Conference, St. Croix, U.S.V.I., Miami Geological Society, P.O. Box 431552, South Miami, FL 33243, U.S.A

diverse populations of regular echinoids. The echinoids *Diadema antillarum* (Family Diadematidae), *Eucidaris tribuloides* (Family Cidaridae) and *Echinometra lucunter* (Family Echinometridae) are particularly abundant. Although information on echinoid distribution and habits is presented in the classic studies of Clark (1919) and Kier & Grant (1965), no data comparing live echinoid distribution with that of subfossil echinoid material exist[1]. Here I determine the amount and nature of taphonomic bias affecting populations of these regular echinoids by comparing the distribution of living and dead individuals and conducting field experiments to determine the rate of decay and disarticulation of freshly-killed specimens. Finally, preliminary work is presented on the relative durability of the echinoids under study as determined by tumbling experiments.

METHODS

Population Censuses

Echinoid populations were censused along two transects constructed in Smuggler's Cove and Rod Bay (Fig. 1). The Smuggler's Cove site was selected because several reef and near-reef environments are present within a relatively short distance. A 720 m transect line was constructed heading due north from the Smuggler's Cove dock. Echinoids were counted in rocky shoreline, *Callianasa*-dominated sandy areas, *Thalassia*-dominated grass beds, patch reef, reef tract and shallow (water depth 1.5 m) and deep (water depth 12 m) forereef environments. At stations 60 m apart a 1 m^2 quadrat was placed adjacent to the transect line and live and dead echinoids within the quadrat were counted. The quadrat was then flipped over and another m^2 was censused. This process was repeated ten times at each station resulting in a census of a 1 x 10 m^2 "column" situated perpendicular to the transect line and occurring every 60 m. Surficial sediment samples were collected from the first quadrat censused at each station for later analyses to determine the contribution of echinoderm skeletal elements.

The Rod Bay site was selected because regular echinoids were observed to be particularly abundant. A 50 m transect was constructed, and the census proceeded in the same fashion as in Smuggler's Cove except that sampling stations were 10 m apart. Within the 50 m transect, rocky

[1]Although Serafy (1979) recorded the occurrence of live and dead echinoids collected by dredging along transects constructed adjacent to the Gulf Coast of Florida.

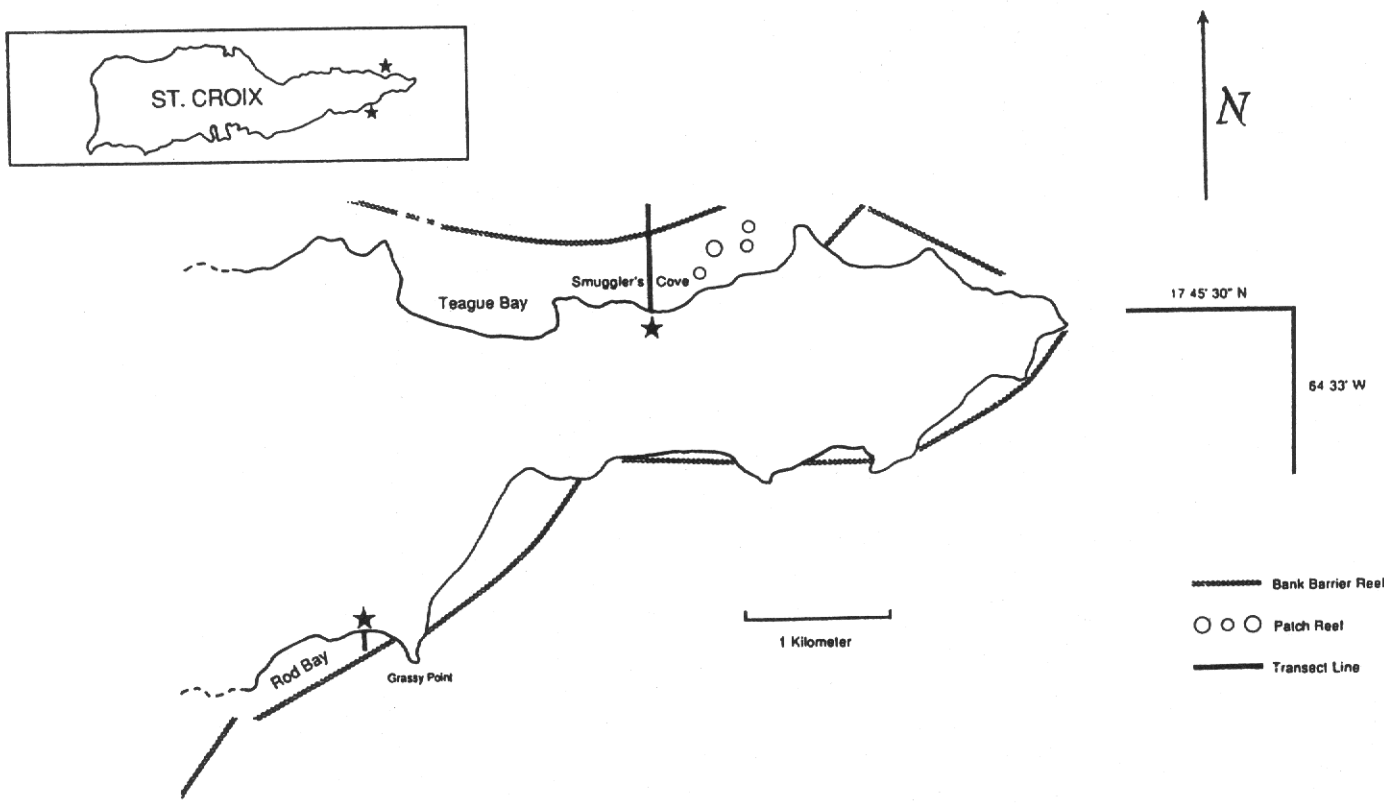

Figure 1- Transect localities adjacent to St. Croix. Each transect is marked with a star.

shoreline, *Thalassia*-dominated grass beds, a zone of coral-algal rubble and an environment of very small patch reefs were censused. Surficial sediment samples were also obtained.

Constituent Particle Analysis

Sediments obtained from stations along both transects were dried, impregnated with epoxy and ground into standard thin sections. Thus, all size fractions were represented in thin section to mitigate for the possibility that different echinoids would break down into different size fractions. The thin sections were point counted on a 1 mm^2 grid following the method of Ginsburg (1956). Echinoderm skeletal elements were counted by taking advantage of the unit extinction they exhibit in cross-polarized light, and their percent contribution to the sediment was calculated.

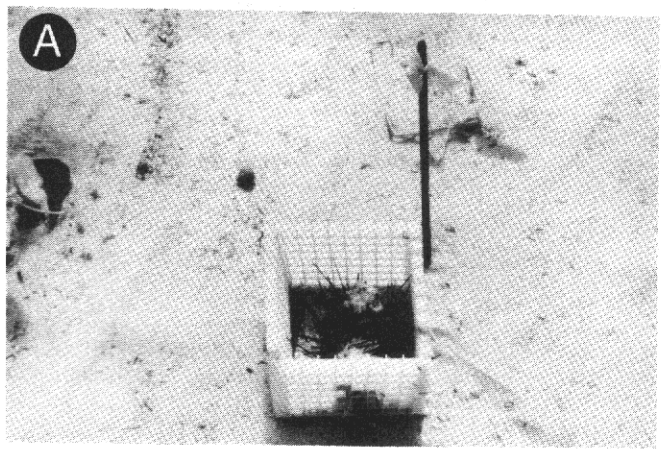

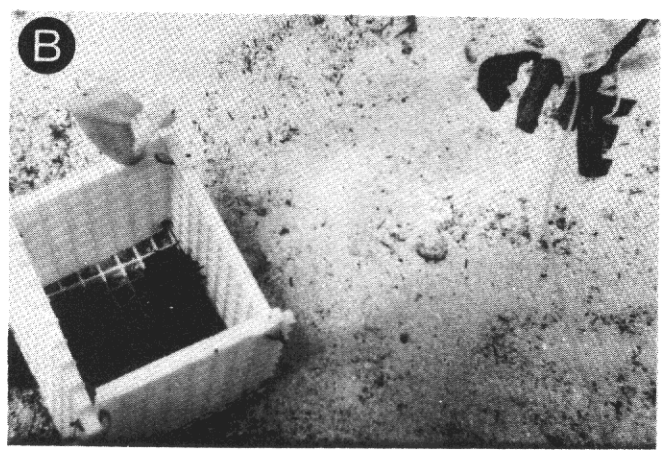

Figure 2- Echinoids placed in cages in the backreef (water depth 3 m) in Smuggler's Cove, A) Specimen of *D. antillarum*; B) Specimens of *E. lucunter* and *E. tribuloides*.

Field Experiments

Freezer-killed specimens of *Diadema antillarum* , *Eucidaris tribuloides* and *Echinometra lucunter* were placed in cages with open tops and a mesh size of 2 cm^2 . These "open" cages were used to contain the dead echinoids somewhat while leaving them exposed to large and small scavengers. The cages were placed on a wave-rippled, sandy substrate immediately behind the reef tract in Smuggler's cove in 4 m of water (Fig. 2). Additional cages were buried at 10 and 20 cm intervals in the sediment at the same location.

Tumbling Experiments

Specimens of *Echinometra lucunter* and *Diadema antillarum* were preserved in 95% ethanol in order to transport them intact from the field to the laboratory. The specimens were then placed in a 4:1 solution of bleach and water to oxidize all of the organic tissue contained within the skeleton . The resulting mass of spines, test and lantern elements was dried, weighed and placed in seawater in a baffled plastic tumbler attached to a variable speed motor (Fig. 3). Two trials of 1, 10 and 100 hours were run at 25 rpm for each echinoid. At the end of each trial the contents of the tumbler were wet-sieved through a stack of nested sieves and the >2mm, 1-2mm, 500μ-1mm and 125μ-500μ size fractions were isolated for analysis. Individual pieces of spine, test and lantern occurring in the three largest size fractions were counted and weighed. The 125μ-500μ size fraction was weighed only.

RESULTS AND DISCUSSION

Population Censuses

A total of 130 square meters were censused in Smuggler's cove (Fig. 4). Live *Echinometra*

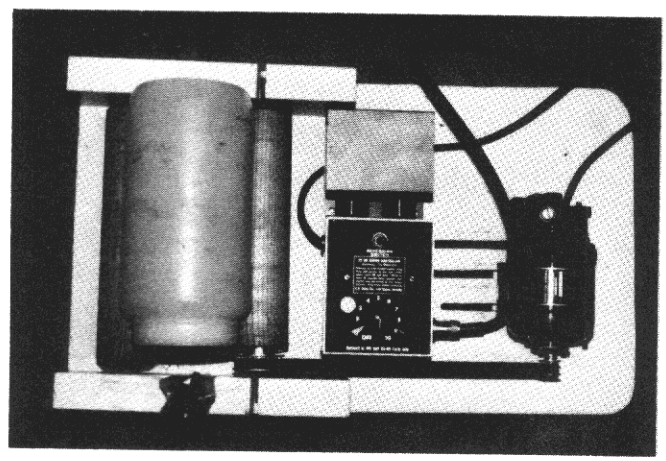

Figure 3- Tumbling device used in this study. Variable speed motor was set at 25 rpm.

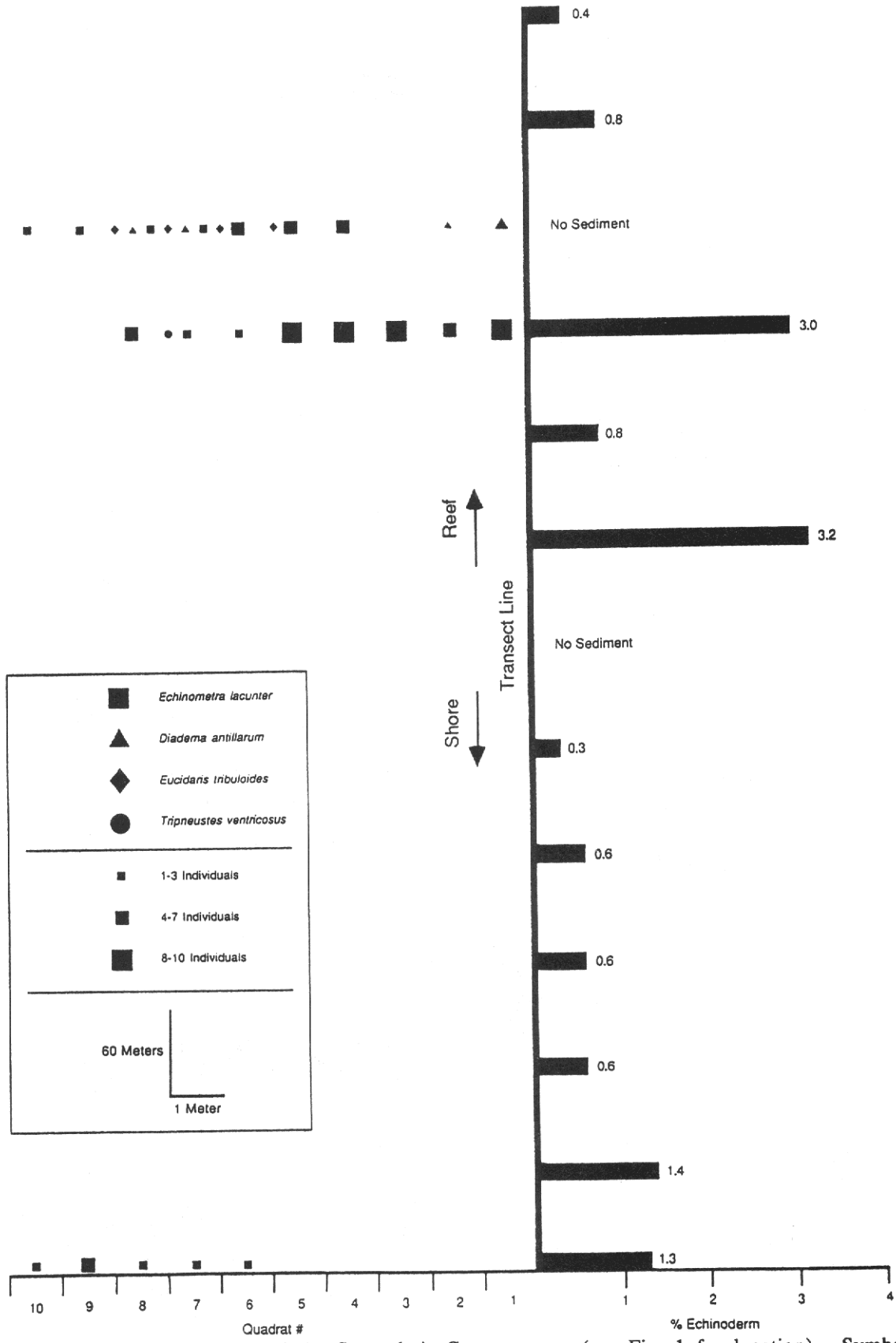

Figure 4- Schematic representation of the Smuggler's Cove transect (see Fig. 1 for location). Symbols to the left of the transect line indicate live echinoid abundance. Water depth reaches a maximum of 4 m in the backreef/ seagrass bed environment and 12 m in the fore-reef. Histogram to the right of the transect line shows the percent echinoderm grains point-counted in sediment samples.

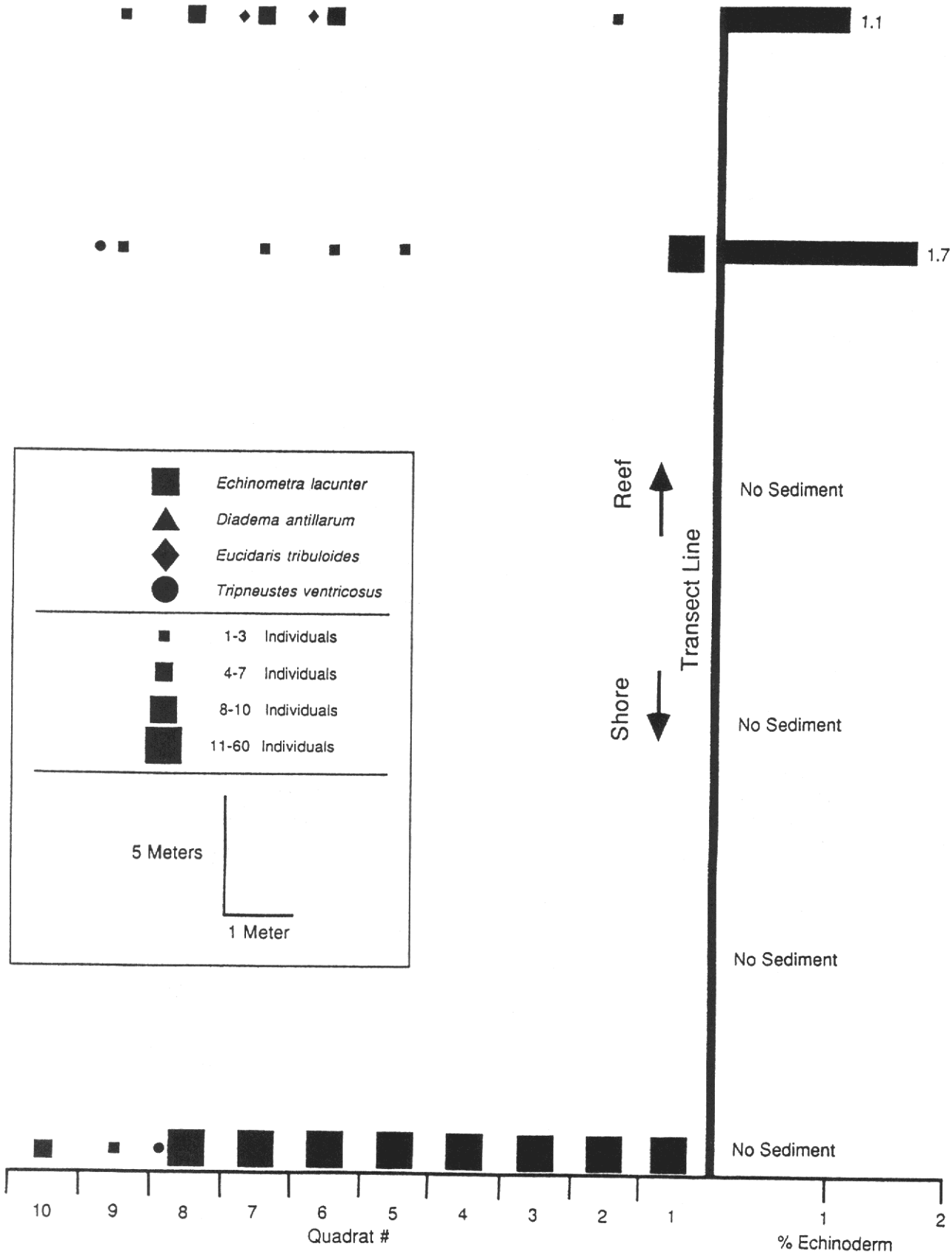

Figure 5- Schematic representation of the Rod Bay transect (see Fig. 1 for location). Symbols to the left of the transect line indicate live echinoid abundance. Maximum water depth along the transect is 1 m. Histogram to the right of the transect line shows the percent echinoderm grains point-counted in sediment samples.

lucunter were observed in low numbers along the rocky shoreline and no living echinoids were observed again until the same species was encountered in slightly higher numbers at the reef tract . Highest echinoid diversity occurred in the shallow forereef environment, with individuals of *D. antillarum*, *E. lucunter*, and *E. tribuloides* present in relatively low numbers. Live echinoids were not observed in the deeper forereef environment. No intact or partial tests of dead echinoids were observed in any quadrat studied along the entire transect.

Comparison of living and dead echinoids yielded essentially the same results in Rod Bay, where a census of a total of 60 square meters was conducted (Fig. 5). Although numbers of *Echinometra* were relatively high along the rocky shoreline (reaching a maximum of 59 individuals per square meter) no intact or partial tests of any echinoids were observed associated with the living fauna. Two individuals of *Tripneustes ventricosus* and four individuals of *Eucidaris tribuloides* were counted along with additional individuals of *Echinometra* at 40 and 50 meters along the transect, respectively. Dead echinoid material was not observed in any quadrat studied. In addition, very little sediment had accumulated in the area in which the transect was constructed, preventing collection at all but two stations.

Constituent Particle Analysis

Echinoderms at both localities are minor contributors to the sediment comprising, on average, 1.2% of the constituents and ranging from 0.3%-3.2%. The percentages of echinoderm skeletal elements in the sediment does not correspond to the distribution of echinoids (Figs. 4 & 5). In fact, the largest amount of echinoderm material occurred at a station where no echinoids were counted (Fig. 4). It should also be noted that the highest echinoid diversity and abundance occurred in an environment where no sediment was available to sample. Thus sediment compositon was an unreliable indicator of echinoid distribution in the two areas studied.

Field Experiments

The lack of correspondence of living echinoids to macro- and microscopic skeletal material suggests that the echinoids under study are rapidly acted on by biostratinomic processes. The field experiments were conducted to assess the rapidity with which this could occur. Within six days, all the echinoids placed in the back-reef environment in Smuggler's Cove were devoid of any organic material (Fig. 6). Few spines were observed within the cages and the tests of *E. tribuloides* and *E. lucunter* were filled with sediment and intact. The test of *D. antillarum* was also filled with sediment and appeared intact. Closer examination revealed, however, that the test had begun to separate along its ambulacral sutures. No elements of the Aristotle's Lantern of any of the echinoids were observed. Within 12 days, no spines were left within the cages and the tests of *Eucidaris* and *Echinometra* were still intact. The test of *Diadema* had completely disarticulated along its ambulacral sutures resulting in the presence of several large sections of interamb (Fig. 7).

The results of the field experiments help to partially resolve the lack of correspondence of the live and dead fauna. The rapid dissemination of spines and lantern elements from the cages indicates that they do not remain near the test that produced them. The patchy distribution of live echinoids observed in Smuggler's Cove and Rod Bay would therefore be expected to produce a scattered distribution of these skeletal elements which, even if time-averaged, would comprise a small proportion of the sediment.

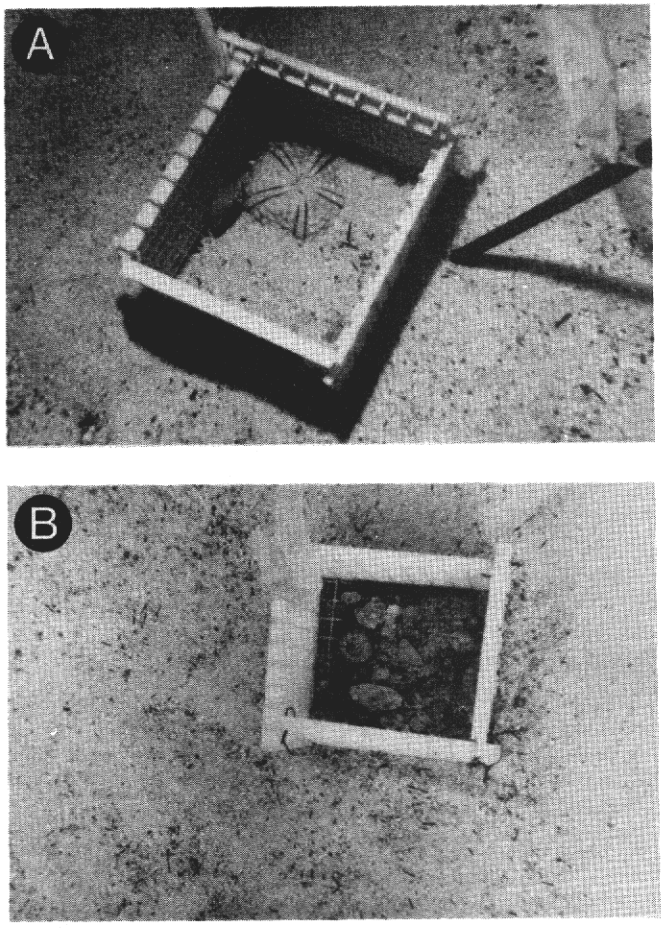

Figure 6- Echinoids in cages in backreef of Smuggler's Cove after six days, A) *D. antillarum*; B) *E. lucunter* and *E. tribuloides*. Note absence of organic tissues and spines.

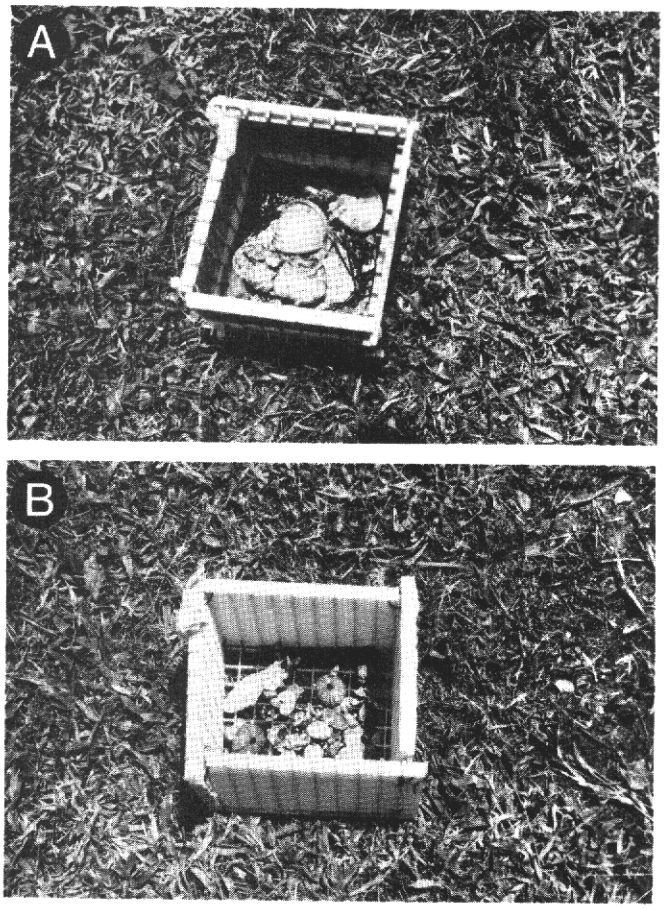

Figure 7- Cages containing echinoid specimens upon removal from the backreef in Smuggler's Cove. Cages were removed 12 days after the experiment was started, A) *D. antillarum*; B) *E. lucunter* and *E. tribuloides*. Note the difference in the condition of the tests.

The rapid degradation of the *Diadema* test relative to the other echinoids was expected. Of the echinoids studied, *Diadema* possesses the least durable test because very little interlocking of the stereom occurs at plate sutures (Smith, 1984). Thus no intact or partially intact tests of *Diadema* would be expected to occur in concert with live individuals, particularly since individuals of *Diadema* were observed in the shallow forereef environment where wave energy was quite high.

Echinometra represents the other end of the "durability spectrum" for the echinoids studied. A great deal of stereomic interlocking occurs across plate boundaries resulting in a test that is highly resistant to fracturing (Smith, 1984). However, no intact dead tests of this echinoid were found. Thus possession of a highly resistant test as well as relatively high abundance does not make the preservation of this echinoid any more likely than preservation of *Diadema* in the environments studied.

Tumbling Experiments

The purpose of the tumbling experiments was to assess whether any taxonomically-controlled difference in the breakdown of the echinoid skeleton contributes to taphonomic bias. Specimens of *Diadema* and *Echinometra* were selected because they represent the most fragile and the most sturdy of the echinoids studied. Data are expressed as weight percent of the entire skeleton to mitigate for the difference in size of the specimens. Average values of the two trials are presented.

The difference in test strength became apparent immediately as *Diadema* tests broke apart into the >2mm and 1-2mm size fractions within a few minutes of starting a tumbling trial whereas *Echinometra* tests remained intact in the >2mm size fraction after 100 hours of tumbling (compare Fig. 8 and Fig. 9). With increased tumbling time however,

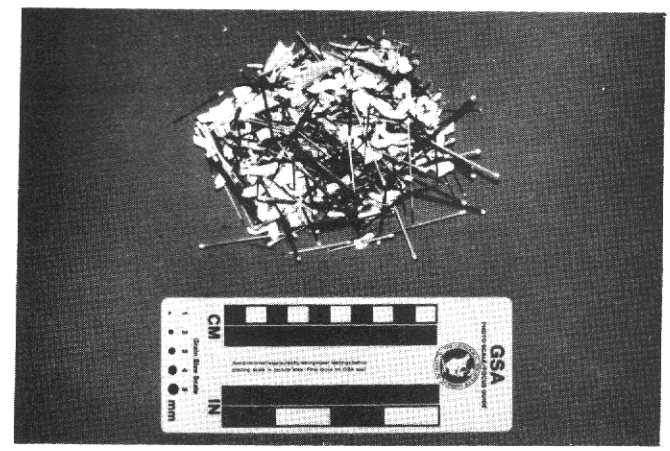

Figure 8- *D. antillarum* after one hour of tumbling. Note the considerable disarticulation of the test. The test was observed to disarticulate within minutes of starting the tumbler.

Figure 9- *E. lucunter* after one hour of tumbling. Note that the test is intact. Tests remained intact after tumbling periods of 100 hours.

there was little change in the proportions of either skeleton present in the three size fractions studied (Figs. 10 and 11). This indicates that no further abrasion of the skeletal elements occurred in the tumbler after initial disarticulation took place. Thus the fact that *Diadema* possesses a more fragile test than *Echinometra* only results in its much more rapid initial disarticulation and not in a greater proportion of the test contributing to the smaller size fractions. Spines of both echinoids are present in all the size fractions and lantern elements of both echinoids were present in only the >2mm size fraction (Figs. 12C and 13C).

The tumbling experiments suggest that, all things being equal, intact tests of *Echinometra*, larger lantern elements of both echinoids and spines of both echinoids should be apparent in close proximity to the live populations studied. Factors other than taxonomically-controlled patterns of test disarticulation are clearly at work to bias subfossil echinoid assemblages adjacent to St. Croix. Results of field work and laboratory experiments indicate that the echinoids studied are rapidly acted on by biostratinomic processes which initiate complex taphonomic histories. Although taxonomically-governed differences in skeletal strength do exist,

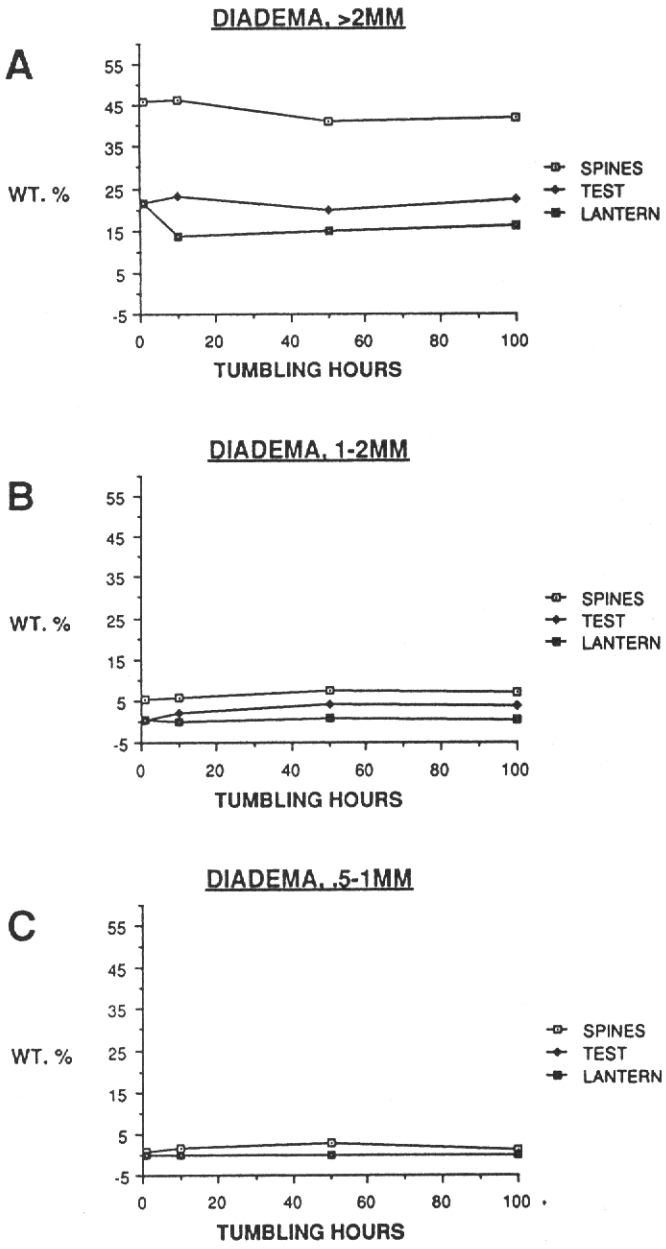

Figure 10-Tumbling results expressed as weight percent of the entire *Diadema* skeleton, A) >2 mm size fraction; B) 1-2 mm size fraction; C) 500 μ-1 mm size fraction.

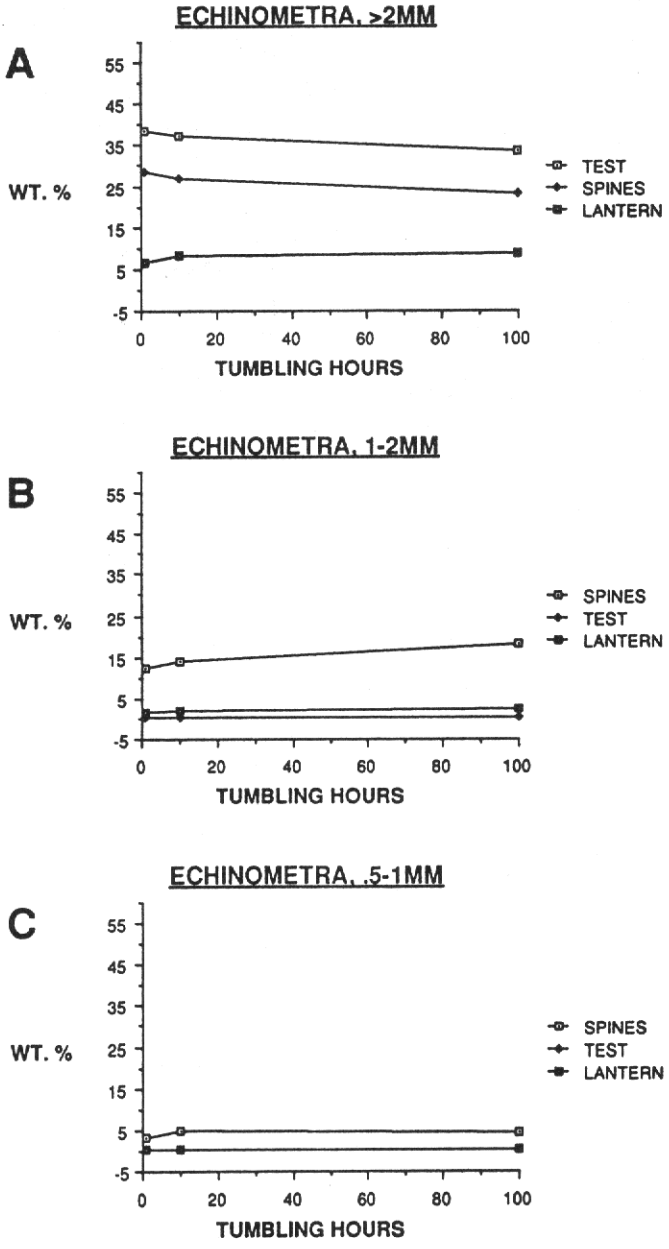

Figure 11-Tumbling results expressed as weight percent of the entire *Echinometra* skeleton, A) >2 mm size fraction; B) 1-2 mm size fraction; C) 500 μ-1 mm size fraction.

there is no *a priori* reason to assume that a stronger test makes preservation more likely in the environments studied in Smuggler's Cove. Thus it may be that, in the environments studied, extraordinary events are required to preserve the regular echinoids living there. Mass mortality of populations of *Diadema antillarum* occurred in St. Croix in 1984 and may have provided such an event.

Preservation of Echinoid Mass Mortality

During 1983-84 populations of *Diadema* were decimated, possibly by disease, throughout the Caribbean and tropical Western Atlantic (Lessios et al., 1984). Greenstein (1989) demonstrated that no signature of the event was present in surficial sediments accumulating in and around a fringing reef in Bonaire, Netherlands Antilles. However, active transport of sediment continually occurs in the area studied (Kobluk & Lysenko, 1984). In St. Croix, intact tests of *Diadema* were observed accumulating in sea grass beds leeward of the reef tract in Smuggler's Cove (Miller, pers. comm.). Sea grass beds are areas of net sediment accumulation (Ginsburg & Lowenstam, 1958). Thus one would expect that a sea grass bed might preserve, as a

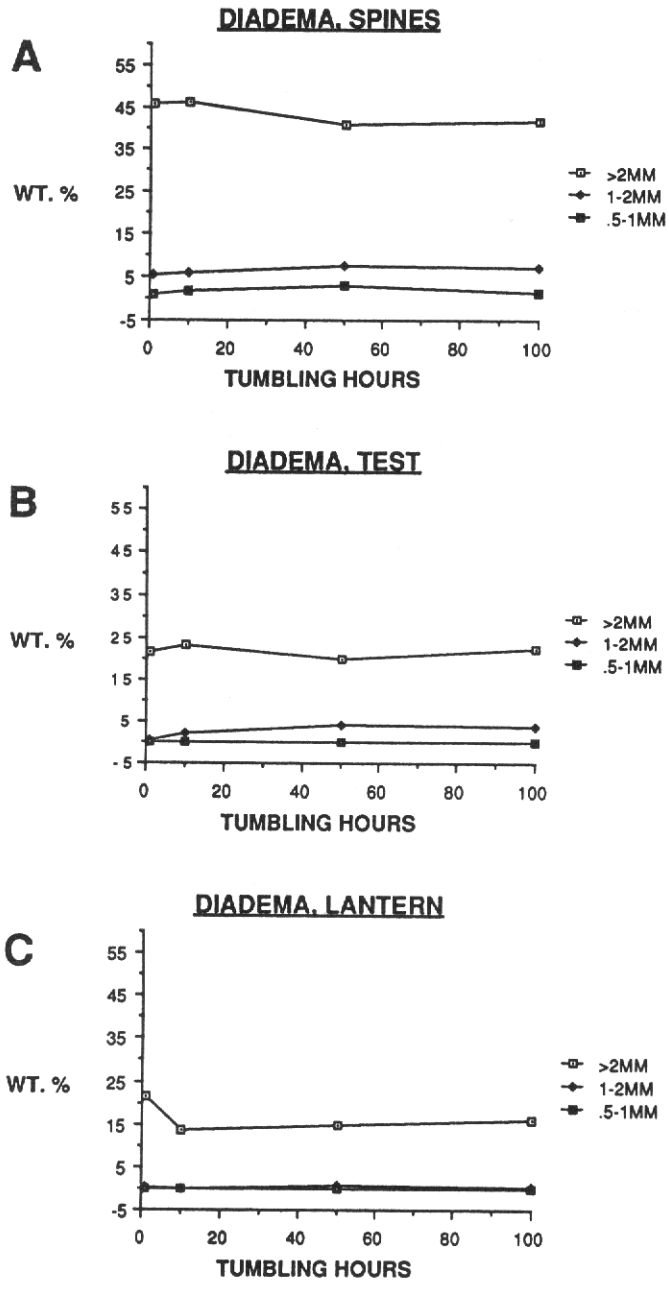

Figure 12-Tumbling results expressed as weight percent of the entire *Diadema* skeleton, A) spines; B) test plates; C) lantern elements.

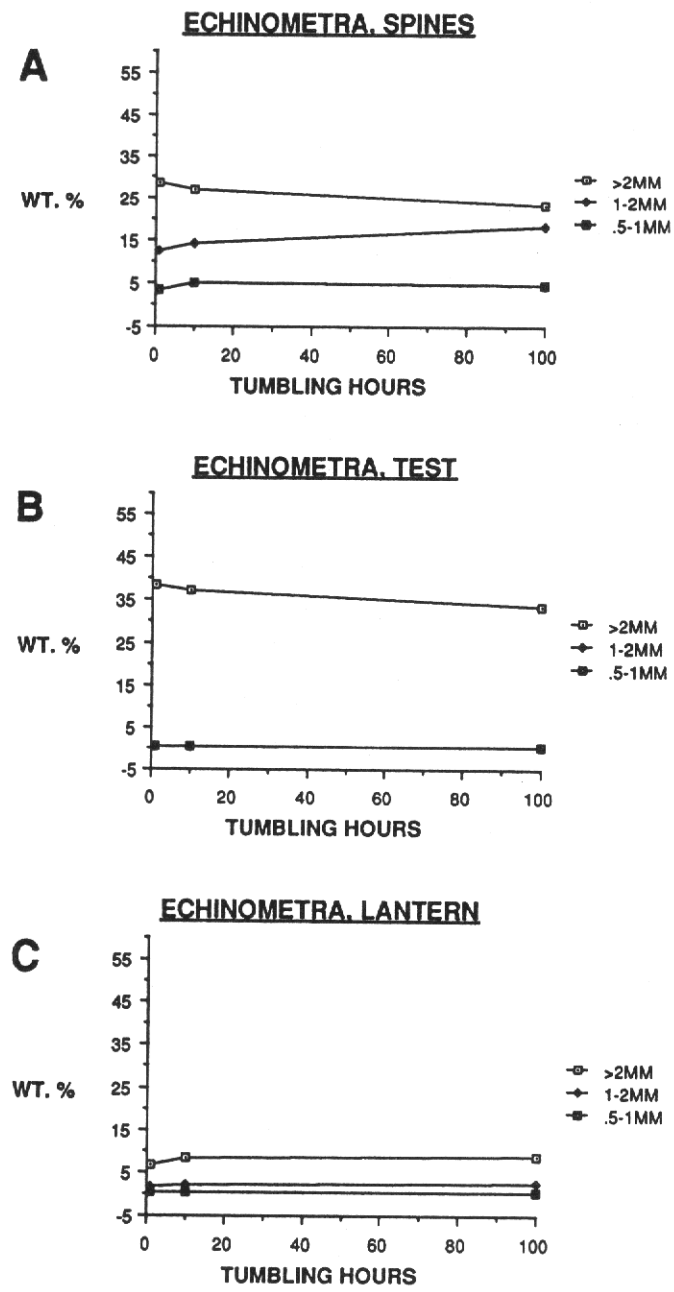

Figure 13-Tumbling results expressed as weight percent of the entire *Echinometra* skeleton, A) spines; B) test plates; C) lantern elements.

distinct horizon unusually rich in echinoderm material, an event that produced higher than normal amounts of subfossil echinoid material. In 1988 a 70 cm piston core was taken through a sea grass bed situated leeward of the reef tract in Smuggler's Cove to determine if such a horizon existed. The core was examined macroscopically on a centimeter scale for evidence of an echinoderm-rich layer in the larger size fractions and none was observed. Thin sections were made of material obtained at alternate-centimeter intervals and point counted using the same method described above.

Results of thin section analysis (Fig. 14) indicate that echinoderm grains comprise a small proportion of the sediment constituents in the core, ranging from 0.3-3.4%. The upper limit of a 95% confidence interval computed about the mean of the values is 1.95%. Approximately one-third of the values (10 of 33 samples) are higher than this value. Thus the variation in the amount of echinoderm material present does not produce an "echinoderm-spike". If the highest value of 3.4% is the result of the *Diadema* mass mortality, it is doubtful that the slight increase in echinoderm material would be recognizable in a stratigraphic succession. Thus, transport of innumerable intact tests of *Diadema* into an environment of net sediment deposition did not enhance their preservation potential.

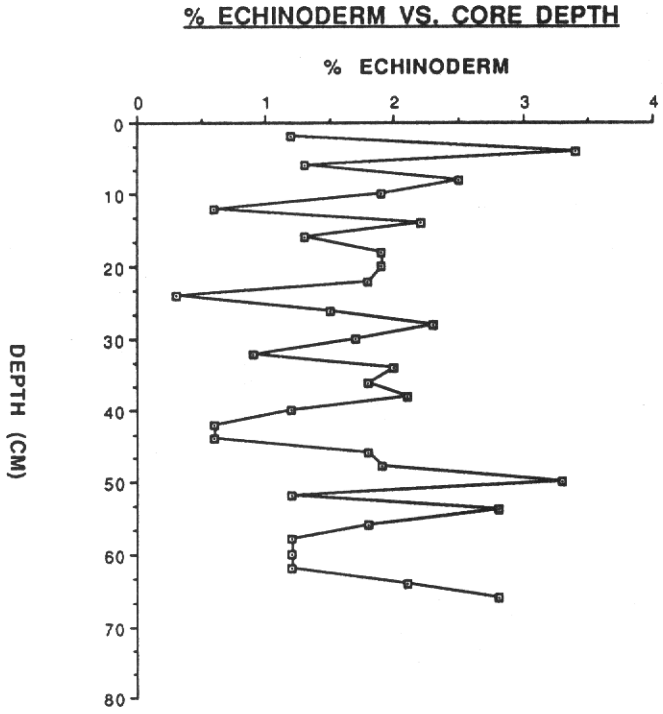

Figure 14-Percent echinoderm material vs. depth down core obtained from a seagrass bed leeward of the reef tract in Smuggler's Cove. Values obtained by point-counting.

IMPLICATIONS FOR ECHINOID FOSSIL RECORD

Results of the population censuses emphasize the rapidity with which populations of regular echinoids are reduced to essentially unrecognizable grains of carbonate sand. *Diadema* appears to be particularly vulnerable to taphonomic bias given the lack of signature of its mass mortality. The data obtained from the various facets of this study make it possible to predict the nature of the fossil records of each group represented by the species studied. Thus one would expect that in the absence of unusual taphonomic circumstances fossil species belonging to the Diadematidae might be represented by lantern or spine elements whereas intact tests of Echinometrids would more commonly be preserved. *Eucidaris tribuloides* and *Tripneustes ventricosus* were also subjected to rapid taphonomic bias in Smuggler's Cove. Although analysis of the disarticulation of their skeletons is ongoing, preliminary results indicate that fossil specimens of related forms would be expected to be preserved as skeletal fragments.

An analysis of the recorded occurrences of fossil species belonging to each family is currently underway. Type specimens of all species belonging to each of the four families are characterized according to preservational style, stratigraphic position and lithology of the enclosing unit. The literature-derived data, obtained for over 1000 species, will serve as a test of the predictions derived from the results of this study. Preliminary results suggest that, in addition to occurrences of well-preserved fossil species that are the result of extraordinary taphonomic circumstances (see for example Aslin, 1968, Bloos, 1973, Rosenkranz, 1971, Poborski, 1954 and Gill & Cobban, 1966), many species are described on the basis of fragmentary remains. This is particularly true of the Family Cidaridae, whose members comprise the longest and most diverse evolutionary history of the groups studied. Further analysis of the literature data will determine whether preservational style can be attributed to taxonomic, stratigraphic or lithologic factors.

CONCLUSIONS

1. The distribution of macro- and microscopic echinoid skeletal material does not reflect the distribution of living populations of *Diadema antillarum, Echinometra lucunter, Eucidaris tribuloides* and *Tripneustes ventricosus* in Smuggler's Cove or Rod Bay, St. Croix, suggesting that dead echinoids are rapidly acted on by biostratinomic processes.

2. Specimens of individual echinoids are divested of organic material, spines and lantern elements

within six days of death. In addition, tests of *Diadema antillarum* had begun to disarticulate along plate sutures.

3. High relative abundance and the possession of a relatively sturdy test do not make *Echinometra lucunter* any less vulnerable to taphonomic bias than the other echinoids studied.

4. Skeletons of *D. antillarum* disarticulate more rapidly than skeletons of *E. lucunter* when tumbled although no further breakdown of either skeleton occurs after initial disarticulation.

5. Results of tumbling experiments suggest that, in the absence of unusual taphonomic conditions, lantern elements and intact tests of Echinometrids may be expected to occur as fossils whereas spines, lantern elements and test fragments might represent Diadematids as fossils.

6. No echinoderm-rich horizon occurred in a seagrass bed core indicating that the generation of innumerable intact tests of *Diadema antillarum* and their transport into areas of net sediment accumulation was insufficient to preserve any record of widespread mass mortality.

7. Predictions concerning the preservational style of fossil species belonging to each family are currently being tested by an extensive review of the literature.

ACKNOWLEDGEMENTS

Financial support from a Sigma Xi Grant-in-aid-of-Research, the Caster Fund (University of Cincinnati) and a Departmental Research Grant (University of Cincinnati) is gratefully acknowledged. The facilities and staff of the West Indies Lab, St. Croix were indispensible to this study.

REFERENCES

Aslin, C.J., 1968, Echinoid preservation in the Upper Estuarine Limestone of Bilsworth, Northamptonshire: Geological Magazine, v. 105, p. 506-518.

Bloos, G., 1973, Ein fund von seeigeln der Gattung *Diademopsis* aus dem Hettangium Württembergs und ihr Lebensraum: Stuttgarter Beitrage Naturklasse (B), v. 5, p. 1-25.

Clark, H.L., 1919, The distribution of the littoral echinoderms of the West Indies: Papers from the Department of Marine Biology of the Carnegie Institution of Washington, v. 12, p. 51-73.

Gill, J.R. & W.A. Cobban, 1966, The Red Bird section of the Upper Cretaceous Pierre Shale in Wyoming: U.S.G.S. Professional Paper 393-A, U.S. Government Printing Office.

Ginsburg, R.N., 1956, Environmental relationships of grain size and constituent particles in some south Florida sediments: American Association of Petroleum Geologists Bulletin, v. 40, p. 2384-2387.

Ginsburg, R.N. & H.A. Lowenstam, 1958, The influence of marine bottom communities on the depositional environment of sediments: Journal of Geology, v. 66, p. 310-318.

Greenstein, B.J., 1989, Mass mortality of the West-Indian echinoid *Diadema antillarum* (Echinodermata: Echinoidea): A natural experiment in taphonomy: Palaois, v. 4(5), p. 487-492.

Greenstein, B.J. & D.L. Meyer, 1985a, Mass mortality of the West Indian echinoid *Diadema antillarum*: A natural experiment in taphonomy: Geological Society of America Abstracts with Programs, v. 17(7), p. 598.

Greenstein, B.J. & D.L. Meyer, 1985b, Actuopaleontology of reef-dwelling echinoderms at Bonaire, Netherlands Antilles: Ohio Academy of Science Annual Meeting, Abstracts with Programs, v. 85(2), p. 19-20.

Kier, P.M., 1977, The poor fossil record of the regular echinoid: Paleobiology, v. 3, p. 168-174.

Kier, P.M. & R.E. Grant, 1965, Echinoid distribution and habits, Key Largo Coral Reef Preserve, Florida: Smithsonian Miscellaneous Collections, v. 149(6), p. 1-68.

Kobluk, D.R., and Lysenko, M.A., 1984, Carbonate rocks and coral reefs, Bonaire, Netherlands Antilles: Geological Association of Canada, Mineralogical Association of Canada Joint Annual Meeting Field Trip 13, 67 p.

Lessios, H.A., Robertson, D.R., and Cubit, J.D., 1984, Spread of *Diadema* mass mortality through the Caribbean: Science, v. 226, p. 335-337.

Poborski, S.J., 1954, Virginia formation (Triassic) of the St. George, Utah area: Geological Society of America Bulletin, v. 65, p. 971-1006.

Rosenkranz, D., 1971, Zur sedimentologie und Ökologie von echinodermen-lagerstätten: Neues Jahrbuch für Geologie und Palaöntologie Abhandlungen, v. 138, p. 221-258.

Schäfer, W., 1972, Ecology and paleoecology of marine environments: Oliver and Boyd, London, 568 p.

Serafy, D.K., 1979 Echinoids (Echinodermata: Echinoidea): Memoirs of the Hourglass Cruises, v. 5(Part 3), Florida Department of Natural Resources Marine Research Laboratory, 119 p.

Smith, A., 1984 Echinoid Palaeobiology: Special Topics in Palaeontology 1, George Allen and Unwin, London, 190 p.

CRETACEOUS TECTONIC COMPLEX, ST. CROIX

Robert Speed
Department of Geological Sciences
Northwestern University
Evanston, IL 60208

James Joyce
Department of Geology
University of Puerto Rico
Mayaguez, PR 00708

ABSTRACT

A tectonic complex of Cretaceous sedimentary rocks underlies St. Croix, possibly to substantial depth. The sedimentary rocks are almost entirely volcanigenic, derived from contemporaneous arc volcanoes in the duration, Cenomanian or Turonian through Maastrichtian. Minor pelagic beds (chert) also occur. All the volcanigenic sedimentary rocks are deep marine and can be assigned to turbidite facies from outer to inner fan. The depositional site was a basin floor near the base of slope of a Late Cretaceous island arc whose duration of activity was at least 14 ma and perhaps, greater than 30 ma. The basin may have been a trench floor. The tectonic complex in which all the Cretaceous strata occur is an assembly of thrust sheets (= nappes). Beds in all the sheets were folded and cleaved to varied degrees and in varied sequences before a short episode of late Maastrichtian igneous intrusion. Early deformations are S- to SW-verging. The tectonic complex is interpreted as a product of accretion during Late Cretaceous convergence in which the downgoing plate had a component of N to NE transport in today's coordinates.

INTRODUCTION

Cretaceous sedimentary and intrusive igneous rocks underlie all of St. Croix's surface except for a central region of unconformable Miocene and younger cover (Fig. 1). The depositional realms and pre-Miocene structural evolution of the largely volcanigenic Cretaceous strata are the focus of this paper with the aim of understanding the early tectonics of St. Croix. Our field work in St. Croix was in the middle seventies and 1988; some of these results are Speed (1974), Joyce (1979), and Speed et al. (1979). Earlier publications providing data on the Cretaceous rocks were Quin (1907), Cedarstrom (1950), and Whetten (1966), and a later one by Stanley (1988). Our studies focused more closely on outcrop-scale structural analysis, structural synthesis, and dating than those of other workers and had the benefits of advances in turbidite facies analysis.

The magmatic character of St. Croix's Cretaceous intrusions and the metamorphism of Cretaceous sedimentary rocks are important facets of St. Croix's early evolution not dealt with this paper. Whetten (1966) provides discussions on these subjects.

ARCHITECTURE OF ST. CROIX

The island of St. Croix is a peak on the submarine St. Croix platform which is a bathymetric ridge and probable extensional fault block in the southeasternmost Greater Antilles. At the surface, St. Croix is underlain by Cretaceous sedimentary rocks that occupy a Cretaceous tectonic complex, Cretaceous igneous intrusions, and Cenozoic strata (Fig. 1).

The Cretaceous tectonic complex is composed of folded, cleaved, and faulted sedimentary rocks of Cretaceous depositional ages. Our studies to date indicate that strata of the complex are probably not in a depositional succession. Rather, the complex may be an assemblage of tectonic sheets or nappes, each bounded by shallowly dipping faults that we interpret to be thrusts. Figure 1 shows the six nappes (K1-6) identified to date. Differentiation of the nappes is based on differences in stratal character and structural sequences given in Table 1. Their fault contacts are exposed in isolated outcrops, and most of the nappe boundary traces in Figure 1 are interpolated below extensive vegetation and Recent cover. Future work may show that these large nappes are divisible into smaller fault-bounded units.

Igneous intrusions at least partly of Maastrichtian age occur as dikes and sills throughout the tectonic complex and as plutons, one in western and the other in eastern St. Croix (Fig. 1). These appear to be a consanguinous suite, judged petrographically to be of island arc magma. Some dated intrusions followed the main assembling of the tectonic complex, thus proving the complex is Cretaceous. Other intrusions, mainly sills, were folded and (or) cleaved in early deformations. These pre- and syncomplex intrusions are not yet dated radiometrically and are known only to be postdeposition, hence Late Cretaceous.

The Cretaceous tectonic complex and Cretaceous intrusions may extend to substantial depth because similar igneous and metasedimentary rocks have been dredged off the north flank of St. Croix at depths of 1.5 km (Bouysse et al., 1985) and because a refraction layer with velocity of about 4.7 km/sec extends from the surface of St. Croix to a depth of about 8 km (Officer et al., 1987).

The central region of St. Croix is underlain by little deformed Cenozoic sedimentary cover (Fig. 1) (Gill, 1989). The cover occupies a deep basin that may be a full graben as shown on Figure 1. Cenozoic strata unconformable on Cretaceous rocks at the basin flank are as old as middle or early Miocene (Multer et al., 1977) but could be pre-Miocene in the deeper reaches of the graben (Whetten, 1966; Lidz, 1988). The Miocene and Pliocene normal faulting associated with subsidence of the graben is probably related to regional extension that has developed the St. Croix platform and adjacent basins.

Larue, D.K., and Draper, G. (eds.),
Transactions of the 12th Caribbean Geological Conference, St. Croix, U.S.V.I., Miami Geological Society, P.O. Box 431552, South Miami, FL 33243, U.S.A

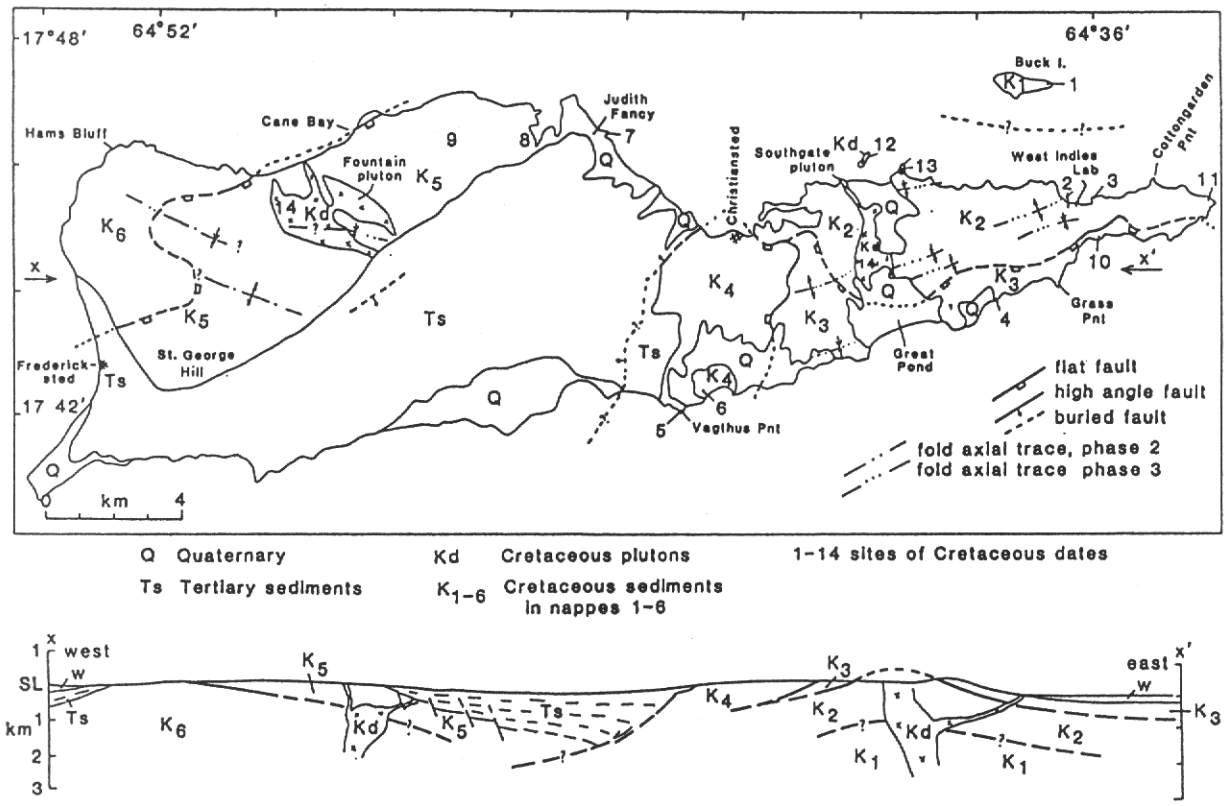

Figure 1. Map of St. Croix showing outcrop areas of Cretaceous and Cenozoic rocks, nappes K1-K6 of Cretaceous rocks, diagrammatic cross section, axial traces to some macroscopic folds, and sites of samples dated by fossils or KAr (Table 2).

CRETACEOUS LAYERED ROCKS

Introduction: The Cretaceous layered rocks of St. Croix are almost entirely volcanigenic sediments together with minor pelagic sediment that accumulated in subwavebase, probably deep marine sites. There are no lavas or proved pyroclastic deposits, contrary to claims by Lidz (1988).

Each of the nappes of the Cretaceous tectonic complex probably or possibly contains a coherent stratigraphy (K2, K4, K5 are probable, others possible), but correlations cannot be made between adjacent nappes. There is thus no islandwide stratigraphy of Cretaceous strata. Moreover, because the Cretaceous rocks in different nappes did not necessarily come from a single original stratigraphic sequence, there can be no valid estimate of composite thickness (such as given by Lidz, 1988). Whetten's (1966) organization of an islandwide stratigraphy showed great complexity which he attributed to facies changes that were expectable for what he correctly perceived as a turbidite realm of deposition. Our observation of fault boundaries between parcels of strata with mainly different characteristics (Table 1), however, implies the abrupt juxtapositions are tectonic, not generally depositional. Whetten's (1966) formational names, not used here, are still convenient for discussion of stratal types (i.e., Caledonia for thin bedded sandy-muddy turbidite and Judith Fancy for thick coarse lithic-rich beds) but should not be used to convey stratigraphic position. Correlations of bed sequences within nonadjacent nappes may ultimately be valid, given new dating; suggestions for such correlation by general lithic lookalikes were aptly made by Whetten (1966)—for examples, parts of nappes K2 and K6.

Depositional Ages: Fossil evidence for ages of deposition now exists from ten samples at eight sites, and a radiometric age exists for an igneous clast in sandstone at a ninth site (Table 2). Of these, only two of the eleven samples can be taken as probable age of deposition. The two are ammonites, one found as an isolated individual at the top of a distal turbidite (Perinoceras) and the other as float on a hilltop in similar beds (Tarrantoceras). Neither is associated with other fossils, and each is much larger than any associated grains. The ammonites are therefore probably pelagic. The other dated samples are resedimented and give only a maximum age of deposition. The planktic forams at sites 4 and 6 (Table 2) are considered resedimented because of their association with resedimented megafossils.

A minimum age of deposition of the Cretaceous strata is probably given by dates of the intrusive rocks (Table 2). The similarity of radiometric dates from postcomplex igneous rocks from seven sites and of petrography makes a compelling argument for nearly synchronous emplacement of such igneous bodies throughout St. Croix. No dates exist, however, for dikes in nappes K1, K4, and K6, and we must assume such dikes are also Maastrichtian. The average mean value date for

Table 1: Characteristics of Nappes in Cretaceous tectonic complex

Nappe	Lithotypes	Known Depositional Ages	Structures
K1	thin bedded graded sandy turbidite and nongraded ss, both loc. calcarenite; massive mst; minor pebbly ss with nonvolc + volc lithoclasts; ss are fsp > lith > skel > pyx	Campanian or Maastrichtian	subvertical homoclinal bedding and S1 cleavage + steep F1 fold axes; steep and flat shear zones with F2 folds, S2 cleavage, and quartz veins; late kinks
K2	thin and med bedded sandy-muddy turbidite with cherty tops; intervals of thick graded volc ss±debris flow up to 20 m thick; bedded chert; ss are fsp>>lith > pyx=skel	Cenomanian or Turonian and Coniacian	4 phases: 1) local zones of isoclines; 2) pervasive SW-verging close major and minor folds + cleavage; 3) upright macrofolds of beds + cleavage; 4) steep and flat faults + related folds and kinks
K3	massive and laminated mst, loc cherty and muddy turbidite; thick bedded graded or massive or pebbly ss; skeletal debris flow; ss are fsp > lith > pyx > skel	late Campanian or Maastrichtian	similar to K2 phases 2-4
K4	thick bedded massive or graded coarse wacke, mainly pebbly, and sed breccia; thin bedded sandy turbidite; ss are lith > fsp=pyx; loc skel-rich	late Campanian and Maastrichtian	major and minor SW-verging open or close folds with local cleavage; later faults and related local folds
K5	thick bedded graded and massive ss and sandy turbidite alternate with intervals of thin-med bedded sandy-muddy turbidite; also massive mst and debris flow; ss are lith > fsp > pyx > skel	Campanian or Maastrichtian	major upright or S-overturned folds with local cleavage; late faulting
K6	thin bedded muddy-sandy turbidite, loc with cherty tops; intervals thick graded-lam or massive ss ± pebbly ss ± debris flow; ss are fsp > lith > skel > pyx	undated	early minor folds and pervasive cleavage with SW vergence plus flattened cgls; late minor folds of bedding and cleavage

postcomplex igneous rocks is about 69 ma which is late Maastrichtian according to Kent and Gradstein (1985), and the oldest mean value is 71.8 ma, early Maastrichtian. These dates on igneous hornblende can be regarded as accurate because of fresh mineral separates and the absence of postemplacement heating or burial (Speed et al., 1979).

Dating indicates (Table 1) that nappes K1, K3, K4, and K5 contain beds of Campanian and/or Maastrichtian age, and K2 contains substantially older beds, Cenomanian or Turonian and Coniacian. K6 is undated and can only be assumed to be Maastrichtian or older. It is important to note that each nappe probably contains a thick stratal sequence, and current dating does not sample the full sequence of any nappe. The dated sites in K2 are probably low in its sequence, and because K2 is mainly thin bedded and probably not rapidly deposited, it may continue well up in the Late Cretaceous.

The time span represented by dates of the Cretaceous strata is about 28 ma at maximum (base Cenomanian to 69 ma) and about 15 ma at minimum (mid-Turonian to base Maastrichtian), using the Kent and Gradstein (1985) correlations.

Volcanigenic Lithotypes: Nearly all (>99%) of the Cretaceous sediments of St. Croix have generally related compositions: arc volcanigenic with varied minor proportions of skeletal and intraclastic debris (Table 3). Clast types outside this realm are very rare, and in particular, no sediment derived from continental or highgrade metamorphic terranes has been recognized. The volcanigenic particles were probably all derived from a region of contemporaneous volcanism, not from an ancient terrane. Whetten's (1966) distinction of tuffaceous vs epiclastic volcanigenic debris is not supported by our observations; the sediments he called epiclastic are at higher grades of in situ metamorphism, which may account for perceived mineralogical differences. A radiometrically dated volcanic clast in K3, a pyroxene-hornblende porphyry, is 75.3 ±4.3 ma (Table 2), indicating that the maximum duration of extrusion, transport, deposition, and deformation before late Maastrichtian postcomplex intrusion was about 6 ma. It is probable that extrusion and deposition were concurrent at 75 ma and that the tectonic complex took 5 or 6 ma to build up.

The only clast type suggestive of an unroofed source region is rare diorite, but these may have emerged from the volcano as inclusions in extrusions.

Table 2: Depositional ages of Cretaceous sedimentary and igneous rocks

Site[1]	Fault Packet	Basis	Age[2]	Reference
1. Buck Island	K1	coral	Campanian or Maastrichtian (max. age)	Whetten (1966)
2. Tague Bay	K2	ammonite, *Tarrantoceras*(?)	probably Cenomanian, possibly early to middle Turonian	Speed et al. (1979)
3. Romney Pnt.	K2	ammonite, *Perinoceras*[3]	Coniacian	this paper
4. Robin Bay	K3	hbl KAr on igneous clast in pebbly sandstone	75.2±4.3 ma, Maastrichtian or late Campanian (max. age)	Speed et al. (1979)
5. Vagthus Pnt.	K4	planktic forams	Campanian or Maastrichtian (max. age)	Whetten (1966)
		rudist, *Titanosarcolites*	Maastrichtian (max. age)	Whetten (1966)
		"benthic microfauna"	Maastrichtian (max. age)	Andreieff et al. (1986)
6. Diamond Keturah	K4	planktic forams	late Campanian (max. age)	Whetten (1966)
7. Judith Fancy	K5	rudist, *Barrettia* sp.	Campanian (max. age)	Whetten (1966)
8. Sugar Bay	K5	rudist, *Barrettia* sp.	Campanian (max. age)	Whetten (1966)
9. Clairmont	K5	benthic forams	Campanian (max. age)	Whetten (1966)
10. Grapetree Pnt.	—	mafic porphyry dike; hbl KAr	70.1±3.9 ma, Maastrichtian	Speed et al. (1979)
11. East Point	—	ditto	71.8±2.2 ma, Maastrichtian	Speed et al. (1979)
12. Green Cay	—	ditto	66.1±1.8 ma, Maastrichtian to early Paleocene	Speed et al. (1979)
13. Pull Point	—	Southgate pluton, hbl KAr	66.0± 3.2 ma, Maastrichtian to early Paleocene	Speed et al. (1979)
14. plutons; sites uncertain	—	3 hbl KAr dates, presumably from Fountain and Southgate plutons (Fig. 1)	mean values 69 to 71 ma	Lidz (1988)

[1] numbered sites on Figure 1

[2] radiometric-geologic time scale correlations from Kent and Gradstein (1985)

[3] identified by W. A. Cobban, written commun., 1988.

Most volcanic lithoclasts are angular but some are subrounded, indicating that residence times in the littoral or subaerial environments at the source volcanoes was generally short to vanishing. The skeletal debris is widely distributed as broken fragments in trace amounts in medium and in coarse-grained sandstone but locally concentrated as unbroken fossils in some grain- and debris flows. Such particles (Table 1) are resedimented from neritic and/or littoral environments.

The volcanic rock fragments in Cretaceous sediments throughout St. Croix have ranges of properties: color index, phenocryst/matrix ratio, pyroxene/hornblende ratio, presence of quartz, and vesicularity. Such properties may vary greatly in a given bed, but the ranges are not conspicuously different among the six nappes.

The principal lithic distinctions among the six nappes are of general particle size distribution and the nonindependent parameters of sand composition and mean layer thickness (Table 1). Thus, for example, nappes K2 and K6 ("Caledonia") are relatively fine grained (sand/mud ~1), rich in feldspar relative to other sand particles, and thinner bedded. Sandstones of these nappes contain, however, minor but ubiquitous pyroxene and/or hornblende, and volcanic rock fragments, as well as local intervals of very thick sandstone and debris flow. On the other hand, K4 and K5 are relatively coarse-grained as a whole (sand/mud >3), have more nearly equal contents of dark minerals and lithics to feldspar, and have greater proportions of thick beds. Nappe K3 is bimodal, characterized by massive mudstone and channel-filling coarse and pebbly sandstone and rarer beds of intermediate size grade. Nappe K1 has high proportions of fine sandstone and detrital carbonate compared to other nappes. K1 also has a couple of pebbly sandstones that are distinctive for their content of nonvolcanic lithoclasts: rounded radiolarite, chert, and siliceous carbonate, which do not evidently exist in other nappes.

Layer Styles and Transport Mechanisms: The Cretaceous volcanigenic sediments of St. Croix occur in a vast range of depositional unit thicknesses, from 1 cm to > 30 m. Commonly related variables are grain size distribution, sand composition (discussed above), and the existence of channeled bases. All layers are sediment-gravity flows, except perhaps for certain thick massive mudstones which might be hemipelagic. Of the sediment-gravity flows, both turbidites and nonturbidites occur in varied proportions in each nappe. We call layers turbidite if they are generally tabular, upward fining, and have two or more consecutive Bouma zonations.

Turbidites of St. Croix are of three general types:

1. muddy: these are thin-bedded, mud-rich (ss/mst 0.1 to 1), base absent and top present, nonchannelized, and have sand rarely coarser than fine-grained; examples: Lamb Point to East End section; east Butzberg.

2. thin sandy: these are thin and medium bedded, sand-rich (ss/mst >1), generally base absent, top present or absent, mainly nonchannelized, have sand rarely coarser than medium-grained; examples: northern St. George quarry; Point Cudejarre, Buck Island, Allandale.

3. thick sandy: these are layers 0.5 to 3 m thick, commonly in upward-thickening sequences; they have ss/mst >5, are base present and commonly have pebbly (lithoclastic) basal zones and scoured bases; such beds may have full Bouma zonation or be top absent; intraclasts are commonly concentrated in the Tb zone; interesting Tbcbc... repetition occurs within some individual turbidites, examples: Grapetree Point, Tague Point, Hams Bluff, Crique Dam.

Nonturbidites are of widely varying types: thick mudstone, thin ungraded sandstone, thick massive sandstone, and sedimentary breccia.

Table 3: Lithic properties of Cretaceous strata

	constituent grains	granulometry	matrix-cement	rock types
SEDIMENTARY BRECCIA	**volcanic fragments:** chiefly porphyritic, occasionally equigranular basalt, pyrox. andesite, hbl-pyrox. andesite, dacite, pyrox. dacite, plag.-pyrox-chlorite rock, and altered equivalents; scoria **skeletal fragments:** rudist, bivalve, gastropod, coral **sedimentary rock fragments:** lithic-feldspar wacke and arenite, mudstone, chert; limeclasts, locally stromatolitic **mineral fragments:** framework components in microbreccia; same as in sandstone	granule to cobble size; chiefly angular; local accumulations of sub-rounded coarse fragments.	matrix is variable mixture of sand-sized particles (of types in sandstones) in coarse-grained breccia and chlorite, 10A mica, zeolite, and hydrocalcsilicate minerals; locally dominant CO3 cement.	lithic breccia lithic-feldspar microbreccia lithic-skeletal breccia/ microbreccia megabreccia (partly brecciated slump masses)
SANDSTONE	feldspar (plagioclase) pyroxene quartz lithic clasts: very fine-grained andesite, dacite chloritic rocks, chert skeletal particles hornblende	very fine-grained to coarse-grained sand; generally angular; subrounded coarse-grained sand at places	wacke: chlorite, 10A mica arenite:carbonate cement, minor clay, zeolite, prehnite	fine-grained feldspar-lithic wacke medium- to coarse-grained feldspar-pyroxene-quartz-lithic wacke ditto: arenite
MUDSTONE	variable proportions of silt- to very fine-grained sand size feldspar-quartz-skeletal particles and finer-grained chlorite, 10A mica, carbonate, and cherty quartz; abundant silica microveinlets; gradations in proportion of SiO2 between mudstone and chert.			laminated siltstone-mudstone silty (sandy) mudstone homogeneous mudstone porcellainite
CHERT	microcrystalline quartz; veinlets of calcite and quartz abundant; frequent sprinkling of silt-sized quartz (no indications they are biogenic); smears of opaque substance.			chert silty chert

Thick mudstone is either massive or vaguely laminated and may or may not include laminae of thin ungraded sandstone or chert. The mudstone is commonly organic-rich (black). We have not investigated the microstructure of such rock and are uncertain whether it is a very muddy turbidite, perhaps locally or widely homogenized by bioturbation, or it is due to hemipelagic deposition; examples are Hughes Point, Grass Point, Cane Bay, Mt. Fancy.

Thin ungraded sandstones are well sorted, fine to coarse grained, tabular, and plane-bottomed. They commonly occur in sections with muddy or thin sandy turbidites and have higher proportions of cement (carbonate, calcsilicate) and lower matrix than turbiditic sand. They are generally massive except in coarser layers where they are conspicuously cross-laminated. These were interpreted as either a product of reworking of turbidites by bottom currents or, for the coarser beds, grain flow by Speed (1974). Stanley (1988) subscribes to the first explanation. Examples are at Buck Island southshore and East End.

Thick massive sandstones are channelized deposits associated with slumps and debris flow. They are coarse grained, commonly pebbly, and may have a rude plane lamination. Nonequant particles are well aligned, indicating a fully turbulent flow. The top few percent of the layer, if present, is commonly upward fining. Examples are at Tague Point, Isaac Point, Robin Bay, Recovery Hill, and Crique Dam.

Sedimentary breccia consists partly of thick fragment-touching piles of angular lithoclasts and poorly sorted muddy-sandy matrix. These deposits are debris flows, and although locally plane and concordantly bottomed, they occur in lenticular, channelized coarse grained sedimentary sequences. Their moderate to good clast alignment and locally graded tops indicates generally fluid flows. Slumps form another type of sedimentary breccia. These consist of slabs and folded masses of intraclastic turbidite and other layer types together with lithoclasts and occur in association with debris flows and/or massive sandstone. Examples are Grass Point, Shoy Point, Tague Point, Hams Bluff, Judith Fancy, and Vagthus Point.

Layer Sequences: Upward thickening and coarsening sequences can be recognized on two scales. Gradual thickening over 100's of meters occurs at East End to Point Cudejarre, indicating progressive progradation, probably over a broad outer fan. More abrupt thickening sequences over 10's of meters, commonly culminating in channelized deposits, can be seen at Grass Point, Grapetree Bay, Cramer Park, and Crique Dam. Upward thinning sequences are less evident.

Chert and Pelagic Rocks: Aside from sediment-gravity flows of volcanigenic particles, pelagic deposits probably form the rest, a tiny fraction, of the Cretaceous strata. They are mainly in sections of thin bedded volcanigenic rocks. The evidence for pelagic constituents is inferred from the existence of bedded chert (Speed, 1974) which is the result of thorough diagenetic transformation. Chert occurs both as a layered vitreous type and as grainy rock in the top few centimeters of muddy and sandy turbidites. Vitreous chert almost certainly arose from in situ biogenic particles, although no tests have been recognized in dissolution residues (D. L. Jones, written comm., 1980) and by microscopic study. The grainy cherts are an evident replacement product and pore filling at bed tops, implying that soluble biogenic pelagic particles accumulated between successive turbidites.

Chert diagenesis occurred early in the history of the Cretaceous sediments because 1) it is cut by sandstone dikes, 2) it occurs in intraclasts in channelized deposits, and 3) chert-rich zones took up displacements by buckling in the first deformation whereas other stratal types deformed without flexing, probably by pore volume loss.

Examples of chert are at Cramer Park and Buck Island.

Sand Loading and Intrusion: The Cretaceous rocks of nappes K2, K3, and K6 contain remarkable loading features, called linear load casts by Speed (1974) and Speed et al. (1979), and abundant sandstone intrusions occur throughout.

Linear load casts are highly elongate protrusions of the bases of sandstone layers into subjacent mudstone, in association with flame structures of mudstone. They differ from standard loads which are equant in the bedding plane, by their axiality and parallelism (Fig. 2). They are postdepositional (not flutes) because they deform lamination in subjacent layers. Moreover, they are related to tectonic deformation because axial plane cleavage parallels the bisecting plane of the linear loads and flames and tectonic fold axes parallel the linear load axes (Fig. 2). These are interpreted (Speed, 1974) to have arisen during layer-parallel tectonic compression when sands were incompressible but incohesive and mudstone was contractable by cleavage development and pore collapse. The vertical exchange of sand and mud in planes normal to maximum compression permitted the sand layers to shorten without detachment from adjacent mudstone. The upshot of this is that tectonism and cleavage development began in nappes K2, K3, and K6 before lithification of at least the basal parts of many sandstones. Examples of linear load casts are at Coakley Bay, Romney Point, Grapetree Point, and Caledonia Quarry.

Sandstone dikes and irregular intrusions occur widely in St. Croix. Such bodies transferred coarse sand fractions up or down from a sand source beds. Sandstone dikes intruded before, during, and after cleavage development, but there is no evident dike alignment relative to strain axes. Interesting sandstone phacoliths occur in folds at places where sand intruded hingeward during folding. As with linear load casts, sand intrusions indicate some sands remained unlithified through at least early tectonism. Examples of intrusions are at Cramer Park, Vagthus Point, and Judith Fancy.

Depositional Realm: Because all the Cretaceous nappes of St. Croix contain turbidites with marine skeletal particles, a general environment of deposition can be established as marine and subwavebase. The absence of planktic calcareous fossils, except at Vagthus Point and Diamond Keturah (Whetten, 1966), suggests the depth was below the carbonate compensation depth, assuming that cherts came from siliceous plankton and that diagenesis was not the cause for the near-absence of calcareous tests. Moreover, the planktic forams at the two exceptional sites are probably resedimented, as discussed earlier, and thus were buried too rapidly for dissolution in deep ocean water. The occurrence of intraclasts and slumps of turbiditic and other layers in channel filling beds and turbidites above channel fills implies the channels formed in the same deep water environment.

It is generally convenient and useful to relate such layer sequences to model turbidite fan facies (for example, Walker, 1984). We do not infer, however, that the Cretaceous rocks of St. Croix occupied any particular original fan geometry, and it is possible they may never have occupied a single initial stratigraphic succession.

The turbidite layers occur in greater or lesser abundance in all nappes. These are probably outer fan or fan fringe facies because of their tabularity and lateral continuity (where this can be seen such as at East End) and intervals of upward thickening that imply source progradation without erosion. The variations about the outer fan theme differ to degrees among nappes. Nappes K2 and K6 ("Caledonia") are principally outer fan deposits that include sporadic thick channel fills (10->50 m) which were emplaced and covered by thin turbidites. This indicates that the channeling was not due to systematic migration or reconfiguration of the fan system.

K1 has facies with abundant discrete fine sand and mud which may represent either or both bottom current reworking and interchannel plus crevasse splay deposits. The fineness of grain and paucity of sedimentary structures in such rocks may suggest the former, and the association with channelized pebbly sandstone and carbonate grain flows, the latter.

In K3, the abundant nonturbidite (?) mudstone and thick channel filling sequences suggest either an upper fan interchannel regime or fan-abandonment facies with sudden reactivation.

Nappe K4 may contain midfan and upperfan channel mouth deposits together with outer fan intervals (Whetten's (1966) Recovery Hill member). K5 has outer and midfan facies in western outcrops and upperfan channel deposits at Clairmont and Judith Fancy.

The provenance of sediment in the sediment-gravity flow deposits was an active, emergent island arc with volcanic edifices emitting magmas of varied composition, from basalt to dacite, and with neritic and/or littoral carbonate banks that flanked parts of the volcanic edifices. The source terrane is known to have supplied sediment for at least 14 ma and perhaps 30 ma or longer.

Whetten's (1966) interpreted flow directions in St. Croix turbidites as southerly. Our measurements, corrected for tectonic rotation, however, indicate varied directions and dispute claims to any preferred direction. All such measurements must take into account steeply plunging fold axes (to 60°) whose axial trends vary with position (Speed, 1974). Thus, the sedimentology of the Cretaceous rocks does not indicate the source-basin direction.

The fan facies of the Cretaceous strata suggest a basin floor rather than a slope as the general depositional site because of the general preponderance of turbidites and rarity of rocks typical of slopes such as mudslumps, pebbly mudstone, and channellized fine-grained sandstone. The basinal site was probably close to base of slope as implied by innerfan and fan-channel facies.

Tectonic Setting of Basin: The basinal sites were evidently in the vicinity of an active Late Cretaceous island arc. Three general settings can be envisioned: fore-, back, and intra-arc. The expected stratal and structural products for deposits in such settings differ as follows.

In case of a forearc, the basinal site was likely to have been an unfilled bathymetric trench because the width of the forearc was probably narrow and arc-derived sediment funneled directly to the slope base, as in Pacific arcs. Evidence suggesting a narrow forearc is the lack of continental sediments and the absence of pelagic carbonate beds which might imply deposition above CCD in a forearc basin or slope basins on a wide forearc. The exception to an exclusively volcanigenic and fringing reef-derived sediment population is the clasts in pebbly sandstone of nappe K1 (Buck Island) which indicates unroofed radiolarian pelagic rocks; these were perhaps resedimented within the forearc. In a trench, fan facies would have developed a complex pattern by flow parallel to and across the trench axis (for example, Graham et al., 1975; Schweller and Kulm, 1978). Further, most sediments deposited in a trench would have probably accreted within a few million years of their accumulation. Therefore, accretion (imbrication and folding) and sedimentation were continuing and contemporaneous phenomena, and strata in adjacent imbricate sheets would not generally have been in a single initial stratigraphic succession.

A backarc basin site, on the other hand, would probably have been tectonically relatively stable during sediment accumulation. A vertical succession of strata in radial fans (Walker, 1984) would be predicted. Then, the onset of a phase of tectonic activity, not specifically predicted by plate tectonic theory, is required to have imbricated the succession. Such activity can be envisioned as a Maastrichtian subduction of backarc basin lithosphere below the arc, in which case the arc-trench system would have been N or NE facing in today's coordinates.

An intraarc basin occurs within the magmatic arc platform, probably steep-walled graben caused by extension that accompanies arc-building. Deposits in such basins are probably like those in backarc basins but with sediment sources from both sides of the graben. Beds deposited in an intraarc basin might be expected to include calcareous pelagic rocks unless the rate of turbidite accumulation were too great to permit discrete pelagic deposits. A major distinction between intraarc and backarc or trench/forearc basins is the much greater probability of magmatism during sedimentation.

Several observations suggest a forearc site is the more likely. First, the imbricate sheets do not repeat an evident stratigraphic succession. Second, the imbrication and deformation of Cretaceous strata in nappes K1, K3, K4, and K5 occurred shortly after their deposition (0-10 ma) and the sand mobility in all nappes indicates incomplete lithification before imbrication. In contrast, the intrusion of sills and dikes in at least two and probably more stages within the Late Cretaceous suggests an intraarc basin may have been more likely.

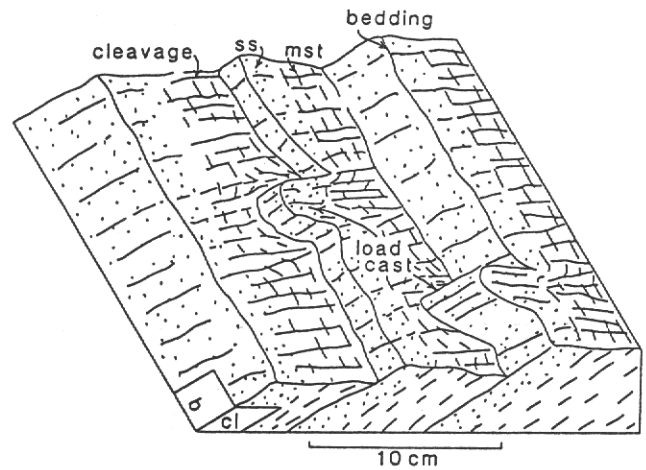

Figure 2. Three dimensional illustration of relations among linear load casts, bedding, and cleavage.

STRUCTURES OF CRETACEOUS STRATA

All the Cretaceous strata of St. Croix are deformed. The structures and their sequence of development differ nappe to nappe, but certain common elements exist among nappes. Each nappe underwent at least one phase of deformation before the youngest phase (postcomplex) of igneous intrusion in the Maastrichtian (66-72 mybp). The timing of some later phases of deformation relative to intrusion is uncertain.

Table 4 summarizes principal structures in sequence for nappes K1-6.

Table 4: Structures in sequence in Cretaceous nappes
(sequence numbers not necessarily correlative nappe to nappe)

Nappe	
K1	D1: subvertical to overturned homocline, E striking and S facing; foliation (S1) steeply N dipping; tight minor folds (F1) with axial planes in foliation plane and N verging; homocline probably a flank of a S verging major fold. D2: flat and steep fault zones with central shear zones with foliation and quartz veins; open to tight folds of bedding and S1 in shear zone walls; folds are mainly flat, some doubly hinged.
K2	D1: local isoclines in chert-rich sections, folded nearly homoaxially by F2 folds; detached from adjacent strata. D2: pervasive close S verging major folds (F2) with axial plane cleavage (S2) and trains of harmonics with vergence appropriate to limb position; axial planes dip between N and W (folded in D3); F2 axes plunge steeply in S dipping great circle. D3: major folds of D2 elements; D3 axial traces defined mainly by formlines of D2 cleavage (Fig. 4); D3 axial planes strike ENE, dip 70°S to 90° (Fig. 4); rotation of F2 axes in D3 suggests horizontal maximum elongation. D4: late fault-related folds and kinks. Orientation data for K2 in Speed (1974).
K3	D1: isoclinal folds in pelitic rocks with strong axial plane cleavage, dipping between N and W, and major S verging folds of thick layer sequences. D2 and D3: same as D3 and D4 of nappe K2.
K4	D1: sporadic close major and macroscopic folds with S vergence or overturning; local S1 axial plane cleavage in muddy beds, poorly developed; cleavage and folds with varied orientation suggest D2 event and rotation of cleavage about a N plunging axis.
K5	D1: sporadic cleavage in muddy rock; dips between N and E, modally NE. D2: major close folds (Fig. 1) with WNW striking, steeply N dipping axial planes, and S overturning; F2 axes plunge steeply E.
K6	D1: minor folds with axial plane cleavage (S1) dipping NNE to NE; F1 axes plunge ENE; sedimentary breccia flattened in cleavage plane (NE dip) and X/Y = 1 to 3, X (max. elongation) N plunging. D2a: minor chevron and kink folds of bedding and cleavage; S2 axial planes conjugate, dip N and S; F2 axes steeply E plunging. D2b: major gentle syncline with WNW axial trace (Fig. 1), probably continuous with D2 syncline of K5.

Major Features: Beds in all the nappes are in early folds with harmonic content that varies with layer thickness implying a buckling rather than fault-bend origin. The number of fold superpositions varies among nappes; most have two, but K2 has four. Axial planes and related cleavage all had initial strikes between E and NE and northerly dips. Vergences of major folds are southerly in all nappes. Axes of all folds plunge easterly, generally between 30° and 70°; except for some reoriented early folds.

Cleavage occurs in all nappes, but its development varies. It is strongly developed in the structurally lower nappes (K1, K2, K3, K6) which are more generally muddy. There, it is closely spaced and pervasive and at least partly a product of pressure solution. Its occurrence is more sporadic in higher nappes (K4, K5), even in muddier intervals. This seems to reflect initial development rather than degree of contact metamorphic obscuration. Structural depth may have been the controlling parameter to cleavage development.

No penetrative tectonic lineations have been recognized in St. Croix, implying strains were flattening rather than constrictional. This is supported by clast shapes in strained sedimentary breccias where X/Y = 1 to 3 within the cleavage plane.

Late major folds have been superposed on earlier fold sets in at least four nappes (K2, K3, K5, K6). These have approximately E striking axial planes with steep dips. They are discussed further below.

Late brittle faults and related folds and kinks in their walls affect all the nappes. Their orientations and slip sense are highly varied: normal-oblique, reverse, thrust, and horizontal. They probably formed in several stages and almost certainly are not all synchronous. Some normal faults were clearly contemporaneous with Maastrichtian diking and are followed by dike tips and diatremes. At the East End, such faults indicate ENE-WSW horizontal extension during diking. It is probable that some sets of late faults are related to the central graben of Cenozoic age (Fig. 1).

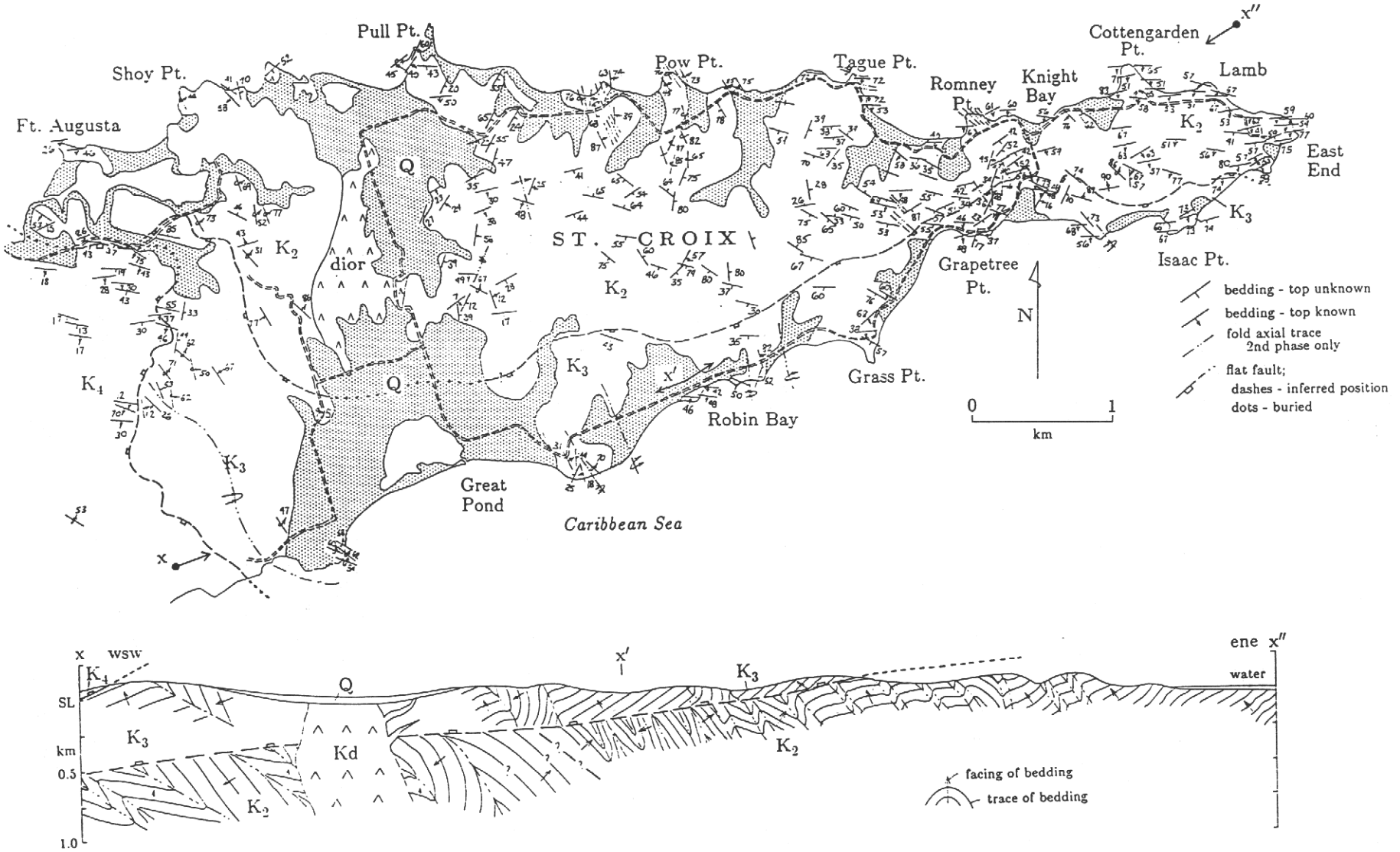

Figure 3. Map and section of eastern St. Croix showing distribution of bedding attitudes, approximate nappe boundaries, and axial traces of folds of most intense deformation phase (phase 2 in K2, phase 1 in K3).

East End Structures: Figure 3 shows a map of bedding and cross sections for eastern St. Croix. The principal features are the south to west vergent folds of nappes K2 (F2) and K3 (F1) where exposures permit them to be identified.

Because both nappes possess the same fold train, they were either 1) juxtaposed before this folding event or 2) folded at different sites under the same kinematic regime and then juxtaposed without rotation. At the three places where the K2-K3 boundary is exposed, the fault cuts cleavage, implying the fault is younger than this fold train. Therefore, the second explanation has support.

Figure 4A shows the orientations of cleavage related to the principal folding of K2 (S2) and K3 (S1), together with form lines to assess axial trace orientation of late major folds that cause the 90° variation in cleavage strike. Figure 4B (Equal area net lower hemisphere) shows that poles to cleavage form a girdle with easterly plunging axis. Figure 4C shows that the constructed axial plane for the late major fold is ENE striking and steeply dipping.

The emplacement of nappe K4 on K3 and K2 was after the early deformations of the lower nappes (D2 in K2, D1 in K3) because the boundary cuts their cleavage. It is unclear whether the late major folds affect K4 or not.

West End Structures: Figure 5 shows structural data and interpretation for a part of western St. Croix from our field studies, chiefly by J. Joyce, together with some bedding attitudes from Whetten (1966). The position of the K5-K6 fault boundary is interpolated among three exposures at Cane Bay, Annaly Trail, and near Oxford.

The lower nappe, K6, contains two deformation phases (Table 4). The first includes minor folds, F1, and axial plane cleavage, S1, from the northern coast to Sprat Hall (Fig. 5). Poles to S1 occupy a short girdle whose maximum plunges SW. The F1 axis maximum plunges steeply ENE. South of Sprat Hall, K6 may include the vertical or overturned limb of a major F1 fold (section, Fig. 5). F2 folds in K6 have E striking axial planes; these are not included on the section of Figure 5 because their occurrence is sporadic and amplitude small.

The upper nappe, K5, contains major folds of bedding and sporadic local cleavage (Table 4). Because the major folds' axial planes (WNW strike, steep NNE dip) are not apparently coplanar with cleavage (NW strike, moderate NE dip) (Fig. 5), the two structures are provisionally considered to be sequential. Although the data are sparse, owing to limited exposure, cleavage seems not to be folded; hence, the major folds are taken as D1 and cleavage, D2.

The K5-K6 boundary was an active fault during and/or after D1 of K6 because S1 cleavage is deflected at the boundary. The nappe boundary was also active during D1 of K5 because it partly cuts out the major fold limbs (Fig. 5). The nappe boundary and homoclinal bedding of K6, however, are in low amplitude folds with axial traces approximately coincident with those of D1 folds in K5. This implies that K5 and K6 locked together before the cessation of folding in K5. Perhaps, D2 deformations in both nappes are a further response to contraction after nappe locking.

Timing of Structures: In eastern St. Croix, the juxtaposition of nappes K2 and K3 and deformations D1+2 in K2 and D1 in K3 occurred before latest Maastrichtian intrusion. Evidence includes cutting of structures by undeformed dikes and contiguity of the area of strong contact metamorphism by the Southgate pluton (Fig. 1) across the nappe boundary. The age of late major folding (D3 in K2, D2 in K3), however, is unknown within the range, Maastrichtian - early Miocene. The range is supplied by D1 in K3 and earliest known ages of little deformed cover to the Cretaceous of St. Croix. The intrusions do not date the late folding because such folds have large wavelengths and the dikes had no uniform initial attitude.

The age of juxtaposition of nappe K4 is unconstrained after rock deposition in the Maastrichtian. Until disputed by new evidence, we assume it to have been during the Cretaceous as with K2 and K3. A plausible alternative, however, is that the base of K4 is a Cenozoic low-angle normal fault related to tectonics that caused the central graben of St. Croix.

In western St. Croix, D2 (cleavage) of K5 and D1 of K6, hence juxtaposition of K5 and K6, preceded intrusion and are probably of Maastrichtian age. The key evidence is that metamorphism in dike walls is postcleavage in both nappes, but use of this to date cessation of relative movement of the nappes pivots on the argument that cleavage of K5 is contemporaneous with or later than cessation. The age of D2 in K5 is unconstrained.

Structural Evolution: The principal structures of the Cretaceous strata of St. Croix, nappes, early folds, and foliation provide evidence for contraction and imbrication in Late Cretaceous time, probably mainly or entirely Maastrichtian. Such deformation can be interpreted as a product of thrust imbrication even though the ages across nappe boundaries are unknown.

Because the imbrication took place at or near the base of slope of an island arc, the displacement zone was almost certainly a convergent plate boundary. The thrust stacking accreted sediment sheets to the front of an overriding plate from a downgoing one. The pervasive SW to S vergence and/or overturning of structures within the imbricated sheets implies the downgoing plate had a component of Late Cretaceous relative motion between N and NE in today's coordinates. The late folding in nappes K2 and K3 can be interpreted as representing progressive NS shortening of the imbricated sediments after accretion.

The relationships of Cretaceous strata before imbrication are unclear. The lack of stratigraphic correlations among adjacent nappes indicates either that 1) the strata were sequentially deposited and accreted, as in a trench wedge, or 2) that both emergent thrusting and duplexing occurred in an initially continuous stratigraphic sequence.

Tectonics: Current understanding permits two alternative schemes for the early tectonic evolution of St. Croix's Cretaceous tectonic complex. First is the deposition of Late Cretaceous volcanigenic strata on a trench floor to the present south and west of the magmatic arc platform. Such strata were progressively driven into and scraped off at the toe of the island arc's accretionary prism. This hypothesis accounts well for the structure and stratigraphic differences of nappes. It suffers, however, in the attempt to explain two or more phases of magmatism within the basin during and after sediment accumulation and deformation.

Second is the deposition of the Cretaceous strata in an intraarc basin which collapsed in Maastrichtian time. Basin collapse may have had vergence either toward the fore- or backside of the arc or conceivably was bivergent. Therefore, an intraarc basin origin provides no implications for arc polarity. An intraarc basin origin is supported by the intrusion of Late Cretaceous arc magmas into the basinal strata before and after deformation. Such an origin may be disputed, however, by the lack of carbonate pelagic beds.

To conclude, origins of Cretaceous sediments as trench fill or intraarc basin deposits are currently permissible. Further studies are required to discriminate these origins.

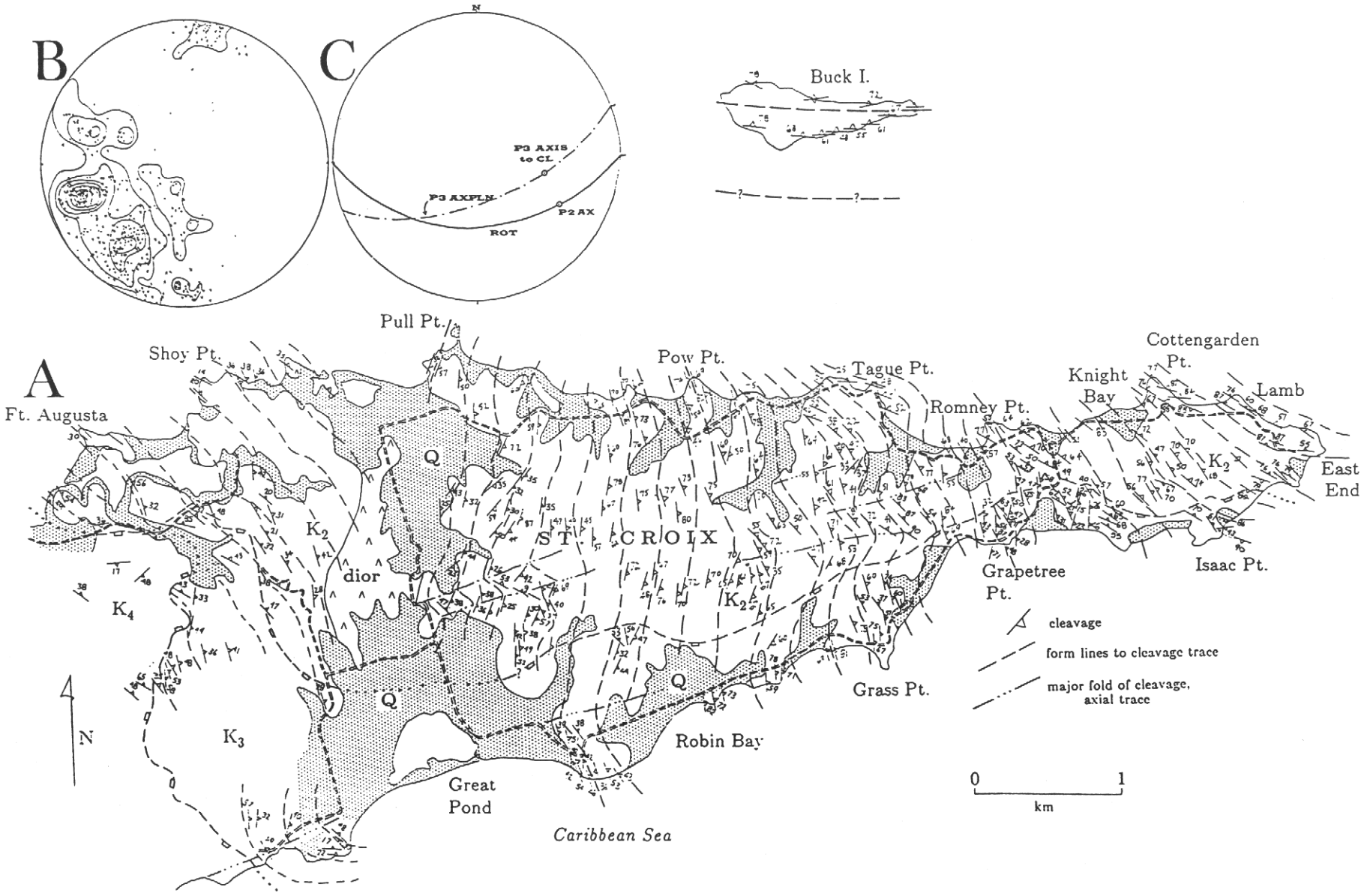

Figure 4. Map of eastern St. Croix showing distribution of cleavage attitudes and axial traces of some late stage macroscopic folds of cleavage (phase 3 in K2, phase 2 in K3). Orientation diagrams (equal area, lower hemishpere): B) poles to cleavage (x) and axial planes (dots) that are phase 2 in K2 and phase 1 in K3; C) calculated axial plane (dash-dot line) for late stage (phase 3) macrofolds from average axial trace (map) and axis to elements in B; solid great circle is rotation path of phase 2 fold axes.

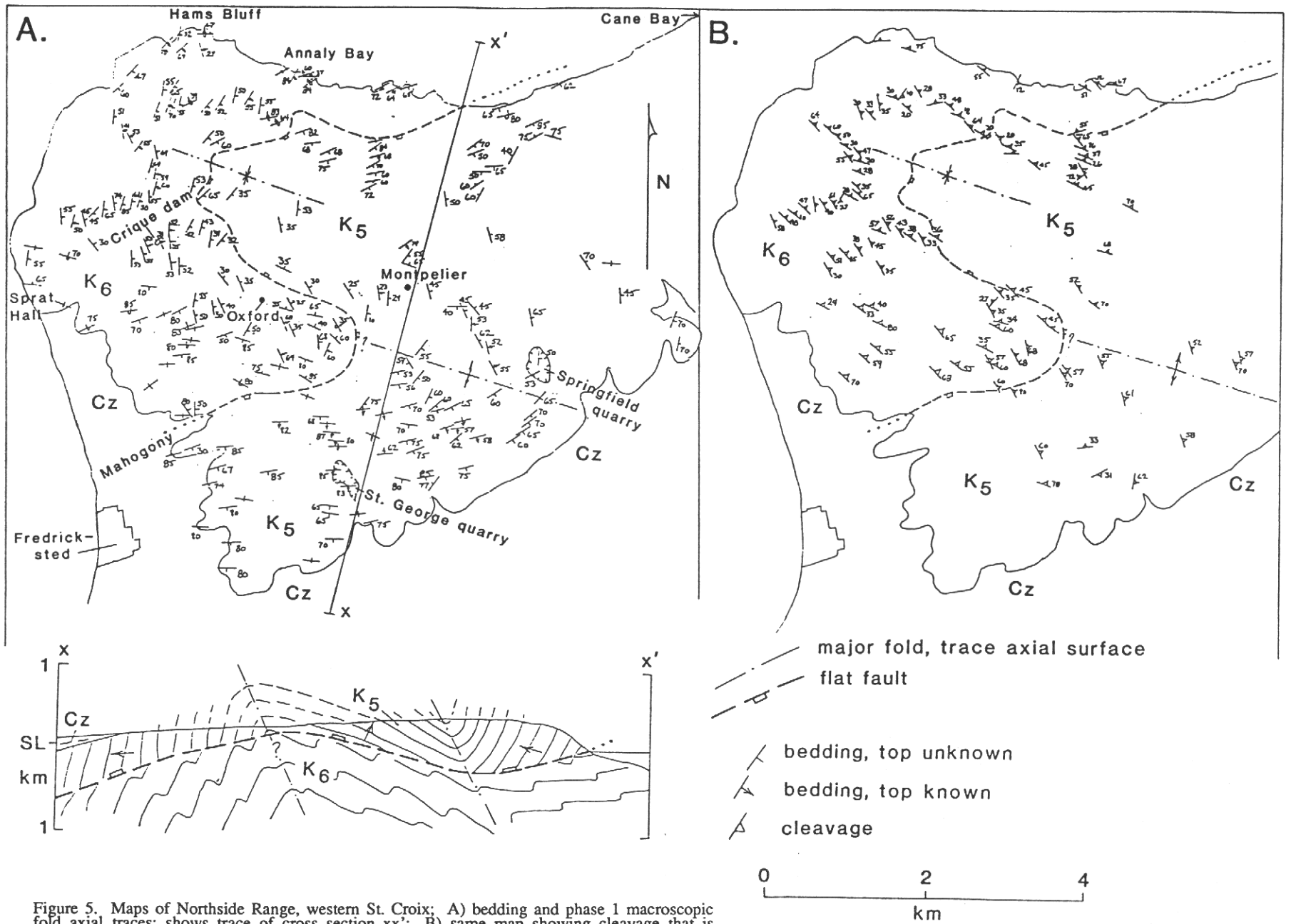

Figure 5. Maps of Northside Range, western St. Croix; A) bedding and phase 1 macroscopic fold axial traces; shows trace of cross section xx'; B) same map showing cleavage that is probably second phase.

CONCLUSIONS

1. The exposed sub-Cenozoic rocks of St. Croix are deep marine volcanigenic sedimentary rocks with minor pelagic interbeds. Their depositional ages range from Cenomanian or Turonian to Maastrichtian. There are no magmatic rocks, but the volcanigenic constituents came from an active island are throughout this duration.
2. The Cretaceous strata occupy a tectonic complex that probably comprises thrust-bounded sheets (nappes). No islandwide stratigraphic succession exists.
3. The Cretaceous strata are in outer to innerfan facies. They were deposited at or near the base of slope of a Late Cretaceous island arc. The basin was probably a trench adjacent to the convergent boundary of the island arc system or a basin (intraarc) within the magmatic arc platform.
4. Island arc magmatism at the sediment source was ongoing for at least 14 ma and perhaps, more than 30 ma.
5. Imbrication of the Cretaceous strata was accompanied by folding and cleaving with vergence or overturning between S and SW in today's coordinates. The imbrication was followed by later NS horizontal contraction.
6. Imbrication was completed in Maastrichtian time. It is interpreted as representing the accretion of sediment to the forearc toe above a downgoing plate with a component of N to NE transport relative to the island arc or the collapse of an intraarc basin with either fore- or backthrusting.

ACKNOWLEDGEMENTS

This study resulted in part from research sponsored by NSF Grant EAR-8803633. I am grateful to D. Larue, and H. Ave-Lallement for challenging commentary in the field and to G. Draper for showing me a cleaved sill at Knights Bay.

REFERENCES

Andreieff, P., Mascle, A., Mathieu, Y., and Muller, C., 1986, Les carbonates néogènes de Sainte-Croix (les Vierges): Etude stratigraphique et petrophysique: Rev. Inst. français du pétrole, v. 41, p. 335-349.

Cedarstrom, D. J., 1950, Geology and groundwater resources of St. Croix, Virgin Islands: U.S. Geol. Survey Water Supp. Paper, v. 1067, 117 p.

Graham, S. A., Dickinson, W. R., and Ingersoll, R. V., 1975, Himalayan-Bengal model for flysch dispersal in Appalachian-Ouachita system: Geol. Soc. America Bull., v. 86, p. 273-286.

Joyce, J., 1979, Structures and lithology of the West End, St. Croix, USVI [M.S. report]: Evanston, IL, Northwestern Univ.

Kent, D. V., and Gradstein, F. M., 1985, A Cretaceous and Jurassic geochronology: Geol. Soc. America Bull., v. 96, p. 1419-1427.

Lidz, B., 1988, Upper Cretaceous (Campanian) and Cenozoic stratigraphic sequences, northeastern Caribbean (St. Croix, USVI): Geol. Soc. America Bull., v. 100, p. 282-298.

Multer, H. G., Frost, S. H., and Gerhard, L. C., 1977, Miocene "Kingshill Seaway"—A dynamic carbonate basin and shelf model, St. Croix, U.S. Virgin Islands: in Reefs and Related Carbonates - Ecology and Sedimentology, Amer. Assoc. Petrol. Geol. Studies in Geology 4, p. 329-352.

Quin, J. T., 1907, The Building of an Island: New York, Chauncy Holt, 106 p.

Schweller, W. J., and Kulm, L. D., 1978, Depositional patterns and channelized sedimentation in active east Pacific trenches, *in* Stanley, D. J., and Kelling, G., eds., Sedimentation in Submarine Canyons, Fans, and Trenches, Stroudsberg, Penn.: Dowden, Hutchinson, and Ross, p. 311-324.

Speed, R., 1974, Depositional realm and deformation of Cretaceous rocks, East End, St. Croix: West Indies Lab. Spec. Publ. 5, p. 189-200.

Speed, R. C., Gerhard, L. C., and McKee, E. H., 1979, Ages of deposition, deformation, and intrusion of Cretaceous rocks, eastern St. Croix, Virgin Islands: Geol. Soc. America Bull., v. 90, Pt. I, p. 629-632.

Stanley, D. J., 1988, Deep-sea current flow in the Late Cretaceous Caribbean: measurements on St. Croix, U.S. Virgin Islands: Marine Geology, v. 79, p. 127-133.

Walker, R. G., 1984, Facies Models, Geosci. Canada Reprint Series 1, 317 p.

Whetten, J. T., 1966, Geology of St. Croix, U. S. Virgin Islands: Geol. Soc. America Mem., v. 98, p. 177-239.

A NOTE OF THE RELATIVE TIMING OF CLEAVAGE FORMATION AND MAGMATISM IN THE CRETACEOUS ROCKS OF ST. CROIX, U.S. VIRGIN ISLANDS

Grenville Draper and Jamie M. Bartel
Department of Geology
Florida International University
Miami, Fl 33199, U.S.A.

ABSTRACT

The Cretaceous sedimentary rocks of St. Croix are characterized by a pervasive slaty cleavage. The timing of the development of this cleavage relative to the emplacement of various major and minor igneous plutons was previously regarded as uncertain, but generally was considered to have taken place before the intrusions. We report the presence in the East End of St. Croix of cleavage in a pyroxene porphyry sill and a diatreme dike. These features indicate at least some of the magmatic activity on St. Croix preceded the cleavage forming deformation. We further suggest that folded quartz veins in the West End of St. Croix, that were involved in the later stages of cleavage formation, may have been derived from cooling igneous bodies at depth. These observations indicate that at least some magmatic activity pre-dated or was approximately synchronous with cleavage formation. If the observed igneous bodies were formed in the same interval as other minor intrusions, this implies that the cleavage formed during or post Maastrichtian - early Paleocene time.

INTRODUCTION

The island of St. Croix is the peak of the St. Croix platform which forms a submarine ridge in the southeastern Greater Antilles. The island is composed of deformed, Upper Cretaceous sedimentary rocks and igneous intrusions (Whetten, 1966; Lidz, 1988; Speed and Joyce, 1989; see also Fig. 1), except for a central graben (Whetten, 1966), or half graben (Speed and Joyce, 1989), which is occupied by limestones of Miocene and younger age.

Whetten (1966) considered the Cretaceous sedimentary rocks to be composed of four stratigraphic units: the Caledonia, Allendale, Cane Valley and Judith Fancy Formations. In contrast, Speed and Joyce (1989) were of the opinion that no coherent stratigraphy can be established and that the Cretaceous rocks are composed of six structural packages, or nappes, labeled K1 through K6 (Fig 1). The Caledonia Formation (nappes K1, K2, K3, K6 of Speed and Joyce, 1989) are composed of turbidites and contourites (Speed, 1974; Speed and Joyce, 1989; Stanley, 1989) containing detrital carbonate, quartz and feldspar grains, with minor chert and debris flow beds. The Allandale, Cane Valley and, in particular, the Judith Fancy (K4, K5) are composed of volcanogenic (?tuffaceous) sandstones and siltstones.

Structurally, the most obvious feature of these rocks a penetrative slaty cleavage (Fig. 2) that is pervasive throughout all units except the Judith Fancy Formation where it is only locally developed in fine grained lithologies (Speed and Joyce, 1989, and authors' own observations). Speed and others (1979) and Speed and Joyce (1989) assert that this structure was formed before the intrusion of major and minor igneous bodies. Hornblende K-Ar dates obtained from minor intrusions (referred to as "dikes" in Speed and Joyce, 1989, but many are sills) range from 71.8 to 66.1 Ma (Speed and others, 1979), but igneous clasts in a pebbly sandstone at Robin Bay yield and age of 75.2 Ma. The sills and dikes are presumed undeformed, and hence the conclusion of Speed and others (1979) and Speed and Joyce (1989) is that the tectonite fabric of the sedimentary rocks took place between 75.2 and 71.8 Ma.

In this note, we describe occurrences of intrusive igneous bodies that either possess a cleavage or were deformed in the later stages of cleavage formation. These observations imply that least some magmatic activity pre-dates or is synchronous with tectonism, and therefore, that cleavage formation in St Croix may have been later than previously suggested.

Larue, D.K., and Draper, G. (eds.),
Transactions of the 12th Caribbean Geological Conference, St. Croix, U.S.V.I., Miami Geological Society, P.O. Box 431552, South Miami, FL 33243, U.S.A

CLEAVAGE IN CRETACEOUS SEDIMENTARY ROCKS

Our observations indicate the Cretaceous sediments consist of mainly of impure, arkosic calcarenites with minor quartz clasts, with lesser amounts of calcareous arkoses and graywackes. Beds of chert are present in the East End of St. Croix (Speed and Joyce's K2 nappe), as are arkosic grits (within Speed and Joyce's K3 nappe; Whetten's Grass Point Member).

In outcrop and hand specimen, the cleavage in the sedimentary rocks appears as a planar penetrative fabric, usually at a high angle to bedding (Fig. 2). Our preliminary examination indicate that the cleavage in the rocks of the Caledonia Formation results from several fabric elements:

1) alignment of ellipsoidal carbonate grains (formed form originally equant detrital grains)
2) pressure solution seams, usually anastamosing, of finite length which varies in length from "short" (one to two grain diameters) to "long" (many grain diameters). These are comparable to varieties of "disjunctive" or "wispy" seams of Borradaile and others (1982, p.34).
3) alignment of phyllosilicate grains, some of which are distributed throughout the rock, others of which are concentrated as lenticular pods.

The degree of development of these features are a function of finite strain and mineralogical composition. In general, quartz and feldspar grains are not deformed internally.

SILL LOCATED WEST OF COTTONGARDEN BAY

A sill of andesitic pyroxene porphyry occurs in outcrops on a wave cut platform west of

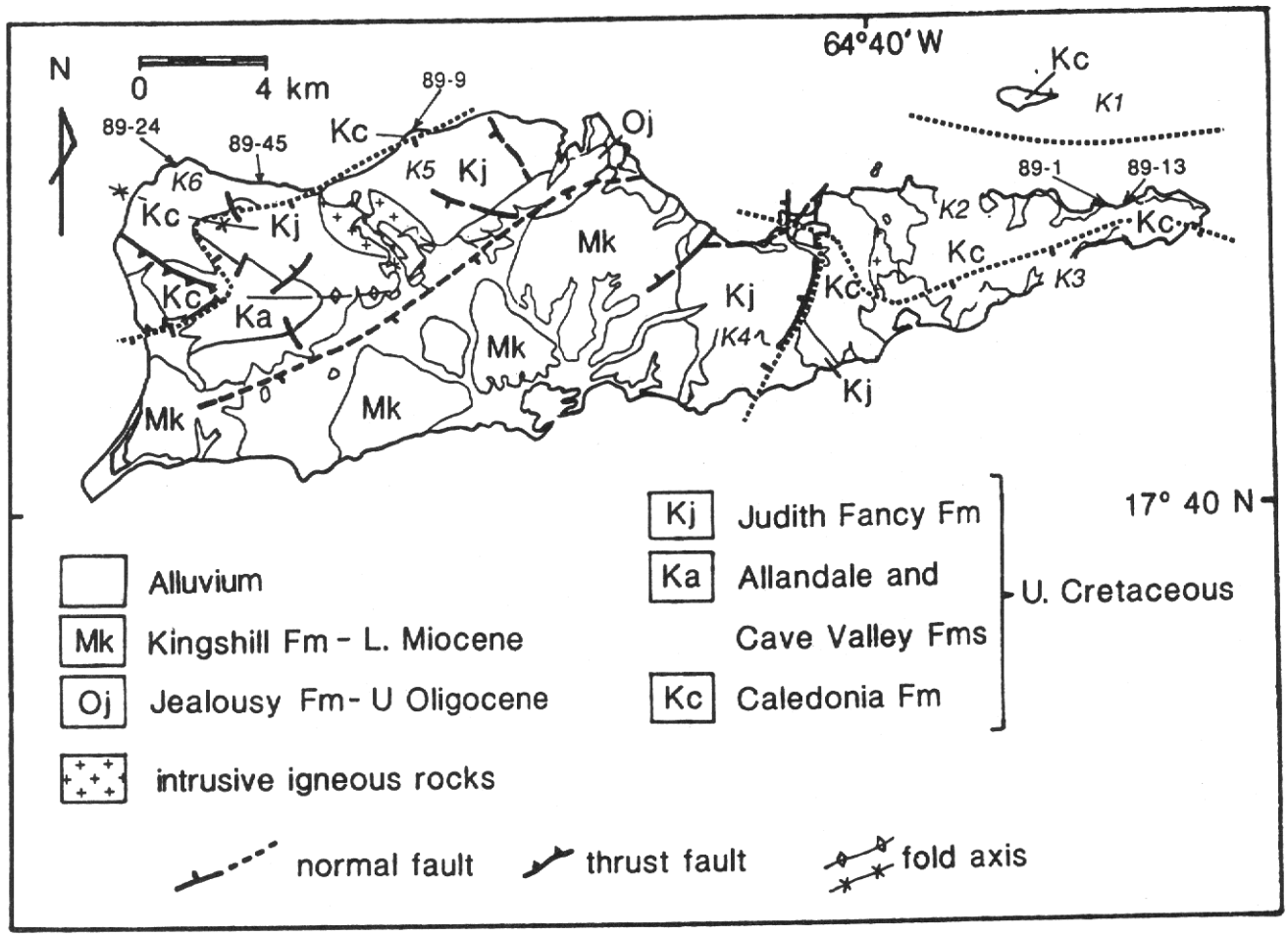

Fig. 1 Geologic map of St. Croix based on Whetten (1966). Boundaries of the nappes of Speed and Joyce (1989) are shown by the dotted lines and labeled in italics. Localities referred to in text are: 89-1 Knight Bay, 89-13 West of Cottongarden Bay, 89-24 Hamm's Bluff, 89-45 west of Annaly Bay.

Cottongarden Bay (grid reference 313642). The 28-30 cm. thick sill occurs in intercalated beds of sandstone, siltstone and chert which strike 108^0 and dip 79^0N . Slaty cleavage in the surrounding sedimentary rocks strikes 004^0 and dips $38\text{-}40^0$E. Cleavage in the sill, which is sub-parallel to the cleavage in the country rock, can easily be observed in the outcrop in the intertidal zone, but is hard to perceive in the more weathered rock exposed in the cliff face.

In thin section, the cleavage is developed as a series of lenticular 2-3mm by 0.4 mm domains of sinuous, anastamosing seams of fine-grained phyllosilicates irregularly distributed throughout the rock.

DIATREME DIKE AT KNIGHT BAY

A small diatreme (explosively emplaced breccia) dike can be observed cutting black siltstones on the east side of Knight Bay (grid reference 312640). The dike has irregular boundaries and is variable in thickness from 30 to 100 cm. Angular clasts in the dike are composed of both volcanic and sedimentary rocks which are up to 10 cm in diameter. The larger volcanic clasts consist of leucocratic, seriate textured dacite and quartz microphenocryst bearing rhyolite. Neither of these igneous lithologies have previously been reported from St. Croix. Devitrified glass shards are found as small (>3mm) clasts in the dike and their presence confirms the interpretation that this body represents an igneous rather than sedimentary intrusion (Speed, personal commuinication).

Mesososcopic scale clasts in the diatreme are deformed into approxomately ellipsoidal shapes with their short axes perpendicular to cleavage planes. Cleavage is developed in the both the sedimentary clasts and the matrix of the diatreme, and has the same orientation in each of these, indicating that cleavage formed after emplacement of the diatreme. The cleavage morphology and architecture in the sedimentary clasts of the dike are identical to those found in the surrounding sedimentary rocks of the Caledonia Formation in that they are defined by (a) preferred orientation of ellipsoidal carbonate grains, (b) phyllosilicate aggregates and (c) anastamosing pressure solution seams. The fabric of the matrix is defined by anastamosing, discontinous pressure solution seams, concentrated on the boundaries of undeformed feldspar and quartz grains, and oriented aggregates and isolated grains of a brown pleochroic phyllosilicate (?stilpnomelane). With the exception of the devitrified glass shards, the igneous clasts have not developed a cleavage.

Fig. 2 Cleavage in arkosic calcarenites (with minor chert beds) at Knight Bay (locality 89-1), East End, St. Croix. Cleavage parallel to hammer handle (30 cm). Exposed face trends NNE-SSW.

FOLDED QUARTZ VEINS IN THE WEST END OF ST. CROIX

Well developed quartz veins and segregations are found at several locations in the West End of St. Croix and are particularly well displayed at localities at Hamm's Bluff (grid reference 013658) and west of Annaly Bay (grid reference 036652) . At both these localities, the quartz veins form ptygmatic folds (Fig 3) whose axial planes are parallel or sub-parallel to the cleavage (Joyce,1979, personal communication; othors own observations). This relation suggests that the veins were formed and folded in the latter stages of cleavage formation. As most of the Cretaceous sediments are calcareous, the source of the silica of the quartz veins is puzzling. It is possible that quartz rich sequences underlie the Caledonia Formation and that the silica was released during as a result of pressure solution of these hypothetical sediments. We suggest that a more likely source of silica is from cooling intermediate to felsic intrusions and therefore infer that the cleavage forming deformation in the West End is approximately synchronous with magmatic activity.

CONCLUSIONS

The features described: (1) cleavage in a porphyryitic sill, (2) cleavage in a diatreme and (3) axial planar cleavage developed in association with folded quartz veins possibly derived from cooling igneous intrusions, demonstrate that at least some igneous activity on St Croix was took place before, or was syncronous with, the tectonism which formed the slaty cleavage in the sedimentary rocks. The site west of Cottongarden Bay may be particlarly revealing. As a result of the fortuitous weathering of the outcrop close to sea level, the cleavage in the sill is easily observed. Cleavage in other intrusive rock bodies may be present but, with other weathering states, may not be so obvious. It is also possible that many intrusive bodies emplaced before tectonism may not have developed any cleavage, because they are so strong compared to the surrounding sedimentary rocks, and hence nearly all the strain (and hence slaty cleavage development) will have been accommodated by surrounding sedimentary rocks rather than by the sills. Thus, even if other intrusions predate deformation, they may only have a weak cleavage if it is detectable at all.

Our contention, therefore, is that a large part of the magmatic activity affecting St Croix preceded or was synchronous with the cleavage forming deformation. This deformation must have taken place, therefore, in the interval recorded by

Fig. 3 Folded quartz veins at Hamm's Bluff, West End, St. Croix. Bedding is subhorizontal in photograph, Regional cleavage is parallel to hammer handle, but locally is refracted into parallelism with the axial planes of folds in quartz veins.

K-Ar dates of the minor intrusions of the East End (between 71.8 and 66.1 Ma - Maastrichtian to earliest Paleocene), or later.

To resolve the question of the age of cleavage forming tectonism on St, Croix, further geochronologic studies on the intrusive rocks must include careful outcrop observations, and examination of oriented samples in thin section, to determine if tectonite cleavages, or associated syn-cleavage structures (such as folded sills with axial planar cleavages in accompanying sedimentary layers), are present.

ACKNOWLEDGEMENTS

We thank Denny Hubbard and other staff members of the West Indies Laboratory for their help and cooperation. We are greatful to Jim Joyce and especially Bob Speed for free exchange

of ideas and information at the outcrop. Gautam Sen reviewed the original manuscript and suggested many improvements. Financial support was provided in part by a Summer Grant from the provost of Florida International University.

REFERENCES

Borradaile, G.J., Bayly, M.B. and Powell, C. McA., 1982, Atlas of deformational and Metamorphic Rock Fabrics, Springer-Verlag, New York, 551 pp.

Joyce, J., 1979, Structures and lithology of the West End, St. Croix, U.S.V.I., unpublished M.S. thesis, Northwestern University.

Lidz, B., 1988, Upper Cretaceous(Campanian and Cenozoic stratigraphic sequences, northeastern Caribbean (St. Croix, USVI), Geological Society of America Bulletin, v. 100, p.282-298.

Speed, R.C., 1974, Depositioanal realm and deformation of Cretaceous rocks, East End, St. Croix: West Indies Laboratory, St. Croix, secial publication no. 5, p.189-200.

Speed, R. C., Gerhard, L.C. and McKee, E.H., 1979, Ages of deposition, deformation and intrusion of Cretaceous rocks, eastern St. Croix. Virgin Islands, Geological Society of America Bulletin, v. 90, p.629-632.

Speed, R., and Joyce, J., 1989, Depositional and structural evolution of Cretaceous strata, St. Croix: *in* Hubbard, D.K.,(ed.) Terrestrial and marine geology of St. Croix, U.S. Virgin Islands, special ublication no. 8, West Indies Laboratory, St. Croix, p.23-35.

Stanley, D.J., 1989, Sedimentology amd paleogeography of Upper Cretaceous rocks, St. Croix, U.S. Virgin Islands: new interpretations: *in* Hubbard, D.K.,(ed.) Terrestrial and marine geology of St. Croix, U.S. Virgin Islands, special ublication no. 8, West Indies Laboratory, St. Croix, p.37-47.

Whetten, J.T., 1966, Geology of St. Croix, U.S. Virgin Islands: Geological Society of America Memoir 98, p. 177-239.

CHARACTERISTICS OF VOLCANIC CENTERS FROM THE LESSER ANTILLES

A.L. Smith and M.J. Roobol
Department of Geology
University of Puerto Rico 00708

ABSTRACT

The active volcanoes of the Lesser Antilles are characterized both by effusive eruptions producing lava flows and domes, and by explosive eruptions producing various types of pyroclastic deposits. Five major styles of explosive eruptions have been distinguished, these styles and their products are:

Pelean - block and ash flows, dense andesite surges, ash and dust falls;
St. Vincent - scoria and ash flows, scoriaceous surges, lapilli-, and ash-falls;
Plinian - pumice and ash flows; ash hurricanes, pumiceous surges, lapilli-, and ash-falls;
Asama - semi-vesicular block and ash flows;
Phreatomagmatic/Phreatic - block flows, base surges, ash falls.

Based on their eruptive products the volcanoes of the Lesser Antilles can be grouped into five types:

a) Centers composed almost entirely of pyroclastic deposits - Mt. Pelée (Martinique), the Quill (St. Eustatius);
b) Centers composed of dome clusters and associated aprons of block and ash flow deposits (produced by Pelean eruptions) - Saba island, Soufriere Hills (Montserrat);
c) Centers with numerous dacitic pumice and ash flows - centers on Dominica, south-central St. Lucia;
d) Centers with significant lava flows associated with pyroclastic deposits of various types - the Peak (Nevis), Soufriere (St. Vincent);
e) Centers composed of basic and intermediate lava flows and associated fall deposits- South Soufriere Hills (Montserrat);

The pyroclastic deposits from all volcanic centers are often reworked soon after eruption by fluviatile processes so that stratigraphic sections commonly show intercalations of pyroclastic deposits with their epiclastic derivatives. Eruptions from Lesser Antillean volcanoes also produce submarine deposits such as subaqueous ash falls, subaqueous volcaniclastic flows and ash turbidites.

INTRODUCTION

The Lesser Antilles island arc extends from the Anegada Passage, east of the Virgin Islands, to just north of the South American continent. The active arc (Fig.1) includes, from north to south, the islands of Saba, St. Eustatius, St. Kitts, Nevis, Redonda, Montserrat, Basse Terre of Guadeloupe, Dominica, Martinique, St. Lucia, St. Vincent, the Grenadines and Grenada, as well as a number of submarine centers, including the active volcano of Kick'em Jenny (Robson and Tomblin, 1966; Bouysse et al, 1980; Roobol and Smith, 1989). Eruptions from the subaerial volcanoes are both effusive and explosive, with the latter representing the dominant eruptive style (Roobol and Smith, 1989).

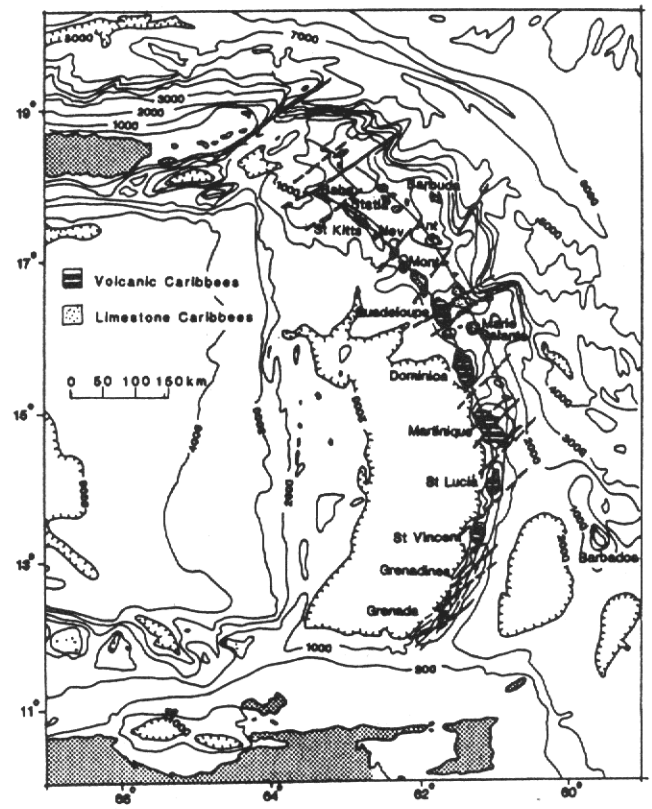

Figure 1. Map of the Eastern Caribbean and Lesser Antilles island arcs. Isobaths in meters; proposed transverse faults after Westercamp (1979). Mont - Montserrat; Ant - Antigua; Nev - Nevis (After Smith and Roobol, in press.)

ERUPTIVE STYLES

Effusive eruptions have produced both lava flows and domes and range in composition from basalt to rhyolite. Lava flows are usually basalt or andesite in composition and have been produced by both central and flank eruptions. Many flows exhibit a massive or columnar jointed core with a blocky or rubbly surface (when preserved) (Fig.2). Most have high-aspect ratios, having flowed usually only a few kilometers from their source. Aspect ratio is V/H where V is the average thickness of the flow or deposit in meters and H is the diameter of a circle covering the same areal extent as the flow or deposit in kilometers (Walker, 1973, 1983). Domes have been extruded from both central vents, for example, the 1902-05 dome of Mt. Pelée, Martinique (LaCroix, 1904), and from parasitic vents, for example,Great Hill, Saba, (Westermann and Kiel 1961), and are usually andesitic or dacitic in composition. All historic domes are covered by a carapace of blocks: these are often lacking on the older domes because of erosion. A section through The Great Hill dome on Saba is shown in Figure 3. This dome is cut by a number of fractures

Larue, D.K., and Draper, G. (eds.),
Transactions of the 12th Caribbean Geological Conference, St. Croix, U.S.V.I., Miami Geological Society, P.O. Box 431552, South Miami, FL 33243, U.S.A

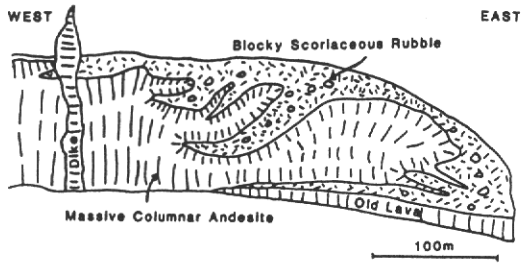

Figure 2. Section through a pre-historic lava flow exposed in the northern crater wall of Soufriere volcano, St. Vincent (After Sigurdsson, 1981).

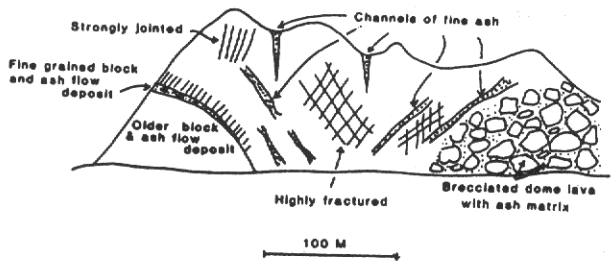

Figure 3. Sketch of a section through Great Hill dome, Saba.

which are filled with fine ash and has a breccia-like outer margin on one side in which blocks of dome lava are enclosed in an ash matrix.

Explosive eruptions have produced various types of pyroclastic deposits including flow, surge and fall. Most of the pyroclastic flow deposits from Lesser Antillean volcanoes are of high - aspect ratio type and form valley infills, although some low-aspect ratio deposits, eg ash hurricanes, do occur (Smith & Roobol, in press). Pyroclastic surges may occur either associated with pyroclastic flows (ground surges and ash-cloud surges), or as independently derived low density flows (base surges, groundsurges). Various mechanisms proposed for the production of pyroclastic flows and surges are shown in Figure 4. Fall deposits from eruptions of Lesser Antillean volcanoes range from coarse Plinian lapilli deposits to fine ash and dust deposits characteristic of Pelean and phreatic or phreatomagmatic eruptions. The distribution pattern of fall deposits depends on the interaction of the height of the eruption column and the velocity and direction of the wind at various heights in the atmosphere (Figure 5). For the Lesser Antilles, which are located in the belt of the Trade Winds, relatively low eruption columns generate deposits elongated towards the west (Fig. 6a). In contrast eruption columns that reach the upper troposphere produce deposits that have a distribution pattern to the east or southeast (Figure 6b).

Five major styles of explosive activity have been identified for the volcanoes of the Lesser Antilles. Each style has produced a variety of distinct deposits (Table 1). Pelean-style eruptions (LaCroix, 1904) are characterized by the growth of a dome throughout the eruption. Partial or complete destruction of this dome by explosions produces the large angular blocks which give the pyroclastic flow deposits generated by these eruptions their characteristic appearance - block and ash flow deposits (Fig.7). Most Pelean- style eruptions tend to affect only a limited sector of the volcano's flanks (Fig. 8) (Westercamp and Traineau, 1983; Roobol and Smith, 1975; Smith and Roobol, in press). St. Vincent- and

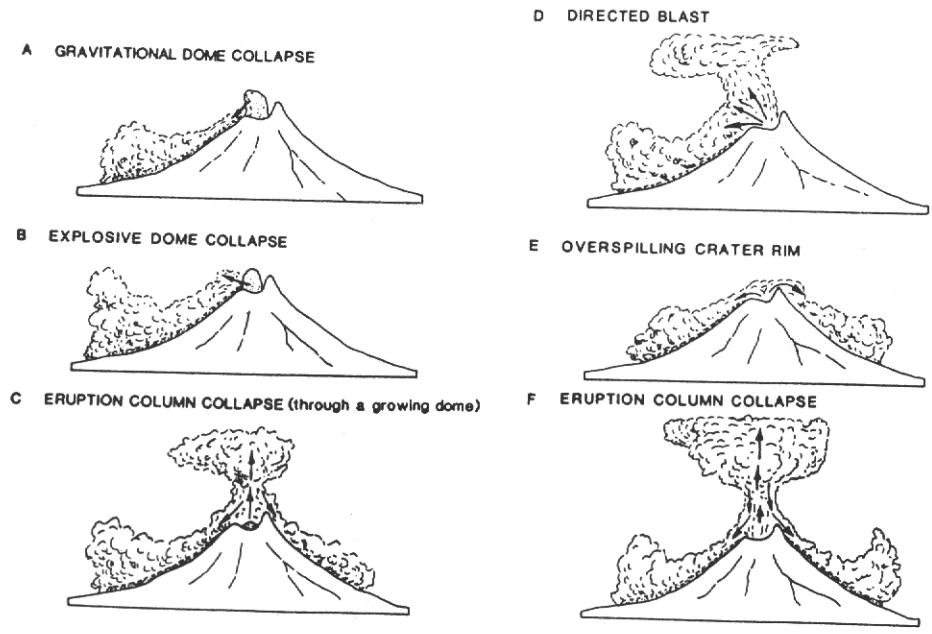

Figure 4. Diagram showing the different mechanisms proposed for the generation of pyroclastic flows (After Smith and Roobol, in press).

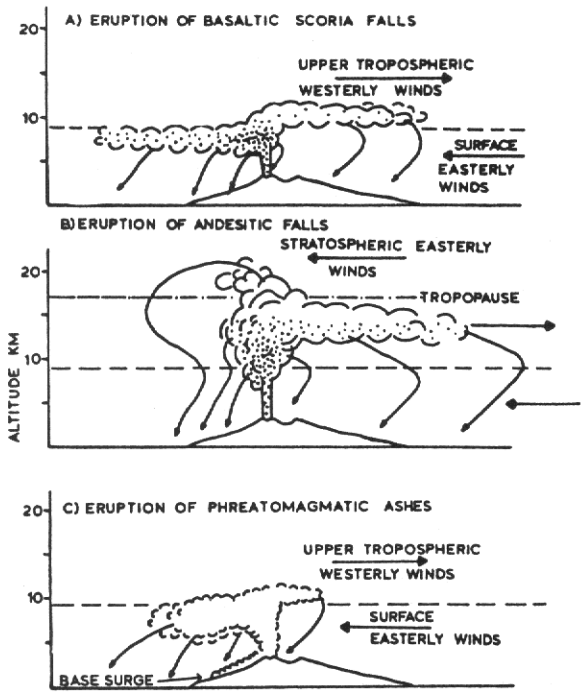

Figure 5. Schematic diagrams showing the effects of a layered atmospheric system and eruptive column heights on the dispersal of airfall ejecta from the Lesser Antilles. The heights given, correspond to data from today's wind system in the vicinity of St. Kitts where the lower Trospospheric easterlies are confined to altitudes of 5-9 km depending on the season. The tropopause is shown at about 17 km. Trajectories are schematic transport paths of airfall ejecta (After Roobol et al., 1985).

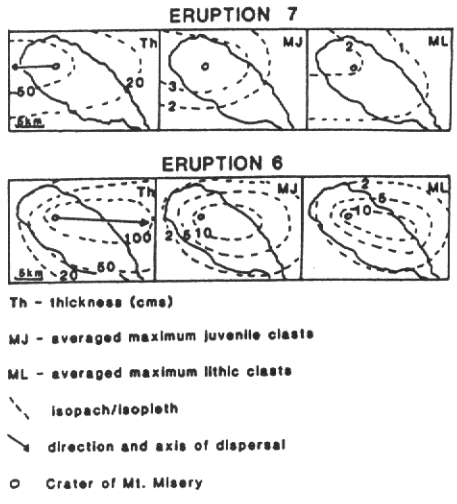

Figure 6. Dispersal maps for fall deposits for the Mansion Series, St. Kitts, A) Basaltic scoria fall deposit of eruption 7 (Unit B, Black Cinders) B) Andesite fall deposits of eruption 6 (Unit C, Upper Green Lapilli) (After Roobol et al., 1985)

Table I . Deposits produced by the Eruptive Styles Characteristic of Lesser Antillean Volcanoes

Eruptive Style	Deposits
PELEAN	Block and ash flow (high aspect ratio): Block and ash flow (low aspect ratio): Dense andesite surge; ash and dust falls
ST. VINCENT	Scoria and ash flow (high aspect ratio): scoriceous surge; lapilli-and ash-falls
PLINIAN	Pumice and ash flow (high aspect ratio): ash hurricanes (low aspect ratio): lapilli- and ash-fall
ASAMA	Semi-vesicular block and ash flow (high aspect ratio)
PHREATIC/PHREATOMAGMATIC	Block flow; base surge; lapilli-ash and dust falls

Plinian- style eruptions both occur from open craters and their pyroclastic flows are generated by eruption column collapse (Fig. 4). Pyroclastic flows from both eruptive styles can affect all flanks of a volcano, with coarse high - aspect ratio flow deposits occupying the valleys, and, in the case of Plinian eruptions, low- aspect ratio ash hurricane deposits extending out to tens of kilometers from the central vent (Roobol and Smith, 1980; Smith and Roobol, in press). Fall deposits are usually associated with both of these eruptive styles (Fig. 8). Asama-style activity describes eruptions which produce very low eruptive columns so that the pyroclastic flows essentially only overtop the crater rim and flow down the flanks of the volcano under gravity. Fall and surge deposits associated with this eruptive style have not been identified in the Lesser Antilles. Phreatic and phreatomagmatic deposits are very common on the "wet" volcanoes of the Lesser Antilles. Most of the historic activity has been of this style (Roobol and Smith, 1989) and many of the deposits from supposedly magmatic eruptions show evidence of water/magma interaction (Roobol et al, 1985, Smith and Roobol, in press). Phreatic/ phreatomagmatic eruptions are mostly of limited lateral extent.

VOLCANIC CENTERS

A summary of the activity recorded from the different islands/volcanoes of the active arc of the Lesser Antilles is given in Table 2. Based on the relative abundance of the different types of eruptive products, the volcanoes of the Lesser Antilles can be subdivided into five types of centers.

I - Centers composed almost entirely of pyroclastic deposits eg. Mt. Pelée, Martinique and the Quill, St. Eustatius. Both of these volcanoes, with the exception of a few dome and lava flow remnants in the summit region, are composed entirely of pyroclastic deposits (Fig.9) and their epiclastic derivatives.

II - Centers composed of Pelean-dome clusters and associated aprons of block and ash flow deposits: The dominant mode of activity on the island of Saba has been the extrusion of summit and flank domes, some of which

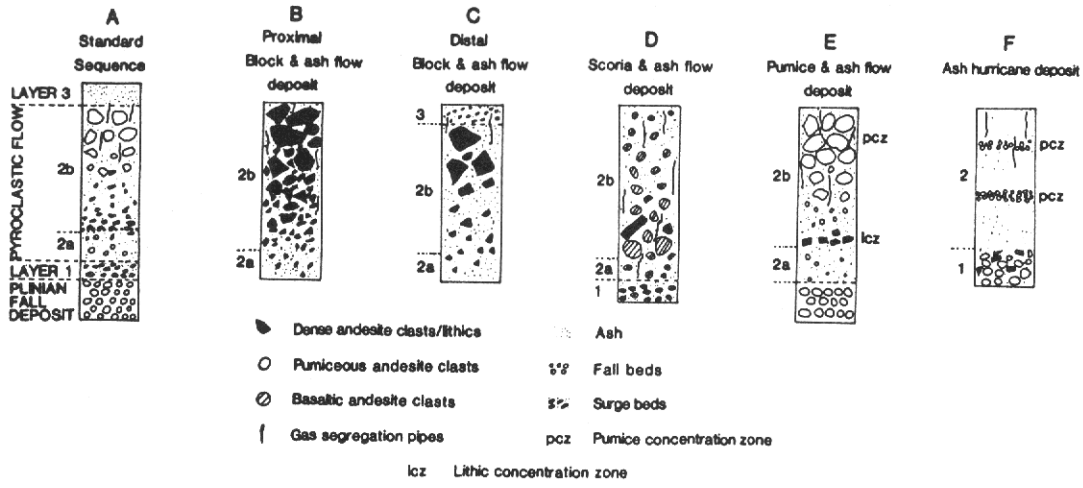

Figure 7. Diagrammatic sections through pyroclastic flow deposits. Layer 1 can be either a ground layer or a ground surge deposit; Layer 2a is the fine-grained basal layer of the pyroclastic flow; Layer 2b is the overlying "body" of the pyroclastic flow; Layer 3 is a co-pyroclastic flow airfall or an ash-cloud surge. Thickness of all the types of deposits, except the ash hurricanes, can range from 1 meter upto 50 meters; the ash hurricanes do not exceed 3 meters.

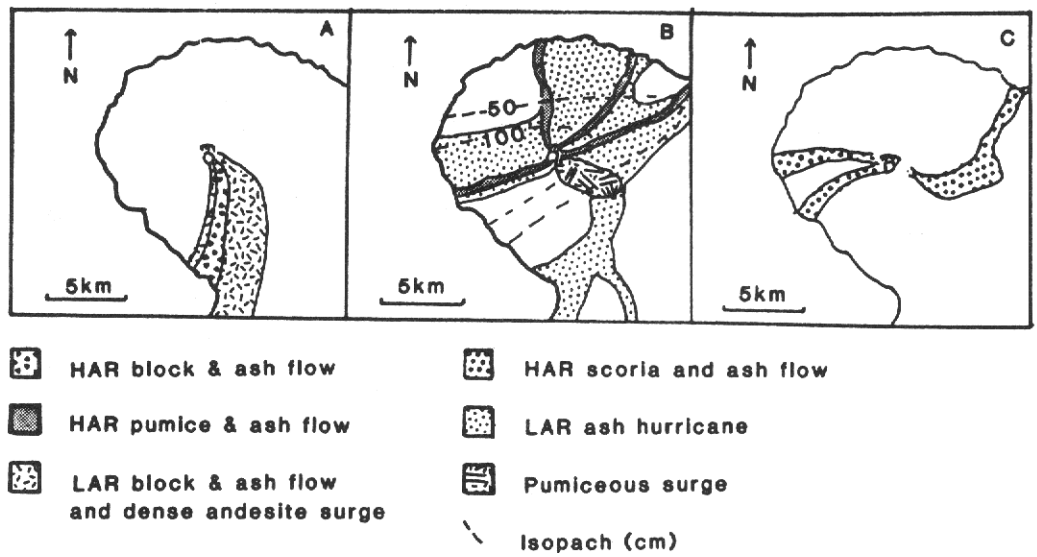

Figure 8. Maps showing distribution of deposits from prehistoric eruptions of Mt. Pelée. A - Pelean-style eruptions of stratigraphic subunit 14 (5,000-5,300 years BP); B - Plinian-style eruption - stratigraphic subunit d (1,800-2,200 years BP); C - St. Vincent- style eruption - flow A (~25,500-28,000 years BP) (After Smith and Roobol, in press).

have produced small short lava flows, and the associated eruption of block and ash flows. Although other types of volcanic activity have occurred on the island, their deposits only form a small percentage of the eruptive products (Fig.10).

III - Centers that have produced extensive andesite/dacite pumice and ash flow deposits: The youngest major eruptive activity on the islands of St. Lucia and Dominica (Figs. 11 and 12) have been of this type. On these islands numerous pumice and ash flows have flowed down most of the large valleys radiating away from the vent regions. On Dominica, many of these vents were subsequently blocked by the extrusion of Pelean domes, which are associated with the eruption of relatively small- volume block and ash flow deposits (Fig. 12).

IV - Centers with significant lava flows associated with pyroclastic deposits of various types: Mt. Misery, St. Kitts is an example of this type of center. During the last 40,000 years the volcano has erupted basic and intermediate composition lava flows, basaltic/basaltic andesite scoria falls, andesitic sub-plinian falls, lithic-rich scoria and ash flows and phreatic/pheatomagmatic falls and surges (Baker, 1969; Baker 1985, Roobol et al 1981, Roobol et al, 1985, 1987) (Fig.13).

V - Centers composed of basic and intermediate lava flows and associated fall deposits: The South Soufriere Hills on Montserrat with a thick sequence of basaltic and andesitic block, scoriaceous lapilli and ash fall deposits (White River Succession), and associated lava flows and domes, is an example of this type of center (Fig. 14).

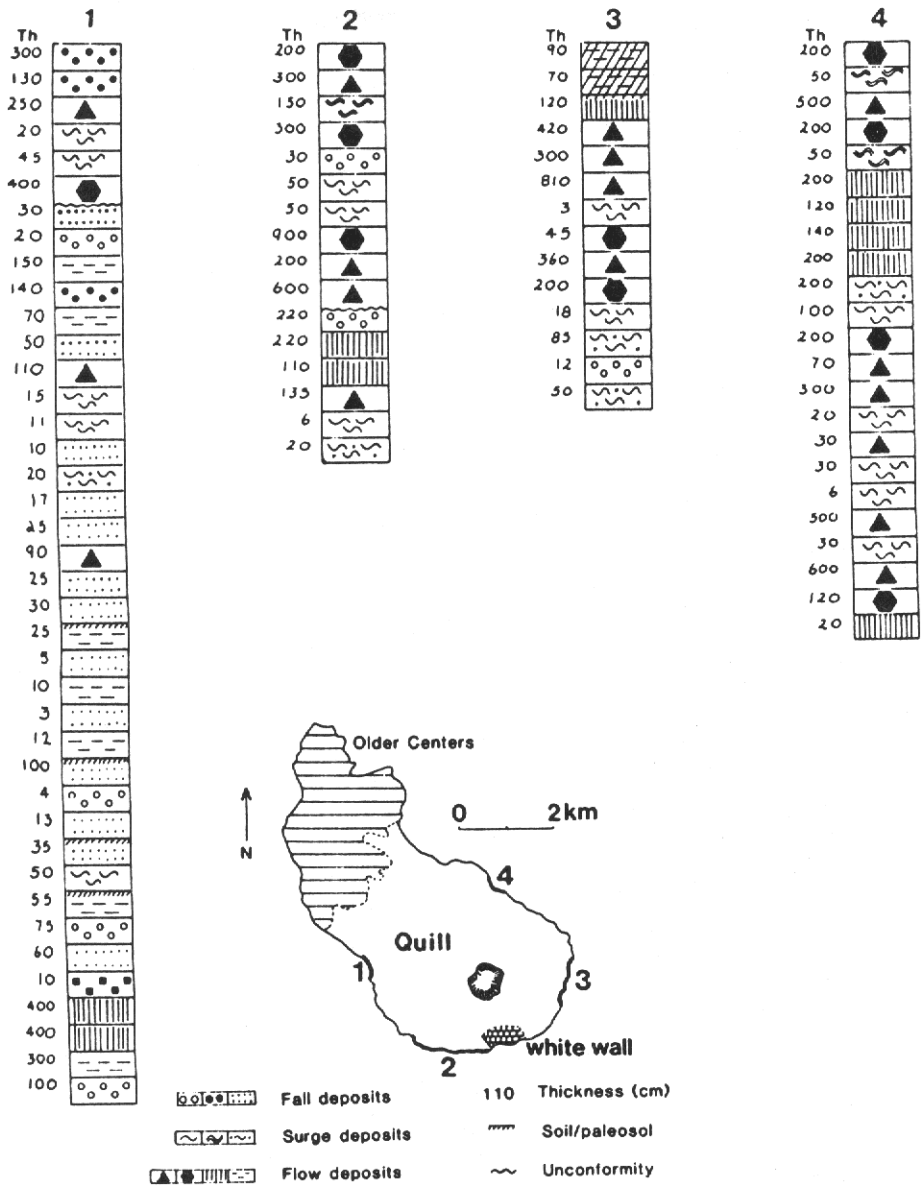

Figure 9. Stratigraphic sections through deposits from the Quill, St. Eustatius. Also shown is the uplifted limestone block of the White Wall and the older Northern Centers.

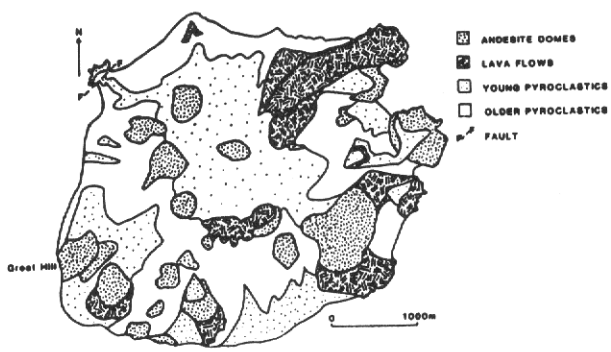

Figure 10. Geologic Map of Saba showing distribution of domes, lava flows and older and younger pyroclastic deposits (dominantly andesitic block and ash flows).

EPICLASTIC DEPOSITS

The pyroclastic deposits from all eruptive styles are commonly reworked by rainwash and fluviatile processes soon after eruption, so that stratigraphic sections commonly show intercalations of pyroclastic deposits with their epiclastic derivatives. For relatively small eruptions the primary pyroclastic deposits may be almost completely reworked and eroded so that hardly any evidence of the eruption remains in the stratigraphic record (Smith and Roobol, in press). In the lower part of Stratigraphic Division A of Mt. Pelée, Martinique epiclastic deposits make up approximately 75% of the stratigraphy (Fig. 15). These deposits are dominantly fluviatile conglomerates composed of boulders of dense andesite which alternate with fluviatile sandstones rich in andesitic pumice (Smith and Roobol in press). The former are thought to represent reworked Pelean block and ash flow deposits and the latter reworked Plinian fall and flow deposits.

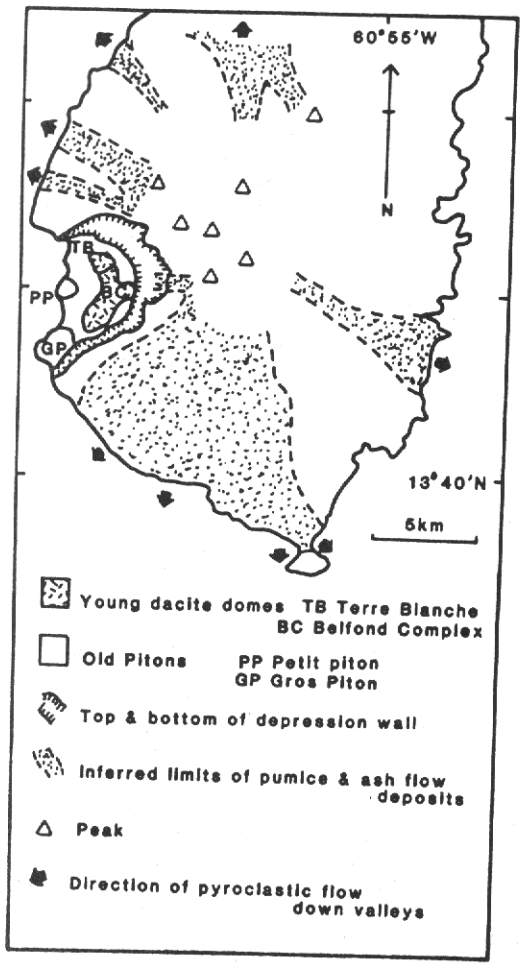

Figure 11. Map of southern and central St. Lucia showing radial distribution of pumice and ash flow deposits from a possible source in the central rainforest. (After Roobol et al, 1983; Wright et al., 1984).

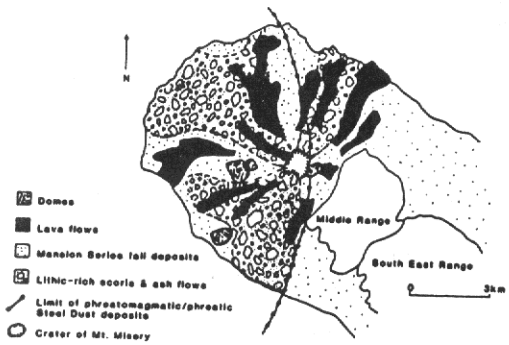

Figure 13. Map showing distribution of young (<45,000 years BP) volcanic deposits from Mt. Misery St. Kitts. Steel Dust Series deposits occur to the west of the line designating their limit (After Baker,1969; Roobol et al., 1987).

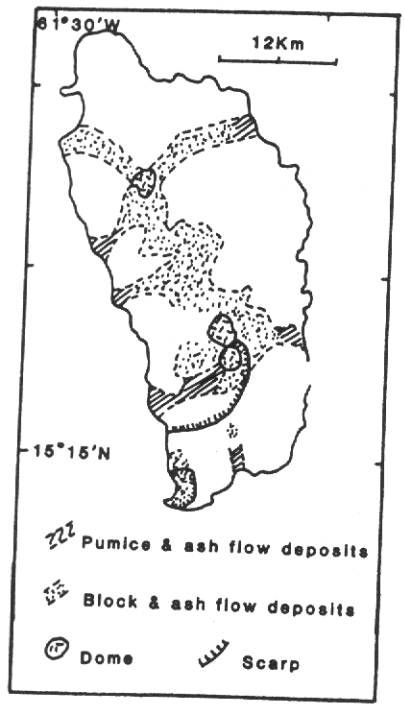

Figure 12. Distribution of youngest pyroclastic flow deposits in Dominica (After Carey and Sigurdsson, 1980; Roobol et al., 1983).

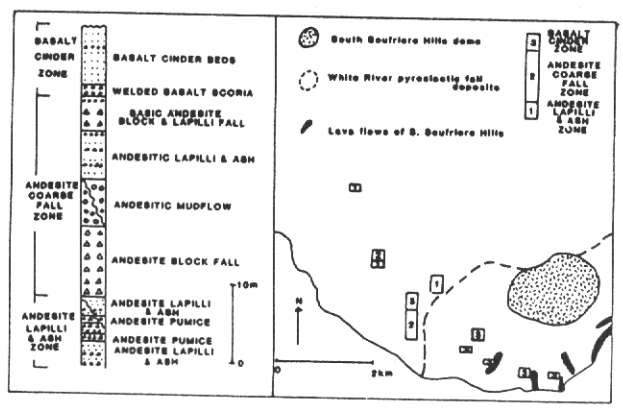

Figure 14 Map of southeastern Montserrat showing distribution of White River pyroclastic deposits and location of associated lava flows and the South Soufriere Hills dome (After Rea, 1974).

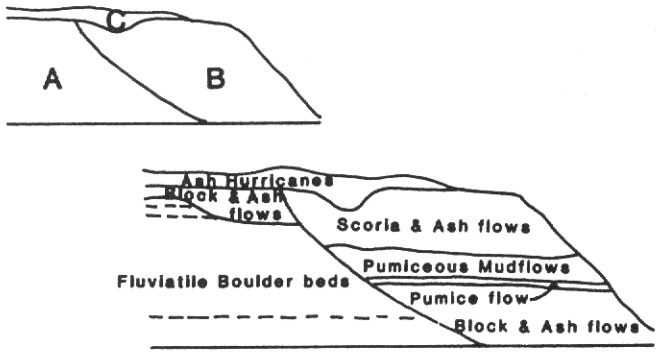

Figure 15. Sketch of the geology in the sea cliffs to the east of the town of Grande Riviere, Martinique.Dashed lines in fluviatile boulder beds represent crude stratification; the small inset shows the stratigraphic divisions. (After Smith and Roobol, in press).

Thus the alternation in eruptive style between Pelean and Plinian, so characteristic of the younger deposits of Mt. Pelée, can also be seen in the fluviatile reworked core of the volcano (Roobol and Smith, 1976, Smith and Roobol in press).

Mudflows also occur within the stratigraphic sequences. Some of these may represent lahars produced directly by volcanic activity, for example, the lahar of May 7th, 1902 that destroyed the Le Guerin sugar factory on Martinigue (LaCroix, 1904), others are purely secondary in origin. Mudflow deposits can often be confused with block and ash flow deposits as both have similar lithologies. For the Lesser Antilles two criteria have proved useful to distinguish between them. These are the presence, of gas escape structures and carbonized wood in the pyroclastic deposits. The former are not found in mudflows, and, although mudflows can contain wood, it is not usually carbonized (Smith and Roobol, in press).

SUBMARINE DEPOSITS

The Lesser Antilles represent a chain of relatively small volcanic islands so that much of the material erupted from the subaerial volcanoes is deposited on the surrounding sea floor. It has been estimated that for large explosive eruptions only about 5% of the magma erupted is deposited on land (Cary and Sigurdson 1980). Thus, in order to described the volcanic products from Lesser Antillean volcanoes, one must take into account the submarine deposits . The main types of subaqueous deposits described from subaerial eruptions from the Lesser Antillean volcanoes are: fall deposits, subaqueous volcaniclastic flow deposits and ash turbidities (Sigurdsson et al, 1980). These authors showed that most of the fall deposits occur to the east of the islands as a consequence of the effects of the upperTropospheric winds. In contrast, volcaniclastic flow deposits and ash turbidites are most abundant in the Grenada basin to the west. Stratigraphic evidence suggests that volcanic activity in the Lesser Antilles has, for the last 100,000 years, been predominantly subaerial in nature, and subaqueous volcaniclastic flow deposits have been produced by two main mechanisms. First, the entry of subaerial pyroclastic flows into the sea, for example, Mt.Pelée, 1902 (LaCroix,1904), and second the slumping of littoral or submarine accumulations of pyroclastic deposits into deeper water, for example, St. Vincent, 1902 (Anderson and Flett, 1902). Dilution of these subaqueous volcaniclastic flows by mixing with sea water eventually generate ash turbidities. The abundant ash turbidities described from the Grenada Basin (Sigurdsson et al, 1980) indicate that this is a common occurrence. A third mechanism for the generation of subaqueous volcaniclastic flow deposits is the sector collapse of the flanks of volcanic edifices. Such collapse would give rise to subaqueous debris fans and associated slump and debris flow deposits. Such a process has been well described for Piton de la Fournaise volcano on Reunion island (Duffield et al., 1982; Rousset et al., 1987) and has been proposed as the mechanism to explain the arcuate depressions on the western flanks of Soufriere volcano, St. Vincent, the Soufriere area of St. Lucia and areas in southern Dominica (Roobol et al, 1983).

VOLCANICLASTIC FACIES

Based on the above discussion it is evident that different volcaniclastic facies can be described for the volcanoes of the Lesser Antilles. The major facies division is between the subaerial deposits and the more voluminous submarine deposits. The subaerial facies, within approximately 10km of the crater, would be composed of high level intrusions/extrusions, lava flows, high-aspect ratio pyroclastic flows showing an irregular distribution (i.e confined to valleys) between which would be finer grained deposits derived from surges, low-aspect ratio pyroclastic flows and coarse- to medium- grained fall deposits. Beyond this limit would be found fine- grained fall deposits and deposits from the more extensive low-aspect ratio pyroclastic flows. The subaerial deposits would pass, at the shore line, into subaqueous debris flow and volcaniclastic flow deposits. Such deposits would be concentrated off the mouths of the valleys down which the subaerial pyroclastic flows travelled. For the Lesser Antilles, with their relatively steep western margin, extensive deep water subaqueous volcaniclastic flows are concentrated on the west. On the eastern side of the islands with their broad insular shelves, most subaqueous volcaniclastic flow deposits accumulate relatively close to shore, so that the dominant volcanic component offshore are fall deposits.

Further from shore the subaqueous volcaniclastic flow deposits would became finer grained and less common, only being represented by the deposits from the larger eruptions. These flow deposits would, through eventual intermixing with water pass into ash turbites. Interbedded with all these subaqueous volcaniclastic deposits would be marine pelagic and hemipelagic sediments and turbidites produced by non-volcanic mechanisms. (Figs. 16A and 16B).

ACKNOWLEDGEMENTS

Research was supported by grants from the National Science Foundation (EAR 73-00194, EAR 77-17064, RII 85-13533) the University of Puerto Rico (Mayaguez), and the American Philosophical Society (Johnson Fund #958, Hays Fund #106). Thanks to J.H. Schellekens and D. Larue for helpful discussions and to I. Díaz for typing the manuscript and G. Otero for drafting some of the figures.

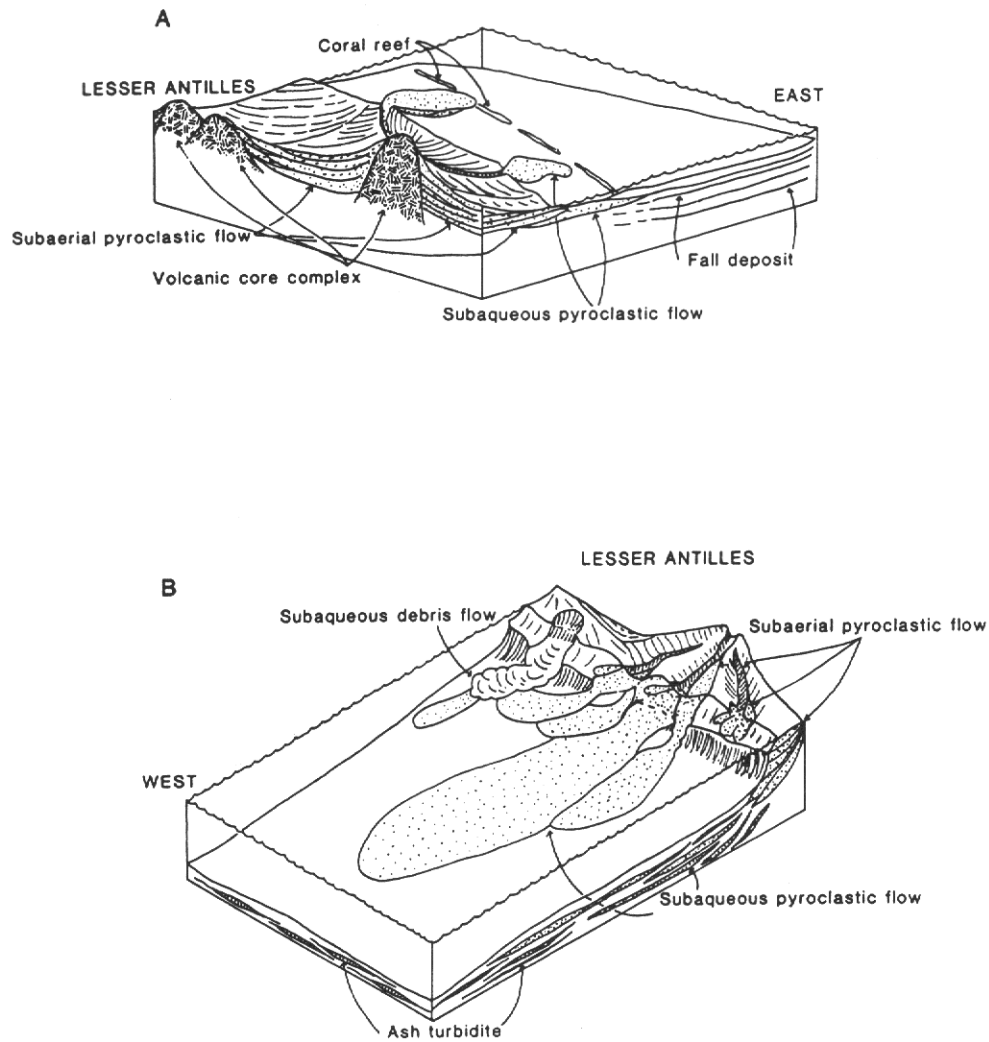

Figure 16. Schematic block diagrams showing potential distribution of volcaniclastic deposits (subaerial and submarine) in the Lesser Antilles. A - looking towards the east; B - looking towards the west.

TABLE 2. SUMMARY OF ERUPTIVE ACTIVITY FOR THE ACTIVE CENTERS OF THE LESSER ANTILLES

	EXPLOSIVE						EXTRUSIVE		
	Pyroclastic flows			Falls					
Island/ Volcano	Block & Ash	Scoria & Ash	Pumice & Ash	Pumice & Ash	Scoria & Ash	Dense/ Andesite	Domes	Lava-flows	Types of Center
Saba	A	S	S	S	S	S	A	M	II
Quill (St. Eustatius)	A	A	M	M	S	M	S		I
Mt. Misery (St. Kitts)		A	S	A	M	M	M	M	IV
Nevis Peak (Nevis)	A					S	A	A	II/IV
Soufriere Hills (Montserrate)	A			S	S		A		II
S. Soufriere Hills (Montserrate)				A	A		M	A	V
Soufriere (Guadeloupe)	M	M	M			A	A	M	IV
Monts Caraibes (Guadeloupe)					A			A	V
Dominica (latest volcanics)	M		A	A			M		III
Mt. Pelée (Martinique)	A	M	A	A	M	S	A	S	I
St. Lucia (lastest volcanics)	A		A	A			A		III
Soufriere (St. Vincent)	M	A			A		S	A	IV

A - abundant

M - moderate

S - scarce

FALLS

Deposits	Type
Pumice & Ash	Plinian/subplinian
Scoria & Ash	St. Vincent
Dense andesite & ash	Pelean/Phreatic

REFERENCES

Anderson, T., and Flett, J.S., 1903, Report on the Eruptions of the Soufriere in St. Vincent in 1902 and on a visit to the Montagne Pelée in Martinique, Part I: Phil. Trans. Roy. Soc. London , Ser. A, v. 200, p. 353-553.

Baker, P.E., 1969, The geological history of Mt. Misery volcano, St. Kitts, West Indies: Over. Geol. Min. Res., v.10, p. 207-238.

Baker, P.E., 1985, Volcanic Hazards on St. Kitts and Montserrat, West Indies: Geol. Soc. Lon. Jour., v. 142, p. 279-295.

Bouysse, P. Andreieff, P. and Westercamp, D., 1980, Evolution of the Lesser Antilles island arc, new data from the submarine geology: Trans. IXth Carib. Geol. Conf., Santo Domingo, p. 75-88.

Carey, S.N., and Sigurdsson, H., 1980, The Roseau ash: deep sea tephra deposits from a major eruption on Dominica, Lesser Antilles arc: Jour. Volcanol. Geotherm. Res. , v. 7, p. 67-86.

Duffield, W.A., Stieltjes, L., and Varet, J., 1982, Huge landslide blocks in the growth of Piton de la Fournaise, la Reunion and Kilauea volcano, Hawaii: Jour. Volcanol. Geotherm. Res., v. 12, p. 147-160.

LaCroix, A., 1904, La Montagne Pelée et ses eruptions: Paris, Masson et cie, 662 p.

Rea, W.J., 1974, The volcanic geology and petrology of Montserrat, West Indies: Geol. Soc. London Jour. , v. 130, p. 341-366.

Robson, G.R. and Tomblin, J.F., 1966, Catalogue of the Active Volcanoes of the World, including Solfatara Fields, Part XX: West Indies: Inter. Assoc. Volcanol., Rome, 56 p.

Roobol, M.J.,and Smith, A.L., 1975, A comparison of the recent eruptions of Mt. Pelée, Martinique and Soufriere, St. Vincent: Bull. Volcanol. , v. 39, p. 1-27.

Roobol, M.J., and Smith, A.L., 1976, Mt. Pelée, Martinique: a pattern of alternating eruptive styles: Geology, v. 4, p. 501-524.

Roobol, M.J., and Smith, A.L., 1980, Pumice eruptions of the Lesser Antilles: Bull. Volcanol. , v. 43, p. 277-286.

Roobol, M.J. , and Smith, A.L.,1989, Volcanic and Associated Hazards in the Lesser Antilles: Proc. Volcanol. , v. 1, p. 57-85.

Roobol, M.J., Smith, A.L., and Wright, J.V., 1981, Revisions in the pyroclastic stratigraphy of Mt. Misery volcano, St. Kitts, Lesser Antilles, 14C ages and recognition of pyroclastic flow deposits: Geol. Soc. London Jour. , v. 138, p. 713-718.

Roobol, M.J., Wright, J.V., and Smith, A.L., 1983, Calderas or gravity-slide structures in the Lesser Antilles arc?: Jour. Volcanol. Geotherm. Res. v. 19, p. 121-134.

Roobol, M.J., Smith, A.L. , and Wright, J.V., 1987, Lithic Breccias in Pyroclastic Flow Deposits on St. Kitts, West Indies: Bull. Volcanol., v. 49, p. 694-707.

Roobol, M. J., Smith, A.L., and Wright, J.V., 1985, Dispersal and Characteristics of Pyroclastic Fall Deposits from Mt. Misery Volcano, West Indies: Geol. Rundsch., v. 74, p. 321-335.

Rousset, D., Bonneville, A., and Lenat, J-F., 1987, Detailed gravity of the offshore structure of Piton de la Fournaise volcano, Reunion Island: Bull. Volcanol., v. 49, p. 713-722.

Sigurdsson, H.,1981, Geologic observations in the Crater of Soufriere volcano, St. Vincent: Univ. West Indies, Seismic Res. Unit Spec. Pub. No. 1981/1, 25 p.

Sigurdsson, H., Sparks, R.S.J., Carey, S.N., and Huang, T.C., 1980, Volcanogenic sedimentation in the Lesser Antilles Arc: J. Geol., v. 88, p. 523-540,

Smith, A.L., and Roobol, M.J., in press, Mt. Pelée, Martinique - A Study of an Active Island Arc Volcano: Mem. Geol. Soc. Am., 175 .

Walker, G.P.L., 1973, Lengths of Lava flows: Phil. Trans. Roy. Soc. London, v. 274, p. 107-118.

Walker, G.P.L., 1983, Ignimbrite Types and Ignimbrite Problems: Jour. Volcanol. Geotherm. Res. v. 17, p. 65-88.

Westercamp, D., 1979, Diversité, controle structural et origines du volcanism recent dans l'arc insulaire des Petites Antilles: Bull. B.R.G.M., sect. IV, No. 3/4, p. 211-226.

Westercamp, D., and Traineau, H., 1983, The past 5,000 years of volcanic activity at Mt. Pelee, Martinique (F.W.I.): implications for assessment of volcanic hazards: Journ. Volcanol. Geotherm. Res., v. 17, p. 159-185.

Westerman, J.H. and Keil, H., 1961, The geology of Saba and St. Eustatius: Uitg. Natuurwet. Studietering Suriname Ned. Antilles, v. 24, 175 p.

REEFS OF ANTIGUA, WEST INDIES: CHANGES OVER 40 YEARS

Malcolm P. Weiss
Department of Geology, Northern Illinois University
DeKalb, Illinois 60115

ABSTRACT

Changes in the reefs and shallow sediments off Antigua are tallied by comparison of aerial photographs from 1941 and 1954/58, and by summary of an earlier report (Weiss and Multer, 1988) on the period 1954/58 to 1981. Depletion of coralgal communities is the most serious change observed (241 hectares in the first period and 43 in the second), mostly on fringing reefs in developed areas. Patch reefs on the windward side lost coral from the reef tops during 1941-1954/58, apparently through a natural cycle of depression, for some subsequent recovery has occurred. Large areas of both grassy and mixed coral-and-grass bottom have been altered severely by dumping of dredge spoil and by drift of suspended sediment disturbed by dredging. On the leeward side of Antigua some areas of sand bottom have lost grass cover and others have gained grass cover, apparently as results of changes in the sediment load brought to the shallow shelf. Important areas of "scrolled sand" on that leeward shelf seem to alternate between arcuate ridges of bare sand on grassy bottom and bottoms in various stages of sediment removal, during which the loose sand is torn away, leaving linear blowouts in the grassy sea floor. Development since WW II has clearly altered Antigua's marine shallows, including loss of clarity of the waters of some bays. This study extends that of Weiss & Multer (1988), so that a 40-year record of the nearshore bottom is now available (1941-1981).

INTRODUCTION

Antigua (Fig. 1) is a large island (284 km^2; 108 mi^2) in the Limestone Caribbees, the outer chain of islands in the northern Lesser Antilles. It is one of the two islands belonging to the state of Antigua & Barbuda that lie on the Barbuda Bank, which is near the northern end of the Lesser Antilles chain. Like other islands in the Limestone Caribbees, it consists partly of Early Tertiary limestone laid on a foundation of volcanics of similar age. Antigua is favored by large areas of fringing, bank-barrier and patch reefs, and fine beaches, all important features for the tourist industry, which is perhaps the most important part of the Antiguan economy. The condition of these marine features should be of utmost concern to the government and commercial interests there.

A submarine geological map of the reefs and modern sediments of Antigua (Weiss and Multer, 1988) shows the areas and classifications of reefs and various types of sediments as of 1981, the latest date for which aerial photographs of the whole island were available. The planimetry of areas mapped was controlled on a stereoplotter with aerial photographs made in 1954 and 1958; changes between then (1954/58) and 1981 were fitted to the plotted sheet by direct comparison of the younger and older photographs. An abstract describing the map appears elsewhere in this volume (Weiss & Multer, 1990), and a summary of the changes in bottom conditions 1954/58 to 1981 is included in this report.

During the years of field checking and cartographic preparation of the reefs map it was learned that aerial photographs of Antigua had been taken much earlier than 1954--in 1941, in fact. They were taken by the US Army Air Force in August of 1941 (British Ordnance Survey files say March 8th, but the photographs all read Aug., 1941), in preparation for the establishment of a US Army air base on Antigua, as part of the "destroyers-for-bases" deal worked out by President Roosevelt and Prime Minister Churchill in September of 1941. The 1941 photographs were given to the Ordnance Survey of Great Britain by the US Defense Department (probably in 1947, when the 1942 photos were transferred), and all record of their existence was deleted from files in Washington. As several newer series of photographs were made, by the United States in 1942, 1954 and 1958, by the British government in 1968 and by the Royal Air Force in 1975, the availability of the 1941 photos was obscured. Having learned about them during a visit to the Ordnance Survey in 1985, it took until 1989 to obtain copies, for the US-British agreement provided that US permission be required before the photographs could be copied--and, as Washington denied their existence, they would not give permission!

This paper undertakes to compare the status of reefs and other bottom deposits as they were in 1941 with those of 1954/58, though the 1958 photographs were the principal control for the published map (Weiss & Multer, 1988). The 1954 series (1:10,000) covered no more than 10 percent of the island of Antigua, and none of the sea to east and west, although it does display well the large bank-barrier reefs off the north coast. Differences between conditions of the late 1950's and 1981 are expressed on the map (Weiss & Multer, 1988), and summarized herein for continuity (Figs. 2-8 and Table 3). This report, then, reaches back in time to compare the nearly virgin marine environment of Antigua (1941) with its status in the late 1950's, a time when much of the postwar development that has beset this tropical paradise was already in place. With the map (Weiss & Multer, 1988) and this paper, it is possible to reconstruct the many changes--mostly results of development--that have occurred between the island's pristine state and its current state (little change in the type and magnitude of development or of population pressure has occurred on the island since 1981). Descriptions of the major reef types in their present state, and examples of the principal biota, are given in Multer et al. (1986).

Larue, D.K., and Draper, G. (eds.),
Transactions of the 12th Caribbean Geological Conference, St. Croix, U.S.V.I., Miami Geological Society, P.O. Box 431552, South Miami, FL 33243, U.S.A

PURPOSE

This paper has the obvious and implicit purpose of extending the record of changes in the reefs and associated sediments over a period nearly twice as long as that expressed in the reefs map (Weiss & Multer, 1988). As a contribution to science, it is a small step in the accumulation of dynamic data, which should be taken account of by commerce and government while planning further changes to the natural state of Antigua's marginal marine environment. Van Duyl (1985) expresses these and other sound purposes for areal studies of reefs most effectively and gracefully: reefs are protective ramparts and sources of food, income from tourists, building materials, and reef biota and products for trade. She also points out that baseline data such as these are required if we ever are to learn the degree of coastal urbanization, development and exploitation that reefs and other communities can withstand.

This paper and the earlier map (Weiss & Multer, 1988) with which it draws comparisons treat the reefs at a scale 10 times smaller than that of Van Duyl's map (Van Duyl, 1985). Her work, furthermore, makes much finer distinctions of ecologic and morphologic types than was possible for this study.

METHOD

The qualities and properties of the 1941 photographs are important to their comparison with later, and in some ways technically better photographs. The 1941 prints are 7 x 9 inches, with the short dimension in the direction of the flight path; those used are matte prints. The scale is larger than most series flown in the years since: 1:10,000, with a high degree of consistency; a spot check shows variations of only 1 percent smaller to 3 percent larger scale. The condition of the sea was rather rough, with a conspicuous chop over the whole area (August, 1941; no day given). The area of the sea floor visible in these prints is much less than on younger photos, but this is due only partly to the rough sea. The film used was Eastman Regular Safety, and its ability to display the bottom is much less than that of more modern films: to only 3-4 meters of depth in these prints, compared to 20 meters depth in many of the more modern series. Clouds were scattered in August of 1941, but they obscure very little area because the plane flew so slowly that successive frames show the cloud moved off, in many cases!

Defects in the film are numerous, in marked contrast to later series. Most are operational: finger- and tape-marks made on the negatives, and numerous blobs and smudges that seem to result from careless handling in the darkroom. Even so, these do not much impair the prints for study.

The main problem for this study is the degree of coverage of the 1941 photographs. The flights were planned to assist the development of the military base, and the waters around Antigua were of no concern. Thus the photographs do not show much offshore, except in the northeastern quadrant where all of North Sound was covered in order to include the many islands there. The 1941 photographs cover only about 20 percent of the marine area mapped by Weiss & Multer (1988). Although the 20 percent includes all the bays around the island, the limited penetration of the film then used renders the deeper and grass-held (less reflective) parts of those bays invisible. The 1941 photographs do show the shallow bottoms close to the shore, however, and thus the fringing reefs. The bank barriers are also shallow enough to be interpreted readily, but only those on the east side are included in the flight paths. Patch reefs shallow enough to refract waves (less than 2 m) are clearly shown; some deeper ones lurk as dark hulks, particularly in the northeastern quadrant, and some are so deep as to be invisible on the 1941 photographs. In summary, perhaps half of the patch reefs in the bays on the northeast and east coasts can be studied from those photographs. Even so, such old photographs are the only pre-development record of conditions on and around Antigua that we have, and are thus an important part of the series of aerial investigations from which an assessment of the shallow marine realm can be discerned. A detailed investigation of any area should include study of the 1942 photographs as well.

USE OF THE FIGURES AND TABLES

A full-blown map of Antigua, with numerous geographic points identified, is beyond the scope of this volume. But the sketch maps herewith (Figs. 2-8) and the graphic data summarized in their captions express the differences between the reefs of 1941 in their natural state and those of 1954/58 (Weiss & Multer, 1988). The accompanying maps may be used simply as a record of the most important 17 years of change, or they may be studied in comparison with any of several maps of Antigua: the map of modern reefs and sediments (Weiss & Multer, 1988, 1:40,000), the standard topographic map of the island, which shows the location of most of the reefy masses by conventional symbols (Ordnance Survey of Great Britain, 1980, 1:50,000), or the US Defense Mapping Agency Hydrographic Office chart No. 25BHA25570 (1:50,000) of recent date.

Where figures overlap, the data concerning areas that have undergone change appear on the map figure of lower number, and are included with that figure caption.

TYPES OF BOTTOM CHANGES AND SYMBOLS

Coastline

The perimeters of the island of Antigua and its satellite islands, shown in Figures 2-8, are the water's edge; coastal mangrove swamps, mapped by Weiss & Multer (1988), are not shown here. The nature of the coast in Figures 2-8 is expressed by different kinds of line: solid line = rocky or earthen coast, dashed line = mangrove fringe or edge of mangrove swamp, and dotted line = sand beach.

Water Clarity

Comparison of the photographs of the principal harbors, as shown in both the 1941 and younger photographs, shows that the water in them was much clearer in 1941 than it is now, after much development. These are St. Johns Harbour, on the northwest coast (Fig. 8), and Falmouth Bay and English Harbour on the south coast (Fig. 5). St. Johns is the capital city and is surrounded by the heaviest population concentration. It was the first harbor to be improved and deepened for large sea-going vessels, and still the only one into which large cruise ships can enter. Falmouth Bay and English Harbour are among the most important recreational sailing ports in the Caribbean, and are heavily used year-round. Given the serpentine shape and narrow entrance of English Harbour (Fig. 5)

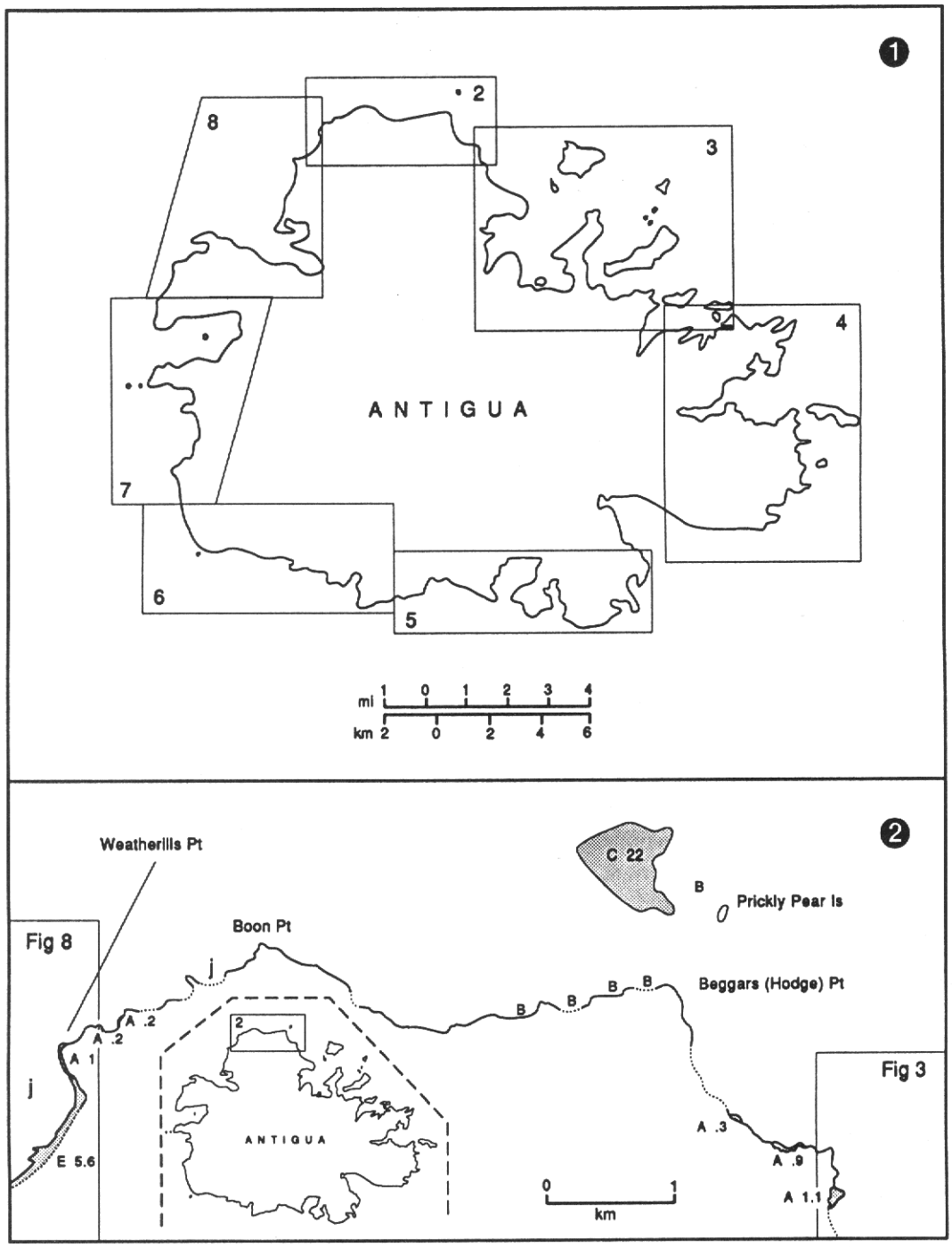

Figure 1 - Outline map of Antigua, showing outlines of areas covered by Figures 2-8, in each of which changes of bottom material are keyed to Tables 1, 2 and 3 by letters and symbols.

Figure 2 - The north coast of Antigua, with inset of the whole island. Rocky coast is shown by a solid line, mangrove fringe by dashed line and sand beach by dotted line. Here and on following figures changes from 1941 to 1954/58 are represented by capital letters and Roman numerals; the areas affected, in hectares, are given by the Arabic numbers. The lower-case letters and (+) symbols locate changes between 1954/58 and 1981, although no areas are cited.

Affected areas in hectares (numbers) sum to: (A) 3.7, (C) 22, (E) 5.6; several unmeasured (B) areas also occur.

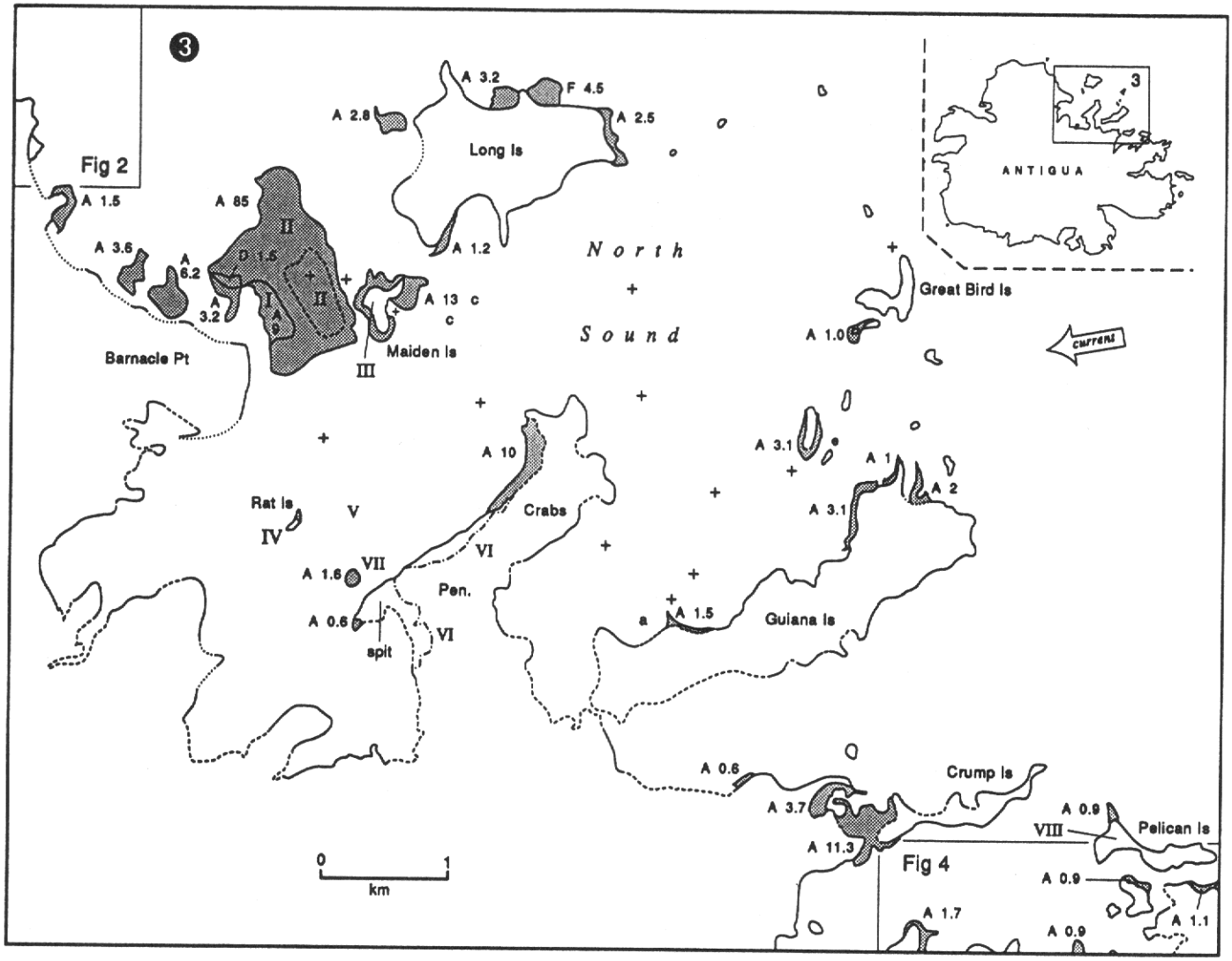

Figure 3 - The northeastern quadrant of Antigua, including all of North Sound.

I - This area was a "deeper reef" in the usage of Weiss & Multer (1988), a terrace below the fringing reef.

II - This large area was sand mottled with numerous coral clusters (5c of Weiss & Multer, 1988) in 1941.

The part enclosed within dashed line was a coral-dotted bank with deeper channels to east and west of it. Seawater piled into North Sound from the east by NE Tradewinds and the North Equatorial Current escaped to the northwest through these channels and the one between Maiden and Long Islands.

The area has since deteriorated to muddy sand by the dredging of ship channels close to Maiden Island and farther south in North Sound.

III- For the record, Maiden Island is shown in its original shape, before being altered by heaps of dredge spoil. Further, the former fringing reef there is not so much deteriorated as it is buried by dredge spoil (see Weiss and Multer (1988)).

IV - Rat Island has been enlarged by 150 percent since 1941. The older, bedrock part is the small, northern oval; a large heap of skeletal sand and gravel has been built southwestward from the bedrock nucleus.

V - The former Mouse Island was barely awash in 1941, but now wholly submerged. It may have been a sand bank, as suggested by Weiss & Multer (1988), but its progressive diminution makes it more likely that it was originally a low-lying mass of weak Antigua Limestone.

VI - The dot-dash line shows the original bedrock margin of Crabs Peninsula. It has been straightened by development--both fill and dredging--on the northwest coast. A narrow sand spit at the southwest corner has not changed much in length since 1941, when it had a mangrove swamp behind it. But now the spit is 2-3 times wider and the swamp behind it has been loaded with sand to the degree that the mangroves have given way to terrestrial scrub vegetation, and the shore behind the spit has the modern configuration shown on maps (cf note VII).

VII- This was a coral-covered patch reef in 1941. The eminence on the sea floor shows in later photographs, but is indistinguishable from neighboring grass-held sand bottom. The coral community has been mantled by debris from the development of the northwest shore of Crabs Peninsula (cf note VI).

VIII-In 1941 Pelican Island had a narrow rim of coral fringing the west and south shores. By 1958 it had been mantled by skeletal sand, as it remains today.

Affected areas in hectares sum to: (A) 176.2, (D) 1.5, and (F) 4.5.

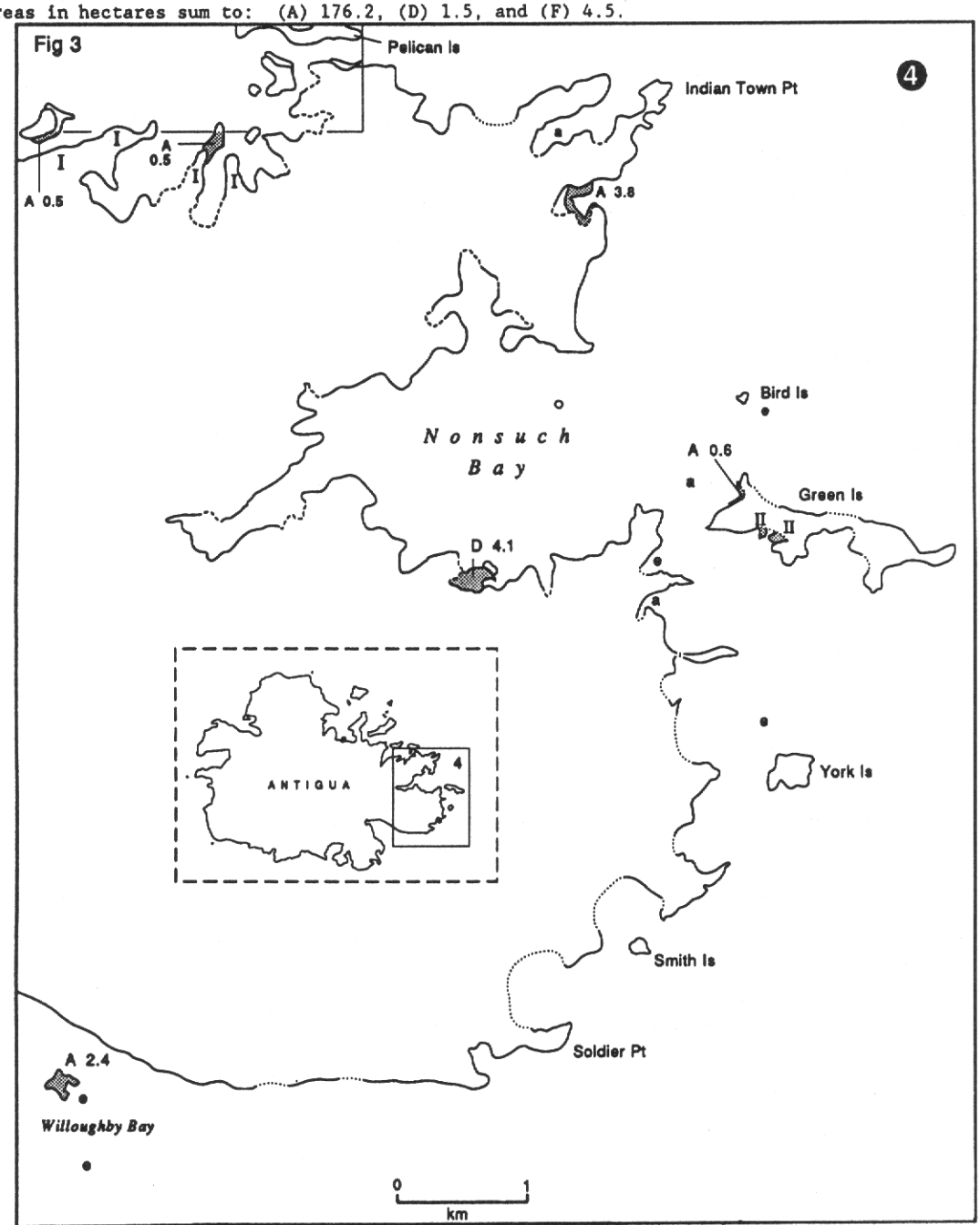

Figure 4 - the eastern sector of Antigua, from Pelican Island at the north to Willoughby Bay on the south. The largest bank barrier of the windward coast lies off Nonsuch Bay, between Green Island and Indian Town Point.

I - A very narrow mangrove rim occurred in 1941 at the toe of the steep rocky banks in this area, but was gone by the late 50's. Development has not occurred here: can a slight sea-level rise have destroyed the narrow, linear ecologic niche on these steep slopes?

II - Two small patches were grass-held sand in 1941 and are mapped, in error, as fringing reef by Weiss & Multer (1988). Grass-held sand remains on these two places, which were not affected by the post-1958 damage, mapped by Weiss & Multer (1988).

Affected areas in hectares sum to: (A) 9.2 and (D) 4.1.

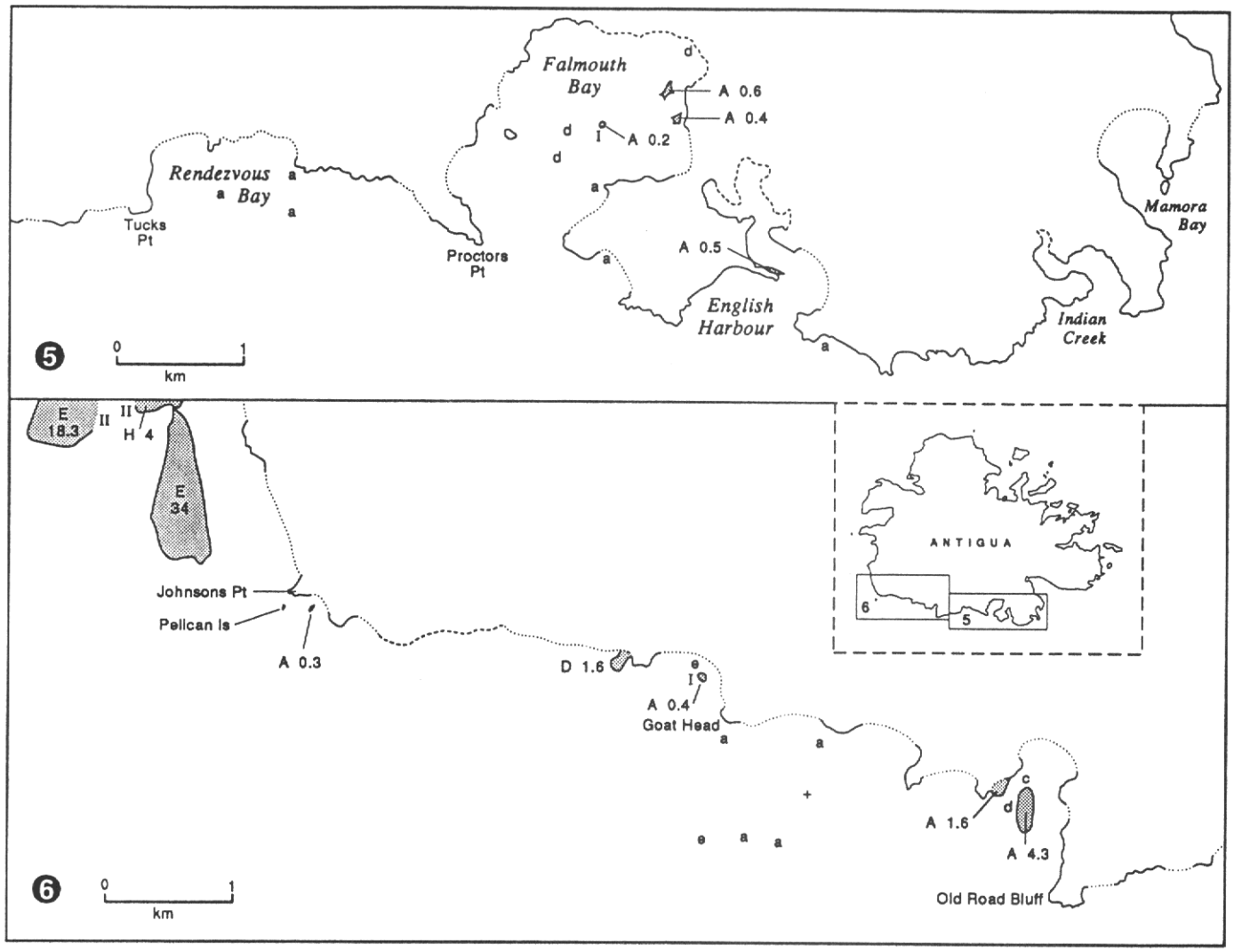

Figure 5 - The south-central coast of Antigua includes the two busiest sites of yachting activities: Falmouth Bay and English Harbour.

I - This small area was a pinnacle or patch reef, rising from the Millepora-Porites bank, now degraded to a bump of the latter community.

Affected areas in hectares sum to: (A) 1.7.

Figure 6 - The southwestern quadrant of Antigua. The very large bank-barrier reefs that lie west of Old Road Bluff and extend beyond Johnsons Point are not included in the 1941 photographs. Fringing reefs are narrow along the south coast. The largely sand-covered shelf on the west side of the island begins in the current shadow of Antigua, northwest of Johnsons Point.

I - A small patch reef has been covered by sediment.

II - Cloud cover obscures the sea floor. Values of areas in hectares apply only to those visible.

Affected areas in hectares sum to: (A) 6.6, (D) 1.6, (E) 52.3), and (H) 3.95.

it does not flush as readily with tidal change as either of the other two. Now these waters, particularly St. Johns and English Harbours, are heavily loaded with suspended sediment, both mineral and organic particles. The bottom muds are foul, sulfurous and black (Kamm, 1981). The 1941 photographs show about 2 m of clear water over nearshore shallows in English Harbour and the outer half of St. Johns Harbour; little can be seen there now, for transparency is a fraction of a meter.

A general decrease of clarity of water and increase of suspended sediment in the shallow waters of Antigua may be indicated by the large plumes of suspended sediment seen in the more recent aerial photographs in the lee of the headlands and of the whole island. Even though the conditions of the sea were rougher during the 1941 photography than during 1954, 1958, or 1981, few such plumes are to be seen in the older photographs, and they are small and closely related spatially to beaches on the west coast. Such plumes and sheets of turbid water now sometimes cover

many square kilometers in the northwest and southwest quadrants of the island, and over wide areas off the west coast, all in the lee of the North Equatorial Current that bathes the Lesser Antilles. Of course it is possible that such large plumes are episodic and storm-generated, and that only certain ones are caught by the camera.

It is certain that the development of Antigua's bays and shores has contributed to the fouling of some of the former and the loss of sediment to the narrow shelf and open sea to the west of the island. Some of the disturbance and loss of sediment may of course be due to sea-level rise, but I believe that dredging of ship channels (e.g., Fig. 3, II) and local alterations of the beaches have played an important part. Regrettably, no way presents itself to quantify the changes. Kamm's study (1981) will, however, serve as a benchmark for future studies of the shallow marine and coastal sediments.

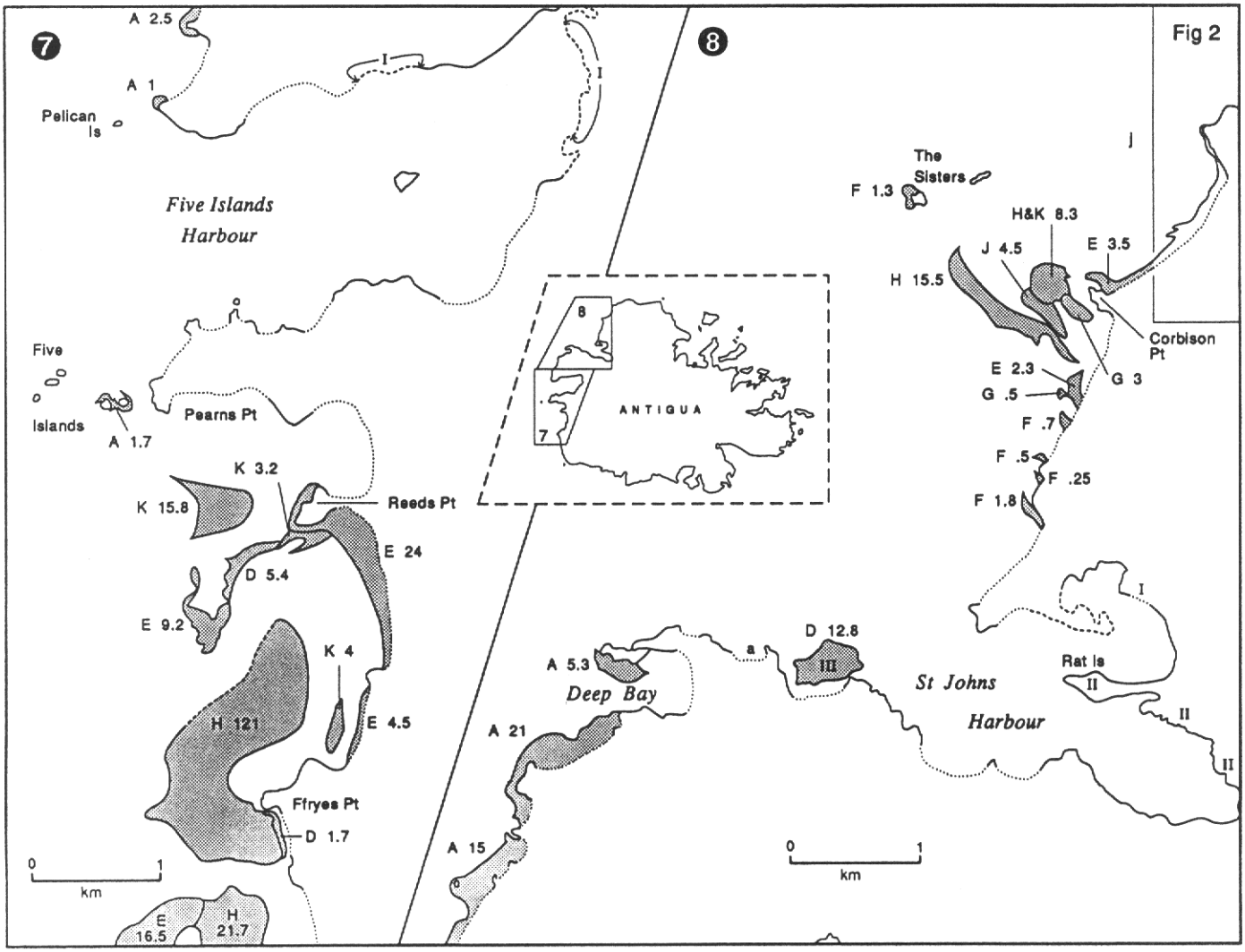

Figure 7 - The west-central coast of Antigua includes the large Five Islands Harbour with a shallow bottom mostly of mud. The bottom on the shallow shelf off the west side of Antigua has little coral and large areas of sand and grass-held sand.

I - Mangrove fringe has taken over sand beach in the two zones, totalling 1700 meters.

Affected areas in hectares sum to: (A) 5.2, (D) 7.1, (E) 54.2, (H) 142.7, and (K) 23.

Figure 8 - The northwestern quadrant of the island of Antigua, centered on St. Johns Harbour. The city of St. Johns, the capital and largest population center, surrounds the southeast end of the harbor.

I - A sandy beach has developed since 1941, perhaps by sea-level rise, or accumulation of dredge spoil?

II - Changes of the shore and commercial structures along the rim of St. Johns Harbour are not tallied, although the causeway to and docks on Rat Island are much wider now than before development set in.

The shallow waters at the margin of the outer harbor were clear in 1941; by 1958 the harbor bottom was everywhere obscured by suspended sediment, even in the shallowest parts.

III- A large area of sand with little vegetation was probably formed by dumping of dredge spoil there from the ship channel.

Affected areas in hectares sum to: (A) 41.3, (D) 12.8, (E) 5.8, (F) 4.55, (G) 3.5, (H) 15.5, (J) 4.5 and (H & K) 8.3.

Changes to Reefs and Bottom Sediments

1941 to 1954/58

The changes are described in terms expressing the difference from 1941 conditions to those of 1954/58. It is important to remember that much of the non-reef bottom, all of the deeper reefs (Weiss and Multer, 1988), perhaps half of the patch reefs, and the bank barriers off the north and south coasts are invisible, or not covered, by the 1941 photographs. The sorts of changes described in Table 1, and recorded in Figures 2-8 are minima of what may actually have occurred as Antigua was transformed from an agricultural, undeveloped island to a busy, modern, tourist mecca with large populations of visitors, ships and yachts, plus all the modern infrastructure and transport necessary to the new economy and way of life. The several types of changes (Table 1) are identified by letters, which appear on the maps and in their captions. The numbers associated with the letters (except B), on the maps (Figs. 2-8) and in Table 2 refer to the area(s) affected in hectares (1 ha = 10,000 m^2, 2.47 acre, or 107,099 ft^2.)

Table 1 - TYPES OF CHANGES OF BOTTOM SEDIMENT

Changes 1941 to 1954/58 are marked with capital letters in the table and on Figures 2-8.

A/a - Deterioration of vigorous coralgal community by loss of coral and increase of or burial by bare skeletal sand or grass-held sand

B - Seagrass flats on tops of reefs, behind the reef front, are less heavily vegetated

C/c - Mixed coral and sand, or sand mottled with small clumps and boilers, has lost much of the stabilizing vegetation and the boilers are reduced in size; also includes some burial by sand

D/d - Grass-held sand meadows have been buried by bare sand

E/e - Bare sand has grassed over; or the density of the grass has increased conspicuously

F - Former submarine outcrop now sand covered

G - Submarine outcrop now exposed by removal of former sand cover

H - Grass-held sand has become "scrolled" (see subsequent discussion)

J/j - "Scrolled-sand" bank overspread by bare sand

K - "Scrolled-sand" bank smoothed or buried and covered by sea grasses

Changes 1954/58 to 1981 (described by Weiss and Multer, 1988) are located on Figures 2-8 by lower-case letters corresponding to certain of the capitals above: a, c, d, e, j. Sites of increase of coral and grass from 1954/58 to 1981 are marked on Figures 2-8 by (+).

Table 2 - SUMMARY OF CHANGES, 1941-1954/58, IN HECTARES

CHANGES SYMBOL \ FIG.	2	3	4	5	6	7	8	SUM
A	3.7	176.2	9.2	1.7	6.6	5.2	41.3	244
B	(not measured)							
C	22							22
D		1.5	4.1		1.6	7.1	12.8	27.1
E	5.6				52.3	54.2	5.8	118
F		4.5					4.6	9.1
G							3.5	3.5
H					4	142.7	19.6	166.3
J							4.5	4.5
K						23	4.2	27.2

1954/58 to 1981

The map prepared by Weiss and Multer (1988), described elsewhere in this volume, covers an area much larger than the scope of the 1941 aerial photographs. Thus some of the changes of bottom sediments occurring from 1954/58 to 1981 cannot be represented on the figures accompanying this report.

Even so, in order to give a 40-year view of sedimentary environment dynamics, the locations of most of the 1954/58-1981 changes, as well as their natures, are illustrated in Figures 2-8 of this paper; they are symbolized together with the older changes already described by using lower-case letters corresponding to the capital letters in Table 1. Some changes seen in the later period are not recognized from the earlier, particularly the increase of coral on some windward patch reefs and the colonization of old dredge spoil by small coral clumps. These are represented by (+) symbols on the maps, especially in North Sound (Fig. 3).

Repetition here of the areas affected during the 1954/58-1981 interval from the published map (Weiss and Multer, 1988) would clutter Figures 2-8 and make them ineffective. However, the sites of those changes and their natures are indicated in the figures, and a summary of their magnitudes is given in Table 3.

Table 3 - SUMMARY OF CHANGES, 1954/58 - 1981, IN HECTARES

a - Loss or depletion of coral and gain of sand	31
c - Mixed, patchy coral and grass-held sand has lost vegetation and coral	11.5
d - Grassy "meadows" buried by or gone to sand	7.8
e - Bare sand grassed over or grass density increased	60.9
j - "Scrolled" sand spread smooth or covered by sand	3.9
+ - Increased area of coral (17.9 ha) or increase of coral density (11.9 ha)	29.8

Of these, the first three may be regarded as destructive, erosive, etc.; the fourth and sixth may be considered healing or constructive. The changes summarized here are described fully by Weiss and Multer (1988), as well as a few other instances not illustrated in Figures 2-8.

SPECIAL FEATURES

Upon comparison of the areas of the marine bottom shown in both the 1941 and 1954 and 1958 photographs, two aspects were distinguished that cannot be presented effectively in the maps. They require discussion, partly because their causes and stages of development are unknown, and partly because the magnitudes of the areas affected are uncertain and therefore not measurable.

Sand on Patch Reefs

Several score of patch reefs occur around Antigua (Weiss and Multer, 1988), particularly in the areas shown in Figures 3 and 4. As was explained earlier, fewer than half of these show well on the 1941 photographs, partly because of the insensitivity of the film used to the dim light reflected from depths of more than about three meters and partly because the patch reefs had less sand cover then and were less reflective.

Those patch reefs clearly visible in the 1941 photographs, including many in North Sound (Fig. 3) and in the large bays south of it (Figs. 3, 4), all have dark upper surfaces. They appear to have a rough, furry texture that shows clearly that they were capped by dense, vigorous colonies of living coral. No brightly reflecting light spots suggest the presence of skeletal sand. The patch reefs having this dark appearance are those that cause refraction of the waves, and probably were then less than 2 meters below sea level.

These same patch reefs had conspicuous patches of sand on their tops by 1958, and these persist today. On the smaller patch reefs the sand occurs in small patches among the clumps and heads of living coral; on the larger ones the living coral tends to be concentrated around the margin of the patch reef and the top can be mostly sand--microatolls, in effect. Direct inspection of such microatolls does not give one the impression of deterioration; the coral is healthy, and patch reefs with sandy patches on top are in no way abnormal. But there was a significant change in the ratio of coral to sand on many patch reefs in the areas of Figures 3 and 4, and to a lesser extent elsewhere around Antigua, between 1941 and 1958.

It would be easy to speak of abuse or pollution, but difficult to prove. Further, these changes have occurred at sites which are washed by normal seawater, and are up-current from the sites of dredging and other major disturbances of the bottom that development has brought. Nearby sources of pollution are very scarce in the area affected: one hotel exists on Long Island (Fig. 3), but was not there in 1958 and, although the north shore of Crabs peninsula (Fig. 3) was altered before 1958, the industrial development, marina, and motel are all post-'58.

A more likely explanation for the decrease in the ratio of coral cover to skeletal sand on the tops of the patch reefs is some natural trend of coral depletion, of the sort that has now been observed on St. Croix, and elsewhere (Bythell et al., 1989; Hubbard, 1989). It is also possible that a hurricane tore up the patch reefs of the northeast quadrant of Antigua between 1941 and 1958, but the bank-barrier reefs off the east coast show no significant differences across the time period, and this explanation is not considered likely. Two "serious" hurricanes passed rapidly over Antigua in August of 1950 (D.V. Nicholson, personal communication, November, 1989).

"Scrolled sand"

Many areas of the sandy bottom in the lee of Antigua have a pattern and texture (Fig. 9) different from the bare sand and grass-held sand bottoms to the north, east and south of Antigua. The pattern is of wavy streaks of light-colored bottom (bare sand) that join and separate along their length, and crudely resemble festoons of drapery or bunting (Fig. 9). The light-colored streaks are conspicuous because the background is dark, grass-held sand. Small, linear patches of this "scrolled sand" occur close to shore at the northwest and southwest corners of the island, where the persistent currents refract onto the open shelf west of Antigua. Larger patches of the same sort of texture occur on the shelf, off the west coast, caused perhaps by the beat of refracted wave sets. Very small areas with similar patterns occur just within the openings of Falmouth and Mamora Bays (Fig. 5), where entering currents slow and drop sediment.

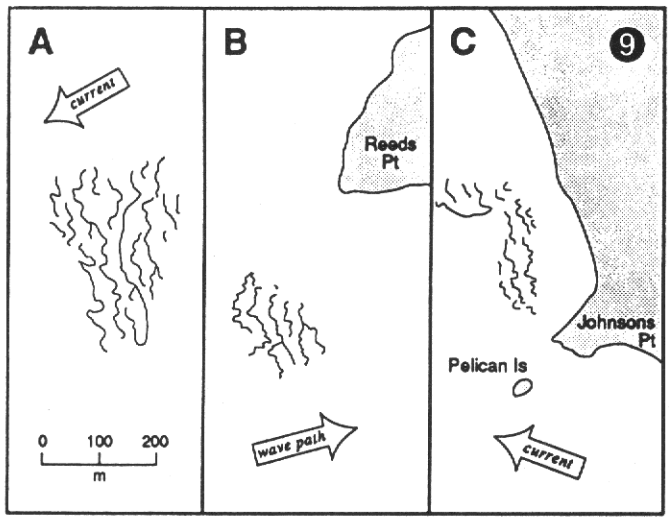

Figure 9 - "Scrolled sand" patterns. The lines show the bands of bare sand as they appear against the background of grass-held sand. Sketches are oriented with North at the top and all have the same scale; the coastline shows in B and C.

A) Patch 0.8 km northwest of Corbison Point (see Fig. 8). The bare-sand festoons seem to have been elevated above the grass in 1941, but are known to have been blowouts in 1983.

B) Off Reeds Point (see Fig. 7). Wave refraction in lee of Antigua brings waves directly to shore. Relative elevation of the bare and grassed sand in 1941 cannot be determined definitely.

C) Off Johnsons Point (see Fig. 6). Here the festoons of bare sand definitely were elevated above the grassed sand in 1941, and also stepped downward away from the shore. Spread of current threads and wave refraction turn energy toward shore.

During aerial reconnaissance for the submarine geologic map (Weiss & Multer, 1988), these "scrolled sands" seemed to be areas in which abundant sand moving across the sea floor had piled up into irregular "windrows," rather like broad parabolic dunes. Diving on those off the northwest coast, in the early 1980's, showed that the sand streaks were not elevated above the grass-held parts of the sea floor, but were depressed. These were examples of the linear blowouts of sand and, presumably, grass that were first described by Wanless (1981). These areas were mapped by Weiss & Multer (1988) as "sandy mud and sand with parallel blowouts," having maximum "wavelengths" of 10 to 30 meters.

The 1941 photographs (scale 1:10,000) show that some of the "scrolled sand" bottoms have the light bands standing above the grass-held surfaces (Fig. 9). This is seen off Corbison Point (Fig. 9A) and near Johnsons Point (Fig. 9C). At other areas (Fig. 9B) the relative elevation of the bare sand cannot be demonstrated from the old photographs.

That the areas of the bottom having this "scrolled" texture change over time is demonstrated by the fact that instances of former sand elevation have since been observed to be sand blowouts, in the area of Figure 8. Thus the texture of the bottom is not constant, although the pattern on the bottom may be nearly so. Further, large areas off the west coast of Antigua have changed pattern as well, from "scrolled" to mottled (i.e., grass in patches, rather than streaks) or from mottled to "scrolled." The changes, insofar as they can be observed, are expressed by the symbols H, J, and K in Table 1 and Figures 6, 7 and 8.

Although these sand banks are dynamic, the areas affected remain about the same; the smaller patches near the northwest and southwest corners of Antigua, and in the mouths of Falmouth and Mamora Bays, have not changed their size or shape from 1941 to 1981, the date of our last photographs. The distribution of grass on the sandy bottom can change, and the bare sand may stand now above or now below the grass-held sand surface. Each of these sites is in a current shadow--some broad, some narrow--where suspended sediment is dropped from the rapid currents streaming by the north and south coasts of Antigua (e.g., Figs. 9A, C). Others seem to be controlled by wave paths (Fig. 9B). Some sand is spread in sheets that become vegetated randomly (mottled), and some is dropped so abundantly that the mass accumulates as low dunes over a grass-held surface.

Changes from such dunelets to blowouts result from episodic storms or storm surges, which entrain the bare sand, held only by mucilaginous algal mat, and leave the grass-held sand relatively undisturbed. Changes from "scrolled" sand bottom (J or K of Fig. 7 or 8) must result from major changes in the amount of sand swept into the shelf west of Antigua; such might be episodic and natural or the result of changes of the nearshore environments under development. As such development has affected the north shore much more than the south, and there is no corresponding skewness of the sediment changes, the cause is probably natural. If the process is natural, it is easier to explain the changes of bottom texture and pattern occurring within the same perimeters over 40 years. Probably the work is done by major storms or swells, and not just the routine currents and refracted waves.

Although no attempts have been made to study the sedimentary structures within any of these sandy bottoms, one wonders what they might be.

CONCLUSIONS

The map of reefs and modern sediments prepared by Weiss & Multer (1988) provides a benchmark of bottom materials around Antigua in 1981, one which can be useful in planning for further development and utilization of its marine resources. It also records changes of small areas over time (1954/58 to 1981). This paper extends the series of changes of bottom materials, and the areas affected, from 1954/58 back

to 1941, the date of the earliest aerial photographs taken of Antigua and its marginal shallows, and a time, also, when those shallows were virtually in their native state. Colonialism had changed the island significantly, but without affecting the sea, beyond the fouling of St. Johns and English Harbours. This paper, together with the map of Weiss & Multer (1988) records the changes of shallow marine materials from pre-development times to the current condition, a state of development that has reached very nearly its peak. The specific conclusions listed below refer only to changes from 1941 to 1954/58.

1. Fringing reefs, particularly on the north and northeast coasts, have been diminished in numbers, area, and the abundance of coral (particularly on the reef flats behind the crest). The geographical skewness points to marine and coastal development: dredging, construction of shore facilities--ramps and docks, pollution from sewage released directly into the sea, and minor filling on the shore associated with residential and commercial construction on the beaches and sea cliffs.

2. Associated with the loss of coral on some fringing reefs is a loss of sea grasses on the reef flats, particularly along the north coast (Fig. 2, B), which is rimmed with private homes and hotels.

3. The two bank-barrier reefs photographed in 1941, that passing southeast through Great Bird Island along the whole east side of Figure 3 and that extending from Indian Town Point to Green Island (Fig. 4), show no appreciable change over the interval.

4. The patch reefs recorded in 1941, perhaps half of the more than 100 extant (mostly in the area of Figures 3 and 4), show a marked loss of coral from the tops of the patches, without apparently, any loss of vigor of the marginal coral community, and certainly no loss of area or height. It is suggested that this is a consequence of the natural cycle of reef communities wherein the ratio of living to dead coral changes.

5. Large areas of bare skeletal sand have been grassed over, or the grass has become more dense. This is regarded as a progressive, stabilizing trend, but occurred almost entirely on the shelf west of Antigua.

6. Some areas in current shadows appear to accumulate large amounts of loose sand, which is heaped, or scoured, or grassed over, repeatedly, within about the same areas of the sea floor. These areas are most important on the shelf west of Antigua, and are thought to change in response to storm attack or storm surge, from time to time.

7. The persistence of shape and scope of mangrove fringes and swamps over time is remarkable, although not mapped on the figures. The narrow fringes persist, except where destroyed by man, apparently because their narrow niche is controlled by steep coasts. Within the broader swamps that fill lowlands at the heads of some bays the shapes and widths of the sinuous inlets in the dense mangrove also have not changed.

8. That the loose sediment on the shallow sea floor is unstable we certainly would expect. Convincing evidence is given by those few areas in which submarine outcrops of bedrock have either been covered or uncovered over time.

Lisa Paulson prepared the figures and Amy Polzin composed the text. Clarity of the report was improved by David Larue and Elizabeth Burton.

REFERENCES

Bythell, J.C., Gladfelter, E.H., Gladfelter, W.B., French, K.E. and Hillis, Z., 1989, Buck Island Reef National Monument - Changes in modern reef community structure since 1976, in D.K. Hubbard, Ed., Terrestrial and marine geology of St. Croix, U.S. Virgin Islands: Fairleigh Dickinson University West Indies Laboratory, Spec. Pub. 8, 145-153.

Hubbard, D.K., 1989, Modern carbonate environments of St. Croix and the Caribbean: a general overview, in D.K. Hubbard, Ed., Terrestrial and marine geology of St. Croix, U.S. Virgin Islands: Fairleigh Dickinson University West Indies Laboratory, Spec. Pub. 8, 145-153, plus field trip log to Boiler and Lamb Bays (5 p.).

Kamm, J.L., 1981, Trace-element concentration and distribution in the sediments of Antigua, British West Indies: Unpubl. Master's Thesis, Northern Illinois University, DeKalb, 78.

Multer, H.G., Weiss, M.P. and Nicholson, D.V., 1986, Antigua: reefs, rocks and highroads of history: Leeward Islands Science Associates, Contr. No. 1, 116.

Van Duyl, F.C., 1985, Atlas of the living reefs of Curaçao and Bonaire (Netherlands Antilles): Uitgaven "Natuurwetenschappelijke Studiekring voor Suriname en de Nederlandse Antillen," No. 117, 37, 42 pls, Utrecht.

Wanless, H.R., 1981, Fining-upwards sedimentary sequences generated in seagrass beds: J. Sedimentary Petrology, 51, 445-454.

Weiss, M.P. and Multer, H.G., 1988, Map of modern reefs and sediments of Antigua, West Indies: Department of Geology, Northern Illinois University, DeKalb, Scale: 1:40,000.

MAP OF MODERN REEFS AND SEDIMENTS OF ANTIGUA, WEST INDIES

M.P. Weiss
Dept. of Geology
Northern Illinois University
DeKalb, Illinois 60115

H. Gray Multer
9855 Canaseraga Road
Arkport, New York 14807

A colored geologic map of the submarine geology around Antigua is 70.5 x 103 cm (27.75 x 40.5 in) in size, with a scale of 1:40,000, was displayed at the Conference on St. Croix, August 7-11, 1989. The reefs and bottom sediments are mapped to a depth of about 20 m (10 fms). Five main submarine geologic units are mapped: 1) grass-held sediment, 2) linear reefs, 3) patch reefs, 4) deeper reefs, and 5) sand. Sixteen divisions of these main types are also shown. the coast of Antigua and its nearby islands is distinguished by symbols as rocky, sand beach or mangrove fringe. Certain special features, such as steep scarps, sand-filled channels in coral, and underwater bedrock outcrops are also shown.

The map was constructed photogrammetrically on a stereoplotter, using aerial photographs taken in 1954, 1958 and 1981. "Ground-truthing" was accomplished by swimming traverses, observations and sampling from boats, inspection from the shore, and some drilling. The various seafloor environments/communities are described and illustrated in color on the back of the map.

A special feature is the recognition of changes in bottom environments over time; 49 such areas are mapped, and the nature of the changes described. The sizes of such areas are also tabulated. Most show the effects of commercial and residential development on Antigua since World War II. A summary of those changes and their locations is included in the report by Weiss (this volume).

Looking to the future, the map (published in 1988) will serve as a benchmark of shallow-water environments against which to compare future observations and mapping. Copies are available for purchase from Northern Illinois University.

Reference

Weiss, M.P. and Multer, H.G., 1988, Map of modern reefs and sediments of Antigua, West Indies: Department of Geology, Northern Illinois University, DeKalb, Scale: 1:40,000.

Larue, D.K., and Draper, G. (eds.),
Transactions of the 12th Caribbean Geological Conference, St. Croix, U.S.V.I., Miami Geological Society, P.O. Box 431552, South Miami, FL 33243, U.S.A

THE CRETACEOUS AGE SEDIMENTS OF THE SABA BANK AND THEIR PETROLEUM POTENTIAL

ARIEL J. WARNER Jr.
ALADDIN PETROLEUM CORPORATION
WICHITA, KANSAS

ABSTRACT

The Saba Bank area has been under active exploration for hydrocarbons since the early 70's. There has been 3600 plus km of seismic data acquired over the bank, two wells drilled and numerous reports on the area's petroleum potential published. The work proved the existence of good source and reservoir rocks within the Tertiary section. The well data also proved the Tertiary section to be too immature to have produced the hydrocarbon shows found during the drilling. The available data suggests the existence of a Late Cretaceous sedimentary section underlying the drilled Tertiary section. This section may have provided the source rocks for the hydrocarbons present.

INTRODUCTION

The Saba Bank is 13.5 km (8 mi) southwest of the island of Saba and 135.5 km (84 mi) east-southeast of St. Croix, U.S. Virgin Islands (fig. 1). The bank is a completely submerged carbonate platform raised approximately 1,000 m (3,290 ft) above the general seafloor. The area has had two (2) exploratory wells drilled on the permit since 1977 (fig. 1). Both wells reached total depth in a Paleocene-Eocene Age andesite (Larue, 1988; Warner, 1989).

The Saba Bank area belongs to the very complex tectonic framework of the Caribbean Sea (Case, 1980) and so far no completely satisfactory theory of the tectonic history of the region exists. In discussing the geological history and petroleum potential of the Saba Bank several things must be considered: (1) Is The Saba Bank genetically related to the Greater Antilles, the Lesser Antilles or both? (2) Is the Saba Bank a northern extension of the Aves Ridge (Bouysse, 1985)? (3) Do sediments of Early Eocene age and older exist beneath the platform? Saba Island is usually considered as part of the Tertiary Island Arc system along the Eastern edge of the Caribbean Plate, yet geologically Saba Bank or a part might belong to the Greater Antilles.

STRATIGRAPHY

There were four major stratigraphic units drilled in the two wells (fig. 2). The units range, in age, from Early Eocene through Early Pliocene (Fina, 1982a, 1982b; Marathon 1977a, 1977b). The units from top to bottom are as follows:

Upper Carbonate Unit

This unit is primarily pale yellow to translucent, crystalline to microcrystalline limestone. Age dating and the fossil recoveries suggest this section ranges from Middle Miocene to Early Pliocene in age.

Volcano Clastic Section

This unit in Saba Bank No. 1 consists of conglomerates, sandstones, alternating siltstone and claystone facies. In the Saba Bank No. 2, the central unit is finer grained and contains no conglomerates. The volcano-clastic unit ranges in age from Early Eocene to Middle Miocene. The environment of deposition of the unit is a near-shore deltaic-neritic at S. B. No. 1 and a neritic to deep water submarine fan environment at S.B. No. 2.

Lower Carbonate Unit

In Saba Bank No. 1, a Mid to Late Eocene age limestone was encountered. Marathon (1977a) has described the limestone as being:

> . . . mostly micritic or well cemented clean limestones with little porosity, but includes interbeds of poorly cemented, fine grained carbonate sand that have excellent porosity.

Larue, D.K., and Draper, G. (eds.), *Transactions of the 12th Caribbean Geological Conference, St. Croix, U.S.V.I.*, Miami Geological Society, P.O. Box 431552, South Miami, FL 33243, U.S.A

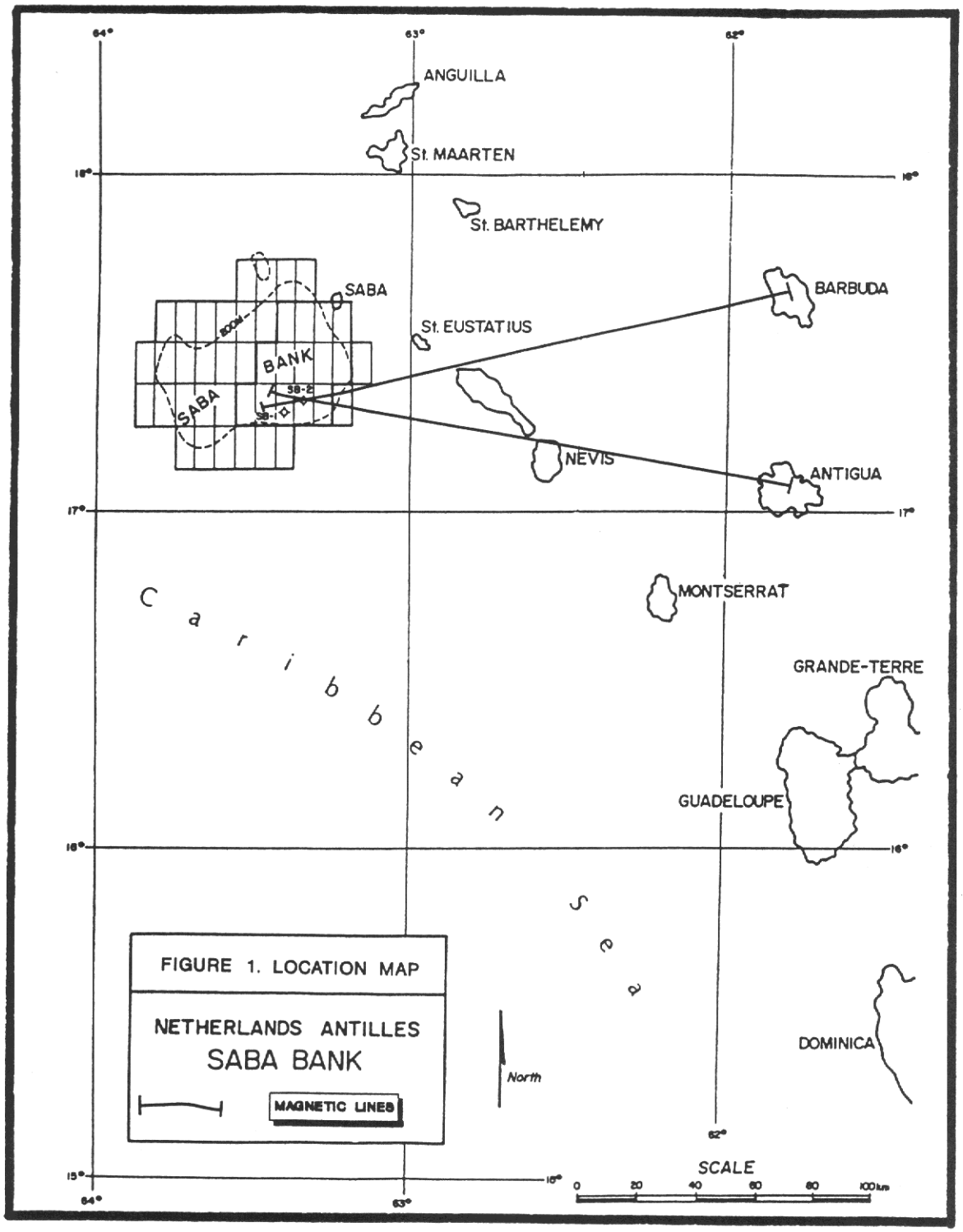

FIGURE 1. LOCATION MAP

NETHERLANDS ANTILLES
SABA BANK

MAGNETIC LINES

The lower unit in Saba Bank No. 2 is not a carbonate but rather a turbidite. This unit consists mainly of silty claystones and argillaceous siltstones, with several sandstone beds encountered in the lower portion (Fina, 1982a).

Conglomerate Found In S.B. No. 1

In the S.B. No. 1, a basal conglomerate was encountered above the andesite. The conglomerate was not cored. It was described (Marathon, 1977a) as being composed of quartz grains ranging from fine grained to conglomeratic with a

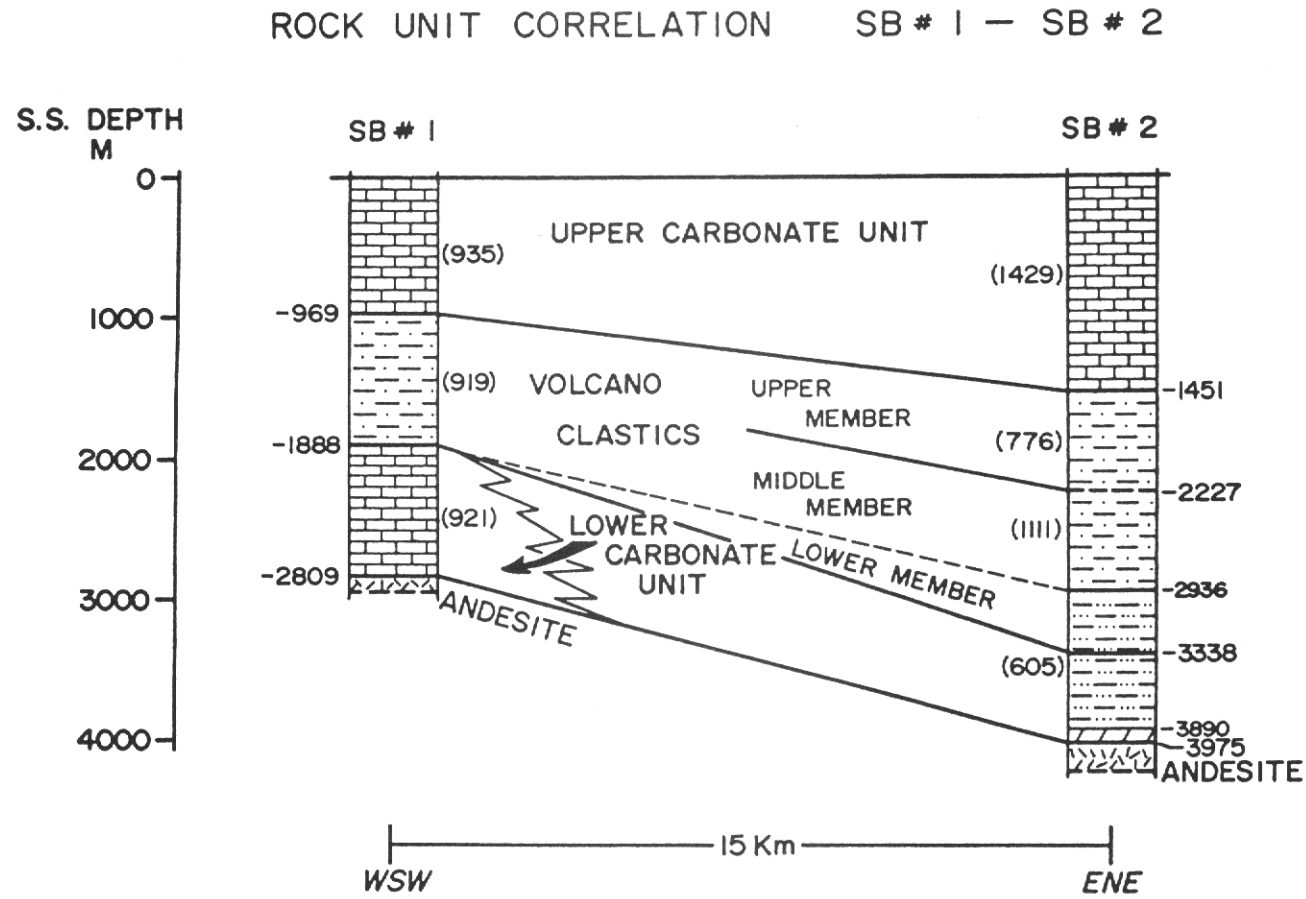

(THICKNESS IN M INDICATED BRACKET)

FIGURE 2.

After Fina 1982a.

silica cement in a non calcareous clay matrix with disseminated pyrite. The unit is green-gray with a "weathered Kaolinite appearance. (Marathon, 1977a) It is clear from the interval of altered conglomerate rocks resting on these volcanics that a significant unconformity which may represent part of the Late Paleocene and/or Early Eocene time caps the volcanic sequence. In the S.B. No. 2. this conglomerate was not found Fina described several basal sands that could possibly represent weathered andesite.

Andesite

Both exploratory wells reached total depth in an andesite porphyry that is dated between Early Paleocene to Early Oligocene. See table No. 1. The original dating on the andesite under S.B. No. 1 is a closer approximation of the actual age of the andesite. The dates were recorded from separated hornblende crystals. Whereas the S.B. 2 dates were from whole rock samples. From the samples recovered, the consensus is that the andesite represents either a surface intrusion or a near surface volcanic feeder system. In the Saba Bank No. 1, the top of the andesite is at 2,856 m (9,370 ft). In the Saba Bank No. 2, the unit is at 4,032 m (13,228 ft).

GEOCHEMISTRY

Marathon's S.B. No. 1 Data

Nine composite samples of cuttings were analyzed for total hydrocarbons, saturates and aromatics. The samples yielded total hydrocarbons of 234 to 593 ppm. All the composites gave the appearance of containing good source rocks for oil. (figure 3.) Marathon's stated:

> ...the rocks give the appearance of good but

TABLE 1.
AGES OF ANDESITE

LABORATORY	ROCK TYPE	SB 1	SB 2
GEOCHRON USA	HORNBLENDE	64.5MY	
BRUSSELS UNIV.	WHOLE ROCK	37.3MY	
" "	FELDSPATH		34.4MY
ROBERTSON RESEARCH	WHOLE ROCK		38.4MY
" "	WHOLE ROCK		54.3MY

MARGIN OF ERROR 1.4 TO 3.7 MY

BASED ON K-AR DATING METHODS

immature source rocks for oil. If similar rocks occur deeper, or if rocks stratigraphically equivalent are more deeply buried elsewhere, they should make excellent source rocks.. (Marathon 1977a) (figures 4 and 5.)

GEOCHEMICAL STUDY OF S.B. NO. 1
FIGURE 3

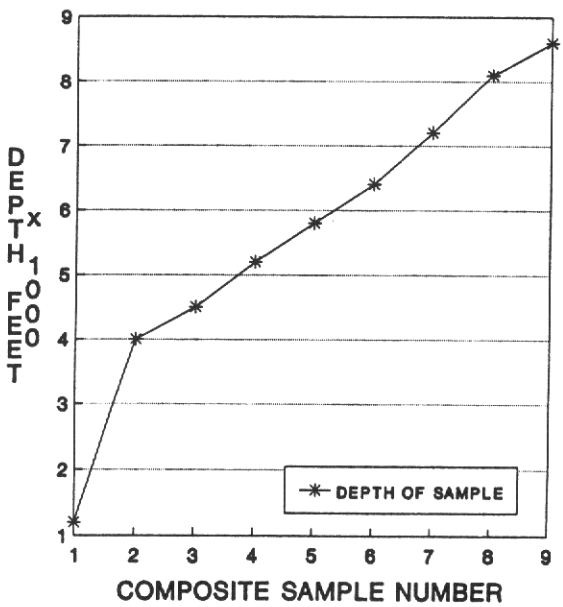

BASED ON MARATHONS DATA

S.B. NO. 1 HYDROCARBONS AND ORGANIC CARBON FIGURE 4.

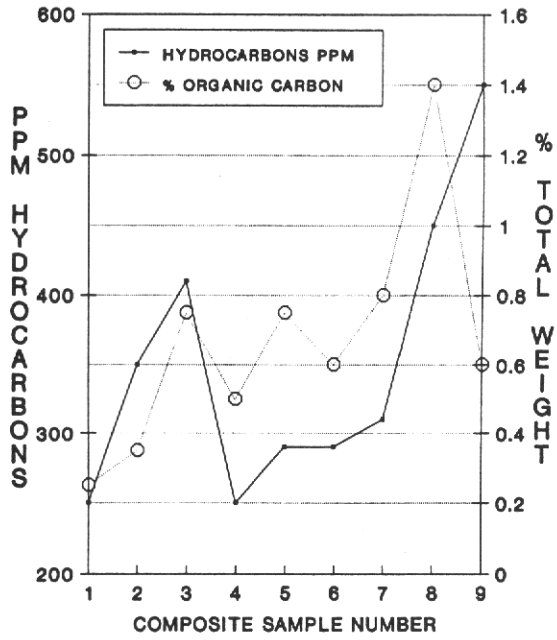

BASED ON MARATHONS DATA

OIL WINDOW OF S.B. NO. 1
FIGURE 5

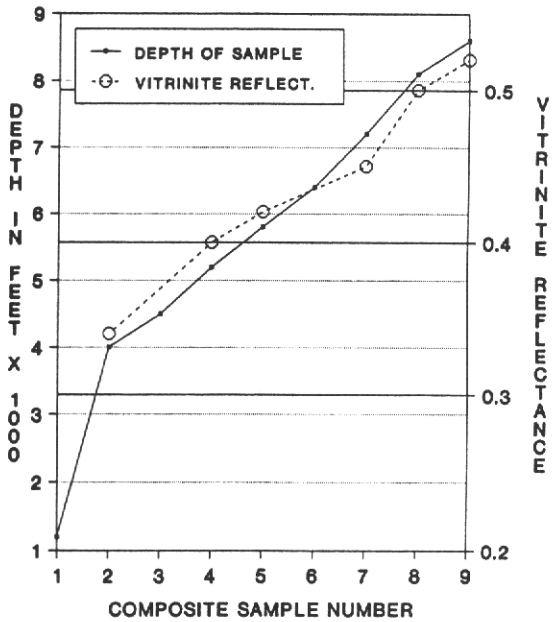

BASED ON MARATHONS DATA

Petrofina's S.B. No. 2 Data

Petrofina S.A. contracted Robertson Research U.S. Inc. to conduct the various analyses on the S.B. No. 2 samples. Twelve core samples from 3,422.3 m. (11,190.9 ft.) to 3,795.6 m. (12,411.6 ft.) were analyzed to determine total organic carbon content and vitrinite reflectance. (figure 6.)
Robertson Research concluded that:

> Geochemical data on representative samples from two cored intervals in the S.B. - 2 well reveal only limited quantity of low yield, gas-generating organic matter is present and the sampled interval, therefore, has very little capacity to generate hydrocarbons. Sufficient burial and thermal maturation for oil generation does exist but the samples are only in the early stages of gas generation.

PREANDESITE FORMATIONS

The thesis that there exists pre-Eocene sedimentary rock units rests heavily upon three major facts: (1) the Cretaceous clastic rock samples recovered from the two Saba Bank wells; (2) the deep sedimentary basin beneath Saba Bank revealed by the airborne and surface magnetic; and (3) seismic data which includes an abundant amount of slower velocity seismic reflections that exist below the 64 my andesite (Daly 1983). (figure 7.)

In both the S.B. No. 1 and S.B. No. 2 reworked Cretaceous rocks were found. The samples contained reworked calcareous nannofossils. The nannofossils found in S.B. No. 2 were in the central sedimentary section from 1770 - 1930m (5805 -6330ft) and 2860 - 3994m (9380 -13100ft). (Robertson Research 1982) Marathon in their reports on the S.B. No. 1 discuss the calcareous nannofossils but, like Robertson Research, fail to give a listing of the individual species present. A sidewall core in S.B. No. 1 taken at 1679m (5507ft) contained a very large amount of organic matter including much fungal material, pieces of light brown cuticle, fusinite and wood. (Daly 1989) Joe Guennel of Marathon described the material as " ...Mesozoic in age and I suspect that they are associated with the coaly material, especially the fungal remains. A Cretaceous coal or lignite may thus be one of the sources for some to the allochthonous organic material in this sample". (Marathon 1977b)

A sample in the S.B. No. 2 well at 3,920 m. (10,758 ft.) was dated using K/AR at 90.2 my (Fina 1982a). This date was acquired from what appears to be reworked Cretaceous volcanics. Petrofina failed to give a good description of this sample so its exact composition is unknown. There is no definite

S.B. NO. 2 TOTAL ORGANIC CARBON AND CARBONATE BY % WEIGHT. FIGURE 6.

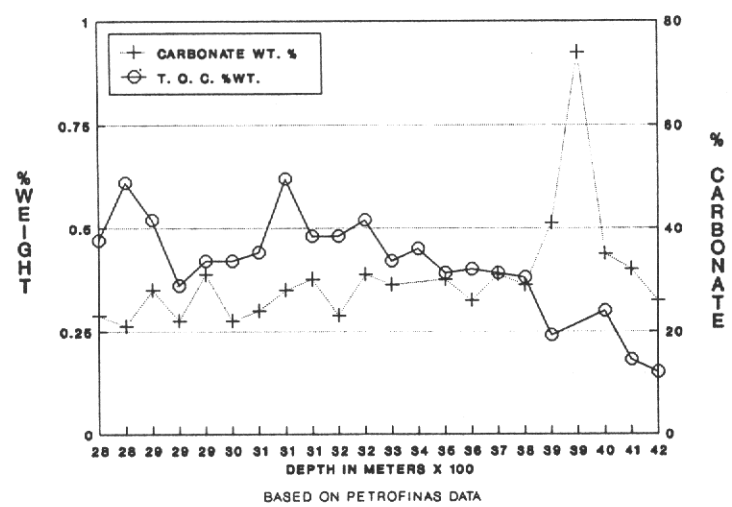

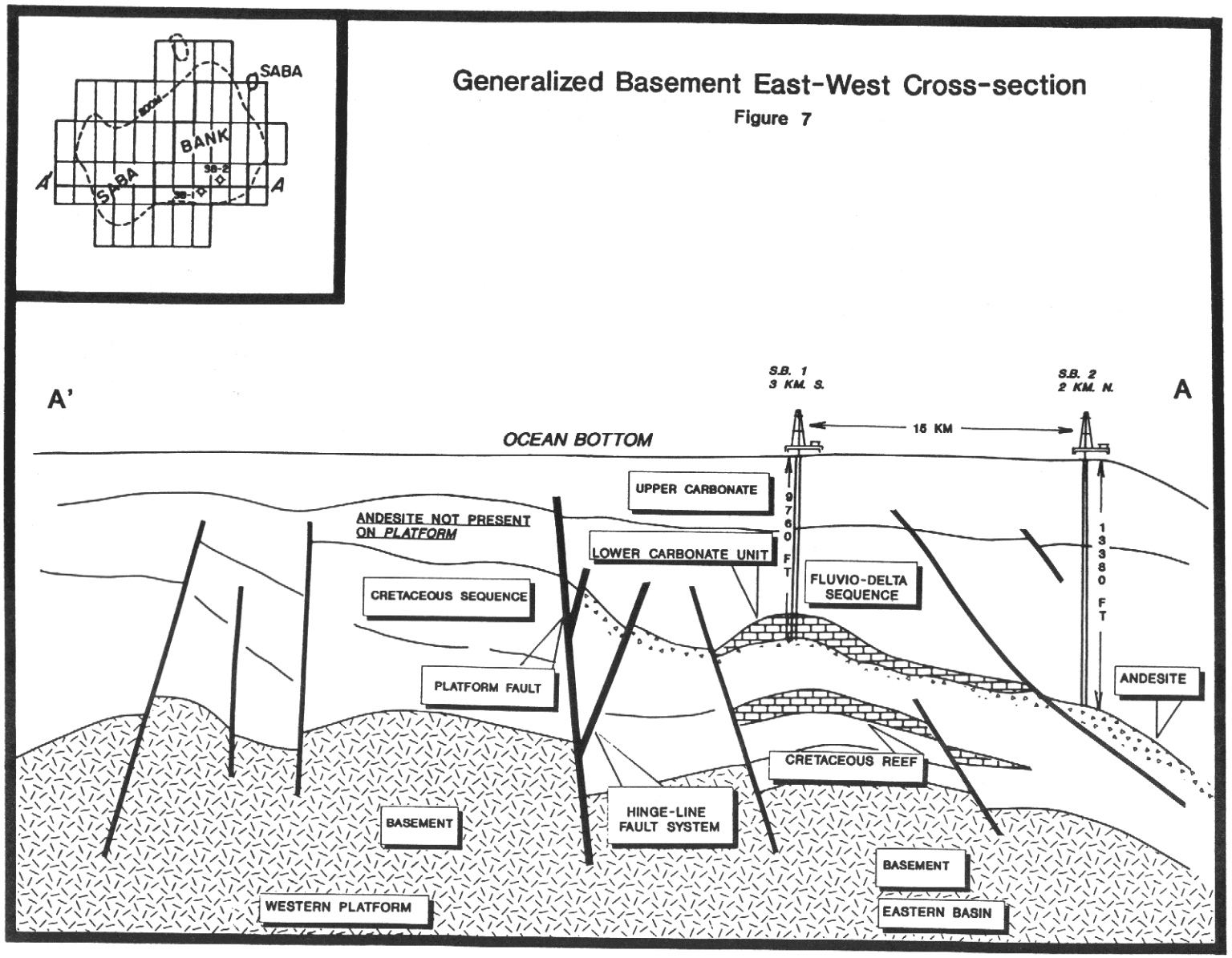
SABA
BANK
SABA
A
A
38-2
38-1
Generalized Basement East-West Cross-section
Figure 7
A'
A
S.B. 1
3 KM. S.
S.B. 2
2 KM. N.
15 KM
OCEAN BOTTOM
UPPER CARBONATE
ANDESITE NOT PRESENT
ON PLATFORM
LOWER CARBONATE UNIT
9760 FT
13380 FT
FLUVIO-DELTA
SEQUENCE
CRETACEOUS SEQUENCE
PLATFORM FAULT
ANDESITE
CRETACEOUS REEF
BASEMENT
HINGE-LINE
FAULT SYSTEM
BASEMENT
WESTERN PLATFORM
EASTERN BASIN

proof that older sediments exist, but my interpretation of the data infers the existence of an older sedimentary section. Figure 7 is a reconstruction of the sedimentary sequence underlying the Saba Bank based on seismic information and results from the S.B. No. 1 and S.B. No. 2. Both Saba Bank No. 1 and 2 penetrated into the Eocene age Andesite. The magnetic and gravity data suggests volcanic basement at approximately 17,000 ft and 23,000 ft under the Saba Bank No. 1 and 2 respectively. In the Saba Bank area seismic data strongly suggest the presence of a thick pre-Tertiary sedimentary section. The reworked Cretaceous found rocks in the Tertiary sediments on Saba Bank show that the Bank may have been attached or adjacent to St. Croix during Mid to Late Cretaceous (Speed 1974). If this is the case, then the proposed Cretaceous section underlying the andesite at Saba Bank would be similar to that found exposed at St. Croix. Lidz (1988) describes the St. Croix Cretaceous section as follows: " Strongly folded Upper Cretaceous deep water (oceanic) calcareous turbidites and volcaniclastics (>10.6 km. thick; 34,700 ft.)..."

Recent evidence suggests that rocks on St. Croix represent 5 to 7 Cretaceous nappes such that only a structural thickness can be estimated (Speed, 1989; Speed and Joyce, 1989). The Cretaceous layered rocks on St. Croix are mostly volcanogenic strata that accumulated probably at deep-marine sites (Speed, 1989; Speed and Joyce, 1989). Essentially, all of the exposed Cretaceous section on St. Croix has experienced low grade regional and contact metamorphism and would therefore be considered unfavorable for hydrocarbon production. If this is correct, then relating the Saba Bank to the Greater Antilles rules out any hydrocarbon potential in the older Saba Bank sediments. However, if the Saba Bank region is related to the present Lesser Antilles volcanic arc, then the sediments expected in the area would be no older than the Mid Miocene to Oligocene and be primarily volcanic or volcano clastic in origin (Malfait and Dinkelman, 1972; Tomblin, 1975).

Offshore St. Croix along the base of the north insular slope, dives by the Alvin have revealed a thick sedimentary section that might contain some of the oldest exposed sedimentary formations of the Caribbean Region. Lidz (1988) reported that:

> . . . Alvin dives about East End Range showed sedimentary rocks 3.7 km. (12,000 ft.) below sea level dipping gently (10^{o}-20^{o}) westward under the Cretaceous strata. Although not sampled, these sandstones and conglomerate beds indicate a thick sedimentary section under the island. Seismic reflection data collected on the Fredericksted plateau at the west end of the island and cooperative dives in the DSRV Aluminaut revealed that the plateau is formed by synclinal valley-fill sequence underlain by unknown thickness of stratified, moderately deformed sedimentary and metasedimentary rocks.

Presence of reworked unmetamorphosed mature organic matter (coal fragments?) and calcareous nannofossils of Cretaceous Age, found in the S.B. 1 and S.B. 2 wells, tends to prove the proximity of a Cretaceous section which has not undergone the metamorphism seen in surface exposures on St. Croix. This also suggests that Cretaceous rocks of Saba Bank were not deposited in the same environment as the exposed Cretaceous section on St. Croix.

It is, therefore, incorrect to generalize the idea of an Early Cretaceous economic basement throughout the region. If the above is the case, the Saba Bank being genetically related to the St Croix region would not preclude hydrocarbon production.

STRATIGRAPHIC RECONSTRUCTION

The Platform Fault (figure 7.) appears to have been first activated during the Middle to Upper Cretaceous when the western platform area was uplifted with the eastern Saba Bank slowly subsiding. The eastern area remained at or near sea level long enough to allow for the Cretaceous reef under the Saba Bank No. 1 to grow. (figure 8.) The eastern area continued to drop relative to sea level creating a basin that was receiving sedimentary influx from the uplifted Cretaceous Platform.

Around Mid to Late Paleocene the andesite that was encountered in the two wells was emplaced. The andesite was either a surface flow or a near surface volcanic feeder system emplaced along the platform

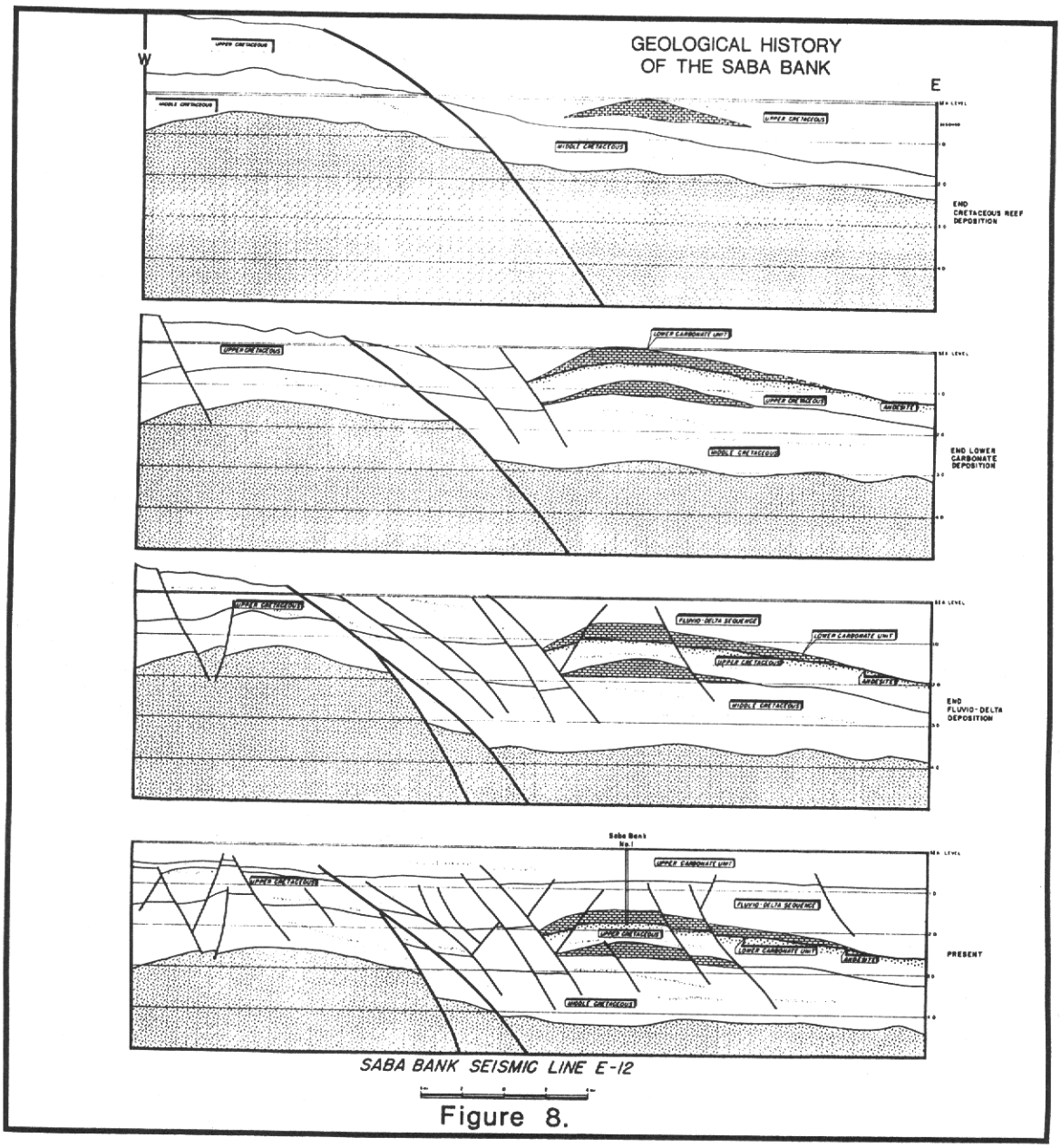

Figure 8.

fault system. The andesite is probably evidence of the final volcanic activity from the Aves Ridge (Pinet, 1985). Neither Marathon nor Petrofina made any comment about finding reworked andesite in the sedimentary sections of the two wells but diagenesis may have destroyed the evidence. In both wells there is no indication of thermal alteration to the sediments overlying the andesite, suggesting that the sedimentary section overlying the andesite was removed before the deposition of the carbonate, or the andesite was a surface extrusion that cooled quickly prior to the western area submerging. As the eastern basin was filling, post andesite emplacement, the basin became shallow enough to allow for the reefal buildup that was tested in S.B. No. 1. This reef continued to build until Late Eocene. The reef created an effective dam stopping what sediments were being eroded from reaching the deep basin found in the S.B. No. 2.

The area north and west of the Platform Fault was a positive during Late Eocene time with the present hinge-line being the shoreline. Carbonates were building in the shallow marine zone east of the hinge-line fault. The slope was narrow with the sea floor plunging rapidly to the east creating the basinal area tested by S.B. No. 2. Sediments found in the S.B. No. 2 are younger than the Lower

Carbonate, suggesting a period of nondeposition during Late Eocene in the deeper basinal areas. The above suggests that the Western Platform area did not have great relief and was not subject to extensive erosion during Late Eocene.

During Oligocene to Middle Miocene time, the Platform Fault was reactivated with the Western Platform being uplifted and the eastern area subsiding rapidly. Seismic data shows progradation from the platform to the east and southeast. In the S.B. No. 1 area, an increase in sandstone and conglomerate deposition is seen where claystones were reported to have been deposited at the S.B. No. 2. This suggests that S.B. No. 1 is closer to the depositional source i.e., the platform.

During the Middle to Late Miocene, the whole Saba Bank area was peneplained preceding the deposition of the Upper Carbonate. This was probably caused by a general uplift of the whole bank area with the eroded sediments being deposited off the bank into the deeper basinal areas. This general uplift may have been brought about by the changes that took place along the Outer Island Arc at this time. During the Middle Miocene to Early Oligocene the outer arc became an inactive volcanic arc and the Inner Island Arc became the active Volcanic Arc.

1988 SEISMIC DATA

Approximate Cretaceous Tertiary Boundary

The Approximate Cretaceous Tertiary Boundary Horizon varies in depth below sea level from 2,850 milliseconds on the downthrown side of the Platform hinge-line to 600 milliseconds on the upthrown side of the Platform hinge-line. The horizon appears to represent seismic anomalies relative to the sedimentary hiatus between Tertiary sediments and the underlying Cretaceous sediments (figure 9).

Site 146 of leg 15 of the D.S.D.P., in the central Caribbean Basin proved the existence of a Late Cretaceous sea level low stand, thus allowing Late Cretaceous carbonate buildups to be generated (Edgar, 1973). At the S. B. No. 1 site, line E-12 shows one such Cretaceous reefal buildup.

One of the questions from previous seismic work was: Did the andesite cover the platform area and if so, does the Approximate Cretaceous Tertiary Boundary Event represent the andesite seismically on the platform? The lack of reworked andesite in the sediments overlying the basal carbonate buildup under S. B. No. 1 suggests that the andesite was not present on the uplifted platform, and if the andesite was emplaced on the platform, all sedimentary evidence has been destroyed. If the andesite is the Approximate Cretaceous Tertiary Boundary Event on the platform, it would have to be older than the dating indicates. This assumption is made because in the central sedimentary sequence penetrated in the S.B. No. 1, reworked Cretaceous was found; therefore, the source for these sediments must be Cretaceous in age. If the Approximate Cretaceous-Tertiary Boundary Event on the platform is the andesite, it would have to be at least Mid to Late Cretaceous (90 my) not Paleocene-Eocene in age. Between the S.B. No.1 site and the uplifted platform, there is a character change in the reflection of the andesite such that it is no longer traceable as a continuous event. The seismic characteristics go from a high amplitude reflection to a lower frequency event.

Mid Cretaceous Event

The Mid Cretaceous Event Horizon varies in depth from 4.0 seconds below sea level under the S.B. No. 1 location to roughly 1.4 seconds on the platform. This reflection is correlative across the platform, and as interpreted, appears to represent a Mid Cretaceous event. The seismic also suggests an additional section below the horizon. From the reflection characteristics, these events are sedimentary in nature. (figure 10.)

PROSPECTS IDENTIFIED ON THE SABA BANK

The prospects on the Saba Bank can be divided into two groups, the Tertiary Prospects proven by the Saba Bank wells and the Cretaceous prospects indicated by the new seismic and the reworked Cretaceous sediments found in both wells. The Tertiary Prospects are limited to the downthrown eastern basins.

TERTIARY PROSPECTS

Carbonate Buildups

The Saba Bank wells proved that along the platform hinge-line an ancient shelf existed. Carbonate

Drilling Targets on Eastern Saba Bank

Figure 9.

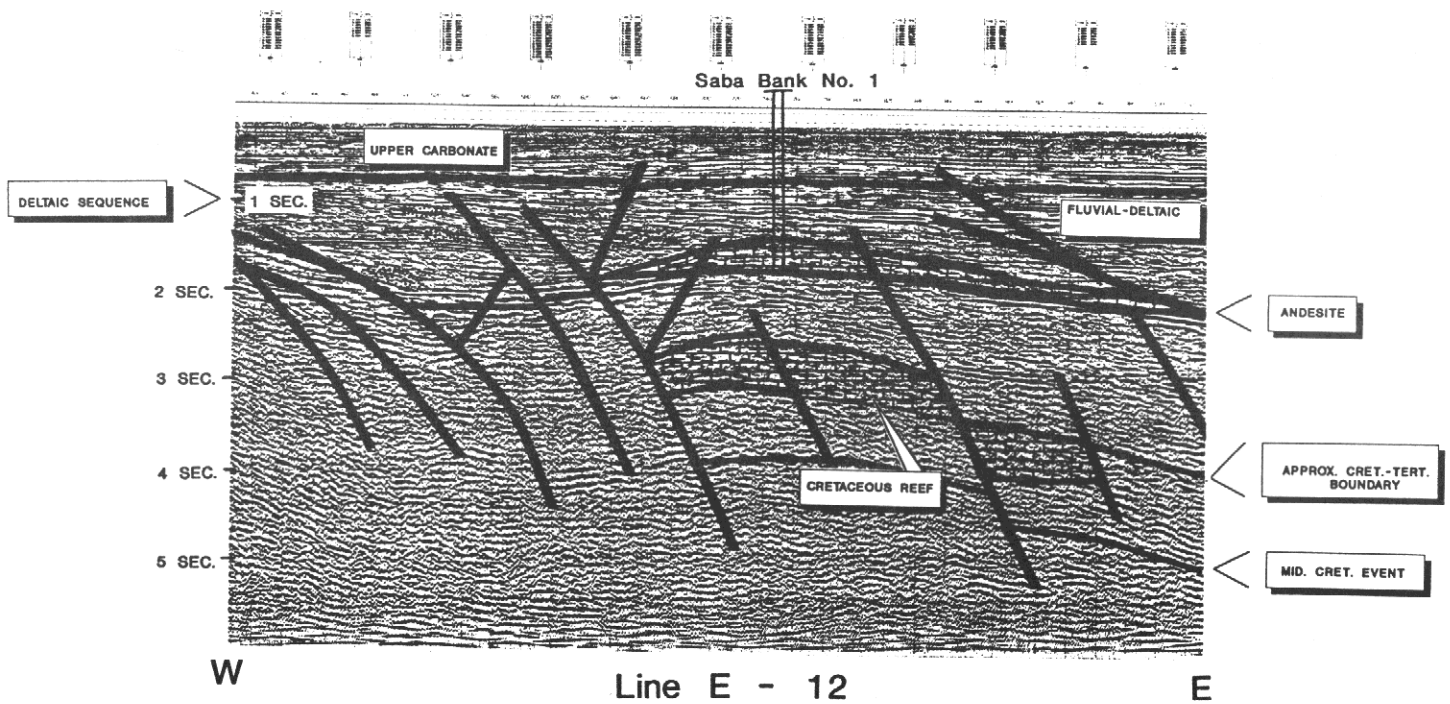

Deeper Cretaceous Section on Northwest Platform

FIGURE 10.

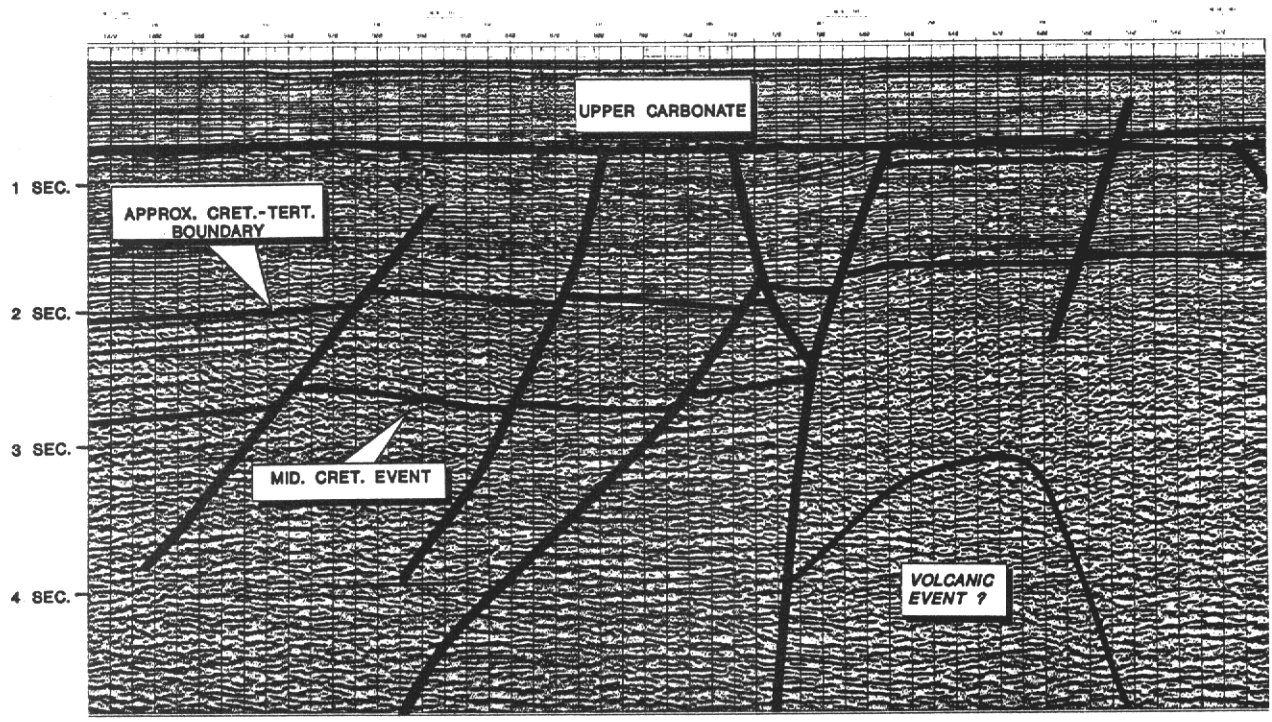

buildups and associated reef facies have been seismically recognized along this shelf. (Figure 11.) Petrofina described several good drilling targets in the shelf area (Fina 1983). The reservoirs are carbonates similar to that encountered in the Saba Bank No. 1. The fair to good source rocks encountered in the S.B. No. 1 & 2 should be developed within the area of this prospect. The reef drilled under the S.B. No. 1 location showed some asphalt in the basal portion. This unit had TOC values that ranged from 732 to 434 ppm and % organic carbon values of 1.33 to .64% of total weight. The analysis of the carbonate samples showed it to be a good to superior source for oil yet, immature. (Marathon 1977a) The analysis of the depositional history of these prospects indicates that they lie within the oil window. Furthermore, the faulting that is indicated through the andesite will, in some cases, allow migration from the older Cretaceous sediments. The logs from S.B. No. 1 show the basal carbonate contained adequate porosities to be productive but was immature.

Fluvial-Deltaic Sequence

Seismic line E-12 (figure 9.) from shot point 380 to 700 shows a sedimentary basin 2,137 m. (7,000 ft.) deep. The sedimentary sequence of this basin is expected to be deltaic deposits, i.e., sandstone with interbedded shales. The basin can be traced along the ancient shelf line trending north, northeast, and east. In the S.B. No. 1 the central sequence contained several zones of sandstone and fine grained conglomerates that would make good reservoirs, but immature. This sequence is further from the depositional source than the above described delta systems and should be finer grained than the sediments within the systems. These deltaic systems overlie the platform hinge-line fault system, where the seal of the andesite should be broken, thus allowing the migration of hydrocarbons from the underlying Cretaceous sediments.

Turbidite Prospects

Evaluation of the seismic data revealed that the S.B. No. 2 was

drilled on a paleo-ridge and due west of the S.B. No. 2 location is a north-south trending trough. Although poor to fair data quality and limited resolution was experienced, reliable seismic mapping of the prospects was achieved. This early paleo-ridge restricted the eastward flow of the turbidite sequences, resulting in north-south trending sand bodies which form stacked bundles of sands and, in consequence, multiple pay targets. S.B. No. 2 was located in a paleogeographic position not favorable for the buildup of clean sand bodies. Therefore, channel margin facies were encountered with poor reservoir characteristics. The S.B. No. 2 well did, however, have good gas indications. In correlating these shows with the proposed turbiditic sequence, an environment favorable for accumulation of hydrocarbons should be developed west of the well. The C_1 to C_5^+ gas component ratios recovered from the well test indicate that the turbidite sand reservoirs will be liquid hydrocarbon bearing.

Cretaceous Plays

At D.S.D.P. site # 146, in the central Caribbean Basin, is an Upper Cretaceous (90 +/- my.) limestone that varies from reefal to biogenic in nature. This limestone is evidence for a sea level low stand in the Caribbean Basin during this time period. Above the limestones are several bituminous layers with up to 12% total organic carbon. These layers may represent a period of bottom stagnation that was brought about by the lowering of sea level and may be equivalent to the reworked bituminous layers found in the two Saba Bank wells.

Two oil seeps have been reported in Puerto Rico in outcrops of Cretaceous rocks. One consists of drops of oil in calcareous concretions in a shale near Coamo. The other seep consists of oil-impregnated soil in the bottom of Largo No. 1, 8 km. northeast of Ponce. The petroleum apparently comes from the Cretaceous or Eocene rocks beneath the lake.

The seismic survey of the Saba Bank Platform reveals a thick sedimentary section in the Northwestern portion. (figure 11.) The area is either a downdropped block respective to the remainder of the platform, or a piece of the original Cretaceous platform that was not uplifted, but remained stable during the activation of the platform fault system. Regardless of whether the additional section is of Tertiary Age or if the additional section is Cretaceous and is similar to the section that provided sedimentary detritus for the Eastern Bank sediments, good drilling targets should be present.

On the Eastern Saba Bank, the Tertiary sediments proved to be immature for hydrocarbon generation, but both wells proved that good reservoir rock existed. If the andesite acts as an effective seal for the Cretaceous rocks as believed, then where the andesite is not present, i.e., the Platform, the overlying Tertiary sediments should be productive. Reworked Cretaceous detritus, in the sediments, at the two Saba wells suggests that both good source and reservoir rocks exist in the eroded sections. These Cretaceous rocks, when encountered, should be mature for hydrocarbon production as indicated by the migrated hydrocarbons found in both Saba wells. In addition, these Cretaceous sediments would have been within the oil window prior to the uplift of the platform. Both stratigraphic and structural traps are seismically mappable in this thicker sedimentary sequence.

Underlying the andesite at the S.B. No. 1 location, the seismic indicates an additional sedimentary section. Within this section is a thick reefal buildup approximately 4,114 m. (13,475 ft.) below ocean bottom. The seismic reflections indicate an onlapping reefal buildup. The western edge of the buildup appears from the seismic data to have experienced a similar deposition history as the shallower reef. The velocities and the amplitude of the reflectors indicate that the western edge of the buildup is very dense. The upper reef experienced a sedimentary loading which either created conditions of porosity filling or matrix collapse, thereby giving the dense character that the seismic reflections indicate. The S.B. No. 1 well proved that adequate reservoir porosities were present within the penetrated carbonate, but the Tertiary rocks were immature. The lower reefal buildup is within the known oil window, that was 10,000 +/- ft under the S.B. No. 1. Figure 6 shows the location of a Cretaceous age shelf where numerous Cretaceous reefal buildups are suggested by the seismic data. These reefs trend generally east-west beginning in the southwestern Saba Bank and ending under the location of S.B. No. 1. The seismic data suggests that these buildups are considerably larger than the reef found under S.B. No. 1.

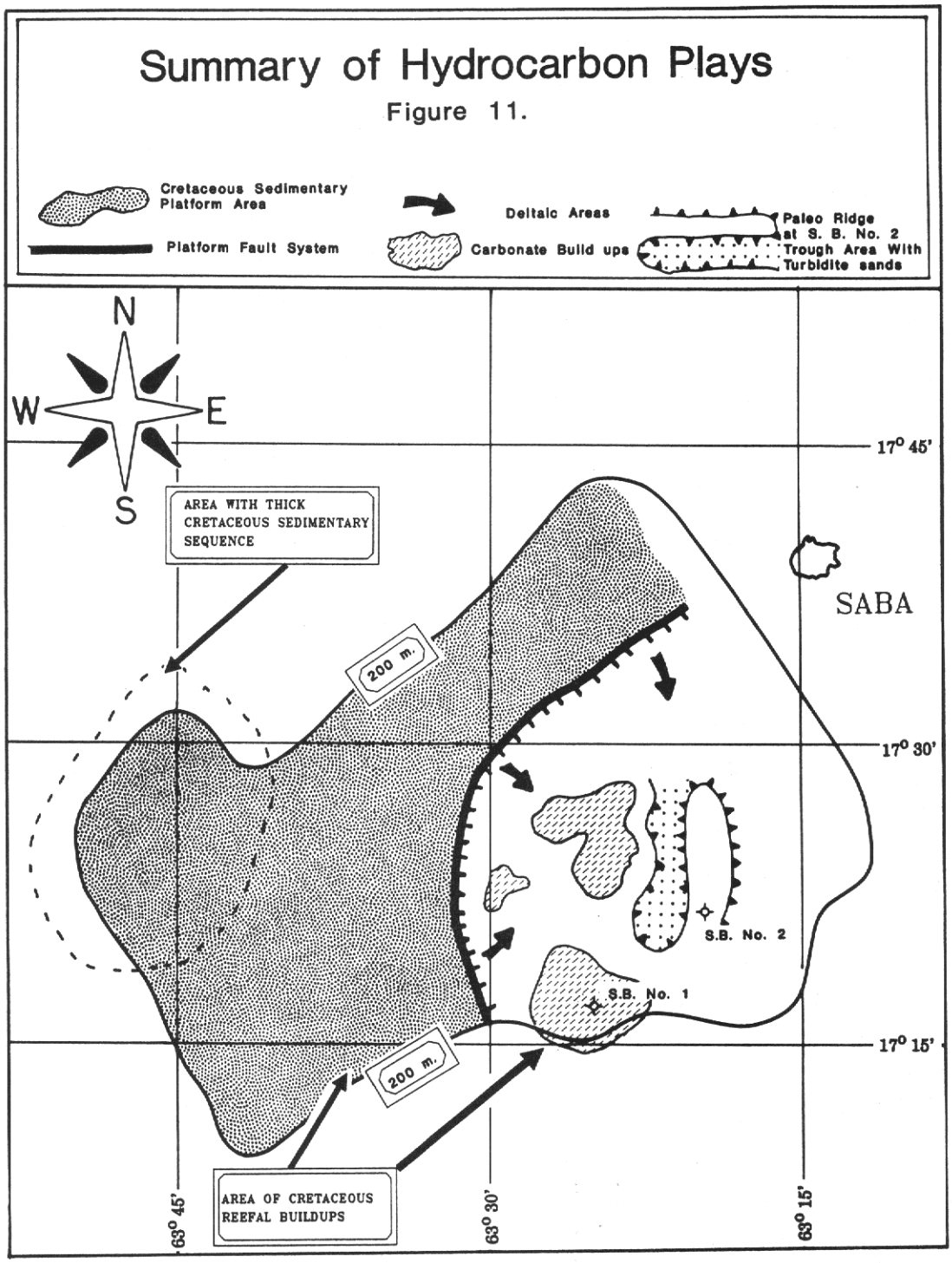

SUMMARY

The well, seismic, and magnetic data on the Saba Bank all allude to the conclusion that there exists a thick sedimentary section beneath the andesite. The age dating results suggest this section will be younger than Early Eocene and probably as old as Early Cretaceous. The live hydrocarbon shows in Saba Bank No. 2 are from migrating oil that has moved through the zone. The underlying Cretaceous section represents the most logical source for these hydrocarbons. In both Saba Bank No. 1 and Saba Bank No. 2, the oil window was just being entered as total depth was being reached. The Cretaceous section has been buried to a sufficient depth to allow for full maturation of the source rocks. This is based on live oil found in Saba Bank No. 2 that was not in situ

but migrated from underlying deposits, i.e., the Cretaceous section. (figure 11.)

The reworked bituminous layers and calcareous nannofossils indicate the Cretaceous rocks should vary from terrestrial to neritic in origin, giving both good reservoir and source rock potential to the section. Evidence suggests that an unmetamorphosed Mid to Late Cretaceous sedimentary section exists beneath the Saba Bank and that the section should not only contain good reservoirs but also the source rocks for the hydrocarbons found in S.B. No. 1 and No. 2

References cited

Bouysee, P. H., The Lesser Antilles Island Arc: Structure and geodynamic evolution, Deep Sea Drilling Project Report, 78, 83-103, 1982.

Case, J. E., Geological-tectonic map of the Caribbean Region, U.S.G.S. Misc. inv. map 1-1100, 1980.

Daly, Thomas, E., Petroleum Prospects Saba Bank Area Netherlands Antilles, Unpublished report 14 p., 1989.

Daly, Thomas, E., Saba Bank petroleum geology, NE Caribbean, Oil and Gas Journal, 83, 112-118., 1983.

Edgar, N. T., Saunders, J. B., et al., 2. Site 146/149. In Edgar, N.T., Kaneps, A. G., and Herring, J.R., eds. Initial reports of the Deep Sea Drilling Project, 15, Washington (govt. Printing Office. 17-80, 1973.

Fina Petroleum, Final well report Saba Bank - 2 part 1 geological report, Unpublished report, 100+, 1982a.

Fina Petroleum, Final well report Saba Bank - 2 part 2 geological report, Unpublished report, 100+, 1982b.

Fina Petroleum, Saba Bank permit farmout proposal. Unpublished report, 23, 1983.

Larue, D.K., Tectonics and petroleum potential of the Caribbean Region, 7th Annual Symposium on Caribbean Geol. 15, Feb. 24-28 1988.

Lidz, Barbara, H., Upper Cretaceous (Campanian) and Cenozoic stratigraphic sequence, Northwest Caribbean St Croix U.S. Virgin Islands, Geol. Soc. Am. Bull., 100, 282-298, 1988.

Malfait, B. T., Dinkleman, Menno, G., Circum-Caribbean tectonic and igneous activity and the evolution of the Caribbean Plate, Geol. Soc. Am. bull., 83, 251-272, 1972.

Marathon Oil Co., Well history Saba Bank No. 1, Unpublished Report, 30, 1977a.

Marathon Oil Co. Research Center, Evaluation of geology and source rock possibilities: Saba Bank - 1, Unpublished Report, 30, 1977b.

Pinet, B. Structure of Aves Ridge and Grenda Basin from multichannel seismic data, Geodynamque des Caribes, 27, 53-64, 1985.

Robertson Research (U.S.) Inc. Saba Bank-2 Well, Netherlands Antilles. Volume 1: Biostratigraphy, Project No. RRUS 812/I/T/87, 33 p., 1982

Speed, R. C., Depositional realm and deformation of Cretaceous rocks, East end, St Croix, in Guidebook to the geology and ecology of some marine and terrestrial environments West Indies Lab., 5, 189-200, 1974.

Speed, R. C., Tectonic evolution of St Croix: Implications for tectonics of the northeastern Caribbean: in Terrestrial and marine geology of St. Croix, U. S. Virgin Islands, West Indies lab., 8, 9-22, 1989.

Speed, R. C. and Joyce, James, Depositional and structural evolution of Cretaceous strata, St. Croix: in Terrestrial and marine geology of St. Croix, U. S. Virgin Islands, West Indies lab., 8, 23-36, 1989.

Tomblin, John Frederick, The Lesser Antilles and Aves Ridge: in The ocean basins and margins Vol.3 the Gulf of Mexico and the Caribbean, 476-500, 1975.

Warner, A. J. Jr., and Kubena Reed, The Petroleum Potential of the Saba Bank: an interpretation, Unpublished Paper, 35, 1989.

STRESS INDUCED MODIFICATION OF SEDIMENT MASS PHYSICAL PROPERTIES DURING ACCRETION: A RECONSTRUCTIONAL APPROACH

Warner Brückmann, GEOMAR–Research Center
for Marine Geosciences, Kiel, FRG

ABSTRACT

The impact of lateral stress on mechanical diagenesis of marine sediments can be estimated using sediment physical property data.

The depth dependent compactional behavior of a set of standard sediment types is described by a number of type curves developed in a statistical analysis of the Deep Sea Drilling Project (DSDP) sedimentological and mass physical property database (legs 1–96). The typecurves define compactional behaviour of mainly pelitic and psammitic sediments of low carbonate content. They are employed as a reference tool for the quantification of tectonically induced consolidation in a growing accretionary wedge.

Based largely on these typecurves and sediment physical property data from DSDP– and ODP–legs 78A and 110 (Barbados Ridge), a simple palinkinetic reconstruction procedure was employed to determine porosity changes during accretion. Palinspastically removing the compactional effects of burial diagenesis caused by imbricate stacking of wedge slices, a synthetic preaccretion porosity vs. depth profile could be modeled, which bears strong resemblence to characteristic profiles from 2 reference drill holes in front of the accretionary wedge (Sites 543 and 672). Comparison of synthetic and reference profiles reveals a lithologically controlled exponential relationship between depth and porosity divergence. Reevaluation of the reconstruction procedure in terms of involved stresses yielded a semiquantitative estimate of the relative and absolute impact of the lateral stress component on sediment consolidation in this part of the convergent plate margin.

This semiquantitative definition of compactional response to the lateral stress component provides an important constraint for further modeling of deformational behavior of accreted sediments.

INTRODUCTION

Convergent plate boundaries are in many instances characterized by the development of a wedge shaped accretionary superstructure, that derives from the process of continuous offscraping and subsequent addition of marine sediments from subducting oceanic plates to the overriding plate. Formulated by SEELY, VAIL & WALTON, 1974 the "trench slope model" postulated the development of submarine complexes of great lateral extension in the slope of trenches above subduction zones. It was based on earlier work and on seismic observations by SEYFERT, 1969, von HUENE, 1972, DICKINSON, 1973, and KARIG, 1969.

The popular subduction accretion model assumes the growth of such structural complexes by frontal accretion of imbricate thrust slices of sediments scraped off a downgoing oceanic plate (AOKI et al., 1982 BIJU-DUVAL et al., 1982, MOORE & BIJU-DUVAL, 1984, MOORE & SILVER, 1987).

Since the frontal accretion and imbrication of semilithified sediments constitutes a mechanical analogon to the tectonic style of fold and thrust belts on land (BOYER & ELLIOT, 1982), similar structural expressions are often inferred (MOORE & SILVER, 1987, SILVER et al., 1986, SAMPLE & FISCHER, 1986). Duplex structures, regular series of imbricately stacked thrust packages, which are a common feature in the frontal part of alpine nappes, are also believed to dominate the tectonic style of accretion. This rather regular mode of accretion constrains the style of deformation in the frontal zone of an accretionary wedge, often termed "wedge toe".

While a large part of the crustal convergence is compensated in the wedge toe (and beyond that) through imbrication, deformation and enhanced compaction of semilithified sediments during the process of accretion can also account for some degree of shortening.

Accreted sediments have experienced a multiphase deformational history that has a strong impact on their physical properties.

One of the most important factors in establishing a "steady state" accretionary wedge is the availability of pore fluids that are supplied by compaction, low grade metamorphic dehydration reactions and thermal expansion at depth. HUBBERT & RUBEY, 1959 and RUBEY & HUBBERT, 1959 were the first to point out the fundamental importance of overpressured pore fluids in the initiation of detachment zones and in the transport of thrust slices over long distances. The tectonic and geometrical analogy of accretionary imbrication zones with the frontal parts of alpine nappes suggests similar processes of mechanical decoupling along zones of overpressured pore fluids.

Assuming a Coulomb failure criterion CHAPPLE, 1978, WESTBROOK, 1982 and DAVIS et al., 1983 used the slope angle to estimate the basal shear stress of a sliding wedge. They calculated the relation of hydrostatic and lithostatic pressure necessary for mechanical decoupling along the basal décollement. In the case of the Barbados Ridge a relation of 0.92 is necessary for mechanical decoupling of subducted and accreted sediments. These calculations are supported by observations of overpressured pore fluids along

Larue, D.K., and Draper, G. (eds.),
Transactions of the 12th Caribbean Geological Conference, St. Croix, U.S.V.I., Miami Geological Society, P.O. Box 431552, South Miami, FL 33243, U.S.A

a number of convergent plate margins (von HUENE & LEE, 1983). Other indicators are mud volcanoes that are developing in many convergent settings, in some cases far away from the deformation front (WESTBROOK & SMITH, 1983). The oceanic reference Site 672 of ODP Leg 110 in front of the Barbados Ridge Complex penetrated a layer of sediments rich in methane which are derived from the accretionary prism indicating the existence of hydrologic preformation of a fore-runner for the future dcollement in the hitherto undeformed strata.

Deformation and mass physical properties of accreted sediments

Due to the unique structural and tectonic properties of accretionary wedges the constituting sediments are characterized by an anomalous development of their mass physical properties porosity, density and shear stress. The compressive tectonic setting of convergent plate margins can be treated as a natural laboratory, in which the deformational reaction of semilithified marine sediments to excessive lateral stress can be studied. The overall deformational behavior of accreted sediments and their soil mechanical properties are in close relationship with large scale geometry of an accretionary wedge.

Porosity as an important index parameter for the compaction is a function of lithology and burial depth as well as the orientation and magnitude of in situ total and shear stress. It is well known, that marine sediments undergoing accretion are developing a significantly lower porosity than those that are compacted in undisturbed basinal sequences (MOORE & KARIG, 1978, CARSON, 1977, WESTBROOK et al., 1982, FOWLER et al., 1985). This observation has not been quantitatively described, as was stated by BRAY & KARIG, 1985:

"However this conclusion has not been adequately documented, and neither the gradient with which porosity decreases with depth within an accretionary prism nor lateral changes in that gradient have yet been explored."

KARIG, 1985 proposed a rapid porosity decrease with depth and with distance from the wedge toe in the frontal parts of an accretionary wedge, leveling off gradually with increasing distance from the deformation front. Deformation and tectonic consolidation are concentrated in the upper part of the wedge toe. DAVIS & von HUENE, 1987 assumed that the bulk of active compressional deformation is concentrated in the first 5 to 15 km of the Barbados, Nankai and Middle America accretionary prisms.

Qualitative and quantitative modeling

During the late seventies to early eighties, when the basic concepts for the genesis of accretionary prisms were developed, these structures were relatively inaccessible to direct sampling by drilling, the only information available were derived from seismic profiles.

Based on seismic data a number of modeling attempts were made to gain a more thorough insight into the basic processes that shape and modify accretionary wedges.

Several physical modeling attempts succeeded in replicating the overall geometry of accretionary wedges in squeezze boxes and other mechanical devices in which artificially deposited clays were subjected to lateral compression (COWAN & SILLING, 1978, DAVIS, SUPPE & DAHLEN 1983, CARSON & BERGLUND, 1986). With poorly constrained boundary conditions and many problems of scaling, and through negligence of the hydrologic regime many of these models had only limited applicability to real world situations.

Aside of these techniques there have been several attempts of using FE/FD (finite element / finite difference) methods to model accretionary wedge deformation assuming viscous, plastic or, most successfully, Coulomb rheological behavior. Numerical methods were applied in a number of cases to define the overall geometry and gross deformational behavior of accretionary wedges in general. Early studies by WOODWARD, 1976, CHAPPLE, 1979, PARK, 1981 and STOCKMAL, 1983 attempted to model the stress field associated with accretionary wedges in general. NGOKWEY, 1984, 1985 developed a FE model that successfully incorporated data on Leg 78A to describe the framework of deformation in the Barbados Ridge Complex.

A common problem to all these models is the strong dependence on the type of assumed rheological properties of accreted sediments. There are three basic types of rheological behaviour that can be applied — Coulomb, plastic and viscous (MOORE & SILVER, 1987). Under the assumption of brittle deformation and constant rate of plate convergence Coulomb–type models predict the development of a stable continuum. In this "steady state trench"–situation the slope angle, internal pore pressures and the mass gain at the wedge toe are in equilibrium with the overall geometry of the wedge. STOCKMAL, 1983 using a plastic rheology to define a stress field around an idealized accretionary wedge proposed listric faults in the toe section. CLOOS, 1982 proposed mass transfer through convective return within the whole wedge assuming viscous material properties.

Nevertheless, realistic modeling of the deformational behavior of accreted sediments is still seriously hampered by the lack of good in situ data.

Apart from this, hydrological modeling mostly done by Shi and Wang has dominated the published work in recent years (WANG, 1984, SHI & WANG, 1985, 1987, 1988, and SHI, 1986).

Thermal modeling is another relatively new field, that has been developed in close relationship with the above mentioned techniques (DAVY & GILLET, 1978, SHI & WANG, 1987, and PEACOCK, 1987).

PALINSPASTIC RECONSTRUCTION OF PHYSICAL PROPERTIES

The problem that shall be adressed in this paper is the quantification of the magnitude of lateral stress in terms of its deformational impact on accreted sediments — as it can be deduced from compaction phenomena in these environments.

The concept that will be applied here, is to reconstruct a synthetic pre-accretionary porosity-depth profile from available drillhole data from an accretionary wedge taking into account all known parameters contributing to compaction and comparing it to a standard reference profile of comparable lithology.

This approach is somewhat different from the normally taken path: instead of relying on a set of functions relating the basic properties of the modeled structure, here only actually determined data points were used as a model input. As many as possible original data were incorporated to reconstruct a physical property profile such as additional gravitational loading due to imbrication.

By discounting the known processes it will be possible to define the magnitude of any additional process specific to the convergent accretionary environment.

DSDP Leg 78A and ODP Leg 110: BARBADOS RIDGE COMPLEX

An important drawback is the scarcity of actual data from accretionary wedges, since they are very inaccessible to direct sampling.

One of the main sources of information concerning sedimentological and sediment physical property data from accretionary wedges were the drilling operations of the Deep Sea Drilling Project (DSDP) and its successor Ocean Drilling Program (ODP).

Drilling the circumpacific forearc areas provided a wealth of data, yet only DSDP Leg 78A and ODP Leg 110 in the Barbados Ridge Complex succeded in reaching and penetrating the basal décollement zone, that is separating subducted and accreted sediments at the base of the prism. Both legs gained physical property data hitherto unavailable especially in the areas close to detachment planes and shear zones.

Regional setting

In the southern part of the Lesser Antilles island arc, continuing subduction of the North American plate under the Caribbean plate has produced an unusually broad accretionary prism varying in width from 80 to 300 km. Here the incoming sedimentary pile consists of up to 7 km of terrigenous material, derived mainly from the Orinoco Fan of the nearby South American continent.

The Leg 78A and 110 drilling area, located in the northernmost section of the Barbados Ridge Complex (Fig. 1, 2) is characterized by the input of 700 m of pelagic to hemipelagic clays. In this area the topographic high of the Tiburon Rise is shielding the subducted sedimentary sequence from the influx of terrigenous material. Drilling results as well as seismic profiles strongly suggest successive growth of the accretionary wedge by imbricate thrusting and stacking of offscraped sediment slices at the deformation front (Fig. 3). In the drilling area the upper 200 m of the incoming sedimentary sequence are scraped off from the subducting Atlantic plate and attached to the accretionary wedge. Shear and detachement zones in the wedge toe area are characterized by near lithostatic pore fluid pressures that are believed to facilitate the movement of large thrust slices.

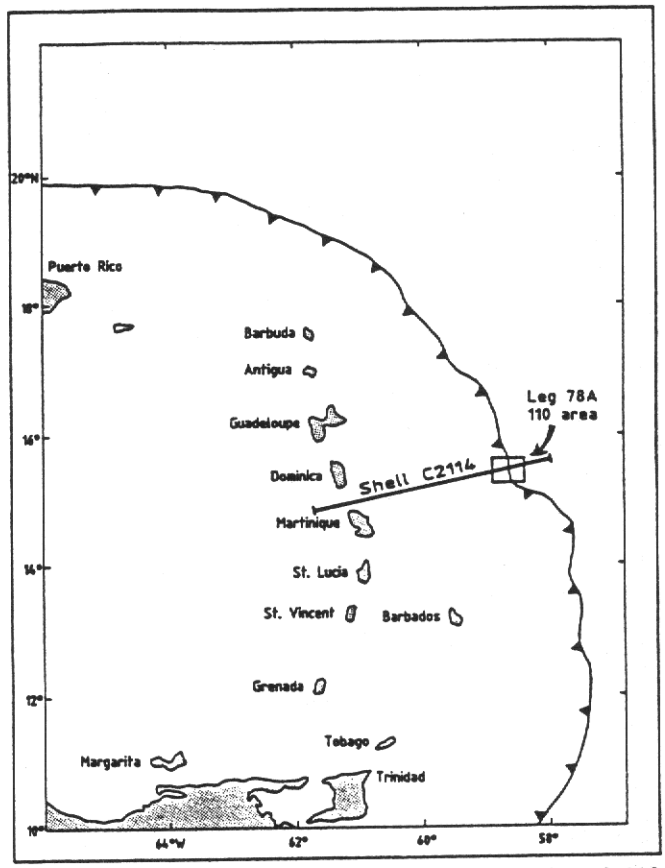

FIG. 1. Regional location map for the Leg 78A and 110 drilling area (from DAVIS & HUSSONG, 1984)

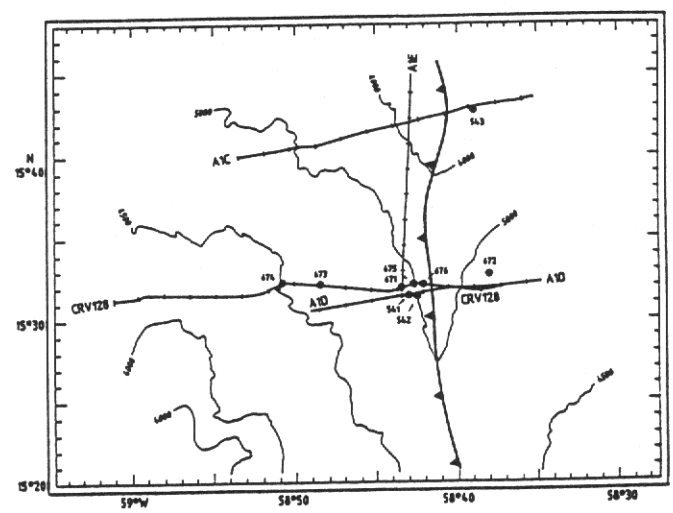

FIG. 2. Site location map for the Leg 78A and 110 drilling area (modified from MOORE & BIJU-DUVAL, 1984)

Sedimentological, stratigraphic and sediment physical property data on Legs 78A and 110 are utilized in this study to develop a palinspastic model to examine the compactional effects associated with initial deformation in imbricated thrust slices at the wedge toe.

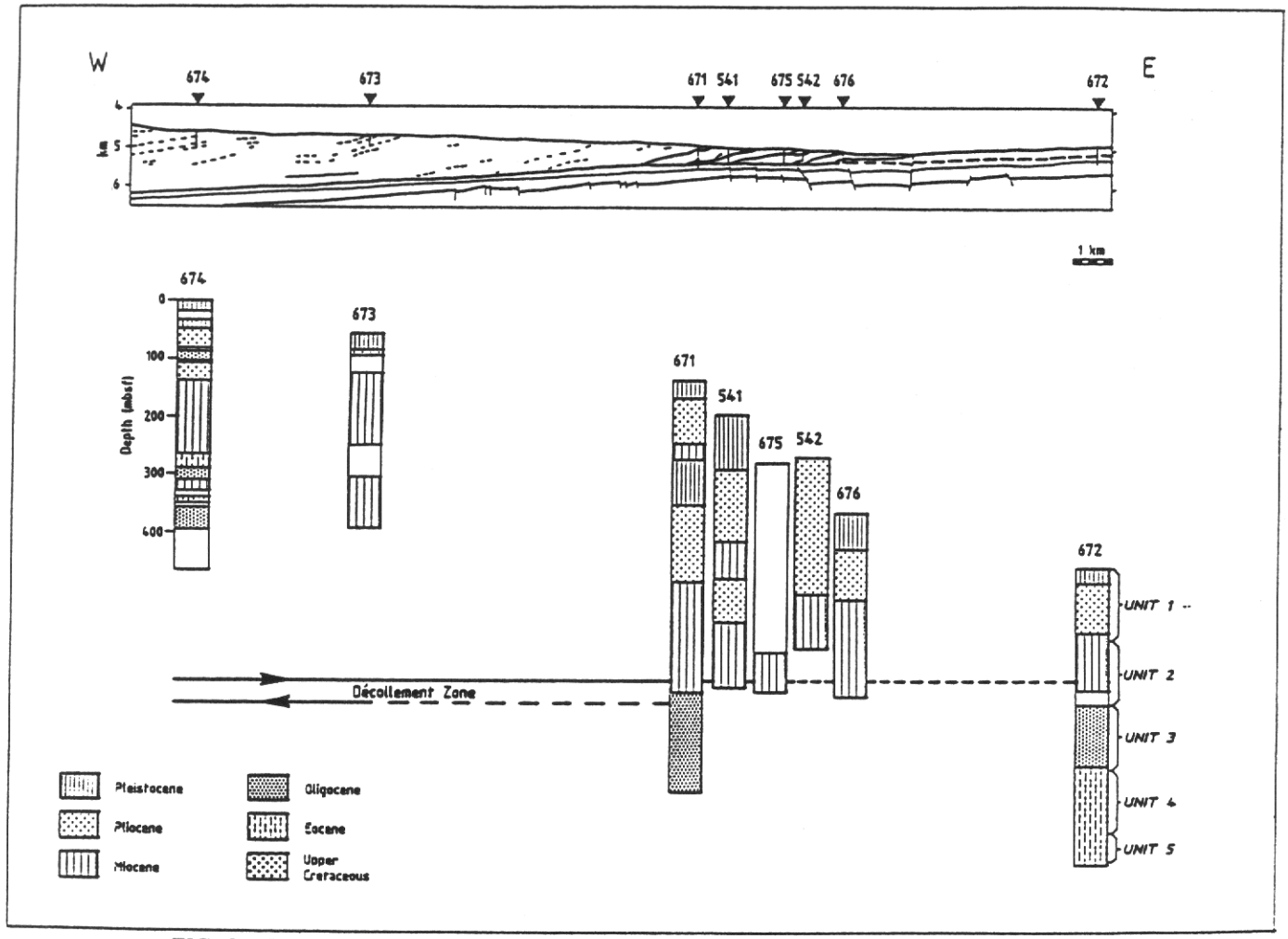

FIG. 3. Leg 78A and 110 sites projected onto an interpreted cross section along seismic Line C2114 (modified from MOORE, MASCLE et al, 1988)

The data fulfill a number of pre-requisites essential to the application of the reconstructional approach outlined above:

- all seven drill sites in the frontal part of the wedge toe as well as two reference sites in front of the deformation zone are located along one seismic line. There is good stratigraphic correlation among all sites, with the reference sections reaching stratigraphic levels below the lowermost sections recovered in the accreted sequences.
- Coring of holes was adequate to provide a good physical property data coverage of all sites.

There are four basic steps involved in the implementation of the proposed reconstruction procedure:

1. Data input

All physical property data that were routinely determined during Leg 78A were supplied through the DSDP database system; relevant physical property data on Leg 110 were made available by a shipboard scientist (J. Behrmann, Giessen). Error checking revealed only few serious data inconsistencies, that made correction or omission necessary.

2. Definition of correlation table

Using the biostratigraphic information given in MOORE & BIJU- DUVAL et al., 1984 and in the ODP-Preliminary-Report on Leg 110 a correlation table was defined to relate the position and vertical extension of the major lithological units in the wedge sites and the reference sites.

3. Resequencing

This information was utilized to carry out a resequencing procedure. All the data locations from the wedge sites were rearranged into the correct biostratigraphic order according to their original position in the reference section to establish a synthetic composite profile.

4. Decompaction

The decompaction procedure was carried out using a simple exponential compaction equation, the parameters of which were determined using the DSDP sediment physical property database of Legs 1-96.

5. Synthesis

The final steps of the reconstruction procedure involved the combination of all reassembled and decompacted data.

Implementation of proposed reconstruction procedure

Resequencing was carried out using the above defined correlation tables. Respective new data positions were calculated using the following scheme:

$$(1.1)\quad POS_{new} = LB_{act} + ((POS_{old} - UB_{act}) + \frac{UB_{act} - LB_{act}}{UB_{ref} - LB_{ref}}$$

POS_{old}, POS_{new} represents the actual (old) and the calculated (new) positions in the hole (mbsf), LB_{ref} and UB_{ref} indicat the lower and upper boundary of the reconstructed unit in the reference drillhole. LB_{act} and UB_{act} represent the lower and upper boundary of the reconstructed unit (mbsf). The difference between POS_{new} and POS_{old} determines the amount of decompaction necessary to account for the difference in vertical gravitational loading.

Decompaction is accomplished using an exponential porosity vs. depth relation of the type:

$$(1.2)\quad n(z) = n(0) * e^{(\beta * z)}$$

were z represents depth in mbsf, n fractional porosity, $n(0)$ porosity at the seafloor (1 mbsf). This type of compaction equation was first proposed by ATHY, 1930, and is generally accepted as a good approximation for gravitational compaction. The value of the dimensionless constant β is lithology controlled. Using the old and reconstructed depth data calculated in (1.1), decompacted porosities can be calculated for the respective depths by:

$$(1.3)\quad n_{new} = n_{old} + ((n_0 - e^{(POS_{new} * \beta)}) - (n_0 - e^{(POS_{old} * \beta)})$$

Appropriate values for β were derived from a statistical analysis of the DSDP sedimentological and mass physical property database. Type curves were defined for the compactional behavior of pelitic and psammitic sediments of low carbonate content.

After completion of the resequencing and decompaction procedures the effects of additional gravitational loading due to imbrication alone have been removed. Reference curve and reconstructed partial curves should be congruent if the difference in loading were the only factor modifying porosity in an imbricated stack of accreted sediments. All resequenced and decompacted porosity vs. depth data were finally combined into a composite scattergram. In the following the reconstructed profile encompassing all sites is allways compared to the reference site 672.

Results of porosity reconstruction

Since most of the reconstructed data belong to either units 1 or 2 (Table 1), the reconstruction is well constrained by the large number of data from all sites in the uppermost 200 m.

Table 1: Site 672 : Lithology

UNIT 1 :	0 – 123 m	(Early Pleistocene to Late Miocene) Calcareous clay and mud, frequent ash layers, traces of biogenic siliceous components. $CaCO_3$: 20 to 45 %
UNIT 2 :	124 - 228 m	(Late Miocene to Late Oligocene) A: Mudstone, claystone, few ash-layers, $CaCO_3$ low B: Claystone, siliceous claystone, ash layers C: Claystone, mudstone, laminated silt intervals
UNIT 3 :	229 - 332 m	(Late Oligocene to Early Oligocene) Interbedded claystone, calcareous mudstone and marl; thin quartz–silt laminae, $CaCO_3$: 0–50 %
UNIT 4 :	333 - 446 m	(Early Oligocene to Middle Eocene) Interbedded claystone, laminated calcareous mudstone, micritic limestone and calcarenite; glauconitic sand layers; $CaCO_3$: 0 to 60 %
UNIT 5 :	447 - 494 m	(Middle Eocene to Early Eocene) Siliceous claystone, shaly in lower part, $CaCO_3$ nil

Visual comparison revealed some similarity in the data distributions of both reconstruction and reference scattergrams. To quantify this observation, the original as well as the reconstructed data sets were treated with a moving average (single pass) smoothing procedure. Comparison of the reference and reconstruction (Fig. 4) shows close correlation of both curves, that are following the same general trend with depth, the reconstruction being always a little lower than the reference. They are parallel even in the range between 100 and 200 m, were an anomalous pattern of lithologically controlled porosity increase with depth also marks the stratigraphic niveau of décollement. A closer look at the depth range from 0 to 250 mbsf which is best supported by data, suggests that the difference between both curves is not randomly distributed but closely correlated with lithological composition of the reference section (Fig. 5 A). A comparison with the table of lithological units (Tab. 1) shows that the divergence in porosity is regularly in– and decreasing from top to bottom being smallest close to unit boundaries. This effect is clearly visible in unit 1.

In yet another closeup encompassing mainly unit 1 (0 – 123 m) — porosity divergence again shown separately on the left — it is clearly visible, that the porosity gap is increasing with depth (Fig. 5 B). This divergence can very well be approximated by the simple exponential regression (Fig. 6).

$$(1.4)\quad \delta_{POR} = 3.783 * (1 - e^{(-0.02418 * z)})$$

This function is quantifying the modeled additional porosity reduction as a function of depth. This additional compaction compared to normal consolidation is due mainly to the stress conditions present in the accretionary wedge.

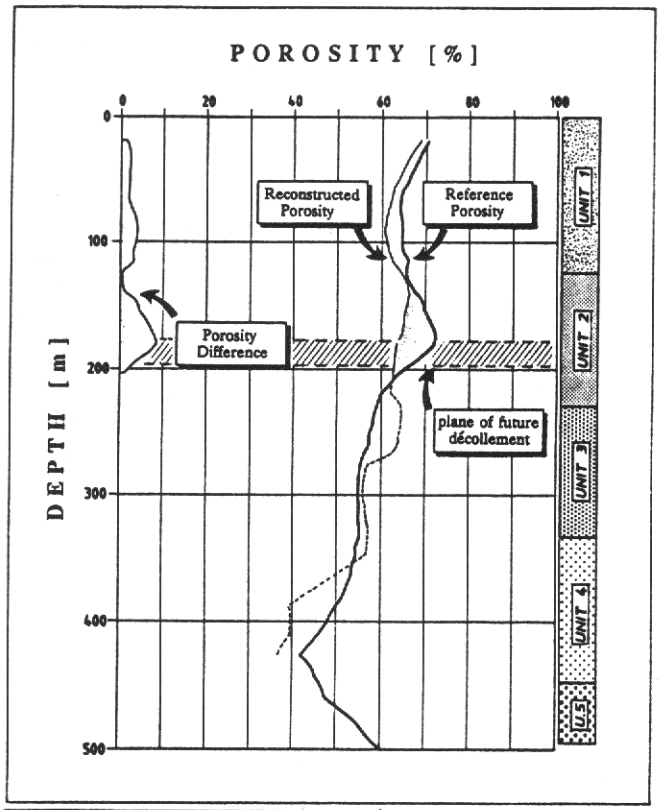

FIG. 4. Comparison of reconstructed and reference porosity–depth profiles. Stippled lines indicate areas of poorly constrained data. Porosity difference marked separately on the left.

Implications and applications

The next logical step in the analysis of the state of stress in the wedge is therefore the substitution of the parameter depth in the last equation with stress. This reassesment of the relation can be accomplished using site 672 data (MASCLE, MOORE et al, 1988, p. 242, fig. 42 – lithostatic stress) on the stress vs. depth relation. Assessment of the necessary amount of additional lateral loading is easiest accomplished by application of the same general reconstruction procedure again, using a stress vs. porosity instead of a depth vs. porosity relation. This was done by applying a linear relation between total stress and depth to (1.4) from which ultimately a homologous relation between porosity and stress can be defined. It presents the reconstruction–reference discrepancy with depth in a similar fashion.

$$(1.5) \quad \sigma_v = -3423 * \left(1 - e^{(0.1015 * \delta_{POR})}\right)$$

σ_v (effective vertical load) is expressed as a function of δ_{POR}, the appropriate regression curve (fig. 6 B) demonstrates the interrelationship of additional porosity reduction and the inferred total vertical loading. To understand

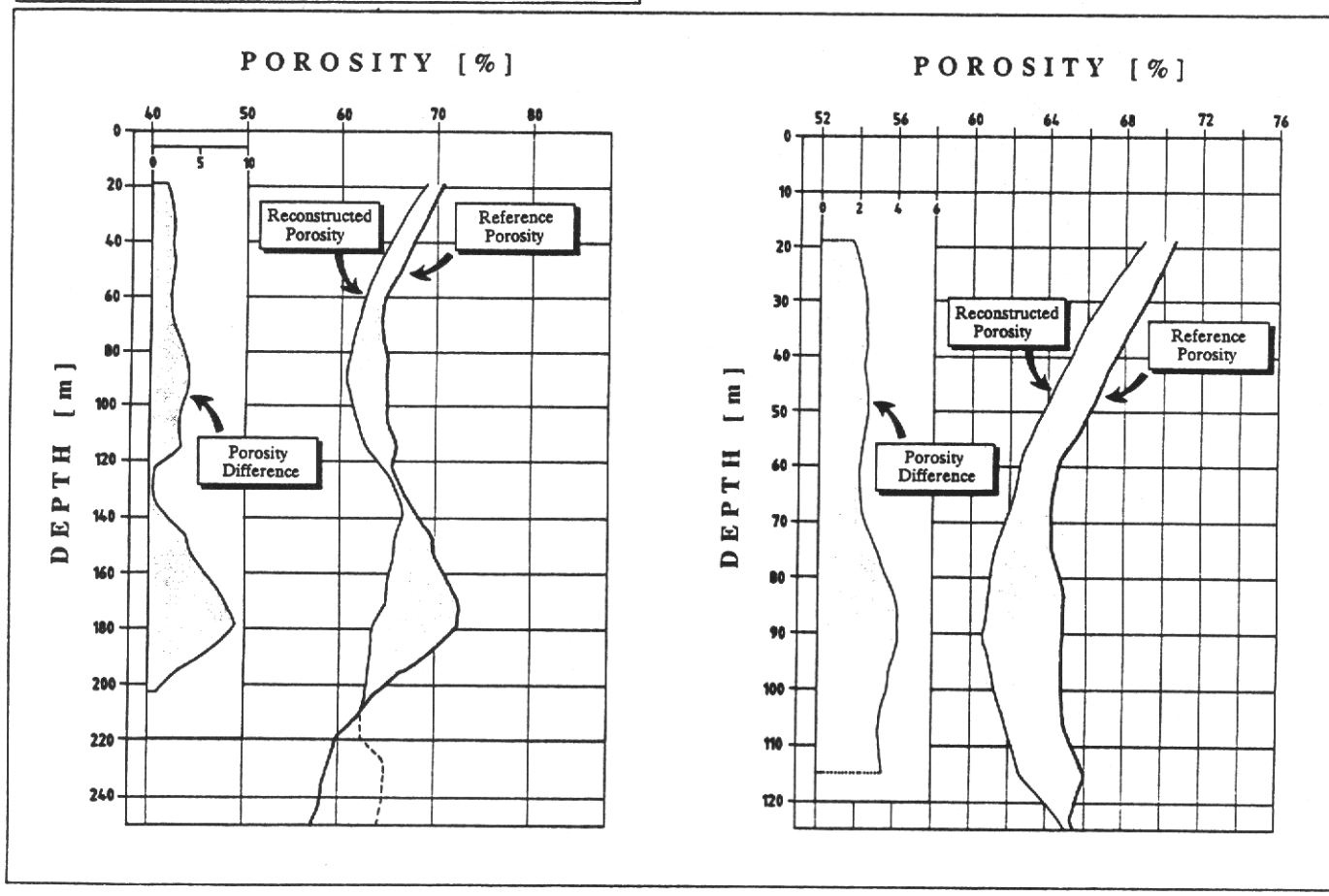

FIG. 5. Comparison of reconstructed and reference porosity–depth profiles
(A) Depth range 0 – 250 m (unit 1 and unit 2)
(B) Depth range 0 – 125 m (unit 1)

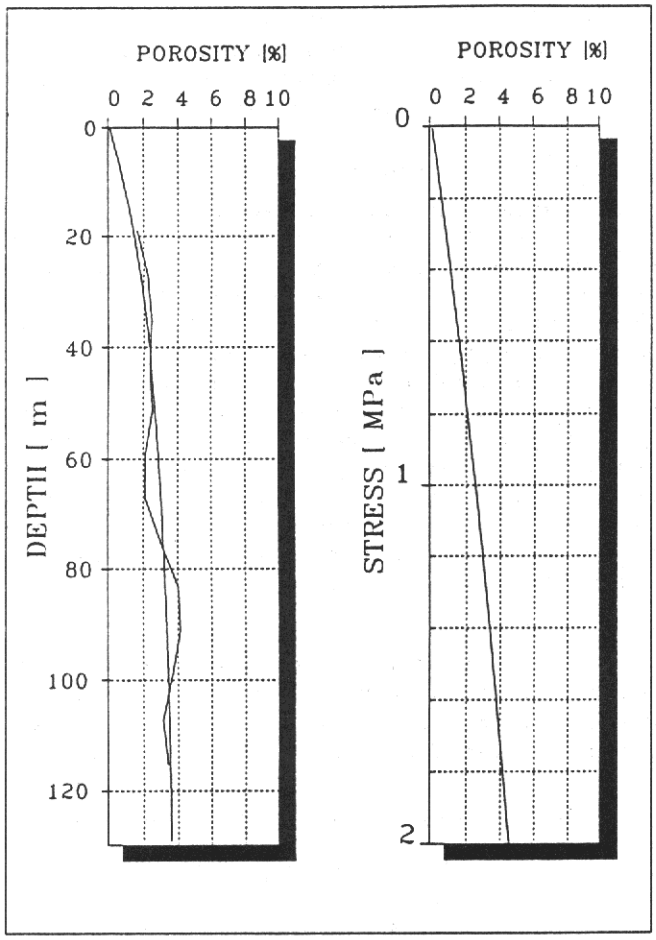

FIG. 6. (A) Regression of modeled porosity difference vs. depth
(B) Regression of modeled porosity difference vs. effective vertical stress

the relevance and possible implications pertinent to this function, some basic soil mechanical aspects of sediment compaction must be understood. During "normal" (uniaxial loading) gravitational consolidation a constant ratio K_0 of σ_v and lateral loads (σ_h) is maintained (eq. 1.6).

(1.6) $K_0 = (\sigma_v/\sigma_h)$

K_0 is a lithology dependent constant that is related to angle of internal friction by:

(1.7) $K_0 = (1 - \sin\Phi)$

This relation is valid for sediments under loading pressures of up to 100 MPa (LAMBE & WHITMAN, 1979). K_0 values of 0.6 are characteristic for marine sediments of the type discussed here (MOORE & BYRNE, 1986). Inserting this K_0-value into equation (1.6) the following relative amount of σ_v can be inferred for a normal uniaxial loading situation:

(1.8) $\sigma_v = 1.67 * \sigma_h$

This relative estimate of σ_v is valid for normal K_0 consolidation. It can be applied to determine the proportion of the lateral stress component in the convergent setting of the Barbados Ridge Complex. Redefining the modeled relation of additional porosity reduction and necessary additional vertical loading (eq. 1.5) using eq. (1.8) the following new equation holds:

(1.9) $\sigma_{h+} = (-3423 * (1 - e^{(0.1015 * \delta_{POR})})/1.67)$

were σ_{h+} expresses the amount of lateral stress necessary to cause the additional porosity reduction modeled for unit 1 sediments in the wedge. Comparison of the relative proportions of normal vertical, normal horizontal and additional horizontal stresses acting on unit 1 sediments facilitates the analysis of in situ stress conditions in the frontal on the wedge (Fig. 7). The relative impact of the modeled additional (or excess) stress on the observed compaction of unit 1 sediments is largest near the surface. Normal vertical and normal horizontal stress exceed the impact of additional lateral stress around 15 m and 75 m respectively.

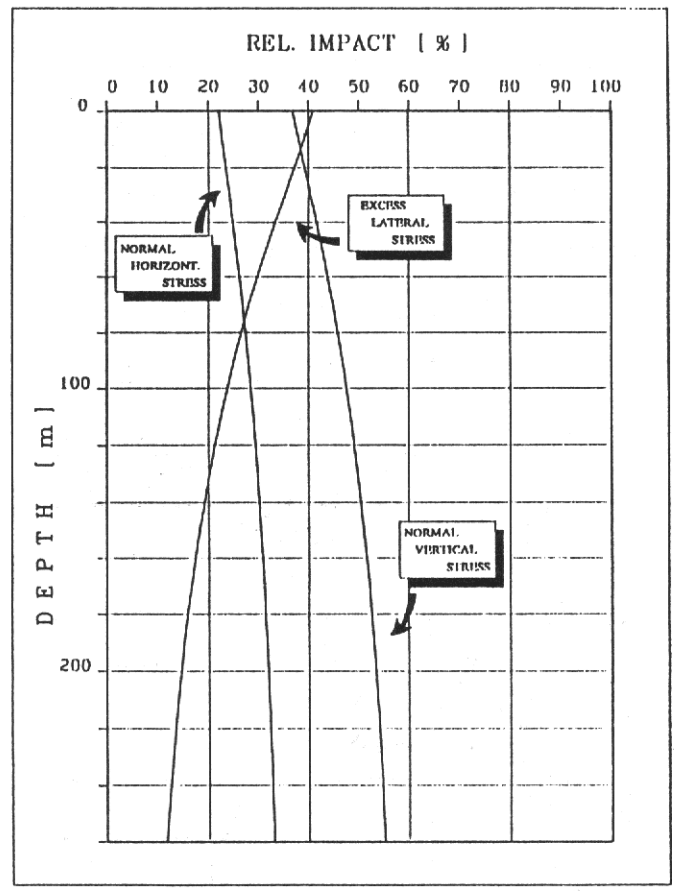

FIG. 7. Relative contribution of excess lateral, normal horizontal and vertical stress to total deformation

In a diagram of mean normal effective stress vs. shear stress — commonly termed σ–τ–diagram — the rest state consolidation path is identified by a straight line (Fig. 8).

(1.10) $\tau = (\sigma_v - \sigma_h)/2$

(1.11) $\sigma = (\sigma_v + \sigma_h)/2$

Stress paths that extend into the field of negative shear stress values are indicative of horizontal shortening and

thrust faulting, in soil mechanics called passive state and passive failure respectively (LAMBE & WHITMAN, 1969). During normal undisturbed consolidation sediments will follow a straight K_0–deformation path with σ and τ increasing with a constant ratio. Upon approaching a subduction zone sediments will deviate from the normal K_0–path. With horizontal stress here exceeding the vertical stress, the stress path is departing from the normal consolidation path, until shearing and detachment of a new wedge slice occurs (Fig. 8). This process has been described only qualitatively, since boundary conditions for sediment compaction in this tectonic setting are poorly known and physical properties of the involved sediments were rarely determined. Several stress path configurations previous to sediment failure are possible, depending on the type rheological properties assumed (in Fig. 8 indicated by E–T, E–O, E–P).

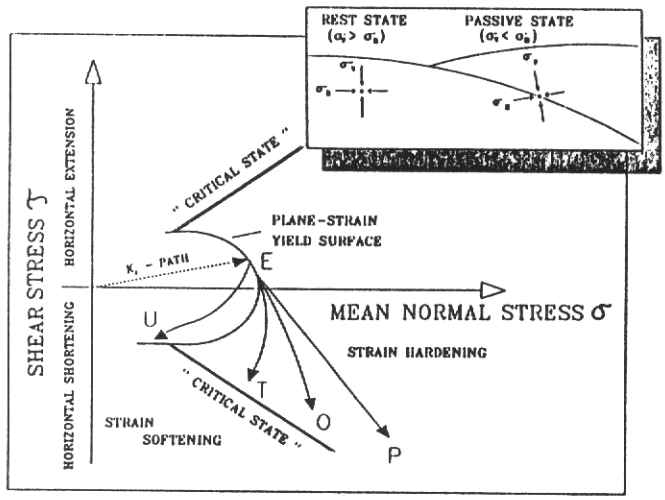

FIG. 8 Possible stress paths during accretion (modified from BRANDON, 1984)

Expressing the modeled and inferred vertical and horizontal stresses in terms of shear stress and mean normal effective stress it is possible to determine the state of stress for reconstructed unit 1 sediments. To do so, σ_{h+} has to be included in eq. (1.10) and (1.11):

$$(1.12) \quad \tau = (\sigma_v - (\sigma_h + \sigma_{h+}))/2$$

$$(1.13) \quad \sigma = (\sigma_v + (\sigma_h + \sigma_{h+}))/2$$

Thereby it is possible to present the in situ state of stress of unit 1 sediments as it can be inferred from the modeled additional lateral stress (Fig. 9).

DISCUSSION

The curve representing all reconstructed shear stress values for unit 1 sediments lies completely in the negative field of the diagram. The distribution of negative τ–values with depth is asymetric towards the upper part of unit 1. The obvious conclusion, that convergence–related lateral stress was compensated most intensively in the middle part of unit 1 is misleading. A realistic assessment of the compactional response of unit 1 sediments has to be based on a comparison of K_0–deformation path and the reconstructed in situ path, as indicated in Fig. 9. The strongest deviation from the normal isotropic consolidation path occurs at the base of unit 1, not in the middle part. This is indicated by a set of parallel stress vectors at random depths, that are connecting corresponding depths on the K_0–curve and the in situ–curve. The inclination of the stress vectors is in good agreement with a stress–path E–O (Fig. 8), which BRANDON, 1984 assumed to be typical for ductile deformation without failure in normally to underconsolidated sediments.

This result is supported by the observation, that few mayor shear zones or detachement planes or located in unit 1 sediments.

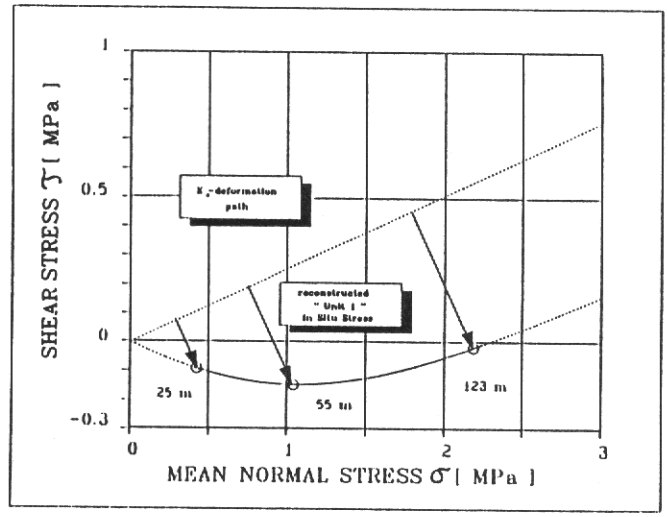

FIG. 9. State of stress during normal consolidation and during accretion (unit 1 sediments). Solid curve indicates reconstructed unit 1 data, the stippeled part their extrapolation. The straight line identifies normal K_0–consolidation path. See text for explanation.

CONCLUSIONS

A palinspastic reconstruction scheme, developed to study porosity changes in marine sediments during accretion was sucessfully applied to sediment mass physical property data from the accretionary Barbados Ridge Complex. From the results the following conclusions can be drawn:

- A restored composite porosity vs. depth profile exhibits strong similarity to an original profile from undeformed strata prior to accretion.
- After accounting for the effects of structural disruption and differential loading during accretion, porosity differences between undeformed sediments and their accreted counterparts remain significant, ranging from 2% to 9%.
- This phenomenon, which is best seen for the uppermost section of the reference site, can be approximated by an exponential function that relates the mode-

led additional porosity reduction to additional lateral loading.

- This quantification of the excess lateral stress can be employed in the analysis of the stress pathways sediments take during the process of accretion.
- Sediments of unit 1 in the oceanic reference section experienced strong lateral deformation during accretion, causing them to depart from the normal isotropic consolidation path. The prevailing consolidational process during accretion in this unit is ductile deformation without failure.

REFERENCES

AOKI, Y., TAMANI, T. & KATO, S., Detailled structure of the Nankai Trough from migrated seismic sections, In: Studies in Continental Margin Geology, Watkins, J.S., & Drake, C.L.(ed.), Am. Ass. Pet. Geol. Memoir, 34: 309–322, 1982.

ATHY, L. F., Density, porosity, and compaction of sedimentary rocks, Am. Ass. Pet. Geol., 14 (1): 24.

BALDWIN, B., & BUTLER, C.O., Compaction curves, Am. Ass. Pet. Geol. Bull., 69 (4): 622–626, 1985.

BIJU-DUVAL, B., LE QUELLEC, P., MASCLE, A., RENARD, V., & VALERY, P., Multibeam bathymetric survey and high resolution seismic investigations on the Barbados Ridge Complex (Eastern Caribbean): A key to the knowledge and interpretation of an accretionary wedge, Tectonophysics, 86: 275–304, 1982.

BOYER, S. E., & ELLIOT, D., Thrust systems, Am. Ass. Pet. Geol. Bull., 66, (9): 1196–1230, 1982.

BRANDON, M.T., A study of deformational processes affecting un– lithified sediments at active margins, Unpubl. PhD thesis, University of Washington, Seattle, Washington. 159 p., 1984.

BRAY, C.J., & KARIG, D.E., Porosity of sediments in accretionary wedges and some implications for dewatering processes, J. Geophys. Res., 90 (B1): 768–778, 1985.

BRÜCKMANN, W., Typical modes of sediment compaction and their modification in an active accretionary wedge (Barbados Ridge), PhD thesis (in German), Beitr. Geol. Inst. Univ. Tübingen, Rh. A, 6: 1–135. 1989.

CARSON, B., Tectonically induced deformation of deep–sea sediments off Washington and Northern Oregon: Mechanical consolidation, Marine Geol., 24: 289–307, 1977.

CARSON, B., VON HUENE, R., & ARTHUR, M., Small–scale deformation structures and physical properties related to convergence in Japan Trench slope sediments, Tectonics 1 (3): 277–302, 1982.

CARSON, B., & BERGLUND, P.L., Sediment deformation and dewatering under horizontal compression: Experimental results, In: MOORE J.C.(Ed.): Structural fabric in Deep Sea Drilling Project cores from forearcs, Geol. Soc. Am. Mem., 166: 135–150, 1986.

CHAPPLE, W.M., Mechanics of thin–skinned fold–and–thrust belts, Geol. Soc. Am. Bull., 89: 1189–1198, 1978.

COWAN, D.S., & SILLING, R.M., A dynamic, scaled model of accretion at trenches and its implications for the tectonic evolution of subduction complexes, J. Geophys. Res., 83 (B11): 5389–5397, 1978.

DAVIS, D. M., & VON HUENE, R., Inferences on sediment strength and fault friction from structures at the Aleutian Trench, Geology, 15: 517–522, 1987.

DAVIS, D. M., & HUSSONG, D. M., Geothermal observations during Deep Sea Drilling Project Leg 78A, In: BIJU–DUVAL, B. MOORE, J.C. et al., Init. Repts. DSDP, 78: 593–598, 1984.

DAVIS, D.M., The compressive mechanics of accretionary wedges applied to the Leg 78A study area near Barbados, In: BIJU– DUVAL, B. MOORE, J.C. et al., Init. Repts. DSDP, 78: 569–579, 1984.

DEMARS, K.R., & NACCI, V.A., Significance of Deep Sea Drilling Project sediment physical property data, Marine Geotechn., 3: 151–170, 1977.

DICKINSON, W.R. & SEELY, D.R., Structure and stratigraphy of forearc regions, Am. Ass. Pet. Geol. Bull., 63 (1): 2–31, 1979.

FOWLER, S.R., WHITE, R.S., & LOUDEN, K.E., Sediment dewatering in the Makran accretionary prism, Earth and Planetary Science Letters, 75: 427–438, 1985.

GRETENER, P.E., Pore pressure, discontinuities, isostasy and overthrusts, In: LEGGET, J.K.: Thrust and Nappe Tectonics, Geol. Soc. Spec. Publ., 9: 33–39, 1981.

HAMILTON, E.L., Prediction of deep–sea sediment properties: state of the art, In: INDERBITZEN, A.L.: Deep–sea sediments, physical and mechanical properties . Plenum Press, New York. 1–43., 1974.

HAMILTON, E.L., Variations of density and porosity with depth in deep sea sediments, J. Sed. Petr., 46 (2): 280–300, 1976.

JONES, M.E., & ADDIS, M.A., The application of stress path and critical state analysis to sediment deformation, J. Struct. Geol. 8, (5): 575–580, 1986.

KARIG, D.E., & SHERMANN III, G.F., Subduction and accretion in trenches, Geol. Soc. Am. Bull., 86: 377–389, 1975.

KARIG, D.E., Physical properties and mechanical state of accreted sediments in the Nankai Trough, Southwest Japan Arc, In: Moore, J.C.: Structural fabric in Deep Sea Drilling Project cores from forearcs, Geol. Soc. Am. Mem., 166: 117–133, 1986.

KNIPE, R.J., & NEEDHAM, D.T., Deformation processes in accretionary wedges — examples from the SW margin of the Southern Uplands, Scotland, In: COWARD, M.P., & RIES, A.C.(eds.): Collision Tectonics, Geol. Soc. Spec. Publ., 19: 51–65, 1986.

LAMBE, T.W., & WHITMAN, R.V., Soil mechanics, New York, John Wiley & Sons, 553 p., 1969.

LUCAS, S.E., & MOORE, J.C., Cataclastic deformation in accretio– nary wedges: Deep Sea Drilling Project Leg 66, southern Mexico, and on–land examples from Barbados and Kodiak Islands, In: MOORE, J.C.: Structural fabric in Deep Sea Drilling Project cores from forearcs, Geol. Soc. Am. Mem. 166: 89–104, 1986.

MAGARA, K., Water expulsion from clastic sediments during compaction – directions and volumes, Am. Ass. Pet. Geol. Bull. 60 (4): 543–553, 1976.

MAGARA, K., Compaction and fluid migration. Developments in Petroleum Science, Amsterdam (Elsevier), 319 p., 1978.

MARLOW, M.S., LEE, H.J., & WRIGHT, A.W., Physical properties of sediments from the Lesser Antilles Margin along the Barbados Ridge: Results from Deep Sea Drilling Leg 78A, In: BIJU–DUVAL, B. MOORE, J.C. et al., Init. Repts. DSDP, 78: 548–558, 1984.

MASCLE, A., BIJU–DUVAL, B., LETOUZEY, J., MONTANDERT, L., & RAVENNE,C., Sediments and their deformation in active margins off different geological settings, In: International Symposion on Geodynamics in the Southwest Pacific, Noumea, 1976. Paris (Ed. Technip), 327–344, 1976.

MASCLE, A., MOORE, J.C. and shipboard scientific party, Site 672, Proc. ODP, Part A, Init. Repts., Leg 110, 205–310, 1988.

MASCLE, A., MOORE, J.C. et al., Accretionary complex penetrated, defined, Geotimes, 32: 13–16, 1987.

MOORE, J.C, ROESKE, S., LUNDBERG, N., SCHOONMAKER, J., COWAN, D.S., & GONZALES, E., Scaly fabrics from Deep Sea Drilling Project cores from forearcs, Geol. Soc. Am. Mem., 166: 55–74, 1986.

MOORE, J.C., & BIJU–DUVAL, B., Offscraping and underthrusting of sediment at the deformation front of the Barbados Ridge: Deep Sea Drilling Project Leg 78A, Geol. Soc. Am. Bull., 93: 1065–1077, 1982.

MOORE, J.C., & BIJU–DUVAL, B., Tectonic Synthesis, Deep Sea Drilling Projekt Leg 78A: Structural evolution of offscraped and underthrust sediment, Northern Barbados Ridge Complex, In: BIJU–DUVAL, B. MOORE, J.C. et al., Init. Repts. DSDP, 78: 601–621, 1984.

MOORE, J.C., & BYRNE T., Thickening of fault zones: A mechanism of melange formation in accreting sediments, Geology, 15: 1040–1043, 1987.

MOORE, J. C, & MASCLE, A. et al., Tectonics and hydrology of the northern Barbados Ridge: Results from Ocean Drilling Program Leg 110, Geol. Soc. Am. Bull., 100: 1578–1593, 1988.

MOORE, J.C., & SILVER, E.A., Continental margin tectonics: submarine accretionary prisms, Reviews of Geophysics, 25 (6): 1305–1312, 1987.

NGOKWEY, K., Numerical modeling of sediment deformation linked to subduction: Mechanical model and comparison with Barbados ridge complex, In: BIJU–DUVAL, B. MOORE, J.C. et al., Init. Repts. DSDP, 78: 559–568, 1984.

PARK, M.J.M., Numerical analysis of deformation in the upper part of subduction zones. Unpubl. PhD thesis, University of Durham, Durham, England ,165 p., 1981.

SHI, Y., & WANG, C.Y., High pore pressure generation in sediments in front of the Barbados Ridge complex, Geophys. Res. Letters, 12 (11): 773 –776, 1985.

SHI, Y. & WANG, C.Y., Two dimensional modeling of the P–T–t paths of regional metamorphism in simple overthrust terrains, Geology, 15: 1048–1051, 1987.

SEELY, D.R., VAIL, P.R. & WALTON, G.G., Trench slope model, In: BURK, C.A. & DRAKE, C.L. (Eds.): The geology of continental margins. Springer (New York), 249–260, 1974.

SEYFERT, C.K., Undeformed sediments in oceanic trenches with sea floor spreading, Nature, 222: 70, 1969.

SILVER, E.A., ELLIS, M.J., BREEN, N.E., & SHIPLEY, T.H., Comments on the growth of accretionary wedges, Geology, 13: 6–9, 1985.

SPEED, R.C., Geology of Barbados: implications for an accretionary origin, Oceanologica Acta, 28: 259–265, 1981.

STOCKMAL, G.S., Modeling of large scale accretionary wedge deformation, J. Geophys. Res., 88 (B10): 8271–8287, 1983.

SUESS, E., KULM, L.D., CARSON, B. & WHITICAR, M.J., Fluid flow and methane fluxes from vent sites at the Oregon subduction zone, EOS, 68 (44): 1486, 1987.

TORRINI, R., SPEED, R.C., & MATTIOLI, G.S., Tectonic relations between forearc basin strata and the accretionary complex at Bath, Barbados, Geol. Soc. Am. Bull., 96: 861–874, 1985.

VON HUENE, R., Long décollements and mud volcanoes: Evidence from the Barbados ridge complex for the role of high pore fluid pressure in the development of an accretionary complex, Geology, 2: 279–283, 1983.

VON HUENE, R., Structural diversity along modern convergent margins and the role of overpressured pore fluids in subduction zones, Bull. Soc. Geol. France, XXVI (2): 207–219, 1984.

VON HUENE, R., & LEE, H.J., The possible significance of pore fluid pressure in subduction zones, Am. Ass. Pet. Geol. Memoir, 34: 781–791, 1983.

WESTBROOK, G.K., SMITH, M.J., PEACOCK, J.H. & POULTER, M.J., Extensive underthrusting of undeformed sediment beneath the accretionary complex of the Lesser Antilles subduction zone, Nature, 300: 625–628, 1982.

WOODWARD, D.J. Viscoelastic Finite Element analysis of subduction zones, Unpubl. PhD. thesis, University of Durham, Durham, England, 1976.

WRIGHT, A.W., Sediment distribution and depositional processes operating in the Lesser Antilles Island Arc, Eastern Caribbean, In:BIJU-DUVAL, B. MOORE, J.C. et al., Init. Repts. DSDP, 78A: 301–324, 1984.

ZHAO, W.L., DAVIS, D.M., DAHLEN, F.A., & SUPPE, J., Origin of convex accretionary wedges: Evidence from Barbados, J. Geophys. Res., 91 (B10): 10,246–10,258, 1986.

ORIGIN AND GEOLOGIC IMPLICATIONS OF DIAGENETIC LIMESTONE IN FAULT ZONES OF BARBADOS

Rudolph Torrini, Jr.
Woodward-Clyde Consultants
5055 Antioch Road
Overland Park, Kansas 66203

Robert C. Speed
Department of Geological Sciences
Northwestern University
Evanston, Illinois 60201

George E. Claypool
Mobil Research and Development
1377 Midway Road
Dallas, Texas 75244-4312

ABSTRACT

Fault zones and mud diapirs that crop out on Barbados Island in the crestal zone of the Barbados accretionary prism contain nodules and crusts of diagenetic limestone, limestone chimneys, molluscan fossils, and probable fossil tube worm casts. The limestone is only in fault zones that formed or were reactivated during the late (Miocene-Pliocene) history of the prism and is ^{13}C-depleted relative to marine carbonate sediments and seawater. Geologic and isotopic evidence exists for both gaseous and nongaseous petroleum precursors to the light limestone nodules. Overthrust outer forearc basin strata of the Oceanic allochthon provided a relatively impermeable seal to upward migrating fluids. The fault zones and diapirs were evidently the preferential pathway of fluid advection and escape. The association of the diagenetic limestone with limestone chimneys, molluscan fossils, and probable fossil tube worms suggests the emergence of fault zones at the seabottom and the existence of fluid escape vents like those at modern active margins. A thermogenic origin of the hydrocarbon is indicated, with source depths ranging from 3 to 20 km. Thus, hydrocarbon source rocks could include both shallow offscrape and deeper underplated rocks. Geologic and isotopic data suggest precipitation of limestone at low temperatures (5°-29°C) and shallow depths, perhaps at or near the seabottom. The occurrence of petroleum-derived carbonates in mud diapirs as well as fault zones suggests that fluid overpressure and advection of hydrocarbons may have been linked. Migration of hydrocarbons may have been induced or enhanced by water released during the smectite-illite transformation within overpressured rocks at depth.

INTRODUCTION

Fault zones and mud diapirs that crop out on Barbados Island in the crestal zone of the Barbados accretionary prism (Fig. 1A) contain nodules and crusts of diagenetic limestone, limestone chimneys, molluscan fossils, and probable fossil tube worm casts. The limestone is only in fault zones that formed or were reactivated during the late (Miocene-Pliocene) history of the prism and is ^{13}C-depleted relative to marine carbonate sediments and seawater. Its stable isotopic compositions and associated hydrocarbon residues provide important constraints on sources, source depths, temperatures, and principal migration paths of advecting fluids within the Barbados accretionary prism. In this paper, we describe the petrography, mineralogy, and stable carbon and oxygen isotopic compositions of the diagenetic limestone and discuss the geologic implications of the limestone for the defluidization processes within the Barbados accretionary prism. A companion paper (Torrini et al., 1990) describes early diagenetic carbonate that occurs in terrigenous and hemipelagic strata in the basal complex of Barbados.

43 samples of diagenetic limestone were collected from various fault zones and diapirs in the Scotland District of Barbados (Fig. 1B). The mineralogy of individual samples was determined by powder X-ray diffraction (XRD) using quartz as an internal standard, and separates of all powdered samples were analyzed at the U. S. Geological Survey, Lakewood, Colorado for carbon and oxygen isotopic composition. Standard isotopic analysis techniques were used, and data for both oxygen and carbon are presented in the normal δ notation with reference to the PDB standard.

GEOLOGY OF BARBADOS

The island of Barbados exposes the structural high of the accretionary prism of the active Lesser Antilles forearc (Fig. 1A) (Speed and Larue, 1982; Speed, Westbrook et al., 1984). The Scotland District of Barbados (Fig. 1B) is an erosional window through Pleistocene reef that caps the majority of the island. Outcrop and well studies indicate the existence of three major tectonic units beneath the reefcap (Fig. 1B) (Speed, 1988 and references therein). The highest unit is the Oceanic allochthon, whose beds were thrust east above the prism's structural high from the adjacent forearc basin. The Oceanic beds consist of terrigenous-free successions of lower bathyal-abyssal pelagic strata, mainly smectite-nanno-rad-foram marl and radiolarian mudstone, and interbedded volcanogenic turbidites and waterlaid tuffs that range in age from early middle Eocene to early middle Miocene (Torrini, 1988; Torrini et al., 1985). The intermediate unit is sporadically occurring prism cover of Miocene and possibly Oligocene age (Speed, 1988). The lowest unit is the basal complex, which is an assemblage of fault-bounded packets of terrigenous submarine fan and hemipelagic strata of probable early to late Eocene depositional age. The basal complex, which forms the foundation of the structural high of the accretionary prism and extends to depths $\geq$4 km, is thought to have formed by offscrape and accretion in late Eocene time. Organic carbon-rich mud diapirs cut the basal complex (Larue and Speed, 1984) and locally, the Oceanic allochthon (Torrini et al., 1985; Larue, 1988). The diapirs consist of angular blocks of sedimentary rocks from sand to 100 m sized, green mudstone granules, and foliated organic carbon-rich sandy mudstone matrix.

Evidence for modern emergence of fluids from the structural high of the prism include: (1) mud diapirs on and around Barbados (Torrini and Speed, 1989), (2) oil seeps from fault zones on Barbados, and (3) melt breccias on Barbados that indicate combustion around local vents of hydrodarbon gas.

DIAGENETIC LIMESTONE

The diagenetic limestone described in this paper occurs exclusively within organic carbon-rich mud diapirs and fault zones, including *intra-Oceanic fault zones* (OFZ) that separate nappes of Oceanic beds

Larue, D.K., and Draper, G. (eds.),
Transactions of the 12th Caribbean Geological Conference, St. Croix, U.S.V.I., Miami Geological Society, P.O. Box 431552, South Miami, FL 33243, U.S.A

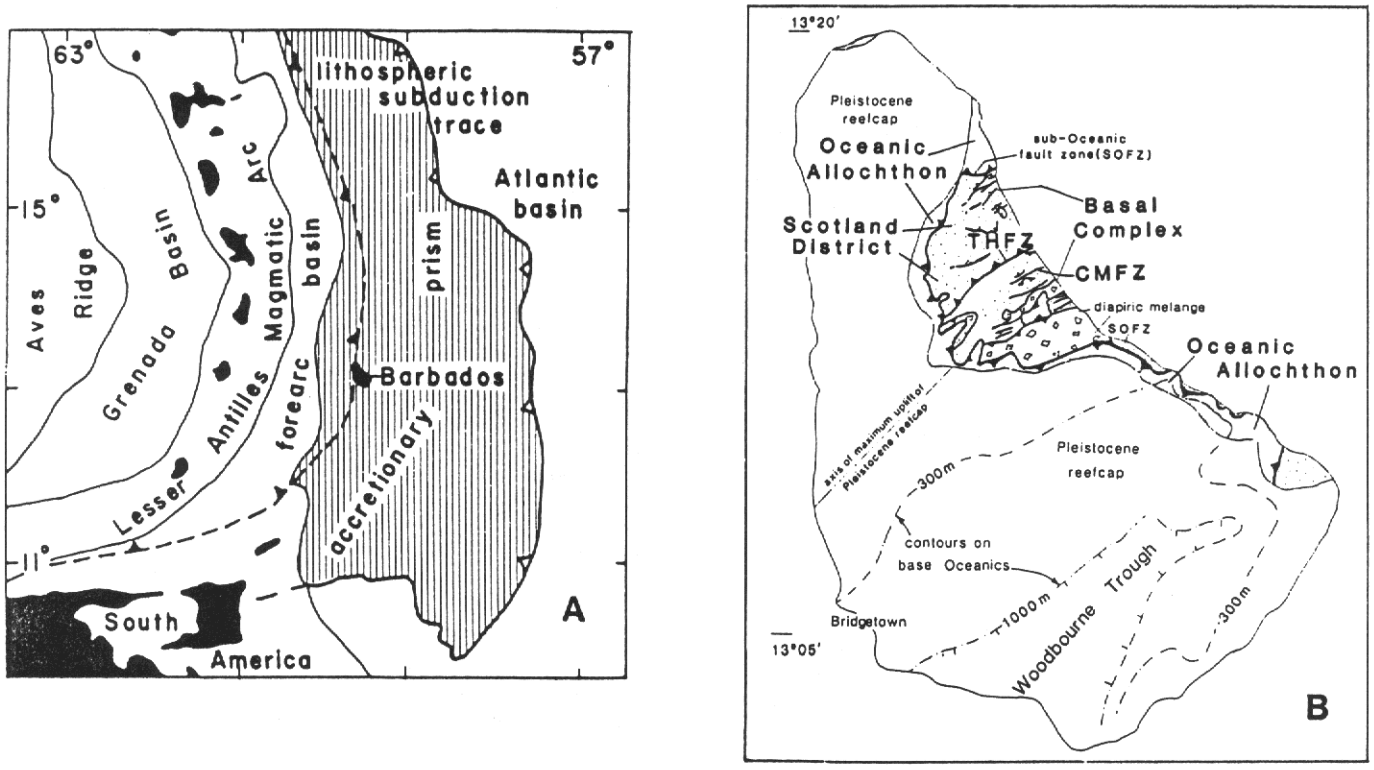

Figure 1. A) Index map showing location of Barbados Island at structural high of Lesser Antilles forearc; B) Generalized geologic map showing major tectonostratigraphic units of the Scotland District of Barbados. SOFZ, Sub-Oceanic Fault Zone; CMFZ, Chalky Mount Fault Zone; THFZ, Turner Hall Fault Zone.

within the Oceanic allochthon, the *sub-Oceanic fault zone* (SOFZ), which is the sole fault of the Oceanic allochthon, and *reactivated fault zones within the basal complex*, including the Turner Hall fault zone (THFZ) and the Chalky Mount fault zone (CMFZ) (Fig. 1B). The OFZ and SOFZ are semitabular zones of variable thickness that consist of one or more discrete striated fault surfaces whose walls contain foliated clay-rich insoluble residues that are relics from dissolution of carbonate in Oceanic beds. Motions in the OFZ and SOFZ are no older than Miocene, the age of emplacement of the Oceanic allochthon according to paleontological constraints (Speed, 1988). Reactivated fault zones of the basal complex are distinguished by the existence of late structures that represent departures from early kinematics and apparently reflect late intraprism contraction (Speed, 1983). The age of reactivation of the CMFZ is unknown, but renewed motion on the THFZ probably includes Miocene and (or) Pliocene components. Displacements in the above mentioned fault zones were taken up under shallow, brittle conditions, resulting in the formation of cleavage, microfractures, and broken formation that clearly increased the permeability of fault zone rocks relative to wall rocks.

The main features of the limestone nodules and crusts are their occurrence as discrete bodies and evidence for a diagenetic rather than depositional or biostromal origin. The limestone bodies are composed strictly of calcite. They are sharply bounded but are variably tabular to equant, centimeter to several meters in length, and dispersed or concentrated. Most are massive, but some contain relict sedimentary lamination. In fault zones, limestone nodules are commonly aligned in horizons that parallel the local fault zone boundaries (Torrini et al., 1985). Fault zones at several localities include limestone chimneys, molluscan limestone, and limestone tubes in sinuous, intertwined clusters (Larue and Suess, 1985; Speed et al., 1985). The limestone chimneys are evidence of ancient fluid escape at seabottom vents, and the molluscan limestone and limestone tubes are interpreted as associated vent-based benthic communities (mollusks, tube worms). Thus, at least part of the diagenetic limestone is thought to have precipitated at or near the sediment/water interface.

Four different diagenetic textures are recognized amongst the limestone: (1) radiaxial calcite in replacive radiating sheaves (microcabbageheads) and in microveinlets, often in cross-cutting sets, (2) pore-filling blocky calcite, (3) replacive micritic calcite, and (4) replacive rhombohedral calcite. Two or more of the textures commonly occur within a single specimen. Precursor material, preserved in vanishing to moderate quantities, includes quartz, feldspar, clay, siliceous tests, and solid organic substances. Calcareous biogenic particles are generally absent. Masses of diagenetic calcite locally cross-cut and replace foliated fault zone rock, clearly indicating that limestone precipitation was syn- or post-faulting.

The preferential occurrence of isotopically light limestone in the SOFZ, OFZ, and reactivated fault zones of the basal complex suggests that fluid migration and limestone precipitation were genetically related to late intraprism contraction and emplacement

of the Oceanic allochthon in Neogene time. Thus, limestone precipitation probably began no earlier than early Miocene. Limestone nodules in mud diapirs may be fault-zone related protoliths or diagenetic products of hydrocarbon degassing during diapirism. Such diapirism is thought to have occurred at least partly since early Miocene time (Larue and Speed, 1984; Speed, 1988). It may have been generally coeval with contraction and uplift in the crestal zone of the prism and with the Neogene reactivation of old accretionary surfaces in the basal complex and emplacement of the Oceanic allochthon.

ISOTOPIC COMPOSITIONS AND INTERPRETATIONS

The $\delta^{13}C$ and $\delta^{18}O$ values of the diagenetic limestone range from -15.1 and -54.5 o/oo and -1.42 to +2.12 o/oo (PDB), respectively (Fig. 2). The $\delta^{13}C$ compositions are atypical of marine carbonate sediment and indicate that the carbon in the calcite is at least partly organic. Approximately one third of the $\delta^{13}C$ values are lighter than those of carbon of nongaseous organic material (-21 to -28 o/oo), indicating a conctribution of carbon from hydrocarbon gases, presumably methane. The confined occurrence of isotopically light limestone to fault zones and diapirs suggests that the methane migrated along fault zones and diapiric pathways from depth and was not a stratiform accumulation generated by shallow, in situ bacterial decay of organic matter. Geologic and isotopic evidence exists for both gaseous and nongaseous petroleum precursors to the light limestone nodules, and the majority of $\delta^{13}C$ values are inconsistent with inorganic carbon precursors. The methane source was probably mainly thermogenic, not biogenic because the compositional range of the limestone nodules does not include any $\delta^{13}C$ values that can be uniquely attributed to a biogenic methane precursor (e.g. -75 to -90 o/oo; Rice and Claypool, 1981) and because oil seeps and asphaltic hydrocarbon residues found in certain fault zones were generated at temperatures ≥100°C.

Because of geologic evidence for precipitation of at least part of the limestone around ancient seabottom fluid escape vents, the water fraction of the limestone-forming fluids may have consisted of various proportions of diagenetic pore water and sea water. The $\delta^{18}O$ value of the fluids was probably ≥ -2.0 o/oo because more negative values yield calculated equilibration temperatures colder than the minimum known temperature of bottom water (2°C; Kennett, 1982). Precipitation of the limestone is thought to have occurred in Neogene time when major glaciation certainly affected the $\delta^{18}O$ composition of the world oceans (Kennett, 1982). Accordingly, we have calculated temperatures of formation of the limestone (Craig, 1965) assuming isotopic equilibration with $\delta^{18}O$ fluid compositions of -1.2 o/oo (SMOW, nonglacial oceans; Shackleton and Kennett, 1975)) and +1.2 o/oo (SMOW, oceans at glacial maxima; Kennett, 1982; E. Birchfield, personal communication, 1986). The calculated isotopic equilibration temperatures, which range from 5°-29°C, are relatively low, supporting our geologic interpretation that precipitation of the limestone in fault zones and diapirs occurred at shallow depths, perhaps at or near the seabottom.

The hydrocarbon-derived component of the diagenetic fluids originated from both solidified oil and methane. Estimated source depths for the oil and methane based on the temperature range for thermal catagenesis (75°-300°C) and a geothermal gradient on Barbados of 15°C/km (Larue et al., 1985) range from 3 to 20 km. This indicates that hydrocarbon source

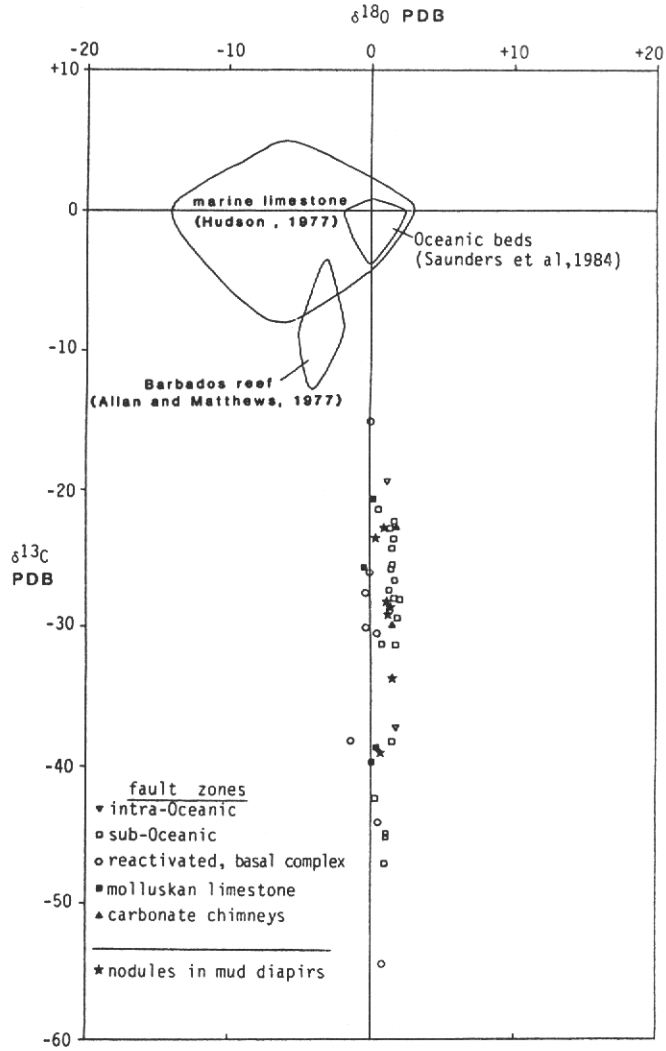

Figure 2. Stable carbon and oxygen isotopic compositions of diagenetic limestone nodules in fault zones and mud diapirs of Barbados.

rocks could include both shallow offscraped and underplated rocks at the base of the accretionary prism. Geologic and isotopic lines of evidence suggest precipitation of the limestone at relatively low temperatures (5°-29°C) and shallow depths, perhaps at or near the seabottom. Thus, potential sources of the water fraction of the diagenetic fluids are: (a) seawater that was contemporaneous with emergent faulting and (or) seabottom fluid venting, (b) shallow origin diagenetic pore water from the Oceanic allochthon or shallow levels within the prism, or (c) deep origin diagenetic pore water that cooled during advection from deeper levels within the prism. The occurrence of petroleum-derived nodules in mud diapirs as well as fault zones suggests that fluid overpressure and advection of hydrocarbons were linked. Migration of hydrocarbons may have been induced or enhanced by water released during the dehydration of expandable layer clays within overpressured rocks at depth.

Oxidation of hydrocarbons probably ocurred by one or more of the following mechanisms: 1) exposure to oxygenated seawater in the aerobic zone (≤1 m), 2)

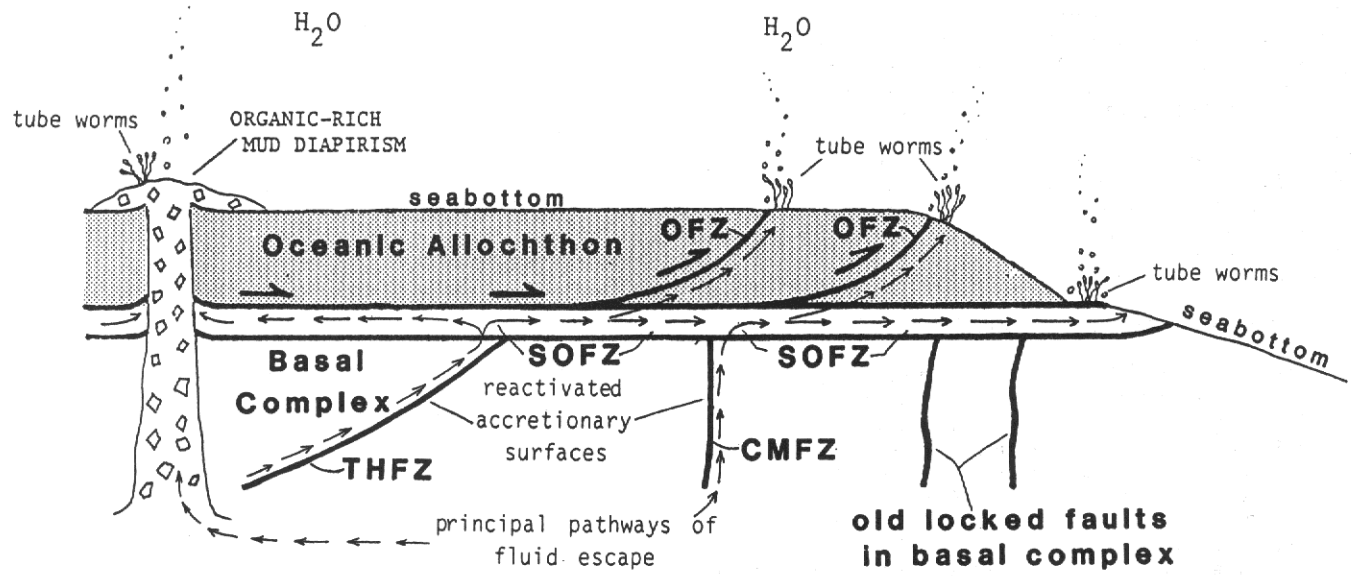

Figure 3. Schematic diagram showing principal pathways of fluid migration and escape from the crestal zone of the Barbados accretionary prism; heavy lines are faults; CMFZ, Chalky Mount Fault Zone; THFZ, Turner Hall Fault Zone; SOFZ, Sub-Oceanic Fault Zone; OFZ, Intra-Oceanic Fault Zones. Tube worms thrive at seabottom where methane-bearing fluids are expelled.

circulation of oxygenated seawater through fault zones, or 3) anaerobic bacterial processes within the zone of sulfate reduction (Hudson, 1977; Rice and Claypool, 1981). We speculate that oxidation of the hydrocarbons generated light CO_2 which increased the acidity of the upward-migrating fluids and led to dissolution of marine carbonate rock in fault zone walls. The consequent introduction of HCO_3 from calcareous wall rocks would have increased the pH, causing biogenic silica and phyllosilicates to dissolve and calcite to precipitate.

GEOLOGIC IMPLICATIONS

Late events in the history of the accretionary prism are recorded by structures in the basal complex, Miocene prism cover, and the Oceanic allochthon. These include Neogene arcward tectonic wedging of the prism into the forearc basin succession and associated oceanward thrusting of outer forearc basin strata of the Oceanic allochthon above the prism's structural high. Such Neogene motions were accompanied by intraprism contraction by motions on reactivated faults in the basal complex and mud diapirism. During these later stages, turbiditic sandstone interbeds in the basal complex were relatively impermeable due to cementation by early diagenetic carbonate (Torrini et al., 1990). Moreover, smectite-rich beds of the overthrust Oceanic allochthon provided a relatively impermeable seal to advecting fluids of the accretionary prism. Thus, mud diapirs, reactivated fault zones of the basal complex, and the sub- and intra-Oceanic fault zones of the Oceanic allochthon were the principal pathways of fluid advection and escape from the accretionary prism (Fig. 3). Secondary (fracture) permeability was clearly important in providing an avenue for fluid escape.

A record of early (Eocene) fluid venting from the accretionary prism apparently is lacking, at least from exposures on Barbados. The petroleum-derived diagenetic limestone described in this paper occurs only in fault zones with late (Neogene) displacements. The absence of a diagenetic record of early fluid venting might be explained by: (a) erosion of shallow prism rocks that contained the early diagenetic carbonate record, (b) lack of carbonate precipitation due to trapping of methane in gas hydrate, or (c) lack of carbonate precipitation due to local anoxia that discouraged oxidation of methane for incorporation into diagenetic carbonate.

CONCLUSIONS

Fault zones and mud diapirs on Barbados contain petroleum-derived diagenetic limestone nodules and crusts. The diagenetic limestone is only in fault zones that formed or reactivated during the late (Miocene-Pliocene) history of the accretionary prism. Fault zones and diapirs were evidently the preferential pathway of fluid advection and escape (Fig. 3). Overthrust outer forearc basin strata of the Oceanic allochthon provided a relatively impermeable seal to upward migrating fluids. The association of the diagenetic limestone with limestone chimneys, molluscan fossils, and probable fossil tube worms suggests the emergence of fault zones at the seabottom and the existence of fluid escape vents like those at modern active margins. A thermogenic origin of the hydrocarbon is indicated, with source depths ranging from 3 to 20 km. Thus, hydrocarbon source rocks could include both shallow offscrape and deeper underplated rocks. Geologic and isotopic data suggest precipitation of limestone at low temperatures (5°-29°C) and shallow depths, perhaps at or near the seabottom. The occurrence of petroleum-derived carbonates in mud diapirs as well as fault zones suggests that fluid overpressure and advection of hydrocarbons may have been linked. Migration of hydrocarbons may have been induced or enhanced by water released during the smectite-illite transformation within overpressured rocks at depth.

ACKNOWLEDGEMENTS

This research was supported by Department of Energy Grant No. DE-AC21-84 MC21132, National Science Foundation Grant INT82-12272, and PRF Grant 12669-AC2, all to R. C. Speed. We are grateful to the U. S. Geological Survey for use of facilities for isotopic analyses.

REFERENCES CITED

Allan, J. R., and Matthews, R. K., 1977, Carbon and oxygen isotopes as diagenetic and stratigraphic tools: Surface and subsurface data, Barbados, West Indies: Geology, v. 5, p. 16-20.

Craig, H., 1965, The measurement of oxygen isotope paleotemperatures: in Proceedings, Speleto Conference on Stable Isotopes: Oceanographic Studies and Paleotemperatures, no. 3.

Hudson, J. D., 1977, Stable isotopes and limestone lithification: J. Geol. Soc. London, v. 133, p. 637-660.

Kennett, J. P., 1982, Marine Geology: Englewood Cliffs, New Jersey, Prentice Hall, Inc., 813 p.

Larue, D. K., 1988, Nappe Dismemberment by Melange Intrusion, Cattlewash, Barbados: Trans. 11th Carib. Geol. Conf. (1986), p. 30:1-30:14.

----------, Schoonmaker, J., Torrini, R., Jr., Lucas-Clark, J. Clark, M., and Schneider, R., 1985, Barbados: maturation, source rock potential and burial history within a Cenozoic accretionary complex: Marine and Petroleum Geology, v. 2, p. 96-110.

----------, and R. C. Speed, 1984, Structure of the accretionary complex of Barbados, II: Bissex Hill: Geol. Soc. America Bull., v. 95, p. 1360-1372.

----------, and Suess, I., 1985, Eocene Subduction-driven Vent Community, Joes River Melange, Barbados: (abstract), Trans., American Geophysical Union, v. 66, no. 46, p. 1097.

Rice, D. D., and Claypool, G. E., 1981, Generation, accumulation, and resource potential of biogenic gas: Am. Ass. Pet. Geol. Bull., v. 65, no. 1, p. 5-25.

Saunders, J. B., Bernoulli, D., Muller-Merz, E., Oberhansli, H., Perch-Nielsen, K., Riedel, W. R., Sanfilippo, A., and Torrini, R., Jr., 1984, Stratigraphy of the late Middle Eocene to Early Oligocene in the Bath Cliffs Section, Barbados, West Indies: Micropaleontology, v. 30, no. 4, p. 390-425.

Shackleton, N. J., and Kennett, J. P., 1975, Paleotemperature History of the Cenozoic and Initiation of Antarctic Glaciation: Oxygen and Carbon Isotope Analyses in DSDP Sites 277, 279, and 281: in Kennett, J. P., Houtz, R. E., and others, Initial Reports of the Deep Sea Drilling Project, Volume 29: Washington, D. C., U. S. Government Printing Office, p. 743-755.

Speed, R. C., 1983, Structure of the accretionary complex of Barbados,I: Chalky Mount: Geol. Soc. America Bull., v. 94, p. 92-116.

----------, 1988, Tectonostratigraphy of Barbados: A Preliminary Synthesis: Trans. 11th Carib. Geol. Conf., Barbados (1986), p. 29:1-29:11.

----------, and Larue, D. K., 1982, Barbados: Architecture and Implications for Accretion: J. Geophys. Res., 87, No. B5, p. 3633-3643.

----------, R. Torrini, Jr., and G. E. Claypool, 1985, Ancient fluid escape vents in a Cenozoic accretionary complex: 98th Annual Meeting of the Geol. Soc. Am., Abs. with Prog., 17, p. 723, 1985.

----------, G. K. Westbrook, et al., 1984, Atlas 10 Ocean Margin Drilling Program, Lesser Antilles and Adjacent Ocean Floor: Marine Science Institute Publications, Woods Hole, Massachussets.

Torrini, R., Jr., 1988, Structure and Kinematics of the Oceanic Nappes of Barbados: Trans. 11th Carib. Conf., Barbados (1986), p. 15:1-15:15.

----------, and Speed, R. C., 1989, Tectonic Wedging in the Forearc Basin/Accretionary Prism Transition, Lesser Antilles Forearc: J. Geophys. Res., v. 94, no. B8, p. 10549-10584.

----------, Speed, R. C., and Claypool, G. E., 1990, Stable Isotopic Compositions of Diagenetic Carbonate in Hemipelagic and Terrigenous Submarine Fan Strata, Barbados, West Indies: Trans. 12th Carib. Geol. Conf., St. Croix, this volume.

----------, Speed, R. C., and Mattioli, G. S., 1985, Tectonic relationships between forearc basin strata and the accretionary complex at Bath, Barbados: Geol. Soc. America Bull., v. 96, p. 861-874.

STABLE ISOTOPIC COMPOSITIONS OF DIAGENETIC CARBONATE IN HEMIPELAGIC AND TERRIGENOUS SUBMARINE FAN STRATA, BARBADOS, WEST INDIES

Rudolph Torrini, Jr.
Woodward-Clyde Consultants
5055 Antioch Road
Overland Park, Kansas 66203

Robert C. Speed
Department of Geological Sciences
Northwestern University
Evanston, Illinois 60201

George E. Claypool
Mobil Research and Development
1377 Midway Road
Dallas, Texas 75244-4312

ABSTRACT

Diagenetic carbonate nodules and cements occur in organic carbon-rich terrigenous and hemipelagic strata of the basal complex on Barbados Island in the crestal zone of the Barbados accretionary prism. The carbonate has no apparent association with deformational structures, and various lines of geologic evidence suggest that it is a product of early diagenesis. Isotopic compositions of such carbonate can be successfully interpreted using a standard model of organic burial diagenesis. Some of the diagenetic carbonate has positive $\delta^{18}O$ values and zoned or highly negative $\delta^{13}C$ values indicative of precipitation at relatively low temperatures and shallow depths (0-100 m) in the aerobic and sulfate reduction zones and (or) near the top of the carbonate reduction zone. Other carbonate has more negative $\delta^{18}O$ values and positive $\delta^{13}C$ values, suggestive of at relatively greater temperatures and depths (≥500 m) within the zone of carbonate reduction and (or) early thermal diagenesis. The early diagenesis probably occurred in early-late Eocene time, prior to offscrape and accretion of beds of the basal complex. Lack of systematic correlation between $\delta^{13}C$ and $\delta^{18}O$ of the diagenetic carbonate suggests spatial and (or) temporal variability in depth of organic burial diagenetic zones in the predeformed succession of marine strata.

INTRODUCTION

Carbonate nodules and cements of probable early diagenetic origin occur in organic carbon-rich terrigenous and hemipelagic strata that crop out on Barbados Island in the crestal zone of the Barbados accretionary prism (Fig. 1A). In this paper, we describe the petrography, mineralogy, and stable carbon and oxygen isotopic compositions of the early diagenetic carbonate and give interpretations of the significance of $\delta^{13}C$ and $\delta^{18}O$ compositions for the relative ages, temperatures, and depths of carbonate precipitation. A companion paper (Torrini et al., 1990) describes diagenetic carbonate of probable late origin that occurs exclusively in fault zones and mud diapirs of Barbados.

Thirty-five samples were collected from the freshly fractured faces of beds and nodules. For certain nodules, cores were sampled along with rims and cross-cutting veins. The mineralogy of individual samples was determined by powder X-ray diffraction (XRD), and separates of all powdered samples were analyzed at the U. S. Geological Survey, Lakewood, Colorado for carbon and oxygen isotopic composition. Calcite, dolomite, and siderite were identified based on their characteristic d(104) spacings. Ferroan dolomite was identified based on its rhombohedral morphology in thin section and on the dominance of iron vs. calcium and magnesium on its EDX spectrum. Data for both oxygen and carbon isotopes are presented in the normal δ notation with reference to PDB standard.

GEOLOGY OF BARBADOS

The island of Barbados exposes the structural high of the accretionary prism of the active Lesser Antilles forearc (Speed and Larue, 1982; Speed, Westbrook et al., 1984). The Scotland district of Barbados (Fig. 1B) is an erosional window through Pleistocene reef that caps the majority of the island. Outcrop and well studies indicate the existence of three major tectonic units beneath the reefcap (Fig. 1B) (Speed, 1988 and references therein). The highest unit is the Oceanic allochthon, which consists of interbedded pelagic and volcanogenic Cenozoic rocks that were thrust east above the prism's structural high from the adjacent forearc basin. The intermediate unit is sporadically occurring prism cover. The lowest unit is the basal complex, which is an assemblage of fault-bounded packets of siliciclastic turbidites and hemipelagic strata of probable early to late Eocene depositional age. The basal complex, which forms the foundation of the structural high of the accretionary prism and extends to depths ≥4 km, is thought to have formed by offscrape and accretion in late Eocene time. Diapirs of organic carbon-rich, mud-matrix melange cut the basal complex and locally the Oceanic nappes (Speed, 1988).

Rocks of the Basal Complex

There are no evident correlations among sequences of beds in different fault-bounded packets of the basal complex. Relative stratigraphic positions are known only on an intrapacket basis.

Terrigenous beds of the basal complex are about half quartz-rich turbiditic sandstone and half illite- and kaolinite-rich mudstone (Larue and Speed, 1985). Mudstones contain Type III kerogen and 0.3 - 4.0 wt% total organic carbon. With the exception of rare planktics (nannofossils) and coarse resedimented shallow-water fossils, the terrigenous strata are virtually noncalcareous. The terrigenous sediment, of continental provenance, was derived from cratonal South America and probably deposited in a trench wedge and (or) varied sites on one or more submarine fans (Larue and Speed, 1985; Kasper and Larue, 1986).

Hemipelagic rocks of the basal complex include radiolarite, radiolarian mudstone, and radiolarian-bearing muddy, quartzose turbidites of early and middle Eocene age. Such rocks are generally more smectite-rich than terrigenous strata of the basal complex, contain both Type II and Type III kerogen, and have total organic carbon values of 1.8-10.7 wt.%.

Larue, D.K., and Draper, G. (eds.),
Transactions of the 12th Caribbean Geological Conference, St. Croix, U.S.V.I., Miami Geological Society, P.O. Box 431552, South Miami, FL 33243, U.S.A

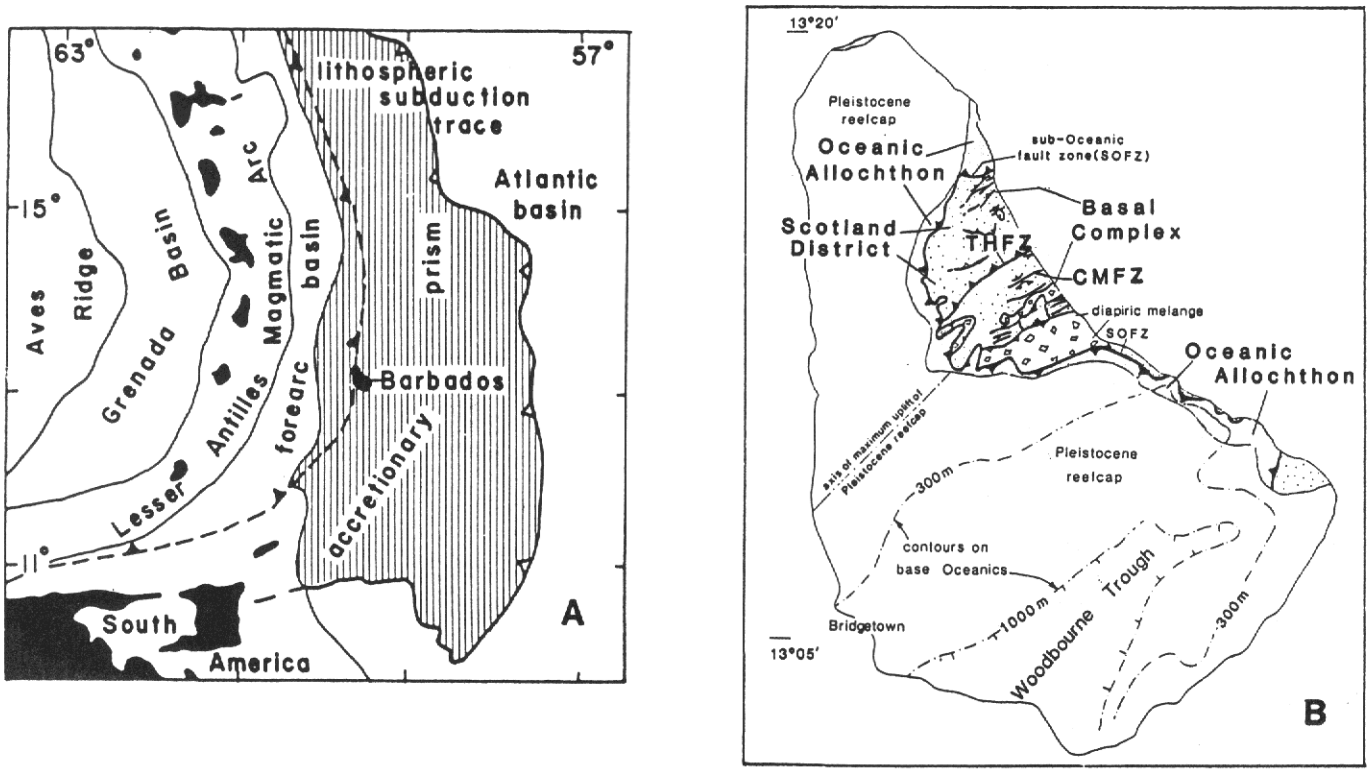

Figure 1. A) Index map showing location of Barbados Island at structural high of Lesser Antilles forearc; B) Major tectonostratigraphic units of the Scotland District of Barbados.

TYPES AND OCCURRENCES OF DIAGENETIC CARBONATE

Five different types of diagenetic carbonate have been identified among strata in the basal complex of Barbados: (1) calcite nodules, (2) calcite cement, (3) cone-in-cone calcite, (4) clay ironstone (Fe-bearing carbonate), and (5) dolomite cement. *Calcite nodules* occur within quartzose sandstones. The nodules are spherical to ellipsoidal and concentrated along certain stratal horizons or intervals. Sedimentary structures (convolute bedding, plane- and cross-lamination) are preserved within some of the nodules, and sedimenatary lamination in adjacent sandstone typically deflects tangentially about the nodules. Continuous or blocky, pore-filling sparry *calcite cement* also occurs in quartzose sandstones, whose detrital framework and sedimentary structures are well preserved. *Cone-in-cone structures* occur in terrigenous mudstone as semicontinuous horizons of nested or interfering conical structures with lengths $\geq$ 3 cm, variable apical angles, and axes oriented orthogonal to bedding. Individual cones and cone segments are composed of fibrous calcite and are commonly separated by annular, cross-cutting seams of fine-grained noncalcareous particles, mainly clay minerals and quartz. *Clay ironstones* are gray to deep red, iron carbonate-cemented horizons in organic carbon-rich radiolarian mudstone and fine-grained, laminated sandstone. Diagenetic carbonate minerals in the ironstones include siderite and ferroan dolomite. The *Dolomite cement* with rhombohedral crystal morphology occurs in hemipelagic rocks.

RELATIVE AGE OF THE DIAGENETIC CARBONATE

All such diagenetic carbonate is interpreted as a product of early (predeformation) diagenesis from the following lines of evidence. Firstly, sedimentary laminae deflect tangentially about the rims of large carbonate nodules, indicating precipitation of nodules prior to major compaction and porosity loss. Secondly, the carbonate has no apparent association with deformational structures such as folds, foliation, broken formation, or fault zones. Long axes of elliptical concretions and horizons of concretions and cone-in-cone carbonate are concordant to stratigraphic layering, even where such layering is folded. Thirdly, the orthogonal orientation of cone-in-cone axes with respect to host bedding is generally interpreted as a product of compaction during early diagenesis (Franks, 1969; Gilman and Metzger, 1967). Finally, at least some of the calcite-cemented sandstones and calcite nodules in sandstone have relatively high carbonate content (43-93 wt%; avg. $\approx$ 70 wt%). The values are higher than the maximum porosity of unconsolidated sand (~50%), suggesting displacement of sand grains during calcite crystal growth prior to major burial and compaction. Assuming that the diagenetic carbonate is a product of early diagenesis, its precipitation age probably is Eocene, the probable depositional age of strata in the basal complex of Barbados (Speed, 1988).

ISOTOPIC COMPOSITIONS AND INTERPRETATIONS

$\delta^{13}C$ and $\delta^{18}O$ compositions of the diagenetic carbonate range from -41.8 to +24.2 o/oo and -6.69 to +5.24 o/oo, respectively (Table 1; Fig. 2). Given an early diagenetic origin for the carbonate, the broad range of $\delta^{13}C$ values is most simply explained by a standard model of precipitation in various depth-related zones of organic burial diagenesis where $\delta^{13}C$ of dissolved CO_2 varies in response to differing modes of bacterial degradation of organic matter (Fig. 3;

Claypool and Kaplan, 1974; Gautier and Claypool, 1984). These zones are, from top down (Fig. 3): (1) the aerobic zone, (2) the sulfate reduction zone, (3) the zone of carbonate reduction (bacterial methanogenesis), and (4) the zone of thermal catalytic degradation and decarboxylation. Isotopic equilibration temperatures were calculated assuming equilibration with pore fluid compositionally equivalent to seawater of the nonglacial (Eocene) oceans ($\delta^{18}O$ = -1.2 o/oo, SMOW; Shackleton and Kennett, 1975). The temperatures range from 9°-39°C. Organic diagenetic zones of carbonate precipitation can be interpreted based on carbon isotopic compositions and zonations, iron content, and differences in $\delta^{18}O$ composition and calculated equilibration temperature.

Isotopically heavy diagenetic carbonates (highly positive $\delta^{13}C$ values) probably precipitated in the zone of carbonate reduction (Fig. 3) where dissolved carbonate becomes ^{12}C-depleted due to preferential removal of light CO_2 to form biogenic methane (Claypool and Kaplan, 1974; Irwin et al., 1977).

The origins of isotopically light diagenetic carbonates are more difficult to interpret because each of the four zones of organic diagenesis may theoretically include ^{13}C-depleted CO_2 (Fig. 3). Although carbonate generally does not precipitate in the aerobic zone due to rapid loss of CO_2, it may do so in rare cases and is iron-free due to the absence of reduced iron (Gautier, 1985). Carbonate precipitated in the sulfate reduction zone is also generally iron-free due to the preferred complexing of ferrous iron with reduced sulfur to form pyrite (Gautier and Claypool, 1984). Thus, iron-bearing ^{13}C-depleted diagenetic carbonate (clay ironstones, Fig. 3) probably precipitated in the zone of carbonate reduction rather than the aerobic or sulfate reduction zones. Rims and cross-cutting veins of iron-free calcite nodules (cannonballs, ellipsoids) are ^{13}C-depleted relative to their cores, suggesting precipitation during progressive burial at shallow depths in the aerobic and (or) sulfate reduction zones.

The organic diagenetic zones in which other samples of iron-free ^{13}C-depleted diagenetic carbonate originated are less certain but can be interpreted from $\delta^{18}O$ values and estimated relative precipitation depths. Samples with more negative $\delta^{13}C$ values (-29 to -40.2 o/oo) have positive $\delta^{18}O$ values (+0.14 to +0.58), suggesting precipitation at temperatures corresponding to relatively shallower depths near the boundary between the zones of sulfate and carbonate reduction (Fig. 3). In contrast, samples with less negative $\delta^{13}C$ values (-7.8 to -14.5 o/oo) have negative $\delta^{18}O$ values (-2.75 to -6.53 o/oo), suggesting precipitation at temperatures corresponding to relatively greater depths within the zone of carbonate reduction (Fig. 3).

Table 1. Stable isotopic composions of diagenetic carbonate

Type of Diagenetic Carbonate	$\delta^{13}C$ (o/oo)	$\delta^{18}O$ (o/oo)
cone-in-cone calcite in terrigenous mudstone	-11.1 to +19.4	-4.41 to +0.49
calcite concretions in quartz sandstone	-41.8 to -8.0	+0.05 to +0.79
clay ironstones	-21.8 to -11.7	-3.83 to +2.41
calcite cement in quartz sandstone	-40.2 to +13.7	-6.53 to +0.58
dolomite cement in hemipelagic strata	-2.5 to +24.2	-6.69 to +2.97

DEPTH OF PRECIPITATION

The oxygen equilibration temperatures of the early diagenetic carbonate can be used to calculate maximum precipitation depths. Assuming an Eocene bottom water temperature of 10°C (Savin et al., 1975) and a geothermal gradient on Barbados of 15°C/km (Larue et al., 1984), the calculated temperatures correspond to depths between 0 and 1,900 m below the seabottom.

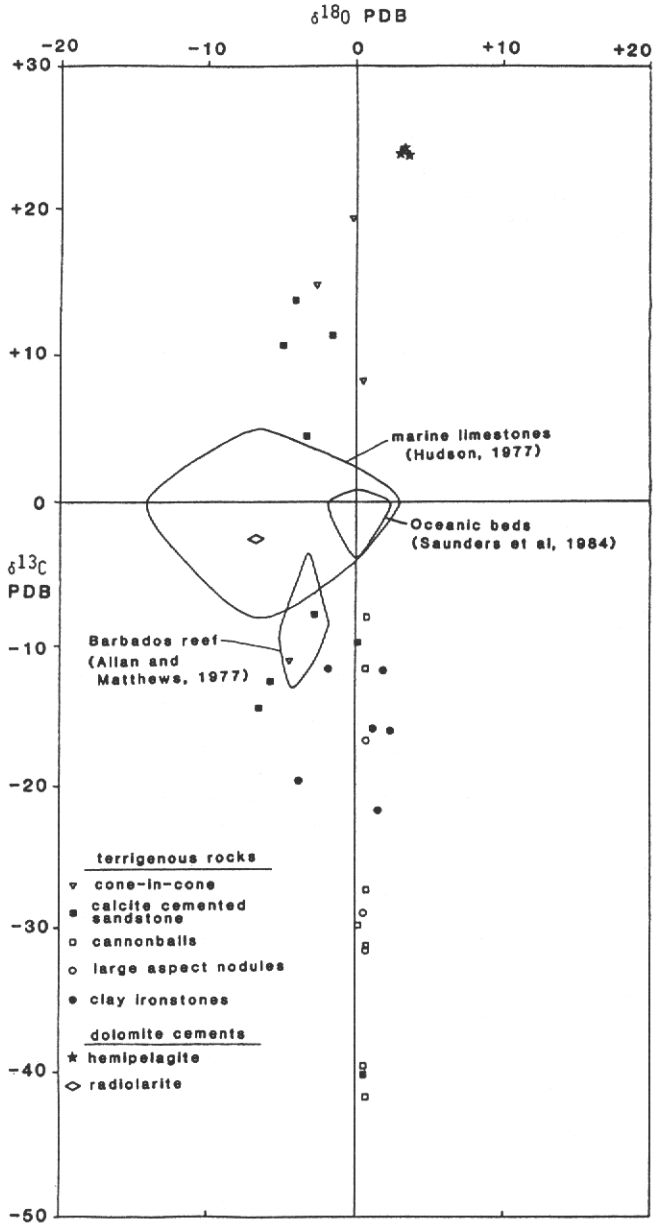

Figure 2. Stable carbon and oxygen isotopic compositions of early diagenetic carbonate in terrigenous and hemipelagic strata of Barbados. See text for discussion.

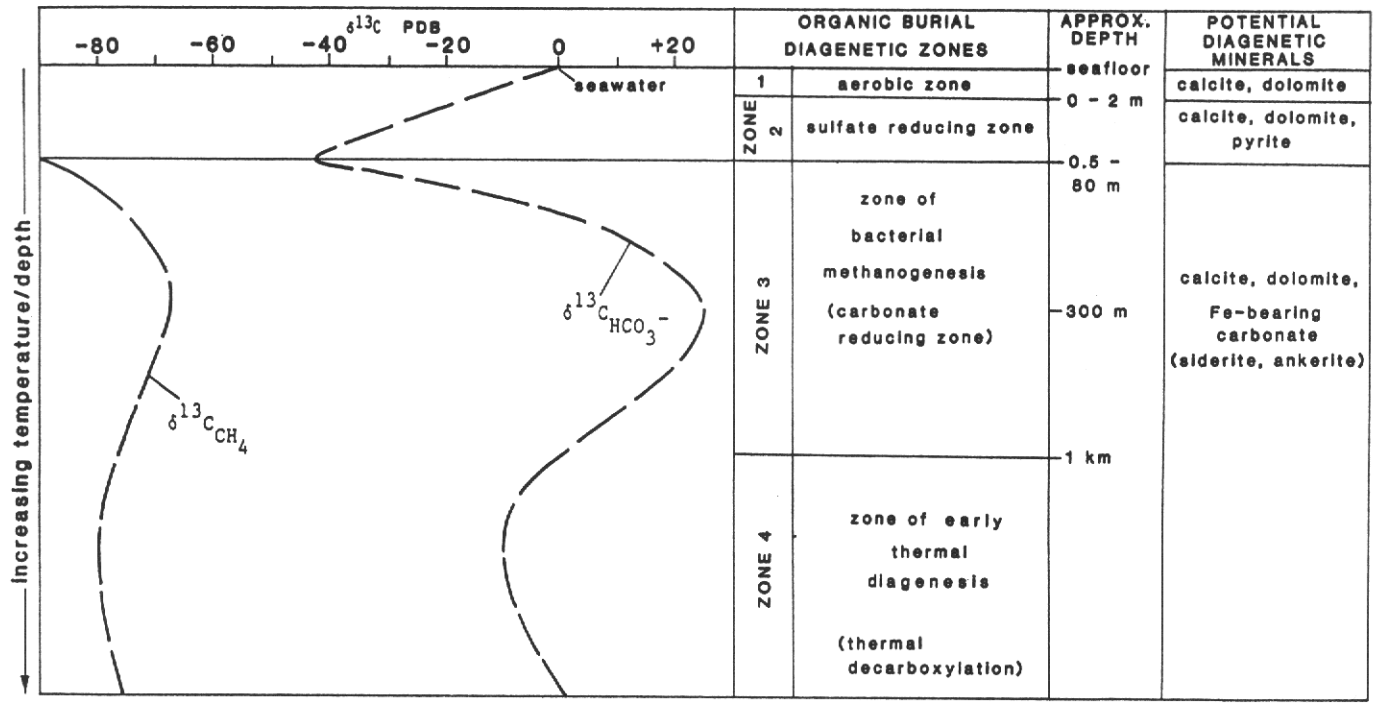

Figure 3. Generalized diagram showing succession of depth and temperature related zones of organic diagenesis and associated $\delta^{13}C$ compositions of CH_4 and HCO_3- available for precipitation of diagenetic carbonate.

Carbonates formed in the aerobic and (or) sulfate reduction zones precipitated at depths ≤500 m and probably ≤100 m, based on the following reasoning. Firstly, outcrop evidence and high carbonate content indicate precipitation of such calcite nodules prior to major compaction and porosity loss. Secondly, the observed depth to the base of the sulfate reduction zone at DSDP sites of rapid terrigenous sediment deposition is generally ≤100 m. Finally, the $\delta^{18}O$ compositions of samples interpreted to have formed at shallow depths in the aerobic and (or) sulfate reduction zones (+0.05 to +0.79 o/oo) yield equilibration temperatures (9°-12°C) like those of Eocene bottom water in the Atlantic Ocean (Savin et al., 1975). Regardless of the reality of such temperatures, the oxygen isotopic compositions are like those of benthic foraminifera in Eocene-Oligocene Oceanic beds (-0.03 to +2.30 o/oo; Saunders et al., 1984), indicating precipitation at or near the sediment/water interface.

The oxygen isotopic compositions of carbonates precipitated in the zone of carbonate reduction yield equilibration temperatures of 10°-39°C. The temperature range and variable carbonate content of such samples suggest precipitation over a range of depths. Some have high carbonate content and $\delta^{18}O$ values like those of carbonate of the suprajacent sulfate reduction zone, suggesting precipitation near the top of the carbonate reduction zone at shallow depths (≤100 m) prior to major compaction and porosity loss. Others have low carbonate content and more negative $\delta^{18}O$ values, suggesting precipitation deeper within the carbonate reduction zone, at depths ≥500 m.

CONCLUSIONS

Diagenetic carbonate in terrigenous and hemipelagic rocks of the basal complex without apparent association with deformational structures is a product of early diagenesis. Isotopic compositions of such carbonate can be successfully interpreted using a standard model of organic burial diagenesis. The early diagenesis probably occurred in early-late Eocene time, prior to offscrape and accretion of beds of the basal complex. Some of the diagenetic carbonate has positive $\delta^{18}O$ values and zoned $\delta^{13}C$ values indicative of precipitation at relatively low temperatures and shallow depths (0-100 m). Other carbonate has more negative $\delta^{18}O$ values and positive $\delta^{13}C$ values, suggestive of precipitation at relatively greater temperatures and depths (500-1,900 m). Lack of systematic correlation between $\delta^{13}C$ and $\delta^{18}O$ of the diagenetic carbonate suggests spatial and (or) temporal variability in depth of organic burial diagenetic zones in the predeformed succession of marine strata.

ACKNOWLEDGEMENTS

This research was supported by Department of Energy Grant No. DE-AC21-84 MC21132, National Science Foundation Grant INT82-12272, and PRF Grant 12669-AC2, all to R. C. Speed. We are grateful to the U.S. Geological Survey for use of facilities for isotopic analyses.

REFERENCES CITED

Allan, J. R., and Matthews, R. K., 1977, Carbon and oxygen isotopes as diagenetic and stratigraphic tools: Surface and subsurface data, Barbados, West Indies: Geology, v. 5, p. 16-20.

Claypool, G. E., and Kaplan, I. R., 1974, The origin and distribution of methane in marine sediments, in Kaplan, I. R. (ed.), Natural Gasses in Marine Sediments: New York, Plenum Press, p. 99-139.

Franks, P. C., 1969, Nature, origin, and significance of cone-in-cone structures in the Kiowa Formation (Early Cretaceous), North Central Kansas: J. Sed. Pet., v. 39, no. 4, p. 1438-1454.

Gautier, D. L., 1985, Interpretation of early diagenesis in ancient marine sediments: in Relationship of Organic Matter and Mineral Diagenesis, S. E. P. M. Short Course No. 17, p. 6-78.

Gautier, D. L., and Claypool, G. E., 1984, Interpretation of Methanic Diagenesis in Ancient Sediments by Analogy with Processes in Modern Diagenetic Environments, in McDonald, D. A., and Surdam, R. C. (eds.), Clastic Diagenesis: Am. Ass. Pet. Geol., Mem. No. 37, p. 111-123.

Gilman, R. A., and Metzger, 1967, Cone-in-cone concretions from western New York: J. Sed. Pet., v. 37, p. 87-95.

Irwin, H., Curtis, C., and Coleman, M., 1977, Isotopic evidence for source of diagenetic carbonates form ed during burial of organic-rich sediments: Nature, v. 269, p. 209-213.

Kasper, D. A., and Larue, D. K., 1986, Paleogeographic and tectonic implications of quartzose sandstones of Barbados: Tectonics, v. 5, p. 837-854.

Larue, D. K., and Speed, R. C., 1985, Quartzose turbidites of the accretionary complex of Barbados, I: Chalky Mount succession, J. Sed. Pet., v. 53, p. 1337-1352.

Larue, D. K., Schoonmaker, J., Torrini, R., Jr., Lucas-Clark, J. Clark, M., and Schneider, R., 1985, Barbados: maturation, source rock potential and burial history within a Cenozoic accretionary complex: Marine and Pet. Geol. , v. 2, p. 96-110.

Saunders, J. B., Bernoulli, D., Muller-Merz, E., Oberhansli, H., Perch-Nielsen, K., Riedel, W. R., Sanfilippo, A., Torrini, R., Jr., 1984, Stratigraphy of the late Middle Eocene to Early Oligocene in the Bath Cliffs section, Barbados, West Indies: Micropaleontology, v. 30, no. 4, p. 390-425.

Savin, S. M., Douglas, R. G., and Stehli, F. G., 1975, Tertiary marine paleotemperatures: Geol. Soc. America Bull., v. 86, p. 1499-1510.

Shackleton, N. J., and Kennett, J. P., 1975, Paleotemperature History of the Cenozoic and Initiation of Antarctic Glaciation: Oxygen and Carbon Isotope Analyses in DSDP Sites 277, 279, and 281: in Kennett, J. P., Houtz, R. E., et al., Initial Reports of the Deep Sea Drilling Project, v. 29: Washington, D. C., U. S. Govt. Printing Office, p. 743-755.

Speed, R. C., 1988, Tectonostratigraphy of Barbados: A Preliminary Synthesis: Trans. 11th Carib. Geol. Conf., Barbados, p. 29:1-29:11.

Speed, R. C., G. K. Westbrook, et al., 1984, Atlas 10, Ocean Margin Drilling Program, Lesser Antilles and Adjacent Ocean Floor: Marine Science Institute Publications, Woods Hole, Massachussets.

Speed, R. C., and Larue, D. K., 1982, Barbados: Architecture and Implications for Accretion, J. Geophys. Res., v. 87, No. B5, p. 3633-3643.

Torrini, R., Jr., Speed, R. C., and Claypool, G. F., 1990, Origin and Geologic Implications of Diagenetic Carbonate in Fault Zones of Barbados: Trans. 12th Carib. Geol. Conf., St. Croix, 1989, this volume.

PATCH REEF ECOLOGY, SEDIMENTOLOGY AND DISTRIBUTION BUCCOO REEF COMPLEX, TOBAGO

D. Hudson
Exploration Department
Trinidad & Tobago Petroleum Company Limited
Santa Flora, Trinidad and Tobago

E.W. Mountjoy
Department of Geological Sciences
Mc Gill University, Montreal, Quebec, Canada

ABSTRACT

Four distinct patch reef types have been identified in the back-reef and lagoonal areas of the Buccoo Reef Complex, Southwestern Tobago. This differentiation is based on ecology, associated sediment distribution, and their geographic location within the reef environment.

Algae - Porites patch reefs are elongate to sub-circular in plan view, and dominated by algal-encrusted Porites coral rubble and Halimeda opuntia, and minor clumps of Porites porites and Thalassia testinidium. Elongate-shaped Acropora patch reefs are composed of thickets of Acropora cervicornis, with minor stands of A. prolifera and species of Siderastrea, Agaricia, Montastrea and Diploria. Acropora-Millepora assemblages which are elongate to sub-elliptical in shape, are compositionally similar to the Acropora assemblages, except for the introduction of extensive occurrences of the hydrozoan Millepora. A single occurrence of the elongate to tabular-shaped Montastrea assemblage is predominated by coral heads of Montastrea annularis.

Extensively fragmented Halimeda plates are the dominant sediment particles associated with Algae - Porites patch reefs. Particles of coral, coralline - algae, Halimeda, and mollusc grains in varying percentages, occur on the substrates of the Acropora and Acropora - Millepora assemblages.

A systematic change, relative to their distinctive ecology, occurs in the distribution of patch reefs in the lagoonal and back-reef areas of the reef complex. This geographic distribution and specific ecological characteristics are primarily controlled by the degree of wave exposure, and are moderately influenced by water circulation and turbidity.

INTRODUCTION

Physical Setting

The island of Tobago is situated in the southeastern Caribbean, near the junction of the Lesser Antillean outer sedimentary arc or accretionary prism to the northeast, the Atlantic Basin to the southeast, and the South American Mainland to the southwest (Case, 1975, Mascle et al., 1979). It is located at approximately 11°N latitude and 61°W longitude, 32.2 km northeast of Trinidad. Covering an area of 301 km², the island is 42 km long and 12 km wide at its widest point.

The Buccoo Reef Complex and its associated environs are situated in the southwest corner of the island of Tobago (Fig. 1). Encompassing an area of approximately 7 km², the coralgal reef forms a broad arc around the lagoonal area. It is composed of 5 discontinuous reef flats, with numerous patch reefs in the back-reef and lagoonal areas (Fig. 1). From west to east, the reef flats are named Pigeon Point, Western, Northern, Outer and Eastern (Kenny, 1976). The Reef Lagoon, Inner and Outer Bon Accord Lagoons are enclosed by these reefs flats.

Average depths of 2 - 5 m in the Reef Lagoon, and 2 - 4 m in Inner and Outer Bon Accord Lagoons with a few deep depressions were observed. Surface currents exhibited simple circulatory patterns of low to moderate strength (2 to 6 cm/s), controlled chiefly by the Antillean current, prevailing Northeast Trade Winds and tidal variations (Kenny, 1976).

Purpose of Study

The patch reefs or coral-rich areas in the back-reef and lagoonal areas of Buccoo Reef Complex have not been previously described in any detail (Kenny, 1976). In order to provide scientific data on this component of the Buccoo Reef System, this study was carried out:

(1) To describe patch reefs of the reef complex, with special emphasis on their stage(s) of development.
(2) To determine the nature of patch reef sediments.
(3) To explain the geographic distribution of the patch reefs in the back-reef and lagoonal environments of the reef system.

Methodology

During a marine geological survey of the Buccoo Reef Complex in June-August, 1980, dissimilar patch reefs were mapped in detail along north-south traverses at 10 m intervals(Fig. 1), and 31 other reefs were studies in general. These field observations were supplemented by aerial photographic analyses, where the colour contrasts on the photographs were utilized for defining the boundaries of patch reefs at that time.

PATCH REEF ENVIRONMENTS

Ecology

Four different patch reefs were identified in the lagoonal and back-reef areas of the Buccoo Reef Complex (Fig. 1). They are as follows:

1. Algae - Porites;
2. Acropora;
3. Acropora-Millepora;
4. Montastrea.

Thirty-four patch reefs were mapped and located. Of these, 17 were Algae - Porites, 13 were Acropora, 3

Larue, D.K., and Draper, G. (eds.),
Transactions of the 12th Caribbean Geological Conference, St. Croix, U.S.V.I., Miami Geological Society, P.O. Box 431552, South Miami, FL 33243, U.S.A

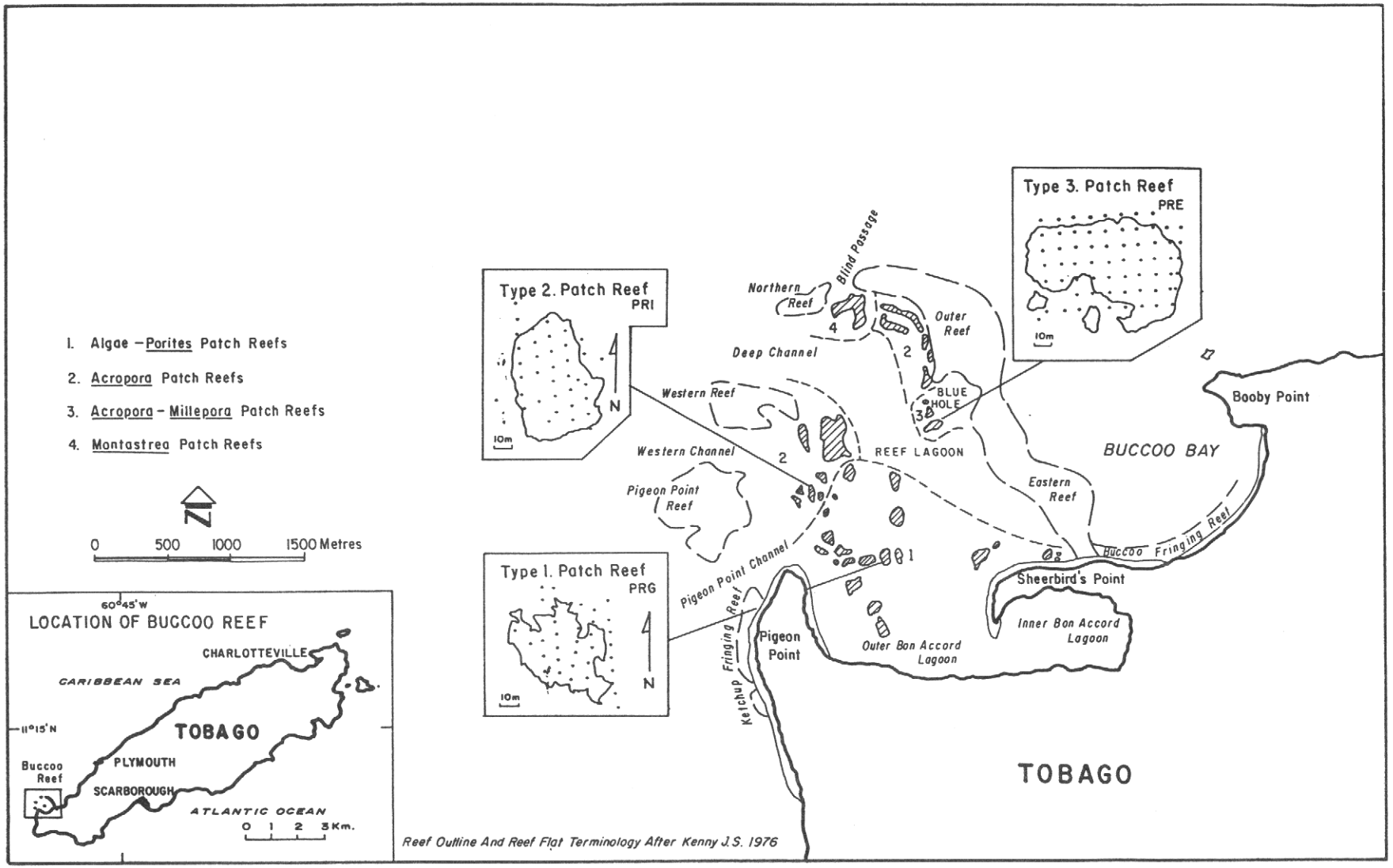

Fig. 1 - Map of Buccoo Reef Complex showing distribution of various patch reefs. Inset maps indicate patch reefs studied in detail and location of Buccoo Reef.

were Acropora - Millepora, and 1 of the Montastrea variety (Fig. 1).

Algae - Porites Patch Reefs

Algae - Porites patch reefs are located in the south-central areas of Reef Lagoon, and south-western portions of Outer Bon Accord Lagoon (Fig. 1). They are elongate to sub-circular in shape, forming shallow, rather subdued mounds which rise from depths of 2 - 5 m in lagoonal areas, to less than 0.5 m below sea level in some cases. These mounds range in size from 50 to 5000 m^2.

For a more detailed examination of these organism-rich areas, a patch reef located on the northern margin of Outer Bon Accord Lagoon, approximately 500 m to the west of Pigeon Point was chosen as a typical example (Fig. 1). Referred to as Patch Reef Giselle (PRG), it is approximately 4000 m^2 in area, and rises from depths of 2 - 3 m in surrounding lagoonal waters to approximately 0.5 - 1 m in its north-central portion (Fig. 2A).

Ecologically, living corals are very sparse (5%) and confined to small clumps of Porites porites (Fig. 2B). Porites coral rubble and extensive H. opuntia are the predominant constituents on the substrate of this patch reef (Figs. 3A and 3B). Porites coral and coral rubble are both heavily encrusted by Halimeda spp., coralline-red algae, boring molluscs and serpulid tubes. Growth of Halimeda spp. on sand substrates occurs towards the margin of the patch reef. Minor occurrences of Thalassia testinidum and burrow mounds are also present. Living organisms, e.g. molluscs, brittle stars, sea anemones, sponges, and sea urchins, are associated with the coral rubble.

The percentage of living Porites coral increases to about 20% in the Algae - Porites patch reefs located in the Reef Lagoon. Minor sea fans and sea whips are also present.

Acropora Patch Reefs

Acropora patch reefs are located in southwestern and northeastern Reef Lagoon; to the east of Pigeon Point and Western reef flats, and bordering the Outer Reef Flat respectively (Fig. 1). The reefs are elongate to tabular in shape. These patch reefs form coral-rich banks which are approximately at 1 m elevation above the lagoon floor towards their centre. They range in area from 50 to 60,000 m^2, and are subaerially exposed during extreme spring tidal lows.

Patch Reef Ivy (PRI) was selected as a typical example of these Acropora - rich areas (Fig. 1). PRI is located approximately 400 m north of Pigeon Point peninsula and 350 m west of Pigeon Point Reef Flat. It is approximately 4500 m^2 in area, and rises to within 1 m of sea level on its south and southeastern sections (Fig. 4A).

Living corals average about 30 - 40% on Patch Reef Ivy, and are dominated by thickets of Acropora cervicornis (Fig. 4B). Patch reef stabilization is achieved by the interlocking, growth framework of the branching Acropora colonies. Minor patches of diverse coral species of Siderastrea, Agaricia, Montastrea and Diploria, and the hydrozoan Millepora are also present. Easily fragmented A. cervicornis accounts for an extensive coral rubble (Fig. 5A) which is moderately encrusted by coralline-red algae. Halimeda sp. growth occurs at the base of dead coral branches (Fig. 5B). Minor occurrences include sea fans, sea whips, molluscs, sponges and the conch Strombus gigas. Burrow mounds on bare sand areas are also present.

Acropora - Millepora Patch Reefs

Acropora - Millepora patch reefs are located in the eastern portion of Reef Lagoon bordering the Blue (Deep) Hole (Fig. 1). They are elongate to sub-elliptical in shape and form coral-rich banks similar in appearance to the Acropora patch reefs. The Acropora - Millepora patch reefs rise from lagoonal depths of 2 m to less than 1 m below sea level toward their centres. They range in area from 600 to 6000 m^2.

Patch Reef Elsa (PRE) represented a typical example of the Acropora - Millepora coral-rich areas (Fig. 1). It is located on the western margin of the Blue (Deep) Hole, and is approximately 6000 m^2 in area. It rises to within 1 m of sea level (Fig. 6A).

The hydrozoan Millepora along with living coral species dominated by A. cervicornis, cover 10-50% of the substrate of Patch Reef Elsa (Fig. 6B). M. alcicornis with minor occurrences of M. complanata are the main hydrozoan species present. Minor Diplora sp. and Siderastrea sp. also occur on this patch reef. Similar to the Acropora Patch Reef (PRI), patch reef stabilization is achieved on PRE by the interlocking, growth patterns of A. cervicornis. Fragmented coral and Millepora rubble encrusted by Halimeda spp. and coralline-red algae are very abundant (Figs. 7A and 7B). On the southwestern margin of the patch reef, dead coral and Millepora skeletons are extensively overgrown by a green algae. Burrow mounds occur in bare sand areas, and molluscs and sea anemones are also present.

Montastrea Patch Reef

A Montastrea-dominated patch reef is located at the lagoonal entrance of the Blind Passage, on the southern border of the northwestern tip of Outer Reef Flat (Fig. 1). This area, due to its prolific coral growth, is referred to as the Coral Gardens. The patch reef is approximately 9500 m^2 in area and elongate-tabular in shape. Coral growth begins in back-reef areas at depths of 2 m, continuing towards the Reef Lagoon in increasing depths up to 10 m (Kenny, 1976).

The coral-rich area was not examined in detail. The shallower portions of the patch reef (depths of 2 - 4 m) are dominated by coral heads of Montastrea annularis, interspersed with a variety of sea fans, sea whips and the hydrozoans Millepora. Numerous eroded coral heads, probably destroyed by grazing parrot fish and the sea urchin Diadema are also common in this area. At mid-depth (3 - 7 m), scattered M.

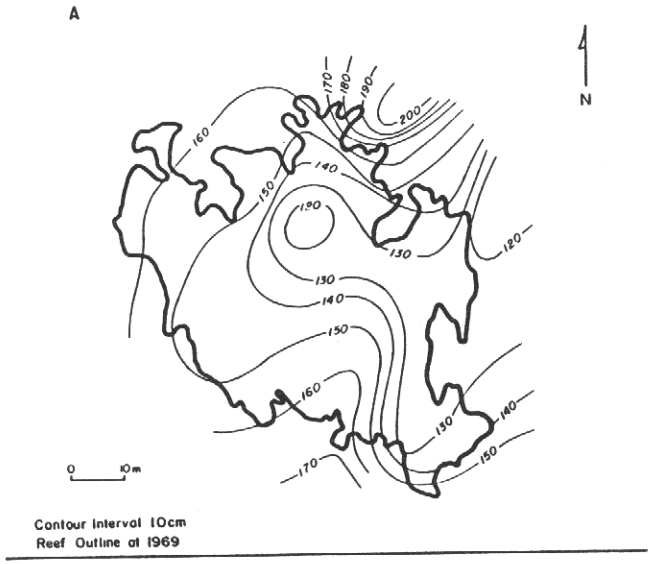

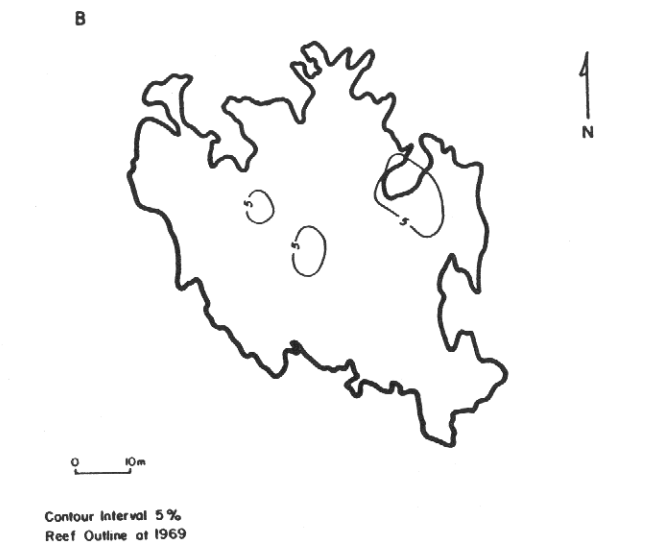

Fig. 2A - Bathymetric map of Patch Reef Giselle, an Algae - Porites Patch Reef

Fig. 2B - Contour map of percentage occurrences of the living coral Porites on Patch Reef Giselle, an Algae - Porites Patch Reef

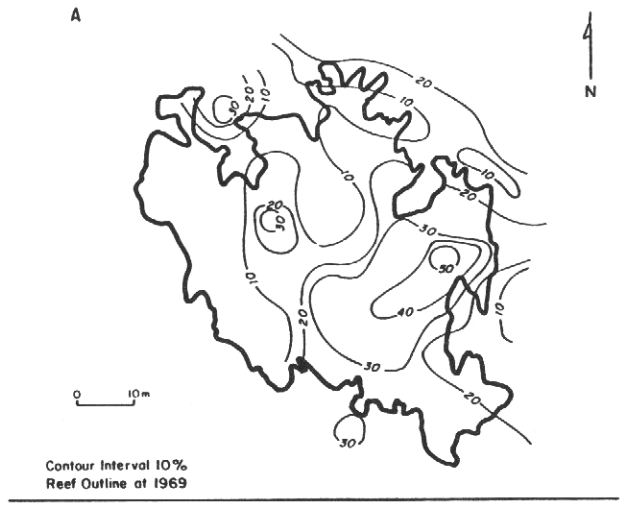

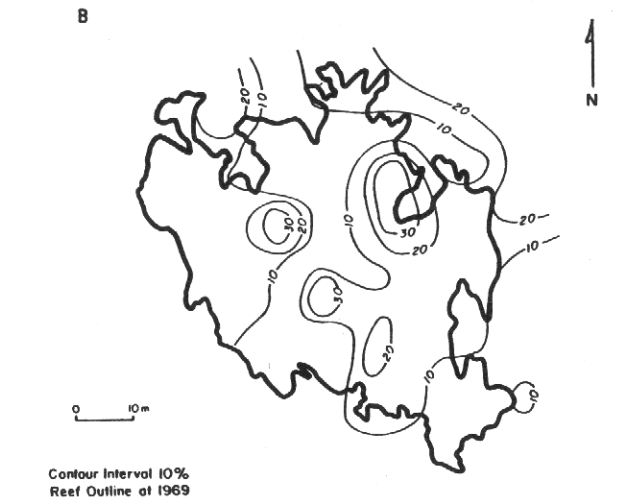

Fig. 3A - Contour map of percentage occurrences of Porites coral rubble on Patch Reef Giselle, an Algae - Porites Patch Reef.

Fig. 3B - Contour map of percentage occurrences of Halimeda on Patch Reef Giselle, an Algae - Porites Patch Reef.

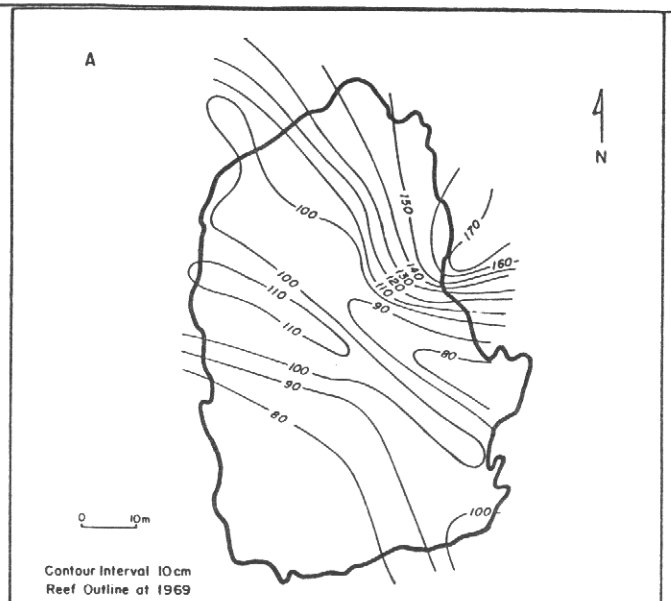

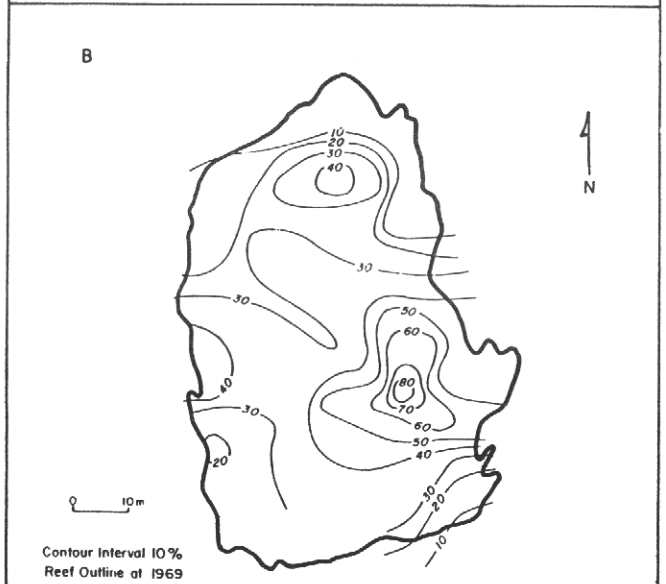

Fig. 4A - Bathmetric map of Patch Reef Ivy, an Acropora Patch Reef.

Fig. 4B - Contour map of percentage occurrences of the living coral Acropora on Patch Reef Ivy, an Acropora Patch Reef.

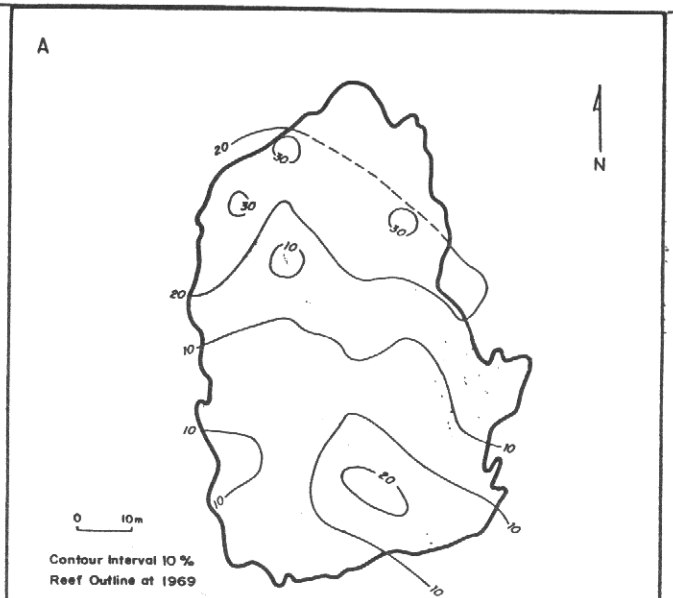

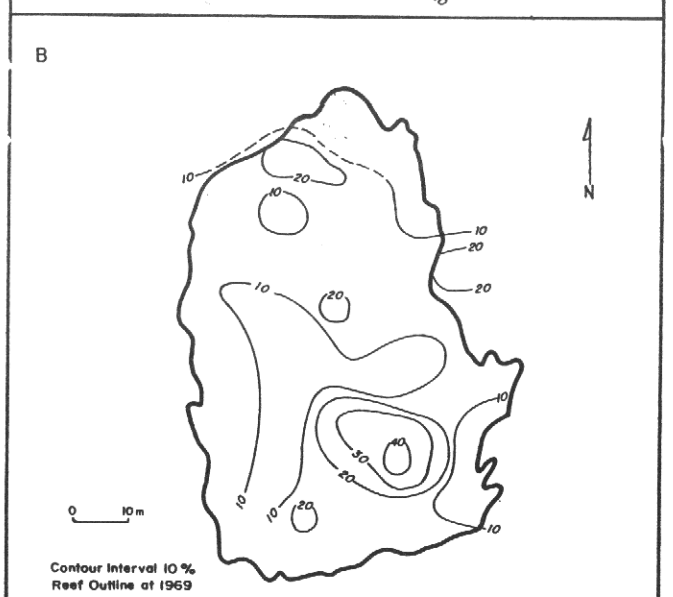

Fig. 5A - Contour map of percentage occurrences of coral rubble on Patch Reef Ivy, an Acropora Patch Reef.

Fig. 5B - Contour map of percentage occurrences of Halimeda on Patch Reef Ivy, an Acropora Patch Reef.

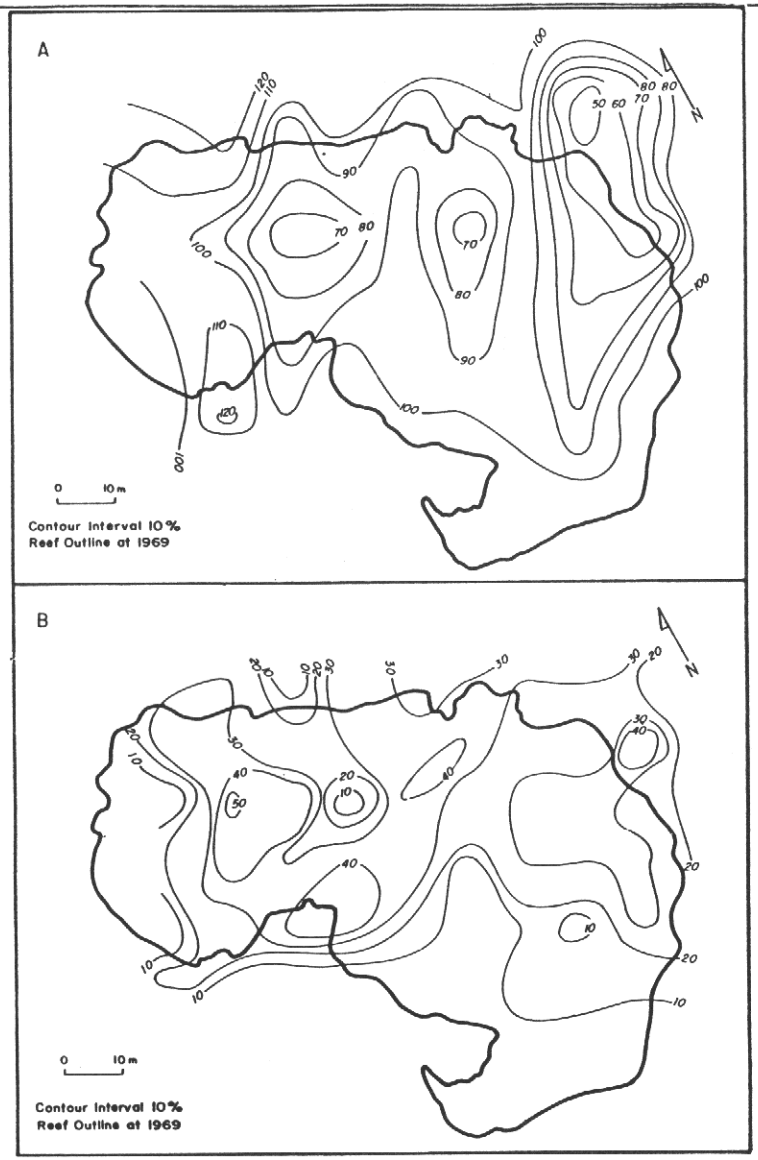

Fig. 6A - Bathymetric map on Patch Reef Elsa, an Acropora - Millepora Patch Reef.

Fig. 6B - Contour map of percentage occurrences of coral and the hydrozoan Millepora on Patch Reef Elsa, an Acropora - Millepora Patch Reef.

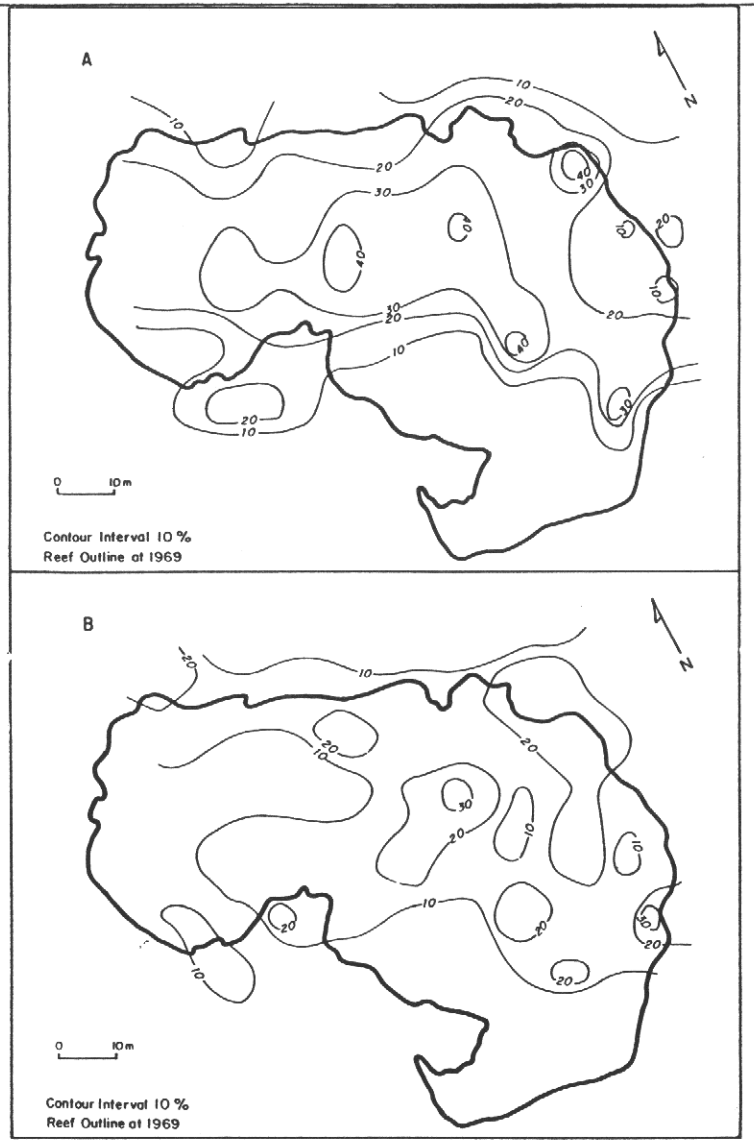

Fig. 7A - Contour map of percentage occurrences of coral (including Millepora) rubble on Patch Reef Elsa, an Acropora - Millepora Patch Reef.

Fig. 7B - Contour map of percentage occurrences of Halimeda on Patch Reef Elsa, an Acropora - Millepora Patch Reef.

annularis are associated with occasional colonies of Acropora palmata, A. cervicornis and Porites astreoides. Coral colonies in the deepest areas (>7m) consist of heads of M. annularis, M. lamarkana, Diploria strigosa, D. labrynthiformis, Colpophyllia natans and Siderastrea sidera (Kenny 1976).

Sediments

Sediments in the Algae - Porites patch reefs are generally composed of Halimeda particles. Minor amounts of coral, coralline-algae and mollusc grains, along with gorgonacea and sponge spicules are also present. Of significance are minor amounts of terrigenous quartz silt in all sediment samples of the Algae - Porites patch reefs (Table 1). Most particles are extensively abraded. These sediments are predominantly of a coarse sand size and poorly to moderately sorted (Table 2).

PATCH REEF	MEAN Ø		SORTING Ø	
Algae - Porites	0.57	Coarse sand	1.64	Poorly sorted
	1.00	Coarse sand	1.27	Poorly sorted
	0.94	Coarse sand	0.79	Moderately sorted
	0.93	Coarse sand	1.37	Poorly sorted
	0.92	Coarse sand	1.21	Poorly sorted
Acropora	1.56	Medium sand	1.23	Poorly sorted
	0.91	Coarse sand	1.81	Poorly sorted
	1.04	Medium sand	1.30	Poorly sorted
	0.99	Coarse sand	1.46	Poorly sorted
	1.64	Medium sand	1.46	Poorly sorted
Acropora - Millepora	1.08	Medium sand	1.05	Poorly sorted
	1.18	Medium sand	1.16	Poorly sorted
	1.32	Medium sand	1.16	Poorly sorted
	1.08	Medium sand	1.17	Poorly sorted
	1.08	Medium sand	1.18	Poorly sorted

Table 2: Grain Size Analysis of Some Representative Samples of Patch Reef Sediments

The Acropora patch reefs are characterized by sediments composed of Halimeda grains, with occurrences of coral, coralline - algae and mollusc fragments, which are in a greater abundance compared to the sediments of the Algae-Porites patch reefs (Table 1). These patch reef sediments are not excessively fragmented, and several particles are encrusted by worm tubes, benthonic foraminifera, and coralline algae. The sediments range in size from medium to coarse sand, and are generally poorly sorted (Table 2).

The sediments of the Acropora - Millepora patch reefs are similar in composition to the Acropora patch reef sediments (Table 1). These sediments are extensively fragmented, and coral grains are well rounded. Some mollusc particles are heavily bored. Sediments are of a medium sand size and poorly sorted (Table 2).

Geographic Distribution

A systematic change in the distribution of patch reef types occurs in the lagoonal areas of the Buccoo Reef Complex. With their distinct ecology and associated communities, this systematic change outlines a general geographic distribution of the patch reefs (Fig. 1). Algae - Porites patch reefs occur in the southern lagoonal areas at south-central Reef Lagoon and western Outer Bon Accord Lagoon. Acropora patch reefs are located in central and northern lagoonal areas, on the south-western and northeastern margins of Reef Lagoon. Acropora - Millepora patch reefs are restricted to central lagoonal areas, bordering the Blue (Deep) Hole. The Montastrea patch reef is confined to the northern lagoonal areas adjacent to the entrances of the Blind Passage and Deep Channel (Fig. 1).

DISCUSSION AND SUMMARY

Table 3 summarizes the major characteristics of the patch reefs in the lagoonal areas of the Buccoo Reef Complex. Similar patch reef communities occur in Watering Bay, Grenada (Pendlebury, unpublished), and Glovers Reef Atoll, Belize (Wallace and Schafersman, 1977).

Reef-Building Framework

The Algae - Porites patch reef form constructive elements, despite their non-rigid framework, owing to the trapping and binding of sediment by Porites coral rubble. The rubble is not cemented to the substrate, but held in place by the intergrowth of green algae Halimeda, a feature observed in the development of the Rodriguez Mudbank (Turmel and Swanson, 1976). In addition, the baffling effect on sediments by the blue-green algae H. opuntia, and marine grass T.testinidum further stabilizes these patch reefs (Multer and Zankl, 1985).

Growth and colonization of Acropora and Acropora - Millepora patch reefs are probably initiated by asexual regeneration of broken A. cervicornis branches. That is, the broken branches healed their ends and started budding. Further stabilization and framework development in these patch reefs are achieved by the fusing of A.cervicornis branches with each other, and with the surrounding substrate (Gilmore and Hall, 1976). In addition, organic cementation by coralline-red algae and benthonic foraminifera contributes to the process of fusion (Multer and Zankl, 1985). Similar to the Algae - Porites patch reefs,

TABLE 1: PERCENTAGE COMPOSITION OF SOME REPRESENTATIVE SAMPLES OF PATCH REEF SEDIMENTS

PATCH REEF	Halimeda	Coral	Coralline - Algae	Molluscs	Benthonic Foraminifera	Echinoid Spines	Spicules	Quartz Silt	Other
	72	6	-	10	-	2	4	5	1
	74	4	2	10	1	1	3	4	1
Algae -	83	3	4	6	-	-	1	2	1
Porites	74	5	1	14	-	-	3	1	2
	69	1	2	16	1	1	4	2	4
	30	12	33	20	-	1	2	1	1
	58	7	13	16	-	-	4	1	1
Acropora	41	27	15	10	1	-	3	1	2
	57	13	15	10	1	-	1	1	2
	55	22	14	5	-	-	2	1	1
	31	36	17	13	1	-	-	<1	2
	53	18	14	8	1	-	3	1	2
Acropora -	53	19	16	8	<1	-	1	1	2
Millepora	39	27	24	8	<1	-	1	<1	<1
	53	10	21	15	1	-	<1	<1	<1

Other grains are mainly pelagic forminifera and worm tubes.

TABLE 3: SUMMARY OF CHARACTERISTICS OF PATCH REEFS IN THE LAGOONAL AREAS OF THE BUCCOO REEF COMPLEX

PATCH REEF TYPES	ALGAE - PORITES	ACROPORA	ACROPORA - MILLEPORA	MONTASTREA
Location	South-central Reef Lagoon; Western Outer Bon Accord Lagoon	Southwestern and Northeastern Reef Lagoon	Eastern Reef Lagoon	Lagoonal entrance of Blind Passage
Shape	Elongate to sub-circular	Elongate to tabular	Elongate to sub-elliptical	Elongate - tabular
Area (m^2)	50 - 5000	50 - 60,000	600 - 6500	4500
Major Communities	Porites coral rubble; Halimeda opuntia	A. cervicornis; Acropora rubble; Halimeda sp.	A. cervicornis; M. alcicornis; Acropora and Millepora skeletons; Halimeda sp.; fleshy green algae	M. annularis
Minor Communities	P. porites; T. testinidium; coralline-red algae; molluscs; sponges; sea urchins	A. prolifera; Siderastrea; Agaricia; Montastrea; Diploria; Millepora; sea fans; sea whips; coralline-red algae	A. prolifera; Diploria; Siderastrea; M. complanata; sea fans; sea whips; coralline-red algae	Millepora sp.; A. palmata; A. cervicornis; P. astreoides; M. lamarkana D. strigosa; D. labrynthiformis; C. natans; S. siderea; M. areolata; E. fastigiata; sea fans; sea whips; sea urchins
No. of Significant Patch Reefs >50 m^2	17	13	3	1

Acropora and Millepora rubble also trap and bind sediment, which contributes to the framework building process.

The interlocking, growth patterns observed on Acropora and Acropora - Millepora patch reefs result from the fusion process of A. cervicornis described above.

The Montastrea Patch Reef forms a rigid framework, built up of coral heads of M. annularis. The ability of M. annularis to exclude almost all other corals competing with it for the same space, by extracoelenteric digestion (polyps of M. annularis extrude mesenterial filaments which dissolve the tissues of other corals), ensures its dominance on this patch reef as the primary reef builder (Lang, 1973; Scatterday, 1977).

Lack of Coral Diversity

The patch reefs of Buccoo Reef Complex generally exhibit a lack of coral diversity (Table 3). This aspect is probably due to the limited depths in which these patch reefs occur (generally 1 - 4 m), inhibiting vertical development and probable ecological zonation.

The weakly defined ecological zones (M. annularis 2 - 4 m; M. annularis, Acropora spp. 3 - 7 m; mixed coral head zone, >7 m) in the Montastrea Patch Reef, have developed because of its occurrence in deeper waters, which allowed for some vertical development. In addition, extensive biological erosion of M. annularis coralla by parrot fish and sea urchins, provides available substrate for other coral species to develop (Frydl, 1977; Scatterday, 1977).

Stages of Development

Based on observations and detailed mapping, four stages of development for patch reefs in the lagoonal areas of the Buccoo Reef Complex can be recognised, using Multer's (1975) model for the evolution of Florida patch reefs (Fig. 8):

(1) An initial stage with incipient development of corals.
(2) A youthful stage exhibiting luxuriant coral growth.
(3) A mature stage which is characterized by decreased coral growth and increased rubble deposits.
(4) An old age stage predominated by coral rubble which is encrusted with coralline and fleshy algae.

The Algae - Porites patch reefs are present in the mature and old age stages. These patch reefs would have been initiated by the incipient development of P. porites on stable sand or bare rock substrate. They would then progress to the youthful stage where P. porites would be dominant with minor occurrences of Porites rubble. Moderate to extensive Porites rubble encrusted by Halimeda and coralline-algae, characterise the mature and old age stages respectively, for Algae - Porites patch reefs observed at present (Fig. 8).

The Acropora patch reefs occur in the incipient, youthful and mature stages of development. The colonization of stable sand substrates by initial growth of A. cervicornis, the incipient stage of Acropora patch reefs, is present as discrete thickets in the Reef Lagoon. The youthful development stage of these patch reefs also occurs in Reef Lagoon as A. cervicornis coral-rich areas with minor Acropora rubble. Breakage of Acropora branches result in the formation of extensive coral rubble encrusted by Halimeda, which define the mature stage of development. The old age stage of Acropora patch reef development, which would probably be dominated by coral rubble with minimal coral growth was not observed (Fig. 8).

Acropora - Millepora patch reefs are restricted to the mature stage of development. The incipient stage of these patch reefs would also be the A. cervicornis thickets from which the Acropora patch reefs evolve. However in certain sections of Buccoo Reef lagoons where medium to high energy wave conditions occur, the hydrozoan Millepora will begin to replace A. cervicornis colonies (Adey and Burke, 1977). Millepora and Acropora communities and associated rubble, encrusted by Halimeda, coralline-red and fleshy green algae are observed, and characterize the mature development stage of Acropora - Millepora patch reefs. The old age stage of extensive Acropora and Millepora rubble encrusted by fleshy algae and probably Palythoa spp. has not yet developed (Fig. 8).

The Montastrea patch reef would have developed by the initiation of Montastrea growth on suitable substrates. This would have been followed by a M. annularis dominated patch reef in its youthful stage. At present, the Montastrea Patch Reef is transitional between the mature and old age stages of development. The dominant M. annularis coral heads exhibit extensive biological erosion, and these bare surfaces and other areas have been colonized by diverse coral species. Dead coral heads and coral rubble are observed in certain areas (Fig. 8).

Sediment Characteristics

Extensive occurrences of H. opuntia on the substrate and encrusting Halimeda spp. on Porites coral rubble (Figs. 3A and 3B) result in the predominance of Halimeda fragments in the sediments of the Algae - Porites patch reefs. In contrast, larger percentages of living corals and hydrozoans, encrusted by various organisms (Figs. 4B, 5A, 5B, 6B, 7A and 7B) result in a more equitable distribution of Halimeda, coral, coralline - algae and mollusc particles in the sediments of the Acropora and Acropora - Millepora patch reefs. Patch reef sediments therefore generally occur in situ. This factor is further supported by their medium to coarse sand size and poorly sorted nature.

The presence of fine size quartz silt in the sediments of the Algae - Porites patch reefs is indicative of a terrigenous input to these areas, through the canals and streams draining into the Inner and Outer Bon Accord Lagoons.

Factors Controlling Patch Reef Occurrences and Development

The geographic zonation of the different patch reefs in the lagoonal areas, their distinct ecological characteristics and various stages of

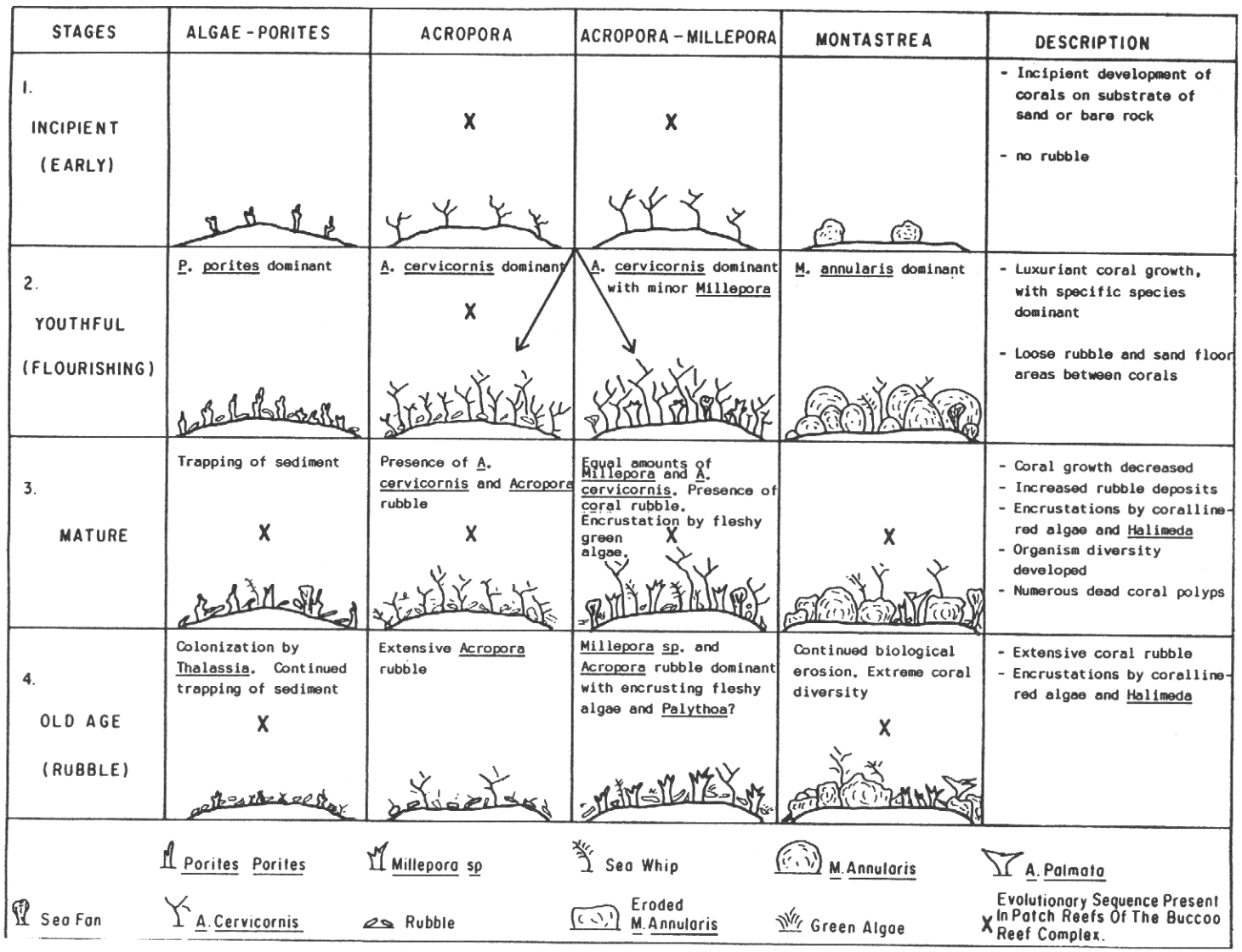

Fig. 8 - Schematic illustration showing suggested evolutionary sequences of patch reefs in the Buccoo Reef Complex. Zones without x's do not occur at present on the reef.

development are probably controlled by a combination of environmental parameters which include bathymetry, wave exposure, water circulation, salinity and turbidity, and the nature of the substrate.

The Porites coral is extremely adaptable to environmentally-stressed areas. For example, it has the ability to reject sediment much better than other varieties (Hubbard and Pocock, 1972). Therefore Porites coral initially colonized the southern lagoonal areas of Buccoo Reef Complex (Fig. 1) which is shallow and turbid, and exhibits low wave energy and moderate water circulation.

Low salinity levels and influx of terrigenous sediment in southern lagoonal areas, especially after very heavy rainfall probably resulted in the death of Porites coral, and the development of extensive coral rubble. Terrigenous sediment (quartz silt) is still being deposited in these areas, as indicated by the sediment analysis. The trapping of sediment by the coral rubble further retarded the growth of Porites, owing to an unstable sediment substrate and increased levels of turbidity. These factors explain the occurrences of the mature and old age stages of development for the Algae - Porites patch reefs.

Acropora communities are well suited to the shallow, well circulated, moderate wave energy conditions of the central and northern lagoonal areas (Fig. 1).

In the southwestern Reef Lagoon, which experiences low to moderate wave energy conditions, breakage of Acropora branches are not extensive, and the patch reefs are in the youthful stage of development. In northeastern Reef Lagoon, where the Acropora patch reefs are more exposed to the waves, damage to the coral branches are more extensive. This results in the formation of coral rubble and the mature stage of development in these patch reefs.

Owing to the increase in wave height, after passing over the deeper waters of the Blue (Deep) Hole, Millepora communities have colonized and replaced Acropora corals in this area (Fig. 1). This results in the formation of Acropora - Millepora patch reefs. Field studies in the Caribbean (Adey, 1975; Adey and Burke, 1977) have shown that Millepora is very adaptive to moderate and high-energy wave conditions. These conditions also restrict the grazing of ecological communities by fish and other invertebrates, resulting in the occurrence of fleshy green algae in these patch reefs.

Extensive damage to Acropora and Millepora colonies by high wave energy, results in extensive rubble development, hence the occurrence of the mature stage of development for Acropora - Millepora patch reefs.

The massive domal-shaped coral heads of the Montastrea Patch Reef develop in the deeper waters of northern lagoonal areas, adjacent to the Blind Passage and Deep Channel (Fig. 1). Montastrea corals are also adaptive to the lower wave energy and decreased light conditions in this area. Low to moderate wave energy conditions in this area as a result of deeper water conditions do not inhibit grazing by fish and other invertebrates. Therefore the coral heads are subjected to extensive biological erosion, resulting in the toppling of some Montastrea corals, and colonization by other corals on these bare surfaces. This feature of coral erosion by organism grazing, and increased coral diversity defines the mature - old age transitional stage of the Montastrea Patch Reef.

Geographic distribution, ecological characteristics and development stages of the four different patch reef types in the Buccoo Reef Complex are therefore primarily controlled by the degree of wave exposure; and moderately influenced by degree of water circulation and turbidity. Geister (1977) also indicated previously that ecological zonation of Caribbean corals are to some extent dependent on the degree of wave exposure. With respect to the major environmental parameters: wave exposure, degree of water circulation and turbidity, which affect the patch reefs of Buccoo Reef, it can be summarized that:

(1) The Montastrea Patch Reef has developed in low wave energy, low water circulation and high turbidity environment.
(2) The Algae - Porites patch reefs are characterized by an environment of moderate water circulation, low wave energy and high turbidity.
(3) The Acropora patch reefs are located in a low to moderate wave energy, moderate water circulation and low turbidity environment.
(4) The Acropora - Millepora patch reefs occur in an environment characterized by high wave energy, strong water circulation and low to high turibdity.

ACKNOWLEDGEMENTS

D. Hudson carried out this study as part of his M.Sc. research at McGill University, under the guidance of Dr. E.W. Mountjoy, whose supervision is gratefully acknowledged. Funding for this research was provided by McGill University, along with a National Science and Engineering Research Grant A 2128 to Dr. E.W. Mountjoy.

In addition the authors are thankful to the Institute of Marine Affairs, Trinidad for field support; Messrs. A. Cummings and R. Ramkissoon for draughting the figures; Mr. B. Dyer for his assistance during the field work; and Mrs. M. Croney for her invaluable typing skills.

The assistance of the Drawing Office, Exploration Department of the Trinidad and Tobago Petroleum Company is also acknowledged.

REFERENCES

Adey, W.H., The Algal ridges and coral reefs of St. Croix - their structure and Holocene development, Atoll Research Bull. 187, The Smithsonian Institution, Washington D.C., 1975.

Adey, W.H., and Burke, R.B., Holocene bioherms of Lesser Antilles - Geologic control of development, 67-81 in Frost, S.H., Weiss, M.P., and Saunders, J.B., Eds., Reefs and Related Carbonates, Amer. Assoc. Petroleum Geologists, Studies in Geology 4 421, 1977.

Case, J.E., Geologic Framework of the Caribbean, 3-26 in Weaver, J.D., Ed., Geology Geophysics and Resources of the Caribbean, Report of the Caribbean Region and its Resources, Kingston, Jamaica, 17-22 February, 1975, 150, 1975.

Frdyl, P., The geological effect of grazing by parrotfish (Scaridae) on a Barbados coral reef, M.Sc. Thesis, Technical Report 77-3, Dept. of Geological Sciences, McGill University, 136, 1977.

Geister, J., The influence of wave exposure on the ecological zonation of Caribbean coral reefs, Proc.of the 3rd. Int. Coral Reef Symposium, Miami, Florida, 23-29, 1977.

Gilmore, M.D., and Hall, B.R., Life history, growth habits and constructional roles of Acropora cervicornis in the patch reef environment, Jour. Sed. Petrology 46, 18-22, 1976.

Hubbard, J.A.E.B., and Pocock, Y.P., Sediment rejection by Recent scleractinian corals: a key to paleoenvironmental reconstruction, Geol. Rundschau 61, 598-626, 1972.

Kenny, J.S., A preliminary study of Buccoo Reef/ Bon Accord Complex with special reference to development and management, Dept. of Biological Sciences, University of the West Indies, St. Augustine, 123, 1976.

Lang, J., Interspecific aggression by scleractinian corals. 2. Why the race is not only to the swift, Bull. Marine Sci., 23, 260-279, 1973.

Mascle, G., Lajat, D., and Nely, G., Sediments deformation linked to subduction and to argillokinesis in the southern Barbados Ridge from multichannel seismic surveys, Transactions of the 4th Latin Amer. Geol. Congress, Port-of-Spain, 873-882, 1979.

Multer, H.G., Ed., Field guide to some carbonate rock environments, Florida Keys and Western Bahamas, Contribution 40, Dept. of Earth Sciences, Farleigh Dickinson University, New Jersey, 175, 1975.

Multer, H.G., and Zankl, H., Distribution, structure and origin of Holocene patch reefs in the West Indies, Proc. of the 5th. Int. Coral Reef Congress 3, Tahiti, 227-228, 1985.

Scatterday, J.W., Low-water emergence of Caribbean reefs and effect of exposure on coral diversity - observations off Bonaire, Netherlands, Antilles, 155-169 in Frost, S.H., Weiss, M.P., and Saunders, J.B., Eds, Reefs and Related Carbonates, Amer. Assoc. Petroleum Geologists, Studies in Geology 4, 421, 1977.

Turmel, R.J., and Swanson, R.G., The development of Rodriguez Bank, a Holocene mudbank in the Florida reef tract, Jour. Sed. Petrology, 497-518, 1976.

Wallace, R.J., and Schafersman, D., Patch-reef ecology and sedimentology of Glovers Reef Atoll, Belize 37-52 in Frost, S.H., Weiss, M.P., and Saunders, J.B., Eds., Reefs and Related Carbonate, Amer. Assoc. Petroleum Geologists, Studies in Geology 4, 421, 1977.

STRATIGRAPHIC AND STRUCTURAL RELATIONSHIPS ON TOBAGO, WEST INDIES, AND SOME TECTONIC IMPLICATIONS

A.W. Snoke, J.D. Yule[1], D.W. Rowe[2]
Department of Geology and Geophysics
University of Wyoming
Laramie, WY 82071-3006, USA

G. Wadge
Department of Geography
University of Reading
Reading RG6 2AB, UK

W.D. Sharp
Department of Earth and Space Sciences
State University of New York
Stony Brook, NY 11794, USA

Present addresses:
[1]Division of Geological & Planetary Science, California Institute of Technology, Pasadena, CA 91125, USA
[2]WESTGOLD, 2104 Reserve, Missoula, MT 59801, USA

ABSTRACT

Tobago is principally composed of igneous and metamorphic rocks that comprise a natural cross-section through a fragment of the allochthonous, Mesozoic oceanic-arc of the southern Caribbean. The pre-Cenozoic rocks of Tobago can be divided into four, approximately east-west-striking belts that transect the island: North Coast Schist (NCS), amphibolite-facies aureole (dynamothermal metamorphism of NCS rocks), ultramafic to tonalitic plutonic complex, and Tobago Volcanic Group (TVG). A mafic dike swarm widely intruded the plutonic complex and TVG, whereas only scattered post-metamorphic dikes occur in the NCS and amphibolite-facies aureole belts.

Radiolaria in argillite layers from a distinctive epiclastic unit in the TVG suggest an Aptian-Albian age, and ammonite molds from the same unit indicate an Albian age. $^{40}Ar/^{39}Ar$ hornblende plateau ages from the plutonic-volcanic-dike complex indicate that this rock suite evolved principally during the Albian (ca 105-103 Ma). One representative of the mafic dike swarm yielded a hornblende plateau age of ca 91 Ma, indicating that mafic magmatism apparently extended into the early Late Cretaceous. The age of the NCS is at least Aptian and perhaps as old as Late Jurassic ($^{40}Ar/^{39}Ar$ data on relict igneous hornblende from greenschist-facies tuff breccia).

Quaternary coralline limestone forms a low relief platform at the southwestern end of the island. Other Cenozoic map units are the Rockly Bay Formation (Pliocene), sandstone, conglomerate, and limestone of Montgomery (Pleistocene to Pliocene?), and Quaternary alluvium.

The NCS rocks are lower greenschist facies, multiply-deformed volcanogenic rocks. Detailed geologic mapping indicates that the NCS was wallrock for the plutonic complex. A selvage of amphibolitic rocks (<250 m structural thickness) forms a mappable belt between the NCS and the plutonic complex. Metamorphic grade in the aureole decreases with increasing structural depth, thereby exhibiting an inverted metamorphic gradient. The primary igneous contact between the intrusive plutonic rocks and the metamorphosed NCS rocks is only locally preserved, and more commonly this boundary has been overprinted by brittle deformation and retrogression. Where preserved, the primary igneous contact is interpreted as the margin of a zone of high shear strain which developed as a hot, nearly crystallized mass of ultramafic-mafic rocks dynamothermally metamorphosed older greenschist facies rocks during emplacement into the upper crust. During the progressive upward emplacement of the plutonic suite, this zone evolved from a plastic shear zone into a brittle fault zone referred to here as the "back-aureole (reverse) fault". Although the back-aureole fault virtually transects the island, it is related to the emplacement of the intrusive plutonic complex and not a regional compressive stress regime. Furthermore, in that this fault zone appears to have developed in close association with the mid-Cretaceous plutonic suite, it is inferred to be a Cretaceous fault system.

Both normal and oblique-slip faults have fragmented and offset the back-aureole fault. A normal fault system subparallel to the back-aureole fault has greatly complicated relationships by attenuating the amphibolite aureole and juxtaposing various elements of the four main belts into anastomosing, fault-bounded slices. A still younger system of high-angle, cross-cutting faults strike approximately NNW and chiefly display left-lateral separation. This separation is probably a result of a complex oblique-slip displacement history. The age of the normal and oblique-slip faulting is uncertain but may be related to the broad strike-slip regime that apparently existed in the southeastern Caribbean during the Neogene.

Tobago is the easternmost part of a composite oceanic-arc terrane that initially collided with the northwestern margin of South America in the mid-Late Cretaceous. Subsequently, parts of this allochthonous terrane were progressively accreted from west to east along the northern rim of South America. Displaced fragments of the originally composite, Mesozoic oceanic-arc preserved in the southeastern Caribbean include: the Aruba-Blanquilla island chain, Aves Ridge, the Villa de Cura klippe (Venezuela), the El Copey Formation (Araya Peninsula), and Tobago, West Indies.

INTRODUCTION

Tobago, West Indies, is an island that forms part of a structural high composed chiefly of Mesozoic igneous and metamorphic rocks at the northeasternmost corner of the present-day South American continental shelf (Figure 1; Case and

Larue, D.K., and Draper, G. (eds.),
Transactions of the 12th Caribbean Geological Conference, St. Croix, U.S.V.I., Miami Geological Society, P.O. Box 431552, South Miami, FL 33243, U.S.A

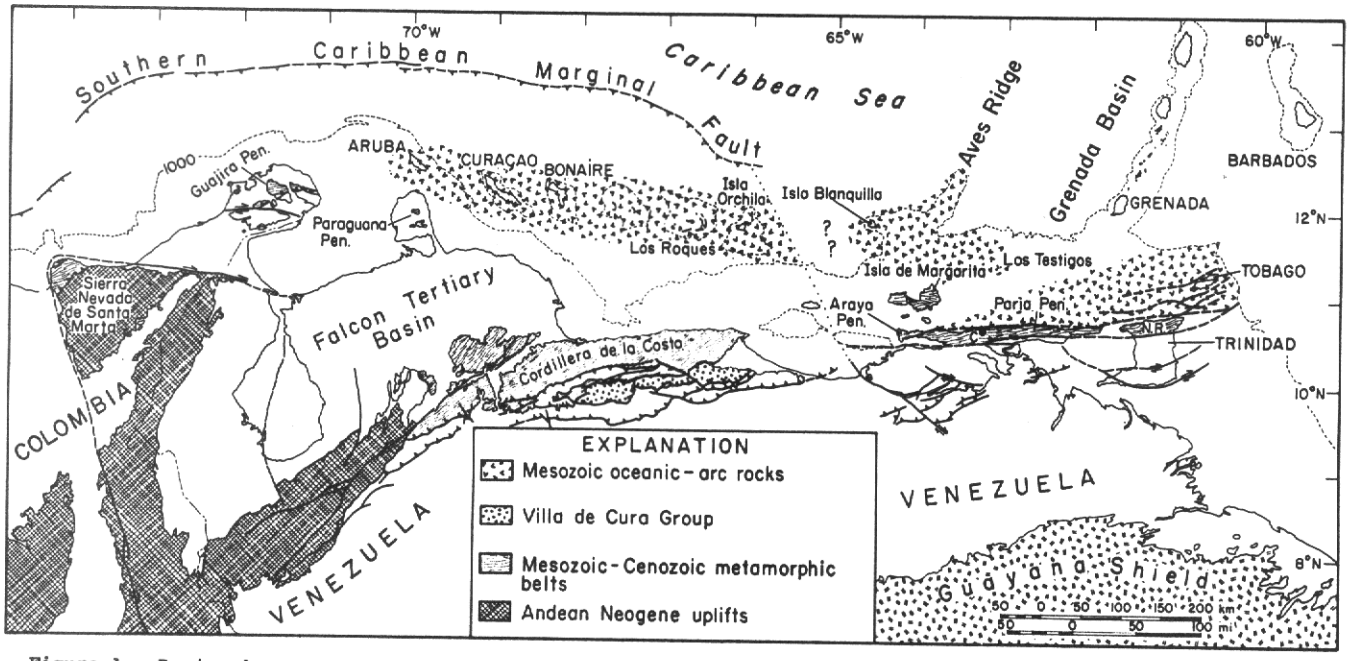

Figure 1. Regional geotectonic map of the southern Caribbean region showing the inferred distribution of fragments of the accreted Mesozoic oceanic-arc and associated geological terranes. N.R. = Northern Range. C = Carúpano.

Holcombe, 1980). However, petrochemical data indicate an oceanic island arc character (Frost and Snoke, 1989), implying an allochthonous history since petrogenesis. Tobago, therefore, has a definite affinity with allochthonous oceanic-arc rocks that occur as scattered fragments along the northern rim of South America (e.g., Stephan et al., 1980; Figure 1). It is thus the easternmost element of the Caribbean Mountain system (Bellizzia, 1972). Tobago's position and relationships with the southern Lesser Antilles island arc and associated accretionary prism are more uncertain, and have prompted substantial speculation. Could the Paleogene platform of the southern Lesser Antilles volcanic arc be built upon a Mesozoic igneous and metamorphic basement similar to Tobago (Westbrook and McCann, 1986; Bouysse, 1988)? Is Tobago part of an accretionary complex that is obliquely overriding the northeast continental margin of South America (Speed, 1985, 1986; Speed and others, 1989)? Is Tobago a fault-bounded sliver that has been transported hundreds of kilometers along the Caribbean-South American plate boundary (Robertson and Burke, 1988)?

Obviously, a detailed knowledge of the geologic history of Tobago would provide some important constraints for these and other tectonic models for the southeastern Caribbean. The purpose of this article is therefore to present a preliminary overview of the stratigraphic and structural relationships of the Mesozoic rocks exposed on Tobago, West Indies, and to highlight the implications of these relationships for the tectonostratigraphic history of the allochthonous, Mesozoic oceanic-arc of the southern Caribbean.

We begin our overview with descriptions of the broad-scale subdivisions of the Mesozoic igneous-metamorphic complex of Tobago (Table 1); the distribution of these rock units is shown on Figure 2. A summary of new $^{40}Ar/^{39}Ar$ radiometric studies (Table 2) which provides important geochronological constraints on the evolution of the Mesozoic rock suite is also presented. In the second part of the article, we summarize the main structural features of the island, and two geologic cross-sections (Figure 3) allow one to visualize these relationships at depth. Finally, these data, analyzed within the regional framework of the southern Caribbean, are used to provide a preliminary evaluation of four fundamental aspects of the geology of Tobago:

1) the cogenetic nature of the mid-Cretaceous plutonic and volcanic rocks on Tobago;

2) the development of a composite oceanic island-arc terrane;

3) the affinity of the Tobago terrane to other lithological units in the southern Caribbean; and

4) the displacement history of the Tobago terrane.

ROCK UNITS

The Mesozoic rocks of Tobago (Table 1) can be divided into four main groups: the North Coast Schist (NCS), amphibolite-facies aureole (dynamothermal metamorphism of the NCS rocks), the ultramafic to tonalitic plutonic complex, and the Tobago Volcanic Group (TVG). These broad lithologic subdivisions form approximately east-west-striking belts which transect the island (Maxwell, 1948). A mafic dike swarm widely intruded the plutonic complex and TVG, whereas only scattered post-metamorphic dikes occur in the NCS belt. The Mesozoic rocks of Tobago represent an exceptional natural cross-section through a part of a composite oceanic-arc terrane (Frost and Snoke, 1989).

A systematic $^{40}Ar/^{39}Ar$ study was carried out

TABLE 1. LITHOLOGIC SUBDIVISIONS OF PRE-CENOZOIC ROCKS OF TOBAGO, WEST INDIES

I. North Coast Schist (inferred stratigraphic order, oldest to youngest)

Parlatuvier Formation - intermediate to mafic tuff and tuff breccia, and pre-metamorphic andesite dikes

Mt. Dillon Formation - siliceous tuff (locally silicified), graphitic siliceous schist, graphitic quartzose phyllite, chert, and scarce premetamorphic andesite dikes

II. Tobago Volcanic Group [stratigraphic order uncertain, apparent order oldest to youngest given; the designations of Maxwell (1948) in parentheses]

Hornblende + plagioclase + clinopyroxene-phyric tuff breccia and lapilli tuff

Plagioclase + clinopyroxene-phyric tuff breccia, lapilli tuff and lava (Goldsborough and Hawk's Bill formations)

Argillite (contain Aptian(?)-Albian radiolaria and Albian ammonites) and volcaniclastic breccia, grit, and sandstone

Clinopyroxene + plagioclase-phyric tuff breccia, lapilli tuff, and scarce lava (Bacolet and Merchiston formations)

III. Plutonic complex (oldest to youngest, based on intrusive relations)

Older deformed mafic plutonic-volcanic complex

Dunite, wehrlite, olivine clinopyroxenite, hornblendite, hornblende plagioclase pegmatoid

Hornblende ± clinopyroxene gabbro, diorite, quartz diorite

Biotite ± hornblende tonalite

IV. Mafic dike swarm (chiefly intrudes plutonic complex and Tobago Volcanic Group but also common in the amphibolitic aureole; only scattered post-metamorphic dikes in the North Coast Schist)

Hornblende microdiorite, hornblende gabbro, acicular hornblende-phyric diorite, dolerite, hornblende + clinopyroxene-phyric melagabbro.

during geologic mapping and structural analysis of Tobago. A detailed report analyzing these new data is in preparation (Sharp and Snoke, in prep., 1990). However, as a chronological framework for this article, we have prepared a brief summary of the new radiometric data (Table 2). These data indicate the following age constraints:

1) $^{40}Ar/^{39}Ar$ hornblende dates from the volcanic-plutonic complex indicate a contemporaneous magmatic evolution in the mid-Albian (ca 103-105 Ma);

2) Hornblende plateau ages from the mafic dike suite indicate two emplacement ages: early dikes, only slightly younger (ca 102-103 Ma) than the volcanic-plutonic complex and a distinctly younger suite (ca 91 Ma); and

3) a primary protolith age on the volcanogenic Parlatuvier Formation of the North Coast Schist >120 Ma.

The Cenozoic rock record on Tobago, exclusive of Holocene surficial deposits, consists of the following deposits (oldest to youngest): Rockly Bay Formation (Pliocene); sandstone, conglomerate, and limestone of Montgomery [Pleistocene - Pliocene(?)]; and the coralline limestone of Booby Point (Quaternary). These deposits represent various shallow marine accumulations and their preservation therefore records tectonic uplift and/or sea level change. These shallow marine deposits are conspicuously fossiliferous and consequently several studies have been completed on these rocks (for specific details see: Trechmann, 1934; Maxwell, 1948; Saunders and Muller-Merz, 1985). The distribution of these deposits is shown in Figure 2.

North Coast Schist

This extensively exposed rock unit forms the northern third of the island, including the rugged and densely vegetated backbone of Tobago known as the Main Ridge. This lithologically diverse and strongly deformed unit was named by Maxwell (1948) and differs significantly from the schistose rocks of the Northern Range of Trinidad because it has evolved from volcanogenic protoliths (Rowe and Snoke, 1986). The NCS rocks were pervasively

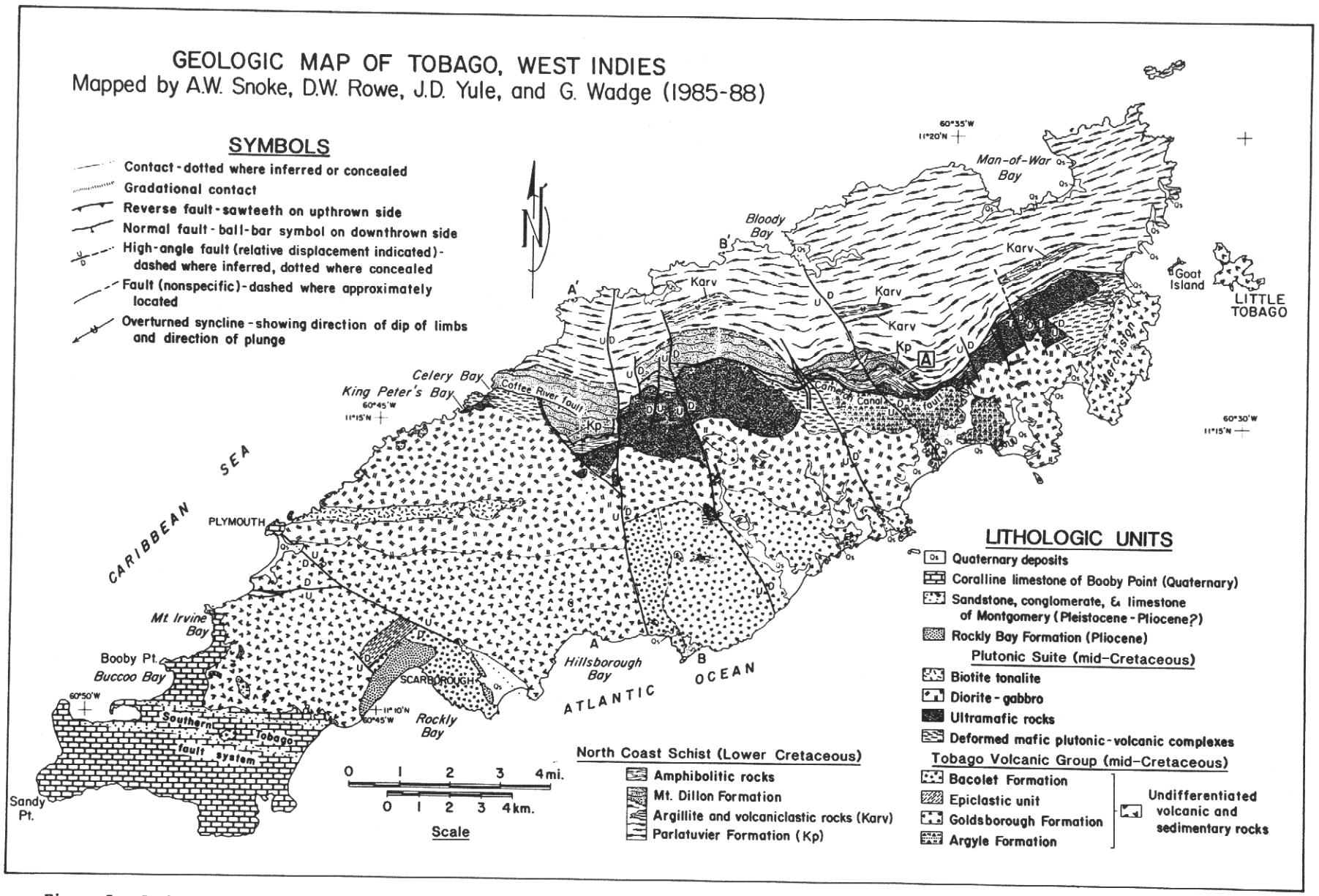

Figure 2. Geologic map of Tobago, West Indies.

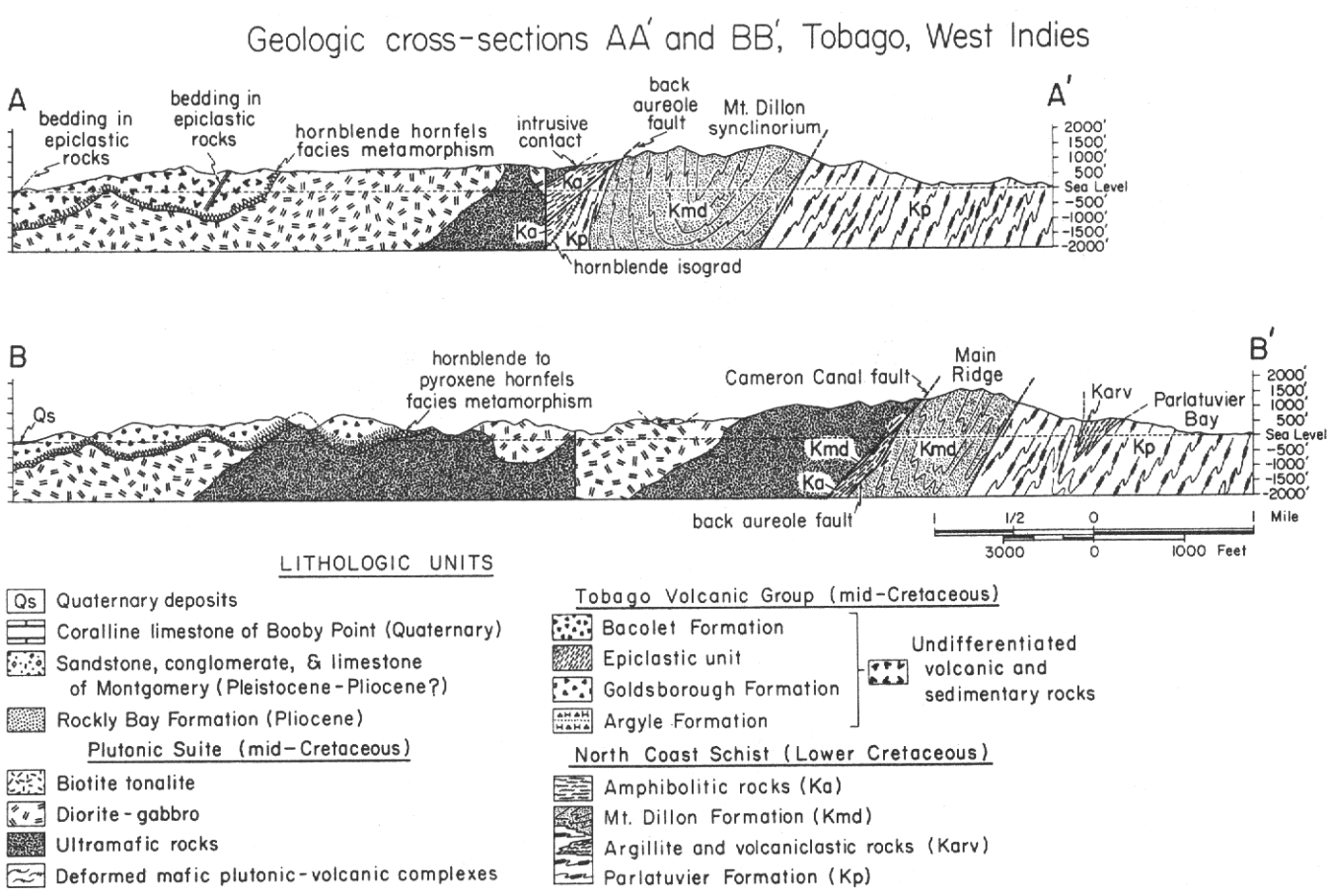

Figure 3. Geologic cross-sections across Tobago, West Indies.

metamorphosed during the mid-Mesozoic (Sharp and Snoke, 1988) and ubiquitously contain lower greenschist-facies mineral assemblages (e.g., chlorite, epidote, actinolite, and albite in mafic protoliths). Along its southern margin, the NCS has been intruded by the ultramafic rocks of the plutonic suite thereby transforming the greenschist-facies rocks to a much higher metamorphic grade characterized especially by the development of hornblende and more calcic plagioclase (oligoclase and andesine). This distinct belt of hornblende schists can be mapped virtually across the island and is referred to as the "amphibolite-facies aureole". These hornblende schists locally grade into typical greenschist-facies NCS rocks, but more commonly, a reverse fault (i.e., the so-called "back-aureole" fault) forms the boundary between the NCS and the strongly metamorphosed and deformed rocks of the amphibolite aureole.

Although the NCS is unfossiliferous, field relationships coupled with radiometric dating indicate that the NCS is apparently the oldest rock unit exposed on the island. As noted above, the NCS served as wallrock for the younger plutonic suite. Furthermore, $^{40}Ar/^{39}Ar$ radiometric dating of relict igneous hornblende from the NCS indicates a pre-Aptian protolith age (>120 Ma) and perhaps as old as Late Jurassic (Table 2).

We have recognized two fundamental lithologic facies that constitute the NCS: Parlatuvier Formation= basaltic andesite lapilli tuff and crystal-lapilli tuff and associated subvolcanic mafic intrusives, and Mt. Dillon Formation= dacitic crystal-lapilli tuff, volcanogenic argillite and siliceous argillite, and siliceous hydrothermal replacement deposits (volcanogenic chert, originally designated "quartzite" by Maxwell, 1948). Although these rocks have been metamorphosed and locally intensely deformed, relict volcanic textures are locally very well-preserved. Coarse volcaniclastic tuff breccia in the Parlatuvier Formation is especially spectacular, consisting of large lithic clasts (sometimes > 30 cm across) in a fine-grained matrix of albite, quartz, epidote, chlorite, calcite, and various accessory minerals.

The Parlatuvier Formation comprises the majority of the NCS, and fresh samples always possess a distinctive dark green to gray-green hue (i.e., a manifestation of the greenschist facies mineral phases). The Mt. Dillon Formation is chiefly exposed in the southern and western parts of the NCS (Fig. 2). This unit is characteristically more siliceous than the Parlatuvier, including both tuffaceous and sedimentary rocks, and when fresh, hand specimens are characterized by dark grayish hues. Weathered massive buff-colored tuff is also very distinctive of the unit, especially in roadcuts or along trail exposures.

The volcaniclastic protoliths of the NCS represent a rock suite deposited subaqueously in a basin adjacent to a volcanic arc. Proximal coarse-grained tuff breccia and crystal-lapilli tuff

TABLE 2. A SUMMARY OF $^{40}Ar/^{39}Ar$ RADIOMETRIC AGE DATA, TOBAGO, WEST INDIES

All ages are based on $^{40}Ar/^{39}Ar$ incremental heating analyses of hornblende. Age assignments are based on consideration of age spectra, K/Ca ratios of individual gas fraction, and isotope correlation diagrams as well as the geologic history of the samples.

Sample 2D-14: A 1-meter-wide dike of hornblende gabbro which intrudes biotite tonalite yielded a plateau age of 91.4±2.2 Ma, interpreted as the age of igneous crystallization.

Sample 1C-30: A 1-meter-wide dike of hornblende melagabbro which intrudes biotite tonalite yielded a plateau age of 102.9±1.1 Ma, interpreted as the age of igneous crystallization.

Sample 1C-29: A 2-meter-wide dike of hornblende porphyry which intrudes biotite tonalite yielded a plateau age of 102.8±1.2 Ma, interpreted as the age of igneous crystallization.

Sample 1C-5: Poikilitic hornblende (quartz-bearing) diorite, a phase of the gabbro-diorite pluton yielded a linear array on an isotope correlation diagram indicating an age of 104.7±1.6 Ma, corresponding to its age of igneous crystallization.

Sample 2D-35: A dikelet of hornblende gabbro pegmatite, representing a late, water-rich phase of the clinopyroxene-rich ultramafic rocks of the intrusive plutonic suite yielded a linear array on an isotope correlation diagram indicating an age of 103.6±1.4 Ma, corresponding to its age of igneous crystallization.

Sample T827: A lithic clast of hornblende-plagioclase porphyry from the Tobago Volcanic Group yielded a plateau age of 104.2±1.3 ma, corresponding to the eruptive age of the enclosing volcaniclastic strata.

Sample DR245: Relict igneous hornblende from a clast of hornblende-phyric andesite in a tuff from the greenschist facies North Coast Schist yielded a complex release spectrum indicating an igneous age of $\geq$120 Ma.

Low temperature parts of release spectra from several samples interpreted to contain intergrowths of phyllosilicates yield ages of about 92 Ma, interpreted to indicate that cooling below about 280°C took place by this time.

(Parlatuvier Formation) interfinger with more distal, fine-grained tuff and hemi-pelagic sedimentary rocks (Mt. Dillon Formation). A possible modern analog of the depositional environment of the NCS is the depositional setting of volcanogenic deposits of the Lesser Antilles island arc in the Grenada basin where coarse, subaqueous pyroclastic debris-flow deposits interfinger with fine-grained basinal facies sediments (Sigurdsson and others, 1980).

Ultramafic to tonalitic plutonic complex

A heterogeneous suite of plutonic rocks forms an intrusive complex immediately south of the NCS. These plutonic rocks have intruded and dynamothermally metamorphosed the NCS wallrocks, and roof pendants of TVG rocks form a south-dipping carapace above the intrusive complex.

The plutonic suite consists of four mappable units: 1) deformed and metamorphosed mafic rocks; 2) ultramafic rocks; 3) gabbro-diorite; and 4) biotite tonalite. Unit 1) was penetratively deformed under hornblende-hornfels to pyroxene-hornfels facies metamorphic conditions during the emplacement of adjacent intrusive ultramafic masses. The protolith for this deformed oldest unit ranged from porphyritic gabbroic bodies to mafic fragmental volcanic rocks (i.e., TVG). The ultramafic rocks form several discontinuous lenticular masses that can be mapped across the island. The ultramafic rocks are commonly clinopyroxene-rich, varying from wehrlite to hornblende clinopyroxenite; however, locally dunite forms distinct masses within the ultramafic complex. Orthopyroxene has not been recognized as a pyrogenetic phase in these ultramafic rocks, and the rocks are not tectonites. These characteristics clearly suggest an affinity with Alaskan-type ultramafic-mafic complexes rather than ophiolitic suites (Snoke et al., 1982). These ultramafic rocks are interpreted as crystal accumulations that were segregated during magmatic differentiation of an originally basaltic magma in a mid-crustal magma chamber. Subsequently, the crystal-rich portions of the magma chamber were re-mobilized and emplaced higher in the crust as hot, nearly solid crystal aggregates. The emplacement of these hot crystal-rich aggregates caused intense deformation of the wallrocks. The NCS was dynamothermally metamorphosed at amphibolite-facies conditions (i.e., the amphibolite-facies aureole), and older parts of the plutonic complex (e.g., unit 1) were also metamorphosed and deformed adjacent to the ultramafic masses. A heterogeneous gabbro-diorite unit subsequently intruded both units 1 and 2, and forms the most extensive plutonic unit on the

island. Variations in mineral content and texture of the gabbro-diorite unit are extreme; compositionally the plutonic rocks of this unit range from quartz diorite to melagabbro, texturally from uniform, medium-grained to pegmatitic. In many parts of the gabbro-diorite unit, extreme textural and compositional variations are common in a single set of exposures, although locally the gabbro-diorite unit can also be strikingly homogeneous. The youngest unit in the plutonic suite is biotite +/- hornblende tonalite that forms an EW-striking, dike-like body that has been mapped from the Caribbean coast near Plymouth to its exposed surface end about 7 1/2 km inland (Fig. 2). Analysis of aeromagnetic data suggests that this intrusion may continue in the subsurface at least several kilometers east of its surface termination (Wadge and Snoke, in prep.).

Tobago Volcanic Group

The volcanic rocks (TVG) that form a carapace above the plutonic suite can be traced from Rocky Point to Little Tobago island (Fig. 2). Cupolas of mafic and ultramafic plutonic rocks locally intrude the volcanic rocks indicating the proximity of the plutonic body beneath the volcanic carapace (Figs. 2, 3). The thickest section of the TVG is exposed near Scarborough where a generally poorly-exposed stratigraphic section of TVG rocks dip moderately (ca 40-50^{o}) to the southeast. In this section, a fossiliferous epiclastic unit has been delineated (Fig. 2). This unit consists of black argillite, sandstone, and sedimentary breccia. Radiolaria in the argillite suggest an Aptian-Albian age (P. Noble, per. comm., 1990), and ammonite molds from several horizons in this unit indicate an Albian age (W.A. Cobban, pers. comm., 1988). Hornblende from TVG tuff breccia collected on Little Tobago island has yielded a plateau age of ca 104 Ma, indicating an Albian age also for this part of the TVG (Table 2).

The TVG rocks are chiefly volcaniclastic breccias, ranging from block-and-ash flow deposits to subaqueous debris-flow deposits; however, locally lava (sometimes pillowed) forms prominent accumulations in the volcanic pile. These volcanic rocks were probably deposited on the flanks of a submarine volcanic center. The following characteristics support a proximal submarine depositional history:

1) pillowed lavas (submarine eruption of lava);

2) the intercalation of marine sedimentary rocks (i.e., fossiliferous argillite);

3) the coarse fragmental texture of much of the rock units;

4) the absence of virtually all non-volcanogenic material;

5) extensive metasomatic alterations (Jackson and Smith, 1985; and Frost and Snoke, 1989).

The laterally discontinuous sedimentary sequences may represent local "ponded" basins along the flanks of the volcanic arc that accumulated hemipelagic and epiclastic sediments between the volcanic eruptions.

Mafic dike swarm

Numerous mafic dikes intrude the plutonic suite and TVG rocks. The most common mafic dikes are fine-grained with microscopic acicular hornblende and subequant plagioclase. The dikes are tabular bodies that form distinctive dark-colored bands in the older plutonic or volcanic wallrock and commonly range in width from about 15 centimeters to a meter. $^{40}Ar/^{39}Ar$ radiometric dating on hornblende from representative samples of the mafic dike swarm indicate two distinct episodes on dike injection. The early, and perhaps most widespread, phase is ca 103 Ma, whereas one member of the dike swarm has yielded a hornblende plateau age of ca 91 Ma.

STRUCTURAL FEATURES

Deformational history of the NCS

Strong penetrative plastic deformation accompanied the greenschist facies metamorphism of the NCS. These volcanogenic rocks were converted into foliated and lineated metamorphic tectonites. Mesoscopic structural features in the NCS include: two foliation surfaces (S_1 and S_2), four fold generations [F_1, F_2 (see Fig. 4), chevron, and kink bands], a stretching lineation (L_{str}), and three intersection lineations (L_{0x1}, L_{0x2}, L_{1x2}). S>L- or S-tectonites are most common, but L>S- or L-tectonites are locally conspicuous. All these features, except perhaps some of the angular folds, were formed during a continuous deformational history that pre-dated the evolution of the mid-Cretaceous plutonic-volcanic-dike complex.

The primary foliation surface in the NCS is S_1 defined in part by the planar orientation of platy metamorphic minerals such as chlorite and white-mica or tectonically flattened volcanogenic fragments (i.e., lapilli). S_1 is subparallel to the axial surfaces of F_1 folds (synmetamorphic) which dip southward across the island. These folds plunge gently to moderately NE-ENE or SW-WSW, but verge consistently northward (i.e., toward the Caribbean Sea). The stretching lineation (L_{str}) is subparallel to the hingelines of the F_1 folds and therefore also plunges gently to moderately NE-ENE or SW-WSW. The hingelines of F_2 folds (late metamorphic) are also broadly subparallel to the hingelines of F_1 folds and the stretching lineation. Therefore, this common coaxiality of fabric elements is interpreted to indicate that both the synmetamorphic and late metamorphic fold phases and the stretching lineation developed during the same progressive, polyphase deformation. Sheath folds have not been recognized in the NCS, and many of the F_1 folds are near-cylindrical in form. The full kinematic significance of these relationships is not fully understood; but it appears likely that the F_1 folds were not rotated into parallelism with the stretching lineation. The folds and stretching lineation evolved concurrently during a period of complex plastic deformation with a strong extensional component parallel to the stretching lineation (i.e., X axis of the finite strain ellipsoid). The overall orientation of the stretching lineations and not the vergence of the folds is the best indicator of the slip line during this plastic deformation.

Deformational features within the amphibolite-facies aureole

The amphibolite aureole occurs as a largely continuous, narrow strip between the NCS and the intrusive plutonic complex (Fig. 2). Where absent, the aureole has been truncated by a NW-striking, right-lateral, oblique-slip(?) fault (Fig. 2). Metamorphic grade within the aureole decreases with

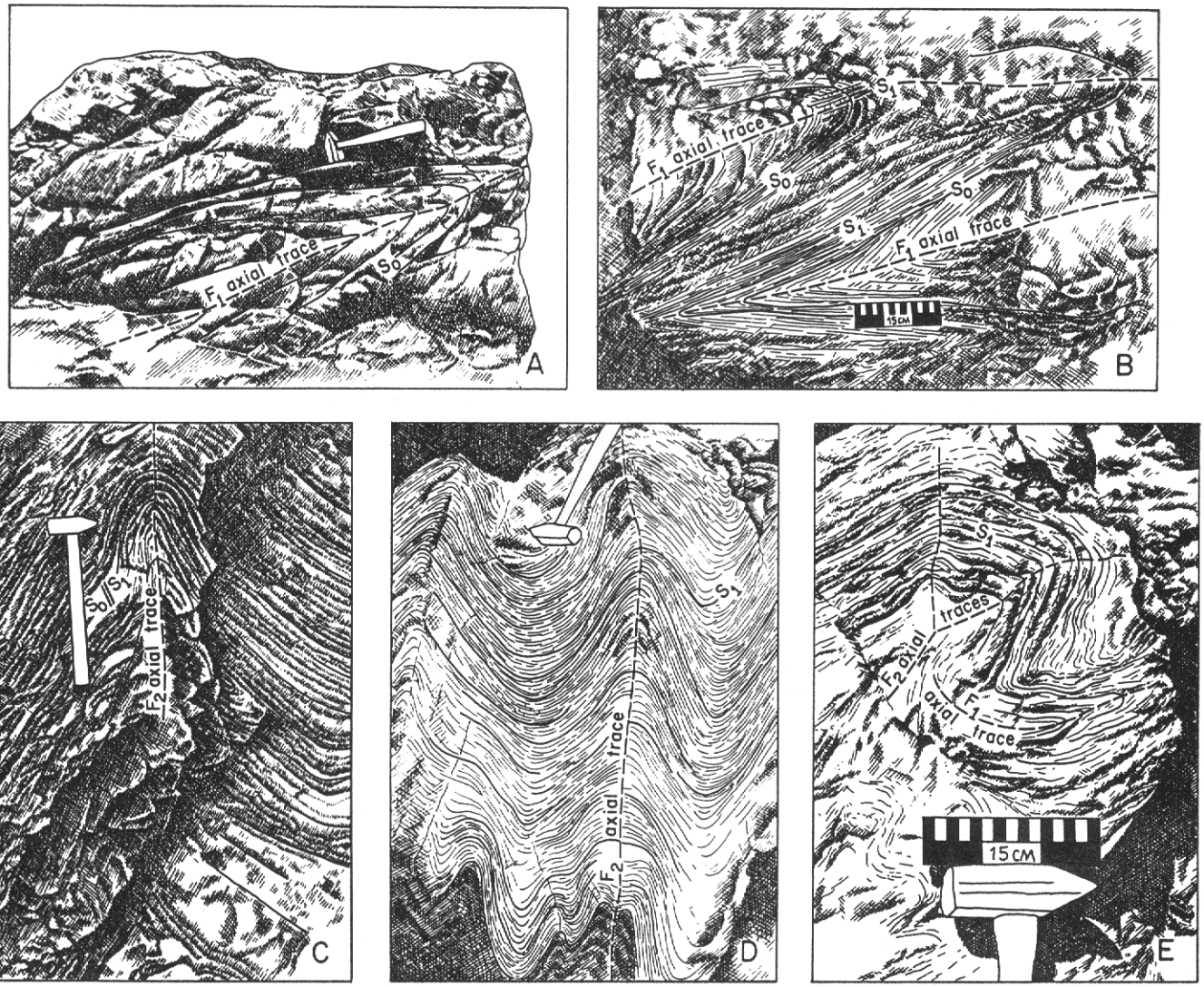

Figure 4. Fold styles in the North Coast Schist. A, S_o, original bedding in the Parlatuvier Formation, deformed by a F_1-style fold, S_1 cleavage subparallel to the F_1 axial surface, Dead Bay River; B, F_1-style, "Z-shaped" fold in the Mt. Dillon Formation, Mt. Dillon trace, note the convergence of S_1 cleavage near the lower hinge; C, Upright, F_2-style fold that deformed both S_o and subparallel S_1 foliation in the Parlatuvier Formation, roadcut along dirt road (Northside Road) approximately 1.3 km northeast of Anse Fourmi; D, S_1 foliation folded by upright, F_2-style flexural flow folds in the Parlatuvier Formation, Bloody Bay River; E, Late F_2-style boxfold that refolded a F_1-style isoclinal fold in the Parlatuvier Formation, Englishman's Bay. Sketches by Phyllis A. Ranz from photographs by A.W. Snoke.

increasing structural depth, thereby exhibiting an inverted metamorphic gradient. The inner parts of the aureole are characterized by a black to gray, locally gneissic, intensely foliated and lineated amphibolite. Toward the outer part of the aureole, the rocks are gray-green to green, epidote-rich, and the intensity of the penetrative fabric is less conspicuous. The northern boundary of the aureole is the "back-aureole" reverse fault which typically truncates amphibolite-facies aureole rocks emplacing them directly adjacent to greenschist-facies Parlatuvier or Mt. Dillon formations. However, in one area, the amphibolite-facies rocks gradually grade into lower greenschist-facies metavolcanic rocks characteristic of the Parlatuvier Formation (Figure 2, locality A). The back-aureole fault in turn truncates these greenschist-facies Parlatuvier rocks, emplacing them above greenschist-facies Mt. Dillon Formation. The protolith for the rocks of the amphibolite-facies aureole therefore is interpreted as the Parlatuvier Formation, albeit on the overturned limb of the Mt. Dillon synclinorium (Fig. 3, section AA').

Structural elements of the aureole include a synmetamorphic foliation and mineral lineation, and a post-metamorphic open fold phase. The foliation is defined by the planar alignment of hornblende and plagioclase grains and locally by alternating hornblende-rich and plagioclase-rich segregation layers. On the foliation plane, a mineral lineation defined by elongate hornblende and plagioclase grains is common. The orientation of the foliation varies but commonly strikes subparallel to the inferred strike of the contact with adjacent intrusive plutonic rocks and dips beneath the plutonic complex. The azimuth of the lineation is also variable but commonly plunges gently to

moderately down the dip of the foliation (i.e., to the south or southeast).

Brittle fault systems

Brittle faults of variable slip delineate several fault systems that have fragmented the Mesozoic lithic belts of Tobago. The oldest fault system is a high-angle, reverse fault that commonly forms the northern contact of the amphibolite-facies aureole. The trace of this fault is closely associated with the greenschist-amphibolite metamorphic facies transition within the aureole, consequently, the fault's displacement history appears linked with the emplacement of the plutonic suite. Our interpretation of these relationships is that a high-temperature, plastic shear zone developed in NCS wallrocks (i.e., the amphibolite-facies aureole) marginal to intrusive ultramafic rocks. As the plutonic suite and its attached aureole rose higher in the crust, a distinct brittle, reverse fault formed in the transition zone between greenschist facies NCS rocks and amphibolite facies rocks of the aureole. This "back-aureole" reverse fault therefore evolved along the outer edge of the amphibolite aureole during the late stage emplacement history of the plutonic suite.

The back-aureole fault has been offset by both younger normal and oblique-slip faults. The best-studied normal faults are the Coffee River and Cameron Canal faults. Both strike approximately EW with hanging wall down to the south (Figs. 2 and 3). These normal faults that are subparallel to the trace of the back-aureole fault locally truncate it or re-use its fault surface in a normal-sense displacement. Both the back-aureole and normal faults are offset by north-northwest-striking high-angle faults. These faults are characterized by left-lateral separation. This separation is probably a result of a complex oblique-slip displacement history. The age of the normal and oblique-slip faulting is uncertain but may be related to the broad strike-slip regime that some geologists have suggested for the southeastern Caribbean during the Neogene (e.g., Robertson and Burke, 1988). A prominent NW-striking, high-angle fault does not fit this evolutionary history. Foliation and lithologic trends clearly indicate a dextral sense-of-slip for this fault. Furthermore, it truncates the back-aureole fault, but is truncated itself by the Coffee River normal fault. The NNW-striking faults also truncate this dextral-slip fault. Oblique-slip faulting therefore both predated and postdated normal faulting, but clearly postdated the development of the back-aureole fault. In this light, we tend to consider the back-aureole fault as Mesozoic, but all other brittle faults as Tertiary. These data suggest that brittle faulting commenced in the Cretaceous during the emplacement of the plutonic suite, but later faulting was superimposed on this system and involved a grossly different slip and probably stress regime.

Perhaps the youngest faults on Tobago are associated with the EW-striking Southern Tobago Fault System. Recurrent earthquake swarms beneath southern Tobago indicate that the system is active (Morgan et al., 1988). Stratigraphic correlations between onland boreholes suggested to Wadge and Hudson (1986) that at least two buried EW-striking faults with a down to the south sense-of-displacement were buried beneath the Quaternary limestone of Booby Point (uplifted coralline reef platform). A normal fault cutting Rockly Bay Formation in a sea cliff near Ju-C Beverages Bottlers Limited, Lower Scarborough, is oriented N85E 54^{o}S and is the only known exposed fault cutting Cenozoic deposits. Immediately south of Black Rock village a distinct EW-striking topographic escarpment occurs within the TVG, and a zone of faults is mappable associated with the topographic break. Some of these faults may have an old and complex movement history, but late Neogene reactivation (south side up displacement) is a reasonable explanation for the escarpment. Significant lithologic contrasts across the fault zone that might suggest an origin of differential erosion for the topographic escarpment are absent. The late Neogene tectonic history of Tobago is poorly understood, but the island does lie within a complex tectonic belt that may serve as a transition zone from strike-slip faulting associated the Caribbean-South American plate boundary to subduction associated with the interaction of the southern Lesser Antilles and the Atlantic plate (Wadge and Hudson, 1986).

DISCUSSION

Cogenetic nature of the plutonic suite and the TVG

The new $^{40}Ar/^{39}Ar$ data (Table 2) coupled with recent paleontological discoveries (A.W. Snoke, W.A. Cobban, and P. Noble, unpublished data), new geochemical data (Frost and Snoke, 1989), detailed mineralogical studies (Girard, 1981), and the overall field relationships provide very strong support for Maxwell's (1948) hypothesis of broad contemporaneity between the TVG and the intrusive plutonic complex. Likewise, many members of the mafic dike swarm were consanguineous with the Albian volcanic-plutonic suite. However, one dike yielded a well-defined $^{40}Ar/^{39}Ar$ hornblende plateau age of ca 91 Ma (Table 2, sample 2D-14), clearly indicating that some mafic magmatism continued into the early Late Cretaceous. Late, broad-scale heating of this general age is also indicated by Ar-loss in the low temperature parts of release spectra for several samples (Table 2) and by fission-track zircon dates (P.F. Cerveny III and A.W. Snoke, unpublished data).

The TVG rocks occur as discrete roof pendants above the intrusive plutonic suite and cupolas of ultramafic to mafic rocks occur within the TVG suggesting that the plutonic suite underlies much of the TVG (Figures 2 and 3). Commonly the TVG rocks are only hornfelsic adjacent to contacts with the gabbro-diorite pluton. However, an enigmatic element of the volcanic-plutonic complex are discrete, highly deformed and metamorphosed complexes referred to on Figure 2 as "deformed mafic plutonic-volcanic complexes". Metamorphic mineral assemblages chiefly indicate hornblende-hornfels facies conditions, but locally pyroxene-hornfels facies assemblages (i.e., coexisting clino- and orthopyroxene) have been found in these metamorphosed mafic rocks (Yule, 1988). Based on detailed geologic mapping of gradational boundaries from weakly metamorphosed TVG rocks into the deformed and metamorphosed mafic complexes (Fig. 2) and relict igneous textures, the deformed mafic rocks appear to be early volcanic and hypabyssal components of the mid-Cretaceous volcanic-plutonic complex. These early mafic rocks were dynamothermally metamorphosed during the subsequent emplacement of the clinopyroxene-rich ultramafic rocks in much the same way that the NCS was metamorphosed to the amphibolite-facies aureole along its contact with the ultramafic rocks. Mafic

dikes, a conspicuous component in both the TVG and plutonic suite, also are common in the "deformed mafic plutonic-volcanic complexes". A somewhat similar amphibolitized gabbroic suite was described by Irvine (1974) as surrounding the Alaskan-type, Duke Island ultramafic complex. Irvine (1974) interpreted this deformed mafic suite as metamorphosed wallrock for the younger ultramafic complex. As noted above, we also believe that the deformed mafic rocks were intruded and metamorphosed by intrusive, hot ultramafic rocks, but consider these deformed rocks as early phases of the volcanic-plutonic suite, whereas Irvine (1974) considered the amphibolitized gabbros as unrelated to the younger ultramafic complex.

The development of a composite Mesozoic oceanic-arc terrane

Nd isotopic data reported by Frost and Snoke (1989) clearly indicate an oceanic-arc petrogenesis for all pre-Cenozoic rocks exposed on Tobago. The NCS, the oldest and most deformed element of the oceanic-arc terrane, included metasedimentary rocks that suggested the involvement of no continental detritus during arc growth, whereas argillite from the younger TVG suggested an important continental contribution during arc growth. The mid-Cretaceous volcanic-plutonic complex is welded to the NCS along the amphibolite-facies aureole, and detailed structural and petrographic studies (Rowe, 1987; Yule, 1988; Yule et al., 1988) suggest that this boundary is a deformed intrusive contact and not a terrane boundary (i.e., suture). Therefore, we hypothesize that the pre-Cenozoic oceanic-arc rocks of Tobago represent a partial cross-section through a composite Mesozoic oceanic island arc. During the early stages of this arc [Late Jurassic(?) - Early Cretaceous], it was situated such that continental detritus was not involved in magma petrogenesis. During the mid-Cretaceous, the situation had apparently changed and a continental component was available during magma petrogenesis and arc growth. This important change in the involvement of continental detritus during arc growth may signal an important shift in the overall plate tectonic geometry related to the developmental history of the "Great Arc of the Caribbean" (Burke, 1988). The structural history of the inferred composite oceanic-arc terrane also suggests an important hiatus in arc growth. The NCS rocks were penetratively deformed under greenschist facies metamorphic conditions prior to the magmatic evolution of the mid-Cretaceous volcanic-plutonic complex. This history therefore suggests penetrative deformation within the Mesozoic oceanic-arc during its early developmental history. The tectonic regime under which this penetrative deformation occurred is uncertain; however, the strong subhorizontal, strike-parallel stretching lineation of the NCS suggests that a transpressive shear zone is a possible model. Deformation within such a shear zone must have pre-dated the mid-Cretaceous, for the TVG are only locally penetratively deformed. Furthermore, the local deformation of the TVG is interpreted as related to the emplacement of hot, partially crystalline ultramafic rocks and not a regional stress field. The mid-Cretaceous oceanic-arc suite therefore appears to be built on an older, deformed oceanic-arc suite whose underpinnings are not exposed. The basement of this early arc suite was most likely ophiolitic such as the complexes preserved in the Western Cordillera of Colombia (Bourgois et al., 1987).

Affinity of the Tobago terrane with other possible fragments of the accreted Mesozoic oceanic-arc in the southeastern Caribbean

The delineation of discrete tectono-stratigraphic terranes in the southern Caribbean evolved rapidly in the 1980s (e.g., Case et al., 1984; Speed, 1985). The early syntheses tended to include Tobago with the metamorphic belts of the Cordillera de la Costa of Venezuela or the Northern Range of Trinidad. However, Rowe and Snoke (1986) emphasized the overall volcanogenic nature of Tobago in constrast to the continental margin sedimentary character of protoliths for Northern Range metamorphic rocks. Furthermore, Wadge and Macdonald (1985) demonstrated that the metabasaltic rocks of the Sans Souci Formation of Trinidad were petrographically and geochemically distinct from the low-grade metavolcanic rocks of the TVG. These studies as well as this preliminary summary indicate no direct geologic linkage between the Mesozoic rocks of Tobago and Trinidad. Recent syntheses of the southeastern Caribbean indicate a major fault zone between northern Trinidad and Tobago (Robertson and Burke, 1989; Speed et al., 1989). Speed et al. (1989) have delineated this fault zone far to the west and suggest that it actually may outcrop on the Araya-Paria peninsulas of northeastern Venezuela (e.g., see Vignali, 1979). Near Carúpano, a northward-dipping thrust fault which separates a hanging wall of greenschist-facies, volcanogenic El Copey Formation from a footwall of metasedimentary Carúpano Formation (i.e., calcareous phyllite, metalimestone, graphitic-calcareous quartz-mica schist, and scarce metaconglomerate) has been delineated (Bladier, 1977; Vierbuchen, 1984). Lenticular serpentinite intercalations and numerous mesoscopic thrust faults suggest important tectonic disruption within the El Copey Formation (Schubert, 1971; Vierbuchen, 1984). Therefore, this thrust fault as well as the North Coast fault zone of Robertson and Burke (1989) may be the southern margin of the allochthonous Tobago terrane (Speed et al., 1989). Possible delineation of the Tobago terrane farther to the west is uncertain, for the Salazar fault truncates the low-grade metamorphic rocks of the Araya Peninsula and amphibolite facies rocks of the Manicuare Formation form the westernmost part of the Araya Peninsula (Schubert, 1971; Vignali, 1979). Nevertheless, Wadge and Macdonald (1985) and Frost and Snoke (1989) have argued that Tobago, the Villa de Cura klippe, the Netherlands Antilles, and various Venezuelan offshore islands (e.g., La Blanquilla) were members of a composite Mesozoic oceanic-arc terrane that was gradually accreted to northern South America, perhaps beginning as early as mid-Late Cretaceous (Pindell et al., 1988; Pindell and Barrett, in press). This correlation was principally based on petrochemical characteristics and scarce radiometric and paleontological age determinations. Much more detailed structural, geochemical, and geochronometric data are required to clearly understand how these various elements of the proposed allochthonous Mesozoic oceanic-arc were interrelated.

Metavolcanic units mapped as part of the Villa de Cura klippe possess clear petrographic affinities with rocks of the TVG. Perhaps the most obvious characteristic is the conspicuously clinopyroxene-phyric nature of the mafic metavolcanic rocks as emphasized by Shagam (1960) for the Villa de Cura Group and originally noted by Maxwell (1948) for the Bacolet Formation of the TVG. This distinctive hallmark is characteristic of many oceanic-arc

volcanic suites throughout the western North American Cordillera (Snoke et al., 1982). Also equally distinctive is that clinopyroxene-rich ultramafic rocks are commonly associated with these metavolcanic rocks in the North American Cordillera, and detailed petrochemical studies of the clinopyroxenes in the volcanic and ultramafic rocks invariably suggest a distinct petrologic lineage (e.g., Irvine, 1973). This characteristic is also shared by both Tobago and the Villa de Cura klippe where mid-Cretaceous clinopyroxene-rich ultramafic rocks (Murray, 1972; Hebeda et al., 1984; Sharp and Snoke, 1988) have intruded and metamorphosed associated clinopyroxene-phyric metavolcanic rocks. Nevertheless, the blueschist facies metamorphism associated with penetrative deformation experienced by part of the Villa de Cura Group (Piburn, 1967) indicates an important difference in the petrotectonic history of the Villa de Cura Group as compared to the static prehnite-pumpellyite metamorphic history of the TVG. A clear understanding of why two apparently similar elements of the Mesozoic oceanic-arc experienced such different metamorphic and deformational histories requires more detailed comparative studies between the two regions.

Rocks units exposed on the Netherland Antilles and considered part of the accreted Mesozoic oceanic arc include the Curaçao Lava Formation, Washikemba Formation, Aruba Lava Formation, and Aruban batholith (Beets et al., 1984). The stratified and locally fossiliferous volcanogenic formations on an individual basis differ in stratigraphic age but when taken together range from mid-Albian(?) to Coniacian (Beets et al., 1984). The igneous crystallization age of the Aruba batholith has been estimated as 88.5+/-0.8 Ma based on a combination of Rb-Sr whole-rock data and K-Ar mineral ages (Priem et al., 1986). These data when combined with the previously enumerated geologic and age relationships of pre-Cenozoic rocks exposed on Tobago further emphasize the composite nature of the accreted Mesozoic arc. The olivine-phyric to plagioclase-pyroxene phyric lavas of the Curaçao Lava Formation record the accumulation of a great submarine, basic volcanic pile (more than 5 km thick) that may correlate with an Albian stage of primitive oceanic-arc growth (Beets et al., 1984; but see Donnelly et al., in press for another interpretation). This stage would be equivalent to much of the TVG. The apparently younger Washikemba and Aruba Lava formations record continued growth of this arc, but the Washikemba Formation includes more evolved magma types such as basaltic andesite (50-60 percent SiO_2) and rhyolite (70-75 percent SiO_2) (Beets et al., 1984). The youngest element of the oceanic-arc assemblage in the Netherland Antilles is the Aruba batholith. This intrusive plutonic complex ranges in composition from (quartz)-norite and quartz-hornblende gabbro to tonalite, and geochemical data from this complex appear to define a calc-alkaline trend (Beets et al., 1984). The Aruba batholith therefore represents a major late Cretaceous magmatic event in Mesozoic ocean-arc evolution, and as concluded by Beets et al. (1984), must pre-date accretion with continental South America.

Elements of the Mesozoic ocean-arc are probably also exposed on the various Venezuelan offshore islands (Dependencias Federales) including: Gran Roque, La Orchila, La Blanquilla, Los Hermanos, Los Frailes, and Los Testigos (Santamaria and Schubert, 1974). However, some radiometric ages (K-Ar, mineral ages) from these islands (e.g., La Blanquilla and Los Testigos) have yielded anomalously young, latest Cretaceous to early Tertiary dates (Santamaria and Schubert, 1974). These dates are difficult to integrate with most recent plate tectonic models for the southern Caribbean (e.g., Beets et al., 1984; Burke, 1988; Pindell et al., 1988), and we tentatively consider these dates as cooling ages unrelated to the initial age of igneous crystallization or metamorphism. However, Loubet et al., (1985) reported similar dates from Margarita Island and interpreted them as evidence of early Tertiary metamorphism. Much more detailed geologic mapping and coordinated geochronometric studies are necessary to make detailed correlations between the Venezuelan offshore islands and the other inferred parts of the Mesozoic oceanic-arc terrane.

Dredge hauls from the southern end of Aves Ridge indicate that this submarine feature is, at least in part, comprised of Mesozoic granitic rocks (Fox et al., 1971; Walker et al., 1972), and therefore, should also be included as part of the Mesozoic oceanic-arc terrane. These granitic rocks would seem to most logically correlate with the granitoid exposed on La Blanquilla (i.e., Garanton trondhjemite of Schubert and Moticska N., 1973). However, such a correlation is not straightforward as judged from the published geochemical analyses of the Garanton trondhjemite (Santamaria and Schubert, 1974) as compared to the petrographic and geochemical data derived from the dredged granitic rocks of the southern Aves Ridge (Fox et al., 1971; Walker et al., 1972). In particular, the granitic rocks from the southern Aves Ridge are more potassic and petrographically are granodioritic rather than trondhjemitic. Nevertheless, K-Ar mineral ages from the dredged granitoids have also yielded late Cretaceous to early Tertiary K-Ar mineral dates (89, 78, 67, 65, 58, 57 Ma)(Fox et al., 1971).

Granitic rocks ranging in composition from trondhjemite to tonalite to granodiorite were part of the Mesozoic oceanic-arc terrane. The apparently oldest representative of these quartz-rich granitoids is a dike-like intrusion of biotite +/- hornblende tonalite which is the youngest plutonic phase of the mid-Cretaceous Tobago pluton. Younger tonalitic rocks are also part of the late Cretaceous, calc-alkaline Aruban batholith and similar rocks apparently form a poorly studied igneous basement from Gran Roque to the southern end of Aves Ridge. These granitoids and the plutonic complexes which they are associated commonly intruded and metamorphosed a chiefly mafic volcanic sequence which ranged in age from mid-Albian to Turonian. Only on Tobago are rocks clearly older than Albian part of the Mesozoic oceanic-arc terrane (i.e., North Coast Schist), although analogous rocks may also be preserved in the Venezuelan offshore islands (Santamaria and Schubert, 1974).

Displacement history of the Mesozoic oceanic-arc terrane

The present geographic position of Tobago has been recognized as a geological anomaly for many years (Maxwell, 1948). Furthermore, the role of strike-slip displacement along the northern margin of South America is controversial. In some syntheses large strike-slip motion is inferred (Burke, 1988; Robertson and Burke, 1989; Erlich and Barrett, 1990), whereas other plate-kinematic models employ oblique collision with only modest strike-slip displacement (Speed, 1985). The resolution of these contrasting models is not completely apparent from the presently available data. However, an

impressive set of diverse data argue for a Pacific origin for the Caribbean plate (Pindell et al., 1988; Pindell and Barrett, in press; Pindell, this volume), thereby implying significant displacement of the inferred fragments of the Mesozoic oceanic-arc from their site of origin. Furthermore, the oceanic-arc petrochemical character of all pre-Cenozoic rocks on Tobago (Frost and Snoke, 1989) clearly indicates an allochthonous history in respect to Tobago's present geographic position as part of the northeastern corner of the South American continental shelf. Such an allochthonous history suggests an important strike-slip component during the final emplacement and accretion of the Mesozoic oceanic-arc along the northern margin of South America. If Tobago, the Villa de Cura klippe, Aves Ridge, and the Aruba-Blanquilla arc were originally part of the "Great Arc of the Caribbean" (Burke, 1988), their accretion history and present geographic position may chiefly reflect a broad zone of transpressional strain between South America and the eastward migrating Caribbean plate which started with an initial collision in the mid-Late Cretaceous and continues to the Present.

CONCLUSIONS

The Mesozoic igneous and metamorphic rocks of Tobago, West Indies constitute a cross-section through a fragment of an allochthonous, composite oceanic-arc terrane (Fig. 5; Frost and Snoke, 1989). New geologic mapping coupled with petrochemical and geochronometric studies indicate:

1) the protolith for the oldest exposed part of the oceanic-arc terrane (NCS) is pre-Aptian and perhaps as old as Late Jurassic;

2) the NCS experienced pre-Albian penetrative deformation and lower greenschist facies metamorphism;

3) the Tobago plutonic complex and volcanic group are cogenetic and evolved in the mid-Albian;

4) ultramafic rocks of the plutonic suite intruded and dynamothermally metamorphosed the NCS forming an inverted, amphibolite-facies metamorphic aureole;

5) a mafic dike swarm widely intruded into the volcanic-plutonic complex and locally intruded the amphibolite-facies aureole and NCS;

6) the mafic dikes are chiefly mid-Albian and therefore were clearly coeval with the volcanic-plutonic suite, although a member of the swarm has also yielded an igneous crystallization age as young as 91 Ma;

7) the Mesozoic lithic belts of Tobago have been been attenuated and offset by brittle fault systems which were related both to the late stage emplacement history of the mid-Cretaceous plutonic complex as well as much later Cenozoic strike-slip faulting; and

8) the Cenozoic deposits on Tobago represent various shallow marine accumulations and their preservation therefore records tectonic uplift and/or sea level change.

ACKNOWLEDGEMENTS

Financial support for this research was provided by NSF grant EAR-8418139 awarded to A. W. Snoke and C. D. Frost. We thank Phyllis A. Ranz for her superb help in preparing the illustrations for this article. The critical review comments of David K. Larue were helpful in preparing the final version of the paper.

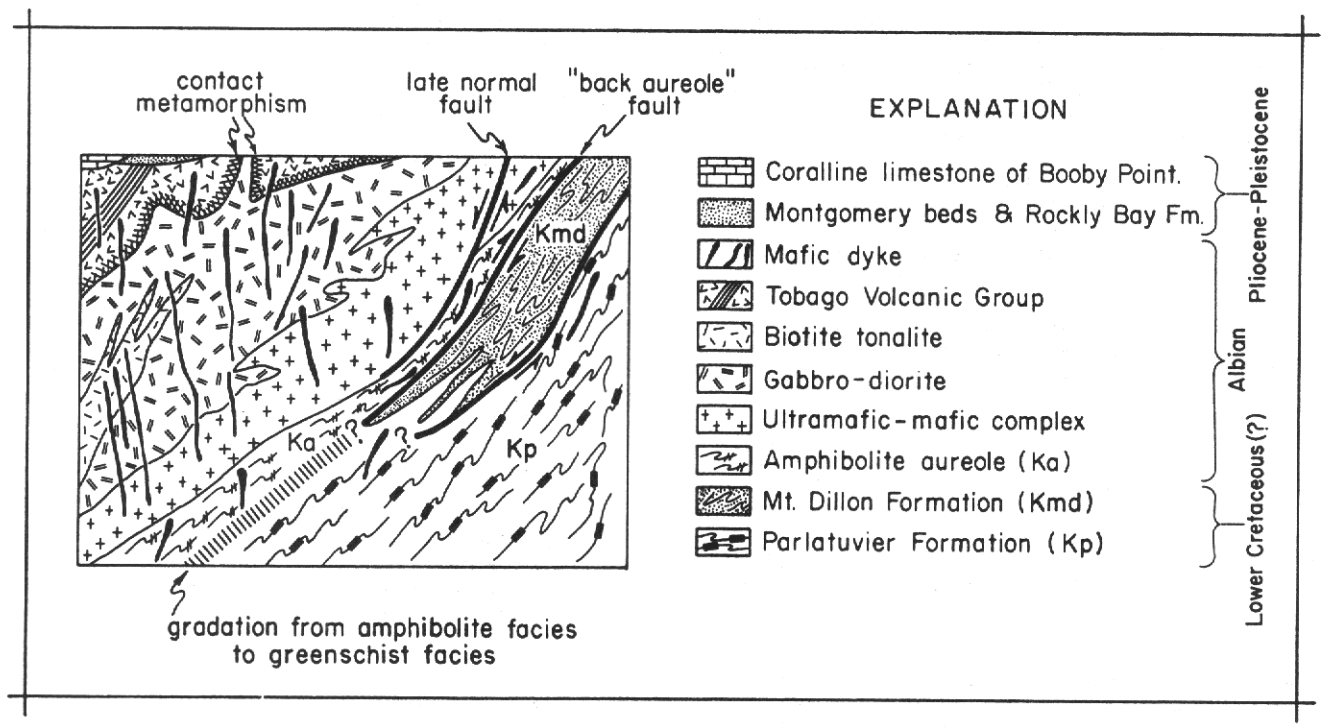

Figure 5. Schematic structural-stratigraphic diagram for Tobago, West Indies.

REFERENCES

Beets, D.J., Maresch, W.V., Klaver, G. Th., Mottana, A., Bocchio, R., Beunk, F.F., Monen, H.P., 1984, Magmatic rock series and high-pressure metamorphism as constraints on the tectonic history of the southern Caribbean, in Bonini, W.E., Hargraves, R.B., and Shagam, R., eds., The Caribbean-South American plate boundary and regional tectonics: Geol. Soc. America Mem. 162, p. 95-130.

Bellizzia G., A., 1972, Is the entire Caribbean Mountain belt of northern Venezuela allochthonous?, in Shagam, R., et al., eds., Studies in Earth and Space Sciences, Geol. Soc. America Mem. 132, p. 363-368.

Bladier, I., 1977, Rocas Verdes de la region de Carúpano, Venezuela, plano de Despeque de Corrimientos, in Boletin de Geodinamica, Comision Internacional de Geodinamica, Grupo 2, Caras, p. 35-49.

Bourgois, J., and 9 others, 1987, Geological history of the Cretaceous ophiolitic complexes of northwestern South America (Colombian Andes): Tectonophysics, v. 143, p. 307-327.

Bouysse, P., 1988, Opening of the Grenada back-arc basin and evolution of the Caribbean plate during the Mesozoic and Early Paleogene: Tectonophysics, v. 149, p. 121-143.

Burke, K., 1988, Tectonic evolution of the Caribbean: Ann. Rev. Earth Planet. Sci., v. 16, p. 201-230.

Case, J.E., and Holcombe, T.L., 1980, Geologic-tectonic map of the Caribbean region: U.S. Geol. Surv. Misc. Inv. Ser. Map I-1100, scale 1:2,500,000.

Case, J.E., Holcomb, T.L., and Martin, R.G., 1984, Map of geologic provinces in the Caribbean region, in Bonini, W.E., Hargraves, R.B., and Shagam, R., eds., The Caribbean-South American plate boundary and regional tectonics: Geol. Soc. America Mem. 162, p. 1-30.

Donnelly, T.W., and 10 others, in press, History and tectonic setting of Caribbean magmatism, in Dengo, G., and Case, J.E., eds., The Caribbean region: Boulder, Colo., Geological Society of America, The Geology of North America, v. H.

Erlich, R.N., and Barrett, S.F., 1990, Cenozoic plate tectonic history of the northern Venezuela-Trinidad area: Tectonics, v. 9, p. 161-184.

Fox, P.J., Schreiber, E., and Heezen, B.C., 1971, The geology of the Caribbean crust: Tertiary sediments, granitic and basic rocks from the Aves Ridge: Tectonophysics, v. 12, p. 89-109.

Frost, C.D., and Snoke, A.W., 1989, Tobago, West Indies, a fragment of a Mesozoic oceanic island arc: petrochemical evidence: Jour. Geol. Soc. London, v. 146, p. 953-964.

Girard, D., 1981, Petrologie de quelques series spilitiques Mesozoiques du domaine caraibe et des ensembles magmatiques de l'ile de Tobago: implications geodynamiques [These]: l'Universite de Bretagne Occidentale, 230 p.

Hebeda, E.H., Verdurmen, E.A.Th., and Priem, H.N.A., 1984, K-Ar hornblende ages from the El Chacao complex, north-central Venezuela, in Bonini, W.E., Hargraves, R.B., and Shagam, R., The Caribbean-South American plate boundary and regional tectonics: Geol. Soc. America Mem. 162, p. 413-414.

Irvine, T.N., 1973, Bridget Cove volcanics, Juneau area, Alaska: possible parental magma of Alaskan-type ultramafic complexes: Carnegie Inst. Yr. Bk. 72, p. 478-491.

_____ 1974, Petrology of the Duke Island ultramafic complex, southeastern Alaska: Geol. Soc. America Mem. 138, 240 p.

Jackson, T.A., and Smith, T.E., 1985, Metasomatism in the Tobago Volcanic Group, Tobago, W.I., in Rodrigues, K., ed., Trans. First Geol. Conf. Geol. Soc. Trinidad & Tobago, p. 34-39.

Loubet, M., Montigny, R., Chahati, B., Duarte, N., Lambert, B., Martin, C., and Thuizat, R., 1985, Geochemical and geochronological constraints on the geodynamical development of the Caribbean chain of Venezuela, in Mascle, A., ed., Geodynamique des Caraibes: Editions Technip, Paris, p. 553-566.

Maxwell, J.C., 1948, Geology of Tobago, British West Indies: Geol. Soc. America Bull., v. 59, p. 801-854.

Morgan F.D., Wadge, G., Latchman, J., Aspinall, W.P., Hudson, D., and Samstag, F., 1988, The earthquake hazard alert of September 1982 in southern Tobago: Bull. Seism. Soc. Am., v. 78, p. 1550-1562.

Murray, C.G., 1972, Zoned ultramafic complexes of the Alaskan type: feeder pipes of andesitic volcanoes, in Shagam, R. et al., eds., Studies in earth and space sciences: Geol. Soc. America Mem. 132, p. 313-335.

Piburn, M.D., 1967, Metamorphism and structure of the Villa de Cura Group, northern Venezuela [Ph.D. thesis]: Princeton, New Jersey, Princeton Univ., 148 p.

Pindell, J.L., Cande, S.C., Pitman, W.C., III, Rowley, D.B., Dewey, J.F., LaBrecque, J., and Haxby, W., 1988, A plate-kinematic framework for models of Caribbean evolution: Tectonophysics, v. 155, p. 121-138.

Pindell, J.L., and Barrett, S.F., in press, Geologic evolution of the Caribbean: a plate-tectonic perspective, in Dengo, G., and Case, J.E., eds., The Caribbean region: Boulder, Colo., Geological Society of America, The Geology of North America, v. H.

Priem, H.N.A., Beets, D.J., Boelrijk, N.A.I.M., and Hebeda, E.H., 1986, On the age of the Late Cretaceous tonalitic/gabbroic batholith on Aruba, Netherlands Antilles (southern Caribbean borderland): Geol. Mijnbouw, v. 65, p. 247-256.

Robertson P., and Burke, K., 1989, Evolution of southern Caribbean plate boundary: Am. Assoc. Petroleum Geologists Bull., v. 73, p. 490-509.

Rowe, D.W., 1987, Structural and petrologic history of northeastern Tobago, West Indies: A partial cross-section through a composite oceanic arc complex [M.S. thesis]: Laramie, Univ. Wyoming, 165 p.

Rowe, D.W., and Snoke, A.W., 1986, North Coast Schist Group, Tobago, West Indies: important constraints on tectonic models for the southeastern Caribbean region: Geol. Soc. America Abs. with Programs, v. 18, p. 734.

Santamaria, F., and Schubert, C., 1974, Geochemistry and geochronology of the southern Caribbean - northern Venezuela plate boundary: Geol. Soc. America Bull., v. 85, p. 1085-1098.

Saunders, J.B., and Muller-Merz, E., 1985, The age of the Rockly Bay Formation, Tobago: Fourth Latin Amer. Geol. Cong., Trinidad & Tobago, p. 339-344.

Schubert, C., 1971, Metamorphic rocks of the Araya Peninsula, eastern Venezuela: Geol. Rundschau, v. 60, p. 1571-1600.

Schubert, C., and Moticska N., P., 1973, Reconocimiento geológico de las Islas Venezolanas en el Mar Caribe, entre Los Roques y Los Testigos (Dependencias Federales). II: Islas orientales y conclusiones: Acta Cient. Venezolana, v. 24, p. 19-31.

Shagam, R., 1960, Geology of central Aragua, Venezuela: Geol. Soc. America Bull., v. 71, p. 249-302.

Sharp, W.D., and Snoke, A.W., 1988, Tobago, West Indies: geochronological study of a fragment of a composite Mesozoic oceanic island arc: Geol. Soc. America Abs. with Programs, v. 20, p. A60.

Sigurdsson, H., Sparks, R.S.J., Carey, S.N., and Huang, T.C., 1980, Volcanogenic sedimentation in the Lesser Antilles arc: Jour. Geology, v. 88, p. 523-540.

Snoke, A.W., Sharp, W.D., Wright, J.E., and Saleeby, J.B., 1982, Significance of mid-Mesozoic peridotitic to dioritic intrusive complexes, Klamath Mountains-western Sierra Nevada, California: Geology, v. 10, p. 160-166.

Speed, R.C., 1985, Cenozoic collision of the Lesser Antilles arc and continental South America and the origin of the El Pilar fault: Tectonics, v. 4, p. 41-69.

_____ 1986, Cenozoic tectonics of the southeastern Caribbean and Trinidad, in Rodrigues, K., ed., Trans. First Geol. Conf. Geol. Soc. Trinidad & Tobago, p. 270-280.

Speed, R.C., Torrini, R., Jr., and Smith, P.L., 1989, Tectonic evolution of the Tobago trough forearc basin: Jour. Geophys. Research, v. 94, p. 2913-2936.

Stephan, J-F., Beck, C., Bellizzia, A., and Blanchet, R., 1980, La chaine caraibe du Pacifique a l'Atlantique, in Geologie des chaines alpines issues de la Tethys: Memoire du B.R.G.M., no. 115, p. 38-59.

Trechmann, C.T., 1934, Tertiary and Quaternary beds of Tobago, West Indies: Geol. Magazine, v. 71, p. 481-493.

Vierbuchen, R.C., 1984, The geology of the El Pilar fault zone and adjacent areas in northeastern Venezuela, in Bonini, W.E., Hargraves, R.B., and Shagam, R., eds., The Caribbean-South American plate boundary and regional tectonics: Geol. Soc. America Mem. 162, p. 189-212.

Vignali, M., 1979, Estratigrafia y estructura de las cordilleras metamorficas de Venezuela oriental (Peninsula de Araya - Paria e Isla de Margarita): GEOS, v. 25, p. 19-66.

Wadge, G., and Macdonald, R., 1985, Cretaceous tholeiites of the northern continental margin of South America: the Sans Souci Formation of Trinidad: Jour. Geol. Soc. London, v. 142, p. 297-308.

Wadge, G., and Hudson, D., 1986, Neotectonics of southern Tobago, in Rodrigues, K., ed., Trans. First Geol. Conf. Geol. Soc. Trinidad & Tobago, p. 7-20.

Walker, B.M., Vogel, T.A., and Ehrlich, R., 1972, Petrogenesis of oceanic granites from the Aves Ridge in the Caribbean basin: Tectonophysics, v. 15, p. 133-139.

Westbrook G.K., and McCann, W.R., 1986, Subduction of Atlantic lithosphere beneath the Caribbean, in Vogt, P.R., and Tucholke, B.E., eds., The Western North Atlantic Region: Boulder, Colo., Geological Society of America, The Geology of North America, v. M., p. 341-350.

Yule, J.D., 1988, Petrology and structure of south-central Tobago, West Indies: Part of a displaced fragment of a Mesozoic oceanic island arc terrane [M.S. thesis]: Laramie, Univ. Wyoming, Laramie, 226 p.

Yule, J.D., Snoke, A.W., and Rowe, D.W., 1988, A dynamothermal inverted metamorphic aureole on Tobago, West Indies: a product of megathrusting or forceful intrusion?: Geol. Soc. America Abs. with Programs, v. 20, p. A60-A61.

STRUCTURAL FEATURES ASSOCIATED WITH THE LOS BAJOS FAULT AND THEIR INTERPRETATION IN THE LIGHT OF CURRENT THEORIES OF STRIKE-SLIP TECTONICS

Llewellyn Tyson
Trinidad and Tobago Oil Company Limited
Pointe-a-Pierre, Trinidad

ABSTRACT

The Los Bajos Fault is a member of a family of NW-SE oriented strike-slip faults present in northern South America. It has an average direction of 113° from north, and a horizontal displacement of roughly ten (10) kilometers. Structural features present along the fault depend on two factors - (1) fault terminii and (2) changes in the direction of the fault:

(1) The northwestern terminus of the Los Bajos Fault is a point of divergence of the former from the Warm Springs (strike-slip) Fault. This area is therefore the site of extensional tectonics, of which the North Soldado Graben is a part. The southeastern terminus of the fault is in a basement-involved reverse fault forming the core of the E-W oriented Southern Range.

(2) Where the direction of the fault trace is less than 113° from north, motion was transpressional, and anticlines developed. These have been somewhat displaced by the Los Bajos Fault, resulting in present day half-anticlines, e.g.the East Soldado, Point Fortin and Los Bajos. Where the direction of the fault trace is greater than 113° from north, motion was transtensional and features such as the Coora and (in part) North Soldado Grabens were formed.

INTRODUCTION

The island of Trinidad is located at the southern terminus of the chain of islands forming the Eastern Caribbean, and is just off northeastern Venezuela. The Los Bajos Fault (refer to Fig. 1) cuts across the island and extends into the shallow sea - the Gulf of Paria - between Trinidad and Venezuela.

The area around the fault has been the focus of intense drilling by oil companies for several decades, because of the occurrence of a giant accumulation along it. This accumulation, of which greater than 800 million barrels of oil have already been recovered, extends over the following areas - East Soldado, Point Fortin, Guapo, Brighton, Forest Reserve, Fyzabad, Palo Seco, Coora and Quarry. The essential results of the geological work by the various companies have been published by Wilson (1958, 1965). In his classical papers, Wilson established:

(1) the magnitude of the strike-slip motion on the fault as being ten (10) kilometers;

(2) the presence of geological structures along the fault on land; and

(3) hypothesized on the relationship between these geological structures and oil entrapment.

In addition, several geologists have published papers pertaining to oil accumulation along discrete parts of the fault. However, there is no publication that studies the Los Bajos Fault in its entirety, i.e. both land and marine areas.

The objectives of this paper are two-fold. In the first place, it is intended to document all of the major structural features along the Los Bajos Fault, and secondly, to interpret these in the light of modern theories of strike-slip tectonics. In this paper the terms "strike-slip", "transcurrent" and "wrench" are used synonymously.

REGIONAL TECTONIC SETTING

Many of the structural elements of northeastern Venezuela extend into Trinidad. For simplicity, these can be grouped into three (refer to Fig. 1):

(1) Belt of low grade metamorphic rocks - this belt extends in an east-west direction across most of northern Venezuela and northern Trinidad. The rocks are predominantly low grade metamorphics including phyllites, schists, slates and marbles. Most of these rocks which are Late Cretaceous in age, crop out just north of the El Pilar Fault.

(2) Middle Miocene fold-thrust belt - this belt which has a width of up to 100 km. consists of a series of NE-SW oriented thrusted anticlines, developed as a result of Middle Miocene tectonism. In surface maps of Eastern Venezuela, this structural style is most conspicuous as the Serrania del Interior, and similarly in surface geology maps of Trinidad as the Naparima-Nariva thrust belt. In both countries the southern portions of the belt are buried under a thick clastic sequence of Late Miocene to Pleistocene age.

Larue, D.K., and Draper, G. (eds.),
Transactions of the 12th Caribbean Geological Conference, St. Croix, U.S.V.I., Miami Geological Society, P.O. Box 431552, South Miami, FL 33243, U.S.A

(3) Belt of strike-slip and associated faulting - This deformation is of Late Pliocene age and is superimposed on the fold-thrust belt. It includes such prominent NW-SE directed faults as the Urica, San Francisco, Soldado, Warm Springs and Los Bajos Faults. All of these terminate in prominent ENE-WSW directed compressional lineaments, including such structures as the Tonoro-El Lirial, the Pedernales and the Southern Range - Galeota Highs.

BASIC CONCEPTS OF STRIKE-SLIP TECTONICS

Before proceeding any further, it is necessary to elaborate on two basic concepts of strike-slip tectonics which impact directly on the remainder of the paper.

The first concept is a model for the development of a strike-slip fault (refer to Fig. 2). This model, which is a synthesis of the ideas of several geologists, illustrates the development of a dextral strike-slip fault. In the first place, as a result of the oblique stresses a line of weakness develops. The latter in reality consists of a series of discontinuous smaller lines of weakness within the basement, arranged at varying angles to each other (Fig. 2(i)). With further compression, left turning or restraining bends become the site of en echelon anticlines in the basement's sedimentary cover. On the other hand, right turning or releasing bends become the site of en echelon synclines in this cover. Hence, at this stage of development a series of en echelon folds and discontinuous faults are characteristic (Fig. 2 (ii)). By the third stage, further compression and extension result in more complex structures - thrusted anticlines, grabens and a through-going fault (Fig.2 (iii)). In the fourth stage (Fig. 2 (iv)), the throughgoing fault results in displaced half anticlines and grabens along it. In more advanced stages of development (not illustrated here), the structural features present along the strike-slip fault become obliterated as a result of uplift and erosion, exposing a very complex shear zone. This latter stage of development is not applicable to the Los Bajos Fault. The salient point to be noted here is that structural features developed along a strike-slip or transcurrent fault depend on the direction of the fault trace. This "snaking" produces restraining and/or releasing bends which correspondingly result in the development of en echelon compressional and extensional features.

The second concept refers to the terminii associated with strike-slip faults developed wholly within continental crust. Such faults, because of the finite nature of continental crust, obey what may be termed a law of conservation of continental crust - i.e. continental crust cannot be created or destroyed by a strike-slip fault, but can be converted from one form to another. Conversion from one form to another dictates that at the respective fault terminii, compression and/or extension occur, complementary to each other. Hence, intra-continental transcurrent faults develop what may be termed a compressional-transcurrent-extensional fault triad (refer to Fig. 3). The "action" of crustal extension at one end is transferred by strike-slipping to the other end, where there is "reaction" in the form of crustal shortening. Within the region, perhaps the best example of this fault triad is the El Tuy-Cariaco Basin (crustal extension) - Urica Fault (strike-slip) - Tonoro- El Lirial High (crustal compression). The El Tuy-Cariaco Basin is well documented by Goddard (1986) and Schubert (1986), while the Urica Fault and Tonoro-El Lirial High have been discussed in an interesting paper by Murany (1972).

LATE PLIOCENE TECTONICS IN THE TRINIDAD AREA

Fig. 4 is a simplified compilation map showing the Late Pliocene structural elements present in the Trinidad area. Three points are of significance here.

Firstly, there are the basement-involved strike-slip faults - Soldado, Los Bajos and Warm Springs - which terminate in the basement-involved reverse faults of the Central and Southern Ranges. This abrupt termination of strike-slip faults and conversion to basement-involved reverse faults by marked change in direction (Stone, 1969), is characteristic of the concept of intra-continental strike-slip fault terminii discussed in the previous section.

Secondly, is the fact that the Los Bajos Fault is a splay of the Warm Springs Fault. This splaying has resulted in divergent wrenching along the latter fault, hence the preponderance of down-to-the-north and down-to-the-south normal faults on either side of the Warm Springs Fault (Fig.4). The N-S line on Fig. 4 is a seismic line, and is illustrated as Fig. 5. In the interpretation of Fig. 5, the two dextral strike-slip faults are shown as well as the (extensional) normal faulting between them.

The third significant point, is the presence of shallow-rooted folds all oriented NE-SW. Some of these folds are shown in Fig. 6, and include the La Brea, Vance River - Boodoosingh, Lot One, Forest, Bernstein and Penal anticlines. The consistent NE-SW orientation of the folds throughout the island further reinforces the idea of a NW-SE directed compression in the Late Pliocene.

STRUCTURAL FEATURES ASSOCIATED WITH THE LOS BAJOS FAULT

The structural features associated with the Los Bajos Fault can be grouped into five (5) categories - (1) the North Soldado Graben; (2) the East Soldado-Point

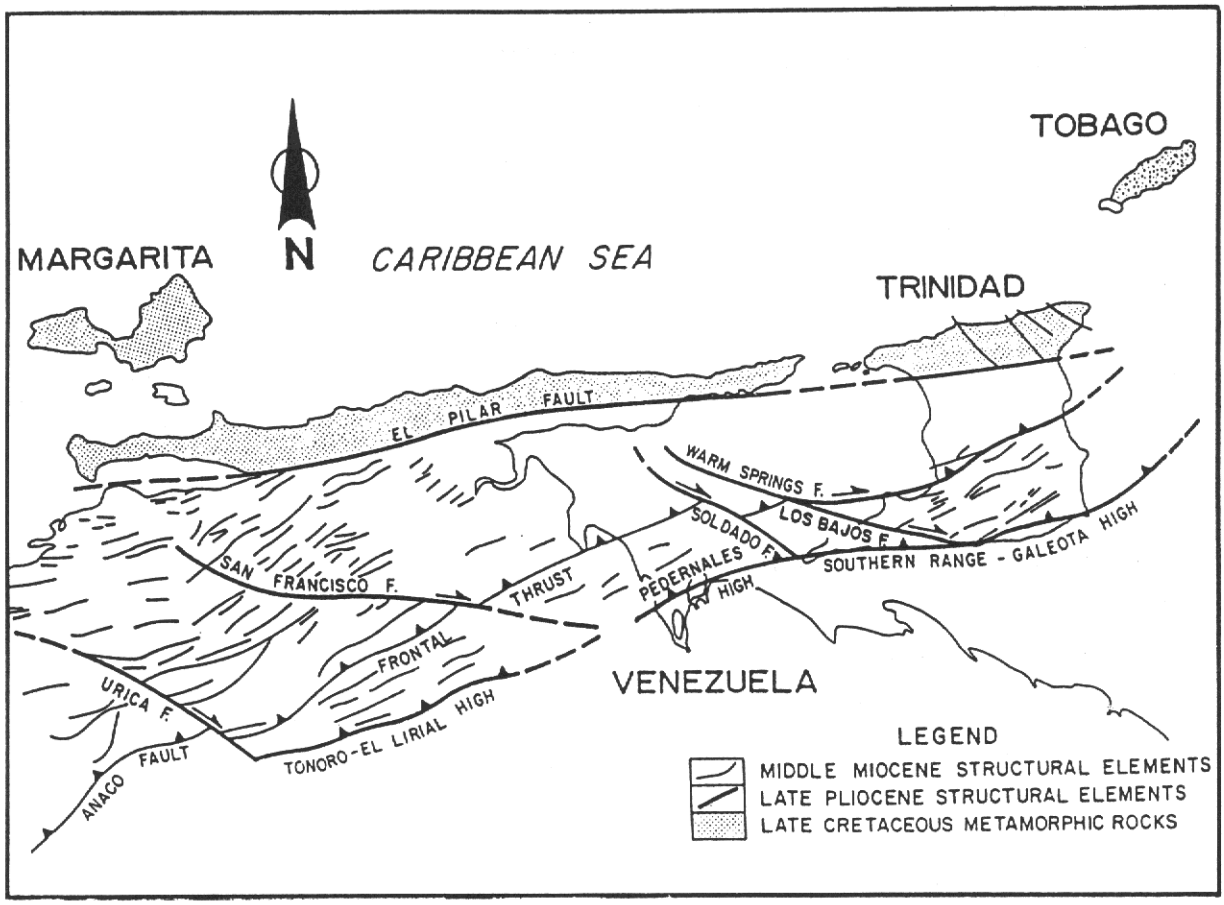

Fig. 1. Location of Los Bajos Fault in relation to the major structural elements of N.E. South America (modified after Salvador and Stainforth, 1965)

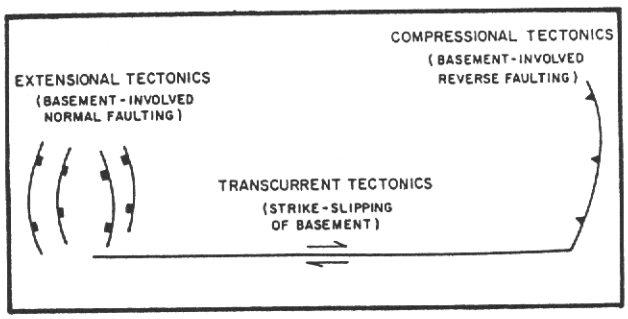

Fig. 3 Model of an extensional - transcurrent - compressional fault triad developed within continental crust

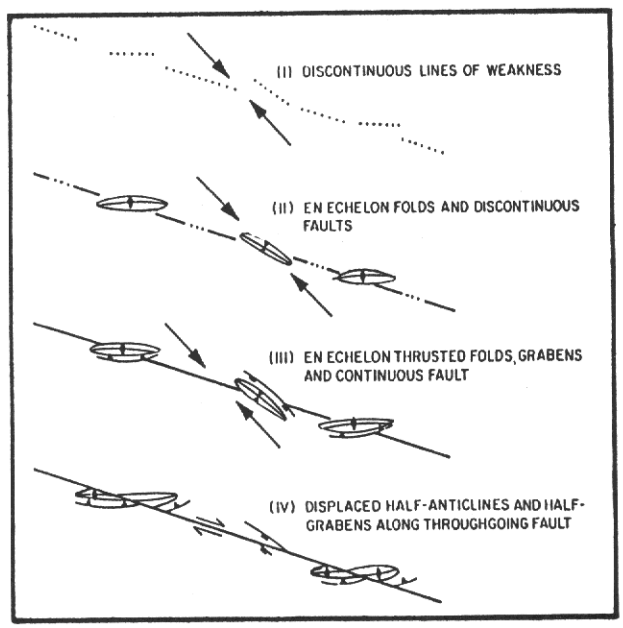

Fig. 2. Model of development of a wrench fault

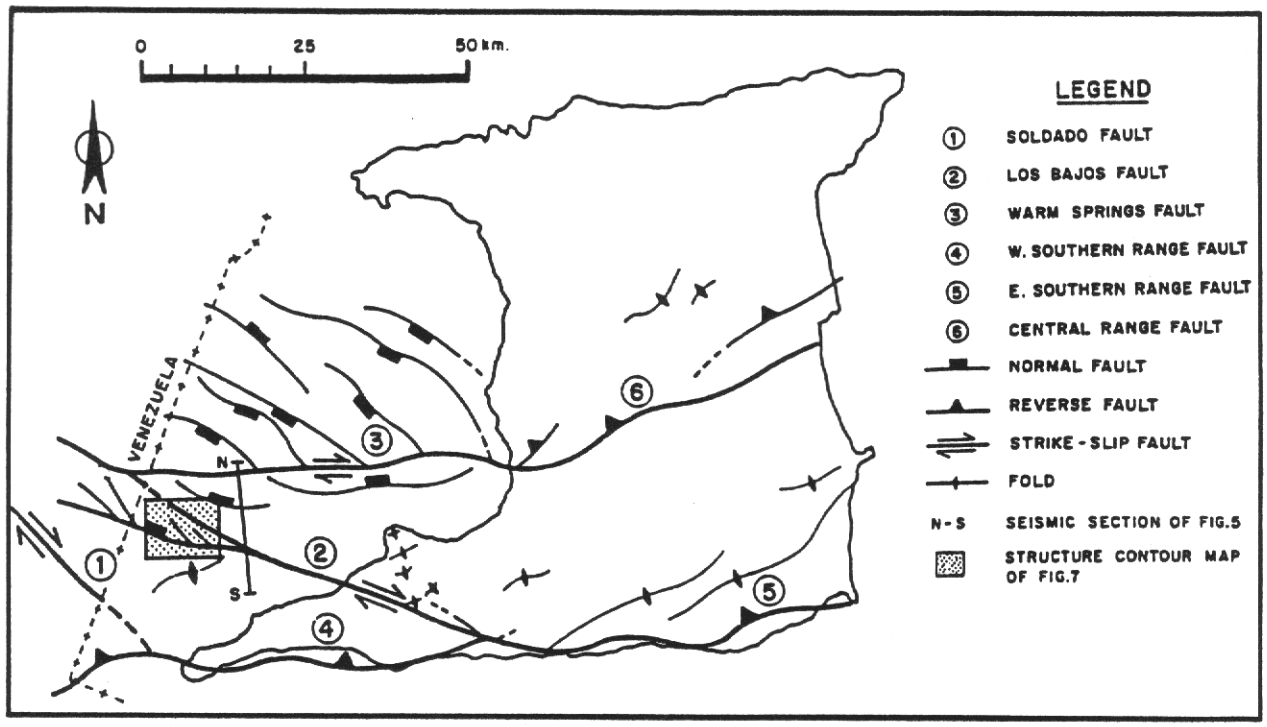

Fig. 4. Compilation map showing Late Pliocene structural elements on land and in the Gulf of Paria, Trinidad

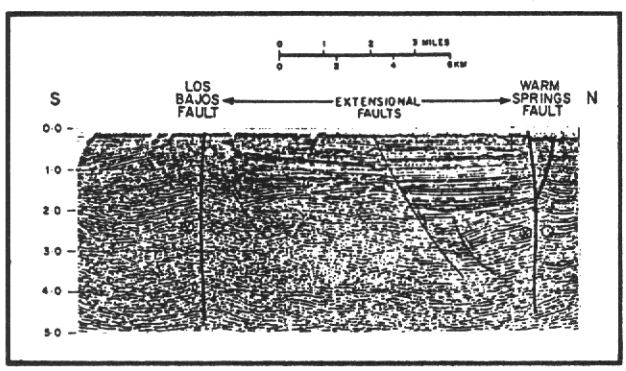

Fig. 5. N-S seismic section across Warm Springs and Los Bajos Faults

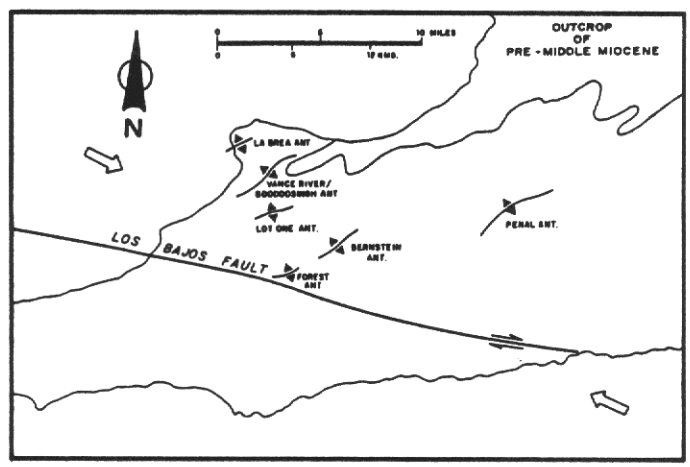

Fig. 6. Map showing shallow - rooted folds in SW Trinidad

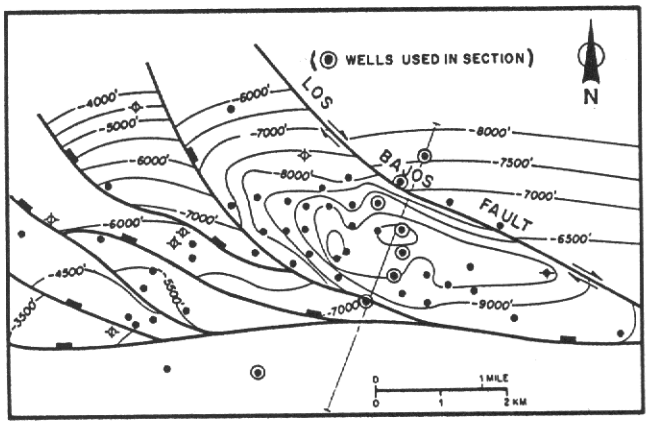

Fig. 7. Structure contour map on top Nariva FM. to illustrate the North Soldado Graben

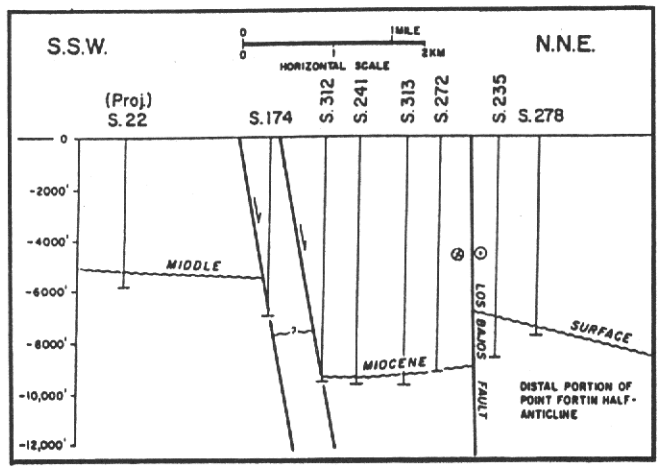

Fig. 8. Structural cross-section across the North Soldado Graben

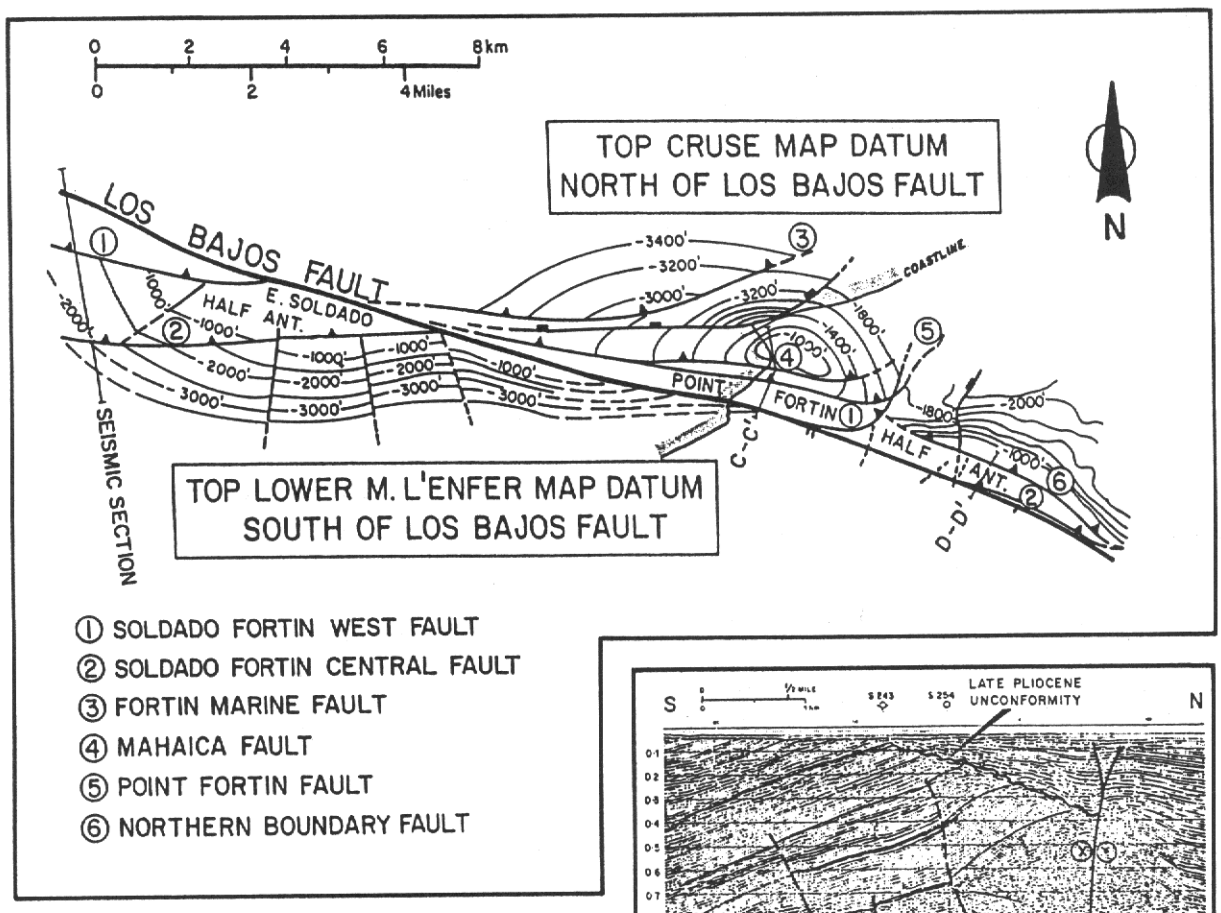

Fig. 9. East Soldado - Point Fortin Anticlinal complex to show interpretation of the major thrust patterns

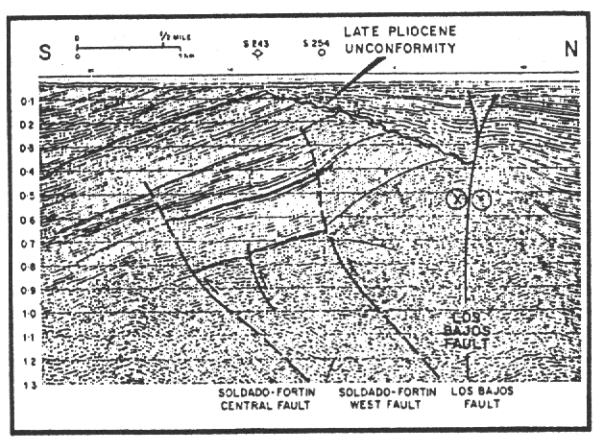

Fig. 10. N-S seismic section across the E-Soldado half anticline

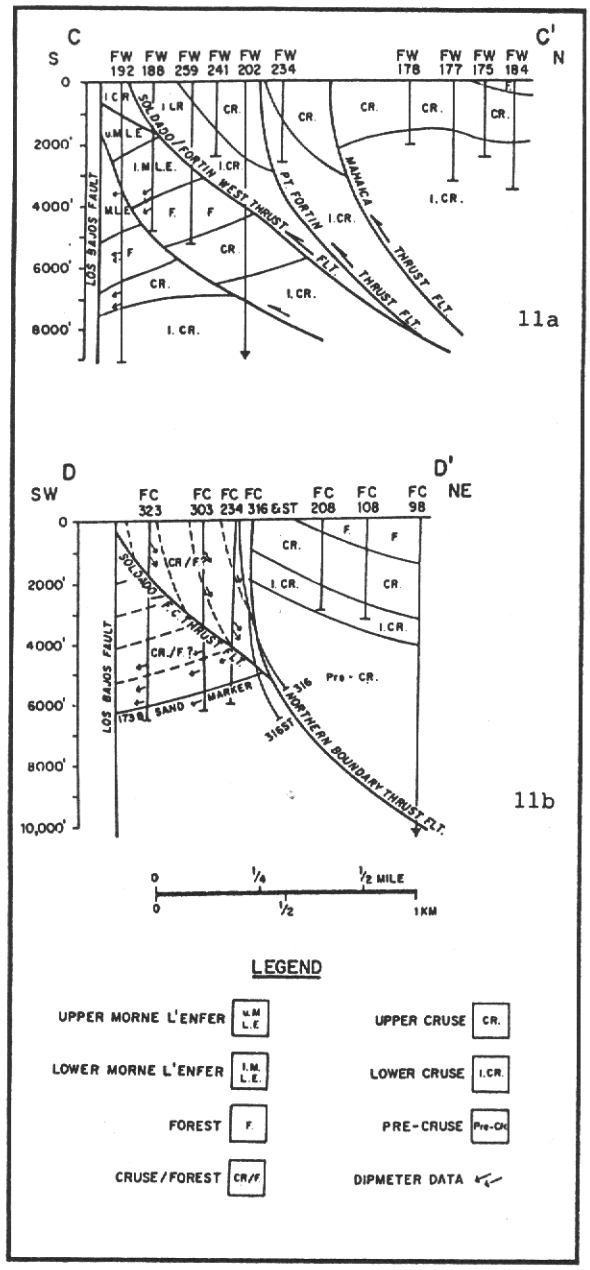

Fig. 11 Structural cross-sections
(a) Point Fortin West C-C'
(b) Point Fortin Central D-D'

Note : All reverse faulting always directed from North.

Fortin Anticline; (3) the Coora Graben; (4) the Los Bajos Anticline; and (5) the Southern Range Basement Reverse Fault. Each of these will now be described in detail.

(1) The North Soldado Graben - This asymmetrical graben structure is located between the WNW-ESE oriented Los Bajos Fault and an E-W trending major normal fault (refer to Fig. 7). Splaying off this normal fault in a NW-SE direction are a series of smaller normal faults, all of which are downthrown to the north or north-east. Consequently, there is a progressive, stepwise downfaulting as is illustrated by the structure contour map on the Middle Miocene datum of Fig. 7. For instance, in the west the datum is at a subsea depth of -3500' and is downfaulted in a stepwise fashion to -10,000' subsea in the axis of the graben. This pattern of faulting is also supported by the SSW-NNE oriented structural cross-section of Fig. 8. The style of faulting in the central Gulf of Paria (refer to Fig. 4) - i.e. down-to-the-south normal faults north of the Warm Springs Fault and down-to-the-north normal faults south of the said strike-slip fault - suggests that the North Soldado Graben is but a part of this larger extensional faulting system.

(2) The East Soldado - Point Fortin Anticline - This feature is really an anticline which has been cut and displaced significantly by the Los Bajos Fault. The East Soldado half-anticline is a complex half-flower on the south side of the Los Bajos Fault (refer to Fig. 9). Associated with this positive half-flower are two major reverse faults, the Soldado Fortin West and Soldado Fortin Central Faults. These two reverse faults are quite clear from the seismic line in Fig. 10. The most uplifted part of this half-anticline has been truncated to form a Late Pliocene unconformity surface, and then onlapped by post - Late Pliocene sediments.

The Point Fortin half-anticline on the northern side of the Los Bajos Fault, is even more complex. There are several reverse faults (refer to Figs. 9, 11) including the Fortin Marine, Mahaica, Point Fortin and Northern Boundary Reverse Faults, as well as the displaced portions of the Soldado Fortin West and Soldado Fortin Central Reverse Faults present in the East Soldado half anticline. The structural cross-section C-C' of Fig. 11a shows the pattern of reverse faulting associated with the western portion of the Point Fortin half-anticline. The basic pattern of faulting is the same in the central and eastern parts of the anticline (refer to cross section D-D' of Fig. 11b), with overthrusting from the north. However, in the central and eastern parts the faulting is much simplified, with only the Northern Boundary and Soldado Fortin Central Reverse Faults being present.

A simplified palinspastic reconstruction of the East Soldado - Point Fortin

anticline is shown in Fig. 12. This "best fit" was achieved by a restoration movement of the northern side of the fault by roughly four (4) miles. In this reconstruction there is a fairly good match-up of the displaced portions of the Soldado Fortin West and Soldado Fortin Central Reverse Faults. The very complex nature of the reconstructed anticlinal structure, with at least six (6) significant reverse faults, suggests that it was an area of intense compression. Furthermore, it can be deduced that this compression was directed from the northwest, which complements the idea that NW-SE directed oblique compressive forces were responsible for the development of the Los Bajos Fault.

(3) The Coora Graben - The Coora Graben is a triangular structure composed of down-to-the-southwest normal faults, subparallel to the Los Bajos Fault (refer to Fig. 13). The structure contour map is drawn on the Coora silt, an easily correlatable marker from well logs. The faults converge with the Los Bajos toward the south-east, but because of a lack of well data their behaviour towards the northwest is not known. Fig. 14 is a N-S cross-section along the line illustrated in Fig. 13, and shows the typical grabenal nature of the area, with the normal faults converging with the Los Bajos Fault at depth.

(4) The Los Bajos Half-Anticline - This structural feature shows up on Kugler's surface geology map (refer to Fig. 15) as a half-anticline, truncated to the north by the Los Bajos Fault. In the core of the structure is the older Cruse Formation, surrounded by the progressively younger Forest and Morne L'Enfer Formations respectively. The structural cross-section Fig.16a, shows a single reverse fault as the cause of the upturning of strata to form the Los Bajos half-anticline. On the other hand, further west along the same structure, this single reverse fault has splayed into a series of smaller reverse faults, as shown in Fig. 16b.

(5) The Southern Range Basement Reverse Fault - Whereas the Los Bajos Fault trends in a NW-SE direction, the Southern Range Basement Reverse Fault has an E-W trend. This remarkable change in direction is responsible for the "death" or "termination" of strike-slip motion on the Los Bajos Fault. The strike-slip motion is "consumed" by basement-involved reverse faulting along the Southern Range Fault, which continues offshore as the Galeota Ridge. Basement-involved reverse faulting along the Southern Range is accompanied by the development of an asymmetrical basin on its southern, underthrust portion (refer to Figs. 17 and 18). This asymmetrical basin is the E-W trending Columbus Channel Syncline. In the latter, as much as 3000 metres of post-Late Pliocene age sediments have accumulated. The tremendous uplift associated with the Southern Range Basement Reverse Fault is best illustrated by Fig.18. The core of this structure is diapiric, and straddles the southern coastline of the island.

ORIGIN AND INTERPRETATION OF STRUCTURES ASSOCIATED WITH THE LOS BAJOS FAULT

Two types of structural features are associated with the Los Bajos Fault. Firstly, there are those associated with the terminii of the fault - the North Soldado Graben and the Southern Range Basement Reverse Fault. Secondly, there are those resulting from the "snaking" or changing of direction of the fault - the East Soldado - Point Fortin Anticlinal Complex, the Coora Graben and the Los Bajos half-anticline. The former features are of much greater magnitude than the latter.

(1) Structures associated with fault terminii :

(a) The North Soldado Graben - The origin of this feature is perhaps linked to two factors. Firstly, it is in the area of the divergence of the Los Bajos and Warm Springs Faults. This area is therefore the site of extension and subsidence, as illustrated by the normal faulting pattern in the Central Gulf of Paria (refer to Fig. 4). Put into perspective, the North Soldado Graben then, is simply one of the down-to-the-north, major normal faults present on the south side of the Warm Springs transcurrent fault. Secondly, and of lesser importance, it owes its origin to the fact that the Los Bajos Fault undergoes a directional change from WNW-ESE to NW-SE in the area just north of the graben (refer to Fig. 7).

(b) The Southern Range Basement Reverse Fault - This represents the southern terminus of the Los Bajos Fault, equivalent to the compressional end of the extensional-transcurrent-compressional fault triad illustrated in Fig. 3. This "killing" of a strike-slip fault by compression, suggests that the Southern Range Reverse Fault and its extension offshore as the Galeota Ridge, must be basement involved. The Tonoro-El Lirial and the Pedernales Highs in Venezuela, as well as the Southern Range-Galeota High in Trinidad are thought by the author to represent present day expressions of an old fundamental fault. Furthermore, the author suggests that it is along this fundamental fault that the compression associated with each of the Late Pliocene strike-slip faults - Urica, Soldado and Los Bajos - is absorbed.

(2) Structures resulting from the changing of direction ("snaking") of the Los Bajos Fault :

Fig. 19 is a plot of the direction from north of the Los Bajos Fault (over 0.3 mile unit intervals) on land, starting from the coastline at Point Fortin, and proceeding southeastwards. The graph shows that

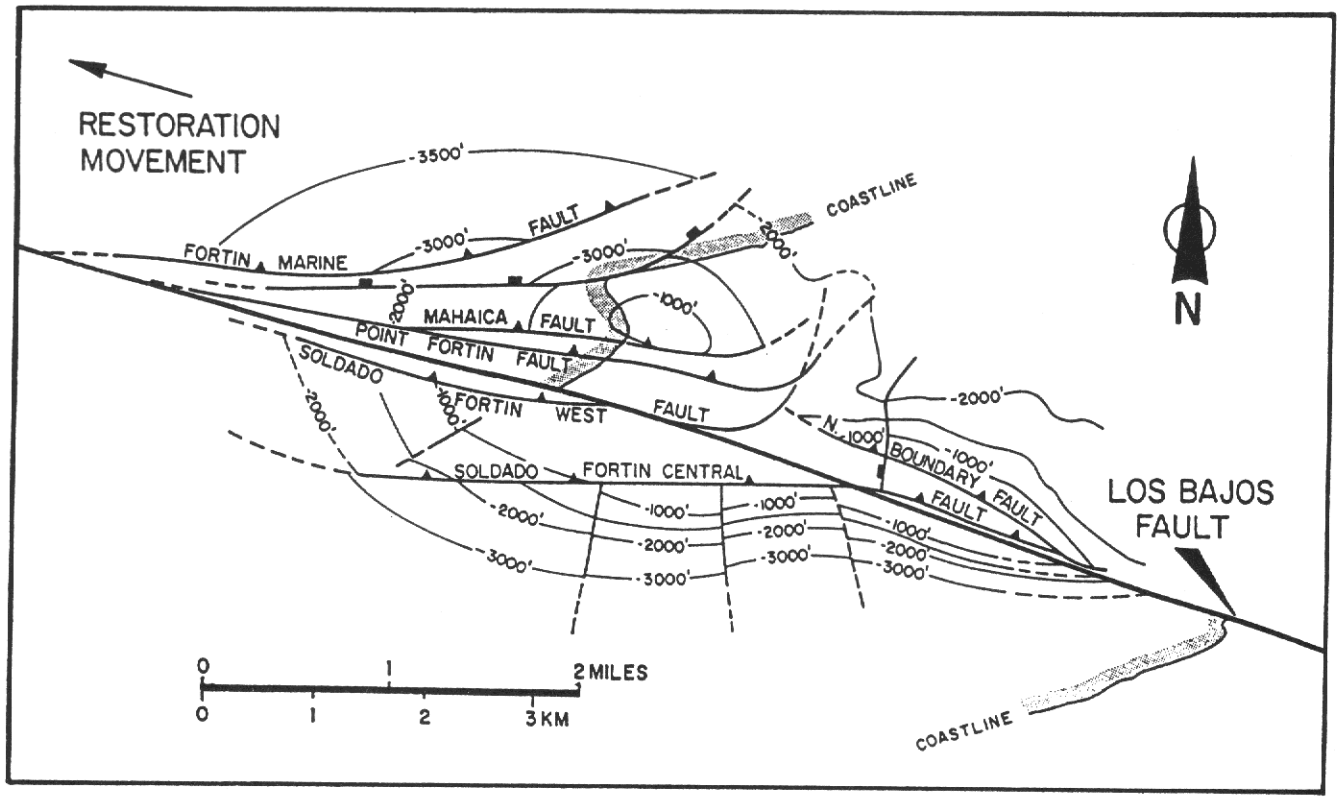

Fig. 12. Simplified palinspastic reconstruction of E. Soldado-Point Fortin anticlinal complex

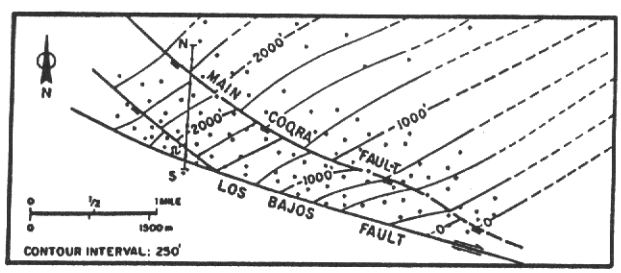

Fig. 13. Structure contour map showing the Coora Graben (modified after Nath 1979)

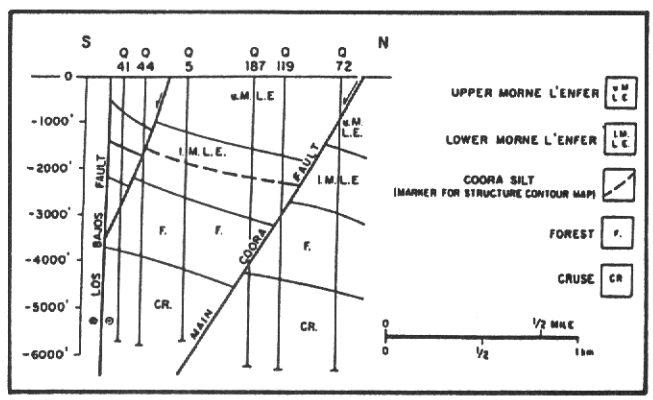

Fig. 14. Structural cross-section across Coora Graben (modified after Wilson 1958)

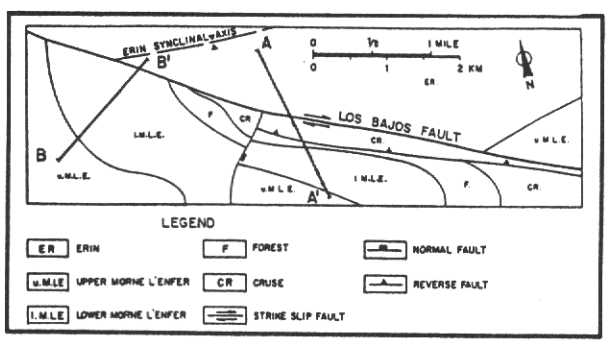

Fig. 15. Los Bajos half-anticline illustrated from surface geology (after Kugler)

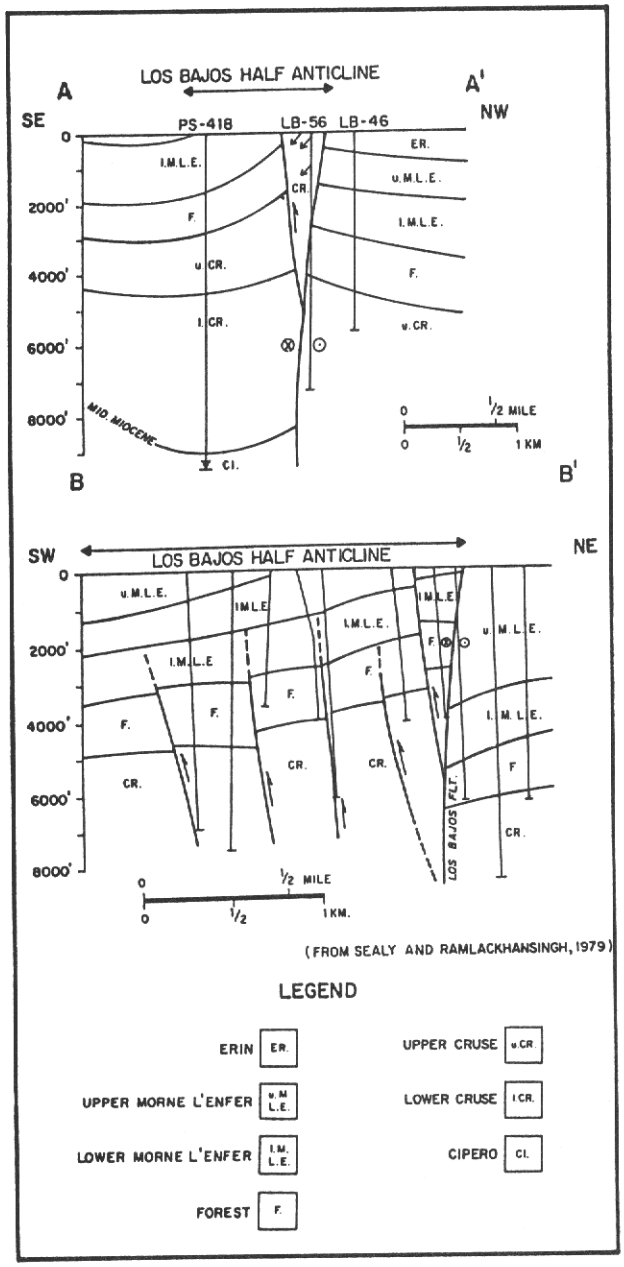

Fig. 16. Structural cross-sections across the Los Bajos half-anticline

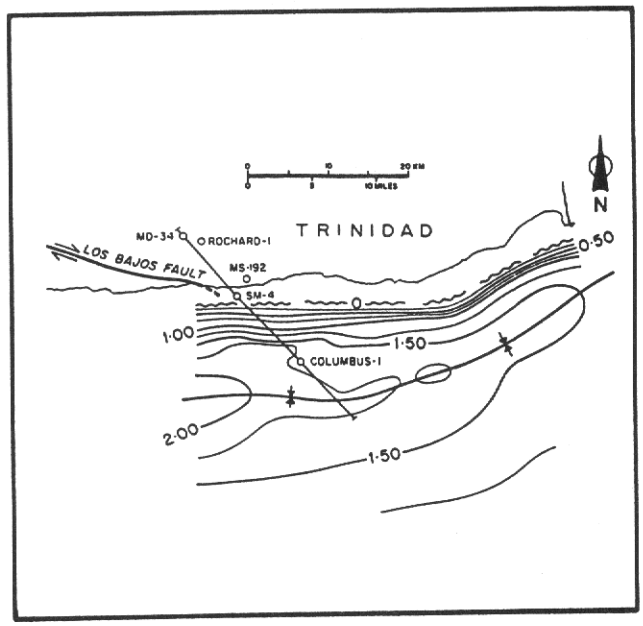

Fig. 17. Structure contour map on Late Pliocene datum of eastern portion of the Columbus Channel Syncline

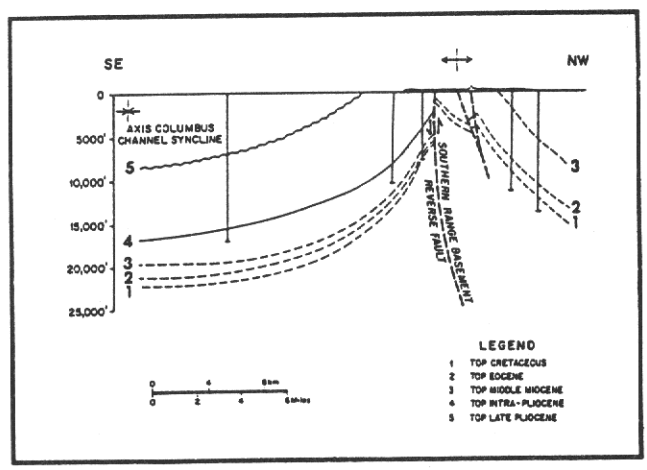

Fig. 18. NW-SE cross section showing the Southern Range basement reverse fault

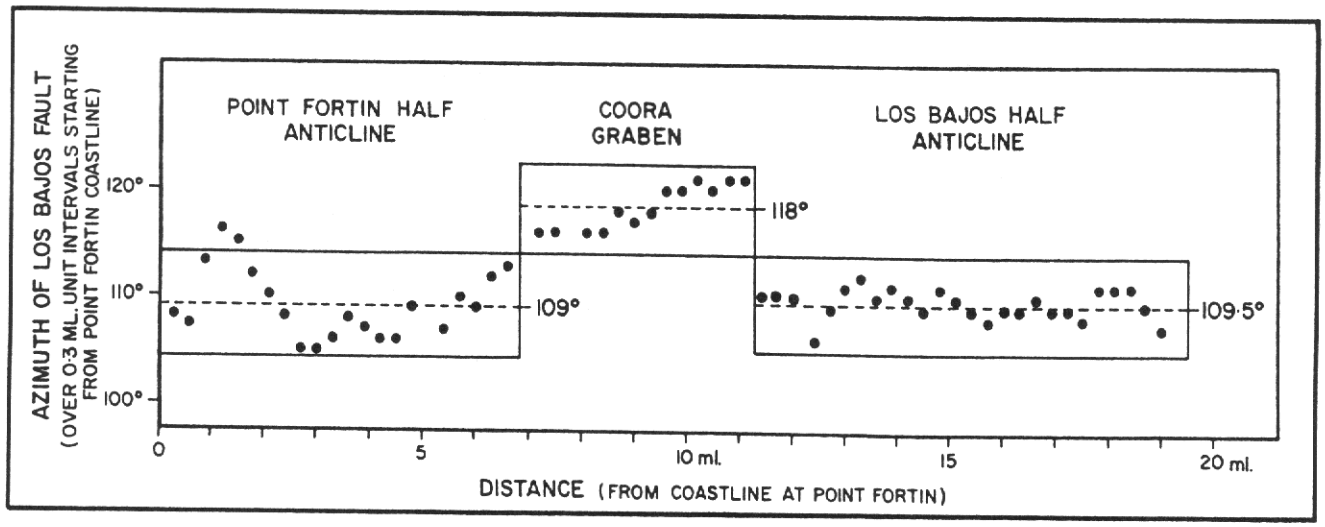

Fig. 19. Relationship of Los Bajos Fault direction and type of structural features developed.

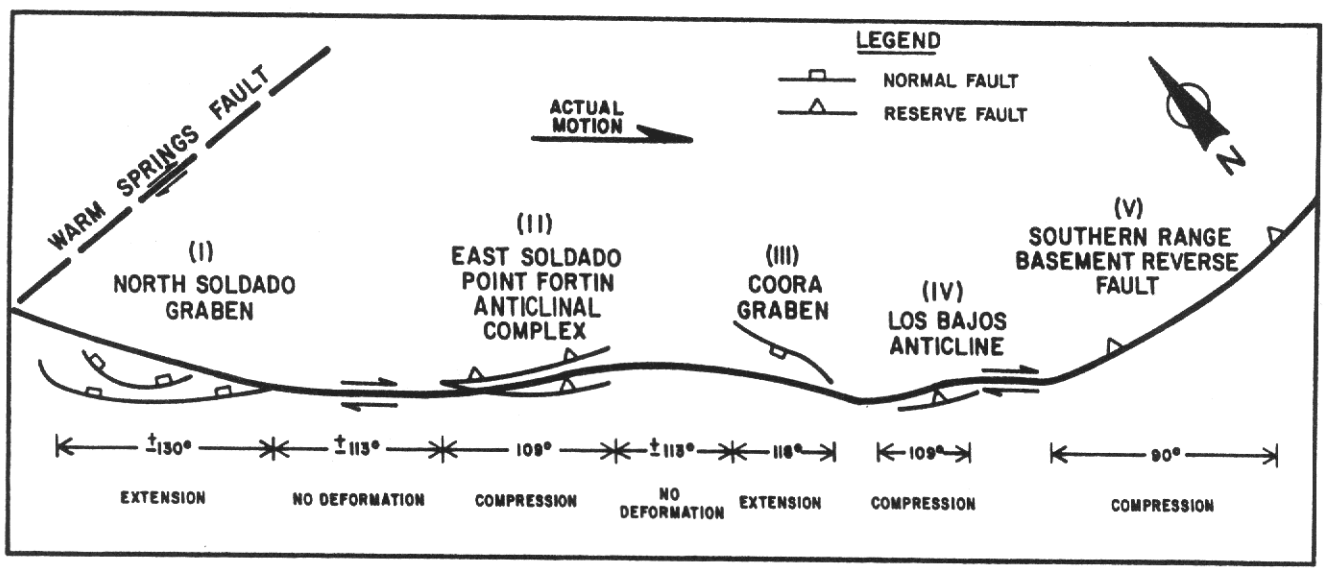

Fig. 20. Schematic illustration of structural features associated with the Los Bajos Fault, and their relationship to change in fault direction

the fault direction can be divided into three parts. The first part, with the exception of two spurious points, corresponds to an ESE direction averaging 109°. The second part averages 118° , whereas the third averages 109.5°. In addition, on the distance axis the positions of each of the three structural features on land have been plotted, and an interesting picture emerges. Average Los Bajos Fault directions from north, corresponding to the Point Fortin and Los Bajos half-anticlines are 109° and 109.5° respectively. These two portions of the fault represent areas of transpression and therefore positive flower development. The change in fault direction to an average of 118° corresponds to the Coora Graben, and represents an area of transtension, and therefore negative flower development. From the correspondence of a fault direction of about 109° to transpression and a direction of 118° to transtension, it is not unreasonable to suppose that parallel wrenching should correspond to an angle of about 113°. The direction of 109° from north for the Los Bajos Fault is maintained as the fault continues offshore into the Gulf of Paria (refer to Fig. 9) just beyond the East Soldado half anticline. The fact that a positive structural feature is still present in the form of the East Soldado half-anticline, fits well the concept that angles like 109° correspond to transpression. In the region of the North Soldado Graben (refer to Fig. 7), the Los Bajos Fault undergoes a change from about 109° to 130° from north, and interestingly enough, this point is associated with transtension. However, as mentioned before, other factors may account for the extensional style of faulting there, i.e. in the North Soldado Graben. Fig. 20 illustrates schematically the role of change of fault direction in influencing the type of structural features present along the Los Bajos Fault.

CONCLUSIONS

(1) There are two types of structural features associated with the Los Bajos Fault - those associated with the fault's terminii and those associated with subtle changes in the fault's direction (Fig.20). The former are of greater magnitude than the latter.

(2) At the WNW terminus of the Los Bajos Fault is the Central Gulf of Paria extensional regime, of which the North Soldado Graben is a part. At the ESE terminus is the basement-involved reverse fault of the Southern Range.

(3) Structural features along the fault are dependent on the changes in direction of the fault (Fig. 20). Where the fault direction exceeds about 113° from north, transtensional features develop, e.g. the Coora and in part North Soldado Grabens. Where the fault direction is less than 113° from north, transpressional features are present, such as the East Soldado, Point Fortin and Los Bajos half anticlines.

REFERENCES CITED

Bertrand, W.G., 1979, Geology of the Point Fortin Field. Trans. 4th Latin American Geological Congress, Trinidad. p. 690-699.

Biddle, K.T. and Christie-Blick, N. eds. 1985, Strike-slip Deformation Basin Formation and Sedimentation, SEPM Special Publication 37, p.375-386.

Charles, D and Cosgrove, P., 1985, A Model for oil exploitation in Trintoc's Point Fortin Anticlinal Area north of the Los Bajos Fault. Trans. 1st Geol. Conf. of the Geol. Soc. of Trinidad and Tobago, p.168-182.

Crowell, J.C., 1974, Origin of Late Cenozoic Basins in Southern California, in Dickinson, W.R. ed. Tectonics and Sedimentation S.E.P.M. Special Publication #22. p. 190-204.

Dibble, T.W., 1977, Strike-slip tectonics of the San Andreas Fault and its role in Cenozoic Basin evolvement, in Late Mesozoic and Cenozoic Sedimentation and Tectonics in California, San Joaquin Geol. Soc. Short Course. p. 26-38.

Goddard, D. 1986. Seismic Stratigraphy and Sedimentation of the Cariaco Basin and surrounding continental shelf, N.E. Venezuela, Trans. 11th Carib. Geol. Conf. Barbados, #34, 1986.

Harding, T.P., 1974, Petroleum traps associated with wrench faults. American Association of Petroleum Geologists v 58 #7p.1290-1304.

Kugler, H.G. 1959, Compilation Geological Map of Trinidad 1:100,000. Orell Fussli, Zurich, Switzerland.

McDougall, A.W., 1979, Geology of the East Soldado Field. 4th Latin American Geological Congress, Trinidad, p. 720-725.

Murany, E.E., 1972, Structural Analysis of the Caribbean Coast, Eastern Interior Range of Venezuela, VI Caribbean Geological Conference, Margarita, p. 295-298.

Nath, M., 1979, Production Geology of the Coora-Quarry Field, 4th Latin American Geological Congress, Trinidad, p. 726-737.

Radovsky, B and Iqbal, J., 1979, Geology of the North Soldado Field. 4th Latin American Geological Congress, Trinidad, p. 759 - 769.

Salvador, A. and Stainforth, R.M., 1965, Clues in Venezuela to the Geology of Trinidad and vice versa. Trans. 4th Carib. Geol. Conf. Trinidad, p. 31-40.

Schubert, C., 1985, Neotectonic Aspects of the Southern Caribbean Plate Boundary, Trans. 1st Geol. Conf. of the Geol. Soc. of Trinidad and Tobago. p. 265 - 269.

Sealy, E. and Ramlackhansingh, A., 1979, The Geology of Trinidad Tesoro's Palo Seco Field including South Erin and Central Los Bajos. 4th Latin American Geological Congress, Trinidad, p. 796 - 802.

Stone, D.S., 1969, Wrench faulting and Rocky Mountain tectonics, Mtn. Geologist, v 6 #2, p. 67 - 69.

Wilcox, R., Harding, T.P. and Seeley, P.R. 1973. Basic Wrench Tectonics. American Association of Petroleum Geologists v 57, #1p. 74-96.

Wilson, C.C., 1958, The Los Bajos Fault and its relation to Trinidad's Oilfield Structures, Jour. Institute for Petroleum, v 44 #413. p.124-136.

Wilson, C.C.., 1965., The Los Bajos Fault, Trans. 4th Carib. Geol. Conf., Trinidad, p. 87-88.

AN EVALUATION OF THE GEOLOGICAL HISTORY AND HYDROCARBON POTENTIAL OF THE LATE MIOCENE - ? PLIO/PLEISTOCENE SEDIMENTS OF THE GOUDRON FIELD - TRINIDAD

Carol P. Telemaque
Geological Department
Trintopec, Santa Flora
Trinidad, West Indies

ABSTRACT

The Goudron Field lies in the Southern Basin onshore Trinidad, on the south-eastern flank of the Rock Dome/Lizard Springs anticlinal trend. A sedimentary sequence of Upper Cretaceous to late Tertiary sediments has been penetrated by the 174 wells drilled in the area. However, to date, only the late Miocene and ? Plio/Pleistocene contain productive hydrocarbon reservoirs.

Two major episodes of late Miocene/ ? Plio-Pleistocene sedimentation have been identified. The older comprised a period of sediment gravity flows into a bathyal environment in the Late Miocene/ ? Early Pliocene which resulted in the deposition of interbedded shales, silts, sands and conglomerates of the Moruga Formation. The younger comprised a period of fluvio-continental deposition in the ? Plio-Pleistocene and resulted in the sands and minor silty clays of the Mayaro Formation.

Deposition of the Moruga Formation was followed by a major tectonic event, resulting in the formation of the Pilote Syncline and the Pre-Mayaro Unconformity. Minor Episodes of ? late Pliocene/Pleistocene faulting are also evident.

The field was discovered in 1927 and has produced 4.6 mm barrels of oil to date and may still ccntain significant reserves to be exploited.

INTRODUCTION

The Goudron Field was discovered in the 1920's, aggressively drilled throughout the 1940's and 1950's, and has been virtually abandoned since that time. Over the period of drilling activity, 174 wells penetrated mainly the shallow, productive Upper Miocene -? Plio/Pleistocene sediments, from which 4.6 mm barrels of oil have been produced. A few wells were also drilled beyond this productive section.

All available data from these wells including electric logs, one dipmeter log, full-hole and sidewall cores, palaeontological reports, and production data were incorporated in the study. Other available data comprised field outcrop and augur samples, Kugler's surface geology map of Trinidad (1959), and geophysical data. The latter consisted of a gravity survey run in 1950, which covered only a small portion of the field and was virtually useless, and an east - west trending seismic (1966) line which provided valuable additional information.

The Goudron Field is situated in the Guayaguayare Sub-basin which lies south of the Rock Dome/Lizard Springs Anticline in the eastern part of the Southern Basin (Fig.1). It lies approximately 30 miles due east of TRINTOPEC's active land operation. The closest TRINTOPEC field under development is Moruga East which lies approximately 5 miles to the west and within which drilling activity has been minimal. Activity in the Goudron Field has been suspended since the 1960's, and much of the existing infrastructure including roads, tanks, pumping station and buildings may require extensive refurbishing and upgrading if an aggressive development/exploration programme is initiated. In the more remote areas, the terrain is rugged and heavily forested, and therefore initial exploration costs may be relatively high.

Abblewhite and Higgins (1965) gave a brief outline of the geology of the field, but since that time no further publications have been made.

STRATIGRAPHY AND SEDIMENTATION

The hydrocarbon-bearing sediments consist of the sands of the older Moruga and younger Mayaro Formations (Figs. 2,3,4). While it is difficult to place these formations in time throughout the late Miocene to Pleistocene, certain pertinent facts have been noted, as follows:

- The basal part of the Moruga Formation is dated late Miocene (post Globorotalia acostaensis).
- The cyclicity of the sedimentation within the two formations could be indicative of eustatic changes

Larue, D.K., and Draper, G. (eds.),
Transactions of the 12th Caribbean Geological Conference, St. Croix, U.S.V.I., Miami Geological Society, P.O. Box 431552, South Miami, FL 33243, U.S.A

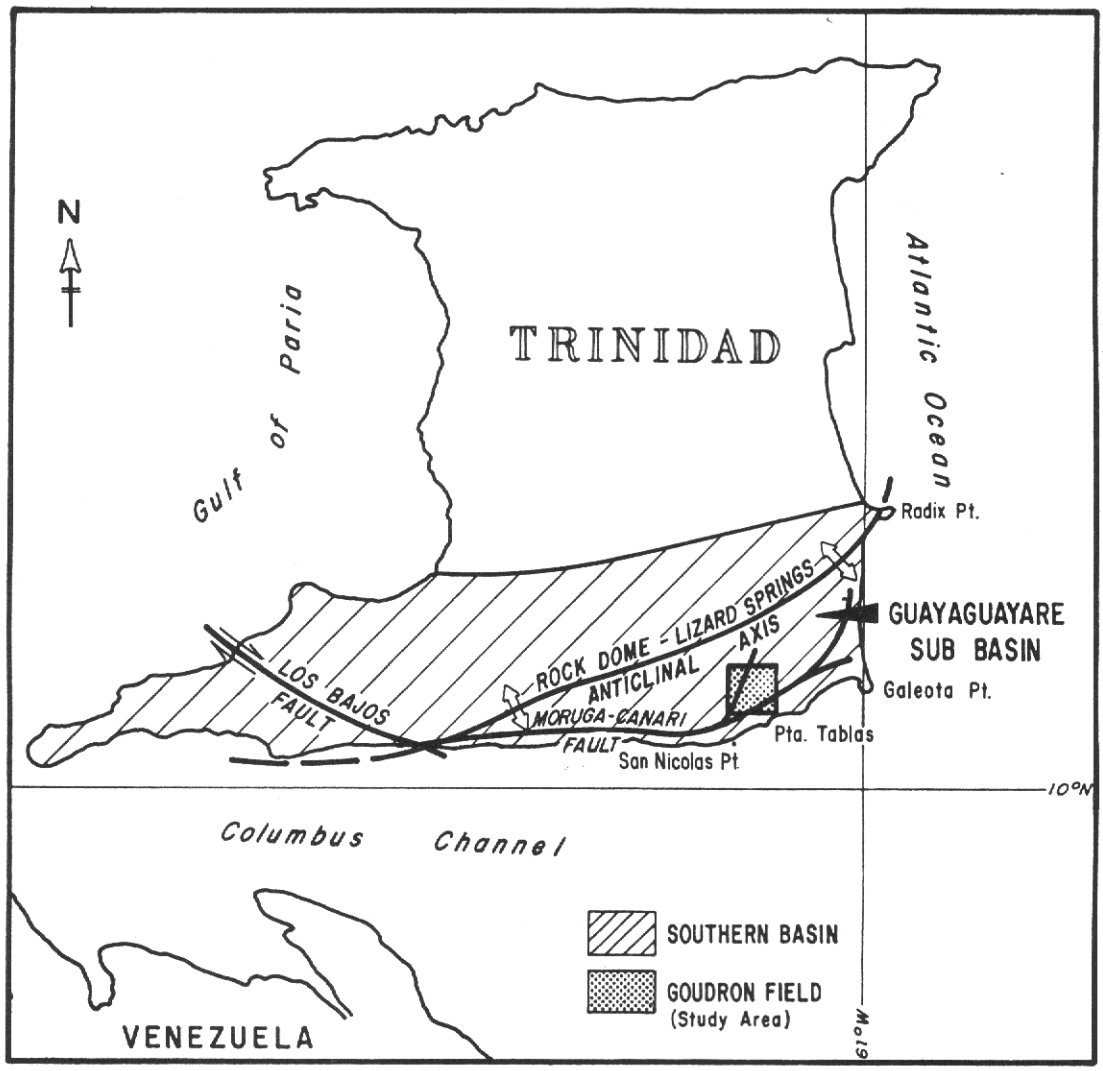

0 10 20 Mls.

Fig. 1 - Location Map

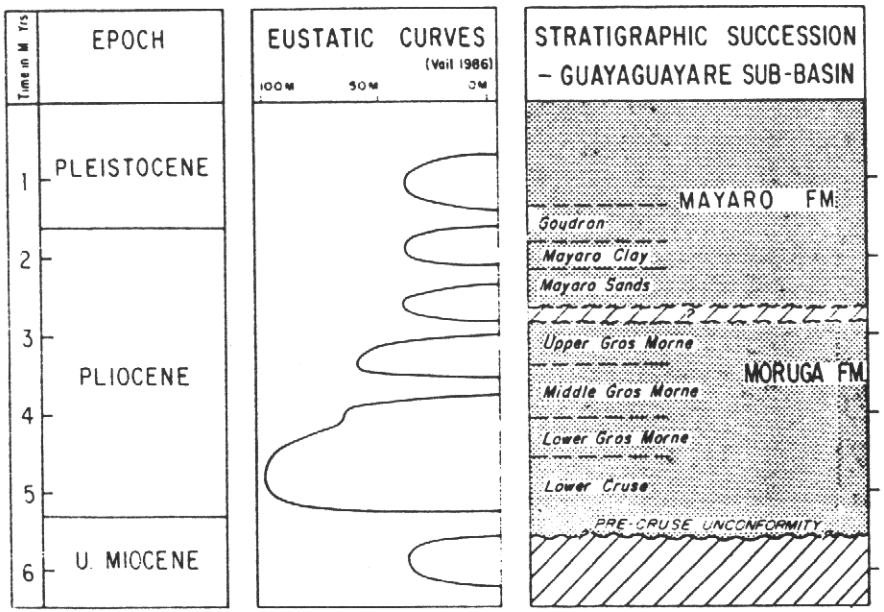

Fig. 2 - Stratigraphic Chart - Guayaguayare Sub Basin with possible relationship to sea-level changes

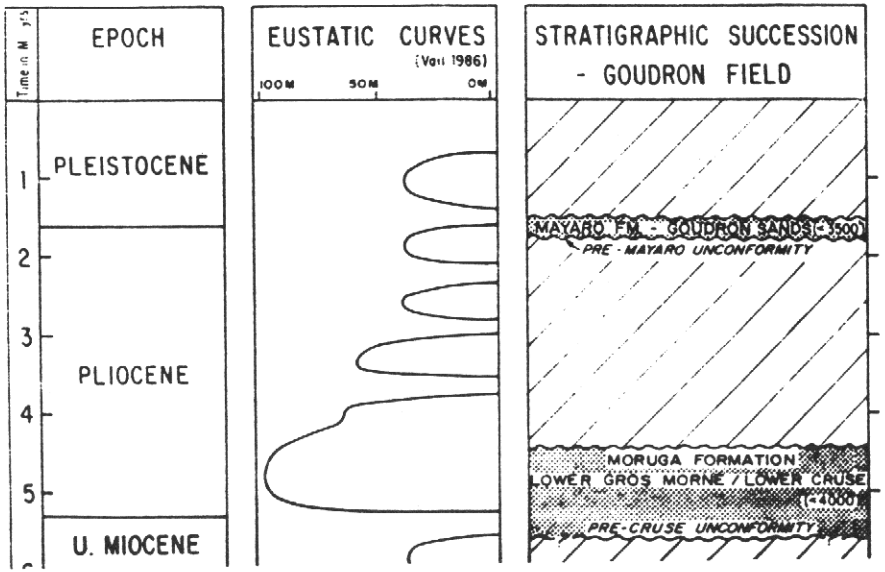

Fig. 3 - Stratigraphic Chart - Goudron Field with possible relationship to sea-level changes

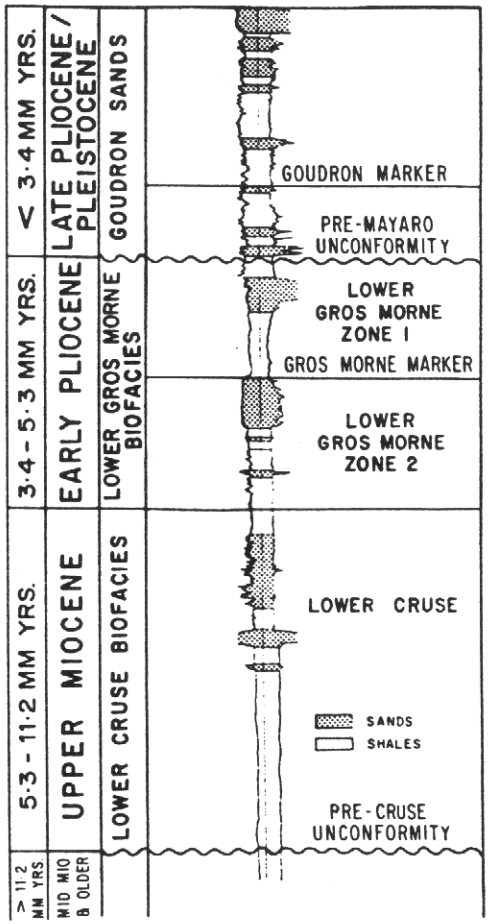

Fig. 4 - Composite Type Log Goudron Field

throughout this time, and there may be correlations between these cycles of deposition and documented worldwide eustatic changes throughout the Miocene - Pleistocene (Figs. 2, 3).

Moruga Formation

The Moruga Formation is late Miocene-?Pleistocene in age,and is underlain unconformably by the Eocene Lizard Springs Formation (Cushman and Jarvis 1928), and the Upper Miocene Lengua (Renz 1942) and Karamat (Suter 1951) Formations, from which it is separated by the Pre-Cruse Unconformity (Figs. 3, 4, 4a). The particular formation which directly underlies the Moruga Formation changes from place to place within the field depending on the formation exposed below the Pre-Cruse Unconformity. The Mayaro Formation unconformably overlies the Moruga Formation.

The Moruga Formation attains a maximum thickness of 4000 feet and is represented within the field by its basal members, the Lower Cruse and Lower Gros Morne Biofacies (Figs. 2, 4). Well-defined lithological markers have been used to subdivide the Moruga Formation into, from oldest to youngest, Lower Cruse, Lower Gros Morne Zone 2 and Lower Gros Morne Zone 1, (Figs. 4, 6, 7, 8). It consists of dark grey to black, immature, slightly calcareous clays, which contain pyrite, mica, glauconite, pebbles and boulders (including chert, calcareous nodules, pepper and salt sandstone, limestone, argilline, marl, clay, mudstone), and sand/silty-sand laminae and beds.

The clays yield a heterogenous fauna consistent with the heterogenous lithologic texture, and these indicate considerable reworking of older Miocene, Oligocene, Eocene, Palaeocene and Cretaceous formations into late Miocene-? Plio/Pleistocene sediments. The fauna are arenaceous and ccmprise predominantly outer-shelf valvulinids, and these indicate deposition in an outer shelf/upper slope environment.

The sands in these zones range in thickness from a fraction of an inch when they occur as laminae to ±300 ft in thickness. They are fine to medium-ccarse grained, silty, and contain pebbles and boulders of siltstone, vuggy limestone and buff-coloured marl. These sands are interpreted as turbidites deposited in an outer shelf/upper slope environment.

Through palaeogeographic reccnstructions, the topography of the surface on which the sediments of the Moruga Formation were deposited ie. Pre-Cruse Unconformity surface, has been defined, and it is apparent that this surface controlled deposition of the overlying turbidite sands of the Late Miocene-? Plio/Pleistocene (Fig. 5). During that period,the depositional surface deepened westward and was characterized by the occurrence cf east-west trending ridges and intervening "lows" within the field area. Dips on the flanks were 14°±. Sands subsequently deposited in this basin became ccnfined to the "lows" between the up-folds, and because of westerly deepening, all the sediments downlap the unccnformity surface eastward, so that younger and younger sediments are in contact with the unconformity surface in that direction (Figs. 6,7,8).

Mayaro Formation

The exact age of this formation is unknown at the present time but it could be Pliocene or as young as the Pleistocene (Figs. 3,4). On-going geological studies may lead to a more exact determination of its age in the future. It is underlain unconformably by the Moruga Formation from which it is separated by the Pre-Mayaro Unconformity, which it onlaps to the west, northwest and southeast (Fig. 11). It outcrops at surface, and is found preserved only in the northern part of the field.

Palaeogeographic reconstruction of the topography of the surface on which the sands of the Mayaro Formation were deposited could be done only in the northern part of the field and indicates close parallels between the features of this surface and the features of the structures created by ? Plio/Pleistocene tectonism which preceded its deposition (Figs. 9, 10). The receiving basin appears to have been traversed by a number of east-west trending, parallel ridges and intervening lows which approximately correspond to the main structural elements of the Moruga structure including the Pilote Syncline, Fault AA', and the northern flank of a southerly upthrust block (Figs. 9, 10).

These facts, coupled with the fact that the present-day structures within the Mayaro Formation closely parallel the palaeotopography in "Mayaro" time, suggest that no tectonism has occurred since the ? Plio/Pleistocene event. (Figs. 9, 10, 12).

The Mayaro Formation is represented by its uppermost member, the Goudron Sandstone, which consists of laminated, cross-laminated and bedded, rippled sandstones, whose sparse fauna, including brackish water miliammina, and lithological character indicate deposition in a nearshore environment (Figs. 3, 4). The sands are fine-very fine grained, fair-well sorted, non-calcareous, silty in part, contain lignite and mica, and are occasionally interbedded with thin shales and silty sand (Figs. 4, 13). The cumulative thickness of these sands exceeds 3000 ft in the east central part of the field (Fig. 11).

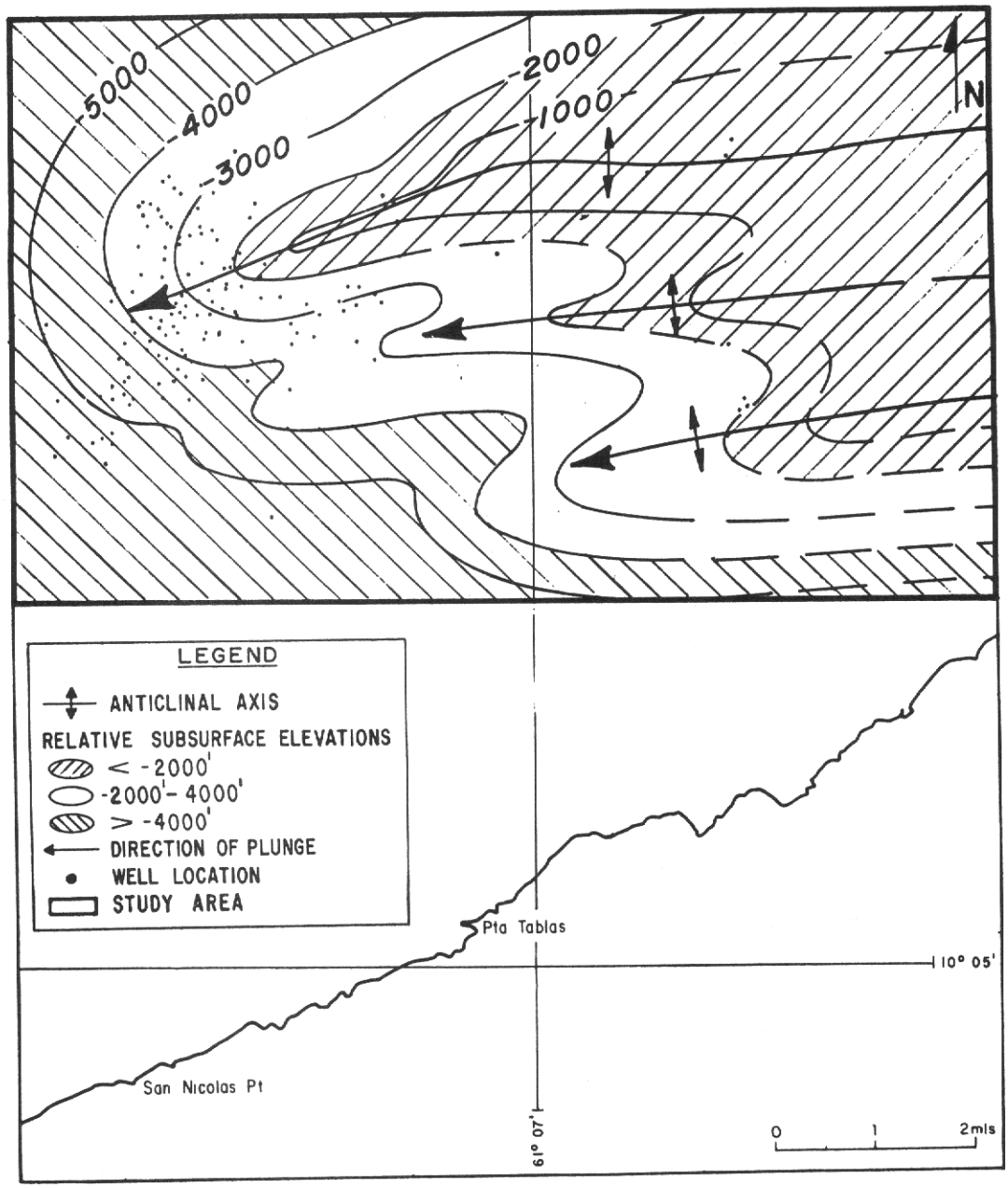

Fig. 5 - Palaeotopography - Late Miocene
(Basin Configuration prior to deposition of Moruga Fm.)

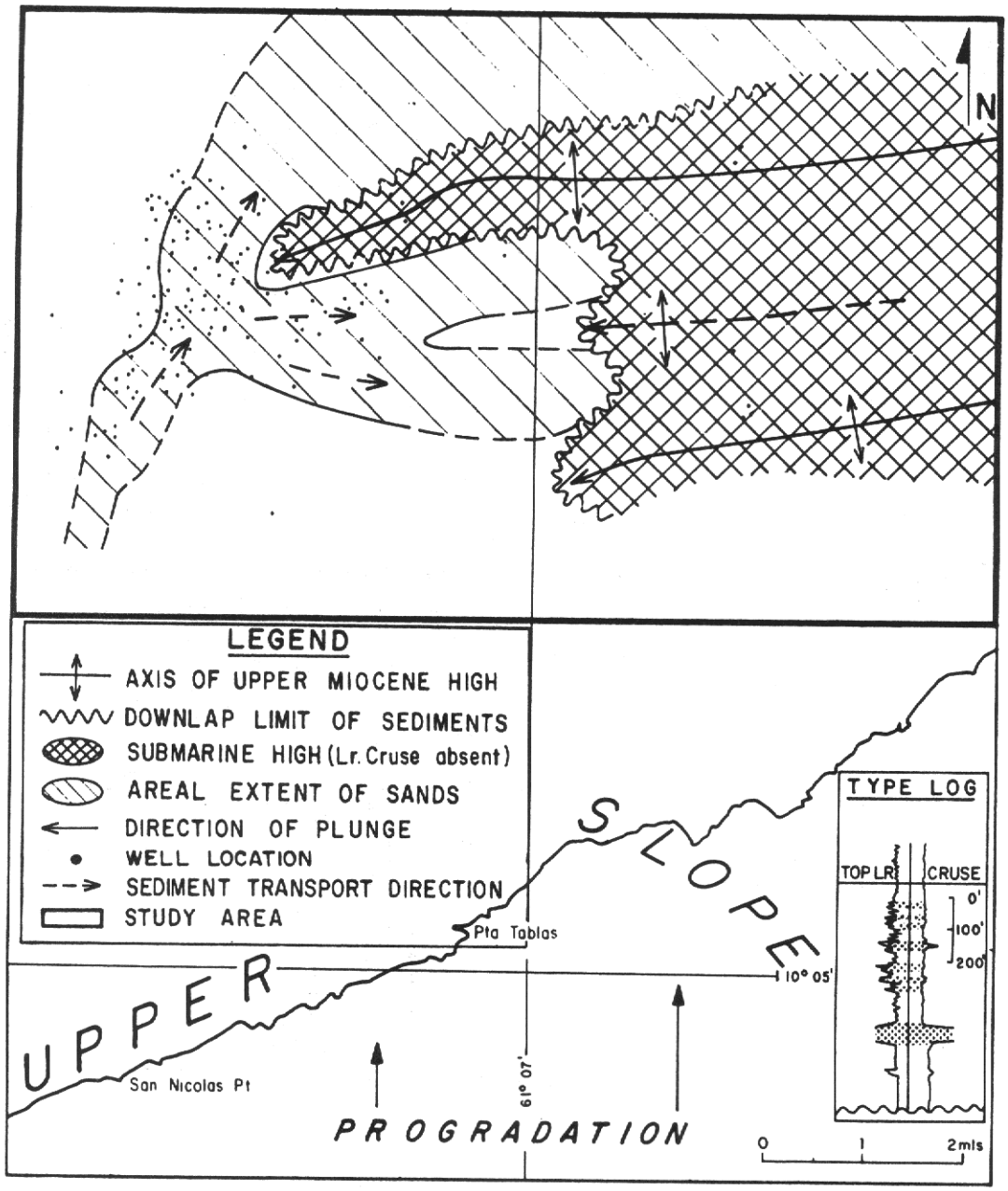

Fig. 6 - Sand Distribution - Lower Cruse

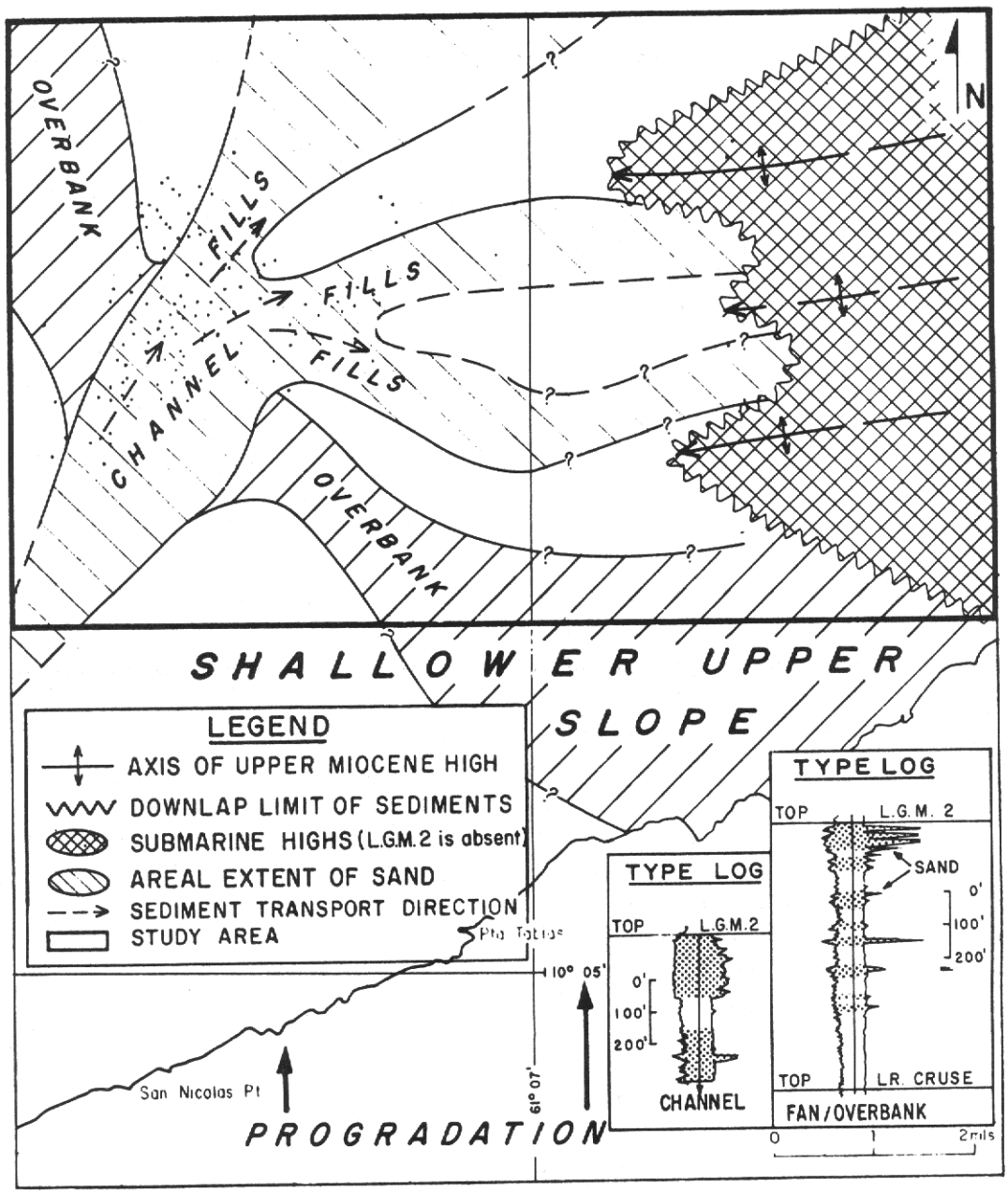

Fig. 7 - Sand Distribution - Lower Gros Morne Zone 2

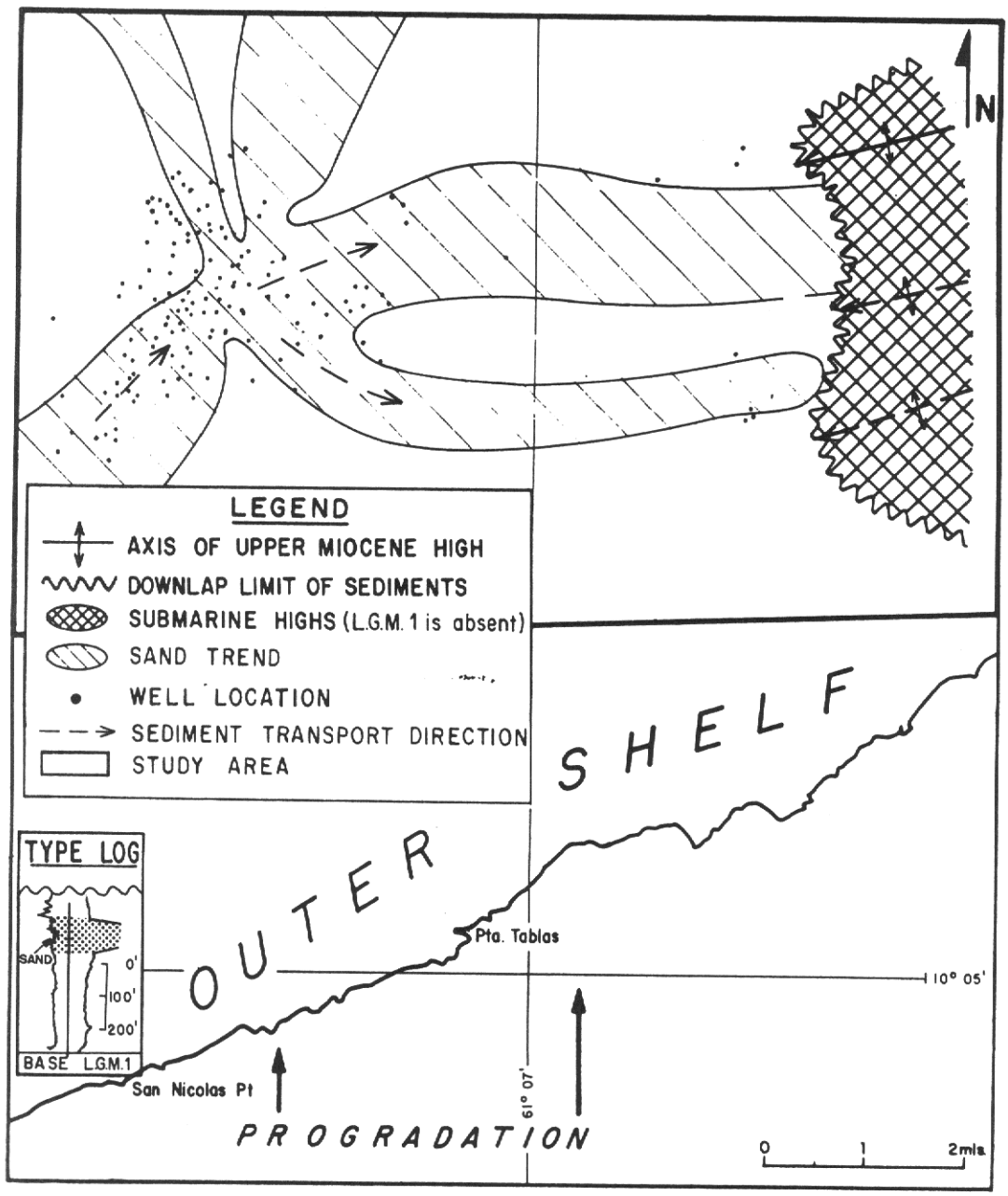

Fig. 8 - Sand Distribution - Lower Gros Morne Zone 1
(Truncation by Pre-Mayaro Unconformity at Top of Section)

STRUCTURE

Well-defined lithological markers were established by well to well correlation of electric logs, and these markers were used to establish the structural history of the late Miocene to?Plio/Pleistocene sediments (Fig. 4a). Two major tectonic events were responsible for the present-day structures within this field. These include a mid-Miocene event and a ? Plio/Pleistocene event (Fig. 3). The former coupled with erosion created the Pre-Cruse Unconformity whose topography influenced deposition of sediments of the Moruga Formation. The latter structured sediments of the Moruga Formation and created the pre-Mayaro Unconformity, whose topography influenced deposition of the sediments of the Mayaro Formation.

Pre-Cruse Unconformity (Figs. 3, 4, 5)

This is a major unconformity resulting from a well-defined mid-Miocene tectonic event, which resulted in the creation of a series of parallel, east-west trending highs running through the field (Fig. 5). Wells which penetrated the unconformity have encountered sediments of mid-Miocene, Eocene, and Palaeocene ages directly below the unconformity surface, depending on their locations. Following the erosion which accompanied the mid-Miocene tectonism, sediments of the Moruga Formation were deposited on the Pre-Cruse Unconformity from as early as the late Miocene.

Structure - Moruga Formation

This structure is the result of a ? Plio/Pleistocene tectonic event that followed deposition of sediments of the Moruga Formation. The exact timing of this event is unknown at this time due to lack of available data.

The Pilote Syncline was one of the major structural features which resulted from this tectonism (Fig. 9). It is a NE-SW trending syncline, whose axis runs through the northern part of the field and plunges to the east. It is asymmetrical, being more steeply dipping on its northwestern flank than on its southeastern flank. As a result, dips vary from 53° E in the west, to 25° straddling the synclinal axis, and 18° N on the southeastern flank of the syncline.

Several major north-south and east northeast -west southwest trending faults dissect the syncline. One fault, AA', is a north-south trending, right lateral, wrench fault and offsets the synclinal axis by .8 km. While this is the present day offset, this displacement is estimated to have been approximately .5 km prior to deposition of sediments of the overlying Mayaro Formation, since lateral displacement along fault AA' is evident, though to a lesser degree in the Mayaro Formation. The other faults are northeast - southwest trending thrust or normal faults, with vertical displacement ranging between 200 ft to 1000 ft.

Pre-Mayaro Unconformity

This is an unconformity which lies between the Moruga and the Mayaro Formations, and is the result of a tectonic event which followed deposition of sediments of the Moruga Formation (Figs. 3, 4, 10). The exact timing of this event is unknown, but could be as early as the early Pliocene or as late as the Pleistocene. The unconformity is only represented in the northern part of the field.

Structure - Mayaro Formation

This "structure" is the result of drape of sands of the Mayaro Formation over the Pre-Mayaro Unconformity, and ?Plio/Pleistocene right-lateral wrench faulting. As a result, the sands of the Mayaro Formation are "folded" into two, sub-parallel, east-west trending synclines whose axes are offset 0.3 km by north-south trending wrench fault, AA'. Both synclines plunge to the east due east of wrench fault AA', and to the west due west of this fault. Dips on the synclinal flanks average 30° east of fault AA' and 25° west of it.

HYDROCARBON POTENTIAL

The Goudron Field has been highly productive in the small area developed in the west-central part of the field. Because of its early abandonment, barely 20% of its productive potential has been realized since its discovery in 1927, from late Miocene to ? Plio/Pleistocene sediments, and though it is presently non-productive, considerable quantities of hydrocarbons, in the order of ±20 mmbo remain to be produced. Oil production in the Moruga Formation is derived from combination structural and stratigraphic traps within structures associated with right-lateral wrenching, and within shoe-string turbidite channel sands interbedded with shales (Figs. 6,7, 8, 13). Some oil is also found in similarly structured overbank fan sands.

While significant production has been obtained from sands of the Mayaro Formation, no well-defined trap is evident, since there is no significant seal. The oil in this formation seems to have a strong affinity to the sands in contact with the pre-Mayaro Unconformity surface. It appears that oil may be currently migrating along the unconformity surface, and that some of it becomes temporarily reservoired in the lowest sands, before being completely lost at surface. (Fig. 13).

It can be inferred that the Moruga Canari Wrench fault system taps the established Cretaceous source rocks at depth beneath the

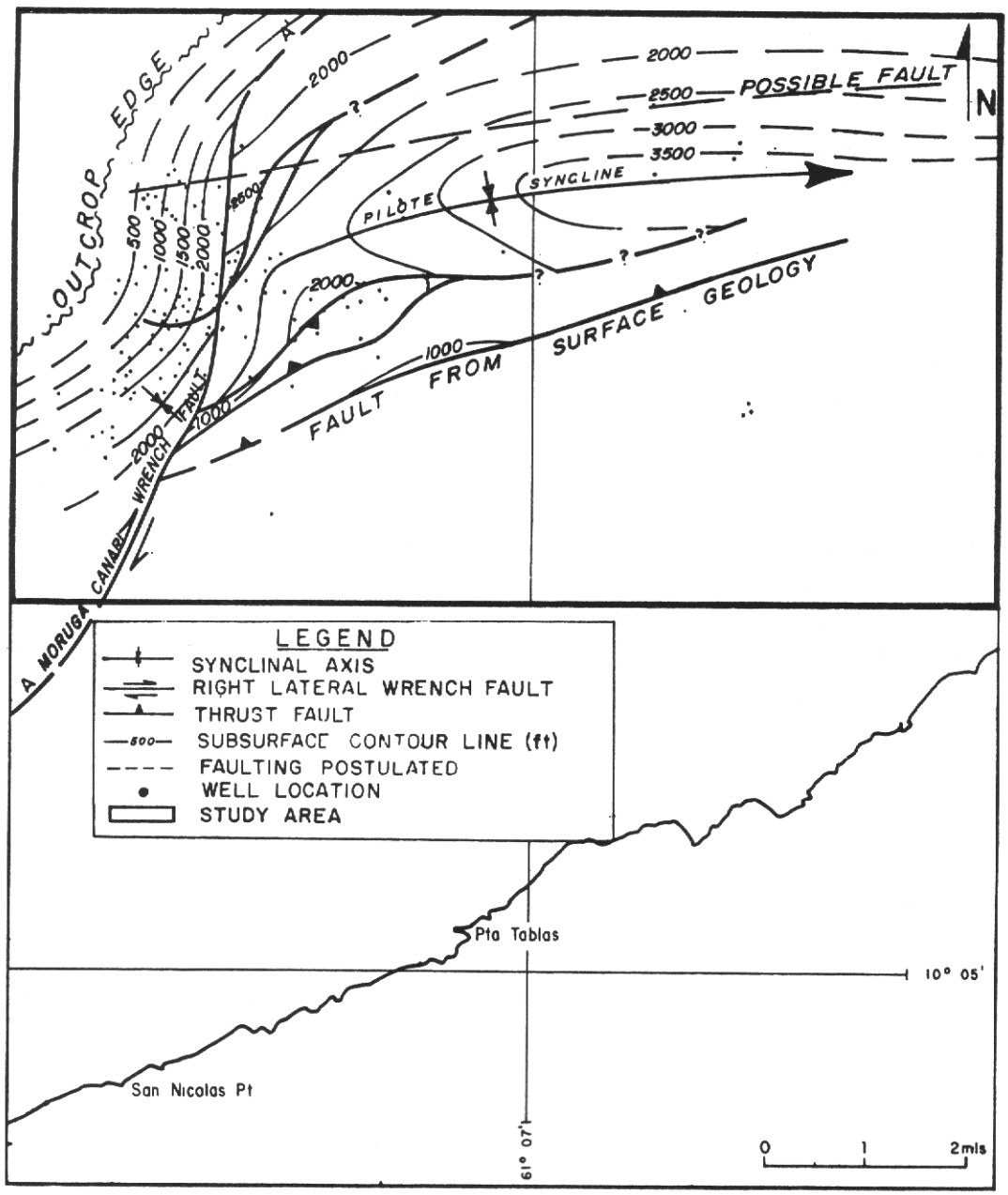

Fig. 9 - Structure Contour Map - Gros Morne Marker

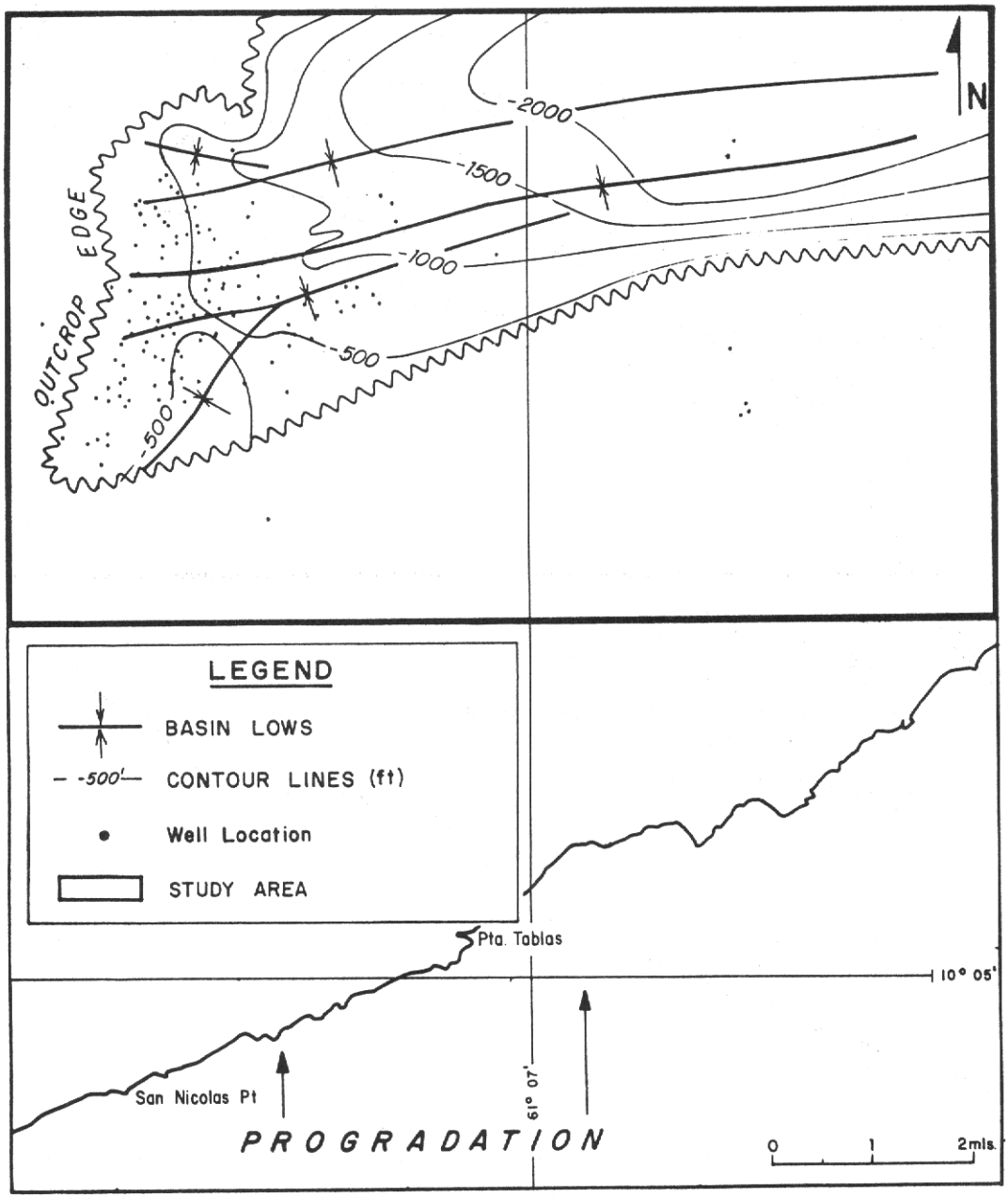

Fig. 10 - Palaeotopography
Late Pliocene/Pleistocene
(Basin Configuration for sedimentation of Goudron Sands)

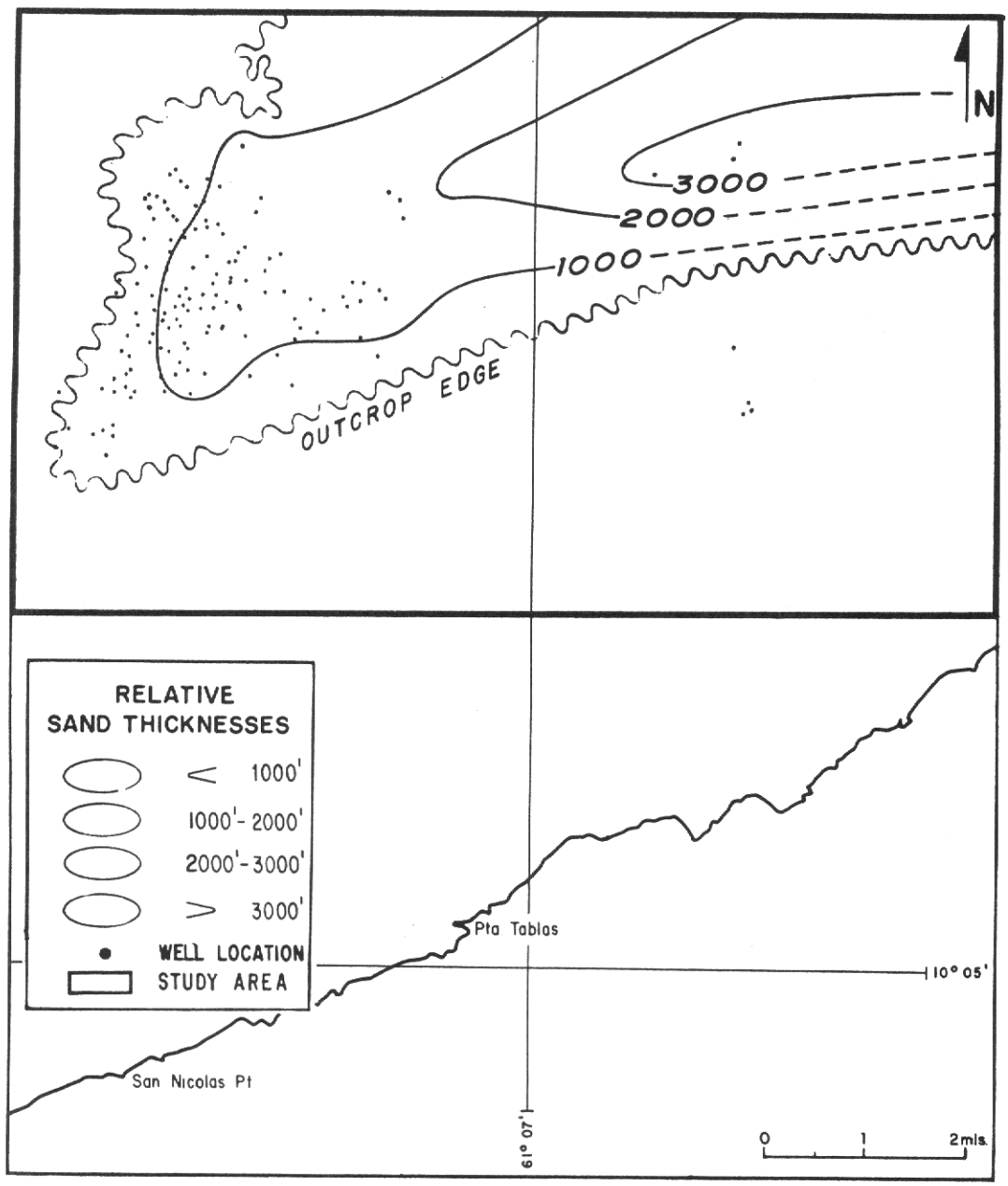

Fig. 11 - Interval Isopach - Goudron Sands

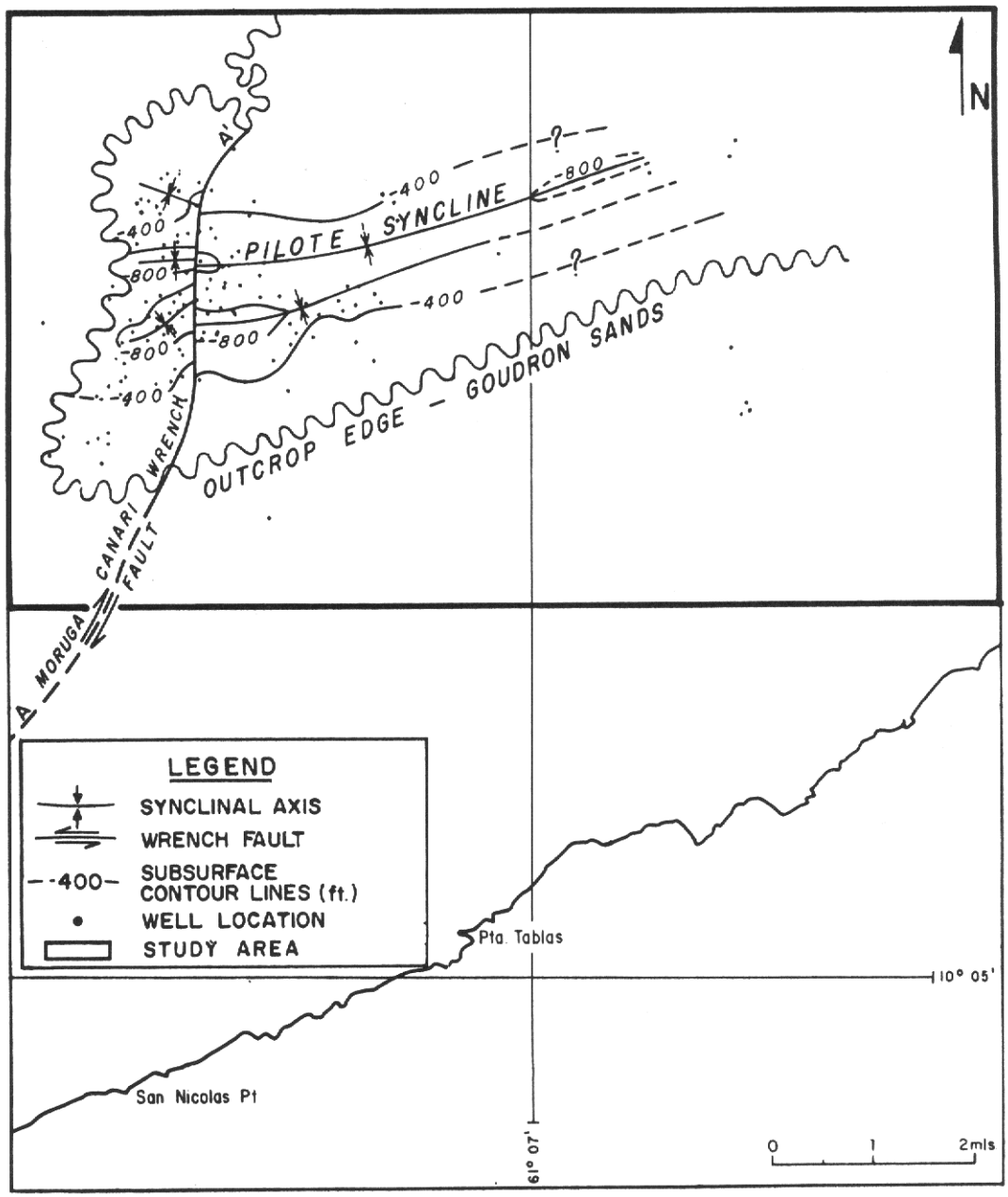

Fig. 12 - Structure Contour Map - Goudron Marker

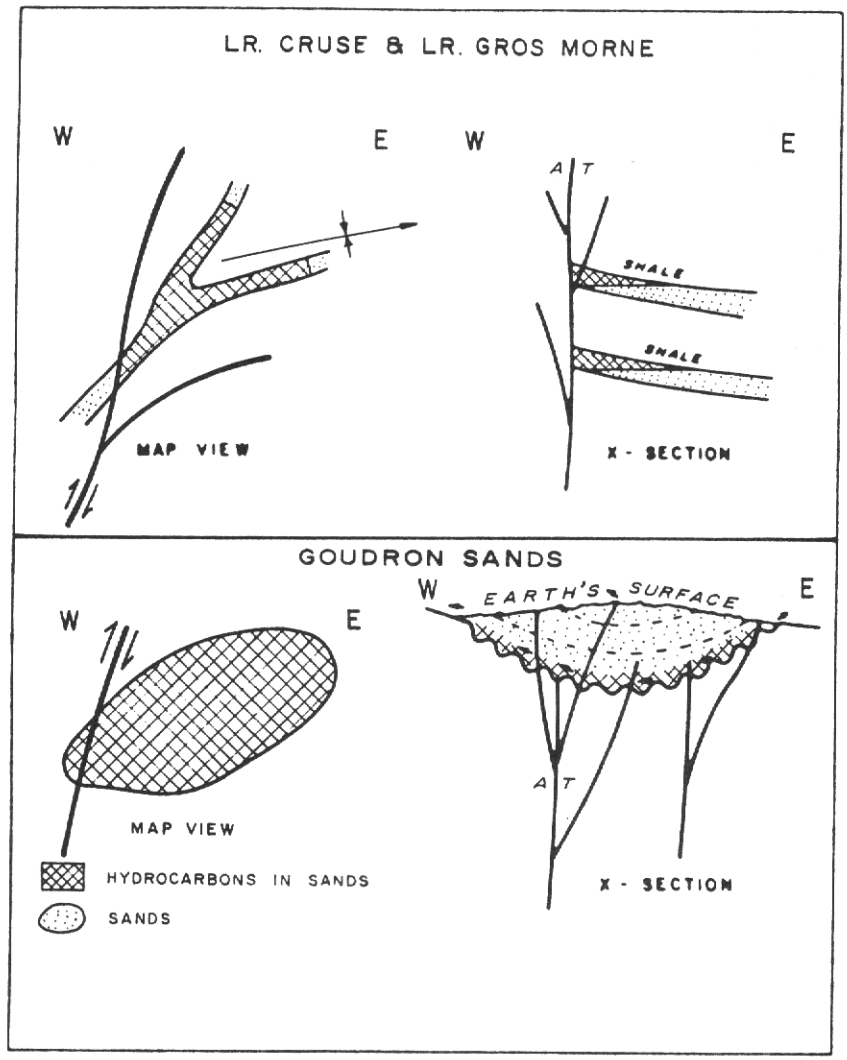

Fig. 13 - Hydrocarbon Potentials

field and beyond the field area, and that some of the faults associated with this system act as conduits for migration into reservoirs in the Moruga and Mayaro Formations.

REFERENCES

Abblewhite, K., and Higgins, G.E., 1965, A Review of Trinidad, West Indies, Oil Development and the Accumulations at Soldado, Brighton Marine, Grande Ravine, Barrackpore-Penal, and Guayaguayare *in* Saunders, J.B. ed., Transactions of the Fourth Caribbean Geological Conference, pp 41-73.

Haq B.U., Hardenbol J, Vail P.R., et al, 1988, Eustatic Curves *in* Vail P.R. ed., Fundamentals of Sequence Stratigraphy Workbook : AAPG course notes.

Kugler H.G. et al, 1956, Stratigraphic Lexicon of Trinidad *in* Lexique Stratigraphique Internationale: Cinq Centre Nationale de la Recherche Scientifique, pp 42-125.

EXPLOITATION OF THE MIDDLE MIOCENE OIL BEARING INTERMEDIATE HERRERA SANDSTONE RESERVOIRS IN TRINIDAD, WEST INDIES

Fazal Hosein
Trinidad and Tobago Oil Co. Ltd.,
Pointe-a-Pierre, Trinidad

ABSTRACT

The Herrera sands contain the major oil producing reservoirs of Miocene age in Trinidad's Southern Basin. They lie within the Upper Cipero shale formation in the Penal/Wilson, Barrackpore/Mandingo and Ortoire fields of south-central Trinidad. These turbidite sands are found at three levels - the "overthrust", "intermediate" and "underthrust" - each level separated by a major thrust fault and associated with a complex structure of a strong overfold and recumbent syncline formed by major tectonic movements at the end of Middle Miocene time.

The Intermediate Herrera sands are confined to a long (17 miles) and narrow (2,000 feet) area trending NE-SW from the Penal/Wilson field to the Barrackpore/Mandingo field. The sands are found at depths of 6,000 to 10,000 feet in a complex structure which plunges to the south-west and is cut by numerous extensional cross faults which delineate separate hydrocarbon pools. Exploration commenced in 1946 and by December 31, 1988 cumulative production was 18 million barrels of oil/condensate and 30 BCF of natural gas. These sands offer the best potential for continued exploitation of an additional 19.5 MM barrels of undeveloped oil/condensate reserves.

INTRODUCTION

Trinidad is located in the south-east corner of the Caribbean and within the eastern Venezuelan Basin (Fig. 1). Geologically, Trinidad has very similar features to Venezuela, having been subjected to the same kind of compressive stress from the north north-west resulting in wrench faults and NE-SW trending folds and thrust faults which are directly associated with oil accumulations in the Miocene age reservoirs of Nariva, Retrench and Herrera sands (Fig. 2).

The Herrera sands are the most important and contain the major oil producing reservoirs of Miocene age in Trinidad's Southern Basin. They lie within the Upper Cipero shale formation in the Penal/Wilson, Barrackpore/Mandingo and Ortoire fields of Southern Trinidad (Fig. 3).

These turbidite sands are found at three levels - the "overthrust", "intermediate" and "underthrust" - each level separated by a major thrust fault. The Intermediate Herrera sands have been exploited in the Penal/Wilson and Barrackpore/Mandingo fields.

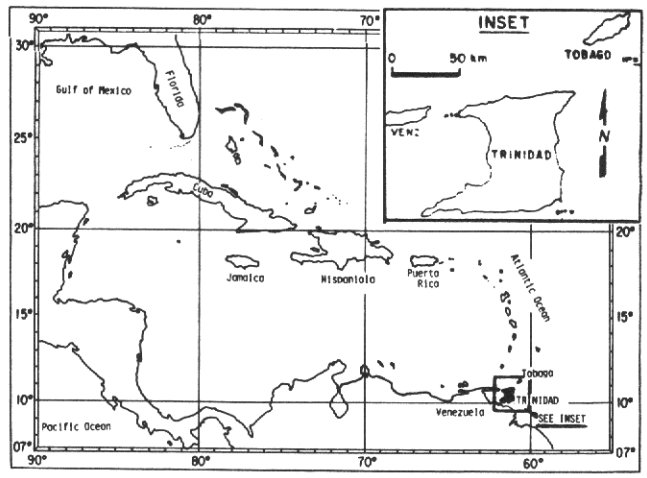

Fig. 1 Location Map showing Trinidad and the Caribbean.

HISTORY OF FIELD DEVELOPMENT

The "overthrust" or shallow Herrera sands were first discovered in 1938 by Shell Oil Company in Penal-23 well. Development drilling of this field continued until 1946 when a field extension well, Penal-92, found the sands missing. The well was deepened to discover the second level or Intermediate Herrera sands well developed and oil bearing below a major thrust fault (Fig. 4). The field was BP-360 drilled in 1954 by the Trinidad leaseholds Ltd. Company which was exploiting the shallow Herrera sands in the area (Fig. 5). Exploitation drilling since then established that the Intermediate Herrera sands are confined to a long (17 miles) and narrow (2,000 feet) area extending from Penal field to the Barrackpore/Mandingo field.

Larue, D.K., and Draper, G. (eds.),
Transactions of the 12th Caribbean Geological Conference, St. Croix, U.S.V.I., Miami Geological Society, P.O. Box 431552, South Miami, FL 33243, U.S.A

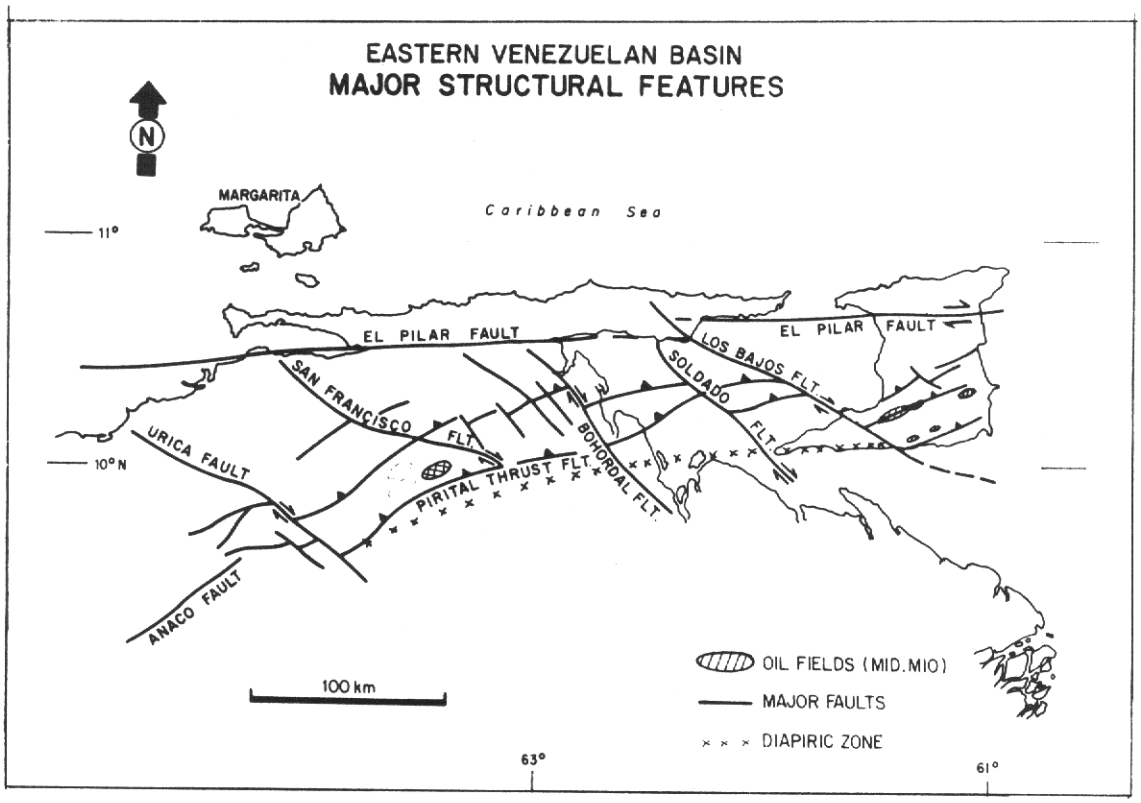

Fig. 2 Regional Map showing the major wrench and thrust faults in Trinidad and Eastern Venezuela.

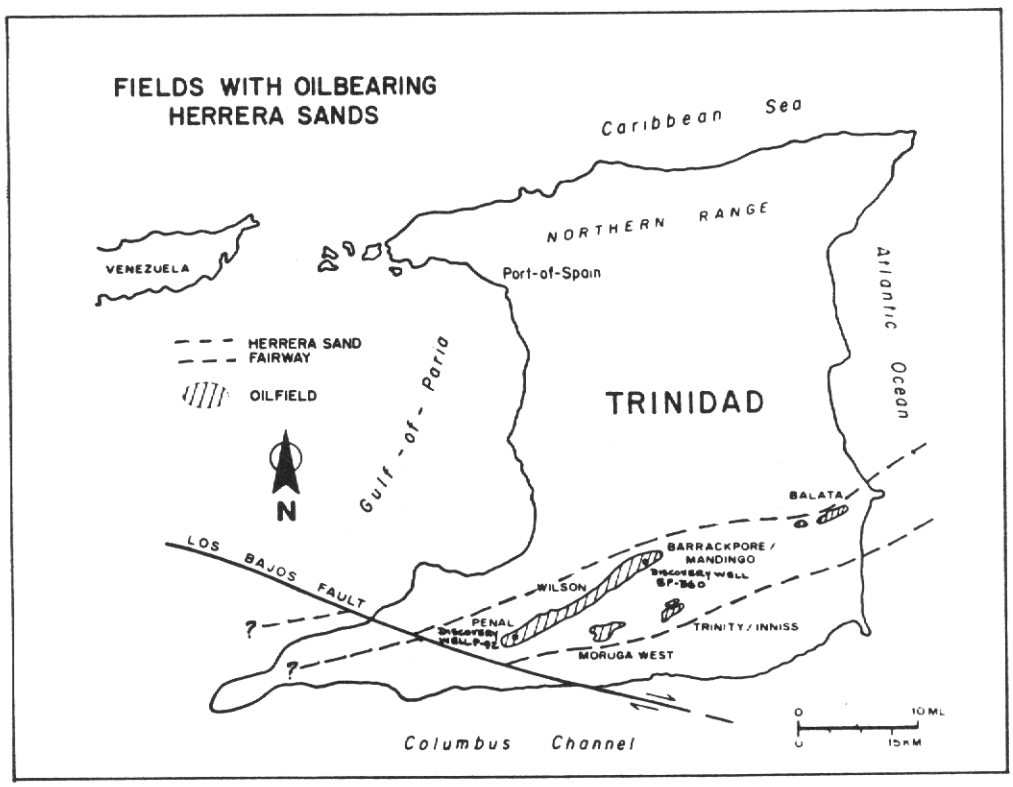

Fig. 3 Location Map showing the fields with oilbearing Herrera sands in Trinidad's Southern Basin.

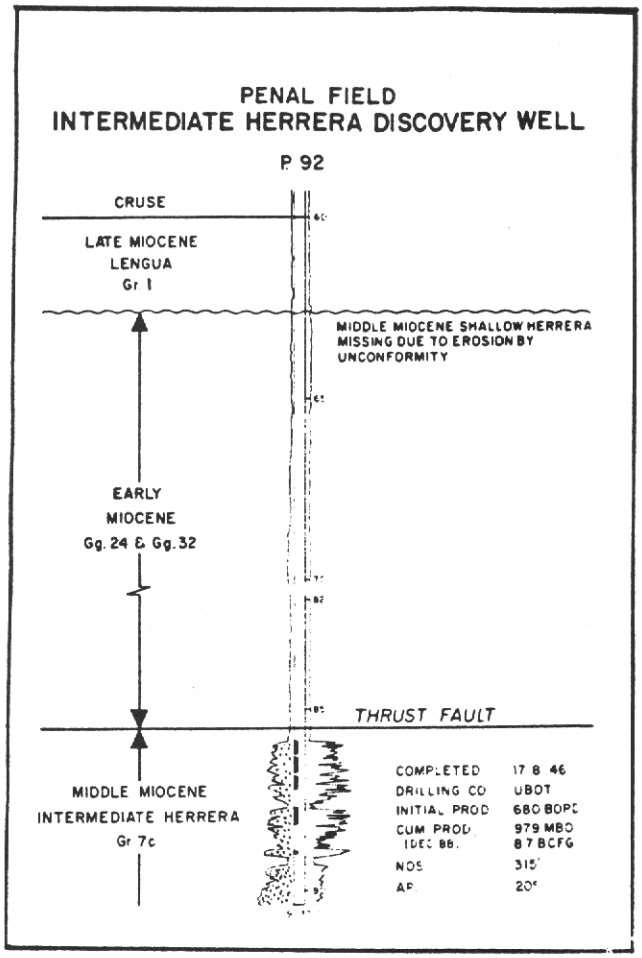

Fig. 4 Gamma Ray-Induction Resistivity Log of Penal-92 well showing well developed Middle Miocene Intermediate Herrera sands.

LITHOLOGY

The Herrera sandstone is generally described as grey, calcareous, fine to coarse and even conglomeratic with a "pepper and salt" appearance. The black "pepper" appearance is due to chert, hard black shale, black limestone and coal fragments. The white "salt" appearance is due to clear quartz grains. The Intermediate Herrera sands range from coarse to very fine grained sands and even siltsize in some areas.

REGIONAL STRATIGRAPHY

The Herrera sands are developed within the Middle Miocene Globorotalia Fohsi zone which form the Upper part of the Cipero formation. The sands were deposited in a marine bathyal environment where the presence of planktonic formaninifera enables zonation using the evolutionary sequence of the Globorotalia Fohsi foraminifera group (Fig. 6).

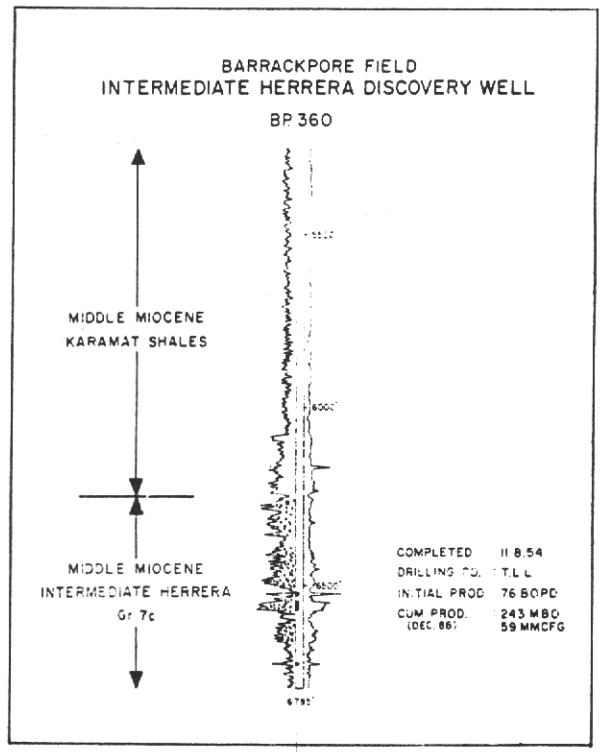

Fig. 5 Gamma Ray-Induction Resistivity Log of Barrackpore-360 well.

Work done by previous authors including P. Bitterli (1958) and W.G. Poole (1965) have already established that the Herrera sands were initially deposited in shallow water and were then transported by turbidity currents into the deeper water environment where they were encased within the Upper Cipero shales. A schematic diagram (Fig. 7) shows the author's model for deposition suggesting a north-westerly source for the Herrera sands which were transported to the shelf edge before being redistributed by turbidity currents into a deep water NE-SW trending trough.

STRUCTURE

At the end of Middle Miocene time, there was strong folding with compression from the north-west which resulted in a complex structure at the Herrera sand level involving a strong overfold with associated faulting and thrusting. A series of NE-SW trending thrust faults developed across Trinidad's Southern Basin. These faults with their associated anticlinal structures provided the traps for oil accumulation in the Intermediate Herrera sands found in an area extending for 17 miles long from south-west Penal to Mandingo field. Using well logs, production data and planktonic foraminiferal zones, the structure of the Intermediate Herrera sands has been mapped over the study area. The Intermediate Herrera sands will be described separately for the Penal/Wilson field and the Barrackpore/Mandingo field.

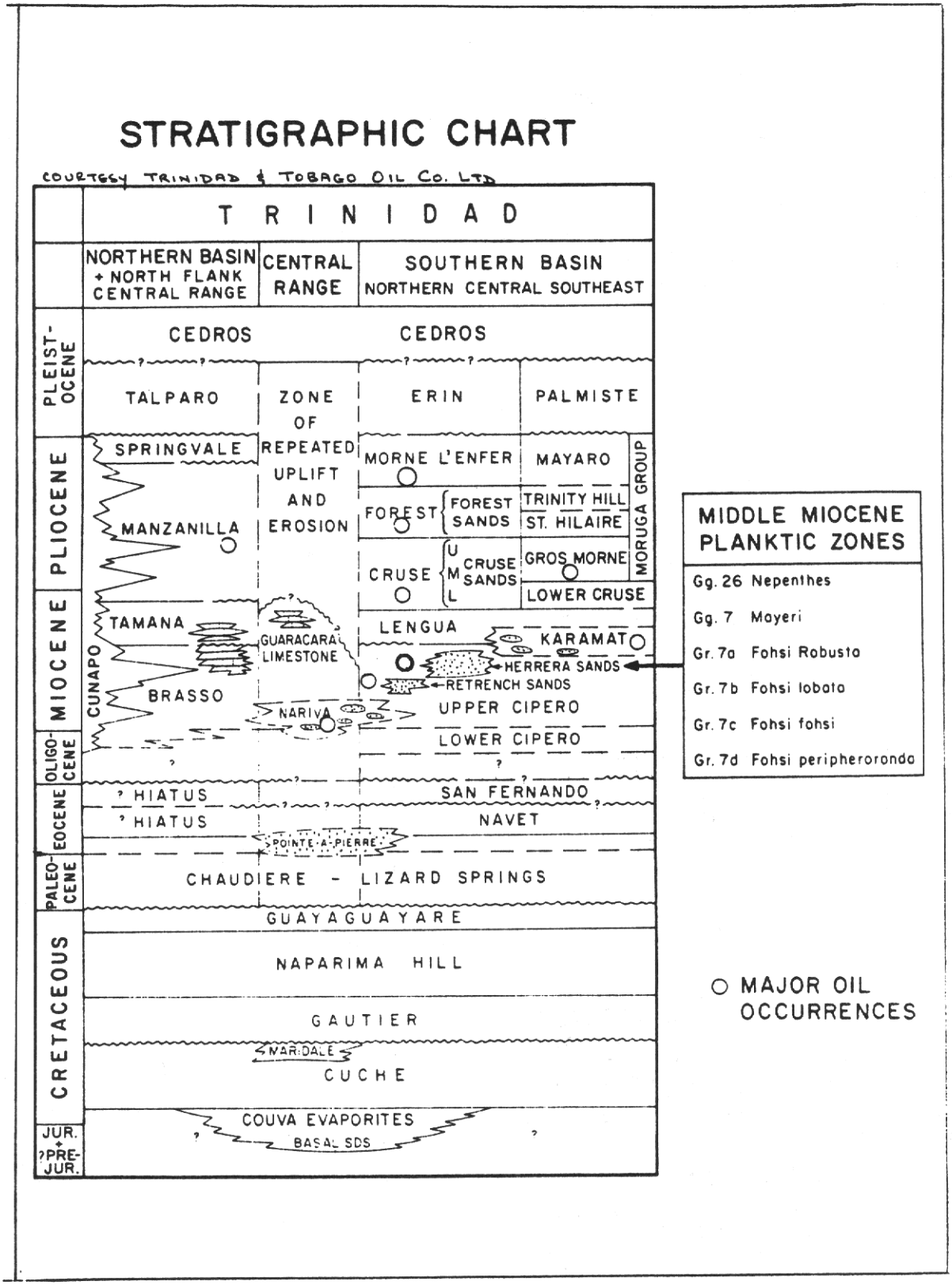

Fig. 6 Stratigraphic Chart of Trinidad. The Herrera sands are found within the Middle Miocene Upper Cipero formation.

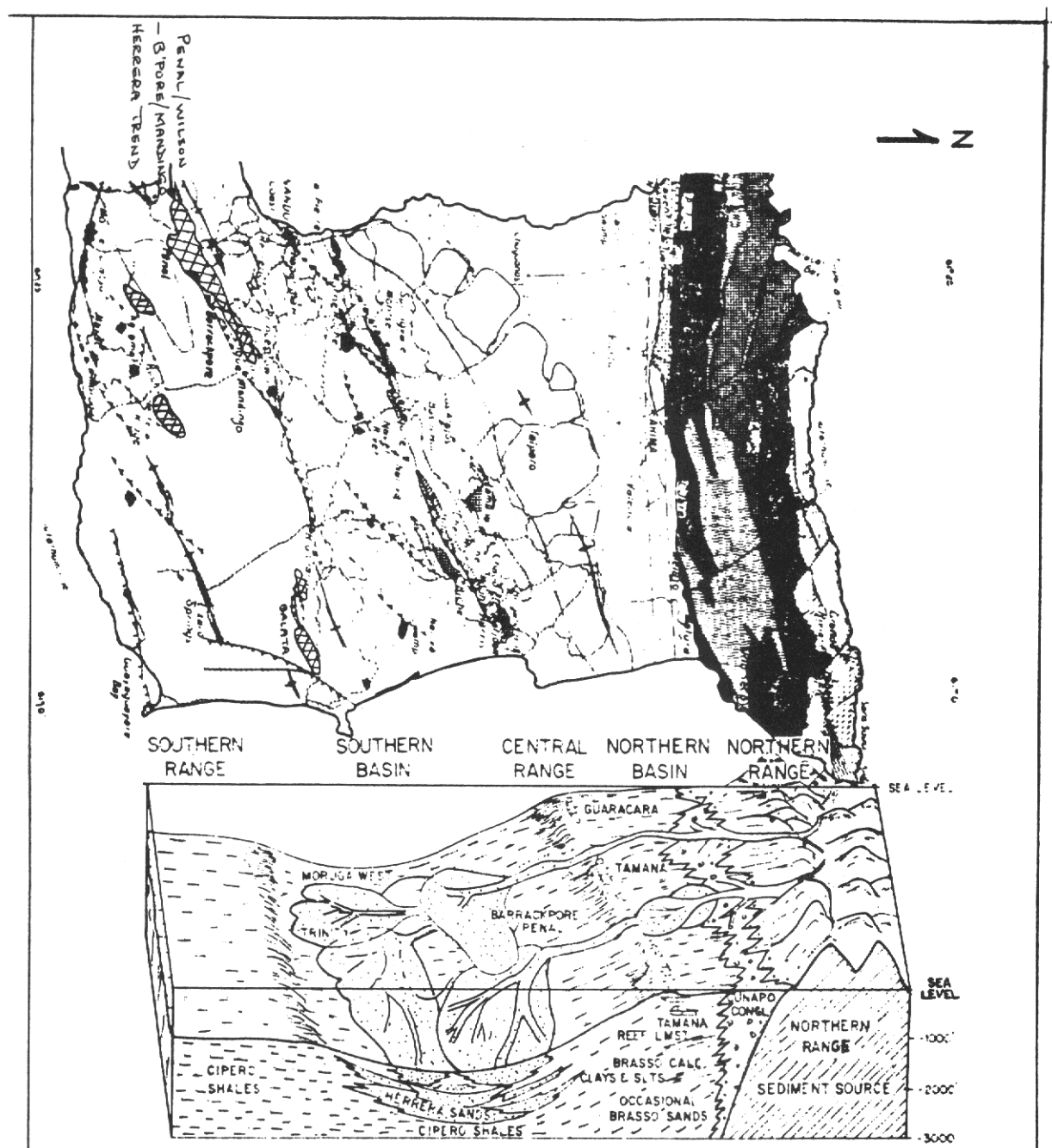

DEPOSITIONAL MODEL FOR HERRERA SANDSTONES DURING MIDDLE MIOCENE Gr 7c AGE

Fig. 7 Depositional Model for the Herrera sands during Middle Miocene Gr 7c age suggest a source from the north-west. Cherts were probably sourced from Cretaceous rocks reworked along the Central Range high.

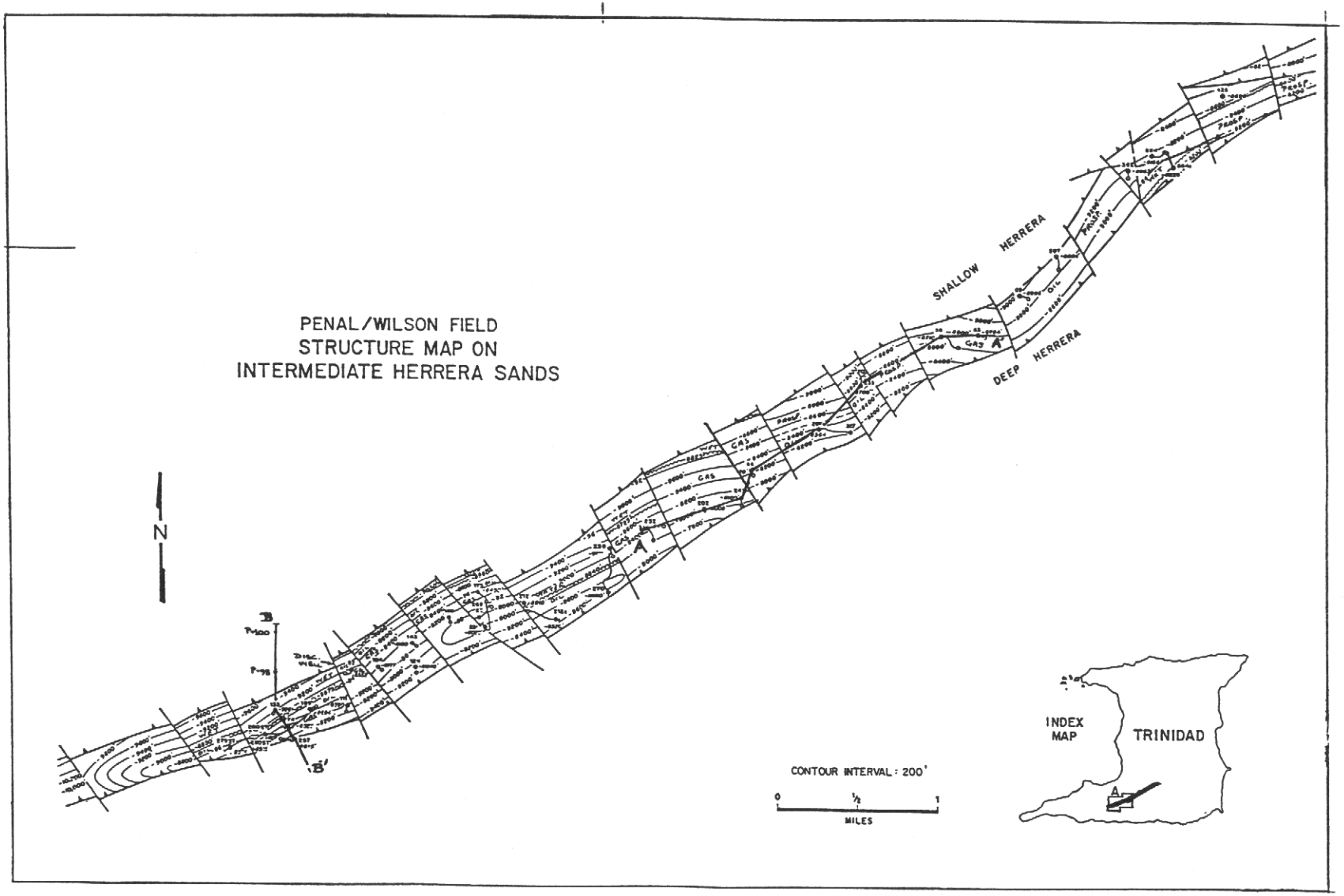

Fig. 8 Structure Map showing the Intermediate Herrera sands between the NE-SW trending thrust faults and NW-SE normal faults. Sands dip to the north-west and are overturned in the Penal area.

PENAL/WILSON FIELD

Structure

The Penal/Wilson field extends for approximately 7 miles over 1,260 acres in a north-east south-west direction (Fig. 8). In the south-west Penal area, the Intermediate Herrera sands have been inverted or overturned with dips ranging from 25° - 60° NW on the northern limb of a recumbent syncline, the axis of which lies within the deep or "underthrust" Herrera sands. The Intermediate Herrera sands are found between two major thrust faults which hade to the north-west and terminate against the Middle Miocene unconformity. In addition to these thrust faults which act as the northern and southern limits of the sands, there are many NW-SE trending normal faults which act as barriers to form separate hydrocarbon accumulations with different formation pressures and water levels (Figs. 9 and 10). The Wilson field is an extension of the Penal field to the north-east where the sands are not overturned but still dip to the north-west.

Stratigraphy

The Intermediate Herrera sands extend over the Penal/Wilson field varying from a massive sand section up to 600 feet thick to a thin sand 35 feet thick. Isopach mapping shows lobes of turbidite sands trending NE-SW and separated in places by areas of thin sand deposition (Fig. 11). Sand thicknesses have been reduced in some wells due to faulting out by the upper and lower thrust faults. Sand packages generally appear to be more continuous in an NE-SW direction (Fig. 12). Wherever the Intermediate Herrera sands are encountered in the same well with the "underthrust" deep Herrera sands, the latter are generally wet as they are in a structurally downdip position (Fig. 13).

Hydrocarbon Manifestations

The hydrocarbons produced from the Penal/Wilson field range from 20° - 30° API black oil to 45° - 56° API condensate, together with associated natural gas. Studies of gravities and gas/oil ratios by L.H. Bolt (1958)-Shell Oil Co., and R. Attai and A. Russell (1984)-Trinidad and Tobago Oil Co. Ltd., indicate a gas/oil contact at approximately 8,575 feet in several fault blocks but varying in the others. The lightest fluid (condensate) and highest gas/oil ratios were found as expected in wells drilled high on the structure. The oil water contact was found to vary from block to block.

Production Characteristics

In the Penal field, the up-dip wells were closed in for gas conservation and to maintain reservoir pressure until the wells completed in the black oil reservoir became high gas/oil ratio producers. The gas/condensate reservoirs were then in the early 1970's produced for gas supplies with a yield of up to 35 bbls. condensate per million cu. ft. of gas. An important characteristic of the field is that the black oil reservoirs in some of the fault blocks e.g. P-175, 189, 279 and 212x, appeared to be reacting to a partial water drive with a slow BHP decline, constant GOR's and increasing water cuts. However, structural mapping of the wells in different fault blocks with varying water levels does not support this theory. Six wells in the field have each produced approximately 1 MMB of condensate with gas production ranging from 8 BCF to 30 BCF per well. Major characteristics of the Penal/Wilson field are summarised in Table 1.

RESERVES

By December 31, 1988, the Penal/Wilson field had produced 14.8 mmbbls. of oil/condensate and 260 BCF of natural gas from the Intermediate Herrera sands in only twenty-six wells.

Together with proven unrecovered reserves of 124 mbbls. of oil and potential possible reserves of 4.4 MMbbls. oil, the total reserves of the Penal/Wilson field are estimated at approximately 19.3 MMbbls. of oil/condensate and 264.5 BCF of natural gas (Table II).

BARRACKPORE/MANDINGO FIELD

Structure

The Barrackpore/Mandingo field extends for 3.75 miles with over 500 acres of productive oil-bearing Intermediate Herrera sands. The sands dip 20° - 25° NNW on the northern flank of a structure formed by NW dipping thrust faults, three of which were mapped in the west and four in the east (Fig. 14). The sands are not overturned and are separated by splay thrust faults which terminate against the Middle Miocene unconformity and which separate the deep Heerera sands to the south-east and the shallow Herrera sands to the north-west (Fig. 15). The field has also been subdivided by several NW-SE trending normal faults which are generally downthrown to the south-west. Small oil accumulations have been found in sands below the thrust fault (Fig. 16).

Stratigraphy

The Intermediate Herrera sands are found throughout the Barrackpore/Mandingo field and vary in thickness from 100 feet to 600 feet between the thrust faults which form the northern and southern boundaries. The sands here are encased within the Cipero shales which in turn undelie the Karamat shales which are characteristic to this area. These karamat shales are well known for its difficult drilling conditions related to swelling shales due to water absorption. Isopach mapping indicates the sands are more continuous in a NE-SW direction supporting deposition in that direction (Figs. 17 and 18).

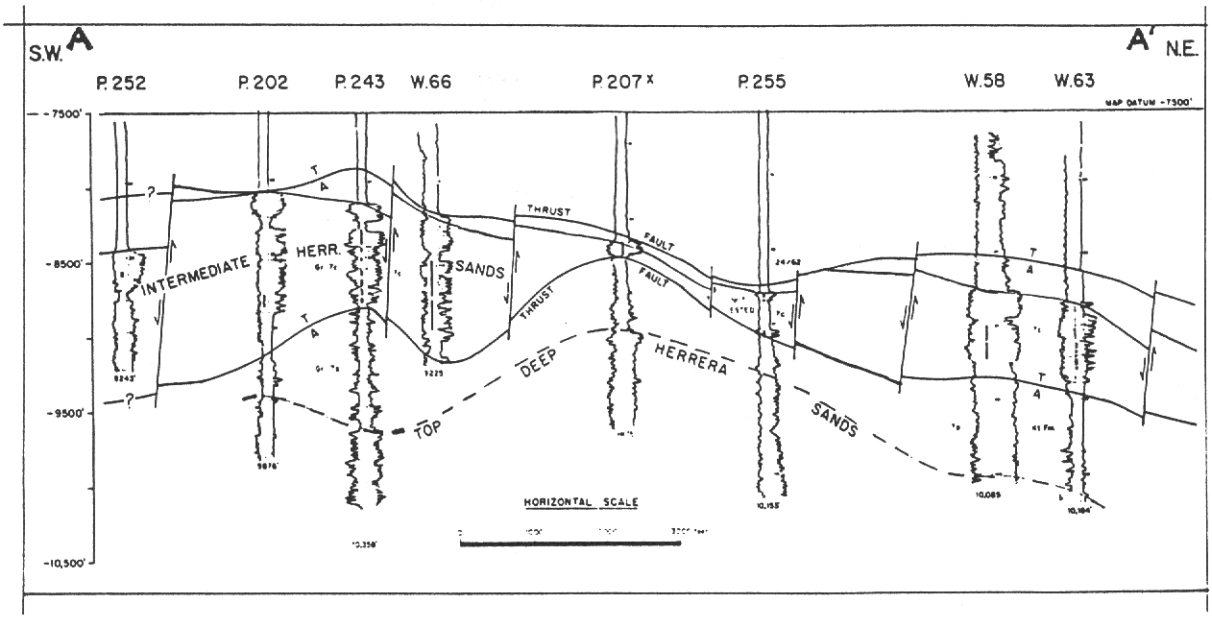

Fig. 9 Strike Section showing Upper and Lower thrust faults displaced by later normal faults.

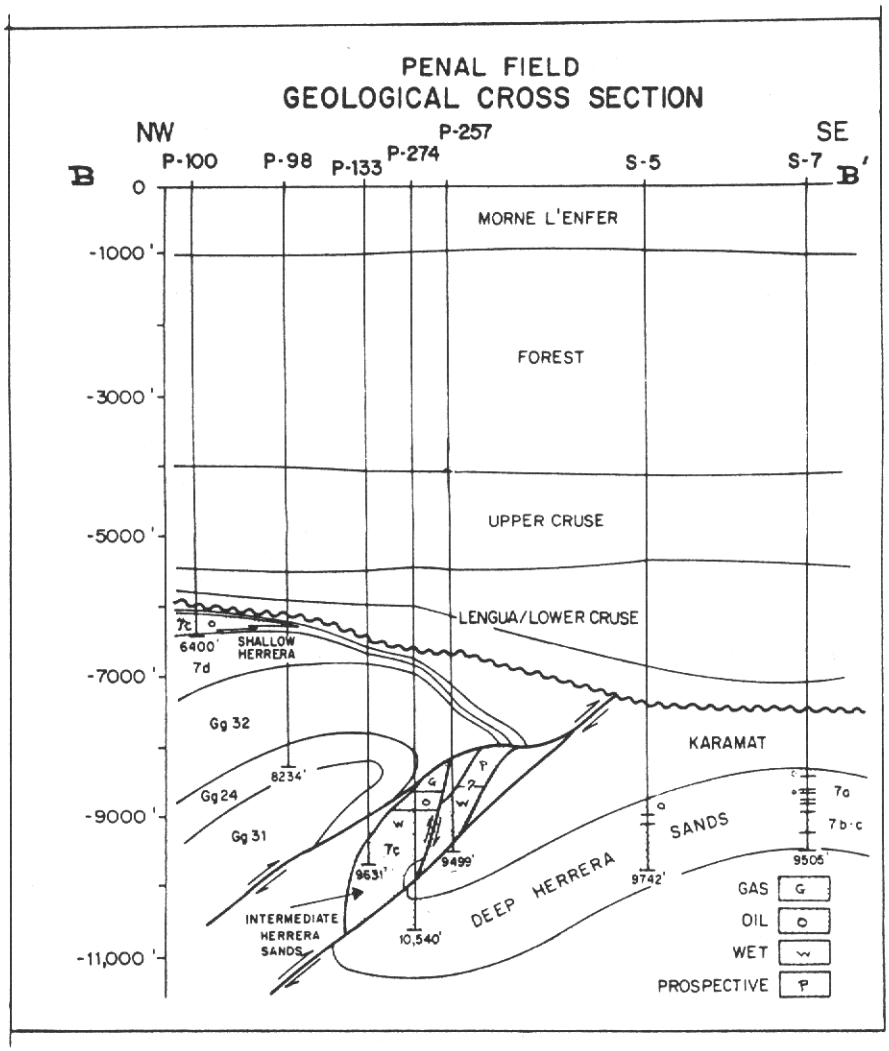

Fig. 10 Overturned Intermediate Herrera sands between two thrust faults in the Penal area.

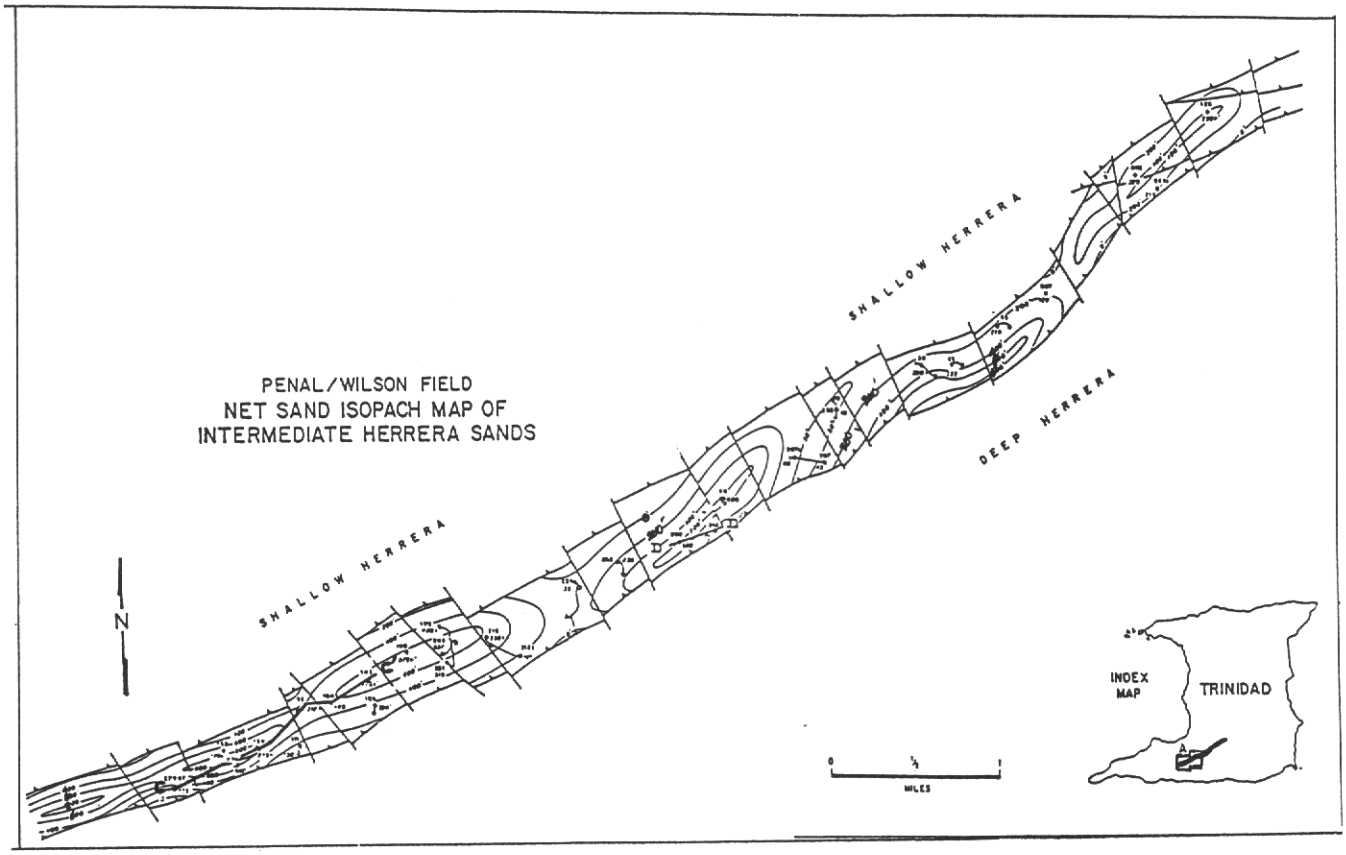

Fig. 11 Isopach Map showing NE-SW trending lobes of Herrera sand deposition.

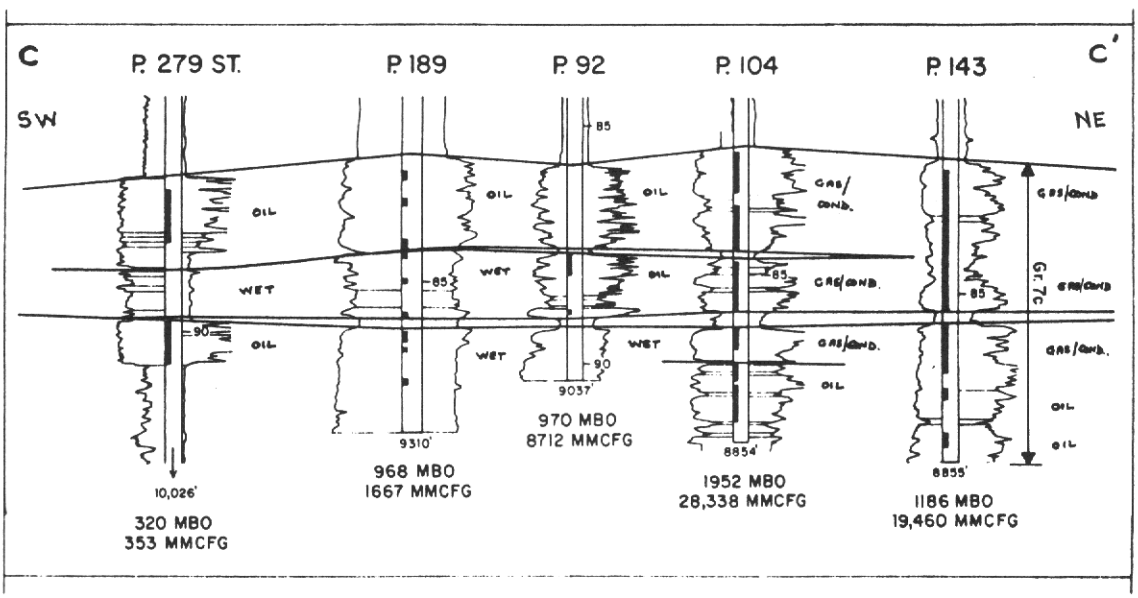

Fig. 12 Stratigraphic Section showing thick well developed oilbearing Intermediate Herrera sands.

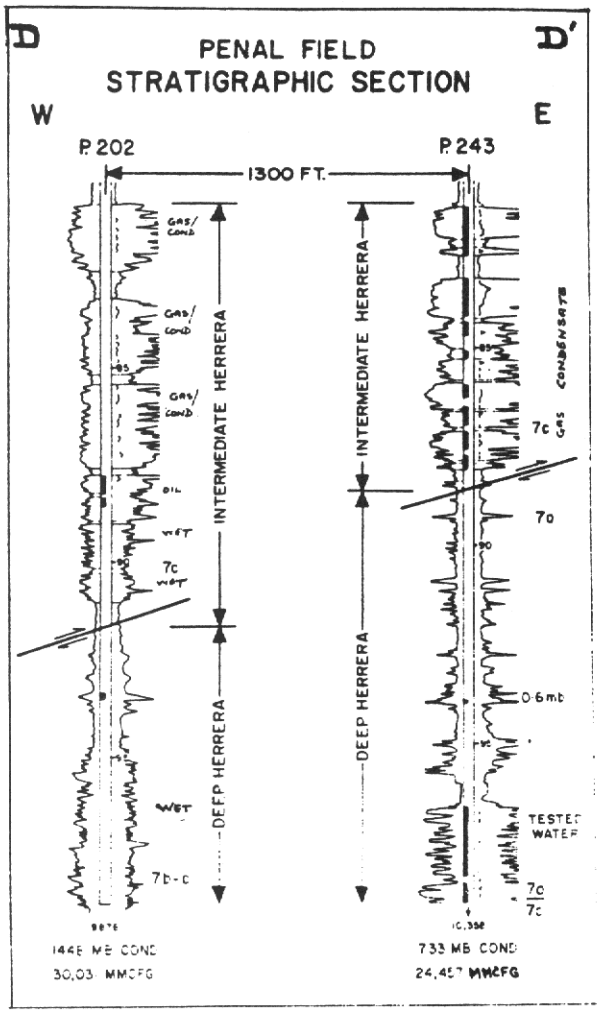

Fig. 13 The Intermediate Herrera sands thrust faulted above the "Deep" sands.

TABLE I
PENAL/WILSON FIELD

INTERMEDIATE HERRERA SAND FIELD & RESERVOIR CHARACTERISTICS

FIRST PRODUCED	1946
FIELD AREA	1260 ACRES
FIELD LENGTH	7 MILES
NO. OF PRODUCTIVE WELLS	26
AVG. DEPTH OF SANDS	8000'-10,500'
APPROX. WELL SPACING	1200 FEET
POROSITY	18-21%
PERMEABILITY	180MD
API GRAVITY (OIL)	20° - 30°
API GRAVITY (CONDENSATE)	45° - 56°
GAS OIL RATIO (GOR)	600-20,000
DRIVE MECHANISM	SOLUTION GAS
TRAPPING MECHANISM	FAULT/SHALE SEAL
AVG. NOS THICKNESS	200-600 FEET

TABLE II
PENAL/WILSON FIELD

INTERMEDIATE HERRERA SAND PRODUCTION AND RESERVES

CUM. PROD. OIL/COND.	14.8 MMB
CUM. PROD. GAS	260 BCF
DAILY PROD. OIL	240 BOPD
DAILY PROD. GAS	1 MMCF
PROVEN UNRECOVERED OIL RES.	124 MBO
PROVEN UNRECOVERED GAS RES.	124 MMCF
POTENTIAL OIL RES.	4.4 MMBO
POTENTIAL GAS RES.	4.4 BCF
PROSPECTIVE ACREAGE	170 ACRES

FIGURES AS OF DECEMBER, 1988

TABLE III
BARRACKPORE/MANDINGO FIELD

INTERMEDIATE HERRERA SAND FIELD & RESERVOIR CHARACTERISTICS

FIRST PRODUCED	1954
FIELD AREA	500 ACRES
FIELD LENGTH	3.75 MILES
NO. OF PRODUCTIVE WELLS	23
AVG. DEPTH OF SANDS	5000'-10,000'
APPROX. WELL SPACING	800 FEET
POROSITY	12-20%
PERMEABILITY	50-100 MD
API GRAVITY (OIL)	22° - 25°
API GRAVITY (CONDENSATE)	—
GAS OIL RATIO (GOR)	800-1000
DRIVE MECHANISM	SOLUTION GAS
TRAPPING MECHANISM	FAULT/SHALE SEAL
AVG NOS THICKNESS	100-300 FEET

TABLE IV
BARRACKPORE/MANDINGO FIELD

INTERMEDIATE HERRERA SAND PRODUCTION AND RESERVES

CUM. PROD. OIL/COND.	3.27 MMB
CUM. PROD. GAS	4.32 BCF
DAILY PROD. OIL	1440 BOPD
DAILY PROD. GAS	1.4 MMCF
PROVEN UNRECOVERED OIL RES.	4.3 MMB
PROVEN UNRECOVERED GAS RES.	4.3 BCF
POTENTIAL OIL RES.	10.4 MMB
POTENTIAL GAS RES.	10.4 BCF
PROSPECTIVE ACREAGE	660 ACRES

Hydrocarbon Manifestations

The hydrocarbons produced from the Barrackpore/Mandingo field are generally black oil of 22° - 25° API with some associated gas. Apart from one well, BP 372, which produced 50° API condensate and one well, BP 524, which was gas bearing, there is no evidence for any major gas-condensate/oil separation as is the case in the Penal field.

Geochemical work by K. Rodrigues (1988) indicates that the oil produced is from Upper Cretaceous Naparima Hill Argillite formation and is a parrafinic oil generated from mixed terrestrial and marine kerogens. A gas chromatogram of a typical Intermediate Herrera crude oil sample is shown in Fig. 19.

Production Characteristics

Most of the oil and gas produced from the Mandingo field has come from twenty wells drilled in the northern thrust fault segment. Some production has been obtained from three wells in the southern thrust fault segment where it seems that poor permeability related to proximity to the thrust fault is causing low productivity. The wells in the eastern part of the field are known to have high water cuts early in the production life, but yet continue to produce oil with cumulatives averaging over 200 Mbbls. per well. In the western part of the field, recently completed wells have little or no water production with cumulative oil production averaging 150 MB oil per well to date with estimated ultimate production of approximately 250 MB of oil per well. Production data indicate that the drive mechanism is solution gas drive. Major characteristics of the Barrackpore/Mandingo field are shown in the Table III.

Reserves

By December 31, 1988, the Barrackpore/Mandingo field had produced 3.32 MM bbls. of oil and 4.52 BCF of natural gas from the Intermediate Herrera sands in twenty-three active wells. Because many of the wells have only recently been drilled and completed, the proven unrecovered reserves are substantial and amount to 4.3 MMbbls. of oil. In addition, it is estimated that potential possible reserves of 10.4 MMbbls. of oil and 10.4 BCF of gas could be present over a minimum of 680 acres. Total reserves for the Barrackpore/Mandingo field are estimated at approximately 18 MMbbls. of oil and 19 BCF of natural gas (Table IV). However, mapping indicates that the Intermediate Herrera structure could extend further eastwards near to the Balata west field. This extension could add substantial amounts of potential oil and gas reserves which could be found in the Intermediate Herrera sands. Potential reserves to the west of the Barrackpore/Mandingo field are also quite substantial, some of which have already been converted to proven reserves by recent drilling since this paper was first written.

SUMMARY

The Middle Miocene age oilbearing Intermediate Herrera sands have been discovered in two fields joined together along a trend 17 miles long and approximately 2,000 feet wide. Discovery of these oilbearing sands was only made possible by drilling deeper in an area complicated at the end of Middle Miocene time by strong overfolding and major thrust faulting which separate the Herrera turbidite sands into three levels, namely the Shallow, Intermediate and Deep. Exploitation of the Intermediate Herrera sands started in 1946 and up to December 31, 1988, 18 MMbbls. of oil/condensate and 264 BCF of natural gas have been produced from the two fields. Ultimate production from this narrow thrust zone between two major faults is estimated at a minimum of 37.3 MMbbls. of oil/condensate and 283.5 BCF of natural gas. This field empahsises the need for drilling deeper in a thrust faulted zone as most of the production has been obtained from a zone which lies below shallower wet overthrust Herrera sands. Identification of and drilling for similar thrusted structure in Trinidad's southern basin may yet find substantial additional hydrocarbon in the prolific oil productive Herrera sands.

REFERENCES

1. Aquing F. 1984 - Evaluation of Intermediate Herrera sands, Penal field. Trinidad and Tobago Oil Co. Ltd., unpublished report.

2. Attai R. and Russell A. 1984 - Reservoir study of the Intermediate and Underthrust Herreras, Penal. Trinidad and Tobago Oil Co. Ltd., unpublished report.

3. Bitterli P. 1958 - Herrera subsurface structure of Penal field, Trinidad, BWI: Bull. Amer. Assoc. Petr. Geol., Vol. 42, No. 1, pp 145-148.

4. Bolt L.H. 1958 - A volumetric estimate of the present oil and gas reserves of Penal Intermediate and Underthrust Herrera sands. Shell Oil Co., unpublished report.

5. Hosein F. 1988 - Evaluation of the Intermediate Herrera sands (Phase I) in the Mandingo field, Victoria Block area. Trinidad and Tobago Oil Co. Ltd., unpublished report.

6. Hosein F. 1989 - Evaluation of the Intermediate Herrera sands (Phase II) in the Barrackpore/Wilson field. Trinidad and Tobago Oil Co. Ltd., unpublished report.

7. Hosein F. 1989 - Evaluation of the Intermediate Herrera sands (Phase III) in Penal field. Trinidad and Tobago Oil Co. Ltd., unpublished report.

8. Poole W.G. 1965 - Some sedimentary features of the Herrera sands of the Clark Road area, Barrackpore Oilfield, Trinidad, West Indies, Fourth Caribbean Geological Conference, pp 101-109.

9. Wildig A. 1973 - Review of oil and gas reserves as at 31-12-72. Shell Oil Co., unpublished report.

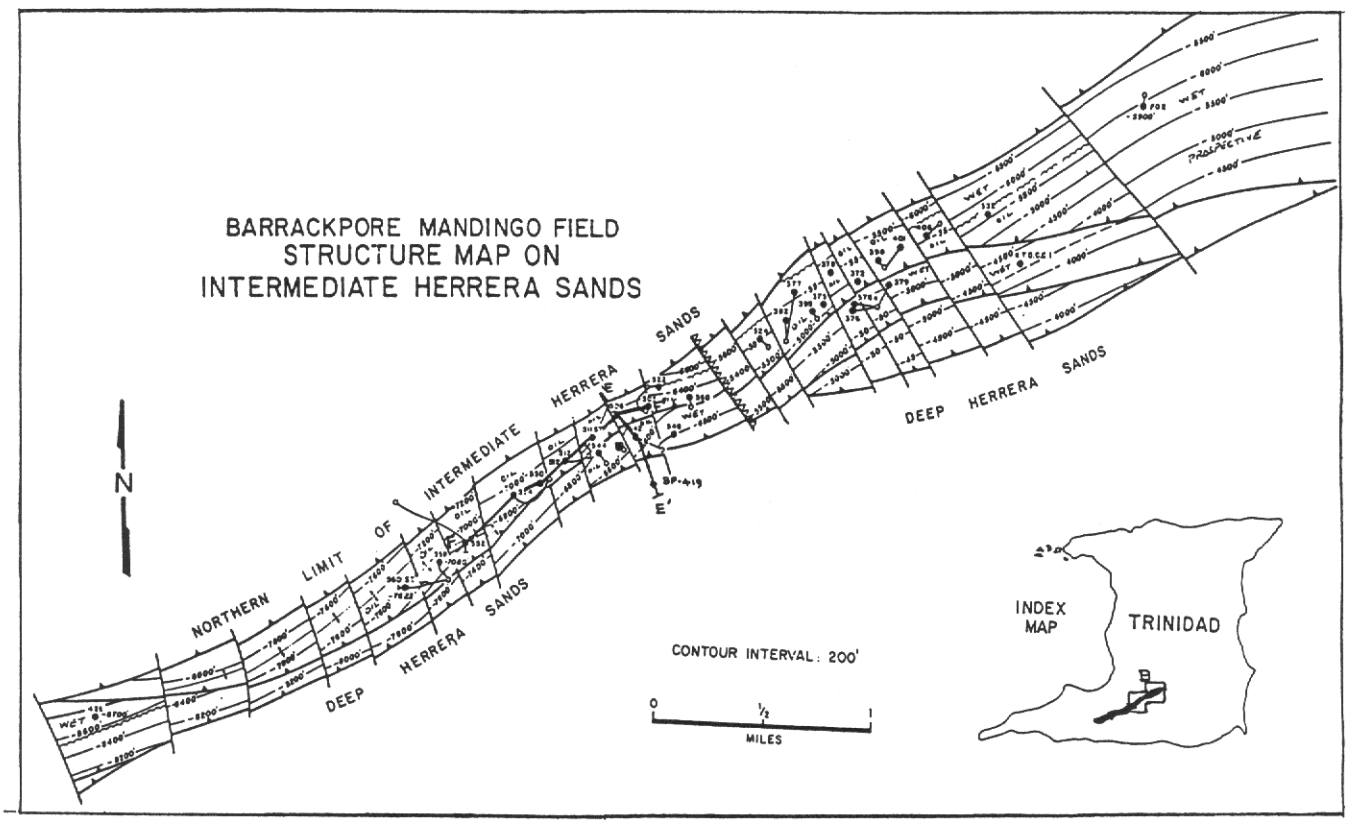

Fig. 14 Structure Map on Intermediate Herrera sands showing NE-SW trending thrust faults and NW-SE normal faults generally downthrown to the south-west. The sands dip to the north-west.

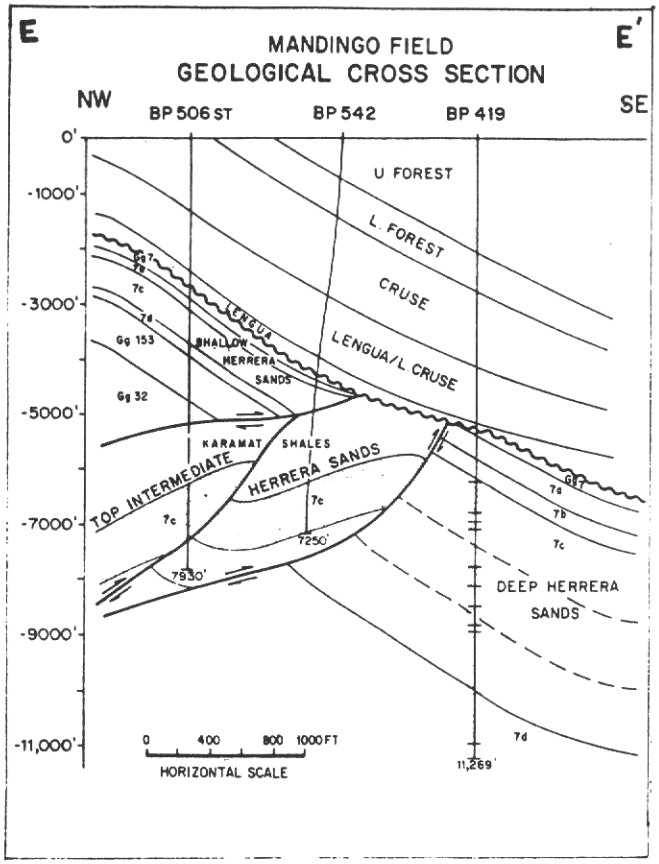

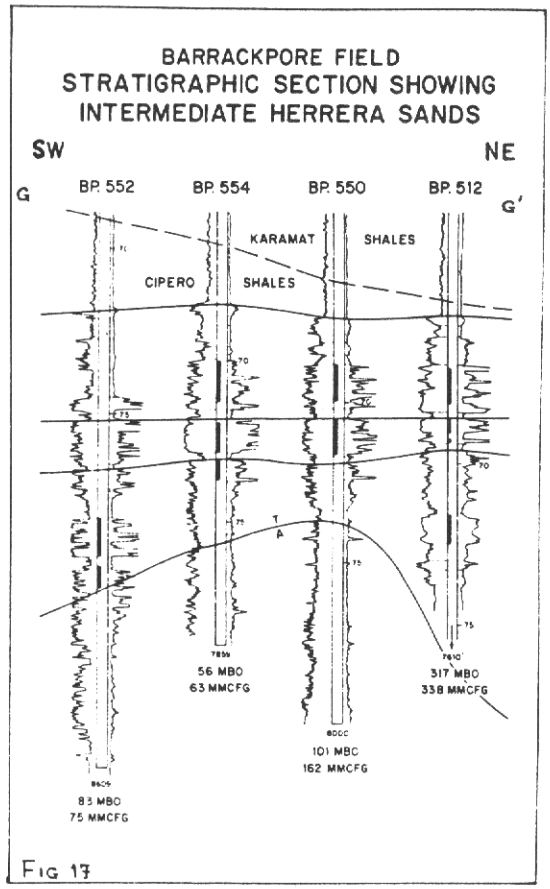

Fig. 15 Section E-E' showing Intermediate Herrera sands between the "shallow" and "Deep" Herrera sands.

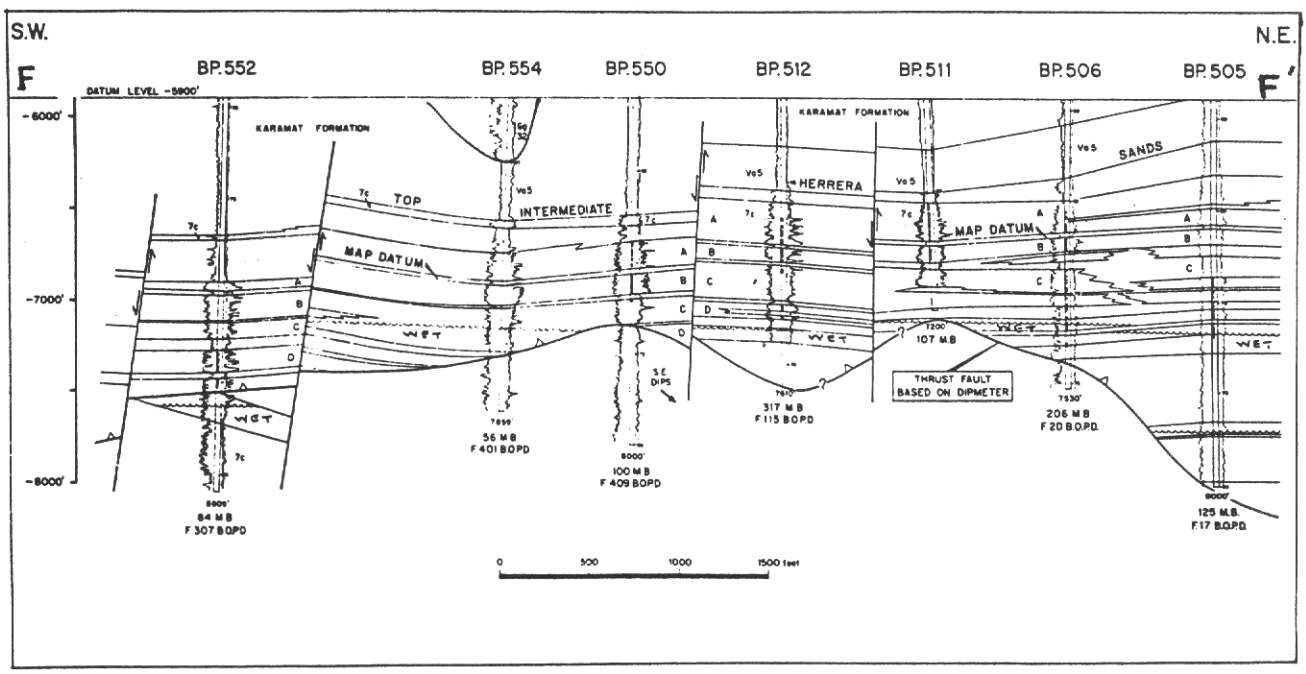

Fig. 16 Cross Section F-F' showing Intermediate Herrera sands cut by normal faults downthrown to the south-west in the Barrackpore-Mandingo field.

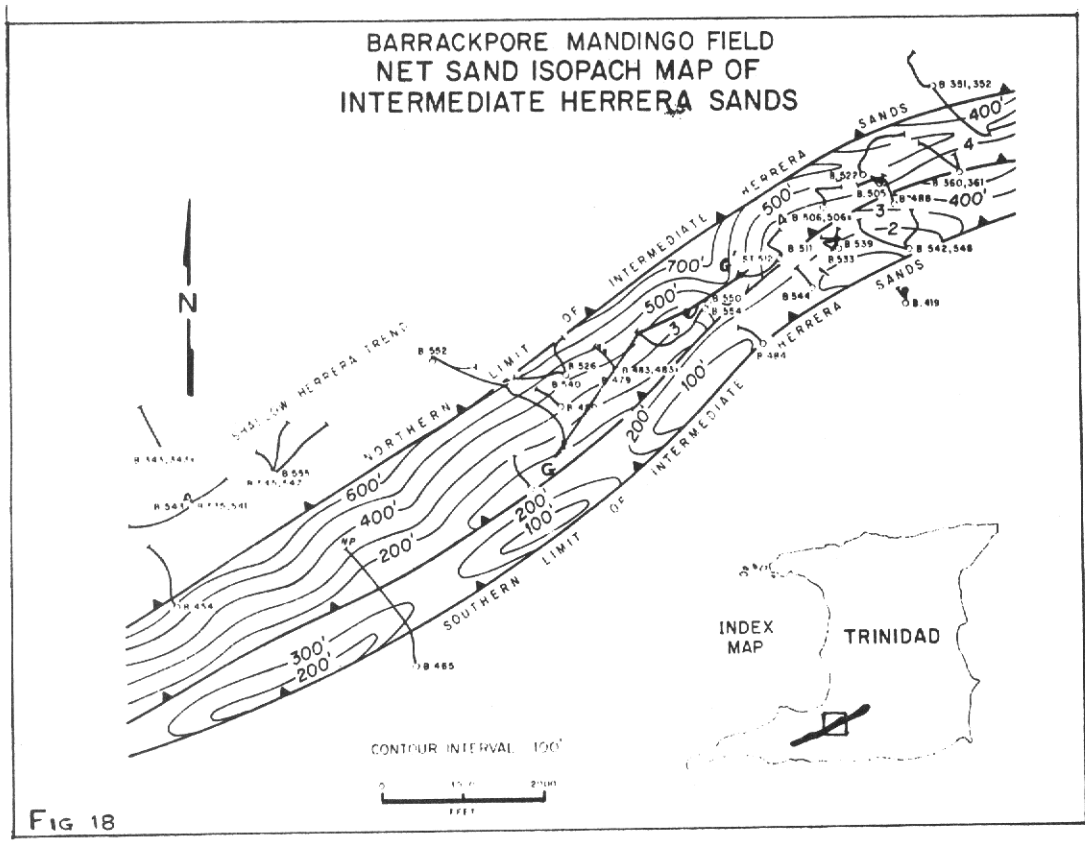
BARRACKPORE MANDINGO FIELD
NET SAND ISOPACH MAP OF
INTERMEDIATE HERRERA SANDS
N
SHALLOW HERRERA TREND
NORTHERN LIMIT OF INTERMEDIATE HERRERA SANDS
SOUTHERN LIMIT OF INTERMEDIATE HERRERA SANDS
600'
400'
200'
300'
700'
500'
100'
INDEX MAP
TRINIDAD
CONTOUR INTERVAL 100'
FEET

FIG 18

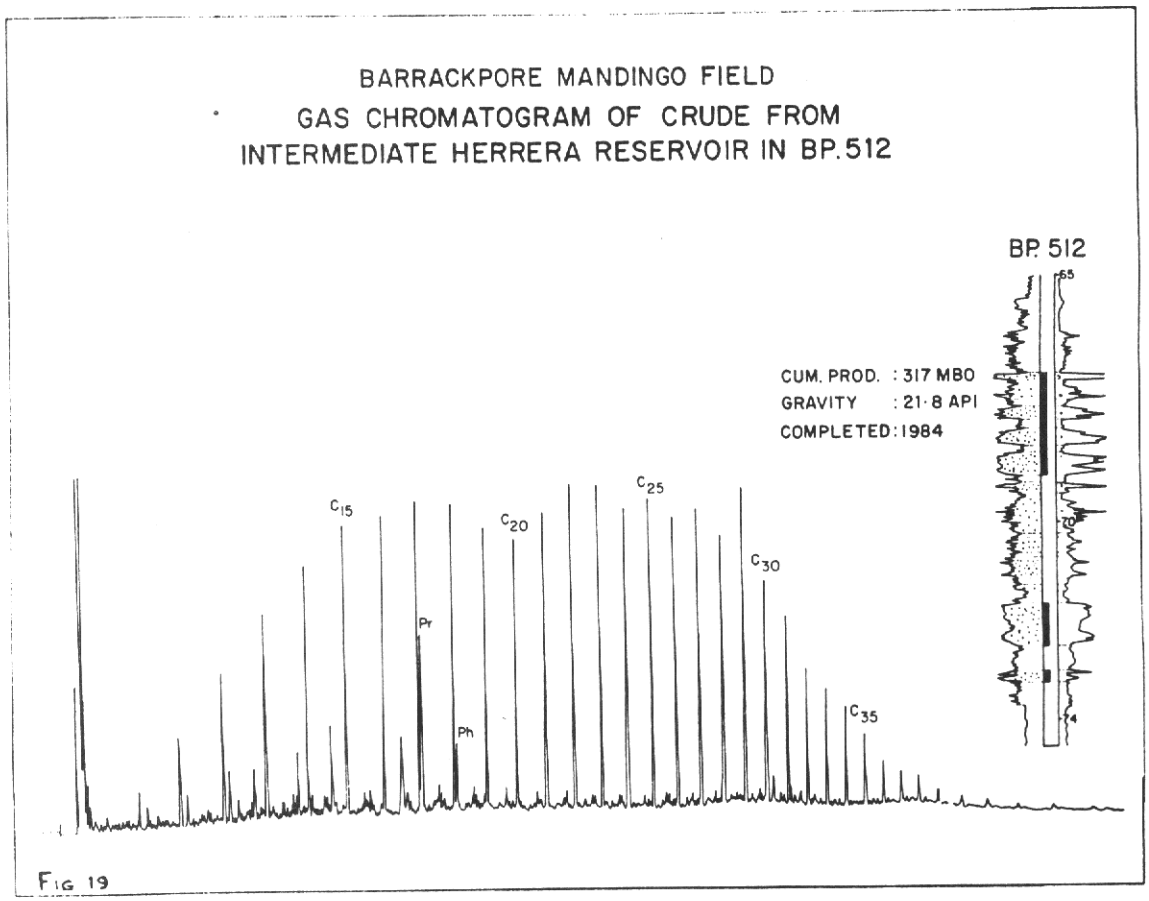
BARRACKPORE MANDINGO FIELD
GAS CHROMATOGRAM OF CRUDE FROM
INTERMEDIATE HERRERA RESERVOIR IN BP.512
BP. 512
CUM. PROD. : 317 MBO
GRAVITY : 21·8 API
COMPLETED: 1984
C15
Pr
C20
Ph
C25
C30
C35

FIG 19

SIGNIFICANCE OF GEOTHERMAL GRADIENTS IN PETROLEUM EXPLORATION IN TRINIDAD

Kirton Rodrigues
Geological Services Laboratory
Trinidad and Tobago Oil Company Ltd
Pointe-a-Pierre, Trinidad

ABSTRACT

The correlation between positive geothermal anomalies and the occurrence of hydrocarbons is based on the premise that water is the major agent of both hydrocarbon migration and heat transfer in sedimentary basins, and suggests a genetic link between geothermal gradients, hydrodynamics and hydrocarbon occurrences. This association has generated growing interest in geothermal studies in relation to the occurrence of petroleum deposits and the importance of the temperature history experienced by the source rock in the maturation process.

Geothermal gradients were derived from bottom hole temperatures recorded on electric logs from 300 exploratory and development wells drilled over Trinidad, including the Gulf of Paria and the North Coast and East Coast marine areas. A study was undertaken to determine the temperature regimes and an iso-geothermal gradient map of Trinidad, showing local and regional variations in heat flow, is presented.

Geothermal gradients over Trinidad vary between 0.8°F and 1.8°F per 100' (15°C and 32°C per km), rarely exceeding 1.5°F/100' (28°C/km), and are comparable to the world-wide average of 1.4°F/100' (25°C/km). These variations are related primarily to: (i) position of basement (heat source) with respect to overlying sediments and (ii) difference in vertical and lateral thermal conductivity of the rocks due to lithologic variation.

INTRODUCTION

For more than 50 years individual geologists (e.g. Van Orstrand, 1934) have observed an association between hydrocarbon occurrences and positive temperature anomalies or 'hot spots' as reflected in higher local geothermal gradients relative to the regional gradient. Geothermal anomalies have been mapped over oilfields in several basins of the world and reported by Ball (1981), Gatenby (1981), Handique and Bharali (1981), Meyer and Mc Gee (1985), Majorowicz et al. (1988), Mc Gee et al. (1989). Structurally as well as stratigraphically controlled fields, and both oil and gas accumulations, show positive geothermal anomalies at producing levels.

Roberts (1981) has reviewed much of the relevant literature and Klemme (1972) has presented evidence to show that high geothermal gradients in clastic rock sequences enhance the processes of oil and gas formation, migration and entrapment.

The correlation between positive geothermal anomalies and the occurrence of hydrocarbons is based on the premise that water is the major agent of both hydrocarbon migration and heat transfer in sedimentary basins, and suggests a genetic association between geothermal gradients, hydrodynamics and hydrocarbon occurrences. This association has generated growing interest in geothermal studies in relation to petroleum deposits. Indeed according to Ovnatanov and Tamrazyan (1970), "Although many methods are used to explore for petroleum, the geothermal method definitely deserves to take its rightful place among the standard exploration tools".

Previous work on geothermal gradients over Trinidad is limited to 2 geothermal gradient maps done by Dominion Oil in 1958 and Shell in 1966. Both these maps were compiled largely from onshore data and are compatible in the recognition of relative hot spots in the northern Gulf of Paria and Balata oilfield areas, although they differ somewhat in the actual magnitude of these anomalies.

Since the last map was compiled in 1966 the North Coast and East Coast Marine Areas have been opened up to exploration and much new temperature data have been generated. Also, more than 400 wells have since been drilled in Trinmar's Soldado area, in addition to other wells drilled onshore, particularly in the Southern Basin. The present study is aimed at updating the 2 earlier geothermal gradient maps using new temperature data available subsequent to 1966, as well as including data from wells which were not available to either Dominion Oil or Shell previously.

The major objectives of this study are as follows:

(1) To determine whether any positive geothermal anomalies or 'hot spots' identified correlate with the presence of oilfields as reported in the literature in other parts of the world.

Larue, D.K., and Draper, G. (eds.), ***Transactions of the 12th Caribbean Geological Conference, St. Croix, U.S.V.I.***, Miami Geological Society, P.O. Box 431552, South Miami, FL 33243, U.S.A.

(ii) To test the hypothesis that these 'hot spots' over oilfields originate in the upward and lateral movement of subsurface formation fluids, including oil, into traps bringing higher temperatures from depth.

(iii) To explain local and regional variations in the geothermal gradients over Trinidad in relation to lithological variations, basement configurations, structure and fluid dynamics.

METHODOLOGY

The temperature underground normally increases with depth below the surface, and the geothermal gradient is a measure of this rate of temperature increase with depth. The geothermal gradient is obtained by dividing the difference between the temperature of the formation and the mean annual surface temperature (ambient) by the depth of the formation, and is usually reported as °F/100' or °C/km.

Ambient temperatures for onshore and offshore wells have been considered uniform in this study and a value of 75°F (24°C) was used. This compares favourably with the 74°F (23°C) used by Talukdar et al. (1988) in Eastern Venezuela.

Most temperatures obtained from oil and gas wells are measured when the hole is under less than stable thermal conditions. Formation temperature is disturbed by the circulation of drilling fluid, which often results in the lower part of the hole being cooled and the upper part heated.

The primary sources of temperatures from wells are:

(i) Electrical logging runs.

(ii) Static bottom hole pressure (BHP) tests or temperature surveys.

(iii) Drill stem tests (DSTs).

Static BHPs and DSTs are the most reliable and provide the most accurate temperature data but are generally not available in large quantities locally. Although being the least reliable, due to the relatively brief time required to run logs, not allowing for subsurface temperatures to stabilize, maximum mud temperature readings recorded on the headings of electric well logs are the most abundant and are the only practical source of enough temperature data in Trinidad.

Due to the non-availability of such data as circulation time, time logger on bottom and time since cessation of circulation, and insufficient logging runs in most wells it was not possible to correct measured bottom hole temperatures (BHTs) for true formation temperature using the Horner technique of Fertl and Wichmann (1977). Since geothermal anomalies are what is being mapped in this study, and therefore the relative differences in geothermal gradients are more important than the absolute values, it is better to use uncorrected BHTs altogether (Handique and Bharali, 1981; Khan and Raza, 1986) rather than BHTs 'corrected' by applying some arbitrary correction factor (eg. 10-15%).

When temperatures were measured at different times the last value was chosen, and the data in each well were checked for consistency at different bottom hole depths (logging depths).

A disadvantage of using BHTs to determine geothermal gradients and temeprature anomalies is that some individual BHT data may be spurious due to careless measurements or recording mistakes. The effects of these are minimised by 'editing' the BHT data for obvious errors (e.g. low temperatures recorded after longer times since circulation stopped, sudden temperature reversals). Also, contouring techniques applied to map geothermal gradients produce a smoothing effect on the data, thus reducing the effects of individual unreasonable data.

Wells were selected on the basis of depth of penetration, both in terms of stratigraphy and footage, and location so as to provide adequate stratigraphic and geographic coverage. More than 1000 wells were examined in the first instance for reliability and consistency of temperature data, and eventually data from 300 wells were used to compile the geothermal gradient map (Figure 1).

Although every effort was made to select wells so as to provide a good geographic spread, this was not possible in some areas simply because of the absence of well data in undrilled areas. Thus only 8 wells are available in the North Coast Marine Area and data from only a few of the more than 200 wells drilled by Amoco off the east coast are accessible. The offshore Soldado area and the onshore Southern Basin, where several thousands of wells have been drilled, naturally have the greatest spread and concentration of data (Figure 1).

RESULTS AND DISCUSSION

The regional present day geothermal gradient map (Figure 1) shows that gradients over Trinidad vary from 0.8°F/100 (15°C/km) to 1.8°F/100 (32°C/km), and rarely exceed 1.5°F/100' (28°C/km). They are comparable to the worldwide average of 1.4°F/100' (25° C/km) and to the 1.3 - 1.4°F/100' reported by Talukdar et al. (1988) for the Maturin Subbasin of Eastern Venezuela.

The lowest gradients (08. - 1.0°F/100') are recorded in the Southeast Coast and North Coast Marine Areas, whereas everywhere onshore and in the Gulf of Paria gradients are >1.1°F/100'. The highest geothermal gradients (>1.5°F/100') are recorded as 10 anomalies or 'hot spots' and are listed as follows (Figure 1):

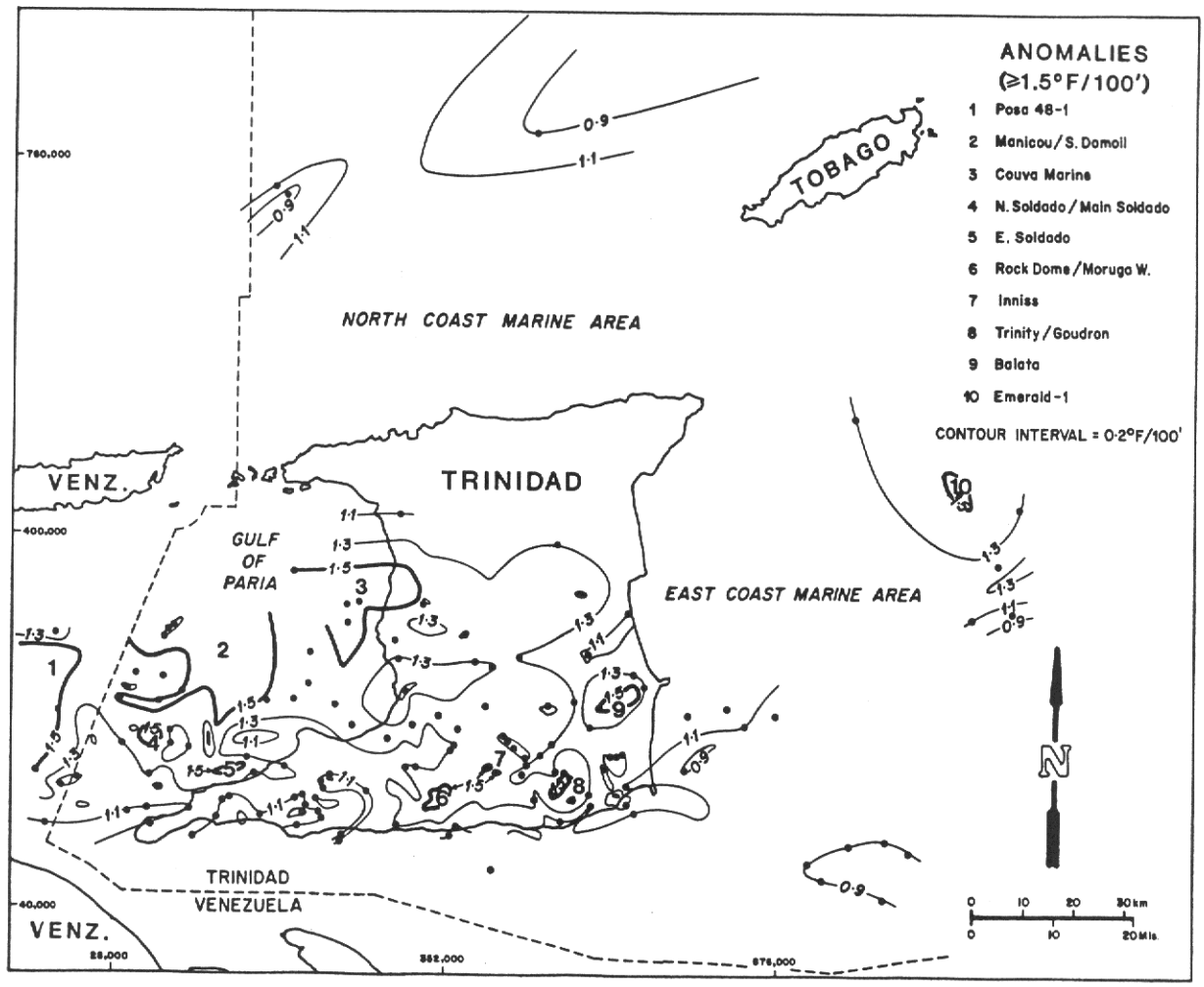

Figure 1. Geothermal gradient map of Trinidad, based on uncorrected bottom hole temperatures.

GULF OF PARIA - (1) Posa-48; (2) Manicou/South Domoil; (3) Couva Marine; (4) Main Soldado; (5) East Soldado;

SOUTHERN BASIN - (6) Rock Dome/Moruga West; (7) Inniss; (8) Trinity/ Goudron (9) Balata

EAST COAST MARINE AREA - (10) Emerald - 1

The principal sources of heat to the upper few miles of the earth's crust are in the outward flow of heat from the central core of the earth, in the presence of igneous magmas that are cooling, in the disintegration of radioactive elements and in the heat of subcrustal thermal convection currents (Levorsen, 1967).

Several factors produce lateral variations or anomalies in the earth's temperature field, resulting in regional variations in geothermal gradients in sedimentary basins. These are discussed by Hitchon (1984) and Meyer and Mc Gee (1985) and some of the more relevant factors are:

(i) Differences in heat flow rate from the source in the basement beneath the basin.

(ii) Lateral and vertical variations in thermal conductivity of the rocks due to a variety of causes (e.g. structural configuration, lithology (Figure 2), cementation, degree of compaction, permeability, fluid content).

(iii) Sources of heat within the rocks as a result of exothermic chemical reactions, mineralogical transformations and radioactive decay.

(iv) Recent intrusive or volcanic activity.

(v) Effects of moving water and other fluids (e.g. petroleum), including connate and meteoric water moving up and down through fractures

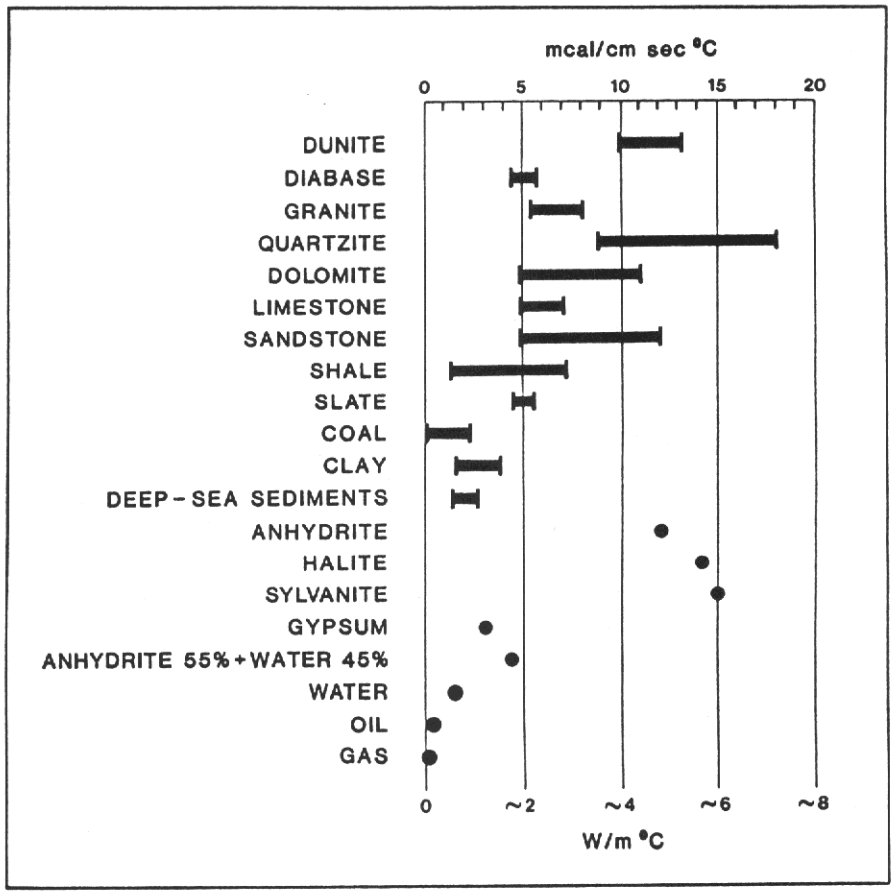

Figure 2. Thermal conductivity of various rocks and pore fluids under near surface conditions modified after Gretener (1981).

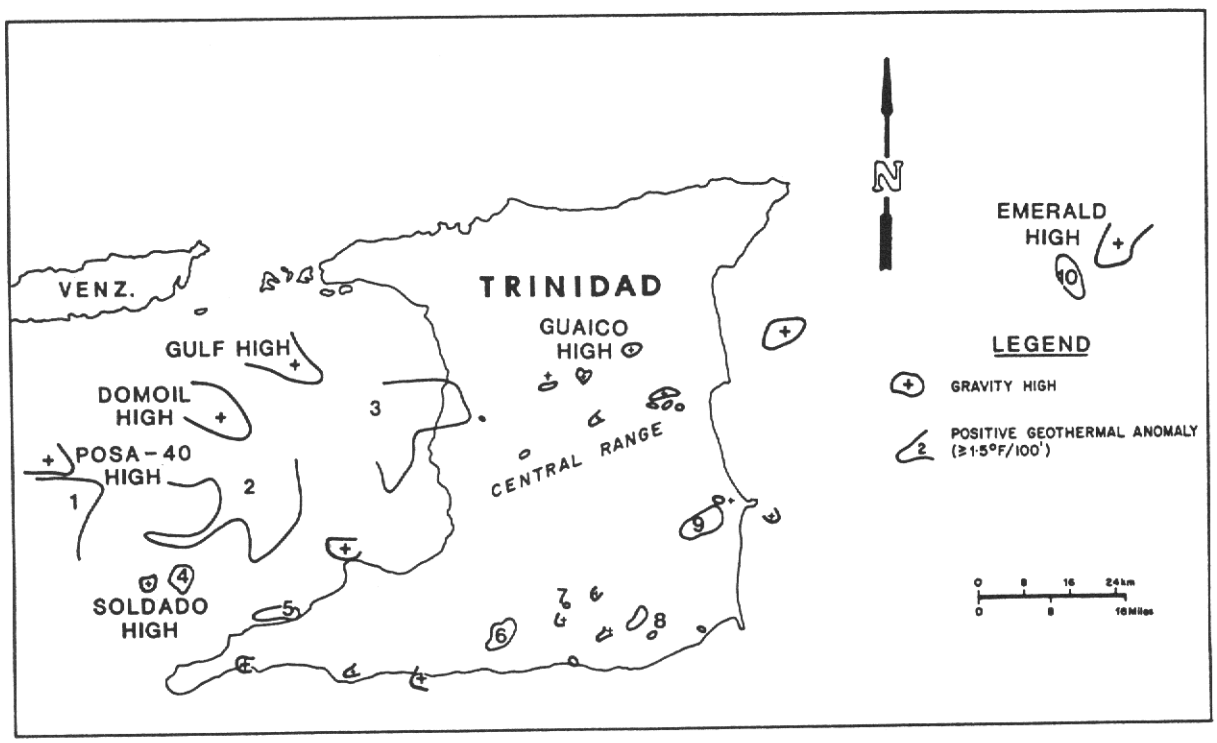

Figure 3. Principal gravity highs over Trinidad, from Bouguer anomaly gravity data. Anomalies numbered 1 to 10 are shown on Figure 1 and are discussed in the text

and pore spaces producing a warming and cooling effect respectively.

(vi) Tectonic friction causing heating.

Not all of these factors are equally important in any sedimentary basin and in some areas most of them can be dismissed as negligible or irrelevant. Factor (ii) is considered one of the primary causes of anomalous geotemperatures in most sedimentary basins. However, factor (v) has recently received considerable attention in the literature as a possible cause for positive geothermal anomalies recognised over oilfields (Meyer and Mc Gee, 1985; Zielinski et al., 1985; Mc Gee et al., 1989).

The geothermal gradient patterns mapped over Trinidad are now discussed in detail and possible explanations offered. The North Coast Marine Area (north of Trinidad and west of Tobago, Figure 1) displays low geothermal gradients ($\leqslant$1.2°F/100'). Basement in this area is mapped at approximately 10,000' and is similar in composition (low grade metamorphics) to what outcrops in the Northern Range to the south. Low heat flow in this area is confirmed by low vitrinite reflectance values (Ro$\leqslant$0.6% at 10,000'). In addition the gas discovered off the north coast is immature biogenic methane typical of low temperature diagenesis.

Basement drilled in the northern Gulf of Paria (Figure 1) is similar in composition and seismic character to that drilled in the northern North Coast Marine Area. The much higher geothermal gradients (1.2 - 1.8°F/100') recorded in the northern Gulf of Paria probably reflect different heat flow regimes related to the presence of at least 10 WNW-trending wrench faults north of the western extension of the Warm Springs Fault and parallel to the Los Bajos Fault, which are not present in the North Coast Marine Area. These faults would have acted as conduits for heat transfer from the heat source in the mantle to the sedimentary section of the earth's crust, possibly by thermal convection.

In the East Coast Marine Area south of Emerald - 1 (anomaly 10, Figure 1) data are limited since most of the wells have been drilled by Amoco. Available data indicate low geothermal gradients (generally $\leqslant$1.0°F/100') and are in very good agreement with the values of 0.85 - 1.15°F/100' reported by Leonard (1983) for the Columbus Basin. Very high sand/shale ratios have been recorded for the Pliocene/Pleistocene section in this area of the east coast, which formed the depocentre of the proto-Orinoco delta (Michelson, 1976). The low geothermal gradients are probably due to a combination of high thermal conductivity of the sand-rich section (Figure 2) and rapid sedimentation rate, not allowing sufficient time for thermal equilibrium to be attained. Indeed Leonard (1983) observed a close correlation between areas with the lowest geothermal gradients and areas with thicker sections of Pleistocene sediments.

Geothermal gradients over onshore Trinidad and the Gulf of Paria vary from 1.1°F/100' to 1.8°F/100' but are mostly $\leqslant$1.4°F/100'. Areas with geothermal gradients >1.5°F/100' are considered positive geothermal anomalies or hot spots and 9 such anomalies are mapped in the Gulf of Paria or onshore Trinidad, with a tenth in the northern East Coast Marine Area (Emerald - 1).

Anomaly 1 in the western Gulf of Paria is centred around Posa-48 (1.8°F/100'). This well encountered Lower Cretaceous limestones at 8800', overlain by Miocene/Pliocene clastics.

The Manicou/South Domoil geothermal anomaly 2 is located east of the Posa-48 anomaly and includes the small South Domoil oilfield (442,000 barrels) and the Manicou gas field. South Domoil - 5 drilled Lower Cretaceous at 7000' overlain by Pliocene/Pleistocene clastics.

Further east, anomaly 3 is centred around the Couva Marine wells (1.6 - 1.8°F/100') and is associated with a small oilfield (227,000 barrels). Miocene and younger shales, sandstones and conglomerates overlie Lower Cretaceous shales at 6500' and a 3000' - 7000' thick evaporite section at 9000' in Couva Marine - 2 and 8000' in Couva Offshore - 1. High heat flow in this area, as evidenced by higher than average geothermal gradients, is supported by high vitrinite reflectance values (Ro>2.0%) measured on Lower Cretaceous shales (Rodrigues, 1988).

As elsewhere (e.g. Shelton et al., 1974; Handique and Bharali, 1981) the geothermal patterns correlate with regional structural and gravity trends. High temperatures recorded as geothermal anomalies mapped in Posa-48, Manicou/South Domoil, Couva Marine and Emerald - 1 correspond to local structural highs which are the expression of basement highs associated with numerous deep-seated faults. Temperatures are highest on the crest of these local structures, decreasing toward the flanks. In addition to the known stratigraphy drilled in these wells, where Lower Cretaceous strata occur at depths of 6000' - 9000', Bouguer anomaly gravity data over Trinidad show gravity highs termed the Posa -40, Domoil, Gulf and Emerald Highs corresponding to anomalies 1,2, 3 and 10 respectively (Figure 3). Gravity highs are in many areas associated with anticlines or with horst blocks, both being structures which bring older denser rocks nearer the surface (Griffiths and King, 1974).

Eight of the 10 positive geothermal anomalies mapped are associated with oilfields (Figure 4): Manicou/South Domoil, Couva Marine, North and Main Soldado, East Soldado, Rock Dome/Moruga West, Inniss, Trinity/Goudron and Balata.

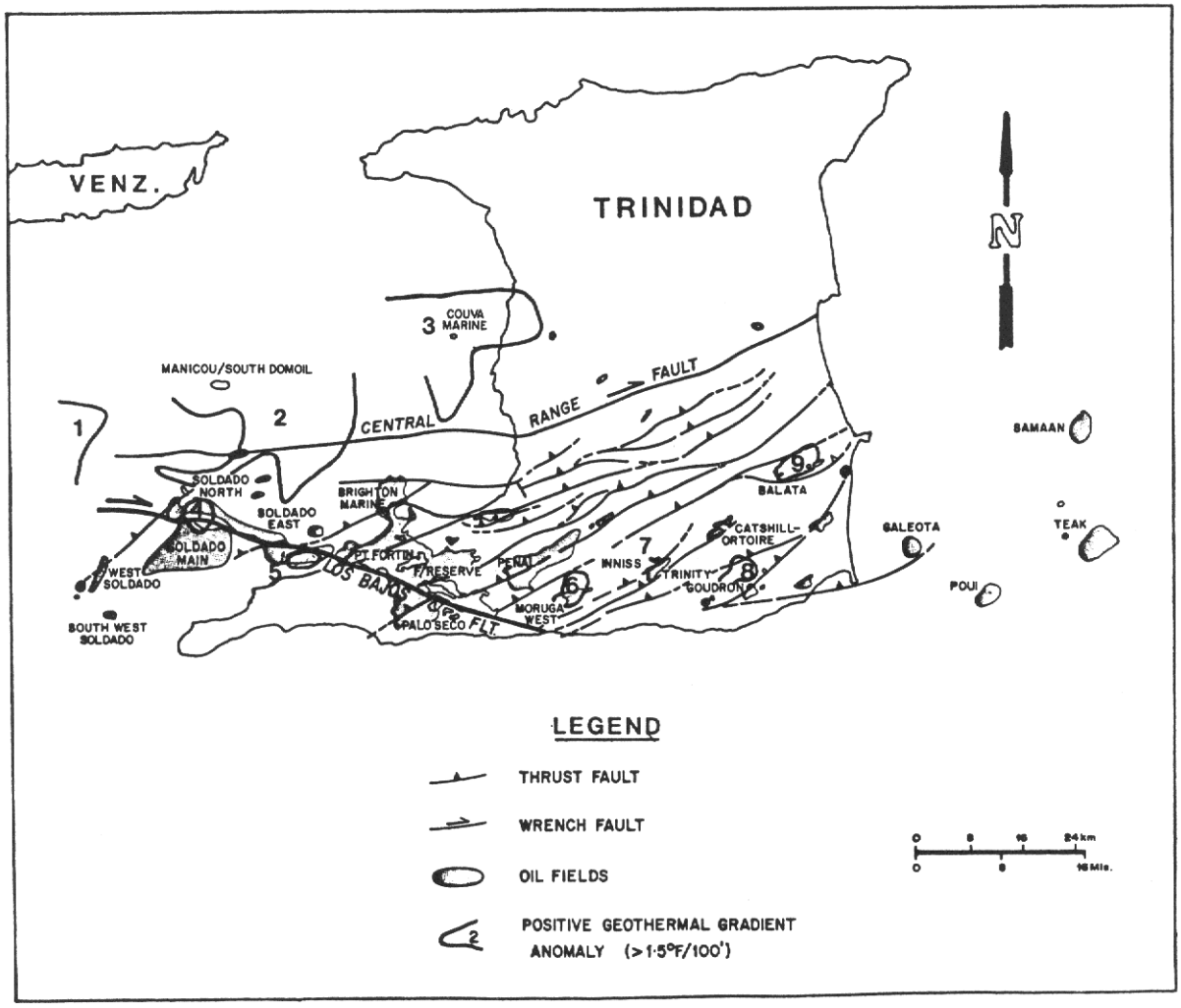

Figure 4. Major lineaments and distribution of producing oilfields, southern Trinidad.

The fact that positive anomalies were not recorded in many other oilfields (e.g. Forest Reserve, Palo Seco, Penal, Brighton Marine etc.) and that 2 positive anomalies (Posa - 48 and Emerald - 1) are not related geographically to producing fields suggest that the association between productive oilfields and positive geothermal anomalies may not be related simply to the presence of hydrocarbons, *per se*.

Gravity highs mapped from Bouguer anomaly gravity data show that 7 of the positive geothermal gradient anomalies are associated with gravity highs (Figure 1 and 3): Posa - 48 (1) Manicou/South Domoil (2), Couva Marine (3), North/Main Soldado (4), Inniss (7), Balata (9), and Emerald (10). On the other hand some gravity highs show no temperature anomalies (e.g. Brighton Marine and those aligned W-E along the Southern Range).

Anomalies 6 (Rock Dome/Moruga West) and 8 (Trinity/Goudron) show no correlation with gravity highs as mapped from Bouguer anomaly gravity data (Figure 3) and in both these areas original gravity data are rather sparse. However, wells drilled in these areas penetrated the Cretaceous at depths of 5000' - 12000' and the temperature anomalies recorded are probably related to the rise of basement configuration, resulting in higher temperatures on the crests of these local structures.

Anomaly 5 (East Soldado) which is also supported by the presence of overpressured shales, is more difficult to explain as this structure is not simple. Mc Dougall (1985) reported Pliocene/Pleistocene uplift along the south side of the Los Bajos fault and steep dips (40°) in the eastern portion of the field as due to mud tectonism producing an anticline or mud-cored uplift. The temperature anomaly may be related to heat influx associated with the upward intrusion of hot overpressured shales and accompanying water (mud tectonism) in the vicinity of the Los Bajos fault.

Both the gravity and oilfield distribu-

tion data (Figures 3 and 4) interpreted with respect to the occurrence of temperature anomalies (Figure 1) indicate that the observed temperature highs over some oilfields may reflect the complex relationship between:

(i) lower thermal conductivity of hydrocarbon bearing reservoir rocks, which result from hydrocarbons (lower thermal conductivity, Figure 2) replacing water in these rocks;

(ii) lateral variations in rock conductivity due to lateral changes in structure or lithology (Figure 2);

(iii) the heat carried along with upward and lateral fluid movement, which becomes trapped when the fluids are trapped.

This study does not support the contention that positive geothermal anomalies are uniquely associated with oil or gas accumulations and hence could be used as an exploration tool.

In the first place, temperatures used in compiling the geothermal gradient map (Fig.1) are not producing level temperatures taken from measurements made during drill stem testing but are bottom hole temperatures. Geothermal gradients computed by taking the difference between the measured temperature at a given depth and the surface temperature at the same location and reporting this difference with respect to the depth of the measurement point actually represent the weighted average gradient of the entire stratigraphic sequence above the recording point. Therefore the value of the geothermal gradient calculated from this method depends largely on the depth of the recording point and the thermal properties of the overlying lithologies. Temperature deviations from the geothermal gradient (i.e. warmer and colder than average areas) may reflect several stratigraphic and lithologic features or the inhomogeneity of the solid matrix and of the fluids that locally affect the heat transfer process, as discussed above.

Secondly, non-hydrocarbon bearing water strata could conceivably produce temperature anomalies by themselves as long as a trap is present.

APPLICATIONS

Accurate temperature measurements are vital to meaningful interpretations of subsurface geothermics. Heat transfer mechanisms affect diagenetic processes, petroleum maturation and migration and the evolution of both the sedimentary basin and its hydrogeologic system.

Geothermal gradient or isothermal surface maps, when constructed from suitable temperature data, offer good reliability and may have several relevant applications:

(1) The geothermal gradient map can be used to determine depths of the oil window over Trinidad, below which liquid hydrocarbons are unlikely to be found. A regional correlation of the depth of oil window (150-300°F) combined with the stratigraphy could be a useful exploration tool.

(2) Low geothermal gradients recorded over southern Trinidad have implications for the timing and duration of oil generation and migration. Low geothermal gradients would mean that Upper Cretaceous source rocks would have attained oil generating maturity only relatively recently (e.g. over the last 5-10 million years).

Similarly, expulsion and migration of petroleum from source rocks are recent phenomena in Trinidad. In the case of the East Coast Marine Area very thick Neogene sediments (possibly >25,000') would mean that Upper Cretaceous source rocks entered and exited the oil window over a very short period of time, because of very high temperatures due to great depths of burial. This time period may be considered almost instantaneous in a geologic sense and would place severe time constraints on source rock maturity and migration avenue and trap availability.

(3) Knowledge of present day temperatures is useful in the delineation of areas with altered oils, especially in Tertiary reservoirs not subject to significant variations in gradients in the past.

(4) Increasing temperatures affect diagenetic reactions in the reservoir, oil to gas cracking, oil and gas volumes, viscosity and fluid pressure.

(5) Since overpressured shales, being an insulator, are often associated with abnormally high temperature gradients (Ovnatanov and Tamrazyan, 1970; Lewis and Rose, 1970) it may be possible to predict the presence of a high pressure zone before drilling into it by observing sudden increases in temperature with depth.

(6) The temperature profile for a new well can be predicted from the geothermal gradient map.

The temperatures recorded and used in this study, even if they were corrected for true formation temperature, are unlikely to be maximum paleotemperatures for the onshore wells due to recent uplift and erosion (which may be as much as 4000' in some areas). Thus present day temperatures may be as much as 35-55°F lower than those attained in the past, and whatever depths are calculated for the oil window or occurrence of biodegraded oils etc. should be considered absolute maxima.

SUMMARY AND CONCLUSIONS

The major objectives of this study were to determine whether positive geothermal anomalies or hot spots identified over Trinidad correlate with the presence of oilfields and can be used as an exploration tool and to explain local and regional variations in heat flow.

In the absence of more reliable temperature data geothermal gradients were calculated for more than 300 wells over Trinidad based on uncorrected bottom hole temperatures and an isogeothermal gradient map compiled.

The map represents the geothermal regime which reflects the summation of a number of geological/geophysical parameters expressed as thermal conductivity, thermal convection and hydrodynamics. Geothermal trends correlate with regional structural and gravity trends and stratigraphic features such as gross lithofacies.

Present day geothermal gradients over Trinidad vary from 0.8°F/100' to 1.8°F/100' but are mostly <1.5°F/100'. Lowest gradients are recorded in the North Coast and East Coast Marine Areas whereas highest gradients (>1.5°F/100') are mapped as 10 hot spots, viz. Posa-48, Manicou/South Domoil, Couva Marine, Main Soldado/North Soldado, East Soldado, Rock Dome/Moruga West, Inniss, Trinity/Goudron, Balata and Emerald - 1.

Some temperature highs are associated geographically with oilfields but this is not an unique association. The positive anomalies correspond to local structural highs which are the expression of basement highs. Lateral and vertical variations in thermal conductivity of the rocks due to a variety of causes (e.g. structural configuration, lithology) seem to be the main factor in producing thermal anomalies over Trinidad.

The geothermal gradient map has several relevant applications, e.g. in defining the depths of the oil window over Trinidad, in delineating areas with bacterially altered oils, in predicting the presence of overpressured shales and the temperature profile of a new well.

Greater effort should be made to ensure that accurate temperatures are measured and recorded at the well site during the drilling, logging and testing of wells.

REFERENCES

Ball, S.M., 1981, Exploration applications of temperatures recorded on log headings: theory, data analysis and examples: AAPG Bull., v.65, p. 1359 (Abs).

Fertl, W.H., and P.A. Wichmann, 1979, How to determine static BHT from well log data: World Oil, Jan. 1977, p. 105-106.

Gatenby, G.M., 1981, Temperature anomalies and Gulf Coast structures: AAPG Bull., v.65 p.1360 (Abs).

Gretener, P.E., 1981, Geothermics: Using temperature in hydrocarbon exploration: AAPG Education Course Note Series#17, 156 pp.

Griffiths, D.H. and R.F. King, 1974, Applied Geophysics for Engineers and Geologists. Pergamon Press, Oxford, 223 pp.

Handique, G.K. and B. Bharali, 1981, Temperature distribution and its relation to hydrocarbon accumulation in Upper Assam Valley, India: APPG Bull., v.65, p.1633 -1641.

Hitchon, B., 1984, Geothermal gradients, hydrodynamics and hydrocarbon occurrences, Alberta, Canada: AAPG Bull., v.68, p.713-743.

Khan, M.A. and H.A. Raza, 1986, The role of geothermal gradients in hydrocarbon exploration in Pakistan: Jour. Petroleum Geology, v.9, p.245-258.

Klemme, H.D., 1972, Heat influences size of oil giants: Oil and Gas Jour., July 17, p.136-144; July 24, p.76-78.

Leonard, R., 1983, Geology and hydrocarbon accumulations, Columbus Basin, offshore Trinidad: APPG Bull., v.67, p.1081-1093.

Levorsen, A.I., 1967, Geology of Petroleum. W.H. Freeman and Company, San Francisco, 724 pp.

Lewis, C.R. and S.C. Rose, 1990, A theory relating high temperatures and overpressures: Jour. Petroleum Technology, Jan. 1970, p.11-16.

Majorowicz, J.A., Jones and K.G. Osadetz, 1988, Heat flow environment of the electrical conductivity anomalies in the Williston Basin, and occurrence of hydrocarbons: Bull. Canadian Petroleum Geology, v.36, p.86-90.

Mc Dougall, A.W., 1985, Geology of the East Soldado Field: 4th Latin American Geological Conference, Transactions, Trinidad. 1979, v.II, p.720-725.

Mc Gee, H.W., H.J. Meyer and T.R. Pringle, 1989, Shallow geothermal anomalies overlying deeper oil and gas deposits in Rocky Mountain region: AAPG Bull., v.73, p.576-597.

Meyer, H.J. and H.W. Mc Gee, 1985, Oil and gas fields accompanied by geothermal anomalies in Rocky Mountain region: AAPG Bull., v.69, p.933-945.

Michelson, J.E., 1976, Miocene deltaic oil habitat, Trinidad: AAPG Bull., v.60, p.1502-1519.

Ovnatanov, S.T. and G.P. Tamrazyan, 1970, Thermal studies in subsurface structural investigations, Apsheron Peninsula, Azerbaijan, USSR: APPG Bull., v.54, p.1677-1685.

Roberts, W.H., 1981, Some uses of temperature data in petroleum exploration, Unconventional Methods in Exploration for Petroleum and Natural Gas II (B.M. Gottlieb, ed.) p.8-49.

Rodrigues, K., 1988, Oil source bed recognition and crude oil correlation Trinidad West Indies: Org. Geochem., v.13 p.365-371.

Shelton, J.W., M.K. Horn and R.H. Lassley, 1974, U.S. geothermal, geologic patterns compared: Oil and Gas Jour., Nov.25, p.173-174.

Talukdar, S., O. Gallango and A. Ruggiero, 1988, Generation and migration of oil in the Maturin Subbasin, Eastern Venezuelan Basin: Org. Geochem., v.13 p.537-547.

Van Orstrand, C.E, 1934, Some possible applications of geothermics to geology: AAPG Bull., v.18, p.13-38.

Zielinski, G.W, J.A. Drahovzal, G.M. De Coursey and J.R. Ruperto, 1985, Hydrothermics in the Wyoming Overthrust Belt: AAPG Bull., v.69, p.699-709.

CONTRIBUTION OF PALEOMAGNETISM IN THE RELATIONS BETWEEN THE PIEMONTIN AND INTERNAL NAPPES OF THE VENEZUELAN CARIBBEAN CHAIN : SYNTHESIS AND NEW DATA.

B. Blin
GDR "Genèse et Evolution des Domaines Océaniques"
6, avenue Le Gorgeu
29287 Brest Cédex (France)

B. Sichler
IFREMER/Centre de Brest
B.P. 70, 29280 Plouzané
(France)

J.F. Stéphan
GDR "Genèse et Evolution des Domaines Océaniques"
6, avenue Le Gorgeu
29287 Brest Cédex (France)

ABSTRACT

The eastward displacement of the Caribbean plate between the two Americas occurs along large transcurrent zones, dextral and sinistral respectively to its south and north boundaries. This particular setting explains the 90° of clockwise rotations shown by the paleomagnetic vectors of the Venezuelan Caribbean mountain chain. In order to define the relations between the Piemontin and internal nappes of the Caribbean chain, a study was undertaken 100 km to the south of Caracas in the Guárico and Cojedes States in 1988. Among the twenty-one drilled sites, two of them are located in the internal nappe of Villa de Cura (in the north), ten in the Piemontin nappe and nine in the autochthonous foreland (in the south).

- In agreement with other paleomagnetic studies, the Villa de Cura nappe shows evidence for a 90° clockwise rotation.
- The Piemontin nappe does not show an overall rotation.
- The results about the foreland indicate a north-south orientation of the paleomagnetic vectors. They are in agreement with the paleomagnetic declinations of the south-american craton and suggest an autochthonous character of the foreland.
- The general north-south orientation of the paleomagnetic vectors deviate near the Guárico and Guaitoco faults (dextral faults).

These results confirm that the Villa de Cura nappe was a north-south oriented island arc, in agreement with the models of Caribbean geodynamic evolution proposed by various authors (Pindell and Dewey, 1982 ; Stephan, 1982 ; Beck, 1986). In contrast, the Piemontin nappe did not rotate and has moved with an orientation similar to its original position. Finally, the autochthonous Oligo-Miocene sandstones, to the south of the Piemontin nappe, show only local rotations near the Guárico and Guaitoco dextral faults.

INTRODUCTION

The Caribbean region is a small lithospheric plate that is moving eastward with respect to the two Americas (Fig. 1). According to Stephan (1982, 1985), Stephan and al. (1985), Beck (1986), its boundaries are formed by :
- in the east, subduction of the Atlantic Plate under the lesser Antilles arc;
- in the west, subduction of the Pacific Plate under Central America;
- in the north, sinistral oblique subduction along the Puorto-Rico trench, with in continuation, the Caiman spreading center in the west. A transform fault zone (Swan, Barlett and Polochic-Motagua) joins the Central America trench to the Tehvantepec Isthmus;
- in the south, a dextral transcurrent zone : the Oca-El Pilar fault system.

Figure 1 shows a summary of the paleomagnetic data of the Caribbean region (Watkins and Cambray, 1971 ; Steinhauser and Vincenz, 1973 ; Vincenz and al., 1973 ; Dasgupta and Vincenz, 1975 ; Mc Donald and Van Horn, 1977 ; Gose and Swartz, 1977 ; Guja and Vincenz, 1978 ; Dasgupta, 1978 ; Hargraves and Skerlec, 1980 ; Skerlec and Hargraves, 1980 ; Stearn and al. 1982 ; Donald and Krushensky, 1983 ; Kerdraon, 1984 and Gose, 1985).

It can be clearly seen that :
- the northern Caribbean boundary exposes paleomagnetic vectors which imply a 80° counterclockwise rotation between the upper Cretaceous and the Miocene;
- the southern boundary of the Caribbean Plate is characterized by paleomagnetic vectors which indicate 90° of clockwise rotation since the upper Cretaceous.

In the Honduras, Gose and Swartz (1977), Gose (1985) suggest a polyphasic rotation, clockwise during the lower Cretaceous and counterclockwise between the upper Cretaceous and the Present.

The available data are in agreement with the kinematic model of the Caribbean Plate. This plate moves to the East and pushes to its boundaries the blocks (islands) which are to its front (Stephan, 1982). The curvature of the actual Lesser Antilles arc expresses perfectly this phenomenon and explains the observed clockwise rotations (in the South) and counterclockwise rotations (in the North).

Larue, D.K., and Draper, G. (eds.),
Transactions of the 12th Caribbean Geological Conference, St. Croix, U.S.V.I., Miami Geological Society, P.O. Box 431552, South Miami, FL 33243, U.S.A

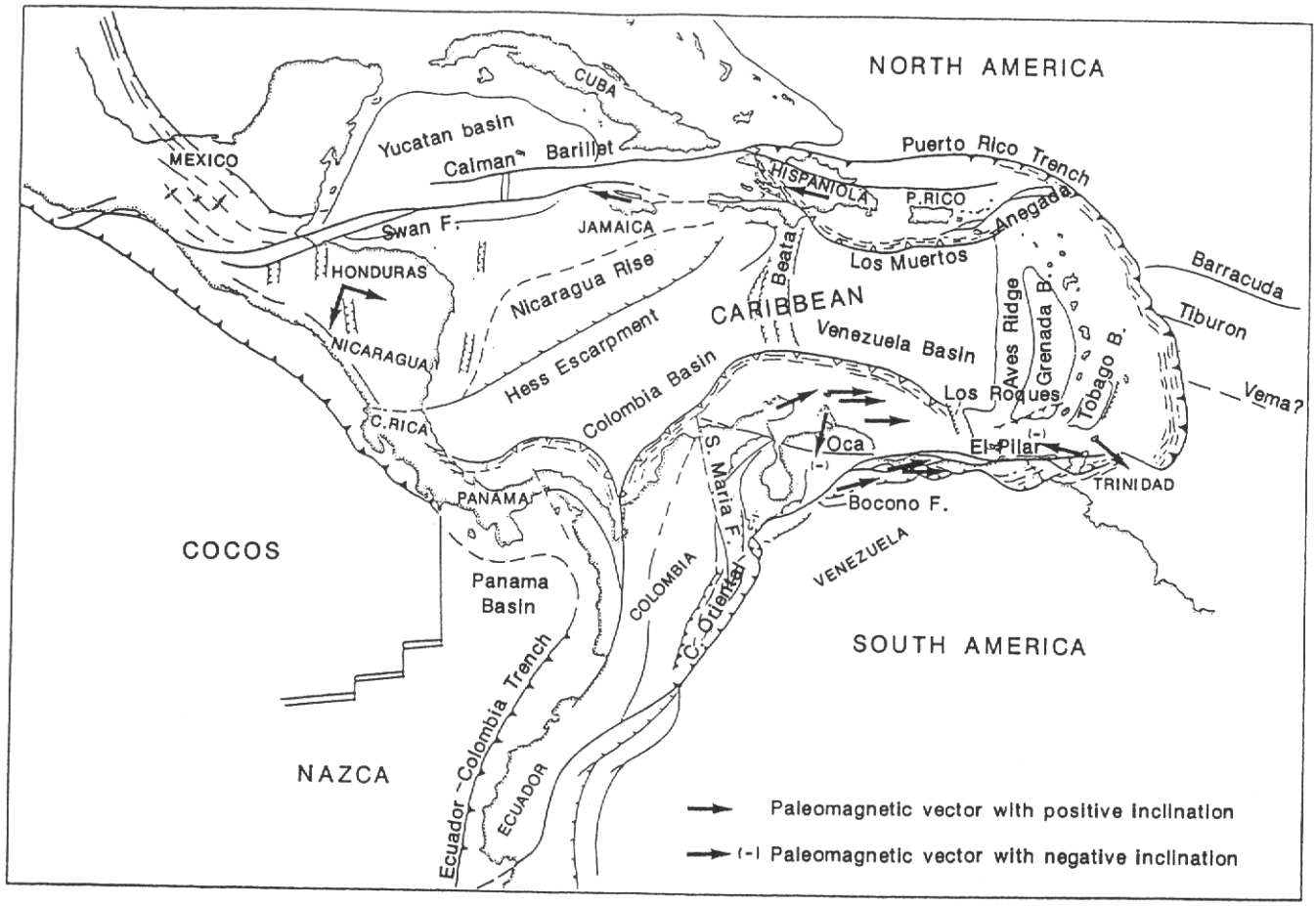

Fig. 1 : Paleomagnetic vectors indicating the tectonic rotations which have occured since the Cretaceous in the Caribbean geodynamic context;Data from various authors.

GEOLOGICAL BACKGROUND OF THE VENEZUELAN CARIBBEAN MOUNTAIN CHAIN

From east to west, the Caribbean mountain chain borders the margin of the South America. This chain is a stack of nappes and shows, from south to north (Stephan, 1977, 1982, 1985 ; Stephan and al., 1980 ; Beck, 1977, 1978, 1986; Santamaria and Schubert, 1974) :

- Paleocene-lower Eocene terrigenous flysch of the Piemontin nappe. This flysch overlays Cretaceous to Paleocene marine sequences.
- the Villa de Cura nappe which is essentially composed of metamorphised volcanic and sedimentary rocks, Coniacian conglomerates and limestones and a volcanic sequence dated with metamorphosed tuffs at 100 Ma (Piburn, 1967, in Skerlec and Hargraves, 1980).
- the Loma de Hierro-Siquisique ophiolitic nappe principally constituted of gabbros and peridotites with a dolerite complex and intruded by microgabbro sills. This unit is unconformably overlain by Maastrichtian sedimentary rocks ;
- the Tinaco-Tinaquillo nappe which is an igneo-metamorphic and ultramafic complex intruded by a 112 Ma old trondjemite (Martin Bellizzia, 1968 in Skerlec and Hargraves, 1980) and middle Albian sills and diabases. The complex is overlain by Turonian calcareous sediments.Paleocene-Eocene conglomerates, overlay unconformably the whole of the underlying rocks.
- the Coastal Fringe unit composed by eclogites, amphibolites and ultramafic rocks intruded in metatuffs and schists. The age of these rocks metamorphosed in green schist facies is upper Jurassic-lower Cretaceous.
- the Coastal Cordillera unit which is a detritic, calcareous and metamorphosed Jurassic-Cretaceous sequence. It is transgressive over a Precambrian and Paleozoic gneissic basement. Granodiorites (80 Ma, Santa Maria and Schubert, 1974) intrude the Coastal Cordillera unit.

PREVIOUS PALEOMAGNETIC DATA FROM VENEZUELA

All the following paleomagnetic data have been compiled in a synthetic review by Kerdraon (1984).

Caribbean Mountain chain (Skerlec and Hargraves, 1980).

The Villa de Cura nappe :
. site 8 : dykes of 100 Ma
. sites 9 and 10 : a 100 Ma ultramafic intrusion
. site 11 : upper Jurassic (?)-lower Cretaceous ultramafic El Chacao complex (Beck, 1983)
the Tinaco unit :
. site 6 : pre-upper Cretaceous ultramafic intrusions

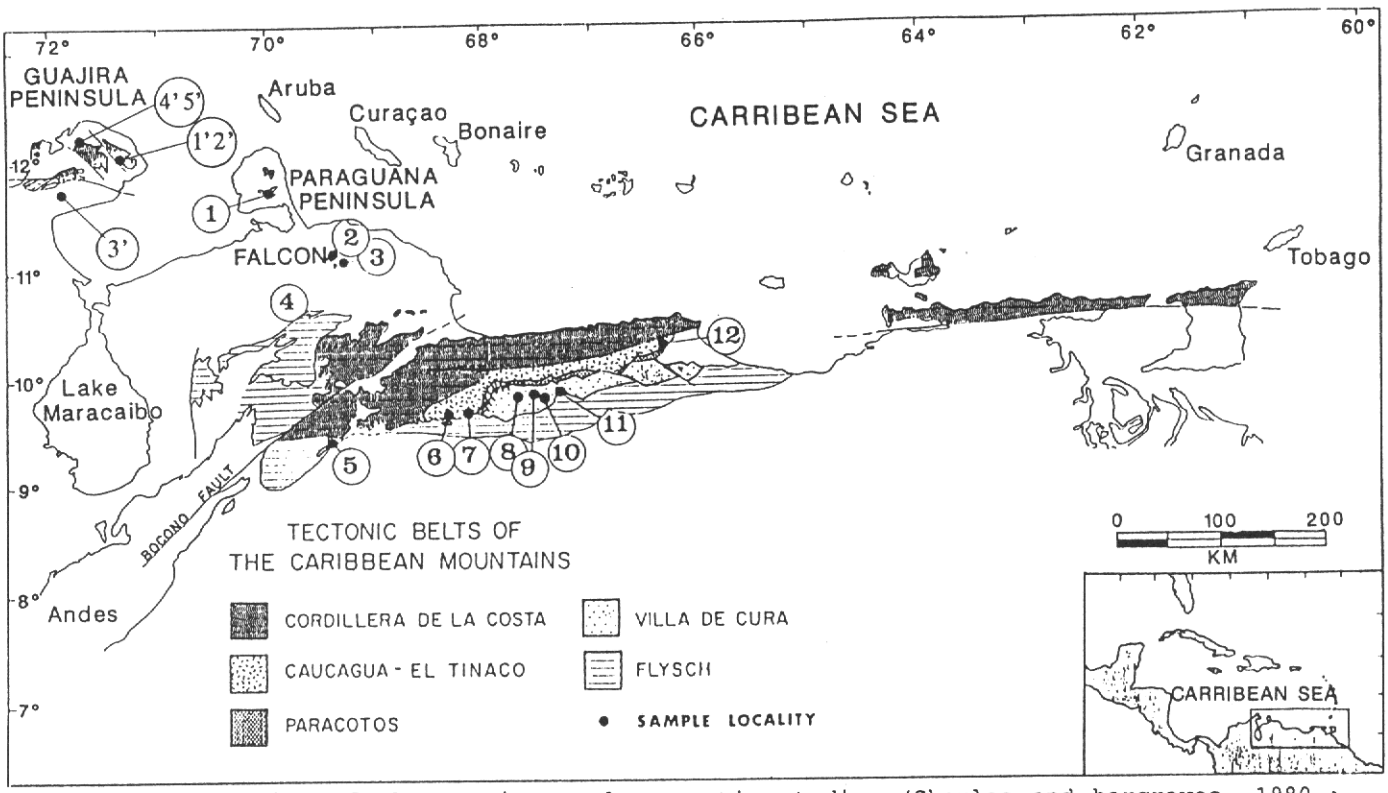

Fig. 2 : Location of the previous paleomagnetic studies (Skerlec and hargraves, 1980 ; Macdonald and Opdyke, 1972).

. site 12 : gabbros intruded in the Gonoropa volcanic rocks which overlay the pre-Mesozoic sequences of the Tinaco unit.

The Siquisique ophiolitic nappe :

. site 4 : gabbros with pyroxenous associated with serpentinites.

The Piemontin unit :

. site 5 : post Paleocene-lower Eocenous ultramafic intrusif (cerro Pelón).

The paleomagnetic results are rather scattered but they indicate a N90E general paleodeclination.

Falcon Basin Guajira and Paraguana Peninsula (Fig. 2).

Falcon Basin : (Skerlec and Hargraves, 1980)

The paleomagnetic studies concern Oligocene gabbroic and dioritic intrusions (site 2). The magnetization vectors indicate a 10° of clockwise rotation.

Paraguana Peninsula : (Skerlec and Hargraves, 1980)

The paleomagnetic data came from gabbros and volcanic rocks of the Santa Ana complex (site 1). The results do not indicate rotation since the lower Cretaceous.

The Guajira Peninsula : (Mac Donald and Opdyke, 1972)

. sites 1' and 2' : Sipana dioritic intrusion and dykes of 195 ±8 Ma.

. site 3' : Rhyodacite (La Teta lava) and diorite of Maruayan respectively of 95 to 120 Ma. and 120 ±4 Ma.

. sites 4' and 5' : Eocene Parashi diorite and dyke.

From the obtained results (Sipana diorites, Teta Lava and Maruayan diorites), the rotation could be estimated to 90° clockwise since the lower Cretaceous. It would have been about only 30° since the Eocene (Parashi diorite and dyke).

Conclusions on the previous paleomagnetic data

The paleomagnetic vector directions, issued from the Venezuelan allochthonous series, show a general 90° clockwise rotation in agreement with the Caribbean plate geodynamic model.

However, it is important to note that the obtained results concern principally the Cretaceous rocks of the southern Caribbean margin. It is more reasonable to consider a 90° clockwise rotation for the allochthonous Cretaceous terranes of the South caribbean region rather than for this whole margin. In this way, we shall see that the Cerro Pelón is not an intrusive in the Piemontin nappe.

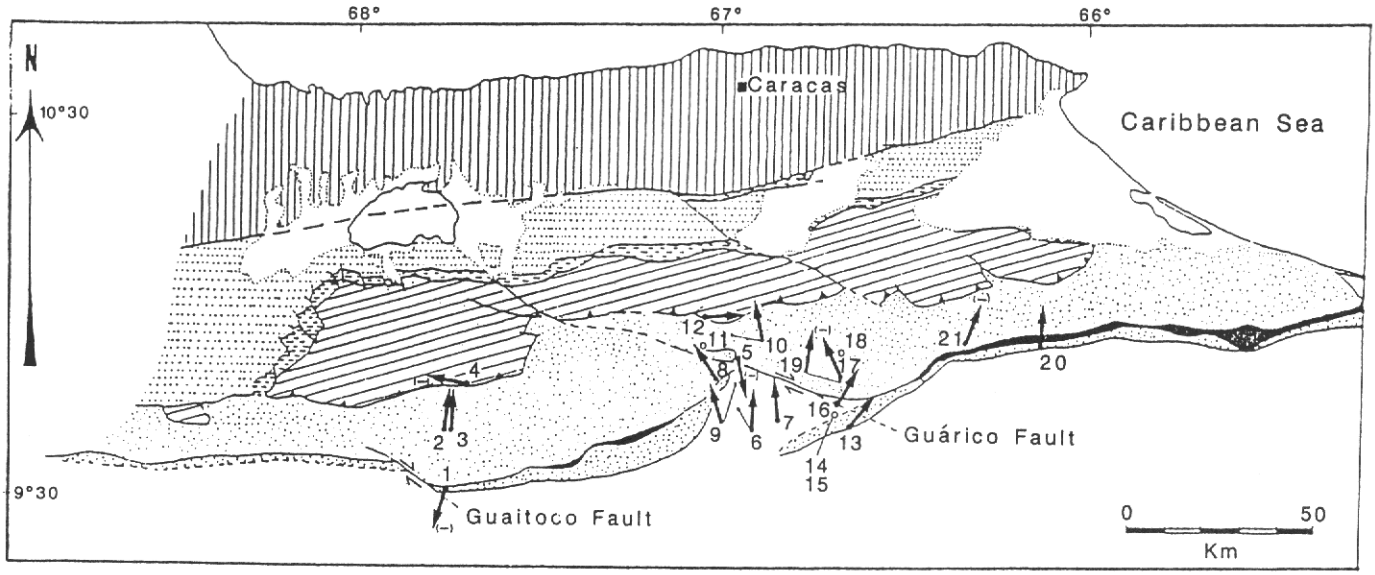

Fig. 3 : Location of the paleomagnetic studies and display of the paleomagnetic vector orientations (this study).

NEW PALEOMAGNETIC STUDY OF THE CARIBBEAN CHAIN PIEMONTIN NAPPE BETWEEN SAN FRANCISCO DE TIZNADOS AND TAGUAY.

The new study of the Caribbean chain front (Blin, 1989) is centered on the Piemontin nappe in order to test possible rotations that affect it, particularly near the Guaitoco and Guárico dextral strike-slip faults.

Sampling was done in the Villa de Cura nappe and in the Oligo-Miocene sandstones of the Quebradón Formation to compare their movements. On the whole 21 sites, 171 samples have been analysed for this study.

Sampling

The figure 3 indicates the position of the studied sites in several unities :
- the Oligo-Miocene sandstones (Fm. Quebradón) : sites 1, 6, 7, 9, 13, 14, 15, 16 and 20;
- the Piemontin nappe : the numerous klippen have permitted to sample the flysch of the Guárico Formation (sites 5, 8, 10, 18 and 21) and the pelites and limestones of the San Antonio Formation (sites 2, 3, 11, 17 and 19);
- the Villa de Cura nappe : the sandstones and microconglomerates with volcanic fragments have been sampled (sites 4 and 12).

For this study, the samples were collected with a thermic portable drill. When it was possible, the oriented samples were taken on the same stratum and in an area of less than a square meter at each site. All the samples therefore have the same magnetic history which gives more credit to the Fisher statistics.

Laboratory Treatment

Natural Remanent Magnetization (NRM) characteristics are measured using a cryogenic magnetometer. To isolate characteristic components of the NRM, stepwise thermal demagnetization procedures which are more effective on the sedimentary rocks, were done up to 480° C.

Results

For all the samples, the demagnetization results are plotted on Zijderveld diagrams and stereograms. We have chosen the demagnetization step the most significant of the primary magnetization. The Fisher statistics have provided the average declination and inclination for each site, after the necessary dip correction. The results are summarized in the Tables 1, 2, 3 and 4 and in Figure 4

Remarks :

. site 1 : Samples 7,8 and 9 are not used because they were collected from a stratum different from the others and not well situated in stratigraphic column.
. site 2 : The sample 9 is insufficiently stable. It is not considered in the average paleovector.
. site 3 : Samples 1, 3, 4 and 5 are not considered because of the bad quality of their Zijderveld diagrams.
. site 8 : The Zijderveld diagrams and the stereograms incoherence do not allow to keep the results of the samples 6, 7 and 8.
. site 12 : the Zijderveld diagrams and the stereograms incoherence of the samples 1, 3 and 4, and the too high inclination of the paleovector of the sample 5, do not allow to keep these

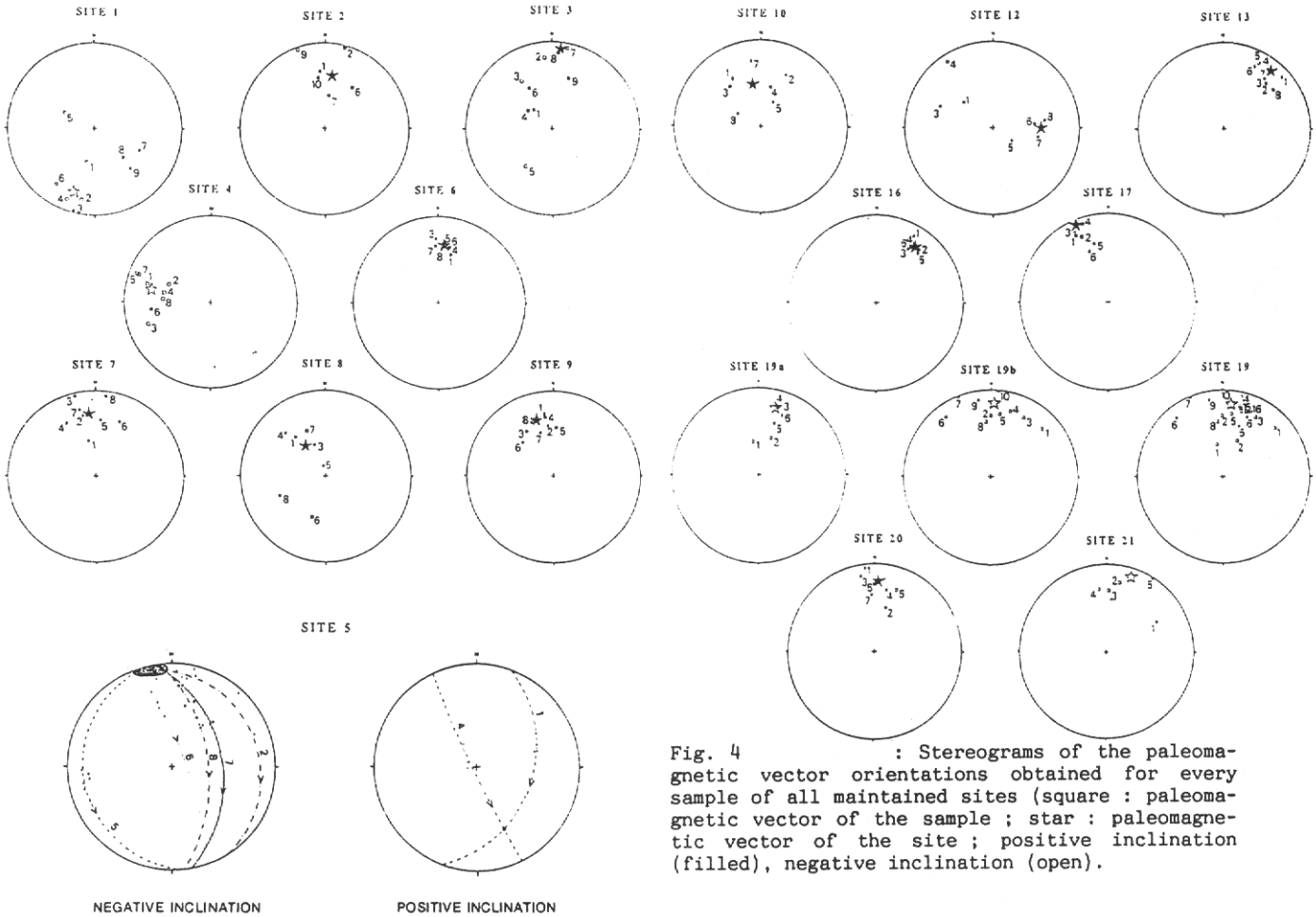

Fig. 4 : Stereograms of the paleomagnetic vector orientations obtained for every sample of all maintained sites (square : paleomagnetic vector of the sample ; star : paleomagnetic vector of the site ; positive inclination (filled), negative inclination (open).

samples for the calculation of the site 12 average direction.
. sites 11, 14, 15 and 18 : The demagnetization curves, the stereograms and the Zijderveld diagrams are not good enough. Under these circumstances it is better to ignore these sites for our study.

Discussion

The figure 3 synthetizes the paleomagnetic results obtained for all sites and it is possible to compare them with the regional geology. We note :

- a 90° clockwise rotation of the Villa de Cura nappe indicated by the East (positive) or West (negative) declinations of the magnetic paleovectors at sites 4 and 12.

- no general rotation in the Oligo-Miocene sandstones of the Quebradón Formation that can explain the North (positive) and South (negative) paleomagnetic vector declinations at sites 1, 6, 7, 9, 13, 16 and 20.

- a few degrees generally counter-clockwise rotation for the Piemontin nappe at sites 2, 3, 5, 8, 10, 17, 19 and 21.

We suggest that these paleomagnetic results indicate that the Villa de Cura nappe was a North-South oriented island arc which rotated over 90° clockwise before overthrusting the Ghuyana craton. These data are in agreement with those of Skerlec and Hargraves (1980).

In Oligo-Miocene sandstones, there are no significative rotations as would be expected by their autochthonous (or parautochthonous) character.

The Piemontin nappe does not show generally large rotations, but up to 30° clockwise occur locally near dextral strike-slip faults. These results are contrary to those of Skerlec and Hargraves (1980) who conclude to a 90° clockwise rotation for the Piemontin nappe from their study of the Cerro Pelón region. A geological study suggests that this massif is a klippe of the Villa de Cura paleoarc (Blin, 1989) and that it cannot be used as a movement marker from the Piemontin nappe.

In detail, we can observe structural effects on the paleomagnetic vector orientations in the Oligo-Miocene sandstones of the Piemontin nappe (fig. 3) :

- the dextral Guaitoco fault may be responsible for the 20° clockwise rotation of the site 1 paleomagnetic vector (table 1).

(I)

SITES	1			2			3			4		
SAMPLES	decl.	incl.	step °C	decl.	incl.	step °C	decl.	incl.	step °C	decl.	incl.	step °C
1	194.8	-47.8	120	355.5	22.5	200	315.5	55.5	200	287	-14.8	300
2	191.7	-10.4	80	14.5	0.7	200	354.1	-11.5	200	292.9	-34.3	300
3	195	L7	150	/	/	/	327.5	-2.4	300	251.6	-15	300
4	202.5	-7.5	200	/	/	/	306.2	50.8	200	282.6	-31.9	380
5	299.3	-46.6	300	/	/	/	217.1	-33.3	380	292	-5.7	350
6	215.3	-14.7	300	33.1	30.5	300	329.8	33.4	300	262.8	20.7	350
7	116.4	30.5	380	6.5	47.1	200	111	-2.9	380	292.1	-7.3	380
8	138	26.8	430	/	/	/	5.8	6.9	350	275.2	-31.8	380
9	135.5	40.5	300	340.1	-L9	200	18.1	27.2	200			
10				352.1	28.7	200						
decl. moy.	200.1			3.2			7.0			282.0		
incl. moy.	-15.6			26.7			4.9			-20.6		
K	15.1			13.4			17.7			19.1		
α_{95}	20.2			21.6			22.4			14.1		
	N.5 (sam. 1,2,3,4,6)			N.5 (sam. 1,2,3,7,10)			N.4 (sam. 2,7,8,9)			N.7 (sam. 1,2,3,4,6,7,8)		

Rq : Site 5 : long.=-66°53,88' / lat.=9°51,35' **Decl : 165° Incl : 4°**

(III)

SITES	10			12			13			16		
SAMPLES	decl.	incl.	step °C	decl.	incl.	step °C	decl.	incl.	step °C	decl.	incl.	step °C
1	329.6	25.1	430	311.5	43.1	150	49.1	6.1	200	14.8	33.1	300
2	26.3	23.2	150	/	/	/	43.7	18.5	200	19.3	43.9	350
3	321.4	29.2	350	292.2	24.5	350	39.6	16.2	200	7.1	41.6	350
4	14	40.1	300	326.1	-5.4	200	34.9	-8	200	15.3	39.8	350
5	26.2	54.9	300	125.6	60.6	300.	28.8	-3.5	200	19.0	46.8	350
6	/	/	/	85.4	38.8	350	27	12.2	200	10.3	40.2	300
7	350.9	14.6	300	101.2	34.2	300	37.4	9.8	200			
8	294.5	54.9	300	80.1	27.9	430	52.4	18.4	200			
9												
10												
decl. moy.	350.0			88.6			39.0			34.7		
incl. moy.	38.5			31.2			8.2			14.1		
K	7.1			67.7			33.2			192.0		
α_{95}	24.3			15.0			9.7			4.8		
	N.7			N.3 (sam. 6,7,8)			N.8			N.6		

.. Before bedding correction (N170, 45 W)

(II)

SITES	6			7			8			9		
SAMPLES	decl.	incl.	step °C	decl.	incl.	step °C	decl.	incl.	step °C	decl.	incl.	step °C
1	14.8	30.5	480	348.5	44.9	200	322.4	30.7	200	352	18	200
2	/	/	/	348.3	19.1	200	/	/	/	354.4	29.4	150
3	357.3	16.8	480	346.2	2	200	340	48.2	200	329.7	27.6	200
4	12.1	23.1	480	331.5	19.9	350	316.5	2L3	200	352	2L1	200
5	5.7	2L7	480	4.8	24	350	346.4	76.5	200	3.8	31	200
6	11.9	21.8	480	23	20.8	200	198.9	-37.3	200	317.8	34.2	150
7	356.3	22.7	480	346.3	13.4	300	337.7	-31.3	200	343.6	34.1	300
8	6.5	24.4	480	7	3.4	150	247.8	29.3	200	338.4	22	300
9												
10												
decl. moy.	6.3			354.4			326.7			344.2		
incl. moy.	23.1			18.9			44.4			21.4		
K	109.2			16.2			10.0			11.5		
α_{95}	5.8			14.1			30.4			17.0		
	N.7			N.8			N.4 (sam. 1,3,4,5,7)			N.8		

* Computed with Zijderveld diagram

(IV)

SITES	17			19a			19b		20		21	
SAMPLES	decl.	incl.	step °C	decl.	incl.		decl.	incl.	decl.	incl.	decl.	incl.
1	344.1	40	150	350	-48		47	-11	353	L98	60	22
2	337.8	16.6	300	22	-42		0	-20	14	34.19	11	-12
3	336.9	24	300	15	-12		29	-14	349	6.87	3	-20
4	350.6	3L1	300	14	-11		16	-14	11	18.67	353	-18
5	8.3	43.8	350	18	27		8	-18	20	-16	32	0
6	339.7	28.3	350	22	17		322	8	0.	14		
7							337	0	357	23		
8							355	-25				
9							350	6				
10							4	0				
decl. moy.	337.5			14.4		6.9	2.6		3.0		19.2	
incl. moy.	L9			-11.6		-10.4	-9.5		12.0		-6.2	
K	33.6			6.6		8.4	9.4		17.0		6.9	
α_{95}	11.7			27.9		13.4	16.5		15.0		3L1	
	N.6			N.6		N.10	N.10		N.7		N.5	

•: Before bedding correction (N30, 38 W)

Table 1, 2, 3 and 4 : Paleomagnetic results (this study).

- the dextral displacement along the Guárico fault could explain the 35-40° rotation observed to the sites 13 and 16 (table 3).

For the sites far from this strike-slip fault, the paleomagnetic vector retains a North-South orientation and testifies to the absence of tectonic movements in these localities.

The site 13 displays a clockwise rotation identical to that of site 16. The evidence of rotation is displayed by the curvature of folds in the Oligo-miocene rocks near the Guarico fault. The geologic map of Venezuela (Ministerio de Energía y Minas, 1976, 1/500000) shows that these folds, originally oriented N60-70E, to the west of the Guárico fault, are oriented East-West direction near the fault. The lack of correspondence of the site 14 and 15 data could result from the position of these sites in a fault zone. The clockwise rotations are thus due to the movement along the Guárico fault (site 16) and to the Oligo-Miocene folds deformation under the Piemontin nappe progression to the South (site 13).

The more or less North-South declinations of the sites 2, 3, 5, 8, 10, 17, 19 and 21 paleovectors indicate that, on the whole, the Piemontin nappe does not significantly rotate within the precision level given by the $\alpha 95$ value, radius of circle of confidence (Fisher, 1953) .

Nevertheless, taking the paleomagnetic declinations of the sites 5, 8, 17 and 19 (keeping the average vector of these two later sites), it can be observed that the paleovectors are more or less perpendicular to the Piemontin nappe meridional boundary. In contrast, in its median part (sites 2, 3 and 10) the vectors remain a North-South orientation. This scheme could represent an image of nappe which flows and where the force lines keep perpendicular to its front. A similar model explains the Hellenic arc structure : the deformation pattern of Aegean zone (Angelier and Le Pichon, 1980) justifies the paleomagnetic declinations obtained by Laj and al. (1982) and Freeman (1983).

Remark :

it is possible that the site 5 had recorded the Guárico fault dextral movement but the demagnetization circle method (used for this site) does not give any $\alpha 95$ value. Then, for our discussion, we have kept the average North-South paleomagnetic vector orientation in this site.

CONCLUSION

These results, associated to the field data, confirm that the Villa de Cura nappe was a north-south oriented island arc rotated 90° clockwise since Cretaceous time, in agreement with the models of Caribbean geodynamic evolution proposed by various authors (Pindell and Dewey, 1982 ; Stéphan, 1982 ; Beck, 1986). In contrast, the Piemontin nappe did not rotate and has moved with an orientation similar to its original position. But near the southern limit of the nappe, the paleomagnetic declinations are often more or less perpendicular to the front and may be due to its southward differential progression, further some deflection may be induced by the Guarico fault. Finally, the autochthonous Oligo-Miocene sandstones, to the south of the Piemontin nappe, do not show rotations excepted locally near the Guárico and Guaitoco dextral faults.

ACKNOWLEGMENTS

This study is a part of a thesis (B.B, 1989). Field study and sampling have been supported by the Corpoven Company. Dr. Emira Cabrera de Molina, Chairman of Geology at Corpoven helped one of us (B.B.) to solve material and field organisation problems. Magnetic measurements were largely performed in the Paleogeophysics Laboratory of Pr. N. Bonhommet at University of Rennes. We thank Dr. C. Beck for helpful comments and suggestions along this study.

REFERENCES

Angelier, J. and Le Pichon, X., 1980, Néotectonique horizontale et verticale de l'Egée : subduction et expansion : 26è Congr. géol. intern., Paris 7-17 juillet 1980, Colloque C5 : Géologie des chaînes alpines issues de la Téthys et Mém. B.R.G.M., n° 115, p. 249-260.

Beck, C., 1977a, Geologia de la Faja Piemontina y del Frene de montana en el noreste del estado Guarico - Venezuela. V Congr. Geol. Venez., Caracas 19 al 23 de noviembre de 1977, V. II, p. 759-786.

Beck, C., 1977b, Sedimentacion y tectonica de la Napa Piemontina y del Frente de montana en la region de Altagracia de Orituco, estado Guarico : V Congr. Geol. Venez., Caracas (1977), guia de la excursion 4.

Beck, C., 1978, Polyphasic Tertiary tectonics of the interior range in the central part of the western Caribbean chain, Guarico state, northern Venezuela. Geologie en Mijnbouw, V. 57, (2), p. 99-104.

Beck, C., 1986, Géologie de la chaîne Caraïbe au méridien de Caracas. Thèse Doct. Etat. Soc. Géol. du Nord, 462 p. Université de Lille.

Blin, B., 1989, Le front de la Chaîne Caraïbe entre la Serrania de Portuguesa et la région de Tiznados (surface et subsurface) - Apport des données paléomagnétiques - Interprétation géodynamique. Thèse Doct., Univ. de Bretagne Occidentale, Brest, 395 p.

Dasgupta, S.N., and Vincenz, S.A., 1975, Paleomagnetism of a Paleocene pluton on Jamaica. Earth and Planet. Sci. Letters., V. 25, p. 49-56.

Donald, E. and Krushensky, R., 1983, A translated terrane exotic to the Caribbean. 10th Carribean Geological Conference, Carthagene, (Colombia).

Fisher, R.A., 1953, Dispersion on a sphere. Proc. Roy. Soc. London, A 217, p. 295-305.

Gose, W.A., 1985, Paleomagnetic results from Honduras and their bearing on Caribbean tectonics. Tectonics : V. 4, p. 565-585.

Gose, W.A. and Swartz, D.K., 1977, Paleomagnetic results from Cretaceous sediments in Honduras : tectonic implications : Geology, V. 5, p. 505-508.

Guja, N.H. and Vincenz S.A., 1978, Paleomagnetism of some late Creaceous and Miocene igneous rock on Jamaica : Geophys. J. Roy. Astro. Soc., 52, p. 97-115.

Hargraves, R.B. and Skerlec, G.M., 1980, Paleomagnetism of some cretaceous-tertiary rocks on Venezuelan offshore islands, Netherlands Antilles, Trinidad and Tobago. 9th. Caribb. geol. Conf., Santo Domingo Dominican Republic (1980), V. 2, p. 509-517.

Horner, F. and Freeman, R., 1983, Palaeomagnetic evidence from pelagic limestones for clockwise rotation of the Ionian zone, western Greece. Tectonophysics, V. 98, p. 11-27.

Kerdraon, Y., 1984, Contribution à l'étude de la plaque Caraïbe : étude géologique de Porto Rico. Synthèse des données sur le paléomagnétisme. Interprétation de profils sismiques sur la fosse de Los Muertos et le passage de Mona. D.E.A., Univ. de Bretagne Occidentale, Brest, 86 p.

Laj, C., Jamet, M., Sorel, D. and Valente, J.P., 1982, First paleomagnetic results from Mio-Pliocene series fo the Hellenic sedimentary arc. Tectonophysics, v. 86, p. 45-67.

Mc Donald, W.D. and Opdyke, N.D., 1972, Tectonic rotations suggested by paleomagnetic results from Northern Colombia (South America), Journ. of Geophys. Res., V 77, p. 5720-5730.

Mc Donald, W.D. and Van Horn T, 1977, Paleomagnetism of the Hawk's Bill formation Tobago. proc. Congr. Geol. Venez., p. 811-834.

Martin Bellizzia, C., 1968, Edades Isotopicas de rocas Venezolanas. Dir. Geol. Bol. Geol., 10, 356-380.

Murray, C.G., 1973, Estudios petrologicos de complejos ultramaficos zonados en Venezuela y Alaska. Boln. Geol. Minist. Minas Venez., v. 12, p. 173-279.

Piburn, M.D., 1967, Metamorphism and structure of the villa de Cura group, Northern Venezuela. Ph. D. dissertation, 148 pp. Princeton Univers.

Santamaria, A.F. and Schubert, C., 1974, Geochemistry and geochronology of the southern Caribbean. Northern Venezuela plate boundary. Geol. Soc. Am. Bull., V. 85, p. 1085-1098.

Skerlec, G.M. and Hargraves, R.B., 1980, Tectonic significance of paleomagnetic data from Northern Venezuela. Journ. of Geophys. Res., V. 85, p. 5303-5315.

Stearns, C., Mauk, F.J., and Van Der Voo, R., 1982, Late Cretaceous-early Tertiary paleomagnetism of Aruba and Bonaire (Netherlands Leeward Antilles). Journ. of Geophys. Res., V. 87, p. 1127-1141.

Steinhauser, P., and Vincenz, S.A., 1973, Paleomagnetism of lower Cretaceous lavas on Jamaica. Arch. Geophys. Biok. S., A22, p. 325-336.

Stéphan, J.F., 1977a, El contacto Cadena Caribe-Andes Meridenos entre Carora y El Tocuyo (edo. Lara) : observaciones sobre en el estilo y la edad de las formaciones cenozoicas en el occidente venezolano. V Congr. Geol. Venez., Caracas 19 al 23 de noviembre de 1977, V. 2, p. 789-816.

Stéphan, J.F., 1977b, Una interpretacion de los complejos con bloques asociados a los flyschs Paleoceno-Eoceno de la Cadena Caribe venezolana : el emplazamiento submarino de la napa de Lara. Abstr. VIIIth. Caribb. Geol. Conf., Curaçao (1977), p. 199-200.

Stéphan, J.F., 1982, Evolution géodynamique du domaine Caraïbe, Andes et Chaîne Caraïbe, sur la transversale de Barquisimeto (Venezuela). Thèse Doct. Etat. Univ. P.M. Curie, Paris VI, 512 p.

Stéphan, J.F., 1985, Andes et chaîne Caraïbe sur la transversale de Barquisimeto (Venezuela) évolution géodynamique. Symposium "Géodynamique des Caraïbes", Paris 5-8 février 1985, A. Mascle Edit., Ed. Technip, p. 505-529.

Stéphan, J.F., Beck, C., Bellizzia, A.and Blanchet, R., 1980, La Chaîne Caraïbe du Pacifique à l'Atlantique. 26è Congr. Géol. intern., Paris 7-17 juillet 1980, Colloque C5 : Géologie des chaînes alpines issues de la Téthys et Mém. B.R.G.M., n° 115, P. 38-59.

Stéphan, J.F., Blanchet, R., and Mercier de Lepinay, B., 1985, Les festons nord et sud-caraïbes (Hispaniola-Porto Rico ; Panama et Colombie-Venezuela) : des pseudo-subductions induites par le raccourcissement est-ouest du bâti continental péri-caraïbe. Symposium "Géodynamique des Caraïbes", Paris 5-8 février 1985, A. Mascle Edit., Ed. Technip, p. 35-51.

Vincenz, S.A. and Dasgupta, S.N., 1978, Paleomagnetic study of some Cretaceous and Tertiary rocks on Hispaniola. Pur. Appl. Geophys., v. 116, p. 1200-1210.

Vincenz, P., Steinhauser, P., and Dasgupta, S.N., 1973, Paleomagnetism of upper Cretaceous ignimbrite on Jamaica. Geophys., v. 39, p. 727-737.

Watkins, N.P. and Cambray, F.W., 1971. Paleomagnetism of Cretaceous dikes from Jamaïca. Geophys. Journ. Roy. Astro. Soc., 22, p. 163.

THE CARIBBEAN-SOUTH AMERICAN PLATE BOUNDARY, ARAYA PENINSULA, EASTERN VENEZUELA

Hans G. Avé Lallemant
Department of Geology and Geophysics
Rice University
P. O. Box 1892, Houston, Texas 77251

ABSTRACT

Preliminary results of a structural geologic study of the low to intermediate P/T metamorphic rocks of the Araya Peninsula, the El Pilar fault zone, and the fold and thrust belt south of the El Pilar fault are consistent with recent plate-tectonic models for the interaction of the Caribbean and South American lithospheric plates. The rocks of the Araya Peninsula underwent two synmetamorphic phases of isoclinal folding (D_{1a} and D_{1b}); the fold axes are parallel to the major principal extension axes (X) which trend east-northeasterly. The D_{1a} and D_{1b} structures are crosscut by north-south striking extensional kink bands, shear zones, and normal faults (D_{1c}) which indicate late synmetamorphic east-west extension. The next phase of folding (D_2) is characterized by tight to open postmetamorphic, northeast trending folds, generally vergent to the southeast and accompanied by southeast vergent thrust faults (northwest vergent folds and thrust faults are relatively rare). The youngest phase of folding (D_3) is characterized by north-northwest trending folds, accompanied by east-northeast and west-southwest vergent thrust faults. The structures in the fold and thrust belt, south of the El Pilar fault, underwent the last two phases of folding (D_2 and D_3) recognized north of the fault. Along the El Pilar fault, upper Tertiary and lower Quaternary rocks are deformed by D_3 structures. It is proposed that the D_{1a}, D_{1b}, and D_{1c} structures formed in an accretionary complex-forearc terrane as the result of right-oblique convergence of the Proto-Caribbean and Farallon plates during the mid to Late Cretaceous. The D_2 structures may have formed during the Oligocene and Miocene as a result of the eastward passing of the Lesser Antilles/Aves Ridge and Leeward Antilles volcanic island arcs along the northern margin of South America. The D_3 structures have formed from Miocene to Recent and are related to "restraining bends" of the east-west striking strike-slip faults which make up the present plate boundary.

INTRODUCTION

The Caribbean-South American plate boundary zone is complex and, in eastern Venezuela, it may be as wide as 300 km (Robertson and Burke, 1989). It is bounded in the north (north of La Blanquilla Island; fig. 1) by a south-dipping thrust fault (Beck, 1985) and in the south by the frontal thrust of the Serrania del Interior foreland fold and thrust belt (Rossi, 1985; Rossi et al., 1987). The boundary zone has been divided into four tectonostratigraphic terranes: the Leeward Antilles volcanic island arc terrane, the Margarita terrane, the Cordillera de la Costa belt, and the foreland fold and thrust belt of the Serrania del Interior (Stephan, 1985; Beck, 1985; Bellizzia, 1986). The first three terranes are separated in the south from the foreland fold and thrust belt by the east-west striking El Pilar fault which is a right-lateral strike-slip fault (Vierbuchen, 1984) and is still active today (Pérez and Aggarwal, 1981). The northern three terranes are tectonically intermixed. In general, though, the Leeward Antilles arc terrane is north, and the Cordillera de la Costa belt south.

Case et al. (1984) defined the Leeward Antilles terrane to consist of the Dutch islands Aruba, Curaçao, and Bonaire and the Venezuelan islands Las Aves, Los Roques, and La Orchilla. The Leeward Antilles (volcanic island arc) terrane is defined here to include Case's Leeward Antilles terrane, but also (fig. 1) the islands La Blanquilla and Los Hermanos and part of Margarita Island, Tobago, and the Carúpano and Tuy-Cariaco basins. Late Cretaceous and earliest Paleogene trondhjemites occur on the islands La Blanquilla and Margarita (Schubert and Moticska, 1973; Santamaría and Schubert, 1974). Late Cretaceous basalt and andesite basement was penetrated by drilling in the Tuy-Cariaco and Carúpano basins (Bellizzia, 1986; Castro and Mederos, 1985). Mid-Cretaceous volcanic and plutonic rocks occur on Tobago (Sharp and Snoke, 1988). Volcanism in the western Leeward Antilles arc ceased at about 80 Ma (Beets et al., 1984), but may have continued till about 64 Ma on La Blanquilla. Mid- to Late Eocene andesites and quartz diorites on the Los Testigos Archipelago (Schubert and Moticska, 1973; Santamaría and Schubert, 1974) and in nearby wells (Bellizzia, 1986) may not be related to the Leeward Antilles arc, but rather to the Lesser Antilles arc (which stretches from Grenada in the south to Saba in the north).

The Margarita terrane (fig. 2, named Coastal Fringe - Margarita terrane by Stephan (1985)) consists of dismembered ophiolite and metasediments containing eclogite and blueschist inclusions. The ophiolitic rocks are found on Margarita (Maresch, 1975; Chevalier, 1987) and on the Araya and Paria peninsulas (Schubert, 1971; Seijas, 1972; González de Juana et al., 1972). In some deep wells in the Carúpano Basin, pre-Tertiary volcanic rocks were recovered which have MORB characteristics (Castro and Mederos, 1985). These rocks have been proposed to be fragments of oceanic lithosphere, formed in the late Jurassic to early Cretaceous when North and South America drifted apart (Maresch, 1975; Beets et al., 1984). Eclogite knockers occur only on Margarita Island. Blueschists have been recovered in deep wells in the Carúpano Basin (Castro and Mederos, 1985; Pereira, 1985). The occurrence of a glaucophane schist has been reported by Campos (in Bellizzia, 1986) on the mainland, east of the Araya Peninsula. These metamorphic assemblages have formed at high pressure (up to 12 kb)/ temperature (P/T) conditions in a subduction complex (Maresch and Abraham, 1981; Navarro, 1981). Most of these rocks were retrograded in the epidote amphibolite and greenschist facies (at pressures of 6 kb and less) during the Late

Larue, D.K., and Draper, G. (eds.),
***Transactions of the 12th Caribbean Geological Conference, St. Croix*, U.S.V.I.**, Miami Geological Society, P.O. Box 431552, South Miami, FL 33243, U.S.A

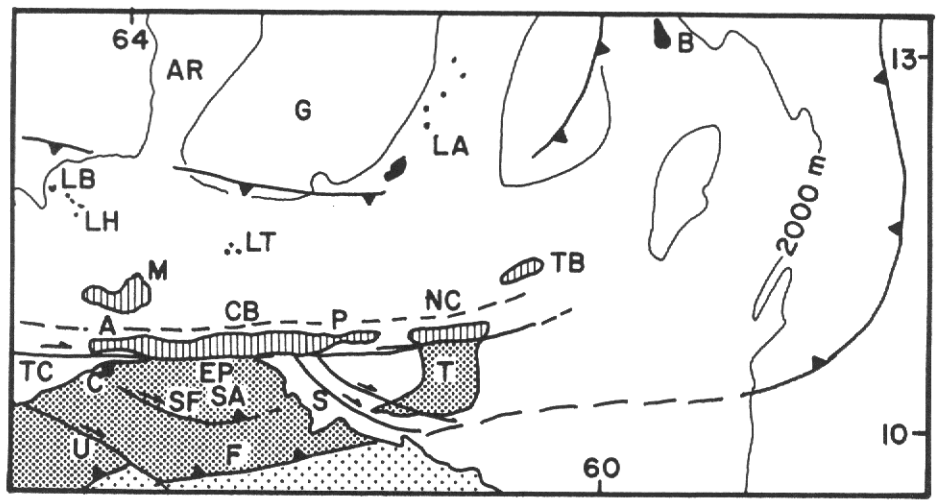

Figure 1. Terrane map of the southeastern Caribbean and northeastern Venezuela (after Stephan, 1985; Beck, 1985; Speed, 1985; Rossi et al., 1987; Robertson and Burke, 1989). Vertically ruled: Margarita and Cordillera de la Costa belts; densely stippled: foreland fold and thrust belt; sparsely stippled: autochthonous; A: Araya Peninsula, AR: Aves Ridge; B: Barbados; C: Cumaná; CB: Carúpano Basin; EP: El Pilar fault zone; F: Frontal thrust; G: Grenada Basin; LA: Lesser Antilles; LB: La Blanquilla Island; LH: Islas Los Hermanos; LT: Los Testigos Archipelago; M: Margarita Island; NC: North Coast fault zone; P: Paria Peninsula; S: Soldado fault zone; SA: Serrania del Interior; SF: San Francisco fault zone; T: Trinidad; TB: Tobago; TC: Tuy-Cariaco Basin; U: Urica fault zone.

Cretaceous (Santamaría and Schubert, 1974; Loubet et al., 1985; Chevalier, 1987).

Most of the Araya (fig. 2) and Paria peninsulas is underlain by metasediments assigned to the Cordillera de la Costa belt (Schubert, 1971; González de Juana et al., 1972; Seijas, 1972). Recently (Bellizzia, 1986; Chevalier, 1987), a large portion of the metasediments of Margarita (Juan Griego Group) has been included in this belt as well, although they contain numerous eclogite and amphibolite knockers. The sedimentary protolith of the Cordillera de la Costa belt may have been deposited on the passive northern continental margin of South America during late Jurassic and early Cretaceous time (Bellizzia, 1986); granitic gneisses in the Cordillera de la Costa belt in north central Venezuela have Paleozoic and Precambrian crystallization ages (Ostos, 1990). The rocks were metamorphosed in the epidote amphibolite and greenschist facies probably during the Late Cretaceous.

The region south of the El Pilar fault (fig. 2) is underlain by a non-metamorphic sequence of Cretaceous and Tertiary sediments. Cretaceous and Paleogene sediments were deposited on the passive continental margin of northern South America and were deformed in a southeast vergent fold and thrust belt during the Oligocene and Miocene (Rossi et al., 1987). The deformed rocks are unconformably overlain by generally coarse-grained sediments of Miocene (partly deformed) and younger age.

Maresch (1974) and Talukdar and Loureiro (1982) were among the first to interpret the geology of northern Venezuela in terms of plate tectonic theory. Their models do not require large displacements: one or more volcanic island arcs and subduction complexes developed off the coast of Venezuela and, ultimately, collided with the mainland resulting in south vergent fold and thrust belts. The interpretation of northern Venezuelan geology changed drastically, however, when more detailed data became available about the relative motions of the North and South American and Pacific basin lithospheric plates through time (e.g. Morgan, 1981; Engebretson et al., 1985). As a result, most recent models (e.g. Duncan and Hargraves, 1984; Ross and Scotese, 1988; Pindell et al., 1988; Pindell and Barrett, 1990) have most tectonic belts of Venezuela formed far to the west, as a result of Cretaceous interaction of the Pacific (Farallon) plate and the South American continent. These belts were thought to have been transported eastward within the Caribbean-South American transform boundary as a result of the relative eastward migration of the Caribbean plate. The emplacement of the terranes onto the South American continent may have been entirely the result of dextral strike-slip motion (Robertson and Burke, 1989) or transpression (Pindell et al., 1988). Speed (1985) proposed that the structures in eastern Venezuela could be best explained by northwesterly subduction and collision of the Lesser Antilles arc with South America.

The present study dealing with the structural evolution of the rocks on the Araya Peninsula (fig. 1 and fig. 2) was carried out in an attempt to test the often conflicting plate tectonic models for the area. The conclusions are preliminary, because this study has not yet been entirely completed and interpretations are often based on poorly-known age relationships. Several samples from the area are being prepared for $^{40}Ar/^{39}Ar$ dating, but results are not yet available.

GEOLOGY OF THE ARAYA PENINSULA

Lithologies

Schubert (1971) divided the metamorphic rocks of the Araya Peninsula into four east-northeast trending belts, each characterized by a particular rock assemblage for which a formation name was coined. These belts or formations are from north to south: Manicuare, Laguna Chica, Carúpano, and

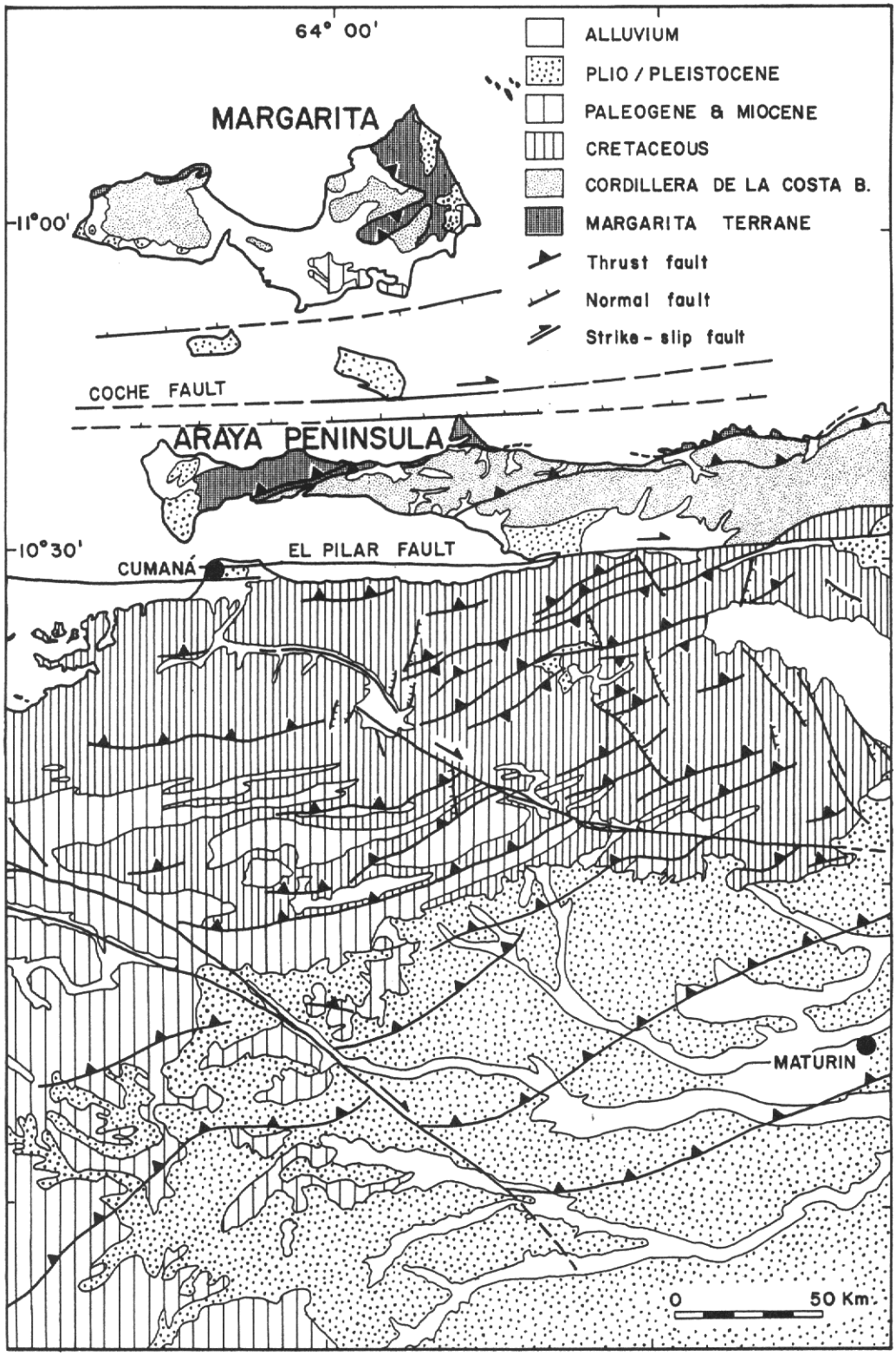

Figure 2. Simplified geologic map of the Caribbean-South American plate boundary zone at the approximate longitude of Isla de Margarita and the Araya Peninsula, after Schubert (1971), Bellizzia et al. (1976) and Rossi (1985).

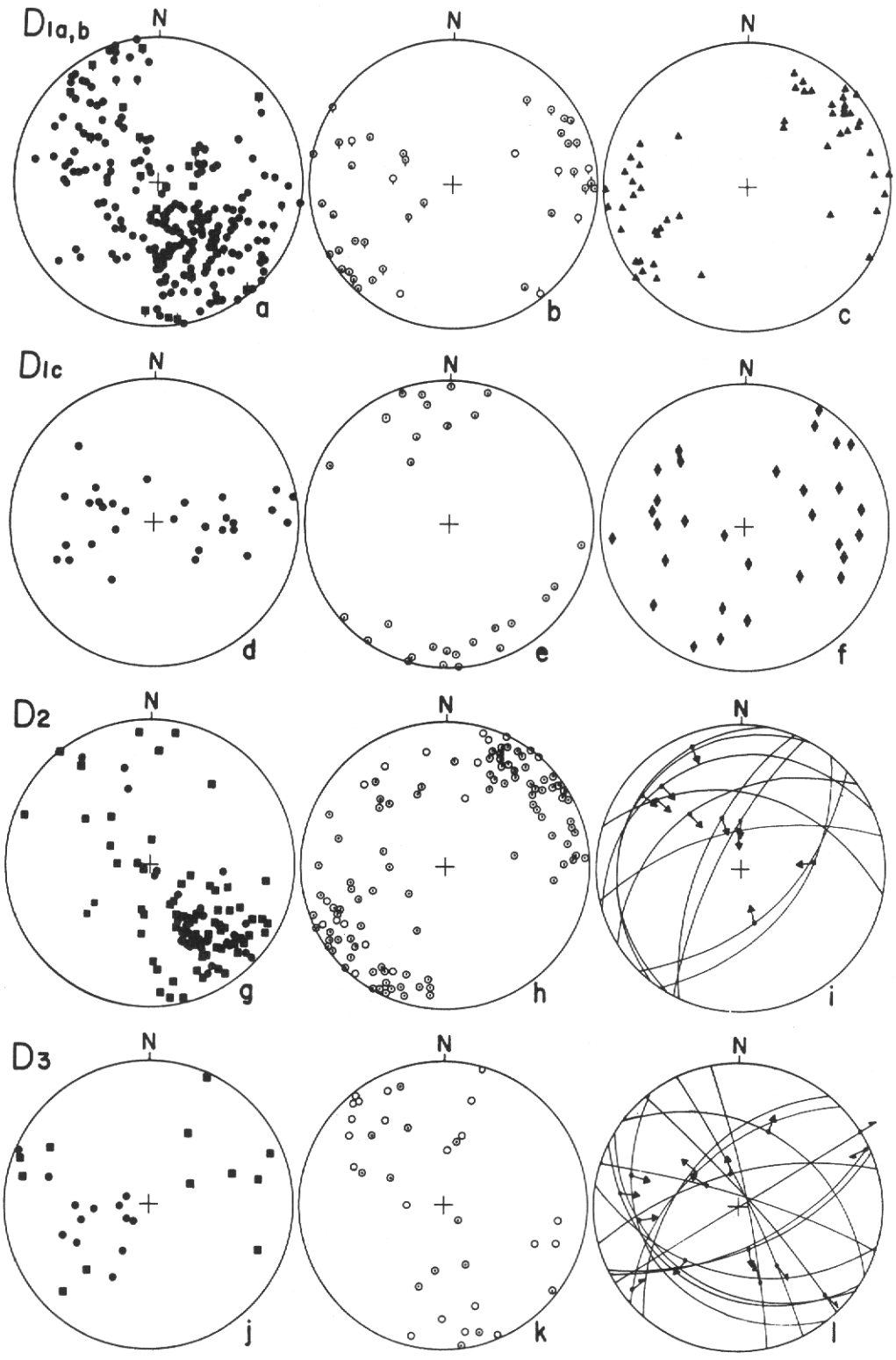

Figure 3. Equal-area, lower-hemisphere projections of structural elements of D_{1a} and D_{1b} (figs. a, b, c; tick marks indicate D_{1b} structures), D_{1c} (figs. d, e, f), D_2 (figs. g, h, i), and D_3 deformation (figs. j, k, l). Poles to foliations and cleavages (dots), poles to fold axial planes (squares), fold axes (circles), intersection and crenulation lineations (dotted circles), stretching lineations (triangles), slip directions (diamonds), faults (great circles; dots on great circle indicate slip direction; arrows pointing outward indicate normal faults or faults with normal component; arrows pointing toward center indicate thrust faults or faults with thrust component; arrows with half arrowhead indicate sense of strike-slip faults).

Tunapui formations. Bellizzia (1986) included the Laguna Chica Formation in the Margarita terrane and the other three formations in the Cordillera de la Costa belt. In the present study, the Manicuare Formation is included in the former, because of its relatively high-pressure metamorphic assemblages. The four belts are separated by steep faults along which the latest displacements resulted from strike-slip motion (Schubert, 1971).

The Manicuare Formation consists of muscovite-biotite schist, kyanite schist, garnet-staurolite schist, quartzite, and two-feldspar gneiss. Kyanite occurs also in quartz veins. The age of the protolith is unknown.

The Laguna Chica Formation consists of quartzite, chlorite schist, amphibole schist, phyllite, and serpentinite. Chevalier (1987) correlated it with the El Copey Formation, east of the Araya Peninsula, which contains similar rocks and, additionally, meta (pillow) basalt, metatuff, metaconglomerate (Seijas, 1972), and epidote-glaucophane schist (Campos, in Bellizzia, 1986). The age of deposition of these rocks is unknown but Vierbuchen (1984) proposed a Lower Cretaceous (Barremian) age on the basis of lithologic similarities with dated rocks east of the Araya Peninsula.

The Carúpano Formation consists of calcareous phyllite, dark gray marble, graphitic and calcareous micaschist, and micro-conglomerate. No fossils have been found in this formation, but Vierbuchen (1984) proposed it to be a lateral facies equivalent of the Albian/Aptian Tunapui Formation.

The Tunapui Formation consists of chlorite-muscovite schist, meta-conglomerate, graphitic phyllite, quartzite, and some limestone. Albian and Aptian ammonites were reported in this formation, east of the Araya Peninsula (Vierbuchen, 1984).

The Manicuare Formation, according to Schubert (1971), was metamorphosed in the epidote amphibolite facies at temperatures of 480°C and pressures of 5 to 6 kb and was retrograded at temperatures of 350° to 450°C and pressures of 3 to 4 Kb. The metamorphic grade of the other three belts is lower (greenschist facies), except for the exotic glaucophane schist reported in Bellizzia (1986). The age of metamorphism on Araya is unknown. An augengneiss on the Paria Peninsula yielded an amphibole K/Ar age of 128± 11.0 Ma and a whole-rock K/Ar age of 53± 3.0 Ma (Santamaría and Schubert, 1974).

Structural Geology of the Araya Peninsula

It has been shown by Schubert (1971) and Vignali (1979) that the structural grain of the Araya Peninsula is controlled by east-northeast to northeast trending folds and faults which deform the metamorphic foliation. Vignali (1979) recognized two generations of isoclinal folds formed during the regional metamorphism. In the present study, five generations of folds were recognized: two generations of isoclinal folds (D_{1a} and D_{1b}), one generation of kink folds related to extensional shear zones (D_{1c}), one generation of northeast trending folds (D_2), and one of north-northwest trending folds (D_3). The D_{1a} structures are the oldest and D_3 folds are the youngest. The first three generations (D_{1a} to D_{1c}) are probably the result of one continuous deformation. Structural elements of the Araya Peninsula are shown in Fig. 3 and simplified models of the structures are shown in Fig. 4. All four belts of the Araya

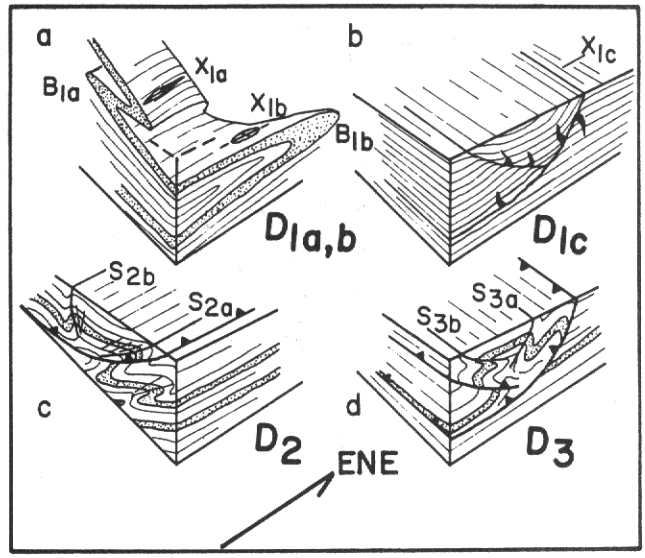

Figure 4. Sketches of deformational structures in metamorphic rocks of the Araya Peninsula. 1) D_{1a} and D_{1b} structures: isoclinal B_{1a} fold, B_{1b} sheath fold, major principal extensions X_{1a} and X_{1b}, all trending northeasterly. b) D_{1c} structures: northeast and southwest dipping extensional shear zones/normal faults with sigmoidal quartz veins (black); major principal extension X_{1c}. c) D_2 structures: southeast vergent thrust fault and fold with rare northwest vergent fold; S_{2a} and S_{2b} are fold-axial planes. d) D_3 structures: northeast and southwest vergent thrust faults and folds; S_{3a} and S_{3b} are fold axial planes.

Peninsula have undergone the same deformational history: every generation of folds (D_{1a} to D_3) is found in each belt. Furthermore, the metamorphic rocks of Margarita Island have suffered the same deformations as those of the Araya Peninsula (Guth and Avé Lallemant, this volume).

Both D_{1a} and D_{1b} folds are synmetamorphic. They are isoclinal. The fold axes of both trend east-west to northeast-southwest (fig. 3b). Thus, they are difficult to separate, except for the rare outcrops where the second is seen to deform the first. Numerous east-northeast trending stretching lineations and stretched pebble elongations (parallel to the major extension axis X of the finite strain ellipsoid) (fig. 3c) were observed. They are related to both D_{1a} and D_{1b} deformations. A few D_{1b} sheath folds were observed indicating east-northeasterly extension. Kinematic indicators suggest that dextral shear has occurred on the S_{1a} foliations.

The third (D_{1c}) deformation is characterized by a conjugate set of north-trending extensional kink bands, extensional shear zones, and normal faults, dipping to the east or the west (fig. 3d) with north-trending fold axes (fig. 3e). Displacement directions trend easterly or westerly (fig. 3f). This deformation is late synmetamorphic, and is characterized by dissolution and deposition of quartz and calcite along the shear planes. No radiometric ages exist for the metamorphic rocks of the Araya Peninsula. However, the deformations on Araya can be correlated with those on Margarita Island (Guth and Avé Lallemant, this volume): radiometric ages of 70 to 80 Ma (K/Ar, amphibole) may date the age of uplift and thus, the age of the

D_{1c} folding event (Santamaría and Schubert, 1974; Loubet et al., 1985; Chevalier et al., 1988).

The fourth generation of folds (D_2) is clearly postmetamorphic. The S_{1a} and S_{1b} foliations (fig. 3a) were folded about northeast trending fold axes (fig. 3h). Most folds are southeast vergent and have northwest dipping axial planes and cleavages (fig. 3g), but northwest vergent folds also occur. Often it can be shown that the D_2 folds are related to thrust faults, mostly northwest and sometimes southeast dipping (fig. 3i). The D_2 event postdates D_{1c} and predates deposition of Pliocene rocks on the Araya Peninsula. This deformation can be correlated with the main deformation in the Serrania del Interior, which according to Rossi (1985) occurred during the Miocene, but may have started in the Oligocene.

A fifth generation of folds (D_3) is characterized by north-northwest trending axial planes and cleavages (fig. 3j) and fold axes (fig. 3k). These folds are related to a conjugate set of thrust and reverse faults which dip northeast and southwest (fig. 3l). East-northeasterly trending normal faults (fig. 3l) may be related to the D_3 phase. The D_3 structures are only locally developed and they are not penetrative. On Araya, no time constraints have been found beyond the fact that these structures postdate D_2 structures. However, they can be correlated with structures along the El Pilar fault (Vierbuchen, 1984), in the hills south of Cumaná (Ascanio, 1972), and along the San Francisco fault zone (fig. 1) suggesting that they formed in Pliocene to Recent time.

PLATE TECTONIC MODEL

Relative plate motion trajectories of South America with respect to North America indicate that from the Late Triassic until the Eocene (49 Ma) North and South America were drifting apart and that from Eocene to Recent, the two plates converged slightly (Pindell et al., 1988). Thus, it is difficult to conceive that the Cretaceous Leeward Antilles volcanic island arc and the Cretaceous metamorphism of the Margarita terrane and the Cordillera de la Costa belt are related to plate convergence, subduction, and collision of the Proto-Caribbean and South American plates. It is much more likely that these terranes are allochthonous and were formed far to the west as the result of the interaction of the Farallon plate and the Proto-Caribbean plate (Ross and Scotese, 1988; Pindell et al., 1988; Pindell and Barrett, 1990). The structures in the Araya Peninsula are compatible with such hypothesis.

The Margarita terrane containing the high P/T eclogite and blueschist knockers, must have formed in a subduction complex (e.g., Ernst, 1988). The D_{1a}, D_{1b}, and D_{1c} structures were formed one after the other at decreasing depth: on Margarita Island D_{1a} formed at 40 km depth and D_{1c} at 20 km (Maresch and Abraham, 1981) and on the Araya Peninsula D_1 formed at 20 km depth, D_{1b} may have formed at 10 km (Schubert, 1971), and D_{1c} at even shallower levels. The major principal extension axes (X-axes) of all three phases are subparallel to the terrane boundaries. Such a situation has been described before in blueschist terranes in Japan (Faure, 1985; Toriumi and Noda, 1986) and was ascribed to suture-parallel simple shear in an oblique subduction zone. Kinematic indicators related to the D_{1a} deformation on Araya suggest that the Venezuelan terranes formed in a right-oblique subduction zone.

The D_{1c} structures clearly indicate suture-parallel extension. Similar structures have been described before in areas of oblique plate convergence; e.g. in the Kuril arc (Kimura, 1986), in the Ryukyu arc (Kuramoto and Konishi, 1989), and the Aleutian arc (Ryan and Scholl, 1989). As the three synmetamorphic deformational phases D_{1a}, D_{1b}, and D_{1c} appear to have formed consecutively while the rocks were being decompressed, it is suggested here that they all formed by suture-parallel extension but with a component of dextral simple shear. This suture-parallel extension may be the result of an increase of obliquity of plate convergence (obliquity is 0°, if the relative plate convergence is perpendicular to the subduction zone; if the obliquity increases to 90°, the plate boundary becomes a transform fault). It is known that forearc terranes, bounded by the subduction zone and a suture-parallel intra-arc strike-slip fault, can be displaced parallel to the subduction zone at a rate equal to the suture-parallel component of the plate convergence velocity (Jarrard, 1986; Avé Lallemant and Oldow, 1988). If the obliquity increases because of the arcuate shape of the volcanic island arc, the suture-parallel displacement rate of the forearc terrane has to increase with the consequence that the terrane will be stretched parallel to the suture. At the same time the subduction component decreases and to reestablish isostatic equilibrium, the subduction complex is uplifted (Avé Lallemant and Guth, 1990). This hypothesis is not inconsistent with plate tectonic models for the Caribbean (fig. 5a). Between about 100 and 70 Ma a fragment of the Farallon plate may have moved northeastward in between North and South America (Ross and Scotese, 1988). The Aves Ridge and the Leeward Antilles (AR and LA in fig. 5a, respectively) were at this time a northeast-facing volcanic arc. Plate convergence was right-oblique and the increase in obliquity (from P to Q in fig. 5a) caused D_1 stretching in and uplift of the accretionary complex as observed on Margarita Island and the Araya Peninsula. At about 80 Ma, the obliquity increased to 90° (point R in fig. 5a), subduction ceased, the Leeward Antilles arc became extinct (Beets et al., 1984), and uplift of the accretionary complex continued. This accretionary complex differs from most other complexes in that it not only includes oceanic rocks (ultramafic and mafic rocks, and deep-water or distal sedimentary rocks), but also continental margin deposits (graphitic and calcareous shales and sandstones, limestone, and conglomerate) and even slivers of Paleozoic and Precambrian granitic gneisses (Ostos, 1990), presumably scraped off northwestern South America.

Between 50 and 65 Ma (Pindell et al., 1988; Ross and Scotese, 1988) the Aves Ridge collided with the Bahama platform and the Caribbean plate started to migrate eastward with respect to South America (fig. 5b). The main contact between the Caribbean and South American plates jumped to the south and the Margarita and Cordillera de la Costa terranes were included in the Caribbean plate. During the eastward migration of the Caribbean, these terranes were situated in a transpressional tectonic setting. It is in this setting that the D_2 structures in the Araya Peninsula were formed. The following hypothesis relates these structures to eastward displacement of the Lesser Antilles/Aves Ridge and Leeward Antilles arcs which acted as a snowplow pushing the allochthonous accretionary wedge and the autochthonous passive margin deposits sideways to the southeast (fig. 6). In the model, the Caribbean plate (CP) moves eastward with respect to the South American plate (SAP) at a rate of ${}_SV_C$. Along the oblique contact P_0Q_0 strike-slip motion occurs at a rate V_T. The component V_N, normal to P_0Q_0, causes a slice (T_1) of the sedimentary apron overlying the South

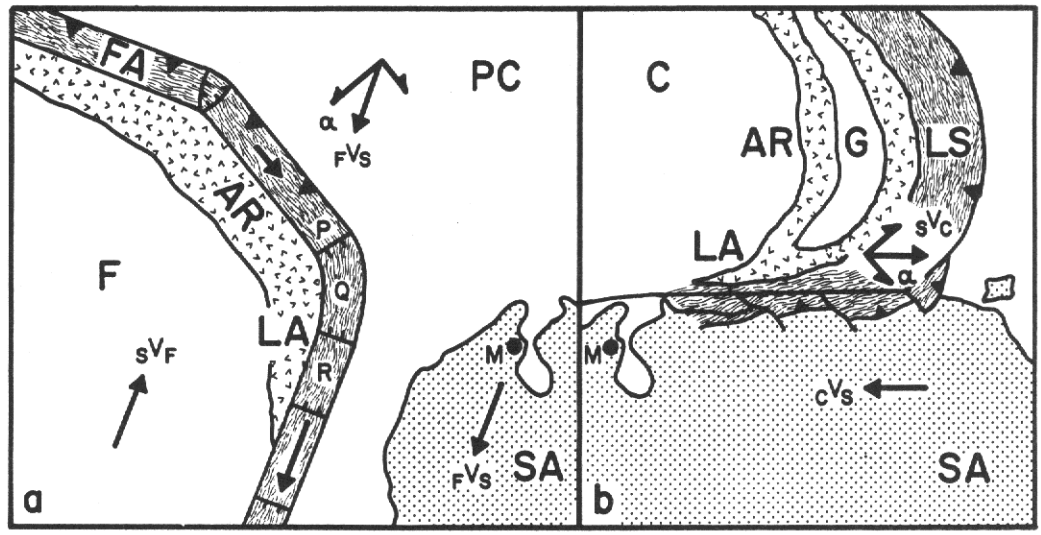

Figure 5. Plate tectonic reconstructions of the southeastern Caribbean for Senonian (a) and Miocene (b) times, modified after Ross and Scotese (1988); AR = Aves Ridge, C = Caribbean plate, F = Farallon plate, FA = forearc terrane, G = Grenada Basin, LA = Leeward Antilles, LS = Lesser Antilles, M = Maracaibo, PC = Proto-Caribbean plate, SA = South America. a) Relative rate of convergence of PC with respect to F is ${}_{F}V_{S}$. At point P, convergence is right-oblique with obliquity a of 30°; suture-parallel velocity of FA is ${}_{F}V_{S}$ sin 30° = $\frac{1}{2}$ ${}_{F}V_{S}$. Plate boundary at R is a transform; thus, obliquity is 90° and the relative velocity of FA at R is ${}_{F}V_{S}$ sin 90° = ${}_{F}V_{S}$. Thus, suture-parallel displacement rate of FA increased by 100% from P to R causing stretching (suture-perpendicular normal faults). b) Relative displacement rate of C with respect to SA is ${}_{S}V_{C}$. Boundary between C and SA is a transform. Southeast-directed thrusting in northern Venezuela is the result of ${}_{S}V_{C}$ sin a.

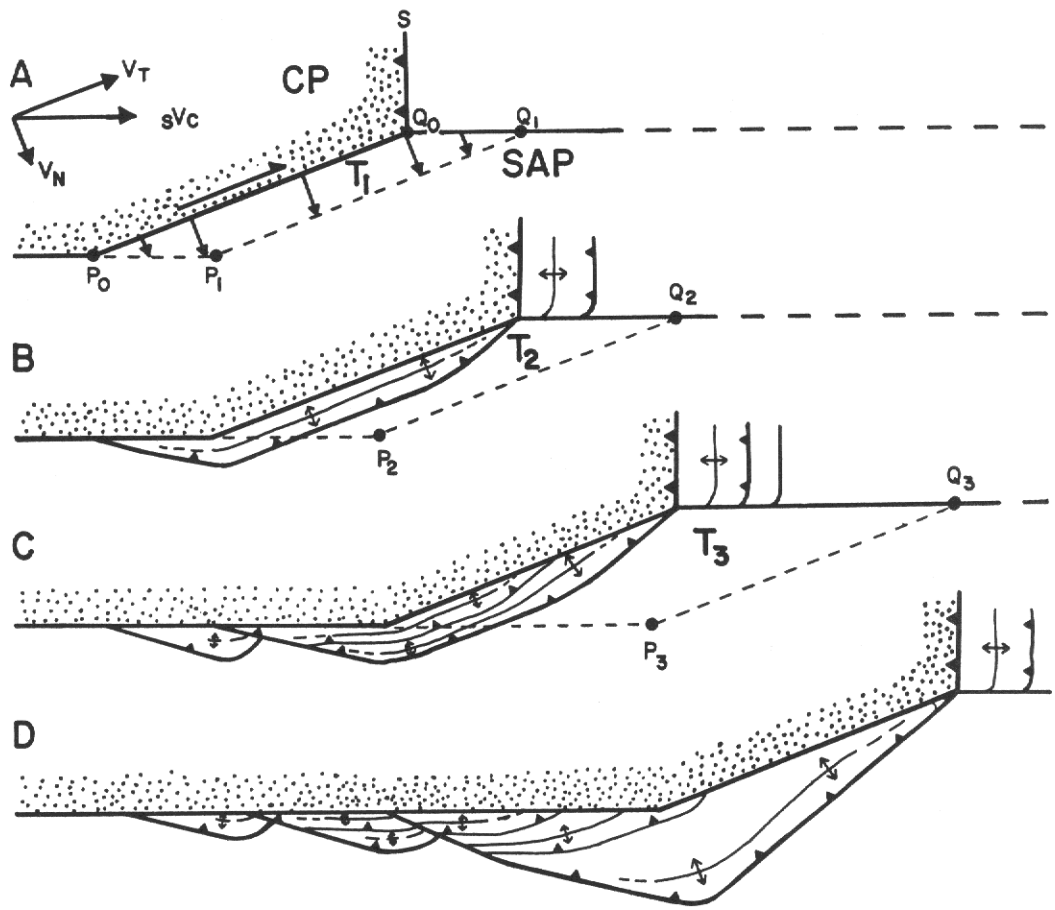

Figure 6. "Snowplow" model for the structural development of the Serrania del Interior fold and thrust belt. See text for explanation.

American basement to be folded and thrust toward the south-southeast. At the same time, relatively thin, distal continental margin sediments are being folded and thrust eastward and partly subducted at the subduction zone S. When the Caribbean plate arrives at P_1Q_1, another slice (T_2) is folded and thrust to the south-southeast. Folds in the first thrust slice (T_1) riding piggy-back style on T_2 may be tightened. This process repeats itself several times (fig. 6C, D). This model is consistent with the decreasing age of deformation and of the basal unconformity in the foreland basin from west to east (e.g. Bellizzia, 1986) and with the style of deformation. However, seismicity along the Urica and San Francisco faults and within the fold and thrust belt (Vierbuchen, 1978) cannot be explained by the snowplow model because the Lesser Antilles arc passed by the area a long time ago. The deformation responsible for the seismicity may be relted to the small convergence between North and South America (Pindell et al., 1988).

The D_3 structures, recognized in the Araya Peninsula, are much better developed near the El Pilar fault (Vierbuchen, 1984) and the San Francisco fault. Similar structures occur in the Miocene to lowermost Pleistocene clastic deposits near Cumaná (Ascanio, 1972). These structures may be related to restraining bends and left stepping of the dextral east trending El Pilar strike-slip fault (fig. 2).

A speculative north-south cross section through the entire Caribbean-South American plate boundary zone at the approximate longitude of Margarita Island and the Araya Peninsula is shown in Fig. 7. The plate boundary zone is almost 300 km wide and consists of allochthonous belts which all share a common decollement surface. This entire zone may be called an "orogenic float" after Laubscher (see Oldow et al., 1989). The cross section is to some extent based on Bellizzia et al. (1976), Biju-Duval et al. (1983), Case et al. (1984), and Rossi (1985). The following eleven comments are related to the locations 1 to 11 in Fig. 7:

(1) The thickness of the Caribbean oceanic crust is taken from Case et al. (1984). It is not known whether it consists of volcanic arc material (Aves Ridge) or of the typical anomalously thick Caribbean oceanic crust.

(2) South-dipping reflectors, north of La Blanquilla Island, may indicate minor Neogene underflow of the Caribbean plate underneath the South American plate (Biju-Duval et al., 1983), related to Neogene convergence between North and South America.

(3) A major positive Bouguer anomaly (Bellizzia et al., 1976) may require the occurrence of a peridotite slab at depth. This slab may have been emplaced during the Oligocene/Miocene D_2 deformation.

(4) The western Leeward Antilles arc was active until about 80 Ma (Beets et al., 1984). Latest Cretaceous/earliest Paleogene biotite K/Ar dates of trondhjemites of La Blanquilla Island (Santamaría and Schubert, 1974) may be uplift ages or may indicate a somewhat later cessation of arc magmatism in the east.

(5) The Atlantic oceanic crust, subducted at the Lesser Antilles subduction zone, is stretched and boudinaged. Presently, it may be a rather wide ductile shear zone.

(6) Serpentinized peridotites, schists, arc plutons, and Eocene sediments exposed on Margarita Island are thrust northward during the Oligocene to Miocene D_2 deformation (Guth and Avé Lallemant, this volume). The contact between the Eocene and older rocks is sheared. Peridotite bodies larger than those exposed on Margarita may occur at depth to explain a major positive Bouguer anomaly over Margarita Island (Bellizzia et al., 1976).

(7) Between Margarita Island and the Araya Peninsula several east-west striking dextral strike-slip faults have been postulated. Here, only one such fault, the Coche fault (Feo-Codecido et al., 1984) is shown; it (fig. 1) may be the continuation of the North Coast fault zone, north of Trinidad (Robertson and Burke, 1989). Several Neogene east-west striking normal faults observed by Biju-Duval et al. (1983) and in Bellizzia (1986) are not shown for simplicity (but see fig. 2).

(8) Several east-west trending faults (not shown in fig. 7 for simplicity) were mapped in the Araya Peninsula (fig. 2) by Schubert (1971). These faults separate higher-grade metamorphic rocks to the north from lower-grade ones to the south. Thus, they can be interpreted as thrust faults which have been active during the Oligocene/Miocene. Slickenside lineations (Schubert, 1971) indicate that they became strike-slip faults subsequently.

(9) The dextral El Pilar strike-slip fault has been active from the Oligocene to the Present (Pérez and Aggarwal, 1981; Vierbuchen, 1984). As Oligocene/Miocene shortening in the foreland fold and thrust belt amounted to at least 40 km (Rossi, 1985) and perhaps even two to three times as much (Felipe Audemard, personal communication, 1990), the El Pilar fault must have migrated southward considerably along the same decollement surface lying beneath the fold and thrust belt.

(10) Several thrust faults (fig. 2) have been mapped in the Serrania del Interior fold and thrust belt (Bellizzia et al., 1976; Rossi, 1985); only five are shown in fig. 7 for simplicity. It should be noted that nothing is known about the deeper parts of the belt.

(11) A strong negative Bouguer anomaly has been interpreted by Potié (1989) to indicate a deep foreland basin which caused a down flexure of the crust. Other alternatives, such as lower bulk densities of the basin sediments and higher densities caused by repeated Cretaceous section in the hinterland may explain the gravity anomaly as well (Felipe Audemard, personal communication, 1990).

PRELIMINARY CONCLUSIONS AND PROBLEMS

The Caribbean - South American plate boundary zone in eastern Venezuela consists of four tectonostratigraphic terranes: 1) the Leeward Antilles volcanic island arc, 2) the Margarita terrane, a subduction complex or forearc terrane, characterized by high P/T metamorphic rocks, 3) the Cordillera de la Costa belt consisting of intermediate to low P/T metamorphic rocks, the protolith of which may have been deposited on a passive continental margin, and 4) the foreland fold and thrust belt of the Serrania del Interior. The first three terranes are probably of Cretaceous age; the fourth consists of Cretaceous and Paleogene passive margin deposits and Neogene orogenic sediments. The contact between the metamorphic belts and the foreland fold and

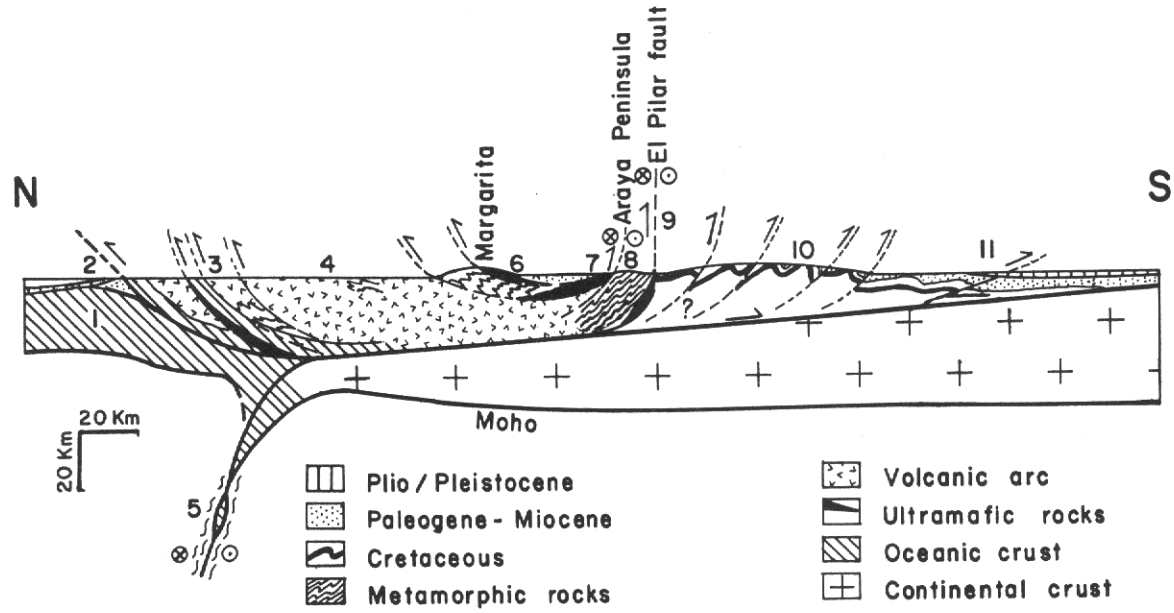

Figure 7. Speculative north-south cross section through the Caribbean - South American plate boundary zone at the approximate longitude of Isla de Margarita and Araya Peninsula. See text for discussion.

thrust belt, is the east trending right-lateral El Pilar strike-slip fault.

All terranes north of the El Pilar fault have undergone the same deformational history. Five generations of folds were recognized. The first three (D_{1a} to D_{1c}) may have formed in the Late Cretaceous; the fourth (D_2) in the Oligocene/Miocene; and the fifth in the Pliocene to Recent.

The first deformation (D_{1a}) is synchronous with high P/T metamorphism in the Margarita terrane and intermediate P/T metamorphism in the Cordillera de la Costa belt. It is characterized by isoclinal folds. The fold axes trend east-northeasterly and are parallel to the principal extension X_{1a}. The D_{1b} structures are coaxial and coplanar with D_{1a}. They formed at lower P/T conditions. The D_{1c} structures are late synmetamorphic. They clearly formed by east-west extension. This stretching parallel to the suture zone may be the result of increased obliquity of plate convergence (increase of the strike-slip component parallel to the suture) and thus of increased suture-parallel displacement rate of the forearc terrane.

The D_2 structures of Araya are mainly southeast vergent folds and thrust faults. They are correlated with the Oligocene/Miocene structures in the foreland fold and thrust belt in the Serrania del Interior. These structures resulted from southeastward displacement which may not have been the result of northwest-southeast convergence of South and North America, but of the eastward migration of the Caribbean plate. The Lesser Antilles/Aves Ridge and Leeward Antilles arcs may have acted as a "snowplow" pushing the terranes sideways toward the southeast.

The D_3 structures are directly related to the displacements along the El Pilar fault. They formed during the Pliocene to the Present.

Many problems are still to be solved. The main problems are related to poor age constraints. There are no faunal nor radiometric ages available for the Araya Peninsula. A few samples are currently being prepared for $^{40}Ar/^{39}Ar$ dating to constrain the age of metamorphism and/or uplift.

The age of formation of the Caribbean seafloor is not well-constrained either. The Caribbean crust is much thicker than normal oceanic crust (Case et al., 1984) and may represent an oceanic plateau formed within the Farallon plate. The collision of the plateau with the Proto-Caribbean plate is thought to be the cause of the flip of the subduction zone and the resulting insertion of this plateau (Caribbean plate) between North and South America (Pindell et al., 1988). The Caribbean plate is often correlated with the B" reflector which may be of Campanian age. If correct, the subduction reversal must be post-Campanian in age (Pindell et al., 1988; Pindell and Barrett, 1987). Ross and Scotese (1988) argue, however, for an Albian (~100 Ma) subduction reversal. Thus, it is imperative to start a deep-drilling program in the Caribbean to learn the composition and age of the Caribbean crust.

Another problem is related to the relatively local nature of the present study. Additional studies are needed in northern and northwestern Venezuela and in Columbia to test the proposed hypotheses. These studies should include structural analysis and age dating.

ACKNOWLEDGMENTS

This study was supported by a grant from the National

Science Foundation (EAR-8517383). Critical comments by David Larue and discussions with Felipe Audemard and Marino Ostos were very helpful.

REFERENCES

Ascanio, G.T., 1972, Geología de los cerros de Caigüire, Cumaná, Estado Sucre: IV Congr. Geol.Venez. Mem., v. 3, p. 1279-1286.

Avé Lallemant, H.G., and Guth, L.R., The role of extensional tectonics in the exhumation of eclogites and blueschists in an oblique subduction setting: northwestern Venezuela: Geology, v. 18, in press.

Avé Lallemant, H.G., and Oldow, J.S., 1988, Early Mesozoic southward migration of Cordilleran transpressional terranes: Tectonics, v. 7, p. 1057-1075.

Beck, C., 1985, Las napas de Aragua-Cadena Caribe central y la historia Mesozóica del margen sur del Caribe a lo largo del meridiano de Caracas: Symposium on Caribbean Geodynamics, edited by Mascle, A., Editions Technip, Paris, p. 541-551.

Beets, D.J., Maresch, W.V., Klaver, G.T., Mottana, A., Bocchio, R., Beunk, F.F., and Monen, H.P., 1984, Magmatic rock series and high pressure metamorphism as constraints on the tectonic history of the southern Caribbean, in The Caribbean - South American plate boundary and regional tectonics, edited by Bonini, W.E., Hargraves, R.B., and Shagam R.: Geol. Soc. America Mem. v. 162, p. 95-130.

Bellizzia, A., 1986, Sistema montañoso del Caribe - una cordillera alóctona en la parte norte de América del Sur: VI Congr. Geol.Venez. Mem., v. 10, p. 6657-6836.

Bellizzia, A., Pimentel, N., and Bajo, R., 1976, Mapa geológica estructural de Venezuela (1:500,000): Venezuela Ministerio de Minas e Hidrocarburos.

Biju-Duval, B., Mascle, A., Rosales, H., and Young, G., 1983, Episutural Oligo-Miocene basins along the north Venezuelan margin, in Studies in continental margin geology, edited by Watkins, J. S., and Drake, C. L.: American Assoc. Petrol. Geol. Mem., v. 34, p. 347-358.

Case, J.E., Holcombe, T.L., and Martin, R.G., 1984, Map of geologic provinces in the Caribbean region, in The Caribbean - South American plate boundary and regional tectonics, edited by Bonini, W.E., Hargraves, R. B., and Shagam, R.: Geol. Soc. America Mem. v. 162, p. 1-30.

Castro, M., and Mederos, A., 1985, Litoestratigrafía de la Cuenca de Carúpano: VI Congr. Geol.Venez. Mem., v. 1, p. 200-225.

Chevalier, Y., 1987, Les zones internes de la chaîne sud-caraibe sur le transect: Ile de Margarita - Péninsule d'Araya (Venezuela): Ph.D. thesis, 464 p., Université de Bretagne Occidentale, Brest.

Chevalier, Y., Stephan, J.-F., Darboux, J.-R., Gravelle, M., Bellon, H., Bellizzia, A., and Blanchet, R., 1988, Obduction et collision pré-Tertiaire dans les zones internes de la Chaîne Caraïbe Vénézuélienne, sur le transect Ile de Margarita-Péninsule d'Araya: C. R. Acad. Sci., Paris, v. 307, s. II, p. 1925-1932.

Duncan, R.A., and Hargraves, R.B., 1984, Plate tectonic evolution of the Caribbean region in the mantle reference frame, in The Caribbean - South American plate boundary and regional tectonics, edited by Bonini, W.E., Hargraves, R.B., and Shagam, R.: Mem. Geol. Soc. America, v. 162, p. 81-93.

Engebretson, D.C., Cox, A., and Gordon, R.G., 1985, Relative motions between oceanic and continental plates in the Pacific basin: Spec. Paper Geol. Soc. America, v. 206, 59 p.

Ernst, W.G., 1988, Tectonic history of subduction zones inferred from retrograde blueschist P-T paths: Geology, v. 16, p. 1081-1084.

Faure, M., 1985, The pre-Cretaceous structure of the outer belt of southwest Japan: Tectonophysics, v. 113, p. 139-162.

Feo-Codecido, G., Smith, F.D. Jr., Aboud, N., and de Di Giacomo, E., 1984, Basement and Paleozoic rocks of the Venezuelan Llanos basins, in The Caribbean-South American plate boundary and regional tectonics, edited by Bonini, W.E., Hargraves, R.B., and Shagam, R.: Mem. Geol. Soc. America, v. 162, p. 213-216.

González de Juana, C., Muñoz, N.G., and Vigali, M., 1972, Reconocimiento geológico de la Peninsula de Paria, Venezuela: IV Congr. Geol.Venez. Mem., v. 3, p. 1549-1586.

Jarrard, R.D., 1986, Terrane motion by strike-slip faulting of forearc slivers: Geology, v. 14, p. 780-783.

Kimura, G., 1986, Oblique subduction and collision: forearc tectonics of the Kuril arc: Geology, v. 14, p. 404-407.

Kuramoto, S., and Konishi, K., 1989, The southwest Ryukyu arc is a migrating microplate (forearc sliver): Tectonophysics, v. 163, p. 75-91.

Loubet, M., Montigny, R., Chahati, B., Duarte, N., Lambret, B., Martin, C., and Thuizat, R., 1985, Geochemical and geochronological constraints on the geodynamic development of the Caribbean Chain of Venezuela: Symposium on Caribbean Geodynamics, edited by Mascle, A., Edition Technip, Paris, p. 553-566.

Maresch, W.V., 1974, Plate tectonics origin of the Caribbean Mountain System of Northern South America: discussion and proposal: Geol. Soc. America Bull., v. 85, p. 669-682.

_____, 1975, The geology of northeastern Margarita Island, Venezuela: a contribution to the study of Caribbean plate margins: Geol. Rundschau, v. 64, p. 846-883.

Maresch, W.V., and Abraham, K., 1981, Petrography, mineralogy, and metamorphic evolution of an eclogite from the Island of Margarita, Venezuela: Journ. Petrology, v. 22, p. 337-362.

Morgan, W.J., 1981, Hotspot tracks and the opening of the Atlantic and Indian Oceans, in The Sea: edited by Emiliani, C., Interscience-Wiley, New York, v. 7, p. 443-475.

Navarro, E., 1981, Relaciones mineralógicas en las rocas eclogitas de la Isla de Margarita, Estado Nueva Esparta: Geos, (Escuela de Geol. Minas, U.C.V.) v. 26, p. 3-44.

Oldow, J.S., Bally, A.W., Avé Lallemant, H.G., and Leeman, W.P., 1989, Phanerozoic evolution of the North American Cordillera; United States and Canada: in The Geology of North America, Vol. A, The Geology of North America - An overview, edited by Bally, A.W., and Palmer, A.R.: Geol. Soc. America, p. 139-232.

Ostos, M., 1990, Tectonic evolution of the south-central Caribbean based on geochemical data: Ph.D. thesis, 411 p., Rice University, Houston.

Pereira, J.G., 1985, Evolución tectónica de la Cuenca de Carúpano durante el Terciario: VI Congr. Geol.Venez. Mem., v. 4, p. 2618-2648.

Pérez, O.J., and Aggarwal, Y.P., 1981, Present-day tectonics of the southeastern Caribbean and northeastern Venezuela: Jour. Geophys. Research, v. 86 (B11), p. 10,791-10,804.

Pindell, J.L., and Barrett, S.F., Geological evolution of the Caribbean region; a plate-tectonic perspective, The Geology of North America, Vol. H, The Caribbean Region: Geol. Soc. America, in press.

Pindell, J.L., Cande, S.C., Pitman, W.C. III, Rowley, D.B., Dewey, J.F., Labrecque, J., and Haxby, W., 1988, A plate-kinematic framework for models of Caribbean evolution: Tectonophysics, v. 155, p. 121-138.

Potié, G., 1989, La Serrania del Interior sur le transect Cumana - Urica et le bassin de Maturin (Vénézuéla): Ph.D. thesis, 226 p., Univeristé de Bretagne Occidentale, Brest.

Robertson, P., and Burke, K., 1989, Evolution of southern Caribbean plate boundary, vicinity of Trinidad and Tobago: American Assoc. Petrol Geol. Bull., v. 73, p. 490-509.

Ross, M.I., and Scotese, C.R., 1988, A hierarchical tectonic model of the Gulf of Mexico and Caribbean region: Tectonophysics, v. 155, p. 139-168.

Rossi, T., 1985, La Serrania del Interior Oriental (Venezuela) sur le transect Cariaco - Maturin: Ph.D. thesis, 369 p., Université de Bretagne Occidentale, Brest.

Rossi, T., Stephan, J.-F. Blanchet, R., and Hernandez, G., 1987, Étude géologique de la Serrania del Interior Oriental (Venezuela) sur le transect Cariaco - Maturin: Rev. Inst. fran. pét., v. 42, p. 3-30.

Ryan, H.F., and Scholl, D.W., 1989, The evolution of forearc structures along oblique convergent margins, central Aleutian arc: Tectonics, v. 8, p. 497-516.

Santamaría, F., and Schubert, C., 1974, Geochemistry and geochronology of the southern Caribbean - northern Venezuela plate boundary: Geol. Soc. America Bull., v. 85, p. 1085-1098.

Schubert, C., 1971, Metamorphic rocks of the Araya Peninsula, eastern Venezuela: Geol. Rundschau, v. 60, p. 1571-1600.

Schubert, C., and Moticska, P., 1973, Reconocimiento geológico de las Islas Venezolanas en el Mar Caribe, entre Los Roques y Los Testigos (Dependencias Federales), II, Islas Orientales y Conclusiones: Acta Cient. Venez., v. 24, p. 19-31.

Seijas, F.J., 1972, Geologia de la región de Carúpano: IV Venez. Geol. Congr. Mem., v. 3, p. 1887-1922.

Sharp, W.D., and Snoke, A.W., 1988, Tobago, West Indies: Geochronological study of a fragment of a composite Mesozoic oceanic island arc: Geol. Soc. America Abst. with Programs, v. 100, p. A60.

Speed, R.C., 1985, Cenozoic collision of the Lesser Antilles arc and continental South America and the origin of the El Pilar Fault: Tectonics, 4, 41-69.

Stephan, J.F., 1985, Andes et chaîne caraïbe sur la transversale de Barquisimeto (Venezuela): évolution géodynamique, Symposium on Caribbean Geodynamics, edited by Mascle, A., Edition Technip, Paris, p. 505-529.

Talukdar, S., and Loureiro, D., 1982, Geología de una zona ubicada en el segmento norcentral de la Cordillera de la Costa, Venezuela: Metamorfismo y deformacíon. Evolucíon del margen septentrional de Suramérica en el marco de la tectónica de placas: Geos, (Escuela Geol. Minas, U.C.V.), v. 27, p. 5-76.

Toriumi, M., and Noda, H., 1986, The origin of strain patterns resulting from contemporaneous deformation and metamorphism in the Sambagawa metamorphic belt: Journ. Metamorphic Geology, v. 4, p. 409-420.

Vierbuchen, R.C., 1978, The tectonics of northeastern Venezuela and the southeastern Caribbean Sea: Ph.D. thesis, 175 p., Princeton University, Princeton.

_____, 1984, The geology of the El Pilar fault zone and adjacent areas in northeastern Venezuela, in The Caribbean - South American plate boundary and regional tectonics, edited by Bonini, W.E., Hargraves, R.B., and Shagam, R.: Geol. Soc. America Mem., v. 162, p. 189-212.

Vignali, M., 1979, Estratigrafía y estructura de las cordilleras metamorficas de Venezuela oriental (península de Araya - Paria e Isla Margarita), Geos, (Escuela Geol. Minas, U.C.V.), v. 25, p. 19-66.

A KINEMATIC HISTORY FOR EASTERN MARGARITA ISLAND, VENEZUELA

L. R. Guth and H. G. Avé Lallemant
Department of Geology and Geophysics
Rice University
P.O. Box 1892 Houston, TX 77251

ABSTRACT

Amphibolites, schists, and minor marble, together with serpentinized ultramafics and leucocratic igneous rocks, make up the metamorphic nucleus of Margarita Island. Knockers of eclogite found within the amphibolites and schists tie the island to similar rocks along the southern Caribbean coast characterized by the occurrence of high pressure metamorphic assemblages. This metamorphic belt is one of several exposed in the Caribbean Mountain System which extends from Tobago to Barquisimeto, parallel to the Caribbean-South American plate boundary.

Five generations of deformational structures have been identified on Margarita Island. The earliest deformation (D_{1a}) is rarely preserved. It occurs as the main foliation in the eclogite knockers and as a crenulated foliation within microlithons bounded by the foliation of the next deformation (D_{1b}). The D_{1b} phase of deformation is synchronous with epidote-amphibolite to greenschist facies metamorphism and formed the dominant metamorphic foliation which is axial planar to associated isoclinal folds. Following this stage of deformation, S-C and quartz c-axis fabrics developed which indicate SW-NE extensional deformation (D_{1c}). All D_1 phases may have occurred in the Cretaceous. In the Oligocene/Miocene, the D_2 phase of deformation folded the D_{1b} foliation into a northwest-vergent anticlinorium that plunges to the SW. The latest brittle deformation (D_3) also shows SW-NE extension.

All fold axes and extensions are aligned SW-NE. This is best explained by a continued component of dextral strike-slip deformation since the mid-Cretaceous. The data are consistent with recent plate kinematic models in which the rocks of Margarita formed far to the west along the Farallon-South American plate margin. The preserved deformations then reflect long-term dextral transport of these rocks along the southern boundary of a Farallon plate fragment as it rafted between the Americas to become the modern day Caribbean plate.

INTRODUCTION

The Caribbean-South American boundary is a complex region of plate interactions. The current boundary is diffuse, encompassing a width of several hundred kilometres and complicated by internal plate deformation (Case and others, 1984; Mann and Burke, 1984; Mascle and others, 1985). Adding to the confusion, most workers (for a review, see table 2 of Pindell and Barrett, in press) now believe that the modern Caribbean plate is a far-traveled oceanic plateau born in the Pacific Basin. Ocean crust, formed during the separation of the Americas, has been subducted beneath the more buoyant Caribbean crust and thus much of the evidence for the early history of the boundary has been destroyed.

Given the above limitations, it is unlikely that the rock record from any one area would contain the necessary and sufficient evidence to completely reveal the Caribbean tectonic history. Study of the current rocks in their current locations can, at best, provide only circumstantial evidence. With enough data from enough areas only a few of the proposed tectonic models will explain all observations. This study on the kinematic history of eastern Margarita Island provides one such line of evidence, that together with other studies elsewhere may help constrain the tectonic history of the southern Caribbean.

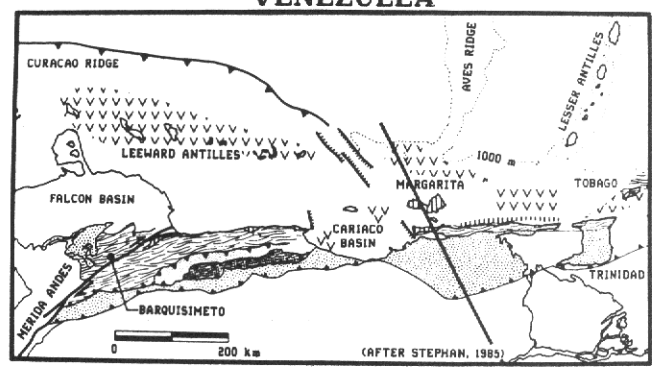

Figure 1. Simplified geologic map of the southern Caribbean and northern Venezuela, after Stephan (1985). The line of the schematic section in figure 2 is shown by the heavy line through Margarita.

REGIONAL GEOLOGY

Margarita Island is located in the southeastern Caribbean Sea (figure 1), where the metamorphic belts of northern South America intersect the arcuate trends of the Aves Ridge, the remains of a Late Cretaceous-Paleogene magmatic arc, and the Neogene Lesser Antilles volcanic arc (Case and others, 1984). The metamorphic belts of the Caribbean Mountain System are defined by lithologic and metamorphic affinities, but age constraints are poor. Some of the most recent descriptions of the metamorphic belts have been published by Case and others (1984), Stephan (1985) and Bellizzia (1986).

Preserved on the Leeward Antilles and Tobago and encountered in some wells drilled between the islands are portions of a Cretaceous magmatic arc. Along the coast, including parts of Margarita Island, is the narrow Coastal Fringe-Margarita nappe characterized by the occurrence of eclogite and blueschist facies rocks. The Cordillera de la Costa nappe is composed of a Paleozoic to Precambrian gneissic basement (Pimentel and others, 1985; Ostos, 1990) unconformably overlain by Mesozoic sedimentary and volcanic rocks (Case and others, 1984; Bellizzia, 1986), all metamorphosed in the Mesozoic to the greenschist facies. Grouped together for simplicity in figure 1 are the rocks labeled Tinaco-Tinaquillo-Paracotos terranes. These include Paleozoic metamorphic rocks of the El Tinaco basement complex (Case and others, 1984; Loubet and others, 1985); the alpine peridotites of the Tinaquillo ultramafic massif (Bellizzia, 1986); the Loma de Hierro

Larue, D.K., and Draper, G., eds.,
Transactions of the 12th Caribbean Conference,
St. Croix U.S.V.I., Miami Geological Society,
P.O. Box 14433, Coral Gables, FL 33114

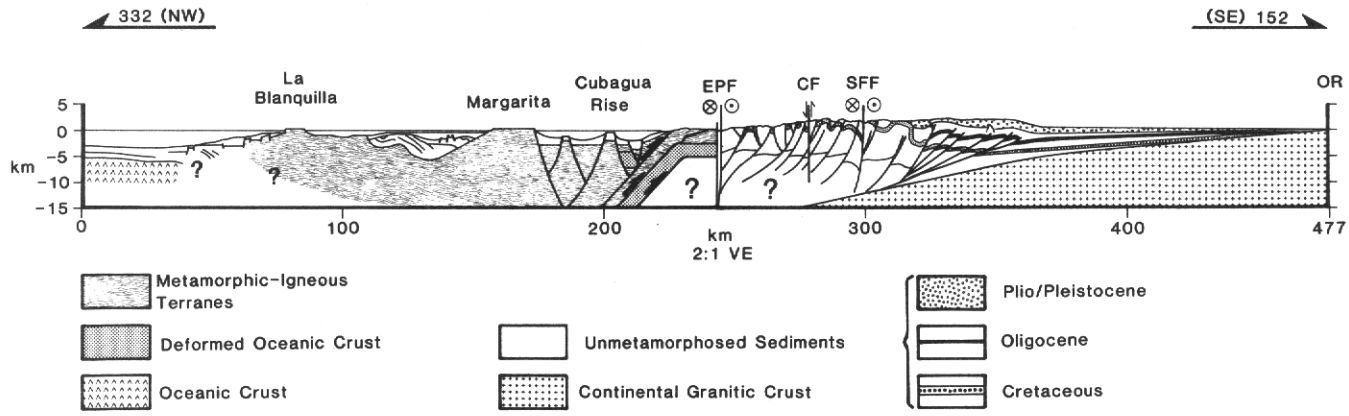

Figure 2. Regional schematic cross section from the Venezuelan Basin to the Orinoco River. The data for this section have been compiled from several published sources (Biju-Duval and others,1983; Ball and others,1971; Vierbuchen, 1984; Rossi and others, 1987; Young and others, 1956). Modifications in these earlier interpretations have been based on the current work and personal communications from F. Audemard (1990). Abbreviations used are EPF = El Pilar Fault, CF = Caripe Fault, SFF = San Francisco Fault, and OR = Orinoco River.

ophiolite; and the Maestrichtian to Early Tertiary Paracotos flysch (Case and others, 1984; González de Juana and others, 1980). The Villa de Cura terrane is composed of interbedded volcanics and sediments metamorphosed to the blueschist facies (Loubet and others, 1985). Stephan (1985) related this terrane with the Cretaceous arc exposed offshore while Ostos (1990) postulated that the Villa de Cura represents oceanic rocks metamorphosed in a Neocomian accreationary wedge.

In the south, unmetamorphosed fold and thrust belts formed as these metamorphic rocks were emplaced onto South America. The age of this deformation decreases from the Paleocene-Early Eocene in the west to the Miocene-Pliocene in the east, related to the progressive emplacement of these metamorphic belts (Pindell and others, 1988; Ross and Scotese, 1988). Figure 2 shows that these unmetamorphosed rocks south of Margarita Island form a south vergent thrust belt with a minimum shortening of 40 km (Rossi and others, 1987), while the actual shortening may be several times that amount (F. Audemard, oral communication, 1990).

The occurrence of ophiolites and rocks associated with magmatic arcs, together with the presence of blueschist and eclogite facies rocks all suggest that these metamorphic belts were formed along a convergent plate margin. Continued strike-slip motion between the Caribbean and South American plates has disrupted these belts, however, so that the regional trends portrayed in figure 1 are, in reality, fairly gross generalizations. This is emphasized in figure 2, where south of Margarita the metamorphic terranes have been disrupted by Neogene extensional faulting in the pull-apart basin at Cubagua and truncated by the El Pilar Fault.

GEOLOGY OF MARGARITA ISLAND

Figure 3a shows a simplified geologic map of Margarita Island, compiled from previous workers (Taylor, 1960b; González de Juana and Vignali, 1970; Muñoz, 1973; Maresch, 1975). The areal distribution of the units is displayed with a minimum of interpretation, since fundamentally different frameworks have been proposed for Margarita.

Earlier workers (Hess and Maxwell, 1949; Taylor, 1960; Maresch, 1971; 1975; Vignali, 1976; 1979) interpreted the metamorphic section in terms of a stratigraphic sequence. Maresch (1971, 1975) believed that the amphibolites of the La Rinconada Group were metamorphosed tholeiitic flows and intrusives formed during rifting (Beets and others, 1984). Amphibolites, quartzofeldspathic schists, graphitic schists, and marbles of the Juan Griego Group, and schists, phyllites, and marbles of the Los Robles Group then represent the metasedimentary cover. The decrease in metamorphic grade from amphibolites to phyllites and the arcuate distribution of the rock units permitted Taylor (1960) to infer an anticlinorium with the axis shown in figure 3a, cored by the La Rinconada Group and plunging to the SW. In this framework, the large serpentinized ultramafic massifs shown in figure 3a are interpreted as the remnants of a large complex infolded and metamorphosed with the other metamorphic rocks (Maresch, 1971; 1975) or thrust sheets capping the mountains of eastern Paraguachoa (Bellizzia and others, 1976; Chachati and Macsotay, 1985).

Chevalier and others (1985; 1988), Bellizzia (1986), and Chevalier (1987) proposed a radically different interpretation - that the serpentinites and the rocks of the La Rinconada and Los Robles Groups represent a metamorphosed ophiolite complex. Guillet and Cannat (1984) found microstructures in some of the rare unaltered olivines characteristic of asthenospheric plastic flow suggesting that the serpentinized ultramafic massifs represent oceanic mantle. The La Rinconada Group is then believed to be metamorphosed tholeiitic MORB crust with its metasedimentary cover represented by the Los Robles Group. This ophiolitic nappe of the Coastal Fringe-Margarita Belt was then emplaced onto the parautochthonous Juan Griego Group belonging to the Cordillera de la Costa Belt and representing a remnant of the old South American passive margin (Bellizzia, 1986).

Figure 3b contrasts these two disparate interpretations. The section by Maresch (1975) shows the steep contacts of rocks infolded within the core of the anticlinorium. The same section by Chevalier (1987) envisions the suite of meta-ophiolitic rocks disrupted by dominantly SE directed thrusts.

Within the La Rinconada and Juan Griego Groups occur lenses and boudins of eclogite. Several studies of these eclogites concluded that these rocks formed under peak metamorphic conditions of P=1.15-1.5 GPa and T=450-700°C (Maresch and Abraham, 1981; Chevalier, 1987). Retrograde trajectories produced partial re-equilibration through metamorphic conditions of P=700-800 MPa and T=400-520°C (Navarro, 1981) down to P<500 MPa and T=480-550°C (Maresch and Abraham, 1981). Chevalier (1987) agreed with Maresch and Abraham (1981) that the eclogite, epidote-amphibolite and greenschist facies metamorphic rocks found on Margarita Island formed in a single Late Cretaceous prograde-retrograde metamorphic cycle. However, other workers used the mineral chemical zonation and the observed reaction textures to infer two discrete metamorphic events (Blackburn and Navarro, 1977; Stephan and others,1980; Navarro, 1981; Talukdar and Loureiro, 1982; and Chevalier and others, 1985). They associated the first of these, a postulated Late Jurassic or Early Cretaceous obduction of oceanic crust onto the South American margin, with the eclogite facies metamorphism. Chevalier (1987) and Chevalier and others (1988), however, relate this obduction with high temperature (T>1000°C) deformation. All workers agree with a Late Cretaceous collision of an island arc with South

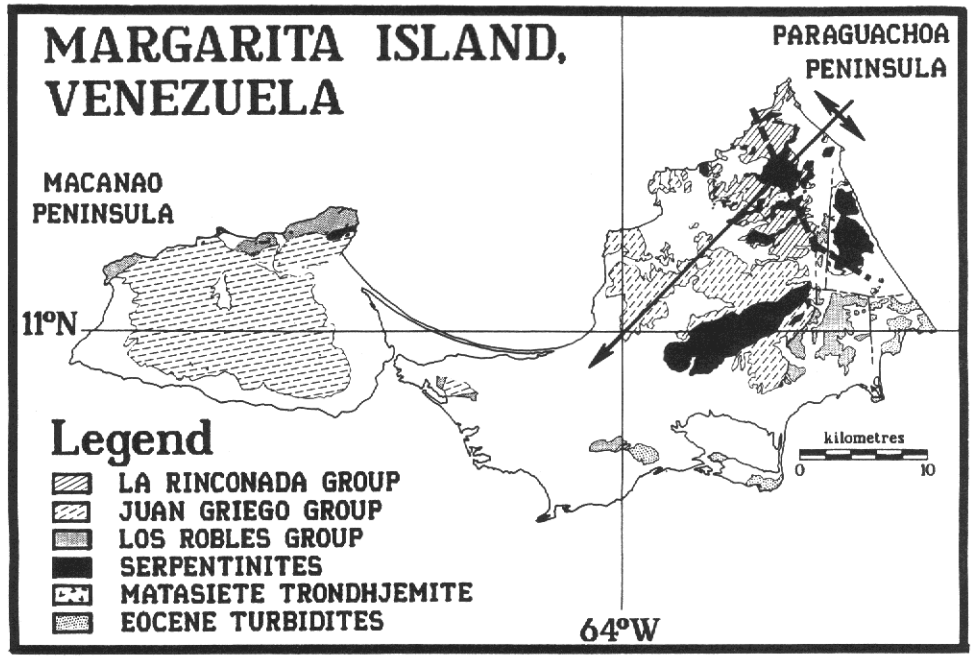

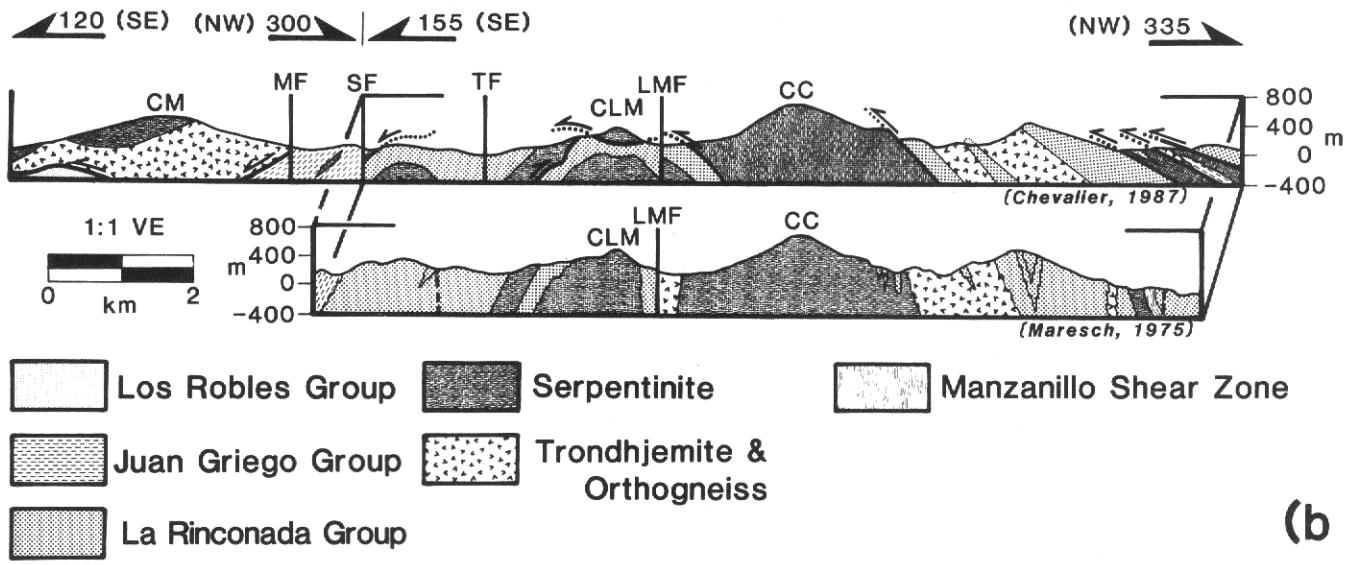

Figure 3a. Generalized geological map of Margarita Island, Venezuela compiled from published sources (Taylor, 1960b; González de Juana and Vignali, 1970; Muñoz, 1973; Maresch, 1975). The axis of the SW plunging anticlinorium inferred by Taylor (1960) is shown, as well as the line of section shown in figure 3b. The unusual shape of the island makes it convenient to refer to the western portion as Macanao and the eastern portion as Paraguachoa.

Figure 3b. Cross sections through Margarita Island from Maresch (1975) and Chevalier (1987). Maresch (1975), using a stratigraphic interpretation, inferred steep contacts within the core of the anticlinorium. Chevalier (1987) re-interpreted many of these contacts to be thrusts, emplacing meta-ophiolites represented by the serpentinites and the La Rinconada Group from the NW to the SE. CM=Cerro Matasiete, CLM=Cerro Los Micos, CC=Cerro Chico, MF=Matasiete Fault, SF=Salamanca Fault, TF=Tacarigua Fault, LMF=Los Micos Fault.

America, with the Coniacian-Campanian time range most often cited (Talukdar and Loureiro, 1982; Beets and others, 1984; Chevalier and others, 1985; 1988).

Leucocratic igneous rocks intruded and were metamorphosed with the La Rinconada and Juan Griego Groups. Most of these bodies are too small to be shown at the scale of figure 3a. However, in a fault bounded block along the eastern coast of the island, a large metatrondhjemite body is capped by serpentinite. Published trace-element analyses of the Matasiete Trondhjemite (Chachati and Macsotay, 1985; Ostos, 1990) plotted on the discrimination diagrams of Pearce and others (1984) indicate that these rocks were formed by subduction-related magmatism and are not oceanic plagiogranites formed along a mid-ocean ridge. Amphibole separates from this unit gave K/Ar ages of 72±5, 74±6 and 72±6 Ma (Olmeta, 1968; Santamaría and Schubert, 1974: recalculated using the Steiger and Jäger 1977 decay constants). However, other published K/Ar ages using various mineral separates from the La Rinconada Group range between 98 and 37 Ma (Loubet and others, 1985; Chevalier, 1987), suggesting a complex thermal history and partial argon loss (Burke, 1988).

Along the southern margin of Margarita Island, unmetamorphosed but folded turbidites are exposed. Hunter (1978)

inferred that these rocks were deposited between the Lower Eocene and the uppermost Middle Eocene based on the microfaunal assemblages, although reworking has introduced conglomeratic or brecciated fragments with Cretaceous and Paleocene fauna (Muñoz and Furrer, 1976; Hunter, 1978; Muñoz, 1983). The folding of these rocks may have occurred in Oligocene/Miocene time. Capping these rocks are relatively undeformed units of Late Miocene age and younger (not shown in figure 3a).

Based on the orientation of the Miocene folds, the island can be divided into 5 regional structural domains. Shown on figure 4, these domains are 1) Macanao Peninsula, 2) the lowland of SW Paraguachoa Peninsula, 3) the La Rinconada, Juan Griego and Los Robles Groups of eastern Paraguachoa, 4) the fault-bounded Matasiete Trondhjemite and 5) the fault-bounded Eocene turbidites on the far eastern corner of the island (Pampatar Formation).

KINEMATIC ANALYSIS

The analysis presented here is confined to the La Rinconada, Juan Griego, and Los Robles Groups of eastern Paraguachoa. Hence, the data all come from a single structural domain - the SW plunging anticlinorium originally described by Taylor (1960) and shown as structural domain 3 in figure 4. The various phases of deformation will be described in order of oldest to youngest, with the corresponding lower-hemisphere, equal-area stereonets shown in figure 5.

The D_{1a} deformation is related to the eclogite facies metamorphism. The data shown in figure 5a are the foliations in the eclogites and the rare planar fabrics preserved in microlithons between the main D_{1b} foliation in the schists. Most of the evidence for this deformation has been destroyed, explaining the sparseness of the data set.

The dominant foliation of the metamorphic rocks on Margarita Island is related to the D_{1b} deformation associated with epidote-amphibolite to greenschist facies metamorphism. A plot of this foliation in figure 5b shows that this fabric has been folded into a great circle distribution with a SW trending fold axis which is the regional D_2 fold axis. Comparison of the D_{1a} and the D_{1b} foliation fabrics shows that they have similar distributions. Talukdar and Loureiro (1982) found comparable deformations in the rocks of the Coastal Fringe-Margarita terrane NW of Caracas; isoclinal folds that developed during the greenschist/epidote-amphibolite facies metamorphism are coaxial and coplanar to the earlier folds formed during blueschist/eclogite facies metamorphism.

The folds on Margarita associated with these two phases of deformation could not be distinguished in the field unless a refolded fold was found. As a result, all fold axes defined by folded compositional layering are plotted together in figure 5c. The most obvious feature of this stereonet is the concentration of the fold axes aligned SW-NE and sub-parallel to the regional D_2 fold axis. Evidence from other domains on Margarita and from similar rocks on the Araya Peninsula (Avé Lallemant, this volume) shows that these fold axes are parallel to the finite strain X (maximum extension) axis. Since these axes are near parallel to the later D_2 fold axis, the D_2 deformation did not significantly rotate these data.

Small scale shears and quartz c-axis fabrics can be used to infer the kinematics of deformation. S-C tectonites form when a penetrative schistosity (S-surface) is offset by shear planes ("cisaillement" or C-surfaces). The angular relationship between the two defines the sense of movement in sheared rocks (Berthé and others, 1979; Simpson and Schmid, 1983; Lister and Snoke, 1984). Asymmetries in quartz c-axis fabrics have also been related to the kinematics (Lister and Williams, 1979; Simpson and Schmid, 1983).

Field measurements of small scale conjugate shear sets and quartz c-axis fabrics from the schists of the Juan Griego and Los Robles Groups define the D_{1c} extensional phase of deformation shown in figures 5d,e,f. The poles to the shear planes are plotted in figure 5d to show that these deformational structures were also

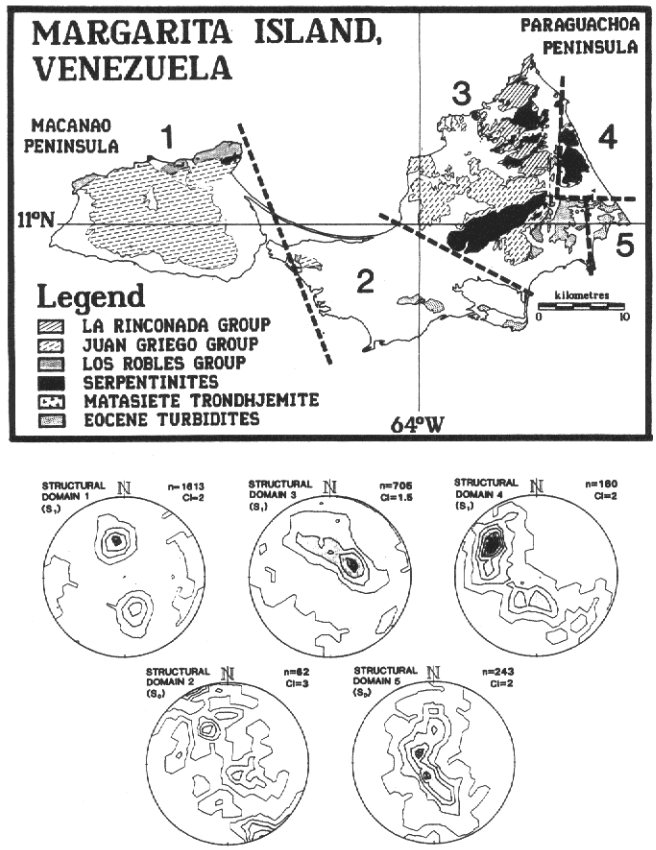

Figure 4. Based on the orientation of the D_2 folding, the island can be divided into the 5 structural domains shown on the smaller version of figure 3a. Boundaries between domains 3, 4 & 5 are known faults; boundaries between domains 1, 2 & 3 are inferred faults. The trends of the La Rinconada and Juan Griego patterns are parallel to the observed D_2 structural trends. The stereonets below the map display the regional structural orientations. These are lower-hemisphere, equal-area projections. CI is the contour interval as % per 1% area and n is the number of measurements used to construct the diagram. The data from structural domains 1 and 2 come from published sources (Hess and Maxwell, 1949; Kugler, 1957; Taylor, 1960b; Rengel, 1961; González de Juan and Vignali, 1969; 1970; Muñoz, 1973), while the measurements from domains 3, 4 and 5 come from this study. In the 2 domains dominated by Eocene outcrop (2 and 5), bedding (S_0) defines the regional structure while in the other domains (1, 3, and 4), foliation (S_1) was used to define the structure.

Figure 5. The structural data from the La Rinconada, Juan Griego and Los Robles Goups of eastern Paraguachoa (domain 3 on figure 4). All stereonets are lower-hemisphere, equal-area projections. CI is the contour interval as % per 1% area and n is the number of data points used to generate the diagram. The 1st row shows structures from the eclogite facies D_{1a} and the epidote-amphibolite facies D_{1b} deformations. The 2nd row shows the greenschist facies D_{1c} extensional structures. The 3rd row illustrates the D_2 features and the 4th row displays the Neogene brittle deformation. In figures 5e, f, and k, the great circles are shear planes and the arrows indicate the direction of motion of the hanging wall across the footwall. Figure 5l shows the orientation of Riedel (R) and conjugate Riedel (R') shears.

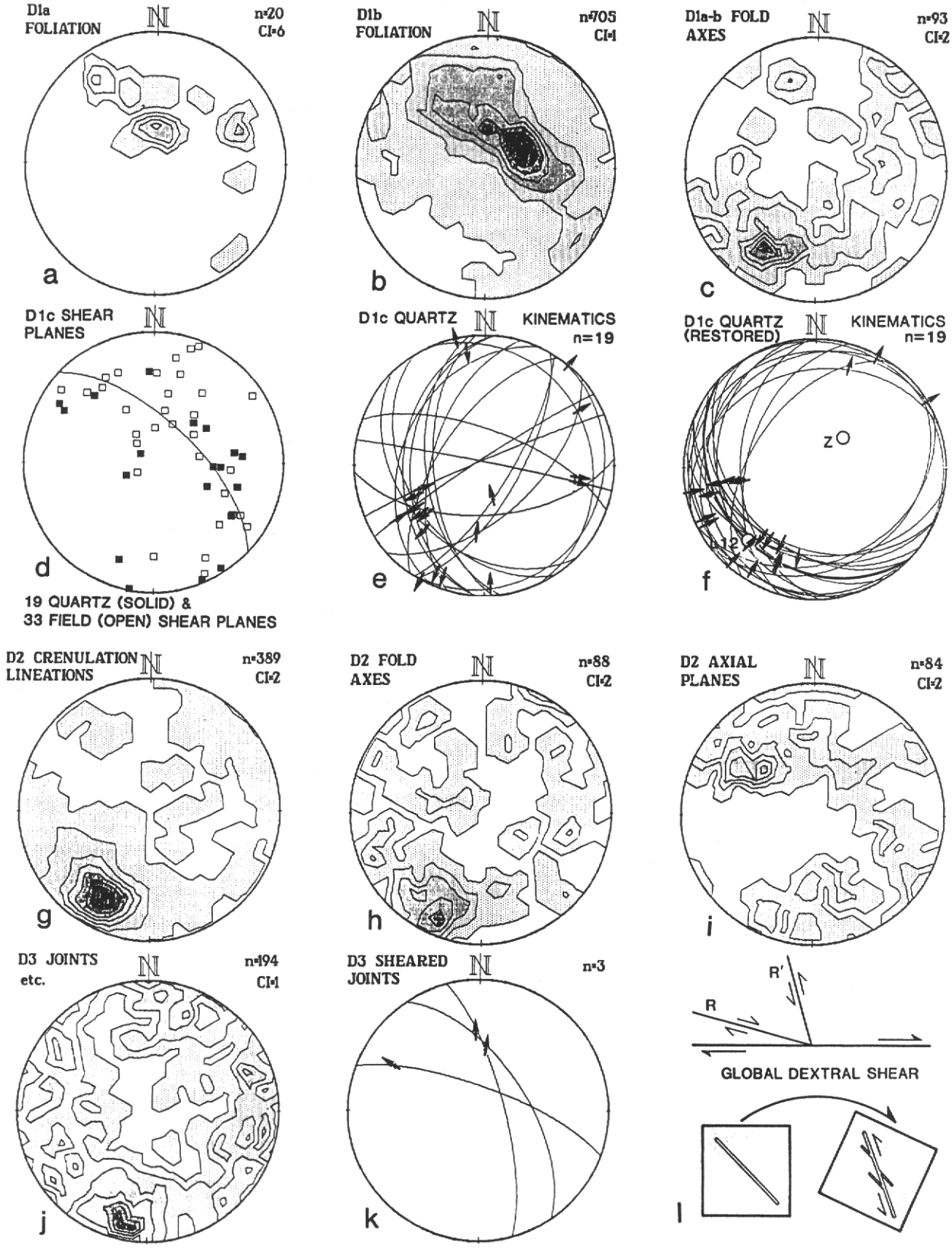

Figure 5. The structural data from the La Rinconada, Juan Griego and Los Robles Groups of eastern Paraguachoa (complete caption on previous page).

folded. The best fit great circle girdle distribution of the foliations shown in figure 5b is plotted on figure 5d to illustrate the similar patterns created by the later D_2 folding. The low angular relationship between foliation and extensional shears make inferences of the slip direction in the field data questionable. Quartz c-axis data therefore form a more reliable data set to define the kinematics, and the results are presented in figures 5e,f. The inferred shear planes are plotted as great circles and the arrows indicate the direction of motion of the hanging wall across the footwall. Of the 20 quartz c-axis fabrics measured, 19 have asymmetric fabrics for which a sense of shear can be determined. Each fabric was generated using 3 mutually perpendicular thin sections with a minimum of 293 c-axes per fabric. Unrestored, there is a wide scatter in the shear planes due to the later D_2 folding but the slip directions are generally SW-NE (figure 5e). With the effects of the D_2 folding removed, the extensional fabric is clearly defined, showing SW-NE extension (figure 5f). The mesoscopic pole to the foliation plane (Z) and crenulation lineation (L12) are shown in their restored positions on figure 5f. The quartz c-axis fabrics demonstrated that the mesoscopic D_2 crenulation lineation could be used to approximate the D_{1c} finite strain X axis.

The structural data for the D_2 folding are shown in figures 5g,h,i. Crenulation lineations and mesoscopic fold axes are parallel, plunging to the SW (figures 5g,h). These folds were observed to be generally NW-vergent, and this is substantiated by the stereonet of the axial planes of the mesoscopic folds measured in the field (figure 5i).

The D_2 deformation folds the Eocene turbidites but not the Mio-Pliocene Cubagua Formation, apparently bracketing the age of folding between the late Middle Eocene and the Late Miocene. However, even these wide age constraints are not accepted by all workers. Vignali (1976, 1979) suggested that the D_2 folding began in the Late Paleocene with maximum activity in the late Middle Eocene and finally ending in the Late Oligocene to Early Miocene. Taylor (1960) and Muñoz (1983) thought that the Eocene turbidites were deposited in a tectonically active basin, so syndepositional folding of these units is not unreasonable. Seismic data from the continental slope north of Margarita Island, correlated with well information, suggests that folding continued through the Middle Miocene (Biju-Duval and others, 1983). The one absolute age date associated with this deformation is the 33±2 Ma feldspar K/Ar age of a pegmatite from Macanao (Santamaría and Schubert, 1974: recalculated with the decay constants of Steiger and Jäger, 1977). Vignali (1976, 1979) found these pegmatites to be influenced by the D_2 folding, but interpreted the date to be the younger limit of the D_2 deformation because of the low blocking temperature of feldspar to argon loss (Harrison and McDougall, 1982; Harrison and others, 1989).

It is tempting to describe the NW-vergent D_2 folding on Margarita Island as the hinterland deformation associated with the Oligocene-Miocene subsidence and the Miocene SE-directed thrusting in the foreland Eastern Venezuelan Basin to the south (González de Juana and Rodriguez, 1951; Cebull, 1970; Vierbuchen, 1984; Rossi and others, 1987; Isea, 1987). However, care must be taken in making correlations across the Caribbean-South American plate boundary. Accepting the 20 $mm \cdot a^{-1}$ relative motion of the Caribbean with respect to South America (Ross and Scotese, 1988; Pindell and others, 1988) places Margarita Island too far west to be directly related with the deformation in the Eastern Venezuelan Basin (figure 6). Curiously, the paleogeographic reconstructions shown in figure 6 place the late Eocene-Oligocene pullapart preserved in the Falcon Basin (Muessig, 1984) and the Quaternary opening of the Tuy-Cariaco Basin (Schubert, 1982) in the immediate wake of Margarita Island.

Clearly, the age of the D_2 folding is not well constrained. Most of the interpretations, however, overlap in the Oligocene through middle Miocene time range.

Figures 5j,k,l show the brittle structures measured in structural domain 3. Figure 5j plots all joints, veins and extensional fractures that post date the D_2 folding. These show SW-NE extension. Some

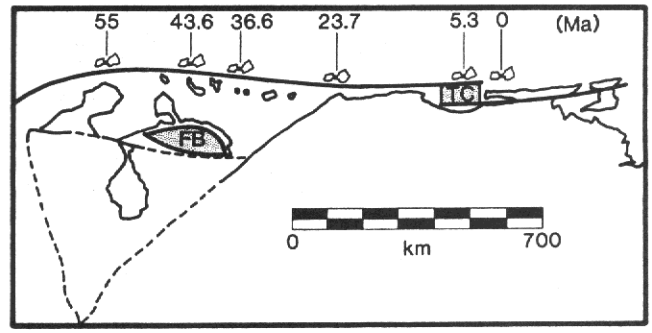

Figure 6. The paleogeographic location of Margarita Island is shown with respect to South America. Dewey and Pindell's (1985) restoration of the Maracaibo Block has been used to estimate the pre-Andean shape of South America. The basins shown are the Falcon Basin (FB) and the Tuy-Cariaco Basin (TC).

joints are sheared, fringed by newer en-echelon extension fractures. Only three were observed in this structural domain (figure 5k) but the data are supported by similar joints and dextral EW faults seen in the other structural domains. In figure 5k, the sheared joints are plotted as great circles and the arrows indicate the direction of motion of the hanging wall across the footwall. These sinistrally sheared joints can form in a global dextral shear environment. Tchalenko (1970) showed that secondary faults associated with a master strike-slip fault often develop into a conjugate set of Riedel shears, one set synthetic (R) to the main fault and one set antithetic (R'). Alternatively, the sheared joints could develop as rotated tension cracks (figure 5l).

The possibility of tectonic block rotations raised in figure 5l for the origin of sheared joints on Margarita Island has a profound affect on the interpretation of the kinematic data, particularly since paleomagnetic data have documented about 90° clockwise rotations in other rocks along the southern Caribbean margin (Skerlec and Hargraves, 1980). Hargraves and Skerlec (1980) measured 35 samples, mostly basic dikes, from 7 sites on Margarita Island. However, pervasive alteration and the resultant weak paleomagnetic signal produce data that are inconclusive (Hargraves and Skerlec, 1980).

A POSSIBLE PLATE TECTONIC MODEL

Figures 5c,e,f,g,h,j show that fold axes and extension directions on Margarita Island always had the same trend. Any permissible tectonic model will have to account for this observation. The simplest explanation extrapolates the present back into the past to conclude that these structures resulted from a continuous component of dextral motion. Based on this data and the data from Araya Peninsula, we propose that the rocks on Margarita Island represent an accretionary complex formed by oblique subduction between the Farallon Plate and South America. As the Farallon Plate entered the gap between the Americas, the increasing obliquity of the subduction zone explains the sequence of synmetamorphic deformations found in this study.

Figure 7a illustrates the model proposed by Avé Lallemant and Guth (in press) to explain how an increasing angle of obliquity can produce the progression of metamorphic grade and structures seen in the synmetamorphic deformation on Margarita. The accretionary wedge can only move with the tangential component of the underthrusting slab (V_T). As the angle of obliquity increases, V_T increases while the convergent motion normal to the plate boundary decreases. The resultant change in velocity of a constant volume accretionary wedge forces plate boundary parallel extension, thinning of the accretionary wedge and uplift of the base of the wedge. When the obliquity is 90°, subduction is totally eliminated and the plate boundary becomes a transform fault. Hence, as hinted by the labeling of the deformations and as shown on figures 7a and b, the eclogite facies D_{1a}, the epidote-amphibolite facies D_{1b}, and

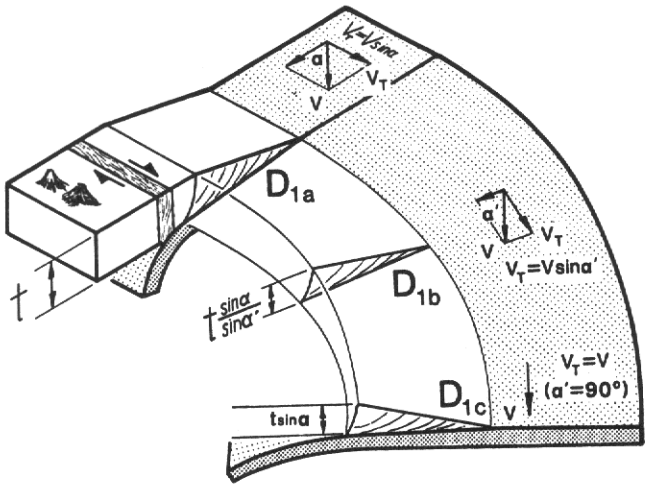

Figure 7a. The inferred deformations within an oblique subduction zone. The shaded plate is the subducting oceanic slab. The total relative plate motion is directed downward, resolved into normal and tangential components. The mechanics of this model is discussed in the text.

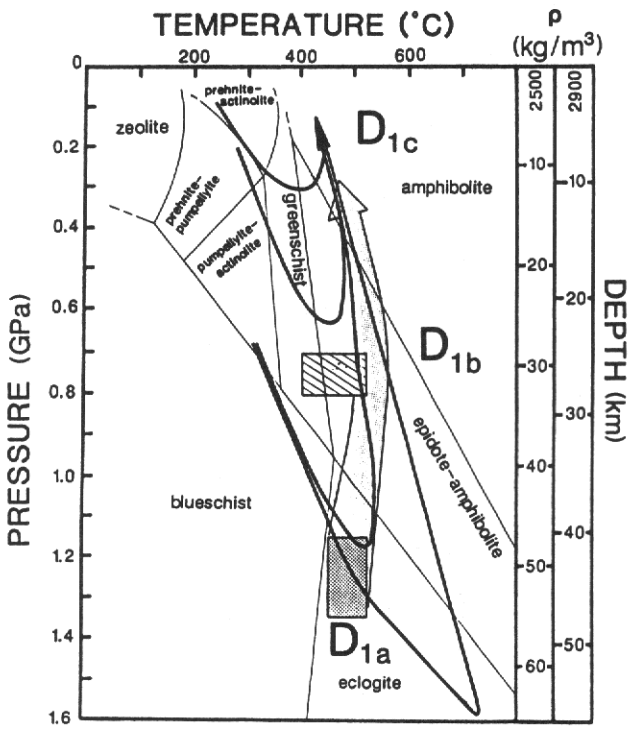

Figure 7b. Pressure-temperature estimates for the Late Cretaceous metamorphism are plotted on the schematic petrogenetic grid of Ernst (1988). The P-T trajectory inferred by Maresch and Abraham (1981) is shown with the stipple patterns, while 4 P-T trajectories from figure 108 of Chevalier (1987) are shown with the heavy lines. The field shown with the diagonal pattern is the P-T estimate for the retrograde metamorphism of Navarro (1981). Depth estimates have been computed for densities of 2500 and 2900 kg/m^3 to model depths in an accretionary prism and island arc, respectively. These values come from Speed and others (1984).

the extensional greenschist facies D_{1c} deformations represent a continuous process and not discrete deformational events.

Figure 7b gives some vertical scale to figure 7a by plotting the metamorphic conditions inferred by earlier workers and the associated deformations found in this study. The peak metamorphic pressures inferred by Chevalier (1987) range from 300 MPa to 1.5 GPa, but the maximum pressure gradient occurs between the middle two curves which show a change in pressure of 600 MPa in samples about 8 km apart. Although Chevalier (1987) proposed a complex tectonic history to explain the geometry, we suggest that the extensional D_{1c} deformation provides a simple mechanism to remove the inferred 16 km of missing section between the two sample sites (assuming a density of 2500 kg·m^{-3})

The later non-metamorphic D_2 folding and D_3 brittle deformations are associated with the dextral Caribbean/South American plate boundary zone. The sequence of deposition and deformation are likely related to restraining and releasing perturbations along the strike-slip boundary.

ACKNOWLEDGEMENTS

Field work was supported by Research Grants 3305-84 and 3437-85 to LRG from the Geological Society of America and by the National Science Foundation Grant EAR-8517383 to HGA. Critical comments by Dave Larue provided helpful guidance in improving the manuscript.

REFERENCES

Avé Lallemant, H.G., 1990, The Caribbean South American plate boundary in the Caribbean Mountains Province, eastern Venezuela: Carib. Geol. Conf., 12th, St. Croix USVI 1989, Trans., (this volume).

Avé Lallemant, H. G., and Guth, L. R., (in press), The role of extensional tectonics in the exhumation of eclogites and blueschists in an oblique subduction setting: Northeastern Venezuela: Geology.

Ball, M. M., Harrison, C. G. A., Supko, P. R., Bock, W., and Maloney, N. J., 1971, Marine geophysical measurements on the southern boundary of the Caribbean Sea, in Donnelly, T. W., ed., Caribbean geophysical, tectonic, and petrologic studies: Geol. Soc. America Mem. 130, p. 1-33.

Beets, D. J., Maresch, W. V., Klaver, G. Th., Mottana, A., Bocchio, R., Beunk, F. F., and Monen, H. P., 1984, Magmatic rock series and high-pressure metamorphism as constraints on the tectonic history of the southern Caribbean, in Bonini, W. E., Hargraves, R. B., and Shagam, R., eds., The Caribbean-South American Plate Boundary and Regional Tectonics: Geol. Soc. America Mem. 162, p. 95-130.

Bellizzia G., A., 1986, Sistema montañoso del caribe - una cordillera alóctona en la parte norte de América del Sur: Cong. Geol. Venez., 6th, Caracas 1985, Mem., v. 10, p. 6656-6836.

Bellizzia G., A., Pimentel M., N., and Bajo O., R. compilers, 1976, Mapa geológico-estructural de Venezuela: Venezuela Ministerio de Minas e Hidrocarburos, Caracas.

Berthé, D., Choukroune, P., and Jegouzo, P., 1979, Orthogneiss, mylonite and non coaxial deformation of granites: the example of the South Armorican Shear Zone: Jour. Structural Geology, v. 1, p. 31-42.

Biju-Duval, B., Mascle, A., Rosales, H., and Young, G., 1983, Episutural Oligo-Miocene basins along the North Venezuelan margin, in Watkins, J. S., and Drake, C. L., eds., Studies in Continental Margin Geology, Am. Assoc. Petroleum Geologists Mem. 34, p. 347-358.

Blackburn, W. H., and Navarro, E., 1977, Garnet zoning and polymetamorphism in the eclogite rocks of Isla de Margarita, Venezuela: Canadian Mineralogist, v. 15, p. 257-266.

Burke, K., 1988, Tectonic evolution of the Caribbean: Ann. Rev. Earth Planetary Sci., v. 16, p. 201-230.

Case, J. E., Holcombe, T. L., and Martin, R. G., 1984, Map of geologic provinces in the Caribbean region, in Bonini, W. E., Hargraves, R. B., and Shagam, R., eds., The

Caribbean-South American Plate Boundary and Regional Tectonics: Geol. Soc. America Mem. 162, p. 1-30.
Cebull, S. E., 1970, Low-angle growth faults in Eastern Venezuelan Basin: Am. Assoc. Petroleum Geologists Bull., v. 54, p. 730-734.
Chachati, B. and Macsotay, O., 1985, Estudio geodinámico y geoquímico de rocas meta-ácidas de Paraguaychoa, Venezuela nororiental: Cong. Geol. Venez., 6th, Caracas 1985, Mem., v. 3, p. 1586-1622.
Chevalier, Y., 1987, Les zones internes de la chaîne sud-Caraïbe sur le transect: Ile de Margarita - Péninsule d'Araya (Vénézuéla): lithostratigraphie, pétrologie, géochimie et évolution tectono-métamorphique, [Ph.D. thesis]: Brest, Université de Bretagne Occidentale, 464 p.
Chevalier, Y., Stephan, J.-F., Blanchet, R., Gravelle, M., and Bellizzia, A., 1985, L'Ile de Margarita et la Péninsule d'Araya (Vénézuéla) jalons d'une collision Crétacé Supérieur sur la paléo-frontiere Caraïbes/Amérique du Sud [abs.]: Symp.Géodynamique des Caribes, Paris 1985.
Chevalier, Y., Stephan, J.-F., Darboux, J.-R., Gravelle, M., Bellon, H., Bellizzia G., A., and Blanchet, R., 1988, Obduction et collision pré-Tertiaire dans les zones internes de la Chaîne Caraïbe vénézuélienne, sur le transect Ile de Margarita-Péninsula d'Araya: Acad. sci. [Paris] Comptes rendus, ser. II, v. 307, p. 1925-1932.
Dewey, J. F., and Pindell, J. L., 1985, Neogene block tectonics of eastern Turkey and northern South America: continental applications of the finite difference method: Tectonics, v. 4, p. 71-83.
Ernst, W. G., 1988, Tectonic history of subduction zones inferred from retrograde blueschist P-T paths: Geology, v. 16, p. 1081-1084.
González de Juana, C. and Rodriguez, L. P., 1951, Fundamental geological characteristics of the Venezuelan oil basins: World Petroleum Cong., 3rd, The Hague, Proc., sec. I (Geology-Geophysics), p. 41-55.
González de Juana, C., and Vignali C., M., compilers, 1969, Mapa geológico Macanao Edo. Nueva Esparta, campo III: Dept. de Geología, Univ. Central de Venezuela.
-------compilers, 1970, Mapa geológico Macanao Edo. Nva. Esparta, campo III: Dept. de Geología, Univ. Central de Venezuela.
González de Juana, C., Iturralde de Arozena, J. A., and Cadillat, X. P., 1980, Geología de Venezuela y de sus Cuencas Petrolíferas, v. I & II: Caracas, Foninves, 1031 p.
Guillet, P., and Cannat, M., 1984, Cinématique de mise en place de l'unité ultrabasique du Cerro Matasiete, île de Margarita, Vénézuéla: Acad. sci. [Paris] Comptes rendus, ser. II, v. 299, p. 133-138.
Hargraves, R. B., and Skerlec, G. M., 1980, Paleomagnetism of some Cretaceous-Tertiary igneous rocks on Venezuelan offshore islands, Netherlands Antilles, Trinidad and Tobago: Carib. Geol. Conf., 9th, Santo Domingo, Dominican Republic, 1980, Trans., v. 2, p. 509-517.
Harrison, T. M., and McDougall, I., 1982, The thermal significance of potassium feldspar K-Ar ages inferred from $^{40}Ar/^{39}Ar$ age spectrum results: Geochim. et Cosmochim. Acta, v. 46, p. 1811-1820.
Harrison, T. M., Spear, F. S., and Heizler, M. T., 1989, Geochronologic studies in central New England II: Post-Acadian hinged and differential uplift: Geology, v. 17, p. 185-189.
Hess, H. H., and Maxwell, J. C., 1949, Geological reconnaissance of the Island of Margarita: Geol. Soc. America Bull., v. 60, p. 1857-1868.
Hunter, V. F., 1978, Notes on the Tertiary stratigraphy of Margarita Island: Geol. Mijnbouw, v. 57, p. 189-192.
Isea, A., 1987, Geological synthesis of the Orinoco Oil Belt, eastern Venezuela: Jour. Petroleum Geology, v. 10, p. 135-148.
Kugler, H. G., 1957, Contribution to the geology of the islands Margarita and Cubagua, Venezuela: Geol. Soc. America Bull., v. 68, p. 555-566.
Lister, G. S., and Snoke, A. W., 1984, S-C mylonites: Jour. Structural Geology, v. 6, p. 617-638.
Lister, G. S., and Williams, P. F., 1979, Fabric development in shear zones: theoretical controls and observed phenomena: Jour. Structural Geology, v. 1, p. 283-297.
Loubet, M., Montigny, R., Chahati, B., Duarte, N., Lambret, B., Martin, C., and Thuizat, R., 1985, Geochemical and geochronological constraints on the geodynamical development of the Caribbean Chain of Venezuela, in Mascle, A., ed., Symp. Géodynamique des Caïbes: Paris Feb. 5-8 1985, Proc., p. 553-566.
Mann, P. and Burke, K., 1984, Neotectonics of the Caribbean: Rev. Geophysics Space Physics, v. 22, p. 309-362.
Maresch, W. V., 1971, The metamorphism and structure of northeastern Margarita Island, Venezuela [Ph.D. thesis] , Princeton, N.J., Princeton Univ., 226 p.
-------1975, The geology of northeastern Margarita Island, Venezuela: a contribution to the study of Caribbean plate margins: Geol. Rundschau, v. 64, p. 846-883.
Maresch, W. V. and Abraham, K., 1981, Petrography, mineralogy and metamorphic evolution of an eclogite from the Island of Margarita, Venezuela: Jour. Petrology, v. 22, p. 337-362.
Mascle, A., Cazes, M., and Le Quellec, P., 1985, Structure des marges et bassins Caraïbes: une revue, in Mascle, A., ed., Symp. Géodynamique des Caïbes: Paris Feb. 5-8 1985, Proc., p. 1-20.
Muessig, K. W., 1984, Structure and Cenozoic tectonics of the Falcon Basin, Venezuela, and adjacent areas, in Bonini, W. E., Hargraves, R. B., and Shagam, R., eds., The Caribbean-South American Plate Boundary and Regional Tectonics: Geol. Soc. America Mem. 162, p. 217-230.
Muñoz J., N. G., 1973, Geología sedimentaria del flysch Eoceno de la Isla de Margarita (Venezuela): Geos [Caracas], no. 20, p. 5-64.
-------1983, Geología del flysch Eoceno de la Isla de Margarita, in Bellizzia G., A., Muñoz J., N. G., Macsotay, O., and Key, C., eds., Guía de la Excursión Geológica a la Isla de Margarita: Sociedad Venezolana de Geólogos, p. 33-37.
Muñoz J., N. G., and Furrer, M., 1976, Cretáceo alóctono en el Eoceno de Margarita, Venezuela: Cong. Latinoamericano Geol., 2nd, Caracas 11-16 Nov. 1973, Mem., v. 2, p. 1321-1328.
Navarro F., E., 1981, Relaciones mineralógicas en las rocas eclogiticas de la Isla de Margarita, Estado Nueva Esparta: Geos [Caracas], no. 26, p. 3-44.
Olmeta, M. A., 1968, Determinación de edades radiométricas en rocas de Venezuela y su procedimiento por el méthodo K/Ar: Bol. Geol. [Venezuela], v. 10, no. 19, p. 339-344.
Ostos R., M., 1990, Tectonic evolution of the south-central Caribbean based on geochemical data [Ph.D. thesis]: Houston, Rice Univ., 401 p.
Pearce, J. A., Harris, N. B., W., and Tindle, A. G., 1984, Trace element discrimination diagrams for the tectonic interpretation of granitic rocks: Jour. Petrology, v. 25, p. 956-983.
Pimentel de Bellizzia, N., Gaudette, H., and Olsewsky, W., 1985, Nuevas dataciones en el "basamento" de la cadena caribe: Cong. Geol. Venez., 6th, Caracas 1985, Mem., v. 3, p. 1979-1994.
Pindell, J. L., and Barrett, S. F., (in press), Geologic evolution of the Caribbean region: a plate-tectonic perspective, in Case, J. E., and Dengo, G., eds. Decade of North American Geology, v. H, Boulder, Geol. Soc. America.
Pindell, J. L., Cande, S. C., Pitman III, W. C., Rowley, D. B., Dewey, J. F., Labrecque, J., and Haxby, W., 1988, A plate-kinematic framework for models of Caribbean evolution: Tectonophysics, v. 155, p. 121-138.
Rengel F., J. M., 1961, Historia del abastecimiento de agua para las islas de Margarita y Coche: Cong. Geol. Venez., 3rd, Caracas 1959, Mem., v. 4, p. 1735-1786.
Ross, M. I., and Scotese, C. R., 1988, A hierarchical tectonic model of the Gulf of Mexico and Caribbean region: Tectonophysics, v. 155, p. 139-168.
Rossi, T., Stephan, J-F., Blanchet, R., and Hernandez, G., 1987, Étude géologique de la Serrania del Interior oriental (Venezuela) sur le transect Cariaco-Maturin: Rev. de L'Institut Français du Pétrole, v. 42, p. 3-30.
Santamaría, F., and Schubert, C., 1974, Geochemistry and geochronology of the southern Caribbean-Northern Venezuela

plate boundary: Geol. Soc. America Bull., v. 85, p. 1085-1098.
Schubert, C., 1982, Origin of Cariaco Basin, southern Caribbean Sea: Marine Geology, v. 47, p. 345-360.
Simpson, C., and Schmid, S. M., 1983, An evaluation of criteria to deduce the sense of movement in sheared rocks: Geol. Soc. America Bull., v. 94, p. 1281-1288.
Skerlec, G. M., and Hargraves, R. B., 1980, Tectonic significance of paleomagnetic data from northern Venezuela: Jour. Geophys. Research, v. 85, p. 5303-5315.
Speed, R. C., Westbrook, G. K., Biju-Duval, B., Ladd, J. W., Mascle, A., Moore, J. C., Saunders, J. B., Schoonmaker, J. E., and Stein, S., eds., 1984, Lesser Antilles and adjacent ocean floor: Ocean Margin Drilling Program Regional Atlas Series, Atlas 10, Woods Hole, Mass., Marine Sci. Inst. Pub.
Steiger, R. H., and Jäger, E., 1977, Subcommission on geochronology: convention on the use of decay constants in geo- and cosmochronology: Earth Planetary Sci. Letters, v. 36, p. 359-362.
Stephan, J-F., 1985, Andes et chaîne Caraïbe sur la transversale de Barquisimeto (Vénézuéla) évolution géodynamique, in Mascle, A., ed., Symp. Géodynamique des Caribes: Paris Feb. 5-8 1985, Proc., p. 505-529.
Stephan, J-F., Beck, C., Bellizzia G., A., and Blanchet, R., 1980, La chaîne caraïbe du Pacifique à l'Atlantique, in Aubouin, J., Debelmas, J., and Latreille, M., eds., Geology of the Alpine Chain Born of the Tethys: Internat. Geol. Cong., 26th, colloque C5, Bur. Recherches Geol. Minieres Mem. 115, p. 38-59.
Talukdar, S. C., and Loureiro C., D., 1982, Geología de una zona ubicada en el segmento norcentral de la Cordillera de la Costa, Venezuela: metamorfismo y deformación. Evolución del margen septentrional de Suramérica en el marco de la tectónica de placas: Geos [Caracas], no. 27, p. 15-76.
Taylor, G. C., 1960, The geology of the Island of Margarita, Venezuela [Ph.D. thesis]: Princeton, N.J., Princeton Univ., 121 p.
-------1960b, Geología de la Isla de Margarita, Venezuela: Cong. Geol. Venez., 3rd, Caracas 1959, Mem., v. 2, p. 838-893.
Tchalenko, J. S., 1970, Similarities between shear zones of different magnitudes: Geol. Soc. America Bull., v. 81, p. 1625-1640.
Vierbuchen, R. C., 1984, The geology of the El Pilar fault zone and adjacent areas in northeastern Venezuela, in Bonini, W. E., Hargraves, R. B., and Shagam, R., eds., The Caribbean-South American Plate Boundary and Regional Tectonics: Geol. Soc. America Mem. 162, p. 189-212.
Vignali, M., 1976, The stratigraphy and structure of the metamorphic eastern Cordillera, Venezuela (Araya-Paria Peninsula and Margarita Island) [Ph.D. thesis]: Zurich, ETH, 129 p.
-------1979, Estratigrafía y estructura de las Cordilleras metamórficas de Venezuela oriental (Península de Araya - Paria e Isla de Margarita): Geos [Caracas], no. 25, p. 19-66.
Young, G. A., Bellizzia G., A., Renz, H. H., Johnson, F. W., Robie, R. H., and Vall, J. M., 1956, Geología de las cuencas sedimentarias de Venezuela y de sus campos petrolíferos: Bol. Geologia [Venezuela], Spec.Pub. no. 2, 140 p.

HISTORY OF GOLDMINING ON THE ISLAND OF ARUBA DUTCH WEST INDIES

Robert Salna
10225 Yonge Street
Richmond Hill
Ontario, Canada
L4C 3B2

ABSTRACT

The island of Aruba, an area of some 190 km2, forms with Curacao and Bonaire, the Leeward Netherlands Antilles, the western section of an E-W running chain of islands and atolls on the Venezuelan continental borderland in the southern Caribbean. This borderland, consisting of ridges and trenches, is a broad orogenic belt of Mesozoic and younger age rock at the boundary of the Caribbean plate withthe South American plate. Its geological history was particularly characterised by strong magmatic activity during the Cretaceous and high structural mobility in Cretaceous and Tertiary times. In this connection the igneous (magmatic) rock series of Aruba, Bonaire and Curacao are considered to belong to a well defined colliding island arc whose highpressure metamorphism resulted of the E-W Aruba-la Blanquilla chain with the South American continental margin. The stratigraphy, structural relations and radiometric dating of the intrusive rocks indicate that the collision took place in Upper Cretaceous time, during the Coniacian/Campanian interval. The igneous rocks consist largely of the Aruba tonalite/gabbro batholith, which is of calc-alkaline composition.

INTRODUCTION

It is interesting to note that the Spanish words "Oro Uba" meaning there was gold, are thought to be the origin of the name "Aruba".

The island of Aruba is located in the Caribbean Sea, 15 miles off the coast of Venezuela centered at 70 00' W longitude and 12 30' N latitude. The island is oriented in a NW - SE direction obtaining a maximum length of approximately 20 miles, and a maximum width of approximately 4 miles.

The major commodity of interest on the island is gold with associated copper and possibly silver. Records from the past indicate that some 35,000 troy ounces of gold has been exported from the island. Most of the gold exported was from narrow high grade mesothermal quartz veins running at various angles within the intrusive contacts. The gold is intimately associated with non-descript sulphides due to the advanced stages of oxidization of the sulphide minerals. Known places where gold has been found include: Tibushi, Alto Vista, Calabas, Ceru Gerard, Ceru Cristal, Bushiribana, Matrividiri, Santa Lucia and Mira La Mar. Placer gold has also been located in the numerous arroys (roois) between and amongst these gold producing areas. (Refer to Fig. 1)

LOCAL GEOLOGY

The island of Aruba has a volcanic and metavolcanic cor consisting of chloritic tuffs and schists with associated volcanic breccias and volcanosediments of primarily mafic (diabase) affinities. Uralitization has taken place in some of the diabase converting the pyroxene to hornblende, due to a late magmatic process. A large batholith has intruded into the original core obtaining a length of nearly 12 miles and a width of 2.5 miles, with a unknown depth. The perimeter of the batholith when in contact with the volcanics displays a very strong contact metamorphic relationship altering the volcanics immensely. The batholith is essentially quartz dioritic in composition grading to a diorite and gabbro along the central northern edge of the island. Porphyritic dykes possibly associated with the intrusion, have entered the volcanics in a more or less east-west direction. Quartz veining is evident through much of the quartz diorite, entering the intrusive as late stage epigenetic masses through zones of weakness (fault zones, fractures and intrusive contacts). These veins are multi-directional and vary in width from a few inches to twenty feet and obtain lengths of up to several thousand feet, with unknown depths. Quaternary limestones lap on and surround the quartz-diorite-volcanic mass. Recent dunes form beaches along the coastline, particularly along the northeast rugged coast, and along the northwest limestone coast.

HISTORY

In March 1824 gold was discovered on the north coast of Aruba in Rooi Fluit, by a young Aruban tending sheep. Tradition has it that he presented this sparkling rock to his father who later showed it to a merchant in the city of Oranjestad. This merchant offered the man $17.00, which was accepted, and the merchant in turn sold it for $70.00. Rumours of this gold discovery spread on the small island until everyone who tended sheep searched the arroys for gold.

The next find was reported near Rooi Daimari and after five months several sizeable nuggets and much fine flour gold had been collected totalling 25 lbs of gold (current 1987 value of $150,000).

An old report by the Aruba Island Mining Company Ltd. dated July 4, 1872, indicated that large quantities of free gold and deposits containing pieces of pure gold weighing from thirty to forty four lbs. were found, some of these are on display in a museum in Leyden, Holland.

The Netherlands government realized the economic significance of finding gold on one of

Larue, D.K., and Draper, G. (eds.),
Transactions of the 12th Caribbean Geological Conference, St. Croix, U.S.V.I., Miami Geological Society, P.O. Box 431552, South Miami, FL 33243, U.S.A

their islands and took measures to curb this new local pastime. All regions where gold was found were declared "not free" and the government sent soldiers to guard these areas. The areas around Diamari, Lagabi (Rooi Fluit) Wacobana, Arikok and Hadicurari were all closed to these primitive prospectors.

The gold was primarily recovered by crude placer mining processes which involved digging clay out of the arroys and allowing it to dry in the sun, all the hardened parts were beaten into small pieces. The large nuggets of gold were plucked out, and the remainder of the clay was ground up (presumably by mortar and pestle) leaving behind the smaller grains of flakes of gold. The remainder of the clay was diluted with water allowing the gold to gravitate to the bottom. In 1854 commercial firms realized that much of the gold was being lost in this antiquated milling method, and they imported crushing mills, establishing them proximal to the main producing areas. Up until this time everyone who looked for gold was required to hand it over to the government for a set price. In 1854 this system was abandoned and concessions were granted to the commercial mining firms. John Taylor and Sons of London England was one of these firms. This company did most of their work on one vein being the "Mira La Mar" just north of Jamanota the highest elevation point on the island. This vein was mined to a depth of 650 feet, and possibly to the 900 foot level. Old records indicate that in the last 8 years of operation "Mira La Mar" processed some 12,000 tons of ore with a average grade of 1.1 oz gold per ton and 0.20 oz silver per ton.

In 1872, Aruba Island Gold Mining Company Ltd., built a milling plant near Bushiribana on the north coast of the island. This mill processed the ore that was mined at Ceru Plat for a period of ten years. (the ruins of which are still standing). In 1899 Aruba Gold Concessions Ltd., built a smelting works at Balashi which apparently processed the ore from the "Mira La Mar" vein and the other veins in the central portion of the island.

In 1916 the materials required to purify the gold ore (amalgams) were no longer available due to World War 1 and gold mining in Aruba ceased. During the 92 years from 1824 to 1916, some 1340 kg of gold bullion had been exported. The production records of gold in Aruba were as follows (translated from dutch to english by Maj. Edward D. Fowler R.A.). Note: these production figures were provided for taxation purposes, who knows how much gold really left the island.

1824-1830	Government	90.396 kg
1830-1854	Free gold digging	Production unknown
1854-1874	Concession de Jongh	1.233 kg
1874-1879	Concession A.I.G.M. Co.	77.070 kg
1895-1900	Concession A.A. Co.	58.500 kg
1901-1908	Concession A.G. Concession	719.829 kg
1909-1916	Concession A.G. Company	391.600 kg
Total		1,338.628 kg

[Current market value at $400 U.S. per ounce, 1340 kg = 35,449.97 troy ounces = $14.2 Million U.S.]

These results, combined with the fascinating mining history of the island enticed Monte Carlo Gold Mines to become interested and to try to re-establish the island as a major gold producer, pending successful exploration results on the island.

Between 1924 and 1987 some minor drilling did take place, however the results showed nothing of significance to the Aruba Gold Project.

PROPERTY (GOLD CONCESSIONS)

In late September 1987 Monte Carlo Gold Mines signed an agreement with Canarub and the Aruban government, granting Monte Carlo Gold Mines exclusive rights to explore for and develop gold on the island.

PRESENT EXPLORATION

Monte Carlo Gold Mines has visited the areas of previous gold production and viewed most of the some 200 veins that have been located, over the past 162 years. It was evident that the primitive Aruban miners which were capable of producing the 35,000 troy ounces of gold used very antiquated mining methods, as well as, gold recovery procedures. Their operations were closed down due to lack of amalgam and cyanide to treat the ore due to the war effort (World War 1) and also the content of gold in the vein systems. Current mining and metallurgical technology would alleviate the problems of the past that the early miners had and would definitely increase the production from any potential minesites, and would increase the bullion production from any ore mined. It is estimated that less than one twentieth of Aruba's gold has been mined to date leaving Monte Carlo Gold Mines with a very good chance of success.

At present, work has focussed on three areas, these being Arikok, Asiboca and Kadoeshi. In each of these situations, rich quartz veins have been previously exploited. The average grade reported in the literature appears to have been about 0.5 oz gold per ton, although bonanza-type values (in the hundreds of ounces per ton) are also known to have been extracted from the surface caps to the veins in the mid to late 1800's. Monte Carlo's strategy is to sample the wallrocks in the old workings, and compile sufficient channel assay data to establish the mineable widths of the vein systems. In the past, the wallrocks (which are often impregnated with smaller auriferous vein networks) have been ignored. Drilling of these and other prospects carried out by James Gill in the 1940's substantiated the depth continuity to some of the veins. In one instance (Mira La Mar lode), the main vein was detected at a vertical depth of 1200 feet. At Arikok, for example, visible gold has been identified in a quartz vein on surface which has been traced for 500 feet +, and has the potential to be extended (on the basis of quartz float), for an additional 1200-1500 feet. In 1987, Robert Salna also discovered several large (50-150 pound) boulders which assayed 2000-8000 oz/t gold in the vicinity of this vein. In 1988, while cleaning out an old pit that was dated about 1820 to 1830 judging from the vintage of some coins that were found nearby, a large quartz sample was found relatively in place which exhibited similar values.

At Asiboca, Monte Carlo has mapped and sampled a number of quartz veins with a known strike length of 1200 feet, which average (to date) 0.22 oz/t over 7 feet, and 0.08 oz/t over 20 feet. Assays of grab samples from trenches on strike with these veins have been recorded up to 8 oz/t. At Kadoeshi, a robust quartz vein has been excavated to a depth of 50 + feet, over a strike length of 300 feet. Samples of wallrock indicate grades ranging from 0.05 to 0.3 oz/t gold. Similar values have been intersected 200-300 feet below surface in historic drilling.

Recent metallurgical testing performed by Casmyn Engineering of Oakville on the various gold

ores of Aruba indicate:

1) That there are no metallurgical problems related to the Aruba ores.
2) Using an 80% grinding to -200 mesh with a cyanide process recovers 90% to 99% of the gold from the ore.
3) Using an agglomeration technique with a 3/8" crush and using a heap leaching technique provides an 80% gold recovery with a ten day leaching cycle.

Monte Carlo Gold Mines, the current holder of the exclusive right to explore Aruba through it's wholly owned subsidiary Canarub N.V., is currently in the process of establishing a 100 ton a day placer mill, and a 200 ton per day heap leach mill in order to process some 75,000 to 100,000 tons of dump material and tailings grading between 0.08 to 0.20 oz gold per ton.

REFERENCES

J.H. Westermann, 1932, The Geology of Aruba

Amyn S. Dahya,P. Eng., April 1990, Casmyn Research and Engineering, Aruba Mining Project

Maj. Edward D. Fowler, R.A., Historical Reports, Aruba Archives

Excerpts taken from reports of:

Neil D. Novak, B.Sc. F.G.A.C., October 1988, Exploration Geologist

Laurence Curtis, PHD, President, 1989, Curtis & Associates Inc., Geological Consultants

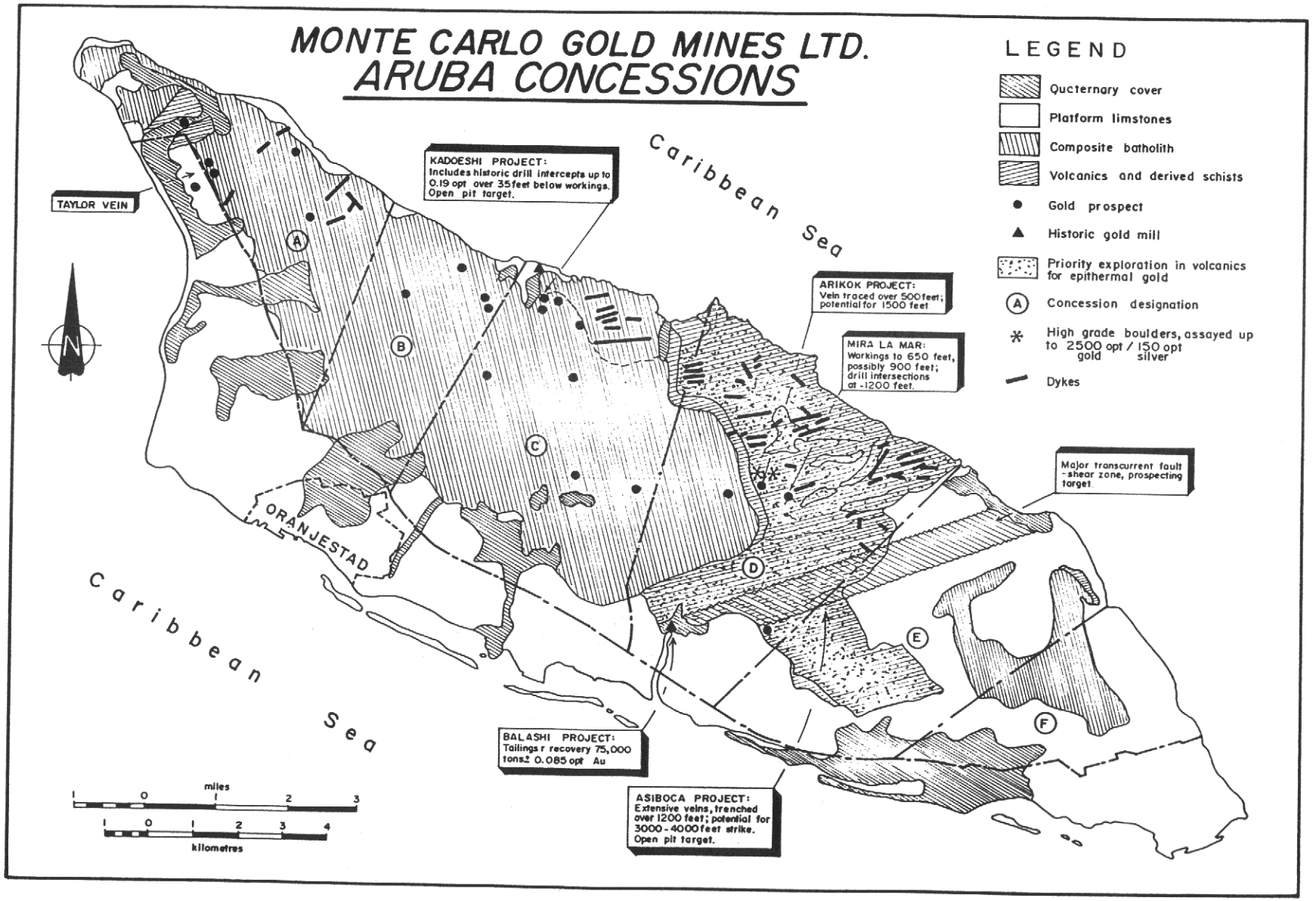
MONTE CARLO GOLD MINES LTD.
ARUBA CONCESSIONS
LEGEND
Quaternary cover
Platform limstones
Composite batholith
Volcanics and derived schists
Gold prospect
Historic gold mill
Priority exploration in volcanics for epithermal gold
Concession designation
High grade boulders, assayed up to 2500 opt / 150 opt gold silver
Dykes
TAYLOR VEIN
KADOESHI PROJECT: Includes historic drill intercepts up to 0.19 opt over 35 feet below workings. Open pit target.
ARIKOK PROJECT: Vein traced over 500 feet; potential for 1500 feet
MIRA LA MAR: Workings to 650 feet, possibly 900 feet; drill intersections at -1200 feet.
Major transcurrent fault - shear zone, prospecting target
ORANJESTAD
BALASHI PROJECT: Tailings r recovery 75,000 tons± 0.085 opt Au
ASIBOCA PROJECT: Extensive veins, trenched over 1200 feet; potential for 3000 - 4000 feet strike. Open pit target.
Caribbean Sea
Caribbean Sea
A
B
C
D
E
F
N
miles
kilometres

EOCENE STRATIGRAPHICAL STUDIES, MARACAIBO BASIN, NORTHWESTERN VENEZUELA

Rosina Pittelli Viapiana
Maraven, S.A. Exploration Department,
P.O. Box 829, Caracas 1010A
Venezuela

ABSTRACT

Benthic foraminiferal analysis were carried out in samples (cuttings, cores) of eight wells and one outcropping section from the Maracaibo Basin, northwestern Venezuela.

The wells located across the basin, from the west to southeast, are in the La Paz, Concepción, Sibucara, Cabimas and Ceuta oil fields; the outcropping Eocene section is near the Misoa Anticline, east of the Mene Grande oil field.

The early Eocene-late middle Eocene sequence includes the siliciclastic Trujillo, Misoa and Paují formations, and the siliciclastic-carbonatic Santa Rita and Jarillal formations.

Five paleobathymetric foraminiferal assemblages, were distinguished: 1) Lower alluvial Trochammina sp. assemblage typifies the Misoa Formation to the west. 2) Deltaic Trochammina - Haplophragmoides assemblages characterizes the Misoa Formation in the entire studied area. 3) A nearshore Quinqueloculina - Agglutinated Foraminifera assemblage recorded at the base and at the top of the Misoa Formation, in the central and eastern parts of the studied area. 4) Inner-Mid neritic Bolivina umbonifera assemblage recognized at the base of the Paují Formation and at the top of the Trujillo Formation. 5) Outer neritic/Upper bathial Sigmoilopsis schlumbergeri - Textularia saggitula assemblage recognized in the Paují and Jarillal formations and locally (to the midwest of the area) in the Misoa and Trujillo formations.

Paleobathymetric changes such as shallowing upward sequences (between the Trujillo and Misoa formations), deepening-upward sequences between the Misoa and Paují formations), and the main changes within the Misoa Formation are related to sediment supply and to eustatic changes of the sea level. However, local changes can be related to paleotopography and possibly to sinsedimentary faulting.

Known reservoirs in the Misoa Formation and at the top of the Trujillo Formation are sand bodies deposited in nearshore and deltaic environments; therefore, faunal assemblage distribution can be used to predict facies changes and consequently reservoir limits.

INTRODUCTION

This paper is a continuation of the studies on the micropaleontology of the Eocene Sediments from the Maracaibo basin.

The objective and scope is to compare the vertical and horizontal lithological-paleontological changes of the early Eocene - late middle Eocene sequence, characterized by the siliciclastic Trujillo, Misoa and Paují formations and the siliciclastic-carbonatic Santa Rita and Jarillal formations.

Eight wells and one outcropping section with good faunal and floral control were selected to provide a stratigraphical correlation across the basin, from west to southeast La Paz, Concepción, Sibucara, Cabimas, Mene Grande and Ceuta oil fields, (Fig. 1). The biostratigraphy of the wells was studied previously by Barbeito et al., 1985; Pittelli, 1985 and Pittelli and Molina 1989.

Sampling: The samples for this study were collected at the wells, micropaleontological analysis were carried out in cuttings, cores and side wall samples. The Trujillo, Misoa and Paují formations were sampled in 1980 by the author at the El Venado near Mene Grande area. The samples were washed through 80 u and 230 u sieves, the residue was split out in three fractions through 40, 180 and 300 sieve, and was handpicked for foraminifera, ostracodes and associated fauna.

STRATIGRAPHY

General Outline

The sequence in the Maracaibo Basin, western Venezuela, is illustrated in (Fig. 2). The stratigraphic column is one of the most interesting ones in Venezuela due to the variety of lithological types that it contains. Four major unconformities are present during the Triassic, Jurassic, Paleocene and the late middle Eocene.

Eocene

Trujillo Formation

Lithology: The Trujillo Formation is predominantely shaly, with laminated dark gray shales and black claystones. The sandstones are of different types: fine to coarse grained, poorly sorted, well cemented; gray, fine grained sandstones, calcareous, interbedded with shaly layers.

Thickness: This unit is absent in la Paz oil field (Well 1). In La Concepción oil field is 190 meters thick (Well 2), and becomes thicker toward the northeast of the studied area to 684 meters (Sibucara oil field and Tablazo Bay, Wells 3, 4 and 5). In the Cabimas oil field it has not been penetrated (Well 6) and is absent toward the southeast of the studied area, Wells 8 and 9, (Fig. 3). Around the outcropping section this unit is present but not included in this study.

Larue, D.K., and Draper, G. (eds.),
Transactions of the 12th Caribbean Geological Conference, St. Croix, U.S.V.I., Miami Geological Society, P.O. Box 431552, South Miami, FL 33243, U.S.A

FIG.1 LOCATION OF THE STUDIED AREA

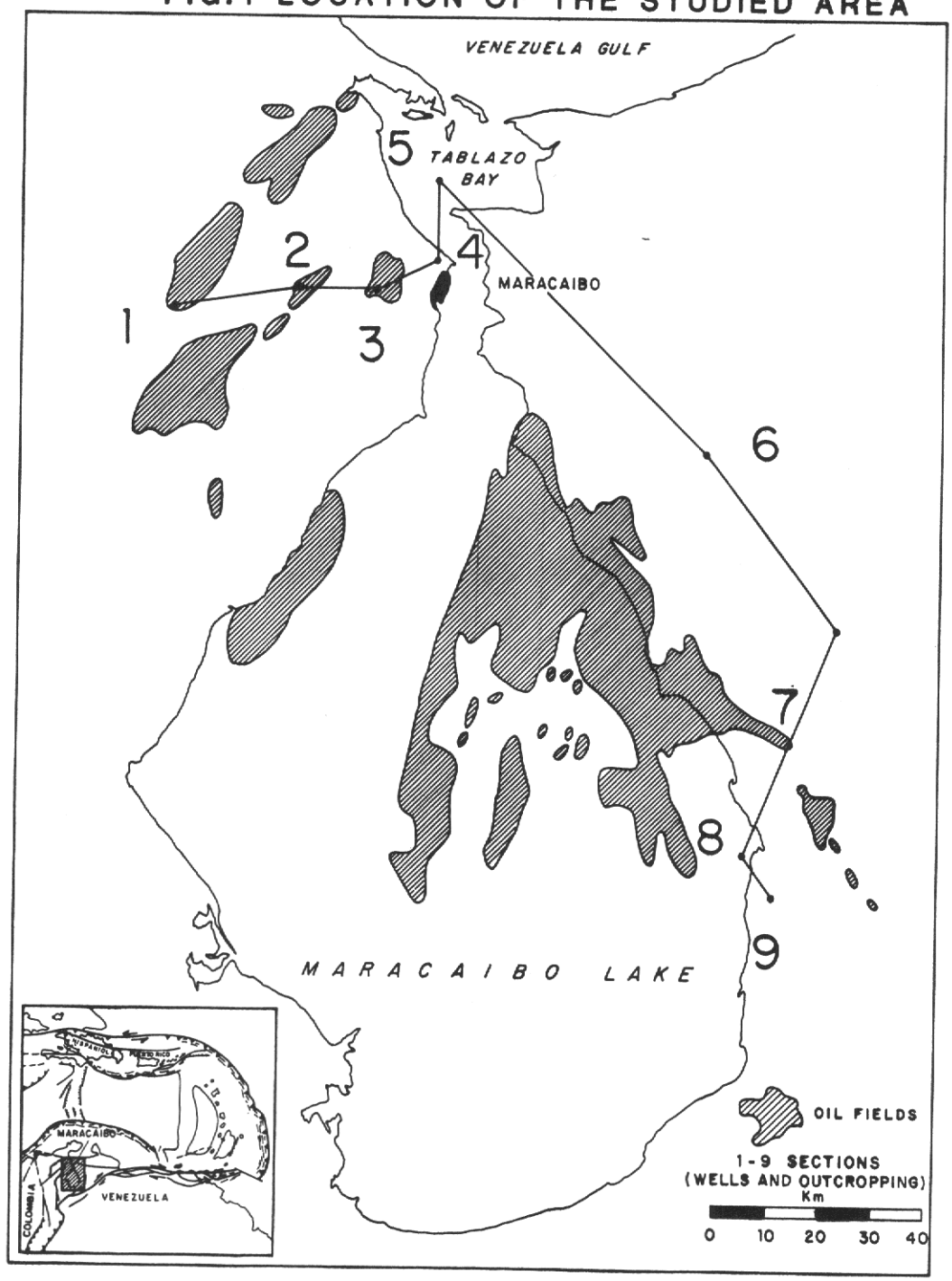

FIG.2 GENERALIZED STRATIGRAPHY

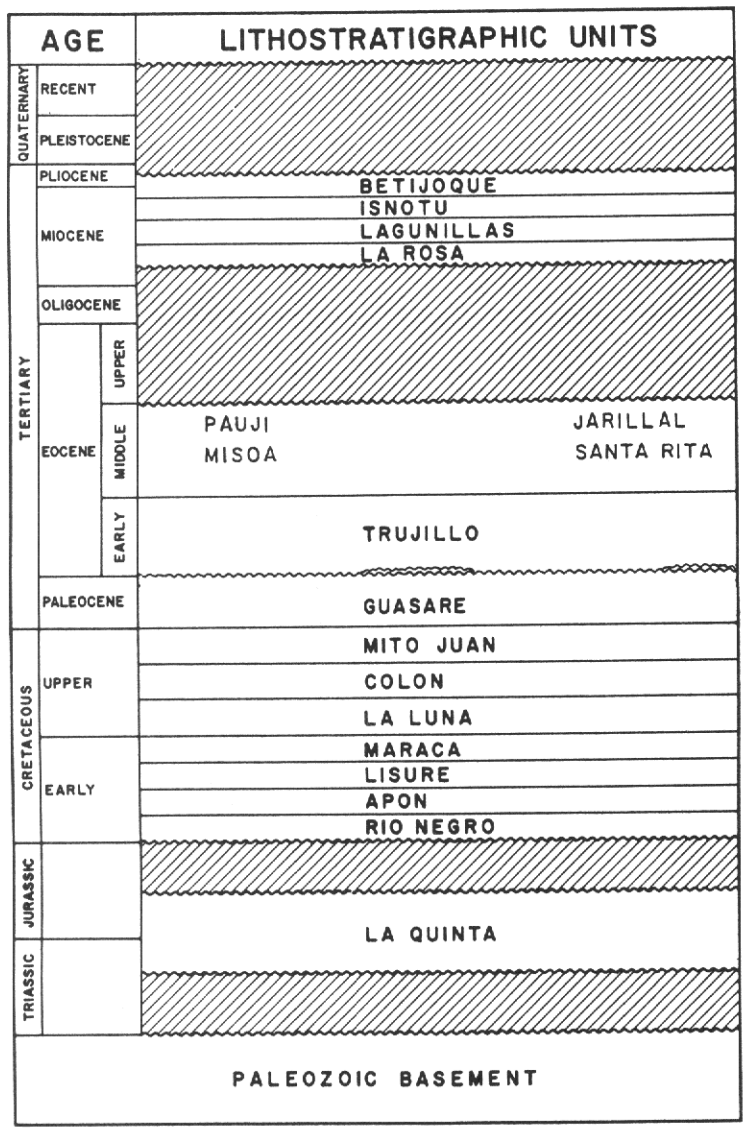

Paleontology and Age: This unit is highly fossiliferous in the middle part of the sequence; throughout its lower and upper parts the faunal contents decrease. The most important genera are represented by Sigmoilopsis schlumbergeri; abundant Plectofrondicularia sp., differents species poor preserved of Ammodiscus spp., Tritaxia spp., Gaudryina spp., Textularia sp., Bathysiphon eocenicus, Haplophragmoides canariensiformis, and Cyclammina cancellata are also present. Toward the upper part the faunal content is poorer and is represented by a Bolivina-Siphonina umbonifera assemblage, associated with some Gyroidina soldanii, and Eocene planktonic foraminifera (badly preserved).

In this unit the palinoflora assemblage is very poor, only some species of Rugotricolporites felix and Echitriporites trianguliformis are present (Barbeito et al.,1985 and Muller J. et al., 1987). The age is early Eocene, based on the presence of the planktonics foraminifera: Hastigerina bolivariana, Pseudohastigerina. aff. wilcoxensis, Acarinina aff. broedermanni, A. pentacamerata and Morozovella edgari, Planktonic zone Morozovella edgari-Acarinina pentacamerata, sensu Toumarkine and Luterbacher, 1985 and P6 - P9, Berggren and van Couvering 1974 (fide Toumarkine and Luterbacher op. cit.).

Misoa Formation

Lithology: Mainly sandy sediments typifie this formation, which consists of light gray to brownish gray, medium to coarse-grained, consolidated sandstones. In the whole formation are subordinate amounts of fine to medium, gray and dark gray, carbonaceous, micaceous, laminated and cross-laminated sandstones. Interbedded with the sandstones are gray to dark gray shales.
Thickness: In La Paz oil field, Well 1, the Misoa Formation is 851 meters thick. Within the La Concepción and Sibucara oil fields, Wells 2, 3, and 4, thicknesses more than 2400 meters have been encountered. Toward the northeast and southeast the thicknesses of the Misoa Formation ranges between 1102 and 860 meters. In the outcropping section, only 760 meters were measured. In Well 9, this formation is thinner, the average thickness is about 320 meters (Fig. 3).
Paleontology and age: In the western part of the studied area the abundant genera Trochammina typifies the Misoa Formation. In the whole area the faunal assemblages are Trochammina spp., Ammobaculites sp. and Haplophragmoides spp. Local changes toward the central and the eastern parts of the studied area, are represented by diversity of fauna such as badly preserved Trochammina, Haplophragmoides, Recurvoides, Quinqueloculina, ostracods and some gastropods. A few planktonics foraminifera were recorded in the Tablazo area: Acarinina gr soldadoensis and Globigerinatheka sp. The palinoflora contents is characterized by the presence of Echitriporites trianguliformis, Retitricolporites guianensis, Bombacacidites soleaformis and Retitricolpites magnus (Barbeito et al., 1985 and Muller J. et al.,1987). The age determination based on palinoflora contents and planktonics foraminifera is late early Eocene to middle Eocene.

Santa Rita Formation

Lithology: The Santa Rita Formation consists of coarse-grained conglomerates, with clasts averaging 5 cm in diameter, confined to the lower portion of the formation, calcareous sandstones, calcareous dark gray shales and marls with subordinate lepidocyclinids-red algal limestones (Fig. 3).
Thickness: This formation is only present in Well 6, where the thickness is 458 meters.
Paleontology and age: Textularia saggitula, badly preserved agglutinated foraminifera, abundant Lepidocyclinida pustulosa, Helicolepidina sp., Nummulites (Paleonummulites) trinitatensis, Melobesioid algae and molluskan debris are all present. The age of the Santa Rita Formation is middle Eocene based on fossils contents.

Paují Formation

Lithology: The Paují Formation contains dark gray silty laminated shales, black claystones, consolidated thin layers of gray, fine-grained sandstones and thin beds of silstone. The sandstones and silstones beds become thicker toward the base of the Paují Formation.
Thickness: The Paují Formation is present only in the southeast part of the studied area (Well 9), where the thickness is 258 meters.
Paleontology and age: Abundant benthonic and planktonic foraminifera such as: Bolivina spp., Textularia saggitula, Truncorotaloides rohri, Turborotalia cerroazulensis cerroazulensis, Globigerina eocaena and Globigerinatheka index are present. The age determination based on planktonic foraminifera is late middle Eocene; planktonic zone Truncorotaloides rohri, sensu Toumarkine and Luterbacher, 1985; and P14, sensu Berggren and van Couvering 1974 (fi and Luterbacher op. cit.).

Jarillal Formation

Lithology: The characteristic lithology of this formation is dark gray to black shales, ocassionally silty and calcareous; light gray consolidated, fine grained, well sorted sandstones and sandy gray limestones.
Thickness: This formation is only present in Well 6 with 1366 meters (Fig. 3).
Paleontology and age: The fossils content is very similar to the Paují Formation, the main difference is the presence of some Nummulites at some calcareous levels near the top of the Jarillal Formation. The age determination is late middle Eocene based on fossil control. Planktonic zone Truncorotaloides rohri, Toumarkine and Luterbacher, 1985 and P-14, sensu Berggren and van Couvering, 1974 (fide Toumarkine and Luterbacher, 1985).

BIOFACIES

According to their foraminiferal contents, five major assemblages were recognized.

Trochammina Assemblage

Characteristics: This biofacies has been defined because of the abundance of the agglutinated foraminifera Trochammina spp. These species have

FIG. 3 REGIONAL CORRELATION

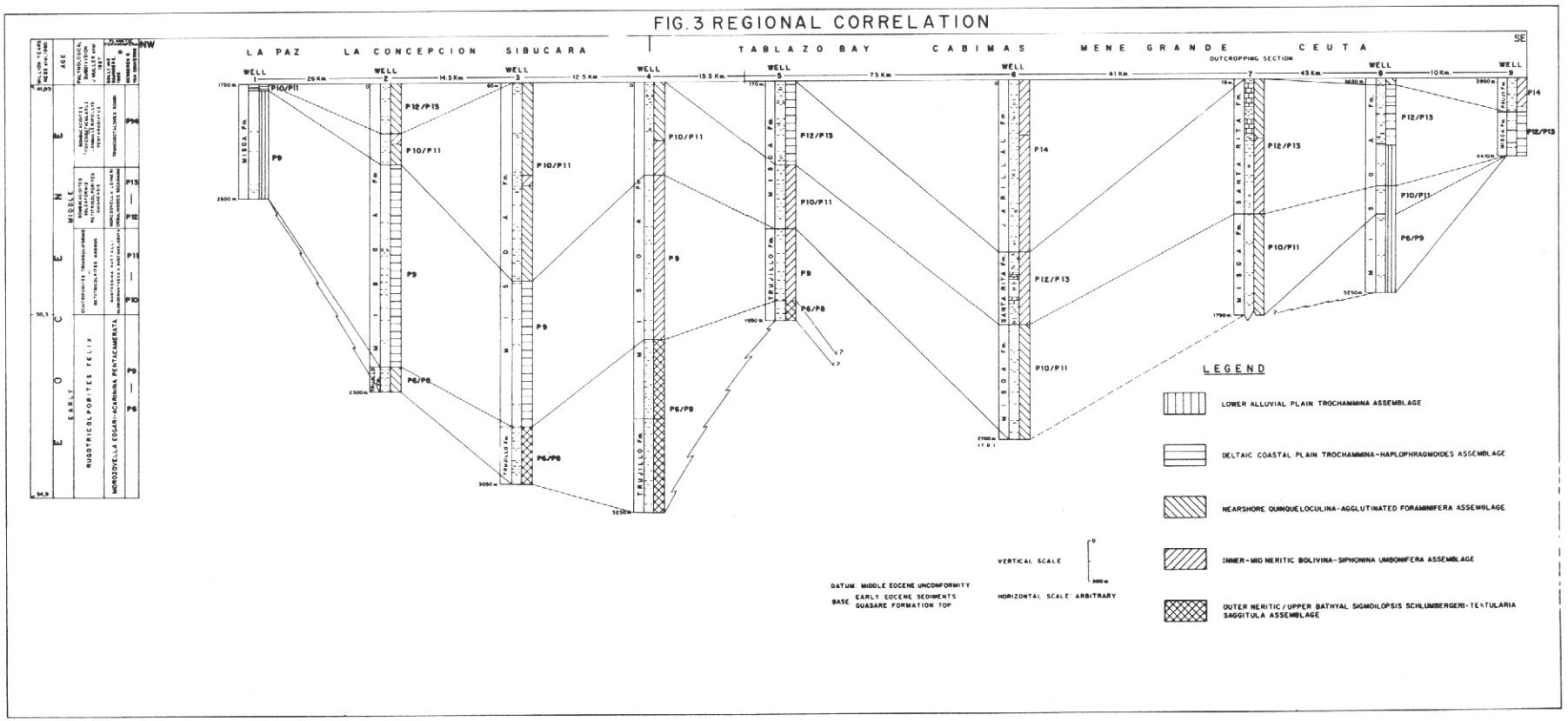

slightly compressed tests, with outlines rounded to ovate, periphery broadly rounded; walls are thin a and very fine grained. The diameter of th test is 0.40-0.70 mm; all the specimens are badly preserved. The others agglutinants have a relative representation of about 30% and include the genera Ammobaculites and Miliammina, also badly preserved.

Depositional environment: The Trochammina Assemblage, according to Barbeito et al, 1985 is typical of lower alluvial plain palaeoenvironment (brackish water).

Geographical distribution: This biofacies is predominantly developed in the western part of the studied area, La Paz oil field, but it appears also to be present in Well 8, southeast of the area (Fig. 3).

Stratigraphic position: In La Paz area, the biofacies occurs within the Misoa Formation in the whole sequence, and in Well 8 is confined to the middle and lower portion of the Misoa Formation.

Trochammina - Haplophragmoides Assemblage

Characteristics: The most abundant species are the agglutinated foraminifera Trochammina spp. and Haplophragmoides spp. The Trochammina are very similar to the first assemblage, the genera Haplophragmoides have a planispirally test, enrolled and evolute; wall finely agglutinated and thin, not alveolar and compressed. The specimens are poorly preserved. Others components of the assemblage, about 20% are agglutinants specimens, which are badly preserved, and difficult to identify.

Depositional environment: According to Barbeito et al, 1985, the assemblage is typical of deltaic coastal plain environments, marsh deposits, brackish water.

Geographical distribution: This biofacies has been recorded in the western part of the area, in La Paz (Well 1) and Concepción oil field (Wells 2 and 3), and in the southeast (Wells 8 and 9). In the center part of the area it is absent (Fig 3).

Stratigraphic position: The biofacies occurs in the upper-most portion of the Misoa Formation toward the west of the area. Toward the southeast, the assemblage have been recorded in the upper portion of the Misoa Formation (Well 8) and in the lower portion of the Misoa Formation (Well 9).

Quinqueloculina - Agglutinated Foraminifera Assemblage

Characteristics: This assemblage is made up basically of diversified agglutinated Foraminifera such as abundant Haplophragmoides spp., Eggerella bradyi, Recurvoides sp., and others arenaceous specimens badly preserved and difficult to identify. The Haplophragmoides specimens are different from those of the Trochammina-Haplophragmoides assemblage. The more conspicuos characteristics of those taxa are: test planispirally enrolled; wall coarsely arenaceous and granular, alveolar. Other components of the assemblage are calcareous foraminifera: small-sized Quinqueloculina sp. and a few species of piritized Bolivina sp.

Depositional environment: This assemblage reflects an increase in marine influence; shallow water, nearshore deposits.

Geographical distribution: The assemblage is more conspicuos in the central and southeast part of the studied area.

Stratigraphic position: Absent in La Paz (Well 1) and in the El Tablazo area (Well 5), this assemblage has been recorded in the upper portion of the Wells 2 and 3 and in the upper most portion of Well 4, (Misoa Formation). Toward the southeast the assemblage has been recorded in the lower portion of Well 6 (only Misoa Formation); upper and lower portion of the outcropping section (Santa Rita and Misoa formations); upper most portion of Well 8 and lower portion of Well 9 (Paují Formation).

Bolivina - Siphonina umbonifera Assemblage

Characteristics:. It is marked almost exclusively by large-sized calcareous foraminifera. Most conspicuos in this assemblage are: Siphonina umbonifera and different species of Bolivina, while the populations of several others are common Lenticulina sp., Gyroidina soldanii, and rare G. neosoldanii. Also present are the large-sized (up to 2 mm) Textularia saggitula, many broken Textularia spp., planktonic foraminifera, and ostracods, pteropods and fish teeth.

Depositional environment: This biofacies represents an interval of open marine fauna, which clearly differs from the mentioned biofacies described before. This assemblage is typical of Inner to mid neritic deposits.

Geographical distribution: It is distributed in the whole area, except in Well 1 and in the southeast Wells 8 and 9 (Fig 3).

Stratigraphic position: This biofacies have been recorded in the upper portion of Wells 2 and 3, probably as a respond to a large marine incursion (Fig. 3). In the central and southeast of the studied area, the assemblage was recognized in the upper and middle portion of the sequences at the base of the Paují Formation, top of the Trujillo Formation and Santa Rita Formation, and within the Jarillal Formation.

Sigmoilopsis schlumbergeri - Textularia saggitula Assemblage

Characteristics: This biofacies is defined by the abundance of open marine fauna. The faunas, are extraordinarily rich and diversified. In its most typical development, the assemblage includes: 60% of large-sized and coarsely arenaceous foraminifera (up to 3 mm), with abundant Sigmoilopsis schlumbergeri and Textularia saggitula; other agglutinants are Eggerella bradyi, Ammodiscus sp., Gaudryina sp., Cyclammina cancellata, and Tritaxia sp. 30% of the assemblage is represented by large-sized calcareous foraminifera Plectofrondicularia sp, Lenticulina sp., Gyroidina soldanii and by thick wall spinose Globigerinids, badly preserved.

FIG.4 EARLY EOCENE: ZONE P9

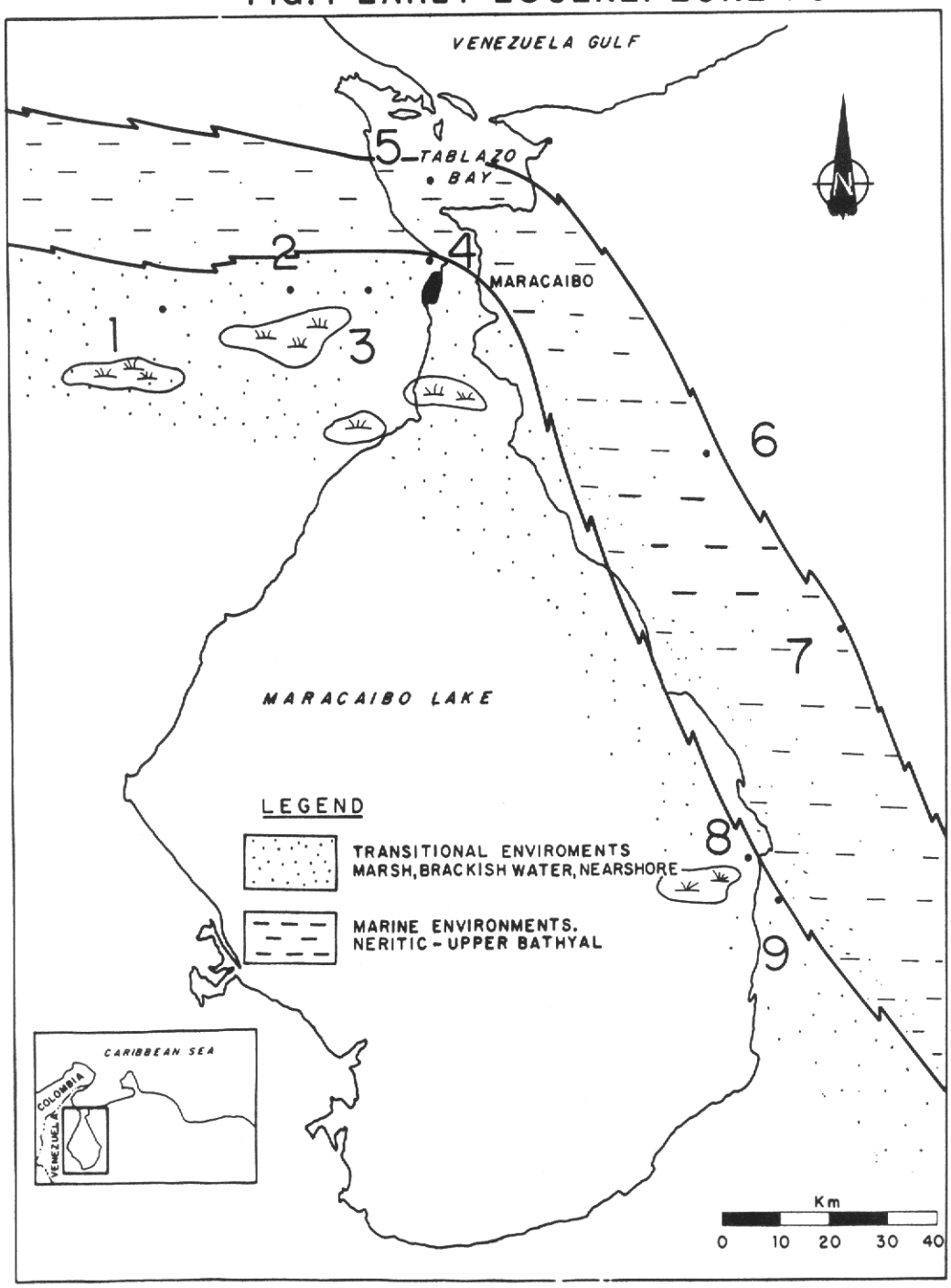

FIG.5 MIDDLE EOCENE: ZONE P10-P11

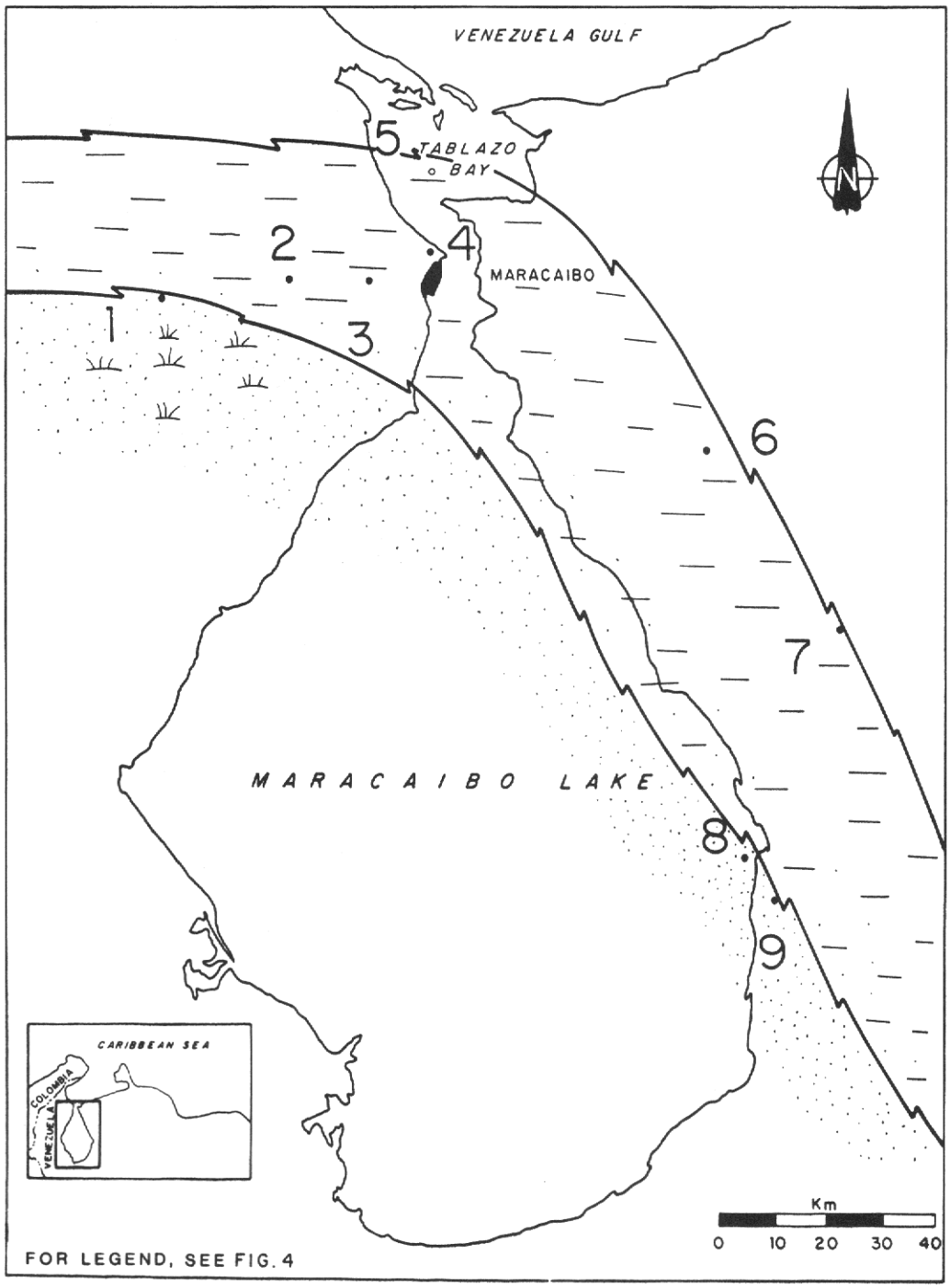

FIG.6 MIDDLE EOCENE: P12-P13

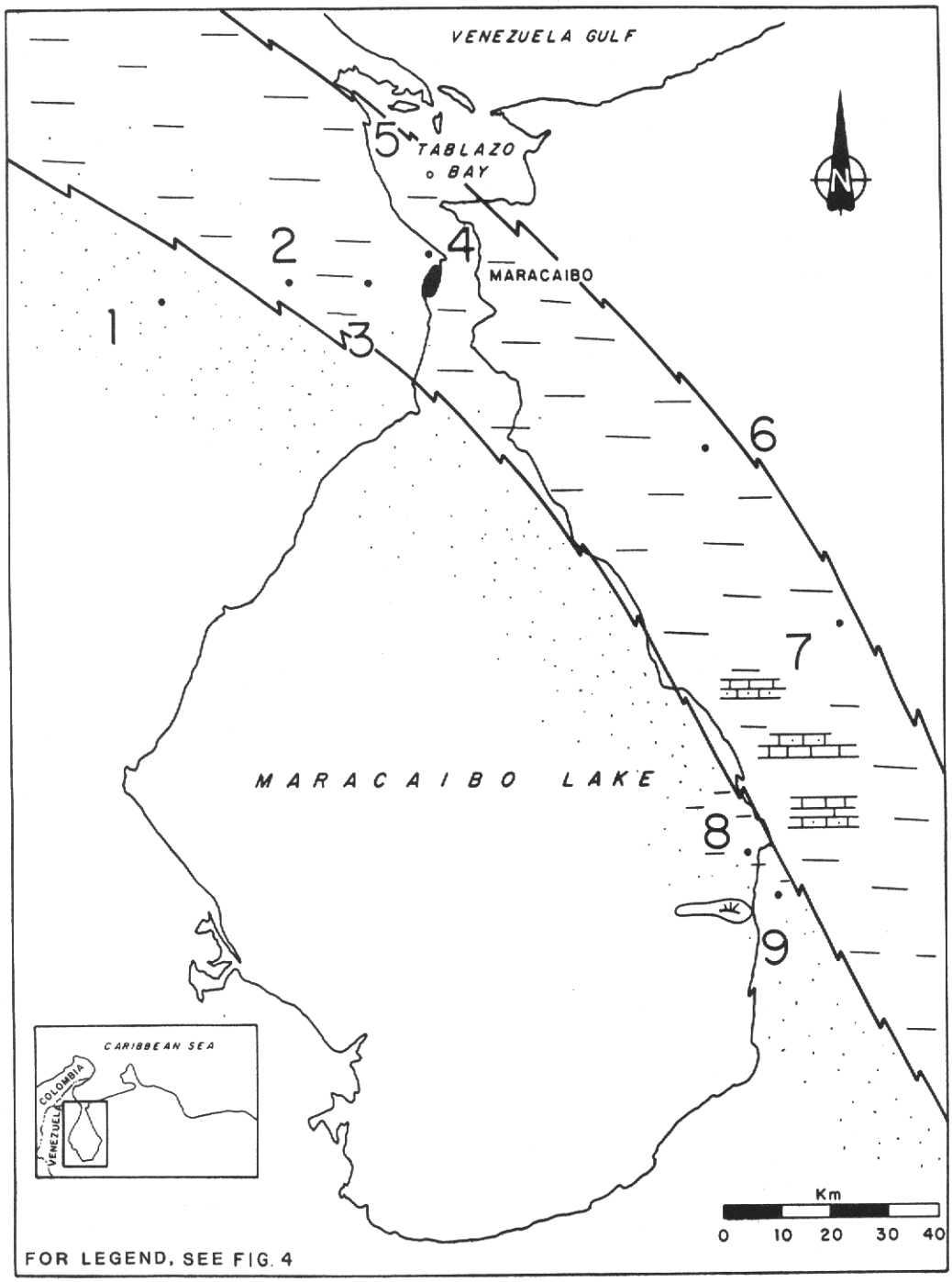

Depositional environment: This assemblage is typical of outer neritic to upper bathyal deposits.

Geographical distribution: It is found in La Concepción, Sibucara and Tablazo area Wells 2, 3, 4 and 5 (Fig. 3).

Stratigraphic position: The assemblage is typical of the Trujillo Formation. It is absent in all the other formations but toward the southeast is present in the lowermost portion of the Misoa Formation. (Fig. 3).

DISCUSSION OF RESULTS

Time vs variation of assemblages

Most of the biofacies discussed here in, are based exclusively on the presence of mostly shallow, brackish-water assemblages of species with no time-stratigraphic significance; because they are environmentally controlled, notably variations in age at different sites within the basin could occur. Exceptions are the faunal marine assemblages, which appear to represent reasonably reliable chronostratigraphic in situ units. Based on the sparse planktonic foraminifera data and palinological biostratigraphy (Barbeito et al, 1985), I correlated the evolution in time of the defined biofacies. According to that scheme, I conclude that the oldest (Zone P9-P10) and shallowest sediments are in the NW, La Paz area (Fig 3).

Paleogeographic map:

In order to clarify the distribution of the several sediment types, I constructed three paleogeographic maps, based on palynological studies (Muller J. et al., 1987) and micropaleontological studies (Pittelli R., 1980, 1985, Barbeito P.J. et al, 1985 and Pittelli R. and Molina A., 1989) they are as follows.

Early Eocene Zone P 9 (Fig. 4): Locally swamp deposits and deltaic sediments are present in La Paz and Concepción oil field and toward the southeast (Wells 8 and 9). The water depth increases gradually to the northeast up to bathyal water depth. A valid exploration target may lie in deltaic sandstones. Sands are apparently absent in the Tablazo and Mene Grande area (Wells 5, 6, and 7).

Middle Eocene Zone P 10 - P 11 (Fig 5): Represents a marine invasion up to Concepción and Sibucara oil fields, with deepest conditions persistently in Tablazo and Mene Grande area. In Wells 1, 8 and 9 deltaic environments are still developed, therefore this is the best area for exploration target; Misoa Formation, Trochammina Assemblage and Trochammina-Haplophragmoides Assemblage.

Middle Eocene Zone P 12 - P 13 (Fig. 6): Stable conditions took place, the marine environment persisted to the north of Wells 1, 8 and 9. Some carbonate sediments are developed in the southeast of the studied area. The most important sands for exploration target are localized in Wells 8 and 9; Misoa Formation, Trochammina-Haplophragmoides Assemblage and Quinqueloculina-Agglutinated Foraminifera Assemblage.

CONCLUSIONS

Five biofacies recognized in the area permitted to determine shallowing-upward sequences between the Trujillo and Misoa formations, and deepening-upward sequences between the Misoa and Paují formations (Fig. 3).

The oldest and shallower sediments are in the La Paz oil field, toward the northwest of the studied area.

Main changes recognized within the Misoa Formation, probably are related to the sediment supply and eustatic changes.

The sediment supply tendency was southwest-northeast.

Relating the biofacies changes to the sedimentary environments and to sands distribution, we can predict facies changes and consequently sandy reservoir limits.

Acknowledgments

The author is thankful to Petróleos de Venezuela (P.D.V.S.A., Caracas) and its affiliate Maraven, S.A. for permission to publish this paper. I am grateful for constructive criticism provided by Francia Galea Alvarez, Emira Cabrera de Molina and Federico Russomanno. Many thanks are due L. Lezama, who helped with the preparation of the poster presented at the St. Croix meeting. The drafting was by the Maraven geology department, drafting department.

REFERENCES

Barbeito P.J.,R. Pittelli and Evans A.M., 1985, Estudios Estratigráficos del Eoceno en el área de Mara - Maracaibo, Venezuela Occidental, basado en Interpretaciones Paleontológicas y Palinológicas. VI Congr.Geol. Venez., Tomo I, 109-139.

Muller J., Di Giacomo E., and van Erve A., 1987, A Palinological Zonation for the Cretaceous, Tertiary and Quaternary of Northern South America. Amer. Assoc. Stratigrap. Palyn. Found. AASP Contributions Series Number, 19, 7-76.

Pittelli R., 1980, Estudio Geológico realizado en el área de Sipayare y El Venado, Distrito Bolivar y Baralt, Estado Zulia, Trab. Espec. de Grado., Inedit, 1980. 125 p.

Pittelli R., 1985, Estudio Geológico Regional de Falcón Occidental. Informe Bioestratigráfico. Private Report. Maraven S.A. 75 p.

Pittelli R. and A. Molina, 1989, El Eoceno medio tardío y Eoceno tardío de la parte occidental de la Cuenca de Falcón. Bol. Soc. Venez. de Geol., 35. In press.

Toumarkine, M. and Luterbacher, H., 1985, Paleocene and Eocene planktic foraminifera in Bolli H. M., Saunders J. B. and Perch-Nielsen K. (editors) Plankton Stratigraphy. Cambridge University Press, 87-154.

INTERPRETATION OF GRAVITY ANOMALIES, MASAYA CALDERA COMPLEX, NICARAGUA

Charles B. Connor
Department of Geology
Florida International University
Miami, FL, 33199, USA

Stanley N. Williams
Dept. of Geology and Geophysics
Louisiana State University
Baton Rouge, LA 70803 USA

ABSTRACT

The Masaya Caldera Complex, Nicaragua, has been the site of major explosive and effusive eruptions in the Quaternary and remains active today. We have interpreted gravity data collected during a regional gravity study by R.L. Williams (1972) in an effort to further delineate geologic structures associated with this unique volcanic feature. A total of 217 gravity stations were occupied in the vicinity of Masaya caldera. Several large amplitude gravity anomalies occur in the area, including a broad +35 mgal high centered on the NE side of Masaya caldera. Upward continuation of the gravity data reveals that this anomaly is similar in shape to the caldera itself: elongate approximately N60°W, parallel to the strike of the Nicaragua Depression, and that it is caused by an anomalous mass located at high levels in the crust. A two and one-half dimensional gravity model suggests that the anomaly is produced by a thin, plate -like body, of density contrast between 300 and 500 kg/m^3. We believe the anomaly is caused by an igneous intrusion, possibly a laccolith or sill, which is approximately 17 km long, 6 to 7 km wide, 2 km thick, and buried at a depth greater than 0.5 km. This body is offset from the caldera and probably intruded prior to the formation of the active caldera. Its presence indicates that the locus of activity has shifted over time, and that volumes of magma, similar to those required by current outgassing models, have intruded to shallow levels previously. Other, negative gravity anomalies occur near the active crater and may be caused by the presence of magma beneath the active crater, conduit geometry or a thick accumulation of tephra.

INTRODUCTION

The Masaya Caldera Complex, Nicaragua (11.98°N, 86.15°W) is an unusual center, which has been very active since the first European exploration of Central America. The shield-like form and fluid basaltic lavas are quite unlike those found at other Central American volcanoes (McBirney, 1956; Mooser et al., 1958; and Simkin et al., 1981). The caldera is well-defined by near vertical bounding faults of zero to 250 m relief and measures approximately 12 x 5 km, elongate in a N60°W orientation, parallel to the axis of the Nicaraguan Depression. Recent volcanic activity at Masaya has been focused at several small pit craters, within the caldera. Santiago Crater, which was formed in 1853 (S.N. Williams, 1983a), is the current site of degassing and extrusive activity. Recent detailed geological and volcanological studies have demonstrated that Masaya has also been the site of at least two Plinian eruptions in the Quaternary (S.N. Williams, 1983b). The latest episode of activity (since late 1979) has involved energetic degassing, through an old lava lake within the Santiago Crater, of a subjacent intrusive mass (Stoiber et al., 1986) and, most recently, the formation of a new lava lake (Cruesot et al., 1989).

The utility of gravity data as an aid in the interpretation of volcanic structures and activity has been amply demonstrated (Yokoyama, 1972; Tsuboi, 1983; Rymer and Brown, 1984; Rymer and Brown, 1986; Brown et al., 1987; and Eggers, 1987). Our recent work at Masaya volcano (Crenshaw et al., 1982; S.N. Williams, 1983a; S.N. Williams, 1983b; Williams and Stoiber, 1983; Stoiber et al., 1986; Walker and Williams, 1986) has established the importance of shallow intrusive magmatic activity and long-term degassing processes at Masaya. In an effort to further improve our understanding of intrusive magma volumes and to delineate geologic structures associated with this major volcanic feature, we have interpreted gravity data collected as part of a regional gravity study by R.L. Williams (1972).

In the gravity study by Williams, a total of 217 stations were occupied in the vicinity of Masaya caldera. Thirty-one stations are located within the caldera itself. Most of these gravity

Larue, D.K., and Draper, G. (eds.),
Transactions of the 12th Caribbean Geological Conference, St. Croix, U.S.V.I., Miami Geological Society, P.O. Box 431552, South Miami, FL 33243, U.S.A

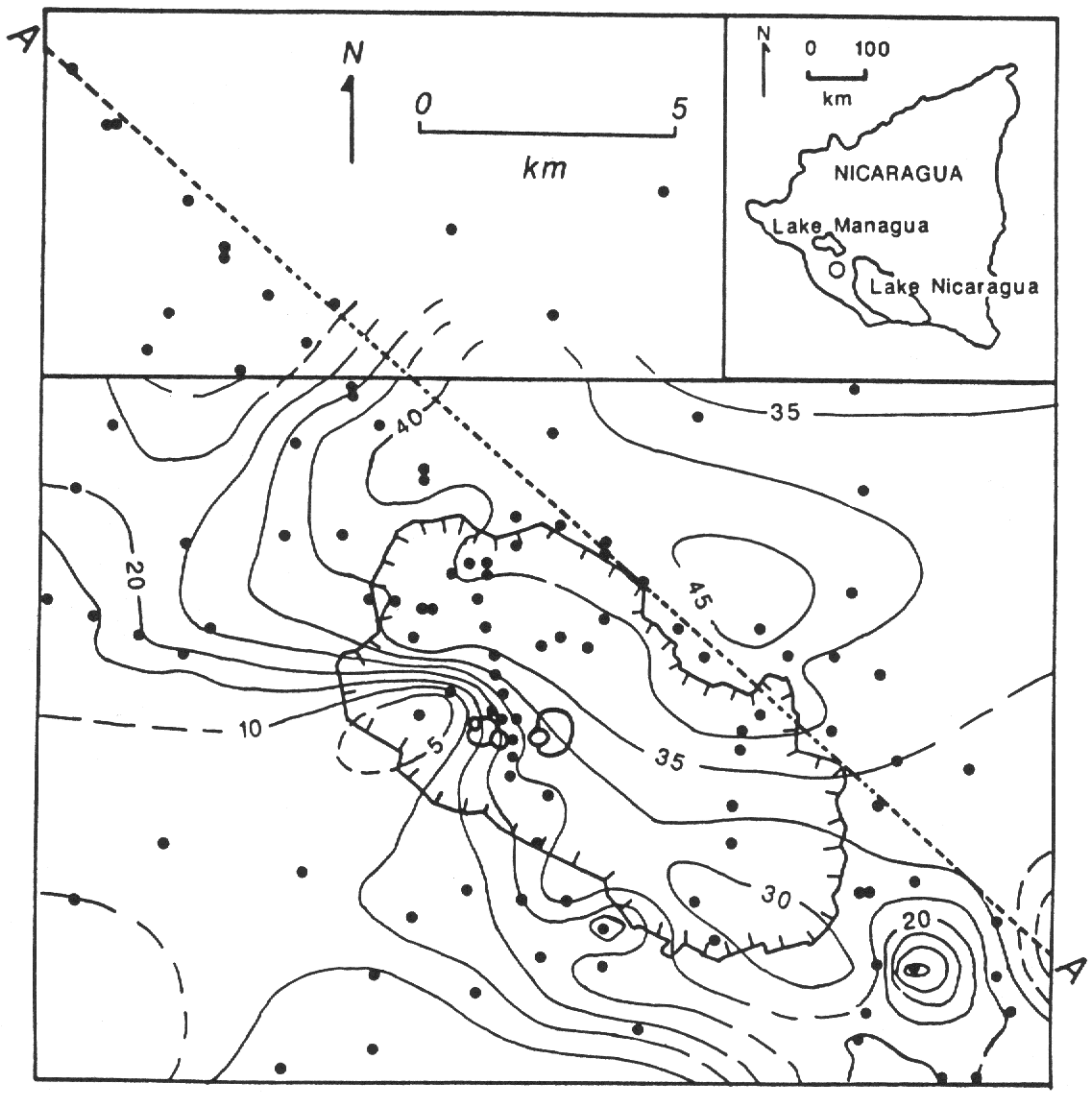

Figure 1. Complete Bouguer anomaly map of the Masaya caldera complex and surrounding area. The contoured area (south of solid line) was contoured using a finite-difference minimum curvature interpolation algorithm (Briggs, 1974), Gravity contour interval is 5 mgal and values are relative to the Managua International Airport station (R.L. Williams, 1972). Gravity stations are shown as solid circles. In this and following figures, the caldera -bounding faults are indicated by solid hachured lines and Santiago and other Recent craters within the caldera are outlined. Profile A-A'; is drawn and modeled in Figure 4. Inset: Nicaragua, with the location of Masaya Caldera Complex indicated by the open circle.

stations are located along roads that transect the area; many of the stations were occupied twice. Line leveling and barometric altimetry provided elevation control for this survey and gravity data were reduced to the complete Bouguer anomaly by R.L. Williams (1972).

GRAVITY ANOMALY MAPS

We utilized these data over an area of approximately 25 x 15 km, centered on the caldera (Figure 1). The data were interpolated to a 50 x 50 grid using a minimum curvature algorithm and contoured (Briggs, 1974; Snyder, 1978). Despite the low sampling density, several large-amplitude gravity anomalies are immediately apparent (Figure 1).

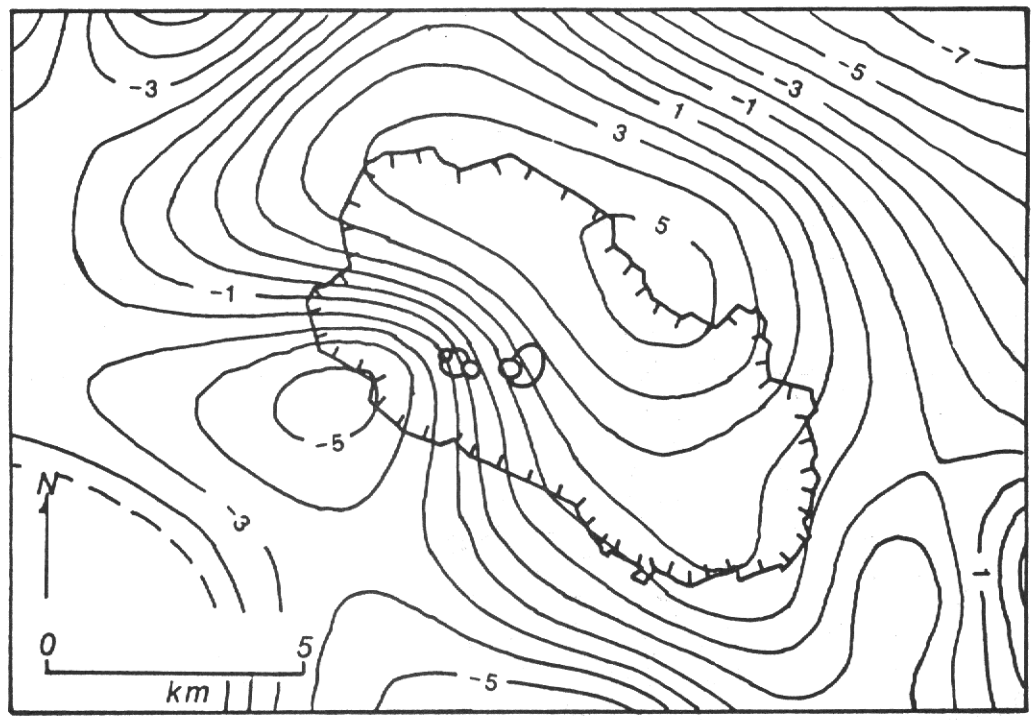

Fig. 2. Upward continuation by 1500m of the interpolated gravity values clarifies the board, large-amplitude anomaly centered on the northeast wall of Masaya Caldera. A best-fit plane was removed prior to making the upward continuation. This continuation was done in the frequency domain using the methods and algorithm of Hildebrand (1983). Contour interval is 1 mgal.

As an aid to the interpretation of these anomalies, a best-fit plane was removed from the interpolated grid and the residuals were upwardly continued (Figure 2). Upward continuation acts to attenuate short-wavelength anomalies caused by local, shallow features. In this case, upward continuation to 1500 m has the effect of isolating a broad positive gravity anomaly, centered on the northeast boundary of the caldera. This positive anomaly is based on a large number of data points and is thought to be a robust signature. Even this anomaly is much attenuated and essentially disappears when the data are upwardly continued to 2500 m, indicating that the source of the anomaly is located at high levels in the crust. A negative anomaly located on the southwest corner of the caldera is only supported by one data point and cannot be treated with as much confidence. The shape and scale of the NE anomaly is like that of Masaya caldera itself, i.e. the anomaly (Figure 2) is elongate approximately N60^{o} W, parallel to the strike of the Nicaragua Depression.

Near-surface, local anomalies were isolated by wavelength filtering. A high-pass, ramped filter was constructed such that anomalies at wavelengths longer than 6 km were strongly attenuated (Figure 3). Of note is a negative anomaly with an amplitude of approximately 15 mgal, located immediately NW of the Santiago Crater. Although the true extent of this anomaly cannot be well constrained from the data (Figure 1), it is clear that a mass deficiency was present here at the time of this survey.

GRAVITY MODEL AND INTERPRETATION

We created a two and one-half dimensional gravity model along a 27 km-long traverse (A-A', Figure 1) near which there is a relatively high density of gravity stations. In two and one-half dimensional modeling, the model is taken as having a finite length perpendicular to the profile, rather than infinite length in this dimension, as assumed in two dimensional gravity modeling (Webring, 1985). The profile, A-A', transects the positive gravity anomaly near the NE rim of the caldera. Gravity values from stations located up to 1.5 km from the traverse line were projected onto the plane of the profile and 9 mgal were subtracted from the value recorded at each station so that the value of the station at point A (Figure

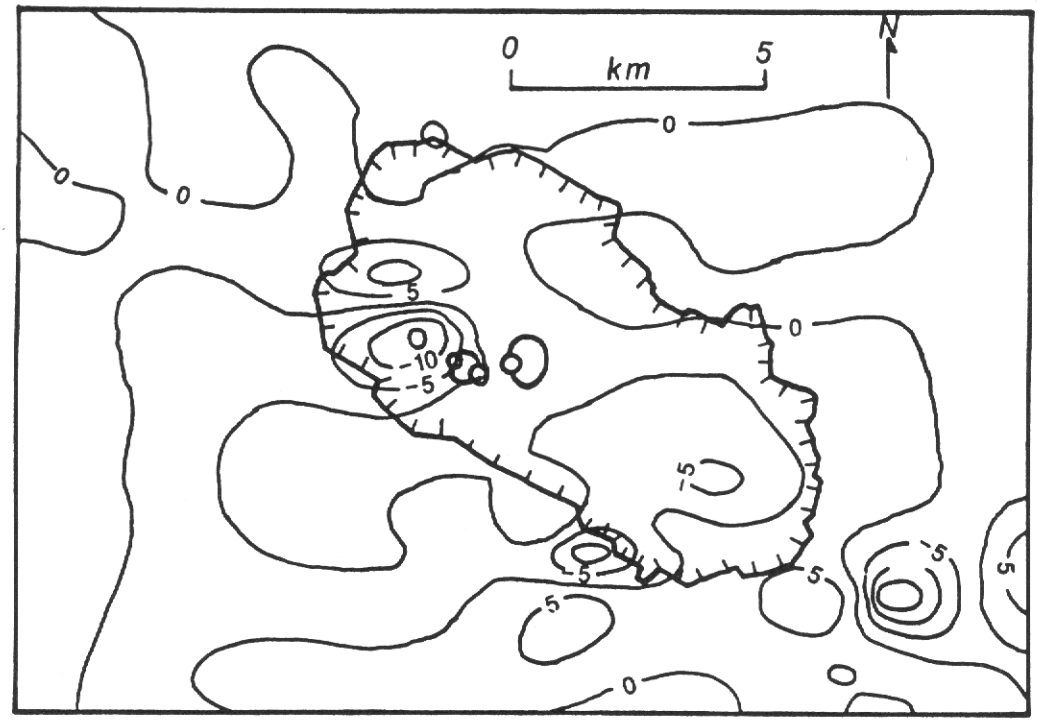

Fig. 3 Filtering the interpolated gravity values using a high-pass filter isolates a 15 mgal negative anomaly, located NW of the Santiago crater. Filtering was done in the frequency domain using a ramp filter: wavelengths greater than 7 km are completely removed, wavelengths less than 5 km are passed. Contour interval is 5 mgal.

1) was zero mgal. The profile and accompanying model are illustrated in Figure 4.

In order to constrain the gravity model, we have incorporated several geologic features into it. The regional geology near Masaya caldera consists of a sequence of Tertiary and younger interbedded lava flows, pyroclastics, and volcanogenic sediment which are generally termed the Las Sierras Formation. The total thickness of this sequence is unknown, but it is at least 600m thick in some locations (Bice, 1980), The details of the stratigraphy and origin of the Las Sierras formation await future studies but it is thought that at least part of the deposits were erupted from Masaya, some as recently as 29,200±200y.b.p. (Williams, 1983a). The detailed geological study of the caldera conducted by one of us (SNW) produced evidence that the present caldera formed as a result of a single catastrophic collapse event triggered by the eruption of voluminous ignimbrites and pyroclastic surges of basaltic composition. The timing of caldera formation is constrained by carbon-14 ages determined on organic debris within the regionally extensive surge deposit (known as the El Retiro in Managua (Bice, 1980) to be between 2,250 and 6,500 y.b.p. After formation of the caldera, renewed magmatism caused the infilling and ultimately, in some areas, overfilling of the caldera with younger lava flows. Eruption rates average from 1.9-5.5 x 10^6 m^3/year, to produce a total erupted volume of lava flows of about 14 km^3 (Williams, 1983a). The historic record of activity at Masaya indicates quite a different character, being dominated by active degassing of large volumes of magma which are rarely or never erupted. The historic eruption rates have been about 0.07 x 10^6 m^3/year or only 1/20 to 1/60th of the recent record. Our data on the total flux of sulfur dioxide (Stoiber et al., 1986) released during the 1979-1987 degassing crisis, combined with the historic record, allows us to calculate that there has been intrusion of approximately 10 km^3 of degassed magma during the past century alone. That could amount to a sill-like body of 180 m thickness, beneath an area equal to the caldera or a sphere of radius 1.3km (for comparison, the diameter of the Santiago Crater (from which all of the most recent degassing emanated) is about 600m).

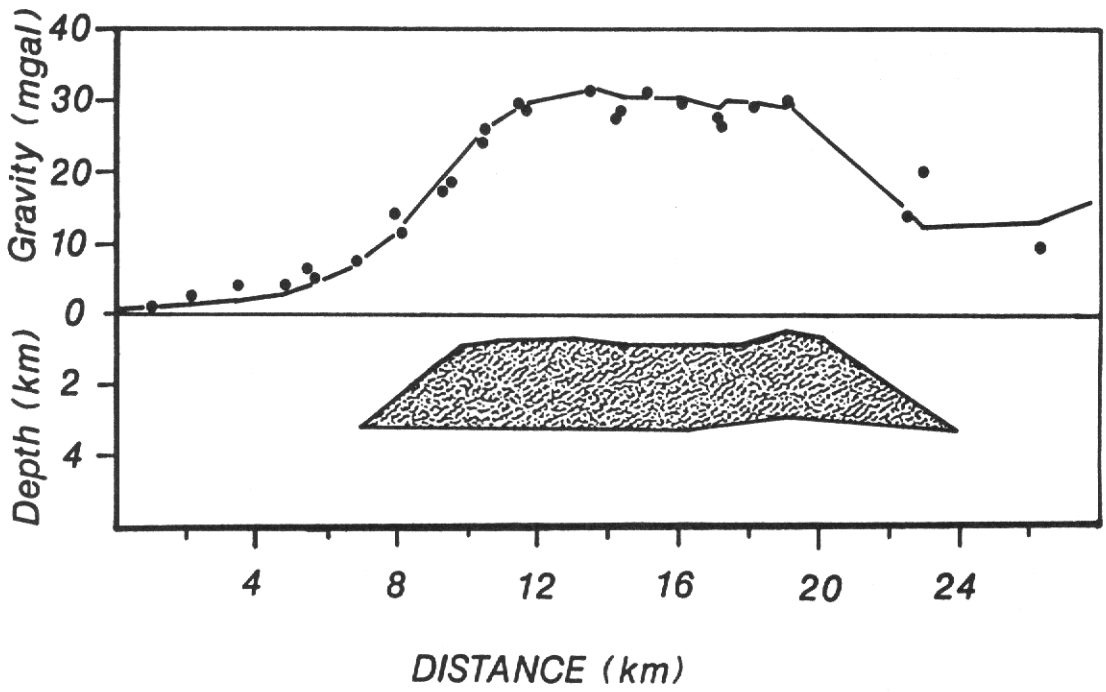

Fig. 4 Observed gravity values (open circle), model of anomalous mass distribution (shaded polygon), and calculated gravity profile (solid curve) along traverse A-A' (Figure 1). In this model, the density contrast between the anomalous mass and surrounding rock is +500kg/m^3. The profile was calculated using the algorithm of Talwani and Ewing (1960) and programs of Webring (1985) and CBC.

No surface geologic contact are readily associated with the broad positive gravity anomaly (Figures 1 and 2), shown in profile in Figure 4. That fact, combined with our knowledge of the geological makeup of the caldera walls convince us that the profile (Figure 4) is most realistically modeled using a completely buried anomalous mass. Regional NW-SE faults, associated with the Nicaraguan Depression, can be projected through Masaya caldera. Strong N-S faulting, related to the location of the caldera at the eastern margin of the central Nicaragua segment boundary (Stoiber and Carr, 1974), is obvious to the north of the caldera, where surficial deposits are offset, and to the south, where vents are aligned in rows. Although there is no vertical displacement of rocks due to regional faults within the caldera, the presence of strong N60^{o}W oriented structures is suggested by the alignments of vents on the caldera floor and the distribution of soil geochemical anomalies within the caldera (Crenshaw et al., 1982). These regional faults may affect gravity gradients, but their affect on the NW-oriented profile should be minimal.

Figure 4 is the one of many models which were considered in our efforts to explain the observed gravity anomaly along traverse A-A'. The key elements of this model are the requirements for a high density contrast (500 kg/m^3) and the thin, plate-like geometry of the anomalous mass. This plate is approximately 17 km long, 2 km thick, and buried below a depth of approximately 0.5 km. The model is most sensitive to the geometry of the plate ends. The presence of the steepest gravity gradient near the crest of the anomaly requires that the contacts dip away from the center of the anomalous mass. This is particularly true on the NW flank of the anomaly, where control is best. Modeling of less well-constrained profiles perpendicular to A-A' indicates that the plate is 5-7 km wide. The model illustrated in Figure 4 uses a model width of 6 km. Finally, a rectangular prism has been added beneath Apoyo caldera, immediately SE of the map area, to account for a regional increase in gravity from NW to SE.

If, as an alternative, an anomalous mass having a density contrast of 300 kg/m^3 is considered, the plate must extend from the present surface to a depth of 5 km. The plate has a length of approximately 20 km and must taper upward, as in the previous model. It is not possible to model the steep gradient observed in the profile with density contrast smaller than 300 kg/m^3.

EXCESS MASS CALCULATION

The excess mass producing the observed gravity anomalies can be computed directly from the gravity observations without assuming that the shape of the causative body is known (eg: Tsuboi, 1983). This involves the application of Gauss's Theorem:

$$E = \frac{1}{2\pi G}\int_{-\infty}^{\infty}\int_{-\infty}^{\infty} g(x,y)\,dx\,dy$$

where E is the excess mass, G is the gravitational constant, and g is the measured gravity anomaly. In this case, the best-fit plane was removed from the observed data and positive residuals were used in the calculation. A grid slightly larger in area and grid point spacing was used, compared to that used in previous calculations. This requires greater interpolation, especially north of the map area (Figure 1), but also provides greater closure about the positive anomaly. The excess mass, calculated in this manner, is 2.9 x 10^{10} metric tons. Given an excess density of 500 kg/ m^3, this corresponds to an excess volume of approximately 116 km^3.

The volume of the model found by forward calculation (Figure 4) is approximately 168 km^3, which is 30% greater than the volume inferred from the excess mass calculation. This disparity may be accounted for in several ways. Most likely, the anomaly is not wholly represented by the residual values, after a best-fit plane is removed; alternatively, the interpolation of gravity values on the north side of the map area may not be adequate. Nonetheless, the general agreement between the model and the excess mass calculation suggests that the predicted mass and size of the causative body is reasonably accurate.

DISCUSSION AND CONCLUSIONS

Gravity anomalies of substantial amplitude and wavelength are found within and around Masaya caldera. Although we have interpreted a regional data set, some patterns in the data do emerge. Filtering the data by upward continuation and wavelength filtering enhances large broad anomalies and local anomalies, respectively. The large-scale feature (Figure 2) is a positive anomaly whose magnitude (35mgal) and wavelength (15km) is quite similar to those found at other basaltic volcanoes from a variety of tectonic settings (e.g. Finn and Williams 1972; Rymer and Brown, 1986), but considerably smaller in magnitude and shorter in wavelength than gravity anomalies associated with shallow (<10 km deep) intrusions at the Hawaiian shields: Kilauea, Mauna Loa, and Mauna Kea (Hill and Zucca, 1987). The long-wavelength anomaly identified at Masaya is not like the positive anomalies found at some andesitic Central American stratovolcanoes, which have shorter wavelengths and generally smaller amplitudes (Brown et al., 1987).

The most surprising result of our analysis is that the large positive anomaly is not concentric with respect to the caldera nor is it contained within the caldera structure, as has been often observed at other calderas for which such data exists (Rymer and Brown, 1986). Upward continuation has demonstrated that the broad positive gravity anomaly is actually offset slightly northward from Masaya caldera itself and is of similar shape. This means that despite the presence of a thick section of caldera-fill of fluid lavas and minor tephra and flow breccia within the caldera, another cause must be responsible for the dominant large-scale anomaly. The steep gravity gradients require a relatively near-surface source. We believe this anomaly (Figures 2 and 4) is likely to be of igneous origin. The geometry of the causative body suggests that it is either an intrusion, possibly a laccolith or sill, or a series of lavas, which have accumulated to substantial thickness over a limited area. A density contrast of 300 to 500 kg/m^3 argues in favor of an igneous intrusions because intrusive igneous rocks have considerably higher densities than the lavas and tephra of the caldera and caldera wall.

If the causative body is an igneous intrusive, similar to those inferred from the history of extraordinary degassing at Masaya (Stoiber et al., 1986), then a volume of 100 to 200 km^3 could

have accumulated in a time frame as short as 1,000 to 2,000 years, during which time the magma may have degassed in a manner similar to that observed historically. It is unlikely, however, even if the anomaly is caused by an intrusion, that it is related to modern activity of Masaya because the anomaly is not concentric with the caldera margin, the high density contrast suggests that the anomaly is caused by solid, rather than molten or partially molten rock, and because no surface deformation or other volcanic features can be unambiguously related to the causative body. For these reasons we believe that the intrusion occurred before the formation of the present caldera. The details of the shapes of the 35 and 40 mgal contours over the caldera walls (Figure 1) are consistent with the possibility that the intrusive body is downthrown by these faults, but greater sampling density is required to adequately test this supposition.

The presence of short-wavelength and large amplitude negative gravity anomalies within the caldera is suggested by measurements at several stations. One of these anomalies is located immediately NW of the active Santiago crater, and may be caused by conduit geometry or the presence of magma at shallow levels. Unfortunately, this anomaly is not tightly constrained by the data. We do know that this location corresponds to the presence of a young open eruptive fissure, which extends from the NW lip of the San Pedro crater (the small older crater which lies on the western edge of the Santiago-Nindiri-San Pedro complex) for at least one km and from which a lava flow emanated (probably within the past 1,000 years). A clearer interpretation of the significance of that anomaly would require more closely-spaced data for that region. However, the negative anomaly is also near a point on the caldera margin which has consistently and exclusively received the deposition of scoriaceous tephra for the entire history of the present Masaya caldera. This results from the extremely consistent tradewinds which blow at the latitudes of Nicaragua. The plinian deposits shown to have been erupted from Masaya about 30,000 years ago (Williams, 1983b) are accumulated to unusual thicknesses in this location. If those same processes have persisted over longer times, the gravity low could be caused by a major accumulation of uncompacted low density tephra. The presence of the anomalies described in this work suggests that future geophysical work at Masaya may be expected to yield further insight into the volcanic processes operating beneath this caldera.

ACKNOWLEDGEMENTS

The research program at Masaya benefitted from the active and enlightened guidance of Dick Stoiber, to whom both of us are grateful. Further assistance was provided by numerous Nicaraguan citizens, including Alejandro Rodriguez, Douglas Fajardo and Julio Garayar of INETER. The people of IRENA, especially Debbie Reid de Jerez and the staff of the Parque Nacional Masaya, also offered important help. Financial support for this research was provided by the National Science Foundation (80LA/R-3, EAR80-20796, and EAR80-25719). We acknowledge the support of the Department of Earth Sciences, Dartmouth College. SNW also wishes to acknowledge the support of the Department of Geology and Geophysics, Louisiana State University and CBC the support of the Department of Geology, Florida International University and the Southeast Regional Data Center.

REFERENCES

Bice, D.C., Tephra stratigraphy and physical aspects of recent volcanism near Managua, Nicaragua, unpubl. Ph.D. dissertation, Univ. Calif. Berkeley, 444p., 1980.

Briggs, I.C., Machine contouring using minimum curvature: Geophysics, 39, 39-48, 1974.

Brown, G.C., H. Rymer and R.S. Thorpe, The evolution of andesite volcano structures: New evidence from gravity studies in Costa Rica, Earth and Planetary Science Letters, 82, 323-334, 1987.

Crenshaw, W.B., S. N. Williams, and R.E. Stoiber, Fault location of radon and mercury detection at an active volcano in Nicaragua, Nature 300, 345-346, 1982.

Cruesot, A., C.M.M. Oppenheimer, D.A. Rothery, B. van Vyk de Vries, O. Castellon, and L. Urbina, Masaya (Nicaragua): Lava Lake develops in new collapse crater, SEAN Bulletin, 14 (2), 7-8, 1989.

Eggers, A.A., Residual gravity changes and eruption magnitudes, Journal of Volcanology and Geothermal Research, 33 (1-3), 210-216, 1987.

Finn, C. and D.L. Williams, Gravity evidence for a shallow intrusion beneath Medicine Lake volcano, California Geology, 10, 503-507, 1982.

Hildebrand, T.G., FFTFIL: a filtering program based on two-dimensional Fourier analysis of geophysical data, USGS Open-File Report 83-237, 54p., 1983.

Hill, D.P., and Zucca, J.J., Geophysical constraints on the structure of Kilauea and Mauna Loa Hawaii, Volume 2, USGS Professional Paper 1350 (R.W. Decker, T.L. Wright, and P.H. Stauffer, eds.), 903-918, 1987.

McBirney, A.R., The Nicaraguan volcano Masaya and its caldera, Trans. Amer.Geophys.Un., 37(1) 83-96, 1956.

Mooser F.H., Meyer-Abich, and A.R. McBirney, Catalogue of active volcanoes of the world, Part VI, Central America, International Assoc. of Volcanol. and Chem. of the Earth's Inter., Naples, 146p., 1958.

Rymer, H., and G.C. Brown, Gravity fields and the interpretation of volcanic structures: geological discrimination and temporal evolution, Journal of Volcanology and Geothermal Research 27, 229-254, 1986.

Simkin, T.L., Siebert, L. McClelland, D. Bridge, C.G. Newhall, and J.H. Latter, Volcanoes of the World, Hutchinson Ross Publ. Co., Stroudsburg, PA, 232p., 1981.

Snyder, W.V., Algorithm 531: Contour Plotting, Collected Algorithms, ACM Transactions on Mathematical Software, 4, 290-294, 1978.

Stoiber, R.E. and M. J. Carr, Quaternary volcanism and tectonic segmentaton of Central America: Bulletin of Volcanology, 37, 304-325.

Stoiber, R.E., S.N. Williams, and B.J. Huebert, Volcanic sulfur and halogen gas geochemistry at Masaya Caldera Complex, Nicaragua: total flux and variations with time, Journal of Geophysical Research, 91(B12), 12,215-12,231, 1986.

Talwani, M., and M. Ewing, Rapid computation of gravitational attraction of three-dimensional bodies of arbitrary shape, Geophysics, 25, 203-225, 1960.

Tsuboi, C., Gravity, George Allen and Unwin, London, 254p., 1983.

Walker, J.A. and Williams, S.N., Shallow magmatic processes beneath Masaya Caldera Complex, Nicaragua (abstract), EOS Trans. AGU, 67 (16), 411, 1986.

Webring, M., SAKI: A Fortran program for generalized linear inversion of gravity and magnetic profiles, USGS Open-File Report 85-122, 108p., 1985.

Webring, M., MINC: A gridding program based on minimum curvature, USGS Open-File Report 81-1224, 41 p., 1981.

Williams, R.L., The geology of western Nicaragua: Tax Improvement and Natural Resources Inventory Project, Final Technical Report, v. 4, Managua, Nicaragua, 1972.

Williams, S.N., Geology and Eruptive Mechanisms of the Masaya Caldera Complex, Nicaragua, Unpublished Ph.D. dissertation, Dartmouth College, Hanover, N.H., 169p., 1983a.

Williams, S.N., Plinian airfall deposits of basaltic composition: Geology, 11, 211-214, 1983b.

Williams, S.N. and R.E. Stoiber, "Masaya-type caldera" redefined as the mafic analogue of the "Krakatau-type caldera" (abstract), EOS Trans, AGU, 64(45), 877, 1983.

Yokoyama, I., Gravimetric, magnetic and electrical methods, in The surveillance and predictions of volcanic activity, pp., UNESCO, Paris, 1972.

ACTIVE TECTONICS OF THE CHORTIS BLOCK

Mark B. Gordon
Department of Geological Sciences
The University of Texas at Austin
Austin, TX 78713-7909, U.S.A.

Michael J. Kozuch
Cuerpo de Paz
Apartado Postal 3158
Tegucigalpa, Honduras
Central America

William R. Muehlberger
Department of Geological Sciences
The University of Texas at Austin
Austin, TX 78713-7909, U.S.A.

ABSTRACT

Internal deformation of the Chortís block (Honduras, El Salvador and environs) is controlled by two well defined, seismically active plate boundaries on the north and on the southwest. Much of the Chortís Block is included in either the Caribbean/Cocos plate boundary zone (convergence rate = 8 $cmyr^{-1}$; Burbach et al., 1984) or the Caribbean/North American plate boundary zone (slip rate < 2 $cmyr^{-1}$; Rosencrantz et al., 1988).

The Nicaraguan depression is a marginal basin responding to subduction from the Middle America Trench and is parallel to the Quaternary volcanic line. The depression crosses the Gulf of Fonseca and continues into El Salvador where it is not as prominent a topographic feature (Wiesemann, 1975). It is absent in Guatemala and the volcano line rests on a topographic ridge.

The Motagua and Polochic faults are the two major, active Caribbean/North American plate boundary faults in Guatemala. Several faults with similar orientations occur south of these faults within the present Chortís block. The most prominent of these faults is the inactive Jocotán-Chamelecón fault and is being cut by north-striking normal faults (Clemons, 1966). However, the Aguan and La Ceiba faults of northern Honduras may be active. The Caribbean/Cocos plate boundary is much more seismically active than the Caribbean/North American plate boundary. The intraplate deformation of the Chortís block, paradoxically, seems to result primarily from motions along the Caribbean/North American plate boundary.

North-trending, normal fault-bounded basins define the Honduras depression (Muehlberger, 1976), a major zone of intraplate deformation entirely within the Chortís block. It is seismically active as demonstrated by instrumentally recorded earthquakes (NEIC Catalog), historical earthquakes (Osiecki, 1981), and Quaternary fault scarps (Everett and Fakundiny, 1976). Recent volcanism is also associated with the Honduras depression (Williams and McBirney, 1969). The principal basins are connected by a series of poorly defined strike-slip faults which strike northwest (Emmet, 1983). These faults are parallel to Late Cretaceous folds and, thus, may be reactivated. Other, smaller basins (e.g., the Jesús de Otoro basin) occur off the principal axis of the Honduras depression. The region as a whole is experiencing northwest-striking dextral shear which reactivates old faults and forms extensional basins between principal fault segments. The most prominent extensional corridor of the Sula valley, Lake Yojoa and the Comayagua Valley (the Honduras depression as defined by Muehlberger, 1976) probably represents the most profound preexisting weakness. Other north-trending extensional basins occur south of the Caribbean/North American plate boundary in Guatemala (e.g., the Guatemala City and Ipala grabens). These basins are active as shown by aftershocks from 1976 Guatemalan earthquake. The aftershocks progressed to the west along the Motagua fault and then to the south along the basin bounding normal faults. This aftershock pattern indicates that north-striking normal faults form within the Chortís block as a result of strike-slip faulting on the plate boundary (Plafker, 1976).

The Guayape fault is the longest, continuous structural feature in Honduras. It extends 300 km southwest from the Caribbean coast to the Jamastrán Valley region. The Choluteca lineament, a possible extension of the fault, continues through Neogene volcanic deposits to the Gulf of Fonseca. Ritchie and Finch (1984) first recognized the Guayape fault as a strike-slip fault. In spite of its sharp, well-defined topographic signature, little seismic activity in this region was found in the NEIC Catalog between 1963 and 1983, or from the historical record (Osiecki, 1981). Our recent geologic mapping in the Catacamas Valley and the geometry of other basins show that the Guayape fault has at present a right-lateral sense of slip, although earlier deformation appears to have been left-lateral (Gordon, 1987). Even though the Guayape fault represents important intraplate deformation, a direct relationship between it and the deformation at the plate boundary is not readily apparent.

REFERENCES

Burbach, G.V., Frohlich, C., Pennington, W.D., and Matumoto, T., Seismicity and tectonics of the subducted Cocos plate, J. Geophys. Res., 89.

Larue, D.K., and Draper, G. (eds.),
***Transactions of the 12th Caribbean Geological Conference, St. Croix*, U.S.V.I.**, Miami Geological Society, P.O. Box 431552, South Miami, FL 33243, U.S.A

7719-7735, 1984.
Clemons, R.E., Geology of the Chiquimula quadrangle, Guatemala, Central America [Ph.D. Diss.], University of Texas, Austin, 124 p., 1966.
Emmet, P.A., Geology of the Agalteca quadrangle, Honduras, Central America [M.A. thesis], University of Texas, Austin, 201 p., 1983.
Everett, J.R., and Fakundiny, R.H., Structural geology of El Rosario and Comayagua quadrangles, Honduras, Central America *in* Informe y trabajos tecnicos presentados en la IV Reunion de Geologos de America Central, Publ. Geol. ICAITI, no. V, 31-42, 1976.
Gordon, M.B., The Guayape fault of Honduras: a major right-lateral fault cutting the Chortis block, EOS (Trans. Am. Geophys. Un.), 68, 423, 1987.
Muehlberger, W.R., The Honduras Depression *in* Informe y trabajos tecnicos presentados en la IV Reunion de Geologos de America Central, Publ. Geol. ICAITI, no. V, 43-51, 1976.
Osiecki, P.S., Estimated intensities and probable tectonic sources of historic (pre-1898) Honduran earthquakes, Bull. Seismol. Soc. Am., 71, 865-881, 1981.
Plafker, G., Tectonic aspects of the Guatemala Earthquake of 4 February, 1976, Science, 193, 1201-1208, 1976.
Ritchie, A.W., and Finch, R.C., Guayape fault system of Honduras, Geol. Soc. Am. Abstr. Progs., 16, 635, 1984.
Rosencrantz, E., Ross, M.I., and Sclater, J.G., Age and spreading history of the Cayman Trough as determined from depth, heat flow, and magnetic anomalies, J. Geophys. Res., 93, 2141-2157, 1988.
Wiesemann, G., Remarks on the geologic structure of the Republic of El Salvador, Central America, Mitt. Geol.-Paläont. Inst. Univ. Hamburg, 44, 557-574, 1975.
Williams, H., and McBirney, A.R., Volcanic history of Honduras, Univ. Calif. Publ. Geol. Sci., 85, 101 p., 1969.

THE CHORTIS BLOCK IS A CONTINENTAL, PRE-MESOZOIC TERRANE

Mark B. Gordon
Department of Geological Sciences
The University of Texas at Austin
Austin, TX 78713-7909, U.S.A.

ABSTRACT

The Chortís block consists of well-dated Mesozoic and Cenozoic formations which unconformably overlie basement of metamorphic rocks which have not been well-dated. The basement rocks are dominantly low grade metasedimentary rocks. One metamorphosed intrusion within the metasedimentary rocks has been dated as Paleozoic in age. The crustal thickness determined from seismic studies demonstrates that the Chortís block has crust with a thickness and seismic velocity typical of continental-type crust. The basement is overlain by sedimentary formations which were deposited under terrigenous or shallow marine conditions. The environment of deposition of these formations suggest that the Chortís block did not experience significant deformation during the Early Cretaceous. Deposition of redbeds occurred during the Late Cretaceous, while volcanic activity was limited in extent. Late Cretaceous limestones were also deposited under shallow marine conditions. Thus, available data clearly demonstrate that the Chortís block has continental-type crust which is pre-Mesozoic in age. During the Mesozoic, the Chortís block experienced platform-type sedimentation. Within the central portion of the block, extensive volcanism occurred only during the Cenozoic.

INTRODUCTION

The Chortís block is the best example of an allochthonous terrane in the Caribbean region, and nearly all workers agree with this interpretation (Dengo, 1969; Case et al., 1984; Gose, 1985; Donnelly, 1989). Because it is an important element of the Caribbean tectonic puzzle, the fundamentals about the geology of the Chortís block need to be widely understood among Caribbean geologists. First of all, we must understand the distinctive basement geology of the block (Dengo, 1969; Table 1). Furthermore, the well-known Mesozoic stratigraphy should be considered when the Mesozoic tectonics of the Chortís block are discussed.

The Chortís Block was defined by Dengo (1969) as the area of northern Central America which is south of the Motagua fault zone (Fig. 1). Although Dengo (1969) did not set a southern limit to the Chortís block, Dengo and Bohnenberger (1969) placed the boundary between northern and southern Central America at latitude 12° 30' N. They used a latitude because a suitable geologic feature had not been recognized as the boundary between two distinct crustal types. Dengo did not attempt to continue the boundaries offshore. Case et al. (1984) suggest that the Chortís block is a superterrane, and discuss the geology of the offshore regions. To the southwest, the Chortís block terminates against the southern Central America province. Case et al. (1984) cite evidence that this oceanic crustal terrane (see Weyl, 1980) extends from Costa Rica offshore to the northwest between the Middle America trench and the Pacific coastline. Based on crustal type (Case et al., 1984), the Chortís block almost certainly continues offshore on the Caribbean side. Basement rocks crop out in the Bay Islands (McBirney and Bass, 1969; Fig. 1) indicating a Chortís-type crust for this region. Part of the Nicaraguan Rise is probably Chortís-type crust. Jamaica is geologically distinct from the Chortís block and has a gravity signature suggestive of oceanic crust (Case et al., 1984). Thus, a boundary between different crustal types occurs within the Nicaraguan Rise. Greater Chortís may be an appropriate name for the part of the northwestern Caribbean which has been rotating past Yucatán since the Eocene. However, Jamaica was probably independent of Chortís during the Mesozoic.

CACAGUAPA SCHIST

The Cacaguapa Schist was named by Fakundiny (1970) after a village surrounded by good outcrop of schist north of Comayagua, Honduras (Fig. 1). Basement rocks of the Chortís block had previously been mapped by Carpenter (1954) and Zoppis Bracci (1961) who used different names. Mapping since 1970 has confirmed that these metamorphic rocks are widespread and are the same rock unit. The dominant rock types are phyllitic and graphitic schists.

Fakundiny (1970) identified two members within the schist: the Humuya Member and the Las Marías Member. The Humuya Member has only been reported from the gorge of Río Humuya (north of Comayagua, Fig. 1). It consists of greenish gray to black schist with intercalated igneous flows. These rocks are interlayered with metaconglomerate and epidote-rich quartzite which suggest a metasedimentary origin for the Humuya Member.

Larue, D.K., and Draper, G. (eds.),
Transactions of the 12th Caribbean Geological Conference, St. Croix, U.S.V.I., Miami Geological Society, P.O. Box 431552, South Miami, FL 33243, U.S.A

CHARACTERISTICS OF BASEMENT ROCKS, CENTRAL AMERICA

Terrane (as defined by Dengo)	Chortís block	Maya block	Southern Central America
Rock type	low grade phyllites Cacaguapa Schist Greenschist metamorphic rocks Some higher grade rocks exposed Some metaigneous rocks exposed (e.g., Simonson 1977)	amphibolitic schist Chuacús Metamorphics garnet amphibolites (McBirney, 1963)	oceanic/ophiolitic Santa Elena complex (Weyl, 1980)
Crustal thickness/ Seismic velocities (km/sec)	37 km 2.6/5.1/6.2/6.6/7.9 (Kim et al., 1982)	43 km 5.0/6.1/6.95/7.6/8.2 (Castro Escamilla, 1980)	43 km 5.1/6.2/6.6/7.9 (Matumoto et al., 1977)
Crustal type	continental	continental	Transitional Ocean/island arc
Age	pre-Mesozoic presumed Paleozoic (see text)	Paleozoic metamorphism 1100 Ma protolith? (Gomberg et al., 1968)	Mesozoic (Weyl, 1980)

Table 1. The terranes of Central America were defined by Dengo (1969) and Dengo and Bohnenberger (1969). The basement rocks of each terrane are distinct. The crustal thicknesses velocities are similar for the three terranes. Matumoto et al. (1977) noted that the geology of southern Central America is oceanic. However, their velocity model indicates that the origin of southern Central America is similar to other circum-Pacific island arcs. Kim et al. (1982) believe that further study is needed to explain the discrepancy between geological data and seismic data for southern Central America.

The Las Marías Member has been found in numerous localities on the Chortís block since the time of Fakundiny, and is similar to the metamorphic rocks described by Carpenter (1954). Greenschist metasedimentary rocks are the most common rock type, although some amphibolite grade rocks may be present (Fakundiny, 1970). The bulk of the unit is chlorite, white mica, and quartz phyllite. Interlayered with the phyllites are marbles (Fakundiny, 1970; Simonson, 1977; Rodbell, 1986; Kozuch, 1989), quartzites (Fakundiny, 1970; Simonson, 1977), and metaconglomerates (Fakundiny, 1970). These rock types demonstrate that the Las Marías member is dominantly metasedimentary. Simonson (1977) mapped metamorphosed mafic igneous rocks and metamorphosed epiclastic rocks which are interlayered with the phyllite. These metavolcanic rocks are volumetrically minor.

Although the phyllite unit is the most common exposed basement rock on the Chortís block, Horne et al. (1976) and Simonson (1977, 1981) have demonstrated that more rock types are present. Horne et al. (1976) found higher grade rocks than had been found in central Honduras. In the Sierra de Omoa (Fig. 1), they recognized almandine amphibolite facies. Hornblende, calcic plagioclase and epidote are widespread in this area whereas garnet and staurolite are only found locally. The rock sequences that they report are mostly metasedimentary because they are interbedded with garnetiferous gneiss, staurolite schist and marble. Low grade phyllite like the Las Marías Member and metaigneous rocks are also exposed in this region.

In the El Porvenir region (Fig. 1), Simonson (1977, 1981) described and mapped five separate members of the Cacaguapa Schist of which three are metasedimentary and two are metaigneous. Some of the metasedimentary rocks are higher grade than had been previously documented in Central Honduras. He called this unit the Garnet Schist Member although it includes several rock types and a variety of minerals. The principal schist member consists of garnet, chlorite, biotite, highly sodic plagioclase and chloritoid. A mafic schist is present. The highest metamorphic grade was epidote-amphibolite facies. Simonson also found quartzite and marble. Quartzite layers tens of meters thick occur throughout the schist, but are not thick enough to be mapped separately. The pelitic nature of most of the member, the presence of the marble member and the common occurrence of quartzite all attest to the metasedimentary nature of this member. The phyllite member mapped by Fakundiny crops out extensively in the El Porvenir quadrangle. Quartzite, marble and mafic schist occur in the phyllite

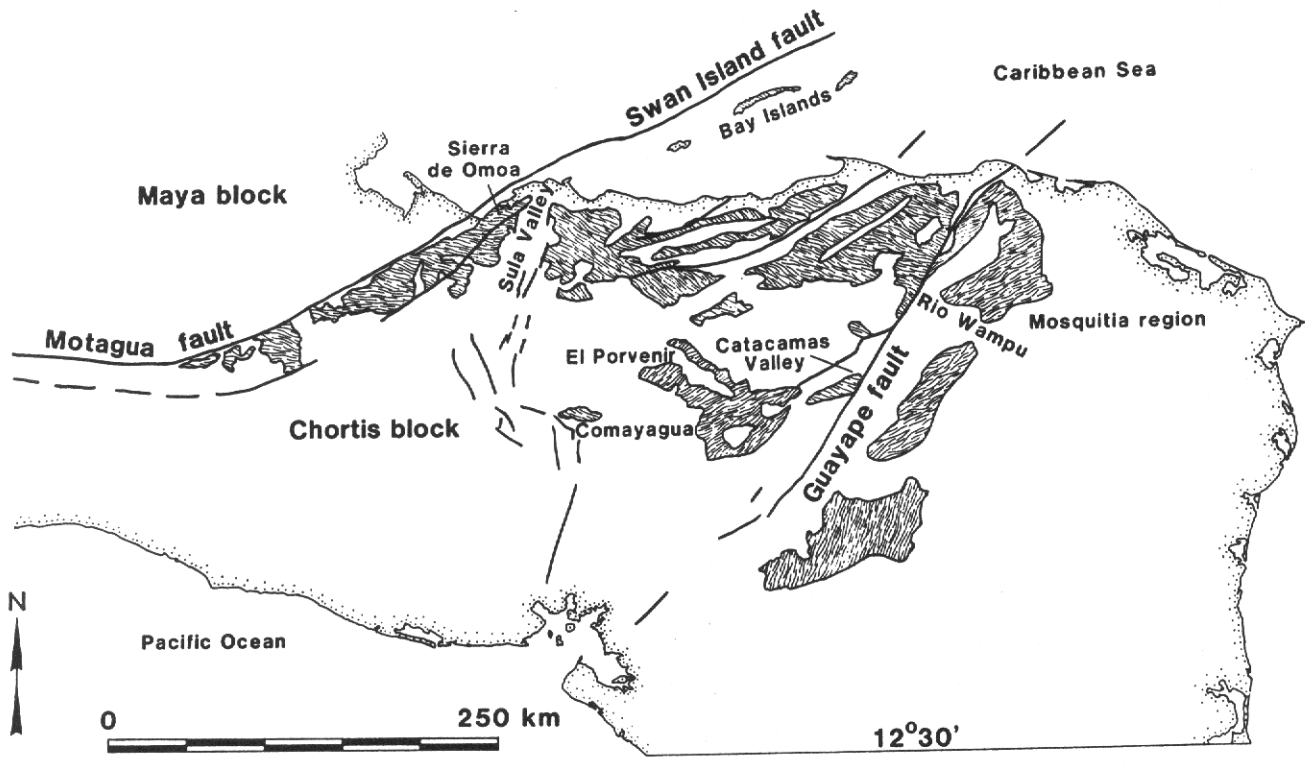

Figure 1. Mapped basement of the Chortís block. Foliations within mapped regions commonly have complex orientations, and pattern is not intended to indicate general strike. Basement rocks have been found under relatively undeformed Mesozoic sedimentary rocks throughout the Chortís block. Much of Honduras has been stripped to the basement, and large regions of nearly exclusive basement exposures exist. Nearly all of Honduras has a basement of metamorphic rocks. Map is modified from Case and Holcombe (1980) based on recent mapping and my reconnaissance studies.

member as well. The member is gray and golden tan, and its mineralogy consists of sericite, chlorite and quartz. Based on their general similarity in bulk composition, Simonson (1977) considered the garnet schist member and the phyllite member as one unit with different metamorphic grades.

Metaigneous rocks have been found in northern Honduras by Horne et al. (1976) and in central Honduras by Simonson (1977). Fakundiny (1971) mapped a mylonitized granite, but did not describe it in detail. A metapluton is exposed on the west side of the Sula Valley at Quebrada Seca (Horne et al., 1976). Phases of the pluton include metatonalite, porphyritic metadacite, metadiorite, and quartz-monzonite gneiss. Horne et al. also described a metapluton from Banaderos, within the Sierra de Omoa. This metapluton includes granodiorite gneiss and tonalite granofels. Simonson (1977, 1981) mapped two distinct types of metaintrusions. Two of these are relatively low-grade mylonite gneisses. The rocks have undergone strain and recrystallization without extensive change in their original mineralogy or texture. If no chemical change occurred during metamorphism, one pluton is metatonalite and the other is metagranite. Simonson's mapping shows that these plutons intruded the metasedimentary rocks prior to metamorphism. Simonson (1977, 1981) also mapped a more highly deformed metaplutonic rock which he called the augen schist member. This member has abundant augens of microcline and recrystallized quartz with white mica and biotite anastomosing around feldspathic augen. Epidote is also present. Simonson (1977) proposes that the augen schist predates the garnet schist. Thus, the augen schist is the oldest metamorphic unit and the metasedimentary rocks were deposited on the augen schist.

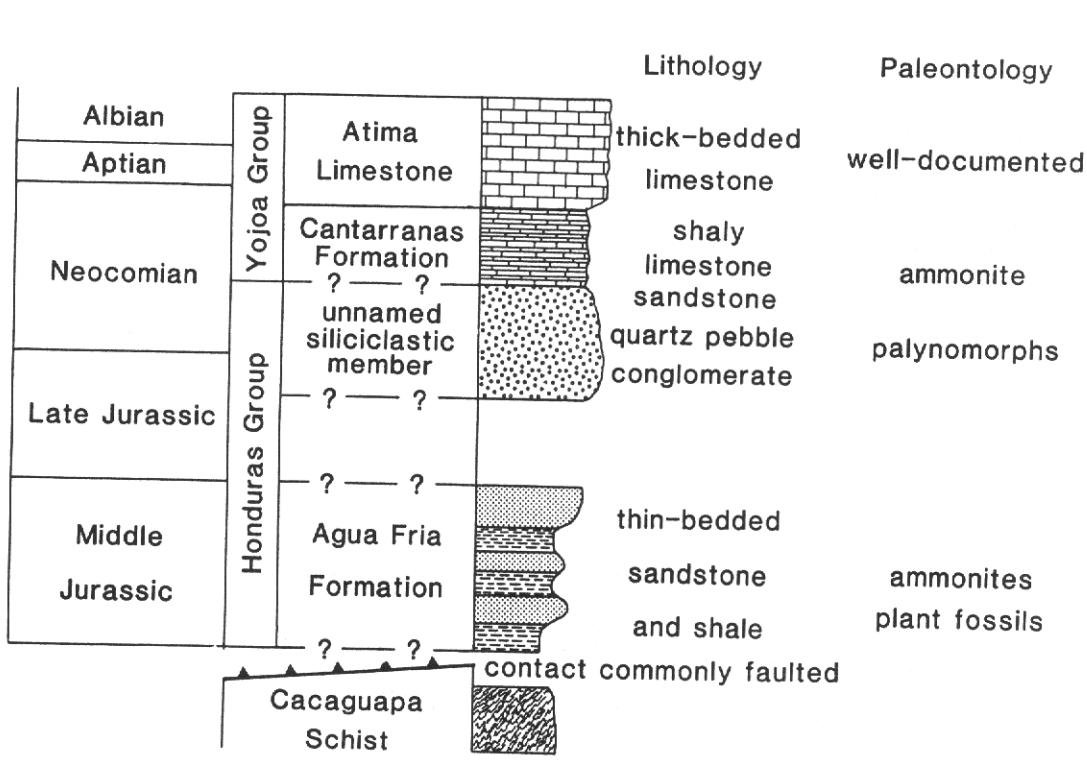

Figure 2. Clastic rocks which crop out beneath the Atima Formation of Mills et al. (1967) were defined as the Honduras Group by Ritchie and Finch (1985). The group consists of two major units, the Agua Fría Formation and the unnamed siliciclastic member. Geologic mapping has not established whether or not the two units occur at the same location. However, the Agua Fría Formation is well-dated (Ritchie and Finch, 1985), and the unnamed siliciclastic member crops out stratigraphically beneath the Atima Formation in numerous locations. The unnamed siliciclastic member is likely Early Cretaceous based on palynomorphs from a few locations, but it has not been well-dated throughout the Chortís block.

Structure

The Cacaguapa Schist experienced several phases of deformation. Its structure has not yet been studied on a regional scale, but local studies have been done in a few widely separated areas. Isoclinal folding has been documented by Fakundiny (1970), Horne et al. (1976) and Simonson (1977). In the Sierra de Omoa, Horne et al. (1976) documented three phases of folding and formation of axial planar foliation and/or cleavage. First generation foliations in the El Porvenir region make a well defined girdle on stereonets indicating folding about a northwest-plunging axis (Simonson, 1977). A second generation foliation is present in the El Porvenir region (Simonson, 1977) which demonstrates that at least two periods of deformation have occurred.

Age

The age of the Chortís basement has not been definitively determined. A limited number of Rb-Sr dates have been determined for the basement rocks. Horne et al. (1976) dated the Quebrada Seca metaigneous pluton by Rb-Sr whole rock dating. Using their data and the new IUGS decay constant ($1.42 \times 10^{-11} yr^{-1}$), L.E. Long (pers. comm., 1990) calculated a date of 300 ± 6 Ma (2σ error) for this rock. It is not clear whether this is a protolith or metamorphic age. However, it clearly demonstrates at least Paleozoic metamorphism occurred on the Chortís block, and that the block is pre-Mesozoic.

Horne et al. (1976) published dates which should not be taken literally because they did not

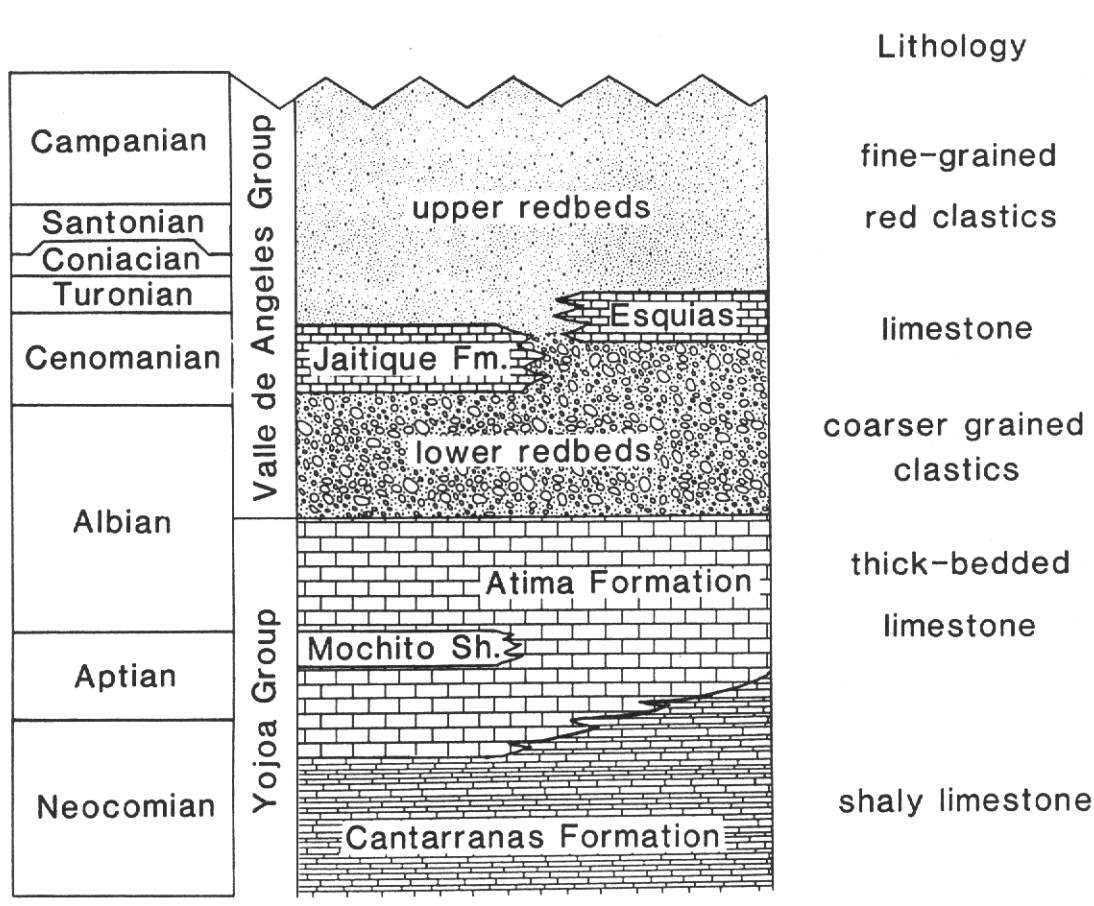

Figure 3) The stratigraphy of Central Honduras is well-known from geologic mapping. Based on this mapping, Finch (1981) revised the stratigraphy of Mills et al., (1967) to incorporate the Cenomanian Jaitique Formation, a limestone unit. This stratigraphy is shown here. The three limestone units have been well-dated with fossils whereas the redbeds have been dated by their stratigraphic position relative to the limestone. A limited amount of palynological data combined with paleomagnetic interpretation suggest that the Valle de Angeles Group does not extend beyond the Campanian (Gose and Finch, 1987).

intend for these dates to be considered precise values. These are either "errorchrons", which assume an initial ratio of $^{87}Sr/^{86}Sr$, or weakly constrained isochrons. The Banaderos metapluton is one that they dated, but the isochron is very poor with large errors. Their date on the Banaderos metapluton is 760 ± 260 Ma (not recalculated because of its large error). The Rb-Sr systematics of the Banaderos pluton may have been disturbed by the intrusion of younger, non-metamorphic quartz monzonite. The errorchrons and the weakly constrained isochrons suggest Paleozoic or Precambrian ages, but do not give tight constraints on the age. Horne et al. (1976) explain the limitations of their isotopic work. Those who cite these data should recognize these problems.

MESOZOIC RECORD

The Mesozoic geology of the Chortís block is dominated by a sequence of clastic sedimentary rocks interlayered with widespread limestone formations (Figs. 2, 3). Volcanic rocks form a relatively minor component of the stratigraphy. Some plutonic rocks have been mapped and dated; with few exceptions these are small bodies. The lack of widespread igneous rocks demonstrates that no long-lasting or pervasive volcanic arc existed on the Chortís block during the Mesozoic.

The Mesozoic stratigraphy has been described by Mills et al. (1967) and Finch (1981). It consists of Middle Jurassic and Early Cretaceous

clastic rocks which are overlain by Aptian-Albian limestone. Recent workers have redefined the stratigraphy below the limestone (e.g., Ritchie and Finch, 1985). These clastic rocks are now called the Honduras Group. Two separate units have been mapped, the Agua Fría Formation and the unnamed siliciclastic member (Fig. 2). The Agua Fría Formation consists of gray shale, sandstone and conglomerate. The sandstones are composed of basement detritus. Ammonites and plant fossil demonstrate that the age is Middle Jurassic (Ritchie and Finch, 1985) although its stratigraphic relationship with other rock formations has not been well established. The unnamed siliciclastic member commonly crops out above the Cacaguapa Schist and beneath the Aptian-Albian limestone. Quartz-pebble conglomerate is a dominant lithology. Quartz veins within the basement form the source for these conglomerates. Sandstones are also composed entirely of basement detritus. Palynomorphs from this formation are Early Cretaceous (Gose and Finch, 1987).

The Atima Formation of Mills et al. (1967) is a widespread, well-dated limestone unit. Either the Atima Formation or metamorphic basement crop out beneath the Tertiary volcanics throughout the region of Guatemala south of the Motagua fault (Case and Holcombe, 1980). The Atima Formation crops out extensively throughout Honduras (Mills et al., 1967), and especially Central Honduras (Finch, 1981). It also crops out in northwestern El Salvador (Weber, 1979) and southeastern Guatemala (Burkart et al., 1973). The age range of the Atima Formation is mostly from the Aptian to the middle Albian. It is dominantly a shallow water, reefal limestone. Because it is a readily identifiable unit, Mills et al. (1967) called it the fundamental stratigraphic datum of Honduras. In central Honduras, the limestone is conformably overlain by the Valle de Angeles Group (Fig. 3), which consists of conglomerate, sandstone, shale, and limestone. The Valle de Angeles group is divided into upper and lower redbeds separated by limestone formations (Fig. 3). The redbeds crop out throughout a wide region as does the Atima Formation. Two Cenomanian-Turonian limestones occur within the Valle de Angeles group in Central Honduras (Finch, 1981; Fig. 3). Another Cenomanian limestone crops out in El Salvador (Weber, 1979). The upper age limit for the Valle de Angeles Group has not been definitively established, but palynological and paleomagnetic results suggest that the youngest deposits are Campanian (Gose and Finch, 1987).

The volcanic content within this stratigraphy is remarkably small. The volcanogenic component of the conglomerates and sandstones of either the Honduras or Valle de Angeles Groups is minor. Basement detritus is much more dominant. Interlayered volcanics occur within the stratigraphy, but they are commonly thin (1 m to 10 m). Mills et al. (1967) report volcanic rocks above the Middle Jurassic rocks in the Río Wampú region in eastern Honduras (Fig. 1). During the course of my mapping, I have found that similar rocks occur in other locations along the east side of the Guayape fault (Fig. 1). However, these rocks are limited in age extent. Simonson (1977) reported several hundred meters of volcanics above the Atima Formation near El Porvenir. These are very limited in map extent, cropping out in only about a 100 km^2 area. I have found several hundred meters of volcanics below the Atima Formation in the Catacamas Valley region. These volcanics are also limited in extent to about 100 km^2. Widespread Mesozoic volcanic rocks do not occur on the Chortís block, and a well-defined volcanic arc did not exist in the Mesozoic in the large region where Mesozoic rocks are exposed. If a volcanic arc was associated with the Chortís block it has subsequently been either buried or tectonically separated from the block (Donnelly, 1989). The hypothesis that the Mesozoic arc has been buried seems unlikely because Mesozoic sedimentary rocks, not Mesozoic volcanic or plutonic rocks, are commonly found beneath the Tertiary volcanic rocks. This record is sharply contrasted to the Cenozoic record in which volcanic and plutonic rocks dominate the geology.

The stratigraphic record shows that the Chortís block was a region of minimal tectonic activity during the Mesozoic. It was not the site of major volcanic arc. Significant deformation would need to be limited to post-Atima time. Deformation synchronous with the deposition of the Valle de Angeles Group has not been documented despite extensive 1:50,000 scale geologic mapping in areas that this unit crops out. The general character of the formation (red sandstones and conglomerates) suggests that it is a syntectonic formation. It could have formed in response to tectonic uplift. However, deformation of both the Atima Formation or the Valle de Angeles Group is relatively minor. The Cretaceous sedimentary rocks are folded and faulted. This deformation did not occur until the collision between the Chortís and the Maya blocks in the latest Cretaceous and the Paleocene (Rosenfeld, 1981; Sutter, 1979).

CONCLUSIONS

The available data demonstrate that the Chortís block is a terrane consisting of continental-type crust. Seismic velocities clearly confirm that the entire crust is continental. The geology of the Chortís block is very different than that of Panama and Costa Rica (Case et al., 1984). The age of the basement rocks has not been definitively established, but it is certainly pre-Mesozoic and is probably Paleozoic. The Chortís block is certainly allochthonous relative to North America. Its Mesozoic history was dominated by deposition of sedimentary rocks without significant volcanogenic component. The most widespread marine formation is the Atima Limestone of Aptian-Albian age. Most of the formation was deposited on a shallow shelf, not deep water. Although the basement rocks are highly deformed,

folding and faulting of the Atima Limestone is not complex in most locations. Mapped intrusions of Mesozoic age are relatively small. Future work on the origin and tectonic history of the Chortís block needs to be done to make Caribbean reconstructions more viable.

ACKNOWLEDGMENTS

Leon E. Long recalculated Rb-Sr dates for me. W.R. Muehlberger and D.K. Larue provided useful reviews. Acknowledgment is made to the Donors of The Petroleum Research Fund, administered by the American Chemical Society, for the support of this research through grant 19990-AC2 to W.R. Muehlberger. I also appreciate the support of the Honduran government through Instituto Geográfico Nacional and Dirección General de Minas e Hidrocarburos.

REFERENCES

Burkart, B., Clemons, R.E., and Crane, D.C., Mesozoic and Cenozoic stratigraphy of southeastern Guatemala, Am. Assoc. Pet. Geol. Bull., 57, 63-73, 1973.

Carpenter, R.H., Geology and ore deposits of the Rosario Mining District and the San Juancito Mountains, Honduras, Central America, Bull. Geol. Soc. Am., 65, 23-38, 1954.

Case, J.E., and Holcombe, T.L., Geologic-Tectonic Map of the Caribbean Region, U.S. Geol. Surv. Misc. Field Inv., Map I-1100, scale 1:2,500,000, 1980.

Case, J.E., Holcombe, T.L., and Martin, R.G., Map of geologic provinces in the Caribbean region *in* Bonini, W.E., Hargraves, R.B., and Shagam, R. (eds.), The Caribbean-South America Plate Boundary and Regional Tectonics, Geol. Soc. Am. Mem., 162, 1-30, 1984.

Castro Escamilla, R.R., Un modelo de la corteza terrestre para el sur de México Mediante el uso de sismos profundos [Ing. Tesis], Universidad Nacional Autónoma de México, 74 p., 1980.

Dengo, G., Problems of tectonic relations between Central America and the Caribbean, Trans. Gulf Coast Assoc. Geol. Soc., 19, 311-320, 1969.

Dengo, G., and Bohnenberger, O., Structural development of northern Central America *in* McBirney, A.R. (ed.), Tectonic Relations of Northern Central America and the Western Caribbean -- The Bonacca Expedition, Am. Assoc. Pet. Geol. Mem., 11, 203-220, 1969.

Donnelly, T.W., Geologic history of the Caribbean and Central America *in* Bally, A.W., and Palmer, A.R. (eds.), The Geology of North America--An overview, Geological Society of America, The Geology of North America, v. A, 299-321, 1989.

Fakundiny, R.H., Geology of the El Rosario quadrangle, Honduras, Central America [Ph.D. Diss.], University of Texas, Austin, 234 p., 1970.

Fakundiny, R.H., Mapa Geológico de Honduras, El Rosario sheet, Instituto Geográfico Nacional, scale 1:50,000, 1971.

Finch, R.C., Mesozoic Stratigraphy of Central Honduras, Am. Assoc. Pet. Geol. Bull., 65, 1320-1333, 1981.

Gomberg, D.N., Banks, P.D., McBirney, A.R., Guatemala: Preliminary zircon ages from the Central Cordillera, Science, 162, 121-122, 1968.

Gose, W.A., Paleomagnetic results from Honduras and their bearing on Caribbean tectonics, Tectonics, 4, 1985.

Gose, W.A., and Finch, R.C., Magnetostratigraphic studies of Cretaceous rocks in Central America, Actas Fac. Ciencias Tierra U.A.N.L. Linares, 2, 233-241, 1987.

Horne, G.S., Clark, G.S., and Pushkar, P., Pre-Cretaceous rocks of northwestern Honduras: basement terrain in Sierra de Omoa, Am. Assoc. Pet. Geol. Bull., 60, 566-583, 1976.

Kim, J.J., Matumoto, T., and Latham, G.V., A crustal section of northern Central America as inferred from wide-angle reflections from shallow earthquakes, Bull. Seismol. Soc. Am., 72, 925-940, 1982.

Kozuch, M.J., Geology of the San Francisco de Becerra quadrangle, Honduras, Central America, Open-file report, Instituto Geográfico Nacional, Tegucigalpa, Honduras, 55 p., 1989.

Matumoto, T., Ohtake, M., Latham, G., and Umana, J., Crustal structure in southern Central America, Bull. Seismol. Soc. Am., 67, 121-134, 1977.

McBirney, A.R., Geology of a part of the central Guatemalan Cordillera, Univ. Calif. Pub. Geol. Sci., 38, 177-242, 1963.

McBirney, A.R., and Bass, M.N., Geology of the Bay Islands, Gulf of Honduras *in* McBirney, A.R. (ed.), Tectonic Relation of Northern Central America and the Western Caribbean--The Bonacca Expedition, Am. Assoc. Pet. Geol. Mem., 11, 229-243, 1969.

Mills, R.A., Hugh, K.E., Feray, D.E., and Swolfs, H.C., Mesozoic stratigraphy of Honduras, Am. Assoc. Pet. Geol. Bull., 51, 1711-1786, 1967.

Ritchie, A.W., and Finch, R.C., Widespread Jurassic strata on the Chortis block of the Caribbean plate, Geol. Soc. Am. Abstr. Progs., 17, 700-701, 1985.

Rodbell, A.A., Geology of the Guaimaca quadrangle, Honduras, Central America, Open-File Report, Instituto Geográfico Nacional, Tegucigalpa, Honduras, 27 p., 1986.

Rosenfeld, J.H., Geology of the Western Sierra de Santa Cruz Guatemala, Central America: An ophiolite sequence [Ph.D. Diss.], State University of New York, Binghamton, 313 p., 1981.

Simonson, B.M., Geology of the El Porvenir quadrangle, Honduras, Central America, Open-file report, Instituto Geográfico Nacional, Tegucigalpa, Honduras, 84 p., 1977.

Simonson, B.M., Mapa Geológico de Honduras, El Porvenir sheet, Instituto Geográfico Nacional, Tegucigalpa, scale 1:50,000, 1981.

Sutter, J.F., Late Cretaceous collisional tectonics along the Motagua fault zone, Guatemala, Geol. Soc. Am., Abstr. Progs., 11, 525-526, 1979.

Weber, H.-S., On the lithology and stratigraphy of the "Estratos de Metapán" in the Republic of El Salvador, Central America, Geol. Jb., B37, 31-54, 1979.

Weyl, R., Geology of Central America, Gebrüder Borntraeger, Berlin, 371 p., 1980.

Zoppis Bracci, L., Estudio preliminar de las mineralizaciones de tungsteno y molibdeno de Macuelizo, Departamento de Nueva Segovia, Bol. Serv. Geol. Nac. Nicaragua, no. 5, 33-52, 1961.

SEDIMENTARY ROCKS OF THE SANTA CRUZ OPHIOLITE, GUATEMALA - A PROTO-CARIBBEAN HISTORY

Joshua H. Rosenfeld
Amoco Production Company
P.O. Box 3092
Houston, Texas 77253

ABSTRACT

The Santa Cruz ophiolite of eastern Guatemala includes sedimentary rocks deposited in the Cretaceous proto-Caribbean ocean. Several conclusions, noted below, are based on preliminary study of these strata.

Intra-basalt chert nodules were deposited during Upper Valanginian/Aptian eruptive activity at the proto-Caribbean spreading center. This oceanic crust was partially blanketed in the Aptian/Albian by upward coarsening volcaniclastic debris derived from the proto-Antillean Island Arc during collision of the western proto-Caribbean with thick Pacific plateau basalt. Chert interbeds date off-axis (seamount?) basaltic eruptions as Albian in age. Argillite melange, possibly Cenomanian in age, formed in an accretionary prism along the leading edge of the advancing Pacific crust. An organic-rich, deep water limestone appears to have been deposited during the widespread Cenomanian Oceanic Anoxic Event.

PURPOSE

With this paper, I propose to accomplish the following:

1) To make available results of a geological reconnaissance originally presented as an unpublished doctoral dissertation (Rosenfeld, 1981.)
2) To place the Santa Cruz ophiolite into the most recent plate tectonic framework.
3) To suggest avenues for further study.

INTRODUCTION

Recent plate tectonic models of the Caribbean (Pindell and Barrett, in press; Donnelly, 1989; Burke, 1988) agree that a "proto-Caribbean" ocean was formed by seafloor spreading between North and South America from the Late Jurassic to the Late Cretaceous. This western arm of the Atlantic Ocean was subsequently consumed beneath a vast slab of thickened Pacific ocean crust ("plateau basalt") which now underlies the oceanic basins of the Caribbean Sea.

Our knowledge of the proto-Caribbean is derived from pieces preserved in ophiolitic terranes obducted during collision of the advancing Pacific crust with continental promontories on the Americas Plate (Yucatan, the Bahamas and northwestern South America).

This paper discusses some aspects of the Santa Cruz ophiolite of eastern Guatemala, a well preserved fragment of the proto-Caribbean which was obducted onto the cratonic Yucatan Block in the Late Campanian. Sedimentary units of the ophiolite have been spared the intense metamorphism, tectonic dismemberment and deep erosion suffered by related ophiolitic fragments smeared along the Motagua-Polochic strike-slip fault zones in Guatemala. These preserved strata provide tantalizing glimpses of proto-Caribbean history.

A more complete description of the Santa Cruz ophiolite, including petrographic, chemical and paleontologic analyses, is found in a doctoral dissertation available from the State University of New York at Binghamton (Rosenfeld, 1981).

REGIONAL SETTING

The Santa Cruz ophiolite underlies the Sierra de Santa Cruz (Figure 1); an east-trending range of jungle covered hills 90 kilometers long and 15 kilometers wide with elevations reaching 1,000 meters. The southern edge of the massif flanks the Izabal pull-apart basin in the Polochic Fault Zone. Post-Middle Miocene left-lateral displacement of about 130 kilometers has been postulated for the Polochic Fault System through palinspastic reconstruction of geological and geomorphological features (Burkart et al, 1987).

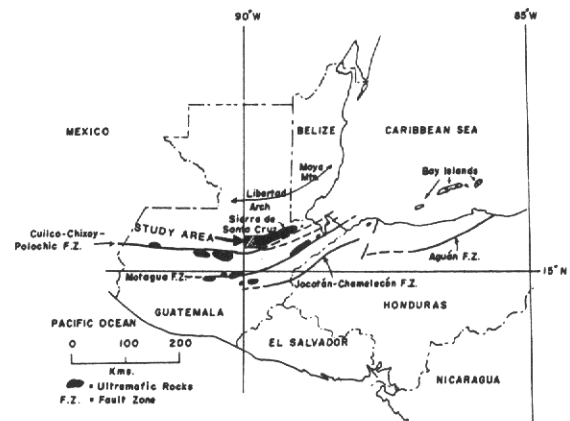

Figure 1 – Major Fault Zones & Ultramafic Exposures of Northern Central America

To its west, north and east, the ophiolite is thrusted over Late Campanian synorogenic turbidite flysch of the Sepur Formation. The Sepur and underlying Cretaceous carbonates are also exposed in windows through the allochthon (Figures 2 and 3). Crystalline basement is a pre-Pennsylvanian gneiss exposed southwest of the ophiolite along the Polochic Fault (Bonis, 1967). The

Larue, D.K., and Draper, G. (eds.),
Transactions of the 12th Caribbean Geological Conference, St. Croix, U.S.V.I., Miami Geological Society, P.O. Box 431552, South Miami, FL 33243, U.S.A.

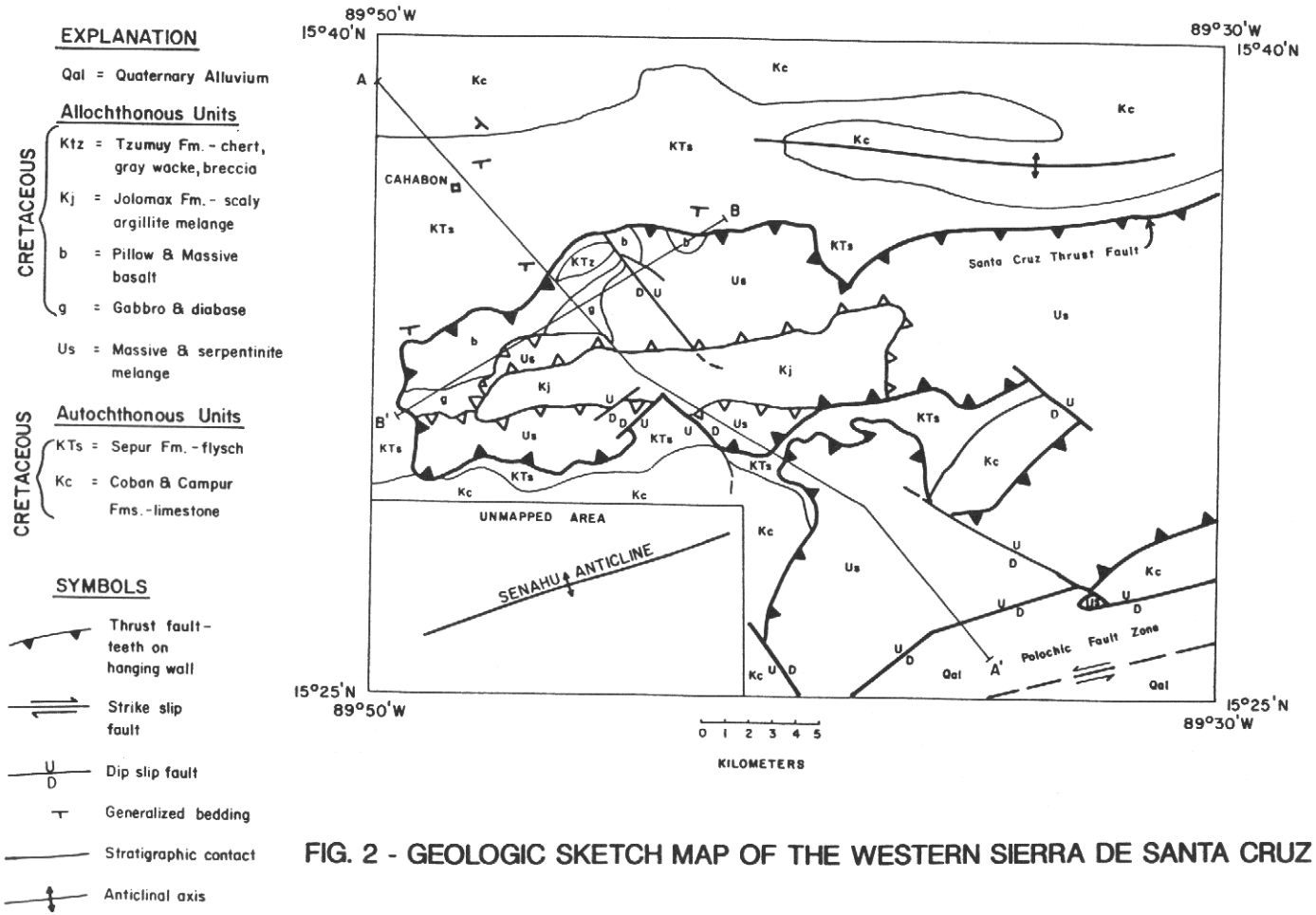

FIG. 2 - GEOLOGIC SKETCH MAP OF THE WESTERN SIERRA DE SANTA CRUZ

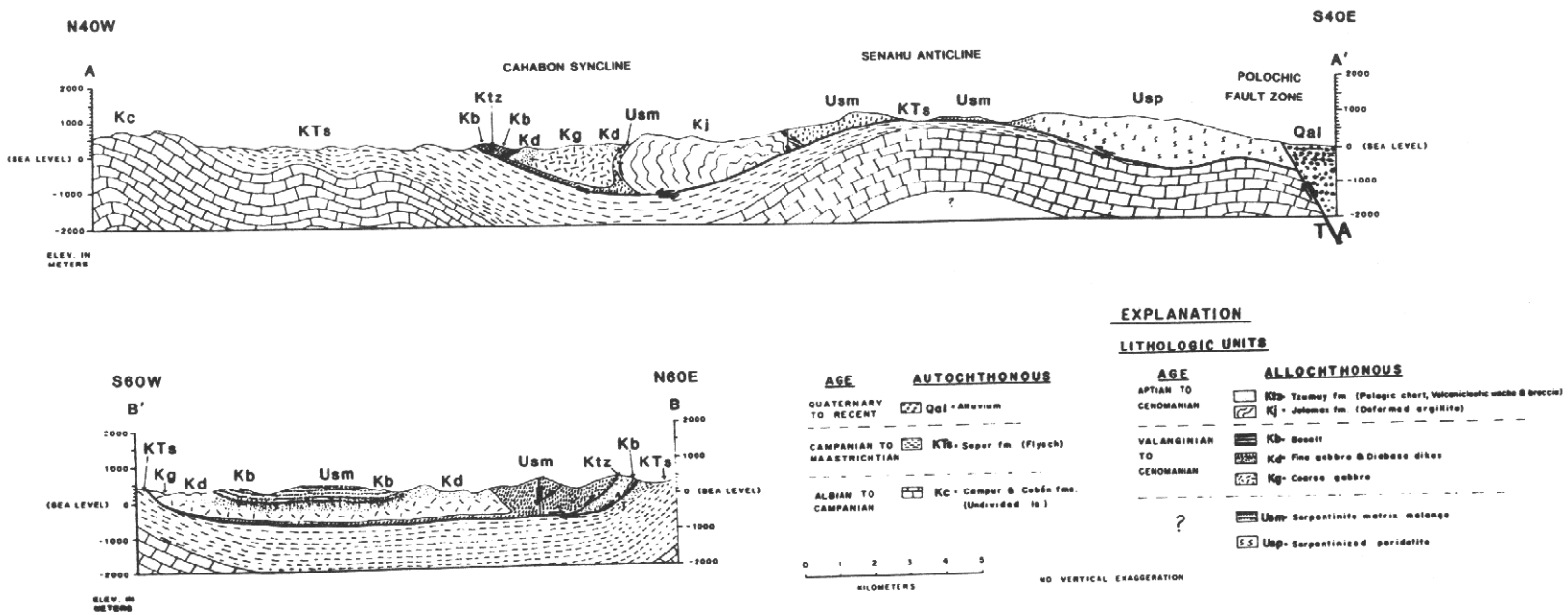

FIGURE 3 GEOLOGIC SECTIONS (LOCATIONS SHOWN ON FIG. 2)

complete Pennsylvanian to Campanian autochthonous sedimentary sequence (Figure 4) crops out in the eroded core of the Senahu Anticline on the western edge of the Sierra de Santa Cruz (Unmapped Area in Figure 2).

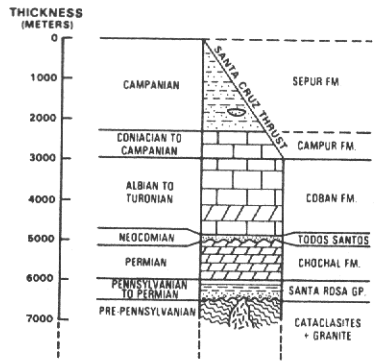

FIG. 4 THE AUTOCHTHONOUS SECTION

The basal decollement of the allochthon is the Santa Cruz Thrust. The translation of the ophiolite slab onto a Campanian turbidite fan occurred as a gravity slide derived from the south (Wilson, 1974, Rosenfeld, 1981).

THE OPHIOLITE

Crystalline Rocks

The ophiolite consists of a layered sequence of serpentinized harzburgite, gabbro, diabase, and hydrothermally altered basalts, whose mafic rocks display typical MORB compositions. Ultramafic cumulates were found in stream boulders, and minor plagiogranite bodies occur within the upper level gabbro and serpentinite melange. The extensive serpentinite melange also encloses blocks of gabbro and amphibolite, as well as disrupted dikes of coarse gabbro, diabase and pyroxenite.

Copper mineralization occurs within basalt and diabase altered to greenschist facies mineralogies. Ore deposition took place in an oceanic hydrothermal system (Peterson and Zantop, 1980; Rosenfeld, 1981; Wilson and Peterson, 1989). Over two million tons of chalcopyrite bearing ore were processed in the 1970's at the Oxec Mine.

Sedimentary Rocks

Intrabasalt Cherts-

Interpillow chert nodules in the lowermost basalts have been dated as Upper Valanginian-Aptian (E. Pessagno, pers. comm.) indicating that seafloor spreading was active at that time. Higher level basalts enclose dark green to black chert beds dated as Berriasian(?)-Albian (P. Whelan-Helwig, pers. comm.). The Albian age is more likely, based on stratigraphic position. Basalts enclosing the younger cherts are less metamorphosed than their deeper counterparts (zeolite vs. greenschist mineralogy), and are amygdular while the older are not. The indication is that eruption of the upper basalts occurred at relatively shallow water depths, and one may speculate that Albian eruptions occurred at an off-axis seamount.

Supra(?)-basalt Limestone-

A single outcrop of black, finely laminated limestone was found in contact with weathered pillow basalt. Coarser laminae contain concentrations of planktonic foraminifera, radiolaria, calcareous nannoplankton and volcanic detritus (euhedral plagioclase, devitrified glass). An analyzed sample contained 1.7% Total Organic Carbon (J. Clendening pers. comm.). Pyrite is abundant in the rock matrix. The age of this sample is probably Cenomanian, (E. Pessagno, L. Balcells-Baldwin, and R. White; see Appendix 1).

The fossil assemblage indicates a purely marine, deep water environment of deposition and the absence of keeled foraminifera suggests that anoxia of the deeper water may have suppressed the deeper water genera which should be abundant in this environment (Jarvis et. al., 1988, p. 87-94.) The high organic carbon content and non-bioturbated lamination of the limestone support this interpretation. Rare benthonic foraminifera and volcanic detritus in some laminae suggest deposition from low energy debris flows originating on a volcanic seamount in the area.

Supra-basalt Volcaniclastics (Tzumuy Formation)-

The lower basalts of the ophiolite are overlain by a 500 meter thick coarsening-upward sequence of bedded chert, turbiditic graywacke and clast supported volcaniclastic breccia of the Tzumuy Formation (Figure 5). These rocks are quite indurated, in contrast to the autochthonous Sepur Formation. Outcrop samples were devoid of usable fossils, but a float fragment yielded a radiolarian age of Aptian-Albian (P. Whelan-Helwig, pers. comm.).

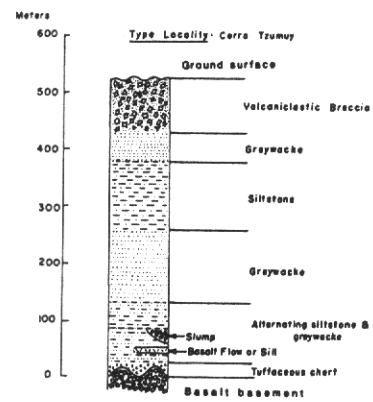

Figure 5- Tzumuy fm. Stratigraphic Section

The volcanic component of the Tzumuy includes pumice shards and euhedral plagioclase grains in the basal cherts. Sandstones contain zoned plagioclase, trachytic textured lithic clasts of dacitic to rhyolitic aspect, and up to 5% quartz presumed to be of volcanic origin. Subangular granule to cobble breccias contain over 95% "arc type" volcanic clasts. A non-MORB, possibly Primitive Island Arc origin has been proposed for these rocks (T. Donnelly, pers. comm.). Although chemistry was not performed on individual volcanic fragments, bulk chemical analyses of the sandstones yielded intermediate range SiO_2 values of 55% to 57%, supporting the interpretation of a volcanic arc provenance for this unit.

This coarsening-upward volcaniclastic sequence, deposited on Aptian oceanic crust, suggests that spreading in this part of the proto-Caribbean occurred near an arc (Figure 6A). It may also be argued that no deep, sediment-trapping trench existed between the arc and this segment of oceanic crust in the Aptian. These suppositions are consistent with the existence of an Aptian Primitive Island Arc at the leading edge of the Pacific plateau basalt (the proto-Antillean Arc of Donnelly, op cit) which "matured" into an intra-oceanic island arc subduction complex during the Albian or Cenomanian as the advancing Pacific crust overrode the western proto-Caribbean (Figure 6B).

Scaly Argillite (Jolomax Formation)-

Sedimentary melange underlies a large area in the core of the ophiolite. Abundant, randomly oriented shear surfaces and mineralized fractures disrupt rarely discernable bedding. The rock is thoroughly metamorphosed in the prehnite-pumpellyite facies.

The fresh rock is dark green to black, weathering to an intense red through oxidation of abundant matrix pyrite. Tightly folded and dismembered chert and volcanic sand laminae comprise a minute percentage of the overall argillite. Included in the melange are large blocks of serpentinite, minor clumps of pillow basalt and small, angular fragments of micritic limestone and chert. Radiolaria occur in the argillaceous matrix but no usable dates have been obtained from the limited original collection (P. Whelan-Helwig, pers. comm.).

The Jolomax Formation may be an accretionary wedge deposit formed at the leading edge of the advancing Pacific crust (Figure 6B). In the absence of age data, the dark color and abundance of pyrite tenuously suggest a dysoxic to anoxic environment of deposition and possible correlation of this unit with the Cenomanian supra-basalt limestone.

DISCUSSION

It is presumptuous to construct a history of the western proto-Caribbean using a few poorly dated sedimentary rocks from a small area of eastern Guatemala. That said, I believe that the Santa Cruz ophiolite contains evidence of Aptian seafloor spreading, Albian-Cenomanian off-axis seamount eruptions, Aptian proto-Antillean island arc activity, and the accumulation of an accretionary prism on the inner wall of a Cenomanian trench. Further speculation links the Cenomanian paleoceanography of the proto-Caribbean to the widespread contemporaneous Oceanic Anoxic Event.

Northward obduction of the Jolomax accretionary prism and a contiguous slab of the proto-Caribbean lithosphere onto the leading edge of Yucatan occurred in the Late Campanian, followed immediately by a northward gravity slide of the allochthon into the Sepur foreland basin. The area was folded in the Paleogene by transpression of Chortis against the southern margin of Yucatan. Neogene strike-slip displacement in the Polochic Fault Zone sliced off and removed to the east the southern continuation of the Santa Cruz ophiolite.

RESEARCH OPPORTUNITIES

This paper highlights an obvious need for further work in the Santa Cruz ophiolite, and in the surrounding flysch where studies may clarify the framework of ophiolite emplacement and the complex interactions of the Yucatan Block, the Antillean Arc and Chortis. I have chosen here to concentrate on the allochthonous sedimentary rocks since they are windows through which proto-Caribbean history may be viewed. Detailed study of these strata would test hypotheses proposed in this paper, and would most certainly lead to more rigorously derived conclusions.

ACKNOWLEDGEMENTS

The original fieldwork and dissertation could not have been possible without the guidance and support of T. W. (Nick) Donnelly and the State University of New York at Binghamton. I owe special thanks to Peter Marsh, geologist and mining engineer, for introducing me to the area and arranging support for the fieldwork. Many colleagues have provided invaluable insights and encouragement. Among others, I would like to thank Fred Nagle, Steve Barrett, Burke Burkart, Peter Muller, Kevin Burke, and the paleontologists cited in the text. Thanks are also due to the management of Amoco Production Company for their continued support and permission to make this contribution.

APPENDIX I

Supra(?)-basalt Limestone Fossil Determinations

from E. A. Pessagno
- Hedbergella delrioensis (Carsey)
- Hedbergella planispira (Tappan)
- Globigerinelloides sp.
- Rotalipora evoluta (Sigal)

from L. Balcells-Baldwin
- Hedbergella delrioensis
- Hedbergella planispira
- Heterohelix sp.
- Marginulinopsis
- Lenticulina

from R. J. White
- Watznaueria barnesae
- Braarudosphaera africana
- Nannoconus truitti

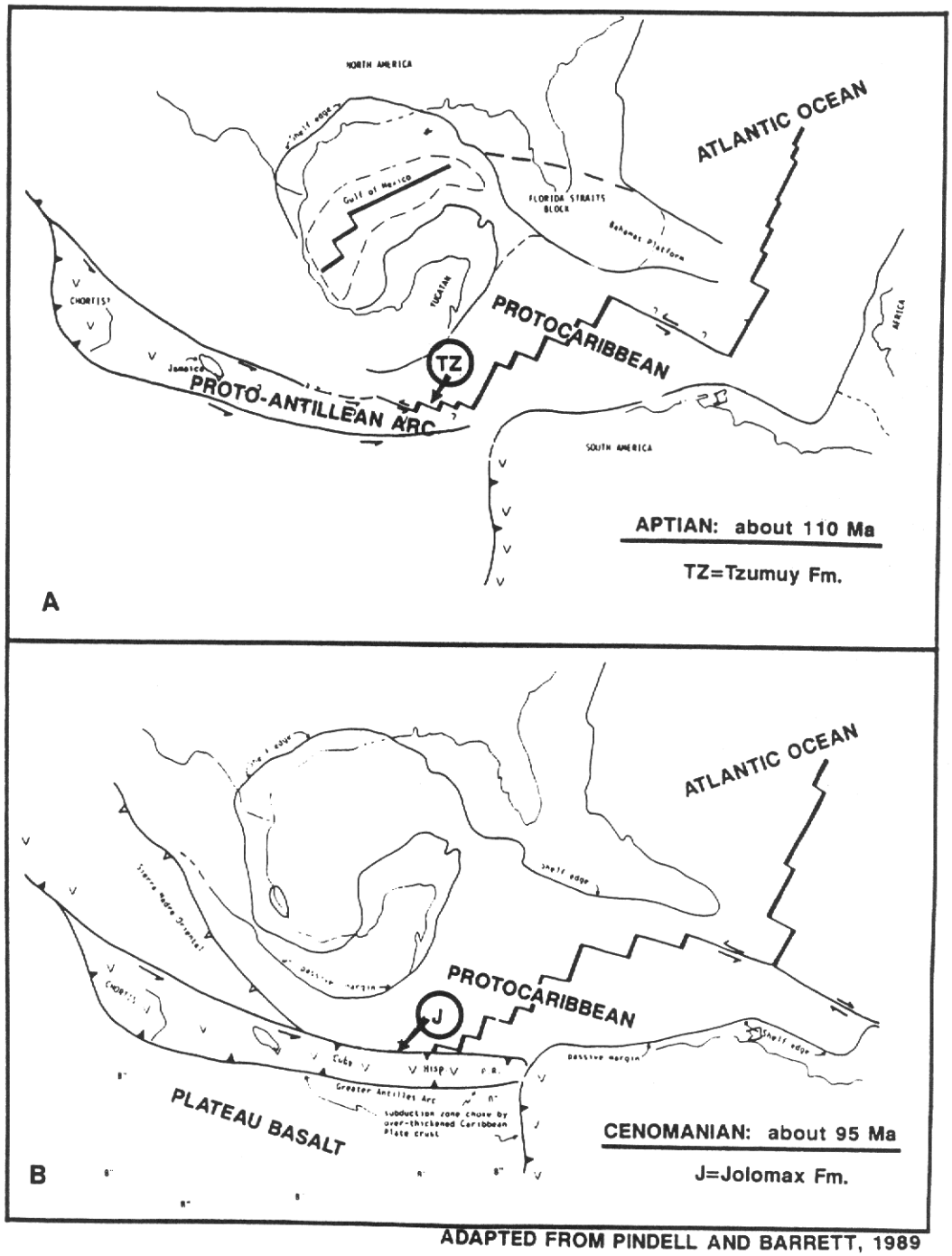

ADAPTED FROM PINDELL AND BARRETT, 1989

FIGURE 6 : PROTOCARIBBEAN RECONSTRUCTIONS

REFERENCES

Bonis, S., Geological Reconnaissance of the Alta Verapaz Fold Belt, Guatemala, Unpubl. Ph.D. Dissertation, Louisiana State University, Baton Rouge, 146 pp., 1967.

Burkart, B., Deaton, B. C., Dengo, C., and Moreno, G., Tectonic Wedges and Offset Laramide Structures Along the Polochic Fault of Guatemala and Chiapas, Mexico: Reaffirmation of Large Neogene Displacement, Tectonics, 6, 411-422, 1987.

Burke, K., Tectonic Evolution of the Caribbean, Ann. Rev. Earth Planet Sci., 16, 201-30, 1988.

Donnelly, T.W., Geologic History of the Caribbean and Central America, in The Geology of North America, Vol. A, Chap. 11, G.S.A., 299-321, 1989.

Jarvis, I. et. al., Microfossil Assemblages and the Cenomanian-Turonian (late Cretaceous) Oceanic Anoxic Event, Cretaceous Research, 9, 3-104, 1988.

Peterson, E. U. and Zantop, H., The Oxec Deposit, Guatemala: an Ophiolite Copper Occurrence, Econ. Geol., 75, 1053-1065, 1980.

Pindell, J. L. and Barrett, S. F., Geological Evolution of th Caribbean Region: A Plate Tectonic Perspective, DNAG Caribbean Region, Vol. H, G.S.A., in press.

Rosenfeld, J. H., Geology of the Western Sierra de Santa Cruz, Guatemala, Central America: An Ophiolite Sequence, Unpubl. Ph.D. Dissertation, State Univ. of New York at Binghamton, 313 pp., 1981.

Wilson, H. H., Cretaceous sedimentation and Orogeny in Nuclear Central America, A.A.P.G. Bull., 59, 1348-1396, 1974.

Wilson, P. N. and Peterson, E. U., Fluid Inclusion Evidence for Fluid Mixing in the Oxec Cyprus-Type Copper Deposit, Guatemala, Econ. Geol., 84, 444-449, 1989.

TECTONICS AND PETROLEUM POTENTIAL OF BELIZE

R. Prasada Rao and R. Ramanathan
Geologists
Office of Geology and Petroleum
Belmopan, Belize
Central America

ABSTRACT

Belize falls in the southern edge of the North American Plate. Three structural units could be discerned - the Belize Basin in the south which is contiguous with the South Peten Basin, the Central Maya Block comprising Paleozoic metasediments and granites, and the Corozal Basin in the north which is the southern continuation of the Yucatan Platform and the eastern continuation of the North Peten Basin. The Belize Basin is structurally complex with folded sediments and thrusts. The Corozal Basin however is characterized by normal faults some of which appear to have strike slip movements.

The regional tectonic framework is one of ancestral basins and rifts known to have formed in Pennsylvanian - Triassic interval. From Jurassic to Mid-Cretaceous the area was surrounded by extensive carbonate shelves, later obliterated at places by Tertiary clastic wedges of deltaic origin. Source rocks appear to be Jurassic to Middle Cretaceous whereas accumulations are likely to be in Middle Cretaceous.

INTRODUCTION

Tectonically Belize forms part of the North American plate and is an extension of the Peten Basin of Mexico and Guatemala and Yucatan platform of Mexico. The boundary between the North American plate and the Caribbean plate is the Motagua-Polochic Fault system and the Swan Fracture Zone in the offshore. This runs very close to the southern extremity of Belize. The northern Belize is named the Corozal Basin which has a sedimentary thickness of over 10,000 ft and is characterized mostly by carbonates and evaporites. The Maya Block comprises Paleozoic metasediments and igneous (granites and rhyolites) intrusives. Further south are exposed Cretaceous and Tertiary sediments. These constitute a folded belt and the sedimentary area is named the Belize Basin (Rao, 1982) which has a thickness of over 16,000 ft predominantly of siliciclastics and limestone. The sedimentary facies, structural style and the tectonic frame work are favorable for the generation, migration and accumulation of petroleum in commercial quantities. The purpose of this paper is to review the geology of Belize including the latest data generated by the Office of Geology and Petroleum, Belmopan and to highlight the oil and gas prospects.

Rock Stratigraphy

Contributions to the stratigraphy of this region include those of Ower (1928), Flores (1952), Dixon (1956), Vinson (1962), Richards (1963), Wilson (1974), Clemons et al (1974), Dengo (1975), Bateson and Hall (1977), Bishop (1980), Peterson (1983), Nair and Cornec (1986), Nair (1987) and others.

The oldest rocks exposed in Belize are the Maya Mountains. These are referred to as Santa Rosa Group and believed to be geosynclinal deposits formed during Pennsylvanian to Permian time. It is not however certain that similar Paleozoic rocks reported from Guatemala, Mexico and western part of the United states were deposited in a single geosynclinal area or in several separate basins. The Santa Rosa Group is intruded by granites of Permian - Triassic age.

Post Triassic sedimentary record of Belize shows somewhat significant differences between the Corozal and Belize Basins, possibly due to the differences in the evolution of these two basins. The salient points of the lithostratigraphy of these two basins are summarized in Fig. 1.

Biostratigraphy

Mega and micro fauna from Belize were reported by earlier workers including Flores

Larue, D.K., and Draper, G. (eds.),
Transactions of the 12th Caribbean Geological Conference, St. Croix, U.S.V.I., Miami Geological Society, P.O. Box 431552, South Miami, FL 33243, U.S.A

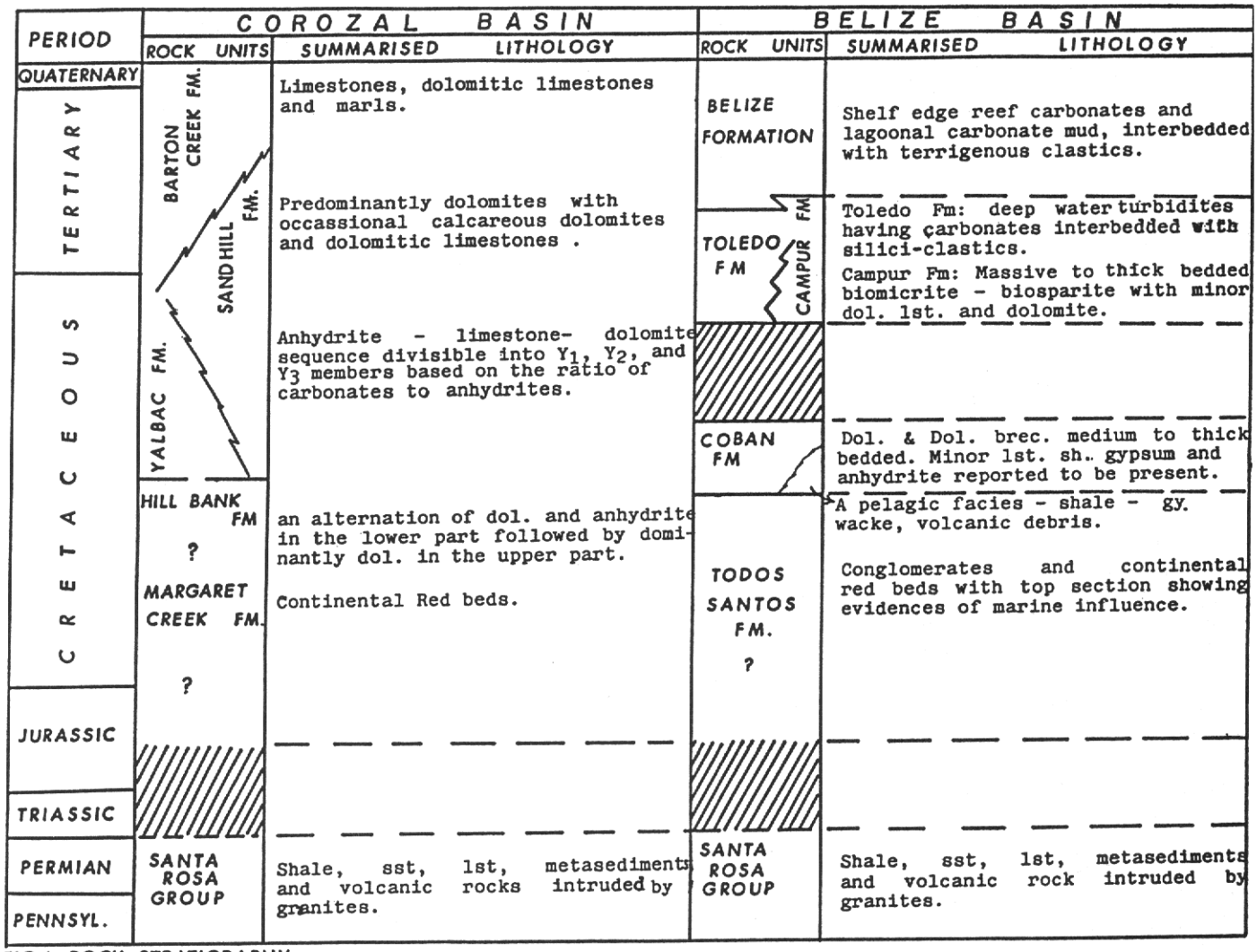

FIG.1 ROCK STRATIGRAPHY

(1952), Dixon (1956) and Bateson and Hall (1977). In addition a few oil companies exploring for petroleum in Belize carried out micro faunal and floral studies both from exposed as well as subsurface sections.

In an attempt to understand paleogeography, paleoecology and depositional history of the sedimentary basins in Belize, foraminiferal biostratigraphic work was initiated by the Office of Geology and Petroleum, Belmopan in 1985. As a result of this a preliminary biostratigraphic zonation has been established for Belize using both planktic and benthic foraminifera. This includes four assemblage zones for Cretaceous and fifteen assemblage and range zones for Tertiary intervals (Ramanathan 1985a,b). These zones together with the major unconformities recognized in Mesozoic and Cenozoic time and the significant transgressive and regressive cycles inferred for a few well sections are given in Fig. 2.

Geologic History

The history of sedimentation in Belize dates back to Late Jurassic-Early Cretaceous, when the weathered peneplained surface of the Santa Rosa Group was faulted down locally. The deposits in these fault bound depressions were fault scree, conglomerate and red shale with occasional anhydrite. (Todos Santos Formation of Belize Basin and Margaret Creek Formation of Corozal Basin).

By the close of Early Cretaceous, there seems to have been extensive diastrophism removing much of the sedimentary cover except from fault bound depressions. The marine transgression that followed seems to be in Albian resulting in the deposition of carbonates in the Belize Basin (Coban Formation) and carbonates and anhydrites in the Corozal Basin (Hill Bank Formation). There seems to be a major unconformity representing non-deposition from Cenomanian to Early

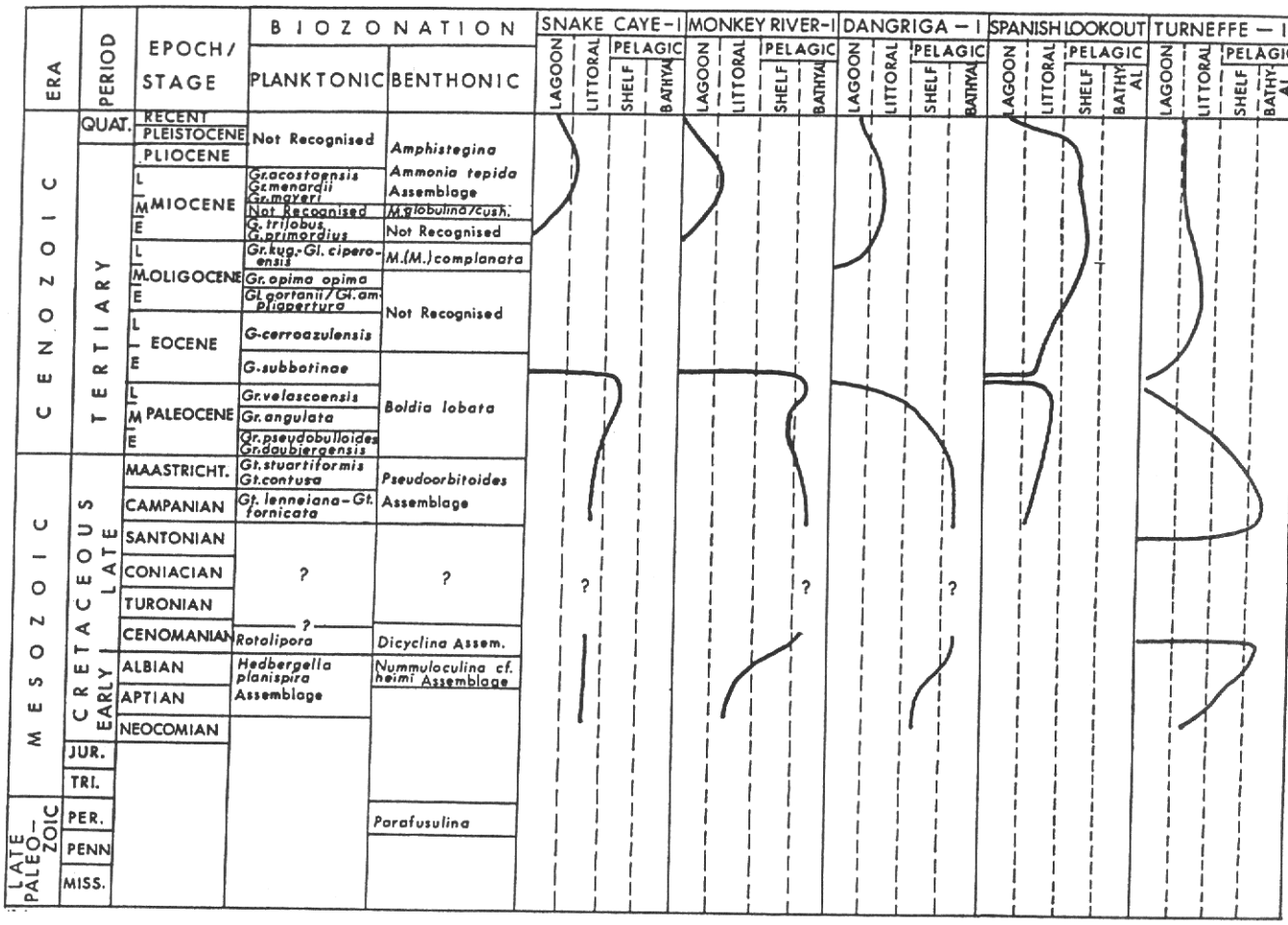

FIG. 2. BIOSTRATIGRAPHY

Campanian in the Belize Basin. However, such a major break in the depositional history is yet to be recognized in the Corozal Basin. Nevertheless, a major transgression in Late Campanian brought these two basins under marine influence. While Belize Basin experienced a deep marine turbidite facies (Toledo Formation) and a shallow marine carbonate facies (Campur Formation) the Corozal Basin continued to be under the influence of hypersaline lagoonal conditions in the western part supporting carbonates and anhydrites (Yalbac Formation) and normal marine conditions in the eastern part accomodating carbonates (Sand Hill Formation).

The major tectonic events witnessed in Belize and Corozal Basins were also responsible for the uplift of the Maya Mountains during Early Eocene. Extensive movements along preexisting fault trends took place during this time. At least some of these movements seem to have been strike slip in conformity with the tectonic style of the period in the region. Extensive development of chert possibly due to hydrothermal activity along some of these faults also took place in part of Corozal Basin.

Except in fault bound depressions, there was again a major break in deposition from Middle Eocene to Early Miocene. Late Miocene witnessed a significant transgression resulting in the deposition of lagoonal shallow shelf and shelf edge carbonates in the Corozal Basin (Barton Creek Formation) and shelf edge reef carbonates interbedded with terrigenous clastics in the Belize Basin (Belize Formation).

STRUCTURE

Regional Considerations

Bouguer anomaly map of the Yucatan Peninsula highlights a regional gravity high in the northeastern part and a large low in the southwestern part, the two apparently separated by a

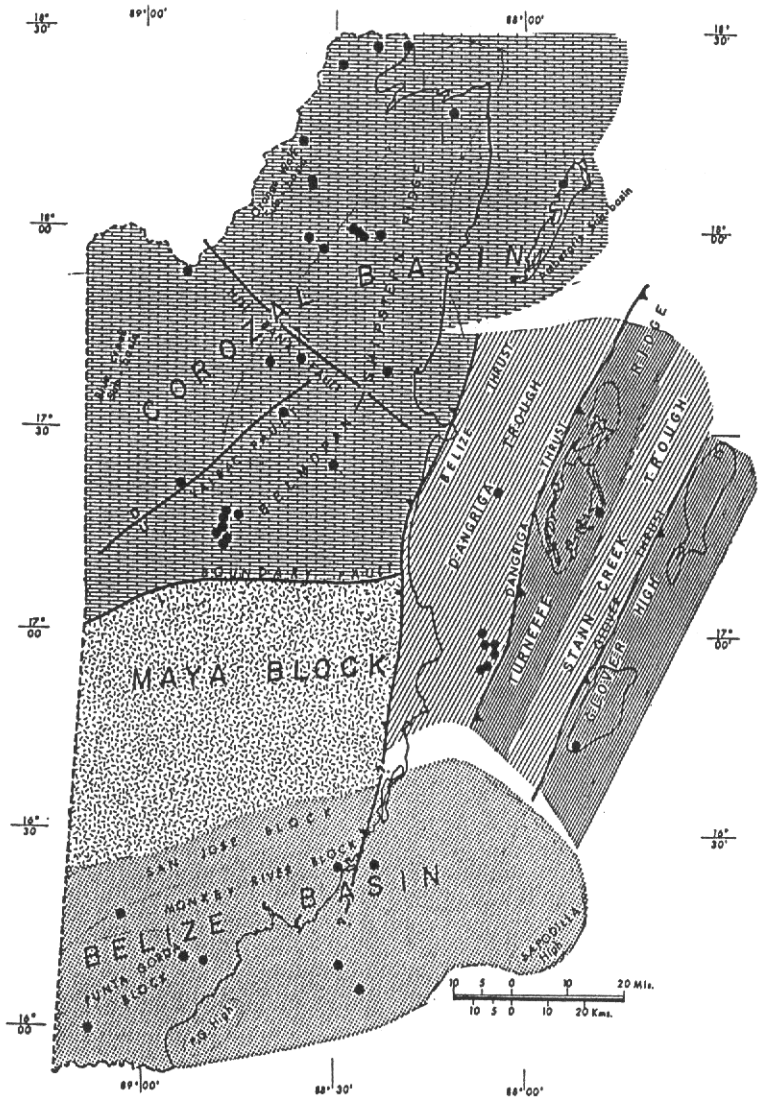

FIG. 3. TECTONIC MAP OF BELIZE

fault. This fault separates the Yucatan Platform from the Peten Basin. The magnetic map is not that clear but in the Yucatan Platform there is a coincidence of the gravity and magnetic lows which could indicate a sedimentary basin. The magnetic map, however, clearly brings out the extension of the Peten Basin into the Blue Creek area of Belize.

Structure of Belize

Aeromagnetic as well as geologic maps confirm the existence of three structural units, the Corozal Basin, the Maya Block and the Belize Basin. In a broad sense, the aeromagnetic map of Belize has two features - the northern Belize (Corozal Basin) with low frequency anomalies and the souther Belize (Maya Block and Belize Basin) with high frequency anomalies (Fig.3).

The Corozal Basin is separated from the Maya Block by a boundary fault, known as Northern Boundary Fault expressed in all the maps - geological, geomorphic, aeromagnetic and gravity. The structure of Corozal Basin is interpreted based on isobath of "basement" prepared from well information, aeromagnetic, bouguer anomaly, geological and geomorphic maps (Fig. 4). The Corozal basin has two significant trends - (i) a large NE - SW ridge named Belmopan-Shipstern Ridge flanked in the East and West by sub-basins and (ii) a NW-SE fault that bisects the Corozal Basin into two parts - the northern half being the extension of the Yucatan Platform and the southern half the continuation of the Peten Basin. The Belmopan Ridge appears to be cut and displaced by this NW-SE tear fault. These faults divide the Corozal Basin into sub-basins and ridges (See Fig.3).

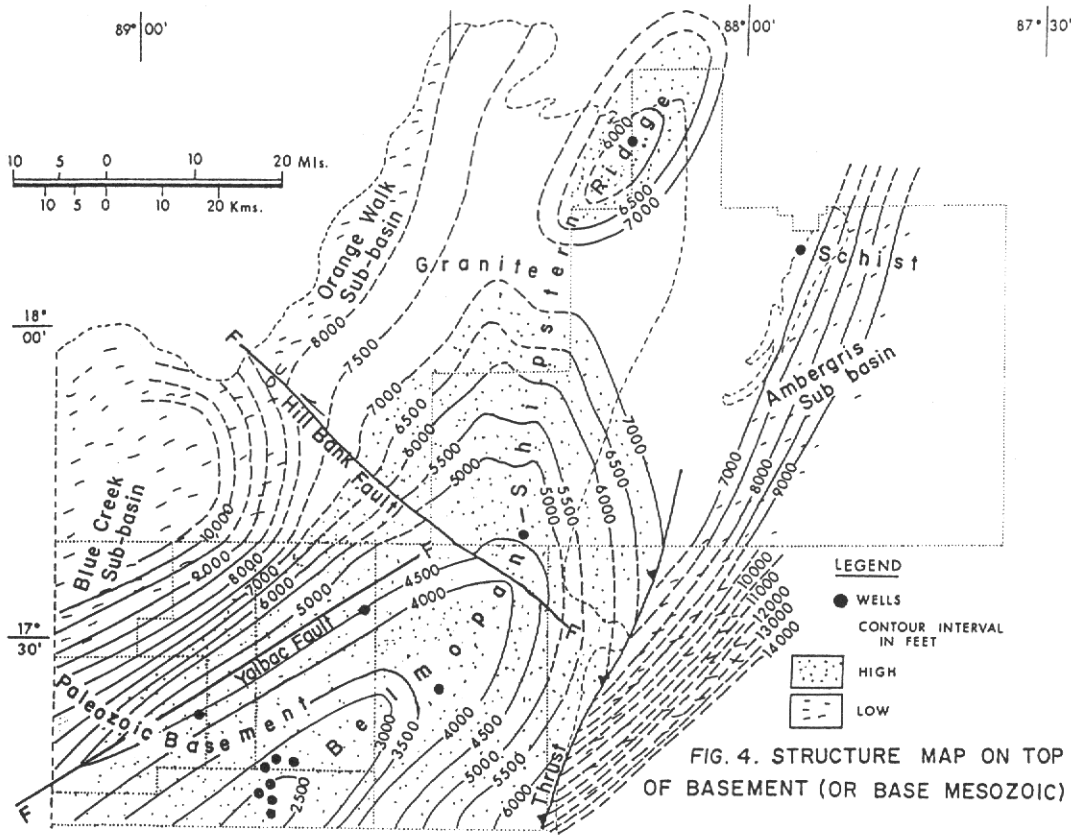

FIG. 4. STRUCTURE MAP ON TOP OF BASEMENT (OR BASE MESOZOIC)

The Belmopan-Shipstern Ridge in the southern part of the Corozal Basin is thrust over the offshore along the Dangriga Trough. This thrust which is NE-SW continues southwards, whereas it dies further north. The northern part of the Corozal Basin as a part of the Yucatan platform appears to have experienced only epeirogenic movements. The western part of the Belmopan-Shipstern Ridge has normal faults heading east and the beds dip in the westerly direction into the Orange Walk sub-basin. The structural style that could be expected here are closures againsts faults. The Belmopan-Shipstern Ridge has a saddle in the northern part and gravity, magnetic and seismic data suggest the presence of an extra sedimentary section, perhaps a Jurassic basin underlying the Cretaceous. Southwest of the Hill Bank Fault, the Yalbac Fault brings the Shipstern-Belmopan Ridge against the Blue Creek sub-basin, which is the eastern extension of the North Peten Basin. The dips on the western flank of the ridge are slightly steeper Fault closures against Yalbac Fault and Hill Bank Fault are the structural styles expected.

The Belize Basin is essentially a folded and faulted belt. In the offshore, the southern part appears to be a "platform" as indicated by the low frequency magnetic anomalies and by a large gravity high. The Belize Basin constitutes several structural units - the San Jose Block, the Monkey River Block, the Punta Gorda Block etc. (See Fig.3). Further northwards in the offshore there are sets of deep sub-basins and ridges. The Maya Block evidently gets cut off by N-S Fault and juxtaposed with a deep basin - the Dangriga Trough with a sedimentary thickness of more than 16,000 ft. These ridges and troughs are very likely the continuation of the Coban Folded Belt. Reverse faults appear to be common - at least in two wells there is repetition of section.

Unlike the eastern part of the Corozal Basin, the Belize Basin and offshore from part of a tectonic setting where the dominant mechanism is strike slip faulting. Sub-basins and ridges in this basin are formed due to suck a mechanism, Structures where entrapment takes place could be fault closures or pinchouts on the margins juxtaposing these with probable source rocks in the deeper parts of the basin.

PETROLEUM GEOLOGY

Temperature Gradient Map

A temperature gradient map (Fig. 5) suggests that the gradients increase towards the Maya

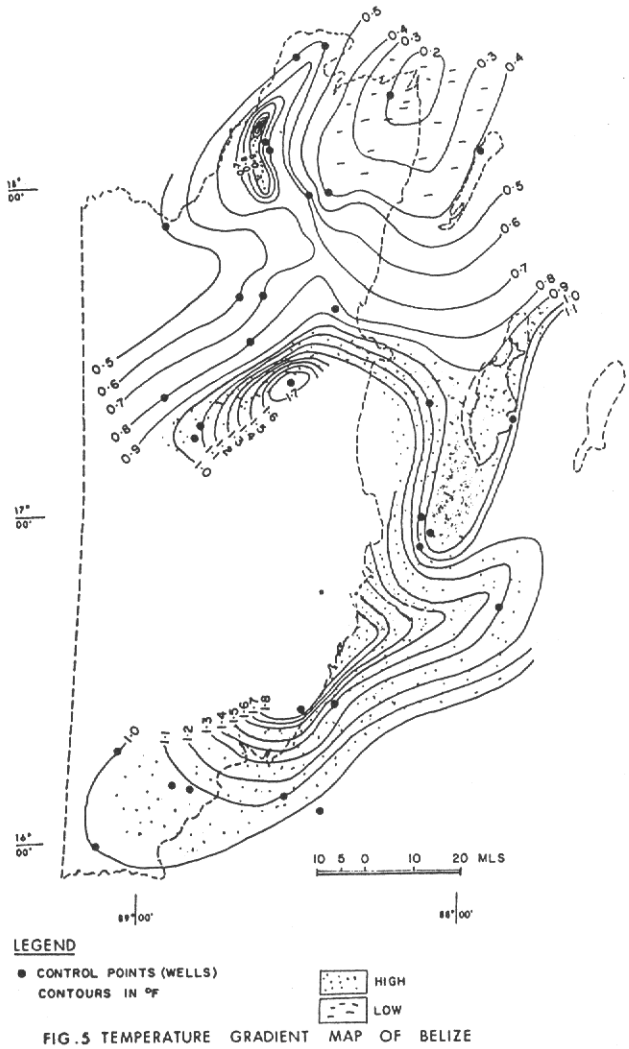

FIG.5 TEMPERATURE GRADIENT MAP OF BELIZE

Mountains. The higher gradient in the north near Belmopan could be related to the boundary fault and in the east (offshore) and south to a system of tear faults. The structures that fall in this wide region of higher geothermal gradients are worth exploring.

Oil Occurrences

Oil occurrences in the Reforma-Campeche-Guatemala area range from Albian to Paleocene. In Corozal Basin oil shows are in Yalbac Formation (Cenomanian - Turonian), whereas in the Belize Basin they are in the Albian part of the Coban Formation.

Oil Seeps

There are at least three surface oil seeps in the Corozal Basin, near Warree Bight, Buena Vista and Roaring Creek (Fig. 6). Others reported are near Bullet Tree Falls and Sibun River. In the Belize Basin, three are at least on seep near Temash and three reported seeps near Punta Gorda (Fig. 6).

Oil Shows

Almost all the wells in the western part of the Corozal Basin (west of Belmopan -Shipstern Ridge) had live oil shows from the Yalbac section. Of the seventeen wells drilled in the Belize Basin eight had live oil shows from the Coban section.

Source Rock

The Tertiary, the Upper Cretaceous and the Lower Cretaceous rocks encountered in the wells of Corozal Basin have thin black shales which are organic rich. These rocks would thicken basinward and organic matter could be rich in the depocenter. This could be especially so in the case of Middle Cretaceous (Turonian) whose equivalent is the Eagle Ford shale of East Texas (Brown and Ruth, 1985). If this is the case, and if proper traps are identified and drilled there could be prolific production.

The oil in S.E. Mexico is supposed to be sourced from the Jurassic-Lower Cretaceous marine shales (Viniegra, 1971, Bishop, 1980, Meyerhoff, 1980, Santiago et. al 1984, Peterson, 1983) which could be the marine equivalent of the Todos Santos Formation. This formation has been penetrated in two wells, Spanish Lookout and Seal Caye. The environment in which it was deposited (in Seal Caye) was continental to begin with and changed to marginal marine passing upward into normal marine shelf and probably pelagic. This formation is correlatable with the Todos Santos Formation of Western Guatemala and Lecho Rojos and San Ricardo Formations of Southern Mexico.

If local basins developed during strike slip movements in Lower Cretaceous and Paleocene, chances of development of richer shales with oil prone - type kerogen would be present. In fact anomalously high heat flows are observed in Dangriga well, and thick sediments reaching oil window are present as for instance in Palmetto Caye well offshore,. Other factors which are speculative are maturity, adequate organic matter, local migration, existence of migration fairways (depositional, tectonic) and trapping within margins of depocentres.

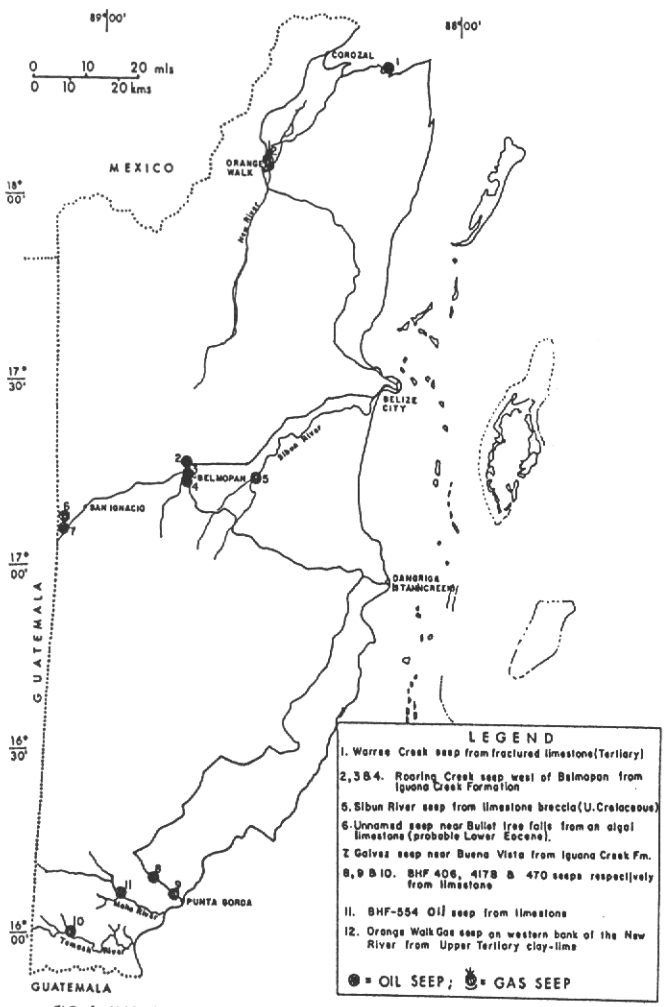

FIG. 6. MAP SHOWING LOCATIONS OF OIL AND GAS SEEPS IN BELIZE

Reservoir and Cap Rocks

In Corozal Basin, the Yalbac Formation which comprises alternations of dolomite and anhydrite is the natural combination of reservoir and cap rock. The underlying Hill Bank Formation is also a dolomite section with anhydrite intervals. In the Belmopan area the shale content of the dolomite varies from 5 to 20% and permeability of 10 millidarcies, with a few intervals going up to 130 millidarcies. The Yalbac Formation however has porosities up to 15% and permeabilities up to 3 millidarcies, a few exceptions however are 50 millidarcies. Core analysis data show low permeabilities at high porosities, which suggests that effective porosities could be increased by formation stimulation. Fracture porosity seems to be present near fault zones.

In Belize Basin, the best reservoir rock appears to be Upper Coban. In one of the wells (Coco Plum-I) a high porosity of 45% and permeability of 37 darcies are reported in one case. One view is that the tallus that is buried in the shale (Punta Gorda Formation is an example) could be a good exploration target. Structures over such basinal margins where such tallus is deposited or "stratigraphic traps" are the areas to look for. Exploration for pure stratigraphic traps is expensive and elusive and so any seismic anomaly located on basin margins is worth drilling. Location of basin margins is possible, provided a high quality seismic exists supported by aeromagmatic data. Numerous structures are already mapped by seismic and if from regional considerations cap rock is identified such areas would be worth testing.

TYPE OF PLAYS EXPECTED

Corozal Basin

In Corozal Basin the major structural feature is the Shipstern Ridge which nearly limits the anhydrites. The western flank of this ridge is characterized by normal faults heading eastwards. Closures developing against these faults are the plays to be tested. The seismic lines bring out some of the fault closures. Other closures expected are the ones against Yalbac Fault and Hill Bank Fault.

Belize Basin (onland and offshore)

Numerous anticlinal closures are mapped by seismic in the offshore, and geologically mapped onshore. Although seismic quality is good it is not clear how many of these structures continue downwards (antiforms?) and whether some of these are cut off by thrust faults. The prospects of these however are very good especially if sub-thrust blocks of these structures are tested.

REFERENCES

Bateson, J.H., Hall, I.H.S., (1977). The geology of the Maya Mountains, Overseas Mem. 3. Inst. Geol. Sciences. Her Majest's Stationery Office, London P. 43.

Bishop, W.F., (1980) Petroleum geology of Northern Central America. Jour. Petroleum Geol. Vol. 3 No. 1, P. 3-59.

Brown & Ruth Laboratories Inc., (1985). Regional petroleum geochemistry of the onshore and offshore sediments of Belize. Unpublished Rep., Houston, Texas, p. 60.

Clemons, R.E., Anderson, T.H., Bohnenberger, O.H., Burkart, B. (1974). Stratigraphic nomenclature of recognized Paleozoic and Mesozoic Rocks of Western Guatemala. Amer. Assoc. Petrol. Geologists, Bull. Vol. 58, p. 313-320.

Dengo, G., 1975. Paleozoic and Mesozoic tectonic belts in Mexico and Central america. In A.E.M. NAIRN, F.G. Stehl, (Eds.). The ocean basins and margins, Vol. 3; The Gulf of Mexico and Caribbean. Plenum Press. N.Y. p. 283-323.

Dixon, C. G., (1956). Geology of Northern British Honduras with notes on adjacent areas. Govt. Printer, Belize, p. 91.

Flores, G., (1952). Geology of Northern British Honduras: Amer. Assoc. Petrol. Geologists, Bull. Vol. 34, p. 404-409.

Meyerhoff, A.A., (1980). Geology of Reforma-Campeche Shelf. Oil Gas Jour. April 21, pp. 121-126.

Nair, K.M., (1980). Stratigraphy of Belize Basin. UNDP/BZE/83/001 Belmopan, Belize (unpublished Report) p. 37.

Nair, K.M., Cornec, J.H., (1985). Pre-Cenozoic stratigraphy of Corozal Basin, Northern Belize. UNDP/BZE/83/001, Belmopan, Belize, (unpublished Report).

Ower, L.H., (1928). The geology of British Honduras. Colonial Survey office, Belize.

Peterson, J.A. (1983). Petroleum geology and resources of Southern Mexico, Nothern Guatemala and Belize. Geological Survey Circular 760. USGS; p.44.

Ramanathan, R., (1985a). Foraminiferal micropaleontological report on Spanish Lookout-I offshore Belize. UNDP/BZE/83/001, Ministry of Nat. Res., Belmopan, Belize, p. 17 (unpublished Rep.).

Ramanathan, R.,(1985b). Foraminiferal micropaleontological report on Monkey River-I onshore Belize. UNDP/BZE/83/001, Ministry of Nat. Res., Belmopan,Belize, p. 12 (unpub. Rep.).

Rao, R.P., (1982). Exploration in Belize gains momentum. Oil and Gas Journal, Sept. 27, 1 982, p.308-318.

Richards, H.G., (1963). Stratigraphy of earliest Mesozoic sediments in Southeastern Mexico and western Guatemala. Amer. Assoc. Petrol. Geologists, Bull. Vol. 47, No. 10, p. 1 861-1870.

Santiago, J.A., Carillo, J.B. and Martell, B.A., (1984). Geología de Mexico. In: Evaluación de formaciones en Mexico. Petroleos Mejicanos and Schlumberger offshore Service, pp. I.1 - I.36.

Viniegra, F. O., (1971). Age and evoluation of salt basins of southeastern Mexico, Amer. Assoc. .Geol., Bull., Vol. 55, No. 3, pp. 478-494.

Vinson, G.L., (1962). Upper Cretaceous and Tertiary stratigraphy of Guatemala. Amer. Assoc. Petrol. Geologists. Bull. Vol. 46, No.4, p. 425-456.

Wilson, H.H., (1974). Cretaceous sedimentation and orogeny in nuclear Central America: Amer. Assoc. Petrol. Geologists Bull. Vol. 58 p.1348-1396.

PRECISIONS SUR LA NATURE, LA STRATIGRAPHIE ET L'EXTENSION DE LA FORMATION DE RIVIERE GLACE (PRESQU'ILE DU SUD D'HAITI).

AMILCAR H.,Bureau des mines et de l'Energie, B.P. 2174, Port-au-Prince, Haiti.

La formation de Riviere Glace a ete observee et decrite d'abord par J. Butterlin (1954;1960) puis par T. Calmus (1983) qui en a propose le terme.
De nature essentiellement detritique, cette formation telle qu'observee dans la localite type, est constutuee d'une serie rythmique de silts calcaro-argileux, les bancs fins augmentant en proportion a mesure qu'on descend dans la serie. D'autres affleurements presentent une sequence silto-greseuse avec des passees de calcarenites a granoclassement typique des turbidites et des figures de base de bancs.

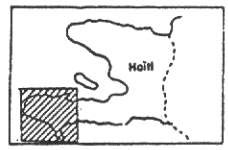

Localisation du secteur d'etude

L'âge de la formation se precise: la limite Cretace-Tertiaire.
Des échantillons prelevés dans deux localites distantes de 40 km environ, ont livré une nanno-flore: Micula prinsi, Thoracosphaera sp. et Watznaueria barnesae indiquant le Maestrichtien terminal-Danien (à noter que Micula Prinsi, forme rare, est un excellent marqueur dont l'apparition n'a duré que 150000 ans environ). Plus au Nord de ces deux localités, un niveau de calcaire gris bleuté, finement détritique, intercalé dans des pélites a fourni des petites globigérines du Danien inférieur, de rares rugoglobigerines, des Gumbelina sp. et de gros lagenides rectilignes.
L'extension géographique de cette formation dépasse les limites connues. On a observé des affleurements à plus de 50 Km à l'Est et 80 Km à l'Ouest de la localité type.
La formation de Rivière Glace, dont l'importance se precise au fur et à mesure de nos investigations, est complexe. Elle semble être l'equivalent de la formation de Beloc.

SUBSURFACE GEOLOGY OF RIO MAJADA AND RIO LAPA VALLEYS, PUERTO RICO

Asencio,E.,and Ramos-Ginés,O., U.S. Geological Survey, Water Resources Division, P.O. Box 4424, San Juan, P.R. 00936

A geophysical study to map the subsurface geology of the Rio Majada and Rio Lapa valleys, located in southern Puerto Rico, was undertaken to delineate geologic controls of the main water supply sources for the Puerto Rico Olympic Committee training facility. Surface geophysical techniques and continuous core samples were used to obtain information about the thickness of the alluvium and gross variations in lithology throughout both valleys.

The seismic refraction sections and electrical resistivity soundings, calibrated with the drill hole lithology, can be divided into three units: 1) alluvial deposits; 2) weathered rocks; 3) unweathered rocks. Alluvium thickness varies from 10 to 35 feet. This thin veneer of alluvium overlies weathered flow breccias and volcanic breccias in the Rio Majada valley; and tuffaceous mudstones, volcanic breccias and pillow lavas in the Rio Lapa valley. The weathering profile is the sequence of layers of materials with different physical properties which have developed in-situ and lies above the unweathered rocks. Three layers within the weathered profile were delineated on the basis of distinct seismic velocity differences, although the irregular and gradational nature of the contacts was poorly defined in the core samples. Weathered volcanic breccias, tuffaceous mudstones and pillow lavas in the Rio Majada and Rio Lapa valleys constitute the most favorable water-bearing units for ground-water development.

APERCU SUR LES TERRASSES PLIO-QUATERNAIRES DU NORD-OUEST D'HAITI

AMILCAR C.,H.,Bureau des Mines et de l'Energie, Port-au-Prince, Haiti.

Les terrasses plio-quaternaires qui bordent la partie nord-ouest de la cote haitienne sont parmi les plus spectaculaires du monde. Très nombreuses et exceptionnellement preservées, elles expriment l'instabilite tectonique de la région qui se situe en bordure de la plaque caraibe. Leur obliquité par rapport à la limite de cette plaque, leurs altitudes et leurs diverses inclinaisons permettent de mesurer avec precision la déformation de la région.

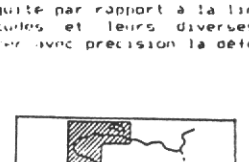

Localisation du secteur d'étude

Les terrasses ne sont pas uniquement des constructions récifales: en effet, d'après l'observation de coupes naturelles de rivières et de falaises, elles se caractérisent par des formations de pentes importantes (couches détritiques obliques) surmontées de dalles massives plus ou moins construites d'où l'importance de l'érosion marine par rapport à la contribution organique, dans la création des terrasses.

LES SEDIMENTS RECENTS DU PLATEAU INSULAIRE GUADELOUPEEN

AUGRIS C., IFREMER, BP 70, 29263 Plouzané, FRANCE
ASSOR R., Université Antilles-Guyane, BP 592, 97167 Pointe-à-Pitre, FRANCE

Le plateau insulaire de l'archipel guadeloupéen a fait l'objet d'une cartographie détaillée de la couverture sédimentaire meuble et de la morphologie sous-marine, à l'aide de différentes techniques complémentaires : sonar à balayage latéral, sismique réflexion haute résolution, bathymétrie, prélèvements de sédiments à la benne, prises de vue, carottage. La reconnaissance quasi complète a été réalisée.

Les résultats montrent :

- la répartition horizontale des formations : massifs coralliens et ensemble sédimentaire. A l'intérieur de celui-ci, en fonction des coefficients de rétrodiffusion des constituants, différents types de sable ont été identifiés, certains pouvant être affectés par des figures de houle.
- la distribution verticale des accumulations, mettant particulièrement en évidence des chenaux fossiles.

Les documents élaborés sont une référence utile pour toute activité liée au domaine marin : enseignement, aménagement, exploitation des ressources, protection du milieu.

THE CARIBBEAN SOUTH AMERICAN PLATE BOUNDARY IN THE CARIBBEAN MOUNTAINS PROVINCE, EASTERN VENEZUELA

AVÉ LALLEMANT, H. G. , Department of Geology and Geophysics, Rice University, P. O. Box 1892, Houston, Texas 77251

Preliminary results of a structural geologic study of the intermediate P/T metamorphic rocks of the Araya Peninsula, the El Pilar fault zone, and the fold and thrust belt south of the El Pilar fault, are consistent with recent plate-tectonic models for the interaction of the Caribbean and South American lithospheric plates. The rocks of the Araya Peninsula underwent two synmetamorphic phases of isoclinal folding (D_{1a} and D_{1b}) which may have resulted from east-directed tectonic transport. The D_{1a} and D_{1b} structures are cross cut by north-south striking listric normal faults/shear zones and kinks (D_{1c}) which indicate east-west extension. The next phase of folding (D_2) is characterized by tight to open postmetamorphic, east-northeast trending folds, generally verging to the south and generally accompanied by south vergent thrust faults (north vergent folds and thrust faults are relatively rare). The youngest major phase of folding (D_3) is characterized by east and west vergent folds, accompanied by east and west vergent thrust faults, respectively. The structures in the fold and thrust belt, south of the El Pilar fault, underwent the last two phases of folding (D_2 and D_3) recognized north of the fault. Along the El Pilar fault, upper Tertiary and lower Cenozoic(?) rocks are deformed by D_3 structures. It is proposed that the D_{1a} and D_{1b} structures formed in a "transpressional terrane" or a "forearc sliver" as a result of interaction of the Farallon plate with northwestern South America during the mid to Late Cretaceous, and that the D_{1c} extensional structures are related to Late Cretaceous uplift and gravitational collapse while the terrane was displaced northeast-ward in a transform margin. The D_2 structures may have formed during mid to late Tertiary time as a result of the eastward passing of the lesser Antilles volcanic arc along the northern margin of South America. The D_3 structures are related to "restraining bends" of the east-west striking strike-slip faults which make up the present plate boundary.

GENETIC AND PROCESS MINERALOGIC ASPECTS OF GOLD-QUARTZ VEIN MINERALIZATIONS, CORDILLERA OCCIDENTAL, COLOMBIA S.A.

BAUM, W., Pittsburgh Mineral & Environmental Technology, Inc., 390 Frankfort Road, Monaca, PA 15061, USA;
GOBEL, V.W., Department of Geology, Stephen F. Austin State University, Nacogdoches, TX 75961, USA

Hydrothermal gold-quartz mineralizations in the Western Cordillera (Cordillera Occidental) of Colombia are mainly associated with high-plutonic tonalite intrusions of Tertiary age. Polymetallic Pb-Zn-Cu-Au-Ag vein systems and impregnations formed from aqueous phases of mixed formational-magmatic origin with a main and also productive stage between 290-210 °C. Intensively altered wall rocks show pyritic propylitization, also kaolinitization and silicification. Present mining operations are relatively small, and their full potential has not yet been utilized. Initial process mineralogic studies used selected composite samples from various gold-quartz mineralizations in the southern part of the Western Cordillera. Substantial amounts of gold occur as coarse to fine or ultrafine inclusions of native gold in base metal sulfides, i.e., pyrite, chalcopyrite, galena, and sphalerite. Virtually all of the native gold exhibits a distinct light yellow colour indicative of elevated silver concentrations of 15-25 wt% . Particle size analyses of gold indicate a bimodal size distribution, with approximately 30-40 % of the Au occurring in the coarse size (+ 200 mesh) fraction and 60-70 % in the fine to ultrafine size range of -200 to -500 mesh. Silver exhibits a more complex mineralogic occurrence with considerable concentrations associated with Ag-bearing tetrahedrite, pyrargyrite, sphalerite, chalcopyrite, and galena.
High grade zones in various parts of the veins may affect sampling and assaying of drill core, channel, and trench samples. Thus, great care is advised during sampling preparation to minimize severe nugget effects due to coarse gold particle sizes. Gold mineralizations frequently extend into hanging and foot walls of the veins where gold is primarily associated with pyritic-propylitic alteration and mineralization.
Process mineralogy indicates that many vein ores should be amenable to physical pre-concentration methods using gravity devices. It is recommended that any further assessment work on these very attractive mineralizations be guided by such evaluations. Increased recovery rates and higher profitability can be expected.

PRESUPUESTO DE SEDIMENTOS, ESPERANZA, VIEQUES, PUERTO RICO (1935-1988): RELACIONADO CON LOS CAMBIOS EN LAS CONDICIONES CLIMATOLOGICAS DEL CARIBE

BARRETO, M., Departamento de Ciencias Marinas, UPR, Mayaguez, Puerto Rico

Estudio de presupuesto de sedimentos en la zona de Esperanza, Vieques, P.R. durante los ultimos cincuenta anos relacionado con los cambios en las condiciones climaticas en el Caribe. Dinamica de transferencia de sedimentos en el sistema es descrita cualitativa y cuantitativamente, atraves del estudio de cambios de perfiles de playa, muestras de sedimentos actuales colectadas mediante dragado y muestras de playa, analisis de patrones de refraccion, comparacion de contornos de batimetria, medidas de corrientes litorales, estudios de fotografias aereas del area a escala de 1:2,000 y datos climatologicos de la zona bajo condiciones de eventos promedios normales y anormales. Analisis de las variables del sistema demuestran un incremento en la tasa de erosion durante los ultimos veinte anos.

SEDIMENT BUDGET, ESPERANZA, VIEQUES, PUERTO RICO (1935-1988): RELATED TO CARIBBEAN CLIMATIC CONDITIONS CHANGES

BARRETO, M., Marine Sciences Department, UPR, Mayaguez, Puerto Rico

This paper presents a sediment budget study at Esperanza, Vieques, P.R. The beach equilibrium has changed during the last fifty years of Caribbean climatic changes. Beach sediment dynamics are described both quantitatively and qualitatively using: monthly beach profiles, analyses of beach and nearshore samples, wave refraction plots, bathymetric changes, current measurements, and weather data. Aerial photos at 1:2,000 were used to measure shoreline changes over a 50 year period. Analysis of the data shows a increase in erosion rates for the last twenty years.

PALEOGENE ACCRETION AND SUSPECT TERRANES IN SOUTHERN COSTA RICA (OSA, BURICA, CENTRAL AMERICA)

BAUMGARTNER, P.O.*, OBANDO, J.A.**, MORA, C.*, CHANNELL, J.E.T.*** AND A. STECK**** * Institut de Géologie, BFSH 2, Univ. of Lausanne, 1015 Lausanne, Switzerland. ** RECOPE, Edificio Colón, Apt. 4351, San José, Costa Rica. *** Dept. of Geology, Univ. of Florida, Gainesville, Florida 32611, U.S.A. **** Institut de Minéralogie, BFSH 2, Univ. of Lausanne, 1015 Lausanne, Switzerland.

Oceanic Basement and associated deep water sediments of the Osa and Burica Peninsulas and the Golfo Dulce area have been globally included with the Nicoya Complex by most authors. Our field studies of the last 5 years lead to a separation of 3 units, which are distinct from the Nicoya Complex and separated from each other by Neogene to Recent fault systems. Each of the units is characterized by a distinct Late Cretaceous-Paleogene sedimentary and tectonic history and significantly different paleolatitudes, leading us to define two suspect terranes.
1. Golfito Terrane. - The Golfito Terrane forms the NE shore of the Golfo Dulce and the isthmus of the Osa Peninsula (Rincón - Boca del Sierpe). It is characterized by oceanic basalts and dolerites (over 95% of volume) and by stratigraphically overlying Campanian-Maastrichtian argillites. Preliminary paleomagnetic data indicate equatorial Late Cretaceous paleolatitudes, which are significantly different from those known for Santa Elena, Nicoya and the Fila Costeña.
2. Burica Terrane. - The Burica Terrane forms the SW shores and the central highs of the Burica Peninsula and is characterized by oceanic basalts, dolerites and hypabyssal rocks stratigraphically overlain by late Paleocene-middle Eocene pelagic and redeposited shallow water sediments. Very proximal shallow carbonate debris flows in the central part suggest a near carbonate platform, whereas dominantly pelagic and turbiditic lithologies in coastal outcrops suggest a paleoslope adjacent to an oceanic seamount with water depths within the photic zone. Preliminary paleomagnetic data indicate a far more southerly Paleocene paleolatitude than for the rest of Costa Rica.
3. Caño Accretionary Complex. - The Caño Accretionary Complex forms the Caño Island and the pre-Neogene of the SW and central Osa Peninsula. The Complex is characterized by strongly deformed and low grade metamorphic turbidites and hemipelagic and pelagic sediments (over 95% of volume). In some places (San Pedrillo-Marenco) 10-100 m sized blocks of oceanic basalts, dolerites and minor amounts of gabbros and acid differentiates occur in a pelagic sedimentary matrix. Central and outer Osa has no igneous basement. Some areas show deformed debris flows and turbidites of shallow water origin. Ages of pelagic and shallow water lithologies which occur as blocks or in turbidites range from Late Cretaceous to Oligocene. It is thought that the Complex is a result of Oligocene and post-Oligocene accretion in the Mid-American Trench. The different types of sedimentary melanges suggest offscraping of the sedimentary cover of the oceanic plate including both oceanic and trench-fill sediments. The latter consist of arc-derived turbidites which contain olistoliths possibly derived from an outer high (Golfito Terrane?) forming the inner wall of the trench. Paleolatitudes, emplacement histories of the terranes and the accretionary history of Osa support current plate tectonic models suggesting a southwestern, pacific origin and a NE-movement of the Caribbean plate between Campanian and Paleocene. The Burica Terrane, however, must have docked on the Caribbean plate in post-Paleocene times, after the formation of the Mid-American Trench.

SEDIMENT SUBDUCTION AT THE LESSER ANTILLES CONVERGENT MARGIN.

BEHRMANN, J.H., IGL, Univ. Giessen, D-6300 Giessen, West Germany.

An interesting question to be addressed in geotectonics is how much sediment is accreted or subducted along convergent plate margins. Sediment subduction influences the geochemical balance of the Earth's mantle, and is a potentially important factor in the formation of island arc magmas. Sediment accretion is one of the long-term limiting factors of continental growth.

Sediment accretion versus sediment subduction at the plate interface Americas-Caribbean is investigated in a steady-state dynamic model. The model accounts for the geological evolution of the Eastern Caribbean borderlands since the Tithonian, and presumes that the "modern" Lesser Antilles subduction zone formed at about 48 mybp. Dynamic variables are: (1) growth rates of the accretionary wedge. (2) Rate of plate convergence. (3) Age of subducted crust through time. (4) Sedimentation rates on the subducting plate through time.

Size and age of the accretionary wedge can be approximated from the age of the Lesser Antilles island arc, and from reconstructed crustal profiles based on geophysical data. Convergence rates are constrained by plate reconstructions and the opening history of the Cayman Trough. A sedimentation rate profile on the oceanic crust east of the Lesser Antilles forearc is calculated from DSDP/ODP drillholes 27, 543 and 672, and is calibrated to finite thicknesses of the sedimentary column in front of the three sections studied across the subduction zone. Results and interpretations are as follows:

(1) In front of the northern Lesser Antilles (Antigua/Anguilla) there is no or very little sediment subduction into the mantle.

(2) The central segment (latitude of Dominica/Martinique) shows non-steady-state behaviour. Early terrigeneous sedimentation and resulting rapid growth of the accretionary wedge is followed by hemipelagic sedimentation and slow wedge growth. This effect is probably caused by the arrival of the Tiburon Rise at the subduction zone. No estimations of sediment subduction are possible.

(3) The southern segment (Grenada/Barbados) shows evidence for massive subduction of terrigeneous sediments into the Earth's mantle.

CONTRIBUTION OF PALEOMAGNETISM IN THE RELATIONS BETWEEN THE PIEMONTIN AND INTERNAL NAPPES : SYNTHESIS AND NEW DATA.

B. BLIN *, B. SICHLER **, J.F. STEPHAN ***

** : GIS "Océanologie et Géodynamique", 6 Avenue Le Gorgeu, 29287 Brest Cedex FRANCE.*
*** : IFREMER, Centre de Brest, DERO/GM, B.P. 70, F-29263 Plouzane FRANCE.*
**** : Institut Géodynamique URA 720 Université de Nice Sophia Antipolis, Parc Valrose 06034 Nice FRANCE.*

The east displacement of the caribbean plate is occuring between the two Americas by larges transcurrente zones, dextral and sinistral respectively to its south and north boundaries.This particular setting explains the 90° of clockwise rotations shown by the paleomagnetic vectors of the venezuelan caribbean Chain. With the end to define the relations between the piemontin and internal nappes of the caribbean Chain, a study was realized in 1988, 100 km to the south of Caracas in the Guárico and Cojedes States. Of the 21 sites perfored, 2 were in the internal nappe of Villa de Cura (to the north), 10 in the piemontin nappe and 9 in the autochtonous foreland (to the south).

- In agreement with the others paleomagnetic data, the Villa de Cura nappe gives evidence for 90° of clockwise rotation.
- The piemontin nappe do not show general rotation.
- The results about the foreland indicate a north-south orientation of the paleomagnetic vectors. They are according to the autochtonous character and to paleomagnetic declinations of the south-american craton.
- Nevertheless, the general north-south orientation of the paleomagnetic vectors can be deviated near the Guárico and Guaitoco faults (dextral faults).

These results, associated to the field data, confirm that the Villa de Cura nappe was a north-south oriented insular paleoarc, in agreement with the models of the caribbean geodynamic evolution proposed by different authors (Pindell and Dewey (1982), Stéphan (1982), Beck (1986)). On the contrary, the piemontin nappe did not rotate and has moved with an orientation similar to its original position. A possible flow of the piemontin unity could explain the declinations perpendicular to the front of this nappe, on which superposes the Guárico fault effect. Finally, the autochtonous oligo-miocenous sandstones, to the south of the piemontin nappe, do not show rotations excepted clockwise near the Guárico and Guaitoco dextral faults.

MUDSTONE MICROFABRICS, DEFORMATION MECHANISMS AND FLUIDS IN THE LESSER ANTILLES FOREARC.

BEHRMANN, J.H., IGL, Univ. Giessen, D-6300 Giessen, West Germany.
and
PRIOR, D.J., Dept. of Earth Sciences, Leeds University, Leeds LS2 9JT, England.

Deep ocean drilling (ODP Leg 110 and DSDP Leg 78A), extensive seismic reflection profiling and on-land structural studies, have made the Lesser Antilles Forearc one of the best constrained active accretionary wedges. Drilling at Site 671 achieved penetration of several active thrust faults, and the basal décollement zone of the accretionary wedge. We have examined in detail the microfabrics of tectonized muds in a discrete thrust at 128m, and in the basal décollement at 600m to 630m below sea floor. The thrust at 128m repeats at least 160m of stratigraphically defined rock column, constraining a total minimum displacement in the order of 600m. The fault rock comprises 6mm of mesoscopically foliated clays, bordered by undeformed wall rock. The 30m thick zone of sheared mudstones in the basal décollement at Site 671 contains a displacement in excess of 2000m.

High resolution backscattered electron images on the scanning electron microscope have been used to examine the microfabric of the forearc sediments. Clays and clasts are pervasively aligned in the immediate hangingwall to the 128m thrust. Microfabric intensity decreases upwards and the sediment is undeformed more than 6mm away from the thrust. In contrast the mudstones of Miocene age in the décollement zone have randomly aligned clays and clasts despite the evidence for significant strains from observed fold structures and balanced section inferences.

Deformation at the 128m thrust and in the basal décollement probably occurred by different mechanisms. One caused grain alignment, and one allowed accomodation of strain without grain alignment. Both are likely to be forms of particulate flow, but with contrasting grain interactions controlled by the fluid environment. The lack of grain alignment in the décollement was probably promoted by high pore fluid pressures and a cation-rich fluid which prevented development of weak clay-clay bonds by cation adsorption on clay surfaces. At higher levels, the 128m thrust for instance, such fluids may have been lost to the surface, and grain interactions were more dominant.

THE ESPINO GRABEN COMPLEX AND THE SOUTH LLANOS LINEAMENT: GRAVITY AND MAGNETIC ANOMALIES OVER A MAJOR UNEXPOSED RIFT ZONE AND MEGASHEAR IN NORTHERN SOUTH AMERICA

BONINI, W. E., Department of Geological and Geophysical Sciences, Princeton University, Princeton, New Jersey, 08544, U. S. A.

Three Mesozoic graben complexes have been identified in northern South America: Takutu in Guyana and Brazil (Crawford and others, 1985); Maracaibo (Burke, 1976) in western Venezuela; and the unexposed Espino (Smith and others, 1984) in eastern Venezuela. Similarities among them are that they are about 30-60 km wide, 4-5 km deep, several 100 km long, and contain red sediments and volcanics.

On the basis of magnetic anomalies it is proposed that the southern margin of the Espino Graben complex - the South Llanos lineament - extends for about 800 km in Venezuela and into Colombia. Interpretation of these anomalies indicates that the South Llanos lineament is a zone characterized by a series of normal faults. South of the Espino drill-hole the fault throw is down to the north, and north of the hole down to the south. The graben zone is over 100 km wide.

Analyses of gravity anomalies indicate that there is "high-density crust" just north of the Espino drill-hole. These data suggest that this portion of the crust underlying the Eastern Venezuela Basin could be related to the Mesozoic rifting event. Gravity-high closures to the southwest of the drill hole may be related to volcanics, similar to those reported in the Espino well.

The geophysical and drill-hole data place constraints on the pattern of the Mesozoic breakup of Pangea, the northern margin of the South American craton, and the development of the Caribbean plate.

LES BASSES TERRASSES CORALLIENNES DE LA GUADELOUPE : IMPLICATIONS NEOTECTONIQUES.

BONNETON J-R. (G.I.R.C.A.S.T.) Université Antilles-Guyane, BP. 592 POINTE-A-PITRE (GUADELOUPE) CEDEX

L'étude des terrasses émiennes (Inter Riss - Würn) sur les îles calcaires de l'archipel guadeloupéen permet de préciser l'histoire récente postérieure à 100.000 ans B.P. de ce secteur de l'Arc des Petites Antilles.
BATTISTINI et al (1986) ont déjà proposé pour ces récifs quaternaires émergés un âge "Eemien" à partir de critères morphologiques et de datations radiométriques.
L'analyse radiométrique des terrasses successives situées à l'extrémité Est de la GUADELOUPE (Grande-Terre) en utilisant 238 U et 232 U comme traceurs (BERNAT), suggère des périodes de haut niveau marin associées à des développements récifaux d'âge compris entre 100.000 et 160.000 ans B.P.
Aucune étude précise sur la déformation de ces niveaux de terrasses n'a été réalisée à ce jour. Ils constituent le marqueur stratigraphique daté le plus récent (≈ 100.000 ans B.P.). Leur position haute émergée, (+ 8 m pour celles de la Pointe-des-Châteaux) associée à des failles normales à rejet métrique indique un état de contrainte en distension avec des déformations en extension radiale.
Ces niveaux fournissent des déformations cassantes les plus récentes et l'âge des derniers rejets des failles. C'est ici un élément important pour l'évaluation de l'aléa sismique.
La fracturation E-W affectant les terrasses est comparable en tout point à celle de MARIE-GALANTE au Sud et à la DESIRADE à l'Est. L'analyse microtectonique pour ces secteurs montre que l'archipel est soumis actuellement et depuis le Pliocène supérieur à une extension radiale.
A MARIE-GALANTE, la faille majeure affecte les basses terrasses émiennes et les niveaux de plage supérieurs avec un rejet d'environ 100 m. Les terrasses et les niveaux de plage sont affectés par des accidents normaux E-W. Leur étude fait apparaître une extension radiale identique à celle de la GRANDE-TERRE.
La Basse Terrasse de la DESIRADE est en position haute (+ 10 m à + 4 m) Elle est surmontée par des plages émergées à galets. Des accidents récents E-W découpent et verticalisent aussi bien les plages supérieures à galets que la terrasse émienne ou les coraux et les brèches corralliennes.
L'interaction des mouvements tectoniques et des oscillations marines sont responsables de l'édification des complexes de terrasses récifales.
On a ainsi la possibilité d'estimer avec une bonne approximation la vitesse moyenne de ces déformations. Ces dernières n'ont rien de comparable avec les terrasses marines des Grandes Antilles (CUBA, HAITI, JAMAIQUE) qui culminent à plusieurs centaines de mètres au-dessus du niveau de la mer.

NOUVELLES DONNEES STRUCTURALES SUR L'ILE DE St CROIX ET DE SON ENVIRONNEMENT.

BONNETON J-R. (G.I.R.C.A.S.T.) Université Antilles-Guyane, BP.592 POINTE-A-PITRE (GUADELOUPE) CEDEX

L'Arc des Petites Antilles se termine par la plateforme d'ANGUILLA - St MARTIN - SOMBRERO. Le passage d'ANEGADA marque le passage aux Grandes Antilles. Il se prolonge par le bassin des Iles Vierges entre VIEQUES et St CROIX. L'île de St CROIX occupe une position excentrée dans ce contexte. La transition Grandes-Antilles - Petites Antilles est marquée par une évolution spatio-temporelle du magmatisme liée à une tectonique polyphasée : l'une d'âge postérieur au Sénonien-Paléogène, l'autre évoluant au Mio-Pliocène.
Les travaux de (BONNETON et BECK, 1987) ont permis de mettre en évidence deux sites fossilifères à Rudistes du Sénonien supérieur (Campanien sup. à Maestrichien) à ISAAC POINT, en plus de ceux mentionnés par WHETTEN (1966) et ANDREIFF et al (1986).
On a donc un âge Sénonien pour toute la moitié orientale de l'île et la possibilité d'un âge Cénomanien dans ce secteur (SPEED 1979) est rejeté. Le secteur NW de l'île (Hamms-Bluff, Springfield, St Georges) a révélé des localités très riches en microfaunes. Ces niveaux sont apparemment en continuité avec la partie Est de l'île avec un passage à Judith Fancy.
D'un point de vue structural on assiste à un basculement généralisé des axes de plis synchisteux tant à l'Ouest qu'à l'Est. Dans la partie occidentale on a de grands cisaillements plats qui ne peuvent en aucun cas être interprétés comme des charriages. Les études microtectoniques montrent plutôt un régime en extension radiale E-W. de part et d'autre du graben central. A l'Est de l'île la tectonique polyphasée y est plus nette. Un régime en extension donne des failles normales associées à des décrochements en compression.
Les séries du Crétacé supérieur-Paléogène tectonisées de St CROIX ont joué en compression (N-S à vergence Nord) comme à TORTOLA mais l'édifice a également fonctionné en distension. L'âge de certains dykes de St CROIX (H. BELLON) serait Eocène supérieur, ce qui placerait une première phase tectonique distensive entre l'Eocène moyen et la base de l'Oligocène.
Plus à l'Est à St MARTIN. Les accidents E-W sont localement décrochants dextres avec des conjugués à SW-NE. Le Miocène supérieur est affecté par une extension radiale pure SW-NE associée à ces décrochements.
De part et d'autre du fossé d'ANEGADA on a des séries paléogènes très peu déformées (St MARTIN, ANGUILLA, CULEBRA). Des séries du Crétacé supérieur Paléogène très tectonisées témoins d'un édifice soumis à une tectonique polyphasée : un régime compressif N-S à SW-NE associé à un régime distensif débutant à l'Eocène moyen et se poursuivant jusqu'au Mio-Pliocène (St CROIX et TORTOLA). Conséquences des coulissages E-W déjà signalés à St THOMAS.

EL MELANGE OFIOLITICO DE HOLGUIN (CUBA NORORIENTAL) Y SU SIGNIFICADO TECTONICO

BEBZSENYÁNSZKY, K.
Oficina Central de Geología, Budapest, Hungría.

El área investigada forma parte del cinturón ofiolítico de Cuba septentrional. Aquí, aflora el contacto entre el margen continental mesozoico norteamericano, representado por la Plataforma de Bahamas y la zona de melange - ofiolítico que actualmente se encuentra en posición alóctona, sobreocorrida sobre el margen continental. El término de "melange" se utiliza según el concepto de Hsü - (1968).

Entre los componentes constitutivos principales del melange, se reconocen fragmentos de tres unidades paleotectónicas del mesozoico tardío: banco carbonatado del margen continental y de su basamento siálico metamorfizado, fragmentos de una asociación ofiolítica completa del fondo oceánico incluyendo sus bloques metamorfizados, y -- fragmentos de un arco volcánico maduro.

La edad de la formación más joven, constituyente del melange, es Eoceno temprano. La cobertura postorogénica - se caracteriza por sedimentos terrígenos del Paleógeno - tardío, mientras el Neógeno se destaca por el predominio de rocas carbonatadas.

Dentro del melange se diferencian mantos de corrimientos con estructura interna frecuentemente escamada, dirigida - con pocas variaciones hacia el Norte. El manto inferior - contacta directamente con el melange continental, mientras los superiores lo sobreyacen tectónicamente.

Las características del melange indican un desarrollo - continuo de la colisión, hasta el cierre gradual de la cuenca suboceánica ubicada entre el margen continental y el arco volcánico. Los momentos culminantes del desarrollo son: cese del vulcanismo en el Campaniano Superior, formación de olistostromas en el Paleoceno y la - conclusión del avance de los mantos de corrimientos en el Eoceno Medio.

El análisis formacional y facial de las rocas componentes del melange, permite la reconstrucción esquemática de la situación paleogeográfica anterior a la colisión, del Cretácico tardío (de Norte a Sur): margen continental pasivo fallado, subcuenca oceánica remanente parcialmente consumida, zona de subducción con buzamiento hacia el - Sur, cuenca de antearco, arco volcánico.

MANIFESTACIONES DEL DIAPIRISMO ARCILLOSO EN EL MARGEN COLOMBIANO DEL CARIBE

Briceño, L.A[1]. Vernette, G[2], Perez R[1]., Geyet J.[2]

RESUMEN.

Utilizando cañones de agua y ecosondas de 3,5 KHz, se tomaron nueve perfiles sísmicos que cubren aproximadamente 1,500 km lineales de información. Se observan variadas manifestaciones del diapirismo arcilloso, que se han clasificado en abombamientos, domos, volcanes, pliegues y plumas diapíricas. Domos y pliegues se encuentran especialmente al sur de la latitud 10°30', y corresponden a movimientos de masas de gran extensión, alcanzado hasta más de 2 s t.d. de espesor ; hecho este que consideramos como el modificador principal de la morfología del margen de este sector. Los volcanes, generalmente situados en la cumbre de domos y pliegues representan la expresión actual del diapirismo a través de los cuales se expulsan tanto arcilla, como fluidos (agua y metano). Las plumas, a diferencia de las otras manifestaciones, en general, no deforman las capas intruidas y su presencia está limitada a la zona de plataforma, hacia el norte de la latitud mencionada, definiendo así dos áreas claramente diferenciables, tanto desde el punto de vista morfológico como sedimentológico y structural.

[1]Universidad Nacional de Colombia, Departamento de Geociencias, A.A. 14490, Bogotá, Colombia.
[2]Université de Bordeaux, Département de Géologie et Océanographie, Av. des facultés, 33405 Talence, France.

GEOLOGICAL SETTING OF SOME POLYMETALLIC MASSIVE SULFIDE OCCURRENCES IN THE MEDIAN BELT, CENTRAL DOMINICAN REPUBLIC

BROUWER, S.B., MACVEIGH, J.G., ESPAILLAT, J., JIMENEZ, J., PIZANO, O., Falconbridge Dominicana C por A., Dominican Republic and Falconbridge Ltd., Canada

The Median Belt, 185 km in length, of mainly metamorphic and mafic volcanic rocks of Cretaceous and possible pre-Cretaceous age, flanks the east and north edge of the Cordillera Central in the Dominican Republic, and contains several polymetallic massive sulfide occurrences. Some of these occurrences are being evaluated by Falconbridge Dominicana, Falconbridge Ltd and Recursos del Caribe S.A. Three occurrences have been selected to show the diverse characteristics and distinct geological environments.

The Sabana Potrero copper prospect is hosted by mafic volcanic rocks (mainly pillow lavas) of the Peralvillo Formation of Late Cretaceous age, at the northeast contact of the Median Belt peridotite. It consists of lenses of fine-grained copper rich massive pyrite which are structurally overlain by a quartz-sulfide stockwork and complexly intruded by mafic rocks.

The Cerro de Maimon deposit contains 2.9 million metric tons of sulfide ore grading 4.06% Cu, 0.07% Pb, 1.83% Zn, 44.9gm Ag/t, 0.47gm Au/t. It is associated with Early or pre-Cretaceous felsic meta-volcanic rocks of the Maimon Formation near the contact with rocks of the Peralvillo Formation. The massive sulfide body is conformable with the enclosing rocks and structurally underlain by an extensive zone of pyritic quartz-sericite rock.

The Amina Formation considered to be the stratigraphic equivalent of the Maimon Formation hosts the El Anon massive sulfide prospect in the northwestern Dominican Republic. The copper-zinc rich massive sulfides are localized within a narrow, four km long belt of pyritic quartz - sericite (chlorite) schists, and fine felsic meta-volcaniclastic rocks. The adjacent rocks are principally laminated and banded mafic meta-volcaniclastic rocks with thin to thick felsic interlayers.

The stratigraphic settings, distribution and types of alteration and mineralization, and metal zoning support a volcanic exhalative origin for the sulfide occurrences and highlights the potential for a diversity of deposit types in a variety of volcanic-tectonic environments.

TECTONIC ESCAPE IN THE EVOLUTION OF THE CARIBBEAN

Burke, K., and Rutherford, E., Dept. of Geosciences, The University of Houston, Houston, Texas.

In tectonic escape, material is displaced laterally from a region of high stress to a region of lower stress. Areas of high stress are usually associated with convergent plate margins and continental collision zones, and areas of low stress state generally involve oceanic free faces. Escape has lately been shown to be a significant factor in the evolution of major orogenic systems, as well as an important control in modifying local geologic relationships. Caribbean plate boundary zones are currently being modified by tectonic escape, and escape has been important at various stages of Caribbean plate evolution.

The best known area of active escape occurs in Colombia and Venezuela and involves the northward motion of the Maracaibo block and related fragments as a result of the collision of Panama with northwestern South America. The net regional displacement due to escape, as well as differential motion between individual fragments, is accommodated by a complex system of strike-slip faults. Displacements on the larger strike-slip faults, for example the Santa Marta and Bocono faults, range to approximately 100 km. The free face to this system lies in the Venezuelan Basin, where it is associated with a broad thrust belt related to the net convergence between the Maracaibo block and the Caribbean plate. Where the southern strike-slip margin of the Caribbean and the escape system meet, South American material carried northward is being sliced off and redistributed to the east along the plate boundary zone.

Tectonic escape appears also to be occurring in the northeastern Caribbean, to the east of Puerto Rico. This area, including the eastern Greater Antilles and northern end of the Lesser Antillean accretionary prism, is in transit from a confined state to an unconfined state as it passes the Bahamas Platform. To the west of this area secondary structures reflect east-west trending strike-slip motion. Past the transition, however, a northeast-southwest trending extensional strike-slip system accommodates northward escape toward a free face in the Atlantic.

A more complex example of Caribbean tectonic escape is discernable in the western tip of Cuba, and is related to the Paleogene collision between the Caribbean plate and the Bahamas platform. Along the northernmost part of the plate boundary, between Cuba and Florida, suitable conditions developed for tectonic escape out of the collision zone and into the Gulf of Mexico. A group of strike-slip faults in western Cuba may represent a part of the escape system.

Modeling sediment compactional response to lateral stress in the Barbados Ridge Complex

W. Brückmann, GEOMAR - Research Center for Marine Geosciences, Wischhofstr. 1-3, 2300 Kiel, W. Germany

The impact of lateral stress on mechanical diagenesis of marine sediments was studied using Deep Sea Drilling Project (DSDP) and Ocean Drilling Project (ODP) sediment physical property data.

A statistical evaluation of the Deep Sea Drilling Project (DSDP) sedimentological and mass physical property database (Legs 1-96) yielded functions for the depth dependent compactional behavior of a set of standard sediment types. These "typecurves" are well constrained for mainly pelitic and psammitic sediments of moderate carbonate content. They are employed as a reference tool for the quantification of tectonically induced consolidation in the Barbados Ridge accretionary wedge.

Based on the developed typecurves and sediment physical property data from DSDP- and ODP legs 78A and 110 (Barbados Ridge) as well, a simple palinkinetic reconstruction procedure was employed to determine porosity changes during accretion. Palinspastically removing the compactional effects of burial diagenesis caused by imbricate stacking of wedge slices, a synthetic preaccretion porosity vs. depth profile could be modelled, which bears strong resemblence to characteristic profiles from 2 reference drill holes in front of the accretionary wedge (sites 543 and 672).

Comparison of synthetic and reference profiles reveals a lithologically controlled exponential relationship between depth and porosity divergence. Reevaluation of the reconstruction procedure in terms of involved stresses yielded a semiquantitative estimate of the relative and absolute impact of the lateral stress component on sediment consolidation in this part of the convergent plate margin.

This semiquantitative definition of compactional response to the lateral stress component provides an important constraint for further modeling of deformational behavior of accreted sediments.

PRE-HOLOCENE SURFACE CONTROL ON HOLOCENE BANK BARRIER REEF DEVELOPMENT, ST. CROIX, U.S. V.I.

BURKE, R. B., North Dakota Geological Survey, P.O. Box 8156, Grand Forks, ND 58202-8156, USA; ADEY, W. H., National Museum of Natural History, Smithsonian Inst., Washington D.C. 20560, USA; MACINTYRE, I. G., National Museum of Natural History, Smithsonian Inst., Washington D.C. 20560, USA; and STUCKENRATH, R., Smithsonian Environmental Res. Cntr., Rockville, MD 20852, USA.

An E-W series of 16 cores drilled along 2.5 km of the reef crest parallel to shore shows the pre-Holocene surface (PHS) dips east (1m/km). In a N-S transect perpendicular to shore, 10 cores showed the PHS dips more gently to the north except at a depth of -8.5m MSL where a 4m bench occurs locally. In the context of Holocene sea level dynamics and consequences, both the easterly dipping shelf and the bench influenced the timing, location, and the development style of the structural facies forming the reef. Fourteen radiocarbon dates show the reef first reached sea level 1455 YBP, near the center of the reef, not reaching sea level to the west until the present, and to the east from 120 to 803 YBP. The large structural elements in the reef cores first appeared 6135 YBP and form the thickest patch reef facies in the center of the reef, whereas rubble and sand increased to both the east and west. The seaward position of the reef is locally determined by the bench. Facies distribution indicates the reef developed as a series of patch reefs aligned parallel to the shore that coalesced into a continuous barrier. Patch reefs reaching sea level prograded seaward.

EPOCAS METALOGENICAS DE CUBA

CABRERA, R., STANEK, P., LAVANDERO, R., FORMELL, F.
Instituto de Geología y Paleontología, MINBAS, Cuba

Las Epocas Metalogénicas (EM) que fieron origen a los principales grupos formacionales de yacimientos minerales de Cuba se determinan en vinculación histórico-geológica durante el proceso de formación de la isla. Para esto se acepta la formación del Caribe a partir del fraccionamiento del Pangea y el desarrollo de una riftogénesis durante el Mesozoico Temprano con la formación sincrónica de los Márgenes Continentales (MC) y la Corteza Oceánica (CO), durante el Jurásico-Cretácico Temprano, seguida con el régimen de Arco Insular (AI) (en dos edades) K y Pg y la deposición del complejo de cobertura a partir del Oligoceno.

Con el régimen riftogénico se desarrolla la primera EM durante el Jurásico Tardío y Cretácico Inferior con la deposición de los yacimientos sulfurosos en el MC pasivo y probablemente la formación de las segregaciones de cromitas en la base de las ofiolitas. Con el complejo del lecho oceánico se asocia los yacimientos de Cu.

Una segunda EM se vincula al régimen de AI Cretácico donde se formaron yacimientos de Cu, Cu-Zn y Pb-Zn. Al final de este período y en relación con las intrusiones de granitoides se formaron yacimientos de Fe-skarn, Cu-Mo y Au.

Durante el Paleógeno relacionado con el AI de esta edad, se desarrollaron los yacimientos de Cu, Pb-Zn y manganeso vinculado al complejo sedimentario. Durante el Eoceno Medio vinculados a la penetración de las intrusiones de granitoides, se formaron yacimientos de Fe-skarn, Cu y Cu-Mo.

Como indicaciones de una EM, todavía poco fundamentado, con poca importancia regional, aparecen las mineralizaciones sulfurosas superpuestas en el Cenozoico.

La EM más reciente se relaciona con los yacimientos surgidos a partir de la acción supergénica sobre los complejos rocosos formados, dando lugar a la formación de yacimientos de Ni-Co-Fe, Fe y Al.

THE CHORTIS BLOCK IS AN OCEANIC MESOZOIC TERRANE

MARIA FERNANDA CAMPA
UNIVERSIDAD AUTONOMA DE GUERRERO
APARTADO POSTAL NO. 197
TAXCO, GRO.
MEXICO

GUSTAVO A. ALTAMIRANO
INMINE-EXPLORACION
APARTADO POSTAL P-105
MANAGUA, NICARAGUA

WE RECOGNIZED AT PRESENT, BELOW THE LATE CENOZOIC CONTINENTAL VOLCANIC ROCKS AND MARINE SEDIMENTS, A COMPLEX FOLDED AND FOLIATED ASSEMBLAGE OF LIMESTONE, SHALE, SLATE, CUARCITE GREWVACKE, TUFF, ANDESITE, DIABASE, SERPENTINE AND OTHER ULTRABASIC ROCKS WHICH CAN BE INTERPRETED LIKE FRAGMENTS OF A LATE MESOZOIC AND EARLY CENOZOIC VOLCANIC ISLAND ARCS AND OCEANIC CRUST.

IN BOTH CRUSTAL PLAINS, SEVERAL WELLS HAVE BEEN DRILLED, SOME OF THEM CONFIRM THE OCEANIC NATURE OF THE BASEMENT. THE CRUSTAL THICKNESS HAVE BEEN ESTIMATED FROM 25 TO 40 KM. AND SEISMIC VELOCITIES INDICATE AN OCEANIC TO INTERMEDIATE CRUST. THE CHORTIS BLOCK AT PRESENT IS MAINLY A COMPOSITE TERRANE SIMILAR OF THOSE OF THE SIERRA MADRE DEL SUR IN MEXICO, THE GREATER ANTILLAS, COSTA RICA AND PANAMA, PROBABLY FRAGMENTS OF A LATE MESOZOIC VOLCANIC-ISLAND ARC AND OCEANIC CRUST SUPRATERRANE ORIGINATE IN THE PANTHALASSA.

IT WAS FOLDED AND INTRUDED BY GRANITE PLUTONS DURING LATE CRETACEUS AND EARLY CENOZOIC SIMILAR TO THOSE OF THE AMERICAN THRUST BELT FORMED DURING THE MAJOR PACIFIC ACRETIONS. THIS OCEANIC MESOZOIC BASEMENT WAS OVERLAPED BY ISLAND ARC ASSEMBLAGES LATE CENOZOIC IN THE PRESENT PACIFIC RANGES, CONTINENTAL VOLCANIC IGNIMBRITES IN THE CENTRAL CORDILLERA AND DELTAIC WEDGE AND CARBONATES IN THE ATLANTIC PLAIN AND SHELF. THE ACTIVE TECTONIC HAVE BEEN BROKEN THE AREA ORIGINATING THE CHORTIS-NICARAGUA ACTIVE PLATE.

GEOMETRY AND TECTONIC REGIME ALONG A MAJOR STRIKE-SLIP FAULT : THE NORTHERN CARIBBEAN TRANSCURRENT PLATE BOUNDARY FROM CUBA TO HISPANIOLA, GREATER ANTILLES (73°W to 77°W)

Eric CALAIS[1], Bernard MERCIER de LEPINAY[1] and Vincent RENARD

Marine geophysical surveys using *Seabeam*, single-channel seismic reflection, gravimetric and magnetic measurements were undertaken along the Northern Caribbean transcurrent plate boundary during the SEACARIB II cruise (R/V Jean-Charcot, 16/11-23/12/1987).
One of the main goals was to explore a poorly-know segment of this plate boundary, located from Cuba to Hispaniola (73°W to 77°W). The collected data alow to better define the geometry and the tectonic regime of this mainly strike-slip area. They support the following results :

1. concerning the tectonic regime along the plate boundary :
a. the eastern part of the Oriente Deep and the Santiago promontory are characterized by **an active compressional tectonics**. We call therefore this area the "Santiago Deformed Belt" extending from 76°40'W to 73°50'W with an east-west general trend. This deformed belt can be longitudinaly divided in three main segments, each one characterized by a particular tectonic style. Its structuration can be related to a **transpressional mechanism** ;
b. in the Windward Passage, the **Saint Nicolas Basin** is a rectangular depression bounded to the south and to the north by normal east-west trending faults. We demonstrate that **it cannot be interpreted as an active pull apart basin**, as done previously.

2. concerning the geometry of the plate boundary :
a. along the southern cuban margin, the **Oriente fault displays a discontinuous trace**. It is composed of at least three main *en relais* segment ;
b. through the Windward Passage this major fault cannot be connected to the subduction front of the atlantic oceanic lithosphere under Puerto Rico and Hispaniola. On the contrary, **it continues eastward on land, into the Cibao Valley in Hispaniola**. Thus, we have for the first time the structural evidence of this connection, as it has been suspected from seismologic data. The Northern Caribbean plate boundary displays therefore a strike-slip/subduction association. Such a structural arrangement is similar to other regions of the wordl such as Sumatra, Andaman, New-Zealand and Philippines.

Our data strongly suggest that a tectonic and kinematic reorganisation recently occured in this area. In comparison with the geological events recorded on land in the Northern Caribbean domain, we can propose a plio-quaternary age for this reorganisation.

1. Institut de Géodynamique, CNRS Sophia Antipolis 1, Bât.3, rue Albert Einstein, 06560 VALBONNE - FRANCE

THE IMPORTANCE OF THE 1988 TREMORS, JAMAICA: A DISASTER MANAGEMENT PERSPECTIVE

CARBY, R.E., Office of Disaster Preparedness,
12 Camp Road, Kingston 4, Jamaica

During 1988 three tremors of magnitude greater than 4.0 affected Jamaica. In addition, many smaller tremors were felt and reported by the public. The three larger shocks were the heaviest felt since the 1957 earthquake (MMI VIII - IX) and provided the opportunity to gather data invaluable to pre-disaster planning and post-disaster response.

Unfortunately, the seismological value of these small earthquakes was lessened by the lack of adequate monitoring and recording equipment at the Seismic Research Unit. They did, however, produce other "positive" results including heightened public awareness of the earthquake hazard and the opportunity for the Office of Disaster Preparedness to assess public reaction and thus indirectly, the effectiveness of its public awareness programme.

This paper discusses the importance of the data gathered and the implications of the lost seismological data.

AGE AND STRATIGRAPHIC STATUS OF THE PALMISTE FORMATION, TRINIDAD, WEST INDIES.

CARR-BROWN, B., Trinidad and Tobago Oil Company, Ltd., Pointe-a-Pierre, Trinidad and Tobago, and
YOUNG-ON, V., Trinidad and Tobago Petroleum Company, Ltd., Santa Flora, Trinidad and Tobago.

The Palmiste Formation has appeared as a stratigraphic unit in publications and internal company reports since 1968, but in the absence of its formal definition confusion exists concerning its age, stratigraphic status, criteria for its recognition and limits of its development.

Onshore, the Palmiste Formation is represented by the Palmiste Clay Member of Kugler (1959) which is developed along the Atlantic coast of the Island between Radix Point and Guayaguayare Bay and has a maximum apparent stratigraphic thickness of more than 1,000 feet. It is separated unconformably from the underlying Mayaro Formation and overlying Quaternary deposits from which it is readily distinguished lithologically and palaeontologically. Between 1966-1968, diagnostic planktic foraminiferal faunas of post-Middle Miocene age were recognised for the first time in Trinidad in samples recovered from the Palmiste Clay and an Early Pliocene **Globorotalia margaritae Zone** age is assigned to the unit on the presence of the zonal marker.

The beds of the Palmiste Formation dip 5° - 35° south beneath Guayaguayare Bay and east to south-east beneath the Atlantic Shelf off Mayaro Bay where the formation is identified with a predominantly clay/shale interval encountered in well Palmiste-2. The interval exceeds 3,000 feet in apparent stratigraphic thickness and can be related to a characteristic seismic stratigraphic sequence observed on seismic data coverage in the area. The offshore unit appears to be restricted between the offshore extensions of the Southern Range and the Naparima-Nariva Thrust Belt, and its eastern limits appear to be fault bounded by a major N-S normal fault which exhibits some component of left-lateral slip. The sequence is assigned an Early Pliocene to possibly Late Pliocene age on planktic foraminifera.

So far correlation with the Late Pliocene Palmiste Formation of Leonard (1983) is not evident. The onshore sequence exhibits onlap westwards and the offshore sequence exhibits onlap relationships along its northern and southern boundaries. From these and other relationships, the Palmiste Formation appears to have been deposited in an arealy restricted sub-basin formed as a result of the onset of uplift in the Galeota area of the Southern Range during the Pliocene. More recent tectonic movements emanating southwards from the Naparima -Nariva Thrust Belt have uplifted the offshore Palmiste Anticline and the Palmiste Formation may have been locally removed by erosion. Uplift of the coastal area has resulted in extensive removal of the onshore sequence.

INTERPRETATION OF GRAVITY ANOMALIES, MASAYA CALDERA COMPLEX, NICARAGUA

Connor, C.B., Dept. of Geology, Florida International University, Miami FL, 33199, USA.
Williams, S.N., Dept. of Geology, Louisiana State University, Baton Rouge LA, 70803, USA.

The Masaya caldera complex, Nicaragua, has been the site of at least two Plinian eruptions in the Quaternary and remains active today. We have interpreted gravity data collected during a regional gravity study by Williams (1972) in an effort to further delineate geologic structures associated with this major volcanic feature. A total of 217 gravity stations were occupied in the vicinity of Masaya caldera. These data were reduced to the complete Bouguer anomaly by Williams (1972). We contoured these data over an area of approximately 25 x 15 km, centered on the caldera, using a minimum curvature algorithm. Several large amplitude gravity anomalies are apparent on this map. These include a broad +35 mgal high on the NE side of Masaya caldera, and a locally steep gradient within the caldera, just NW of the active Santiago vent.

Upward continuation to 1500 m has the effect of isolating the broad positive gravity anomaly. The aspect of this large, positive gravity anomaly is like that of Masaya caldera itself: elongate approximately N60W, parallel to the strike of the Nicaragua Depression. Near surface, local anomalies were isolated by wavelength filtering. A high -pass, ramped filter was constructed such that anomalies at wavelengths longer than approximately 6 km are strongly attenuated. Of note is a negative anomaly, located immediately NW of the Santiago Crater. Although the true extent and amplitude of this anomaly cannot be determined from the data, its presence suggests mass deficiency, spatially associated with the active craters on the caldera floor.

We created a two-dimensional gravity model along a NW -striking traverse, bisecting the large positive anomaly. No surface geologic contacts or discontinuities are associated with the broad positive gravity anomaly and it is modeled as a completely buried anomalous mass. Regional faults, associated with the Nicaragua Depression, can be interpolated through Masaya caldera. Although there is no vertical displacement of rocks due to regional faults within the caldera, the presence of strong N60W oriented structures is suggested by the alignments of vents on the caldera floor and the distribution of soil geochemical anomalies within the caldera. These regional faults may affect gravity gradients, but their affect on the NW -striking profile is minimal. The key elements of the model are a high density contrast, 300 to 500 kg/m^3, and the thin, plate -like geometry of the anomalous mass. This plate is 15 km long, approximately 0.75 - 1.0 km thick, and buried at a depth 0.1 - 0.6 km. A contact dipping away from the center of the anomalous mass is required. We believe this anomaly is likely of igneous origin. The geometry of the causative body suggests that it is either and igneous intrusion, possibly a laccolith or sill, or a series of lavas, which have accumulated to substantial thickness over a limited area. The presence and extent of this anomaly is indicative of the complex volcanic history of this caldera.

Williams, R.L., 1972, The geology of western Nicaragua: Tax improvement and natural resources inventory project, Final Technical Report, v. 4, Managua, Nicaragua.

TECTONIC STYLE AND DEEP CRUSTAL STRUCTURE OF THE EASTERN CORDILLERA (COLOMBIA) FROM A BALANCED CROSS SECTION

B. COLLETTA, J. LETOUZEY, J.L. RUKDIEWICZ, IFP, BP 311, 92506 Rueil-Malmaison Cedex.
Ph. WERNER, F. HEBRARD, TOTAL, Cedex 47, 92069 Paris La Défense.

An E-W transect across the Eastern Cordillera from Yopal in the Llanos Province to Puerto Berrio in the Middle Magdalena Valley has been built using both subsurface and field data. It resulted in a balanced cross section well constrained in Mesozoic and Cenozoic series. The tectonic style in these levels is mostly controlled by low angle thrusting and decollement in the Cretaceous levels. The Cordillera is an assymetrical thrust belt with east-verging faults along most of the transect. West verging structures are restricted to a 50 km wide belt near the eastern border of the Cordillera.

The shortening, estimated through the restoration of the Cretaceous levels to their pre-Neogene state, amounts to 150 km.

An attempt to constraint the deep crustal structure was made through gravity modelling. The assymetry of the Cordillera and its deep structure supports a westverging continental subduction.

CARACTERISTICAS SISMOLOGICAS ASOCIADAS A LA ERUPCION PAROXISMAL DEL VOLCAN NEVADO DEL RUIZ - COLOMBIA

CORAL GOMEZ, Carlos E. - Universidad Nacional de Colombia, Departamento de Geociencias- Apartado Aéreo 14490 Bogotá, Colombia.

CUELLAR RODRIGUEZ, Jairo Y. - Red Sísmica Nacional de Colombia-INGEOMINAS Apartado Aéreo 4865 - Bogotá, Colombia

RESUMEN

Se analizan las principales características de los eventos sísmicos asociados al Volcán Nevado del Ruiz durante 1985 y 1986, como son la magnitud local, el parámetro b, energía liberada, tipo de sismicidad y su comportamiento en el tiempo y el espacio, el mecanismo focal, momento sísmico, tamaño de la ruptura y valor de los esfuerzos liberados.

Se propone la utilización de las fórmulas empíricas para la magnitud de M: 2.82 Log (+) - 246 para los eventos de alta frecuencia (mayores o igual a 4 Hz), llamados tipo A y M = 2.82 Log(t) - 2.34 para sismos de baja frecuencia (menores a 4 Hz), llamados tipo B, los cuales se ajustan mejor a los rangos de magnitud observados en el Nevado del Ruiz. Del análisis de las variaciones del parámetro "b" para los sismos Tipo A y Tipo B parecen estar correlacionados y muestran un incremento de sismos de baja frecuencia de relativa mayor magnitud cuando crece el número relativo de sismos de alta frecuencia de menor magnitud.

Por medio de la acumulación de sismos en el tiempo se establecen tres fases características en cada episodio de actividad volcánica que culmina con uno u otro evento volcánico de importancia. Se nota una disminución de la actividad sísmica y energía sísmica liberada que precede cada erupción. El análisis de estos resultados nos permiten suponer que la disminución en la liberación de la energía sísmica conlleva a un incremento en la energía de deformación del volcán antes de la erupción.

Aunque el estudio de los parámetros focales aún está desarrollándose hemos logrado observar valores muy bajos del momento sísmico, del orden de 10^{17} dinas x cm, radios promedios de ruptura de 0.4 km y valores supremamente bajos de caída de esfuerzos (10^{-3} bares), que parecen aumentar en un orden de magnitud varios días antes de la erupción del 13 de noviembre de 1985.

PARTICULARIDADE GEOLOGO-GEOQUIMICAS DEL ARCO VOLCANICO PALEOGENO Y SU APLICACION EN EL PRONOSTICO METALOGENICO

G. CORREA, M. PEREZ, D. GARCIA, J. L. GUTIERREZ, E./ DUANY, L. PEREZ (Instituto de Geologia y Paleontologia del MINBAS, Cuba).

En el Mapa de Anomalías Geoquímicas de Cuba a escala 1:500 000 se detectaron en la región de la Sierra Maestra 16 anomaliass obtenidas por flujos de dispersión, aureolas secundarias de dispersión en los depositos friables y por aureolas primarias. Estas anomaliass estan relacionadas con mineralización menifera de yacimientos conocidos, manifestaciones o puntos de mineralización.

Hemos asumido que la Sierra Maestra se divide en seis bloques neotectónicos, de oeste a este: Marea del Portillo, Infierno, Turquino, La Bayamesa, El Jobo y Gran Piedra. Estos bloques presentan un desplazamiento vertical de diferente magnitud, presentando por tanto diferente profundidad del corte de erosión.

El Bloque El Jobo es muy conocido pues en el se encuentra el yacimiento El Cobre, así como una serie de manifestaciones de interés. Los bloques Infierno y La Bayamesa presentan carácteristicas similares en cuanto a la disposición de las anomalías en forma de anillo siguiendo las estructuras circulares vulcano-plutónicas. En el bloque La Bayamesa la composición de las anomalías tambien es carácteristica para la mineralización de Cobre-Polimetalico, y en la parte central de la estructura circular es tipica para la mineralización cuprifera relacionada con el intrusivo Guama Sur-Bayamita. Entre estos dos bloques se encuentra el bloque Turquino que es el más elevado de toda la Sierra Maestra, y el menos perspectivo. El bloque Marea del Portillo, es el más occidental de la cordillera, el menos erosionado, y presenta anomalías geoquímicas que pudieran estar relacionas con la manifestación Marea del Portillo conocida en ese lugar. Se indica una probable mineralización ciega en profundidad. El bloque Gran Piedra es el más oriental de la sierra, al este del cual aflora el intrusivo Daiquirí. Las anomalías que se manifiestan tienen las particularidades de la mineralización de cobre polimetalico; controlados por un sistema de fallas, que en ocasiones guardan relación con los yacimientos de Hierro de tipo skarn magnétiticos.

CATALOGO DE LOS MOLUSCOS FOSILES DEL NEOGENO-CUATERNARIO DE CUBA.

ALFREDO DE LA TORRE Y ERNESTINA PEREZ

Instituto de Geología y Paleontología
Calzada #851 Esquina A & 4, Vedado 4, Plaza de la Revolucion
La Habana, CUBA

Se presenta una versión resumida del catálogo de los moluscos fósiles del Neógeno-Cuaternario de Cuba, preparado sobre la base de las colecciones formadas durante años por el autor, así como por los fósiles colectados en los trabajos de levantamiento geológico realizados en el Instituto de Geología y Paleontología. Este constituye el primer aporte (descontando el trabajo de N. FERNANDEZ DE CASTRO de 1876 que nunca llegó a publicarse) que reune información sobre la totalidad de la fauna estudiada, ya que existen muy pocos trabajos anteriores sobre la materia, mayormente desactualizados y que hacen referencia solo a algunas especies pero no a la totalidad de la fauna. Este trabajo incluye reseña histórica, bibliografía más importante, relación taxonómica de especies, subespecies y taxones supraespecíficos representados, con información resumida de autor, fecha de publicación original, de cada especie, subespecie, género o subgénero así como distribución geográfica y estratigráfica, sinonimia mas importante e índice alfabético de especies y subespecies así como algún otro dato que consideramos de especial interés. La pobre preservación de los ejemplares colectados en los estratos del Neógeno cubano constituye una de las razones que explican la escasez de trabajos existentes sobre el tema.

La utilidad práctica de este catálogo es grande para su uso por geólogos y paleontólogos en la determinación rápida de edades de muchas muestras sin recurrir a estudio micropaleontológico. Por otra parte, la reunificación de datos dispersos en gran número de publicaciones, muchas veces antiguas e inasequibles uy la fundamentación del trabajo, principalmente, en el estudio de muestras colectadas dan a este aporte valor científico y teórico.

LA ERUPCION PAROXISMAL DEL VOLCAN NEVADO DEL RUIZ - COLOMBIA

CUELLAR RODRIGUEZ, Jairo V.-Red Sísmica Nacional de Colombia, INGEOMINAS-Apartado Aéreo 4865 - Bogotá, Colombia

CORAL GOMEZ, Carlos E. - Universidad Nacional de Colombia, Departamento de Geociencias - Apartado Aéreo 14490 Bogotá, Colombia.

RESUMEN

Con base en la sistematización de la información geológica se presenta un cuadro general y actualizado del área volcánica conocida como el Parque Natural de los Nevados.

El Nevado del Ruiz es uno de los volcanes del Parque Natural de los Nevados construido en dos etapas: volcán moderno (hace 500.000 años) y volcán antiguo (desde hace un millón de años).

En base a resultados publicados y observaciones propias, se describe un esquema del proceso eruptivo del Nevado del Ruiz. El presente ciclo eruptivo muestra varias etapas de actividad que se definen según el carácter con que se han desarrollado los eventos volcánicos. Estas etapas son: etapa pre-eruptiva, etapa eruptiva preparoxismal, erupción paroxismal y etapa eruptiva post-paroxismal.

La etapa eruptiva parece culminar el 22 de diciembre de 1984, fecha en que ocurrió una serie de temblores de tierra debajo del volcán que dan lugar al inicio de la etapa eruptiva preparoxismal, la cual se prolonga hasta el 13 de noviembre de 1985, cuando se presentó la erupción paroxismal que causó la muerte a cerca de 25.000 personas y pérdidas materiales avaluadas en miles de millones de pesos. A partir del 14 de noviembre de 1985, se inicia la etapa postparoxismal, en la cual se han presentado varios máximos de actividad volcánica, en su mayoría acompañados por extensión de cenizas.

DESCRIPCION DE TRES NUEVOS TAXONES SUBESPECIFICOS DE MOLUSCOS DE LA ETAPA PLIOCENO-CUATERNARIA DE CUBA.

ALFREDO DE LA TORRE Y ERNESTINA PEREZ

Instituto de Geología y Paleontología
Calzada #851 Esquina A & 4, Vedado 4, Plaza de la Revolucion
La Habana, CUBA

En el presente trabajo se ofrece la descripción de tres nuevas formas de moluscos fósiles del Plioceno-Cuaternario de Cuba, las cuales son importantes desde el punto de viste estratigráfico, por lo que la publicación de dichos taxones permitirá su utilización en trabajos bioestratigráficos en nuestro país y en el área correspondiente a la Paleo-Provincia Faunal Malacológica Caribeña, establecida por WOODRING (1965; 1974) para el Mioceno y extendida más tarde por KOJUMDGIEVA y A. de la TORRE (1980) y A. de la TORRE y KOJUMDGIEVA (1985) hasta el Plioceno y existiendo probablemente desde el Eoceno Medio. Se hace referencia asimismo a otras especies asociadas o que corresponden a horizontes estratigráficos equivalentes. Las mismas, conjuntamente con los nuevos taxones descritos en este trabajo coadyavarán a un mejor conocimiento de este lapso geológico en Cuba.

GEOLOGIA DE LA SIERRA DE NEYBA REPUBLICA DOMINICANA

DE LEON, R. Osiris. Corporación de Empresas Estatales. Av. Jiménez Moya, esq. José Contreras. Santo Domingo, Dominican Republic.

La Sierra de Neyba, localizada en la región suroeste de la República Dominicana, está constituida por rocas sedimentarias calcáreas, principalmente calizas terciarias, que se asocian con rocas volcánicas básicas emplazadas en el Eoceno Inferior.

Los flujos volcánicos, integrados fundamentalmente por basaltos, andesitas y piroclastos, datan de 52 millones de años atrás y están estrechamente relacionados con las calizas litográficas pedernalosas de la Formación Neyba, las que fueron depositadas en el Eoceno Medio.

La caliza litográfica de la Formación Plaisance, que es la base calcárea de la región, se concentra en la vertiente noroeste de la sierra, mientras que las calizas cristalinas y margosas de la Formación Sombrerito, que han sido posicionadas concordantemente sobre la Formación Neyba, afloran en la margen sur y en el extremo oriental del sistema montañoso de Neyba.

Las unidades clásticas de la región están representadas por las Formaciones Trinchera y Arroyo Blanco, del Oligoceno y Mioceno respectivamente, encontrándose que mientras Arroyo Blanco es rica en especies de macrofauna, las demás formaciones se caracterizan por la abundancia microfaunística.

La tectónica regional es extremadamente compleja, observándose cabalgamientos de calizas eocénicas sobre grandes mantos de calizas oligocénicas, lo que ha generado un extenso fracturamiento, que permite la rápida infiltración de las aguas meteóricas, las que posteriormente emergen a lo largo del principal plano de falla regional, constituyendo extraordinarios manantiales.

CENOZOIC SEDIMENTARY AND DEFORMATIONAL HISTORY OF THE CENTRAL CORDILLERA SEPTENTRIONAL, HISPANIOLA

DEZOETEN, R., Unocal Corp., International Oil and Gas Division, 1201 W. 5th St., Los Angeles, CA 90017; MANN, P., Institute for Geophysics, Univ. of Texas at Austin, Austin, TX 78759

The transition from convergent to strike-slip tectonics along the northern Caribbean plate boundary is recorded in the Tertiary basins of the Greater Antilles. In Hispaniola, the main zone of Eocene-Recent sinistral displacement at the plate boundary has occurred in the Cordillera Septentrional. Detailed stratigraphic and structural mapping indicate that Paleocene to early Pliocene sedimentary rocks exposed within the central Cordillera Septentrional (500 km^2) can be divided into three lithologically distinct stratigraphic units, each of which are punctuated by a deformational event causing crustal shortening.

The first stratigraphic unit is approximately 250 m-thick, late Paleocene to early Eocene in age, and consists predominantly of suspension deposited, deep marine clastic and carbonate rocks (Los Hidalgos Formation) interbedded with calcalkaline volcanic sills and flows (Palma Picada Formation). Termination of deposition and volcanism in early to middle Eocene time coincides with a major folding and uplift event, believed to have resulted from convergence of the Bahamas Platform and the arc related basins at the leading edge of the Caribbean plate.

The second stratigraphic unit is 4000 m-thick and consists of upper Eocene to lower Miocene conglomerates, sandstones, and shales (Altamira, Las Lavas, and La Toca Formations) deposited by submarine mass-flows within west-northwesterly striking, elongate basins. The composition of framework grains from coeval sandstones changes abruptly across a linear, 100-400 m-wide sinistral shear zone, suggesting that two distinct basins may have been juxtaposed by post-Oligocene faulting. The end of siliciclastic deposition in both basins coincides with a gentle middle Miocene folding event believed to be related to strike-slip faulting.

The third stratigraphic unit is approximately 250 m-thick and consists of upper Miocene to lower Pliocene shallow marine carbonate rocks (Villa Trina Formation). Carbonate deposition ended in early Pliocene time as a result of a folding and uplift event associated with transpression along the Septentrional Fault Zone.

MINERALIZACIONES AURIFERAS EN LOMA NANDITA REPUBLICA DOMINICANA

DE LEON, R. Osiris. Corporación de Empresas Estatales. Av. Jiménez Moya, esq. José Contreras. Santo Domingo. Dominican Republic.

RESUMEN

Las exploraciones geológicas, geoquímicas y geofísicas, así como las trincheras y perforaciones realizadas en una Reserva Fiscal de 6030,25 hectáreas mineras, localiza al noroeste de la ciudad capital de la Republica Dominicana, han permitido detectar la presencia de importantes concentraciones auríferas dentro de múltiples vetas de cuarzo, que cortan las rocas volcánicas de la Formación Duarte.

Esta Formación Duarte, de edad precretácico, y constituida por esquistos verdes, andesitas afaníticas, andesitas porfiríticas, tobas andesíticas y doleritas, ha sido considerada como la fuente de todo el oro aluvional que se mueve a lo largo de las corrientes fluviales que drenan la vertiente norte de la Cordillera Central.

El programa detallado de geoquímica de sedimentos fluviales, llevado a cabo en toda la Reserva Fiscal mediante el sistema de preconcentrados, determino, rápidamente, que las principales mineralizaciones auríferas se concentraban en un área de aproximadamente 350 hectáreas mineras, la cual recibe el nombre de Loma Nandita.

La geoquímica de suelos, orientada hacia la determinación de oro, arsénico y antimonio en los suelos lateríticos del área, reflejó muy pobres resultados, ya que el oro solo se concentra en las vetas de cuarzo, por lo que las rocas y suelos se muestran estériles.

Perfiles electromagnéticos realizados con slingram, detectaron ejes de anomalías que coinciden con la presencia de importantes vetas de cuarzo. Resultados menos concluyentes fueron obtenidos con el programa de polarización inducida (I.P.).

Perforaciones posteriores permitieron confirmar, que algunas de las vetas de cuarzo aurífero registradas en Loma Nandita, continúan por debajo de los 70 metros de profundidad, aunque con valores de oro muy variables, entre cero y 1900 grs. por tonelada, por lo que el trabajo exploratorio debe proseguir en forma sistemática.

STRUCTURE AND ACTIVE TECTONISM OF THE INSULAR MARGIN OFF NORTHWESTERN HISPANIOLA

DILLON, W.P., SCANLON, K.M., U.S. Geological Survey, Woods Hole, MA 02543, AUSTIN, J.A. Jr., University of Texas, Institute for Geophysics, Austin, TX, 78759, EDGAR, N.T., U.S. Geological Survey, Reston, VA, 22092, and PARSON, L.M., Institute of Oceanographic Sciences, Wormley, Surrey GU8 5UB, U.K.

The insular margin off northwestern Hispaniola is a tectonic accretionary wedge, as disclosed by GLORIA broad-range sidescan sonar images and single and multichannel seismic profiles. The data show that the margin is characterized by two principal structural/morphological styles. One style, displayed off northeastern Haiti, has a relatively gentle sea-floor slope (about 4°) that merges gradually into the flat floor of the Hispaniola Basin to the north. Structures associated with this style of margin are broad anticlines separated by thrust faults that dip southward toward Hispaniola, which is acting as a backstop. The anticlines are formed by active syndepositional folding beneath the floor of the basin and at the foot of the insular slope. Subsequently they are sheared off above a main decollement and are thrust beneath the older folds of the accretionary wedge that forms the insular slope. The morphology of this margin type is dominated by slope-parallel anticlinal ridges. A fold-controlled submarine canyon channels turbidity flows to the floor of the Hispaniola Basin, where a fan has formed. The other structural/morphological style occurs off northwestern Haiti and off northwesternmost Dominican Republic, and it is characterized by a much steeper insular slope (as much as 14°). In this type, the foot of the insular slope commonly forms an abrupt angle with the basin floor at a structural front. Internal structure of the insular slope appears to be chaotic in seismic profiles. Areas characterized by the two slope types are adjacent and must have been affected by the same movements and history of plate collision. The differences in structure and morphology may result from variations in dip of the main decollement. Although overall plate motion north of Hispaniola is undoubtedly dominated by transcurrent movement, the structure of the insular slope shows few effects of such motion. Rather, we attribute the insular slope structure observed in our studies to collision, and we assume that strike-slip motion must be taken up to the south. The Hispaniola Basin apparently has been a turbidite basin near the plate boundary for a considerable period, and variations in southward thickening of apparent turbidite layers in the basin may provide a partial history of plate interactions.

OBLIQUE COLLISION BETWEEN THE SOUTHEASTERN BAHAMAS AND HISPANIOLA: PRELIMINARY SEAMARC II/SINGLE-CHANNEL SEISMIC REFLECTION RESULTS

DOLAN, J. F., U. S. Geological Survey, Menlo Park, CA, BREEN, N. A., Lamont-Doherty Geological Observatory, Palisades, NY, MULLINS, H. T., Syracuse University, Syracuse, NY, and SHOR, A., University of Hawaii, Oahu, Hawaii

The shallow-water Silver and Navidad Banks of the southeastern-most Bahamas are obliquely colliding with northeastern Hispaniola along a transpressive segment of the broad, predominantly left-lateral Northern Caribbean Plate Boundary Zone. During June 1989 we plan to study this collision using a combination of SeaMARC II side-scan sonar and digitally recorded single-channel seismic reflection data, to be gathered aboard the R/V Moana Wave. Our study will focus on several major goals: 1) to determine the mode of accretion of the banks to the margin of Hispaniola, with particular emphasis on testing the hypothesis that the banks 'dock' with the overriding margin during an outward jump in the subduction zone, 2) to understand the structural response of the overriding (Hispaniola) plate to collision of the buoyant shallow-water banks, and 3) to determine the role that tectonic activity plays in explaining the small size and erosional margins of the isolated banks of the southeastern Bahamas, which contrast markedly with the large, progradational banks of the tectonically quiescent northeastern Bahamas. Specifically, we want to determine if the narrow, linear troughs that separate the southeastern banks are zones of active faulting associated with the collision. This talk will focus on the preliminary results of the cruise.

EXTENSION AND TECTONIC INVERSION OF AN INTRA-ARC HALF GRABEN: THE WAGWATER BELT, JAMAICA

DRAPER, Grenville, Department of Geology, Florida Inter-national University (The State University of Florida at Miami), Miami, Florida, Fl 33199

The Wagwater Belt, Jamaica, is a belt of Paleocene to Eocene conglomerates, turbiditic sandstones, gypsum and volcanic rocks which separates two areas of Upper Cretaceous island arc rocks. The belt is bordered by two major fault zones: the Wagwater Fault Zone (WWFZ) on the southwest and the Yallahs- Blue Mountain- Plantain Garden Fault Zone (YBPFZ) on the northeast. The rocks within the belt are themselves folded and faulted.

It is suggested that the belt is best modelled as a northeast dipping (relative to modern Jamaica) lithospheric listric normal fault system producing a crustal half graben. The WWFZ and YBPFZ are considered to be two synthetic imbricate listric faults within this major fault system. Such a model can successfully explain (a) the asymmetric distribution of sedimentary facies in the Wagwater Group sediments (b) the low grade metamorphism and 40 my (approx.) K-Ar overprint found in the rocks of the Blue Mountains.

The WWFZ and YBPFZ (and the parent zone) were reactivated (tectonically inverted, in recent jargon) by compressive stresses related to Jamaica's Miocene and later E-W sinistral transcurrent movements. This resulted in reverse motion on the bounding faults of the belt and caused folding and reverse faulting within the belt.

This two phase model for motion on the WWFZ may explain the apparent right lateral offset of the Jack's Hill Granodiorite from the Above Rocks Granodiorite. If extension were oblique on the WWFZ, then eastward oblique slip of the Jack's Hill body down the fault plane during extension, followed by reverse dip slip during reactivation would produce an finite southeasterly displacement. Making certain assumptions about the geometry of the WWFZ, this suggests crustal extension of 20 - 25km.

Other NW-SE trending faults in Jamaica were probably part of the Paleocene- Eocene system of crustal stretching, but, with the exception of the Newmarket-Montpelier Zone, displacement was not sufficient to develop a clastic sedimentary basin. Alternatively, some basins did form, but reverse motion on their bounding faults during Miocene inversion was not enough to expose them, and they remain buried.

RECONSTRUCTION OF THE HISPANIOLA-SOUTHEASTERN CUBA ISLAND ARC AND IMPLICATIONS FOR ITS CRETACEOUS TECTONIC EVOLUTION

DRAPER, Grenville, Dept. of Geology, Florida International University (The State University of Florida at Miami), Miami, Fl 33199.

Northern Hispaniola and southeastern Cuba conatin similar, if not identical, rock suites of Late Cretaceous to Early Eocene age which exist in both regions. It is suggested that these two areas separated along the Oriente transform between mid-Oligocene to Late Miocene time. This separation accounts for only 400km of the proposed 1000 km of left lateral displacement on the northern Caribbean boundary. Other Tertiary faults in northern and central Hispaniola helped accomodate the displacement: Camu (70km), Hispaniola (50km), Guacara (30km), a proposed fault buried in the Cibao Valley (40km), Septentrional (unknown, but probably less than 50km), San Juan - Los Pozos (unknown, but probably less that 15km). If the Tertiary displacements are restored, the Upper Cretaceous island arc can be reconstructed. This exercise reveals that the Upper Cretaceous arc was a broad composite terrane containing a suture zone. It is suggested that the Early Cretaceous arc was generated by a northward dipping subduction zone. Early arc volcanics were deposited on oceanic seamount structure (Duarte Complex). This arc rifted and formed a back arc basin, which was closed by a ?Campanian collisional event that thrust the main arc with its sea mount basement over the remanent arc and caused a flip in the polarity of subduction. The Lower Cretaceous-Lower Tertiary of North-central Hispaniola and southeastern Cuba therefore represents an amalgam of Cretaceous to Lower Tertiary terranes (seamount, Lower to Mid Cretaceous magmatic arc, suture zone, all stitched together by an Upper Cretaceous magmatic arc and accompanied by the Upper Cretaceous forearc terrane). The present structural character of Hispaniola is dominated by Neogene sinistral strike and oblique slip faults which cut obliquely across the the trend of the Cretaceous-Lower Tertiary arc.

NEOGENE TECTONIC DISINTEGRATION OF A CARBONATE EOCENE-EARLY MIOCENE MEGABANK ALONG THE NORTHERN NICARAGUA RISE, CARIBBEAN SEA

DROXLER, A.W., STAPLES, S.A., Dept. of Geology & Geophysics, Rice Univ., Houston, TX 77251; ROSENCRANTZ, E., BUFFLER, R.T., Inst. for Geophysics, Univ. of Texas, Austin, TX 78759; BAKER, P.A., Geology Dept., Duke Univ., Durham, NC 27708

The Northern Nicaragua Rise (NNR) is comprised today of the eastern Honduras/Nicaragua and southern Jamaica carbonate shelves, and a series of relatively small detached carbonate banks (i.e., Pedro, Rosalind, Serranilla and Miskito Banks) separated from each other by intervening basins and seaways. Based on recent seismic surveys of, (1) Walton Basin, located between the Southern Jamaica Shelf and Pedro Bank, (2) seaways on the western side of the NNR (Hine and Hallock Muller, this volume), as well as (3) the middle of the NNR (Univ. of Texas data), we postulate that the present bank and basin configuration evolved from a once continuous mega bank that was present along the entire length of the NNR from Eocene through early Miocene times. In the mid/late Miocene, this mega bank progressively broke up into a series of smaller banks, basins and seaways, mainly as the result of tectonic movements related to the overall strike-slip displacement within the North American and Caribbean Plate Boundary Zone of the Cayman Trench. At the same time, the most eastern portion of the mega bank was uplifted and today forms most of central and south Jamaica. The NNR basins and seaways, because of their common north trending orientation, have been previously interpreted as Paleocene to Recent rifts, becoming progressively younger from Jamaica to Honduras.

Our new interpretation of the NNR general evolution is documented by the results of a recent seismic survey in Walton Basin. The sea floor and subsurface of Walton Basin is clearly dissected by numerous dip-slip and srike-slip faults into a series of faulted and folded blocks as well as horst and garben structures. Most of these tectonic features, currently buried, appear to be inactive; however some faults, displacing the surface sediments, exhibit recent movements. On a detailed bathymetric map of Walton Basin, a plateau, currently at 600 m of waterdepth and comprising one third of the basin floor, clearly appears in our seismic grid as a drowned shallow bank overlain by a wedge of periplatform sediment thinning westwards from the edge of the Jamaica shelf. Smaller banks within Walton Basin, covered today by an average 30 m of water, represent small portions of the former bank that remain with the photic zone due to their location on high standing (faulted or folded) blocks. Intermediate cases are also observed, where small banks compensated for subsidence for some time, but subsequently drowned. Similar features were documented by Hine and Hallock Muller in the western seaways. There, a major (mid-Miocene?) unconformity separates the present arrangement of small banks and seaways from a large underlying carbonate (Eocene-early Miocene?) bank, dissected by near-vertical faults and fault-controlled folds. Interpretation of Univ. of Texas seismic lines from the middle of the NNR suggests that Pedro and Rosalind Banks also were connected until the early Miocene by a continuous bank. According to our new interpretation, the opening of seaways and basins along the NNR after the early Miocene would have initiated the northwestern flow of the Caribbean Current through the NNR. This more western path for the Caribbean Current could explain the initiation of the loop current at that time in the Gulf of Mexico. Since the mid-Miocene, the Caribbean Current has greatly influenced the evolution of the NNR banks and basins.

STRUCTURE AND SPREADING HISTORY OF THE CENTRAL CAYMAN TROUGH

EDGAR, N. T., USGS, Reston, Va USA, PARSON, L. M., Institute of Oceanographic Sciences, Godalming, Surrey, UK, DILLON, W. P., USGS, Woods Hole, Ma., USA, SCANLON, K. M., USGS, Woods Hole, Ma., USA and JACOBS, C.,Institute of Oceanographic Sciences, Godalming, Surrey, UK

The data from this study area in the Central Cayman Trough was obtained from several sources and include GLORIA sidescan sonar images, single-channel seismic profiles, magnetic intensity profiles, and Seabeam bathymetry. This valuable data set demonstrates that features common to rift-transform systems in the Atlantic Ocean are also found in the Cayman Trough. These include transverse ridges, ridge and salients, nodal basins, and a well-displayed transform fault zone.

The sidescan mosaic demonstrates that northerly oriented ridges and valleys generated by seafloor spreading are present not only on the Mid-Cayman Rise, but also that similar ridges on older crust east of the rise are partially buried by sediment. The images also show a series of easterly oriented ridges of oceanic crustal rock in the southern part of the trough that are east of and adjacent to the rift valley. The northerly oriented ridges appear to terminate against the easterly oriented ridges.

The combined data suggest that a major displacement resulting from a ridge jump is not apparent, but minor shifts of the spreading center appear to have occurred, particularly within the rift valley. At least one inactive spreading system can be identified within the valley. A small-displacement jump may account for the presence of a large elevated crustal block lying within the rift valley.

COMPILATION MAPS OF THE ENERGY AND MINERAL RESOURCES OF THE DOMINICAN REPUBLIC

ESPAILLAT, J., LANZO, G., and JIMENEZ, J., Departamento de Recursos Minerales, Universidad Catolica Madre y Maestra, Santiago de los Caballeros, República Dominicana.

Three maps at 1:200,000 and accompanying text have been prepared showing the location and basic information on all the known occurrences of metallic and non-metallic mineral and energy resources in the Dominican Republic.

Gold, with associated silver, is the most important mineral in terms of value and occurs as epithermal, vein and placer deposits. There are more than 100 known significant occurrences of placer gold.

Nickel laterite is the second most valuable mineable metallic resource. Aluminum occurs as terra rossa laterite, but is not presently mined.

Significant occurrences of base metals sulfides of Cu, Zn and Pb with associated Au/Ag have recently been proved. Other occurrences of metals include Mn, Cr, Ti and Fe oxides and minor Pt.

Limestone is the most important non-metallic industrial mineral followed by gypsum, marble, halite (salt), clay minerals, and small amounts of garnet and dolomite. The extensive clay mineral deposits have yet to be evaluated. The semi-precious stones of amber and pectolite are mined.

There are proved reserves of lignite and peat, but these are not presently mined. Non-economic occurrences of oil are known in the southern sedimentary basins.

Five significant hot spring occurrences are known associated with late Cenozoic volcanism and fracture zones in the southeast region. Their potential for geothermal energy has been evaluated.

PETROLOGIA DEL BASAMENTO IGNEO-METAMROFICO DEL NORESTE DE LA CUENCA DE BARINAS-APURE.

ESCALONA, N. Laboratorio Geológico, Corpoven, S.A. Puerto La Cruz Venezuela.

En la región noreste de la Cuenca de Barinas-Apure varios pozos han penetrado rocas metamórficas y sedimentarias consideradas como basamento económico y atribuidas al Precámbrico y Paleozoico indistintamente. El estudio petrológico de la secuencia reconocida en informes y publicaciones de la Industria Petrolera Nacional de Venezuela como argillitas de la Formación Carrizal en los pozos Apure-1, -2 y -3 (perforados entre los años 1947 y 1948) que infrayace a la sección cretácea da por resultado que se trata de dos grupos de rocas metamórficas bien diferenciables.

En los pozos Apure-1 y Apre-2 se encuentra un conjutno de rocas polimetamórficas constituídas por brechas de falla, microbrechas, milónitas (protomilónitas, filónitas, blastomilónitas) y seudotaquilitas. El efecto tectónico (milonítico), asociado a las fallas de Guafita Caño Limón y Apure, se acentúa a profundidad y afecta a rocas sedimentarias originales sobre las que ha actuado un bajo metamorfismo regional en las facies de los esquistos verdes. En el pozo Apure-1 a una profundidad de 2913 m (8828 pies) y asociada a brechas de falla se presenta una roca ígnea (andesita) en gruesas vetas e intercalada con los sedimentos originales, la cual ha sido profundamente alterada y sus componentes máficos marcadamente uralitizados, y metamorfizada conjuntamente con las rocas sedimentarias arriba descritas. Su origen se asocia a los conjuntos de rocas ígneas básicas desarrolladas en margenes continentales activos (suite calco-alcalina).

El pozo Apure-3 exhibe rocas metasedimentarias (metalimolitas arcillosas y metareniscas) con moderado desarrollo de la foliación y escaso fracturamiento y plegamiento. La textura, fábrica y estructura de la roca sedimentaria original son aún claramente observables.

Las rocas metamórficas arriba descrita se pueden incluir todas dentro de una unidad litodémica que en este trabajo se denomina Esquistos de Apure, cuyo holoestratotipo se ubica en el pozo Apure-3.

Similarmente se establece correlación con los esquistos y gneisses de los pozos Agua-Linda-1, SZW-3 y Ticoporo-1, Rosalia-1, Capitanejo-1 (ubicados dentro de esta misma cuenca) cuyas edades se consideran Silúrico temprano (edades radimétricas sobre estas rocas con el método K/A, de tal manera que la faja orogénica paleczóica propuesta en la literatura en la región de los llanos occidentales se amplia al área del Edo. Apure hasta su límite con el precamb. de Guayana(curso Río Arauca).

PETROGRAPHY AND GEOCHEMISTRY OF MAFIC ROCKS OF THE PERALVILLO FORMATION IN THE SABANA POTRERO AREA, CENTRAL DOMINICAN REPUBLIC

ESPAILLAT, J. and MACVEIGH, J.G., Falconbridge Dominicana C por A., Dominican Republic
LEWIS, J.F., The George Washington University, Washington, D.C., U.S.A.

Basalt pillow lavas and minor hyaloclastites intruded by crosscutting dolerites of similar composition, occur immediately north of the El Caribe serpentinized peridotite at Sabana Potrero in the Median Belt of the central Dominican Republic. The occurrence of massive sulphide within the mafic volcanics has given the opportunity for detailed study of samples from drill cores. The structural and stratigraphic information indicate that these mafic volcanic rocks form the base of the Peralvillo Formation of apparent Late Cretaceous age and are equivalent to the vitric and crystalline basalts of the Siete Cabezas Formation to the south of the peridotite belt.

The texture of the volcanic rocks ranges from fine-grained microporphyritic to poorly-developed ophitic to granular textures in the coarse-grained varieties. Clinopyroxene and plagioclase make up 90% of the rocks. The dominant alteration minerals are chlorite, phrenite, and epidote. Iron titanium oxide minerals are ubiquitously replaced by leucoxene.

Mafic lavas and intrusives (dolerites) have been analyzed for major and trace elements mainly for the drill cores of the Sabena Portrero area, but also from surface exposures. Most of the rocks are olivine-hypersthene normative and some contain normative quartz. TiO_2 ranges from 0.43 to 2.8% and varies with the Fe^{tot}/Mg ratio allowing correlations of different flow units between drill holes. Variation diagrams show that both the lavas and intrusive phases belong to a comagmatic sequence and that at least some of the lavas of the Siete Cabezas are comagmatic.

Chondrite-normalized Rare Earth plots show enrichment in Ce over La, depletion in Nd and a positive Eu anomaly. Trace element spider diagrams, normalized to N-Type MORB, show consistent patterns for all samples. Characteristic features are relative enrichment of Ce over La, 2 to 7 times enrichment in Nb and Ta, and slight depletion in Nd. Relative concentrations of Ti, Zr, Hf, Y are constant and similar to those of present-day ocean floor (MORB) basalts. These basalts are chemically distinct from the Duarte metabasalts.

DRILLING SUBMERGED MARINE TERRACES OFFSHORE BARBADOS; AGES, ORIGIN AND SEA LEVEL HISTORY

FAIRBANKS, RICHARD G. (Lamont-Doherty Geological Observatory of Columbia University, Palisades, NY 10964)

Studies of the timing of eustatic sea level changes have been refined using seismic and oxygen isotope data however the magnitudes of sea level changes in the geologic past are not known. Nowhere is this fact more evident than in the discrepancies over estimated sea level during the last glacial maximum. Estimates of mean ocean sea level during the last glacial low-stand range from 80 meters to 165 meters below present level. The exact timing of sea level rise during the last deglaciation is also poorly documented prior to 9,000 years before present.

In the Caribbean, the reef crest coral *Acropora palmata* is one of the dominant reef-framework builders. Its growth is generally restricted to the upper five meters water depth. This species thrives in the surf zone and is presently the best available sea level indicator. *Acropora palmata's* narrrow depth range, abundance in Caribbean reefs, good preservation, and massive size make it superior to molluscs or peats as an indicator of past sea level. Unlike molluscs or peats, corals may be dated by the newly developed 230Th/234U dating method using mass spectrometry. This dating method eliminates the vagaries of C-14 age dating due to varying C-14 composition of local sea water.

In November, 1988, R/V Ranger, outfitted with a wire-line drilling rig and four-point mooring system, drilled sixteen cores into the three submerged terraces located offshore Barbados. More than 1200 feet of reef was cored, resulting in a nearly continuous sequence of *Acropora palmata* between 126 meters and 15 meters below present sea level. The longest core, which was 71 meters long, was collected in 74 meters water depth and sampled the glacial reef and beyond. C-14 measurements were made on several samples during the cruise in order to help guide site selection. C-14 dates indicate that vertical reef growth kept pace with rising sea level, and therefore a complete and detailed record of sea level rise during the last deglaciation is recorded in these cores.

Barbados is the only locality where the marine oxygen isotope record is calibrated against sea level documented with C-14 dated *Acropora palmata*. Similar drilling programs are possible in other tectonic setttings and such studies will test for the first time, the accuracy of isostatic adjustment models.

DIAGENETIC INDURATED MARINE BOTTOMS IN THE SOUTHERN PART OF BARBADOS WEDGE : EVIDENCE OF DEEP FLUID CIRCULATION

by J.C. FAUGERES, R. GRIBOULARD & G. VERNETTE
Lab. Géologie & Océanographie, Univ. Bordeaux I, 33405 TALENCE cedex (France)

The presence of wide indurated bottoms had been observed during DIAPICAR Cruise (Oct.Nov.1987) in the southern part of the Barbados accretionary tectonic prism. These indurated bottoms are located on the top of tectonic relieves (antiform ridges and mud-volcanoes) which result from convergence movement of Atlantic and Carribean plates, involved in very important argilokinetic processes.

The indurated bottoms, upon which deep-sea communities are sometimes established were observed between depths of 1000 and 2200 meters. They present different morphological aspects. They generaly show irregular and disrupted microrelieves (cm to dm) in soft sediments areas supporting some currents-marks. Sometimes the bottom is covered by indurated blocks, scattered in the muddy sediments. They rarely show large concretions (dm to m) and similar to carbonate chimneys observed on Oregon margin. These discontinuous bottoms can covered very large areas (500 m. large and more 10 kms long). The indurated samples collected show brownisch coating constituted of iron and manganese oxides with carbonate origin cement. The soft underlaying sediments show very low carbonate contents (5 to 15%) and with a sometimes high proportion of hydrogen sulphide.

The origin of these encrusting cannot exclusively be linked to a marine environment, as cases of "classical" hard-grounds. We assume that the diagenetical processes responsible for sediment induration are controled by deep fluid circulations and venting.

In fact, chemical analysis of interstitial waters in underlaying soft sediments document dissolve chloride contents (293 and 485 mM/l.) lower than those of sea-water (550 mM/l.). Similar observations are used in O.D.P. Leg 110 sector to identify deep circulation located along the major thrusting faults of the accretionary prism. There, nevertheless, the minimum measured concentration is of 518 mM/l, so, consequently, the membraue filtration and deshydration of clay phenomenon which are invoked seemed insufficient to obtain such chlorinity values. The thermic decomposition of hydrate of methane levels observed on some high resolution seismic profiles (Bottom Simulating reflector) may be accountable of the decrease of chloride and also of an increase of methane concentration. The oxidation of methane into dissolved carbonates favours the precipitation of carbonate cement whilst a part of metallic ions (Fe and Mn) could be result of these fluids.

In conclusion, the indurated bottoms observed on this active margin, can be a main morphosedimentary charactere. Their origin is supposed to be related with carbonate and metallic ions rich environment. They need the lift and venting of deep fluids driven by fractures and their position and expansion along NE-SW and E-W directions emphasize the most actual active structures of this region.

QUATERNARY SEDIMENTS ON THE SOUTH BARBADOS ACCRETIONARY COMPLEX : A COMPARISON BETWEEN MUDDY-DIAPIRIC SEDIMENTS AND SOUTH-AMERICAN RIVER SUPPLIES.

FAUGERES, J.C., GONTHIER, E., PONS, J.C., PARRA, M., Departement of Geology-Oceanography, Bordeaux I, University, Avenue des Facultés - Talence 33405, France.

The tectonic context of the southern termination of the Barbados accretionary complex involves severe deformations as well as a strong dislocation of the prism's sedimentary cover with a tectonic network of various directions. Among these structures, numerous mud-diapiric relieves are present. Their morphology and tectonic features are clearly documented on seabeam and seismic data and allow us to distinguish two kinds of diapiric structures : mud-volcanoes and anticlinal ridges.

Our objective is to characterize diapiric material in order to compare it with the supplies of South American rivers that are deposited in small adjacent basins.

On top of mud volcanoes or anticlinal ridges, the surficial diapiric sediments are clayey silty compact muds, with typical grey-lead or blue-green colors, low carbonate contents and many indurated muddy pebbles. Microfauna is rare and composed of late Miocene-Pliocene pelagical foraminifers. This material is covered by a thin layer of either Holocene soft mud or indurated diagenetic crusts. The clay mineral assemblage is composed of smectite associated with illite, kaolinite, and chlorite.

In the adjacent basins, on the contrary, surficial sediments are recent (last Glacial to Holocene) and are coarse-grained turbiditic layers interbedded in a grey-green slightly compacted mud. Their clay mineral assemblage show a significantly lower smectite content and are similar to the assemblage observed in the sediments provided by the Orinoco and Amazon .

On the slopes of the diapiric structures, the deposits are composed of superposed diapiric material and non-diapiric turbiditic sediments.

According to the age and clay assemblage of diapiric mud, we assume that these sediments are provided by Miocene deep beds : they are first ejected under tectonic stress then they incorporate younger sediments during their uplift.

The diapiric material thus expulsed onto the top of the structures, is scattered on their slopes or into the adjacent basin by gravity processes. Because of the multiplicity of these structures, we suspect that argilokinetic processes are a significant source of sediments for the prism's deposits.

CUBA: FORMACION DE OLISTOSTROMAS EN UN AMBIENTE DE COLISION ARCO INSULAR-MARGEN CONTINENTAL

FLORES R.M., ALBEAR J.F.*

Instituto de Geología y Paleontología
Calzada #851 Esquina A, 4, Vedado 4, Plaza de la Revolucion
La Habana, CUBA

En el territorio de Cuba se desarrollan ampliamente depósitos olistostrómicos de diferente composición, génesis y edad. La formación de los olistostromas cubanos se relaciona con la colisión del arco insular cretácico con el margen continental mesocenozoico de América del Norte. Este proceso se extiende desde el Campaniano hasta la parte baja del Eoceno Medio. Se distinguen tres tipos genéticos. El Tipo I se formó en cuencas superpuestas gracias a movimientos verticales que provocaron el ascenso enérgico del relieve montañoso de las islas del paleoarco insular cretácico. Estos olistostromas están poco deformados y forman horizontes más o menos potentes incluidos por lo general en depósitos terrígenos y se desarrollan en tres intervalos (Maestrichtiano, Paleoceno superior - Eoceno inferior, Eoceno inferior - Eoceno medio). El Tipo II está constituido por depósitos que forman una franja discontinua a lo largo del borde norte de la isla, marcando el cabalgamiento de los complejos del arco insular cretácico y las ofiolitas, sobre el margen continental norteamericano. Son depósitos por lo general polimícticos, potentes, frecuentemente muy deformados, formados en el proceso de colisión del arco insular cretácico con el margen continental (Paleoceno superior - Eoceno medio). El Tipo III (Maestrichtiano-Paleoceno) está constituido por depósitos vinculados al desarrollo de una zona de rift, la cual escindió los complejos del arco insular cretácico a lo largo de la línea Cauto-Nipe. Al N-NW de esta línea (zona Auras), predominaba la compresión y se formó una complica de estructura nape-escamada, acompañada de olistostromas muy deformados en cuya composición entran, fundamentalmente, rocas de la asociación ofiolítica. Al S-SE, en la propia zona de rift, en un ambiente distensional, se produjo la deposición de secuencias terrígenas con olistostromas y turbiditas ultrabásicas que forman un complejo muy particular.

* Instituto de Geología y Paleontología, MINBAS.

EL PROBLEMA DEL EMPLAZAMIENTO DE LOS MACIZOS ULTRABASICOS DE LAS SIERRAS DE NIPE Y CRISTAL Y SU RELACION CON LA DEPOSICION DEL FLYSCH TERRIGENO DE LA FORMACION MICARA

FLORES R.M., ORO J., ALDEAR J.F., (Instituto de Geología y Paleontología, MINBAS, CUBA).

MOSSAKOVSKI A., NEKRASOV G., SOKOLOV S., (Instituto de Geología, Academia de Ciencias de la URSS).

La geología de la región situada al este y sureste del macizo de Sierra del Cristal es una de las claves para comprender la evolución tectónica del territorio de Cuba nor-oriental en el Cretácico Superior Paleoceno. Aquí, se desarrollan los depósitos terrígenos flyschoides de la Formación Míoara ($K_2 - P_1$), los cuales contienen numerosos horizontes de conglomerados polimícticos y de olistostromas de dos tipos: exolitostromas y endolistostromas. Los primeros están constituidos por un amontonamiento de bloques, desde uno hasta varios metros, de rocas fundamentalmente de la asociación ofiolítica (serpentinita, gabros, diabasas, etc.), casi sin cemento. Los segundos, por bloques irregulares del propio flysch encajante, englobados en una matriz aleurolítica de composición vulcanomíctica. Además, aparecen numerosos olistolitos y olistoplacas, hasta de algunos cientos de metros, de serpentinita y turbiditas ultrabásicas. El carácter de la distribución de los sedimentos muestra que la fuente de aporte se encontraba al O-NO, es decir, en dirección al macizo de Sierra de Cristal. Alrededor de este último se extiende, como una aureola, una asociación de ultrabasitas brechosas y turbiditas serpentiníticas, la cual, según todas las evidencias, pudo haber se formado en condiciones de un emplazamiento rápido, acompañado de descomposición brusca, del macizo de Sierra de Cristal, en la paleo-cuenca de deposición de la Formación Míoara. Esta asociación se interdigita en dirección submeridional con los depósitos flyschoides terrígenos de Míoara, los cuales, tal como está establecido, yacen transgresivamente sobre los depósitos arcoinsulares cretácicos. El macizo Moa-Baracoa, como se sabe, cabalga en dirección N-S a los complejos de la zona oriental de desarrollo de Míoara. Por su parte, los macizos de Sierra del Cristal y de Nipe, se vinculan con la posible escisión del arco insular cretácico a lo largo de la línea Cauto-Nipe, ocurrida probablemente en el $K_2 - P_1$, lo cual no había sido considerado hasta ahora.

GEOLOGIA Y DISTRIBUCION DE LAS CROMITAS DE LOS MACIZOS OFIOLITICOS DE MAYARI Y MOA-BARACOA, REGION ORIENTAL DE CUBA.

FONSECA, E., SLADKEVICH, S., MA.STA. CRUZ PACHECO, CAPOTE, C., GARCIA, I., and NAVARRETE, M., Instituto de Geología y Paleontología, Calzada #851 Esquina A y 4, Vedado 4, Plaza de la Revolución, Cuba

En la región oriental de Cuba afloran los mayores macizos ofiolíticos del país, denomicados Mayarí el mas occidental y Moa-Baracoa el oriental. Ambos presentan diferencias en el desarrollo del perfil ofiolítico. En el macizo de Mayarí afloran los complejos ultramáfico metamorfiado, cumulativo ultramáfico y escasamente el málico y los diques paralelos de diabasas. El complejo inferior alfora en la parte mas occidental y se caracteriza por la presencia de harzburgitas y lherzolitas. La mineralizalión de oromitas podiformes con altos contenidos de Cr_2O_3, se dispone en la parte central de este complejo en forma concentrica, empobreciéndose hacia el borde SW del mismo. Los contactos con los complejos cumulatives por el este de diques paralelos de diabasas por el oeste con tectónicos. Em complejo cumulativo se desarrola hacia Sagua de Tánamo y está representado por dunitas, dunitas plagiocláslcas, troctolitas, gabros olivínicos. Se caracteriza por la presencia de cromitas más pobres.

La región de Moa-Baracoa, es una prolongacio del bloque Mayarí. En él predominan los cumulos ultramáficos y málicos, los gabros masivos. Aqui las ultramafitas metamorfizadas afloran poco, sin embargo el complejo basáltico alcanza un gran desarrolo. Los contactos entre todos ellos son tectónicos, las fallas regionales coinciden con el contacto transicional entre la parte inferior y superior de los cumulos. La mineralización cromítica aparece en tres niveles dentro de los cumulos, el inferior en las dunitas enstalíticas con cromoespinelas dactiloscopicas y kotsohubeita intersticial, el segundo nivel corresponde a la zona de transición entre las dunitas y las dunitas plagioclasicas y por ultimo entre los gabros bandeadps y los masivos. Por la distribución de la mineralización, y por las caracteristlsticas, geologicas, se puede adoptar el; modelo de Nicolas y Violette (1982) y suponer que 4el centro de expansión que dio origin a estos macizos ofiolíticos se encontraba en una posición cercana al de Mayarí

GEOQUIMICA DE LA ASOCIACION OFIOLITICA DE CUBA

FONSECA, E., CASTILLO, F., UHANOV, A., and CORREA, G., Instituto de Geología y Paleontología, Calzada #851 Esquina A y 4, Vedado 4, Plaza de la Revolución, Cuba

La asociación ofiolítica de Cuba aflora en diferentes zonas estructurales, principalmente en la región septentrional del territorio y en aislados bloques emplazados en los macizos meridionales metamórficos. Aunque el grade de metamorfismo origina la migración y sustitución de algunos componentes, el quimismo de los complejos es similar. Los cuatro complejos que caracteriza a la asociación ofiolítica se distribuyen irregularmente, el complejo ultramáfico metamorfizado aflora principalmente desde Pinar del Río hasta Villa Clara, disminuyendo su presencia hacia la región oriental del país. A la inversa el complejo cumulativo alcanza su mayor desarrolo en la parte centro-oriental. Los complejos efusivos superiores se distribuyen en todo el territorio donde afloran las ofiolitas.

Geoquimicamente las dunitas del complejo ultramáfico metamorfizado presenta bajos contenidos de Al_2O_3 en tanto en las harzburgitas del mismo complejo estos aumentan. Esto se debe a que la enstatita y las espinelas son los únicos minerales que contienen aluminio. Este elemento en el complejo cumulativo máfico aumenta con la aparición de los minerales félsicos. A medida que ocurre la cristalización fraccionada del complejo cumulativo, se origina un empobrecimiento en el magma de Ni, Co y Cr. En general en estos dos complejos inferiores los alcalis son extremedamente bajos, pero en los superiores existe un aumento progresivo que alcanza un maximo en los basaltos afíricos y boninitas especialmente el sodio. El Sr varia desde O en las ultramafitas hasta 141pmm en los gabroides y en los efusivos alcanza has 196pmm. El V, el Ti, y ell fósforo aumentan desde el complejo ultramáfico metamorfizado al cumulativo, ya qye los dos primeros se concentran en la titanomagnellita y titanoaugita, tan caracteristlsticas en los gabros y diabasas ofiolíticas, y el ultimo por su comportamiento tan semejante al Ti. A veces los contenidos de Nb son más altos en las ultramafitas serpentinizadas que en los gabros, debido a la hidratación de las rocas durante la serpentinización.

Se puede afirmar que la asociación ofiolítica de Cuba, por las variaciones geoquímicas tiene un origen mántico único, pero los complejos cumulativo y efusivo, presentan algunas variaciones litológicas y químicas entre diferentes regiones. Esto se explica para los cumulos por la presencia de camaras igneas aisladas, criterio que tambien pudiera ampliarse a los complejos superiores efusivos de la asociación ofiolítica.

THE MINERALOGY OF BAHAMIAN SOILS

FOOS, A., Geology Department, University of Akron, Akron, Ohio 44325.

The mineralogy of soils occurring on Eleuthera and San Salvador Islands, Bahamas was investigated. These soils represent immature soils forming in a relatively pure carbonate environment. The major factors of soil formation are as follows: 1)The climate is humid tropical savanna with an annual precipitation of 115 cm. 2)The parent material is carbonate eolianite plus airborne dust from North Africa. 3)Relief is low with a maximum elevation is 37 m. 4)The vegetation ranges from low density scrub to dense mixed broad leaf coppice.

Three major soil types, "Bahamas black loam", "Bahamas stony loam" and "Bahamas red loam" occur over consolidated limestones. These soils are thin, stoney and concentrated in shallow karst depressions. The limestone below the solum is altered and occurs as a laminar crust or Ck horizon. The carbonate content of the solum ranges from >90% to 3% and its presence results in a high soil pH (7-8). The mineralogy of the insoluble residue from each soil type is given below.

Soil Name and Type	Minerals Present
Bahamas Black Loam (Leaf mould soil)	Illite, Kaolinite, Quartz, Feldspar
Bahamas Stoney Loam (Immature lateritic soil)	Mixed layered Hy-Al-IC/illite, Kaolinite, Quartz
Bahamas Red Loam (Aluminous lateritic soil)	Hy-Al-IC*, Boehmite, Quartz

*Hy-Al-IC = hydroxy-Al interlayered clay

The "Bahamas black loam" contains unaltered silicate minerals similar to the airborne dust. Partial alteration of primary silicates is observed in the "Bahamas stony loam" which contain mixed-layered clays and lack feldspars. The alteration of the parent material is greatest in the "Bahamas red loam" which contain pedogenic hydroxy-Al interlayered clays (Hy-Al-IC) and boehmite.

Bahamian soils are modern analogs to paleosols which occur within carbonate sequences and represent relatively short intervals of subaerial exposure. An understanding of these soils will improve paleoenvironmental and stratigraphic interpretations of ancient carbonates.

AN INTERPRETATION OF THE GRAVITY FIELD OF THE SE CARIBBEAN PLATE BOUNDARY ZONE

GHOSH, N., BURKE, K., and HALL, S.A.
Dept of Geosciences, University of Houston, Houston TX 77204-5503

To help test various models of its structure, we have studied variations in the character of the gravity field over the southeastern boundary between the Caribbean and South American plates. Crustal sections were constructed along 6 approximately north-south corridors between 60°W and 73°W from published compilations based upon seismic reflection and refraction data as well as geological interpretations. Composite regional gravity anomaly profiles comprising free air data over marine areas and Bouguer values on land were modeled using standard 2-dimensional techniques. Although the geometry of the bodies was varied from profile to profile to optimise the fit with the observed anomaly data, densities of individual bodies were kept constant so as to ensure compatibility between profiles and continuity of sources between adjacent corridors.

Results of the modeling suggest a west to east progressive change from a geometry more indicative of compressive conditions near Valencia to one that is consistent with predominantly strike-slip conditions near Maturin. Modeling of gravity features along a NW-SE profile west of Maracaibo does not require any significant subduction of Caribbean lithosphere beneath South America but rather can be adequately explained by modest amounts of underthrusting. Profiles to the east of the island of Tortuga are compatible with models involving the juxtaposition of arc material and a passive continental margin. Features in the gravity field suggest that the width of this arc material does not substantially change from west to east. At the extreme eastern end of the study area, modeling indicates that the localized loading imparted by the enormous amounts of Orinoco Delta sediments may overlie an oceanic basement.

NEOGENE SEDIMENTARY EVOLUTION OF ST. CROIX, U.S.VIRGIN ISLANDS

GILL, Ivan P., Dept. of Geology, Tulane University, New Orleans, LA 70118; McLAUGHLIN, Peter P., Dept. of Geology and Geophysics, Louisiana State University, Baton Rouge, LA 70803; HUBBARD, Dennis K., West Indies Laboratory, Fairleigh Dickinson University, Teague Bay, St. Croix, USVI, 00820; and MOORE, Clyde H., Jr., Dept. of Geology and Geophysics, Louisiana State University, Baton Rouge, LA 70803.

St. Croix is a dominantly sedimentary island in the northeastern Caribbean and its sedimentary development is therefore of considerable relevance to regional tectonic reconstruction. Previous models of the late Tertiary development of St. Croix assume either that the carbonate sediments were deposited in 1) shallow water or 2) entirely within the confines of an insular graben system. Both models presume a static, isolated island with a self-contained sediment source. Evidence from our drilling program on St. Croix requires modification of both models of basin evolution. Pelagic and hemipelagic carbonates of the Kingshill Limestone overlie blue pelagic and hemipelagic carbonates of the Jealousy Formation with a sharp, diachronous lower-to-middle Miocene boundary that ranges between planktonic foraminiferal zones N8 and N10. The Jealousy Formation itself is a deep-water limestone indistinguishable from the Kingshill Limestone except by color. Based on all known samples taken from it, the Jealousy Formation is a Miocene unit, not Oligocene, and does not outcrop.

Benthic foraminiferal faunes from drill samples suggest that most of the Neogene section reachable by drilling was deposited in the upper bathyal zone. Pronounced shallowing did not occur until the latest Miocene to early Pliocene. Samples collected from the western side of the basin show no sedimentologic or paleoecologic evidence of shallowing, faulting or a nearby landmass during early Miocene deposition of the Jealousy Formation. However, coarse clastic debris in Kingshill Limestone exposures along the eastern fault zone indicate that faulting and graben formation had begun at least prior to the latest middle Miocene.

This evidence indicates that the Jealousy Formation and the Kingshill Limestone began deposition prior to graben formation, and that faulting or horst exposure began later in the middle Miocene. A source external to the present structural basin is required to produce the pre-graben, shelf-derived carbonate components; we suggest that they originated from source areas to the north such as Puerto Rico or the Virgin Islands Platform. It appears likely that St. Croix has migrated and was uplifted in the Neogene, possibly during the opening of the Virgin Islands Basin and the Anegada Passage. The creation of these seismically active features was probably dominated by transtensional movement with a significant left-lateral component of slip.

MAGNETIC ANOMALIES OVER THE COLOMBIAN BASIN, WESTERN CARIBBEAN SEA

GHOSH, N., and HALL, S.A.
Dept of Geosciences, University of Houston, Houston, TX 77204-5503

A new total intensity magnetic anomaly map of the Colombian Basin has been prepared from available marine data using a detailed cross-over analysis to minimize cross-tie errors. Although the anomaly field throughout much of the basin is characterized by low amplitude anomalies, the map also shows several distinct features. These include a series of localized, higher amplitude (200nT) anomalies over the Hess Escarpment and a small area of E-W trending linear anomalies (150-200nT) between 11-15°N, 74.5-77°W. Dominant positive anomalies are found north of the Hess Escarpment and negative anomalies to the south. Anomalies over the northeastern portion of the Lower Nicaraguan Rise are typically 150-250nT with wavelengths of 80-100 km.

To constrain possible sources of the E-W magnetic anomalies, both marine and satellite derived gravity anomaly data were examined for possible correlations. If as has been suggested, the magnetic anomalies are due to basement relief, then there should be corresponding gravity highs and lows. No such features are observed and the anomaly field is found to be rather flat with only a minor NE-SW trend that cuts across the magnetic trends. Seismic reflection and refraction data indicate a thickened sedimentary section which is also not reflected in the gravity data. The absence of a significant gravity low over the area suggests the presence of high density material at shallow depths. Although this material may be intracrustal, refraction data are more compatible with a substantial shallowing of the Moho to depths more consistent with "normal" oceanic crust. The magnetic anomalies are, therefore, interpreted to be those produced by a piece of normal oceanic crust surrounded by thickened, sill-laden crust.

Insufficient features are present to obtain meaningful correlations of the magnetic anomalies with those produced by late Mesozoic spreading. As an alternative approach to determining the age of this oceanic crust, a paleomagnetic pole position has been determined from a deskew analysis of linear anomalies in the Venezuelan and Colombian Basins. Lunes of confidence from this analysis intersect near 45°N, 145°W yielding a pole that places the Colombian Basin at approximately 24°N at the time the oceanic crust formed. The deskew analysis also gives a declination of N 40°W suggesting a counterclockwise rotation of the seafloor since its formation. To determine when the Colombian Basin was located at this latitude and thereby obtain an age for the magnetic sources, we have rotated the area of E-W anomalies about Caribbean-North America rotation poles between 0 and 84 MyBP, and then about Farallon-North America poles between 84 MyBP and 160 MyBP. The area initially tracks westward out of the Caribbean region and then moves northward during the late Jurassic-early Cretaceous crossing 20-25°N sometime in the Jurassic. We therefore interpret the E-W area as a piece of oceanic crust formed at the Farallon Ridge sometime in the Late Jurassic-Early Cretaceous. Such an age is broadly compatible with previous magnetic studies in the Venezuelan Basin which identify the anomalies there as those produced in the Early Cretaceous. Rotation of the Colombian Basin about the North American poles also produces a counterclockwise rotation consistent with the declination given by the deskew analysis.

EVALUATING GROUNDWATER MIXING AND SEAWATER EVAPORATION DURING DOLOMITIZATION, ST. CROIX

GILL, Ivan, Department of Geology, Tulane University, New Orleans, LA, 70118; MOORE, Clyde H. Jr. and AHARON, Paul, Department of Geology and Geophysics, Louisiana State University, Baton Rouge, LA 70803.

This project utilizes the chemistry of the modern groundwater, as well as the chemistry, distribution and petrologic aspects of the dolomite to test various models of dolomitization on St. Croix. Dolomite on St. Croix exists in a highly localized region of outcrops and subsurface strata in a Pliocene reef tract. The dolomite occurs in reef, lagoonal and platform facies that rim the pre-development shoreline of Krausses Lagoon. Below the present water table, dolomitized rock follows the lithified undersurface of the same lagoon. Despite the existence of similar facies elsewhere on St. Croix, the dolomite is found nowhere else. This spatial distribution suggests that the formation of the dolomite was genetically related to hydrologic conditions found in Krausses Lagoon.

The $^{87}Sr/^{86}Sr$ isotopic composition of the dolomite is 0.70887 (±0.00002), which corresponds to the $^{87}Sr/^{86}Sr$ ratio of Miocene seawater. However, the dolomite resides in Pliocene strata, making a Miocene dolomitization event unsupportable and requiring a significant external source of non-radiogenic strontium. St. Croix groundwater $^{87}Sr/^{86}Sr$ ranges from 0.7076 to 0.7085, well below the ratio of both modern seawater and the dolomites. Mixing calculations show that St. Croix groundwater could be a significant source of non-radiogenic strontium in a dolomite formed from a two-component groundwater-seawater mix.

Stable isotopic values for the dolomite ranges from +0.7 to +3.8‰ $\delta^{18}O$ and from +0.6 to +2.4 ‰ $\delta^{13}C$ relative to PDB, with an enrichment trend from the margins to the center of the lagoon. The maximum oxygen isotopic values reached in these dolomites are too enriched in ^{18}O to be formed from groundwater or seawater, even accounting for ice-volume effects. These data imply that dolomite precipitated from fluids enriched in ^{18}O, probably as a result of evaporation. In order to account for the geochemistry and geologic distribution of the dolomites we suggest that dolomitization took place from fluids that were produced from a mixture of evaporated seawater and groundwater. Calculations show that such a scenario is possible, and may be geologically more common than one would suspect. In addition, the calculations show that groundwater effects on the strontium isotopic composition of carbonates cannot be ignored *a priori*, and the dating of carbonates in similar geologic environments should be approached with this in mind.

HIGHSTAND SHEDDING OFF TWO "SEMI-DROWNED" SHALLOW CARBONATE SYSTEMS, PEDRO BANK AND THE SOUTHERN SHELF OF JAMAICA, NORTHEASTERN NICARAGUA RISE

GLASER, K.S., and DROXLER, A.W., Dept. of Geology & Geophysics, Rice Univ., Houston, TX 77251; BAKER, P.A., Geology Dept., Duke univ., Durham, NC 27708

Water depths on (1) Pedro Bank, an isolated carbonate platform and (2) the southern shelf of Jamaica, an attached mixed carbonate/siliciclastic system, average 20 to 30 m. Because the tops of these carbonate systems did not keep up with the Holocene sea level rise, and because they are ususally covered by only a thin veneer of bioclastic (algal-sponge-coral-foram) sandy sediment, they have been considered to be "drowned" or "semi-drowned". Analyses (size fraction separation, carbonate content and mineralogy, radiocarbon dating of bulk sediment and foram biostratigraphy) of four cores from Walton Basin, an open seaway between Pedro Bank and the southern shelf of Jamaica, clearly exhibit current overproduction and highstand shedding of metastable bank derived fine aragonite and magnesian calcite.

For comparative study, we have selected two sets of two 5.5 to 6.0 m long piston cores, located in close proximity to either Pedro Bank or the southern Jamaican shelf. The cores were collected at comparable water depths (300 and 500 m) and close to the bank and shelf edges, 2 to 3 km and 6 to 8 km respectively. The carbonate content of glacial/interglacial sediments just off Pedro Bank, remains almost constant and averages 93%. Whereas, the carbonate content of sediments deposited off the southern Jamaican shelf varies between 45% for Holocene sediments and 70% for sediments deposited during the last glacial to interglacial transition. Based on radiocarbon dating, sedimentation rates during the past 5000 years in the cores nearest to the bank and shelf edges range between 2000 mm/ky off Pedro Bank and 1300 mm/ky off the Jamaican shelf. Sedimentation rates drop significantly for the more distant cores, to 45 mm/ky during the Holocene off Pedro Bank and to 400 mm/ky (carbonate rate) off the Jamaican shelf. Glacial sedimentation rates in the most distant core off Pedro Bank reached only 10 mm/ky. The 3.5 kHz record shows a well defined sediment wedge thinning away from the bank and shelf edges. One of the cores off the southern Jamaican shelf has penetrated the 6 m-thick sediment wedge and has reached its basal erosional unconformity. Based on radiocarbon dates, we can show that this wedge corresponds to the last sea level transgression and the subsequent Holocene flooding of the southern shelf. The drastic changes of sedimentation rates, coarse fraction proportion, carbonate content, and carbonate mineralogy, dated at 9000 years B.P., correspond well with the estimated time of shelf flooding.

FOSSIL ECHINOIDS OF THE LATE PLEISTOCENE FALMOUTH FORMATION (REEF TERRACE 1) OF JAMAICA'S NORTH COAST.

GORDON, CARLA M., Department of Geology, University of the West Indies, Mona, Kingston 7, Jamaica.

It is generally believed that there has been minimal faunal change in the marine community between the last interglacial and the present. This is based primarily on empirical data derived from benthic molluscs (Richards, 1962, Studies on the Marine Pleistocene. Transactions of the American Philosophical Society, 52, 1-141) and coral reef communities. It is not known if this is also true for other marine invertebrate groups. This study attempts to determine whether or not the echinoid faunal composition has changed since the Pleistocene. The highly fossiliferous Falmouth Formation (Reef Terrace 1: approx. 125,000 yr BP) of Jamaica provides an ideal subject for such a study. Furthermore, the Recent echinoid fauna of the Caribbean is a manageable subset of the global echinoid fauna for critical comparison.

In Jamaica there are 17 extant species of echinoid (Clark 1933, A handbook of the littoral echinoderms of Porto Rico and the other West Indian islands. *New York Academy of Science Scientific Survey of Porto Rico and the Virgin Islands, 16, 1-147*; Dr. J.D. Woodley written comm.), yet only 9 fossil species have been described from the entire Plio-Pleistocene interval (approx. 5 Myr) of the island. It is believed that this disparity is only apparent and is partially due to the rapid disarticulation of the multiplated echinoid test. Disarticulated echinoid plates are locally common in the Falmouth Formation.

Research to date has yielded the test from a juvenile *Echinometra* sp. along with abundant radioles test plates from *Astropyga* sp, and/or *Diadema* sp., *Echinometra* sp., and spatangoids. Ossicles of the Aristotle's Lantern and other plates have also been recognised, but have yet to be classified. Additionally, the disarticulated ossicles from ophiuroids have also been found to be abundant.

Irregular echinoids have a better fossil record than regulars but, when dealing with disarticulated material, fragments of regular echinoids are easier to detect and identify.

PALEOCEANOGRAPHIC AND PALEOCLIMATIC RECONSTRUCTION FROM 500 YEAR OLD CORALS, MONTASTREA ANNULARIS, IN THE SHELF OFF LA PARGUERA, PUERTO RICO

GOENAGA, C., Marine Ecology Division, CEER/ University of Puerto Rico and WINTER, A., Department of Marine Sciences, University of Puerto Rico, Mayaguez, Puerto Rico

Specimens of the hermatypic coral Montastrea annularis have been found in the shelf off La Parguera, southwestern Puerto Rico, which are at least 4-5 meters in height. Colonies of this size are uncommon elsewhere in the Caribbean. M. annularis forms distinct annual growth bands which result from the differential deposition of CaCO3 throughout the year. We have counted the growth bands for the entire length of the specimens and calculated their growth rate. These specimens, 4-500 years old, offer the means to reconstruct aspects of the regional climatic and oceanographic history for at least the life of the colony. An important aspect in this study is the potential to separate natural environmental changes from anthropogenic influences, such as the burning of fossil fuel and increased CO_2 in the atmosphere which results in the greenhouse effect.

ACTIVE TECTONICS OF THE CHORTIS BLOCK

GORDON, Mark B., MUEHLBERGER, William R., Department of Geological Sciences, The University of Texas at Austin, Austin, TX 78713-7909, U.S.A., and KOZUCH, Michael J., Cuerpo de Paz, Apartado Postal C-51, Tegucigalpa, Honduras

Internal deformation of the Chortis block (Honduras, El Salvador and environs) is controlled by two well defined, seismically active plate boundaries on the north and on the southwest. Much of the Chortis Block is included in either the CARIB/COCOS plate boundary zone (convergence rate=8 cmyr^{-1}) or the CARIB/NOAM plate boundary zone (slip rate<2 cmyr^{-1}). The Nicaraguan depression is a marginal basin responding to subduction from the Middle America Trench. The depression crosses the Gulf of Fonseca and continues into El Salvador where it is not as prominent a topographic feature. The Motagua and Polochic faults are the two major, active CARIB/NOAM plate boundary faults in Guatemala. Several faults with similar orientations occur south of these faults within the present Chortis block. The most prominent of these faults is the Jocotán-Chamelecón fault which is not active (Clemons, 1966). However, several similar faults may be active, e.g., the Aguan, La Ceiba, and Pueblo Nuevo faults across northern Honduras. The CARIB/COCOS plate boundary is much more seismically active than is the CARIB/NOAM plate boundary. The intraplate deformation of the Chortis block, paradoxically, seems to result primarily from motions along the CARIB/NOAM plate boundary.

North-trending basins with north-striking normal faults define the Honduras depression, a major zone of intraplate deformation entirely within the Chortis block. It is seismically active as demonstrated by instrumentally recorded earthquakes (NEIS Catalog), historical earthquakes (Oslecki, 1981), and Quaternary fault scarps. The principal basins are connected by a series of poorly defined, right-stepping strike-slip faults which strike northwest (Emmet, 1983). These faults may be a reactivation of a Late Cretaceous structural trend. Similar basins occur off the principal axis of the Honduras depression (e.g., the Jesús de Otoro, Talanga, and Santa Bárbara basins) indicating that the region as a whole is experiencing dextral shearing which reactivates old faults and forms extensional basins between principal fault segments. The most prominent extensional corridor of the Sula valley, Lake Yojoa and the Comayagua Valley probably represents the most profound preexisting weakness. Other extensional basins occur south of the CARIB-NOAM plate boundary in Guatemala (e.g., the Guatemala City and Ipala grabens). These basins are actively forming as was shown by the aftershock pattern of the 1976 Guatemalan earthquake (Plafker, 1976). These aftershocks indicate that north-striking normal faults form within the Chortis block as a result of strike-slip faulting on the plate boundary.

The Guayape fault is the longest, continuous structural feature in Honduras. It extends 190 km southwest from the Caribbean coast to the Jamastrán Valley region. An extension of the fault, the Choluteca lineament, may continue through Neogene volcanic deposits to the Gulf of Fonseca. In spite of its sharp, well-defined topographic signature, little seismic activity in this region was found in the NEIS Catalog between 1963 and 1983, or from the historical record (Oslecki, 1981). Our recent geologic mapping in the Catacamas Valley and the geometry of other basins show that the Guayape fault has a right-lateral sense of slip. Even though the Guayape fault represents important intraplate deformation, a direct relationship between it and the deformation at the plate boundary is not readily apparent.

STRATIGRAPHIC IMPLICATIONS OF PALEOMAGNETIC DATA FROM HONDURAS

GOSE, W.A., Department of Geological Sciences and Institute for Geophysics, University of Texas at Austin, Austin, TX 78712-7909 and
FINCH, R.C., Department of Earth Sciences, Tennessee Technological University, Cookeville, TN 38505

Paleomagnetic results from mainly Cretaceous rocks in Honduras delineate a distinctive apparent polar wander path which is well suited for magnetostratigraphy. Our interpretations are based on the comparison of magnetic pole positions of undated rocks with pole positions from rocks which had been dated either by fossils or radiometrically. Using these "calibration points", we were able to resolve stratigraphic problems that have defied normal field mapping and correlation studies. These results demonstrate the power of magnetostratigraphy in the absence of fossils or marker beds, and for areas of discontinuous exposures. For regional interpretations the most important conclusion is that the clastic strata in Honduras, which were formerly assigned to the Todos Santos Formation, were deposited on a different tectonic plate than the true Todos Santos Formation of Guatemala and southern Mexico. The name "Todos Santos Formation" should be abandoned in Honduras and for the entire Chortis Block. The other findings are mainly of local significance: 1. The non-fossiliferous exposures of red beds belonging to the Valle de Angeles Group, can be assigned to either the upper or lower member based on their direction of magnetization. 2. The upper Valle de Angeles beds, at least where sampled for this study, are of upper Cretaceous age, not Tertiary as reported in earlier literature. 3. The Guare limestone is the upper member of the Jaitique Formation as defined by Finch (1981). 4. The Jaitique Formation is older than the Esquías Formation, and the Esquías limestone seems to be younger than the generally quoted Cenomanian age. 5. The Plancitos Formation is of Cretaceous age and probably contemporaneous with the Barremian/Aptian Cantarranas Formation.

A LATE TERTIARY PALYNOFLORA AND TERRESTRIAL PALEOENVIRONMENTS FROM HAITI

GRAHAM, ALAN, Department of Biological Sciences, Kent State University, Kent, Ohio 44242, USA.

In 1923 E. W. Berry published on a small collection of fossil plants made by W. P. Woodring from Haiti. Identifications included the alga Chara, the fern Gymnogramma, and the angiosperms Bumelia, Chrysophyllum, Guettarda, Mespilodaphne, Mimusops, Pisonia, and Simaruba. Early identifications of leaves of tropical plants have proven notoriously unreliable, and the flora has not been studied since Berry's work. Recently permission was received to remove small pieces of the outer matrix of the Haitian specimens to process for pollen and spores. The microfossils recovered include monolete and trilete fern spores, the tree fern Pteris (abundant), pollen of the gymnosperm Pinus (pine; abundant), and pollen of the angiosperms Palmae (palm), Alchornea, Chenopodiaceae/Amaranthaceae, Compositae (common and several types), Engelhardia, Hygrophila (first fossil record), Malpighiaceae, Myrtaceae, Oryctanthus, and various unknowns. From the very general locality data on the specimens they are likely from the Maissada Formation, and the palynomorphs indicate a maximum age of uppermost Miocene to Pliocene. Preliminary results suggest the vegetation was similar to that presently growing on the island, including the pine forests now a prominent community on Haiti. The paleoclimates were also similar to those presently prevailing at low to mid-altitudes.

PALEOMAGNETIC RESULTS FROM THE SOUTHERN CARIBBEAN PLATE BOUNDARY ZONE

GOSE, W.A., Dept. Geological Sciences and Institute for Geophysics, University of Texas at Austin, Austin, TX 78712, USA,
PERARNAU, A. and CASTILLO, J., Dept. Física, Universidad Simón Bolívar, Caracas, Venezuela

We collected 729 rock samples of mainly Cretaceous age at 46 sites in Venezuela for paleomagnetic studies with the aim of assessing the tectonic stability in the southern Caribbean plate boundary zone. 13 sites are located in the Serrania de Perija, 22 sites in the Merida Andes, and 11 sites in the Serrania del Interior. The data are of very good quality and constitute an internally consistent data set, quite in contrast to previously published data from this region.

The samples from the Merida Andes yield well-grouped directions of both polarities. These data imply that the Andes have not undergone any significant motion relative to cratonic South America. This is the expected (and re-assuring) result because the Andes are anchored to the shield by the Precambrian Merida Arch which was a positive structure throughout the Cretaceous.

By contrast, all samples from the Perija Range in western Venezuela have north-east or south-west declinations and the inclinations closely correspond to their present latitude. The data suggest that the Perija range was once a linear continuation of the Santander Massif. In the north, the Perija is truncated by the east-west striking Oca fault for which a right-lateral translation of a few ten's of kilometers has been inferred. The rotation of the Perija could account for about 200 km of dextral offset between the Caribbean and South American plates, a displacement which would not be expressed as a fault offset. This translation is small when compared to the 1100 km of offset along the northern Caribbean plate boundary but future studies in this plate boundary zone may show additional translations.

The data from the Serrania del Interior in eastern Venezuela are in part remagnetized (negative fold test), but most sites indicate no or a small (<10°) clockwise rotation. The lack of significant block rotation in this strike-slip zone implies either that no major strike-slip motion occured between the eastern Caribbean and South America or that plate boundary lies to the north of the coast line.

WINDWARD VS. LEEWARD PLATFORM MARGINS AND THE EFFECT OF LOCALIZED SHELTERING, TONGUE OF THE OCEAN, BAHAMAS

GRAMMER, G. M., GINSBURG, R. N., and MCNEILL, D. F., University of Miami/RSMAS, Comparative Sedimentology Laboratory, Miami Beach, Florida, 33139, USA

Submersible dives to -350m along the platform margin in the southern portion of the Tongue of the Ocean (TOTO), Bahamas indicate distinctive patterns of sediment accumulation related to windward and leeward positioning (see figure). The most striking feature is the variable thickness in the wedge of unconsolidated, fine-grained sediment onlapping the cemented slope. Leeward transects show a significantly higher upper limit of soft sediment onlap (about -215m) than the windward margin (about -340m), presumably as a result of fine-grained sediment being carried off the open platform. Further north, where the leeward margin is partially sheltered by the Exuma chain, less fine-grained sediment accumulates (top at -280m). Total thickness of the near-vertical wall also reflects variations due to windward vs. leeward orientation. Windward margins typically have a wall that extends for 80-100m whereas leeward walls are only 50-60m thick. Variations in wall thickness are probably due to increased sediment supply at leeward margins. Observations indicate that sand-size sediment is transported downslope from the margins of the platform to the cemented slope below. Increased sedimentation rates on leeward margins would result in relative reduction in the vertical expression of the wall. These observations support the concept of rapid lateral growth on leeward margins and suggest that localized variations in sheltering effects may strongly influence carbonate platform growth.

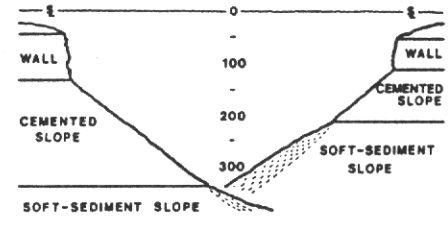

MORPHOLOGY AND DEVELOPMENT OF MODERN CARBONATE SLOPES, TONGUE OF THE OCEAN, BAHAMAS

GRAMMER, G. M. and MCNEILL, D. F., University of Miami/RSMAS, Comparative Sedimentology Laboratory, Miami Beach, Florida, 33139, USA

A thorough understanding of modern slope environments is essential to the interpretation of inclined deposits (clinoforms) from seismic profiles and outcrops of ancient reefs and platform margins. Recent work in the Tongue of the Ocean (TOTO) indicates that modern carbonate slopes are forming by the synsedimentary amalgamation of linear trains of sediment and talus derived from the margin of the platform. In addition, our observations during 94 dives in the research submersible DELTA indicates that the upper slopes of TOTO exhibit a distinctive morphology: 1) the platform margin, which consists of a Holocene sediment wedge situated behind one or more areas of deep reef growth. These deep reefs, where present, are dissected by a series of sediment chutes; 2) the near vertical wall with slopes ranging from 70° to 90°, consists of variable types of deep corals, encrusting coralline algae, sponges, and green algae. The surface of the wall is characterized by small pits, caves, ledges, and vertical overhangs. This zone is capable of producing copius amounts of sediment which is subsequently transported downslope. Transition from the wall to the underlying cemented slope is often characterized by large talus blocks, up to 30m in height; 3) the cemented slope, with a consistent slope angle between 35° and 40°. The surface often shows an irregular surface of hummocks and mogul separated by streams of loose sediment. Samples from this zone reveal submarine cemented sediment and reef talus. In some areas, large promontories project from the slope that may have been formed by the repeated cementing of numerous generations of talus blocks and sediment; and 4) a soft-sediment slope (25°-30°) which onlaps the cemented slope. This sediment wedge exhibits varying surface morphologies ranging from a smooth sediment blanket to a series of large sediment ridges and troughs. Transition between cemented slope and soft-sediment slope is often marked by a zone of talus blocks. The sediment consists of a mixture of platform-margin derived sands and muds, and deep-water planktic material.

These results further refine the upper slope facies and elucidate the complex and heterogeneous nature of slope development.

TAPHONOMIC BIASING OF SUBFOSSIL ECHINOID POPULATIONS ADJACENT TO ST. CROIX, U.S.V.I.

GREENSTEIN, Benjamin J., Department of Geology, University of Cincinnati, Cincinnati, Ohio 45221-0013

The distribution of live and dead echinoids was compared in fore-reef, reef and shallow subtidal environments along a 720 m transect in Smuggler's Cove, and a 50 m transect in Rod Bay, St. Croix. Although echinoids are generally regarded as ubiquitous in shallow reef and adjacent environments, their distributions in Smuggler's Cove and Rod Bay are patchy. No intact tests of dead individuals were found associated with the living fauna, and comparison of live echinoid distribution with sediment composition awaits further constituent particle analyses. The lack of association of live and dead faunas suggests that echinoids are quickly acted on by biostratinomic (post-mortem) processes; their preservation, therefore, may require extraordinary circumstances. One such circumstance may have occurred during March, 1984, when mass mortality decimated populations of Diadema antillarum adjacent to St. Croix. Tests and spines of this species were observed accumulating in seagrass beds immediately leeward of the reef tract in Smuggler's Cove shortly after the mass mortality. In 1988, a piston core taken from one of these beds was analyzed centimeter by centimeter to determine whether an horizon unusually rich in Diadema skeletal elements was preserved as a consequence of the baffling and binding properties of Thalassia. No horizon is evident in the greater than 2 mm size fraction; analysis of the smaller size fractions in thin section is ongoing. The probable lack of a "Diadema spike" in an environment of net sediment accumulation suggests that tests of Diadema degrade so rapidly that increasing the amount of subfossil material as a consequence of mass mortality alone was insufficient to preserve the event.

Decay experiments using specimens of Diadema, Echinometra and Eucidaris indicate that, in the absence of rapid burial, Diadema disarticulates most readily. Spines begin to fall off within 3 days of death and the periostracum begins to decay. After 5 days, the apical system collapses into the corona and the Aristotle's Lantern begins to protrude from the peristome. In this condition, the slightest disturbance causes the test to disarticulate along ambulacral plate sutures. Tumbling experiments with additional echinoid skeletons reveal differences in relative durability of the test as well as the amount of material that is contributed to various size fractions. Results of laboratory experiments and field work suggest that Diadema may be particularly vulnerable to taphonomic bias - a conclusion currently being tested by an extensive review of its fossil occurrences.

COMPOSITION AND DIAGENESIS OF CARBONATE SEDIMENTS ON THE ISLAND SHELF EAST OF HELLSHIRE, JAMAICA.

GREENIDGE, B.H. and HENDRY, M.D., Geology Department, University of the West Indies, Mona, Kingston 7, Jamaica.

Except for the northern region which contains mixed carbonate-siliciclastic material, sediments on the island shelf off the Hellshire coast are essentially pure calcium carbonate.

Major components in order of decreasing abundance are Halimeda plates, cryptocrystalline grains, mollusc fragments, intraclasts and articulated coralline algae. Minor constituents are foraminifera, encrusting coralline algae, echinoderm fragments, bryozoan, octocoral spicules, coral fragments, barnacle fragments and aggregate grains.

The distribution of the major components is influenced by mud dilution in the northern region, availability of hard substrate, biotic environment and physical processes related to wave energy.

Several early diagenetic processes affect the sediments. Encrustation by red algae is quite common. Aggregation has resulted in the formation of intraclasts and aggregate grains, the latter being aided by sediment infilling and cementation within empty scaphopod shells. Grains exhibit varying degrees of micritization ranging from micrite envelopes to cryptocrystalline grains. The following list shows decreasing susceptibility to micritization of various skeletal carbonate grains: Halimeda plates and coralline algae, mollusc fragments, foraminifera, coral fragments, echinoderm fragments. The susceptibility has direct implications regarding preservation of sediment texture during later stages of diagenesis.

KINEMATIC HISTORY FOR EASTERN MARGARITA ISLAND, VENEZUELA

GUTH, L. and AVÉ LALLEMANT, H., Department of Geology and Geophysics, Rice University, P.O. Box 1892, Houston, TX 77251

Amphibolites, serpentinized ultramafics, leucocratic igneous rocks, quartzofeldspathic and graphitic schists and minor marble make up the metamorphic nucleus of Margarita Island. Similar rocks occur along the Caribbean-South American plate boundary region from Tobago to Barquisimeto, exposed in the Cordillera de la Costa belt. The assemblage has been further subdivided into several related Mesozoic metamorphic belts, with Margarita belonging to a narrow band of rocks along the coast characterized by occurrences of high pressure metamorphic assemblages.

On Margarita Island, eclogite knockers in both the schists and the amphibolites spawned considerable work on the metamorphic history of the island. However, the corresponding kinematics were unknown. This study examined small-scale structures to infer a kinematic history for Margarita Island. The results shed light on the origin of the Mesozoic metamorphic belts and the plate tectonics required to form these rocks.

The earliest phase of deformation (D_{1a}) preserved on Margarita Island is rarely observed, seen as a foliation within microlithons bounded by the foliation of the next deformation (D_{1b}). This phase of deformation, synchronous with epidote-amphibolite to greenschist facies metamorphism, formed the dominant metamorphic foliation found on the island which is axial planar to associated isoclinal folds. Late in this stage of deformation, CS and quartz c-axis fabrics show SW-NE extensional deformation. In the Oligocene (?), another phase of deformation (D_2) folded this D_{1b} foliation into an anticlinorium that plunges to the SW. The latest brittle deformation (D_3) also shows SW-NE extension.

All fold axes and extensions are aligned SW-NE. This is best explained by a consistent component of dextral strike-slip deformation since the Cretaceous. The observed changes in deformation reflect variation in depth and local bends in the plate boundary. This model for the kinematic history of the deformation on Margarita Island implies that these rocks were formed far to the west, perhaps in Pacific-South American plate interactions, with the preserved deformation reflecting the long-term dextral transport of these rocks along the Caribbean-South American plate boundary.

UNOCAL EXPLORATION IN HONDURAS AND NICARAGUA - 1961 to 1980

HARDY, L.R., and WILLIAMS, R.E., Unocal Corp. 1201 West 5th St. Los Angeles, California, USA, 90017

An intensive search for hydrocarbons in the Mosquitia Basin of Nicaragua and Honduras began in 1961 when Pure Oil acquired a 5,900 hectare lease in eastern Honduras. By 1981 most exploration operations had ceased, ending a 20-year campaign that saw more than 22 oil companies exploring the basin. A total of 35 wildcats and delineation wells were drilled. Prior to 1961, only 4 wells had been drilled in the basin.

Pure's initial exploration efforts were directed onshore Honduras but shifted offshore in 1966 after Pure merged with Union Oil Company of California (now Unocal). Gravity, magnetics, and 7,800 miles of seismic data were acquired and used to support the drilling of 4 wells in Honduras, one of which yielded subcommercial oil and gas shows. Union's Honduran lease was allowed to lapse in 1977.

Offshore Nicaraguan leases adjacent to the Honduran holdings were secured by Union in 1966 and an exploration program was conducted in concert with the Honduran effort. Additional leases were granted in 1974, bringing the total Nicaraguan holdings to 1,198,000 hectares. Nearly 2,600 miles of seismic data were acquired and 6 wells were drilled. As in Honduras, commercial quantities of oil were not found, despite the fact that several wells flowed low rates of oil. Union's Nicaragua leases were relinquished in 1980.

The lack of success in the Mosquitia Basin was principally credited by Union to a lack of reservoir development. Facies models were used to predict porosity trends and to help select drill sites from numerous structural and reefal anomalies, but these models were not helpful in locating hydrocarbon accumulations. Future exploration efforts will rely on better understanding of sedimentary facies and deeper reservoir objectives.

Ostracode Biostratigraphy of the Titanosarcolites and Oyster Limestone Beds and Associated Facies (Upper Cretaceous) of Jamaica

Joseph E. Hazel
Department of Geology and Geophysics
Louisiana State University
Baton Rouge, LA 70803
USA

Certain Cretaceous lithostratigraphic units of Jamaica of late Campanian to early Maastrichtian age are rich in ostracodes. About 175 species have been identified, nearly all of which are new to science. Important species of the fauna belong to the genera Aequacytheridea, Asciocythere, Brachycythere, Buntonia, Limburgina, Ovocytheridea, Cletocythereis, Eocytheropteron, Schizoptocythere, and Alatacythere. The generic assemblage is distinctly different from the well-known fauna of the North American Coastal Plain. The presence of Ovocytheridea, Buntonia and Schizoptocythere, particularly, relate the Jamaican assemblage biogeographically to Tethyan assemblages described from Africa and southern Asia. At the species level there are three distinct assemblages that succeed each other in time and are proposed as biostratigraphic zones. The oldest of these, which is associated with the Titanosarcolites beds and related shales, has been identified from the Central, Maldon, and Marchmont Cretaceous Inliers. It can be divided into three subzones that are useful for correlation between these inliers. The two younger zones have been found only in the Jerusalem Mountain Inlier of western Jamaica. The oldest of these is associated with the Titanosarcolites beds of this inlier, and the younger zone is found in shales associated with the Lopha arizpensis jamaicensis beds (the oyster limestone). Only two species found in the oldest of the three zones are found in the middle zone, and the youngest and oldest zones share no species. Further, the middle and youngest zones share only three species. Apparently, after an ostracode fauna became established it would be destroyed by a volcanic episode and then the island repopulated from elsewhere in the region. Planktic microfossil data suggest that the three ostracode zones are within in the nannofossil Quadrum trifidum Biochronozone, which is of late Campanian to early Maastrichtian age.

NUEVOS ASPECTOS ACERCA DE LA GENESIS DEL PROTOLITO DEL COMPLEJO ANFIBOLITICO MABUJINA, SUR DE CUBA CENTRAL

HAYDOUTOV,Ivan, BOYANOV, Ivan, and MILLAN, Guillermo, Instituto de Geología y Paleontología, Calzada #851 Esquina A y 4, Vedado 4, Plaza de la Revolución, Cuba

El complejo anfibolítico Mabujina (CM) aflora en la parte sur de Cuba Central, formando una faja de anchura variable que rodea tectónicamente a las secuencias jurásico-cretácicas metamorfizadas que constituyen al macizo de Escambray. Esta constituido principalmente por rocas basicas metamorfizadas en la facies anfibolitica en condiciones de alta relación T/P, deformadas y foliadas de manera muy heterogeneas. Una porción considerable del CM procede de una típica asociación ofiolitica. Esta comprende principalmente anfibolitas y, además, piroxenitas hornblendizadas, microgneises y peridotita serpentinizada. El complejo más caracterizado es el cumulativo bandeado, dado por una laternación de gabros piroxeníticos con diferente granulosidad (desde pegmatíticos) con intercalaciónes frecuentes de piroxenitas con distinto tamaño del grano y en algunas porciones de peridotita. También se destacan anfibolitas de grano fino y microgneises, cuyos protolitos responden al complejo de diques paralelos y al complejo vulcanógeno. Cabe señalar, que los análisis geoquímicos de 8 muestras diferentes demostraron que el contenido de algunos elementos inmóviles estables (TiO_2, - FeO_3, MgO, V, Cr, Sr, Zr) concuerda satisfactoriamente con el campo MORB. Otra parte del CM parece proceder de secuencias pertenecientes al arco volcánico cretácico. Los análisis geoquímicos de 3 muestras diferentes arrojaron una tendencia distinta. A veces se trata de unas anfibolitas esquistosas con numerosos restos de fenocristales de plagioclasa magmatica, la cual es caracteristística para las muestras analizadas. Con esta pueden relacionarse algunos cortes compuestos por metaaglomerado volcánicos y metabasaltos porfiriticos con fenocristales de clinopiroxeno hornblendizado. Tambien tenemos los cuerpos de gneises leucocráticos granaliferos, cuyo protolito corresponde a los propios granitoides vinculados con el arco con el arco volcánico.

De aquí, que el protolito de una gran parte del CM se trata de una sociación ofiolitica que constituyó el fundamento sobre el cual evolucionó el arco volcánico cretácico. Otra porción del CM procede de las propias secuencias de la parte más baja del arco volcánico. Todas estas rocas se metamorfizaron y deformaron conjuntamente en las condiciones de alta relación T/P vinculado geneticamente con el alto gradiente geotermico que tuvo lugar en la región donde se desarrolló el arco volcánico.

EFFECTS OF HURRICANE GILBERT ON THE JAMAICAN COAST WITH PARTICULAR REFERENCE TO DAMAGE AND RECOVERY OF BEACHES

HENDRY, M.D., Geology Department, University of the West Indies, Mona, Kingston 7, Jamaica, and BACON, P.R., Zoology Department, University of the West Indies, Mona, Kingston 7, Jamaica.

The eye of Hurricane Gilbert swept across central Jamaica from east to west on September 12, 1988. This track effectively divided the island into two with respect to damage in coastal areas, the more dangerous north-westerly quadrant of the storm impacting the east and north coasts while the southern coast was in a relatively sheltered position with respect to surge and storm wave effects. Initial post-storm damage inventory was attempted for beach areas by several groups. Along the north coast, impacts were highly variable, ranging from extensive erosion of some beaches and accretion on others, plus damage to coastal structures such as roads, seawalls and groins. Assessment of changes was hampered by two major problems: 1) the apparent absence of standardised recording and reporting techniques and 2) lack of systematic baseline beach observations against which quantitative measurements could be scaled. In addition, there was inadequate information on pre-storm deterioration of coastal infrastructure.

Total estimated insurance loss due to Hurricane Gilbert for private and public facilities islandwide was 50 billion $Ja. However, of expenditure through the Ministry of Construction on post-storm rehabilitation of gullies, drains and rivers, the funds for restoration of coastal infrastructure formed only 3% of the total allocation of $Ja 14m. Accurate figures for the cost of restoration on beaches are not available.

Many beaches that were severely damaged during the storm recovered rapidly within a short period of the event, and costs of hurricane damage must therefore be estimated in relation to likely post-storm beach receovery. We will provide an outline of essential baseline monitoring techniques for coastal areas, and demonstrate how such data can be used to assess the need for artificial post-storm beach recovery and for advising Government and private user groups, such as hoteliers, on the need for coastal defences and appropriate soft-substrate management procedures.

INCORPORATING GEOLOGIC HAZARD INFORMATION INTO DEVELOPMENT PLANNING

HEYMAN, Arthur M., Organization of American States, 1889 F Street NW, Washington D.C., 20006.

The most cost-effective means of reducing the potential impact of natural hazards is by incorporating hazard considerations into the early stages of development planning. The most hazardous geologic phenomena are earthquakes, volcanic eruptions, and tsunamis. Two kinds of information are needed to evaluate earthquake threat to an area: 1) potential severity of an earthquake and 2) likelihood of a damaging earthquake occurring in that area during a particular timeframe. Information is presented for the former in terms of areas that experienced Modified Mercalli Index intensity values of VI or greater and for the latter in terms of percent of conditional probability for ten and 20 year periods. This information is presented at the level of provinces (or equivalent political subdivisions) for South America and Central America. Similar information is presented at the country level for the Caribbean in terms of estimated maximum magnitude M(s) of 4 or greater and scaled likelihood of occurrence of a large earthquake in the near future. Comparable information on Mexico is presented in a different manner. For evaluating volcanic hazards, a list of all volcanoes that have erupted in Latin America and the Caribbean in the last 10,000 years is classified as to location; long- or short-term periodicity; maximum scale of eruption; eruptions that caused deaths or property damage; number of eruptions of each volcano and date of the latest eruption; and associated hazards--explosive eruptions, pyroclastic phenomena, lava flows, and lahars. For tsunamis, wave heights of 2-3m, 3-5m, and 5+m above normal caused by hypothetical earthquakes in seismic gaps on the west coast of South America are shown for population centers from Equador to Chile and information produced by another means is presented for Mexico to Colombia. The information presented should be sufficient for a planner conducting a preliminary regional survey to determine if earthquakes, volcanic eruptions, or tsunamis constitute a significant threat in the survey area.

PATCH REEF ECOLOGY, SEDIMENTOLOGY AND ZONATION, BUCCOO REEF COMPLEX, TOBAGO

HUDSON, D., Institute of Marine Affairs, P.O. Box 3160, Carenage, Trinidad and Tobago and MOUNTJOY, E.W., Department of Geological Sciences, McGill University, Montreal, Quebec, Canada.

Four distinct patch reef assemblages have been identified in the back-reef areas of the Buccoo Reef Complex, Southwestern Tobago. This differentiation is based on ecology, associated sediment distribution, and their geographic location within the back-reef environment.

Algae - Porites assemblages are elongate to sub-circular in plan view, and dominated by algal-encrusted coral rubble, and minor clumps of Porites porites and Thalassia testinidium. Elongate-shaped Acropora assemblages are composed of thickets of Acropora cervicornis, with minor stands of A. prolifera and species of Siderastrea, Agaricia, Montastrea and Diploria. Acropora-Millepora assemblages which are elongate to sub-elliptical in shape, are compositionally similar to the Acropora assemblages, except for the introduction of extensive occurrences of the hydrozoan Millepora. A single occurrence of the elongate to tabular-shaped Montastrea assemblage is predominated by coral heads of Montastrea annularis.

Halimeda plates and mollusc grains are the dominant sediment particles associated with Algae - Porites assemblages. Fragments of coral and coralline - algae, along with Halimeda and mollusc particles in varying percentages, occur on the substrates of the Acropora, Acropora - Millepora, and Montastrea assemblages.

The patch reef assemblages recognized in Buccoo Reef, are ecologically similar to identified zones of coralgal communities on the fore-reef slopes of reef complexes. By a similar comparison, their different geographic locations within the back-reef environment are due to a combination of physical parameters, namely wave exposure, water circulation, water depth, turbidity and salinity.

EXPLOITATION OF THE MIDDLE MIOCENE OIL BEARING INTERMEDIATE HERRERA SANDSTONE RESERVOIRS IN A THRUST FAULTED AREA IN TRINIDAD, WEST INDIES

By

F. HOSEIN, Trinidad & Tobago Oil Co.

The Herrera sands contain the major oil producing reservoirs of Miocene age in Trinidad's Southern Basin. They lie within the Upper Cipero shale formation in the Penal/Wilson, Barrackpore and Ortoire fields of South-Central Trinidad. These turbidites sands are found at three levels, the 'Overthrust', 'Intermediate' and 'Underthrust': each level separated by a major thrust fault, and associated with a complex structure of a strong overfold and recumbent syncline formed by major tectonic movement at the end of Middle Miocene time.

The Intermediate Herrera sands are confined to a long (17 miles) and narrow (2,000 feet) area trending NE-SW from the Penal/Wilson field to the Barrackpore Mandingo field. The sands are found at depths of 6,000 to 10,000 feet in a complex structure which plunges to the southwest and is cut by numerous extensional cross faults which form separate hydrocarbon pools. Exploitation of these pools commenced in 1946 and by December 31, 1988, the cumulative production totalled 18 million barrels of oil/condensate and 30 billion SCF of natural gas. Presently, these sands offer the best potential for continued exploitation of the undeveloped reserves in the area. Additional unrecovered proven reserves are 4.5 MMB oil/condensate and 4.5 BCF of natural gas. Potential reserves in undrilled prospective areas (845 acres) are estimated at 15 MMB oil/condensate and 15 BCF of natural gas.

This paper examines the major aspects of this Miocene play showing the structural and stratigraphic interpretations of the Intermediate Herrera sands and their associated production characteristics. Development trends of the fields are shown and an outline of future plans for exploitation of reserves remaining in the Intermediate Herrera sands is presented.

ENVIRONMENTAL IMPACTS AND CORAL DEGRADATION, BARBADOS COAST

HUNTER, G.T.[1], HOOPER, R.[2], and LAWSON, D.E.[3].
[1]Hunter and Associates, Toronto; [2]Memorial University, St. John's; [3]University of Waterloo, Waterloo, Canada.

Not all is environmentally well in the Barbados coastal zone. The nearshore waters, subtidal reef coral substrate, beaches, backshore and inland zone are all a part of a dynamic interacting environmental system. Environmental deterioration has occurred and is accelerating with adverse effects especially on the west coast.

The intensively developed south and west coast beaches of Barbados have a general post-settlement and recent erosional history due to the degradation and destruction of beach vegetation and inshore fringing coral reefs. The south and west coasts were generally accretional prior to settlement of the island. Convergence of data collected during this study suggests that extensive shallow water coral mortality followed the clearing of the land for sugar cane monoculture. Torrential storm runoff, soil erosion and turbidity accompanying "The Great Hurricanes" may have resulted in the loss of live coral on the inshore fringing reefs and significant shore change.

Accelerated shallow and deeper water coral mortality on the south and west coasts during the past two decades appears to have been coincidental with increasing coastal urbanization and improvements of storm and wastewater drainage systems and introduction of coastal sewage outfalls. Superimposed on these factors are effluent disposal from rum plants, industrial outfalls, and the enrichment of the coastal groundwater circulation not only by wastewater disposal in the soil environment but also to a lesser extent by leaching of fertilizers from the inland canefields. Evidence of eutrophication (nutrient enrichment) in the coastal beach environment is widespread and includes green algal blooms, anaerobic sediments, foul odours, poor underwater visibility and the displacement of live coral on the shallow reefs by crustose algae. Souvenir collectors, boat anchors, periodic dredging, and coastal structures are also factors in reduction of the living coral cover.

Long term protection of Barbados' leeward sandy beaches requires the improvement of water quality in the coastal zone and re-establishment of healthy coral communities. Short term structural beach protection measures will be effective only in the context of long term water quality improvement. Clean up of the coastal environment will make Barbados a more desirable tourist destination and protect its valuable beach resources and improve the quality of life for its residents.

SEDIMENTOLOGY OF THE LATE PLEISTOCENE IRONSHORE FORMATION ON GRAND CAYMAN

HUNTER, Ian G., and JONES, Brian, Department of Geology, University of Alberta, Edmonton, Alberta, Canada T6G 2E3

The Ironshore Formation on Grand Cayman comprises Facies A-G which were deposited in the Ironshore Lagoon. Facies A-F are temporal equivalents; Facies G is a later filling of the lagoon.

Facies A, restricted to the eastern end of the lagoon, consists of abundant bivalves in a matrix of moderately sorted carbonate silt and very fine grained sand. These allochems are predominantly cryptocrystalline grains (recrystallized skeletal grains), *Halimeda*, and benthic foraminifera. Facies B, deposited throughout most of the Ironshore Lagoon, consists of abundant bivalves in a matrix of poorly sorted carbonate sand and silt, composed predominantly of cryptocrystalline grains and *Halimeda*.

Facies C includes a series of patch reefs, which formed near the westward opening of the lagoon. These patch reefs, from 2-3 m to over 300 m in diameter, are dominated by *Montastrea, Diploria, Porites, Siderastrea,* and *Agaricia*. The larger patch reefs, which show a distinct zonation, have a higher diversity than the smaller patch reefs, which are commonly monospecific. Facies D, consisting of carbonate sands and silts, was deposited between the patch reefs.

Facies E comprises a diverse assemblage of corals, similar to those in the patch reefs, but also containing *Meandrina, Acropora, Pocillopora,* and *Dendrogyra*. These corals grew in a reef tract across the western edge of the lagoon, in a back reef environment. Facies F, which consists of well sorted skeletal sands or ooids, crosses Facies E, and is a series of channels through the reef tract.

Facies G consists of oolitic limestones that probably formed in a quiet water setting. This facies was the last filling of the lagoon and overlies Facies C, D and E. The oolitic limestones, with marine trace fossils, are found up to 4 m above present day sea level, indicating that sea level was at least 4 m above present day sea level during the late Pleistocene on Grand Cayman.

POSICIÓN ESTRATIGRÁFICA DE LOS RUDISTAS DE CAMAGÜEY, CUBA

ITURRALDE-VINENT, M., TORRE, A. de la, Museo Nacional de Historia Natural "Felipe Poey", Capitolio Nacional, CUBA

Los yacimientos de rudistas del territorio camagüeyano se encuentran en dos paleoambientes distintos: como parte de un banco carbonatado perteneciente a la margen continental mesozoica de Las Bahamas, y como intercalaciones de calizas en una secuencia efusivo-vulcanógeno-sedimentaria propia de un antiguo archipiélago volcánico.

En el banco carbonatado hay un biostroma con Biradiolites moretownensis de edad ?Campaniano a Maestrichtiano, así como varios horizontes de calciruditas con fragmentos de radiolítidos de mayor antigüedad.

La secuencia efusivo-vulcanógeno-sedimentaria cretácica incluye lavas, tobas, tufitas y varios horizontes de calizas biógenas con rudistas. El nivel más antiguo es del Albiano e incluye Sabinia sp., Tepeyacia corrugata e Ichthyosarcolitas sp. Le sigue probablemente un horizonte con Durania curasavica, D. lopeztrigoi, Vaccinites macgillavri, Torreites tschoppi y Praebarrettia coralli. La ausencia de foraminíferos orbitoidales hace suponer que se trata de un horizonte del Coniaciano ? al Santoniano. Otro nivel con rudistas incluye Barrettia monilifera, Parastroma sanchezi, Antillocaprina acutodentata, Biradiolites acuticostatus, Lapeirousia nicholasi y los foraminíferos orbitoidales Pseudorbitoides sp. y Sulcoperculina sp. Esta asociación puede datarse del Campaniano, pero quizás se extienda al Santoniano.

Discordante sobre la anterior secuencia se encuentra un conglomerado y potente banco de calizas del Campaniano tardío al Maestrichtiano con Biradiolites moretownensis, Titanosarcolites giganteus, Mitrocaprina tschoppi, Antillocaprina annulata, Bournonia thiadensis, Praebarrettia sparcilirata, Bournonia cancellata, Parastroma guitarti y foraminíferos orbitoidales.

VEGETATIVE AND GEOMORPHIC PATTERNS IN RELATION TO MASS WASTING IN A MONTANE-TROPICAL FOREST, PUERTO RICO

CLIFF R. HUPP, USGS, Nashville Tennessee, MANUEL GUARIGUATA, Yale University, and ANGEL J. TORRES, USGS, San Juan, Puerto Rico

An analysis of woody-species distribution was related to aspect, slope declivity, elevation, and landslide features. The study area is located on mountainous slopes of the Caribbean National Forest, Puerto Rico, where landsliding may be the most important surficial-geomorphic agent. Rainfall in excess of 3000 mm per year facilitates the development of diorite derived, saprolite soils, up to 20 m thick, whose weathering profiles strongly affect modes of slope failure. Forty-nine canopy-tree species were identified along transects ranging in elevation from 150 to 800 meters. No significant relations were observed between vegetation pattern and aspect. Vegetation patterns are most affected by slope declivity and elevation; vegetal variation with elevation is well documented and only discussed here to avoid spurious geomorphic interpretation. Mountain palm (Prestoea montana) is strongly associated with concave-upward slopes, having the highest importance values (relative frequency, basal area, and density) in 88 percent of cove transects; it frequently occurs in water-logged soils and on saturated landslide-disturbed surfaces. Convex-upward and intermediate linear slopes tend to have fewer palms and support Micropholis and Cyrilla, at higher elevations (600 - 800 m) where landsliding is most common. Cyrilla, and certain Micropholis and Clusia species are largely restricted to ridge and convex-upward slopes and appear to reflect long periods of slope stability. Thus, most landslide activity may occur in concave-upward slopes. Microtopographic features associated with rotational slumps, debris avalanches, and earthflows affect large-scale species patterns; tree ferns, Cecropia, and Didymopanax tend to dominate during the early stages of landslide regrowth. Trends of basal area and stem density may reflect time since last landslide disturbance and relative stability; basal areas up to 30,170 $cm^2/400\ m^2$ occur on stable, Cyrilla dominated, linear and convex-upward slopes, and may be as low as 9,776 $cm^2/400\ m^2$ on unstable, Prestoea dominated, concave-upward slopes. Vegetation analyses in combination with detailed geomorphic and soil-mechanics analyses may provide a valuable tool in identifying areas of varying landslide susceptability.

RECONSTRUCCIÓN PALEOGEOLÓGICA DEL ARCHIPIÉLAGO VOLCÁNICO PALEOGÉNICO TEMPRANO EN CUBA

ITURRALDE-VINENT, M., Museo Nacional de Historia Natural "Felipe Poey", Capitolio Nacional, La Habana, CUBA.

En el territorio de Cuba se encuentran rocas magmáticas del Paleoceno al Eoceno Superior temprano que se pueden relacionar al arco volcánico "Los Caimanes", que se extendía desde el elevado de Nicaragua-Dorsal de los Caimanes hasta las Antillas Mayores y la Cresta de Aves.

Entre los límites de Cuba se reconocen tres elementos paleogeológicos propios de dicho arco: La zona axial del arco, la cuenca de retroarco, y la zona de influencia del arco. Ellas representan la atenuación de la actividad magmática efusiva en dirección a Cuba-Bahamas.

La zona axial del arco está presente en la Sierra Maestra y se caracteriza por la abundancia de rocas piroclásticas, lavas basálticas hasta riolíticas, y cuerpos subvolcánicos de la misma composición. También están desarrollados los cuerpos apicales de un plutón de dioritas, granodioritas, granitos, plagiogranitos y otras rocas.

La cuenca de retroarco se extiende al flanco N de la Sierra Maestra, las alturas de Moa, Cristal, Baracoa, y los valles del Cauto, Nipe y Guantánamo. Se caracteriza por la abundancia de piroclastitas medio-ácidas que se intercalan con clastitas polimícticas procedentes del N y V. Son escasos los cuerpos efusivos y subvolcánicos.

La zona de influencia del arco se extiende al resto de Cuba. Se manifiesta por las intercalaciones de tufitas de ceniza entre los sedimentos clásticos y carbonatados del Paleoceno al Eoceno Medio. Esto indica que las erupciones explosivas fueron muy frecuentes en el arco.

EVOLUTION PETROGENETIQUE COMPAREE DE LA BASSE-TERRE DE GUADELOUPE ET DE MONTSERRAT

JEREMIE, J.-J., PASCALINE, H., Université Antilles-Guyane
Laboratoire de Géochimie Volcanologie - B.P. : 592 -
97167 - Pointe-à-Pitre CEDEX - F.W.I.

L'étude comparée des schémas d'évolution de la Basse-Terre de Guadeloupe et de l'Ile de Montserrat, sur la base de critères pétrographiques et d'arguments géochronologiques, montre une similitude de l'évolution volcanologique de ces îles.
On distingue dans les deux cas, trois grands ensembles correspondant aux arrivées successives de trois masses magmatiques majeures.
Les évolutions se sont effectuées globalement du Nord vers le Sud le long d'axes de distension N-S.
Les activités volcaniques actuelles se localisent au Sud (Soufrières actives) et à l'Ouest (champs géothermiques) pour les deux îles et le long d'axes structuraux essentiellement orientés NE-SW et NW-SE.

Localisation schématique des trois ensembles (1 à 3) volcaniques en Guadeloupe (à gauche) et Montserrat (à droite)

LITHOLOGIES AND STRATIGRAPHY OF THE PERALVILLO FORMATION IN THE CERRO DE MAIMON AREA, CENTRAL DOMINICAN REPUBLIC

JIMENEZ, J., Falconbridge Dominicana C por A., Dominican Republic
LEWIS, J.F., The George Washington University, D.C., U.S.A.

Preliminary information has been obtained from field observations and drill cores in the Cerro de Maimon area on the Peralvillo Formation which extends as a 0.5 to 2 km wide belt between the El Caribe sepertinized peridotite and the Maimon (schist) Formation to the north, within the Median Belt of the Cordillera Central. The base above the peridotite consists of mafic volcanic rocks intruded by mafic intrusive bodies of variable grain size. This mafic sequence is presumably equivalent to that seen at Sabana Potrero to the east and is overlain by about 200 m of fine mafic tuffs grading into cherty tuffaceous sedimentary rocks. The sedimentary sequence dips at about 45° to the south and is overlain by mafic volcanic rocks consisting mainly of volcaniclastic tuffs and breccias but including flows of amygdaloidal basalt. Drill cores through the upper part of the section below the Maimon contact intersect brecciated recrystallized limestones with carbonaceous horizons and graded felspar-quartz-lithic sandstones and siltstones of definite sedimentary origin. Felsic volcanic rocks (dacites) also occur in the upper part of the section interspersed with the mafic volcaniclastics.

The relationship between the limestones and other calcareous units in the drill cores and the Los Banitos limestone of apparent Early Eocene age mapped by Bowin (1966) has yet to be determined. The contact with the Maimon schists is faulted, and is characterized in drill cores by a 5 - 10 m thick gauge zone of predominantly sheared chloritized rock.

ETUDE DES SOLS LIES AU VOLCANISME ACTIF DES SOUFRIERES DE GUADELOUPE ET DE MONTSERRAT

JEREMIE, J.-J., PASCALINE, H. et CIMEGOTTO, D. - Université des Antilles-Guyane - Laboratoire de Géochimie Volcanologie - B.P. : 592 -
97167 - Pointe-à-Pitre CEDEX - F.W.I.

La comparaison des sols étudiés sur les appareils volcaniques de la Soufrière de Guadeloupe et de la Soufrière de Galway's à Montserrat, a montré que sous climat tropical et sur matériel andésitique peuvent se rencontrer des sols présentant des stades d'évolution très différents.
Les sols observés à la Guadeloupe sur des matériaux jeunes, sont des andosols différenciés riches en substances amorphes (allophanes), alors qu'à Montserrat se rencontrent plutôt des sols peu évolués sans présence de substances amorphes et des sols bruns eutrophes tropicaux sur des matériaux anciens.
Ces différences peuvent s'expliquer par :
- une pluviométrie plus importante à la Guadeloupe qu'à Montserrat,
- la plus grande perméabilité des matériaux volcaniques de la Guadeloupe,
- une vitesse et une intensité d'évolution plus importante en Guadeloupe qu'à Montserrat, du fait de la présence à la Soufrière de Guadeloupe de produits ayant favorisé la séquence évolutive andosolique, tels que les cendres, les lappili et les ponces très perméables, les matériaux argileux hydrothermaux hérités, les solutions acides riches en cations, en silice et en aluminium.

CRETACEOUS RUDISTID PALEOBIOGEOGRAPHY OF THE CARIBBEAN PROVINCE

JOHNSON, C.C., and KAUFFMAN, E.G., Department of Geology, University of Puerto Rico, Mayaguez, PR 00708, and Department of Geological Sciences, CB-250, University of Colorado, Boulder, CO 80309, U.S.A.

Late Jurassic-Early Cretaceous opening of the Caribbean Basin produced a new western arm of the Tropical Tethyan Sea which ultimately connected to the Pacific Ocean to form a circum-equatorial Tropical seaway. Climate models suggest that during eustatic highstand and global warming periods, with elevated atmospheric CO2, the Tropics were possibly divided into three climate/paleobiographic zones; a central zone of higher than normal temperature and salinity termed "Supertethys", flanked by northern and southern Tethyan zones similar to the modern Tropics. The development and disappearance of "Supertethys" strongly influenced paleobiogeographic evolution of Caribbean reef ecosystems. Late Jurassic and earliest Cretaceous coral-algal dominated reefs and associated communities were primarily composed of European lineages, so were the rudistid bivalves that moved into reef niches during the Barremian-Aptian. Lack of Lower Cretaceous provincialism among Caribbean reefs reflected relatively short planktotrophic larval drift distances across the spreading Atlantic ocean. Beginning in the Albian and extending throughout the Maastrichtian, Atlantic spreading exceeded larval drift distances for many coral and rudistid lineages, initiating Caribbean provincialism. Percentages of endemic taxa expanded from subprovincial grade during the middle Cretaceous to provincial grade during the late Cretaceous. Diversity, endemism and the distinctness of Caribbean paleobiogeographic subdivisions diminished during Turonian through Santonian time as a result of volcanism. Campanian through Maastrichtian radiation of rudistids gave rise to significant endemism, especially in central to southern Mexico, Jamaica, Cuba and the Greater Antilles, reflecting continued opening of the Caribbean and relative isolation of northern and possibly southern Tethyan margins. Rudistid reef ecosystems collapsed near the Middle-Late Maastrichtian boundary, at a peak in their evolutionary and paleobiogeographic radiation. Rapid cooling and collapse of the "Supertethyan" zone are proposed causes.

TITLE: PETROLEUM GEOLOGY OF THE WOODBOURNE OIL FIELDS

JOHNSON, M.R.K., and PAYNE, P.L.B., Barbados National Oil Company Limited, Woodbourne, St. Philip, Barbados.

The Woodbourne Oilfield consists of two distincts areas of production-Central Woodbourne and West Woodbourne. The two fields are divided by a minimum of six over thrust fault segments striking nort-east south-west as seen in the surface exposures of the Scotland District.

Oil and Gas Production is from Eocene and Miocene sand stones of the Scotland formation. These reservoirs are heavily interbedded with shale in upward coarsening turbiditic sequences that form complicated multi-level hydrocarbon accumulations. Huge variations in thickness, sand body orientation and geometry, reservoir quality and hydrocarbon type are attributed to the complicated depositional and structural history of the Scotland formation within the Barbados accretionary prism.

The most productive sandstone body [Basal Scotland Series] is postulated as a multistage channel deposit near the distal portion of a submarine fan that has been preserved and rests unconformably on a pelagic shale sequence. A depositional model allowing progressive overlap of distal, intermediate and proximal slope sediments within one vertical sequence, explains vertical variation and many hydrodynamically separated oil and gas reservoirs, where performance trends and reservoir continuity are different between the three main reservoir groups: The Basal Scotlands, Upper Scotlands and Intermediate Unit.

Highly productive wells within the main channel correlate with low sand/shale ratios and structually high positions. Conversely, marginal producers show poor reservoir communication and quality coupled with a low structural position. Cross folding is seen at the main structural element in influencing entrapment.

DISPERSION OF CRETACEOUS TO RECENT VOLCANIC TERRANES IN THE NORTHEAST CARIBBEAN

JOYCE, J., Department of Geology, University of Puerto Rico, Mayaguez, Puerto Rico 00709-5000

Volcanic rocks of the northeastern Caribbean are divided into 6 volcano-stratigraphic groups. The volcanic rock groups are defined as follows: the Basal Group, Late Jurassic-Early Cretaceous oceanic and island arc rocks; Arc 1 Group, middle Cretaceous island arc rocks; Arc 2 Group, Late Cretaceous-Early Tertiary island arc rocks; Arc 3 Group, middle Eocene-early Miocene island arc rocks; Arc 4 Group, Pliocene-Quaternary island arc rocks; Caribbean Group, Cretaceous-Tertiary oceanic igneous and sedimentary rocks. The distribution of these rock groups within and between islands allows for terrane distinction and reconstruction. The terrane reconstruction suggests that Puerto Rico lay south of Hispaniola and that the northern Lesser Antilles lay south of Virgin Islands in the late Eocene. Dispersion of the arc terranes occurred first between Hispaniola and Puerto Rico. Some 300-400km of strike slip translation occurred between these two islands in the late Eocene-early Oligocene. Strike slip motion of 100-150km between the Virgin Islands and the Lesser Antilles occurred during middle Oligocene-middle Miocene. Since middle Miocene about 300km of translation carried northern Hispaniola from north of Puerto Rico and the Virgin Islands to its present location. The present model of terrane dispersion is generally consistant with spreading rates in the Cayman.Trough and the location of Tertiary basins in the northeast Caribbean.

GEOLOGICAL EVOLUTION OF THE OLIGOCENE-MIOCENE BLUFF FORMATION, GRAND CAYMAN

JONES, B., HUNTER, I. G., and NG, K. C. Department of Geology, University of Alberta, Edmonton, Alberta, Canada, T6G 2E3.

The core of Grand Cayman, like the other Cayman Islands, is formed of dolostone which belongs to the Bluff Formation. On Grand Cayman a major disconformity divides it into the lower Cayman Member and the upper Pedro Castle Member.

The Cayman Member is formed of hard, massive, white, microcrystalline dolostone that contains abundant massive and branching corals, bivalves, gastropods, foraminifera, and red algae. This member has high porosity because of (1) leaching of fossils that originally had aragonitic skeletons and (2) dissolution of bedrock associated with karst development. Many of the fossil molds and caves have been partly or totally filled with caymanite (red, white and black), fossiliferous grainstone, terra rossa, and/or flowstone.

The disconformity separating the Cayman and Pedro Castle members is a distinct planar surface that was bored by sponges, worms, and bivalves and locally encrusted by red algae. Sedimentological and diagenetic evidence suggests that the Cayman Member was subaerially exposed and subjected to karst development prior to deposition of the Pedro Castle Member. Corals in the upper part of the Cayman Member suggest that it is of late Oligocene age whereas those in the Pedro Castle Member suggest a middle Miocene age.

The Pedro Castle Member is formed of relatively soft cream to white coloured dolostones that are characterized by abundant foraminifera, rhodolites, and free-living corals. Although porosity is high because of leaching of the corals there is no evidence of dissolution associated with karst development. Only small amounts of white caymanite are present in a few of the coral molds. Although terra rossa occurs in some cavities no fossiliferous grainstone or flowstone has been found.

Petrographic and geochemical evidence suggests that the original limestones of the Bluff Formation underwent only one phase of pervasive dolomitization. $^{87}Sr/^{86}Sr$ isotope ratios suggest that the dolomitization occurred approximately 2 million years ago.

Structural Geology of the West End of St. Croix, U.S.V.I.

Joyce, James, Dept. of Geology, University of Puerto Rico, Mayaguez, Puerto Rico, and Speed, R.C., Dept. of Geologcial Sciences, Northwestern University, Evanston, Illinois 60201.

Analysis of the structural features in late Cretaceous interbedded volcaniclastic sandstones and mudstones on the west end of St. Croix, U.S.V.I., indicates that the initial phase of tectonic activity produced major and minor folds. Such folds are folded about axes which plunge moderately NE-E. Minor fold axial planes and axial plane cleavage strike N50W on the average and dip moderately to the SW. The cleavage varies up to 30° from the average strike, however, within domains only a few feet in size. Several observations suggest that initial folding began before lithification. Mud appears to have flowed during folding producing mud "phacoliths" near hinges of larger minor folds. Wackes and sands also show signs of some flow during folding. Arenite beds intrude under lying mudstones by rounded load casts. The load casts are commonly elongate and define lineations on the base of arenite beds. Load cast linations parallel fold axes of the initial phase of folding, suggesting that loading and folding were contemporaneous. This phase of deformation is correlated with Speed's (1974) east end-tectonic phase 2, which produced open to tight, mainly asymmetric, minor and major folds of bedding possessing axial plane cleavage. Later-phase tectonic activity produced kinks of bedding and cleavage, chevron folds of bedding and cleavage, and faults with assorted offsets. No evidence of flow during this later phase folding was observed. Kinks are similar in orientation to some faults, and some kinks and chevron folds die out into faults. Some later phase folds and faults may have been produced by the same kinmatic event. Average axial plane cleavage attitude is constant over all areas observed indicating no later folding on scales greater than outcrop in size. Many faults strike ENE-WNW with left lateral offsets. Perhaps they are part of the distributed shear related to the Caribbean-North American plate boundary. The present analysis contradicts Whetten's (1966) structural interpretation of the west end of St. Croix wherein E-W axial plane folds have been cross folded by folds with N-S axial planes.

ECOLOGICAL EVOLUTION OF CRETACEOUS CARIBBEAN REEFS

KAUFFMAN, E.G., and JOHNSON, C.C., Department of Geological Sciences, CB-250, University of Colorado, Boulder, CO 80309, U.S.A., Department of Geology, University of Puerto Rico, Mayaguez, PR 00708

During the Cretaceous, Caribbean reefs/frameworks underwent a dramatic evolution in size, distribution, and ecologic composition. Small Lower Cretaceous bioherms and biostromes were dominated by low diversity coral-algal communities; rudistid bivalves occupied lagoonal and inner platform environments as thin lenticular biostromes of recumbent Requienliidae, Caprotinidae and early Caprinidae in paucispecific communities without persistent succession. Middle Cretaceous rudistids rapidly replaced coral-algal communities in prime reef habitats throughout the central Caribbean Tethys. Radiolitidae and Caprinidae dominated loosely-constructed frameworks, shelf margin bafflestone banks, and densely-packed inner platform bioherms with simple two to four stage successions. In northern Tethyan habitats, coral-algal dominated communities persisted in early reef development but were succeeded by caprinid/requienlid-dominated communities in latter stages. These regional differences in succession suggest both broad scale competitive displacement of corals by evolutionarily convergent rudistids, and environmental stress gradients connected with emergence of "Supertethys" (higher temperature and salinity than in normal Tropical settings) favoring more eurythermal rudistid bivalves over coral-algal community elements. Upper Cretaceous platform reefs/frameworks throughout Tethys were strongly dominated by rudistids in all biofacies; corals diversified in secondary habitats. Complex lateral and vertical ecological successions characterized Upper Cretaceous frameworks. Primitive recumbent Caprinidae formed pioneer communities, small erect to recumbent Radiolitidae formed early successor communities, and erect, densely packed (pseudocolonial) Radiolitidae and Hippuritidae formed climax communities in shelf margin and platform reefs. Specially adapted rudistids dominated small biostromal, biohermal, and bafflestone frameworks as these bivalves extensively niche-partitioned latest Cretaceous carbonate and siliciclastic platforms. Epi- and endobiont microcommunities on rudistid framework builders gradually increased in numbers, diversity and levels of microsuccession through the Cretaceous. Intra- and end-Cretaceous extinctions of rudistids decimated the ecologic structure of platform reef/framework communities at peaks in their evolution and may have been related to the breakup and disappearance of the "Supertethyan" zone associated with global cooling.

MICROPLATE TECTONICS OF THE SOUTHWESTERN CARIBBEAN MARGIN

KELLOGG, J., Department of Geological Sciences, University of South Carolina, Columbia, SC 29208, USA.

Since Middle Cretaceous time, two major oceanic island arc terranes have been accreted to the South American continental margin. Structural field studies and gravity and seismic refraction models suggest that during Late Cretaceous time, the West Andean arc was obducted eastward onto the continental margin. This obduction may have been related to the eastward movement of the Aves Ridge past the northern Andes. During Miocene time the Panama arc collided with the West Andes. The Panama arc terrane is defined by exotic Paleocene foraminiferal assemblages. Recently discovered westward verging folding and thrusting between the Western and Central Andes may be associated with the Panama collision. Continued convergence of the Nazca, Caribbean, and South American plates is being accomodated by deformation of the Panama and North Andean microplates (figure). Active folding and thrusting on the southwest Caribbean margin and Wadati-Benioff zones suggest slow amagmatic subduction of Caribbean crust beneath Panama and the North Andes. Active tectonic strain in the southwestern Caribbean is being monitored by the Central and South America (CASA) satellite GPS geodetic network.

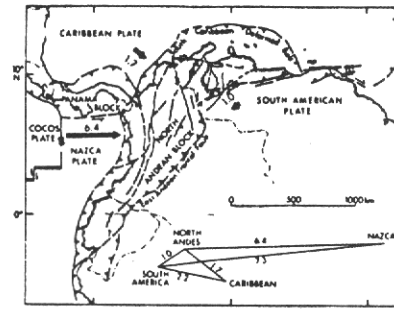

COMPOSITE ASSEMBLAGE BIOSTRATIGRAPHY OF THE CARIBBEAN PROVINCE

KAUFFMAN, E.G., JOHNSON, C.C., and SOHL, N.F., Department of Geological Sciences, CB-250, University of Colorado, Boulder, CO 80309, U.S.A., Department of Geology, University of Puerto Rico, Mayaguez, PR 00708, Paleontology and Stratigraphy Branch, U.S. Geological Survey, National Center, Reston, VA, U.S.A.

Calcareous and siliceous microplankton, ammonites and inoceramid bivalves (in siliciclastic facies), rudistid bivalves, echinoids, nerineid and actaeonellid gastropods, and larger foraminifera (in carbonate platform facies) have been used to construct independent systems of biozonation and correlation in the Tropical Caribbean Province (Tethys). These systems have been limited in resolution by episodic preservation of component taxa, incomplete systematic studies, temporal and spatial mixing of distinct siliciclastic and carbonate biofacies resulting in a lack of stratigraphic continuity of lineages, and where lineages are well known, by the maximum evolutionary rate of component taxa. A new Cretaceous biostratigraphy for the Caribbean Province has been constructed by : (1) more detailed taxonomic studies of certain common molluscan lineages (Actaeonellidae, Inoceramidae, Hippuritacea, Pectinidae and Ostreidae), yielding greater refinement of species ranges; (2) revised biostratigraphic zonations among planktonic foraminifera, nannoplankton, radiolarians and dinoflagellates originally proposed during the last decade; (3) integration of all biostratigraphically useful taxa within major facies and regions of the Caribbean using composite assemblage biozone methodology; and (4) integration of assemblage biozone data from different areas/facies of the Caribbean Province utilizing graphic correlation techniques. This has resulted in an increase in refinement of biozonation for the Caribbean Cretaceous, and more precise correlation to the highly refined biostratigraphic systems of the Western Interior and Gulf Coast regions of North America. Further refinement of Caribbean biozonations will depend upon detailed lineage studies of new groups of marine taxa, especially among Mollusca.

The Petrogenesis of the Washikemba Fm: a primitive island-arc volcanic sequence

G.Th. Klaver*, D.J. Beets** and Pl.Smedley***

*Free University PO Box 7161, 1007 MC, Amsterdam, Netherlands
**SIGO,de Boelelaan 1085, 1081 HV, Amsterdam, Netherlands
***RGD, PO Box 157, 2000 AD, Haarlem, Netherlands

The Washikemba Formation of Bonaire (late Albian to Coniacian) is an over 5 thick submarine succession of lavas, shallow intrusions and subaqeous pyroclastic flows alternating with pelagic sediments. It is estimated that the sequence was formed at a waterdepth of 3500m near the base and 1000m near the top.

The volcanics form a bimodal suite composed of andesites and "rhyolites". Based on their field occurrences the "rhyolites" can be devided in low-viscosity (LVR) and high-viscosity (HVR) types. All rocks have been weathered and altered to low-temperature mineral assemblages. However both unaltered examples of the andesites and "rhyolites" are found.

The HVR have Hyg (Hygromagmatophile elements) patterns roughly similar to those of the andesites but two to three times higher in absolute abundances. The patterns indicate derivation of the HVR from the andesites by fractional crystallization of plag, cpx, apatite and magnetite. The LVR have Hyg elemental patterns scarcely higher than those of the andesites. Unaltered LVR samples indicate an original SiO2 concentration of about 65 wt % for the LVR. Hyg elemental abundances for the altered and unaltered LVR samples are similar. This rules out derivation of the LVR from the andesites by fractional crystallization of plag, cpx, apatite and magnetite. The parental magma(s) of the LVR should have very low Hyg elemental abundances. Basalts with low Hyg elemental abundances indicative for such magmas, do occur in the Washikemba Fm but are very scarce.

DEPOSITIONAL HISTORY AND GEOCHEMISTRY OF THE MID-CRETACEOUS OCEANIC PLATEAUS

G. Th. Klaver[1] and PI Schmedley[2]

(Geomarine Center, Free University PO Box 7161. 1007 MC, Amsterdam, 2 S.I.G.O. de Boelelaan 1085, 1081 HV Amsterdam, Netherlands.

The Mid- to Late Cretaceous oceanic plateaus in the Western Pacific, Indian Ocean and Caribbean represent a major and enigmatic process of formation of oceanic crust. Oceanic plateaus differ from normal oceanic crust in terms of their thickness, extent of flows and geochemistry. Detailed stratigraphy of now on land exposed equivalents (the Curacao and Aruba lava formations) of the oceanic plateaus are here discussed. Both formations consist entirely of basaltic flows, hyaloclastites and shallow-seated sills. Piling up of the basaltic sequences occurred during a short timespan. The basal part of the Curacao lava fromation (>5000 m thick) was formed at a waterdepth of about 5 km and the presence of lapilli tuffs, well sorted conglomerates and a paleosol in the Aruba lava formation (>3000m thick) indicate subaerial volcanism. Trace element characteristics of the Curacao and Aruba lava formations resemble N-type MORB without the Nb, Ta, and LREE relative to chondrites. Nd and Sr systematics indicate that these basalites have oceanic island affinities with radiogenic isotope chracteristics similar to the Easter and Galapagos Island hotspots. Both formations are similar in trace elements and isotope ratios as the majority of the Western Pacific and Caribbean oceanic plateaus.
The narrow range in trace element composition and isotope systematics of all these oceanic plateaus indicate an episode of increased global volcanism in Mid to Late Cretaceous times

REVIEW OF THE UPPER CRETACEOUS ORBITOID LARGER FORAMINIFERA FROM JAMAICA, W.I.

KRIJNEN, J.P., Geological Survey of New South Wales, P.O. Box H5288, Sydney, NSW 20001, Australia

Larger foraminifera are known from most of the Cretaceous inliers in Jamaica. In the western Cretaceous Green Island and Grange Inliers, the Barrettia Limestone is characterized by extremely rich populations of Pseudorbitoides trechmanni. The small Green Island Inlier is the type-locality of P. trechmanni, but in addition, contains Radiorbitoides pectinatus a form regarded to belong to an evolutionary lineage diverged from the Pseudorbitoides-lineage. The revised age of the unit is Late Middle Campanian on the basis of nannoplankton.

In the Sunderland Inlier, the shales of the Sunderland Formation comprise a horizon which contains the evolutionary less advanced Pseudorbitoides chubbi. The overlying Stapleton Limestone contains an abundance of specimens identified as P. trechmanni. Rich populations of Radiorbitoides pectinatus have been described from beds both underlying and overlying the Stapelton Limestone. Based on nannofossils from the Sunderland Inlier, P. chubbi is now regarded as of approximately Middle Early Campanian age (Nannofossil zone 19a), P. trechmanni of Late Middle Campanian age (Nannofossil Zone 21b-21c), while R. pectinatus may range from Late Middle Campanian to possibly Early Late Campanian (Nannofossil Zone 21b-22a).

In the Central Inlier, marls, marly clays and rubbly limestones characterized by a foraminiferal assemblage comprising abundant Kathina, Sulcoperculina, Orbitoides, Vaughanina and minor Asterorbis. Preliminary results of statistical studies on the arrangement of neplonic chambers in Vaughanina reveal that the forms are identical to V. cubensis PALMER. The sequence is succeeded by hard brown limestone with predominantly Sulcoperculina and Chubbina caridenasansis. Throughout the sections the rudists Titanosarcolites, Antillocaprina Chiapasella and Biradiolites jamaicensis are common. The age of the sequence is now considered to range from possibly Late Campanian to Early Maastrichtian.

Two limestone horizons in the Blue Mountain Inlier contain larger foraminifer assemblages which are directly correlatable with the Barrettia Limestone unit (or Stapleton Limestone) from the Green Island-, Grange- and Sunderland Inliers, and with the Titanosarcolites horizons from the Central Inlier. The oldest unit is the Back Rio Grande Limestone which is characterized by an abundance of Pseudorbitoides trechmanni and Sulcoperculina. The fauna occurs in a soft tuffaceous horizon at the very top of 7 m thick sequence of reef-rubbly beds with Barrettia monilifera. P. trechmanni from the Back Rio Grande shows an evolutionary stage of the juvenarium identical to that in forms of Green Island, and a similar Late Middle Campanian age is suggested. The Rio Grande Limestone is an approximately 80 m thick calcarenitic to rubbly bioclastic limestone unit in which spectacular reefs of Distefanella mooretownensis, various species of Titanosarcolites and radiolitids occur in specific beds in the succession. Larger foraminifera comprise an assemblage of abundant Sulcoperculina, Orbitoides, Vaughanina, Vaughanina and to lesser extent Pseudorbitoides. In all the occurrences Pseudorbitoides is regarded to be represented by lis species P. rutteni , which may point to a Maastrichtian age of the Rio Grande Limestone.

Nd-isotopes of authigenic sediments as tracers for the Plate-Tectonic reconstruction of the Caribbean Plate

G.Th. Klaver, J. Smit and C.J. Beets
Free University PO Box 7161, 1007 MC, Amsterdam, Netherlands

All recent Plate-Tectonic reconstuctions for the Caribbean assume that the Caribbean Plate did not form in the present gap between North and South America but rather is a detached part of the Farallon Plate

One way to support this fundamental assumption is to look at the Nd isotopes of authigenic sediments (Cherts, limestones and fish bones). Recent work has shown that Nd isotopic ratios of authigenic sediments from the Pacific and Atlantic are different. This difference in Nd isotopes started at the opening of the Atlantic. It is therefore proposed to measure the Nd isotopic composition of authigenic sediments in a number of time slices to see the change from Pacific towards Atlantic (or specific Caribbean) values. Moreover do the changes in Nd isotopes correspond with major changes in the Plate Tectonic configuration of the Caribbean Plate?

A Pacific origin for the Caribbean Plate has also important consequences for the Cretaceous Tertiary Boundary (KTB). Because of the continuous subduction of the Pacific Plate under the N/S American Continent, little is known about the KTB in the Eastern Pacific. The Caribbean Plate is possibly the only way to obtain information about, for instance, fluxes and integrated amount of iridium , distribution of shocked minerals and K/T spherules, and eventual amount and fluxes of volcanic material in the Eastern Pacific.

To achieve the above objectives we propose to drill a complete section (double HPC/XCB/RCB) through the sedimentary cover, possibly in a number of short overlapping holes in the Venezuelan and/or Colombian basins above B". Basement drilling in these sites can further be used to identify the age and nature of the B" basaltic basement.

THE SEDIMENTOLOGY AND PATROLOGY OF THE HERRERA SANDSTONES OF TRINIDAD W.I.

H.B. Kuarsingh Ph.D. (Lond).,
TRINIDAD AND TOBAGO OIL CO. Pointe-a-Pierre,TRINIDAD, W.I..

Sedimentological and petrological examination of the Herrera sandstones of Trinidad show that these sand bodies were deposited from turbidity currents and are thus turbidites. They were sourced from the North or North West and occur as a series of small turbidite fans (a few kilometers in diameter) trending South West to North East.

The rocks are mostly lith-arenite with occasional quartz-arenite. The principal constituents are quatz, chert, lithic fragments and calcite. The principal accessories are feldsspars and glauconite. The rocks are minerogically immature. Porosity ranges from 0% to 20%. Clasticity index ranges from 0.1 mm to 1.2 mm. Generally the rocks are grain supported, matrix support being very rare.

The rocks have a complex diagenetic history with at least four phases of mineral growth or alteration. There were at least two invasive fluid phases, an earlier acidic phase which led to quartz growth and a later basic phase which led to calcite growth and porosity occulation.

COAL IN THE CARIBBEAN REGION

LANDIS, E.R., and WEAVER, J.N., U.S. Geological Survey, Denver, CO 80225; and CARTER, M.D., and WOOD, G.H., Jr., U.S. Geological Survey, Reston, VA 22092

Coals have been known in the Caribbean Region since 1850, or earlier, and attempts at recovery and utilization began shortly thereafter. Only in Colombia and Venezuela has coal ever been an important part of the nation's energy program. In most of the other nations of the region, the indigenous coal has never been mined to any extent. With increased energy demand, the traditional energy sources such as firewood and wood charcoal, have been replaced, in part, by imported petroleum products. Alternative indigenous sources of energy, such as coal and peat, deserve consideration and investigation.

An extensive literature search provided data for more than 235 locations where coal is known or reported to occur in the Caribbean Region. Most of these locations are in northern South America (108) and Central America (92) with the remainder (37) scattered through the Antillean island nations.

The reported coal locations in the northern part of South America are well explored compared to the coal areas of Central America and the Antillean islands. This is indicated by the distribution of the estimated identified-hypothetical coal resource potential of the region. Of the estimated total of about 11 billion tons, about 10.9 billion are in Colombia, Venezuela and Trinidad, about 350 million tons are in Central America and less than 160 million tons in the Antilles. It must be emphasized that the coal resource data in Central America and the Antilles are incomplete and both the geologic framework and coal quality information are inadequate for a definitive resource assessment in those areas. The required modification of the cited estimates awaits detailed exploration studies.

The 19° Fault, the Mona Canyon Graben, and the Neotectonics of the Puerto Rico Trench

LARUE, D.K., Department of Geology, R.U.M., Mayaguez, PR 00708

The South Samana Bay and Septentrional fault zones of northern Hispaniola can be traced offshore to the east where they are coincident with the Puerto Rico scarp. The Puerto Rico scarp extends to the east, bending around the northwest-trending Main Ridge of the Puerto Rico trench area. The Samana/Septentrional fault zone and its extension as the Puerto Rico scarp is here named the 19° fault, because of its latitudinal position. The fault was previously recognized as one that separates a blueschist terrane from an arc terrane. Motion on the fault zone is problematic: most workers in northern Hispaniola insist that the fault is left-lateral. However, the Mona Canyon, a Plio-Pleistocene graben, crosses the 19° fault, yet is only vertically offset, not laterally, indicating only down-to-the-north motion on the fault. Interestingly, the Mona Canyon graben changes direction across the fault, from north-trending south of the fault, to northwest-trending, north of the fault. GLORIA studies of the Puerto Rico trench to the north of the fault by the U.S. Geological Survey indicate the presence of linear features interpreted to represent strike-slip faults. It is possible that the 19° fault is presently a normal fault near and to the east of the Mona Canyon, and that left-lateral shear is distributed between the fault and the trench, resulting in the rotation of the Mona Canyon graben without appreciable offset. Similarly, the northeast-trending Anomalous Block to the east of the Mona Canyon may have been originally an east-west trending feature. Although the 19° fault east of the Mona Canyon is now a dominantly normal fault, in the past it exhibited strike-slip motion, as indicated by the juxtaposition of different terranes across the fault. The fault makes a releasing bend around the Main Ridge, and basins to the west of the Main Ridge may represent pull-apart or fault-divergence basins, and not true trench-slope basins as was previously proposed. These studies indicate that the Puerto Rico trench is a much more complicated feature than previously thought, and that more neotectonic studies are needed to further resolve the evolution of the region since the Miocene.

EXTENSIONAL ALLOCTHON IN THE MONA PASSAGE

LARUE, D., K., Dept. of Geology, R.U.M., Mayaguez, P.R. 00708

Active normal faults are widespread in the Mona Passage, as seen from an abundance of seismic reflection records on the eastern (Puerto Rican) part of the passage. Normal faults have arcuate shapes with scarp lengths up to 10's of kms, and rotation accompanies deformation in most cases. Faults with greatest displacement are along the Desecheo Escarpment, and the southern part of the Mona Canyon. Displacement seems to be consistently north-south. Maximum vertical and horizontal offsets are several kms. Age of faulting is probably Pliocene to Now, as evidenced from dredge haul data and information from submersibles. The zone of normal faulting can be traced eastward, onto Puerto Rico, where it extends from Aguadilla to approximately Ponce. The extension of the normal fault zone to the west is uncertain, owing to limited data, but may include the Yuma basin, or extend south of the Yuma basin. I propose, based on balanced cross-section constructions, that the normal faults lie above a decollement at approximately 6 kms depth, defining an extensional allochthon. This extensional allocthon toes into the Muertos Trough. The presence of this extensional allochthon helps explain some of the tectonic, seismic and geologic diversity of the eastern Greater Antilles. Another extensional allochthon(s) may be present south of eastern Puerto Rico, in the Whiting basin.

SEDIMENT TRANSPORT ALONG THE BARBADOS COAST

LAWSON, D.E.[a], and HUNTER, G.T.[b]
[a]University of Waterloo, [b]Hunter and Associates, Toronto Canada

The littoral drift systems of the Barbados south coast and west coast are "pulse" driven. Large swells and tropical storms mechanically erode the reef system and also resuspend the biologically eroded reef sediments. Shoreline-refracted storm swell transports these sediments into the nearshore zone. Major sand influxes are cyclical with periods of a decade or more. On the west coast, south-westerly swell opposes northern swell "pulses" of littoral drift. On the south coast, littoral and nearshore drift is generally to the west but local beach cell reversals occur.

Very angular, clear quartz found within the fine sand fraction of the east coast carbonate sands serves as a unique tracer indicating coastal counter-clockwise sediment transport. Transport occurs from the east coast around the northern tip of the island with gradual southerly fall off in abundance downdrift along the west coast.

Size analysis characteristics reinforce the southerly west coast transport interpretation and are suggestive of pulses. Along the southwest coast, relict southeasterly transport paths are indicated. Along the southeast coast, opposing southwesterly transport paths are implied.

The beach cells along the west coast are supplied from northerly littoral drift and from sediments released from local reef and backshore erosion. Sediment transport is partially localised within these smaller scale systems by fringe reefs at the headlands which act as groynes and influence the energy distribution within the cell and resultant sediment transport. Degradation of the coral population has allowed greater wave energy to encroach on the shoreline. Erosional products from the reefs and from the beaches are taken offshore by cellular circulation and are easily resuspended from offshore by storm swells.

Sand influxes from Cobbler's Reef in the 1970's contributed significantly to accretion along the south coast with westerly sediment transport trapped by artificial structures (e.g. Coast Guard Station; Milton - over 10,000 m³ of sand trapped behind breakwater during 1972).

Sediment transport calculations based on 1983/84 field measurements yielded gross transport rates of the order of 12,700 m³ per year for the west coast with a net southerly transport of approximately 7,400 m³. Dominant sediment transport from the north appears to terminate at the Prospect Bulge after which southerly systems may be dominant. Along the south coast an anomalous dominance of easterly transport (71,000 m³/yr) over westerly (33,000 m³/yr) was noted.

EROSION OF THE BARBADOS COAST

LAWSON, D.E.[1], HUNTER, G.T.[2], and HOOPER, R.[3]
[1]University of Waterloo, [2]Hunter and Associates , Toronto
[3]Memorial University

Prior to settlement, the Barbados south and west coasts were accretional. The fringing reefs and sea grass systems, the Manchineel and mangrove association backshore-vegetation formed a shoreline system that advanced seaward at rates of 1-10 m per century interrupted only by occasional severe tropical storms. The beaches were very narrow, nearly continuous, with backshore vegetation growing almost to water's edge.

Since settlement, headlands on the west coast have experienced erosion varying from 15 to 110 m with 40-50 m being common over the past three centuries (as measured by the seaward extent of beach rock and by the width of reef flats). Increasing exposure of beach rock (23% linear increase along the westcoast and 177% along the south coast from 1962-83) is strong evidence of beach retreat. Greatest recessions appear to have been associated with hurricanes prevalent during the late seventeenth to early ninteenth century. Erosion has been renewed again during the past few decades. These two periods of erosion are evidenced by older and younger beach rock at Freshwater Bay headlands and also by an intervening period of secondary coral succession on the fringe reefs. Shoreline erosion "rates" over the past three centuries on the west coast are estimated at 15 m per century with local headland rates varying from 5 to 35 m per century. Headland erosion appears to occur in "pulses" coincident with periodic intense tropical storms followed by accretional recovery cycles. Greatest recession has been observed at the headlands of Fort Denmark, Folkstone, and Freshwater Bay. At many locations the backshore has been "fixed", anchored by revetments and beach structures. As a result, the beaches are rapidly thinning downdrift and are frequently interrupted by eroding foreshores depleted of sands. This discontinuity is a relatively recent phenomenon. Partial removal of beach structures (eg. Golden Palms, Barbados Beach Village) has resulted in marked rejuvenation of the downdrift beaches.

The south coast has been mainly erosional during the post-settlement period. Hurricanes have caused considerable damage resulting in extensive modifications of the shoreline especially at Dover Point where a coastal roadway has been lost and tombolos and embayments appeared and disappeared. Hurricane Janet (1955) made much sediment available for south coast littoral drift during the past two decades. Sea walls and groynes were installed on the south coast throughout this century. The resultant, structurally-trapped artificial beaches do not offer the degree of tropical storm protection provided by natural coral reef-protected and vegetated shorelines. Beach erosion continues in those areas not protected by seaward structures or nature.

Beach profile measurements (1983-84) indicate values of recession and sweep zone widths far in excess of the previous post-settlement rates of beach recessions.

AN EVALUATION OF THE DEPTH OF EMPLACEMENT OF GRANITOID PLUTONIC ROCKS IN THE EASTERN GREATER ANTILLES

LIDIAK, Edward G., Department of Geology and Planetary Science, University of Pittsburgh, Pittsburgh, PA 15260

Electron-microprobe analyses of magmatic hornblendes from granitoid rocks of the San Lorenzo batholith, the Virgin Islands batholith, the batholith on Vieques island, the Utuado pluton, the Morovis stock, the Rio Blanco stock, and other unnamed intrusions in the eastern Greater Antilles have been carried out for the purpose of estimating the pressures at which these intrusions were emplaced. The intrusions have calc-alkalic chemical affinities and consist mainly of quartz diorite, granodiorite, or quartz monzonite. The hornblendes typically occur in association with quartz, plagioclase, K-feldspar, biotite (±), Fe-Ti oxides, and sphene (±).

Utilizing an empirical hornblende geobarometer (Hammarstrom and Zen, 1986, American Mineralogist, v. 71, p. 1297-1313; Hollister and others, 1987, American Mineralogist, v. 72, p. 231-239), the total Al contents of the hornblendes suggest that the intrusions were emplaced at low to medium pressures which correspond to depths of less than about 10 kilometers. Similar pressures of intrusion have been estimated from the metamorphic contact aureoles adjacent to the Virgin Islands and San Lorenzo batholiths. These geobarometric data help characterize the crust in the eastern Greater Antilles and place constraints on minimum crustal thickness in late Cretaceous and early Tertiary time.

DID THE GREATER ANTILLES ISLAND ARC REVERSE SUBDUCTION POLARITY IN LATE CRETACEOUS TIME?

LEBRON, M.C., and PERFIT, M.R., Department of Geology, University of Florida, Gainesville, FL 32611

Several previous workers have postulated a reversal of subduction polarity or "flipping" of the intraoceanic Greater Antilles island arc in Late Cretaceous time. This reversal in subduction polarity from northeast-dipping to southwest-dipping is attributed to attempted subduction of the buoyant oceanic plateau crust, which now outcrops in Cuba, Hispaniola and Puerto Rico beneath the southern Greater Antilles arc. Subsequently, southwestward subduction of oceanic crust of the Atlantic Ocean led to the Eocene collision between the Bahama Platform and the Greater Antilles arc and sudden Eocene cessation of arc activity.

Data used by previous workers to support a Late Cretaceous reversal in subduction polarity include: 1) the present geographic distribution of presumed paired metamorphic belts; 2) compilation of mainly K-Ar radiometric ages from which temporal clusters of ages are assumed to represent major metamorphic events resulting from collision and subduction reversal; and 3) the age, history and composition of arc volcanism in the Greater Antilles.

In order to address the subduction polarity question, we have studied the age, history and composition of Late Cretaceous arc rocks in the little-deformed Cordillera Oriental of eastern Hispaniola. Our studies and those of Bourdon (1985) have shown that the oldest arc rocks (Guamira Basalts) are pre-Aptian in age and consist mainly of mafic tholeiitic volcanic rocks typical of the Primitive Island Arc (PIA) rock suite. These rocks were uplifted and eroded in pre-Aptian time and are unconformably overlain by 200-300 m of shallow-marine limestone. This limestone is overlain by post-Aptian to Maestrichtian intermediate to felsic pyroclastic rocks with calc-alkaline affinities (Loma La Vega Volcanics).

Compilation of results by previous workers in Puerto Rico, Cuba, and other areas of Hispaniola indicate a similar Late Cretaceous arc history punctuated in Aptian-Albian time by uplift and deposition of shallow-marine limestone. We interpret the regional change in magma types from PIA and CA as reflecting a reversal in subduction polarity from northeast-dipping to southwest-dipping. Compositional variation may result from Aptian-Albian reorganization of the arc mantle and the type of sediment subducted (Atlantic vs. Pacific).

METALLOGENESIS OF BASE AND PRECIOUS METALS IN NORTHERN HAITI

K. LOUCA M.SC., PH.D.

LOUCA, K., U.N. Revolving Fund for Natural Resources Exploration, 1 United Nations Plaza, New York, NY 10017

Northern Haiti is dominated by the Massif du Nord, a major anticlinal structure which represents the northwestern extension of Cordillera Central, the "backbone" of the Hispaniola segment of the Greater Antilles Cretaceous-Early Tertiary calc-alkaline volcanic arc. The core of the Massif du Nord is made of the widespread Loma de Cabrera batholith, partly floated by Pre-Albian ophiolite suite rocks, black shale units and Mid-Upper Cretaceous andesitic volcano-sedimentary series. Its periphery is marked by a more or less continuous belt of Upper Cretaceous, intermediate to felsic volcano-sedimentary series (La Mine Series) bordered by the overlying Trois Rivières flysh series and Tertiary limestones.

A spectrum of base and precious metal deposits in the Massif du Nord, is spatially and genetically related to two types of high-level magmatic systems, each characterized by distinct lithologies, alteration assemblages, mineral and geochemical associations. The first system is centered on quartz diorite porphyry stocks, high-level periplutoruc intrusions of the tonalite batholith, emplaced in Pre-Albian formations and in the deeper zones of the Upper Cretaceous andesitic volcanic pile. Mineral deposits related to this system comprise porphyry copper-bearing stocks, limestone replacement deposits (Cu-Au-Ag skarns) copper-rich veins and auriferous quartz veins. Examples of these deposits are Douvray and Blondin with reserves of 200 million tonnes at 0.6 %, Cu and 100 million tonnes at 0.5% Cu respectively, Mémé former undergound mine with potential resource of 3.5 million tonnes at 2% Cu, 1.8g/t Au, 10g/t Ag and Faille B gold deposit with drill indicated reserves of 520,000 tonnes grading 14.1g/t Au.

The second major system sits higher in the stratigraphic sequence and represents epithermal polymetallic mineralization associated with dacitic subvolcanic stocks hosted by the La Mine Upper Cretaceous volcano-sedimentary series. Mineralization exhibits volcano-tectonic fracture control and features strong Cu-Zn-Pb-Au-Ag-baryte associations and enrichment in Hg-As-Mo. The maximum gold and silver contents reported from this type of mineralization are 48.5g/t Au and 640g/t Ag. Mineralization is characterized by large halo of argillic alteration containing zones of chalcedony silica alteration, sulphide stockworks, massive powder-fine pyritization, barite veins, baryte-sulphide lenses and stratabound replacements. Gold oxide deposits associated with this type of mineralization are Morne Bossa and Grand Bois with 2 million at 2.2g/t Au and 4.5 million tonnes at 3.0g/t Au respectively.

PRENEOMORPHIC DIAGENESIS OF CORALS FROM A SUBAERIALLY EXPOSED HOLOCENE REEF, ENRIQUILLO VALLEY, DOMINICAN REPUBLIC

LOVE, K., and WORONOW, A., Department of Geosciences, University of Houston, Houston, TX, 77204-5503.

Analyses of major, minor, and trace elements in corals from a subaerially exposed Holocene reef indicate that significant chemical changes occur prior to the neomorphic transformation from aragonite to calcite. Characterization of these chemical changes affords vital information for 1) interpreting diagenetic environments from postneomorphic chemistries of originally aragonitic constituents; 2) interpreting more realistic chemical "baselines" from petrographically pristine constituents; and 3) discerning the mechanisms by which the preneomorphic changes proceed. In order to characterize the changes, new statistical techniques specific to "closed" data (such as geochemical data) have been used. A suite of corals consisting of thirteen different species, still wholly aragonitic, was collected from an emergent reef in the Enriquillo Valley, Dominican Republic. These corals are being compared chemically, species by species, to living corals from several reefs off the western coast of Puerto Rico. The Puerto Rican reefs were selected because they closely resemble the sediment-stressed conditions inferred for the fossil reef in the Dominican Republic. The Dominican Republic reef was selected as the fossil reef of study due to the excellent preservation of the corals and because the geologic history of the reef is well-documented, allowing chemical changes to be related to a priori information about diagenetic environments. Both the preneomorphic chemical changes and possible mechanisms will be discussed.

SANTONIAN FORAMINIFERA FROM COLOMBIA

J. Ignacio MARTINEZ, Ingeominas, Diag. 53 N°34-53, Bogotá, Colombia S.A.

During a long time it was suggested the lack of Santonian rocks in Colombia excepting some sparse references on Lenticeras baltai-Paralenticeras sieveri a scanty ammonite assemblage found together with Texanites texanus. A rich planktic foraminifera assemblage was found at five localities spread all over Colombia. This fauna consists mainly of Rosita fornicata, Dicarinella asymetrica, D. concavata, Whiteinella inornata, Marginotruncana sinuosa, ? M pseudolinneiana, and Hastigerinoides alexanderi among others. This finding is the first micropalaeontological reference for the Santonian of Colombia, and its biostratigraphic reliability appears to be more practical than those biostratigraphic schemes based on macrofossils.
In the same way, this assemblage has important palaeobiogeographic implications. It allows, for instance to precise the boundary between two previously proposed microfaunal provinces from Central Colombia (Upper Magdalena and Bogotá). The Girardot area, located along this boundary, is characterized by abundant buliminids and rare planktics and suggests shallower conditions than the other samples that are composed enterely of planktic foraminifera. Abundant keeled forms occur, for example, in the Leiva area suggesting offshore (relatively deep water) and anoxic bottom conditions in contrast to previous interpretations that suggested nearshore conditions.

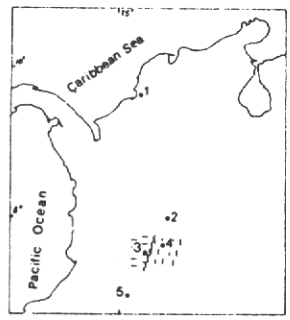

1:100,000 SCALE, GEOLOGIC-TECTONIC COMPILATION MAP, CROSS SECTIONS, AND REGIONAL STRATIGRAPHIC SYNTHESIS OF THE DOMINICAN REPUBLIC

MANN, P., Institute for Geophysics, Univ. of Texas at Austin, Austin, TX 78759; DRAPER, G., Dept. of Geology, Florida International Univ., Miami, FL 33199; LEWIS, J., Dept. of Geology, George Washington Univ., Washington, DC 20052; LEBRON, M.C., Dept. of Geology, Univ. of Florida, Gainesville, FL 32611; DE ZOETEN, R., Unocal International Oil and Gas Division, Los Angeles, CA 90051; HEUBECK, C., Dept. of Geology, Stanford Univ., Stanford, CA 94305; and DOLAN, J.F., U.S. Geological Survey, Menlo Park, CA 94025

The island of Hispaniola is a critical area for understanding the geologic history of the northern Caribbean: 1) the island forms the second largest landmass in the Greater Antilles and completely straddles the 200-250 km wide, present-day North America-Caribbean strike-slip plate boundary zone; 2) rapid late Neogene uplift and deep levels of erosion expose an early Cretaceous-middle Eocene intraoceanic island arc and associated near-arc basins and accretionary prisms; and 3) younger late Eocene-Pleistocene strike-slip-related basins are either exposed in areas of late Neogene uplift or are known from recently released oil company seismic data and exploration wells.

We have prepared a geologic-tectonic compilation map of the eastern two-thirds of the island of Hispaniola (Dominican Republic). The map is divided into four sheets and is accompanied by five regional cross sections and stratigraphic correlation charts. A scale of 1:100,000 was selected in order to display individual structural measurements as well as paleontologic sample sites. A topographic and UTM grid base is used to facilitate use of the map in the field. The map displays lithostratigraphic units (formations, members, etc.) and attempts to maintain as much as possible the stratigraphic nomenclature of early workers. Data sources for the compilation includes over 60 published and unpublished maps, reports, theses, and our own unpublished field data.

The compilation map, sections, and stratigraphic correlations help constrain the geologic history of the following features: 1) Cenozoic juxtaposition of early Cretaceous-middle Eocene intraoceanic island arc terranes across WNW-striking, high-angle faults; 2) extent and structural style of early Miocene-Present fold-and-thrust-belt in central and southwestern Hispaniola; and 3) onshore extension of strike-slip faults related to present-day North America-Caribbean plate motion.

INTRAPLATE DEFORMATIONS IN THE WESTERN CARIBBEAN.

A. MASCLE; Institut Français du Pétrole, BP 311, 92 506, Rueil-Malmaison, France.

Most of the deformations related to the relative displacement of the Caribbean plate with respect to the surrounding plates are taking place along active plate bounderies, either convergent or transcurrent. In the western Caribbean, however, deformations are also taking place in the Caribbean plate itself. Large folds are being formed in the western Colombian Basin together with rifting and transcurrent faulting along the southwestern and southern edge of the Nicaragua Rise.

Some evidence of these deformations is shown by a few seismic profiles shot a few years ago by french oil companies (ELF-Aquitaine, TOTAL-CFP and IFP). They suggest that a new plate boundary is now developing along the southern edge of the Nicaragua Rise. It seems to branch off the main Northern Caribbean plate boundary east of Jamaica, to follow the trend of the Pedro Bank-Bajo Nuevo fault zone and to include the Providencia Trough. Its connection with the Central American active margins however ispoorly understood for the moment.

THE SOUTHEASTERN CARIBBEAN CORNER: A TRIPLE JUNCTION BETWEEN CONVERGENT, TRANSCURRENT AND PASSIVE MARGINS.

A.MASCLE; IFP, BP 311, 92106, Rueil-Malmaison, France. S.GOUYET; ELF-Aquitaine, 64018, Pau, France. T.ROSSI; ELF-Aquitaine, La Défense cedex 45, 92078, Paris-La Défense, France. Ch.BECK; University of Lille, 59655, Villeneuve d'Ascq, France.

Multichannel seismic profiles, field data, and a few wells from the oil industry have been used to prepare regional sections across the passive and active margins of the Southeastern Caribbean Corner. Three margins currently form an active triple junction in the vicinity of Trinidad.

To the south, the Guyana passive margin and the Demerara Rise show three main stages of subsidence that occured in Jurassic-early Cretaceous, Late Cretaceous-Paleogene, and Neogene times. To the north, the southern edge of the Barbados Ridge currently involves the distal part of the Orinoco deep sea fan, with wide eastward verging anticlines, intervening piggyback basins and a few E-W dextral faults. To the west, the southeastern Caribbean margin results from transcurrent dextral shearing and oblique collision between the Lesser Antilles Island arc and the northern South American margin.

A particular feature of the onshore and offshore thrust belts around Trinidad is the presence of mud volcanoes. Overpressuring at depth could result from the difficulty the water has in escaping from the clays when the main compressive stresses are horizontal. Such a stress pattern will prevent the opening of vertical tensional gashes along which the primary migration of water is believed to occur in sediments with initially low permeability.

STRATIGRAPHY AND TECTONIC ANALYSIS OF THE SERRANIA DE TRUJILLO IN THE BOUNDARY OF MARACAIBO BASIN, FALCON RANGE AND CARIBBEAN CHAIN, N W VENEZUELA.

X. MATHIEU *, J.F. STEPHAN **

*: *GIS " Océanologie et Géodynamique", 6, Avenue Le Gorgeu 29287 Brest Cedex FRANCE.*

**: *Institut Géodynamique URA 720 Université de Nice Sophia Antipolis. Parc Valrose 06034 Nice FRANCE.*

The Serrania de Trujillo-Ziruma lies to the East of the Maracaibo Basin, at the junction of three structural provinces : the allochthonous Caribbean Chain (E), the autochthonous of Maracaibo Basin (W), and the Oligo-Miocene Falcon Basin (NE). The Burro Negro fault is an important feature in the studied area since it separates 2 structural trends ; the first corresponds to the southern block with a NW-SE trend. A NE-SW to N-S structural trend is observed near the Valera major Fault zone. Apart from the Jurassic-Cretaceous tectonic wedge situated along the left lateral Valera strike-slip fault zone, the sedimentary deposits that form the Serrania are Tertiary in age. Above the Upper Paleocene shaly limestone, three major sedimentary cycles can be observed. The turbiditic sequences of the Lower Eocene (Fm. Trujillo) are characterized by two conglomeratic levels and olistoliths of cretaceous limestones, and represent the distal flysch of the Lara Complex (allochthonous Caribbean Chain). During the Middle Eocene, Maracaibo Basin fluvio-deltaic complex prograded towards the NE (Fm. Misoa). The Upper Middle Eocene transgression (Agua Negra Group) occurs on deformed structures, (N 160 E Middle Eocene compressive phase).

The Upper Eocene-Oligocene records two tectonic events : a major compressive phase N 110 E and a minor N 20 E.

In Lower Miocene (Burdigalian), the Falcon Basin transgression begins with the sandstone feeding. The major compressive phase (N 130-140 E) which occurs at the end of the Miocene, has reorganized the eocene folds.

The Plio-Quaternary andean uplifting affects the Serrania, showing two tectonic events E-W and N 170 E. The Serrania de Trujillo-Ziruma represents an allochthonous range, with a complex tectonic history, according to a NW-SE to SW-NE compressive stress pattern.

Ref. : MATHIEU X., (1989).- Analyse stratigraphique et tectonique de la Serrania de Trujillo aux confins du Bassin de Maracaïbo, de la chaine du Falcon, et de la Chaine Caraïbe, au N W du Vénézuela. *PhD. thesis* University of Brest, France, June 1989.

GEOLOGICAL MAP OF THE CARIBBEAN

A. Mascle, I.F.P., BP 311, Rueil-Malmaison, France

P. Letouzey, BEICIP, BP 311, Rueil-Malmaison, France

This new geological map of the Caribbean (1:2,500,000th scale) is expected to be published in 1989.

The map has been prepared at the Institut Français du Pétrole, with the collaboration of BEICIP, IFREMER, Elf Aquitaine and Total-Compagnie Française des Pétroles. Special attention has been given to the onshore and offshore sedimentary basins.

A small booklet will accompany the map to explain the structure and evolution of the Caribbean margins.

BIOSTRATIGRAPHY, AND PALEOECOLOGIC SIGNIFICANCE OF CALCAREOUS-SILICEOUS FACIES OF THE NEOGENE MONTPELIER FORMATION, NORTHEASTERN JAMAICA.

MAURRASSE, Florentin J-M.R. Department of Geology Florida International University University Park Campus Miami, Florida 33199, U.S.A.

The Spring Garden Member of the Montpelier Formation exposed on the northeastern coast of Jamaica at Buff Bay includes an interval of calcareous-siliceous facies composed of abundant sponges spicules with varying amount of radiolaria. Triaxon and Tetraxon spicules of the Hyalospongea group dominate the biogenic silica components (60-99%), whereas radiolarian assemblages are empoverished to well diversified. Index radiolarian taxa such as Calocycletta costata, Dorcadospyris dentata and Liriospyris globosa at the base of the exposed outcrop indicates a minimum age of late Early Miocene, Calocycletta costata radiolarian zone, for the occurrence of the calcareous-siliceous facies. This age is in agreement with the foraminiferal assemblage at this level, which comprises Globigerinatella insueta, Globoratalia peripheroronda and Globigerinoides sicanus (without Praeorbulina glomerosa) indicative of the Globigerinatella insueta foraminiferal zone. Therefore the base of the sequence lies within zone N7 or N8 of Banner and Blow.

The upper limit of the calcareous-siliceous facies lies within the upper part of the Brachyospyris alata radiolarian zone of early Middle Miocene age, as indicated by the presence of the nominate radiolarian taxon of the zone, and the absence of Cannartus violina, Calocycletta costata and Cyclampterium lepterum. This zone corresponds to the upper part of the Globoratalia peripheroronda foraminiferal zone as shown by the presence of Globigerinoides sicanus, Orbulina universa, Globoratalia praemenardii, and the absence of Globigerinatella insueta (Zone 8-9 of Banner and Blow). This calcareous-siliceous facies is interpreted to have developed over a neritopelagic bank influenced by strong bottom current, a situation that finds its modern analog in the present area of the Hatton Bank and Rockall Plateau where subsurface flow of the North Atlantic Deep Water (NADW) controls high productivity of Hyalospongia. Radiolaria productivity was irregular and controlled by dynamic divergence which occurred in relation to the paleophysiography of the bank as well as forcing mechanisms associated with minor climatic fluctuations of that time.

EARLY METEORIC DIAGENESIS OF CARBONATE SANDS AT OCEAN BIGHT, GREAT EXUMA ISLAND, BAHAMAS

McCLAIN, M.E., and SWART, P.K., MGG/RSMAS, University of Miami, 4600 Rickenbacker C'way, Miami, FL 33149.

Ocean Bight contains a Holocene strand-plain, deposited in a pocket between two Pleistocene headlands on the island of Great Exuma, Bahamas. Like many similar deposits throughout the Bahamas, the plain consists of multiple ridge and trough couplets which trend parallel to the modern shoreline and represent repeated episodes of beach accretion. Very fine to coarse grained bioclastic carbonate sands compose the deposit. Grain types include coral, green algae (Halimeda sp.), mollusc, coralline algae, and foraminifera fragments. The strand-plain contains a lens of fresh ground water with areal dimensions corresponding to those of the Holocene deposit (~1.5 km^2) and a maximum thickness in excess of 6 meters. As a result of the presence of fresh ground water, diagenetic processes are altering the existing metastable mineral assemblage to low-magnesian calcite. Cementation associated with this alteration is found to occur in the vadose and upper phreatic zones, and is often exposed at ridge crests where deflationary processes have unearthed vadose cementation. In the vadose zone, cementation appears at approximately 10cm below the ground surface. Here, cementation is irregular and somewhat mottled in appearance. Areas of cement are routinely interrupted by areas of completely uncemented, organic rich sands with abundant plant roots. Mottled vadose cement grades downward into more pervasive, fabric selective cement. This transformation occurs within 20cm of the water table (~1-1.5m subsurface). Following this transformation, pervasive cementation usually continues into the upper phreatic zone. An unexpected transformation occurs, however, at depths ranging from 2-3m below the water table. Pervasive void filling cement gives way to a virtual absence of cement despite the presence of fresh ground waters. Of the seven wells drilled into the deposit, all encountered this uncemented zone and further showed it to continue to the Holocene/Pleistocene contact. One explanation for this observation is that the oxidation of organic matter by sulfate derived from aerosols causes a reduction in pH and a consequent undersaturation with respect to all carbonate species. This hypothesis is supported by pH measurements and a strong smell of H_2S. Further analyses of alkalinity, calcium, sulfate, and chloride concentrations should confirm this interpretation.

SEA LEVEL INDUCED EROSIONAL EVENTS IN PLATFORM/PERIPLATFORM SEDIMENTS, AND THE FORMATION OF LOWSTAND DEPOSITS

McNEILL, D.F., RSMAS/University of Miami, Fisher Island Station, Miami Beach, Florida 33139 U.S.A.

Net accumulation curves for Bahamian platform and periplatform carbonates are used to elucidate, with good time control, a regional scale erosional event believed to be triggered by sea level regression. Magnetostratigraphic dating of cores from Little Bahama Bank and San Salvador in conjunction with nearby biostratigraphically and magnetostratigraphically dated periplatform cores collected by the Ocean Drilling Program Leg 101 (sites 633, 630), allow comparison of periods of accumulation and erosion (see figures). These two periplatform cores (and 4 additional ODP cores) show an erosional gap from about 2.2 to over 3.0 Ma, whereas the platform record shows the onset of subaerial exposure at about 2.8 Ma, continuing to about 0.8 Ma. Overlap of these two profiles suggests that a regional scale erosional event, likely slope failure as an avalanching gravity flow, occurred just after initial exposure of the platform between 2.8-2.2 Ma. Net accumulation curves suggest that this event occurred after a prolonged highstand capable of producing and storing large quantities of uncemented sediment. Following the concept of Crevello & Schlager (1980), this large sediment reservoir may have loaded the platform margin and upper slope as sea level and wave base regressed. These data suggest that initial lowering of sea level triggered this regional erosion event on the platform flanks thus moving periplatform sediment basinward, although other triggering mechanisms are possible (i.e. tectonic). This sequence of events may partially explain the lowstand deposits in seismic profiles of pure carbonate environments.

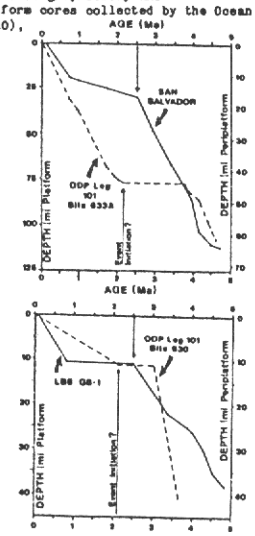

FORAMINIFERA, PALEOENVIRONMENTS, AND BASIN EVOLUTION, S.W. DOMINICAN REPUBLIC

MCLAUGHLIN, P.P., and SEN GUPTA, B.K., Department of Geology and Geophysics, Louisiana State University, Baton Rouge LA 70803

The Azua Basin is an elongate, thrust-fault bounded synclinal sedimentary trough filled with over 2,500 m of Miocene and Pliocene marine sedimentary rocks. The lower part of the sequence reflects a change from a deep carbonate basin setting, represented by the Sombrerito Formation, to a prograding turbidite regime, represented by the Trinchera Formation. The Sombrerito ranges from lower Miocene (Globigerinatella insueta chronozone) to middle Miocene (Globorotalia fohsi robusta c.z.), and its Ojo Largo Member spans the middle-upper Miocene boundary (Globorotalia mayeri c.z. to lower Globorotalia acostaensis c.z.). The Trinchera spans an interval from near the middle-upper Miocene boundary (Globorotalia menardii or Globorotalia acostaensis c.z.) to the lower Pliocene (Globorotalia margaritae c.z.). The upper part of the sequence reflects a transition from shallow-marine to lagoonal paleoenvironments. The Quita Coraza Formation lies in the lower Pliocene (Globorotalia margaritae c.z.). The lower part of the Arroyo Blanco Formation ranges from uppermost Miocene (upper Globorotalia humerosa c.z.) to lower or middle Pliocene (Globorotalia margaritae or Globorotalia miocenica c.z.).

Principal components analysis of rich benthic foraminiferal faunas aided in the recognition of significant species associations based on the loading of species on six factors. Factor 1 represents an uppermost bathyal assemblage, with strong positive factor loadings on Bolivina minima (0.68), Cassidulina norcrossi var. australis (0.73), and Cyroidina regularis (0.71). Lower bathyal species such as Pleurostomella alternans (-0.64), Bolivina peula (-0.62), and Cibicides wuellerstorfi (-0.49) show strong negative loadings. Factor 2 represents middle to upper bathyal assemblages; Oridorsalis umbonatus (0.68), Hoeglundina elegans (0.57), and Uvigerina peregrina (0.51) all have strong positive loadings. Factors 3, 4, and 5 all have positive loadings of neritic species. Factor 3 represents a middle to outer neritic assemblage that includes Angulogerina jamaicensis (0.83), Cassidulina subglobosa (0.59), Cassidulina carinata (0.64), and Cibicidoides pachyderma forma subtilitorella (0.51). Factor 4 has heavy loadings on inner neritic species including Haynesina depressula (0.74), Buliminella elegantissima (0.73), and Roselina concinna (0.66). Species having strong associations with Factor 5 include Cancris sagra (0.69), and Bolivina lowmani (0.59). Factor 6 represents a current-winnowed assemblage. Plots of the factor scores in the stratigraphic sections demonstrate shoaling upward from lower bathyal to inner neritic depths, this trend is paralleled by decreasing diversity and by lithofacies progressions. Cluster analysis reveals seven major sample groupings that correspond almost directly to the faunal zones identified in the Azua Basin by Bermudez (1949).

Placed within the biostratigraphic framework for the basin, the benthic foraminiferal trends indicate migration of paleoenvironments toward the Caribbean during the Miocene and Pliocene, paralleled by a similar time-transgression of lithofacies. This suggests that basin evolution has been controlled by tectonic activity along the northern boundary of the Caribbean Plate, and that it proceeded in two stages: 1) a tectonically quiet open ocean stage before the late Miocene; 2) a subsequent tectonically-active, laterally-constrained clastic basin stage. The large volumes of clastics laid down during stage 2 indicate uplift and erosion of the Cordillera Central. The axis-parallel paleocurrents in the Azua Basin suggest contemporaneous uplift of the Sierra de Neiba as the laterally constraining structure. These events are interpreted to represent rapid filling of a "ramp valley" basin by sediments derived from the uplift of the nearby Cordillera Central, coincident with activation of the Hispaniola restraining bend in the late Miocene.

FROM A VOLCANIC CRISIS TO A VOLCANIC HAZARD ASSESSMENT PROGRAM: THE GUATEMALAN CASE

MERCADO, R. and ROSE, W.I., Michigan Technological University, Houghton, MI 49931 (906-487-2714).

In June, 1986 we undertook an emergency hazard assessment of Tacaná Volcano, Guatemala at the request of the United Nations Disaster Relief Organization. Very little was known about Tacaná, but the start of fumarolic and seismic activity gave rise to fears that a major eruption may take place. Hazard maps and assessments were made and will appear in a forecoming issue of GEOFISICA INTERNACIONAL. Although only minor phreatic eruptions took place, this activity heightened fears concerning the much more active Pacaya, Fuego, and Santiaguito volcanoes. It was clearly seen that hazard assessments were much better carried out on a preventive, rather than an emergency, basis.

Six months later another volcanic crisis occurred in Guatemala as Pacaya had a series of explosive eruptions. The USGS, in cooperation with Instituto Nacional de Sismología, Vulcanología, Meteorología e Hidrología (INSIVUMEH), did a preliminary hazard assessment of Pacaya in February, 1987. Shortly afterwards, the Agency for International Development, USGS, and INSIVUMEH formalized an agreement to develop a local capability for volcanic monitoring and hazard assessment in Guatemala. Because of our familiarity with Guatemalan volcanoes, our group at Michigan Tech was asked to do the hazard assessments and train the Guatemalans in this work. Assessments for the frequently active Fuego and Santiaguito volcanoes have been carried out, in addition to reconnaissance work on the identification of volcanic collapse deposits in the Highlands of Guatemala. A geologist from INSIVUMEH spent 7 weeks at Michigan Tech and at the Cascades and Hawaiian Volcano Observatories getting intense training on volcanological work.

The project is on its second year, but some important issues remain unsolved. Logistic problems are considerable (e.g., obtaining visas for Guatemalan scientists to visit the States for training). Coordination of 3 different bureaucracies (INSIVUMEH, AID, USGS) is also a source of delays (e.g., field seasons can last 8-10 weeks, yet rules at INSIVUMEH allow only 30 field-days for any given project). Local data gathering can be an exercise in frustration (e.g., data from other Guatemalan agencies is almost impossible to obtain). Inter-institutional and personal rivalries in Guatemala also result in slowing down the hazard work. These problems are being addressed and, although not fully solved yet, we have reasons to believe the hazard assessment program in Guatemala will be a success.

VOLCANIC HAZARD ASSESSMENT OF TACANA, FUEGO, AND SANTIAGUITO VOLCANOES, GUATEMALA

MERCADO, R. and ROSE, W.I., Michigan Technological University, Houghton, Mi 49931 (906-487-2714).
MATIAS, O. and GIRON, J., Sección de Vulcanología, INSIVUMEH, 7a Avenida 14-57 Zona 13, Guatemala

Volcanic hazards are a serious concern in Guatemala, a country with several dozen active volcanoes and a population which is concentrated in the same areas. Fuego, Santiaguito and Pacaya are frequently active; Tacaná has given signs of renewing eruptive activity; Tajumulco, Cerro Quemado, Atitlán, and Acatenango have been active in historic times. A program of systematic hazard mapping is currently in effect. We have made hazard maps for Tacaná, Fuego, and Santiaguito. The USGS carried out the assessment for Pacaya.

Tacaná is an andesitic volcano with no historic record of magmatic eruptive activity. Last magmatic activity occurred several centuries ago judging by the degree of revegetation of lava flows. The historic record suggests a pattern of periods of seismic/fumarolic activity spaced 1/4 to 1/2 century apart. At least 2 dacitic prehistoric plinian deposits were discovered. Serious hazards are likely when a magmatic eruption occurs causing ashfall, lava flows, lahars and floods. Evacuation of this remote area will be difficult. Settlement patterns at Tacaná do not indicate any perception of possible volcanic hazards.

Fuego is a frequently active stratovolcano characterized by mafic vertical eruptions from the summit crater accompanied by pyroclastic flows. Last major eruption occurred in 1974; fumarolic activity has characterized the past decade. A radial pattern of pyroclastic flow and lahar hazard zones controlled by the summit crater rim geometry is observed. Lahar and flooding hazards are considerable, and extend at least 25 km to the south. The frequent activity has controlled settlement patterns; the most hazardous areas are uninhabited.

Santiaguito is a continuously active dacitic dome located in the 1902 eruption crater of Santa María volcano. Activity is characterized by 1-5 small ash eruptions/hr from Caliente vent, and avalanching from a 5 km long lava flow. Hazard zonation is controlled by the assymetrical southward slope of basement topography, parallel drainages, and very high rainfall. The 1902 crater symmetry also directs hazards southward. The 1929 dome collapse and associated pyroclastic flows killed as many as 5000 people. In recent years Santiaguito's continued extrusion has triggered extensive lahars and flooding along rivers south of the dome, affecting several towns.

Ashfall hazards are controlled by the seasonal dependence of wind directions, with easterly winds prevailing from June to November, and westerly winds from December to May. Ashfall from Fuego could affect Antigua and Guatemala City, even in the case of minor activity.

All 3 of these volcanoes have a possibility of edifice collapse. Fuego has collapsed twice in the past, producing large debris avalanches. Tacaná is characterized by prominent faulting which could suggest collapse and Santa María's 1902 crater forms a dramatically oversteepened scarp facing SW.

EVOLUCION DE LA ESTRUCTURA DEL MACIZO DE ESCAMBRAY

MILLAN Trujillo, G., Instituto de Geología y Paleontología, Calzada #851 Esquina A y 4, Vedado 4, Plaza de la Revolución, Cuba

Las secuencias jurásico-cretácicas del macizo del Escambray conformaron primeramente una sucesión de nappes y escamas apilados uno sobre el otro, destacandose 6 nappes principales (el más superior se emplazó posteriormente) y diferentes tipos de secuencias. Luego se sometieron a un proceso metamórfico con la ocurrencia de 5 fases (6 etapas) de plegamiento, cada una de las cuales se asocia con un sistema de esquistosidad o olivaje con sus tendencias definidas. El estilo de los pliegues varía en dependencia de la fase y del área; sus órdenes alcanzan hasta muchos centenares de metros. La fase 1 dió lugar a una esquistocidad con una tendencia NE a N-NE y pliegues isoclinales. La fase 2 conformó 2 grandes antiformas con una estrecha sin forma intermedia que se acuna hacia el Norte. La occidental es cupular elongada hacia el NO; mientras que la oriental está elongada más hacia el N-NO, desapareciendo al norte para formar parte del plan estructural de la primera. El sistema de esquistosidad relacional conforma a las antiformas y se asocia con pliegues isoclinales. En ambas antiformas se destaca otra esquistosidad más tardía en su parte axial, dispuesta concordantemente con sus ejes de elongación. La fase 3 - se dispone siguiendo una tendencia arqueada independiente en cada megaestructura. Esta fue intensa en la antiforma occidental y su efecto incrementó el desarrollo de la sinforma hacia el Norte. Las fases 4 y 5 imprimieron la elongación final hacia el O-NO de las antiformas. Finalmente las rocas fueron intensamente fracturadas. Las secuencias primarias del macizo se depositaron en un margen continental. Su apilamiento en nappes, metamorfismo y plegamientos asociados, son consecuencia de una colisión ocurrida en el Cretácico Superior entre este margen y el arco volcánico cretácico; en la parte basal de este último ya se disponía el complejo antibolítico Mabujina (CM). Debido a ello estas secuencias intracorrieron debajo del CM, metamorfizándose y multiplegandose en condiciones de un bajo gradiente temperatura/presión. El CM fue deformado conjuntamente con las mismas y su parte basal parcialmente reelaborada por el metamorfismo. Al desaparecer el estado compresivo vinculado con la colisión, las 2 megaestructuras positivas emergieron en forma diapírica, atravesando las rocas más densas del CM durante la búsqueda del equilibrio gravitacional.

GREAT BAHAMA BANK WHITINGS: CHEMICAL EVIDENCE FOR DIRECT PRECIPITATION

MEYERS, J.B., SWART, P.K., and BURNS, S.J., Univ. of Miami - MGG/RSMAS, University of Miami, 4600 Rickenbacker Causeway, Miami, FL, 33149. SHINN, E.A., and LIDZ, B., U.S. Geological Survey, Fisher Island Station, Miami Beach, FL, 33139. STEINEN, R.P., Dept. of Geology, Univ. of Connecticut, Storrs, CT, 06269-2045.

Whitings are milky clouds of water, rich in suspended carbonate mud, that drift amongst clear waters in carbonate environments. The formation of whitings on the Great Bahama Bank has long been a subject of controversy. Various workers have suggested that whitings can be produced either from direct precipitation or as a result of resuspension of bottom sediment by fish.

In order to further constrain the origin of whitings we have measured changes in alkalinity and pH between the whitings and adjacent 'clear' waters. Sampling was carried out during July and August, 1988, in an area west of Andros (25°00'N lat. 78°45'W lon.) on Great Bahama Bank. Seawater filtrates were later analyzed for chlorophyll concentrations.

Similar to previous workers (Morse, 1984, JGR, 89:3604), we observed a decrease in alkalinity across the bank, consistent with a gradual removal of $CaCO_3$ either as an inorganic or organic precipitate. Individual whitings revealed conflicting results. In some whitings sharp decreases in alkalinity were observed relative to adjacent clear bank waters. In other instances, either slight increases in alkalinity, or no changes were observed. In a previous study, (Morse, 1984) no significant differences in alkalinity were detected between waters inside and outside whitings. One possible explanation for these results is that changes in saturation within the whitings are produced through photosynthetic activity. The process of photosynthesis removes CO_2 thereby increasing pH and supersaturation with respect to calcium carbonate. The resultant change in saturation causes $CaCO_3$ to precipitate and alkalinity to decrease. The varying results in our and previous studies could be explained by differing amounts of photosynthesis and respiration in the whitings at the time of sampling. In support of this idea we note that chlorophyll concentrations were three to four times higher in the whitings than in the surrounding water. Such evidence may give credence to the notion that Bahama Bank whitings precipitate or are formed directly from seawater.

ESQUEMA LITOLOGO-PALEOGEOGRAFICO DE CUBA EN EL INTERVALO PALEOCENO-EOCENO MEDIO

L. MONTERO, G. FURNAZOLA, E. PEREZ, C. DIAZ, J. OHO, P. MEDEROS.

Instituto de Geología y Paleontología
Calzada #851 Esquina A & 4, Vedado 4, Plaza de la Revolucion
La Habana, CUBA

Este esquema se ha confeccionado con el objetivo de que sirva de base para la localización de áreas perspectivas para fosforitas, rocas fosfóricas y prospección de ellas en sedimentos de edad Paleoceno-Eoceno Medio, considerando que en sedimentos de la misma edad se encuentran grandes yacimientos de esta materia prima en la Península de Florida.

Para la preparación de este esquema se estudiaron las siguientes cuencas: Los Palacios, Bahía Honda, Vegas-Mercedes, Santo Domingo, Cienfuegos, Trinidad, Cabaiguan, Cuenca Central, Cauto-Nipe y Guantánamo, analizando las formaciones geológicas que en ellas se encuentran para la descriminación de aquellas con mayores perspectivas.

Los autores consideran que además de la zona occidental de nuestro territorio, donde es conocido el yacimiento La Pimienta, debe centrarse la atención, en los horizontes carbonatados - clásticos de la Cuenca Central que yacen transgresivamente sobre los granitoides que contienen apatito como mineral accesorio y en formaciones de la zona oriental en cuyos espesores toman parte algunas calizas que contienen abundante material órgano-detrítico, además hay otras unidades litoestratigráficas que presentan interés desde el punto de vista facial y genético para la futura prospección de rocas fosfáticas.

También presentan cierto interés, algunas formaciones de la Cuenca Santo Domingo compuestas por secuencias clásticas y carbonatadas que sufrieron la acción de la actividad hidrotermal.

Asimismo en las regiones de Madruga, Cabañas y bahía Honda se conocen secuencias terrígeno-clásticas y carbonatadas donde existen manifestaciones hidrotermales que pudieran acarrear soluciones fosfáticas.

Horizontes con condiciones favorables para la solución de esta materia prima han sido sugeridos para las demás cuencas con menor perspectividad que las antes mencionadas.

EOCENE SHALLOW WATER CARBONATE FACIES WITH LARGER FORAMINIFERA IN THE CAÑO ACCRETIONARY COMPLEX, CAÑO ISLAND AND OSA PENINSULA (COSTA RICA, CENTRAL AMERICA)

MORA, C.*, BAUMGARTNER, P.O.*, and HOTTINGER, L.**
* Institut de Géologie, BFSH 2, CH-1015 Lausanne (Switzerland).
** Geologisches Institut, Bernoullistr. 32, CH-4056 Basel (Switzerland).

The Caño Island is located at the shelf edge 15 km NW off the Osa Peninsula (Bahía Drake, see figure) and 20 km NE of the axis of the Middle American trench, which forms the boundary between the subducting Cocos plate and the Caribbean plate. The island is entirely built by a pervasively tectonized mélange of sedimentary rocks. Massive dark green mylonitic mafic volcanic greywacke (90%) dominate over pelagic limestone, chert and redeposited shallow water carbonates (together 10%) which occur as single dm- to m-sized blocks or in shear-bounded, highly deformed 1-20 m thick bouldery (boudinaged) layers with transitional contacts to the greywacke matrix. These layers are interpreted as tectonized debris flows or turbidites.

On the NE and SE coasts of Caño Island (figure: 1) redeposited shallow water material occurs in isolated blocks of calcarenites and calcirudites showing clasts of lime packstones, grainstones and bindstones and grains of basalt, chert, K-feldspar, and chlorite. The limestone clasts contain the following bioclasts: articulate corralline algae (dominant), larger foraminifera, smaller planktonic and benthic foraminifera, crinoids, siliceous sponge spicules, bryozoans and green algae. The clasts show stylolitized contacts and several phases of fracturing and vein infil by opal-quartz and then calcite. Similar outcrops of shallow water material occur along the NW coast of Osa: Playa Colorado (Bahía Drake, Azema et al. 1983), Punta San José (figure: 2), San Pedrillo and Punta Llorona (figure: 3).

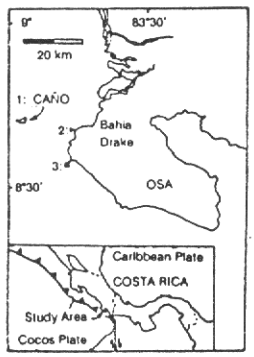

Although the larger foraminifera found at the studied localities are recrystallized, partly silicified and fractured, several different assemblages could be identified (locality number in parentheses): *Amphistegina grimsdalei* (1), *Amphistegina lopeztrigoi* (1), *Amphistegina parvula* (1), *Amphistegina pregrimsdalei* (3), *Amphistegina* sp. (2), *Asterocyclina* sp. (1), *Boreloides* (2), *Discocyclina* sp. (1, 2, 3), *Eoconuloides* sp. (1, 3), *Eolabiania cushmani* (1), *Eolabiania* sp. (1), *Fabiania cubensis* (1, 3), *Helicostegina dimorpha* (3), *Helicostegina polygiralis* (3), *Helicostegina* sp. (2, 3), *Lepidocyclina* sp. (1), *Linderina* sp. (1, 3) *Nummulites floridensis* (1), *Pararotalia* sp. (1), *Sphaerogypsina globulus* (1). These assemblages indicate a middle Eocene age (2, 3) and late Eocene age (1) with reworking of middle Eocene forms.

The intensely deformed sedimentary mélanges found on Caño and Osa are interpreted as arc-derived volcanoclastic slope deposits with associated lime turbidites/debris flows derived from ephemeral platforms. These sediments may represent a trench fill which became accreted to the Middle American arc in post-Eocene times.

TECTONOSTRATIGRAPHY OF THE SAN FRANCISCO RIDGE AREA IN THE NORTHEASTERN CIBAO VALLEY, DOMINICAN REPUBLIC.

NADAI, AGATHE C., Greendale Rd.,Scaredale, N.Y.10583.

Neogene strata exposed along the San Francisco Ridge (SFR as named by the author), which is near the city of San Francisco de Macoris in northeastern Hispaniola record the tectonostratigraphic evolution of a former marine basin, the present day Cibao Valley, which is adjacent to a now uplifted subduction complex, the Cordillera Septentrional. Deep-water calciclastic strata of Miocene age are unconformably overlain by shallow-marine carbonate strata of early Pliocene age. These strata are in turn unconformably overlain by mainly fluvial channel deposits of later Pliocene age or younger.

In the SFR, Miocene strata are folded and faulted which indicates that uplift and deformation occurred since latest Miocene time. The intense deformational event ceased by early Pliocene time as indicated by the much less deformed Pliocene strata. A Pliocene or later deformational event resulted in the present relief of the SFR as evidenced by the broad warping of the Pliocene strata over the SFR.

DOS TIPOS DE COMPLEJOS ULTRABASICOS EN LA ESTRUCTURA DE CUBA ORIENTAL

MOSSAKOVSKI, A.A., NEDRASOV, G.E., SHAVIRINA, M.V., (Instituto de Geología de la Academic de Ciencias de la URSS). ORO J.R. and FLORES R.M., (Instituto de Geología y Paleontología del Minbas, Cuba).

Las ultrabasitas del primer tipo pertenecen a ofiolíticas del Mesozoico Tardío, presentes en las unidades estructurales inferiores de la zona Auras y del alóctono Moa-Baracoa. Estos alóctonos ofiolíticos y tradicionalmente se han considerado como fragmentos de la litosfera de la cuenca oceánica del norte de Cuba y no serán discutidos aquí. Las ultrabasitas del segundo tipo están representadas por cuerpos embudiformes que se hunden verticalmente a gran profundidad, bordeados por campos de cuerpos tabulares, turbiditas y brechas ultrabásicas. Un ejemplo de este tipo de cuerpos ultrabasicos lo constituyen los macizos de Sierra de Nipe y Sierra del Cristal. Este último transiciona hacia el este a una alternancia de ultrabasitas y brechas ultrabásicas, las cuales, a su vez, pasan más al este al flysch de la Formación Mícara, el cual contiene horizontes de brechas, turbiditas ultrabásicas y olistostromas. En contenido de minerales de alta temperatura de las dunitas y harzburgitas del río Arroyón, de fragmentos de hiperbasitas concentrico zonadas con una orla de estructuras columnares radiales (indicador de enfriamiento rápido), indican que el emplazamiento de las rocas ultrabásicas en los depositos de flysch pudo haber concurrido en forma de un diapiro del manto en estado caliente, el cual sufrió desintegración y estratificación del material incandescente de su núcleo en el proceso de salida hacia los horizontes superiores de la corteza terrestre, como resultado de un "choque" térmico y descompresión. Entonces, en forma de una másа fragmentada extrusiva fue exprimido hacia la superficie, a través de una envoltura relativamente fría, produciendo una serie de flujos de brechas y turbiditas ultrabásicas hacia la cuenca de deposición de la Formación Mícara. Esta asociación constituye fragmentos de basamento ultrabásico y de la cobertura flysch-olistostrómica de la depresión suboceanica Cauto-Nipe. La depresión Cauto-Nipe surgio en el Campaniano Superior-Maestrichtiano Inferior en una zona de rift que provocó la apertura de los complejos del arco insular cubano y de la corteza oceanica de la cuenca del Norte de Cuba. Precisamente con la apertura de esta estructura transversal se vincula el sentido del movimiento del alóctono Moa-Baracoa, inverso con relación al sector central de Cuba. Esta zona de apertura representaba, probablemente, la continuación de las fallas de transformación del Atlantico y constituida, al mismo tiempo, el eje de apertura de la Cuenca de Yucatán, cuyos marcos temporales de desarrollo coinciden con los de la depresión Cauto-Nipe.

FORENSIC GEOLOGY: NEW APPLICATIONS OF STANDARD PROCEDURES

NAGLE, Frederick, Department of Geological Sciences, University of Miami, P.O. Box 249176, Coral Gables, Fl 33124.

Two recent court cases involved the theft of cargo and the substitution of sand for the original cargo. In the first case a "piggy-back" cargo container arrived in Miami having traveled by truck from Paraguay to Santos, Brazil and then by freighter to several ports in Brazil and on to Miami. When the container arrived in Miami it was sealed and its papers were in order, the weight having been checked several times enroute. When the container was opened, however, the original cargo was seen to have been replaced by sand. One of several insurance companies was liable but the problem was which one? The question was, where had the switch taken place?

In the second case, a cargo container arrived in Argentina having been shipped from Miami, and again the original cargo had been replaced by sand either in the Miami area or in and around Buenos Aires, Argentina. It was important to the court in Argentina to know whether the switch was done in Miami or Buenos Aires.

In both cases, since the tonnage of sand involved was fairly large, the assumption was made that the sand was taken from a local source near where the switch had taken place. Therefore the problem was to fingerprint these sands and tie them to some local source. The easiest way to do this, it seemed to me, was to do a provenance study by standard grain size analysis and thin section studies and then to try to match the sands to samples in the field. Some likely source areas were selected and others eliminated by studying the route of cargo travel on geologic maps and reference sand samples in the extensive collection at the Department of Geological Sciences, University of Miami and samples from the collections of Dr. Paul Potter at the University of Cincinnati. Both cases were settled on the basis of these studies.

AUTOCTONIA O ALOCTONIA DE LA FAJA DE VILLA DE CURA. UN DEBATE HISTORICO.

NAVARRO, Enrique, Facultad de Ingeniería. Depto. de Geología, Universidad Central de Venezuela, Caracas, Venezuela.

El Grupo Villa de Cura del norte de Venezuela, fué definido como unidad litoestratigráfica por Shagam (1960). Menéndez (1965) y Jarvis (1966) postularon su origen alóctono, lo cual de hecho implicó proponer su formación en algún lugar al norte de la Cordillera de la Costa ("venezuelan northern coast range") y su posterior deslizamiento gravitacional hacia el sur durante el Cretácico tardío - Paleoceno. Para los autores citados, esta hipótesis fué necesaria a fin de explicar los aspectos siguientes: a) El ambiente de depositación de la Formación Paracotos, b) la aparente similitud litológica entre las formaciones Paracotos y Mucaria, c) el supuesto plegamiento pre-Paleoceno evidente tan solo a lo largo del cinturón de Paracotos y en el lado sur del bloque de Villa de Cura y d) supuesta evidencia indicativa de que la fuente de sedimentos del Grupo Caracas fué esencialmente granítica y se encontraba al sur. Autores más recientes han mantenido el mismo criterio sin proporcionar datos adicionales que permitiesen sustentar, más allá de la especulación geológica, la hipótesis mencionada. En contraposición Talukdar *et al.* (1982), Navarro (1983), Ostos y Navarro (1986), Navarro *et al.* (1987a, 1987b, 1988) y Navarro (1988) argumentan en favor de la autoctonía del Grupo Villa de Cura, apoyándose en datos geoquímicos, petrológicos, estructurales y geocronológicos, los cuales permiten explicar el origen del bloque partiendo de un marco tectónico completamente diferente, el cual se basa en la generación de una pequeña cuenca oceánica por expansión en el borde norte del cratón de Guayana (de acuerdo a evidencia presentada por Feo Codecido *et al.*, 1984), en la cual se formaron las rocas correspondientes al grupo citado y unidades asociadas.

TOXIC SUBSTANCES IN THE COASTAL ENVIRONMENT OF THE U S VIRGIN ISLANDS, 1986

COSTDAM, B.L., Millersville University, Millersville PA

Bottom sediment samples collected in March 1986 from four major impact areas off the U S Virgin Islands during the pilot phase of a two-tiered investigation were analyzed for all 129 USEPA priority toxic substances.
Since all organics proved to be below detection limits, the emphasis of the second phase, July/August 1986, was on the 13 USEPA priority toxic trace elements in sediments and seawater sampled from 24 stations around the three major islands: (9 each off St Thomas and St Croix, 6 off St John)

Elevated concentration levels were detected for Ni, Pb, Hg, Zn and Cu, in decreasing order. The rank by overall degree of marine pollution was St Croix >St Thomas >St John. HOVIC Harbor, St Croix, was the most impacted site, showing a heavy degree of pollution by Zn, Cu, Hg and Cr.
The St Thomas Harbors, as well as Gallows Bay, St Croix, were moderately to heavily polluted by Cu, Zn and Pb. Mangrove Lagoon and Benner Bay, St Thomas, were anomalously high in Ni (765 ppm) in sediment, and in Hg (2.5 ppb) in seawater, respectively.
Maximum levels off St John were generally one or more orders of magnitude below those of the other two islands.

Very low toxic concentrations were found at the St Croix STP outfall. Although toxics at the St Thomas STP outfall showed higher concentrations, they were well below levels found both at other USVI sites and at other sewage disposal areas off US mainland coasts.
Concentrations of trace elements in sediments and waters near the VAPA desalination plants on St Thomas and St Croix were low to moderate.

Except for Ni, very poor correlations were found between trace elements in marine sediments and in adjacent rocks and soils. Most of the elevated levels of Cu and Zn are attributed to boat operations and marinas. Distribution of Hg and Pb shows some evidence of atmospheric input.

Comparison with USEPA toxicity criteria indicates little need for concern with levels of Cd, Cr and Zn in USVI marine sediments and seawater, while Hg, Se, Ni and As in USVI waters generally appear to exceed USEPA criteria.

POROSITY AND PERMEABILITY DEVELOPMENT IN THE OLIGOCENE-MIOCENE BLUFF FORMATION, GRAND CAYMAN.

NG, K. C., and JONES, B. Department of Geology, University of Alberta, Edmonton, Alberta, T6G 2E3.

Present day porosity and permeability in the Bluff Formation of Grand Cayman is a result of numerous constructive and destructive processes. Porosity was created by (1) preferential dissolution of aragonitic fossils, (2) solution widening of joints and fissures, (3) development of solution caverns and passages, (4) selective dissolution of the cores of dolomite rhombs, (5) microborings, and (6) tree root borings. The high permeability is related to the extensive network of joints which transect the island and the well developed karst system. Porosity and permeability destruction occurred through the (1) deposition of caymanite, grainstones, terra rossa, and (2) precipitation of speleothemic calcite and carbonate cements. The complex geological development of the porosity and permeability can, however, be deciphered by considering all aspects of the geological history of the island.

The creation and destruction of the porosity in the Bluff Formation was controlled by the interplay of climatic conditions and the successive cycles of regressions and transgressions that have affected Grand Cayman over the last 30 million years. During some regressions porosity was created since the carbonates were exposed to the influx of fresh water. At other times, however, conditions were suitable for the formation of speleothem calcite, calcite and dolomite cements and/or terra rossa and this led to porosity reduction. The onset of transgressive conditions led to porosity destruction since marine sediments were commonly brought onshore and flushed into the cavities via the well developed joint and cave systems.

The combination of constructive and destructive processes has produced a heterogeneous aquifer of which the hydraulic information is difficult to interpret. The integration of hydrogeological data, hydrochemical information and the geological evolution of the island has led to an improved understanding of the manner in which the groundwater behaves because water-rock interactions affects the hydrogeological properties of the aquifer and hence, the ground water flow. Such information is invaluable in the development and management of this valuable resource.

PRECAMBRIAN ROCKS IN THE SOUTHERN EDGE OF THE CARIBBEAN PLATE, VENEZUELA

Marino OSTOS, Enrique NAVARRO and Franco URBANI
Universidad Central de Venezuela, Dept. Geología, Caracas 1051, Venezuela

The Coast Range of northern Venezuela is the most important feature of the southern Caribbean plate margin. The oldest reported rocks (Rb/Sr isochrons) are the Sebastopol Complex (420 Ma, Hurley & Hess, 1972) and the Guaremal Granite (403 Ma, Urbani, 1983).

The metasedimentary rocks of the Caracas Group (Las Brisas and Las Mercedes formations) are the more extensively exposed and have paleontological ages of Late Jurassic - Early Cretaceous (Urbani, 1982). The core of the Coast Range is in part formed by granitic gneisses of the Peña de Mora Formation, previously considered to be equivalent in age with Las Brisas Formation.

Three samples of the Peña de Mora augengneiss from the type locallity and Chichiriviche (location map in Urbani & Ostos, 1989) produce the following Rb/Sr isochron:

Sample	ppm Rb	ppm Sr	$^{87}Rb/^{86}Sr$	$^{87}Sr/^{86}Sr$
PM-86-1	227.4	106.9	6.269	0.84784±0.00012
PM-86-2	227.0	83.9	7.940	0.89125±0.00014
PM-86-3	155.4	162.1	2.793	0.77486±0.00012

$^{87}Sr/^{86}Sr$ (i) = 0.71103±0.00734, best slope 0.02240±0.00121 that allows to calculate an Early Proterozoic age of 1560±83 Ma.

Rocks this old have never been previously reported in the Coast Range and introduces a new element for the interpretation of the tectonic evolution of the southern edge of the Caribbean plate and reinforces the criteria about such evolution given in Navarro *et al.* (1987).

References

Hurley, P. & H.H. Hess (1972) Basamento gnéisico, Cordillera de la Costa, Venezuela. *Circular Sociedad Venezolana Geólogos*, (54): 18.

Navarro, E.; M. Ostos & F. Yoris (1987) Síntesis de un modelo tectónico para la evolucion de la parte norte-central de Venezuela durante el Jurásico medio - Paleogeno. *Iras. Jornadas de Investigación, Facultad de Ingeniería, Univ. Central Venezuela*, Caracas, feb. 1987, *Memoria*, p. 93-98.

Urbani, F. (1982) Comentarios sobre algunas edades de las rocas de la parte central de la Cordillera de la Costa. *GEOS* (UCV, Caracas), (27): 77-85.

------ (1983) Las rocas graníticas del área de Las Trincheras - Mariara, estado Carabobo: geología y edad (Abstract). *Acta Científica Venezolana*, 34(supl. 1): 53.

------ & M. Ostos (1989) El Complejo Avila, Cordillera de la Costa, Venezuela. *Jornadas 50 aniversario Escuela de Geología*, UCV, Caracas, may 1988, *Memorias*, en prensa.

TECTONIC AFFINITY OF MAFIC ROCKS FROM THE CARIBBEAN MOUNTAINS SYSTEM, VENEZUELA

OSTOS, M. (*) and AVÉ LALLEMANT, H.G., Department of Geology and Geophysics, Rice University, P.O. Box 1892, Houston, Texas 77251; (*) also at the Universidad Central de Venezuela, Fac. Ingeniería, Dept. de Geología, Caracas 1051.

The Caribbean Mountains System of Venezuela consists from north to south of the following four east-west trending belts: Cordillera de la Costa Belt (CC), Caucagua-El Tinaco Belt (CT), Paracotos Belt, and Villa de Cura Belt (VC). A petrologic and geochemical study of mafic rocks in these belts was undertaken to determine the tectonic setting of these rocks and their significance with respect to the interaction of the Caribbean and South American lithospheric plates.

Major- and trace-element abundances of thirty-eight (38) samples and rare-earth element (REE) abundances of five (5) samples from the CC were analyzed. These samples were taken from the high P/T metamorphic belt of the CC. All discrimination diagrams suggest that these rocks formed in a mid-oceanic ridge or marginal basin environment (MORB).

Ten (10) hornblende gneiss samples from the CT were analyzed for major- and trace-element abundances, and three (3) for REE abundances. The major- and trace-element contents are typical of tholeiites; trace-element discrimination diagrams suggest a volcanic arc affinity, and the REE patterns indicate association with an Andean-type magmatic arc.

Major- and trace-element abundances of thirty-two (32) metalavas from the VC were analyzed; twenty-five (25) from the high P/T metamorphic Villa de Cura Group and seven (7) from the Dos Hermanas Formation. REE abundances were measured in four (4) samples from the Villa de Cura Group. The trace-element abundances and discrimination diagrams of the high P/T rocks suggest that these rocks were MORB's; the REE contents and patterns are inconclusive. The major and trace elements of the Dos Hermanas metabasalts indicate that they are tholeiites and have formed in a volcanic island arc setting.

Two tectonic models will be proposed. In the first, the entire Caribbean Mountains System is allochthonous and was formed far to the west. In the second the VC is proposed to be parautochthonous.

THE TINAQUILLO PERIDOTITE COMPLEX, VENEZUELA

OSTOS, M. (*) and AVÉ LALLEMANT, H.G., Department of Geology and Geophysics, Rice University, P.O. Box 1892, Houston, Texas 77251; (*) also at the Universidad Central de Venezuela, Fac. Ingeniería, Dept. de Geología, Caracas 1051.

Both the Tinaquillo Peridotite Complex (TPC) and the Tinaco Complex (TC) are part of the Caucagua-El Tinaco Belt. The TPC consists of approximately 70% harzburgite, 20% dunite, and 10% metagabbro. Traditionally, it was thought that the TPC intruded the TC as a crystal mush and that the metagabbro bodies were xenoliths of the TC. Major- and trace-element abundances of twelve and rare-earth element (REE) abundances of three metagabbro samples from the TPC were analyzed. The TiO_2 and trace-element abundances are characteristic of mid-oceanic ridge or marginal basin tholeiites (MORB). Normalized REE patterns of the TPC metagabbros are flat but for positive Eu-anomalies; they also are characteristic of MORB's and are similar to the REE patterns of gabbros of the Semail ophiolite. Major- and trace-element abundances of ten and REE abundances of four metagabbros from the TC were analyzed. The TiO_2 contents are characteristic of volcanic arc basalts. The REE patterns show a light REE enrichment similar to basalts of Andean-type margins. Thus, the metagabbros of the TPC are not xenoliths of the TC. Instead, the TPC may be an ophiolite sutured to the TC during pre-Cretaceous time.

Microprobe analyses of pyroxenes of the TPC peridotites indicate that they underwent at least two thermal events. The first event occurred at approximately 1400°C and the second at about 650°C; the first may be related to crystallization in the upper mantle; the second may be related to the tectonic juxtaposition of the TPC and TC.

The gabbros of the TC near the contact with the TPC have relict granulite facies mineralogies, which may be related to the 650°C event in the TPC. All rocks of the TPC have an intense mylonitic texture which formed during the 650°C event by oblique dextral strike-slip or oblique southeastward underthrusting along the east-west striking, south dipping tectonic contact of the TPC and TC.

INTERPRETACION DE LOS DATOS GEOFISICOS CON FINES DE LA CARTOGRAFIA GEOLOGO-ESTRUCTURAL DE LA REPUBLICA DE CUBA

Manuel E. Pardo Echarte
Instituto de Geología y Paleontología
Calzada #851 Esquina A & 4, Vedado 4, Plaza de la Revolucion
La Habana, CUBA

Se exponen los principales resultados en la interpretación geológica de los datos gravimétricos, aeromagnéticos y aerogammaespectrométricos, con fines de la cartografía geólogo-estructural de la República de Cuba. Se incursiona en el problema de la naturaleza geológica de las principales fuentes de anomalías gravimagnetométricas residuales y, aeroespectrométricas. Como resultado, se establece el carácter, fundamentalmente, rocoso de las primeras y, la probable vinculación de las últimas con la concentración de distintos óxidos en la parte superior de la corteza de intemperismo (suelos), a consecuencia de su evolución en las condiciones de clima tropical. En base a la regionalización conjunta (visual) de los campos gravitatorio y aeromagnético se confecciona un esquema interpretativo geólogo-estructural de la República de Cuba; se delimitan las principales unidades o bloques geólogo-geofísicos y, se comenta, especulativamente, sobre su posible naturaleza y relación. Finalmente, se aborda la identificación de los complejos estructuro-rocosos reconocidos en el esquema anterior, con sus homólogos estructuro-metalogénicos.

LA CONSTITUCION GEOLOGICA DEL MACIZO ISLA DE LA JUVENTUD Y SU METALOGENIA ENDOGENA VINCULADA AL MAGMATISMO ACIDO.

Manuel E. Pardo Echarte
Instituto de Geología y Paleontología
Calzada #851 Esquina A & 4, Vedado 4, Plaza de la Revolucion
La Habana, CUBA

Se argumenta la solución teórica del problema acerca del vínculo entre la estructura dómica regional más joven, superpuesta al cuadro de multiplegamiento y metamorfismo de las secuencias del macizo, y el desarrollo del magmatismo ácido y su metalogenia asociada en la región. Como resultado, se establece que, probablemente, a consecuencia del proceso de formación y evolución estructural del domo, tuvo lugar el emplazamiento de pequeños plutones graníticos (50-100 Km^2), localizados en la intersección del sistema radial de grietas del domo con el sistema anular de fracturas profundas que lo delimita, a través del cual, presumiblemente, penetraron los fundidos anatécticos. A partir de sus apófisis subvolcánicas diferenciados, tuvo lugar, al parecer, la telescopización de las intrusiones fisurales y de la mineralización, fundamentalmente, dentro del sistema radial de grietas. Basado en un mecanismo de herencia metalogénica, se supone que los plutones graníticos formados condujeron a concentraciones minerales, sólo donde éstos sobreyacían a zonas mineralizadas preexistentes y; que la regionalización geoquímica del territorio reproduce la zonalidad geoquímica (y metalogénica) del basamento reelaborado.

Modelo para la evaluación de recursos potenciales (Pronóstico P_3); consideraciones teórico-metodológicas.

Manuel E. Pardo Echarte

Instituto de Geología y Paleontología
Calzada #851 Esquina A & 4, Vedado 4, Plaza de la Revolucion
La Habana, CUBA

Se describe un modelo para la evaluación de recursos potenciales (pronóstico P_3) y el procedimiento de aplicación, a ser utilizado en los casos de regiones poco exploradas, levantadas en escalas medias (1:250 000 - 1:100 000), donde no se dispone de información precisa acerca de la densidad espacial, dimensiones y, ley promedio de los depósitos de interés. El método descrito constituye una generalización del modelo de Finch y Mc Cammon (1987). Este se fundamenta en la derivación del factor probabilístico a partir de la distribución de ocurrencias minerales en el área de estudio y; en la estimación del tonelaje de mena y de la ley del mineral útil, así como del factor de error asociado, a partir de las estadísticas correspondientes a los depósitos tipo mundial. La concepción de este modelo responde a una base teórico-metodológica de límites precisos, la cual se expone en la parte introductoria del trabajo.

MINERALOGIE DES SUBLIMES FUMEROLLIENS AUX SOUFRIERES DE GUADELOUPE ET DE MONTSERRAT

PASCALINE, H. et JEREMIE, J.-J. - Université Antilles-Guyane
Laboratoire de Géochimie Volcanologie - B.P. : 592 -
97167 - Pointe-à-Pitre CEDEX - F.W.I.

PERSON, A., TOUTAIN, J.-P. Université P. et M. Curie - Département de Géologie dynamique - 4, Place Jussieu - 75252 - Paris CEDEX 05

L'analyse minéralogique par diffraction des rayons X d'échantillons de dépôts fumerolliens prélevés aux Soufrières de Guadeloupe et de Montserrat a permis d'identifier une vingtaine de minéraux sublimés dans l'environnement immédiat des évents fumerolliens.
La plupart de ces minéraux de basses températures sont des sulfates. Les minéraux les plus abondants et les plus fréquemment rencontrés sont : le gypse, l'anhydrite, les alumogènes, l'halotrichite, la calcite, les smectites, le soufre, le quartz et la pyrite.
La cristobalite est rencontrée sous les deux phases, basse et haute températures ; cette dernière phase devant appartenir au groupe des minéraux volcaniques associés par entraînement mécanique aux dépôts fumerolliens.
Ces minéraux résultent pour l'essentiel de l'attaque par les gaz volcaniques riches en H_2S du matériel andésitique constituant l'encaissant des dépôts étudiés ; l'action météorique pouvant jouer un rôle secondaire, le gypse étant par exemple probablement le produit de la transformation de l'anhydrite d'origine volcanique.

ANALYSES MINERALOGIQUES ET PETROGENESE DES ROCHES DU VOLCANISME RECENT DE LA BASSE-TERRE EN GUADELOUPE

PASCALINE, H. et JEREMIE, J.-J.-Université des Antilles-Guyane
Laboratoire de Géochimie Volcanologie - B.P. : 592 -
97167 - Pointe-à-Pitre CEDEX - F.W.I.

Sept échantillons représentatifs de la série magmatique du volcanisme Madeleine-Soufrière ont été choisis pour une analyse minéralogique plus approfondie. Toutes les phases minérales ont été repérées et analysées de façon à mettre en évidence l'évolution magmatologique du massif récent.
- La composition de ces phases minérales,
- leur ordre d'apparition,
- les calculs de températures d'équilibre,
- l'existence ou non de certaines phases minérales à certains stades d'évolution magmatique,
- l'observation de traces d'instabilité pour certains minéraux,

ont permis d'aboutir à un modèle basé sur l'étagement de deux réservoirs magmatiques aux profondeurs respectives de 18-20 km et de 8-10 km évoluant chacun par cristallisation fractionnée.
En outre, ce modèle est en accord avec la répartition des foyers des séismes au niveau du massif de la Soufrière.

EOCENE STRATIGRAPHICAL STUDIES, MARACAIBO BASIN, NORTHWESTERN VENEZUELA.

PITTELLI, R., Maraven, S.A., Exploration Department, P.O. BOX 829 Caracas 1010A. Venezuela.

Benthic foraminiferal analysis were carried out in samples (cuttings, cores) of eight wells and one outcropping section from the Maracaibo Basin, northwestern Venezuela.

The wells located across the basin, from the west to southeast, are in the La Paz, Concepcion, Sibucara, Cabimas and Ceuta oil fields; and the outcropping Eocene section is near the Misoa Anticline, eastward the Mene Grande oil field (Text-Fig.1).

The siliciclastic sequence, early Eocene - late middle Eocene in age, is formed by the Trujillo, Misoa, Pauji and Jarillal formations.

Five foraminiferal assemblages, paleobathymetrically related were distinguished: 1) Alluvial Trochammina sp. assemblage typify the Misoa Formation to the west. 2) Deltaic Trochammina - Haplophragmoides assemblage characterize the Misoa Formation in the whole studied area. 3) Nearshore Quinqueloculina - Agglutinated Foraminifera assemblage recorded at the base and at the top of the Misoa Formation, in the central and eastern studied area. 4) Inner-Mid neritic Bolivina - Siphonina usbonifera assemblage recognized at the base of the Pauji Formation and at the top of the Trujillo Formation. 5) Outer neritic/upper bathial Sigmoilopsis schlumbergeri - Textularia saggitula assemblage recognized in the Pauji Formation and locally (to the midwest of the area) in the Misoa and the Trujillo formations.

Paleobathymetric changes such as shallowing upward sequences (between the Trujillo and Misoa formations), deepening upward sequences (between the Misoa and Pauji formations), and the main changes within the Misoa Formation are related to the sediment supply and to eustatic changes of the sea level. However, local changes can be related to paleotopography and possibly to sinsedimentary faulting.

Known reservoirs in the Misoa Formation and at the top of the Trujillo Formation are sand bodies deposited in the nearshore and deltaic environments then, the faunal assemblages distribution can be used to predict facies changes and consequently some sandy reservoir limits.

STRUCTURAL INTERPRETATION OF GRAVIMETRIC AND AEROMAGNETIC DATA FROM THE SERRANIA DEL INTERIOR RANGE AND THE MATURIN BASIN (VENEZUELA) .

G. POTIE * , J.F. STEPHAN ** .

* : *GIS " Océanologie et Géodynamique ". 6 Avenue Le Gorgeu 29287 Brest Cedex FRANCE.*
** : *Institut Géodynamique URA 720 Université de Nice Sophia Antipolis. Parc Valrose 06034 Nice FRANCE.*

The eastern Serrania del Interior lies in northeastern Venezuela, south of the El Pilar dextral strike-slip fault. It represents the foreland fold and thrust belt of the eastern part of the Caribbean Chain. The Maturin Basin lies between the frontal thrust of the range and the Guyana shield.

Both the stratigraphy and the shallow structural pattern of the Serrania have been studied with data from a geological field survey. At a more regional and deeper scale we studied gravimetric and aeromagnetic data.

The Bouguer anomaly increases between Maturin (-160 mGal) and the El Pilar fault zone (0/+10 mGal) . Modelling on the profile Muelle de Cariaco-Aragua de Maturin-Puerto Ordaz has enabled us to confirm the existence of a shallowing in the basement below the northern half of the range, from a thickness of ≈10 km in the sedimentary cover below the Maturin Basin.

The pseudogravimetric transformation of the magnetic anomaly (induced magnetization) shows that the gravimetric and magnetic anomalies share the same origin in the crystalline basement. This is most clearly shown by the same N70 structural trends in both magnetic and gravimetric anomalies.

In addition, we see a N130 lineation in the southeastern sector. This may indicate that the Urica fault, which is seen in the sedimentary cover to the NW, has also involved the basement. However, there is no direct evidence of faulting in the sediments directly above the magnetic lineation. Instead, we propose that the Urica fault was produced by readjustment in the sedimentary cover above a preexisting discontinuity. This is in agreement with our interpretation of the northern Maturin Basin seismic data, which shows the existence of a basal detachment surface.

We finally propose that the shallowing in the basement shown by the gravimetric models is the result of a post-Miocene movement (slab elastic flexure) .

Ref. : POTIE G., (1989) . - La Serrania del Interior Oriental sur le transect Cumaná-Urica et le Bassin de Maturín (Vénézuela). Application des données géophysiques et géologiques à une interprétation structurale. *PhD. thesis* University of Brest (France), 1989, 240 pp., 95 figs., 13 pl.

PATTERN OF FAULT AND FOLD STRUCTURES IN COASTAL PLAIN AREAS OF SOUTHERN PUERTO RICO AND CENTRAL ST. CROIX

RENKEN, R.A., U.S. Geological Survey, WRD, 6481-B Peachtree Industrial Blvd., Doraville, GA 30360 and RODRIGUEZ, Jesús, U.S. Geological Survey, G.P.O. Box 4424, San Juan, Puerto Rico.

Subsurface geologic maps using data from over 500 coastal plain water wells in southern Puerto Rico and central St. Croix indicate that both areas are underlain by a complex series of subsurface fault or fold structures.

Puerto Rico's southern mountains are bordered by six fan-deltas that combine into a narrow (3 to 8 kilometer), but elongate (70 kilometer) coastal plain, forming a coastward thickening sequence (>500 meters) of bedded cobbles, gravel, sand and silt of Miocene (?) to Holocene age. Fan-deltas cover two northwest-trending, left-lateral wrench faults, the Rio Jueyes and Esmeralda faults. Subsurface maps indicate that both faults continue to the southeast as a series of en echelon faults, and combine with northeast-trending cross faults to form a complex of horst and graben structures. Uplifted blocks lie at the discontinous end of major strike-slip faults and graben structures lie between them. To the southwest, an unnamed fault lies parallel to the Rio Jueyes and Esmeralda faults, and extends west-northwest nearly to the western edge of the coastal plain margin. The unnamed fault links with several other faults that strike northeast. These faults, in combination, form the landward edge of the Ponce basin.

A structure contour map of the Jealousy Formation of Oligocene to Miocene age, suggests that several fault block structures vertically displace St. Croix's central carbonate coastal plain sequence. Faults mapped in the subsurface strike in two directions. One group of faults strikes to the northeast and displaces coastal plain strata adjacent to the Northside Range. These faults are complemented by faults that strike northwest. An uplifted fault block or fold structure in the northeastern part of the coastal plain seems to lie in the compressional quadrant of a strike-slip fault. A downdropped block in the south central part of St. Croix lies in the tensional quadrant.

A pull-apart basin tectonic framework is postulated to explain horst and graben structures in southern Puerto Rico. The pattern and orientation of subsurface faults and fold structure that underlie central St. Croix are suggestive of extention and contraction along a buried left-lateral strike-slip fault.

PROBLEMAS DE LA GEODINAMICA DE CUBA

PUSCHAROVSKI, Y.M., MOSSAKOVSKI, A.A., NEKRASOV, G.E. and SOKOLOV S.D. (Instituto de Geología, Academia de Ciencias de la URSS).
FLORES R.M., FORMELL F.A. and CABRERA R. (Instituto de Geología y Paleontología, MINBAS, Cuba.)

La naturaleza tectonica de Cuba muestra una gran complejidad y hetereogeneidad. Los procesos de colisión y de destrucción tuvieron un carácter diferente y asincrónico en diferentes segmentos de Cuba. En el Segmento Central está representada la serie lateral más completa de elementos estructurales de diferentes zonas. Aquí, la formación de la estructura plegada alpina es el resultado de dos colisiones diferentes - Campaniano y Eoceno Inferior-Medio. La primera se debió al choque de un fragmento (desprendido y transportado hacia el Norte) del margen continental de América del Sur, con el arco insular surgido en la paleocuenca del Caribe en el límite Jurásico-Cretácico. La causa de la primera colisión fue la subducción (con buzamiento al Norte) de la corteza oceánica de la depresión meridional, bajo el borde sur del arco volcanico y la consecuencia deriva hacia el norte del fragmento de America del Sur. Como resultado de esta colisión, cesó la subducción y se formó el arco insular protocubano, en cuyos taludes se acumularon, a partir del Campaniano-Maestrichtiano, complejos molasicos y carbonatado-terrigenos. Esta colisión provoco el "salto" de la zona de subducción al borde norte del arco protocubano, con buzamiento al Sur. De esta manera, comenzó el proceso de absorción de la corteza oceánica de la depresión septentriónal, produciendose un acercamiento rápido del continente norteamericano con el arco insular, completándose en el Eocene Inferior-Medio su colisión y la obducción de los fragmentos alóctonos de la depresión suboceanica y delarco insular protocubano, sobre el margen continental. En el Segmento Occidental (al oeste de la Falla Pinar) el carácter de los procesos geodinamicos fue diferente. Aquí en el Paleoceno Superior-Eoceno Inferior-Medio, ocurrion la colisión directa del fragmento continental suramericano y el margen continental norteamericano. La colisión parece ser la única que se produjo en este segmento y provocó una complicada estructural de sobrecorrimientos en los complejos de la cobertura sedimentaria de ambos márgenes.

En el Segmento Oriental los procesos transcurrieron de una forma completamente diferente. Aquí, se produjo tambien el choque del arco insular cretácico con el margen continental norteamericano, el cu l provocó el cabalgamiento en dirección norte de los complejos del primero. Además de ésto, al final del Cretácico Superior (Maastichtiane-Paleoceno) se produjo la escisión del arco insular, a lo largo de la línea Cauto-Nipe, produciéndose un movimiento divergente (al noroeste y al sureste) de las masas rocosas. Al norte ocurrió la colisión de los fragmentos del arco volcánico con el margen continental norteamericano, mientras que en el Sur se produjo el aplamiento tectónico de los complejos del primero, los cuales constituyeron el basamento plegado del arco volcánico del Paleógeno Temprano de Sierra Maestra-Caimán. En el centro de la zona de distensión, posiblemente sobre un diaporo del manto, surgió una depresión riftogénica suboceánica de corto periodo de desarrollo, al parecer relacionada genéticamente con la Cuenca de Yucatán.

WHITING SEDIMENT: BIOLOGICALLY INDUCED NON-SKELETAL PRECIPITATION OF ARAGONITE

ROBBINS, L.L, University of South Florida, Tampa, FL, 33620. BLACKWELDER, P.L., University of Miami, RSMAS, 4600 Rickenbacker Cswy., Miami, FL 33149.

The origin of whiting sediments have been a controversial subject for decades. Although both skeletal and non-skeletal origins have been proposed, none of the evidence thus far has been conclusive. Data collected from several whitings from west of Andros Island, Bahamas in October 1987 and August 1988 suggest that these aragonite laden waters may be the result of high organic content in supersaturated carbonate waters.

During the August cruise, a number of whiting samples were collected and immediately preserved in glutaraldehyde. Scanning and transmission electron microscopy of preserved and non-preserved samples clearly demonstrates a relationship to cellular organics and aragonite crystals. SEM analysis of preserved whiting sediment reveals the presence of clumped spheres of randomly oriented aragonite needles ranging in size from 15-30 microns in diameter. TEM of the samples shows that cells and organics in varying stages of degradation are associated with aragonite needles. Aragonite crystals exhibit a random array, having both perpendicular and parallel orientations to the organic membranes. This type of mineralization implies a biologically-induced precipitation as opposed to a biologically-controlled or matrix mediated mineralization. Further data on the biochemical nature of the organics associated with the whitings indicate the presence of highly negatively charged proteins and macromolecules on which calcium carbonate may precipitate.

These data suggest that some of the Bahama Banks precipitation of aragonite needles may be partially induced by the highly charged microenvironment created by cells in various stages of growth and degradation. Whiting sediments appear to be biologically induced, but of a non-skeletal origin. This mechanism has far reaching implications in the production of lime mud throughout the geological record.

IMPERFORATE LARGER FORAMINIFERA FROM THE OLIGOCENE OF JAMAICA

ROBINSON, E., Department of Geology, Florida International University, University Park, Miami, FL 33199, USA

Assemblages of larger foraminifera in platform carbonates from central and eastern Jamaica contain Praerhapydionina delicata, as well as species of Archaias, Miosorites and other peneropliform genera, from levels correlated with the Oligocene Browns Town Formation. The age and significance of the assemblages are briefly discussed.

PALEOCENE LARGER FORAMINIFERA FROM EASTERN JAMAICA

ROBINSON, E., Department of Geology, Florida International University, University Park, Miami, FL 33199, USA

Species of Ranikothalia and Discocyclina, previously reported from the Paleocene Nonsuch Formation of northeastern Jamaica, are described and illustrated.

SIGNIFICANCE OF GEOTHERMAL GRADIENTS IN PETROLEUM EXPLORATION IN TRINIDAD

RODRIGUES, K., Geological Services Laboratory, Trinidad and Tobago Oil Company Ltd. (TRINTOC), Pointe-a-Pierre, Trinidad.

The correlation between positive geothermal anomalies and the occurrence of hydrocarbons is based on the premise that water is the major agent of both hydrocarbon migration and heat transfer in sedimentary basins, and suggests a genetic link between geothermal gradients, hydrodynamics and hydrocarbon occurrences. This association has generated growing interest in geothermal studies in relation to the occurrence of petroleum deposits and the importance of the temperature history experienced by the source rock in the maturation process.

Geothermal gradients were derived from bottom hole temperatures recorded on electric logs from 250 exploratory and development wells drilled over Trinidad, including the Gulf of Paria and the North Coast and East Coast marine areas. A study was undertaken to determine the temperature regimes, to identify and map the depth range of the oil window in various areas and to delimit the zones of heavy (biodegraded) oils. An iso-geothermal gradient map of Trinidad, showing local and regional variations in heat flow, is presented.

Geothermal gradients over Trinidad vary between 0.9°F and 2.0°F per 100' (17°C and 36°C per Km), rarely exceeding 1.5°F/100' (28° C/Km), and are comparable to the worldwide average of 25° C/Km. These variations are related primarily to: (i) position of basement (heat source) with respect to overlying sediments; (ii) difference in vertical and lateral thermal conductivity of the rocks due to lithologic variation; and (iii) effects of water moving through the sedimentary section.

Caribbean Conference Abstract for Rosencrantz. Oral Presentation

TWO-PART CONVERGENCE ALONG THE CUBAN OROGENIC BELT: OBSERVATIONS AND IMPLICATIONS

ROSENCRANTZ, E., University of Texas Institute for Geophysics, 8701 Mopac Blvd., Austin, TX 78759 USA

The Cuban orogenic belt is commonly considered as arising from the convergence and collision between a northward moving Antilles volcanic arc and a stable Bahamas carbonate platform in Eocene time. However, Cuban stratigraphy and structure suggest that the belt was assembled in two stages, one in the Late Cretaceous and the second in the Early to Middle Eocene. During the Cretaceous, Cuban Zaza Zone volcanic rocks accumulated as an island arc over a north-dipping subduction zone located south of the arc. Remnants of this subduction zone include a buried trench along the southeast margin of Cuba and the metamorphic shear zone mapped along the northern edge of the Escambray massif. Campanian to Maastrichtian radiometric cooling ages of plutonic and related metamorphic rocks north of this suture, and of blueschist minerals located within the suture, suggest that subduction had ceased by this time. Arc rocks were extensively eroded during the Maastrichtian, with local exposure of basal ophiolites. Crust south of this suture, within the Yucatan Basin, includes the Escambray and Isle of Pines metamorphic massifs and the thickened oceanic crust of the Cayman Rise, the presence of which probably contributed to north-dipping subduction stoppage. Post-Maastrichtian North American-Caribbean convergence took place along a south-dipping thrust zone located north of the arc. The overthrust sequence, consisting of Cretaceous arc and Caribbean Basin (Tethys) sediments and basement, obducted onto the Bahamas platform during the Middle Eocene. Platform sediments show little evidence of overthrusting until Upper Paleocene time. Wells drilled in the Havana area penetrate series of platform sequence duplexes emplaced during Late Paleocene to Early Eocene time. Dated melange rocks in central and western Cuban indicate that arc rocks thrust over, and deformed, underlying sediments between Early and Middle Eocene time. During the northward movement of the overthrust plate, a small pull-apart ocean basin, similar to the present-day Cayman Trough, developed within the plate along its western, strike-slip margin adjacent to the Yucatan platform.

Caribbean Conference Abstract for John G. Sclater. Oral Presentation

THE CAYMAN TROUGH: AN ASSESSMENT

ROSENCRANTZ, E., and SCLATER, JOHN G., University of Texas Institute for Geophysics, 8701 Mopac, Austin, TX 78759 USA

The opening of the Cayman Trough has long been used as a measure of the displacement of the Caribbean plate relative to the North American plate and, indirectly, relative to the South American plate. This measure is not absolute as once thought, owing to the observation that the core of the Caribbean plate, as represented by the Colombian and Venezuelan Basins, is separated from the North American plate by one or more EW trending transcurrent fault zones located south of the trough. Nevetheless, the history of trough opening provides important clues as to the age and duration of tectonic events within the northern Caribbean. However, this focus on the trough as an element of tectonic reconstruction tends to obscure the fact that the trough in itself displays several aspects which present a number of interesting problems.

For instance, the Cayman Trough provides the opportunity to study the full evolution of what might be considered a "mature" pull-apart basin. The regional tectonics of the northern Caribbean suggest that the trough originated during the Eocene as a pull-apart along the developing EW trending North American-Caribbean transform shear zone. This is supported by observations that rift blocks at the eastern and western margins of the trough lie oblique to the bounding strike-slip faults, with fault patterns similar to those seen within pull-aparts developed on smaller scales and similar to those documented by experimental work. In contrast, magnetic anomalies and crustal faults originating by seafloor spreading within the trough trend at right angles to the boundary faults. The transition between the rifted margin and oceanic crust is abrupt, with seafloor spreading faults apparently truncating those of the rifted margin.

Another interesting aspect of the Cayman Trough is that its opening direction is tightly constrained by the bounding transforms. The basin opened along a set of "railroad tracks", so to speak, and opening can be reconstructed with an exact match of its conjugate rift margins. This has important implications with regard to rifting sequence and to the nature of the initiation of seafloor spreading within rifted crust.

The Cayman Trough offers the opportunity to examine lithospheric cooling under conditions other than those of deep ocean basins. Measurements of crustal depth and heat flow within the trough show that it is too deep and too cold relative to crustal age as determined from marine magnetic anomalies and regional tectonics. This suggests that lithospheric cooling within the trough is strongly affected by heat loss lateral to the trough, toward the older, colder lithospheric masses of the bounding Nicaragua and Cayman rises. Measurements of basement depth and heat flow within the trough show good correlation to depth and heat flow predicted by small ocean basin cooling models which include lateral as well as vertical cooling of accreting lithosphere. This difference of cooling history, set against probable differences in seafloor crustal composition and structure, can provide additional insight into the mechanics of ocean crust formation.

LATE CRETACEOUS SYNOROGENIC FLYSCH OF EASTERN GUATEMALA - THE SEPUR FORMATION

ROSENFELD, J.H., and BARRETT, S.F., Amoco Production Company, Houston, Texas.

Over 2,700 meters of Late Campanian to Maastrichtian flysch of the Sepur Formation overlie the continental Yucatan (Maya) Block in eastern Guatemala. The flysch and underlying units are folded and thrusted by post-Maastrichtian/pre-Miocene compression attributed to the collision of the Maya Block with an island arc or the Chortis microcontinent.

Clasts in Sepur Formation sandstones and channelized debris flow conglomerates indicate provenance from volcanic, carbonate and ophiolitic terranes. Crystalline "continental" basement clasts are notably rare in eastern Guatemala.

The thick flysch sequence north of the suture zone is diachronous along strike: Late Cretaceous in eastern Guatemala, Paleocene-Eocene in western Guatemala, and Late Cretaceous through Neogene in Chiapas, Mexico. Clast lithologies in the flysch suggest increasing involvement of continental basement westward along the suture trend.

EVOLUTION OF THE HYPOTHESES ABOUT THE ORIGIN OF THE CARIBBEAN

RULL, V., and SCHUBERT, C., I.V.I.C., Apartado 21827, Caracas 1020-A, Venezuela

In general, it can be said that geological research in the Caribbean proceeded in three stages: an initial stage (19th century) of general descriptions; a later stage of reconnaissance, in part oriented by economic motivations; and a final stage of detailed and systematic studies. The general hypotheses on the origin and evolution of the Caribbean can be subdivided into two types: static ones and dynamic ones. The static hypotheses considered that the Caribbean was a submerged continent or a permanent oceanic basin. The dynamic hypotheses can be subdivided into those that do not take into account continental drift, and those that do. Among the first, the most important one is the tectogene hypothesis (postulated by Harry Hess), a crustal zone that is folded downward, originating a negative gravity anomaly, and orogenic, volcanic, and seismic activity. Among the hypotheses that take into account continental drift, there are those that preceeded the hypothesis of plate tectonics, and those that include it. The principal hypothesis that does not include plate tectonics, tries to explain the origin of the Caribbean by sea-floor spreading, from a spreading center located between North and South America. Among the hypotheses that include plate tectonics, one can differentiate between those that postulate an autochthonous origin of the Caribbean, and those that derive it from far away, for example from the Pacific Ocean. A review of the different hypotheses indicates that those that are based on plate tectonics have a similar basis and show a certain refinement with time. On the other hand, those that postulate an autochthonous origin have very diverse bases and show no refinement with time. In general, scientific research tends to progressively increase the amount and quality of data, in order to reduce to a minimum the prejudices of those who interpret them. In the geologic study of the Caribbean, this has been difficult, in large part due to the proliferation of models to explain its origin and evolution. The modern paradigm of geology, plate tectonics, was developed before sufficient data existed to generate an acceptable model for the Caribbean, which was also in accord with the paradigm. The geologic interpretation of the Caribbean began over a century ago; therefore, its history is also a summarized history of geology since the beginning of the century.

ORIGIN OF THE LESSER ANTILLEAN ISLAND ARC: DATA FROM REPTILES AND AMPHIBIANS

ROUGHGARDEN, J., Stanford University

Data on the ecology, systematics, and biogeography of *Anolis* lizards, combined with that on other reptiles and amphibians in the eastern Caribbean, suggest that:

1. The northeastern and southeastern Caribbean have had distinct geologic histories. The line separating these provinces starts between Dominica and Martinique and extends southwest to between Curacao and Bonaire.

2. Within the northeastern province, material in the Guadeloupe-Dominica region has split off from Puerto Rico. The fauna of Guadeloupe and Dominica has had a primarily vicariant origin (i.e., consists of the descendents of populations that were on Proto-Guadeloupe at the time of its original fragmentation from Puerto Rico). This region has then served as a biological source for the younger islands north of Guadeloupe up to the Anegada Passage. Propagules have come north from Guadeloupe by over-water dispersal, in accordance with the prevailing currents.

3. Within the southeastern province, St. Lucia, La Blanquilla and Bonaire seem to be members of a former island arc that was "upstream" of the eastward-moving Caribbean plate. Collision with this island arc resulted in the insertion of St. Lucia between Martinique and St. Vincent, while La Blanquilla and Bonaire were pushed down onto the Venezuelan shelf. The oceanic islands of the southeastern province thus consist of at least four classes of terrains: Curacao—related to Grand Cayman; Bonaire and La Blanquilla—related to St. Lucia; the triplet consisting of Martinique, St. Vincent, and Grenada; and Barbados—an exposed piece of accretionary prism that has formed *in situ* and been colonized recently through local over-water dispersal.

REGIONAL STRUCTURAL AND VOLCANIC EVENTS WITHIN THE COTUI LIMESTONE-SABANA GRANDE CONTACT INTERVAL (LATE CAMPANIAN), SOUTHWEST PUERTO RICO

SANTOS, HERNAN and KAUFFMAN, ERLE G., Department of Geological Sciences, CB-250 University of Colorado, Boulder, CO 80309 U.S.A.

The Campanian Cotui Limestone represents a transgressive carbonate platform which occurs between the Guanajibo and Lajas valleys, Southwest Puerto Rico Terrain. The Cotui disconformably overlies the Lajas Formation (porphyritic lava, minor tuff) and is conformably overlain by the Late Campanian-Maastrichtian Sabana Grande Formation (volcaniclastic conglomerates, sandstones, siltstone, minor limestone lenses). The Cotui Limestone is divided into a lower, thick-bedded, gray mudstone and grainstone containing rudistid and stromatoporoid frameworks, and an upper white-light gray massive grainstone/packstone. Carbonate deposition across the Cotui platform is terminated by rapid inundation of coarse volcanic and limestone breccias in a volcaniclastic matrix, and shallow marine mass flow deposits, suggesting a major structural/volcanic event. The co-occurrence of Durania curasavica? and Barrettia monilifera in the uppermost Cotui Limestone indicates a Late Campanian age; B. monilifera in limestone breccias of the basal Sabana Grande Formation suggests a Late Campanian-Early Maastrichtian age. New field data from the Escuela Padre Rufo area, San German Quadrangle, reveals several episodes of normal faulting during uppermost Cotui-lowermost Sabana Grande deposition associated with major increases in size and amount of volcaniclastic detritus across the southwestern platform. The following series of events were noted: 1) Formation of a half-graben during latest Cotui time; 2) slump of thin carbonate mudstones with flow structures containing large angular volcanic blocks into the graben; 3) temporary quiescence; Cotui Limestone became lithified with early marine cements; 4) renewed movement on the bounding half-graben fault associated with rapid increase in volcanism; mass flow of volcaniclastic debris into the graben incorporating angular blocks of Cotui Limestone; deposition of the Cotui-Sabana Grande transition sediments continued uninterrupted on the north block of the graben; 5) formation of a shallow marine channel within the graben, rounding volcaniclastic pebbles and partially rounding limestone clasts; thin conglomerates spilled over onto the stable block; 6) deposition of shallow marine volcaniclastic sands over the entire area, smoothing fault and channel topography; 7) development of a second normal fault cutting lower Sabana Grande sandstone; the fault dip opposes that of the first fault; and 8) renewal of volcaniclastic sand deposition. This major Campanian event produced tensional faults, rapid initiation of volcanism, and spread of debris flows over much of southwestern Puerto Rico.

THE CARIBBEAN GEOLOGICAL CONFERENCES - PAST, PRESENT AND FUTURE - IDEAS AND PERSONALITIES

SAUNDERS, J.B., Natural History Museum, Basel, Switzerland

The Caribbean Geological Conferences began in 1955 in Antigua with a meeting of only 37 delegates who attended as representatives mainly from the British territories. The series has run without break since then with a three year interval between meetings. The second gathering was held in Puerto Rico with still only 55 delegates. From then onwards, the conferences have been widely advertised and have attracted a broad spectrum of Caribbean geologists and kindred spirits. Conferences today can expect anything up to 200 delegates.

Right from the start, the series has been supported by workers domiciled in the region together with interested participants from further afield who did much, particularly in the early days, to make the connection with academic institutions in North America and Europe. One thinks immediately of Harry Hess from Princeton who had so many students writing theses in the region that, in those heady days, no rum shop from St. Croix to Barquisimeto via Mayagüez was safe from them. Now these students have sent their students who are busy trying to overturn the work of their own masters no doubt.

If the actors have changed, so has the geology - or at least the interpretation of it. At the time of the first meeting the physicists were still telling us there was no way that they would sanction crust sliding about in such a cavalier fashion as the drifters wanted. There was thus still some surreptitious use of land bridges by harassed stratigraphers and palaeontologists.

It was just at the time of the Third Conference in 1962 that the hypothesis of sea floor spreading was first being voiced. In fact, Professor Hess excused his absence from the Fourth Conference because he had to go to Europe to defend his ideas which were still treated with caution if not with disdain by some.

So, the Atlantic was finally opened with some panache, or at least the north and south, but what of the middle? What should be done with the Caribbean? The results from Leg 15 of the Deep Sea Drilling Project were reported at the Sixth Conference in 1971 and this gave the first direct evidence of what lay beneath, or at least, what lay at the top of what lay beneath. At the same conference we were given the first plate model for the development of the Caribbean. This was hot off the press and was to be followed by many others.

Today we know everything, of course. But do we? Perhaps we should go on for a while longer to clean up a few of the new problems that the old answers have created. Where better than at a Caribbean Geological Conference within reach of the sharp tongues of our peers.

DEPOSITIONAL HISTORY OF TERTIARY CARBONATE ROCKS, SUBSURFACE OF NORTHERN PUERTO RICO

SCHARLACH, R. A., HARTLEY, J. R., and WARD, W. C., Dept. of Geology and Geophysics, University of New Orleans, New Orleans, LA 70148

Deep continuous cores taken by the Water Resources Division of the US Geological Survey show that during the late Oligocene and part of the Miocene, the marine shelf (ramp) of northern Puerto Rico was divided into at least four "sub-basins", each with a different depositional history. Vertical and lateral variations in stratigraphy apparently reflect relative sea-level fluctuations resulting from both structural movements and eustatic changes.

L. Oligocene transgression followed by minor regression - A. NW shelf: sand and mud (San Sebastian Fm) interfinger eastward with miliolid-soritid carbonate mud (Cibao Fm). B. W-central shelf: sand and mud (San Sebastian) up into large-foram and red-algae carbonate mud and sand and coral patch reefs (Lares Fm). C. E-central shelf: same as B. D. NE shelf: same as C.

L. Oligocene - E. Miocene transgression - A: marl and carbonate mud with sand and mud (Cibao). B: large-foram red-algae carbonate sand and muddy sand (Montebello Member of Cibao). C: clay and marl with planktonic fossils ("Mudstone Unit") in relatively deep basin (graben?). D: like B with terrigenous sand and mud.

E. Miocene regression - A: quartz-sandy miliolid-soritid carbonate mud (Cibao); possible subaerial exposure in westernmost part. B: quartz-sandy miliolid-soritid carbonate mud and caliche (Cibao). C: like B going into sand and gravel updip. D: skeletal carbonate mud (Cibao) interfingering E with sand and gravel (Mucarabones Fm).

M. Miocene transgression - A: subaerial exposure? (Los Puertos Fm absent?). B: red-algae miliolid-soritid sand with corals (Los Puertos). C: like B. D: carbonate sand (Los Puertos) going E into terrigenous sand (Mucarabones).

M. Miocene regression - A: subaerial exposure?. B: sand and mud and miliolid carbonate mud and caliche (Los Puertos); karst in eastern part (uplifted block?) C-D: miliolid-soritid red-algae sand (Los Puertos/Aymamon).

M. Miocene transgression - A-D: red-algae benthic foram carbonate sand and sandy mud with corals (Aymamon).

L. Miocene regression - A-D: subaerial exposure

E. Pliocene transgression - A-D?: planktonic-foram chalk (Quebradillas Fm).

12th Caribbean Geological Conference St. Croix USVI

COMBINED RADAR AND GLORIA MOSAICS OF PUERTO RICO, THE U.S. VIRGIN ISLANDS, AND SURROUNDING DEEP OCEAN AREAS: TECTONIC INTERPRETATIONS

SCANLON, Kathryn M., U.S. Geological Survey, Woods Hole, MA 02543
SOUTHWORTH, C. Scott, U.S. Geological Survey, Reston, VA 22092

The first high-resolution, geometrically controlled side-looking airborne radar (SLAR) mosaic of Puerto Rico and the U.S. Virgin Islands (USVI's) has been combined with the GLORIA long-range sidescan-sonar mosaic of the surrounding deep ocean areas to provide a unique view of a section of the northern Caribbean plate boundary zone. The GLORIA data provide a reconnaissance view of the structural and bathymetric features of the sea floor; the SLAR data penetrate the persistent cloud cover and dense vegetation that obscure aerial views of the geologic structures and physiographic terrains of the islands. The combined mosaics allow us to map structures across the land-sea boundary and to infer correlations between geomorphic features on land and in the submarine environment.

Puerto Rico and the USVI's lie within a 400-km-wide plate boundary zone between the Caribbean plate and the North American plate. The sense of motion between the two plates is now mainly left-lateral strike-slip, although north-south convergence and active subduction occurred here until about Eocene time. The northern extent of this plate boundary zone is defined by the Puerto Rico Trench. Its sediment-covered floor is clearly visible in the GLORIA mosaic, as are several long, slightly sinuous, east-trending, strike-slip faults. These faults lie in the forearc region between the base of the northern insular slope and the trench floor and presumably accommodate much of the present-day plate motion. The radar mosaic of the Cretaceous and early Tertiary crystalline core of Puerto Rico exhibits lineaments trending approximately N72°W. These lineaments are not discernible in the middle and late Tertiary sedimentary units that flank the older core, which implies that they are relics of the older convergent regime rather than of the more recent strike-slip regime. The Great Southern Fault trends somewhat more north of west (N55°W) than the other lineaments, which it appears to truncate. This suggests that the fault postdates the other lineaments. The GLORIA mosaic of the Mona Canyon area shows fault traces that have the same orientation as the Great Southern Fault. The southern edge of the plate boundary zone is marked by the Muertos Trough, where the GLORIA mosaic reveals a band of deformed sediments at the base of the insular slope.

LATE JURASSIC TO LATE CRETACEOUS DEVELOPMENT OF ISLAND ARC CRUST IN SOUTHWESTERN PUERTO RICO

SCHELLEKENS, Johannes H., MONTGOMERY, Homer, JOYCE, James, and SMITH, Alan L. Department of Geology, University of Puerto Rico Mayaguez, Puerto Rico 00708

Three stages of crustal development can be recognized in Southwest Puerto Rico based on fossil assemblages, radiometric ages, geochemistry, and petrology. The first two stages are preserved in the rocks that occur as relics in the serpentinite of the Bermeja Complex. The third stage unconformably overlies the Bermeja Complex. The first stage is represented by abyssal ocean floor rocks, the second stage formed at bathyal depths due to crustal thickening by island arc or ocean floor volcanism. The third stage represents island arc rocks formed in neritic and subaerial environments following deformation and erosion of the stages one and two. The Bermeja Complex consist of serpentinite, metamorphosed basaltic rocks, cherts, and associated silicified volcaniclastics. The basaltic rocks range in metamorphic grade from weakly metamorphosed prehnite-bearing rocks, through greenstones, to amphibolites. Radiolarian assemblages suggest that stage one is Kimmeridgian - Tithonian, and of northern Tethyan to Boreal paleogeographic origin; stage two is Hauterivian - Aptian; and stage three cherts formed from the Cenomanian to Campanian in the Tethyan Realm. Major, trace, and REE data fail to distinguish between an ocean floor and island arc origin for the basaltic metamorphic rocks. Clinopyroxene compositions for the greenstones, dikes, and two pyroxene gabbro suggest an island arc origin. Radiometric ages indicate a Hauterivian to Albian age for these rocks, corresponding to the second chert forming period. The third chert forming period is coeval with the intrusion of the Maguayo Porphyry diorite, and its associated island arc volcanic series. These volcanics were probably subaerial and are partly covered by Santonian and Campanian reef and shelf limestones.

Volcaniclastic sedimentation pattern and subsequent faunal breaks: An example from the Upper Cretaceous of Jamaica.

by

Winfried Schmidt
Department of Geology
University of the West Indies
Kingston 7, Jamaica

The Upper Cretaceous succession in Jamaica is linked to small scale erosional windows exposing sedimentary rocks of Campanian to Maastrichtian age. The carbonate shoal/volcaniclastic sedimentation pattern is related to tectonic uplift and subsidence of the constricted Caribbean Plate producing clastic sequences and carbonate mounds in a close spatial relationship. Repetitive sequences of sandstones and siltstones are attributed to turbidite/submarine fan sedimentation. Coarse conglomerates and bioclastic limestones are interpreted as near-shore deposits and shallow water rudist reefs, respectively. The rock formations of the Campanian to Middle Maastrichtian times are comparable to facies associations of submarine fan models. Sediment gravity flow mechanics distribute shelf sediments through feeder channels into a deep-water environment, where they are laid down as submarine fans in a arc-related sedimentary basin.

The Middle and Upper Maastrichtian rock record is characterized by rudist build-ups and intercalated fossiliferous shales containing other bivalves, gastropods, solitary corals and echinoids with a near shore to shelf edge affinity. Rudists vanish in the Middle Maastrichtian to the expense of oysters and other fossil groups. The abrupt change from rudist-dominated fossil assemblages to oyster communities cannot be explained by catastrophic events or unconformable contacts. It is suggested that changing substrate conditions in a shallowing upward sequence were responible for the Middle Maastrichtian faunal breaks in Jamaica.

GEOCHEMICAL COMPARISON OF CRETACEOUS BASALTS FROM THE CARIBBEAN, PACIFIC, AND ATLANTIC PROVINCES: ATLANTIC AFFINITY OF THE CARIBBEAN PLATE ?

SEN, G and DRAPER, G., Dept. of Geology, Florida International University, Miami, FL 33199, USA

Major, minor and trace element compositions of rocks of the Cretaceous "basaltic province" of Donnelly are compared with basalts of similar age from Leg 51-53 (Atlantic) and Site 462 (Nauru Basin, Pacific). Data selection from equivalent Pacific and Atlantic MORBs is based on (1) data availability, (2) quality of the data, (3) appropriate age, and (4) basalts with SiO_2=48.5 - 51%. The Caribbean data base includes basalts or their metamorphic equivalents from Leg 15 (Caribbean sea floor), Bath/Dunrobin Fm. and Mt. Hibernia Schists (Jamaica), Dumisseau Fm. (Haiti), Duarte Complex (Dominican Republic), Sans Souci Fm. (Trinidad), and Nicoya Complex (Costa Rica). The Duarte Complex metabasalts appear to be generally different from the others and will not be considered here as a part of this group. The Sans Souci, Nicoya, Mt. Hibernia, lower Dumisseau (LREE-depleted, Ti-poor) and Leg 15 (except Site 151) rocks are very similar to each other. The upper Dumisseau (LREE-enriched, Ti-rich) and Site 151 basalts are similar to each other and are more differentiated than the other rocks of the Caribbean province.

Cretaceous basalts from Leg 51-53 (Atlantic) are distinct from Site 462 (Nauru Basin, Pacific) in several binary element-element plots. The compositional fields of the Caribbean rocks overlap those of the Pacific and Atlantic in most plots except a TiO_2-Sm plot where the Atlantic and Caribbean groups overlap and are fitted by a straight line characterized by a TiO_2/Sm ratio that is distinct from the Pacific ratio (see fig. below).

Given the limited nature of the data from the Pacific, our tentative conclusions are: (1) the compositions of the Caribbean rocks support Donnelly's concept of a Caribbean Cretaceous Basaltic Province (Duarte Complex excluded) (2) basalts of the Atlantic/Caribbean and Pacific(Nauru) tapped distinct mantle sources in Cretaceous time, and (3) the Caribbean basalt province tapped an upper mantle source of Atlantic affinity.

Since present day MORBs from the Atlantic and Pacific are chemically indistinguishable, an interesting corollary of (2) above would be that large scale convective mixing of the mantle sources of the Pacific and Atlantic MORBs must have occurred between Cretaceous and present. Because of the important global implications of our findings, a much larger data base on the Pacific Cretaceous basalts is clearly necessary and is currently being compiled.

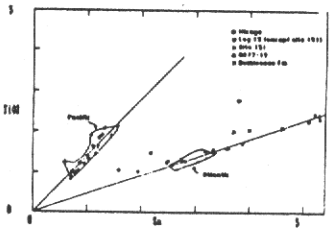

GLAUCONITIC SEDIMENTS IN THE NORTHEAST MEXICAN MID-CRETACEOUS: LIMITS IN THE USE OF GLAUCONITE FOR PALEOGEOGRAPHIC MODELS

SEIBERTZ, E., Institut für Geologie und Paläontologie, Callinstrasse 30, D-3000 Hannover, West Germany

In northeastern Mexico Mid-Cretaceous sediments crop out in barrancas, quarries, and road sections in the Sierra Madre Oriental and in the northern and eastern foothills. The Turonian and Coniacian strata are subdivided lithologically into three units: the Agua Nueva, the San Felipe, and the Méndez Formations. The San Felipe Fm. is subdivided into the underlying La Boca Mb. and the overlying Solis Member. As it is a turbiditic sequence, the San Felipe Fm. yields only few fauna: Inoceramids, found in autochthonous beds, prove an age of Middle and Upper Turonian of these sediments from the region between Monterrey/Nuevo León and Cd. Victoria/Tamaulipas.

The distribution of the mineral glauconite in the turbiditic greensands is of great interest in the view of a paleogeographic interpretation of this region. Due to excellent outcrops it could be proved by a bed-by-bed correlation that the turbidites moved from east to west. The distribution of grain sizes of clastic minerals such as quartz, feldspars, and mica served as sedimentologic caracteristics as well as the occurrence features of the glauconite: In proximal sections glauconite occurs in grains up to one millimeter in size, whereby this diminishes in vertical as well as in lateral directions to the west, north, and south. At the top of the BOUMA-sequences as well as in distal sections glauconite occurs only as matrix.

Being a phyllosilicate with a hardness of only 2 that will not endure large transport, glauconite has been looked upon as an indicator for nearshore depositional environments. Nevertheless, a transport up to 120 km is possible as show the investigation of northeast Mexican Mid-Cretaceous sections. It must be considered, however, that the glauconite grains were moved in a suspension in which they were miniaturized and at least, with decreasing energy, precipitated as a gel to the sediment matrix.

Here we find sediments that were originally deposited as greensands at easterly situated island platforms, and than were transported into a westerly situated subsequent trough (Monterrey Basin), caused by movements of the underground or by atmospheric conditions.

The investigations were sponsored by the Universidad Autónoma de Nuevo León Linares through 1982-84 and by the German Research Foundation through 1985-87.

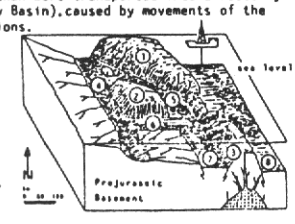

Figure: Compiled Jurassic paleorelief and Late Turonian paleogeography. Stippled areas = cold bottom water. Num. = paleogeographic elements. 3 = Tamaulipas Archipelago.

TECTONIC SIGNIFICANCE OF THE DETERMINATION OF BARIC TYPE FOR ANCHIZONAL AND EPIZONAL ROCKS OF THE ANDES AND CARIBBEAN MOUNTAINS OF VENEZUELA

SHAGAM, R., NADEAU, J.E., Department of Geological and Marine Sciences, Rider College, Lawrenceville, NJ 08648, and PADAN, A., PAMA Oil Shale Co., Negev, Israel.

Use of the b_o lattice parameter of dioctahedral potassic white micas as an index of baric type was developed by Sassi and Scolari (1974). This lattice parameter was measured in samples from anchizonal (sub- greenschist) slates and epizonal (greenschist) slates and schists of the Carboniferous Mucuchachi and Tostos formations in the Andes, and upper Cretaceous formations in the Caribbean Mountains of Venezuala. Cumulative frequency curves were developed for 1.) the Mucuchachi slates, 2.) Tostos schists with biotite, 3.) Tostos schists without biotite, and 4.) slates of the Caribbean Mountains. These cumulative frequency curves were then compared to known terranes to determine baric type. The Mucuchachi slates and Tostos schists with biotite fall at the low end of the baric spectrum and are bracketed by the low-pressure terranes of Boscat and northern New Hampshire. This finding is consistent with the relatively high temperature environment in the Andes which is dominated by thermal rather than baric conditions. Slates of the Caribbean Mountains yield a curve resembling the intermediate pressure terrane of the Swiss Alps. This result is compatible with the metamorphic environment inferred by southward displacement of the Villa de Cura allochton over the upper Cretaceous rocks of the Caribbean Mountains during the Paleocene. The Tostos schists without biotite yield a cumulative frequency curve of intermediate to high pressure baric type approaching that of the Otago schists of New Zealand. The Tostos schists without biotite are commonly assumed to be transitional between lowest greenschist grade Mucuchachi slates and high greenshcist grade Tostos schists with biotite, based on the regional geology. The baric indication, in this case, is inconsistent with expected results. Results, therefore, indicate that baric type determination in the Andes and Caribbean Mountains of Venezuelea for anchizonal slates and epizonal slates and schists using the b_o lattice parameter of white micas cannot be used independently in tectonic interpretation, but must incorporate consideration of the regional geology to insure reliability.

SLOPE-FAILURE PROCESSES IN SAPROLITIC SOILS OF A TROPICAL RAIN FOREST, PUERTO RICO

ANDREW SIMON, USGS Nashville, Tennessee, and MATTHEW C. LARSEN, USGS, San Juan, Puerto Rico

Rotational failures, with associated downslope earthflow component, appear to be the primary mechanism of hillslope denudation in the rainforest of eastern Puerto Rico. Annual rainfall in excess of 3000 mm, and thick sequences (up to 20 m) of residual soils (saprolite) combine to produce specific failure mechanisms. Shear-strength testing and observations of tension cracks indicate that slope failures initiate by tensile failure of saprolite material. The load on a potential failure plane in the subsurface is thereby increased by the additional weight of the detached block and by saturation of the overlying soil. During or shortly after intense and prolonged precipitation, shear failure then occurs along zones of reduced permeability within the saprolite. Fifty-two "naturally occurring" landslides were mapped using aerial photgraphy and field observation. Although forest elevations exceed 1000 m, the majority of these failures were found between 600 to 800 m in elevation,in areas where there is significant concentration of throughflow. Slope failures show no specific trend with respect to slope aspect. More than 100 "road-related" failures were also mapped and can be attributed to such factors as toe-removal, oversteepening, and increased hydraulic gradients. Tensile stresses in the unsaturated, upper-saprolite zone range from 3 - 10 kPa, and have mean seismic-refraction velocities of 476 m/s (+/- 127 m/s). Denser, clay-rich, less permeable saprolitic zones with mean seismic velocities of 1420 m/s (+/- 157 m/s) indicate probable failure planes where excess pore-water pressure decreases shear strength, leading to shear failure. These zones of translocated clay show marked density increases as shown by an order of magnitude increase in blow counts. Slickenside surfaces in the saprolite are found along relict fractures and joints derived from the parent rock-quartz-diorite, and marine-deposited volcaniclastics. This evidence of differential movement suggests that failures, once initiated, occur along specific planes of weakness in the saprolite. However, the largest landslides (areas greater than 25,000 square meters) fail along the saprolite-weathered bedrock boundary. It is therefore apparent that failure planes occur along zones of contrasting density and permeability within the weathered profile.

PETROTECTONIC EVOLUTION OF TOBAGO, WEST INDIES: A FRAGMENT OF A MESOZOIC OCEANIC ISLAND ARC TERRANE

SNOKE, A.W., ROWE, D.W., YULE, J.D., FROST, C.D., Department of Geology and Geophysics, University of Wyoming, Laramie, WY 82071-3006, SHARP, W.D., Department of Earth and Space Sciences, SUNY, Stony Brook, NY 11794, and WADGE, G., Department of Geography, University of Reading, Reading RG6 2AB, UK.

The Mesozoic rocks of Tobago can be divided into three main groups: the North Coast Schist (NCS), the ultramafic to mafic plutonic complex, and the Tobago Volcanic Group (TVG). These broad lithologic subdivisions form three east-west-trending belts that transect the island. A mafic dike swarm widely intruded the plutonic complex and TVG, whereas scattered pre-metamorphic and post-metamorphic dikes occur in the NCS belt.

Radiolaria in argillite layers from a distinctive epiclastic unit in the TVG suggest an Albian to Early Cenomanian age (D.L. Jones and P. Noble, pers. comm., 1987), and ammonite molds from this same unit indicate an Albian age (W.A. Cobban, pers. comm., 1988). $^{40}Ar/^{39}Ar$ hornblende plateau ages from the plutonic-volcanic-dike complex indicate that this rock suite evolved in the Albian (105-103 Ma). The age of the NCS is at least Aptian and perhaps as old as Late Jurassic ($^{40}Ar/^{39}Ar$ data on relict igneous hornblende from greenschist-facies tuff breccia).

Geochemical and Nd and Sr isotope data demonstrate an oceanic island arc character for all the pre-Cenozoic rocks of the island. All suites span the calc-alkaline and tholeiitic regions on discrimination diagrams. Rare earth element (REE) patterns for the NCS, TVG, and plutonic suite are essentially identical and are moderately LREE-enriched (La/Yb = 1.1-2.7). The dikes exhibit the most unevolved REE patterns, and are interpreted as most closely representative of parental liquid compositions.

Detailed geologic mapping indicates that the NCS was wallrock for the plutonic complex; brittle faulting and retrogression have commonly overprinted these relations, but locally the primary intrusive igneous contact between the plutonic complex and the metamorphosed NCS rocks is preserved. This boundary is a zone of high shear strain where a hot, nearly crystalline mass of ultramafic rocks dynamothermally metamorphosed older greenschist facies rocks during high-level emplacement into the crust.

The pre-Cenozoic rocks of Tobago represent an exceptional cross section through a portion of a composite Mesozoic arc system; other parts of which may be found in the Villa de Cura klippe, the Aruba-Blanquilla island chain, and perhaps the Western Cordillera of Colombia and Ecuador.

CHARACTERISTICS OF VOLCANIC CENTERS FROM THE LESSER ANTILLES

A.L. Smith and M.J. Roobol, Department of Geology, University of Puerto Rico, Mayaguez, Puerto Rico 00708

The active volcanoes of the Lesser Antilles are characterized both by effusive eruptions producing lava flows and domes and by explosive eruptions producing various types of pyroclastic deposits. Five major styles of explosive eruptions have been distinguished, these styles and their products are:
Pelean - block and ash flows, dense andesite surges, ash and dust falls;
St. Vincent - scoria and ash flows, scoriaceous surges, lapilli-, and ash-falls;
Plinian - pumice and ash flows; ash hurricanes, pumiceous surges, lapilli-, and ash-falls;
Asama - semi-vesicular block and ash flows;
Phreatomagmatic/Phreatic - ash falls, base surges.
Based on their eruptive products the volcanoes of the Lesser Antilles can be grouped into five types:
a) Centers composed almost entirely of pyroclastic deposits - Mt. Pelée (Martinique), the Quill (St. Eustatius);
b) Centers composed of Pelean dome clusters and associated aprons of block and ash flow deposits - Saba island, Soufriere Hills (Montserrat);
c) Centers with numerous dacitic pumice and ash flows - centers on Dominica, south-central St. Lucia;
d) Centers with at least 50% lava flows associated with pyroclastic deposits of various types - the Peak (Nevis), Soufriere (St. Vincent);
e) Centers composed of basic lava flows and associated fall deposits - South Soufriere Hills (Montserrat).
The pyroclastic deposits from all volcanic centers are commonly reworked soon after eruption by fluviatile processes so that stratigraphic sections commonly show intercalations of pyroclastic deposits with their epiclastic derivatives. Eruptions from Lesser Antillean volcanoes also produce submarine deposits such as subaqueous ash falls, subaqueous volcaniclastic flows and ash turbidites.

ASPECTOS TEORICO-PRACTICOS DE LAS INVESTIGACIONES DEL GRADIENTE VERTICAL ANOMALO DEL CAMPO GRAVITATORIO EN EL TERRITORIO DE CUBA

O.A. SOUSIN, V. BELLO, M. PARDO.
Instituto de Geología y Paleontología, MINBAS, Cuba

Las investigaciones sobre el gradiente vertical anómalo regional (GVAR) del campo gravitatorio presentan un interés teórico y práctico considerable, ya que permiten, por una parte, incursionar en la elaboración de algunas nuevas formas de resolución de las tareas inversas de la gravimetría durante las investigaciones estructurales regionales, y por otra, asegurar la interpretación correcta de los resultados de los levantamientos gravimétricos de escalas medias y detalladas en las regiones montañosas. Es necesario señalar, que, en la práctica mundial, esta cuestión está poco elaborada, en particular, lo relacionado con el esclarecimiento de las causas del GVAR.

De los análisis teóricos se evidencia que el GVAR puede estar provocado por heterogeneidades locales de la densidad, localizadas tanto en la cortoza terrestre, como en el manto superior, así como por zonas características de perturbación de los límites de la corteza y del manto. Los valores del GVAR pueden alcanzar magnitudes significativas (hasta 8.10 mgl/km, según los datos de O.A. Sousin, para las regiones montañosas de Asia) y tener signos diferentes. Magnitudes semejantes de GVAR se destacan también en Cuba Oriental, pero aquí tienen otro significado, ya que están relacionados, probablemente, con una heterogeneidad local de alta densidad y con un levantamiento conforme de la superficie del manto superior. En el trabajo se muestra que para las primeras etapas de las investigaciones del GVAR en Cuba, se debe argumentar con mayor precisión teórica sus magnitudes partiendo de toda la información geofísica y geológica disponible de la región, y después determinar su valor concreto y su distribución areal, primero mediante el análisis de correlación, y posteriormente por investigaciones experimentales. Se muestra también que sin el cálculo de la influencia del GVAR en la parte montañosa de Cuba Oriental se tendrán dificultades serias, no sólo en la interpretación de los trabajos regionales y de búsqueda (en particular, en la búsqueda de cromitas), sino también en la propia confección de los mapas gravimétricos.

EARLY STRUCTURAL EVOLUTION OF ST. CROIX

SPEED, R., Department of Geological Sciences, Northwestern University, Evanston, Illinois, and JOYCE, J., Department of Geology, University of Puerto Rico, Mayaguez, Puerto Rico

St. Croix and perhaps the bulk of the St. Croix Platform are underlain by a Cretaceous tectonic complex composed almost entirely of volcanigenic sedimentary gravity flows of known Cenomanian or Turonian to Maastrichtian depositional ages. The tectonic complex is a pile of thrust sheets that was assembled before intrusion of late Maastrichtian arc magmas. Each nappe contains two or more deformations. Structures in common among the nappes are folds with initial vergence between S and SW, fold related cleavage, and generally steeply E plunging axes.

The early folds and thrusts of St. Croix's Cretaceous strata are interpreted as a product of offscraping trench wedge deposits at the toe of a Late Cretaceous island arc. Later folding in the tectonic complex records NS horizontal contraction (in today's coordinates), possibly in Paleogene time. The Late Cretaceous island arc which supplied the volcanigenic sediments of St. Croix was active for at least 14 ma and perhaps for over 30 ma.

IMPLICATIONS FROM ST. CROIX ON THE PLATE TECTONIC HISTORY OF THE NORTHEASTERN CARIBBEAN

SPEED, R., Department of Geological Sciences, Northwestern University, Evanston, Illinois

Major questions of Cenozoic plate tectonics of the northeastern Caribbean are the duration and total displacement of the Caribbean plate which moves generally east relative to the N. American plate and the precise direction of today's Ca-NA motion. The structural evolution of St. Croix and surroundings implies that the eastern Greater Antilles has undergone transtension since at least early Miocene time and that Ca-NA is more probably ESE than ENE. Troughs between the St. Croix and Virgin Islands Platforms, in the Anegada Gap, and the Puerto Rico Trench may be major breakup zones in this extensional system. Implications of older tectonics from St. Croix are: 1) early Paleogene and(or) end Cretaceous NS convergence affected the eastern Greater Antilles, probably due to a downgoing slab at the precursor to the present Puerto Rico Trench; and 2) convergence occurred on the southern wall of the eastern Greater Antilles in the Late Cretaceous, causing the buildup of the accretionary complex that is the Cretaceous basement of St. Croix. The longitudinal history of St. Croix, however, is still unknown.

GRAVITY AND BOTTOM CURRENT FLOW PATTERNS IN UPPER CRETACEOUS ROCKS, ST. CROIX, U.S. VIRGIN ISLANDS - THEIR PALEOGEOGRAPHIC SIGNIFICANCE

STANLEY, DANIEL JEAN, MEDIBA Program, Division of Sedimentology, NMNH, Smithsonian Institution, Washington, D.C. 20560 (USA)

New measurements of sedimentary structures in rocks on St. Croix, U.S. Virgin Islands, record deep-ocean currents in the northeastern part of the Caribbean during the Late Cretaceous. Flow was directed toward the west, a direction parallel to the surface circulation in this region. Paleocurrent analysis of marine volcaniclastic sections of Late Cretaceous age reveals a two-phase depositional pattern: primary emplacement by turbidity currents flowing toward the south, and the subsequent reworking of these layers by W-flowing bottom currents. Sands were first transported to lower slope aprons, and these were then reworked along bathymetric contours by bottom water flow, probably driven by thermohaline processes. At the end of the Cretaceous, the paleo-Atlantic was much narrower and the Caribbean configuration considerably different than at present. The abundance of current-reworked turbidites and bioturbation structures, however, provide clear evidence of active deep water circulation in the tectonically active island arc setting, and the maintenance of oxygenated conditions on the sea floor, as at present.

[Modified from *Marine Geology*, 79 (1988)]

DOMINANT PALEOCURRENT PATTERNS, ST. CROIX

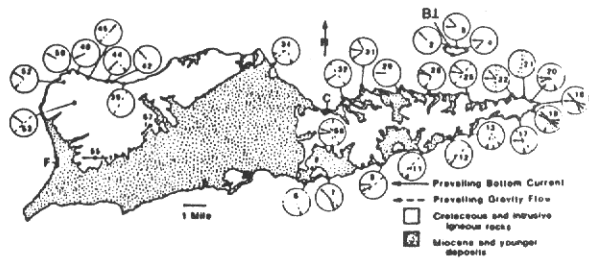

Map showing the prevailing paleocurrent directions (tractive bottom current and gravity flow) measured in Upper Cretaceous sequences at 32 localities on St. Croix and Buck Island (B.I.). Geographic names are listed in Table 1. C - Christiansted; F - Frederiksted.

TURBIDITES, CONTOURITES AND VARIANTS IN UPPER CRETACEOUS STRATA OF ST. CROIX, U.S. VIRGIN ISLANDS - A REVISED SEDIMENTATION MODEL

STANLEY, DANIEL JEAN, MEDIBA Program, Division of Sedimentology, NMNH, Smithsonian Institution, Washington, D.C. 20560 (USA)

A purely turbidite or gravity-emplaced interpretation does not adequately explain the origin of marine volcaniclastic strata in Upper Cretaceous units in St. Croix, U.S. Virgin Islands. Most sandy layers, herein termed intermediate variants, record emplacement in two stages: first by turbidity currents, flowing toward the south, and then a subsequent reworking of these layers by bottom currents flowing toward the west. The sands, accumulating on lower slope aprons, were then displaced along bathymetric contours before burial. A natural continuum of deposits results between downslope-directed turbidity current and bottom current-tractive "sand-member" deposits. The lower part of a variant layer typically preserves the original graded basal (A) turbidite division, while the texturally cleaner middle and upper parts of such a stratum usually show structures more typically associated with tractive transport. An inventory of the diverse suite of reworked sandy lithofacies in St. Croix may be comparable to other cases in the rock record and modern oceans that involve interaction between gravity-driven flows and bottom currents.

[Modified from *Marine Geology*, 78(1987)]

TURBIDITE TO CURRENT-REWORKED SAND CONTINUUM

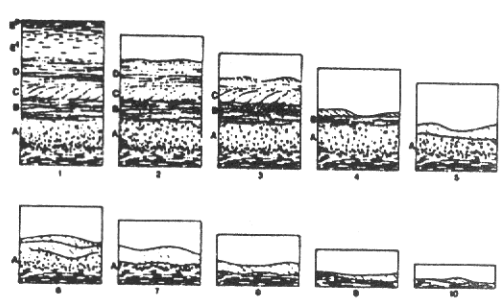

Scheme showing continuum of sediment types which may result from the reworking of a sandy layer originally emplaced as a complete A-E turbidite (1, at left). Reworking would result in partially eroded (2) and partially remolded turbidite (variant) series (3-7), to completely remolded and entirely forereet laminated (8, 9) and to discontinuous starved ripple (10) layers. Stratal types 7 to 10 are the reworked "end-products" in this series. Progressive downward erosion and lateral disruption of the original turbidite layer are depicted.

Evolution of siliceous sedimentary environments in the Nicoya Compex (Costa Rica) during the Jurassic- Cretaceous and its relation to the geotectonic development of the Caribbean Crust.

STEINBERG, ERIK, Escuela Centroamericana de Geología, Apdo 35, 2060 Universidad de Costa Rica, San José/Costa Rica

Recent biostratigraphical and sedimentological studies on the siliceous sedimentary rocks within the ophiolitic Nicoya Complex in NW-Costa Rica yielded a series of new data which shall be presented here.
According to this, three main sedimentary environments belonging to two different basins can be differenciated for these Jurassic to Cretaceous rocks. This is also supported by paleomagnetic data.
Two main sedimentation cycles can be described, one lasting from the Lower Jurassic to the Middle Cretaceous, the other from the Lower to the Upper Cretaceous. The last is partialy represented by bituminaceous sediments which may have a relation to the world wide described Cretaceous anoxic events.
Both basins and their sediments present discriminating caracteristics that allow a direct correlation with the early geotectonic evolution ogf the Central American Landbridge and the Caribbean Crust.
Biostratigraphic data based on radiolarian assamblages permit a more concise subdivision of the siliceous strata, thus yielding a precise timescale for the larger regional geologic events. Furtheron they allow a correlation with international zonations.

ELEVATED MARINE TERRACES ON NORTHWESTERN PUERTO RICO

TAGGART, B.E., Department of Marine Sciences, University of Puerto Rico, Mayagüez, Puerto Rico and **JOYCE, J.** Department of Geology, University of Puerto Rico, Mayagüez, Puerto Rico

We have undertaken a detailed study of marine terraces on northwestern Puerto Rico focusing on correlation of wave-cut geomorphic features and marine terrace deposit stratigraphy. Stratigraphic control is based on C-14 and U/TH coral dates from three localities; Rincón, Borinquen and Quebradillas. The deposits at these localities are dominantly calcareous sandstones and conglomerates derived from mixed marine and terrigenous sources. Corals occur immediately above unconformities and within the coarser conglomerates. The Rincón area contains the most extensive exposures of marine terrace deposits and has yielded the majority of the dated corals. We have correlated deposits and wave-cut features from all other study sites to the Rincón exposures.

U/TH ages of 114,000 (±3,495), 120,000 (±2,950) and 120,000 (±3,084) YBP were obtained for the 10 m surface at Rincón and Quebradillas. It is generally accepted that sea level was 6 m higher than present approximately 125,000 years ago. Therefore, these data suggest that Puerto Rico has been uplifted at an average rate of 0.034 mm/year during the late Quaternary. C-14 ages of 1,590 (±80), 2,050 (±80), 1,460 (±80) and 1,680 (±70) YBP were obtained for the 2 m level at Rincón and Borinquen. U/Th ages obtained for these samples are 3,000 (±150), 3,000 (±150), 8,000 (±470) and 2,000 (±118) respectively. These data imply that there was a change in the rate of uplift from 0.034 mm/year to about 1.5 mm/year. There is no reason to suspect that the rates of tectonic uplift should increase so dramatically during the last 1,500 to 3,000 years. However, the possibility of episodic uplift, as opposed to continuous uplift, cannot be ruled out. An alternative explanation to a radical change in the rate of uplift is that local sea level was approximately 2-3 meters higher than present between 1,500 and 3,000 years ago.

Deep-water limestone deposited during the early Pliocene (Quebradillas Formation) is now found at elevations in excess of 100 m in northwestern Puerto Rico. This is in agreement with the average rate of uplift of 0.034 mm/year obtained using dated late Pleistocene marine terrace deposits and suggests that there has been a slow and constant rate of uplift during the last 3 million years.

CONTROL DESIGN GRADE TOLERANCE FOR SUCCESSFUL WETLAND RESTORATION

STEPHEN, M., Vice President, Coastal Engineering Consultants, Inc., Naples, Florida

This paper presents the colonization and growth rate sensitivity to the initial elevation of the planting substrate for an artificially created mangrove wetland.

Located on Naples Bay in the subtropical climate of Southwest Florida, 15 acres of dredge spoil heavily vegetated with Australian Pine (Casuarina equistifolia) were cleared and scraped to an elevation of + 45 cm above 0.0 N.G.V.D. with a construction tolerance of 15 cm above or below the design grade.

Red Mangrove propagules (Rhizophora Mangle) 20 - 25 cm in height were then planted 1 meter on center.

The initial monitoring survey, conducted 6 months after planting mangrove propagules documented significant growth rate variability as a function of very minor, 10 - 15 cm, difference in elevation of the initial planting surface.

Planting grades at elevations greater than 50 cm above sea level supported volunteer black mangrove (Avicennia germinans) and stunted red mangrove propagule growth.

Planting grades between 35 - 50 cm above sea level supported well developed red mangroves up to 56 cm in height after six months growth.

Planting grades less than 35 cm above sea level suffered high red mangrove propagule mortality. However, in place of red mangrove, substantial oyster and seagrass colonization was recorded.

AN EVALUATION OF THE GEOLOGICAL HISTORY AND HYDROCARBON POTENTIAL OF THE LATE MIOCENE-PLIOCENE SEDIMENTS OF THE GOUDRON FIELD - TRINIDAD

TELEMAQUE, C.P.
Geological Department,
Trintopec, Santa Flora
TRINIDAD, WEST INDIES

The Goudron Field lies in the Southern Basin onshore Trinidad, on the southeastern flank of the Rock-Dome-Lizard Springs anticlinal trend. A sedimentary sequence of Upper Cretaceous to Late Tertiary sediments has been penetrated by the 174 wells drilled in the area. However, to date only the Late Miocene and Pliocene contain productive hydrocarbon reservoirs.

Two major episodes of late Miocene/Pliocene sedimentation were identified. The older comprised a period of sediment gravity flow into a bathyal environment in the Late Miocene/Early Pliocene and resulted in the deposition of the interbedded shales, silts, sands and conglomerates of the Moruga Formation. The younger comprised a period of fluvio-continental deposition in the Pliocene and resulted in the sands and minor silty clays of the Mayaro Formation.

Deposition of the Moruga Formation was followed by a major tectonic event, resulting in the formation of the Pilote Syncline and the Pre-Mayaro Unconformity. Minor episodes of late Pliocene/Pleistocene faulting are also evident.

The field was discovered in 1927 and has produced 4.7 MMBO to date and may still contain significant reserves to be exploited.

PALEOMAGNETIC INVESTIGATIONS IN THE DOMINICAN REPUBLIC (HISPANIOLA)

Stefan THOMAS, Universitaet zu Koeln, Geologisches Institut, Zuelpicher Strasse 49, D - 5000 Koeln 1, W.Germany.

In the Dominican Republic more than 90 outcrops of Cretaceous and Tertiary rocks were sampled for paleomagnetic investigation. Laboratory work is still in progress. A pilot suite of demagnetized samples from different formations gives following results:

Pre-Aptian volcanic rocks including basalts and quartz keratophyres from the Los Ranchos Formation in the Cordillera del Seibo and the eastern Cordillera Central show a stable remanent magnetization. The uncorrected mean direction D = 286.9; I = 33.8 (α_{95} = 12.5; k = 17.9; n = 9) is computed for two localities (distance about 100 km). The directions scatter widely after tilt correction. The data are interpreted to indicate a counterclockwise rotation of the formation after folding of the strata.

Results from the upper Cretaceous EL RIO tonalite batholith in the Cordillera Central coincide with the studies of VINCENZ & DASGUPTA (1978). We found a stable direction of D = 293.1; I = 43.7 (α_{95} = 23.3; k = 9.2; n = 6). The intrusion seemed to be rotated anticlockwise. The rocks of the Rio Los Baos tonalite north of the Bonao fault carry predominantly secondary magnetization of recent origin, characterized by very low coercitive components.

The Paleocene-early Eocene Imbert Formation is located near the village of Imbert in the Cordillera Septentrional. Stable magnetization components of dual polarity were revealed through progressive thermal and alternating field demagnetization of vitric tuffs from the Rio Obispo section. The corrected directions DR = 237.5; IR = 19.5 (α_{95} = 9.8; k = 47.7; n = 6) and DR = 61.3; IR = -20.1 (α_{95} = 19.7; k = 16.1; n = 5) suggest a counterclockwise rotation along the Camu fault.

More data from a field trip in spring 1989 will be presented at the conference. They include results from the lower Miocene Soabrerito Formation and Eocene volcanic and sedimentary rocks of the Sierra de Neita. First results out of this mountain range display anticlockwise rotations of about 60 degrees.

ABSTRACT

"STRUCTURAL FEATURES ASSOCIATED WITH THE LOS BAJOS FAULT"

By

L. TYSON, Trinidad & Tobago Oil Company Limited

The Los Bajos Fault is a member of a family of strike-slip faults present in Northern South America. It has an average azimuth of 113°, and a horizontal displacement of roughly ten kilometres.

Structural features present along it depend on changes in the azimuth of the fault. Where this is less than 113°, transpressional features developed, e.g. the East Soldado, Point Fortin and Los Bajos displaced half-anticlines. Where the azimuth is greater than 113°, transtensional features or grabens developed, e.g. the North Soldado and Coora grabens. Sub-perpendicular folds developed away from the fault include the La Brea, Vance River - Boodoosingh, Lot One, Forest, Bernstein and Penal anticlines.

The terminus of the Los Bajos strike-slip fault is the Southern Range Uplift - a basement-involved thrust fault. This basement-involved uplift resulted in the formation of a linear basin - the Columbus Channel Syncline - over its underthrust limb.

STRATIGRAPHY OF BOQUERON BAY

TORRES, N. DEPARTMENT OF MARINE SCIENCES, UNIVERSITY OF PUERTO RICO, Mayaguez, Puerto Rico 00709

Seven vibro cores and seismic lines have been used to study the stratigraphy of Holocene deposition in Boqueron Bay, Puerto Rico. Boqueron Bay is a 10 square km area bay on the southern west coast of Puerto Rico. It is a shallow bay (10 m depth), bounded on three sides by land and restricted on the fourth side (west) by a shoal reef, which restricts circulation to the open sea to a narrow channel at the north and the south margins of the bay.

The surface sediments are dominantly skeletal carbonate except for a terrigenous quartz-rich component at the west and northwest. The cores show several episodes of mollusc sediments layers, possibly indications rapidly changing environmental conditions. The cores and seismic lines are used to develop a three-dimensional pattern of deposition during Holocene sea transgression.

HOLOCENE OSTRACODA IN AND AROUND LAKE ENRIQUILLO (DOMINICAN REPUBLIC)

VAN DEN BOLD, W. A., Department of Geology and Geophysics, Louisiana State University, Baton Rouge, Louisiana

Fifteen cores of generally about 30-cm length, taken in Lake Enriquillo by Paul Mann, Charlotte Glenn and Ross Maddox (University of Texas, Austin, and University of Houston), show ostracode faunas of very low diversity, but occasionally great abundance of certain species. The top 10-15 cm of four cores exhibits a dominance of Cyprideis salebrosa Bold, accompanied by Limnocythere floridensis Keyser, indicating very low salinity, possibly caused by the presence of fresh water springs. The most common assemblage, occurring in the deeper parts of all cores, and occasionally throughout the cores, is dominated by Cyprideis edentata (Klie), Dolerocypris inopinata Klie and Perissocytheridea cribrosa (Klie). This assemblage is almost identical to the one described by Klie from the saline lagoons of Aruba, Bonaire and Curaçao, and indicates hypersaline conditions, in agreement with the 49 °/.. salinity reported from the lake. Between these two extremes and occupying the middle (and sometimes the upper part) of the cores is an assemblage of Cyprideis similis (Brady) with Dolerocypris inopinata and Perissocytheridea cribrosa. The faunas of the subaerially exposed sediments overlying the Holocene reef around Lake Enriquillo are very different from the fauna of the cores. The basal beds have an almost normal marine fauna with some additional brackish water species (Cyprideis similis, C. salebrosa and Perissocytheridea cribrosa). The overlying beds rapidly become more limnic (?oligohaline), with Cyprideis salebrosa, Limnocythere floridensis and Cytheridella boldi Purper. Intermediate beds yield Cyprideis similis, C. mexicana Sandberg and Paracytheridea setipunctata (Brady), indicating intermediate salinities (?mesohaline). The Cyprideis salebrosa assemblage of the bottom part of a 115-cm-long core in the lake might belong to the similar fauna near the top of the exposed sections, as does the assemblage of a limestone on Isla Cabritos in the lake.

SHORT REVIEW OF THE OSTRACODA OF THE MONTPELIER AND COASTAL GROUPS OF JAMAICA

W. A. van den Bold
Louisiana State University, Baton Rouge

The Montpelier Group (Oligocene - Middle Miocene) contains a mixture of dominant bathyal species, minor outer neritic ones and rare inner neritic taxa. The neritic forms are probably derived from contemporaneous deposits on the shelf. However, in the basal Spring Garden Formation (N 8) redeposited specimens are derived from older (N 1-2) shallow water sediments. The amount of neritic taxa increases slightly in the middle Bonny Gate Formation (N 1), and in the lower Buff Bay Formation (N 14), and there is a steady increase of neritic forms from late Middle Miocene (N 15) to Pleistocene, when more than 75% of the species are neritic. Due to the small number of shallow water species from Oligocene to Late Miocene, it is not surprising that the application of the zonation based on shallow water Ostracoda is not quite satisfactory.

GEOCHEMISTRY OF THE SAN JUAN BASALTS, DOMINICAN REPUBLIC: A REAPPRAISAL BASED ON NEW TRACE ELEMENT DATA

VESPUCCI, P., and LEWIS, J.F., Geology Department of The George Washington University; Direccion de Mineria, Santo Domingo

Basalt lavas of probable Pleistocene age from the northwestern San Juan valley are nepheline basalts, basanites, and alkali olivine basalts. Eleven new samples were analyzed for major elements and for Cr, Ni, Cu, Zn, Rb, Sr, Y, Zr, Nb, Ba, and Rare Earth Elements (REE).

The San Juan basalts are enriched in LIL elements including BA: 1078-2336 ppm and Sr: 1586 - 3466 ppm. Rb/Sr ratios are less than .04. Sr87/Sr86 ratios range from 7059 to .7079, and are higher than calc-alkaline basaltic rocks of similar age in the Valle Nuevo, Padre Las Casas, Yayas de Viajama regions of the eastern Cordillera Central. The San Juan basalts also differ from the calc-alkaline basaltic rocks of the Cordillera Central in having high concentrations of HFS elements (Ti, Nb, Zr) including Nb: 10 - 77 ppm; Zr: 163 - 435 ppm, and TiO2: 1 - 4.1 weight percent.

REE patterns are highly fractionated with chondrite normalized La/Yb ratios ranging from 46 to 85, and La/Sm ratios ranging from 8 to 10. There is minimal enrichment of LIL elements to LRE elements as evidenced by chondrite normalized Ba/La ratios ranging from 1 to 1.5. The behavior of Sr, Ce, La, and Zr is closely related in these basalts.

Numerical petrogenic models indicate that key processes involved in the origin of these basalts include variable degrees of partial melting of an enriched mantle source region and fractional crystallization.

STRUCTURE DE LA MARGE S-W CARAIBE (secteur Cartagena, Colombie)

par

G. VERMETTE[1], C. BOBIER[1], G. BLANC[2], L. BRICEÑO[3], H. CARVAJAL[4], J.GAYET[1], A.MAUFFRET[5], A.MOLINA[6], S. O'CONNELL[7], M. PARGA[1]

Les profils sismiques obtenus au cours de la campagne DIAPICAR (oct.-Nov. 1987) sur la marge SW caraïbe entre le golfe de Morrosquillo et l'embouchure du Magdalena montre l'existence de deux secteurs aux caractères différents :

1) Au Sud, un front de déformation englobant plate-forme et talus continental. Ce front est constitué par une série de plis, rides et dômes d'origine diapirique dont la distribution est en relation étroite avec la structuration régionale de direction principale N30°.

Vers 10°25 de latitude Nord, la base de ce front de déformation s'incurve brusquement à N90° en direction du continent ; c'est une zone de transition où la présence de deux directions structures majeures (N30° pour le banc Tortuga et la presqu'île Baru, N90° pour le chapelet d'îles du Rosaire, cours en dent de scie du Dique) soulignent l'existence de mouvements cisaillants.

2) Au nord, une immense accumulation d'origine deltaïque et qui peut être subdivisé en un éventail fossile centré sur Galerazamba et un prodelta Actuel où les manifestations diapiriques rencontrées sont d'un type différent de celles du secteur Sud.

1 - Département de Géologie et Océanographie - Université de Bordeaux I, France.
2 - Institut de Géologie - Université de Strasbourg, France.
3 - Departamento de Geociencias - Universidad Nacional Bogota, Colombia.
4 - Ingeominas, regional Cartagena, Colombia.
5 - Departement de Géologie dynamique - Université P.M.C. Paris, France.
6 - Centro de Investigaciones Oceanograficas e Hidrograficas Cartagena, Colombia.
7 - O.D.P. Science Operations, Texas A. et M. University, Texas, U.S.A.

GEOLOGICAL EVOLUTION OF THE CRETACEOUS AGE SEDIMENTS OF THE SABA BANK AREA AND THEIR PETROLEUM POTENTIAL

WARNER Jr., A. J., A.J.W. and Associates, Wichita Kansas, and KUBENA, REED, Richmond Texas.

The Saba Bank area belongs to the very complex tectonic framework of the Caribbean Plate and so far no completely satisfactory theory of the tectonic history of the region exists. In formulating a thesis of the area's history, three (3) ideas must be considered: (1) Is Saba Bank genetically related to the Greater Antilles, the Lesser Antilles or a little of both? (2) Is the Saba Bank a northern extension of the Aves Ridge? (3) Do sediments of Early Eocene age and older exist beneath the Saba Bank Platform? During February of 1988 Western Geophysical conducted a seismic survey over the western portion of the Saba Bank. The new seismic revealed that a thick sedimentary section exists below what had been previously considered economic basement. The reworked Cretaceous Age coals and nannofossils found in the Tertiary sediments in both wells drilled on the platform prove that the Cretaceous rocks will not be of deep marine origin. Offshore St. Croix a thick sequence of sandstones and conglomerates has been found. This sequence has not been dated but from its stratigraphic position it should be Mid Cretaceous. These sediments are direct evidence that thick nonmarine Cretaceous sediments do exist in the area. These sediments dip 10 to 20 degrees to the west which, when extrapolated to the east, place them under the Saba Bank Platform. The migrated hydrocarbons found in both Saba Bank wells showed that source rocks exist in the area. Both the seismic data and the well data suggest that a thick nonmarine untested Cretaceous sedimentary section exists under the Saba Bank.

COAL EXPLORATION IN COSTA RICA: A CASE STUDY

WEAVER, J.N., U.S. Geological Survey, MS 972, Denver, CO, 80225; and RAMIREZ, O., MALAVASSI, L., and BOLANOS, K., Refinadora Costarricense de Petroleo (RECOPE), Ap. 4351, Zona 1000, Octavo Piso, San Jose, Costa Rica.

Energy-planning, growth and development problems in Central America cannot be solved without a better understanding of indigeneous energy resources. Developed peat and coal resources can be utilized in a variety of ways, ranging from domestic use through process heat for the coffee, sugar and cement-making industries, and for the generation of electricity. Begining in 1983,the Costa Rican government and the US Agency for International Developemnt (AID) sponsored a cooperative coal development program using United States Geological Survey (USGS) and Refinadora Costarricene de Petroleo (RECOPE) geologists. USGS scientists assisted RECOPE geologists in coal exploration and resource assessment activities with emphasis on technology transfer. Accomplishments of the formal cooperative program include: A) reconnaissance stage investigations were completed in five coal areas (Esparza, Puriscal, El Tablazo, Rio Estrella, and Upala), B) reconnaissance stage investigations and early exploration stage studies were underway in the Zent and Venado coal fields, and C) the first exploratory drill-hole program in the Uatsi Project area of the Baja Talamanca coal field had been completed and a summary progress report had been prepared. As part of the original cooperative agreement, the USGS and USAID helped RECOPE with training and equipment to establish a modern coal analytical facility, designed to provide definitive information on coal quality factors of the coals in Costa Rica.

Since the end of the formal program, RECOPE has continued exploration and development of the Zent coalfield because it is located near main railway and highway systems and could be the source of coal for industries located in the central part of Costa Rica and exploration and development for the Uatsi Project area because of the need for increased electric-generating capacity in that part of the country.

Results to date include: A) the establishment of coal resources of lignite and subbituminous rank of more than 49 million metric tons, of which more than 32 million metric tons are in the Uatsi Project area, almost 15 million metric tons in the Zent coal field B) 700 metric tons of coal were recovered at a surface mining operation in the Zent coal field for testing as a supplemental fuel replacing fuel oil in a cement-making plant C) testing programs for cleaning of coal and improving quality have been conducted and D) preliminary mining designs have been prepared for areas in both the Zent coal field and the Uatsi Project area. As the exploration continues, it is expected that the estimated resources will increase. Planning for further development activities has continued. Coal related hydrologic studies, refraction seismic exploration, and more core-drilling are all planned for the near future.

PETROLOGY OF THE LOWER CRETACEOUS VOLCANIC ROCKS OF NORTHEASTERN PUERTO RICO - INITIAL PRODUCTS OF ISLAND-ARC SUBDUCTION

WEILAND, THOMAS J., Dept. of Geology, Georgia Southwestern College, Americus, Georgia 31709

The Lower Cretaceous pre-Robles formations are the oldest exposed rocks of the central volcanic-plutonic core of Puerto Rico. In northeastern Puerto Rico, pre-Robles rocks include the Daguao Formation at the base, the Figuera Lava and the Fajardo Formation. The Daguao Formation consists of predominantly volcanic breccias, lava flows and tuff. Low silica contents, abundant diopside-augite phenocrysts, common olivine pseudomorphs and calcic plagioclase compositions indicate that these rocks are basalts and basaltic andesites. The Figuera Lava is a thick sequence of albite-rich andesitic and dacitic lava flows with only minor interbedded volcaniclastic rocks. Clear homogeneous albite phenocrysts in these rocks apparently formed during burial metamorphism. The lower Fajardo deposits consist of silicic volcanic breccias and volcaniclastic deposits which represent a continuation in the silica-enrichment trend defined by the underlying Figuera samples. By contrast, the interbedded flows and younger volcaniclastic rocks of the Fajardo Formation record a change to pyroxene-rich intermediate compositions.

Based on whole-rock compositions, modal and normative mineralogy and mineral compositions, the pre-Robles volcanic rocks of northeastern Puerto Rico are subalkaline tholeiites. The low $^{87}Sr/^{86}Sr$ ratios of whole-rock samples, the Cr-rich cores of clinopyroxene phenocrysts, and the similarity between the pre-Robles basalts and experimentally-produced melts of peridotite, indicate that the pre-Robles magmas were probably derived from the partial melting of mantle peridotite. Much of the geochemical and mineralogic variation found in the pre-Robles samples appears related to subsequent crystal fractionation at two or more levels within the crust and upper mantle. Evidence that the silicic and intermediate volcanic rocks were derived from mafic magmas by shallow-level fractionation includes: 1) geochemical trends defined by whole-rock and mineral compositions; 2) temporal relationships of individual flows; and 3) good fit of computer-derived fractionation models.

BEACH DYNAMICS IN THE SAN JUAN METROPOLITAN AREA

WEBB[1], R., and VELAZCO[2], A., [1]Marine Geology Program, U.S. Geological Survey, San Juan, Puerto Rico, [2]Department of Natural Resources, Area of Scientific Research, Section of Marine Resources, San Juan, Puerto Rico.

The north coast of Puerto Rico is a microtidal, high energy environment with a series of separate lunate embayments formed behind eroded eolianites. To quantify the dynamic nature of the beaches in the San Juan area, twenty-four beach sites were profiled on a bi-monthly basis from fall of 1984 through fall of 1985. Wave climate changed over the year with the impact of swells from two tropical storms, Gloria and Kate, being documented. Over the year, eight of the profile stations experienced net losses, with erosion rates in the range of .3 to 11 m/yr; the other sixteen stations were either stable or accreting. In general, areas of wave convergence had the most mobile beaches with low net erosion rates.

Seasonally changing wave energy interacts with the complex bathymetry resulting in little lateral continuity of incident wave energy along any given stretch of shoreline. A variety of seawalls, groins, and jetties have been built to further add to the heterogeneity of the San Juan shoreline. Irregular offshore bathymetry commonly focused incident wave energy into various sections of the embayments and away from the headlands. Results of wave refraction modeling indicated greater potential longshore transport in the embayments than on the headlands. Thus, the vulnerability of a particular beach depended primarily on its position in relation to the foci of wave energy generated by mean and extreme wave conditions.

Each beach reacted differently to periods of extreme wave conditions. In response to the swells generated by Hurricane Gloria in September 1985, eight beaches accreted while ten showed losses. Two months later, Hurricane Kate produced similar responses but on different beaches. Those beaches that had a natural low tide sill near shore were the most stable under any wave condition. Future wave climatology will be the determining factor in the continuing evolution of the beaches in the San Juan area. Measures to mitigate erosion may include perched beaches and possibly engineering solutions involving modification of the offshore eolianites to modify the amount of wave energy entering the area and the refraction patterns developed.

SIGNIFICANCE OF PYROXENE-RICH UNDERSATURATED BASALTS IN THE EARLY TECTONIC EVOLUTION OF PUERTO RICO

WEILAND, THOMAS J., Dept. of Geology, Georgia Southwestern College, Americus, Georgia 31709.

A recent petrographic and geochemical study of volcanic rocks in the Lower Cretaceous formations of central Puerto Rico has located several pyroxene-rich/plagioclase-depleted undersaturated basalts within a thick sequence of less-mafic plagioclase-rich subalkaline lava flows and pyroclastic rocks. These slightly-alkalic undersaturated volcanic rocks include several lava flows, volcanic breccias and tuffs in the partially-correlative Jayuya Tuff, Torrecila Breccia, and Pitahaya Formation of the central tectonic-stratigraphic block of the island. The general absence of plagioclase phenocrysts, Cr-rich diopsidic compositions of pyroxene phenocrysts, high Ni and Cr whole-rock concentrations, high modal concentrations of olivine and clinopyroxene phenocrysts, and normative concentrations of olivine and hypersthene or nepheline in these rocks indicate that they originated from deeper crustal levels than other Lower Cretaceous volcanic rocks of Puerto Rico.

The undersaturated volcanic rocks are located within a stratigraphic sequence that records a rapid change in water depth. Adjacent shallow-marine limestones, interbedded calcareous units with shallow-marine fossils, and possible oxidized units within the sequence indicate that these rocks were erupted in shallow-marine or subaerial conditions. In contrast, the overlying Robles Formation was deposited in predominantly deep-water conditions. Therefore, it appears likely that the pyroxene-rich rocks were erupted concurrently with formation of deep-seated faults that accommodated much of the subsidence in this area.

Based on overlapping whole-rock, mineral and isotopic compositions between the pyroxene-rich undersaturated rocks and the plagioclase-rich subalkaline rocks, both types appear to have been derived from a similar magmatic source but underwent different crystallization histories. The undersaturated basalts apparently were subjected to deep-level fractional crystallization where plagioclase was not a stable phase. In contrast, the underlying and interbedded plagioclase-rich volcanic rocks of the Lower Cretaceous formations must have undergone extensive shallow-level fractionation. The undersaturated basalts were probably erupted during an episode of crustal faulting and subsidence. These rocks appear to have moved rapidly through the crust along deep-seated faults, thereby preventing extensive shallow-level crystallization.

MAP OF MODERN REEFS AND SEDIMENTS OF ANTIGUA, WEST INDIES

WEISS, M.P., Northern Illinois University, DeKalb, Illinois 60115 and MULTER, H.G., RD 1, Box 53, Arkport, New York 14807.

A colored geologic map of the submarine geology around Antigua is 70.5 x 103 cm (27.75 x 40.5 in) in size, with a scale of 1:40,000. The reefs and bottom sediments are mapped to a depth of about 20 m (10 fms). Five main submarine geologic units are mapped: 1) grass-held sediment, 2) linear reefs, 3) patch reefs, 4) deeper reefs, and 5) sand. Sixteen divisions of these main types are also shown. The coast of Antigua and its nearby islands is distinguished by symbols as rocky, sand beach or mangrove fringe. Certain special features, such as steep scarps, sand-filled channels in coral, and underwater bedrock outcrops are also shown.

The map was constructed photogrammetrically on a stereoplotter, with "ground-truthing" accomplished by swimming traverses, observations and sampling from boats, inspection from the shore, and some drilling. The various seafloor environments/communities are described and illustrated in color on the back of the map.

A special feature is the recognition of changes in bottom environments over time; 49 such areas are mapped, and the nature of the changes described. The sizes of such areas are also tabulated. Most show the effects of commercial and residential development on Antigua since World War II.

Looking to the future, the map will serve as a benchmark of shallow-water environments against which to compare future observations and mapping.

MULTIPLE TRANSPORT HISTORY OF MINERAL SANDS ON THE SOUTH JAMAICAN COAST DEDUCED FROM PROVENANCE, SURFACE TEXTURE AND SEA-LEVEL STUDIES

WEST-THOMAS, Jennifer, and HENDRY, Malcolm D., Geology Department, University of the West Indies, Mona, Kingston 7, Jamaica.

Mineralogically mature sediments are rare in the Jamaican rock record, reflecting generally short transport distances from source to depositional site. An exception to this are the quartz-rich sand deposits of the Black River basin on the south west coast of the island. Provenance studies suggest that these sands are derived from the Cretaceous Central Inlier. Consideration of transport pathways indicates that drainage from the inlier to the south coast occurs through the Rio Minho river, the mouth of which reaches the shoreline c. 60 km east of the Black River area.
Surface textures revealed by S.E.M. include evidence of both marine and eolian influences, the latter commonly overprinting the former. Movement westwards along the island shelf, which extends over 25 km south of the island at an average depth of about 40 m could have been facilitated by dominant westerly current and littoral drift directions, after deposition from the Rio Minho. Emplacement of these sediments, which clearly were extensively winnowed during shelf transport, must post date the last interglacial event, because the sands overly an elevated reef of this age at the present shoreline. Sea-level lowering during the Wisconsinan exposed the shelf for an extended period during which time characteristic south-east winds transported the sands to their present location. This proposed fluvial, marine and eolian history has important implications for mineral exploration, because it suggests that the south coast shelf of the island may be extensively veneered by mineral deposits. Metallic minerals found on the shoreline between the Rio Minho and Black River add extra significance to this possibility.